Zhonglin Xu

Fundamentals of Air Cleaning Technology and Its Application in Cleanrooms

Springer

Fundamentals of Air Cleaning Technology and Its Application in Cleanrooms

Zhonglin Xu

Fundamentals of Air Cleaning Technology and Its Application in Cleanrooms

Authored by Zhonglin Xu (in Chinese),
Translated by Bin Zhou

Springer

Zhonglin Xu
China Academy of Building Research
Beijing, China, People's Republic

ISBN 978-3-642-39373-0 ISBN 978-3-642-39374-7 (eBook)
DOI 10.1007/978-3-642-39374-7
Springer Heidelberg New York Dordrecht London

Library of Congress Control Number: 2013950929

Printed on acid-free paper

Springer is part of Springer Science+Business Media (www.springer.com)

Preface

With 50 years of experience in the field of air cleaning technology in China Academy of Building Research, it has been clearly demonstrated that air cleaning technology has become one symbol of modernization in scientific experiment and production activities. In 2001, Professor Yang Chen-Ning, the Nobel Laureate in Physics, pointed out in the speech for the annual meeting of China Association for Science and Technology that there are three major directions for the scientific and technological development in the next 30 or 40 years: (1) widely application of chip, (2) rapid development of medicine and biology, and (3) bioengineering, which cannot be separated from air cleaning technology. In order to advance towards the three major directions, in addition to the process itself, the most challenge is from the air cleaning aspect, where a clean indoor microenvironment must be created.

In 1983, the monograph entitled *Principle of Air Cleaning Technology* was published in Beijing. It has been reprinted by 18,000 copies, but it still cannot meet readers' requirements. With the invitation by Asia Springer Publishing Company in the early 2012, the Chinese manuscript with the title *Fundamentals of Air Cleaning Technology and Its Application in Cleanrooms* was prepared, and the English version was provided by Dr. Zhou Bin, associate professor from Institute of HVAC at Nanjing University of Technology. (Dr. Zhou obtained the doctoral degree from Tongji University and Politecnico di Torino). During the process, undergraduates from the major *Building Environment and Energy Engineering* at Nanjing University of Technology were greatly appreciated. Miss Wu Tianxiang who translated the Japanese language and then performed proofreading was acknowledged. With the encouragement and promotion from Miss Shen Li, this book can be published within 1 year.

Last but not the least, support from the Natural Science Foundation of Jiangsu Province (No. BK20130946) was greatly acknowledged.

Valuable comments and suggestions from readers and friends are welcomed. (To: ph_ph@163.com and zhoubinwx@hotmail.com).

From Xu Zhonglin studio Zhonglin Xu
at Institute of Building Environment and Energy Efficiency,
China Academy of Building Research, Beijing, China
April 3, 2013

Contents

Chapter 1
Particle and Size Distribution

The purpose of air cleaning technology is to get rid of airborne particles as much as possible. Gaseous medium containing dispersed airborne particles is one kind of dispersed systems, which is termed as aerosol.

Exactly speaking, according to ISO definition [1], aerosol system is "the airborne system in gases containing solid particle, liquid particle or solid/liquid particle whose settling velocity could be ignored."

The way that how airborne particles move and distribution is fundamental to air cleaning technology. In order to illustrate easily, particles and size distribution characteristics will be introduced firstly and how particles move indoors in the following chapters.

1.1 Particle Classification

1.1.1 Classification with Particle Formation Methods

1. Dispersed Particles. They are formed into airborne state from solid/liquid under the effect of division, collapse, flow stream, and vibration. Solid dispersed particles could be those with irregular shape or those formed by loosely coagulated particles.
2. Coagulated Particles. They are formed by the process of combustion, sublimation, vapor condensation, and gas reaction. Solid coagulated particles are usually formed by many loose coagulated groups from primary particles with regular crystallization shape or spherical shape. Liquid coagulated particles are smaller than liquid dispersed particles, and the extent of their polydispersity is smaller.

Z. Xu, *Fundamentals of Air Cleaning Technology and Its Application in Cleanrooms*,
DOI 10.1007/978-3-642-39374-7_1, © Springer-Verlag Berlin Heidelberg 2014

1.1.2 Classification with Particle Origin

1. Inorganic Particles. Such as metal dust particle, mineral dust particle, and particles from construction materials
2. Organic Particles. Such as plant fibers, animal skin, hair, horniness, skin debris, chemical fuel, and plastic
3. Living Particles. Such as unicellular algae, fungi, protozoa, bacteria, and virus

1.1.3 Classification with Particle Size

The size range of aerosol is 10^{-7} to 10^{-1} cm, and within this range, the physical characteristic and law will be different when particle size changes.

1. Visible Particle. Visible with eyes and the corresponding particle diameter is larger than 10 μm.
2. Microscopic Particle. Visible with the microscope and the corresponding particle diameter is 0.25–10 μm.
3. Supermicroscopic Particle. Visible with supermicroscope or electronic microscope and the corresponding particle diameter is smaller than 0.25 μm.

It should be noted that particles with diameter 0.1–5 μm are classified as fine particles; those <0.1 μm are superfine particles, and those >5 μm are big particles.

1.1.4 Common Classification Method

In the technical field of aerosol, terms as "dust," "smoke," and "mist" are frequently used. Some definition and concept in air cleaning technology are also usually referred to these terms (such as "dust" concentration in the air and oil "mist" meter). These are the common classifications for particles:

1. Dust. It includes all the solid dispersed particles. The movement of these particles in the air is influenced by the combined effect of gravity and diffusion. It is almost ubiquitous in air cleaning technology.
2. Smoke. It includes solid coagulated particles, particles formed by coagulation effect from liquid and solid particles, and particles from the transition from liquid particle to crystallized particle.

According to ISO definition, smoke is clearly defined as "aerosol formed by solid particles during the metallurgy process. It is the gaseous condensate from the vapor generated after the evaporation of melted material. During the formation process, chemical reaction such as oxidation usually occurs." In the usual circumstance, particles from smoke with diameters much less than 0.5 μm are mainly

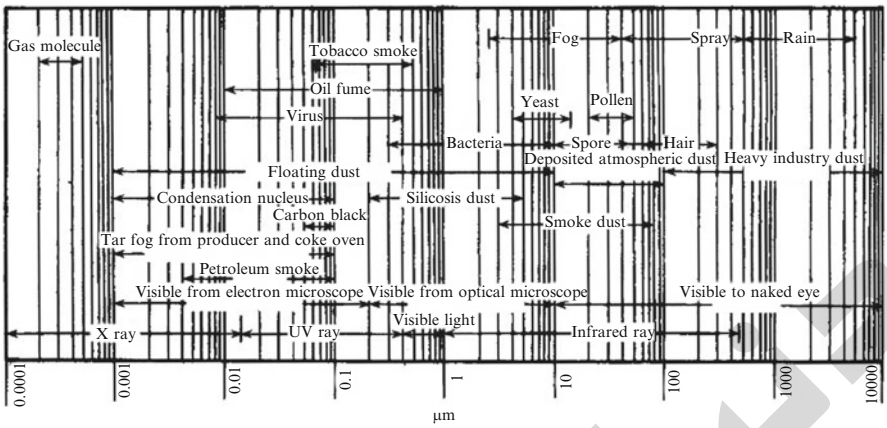

Fig. 1.1 Size range of particles

controlled by Brownian motion effect in the air, which makes the particles strong disperse capacity, and they are difficult to settle down in still air. Smoke stream generated by smoke generator is usually used to detect the leakage on air filters in air cleaning technology field and to perform the experiment for the flow visualization.

3. Fog and haze. Fog includes all the dispersed liquid particles and coagulated liquid particles.

According to ISO definition, mist means "the general term for liquid airborne system in air. In meteorology field it means the airborne system containing droplets which causes the visibility length less than 1 km." Particle size differs with formation state, and it is between 0.1 and 10 μm. Stokes law mainly dominates their movement. For example, sulfate mist generated from SO_2 gas will be transformed into oil mist by the combined effect of heat and compressed air, and oil mist could be the standard aerosol for testing air filter. The combination of fog and fine solid particles is termed as haze.

4. Smog. It includes both liquid and solid particles and both dispersed and coagulated particles. The size ranges from several tenth micrometers to dozens micrometers, such as the combined system formed by coal dust, SO_2, CO, and water vapor, which exist in the air of industrial zone (the typical case is the London mist which is the mixture of smoke and mist, and the FeO smog generated in iron plant). However, according to ISO definition, smog usually represents "visible aerosol generated during combustion process" and "no water vapor included," which means there is a little difference between smog and mist.

Figure 1.1 illustrates the size and range of aerosol particles.

1.2 Evaluation of Particle Scale

1.2.1 Particle Size

Particle size is usually used to represent how big the particle is. However, not all the particles, especially dust particles, have regular geometric shape such as spherical or cubic. Therefore the term "particle size" used frequently does not mean the real diameter of sphere. In the field of aerosol and air cleaning technology, the meaning of "particle size" is some length dimension inside particles, without indication of the meaning of regular geometric shape. When particle scale is analyzed, "particle size" does have this indication.

Exactly speaking, particle size could be divided into two categories:

The first one was measured and defined according to particle's geometric characteristic, such as microscopic method used to determine the particle size. For example, when particles were observed with optical microscopic after the dust sampling, the dust sample was moved towards one direction and through micrometer, where particle was projected onto this scale meter, and the length between two cutting edges by the meter represents the particle size. Particles were measured in a sequential and random way, so the long length was determined when the longer side of particle approached, and the short length was measured when the shorter side approached (shown in Fig. 1.2).

The long and short sides were called directional tangential cutting edge or random diameter. When the number of measured particles was large enough, results could reflect the average cross section of particle sample properly. In this way, it is

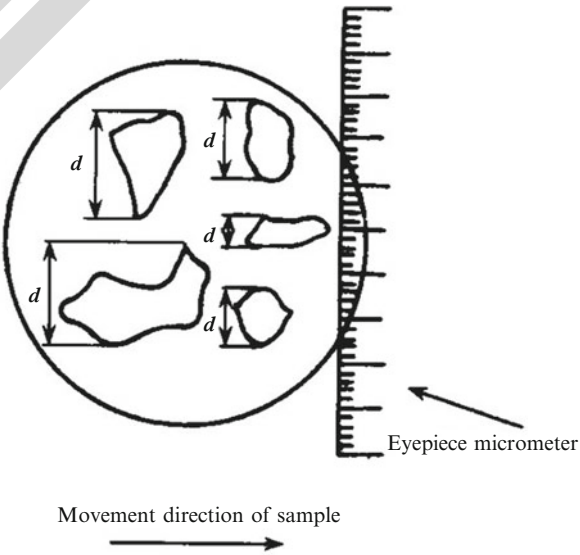

Fig. 1.2 One method to determine particle size

convenient to take measurements. However, in some cases only the maximum projected distance was adopted as particle diameter, such as several standards about cleanroom in the USA. Obviously micrometer must be rotated during measurement, and the location for maximum distance could not be fixed precisely. So the Japanese standard "Measurement of Airborne Particles in Cleanroom" (Japanese Industrial Standards, JIS) suggests no need to rotate micrometer, and instead only the projected maximum length is estimated, which was thought to cause small error. For cubic particles, the diagonal is also used to represent particle size, so it equals with the multiplication of the side length and $\sqrt{3}$. For particles whose projected area is rectangular, the average of long and short side lengths is used, and also the diagonal length could be used based on the short side length. In the following paragraph, NaCl particles will be introduced, and particle size determined by diagonal method is used since the projected area of their crystal is usually quadrate.

The other group was based on the indirect measurement and definition of some physical property of particles. Precipitation method and optic-electrical method are used to determine the particle size. The value obtained is actually an equivalent diameter. In the former Federal German Standard VDI-2083, particle size was defined as the equivalent diameter according to the measuring method, which means some physical property and parameter of referenced particles are equivalent with the counterparts of these particle cloud based on this diameter value. For example, when light scattering air particle counters are used, "particle size" represents the comprehensive effect, i.e., the geometric size range, by comparing the equivalent light scattering intensity between the tested particle and standard particle (such as PSL particles). Setting velocity of particles could be measured, and when the settling velocity in still air calculated by Stokes law in Chap. 6 is equal to that of particles with same density, the spherical diameter of latter is called settling diameter, also Stokes diameter, which is labeled as d_{st}, and it is smaller than other diameter value. Assume the density is 1, the diameter of spherical particles whose settling velocity is the same will also be called aerodynamic diameter, which is widely used in environmental science and labeled as d_a. It is known from Eq. (6.7) that $d_{\mathrm{st}}^2 \cdot \rho_P = d_a^2 \cdot 1$. So the following correlation can be obtained:

$$d_a = d_{\mathrm{st}} \rho_P^{1/2} \tag{1.1}$$

where ρ_P represents the particle density.

American Federal Standards 209C and 209E allowed to use either of (1) maximum visible linear length of particle or of (2) equivalent diameter measured by automatic meter.

1.2.2 Average Particle Size

Since particle shape differs a lot from each other, different values of particle size could be obtained with the above methods, which is inconvenient for application.

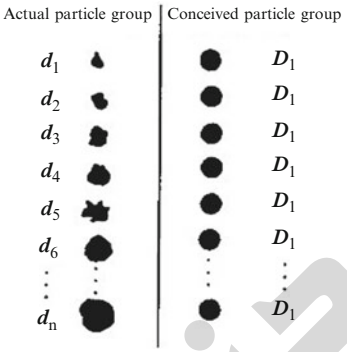

Fig. 1.3 Conceived particle group and average particle size

Therefore, one method to reflect some characteristic by the average particle size from all the particles must be found, and the average value is called "average particle size." This special method is used to represent a hypothesized particle diameter according to some certain characteristic.

Assume the actual particle sizes are $d_1, d_2, \ldots, d_n$, respectively, which is shown in Fig.1.3. These values of particle size were determined by the before-mentioned method. Some certain characteristic (such as light scattering property) could be represented by $f(d_1), f(d_2), \ldots, f(d_n)$, so the property of the particle group $f(d)$ has the following relationship with that of individual particle:

$$f(d) = f(d_1) + f(d_2) + \cdots f(d_n) \tag{1.2}$$

Suppose another particle group contains particles with the same particle size D and its property (such as light scattering property) is the same as that of the actual particle group, so we could get

$$f(d) = f(D) \tag{1.3}$$

where the particle size D means the average particle size of this particle group corresponding to some certain property. D could be defined as the side length of the hexahedron or the diameter of sphere. The latter is usually used, which means the particle group could be treated as a group of spheres with the same diameter.

The simplest case is to assume that the group consists of particles with the same diameter D_1, so the total length of all diameters is the same as that of actual particle group. According to Eq. (1.3), we could obtain

$$\sum n_i d_i = \sum n_i D_i = \sum n_i D_1 = nD_1$$

$$D_1 = \frac{\sum n_i d_i}{\sum n_i} = \frac{\sum n_i d_i}{n} \tag{1.4}$$

This is the arithmetic average diameter. In this equation, d_i is the particle size by any measuring method; m_i is the number of particles with diameter d_i; n is the total particle number.

If the summation of assumed particle areas (projected area or surface area) is the same as that of the actual particle group, we could get the following equation based on Eq. (1.3):

$$D_s = \sqrt{\frac{\sum n_i d_i^2}{\sum n_i}} \tag{1.5}$$

This diameter is termed as average surface diameter.

If the specific length area (i.e., the cross section area per unit length) of the assumed particle group is the same as that of the actual particle group, we could get the following derivation:

$$\frac{\sum n_i \frac{\pi}{4} d_i^2}{\sum n_i d_i} = \frac{n \frac{\pi}{4} d_2^2}{n D_2}$$

or

$$\frac{\frac{\pi}{4} \sum n_i d_i^2}{\sum n_i d_i} = \frac{\pi}{4} D_2$$

Hence

$$D_2 = \frac{\sum n_i d_i^2}{\sum n_i d_i} \tag{1.6}$$

This diameter is termed as specific length diameter.

The same method could be utilized to obtain other average diameters. The cross section could be circular (sphere) or rectangular. Moreover, average diameter could be determined according to the particle size frequency distribution. Table 1.1 lists these average diameters.

By comparison of these diameters, we could get the following sequence:

$$D_{\text{mod}} < D_g < \bar{D} < D_S < D_V < D_2 < D_3 < D_{50}^V < D_4$$

It should be noted for the average particle size names listed in the table. In literature, terms with converse sequence could be encountered. For example, some use “average area diameter,” while others use “area average diameter.” Therefore, the meaning could be clearly understood only when the expression is known. But if we start from the definition, it’s easier to understand the meaning. For example, in Table 1.1, “average area” obviously means all the areas averaged by some quantity

Table 1.1 Average diameter of particles

Symbol	Term	Significance	Calculation method
D_{mod}	Model diameter (or population diameter)	The diameter corresponding with the maximum proportion in the samples. The minimum diameter calculated with the frequency distribution	Obtained from the summit on the distribution curve of particle frequency
D_{50} or D_m	Medium diameter	The number of particles with diameter lager than this value is the same as that with diameter less, and this is called the number medium diameter. The mass of particles with diameter lager than this value is the same as that with diameter less, and this is called the mass medium diameter. All the diameters related to the number are smaller than that related to mass	Obtained at 50 % of the cumulative distribution curve of particle number (or mass)
$\overline{D}$ or D_1	Arithmetic average diameter	It is a kind of arithmetic average values and is the habitually most popular diameter. But small particles occupy the majority in the particle group. So even though the mass may be small, the calculated average diameter will also be greatly reduced. So there is great limit between the real size of particle group and the physical property of this particle group	$D_1 = \frac{\sum n_i d_i}{\sum n_i}$, where n_i is the particle number at each size and Σn_i is the total particle number
D_2	Specific length diameter (length weighted)	It is the division between the projected particle area and the summation of diameters, which is the average diameter per unit length	$D_2 = \frac{\sum n_i d_i^2}{\sum n_i d_i}$
D_3	Specific area diameter (area weighted)	It is the division of the total volume of particles to the summation of cross-sectional area, which is the average diameter per unit area	$D_3 = \frac{\sum n_i d_i^3}{\sum n_i d_i^2}$
D_4	Specific mass diameter (mass weighted, volume weighted)	It is obtained with the surface area per unit mass, namely, the average diameter of unit mass (or volume). It is larger than any other diameter	$D_4 = \frac{\sum n_i d_i^4}{\sum n_i d_i^3}$

(continued)

Table 1.1 (continued)

Symbol	Term	Significance	Calculation method
D_S	Average area diameter	It is the area weighted diameter according to the particle number	$D_S = \sqrt{\frac{\sum n_i d_i^2}{\sum n_i}} = \sqrt{D_1 \times D_2}$
D_V	Average volume (or mass) diameter	It is the volume (or mass) weighted diameter according to the particle number	$D_V = \sqrt[3]{\frac{\sum n_i d_i^3}{\sum n_i}} = \sqrt[3]{D_1 \times D_2 \times D_3}$
D_g	Geometric mean diameter	It is the average of the logarithmic diameters Or it is the nth root of the multiplication of several values	• $\log D_g = \overline{\lg d_i} = \frac{\sum_i^n n_i \lg d_i}{\sum n_i}$ • Expressed with natural logarithm $D_g = \exp\left(\frac{\sum_i^n n_i \lg d_i}{\sum n_i}\right)$
		Or it is the diameter with the maximum frequency from the lognormal distribution, and it is equal with the medium diameter of the particle number. It is always equal to or less than the arithmetic average diameter	• For unclassified data $D_g = \left(\prod_i^n d_i\right)^{1/n}$ • For classified data $D_g = \left(\prod_i^n d_i^{n_i}\right)^{1/n}$ so $\lg D_g = \frac{\sum_i^n n_i \lg d_i}{n}$ or $\lg D_g = \overline{\lg d_i} = \frac{\sum_i^n n_i \lg d_i}{\sum n_i}$ • The summit point can be obtained from the lognormal distribution curve

(such as particle number), so the area is in the numerator. "Area weighted" ("specific area") obviously means per unit area, so the area is in the denominator. As long as we keep in mind of this standard, we will not be confused. As for which average diameter is reasonable, it depends on the purpose of the work. If the gravimetric method is used to measure the particle concentration, diameter D_v which is related to mass should obviously adopted; when the property of light scattering is under investigation, it's better to use average area diameter D_s or average volume diameter D_v, because for different particle size range, the quantity

of light scattering probably depends on the particle area or volume; when the problem is related to the light refraction property, arithmetic average diameter D_1 should be used, because this property depends on the dimension of particle length.

Now let's calculate the average diameter of particles.

During the measurement of particle concentration with the sodium flame method, electronic microscopic could be used to measure the short side length of NaCl particles from 823 samples obtained from the supply air, and we assume the amplification ratio is 30,000 (i.e., include the amplification ratio of electric glass and amplification ratio of reader microscopic for reading values on SEM figures); the lower and upper limits for the group of short side could be calculated by

$$a = \frac{d_p \times 30,000}{\sqrt{3}} \tag{1.7}$$

where

d_p is the upper/lower limit of particle size range
a is the measured value of upper/lower limit of short side

Results for a are as follows:

Particle size interval (μm)	<0.05	0.05–<0.1	0.1–<0.2	0.2–<0.4	0.4–<0.6	0.6–<1.0
a (mm)	<0.87	0.87–<1.7	1.7–<3.5	3.5–<6.9	6.9–<10.4	10.4–<17.3
Number	17	99	429	225	40	13

According to the data from Table 1.2, we could obtain the arithmetic average diameter:

$$D_1 = \frac{\sum n_i d_i}{\sum n_i} = \frac{170.10}{823} = 0.207\,\mu\text{m}$$

Specific length diameter

$$D_2 = \frac{\sum n_i d_i^2}{\sum n_i d_i} = \frac{48.68}{170.10} = 0.286\,\mu\text{m}$$

Specific area diameter

$$D_3 = \frac{\sum n_i d_i^3}{\sum n_i {d_i}^2} = \frac{19.2}{48.68} = 0.394\,\mu\text{m}$$

Specific mass diameter

$$D_4 = \frac{\sum n_i d_i^4}{\sum n_i {d_i}^3} = \frac{9.85}{19.2} = 0.513\,\mu\text{m}$$

Table 1.2 Calculation table for average particle diameter

1	2	3	4	5	6	7	8	9	10	11
Particle size interval (μm)	Avg. value, d_i	Number, n_i	$n_i d_i$	$d_i^2 \times 10^2$	$n_i d_i^2 \times 10^2$	$d_i^3 \times 10^4$	$n_i d_i^3 \times 10^4$	$d_i^4 \times 10^6$	$n_i d_i^4 \times 10^6$	Number frequency (%)
<0.05	0.025	17	0.425	0.0625	1.06	0.16	2.72	0.39	6.63	2.06
0.05–<0.1	0.0725	99	7.425	0.5625	55.69	4.23	418.77	31.64	3,132.36	12.03
0.1–<0.2	0.15	429	64.350	2.25	956.25	33.75	14479	506	200,000	52.13
0.2–<0.4	0.3	225	67.500	9	2,025	270	60,750	8,100	1,822,500	27.34
0.4–<0.6	0.5	40	20.000	25	1,000	1,250	50,000	62,500	2,500,000	4.86
0.6–<1.0	0.8	13	10.400	64	832	5,120	66,560	409,600	5,324,800	1.58
∑		823	170.10		48.68		19.2		9.85	100

Area weighted diameter

$$D_s = \sqrt{D_1 \times D_2} = \sqrt{0.207 \times 0.286} = \sqrt{5.92 \times 10^{-2}} = 0.243\ \mu\text{m}$$

Volume weighted diameter

$$D_V = \sqrt[3]{D_1 \times D_2 \times D_3} = \sqrt[3]{0.207 \times 0.286 \times 0.394} = \sqrt[3]{2.33 \times 10^{-2}} = 0.286\ \mu\text{m}$$

When geometric mean diameter is calculated, we know

$$\lg D_g = \frac{\sum_i^n n_i \lg d_i}{\sum n_i} = -\frac{623}{823} = -0.757$$

Hence we get

$$D_g = 0.175\ \mu\text{m}$$

Reading on the photoelectric flame photometer used in the sodium flame method is proportional with the mass concentration of sodium chloride. Therefore, it is better to use mass ratio diameter D_4 to represent average diameter of sodium chloride particles. In the above example, $D_4 = 0.513$ μm, while the designated value in foreign standard is 0.6 μm.

1.3 Statistical Distribution of Particle Size

A lot of data on particle size will be frequently obtained in the field of air cleaning technology. After sampled on chemical porous membrane, particles with various shapes could be visible with microscope. Different samples will be obtained even though they are sampled simultaneously. Although particles are distributed randomly on the membrane surface, useful "information" is embedded behind those disorderly data. If arrangement and analysis are performed on these data, useful "information" could be extracted fully and correctly, which could be used as the basis for technical measurement adopted in dust measures, dust proof, and dust control. The purpose of data arrangement and analysis is to find the distribution law of particle number with particle size or density. A functional relationship could be used to describe this kind of law. However, there is no special theoretical basis that which kind of law is suitable for particle distribution. It is mainly dependent on experience.

1.3.1 Particle Size Distribution Curve

It is not enough to represent particle characteristic only with calculated average diameter. Particle characteristic depends to a great extent on the law of particle size distribution.

Distribution of particle size also means the dispersity of particles, which represents the number or mass percentage of particles at different size within the group of particle clusters. If particle percentage in the size distribution is introduced with particle number, it is called number frequency distribution (or simplified as frequency distribution). Particle number is usually a big number, so frequency distribution is preferred instead of number distribution in the study of particle size distribution. If particle mass is used for size distribution, it is called mass distribution. If particle surface area is used, it is called surface area distribution. Dispersity of a particle group will be higher for the case of particle cluster with higher percentage of smaller particles and vice versa. Dispersity represents the extent of fragmentation of dispersed material. When dispersity of a particle group is needed, particle size distribution should be obtained.

In the figure of particle size distribution curve, the number of particles within certain range of diameter values, or the ratio (or frequency) of particles in various diameter range segments, will be presented. The curve is obtained by smoothing the frequency distribution in the histogram.

1.3.1.1 Frequency Distribution (i.e., Relative Frequency Distribution) ΔD (%)

It is described with the percentage ratio of certain physical parameter (e.g., number ΔN) of particles with diameters between D_p and $D_p + \Delta D_p$ to the same parameter (e.g., total number ΔN) corresponding to the particle group:

$$\Delta \mathrm{D} = \frac{\Delta N}{N_0} \times 100\ \% \tag{1.8}$$

At first particle diameter is divided into several groups as needed or according to measurement method. It is better to set the diameter distance equally. The upper limit diameter of each group coincides with the lower limit diameter of the neighboring group with lager diameter. If one diameter value equals with the threshold value, it belongs to the larger diameter group. For example, when the diameter group of 0.2–0.4 and 0.4–0.6 are considered, particles with diameter 0.4 μm enters into the second group.

Secondly, particle numbers in each diameter group are countered, and frequency numbers are obtained. When frequency number is plotted as ordinate and diameter as abscissa, histogram could be acquired after rectangles with the height of frequency number are draw. If the ordinate is replaced with frequency (particle number within certain diameter range divided by the whole particle number), the histogram of frequency distribution is acquired.

Figure 1.4 is the NaCl aerosol particles used in the sodium flame method. Figure 1.5 illustrates the situation after its sedimentation and coagulation. Figure 1.6 presents the shape after deformation when wetted [2].

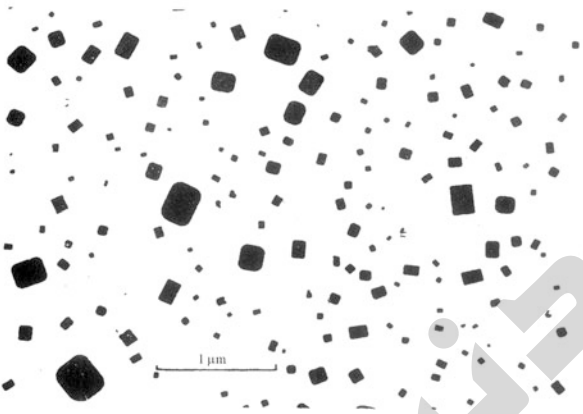

Fig. 1.4 NaCl aerosol particle with magnification of 27,000

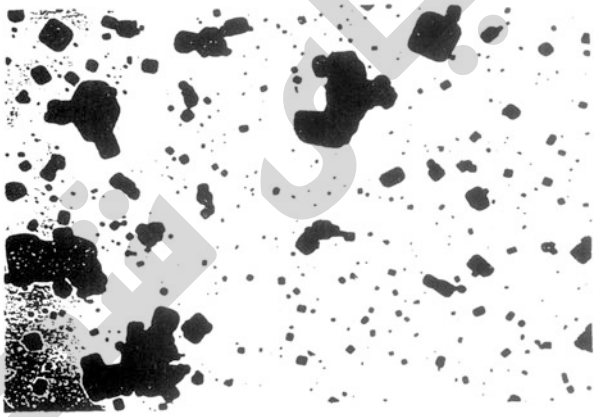

Fig. 1.5 NaCl aerosol particles after sedimentation and coagulation (magnification ratio 13,000)

Table 1.3 shows the number of another group of NaCl aerosol particles with SEM figures, from which we could get the number averaged diameter $\bar{D} = 0.192$ μm.

In Table 1.3, the cumulative mass frequency is obtained from the mass frequency distribution which could be calculated by the product of cubic of mean diameter in the diameter range and particle number.

Relative frequency distribution histogram shown in Fig. 1.7 could be depicted by this table, where the dashed line means the fitted particle distribution curve on the histogram.

Figure 1.8 shows the stereo of NaCl particles [3].

Particle size distribution curves for most particle group are asymmetrical, and they are inclined towards larger diameter. This is almost an intrinsic feature for dust particles since particles with small diameter occupy most portions of the whole dust particles. This kind of distribution is called "right-handed inclination" distribution. Furthermore, there are also "left-handed inclination" distribution and "symmetrical distribution," which are both presented in Fig. 1.9.

Fig. 1.6 NaCl aerosol particles after wet-absorbed deformation (magnification ratio 22,250)

Table 1.3 Number frequency distribution of NaCl aerosol particles

Group (μm)	Frequency	Percentage (%)	Cumulative percentage (%)	Cumulative mass percentage (%)
<0.1	2,895	19.09	19.09	0.11
0.1–<0.2	7,252	47.81	66.90	7.29
0.2–<0.3	2,770	18.26	85.15	19.59
0.3–<0.4	1,314	8.66	93.82	36.52
0.4–<0.5	479	3.16	96.98	49.33
0.5–<0.6	217	1.47	98.41	59.92
0.6–<0.7	116	0.76	99.17	69.25
0.7–<0.8	51	0.34	99.51	75.60
0.8–<0.9	32	0.21	99.72	81.35
0.9–<1.0	14	0.09	99.81	84.88
1.0–<1.1	10	0.06	99.87	88.27
1.1–<1.2	8	0.05	99.92	90.95
1.2–<1.5	8	0.05	99.97	95.28
1.5–<2.0	4	0.03	100.00	100.00

1.3.1.2 Frequency Distribution (i.e., Frequency Density Distribution) $\phi(D)$ ($\% \cdot \mu m^{-1}$)

It is described by the frequency distribution corresponding to the unit particle size range (e.g., 1 μm), i.e.,

$$\phi(D) = \frac{\Delta D}{\Delta D_P} \tag{1.9}$$

When the particle size ranges, especially those in the middle of data, are not equal, the fitted curve from histogram of frequency distribution will not be smooth, and it deviates greatly from the reality.

Take a look at Table 1.4 [4]; we could see the great discrepancy exists between particle size ranges. If histogram is plotted with the frequency data, we could get Fig. 1.10. When the frequency density is used, which is the proportionality of

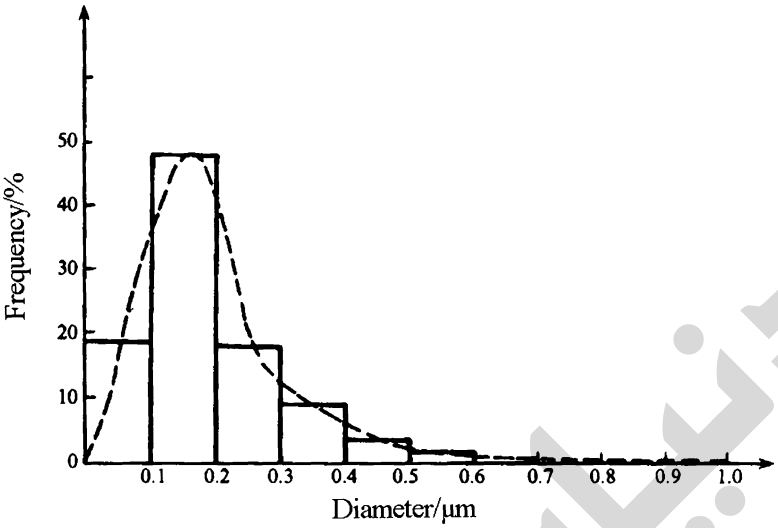

Fig. 1.7 Frequency distribution histogram

Fig. 1.8 Stereo of NaCl particles

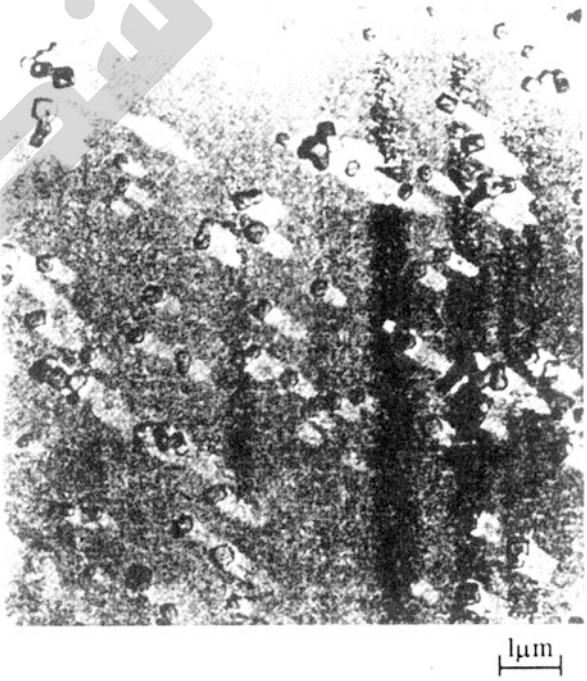

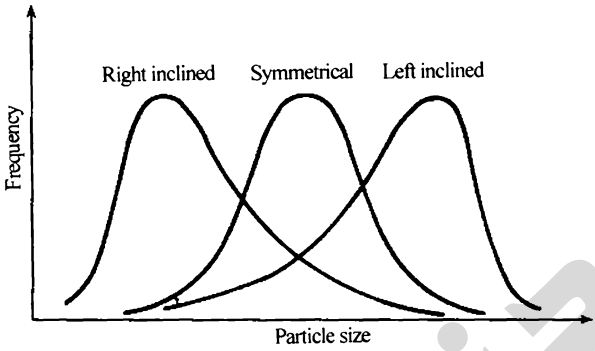

Fig. 1.9 Frequency distribution of particle size

Table 1.4 Classified data with larger interval

Interval (μm)	Number frequency (#)	Percentage (%)	Percentage per micrometer, i.e., channel frequency (%)
0–<4	104	10.4	2.6
4–<6	160	16.0	8.0
6–<8	161	16.1	8.05
8–<9	75	7.5	7.5
9–<10	67	6.7	6.7
10–<14	186	18.6	4.56
14–<16	61	6.1	3.05
16–<20	79	7.9	1.98
20–<35	103	10.3	0.69
35–<50	4	0.4	0.027
<50	0	0	0
Total	1,000	100.0	

particle number per unit size range, we could obtain the histogram as shown in Fig. 1.11. It is obvious that it is difficult to get any smooth curve for the former case. Even if the dashed line was drawn, it is quite different from the dashed line in the latter.

1.3.1.3 Upper Cumulative Frequency Distribution (Abbreviated as Upper Distribution) *R*(*D*) (%)

It is expressed as the percentage of certain parameter of all particles with diameter larger than D_P when compared with the same parameter of whole particle group, i.e.,

$$R(D) = \sum_{D_P}^{\infty} \phi(D)\Delta D_P = \int_{D_P}^{\infty} \phi(D)\mathrm{d}D_P \tag{1.10}$$

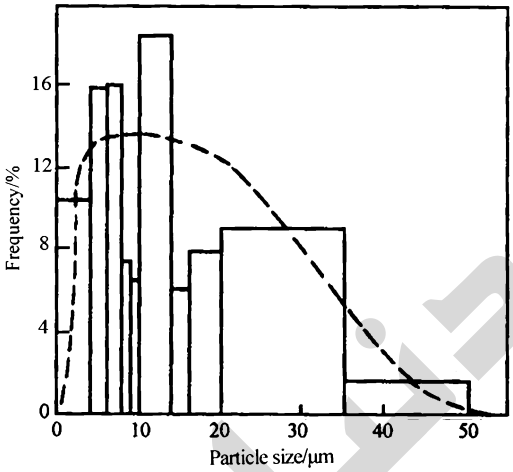

Fig. 1.10 Frequency diagram

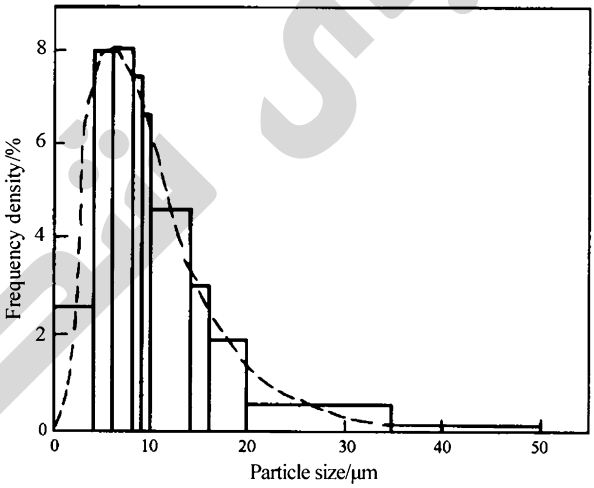

Fig. 1.11 Channel frequency diagram

1.3.1.4 Lower Cumulative Frequency Distribution (Abbreviated as Lower Distribution) $D(D)$ (%)

It is expressed as the percentage of certain parameter of all particles with diameter smaller than D_P when compared with the same parameter of whole particle group, i.e.,

$$D(D) = \sum_{0}^{D_P} \phi(D)\Delta D_P = \int_0^{D_P} \phi(D)\mathrm{d}D_P \tag{1.11}$$

Figure 1.12 shows a typical curve of cumulative frequency distribution.

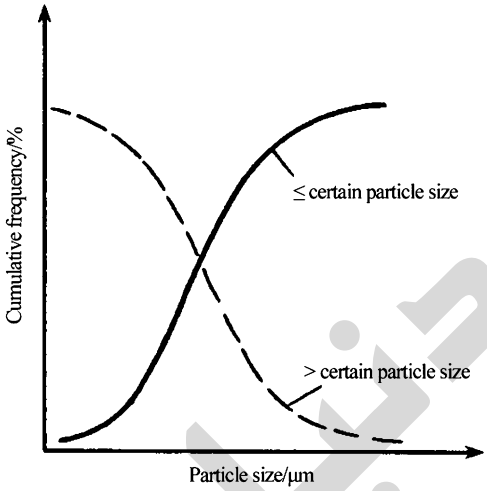

Fig. 1.12 Typical distribution curve of cumulative frequency

Figure 1.13 illustrates the relationship between frequency distribution and upper cumulative frequency distribution. The relationship between frequency distribution and lower cumulative frequency distribution could be derived in a similar way.

1.3.1.5 Bimodal and Multimode Distribution

For some aerosol particles, there will be two or more than two peak values in the frequency distribution curves. The distribution function is comparatively complex, so it will not be introduced here. Some examples are given for reference.

1. Oil mist aerosol. Oil mist is produced by the processes of oil heating, nozzle spraying, and condensation after evaporation. According to the research report [5], this kind of oil mist aerosol has the feature of bimodal distribution, where the main summit located at the diameter 0.133 μm and the second summit at 0.024 μm. The curve shape is independent of the amount of big particles separated. Figure 1.14 shows the curve shape. The reason to form this kind of bimodal distribution is that there are many components and a few nonvolatile materials in the test oil (turbine oil) and these components have respective distribution summit values.
2. Cold DOP aerosol (which can be seen in Sect. 17.2). It is also called pressurized DOP aerosol, which is the liquid mist sprayed from the Laskin nozzle after compressed air goes through the DOP liquid. According to some research report [6], the generated particles have the characteristic of bimodal distribution, no matter how much the compressed air pressure is. The particle size at valley between two summits is equivalent to the median diameter 0.275 μm. Figure 1.15 shows the frequency distribution measured by the channels of laser optical particle counter (every channel corresponds to a certain particle size range,

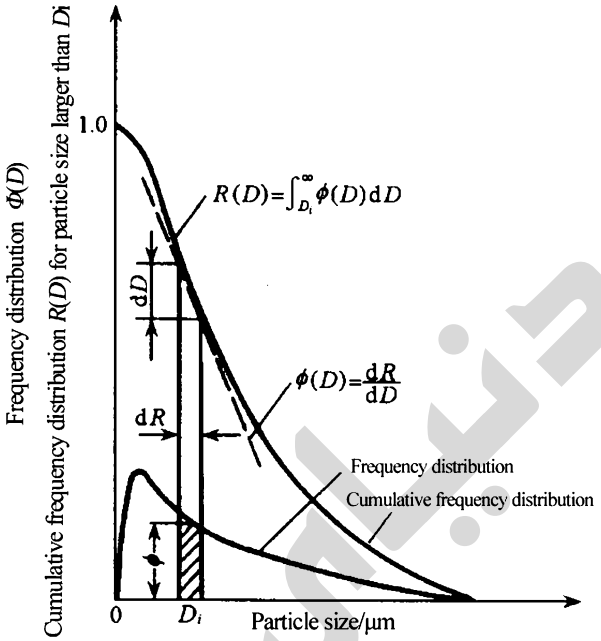

Fig. 1.13 Relationship between frequency distribution and cumulative frequency distribution

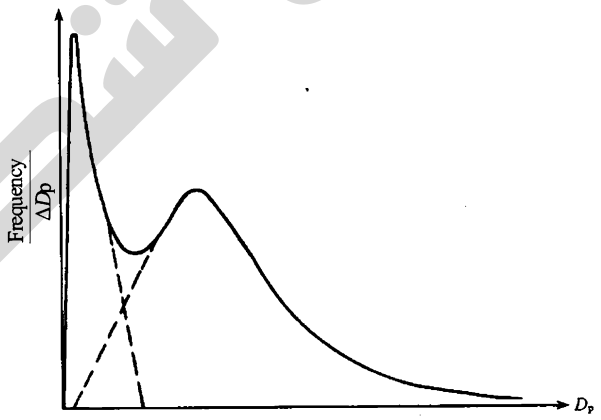

Fig. 1.14 Bimodal distribution of oil mist aerosol

and in the figure the data of particle size were calculated with the channel data from LAS-x particle counter in the test). It is shown that one channel exists between the second peak and the valley and the second peak value is corresponding to 0.3 μm (median diameter). It should be noted that the above experiment was carried out with the laser particle counter which was able to detect the particles with diameter smaller than 0.1 μm (0.09 μm). If the particle counter with the incandescent light was used and the lower detect limit is 0.3 μm, there would be no bimodal distribution [7], and the resultant number median

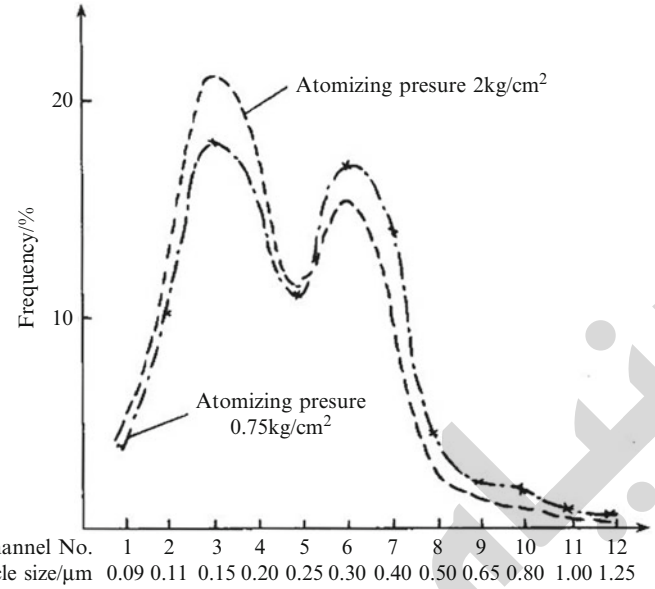

Fig. 1.15 Bimodal distribution of cold DOP aerosol

diameter would obviously be smaller than 0.3 μm, which is different from the above experimental result. Therefore the appearance of bimodal distribution is related to the test method, which needs further investigation.

1.3.2 Normal Distribution and Lognormal Distribution

Normal distribution curve is symmetrical in the middle which is shown in Fig.1.9. There is a highest point in the curve. The curve decreases monotonically towards two sides when the abscissa value of this point is considered as the center. The concept of normal distribution is one of the most important distribution concepts in statistics. In natural and engineering applications, it is the most widely used distribution for continuous data. Now the key points useful for study of particle size distribution will be introduced.

It is known from Figs. 1.9 and 1.10 that a comparatively smooth curve could be obtained from the histogram. Besides, the smooth curve could also be obtained when the sample number increases and the distance of subrange decreases, which is called probability density curve and is usually expressed as

$$y = f(x)$$

where y means the probability density, which is equal to the frequency value per unit abscissa value, and x means the abscissa value, which is the obtained data.

Normal probability density function could be used to represent the normal distribution curve:

$$y = f(x) = \phi(d) = \frac{1}{\sigma\sqrt{2\pi}} \mathrm{e}^{-\frac{(d_i-\overline{D})^2}{2\sigma^2}} \tag{1.12}$$

where

d_t is the particle size;

$\overline{D}$ is the average size, and it is usually the arithmetic mean diameter, so in mathematics it is the average value or expectation; for the case of normal distribution, $\overline{D} = D_m = D_{\mathrm{mod}}$;

σ is the standard deviation of a certain particle group. Since particle number of the particle group sample is very large, it could be expressed as

$$\sigma = \sqrt{\frac{\sum \left\{ n_i \left(d_i - \overline{D} \right)^2 \right\}}{\sum n_i}} \tag{1.13}$$

It is known with calculation that after many times of measurement, the probability for particles with measured diameter in the range of $\overline{D} \pm \sigma$ is 68.3 %, and for particles with $\overline{D} \pm 2\sigma$, it is 95.4 %, while for particles with $\overline{D} \pm 3\sigma$, it is 99.7 %. At the same time, the value of σ could be used to represent the extent of "slim" for the curve. The curve is "fat" with large value of σ, which means data are scattering and vice versa. Figure 1.16 gives the schematic diagram of both situations.

For the case of normal distribution when the abscissa of the highest point on the curve equals with 0 and the standard deviation is 1, it is termed as the standard normal distribution and labeled as $N(0, 1)$. Standard normal distribution curve could be obtained when any nonstandard normal distribution curve is translated, as shown in Fig. 1.17.

Cumulative distribution function $F(x)$ is obtained by integrating probability density function, and it is as follows:

$$F(x) = \int_{-\infty}^{\infty} \phi(x)\mathrm{d}x \tag{1.14}$$

or

$$F'(x) = \phi(x) \tag{1.15}$$

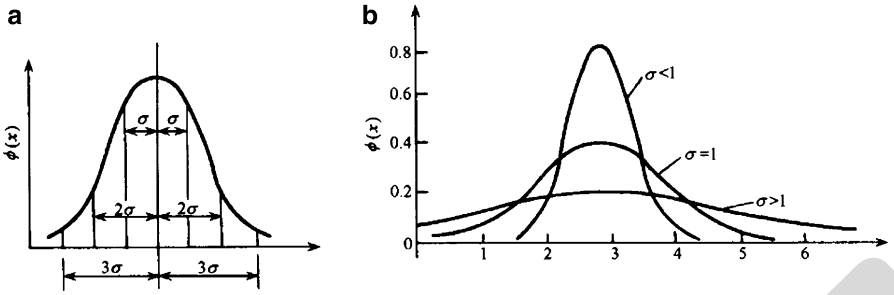

Fig. 1.16 Visual diagram of the meaning of σ (**a**) Relationship between σ and probability. (**b**) Relationship between σ and data dispersity

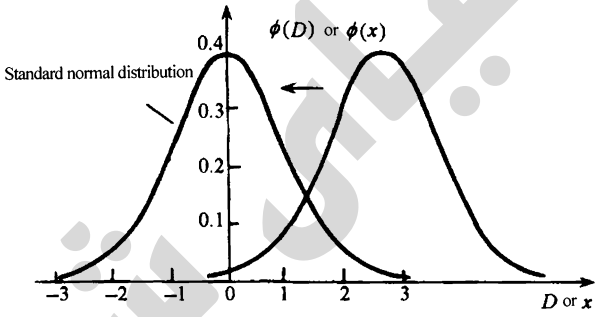

Fig. 1.17 Standard normal distributions

Figure 1.17 presents the curve for probability density function, and Fig. 1.18 is its cumulative distribution function curve.

The relationship between $\phi(x)$ and $F(x)$ is that of derivative and integration. This is the same for other statistical distribution, and it will be used in the process of sampling and measurement.

One special coordinate paper is called normal probability paper shown in Fig. 1.19, where its abscissa uses normal scale while the ordinate is drawn according to the normal distribution feature. If particle diameters follow normal distribution, a straight line will be obtained when the abscissa represents the particle size and the ordinate means the cumulative distribution frequency. This is one simple method to check whether particle size distribution is normal distribution.

Normal distribution could be used to depict specially generated monodisperse aerosols and pollen particles with single diameter, while most particle diameters do not follow normal distribution but close to it. For the case shown in Fig. 1.11, the cumulative distribution curve on the normal probability paper is not straight as noted in Fig. 1.19. The reasons are:

1. In normal distribution, the variable is continuous data (such as length measurement), while only discrete data are available in the particle sizing process. As detection means develops, the grouping range will be closer and the measured data will be more continuous, so it will approach the normal distribution.

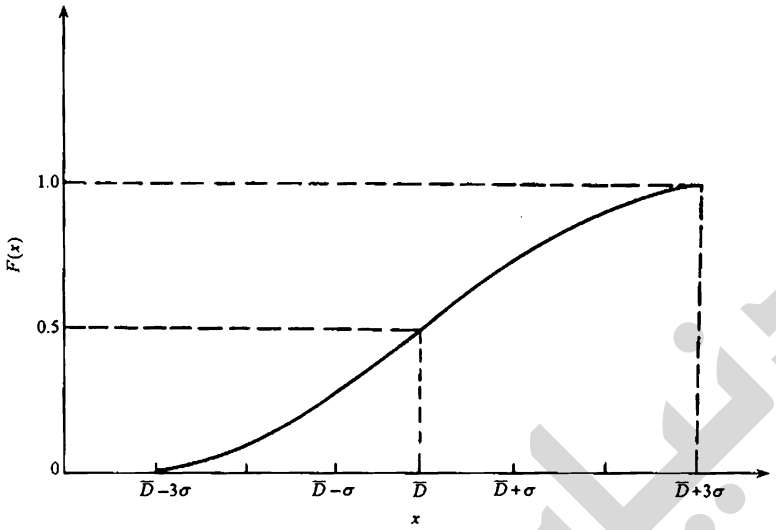

Fig. 1.18 Curve for cumulative distribution function

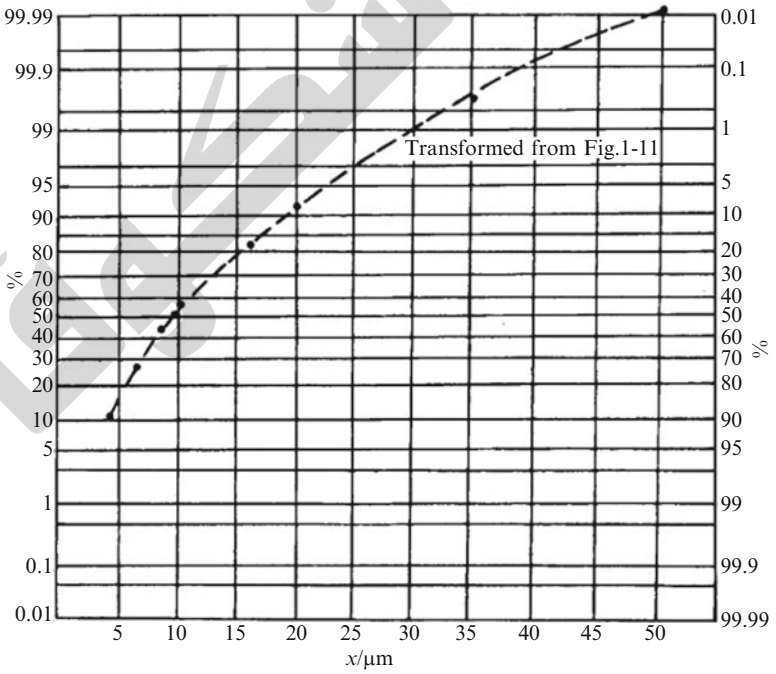

Fig. 1.19 Normal probability paper

Table 1.5 Logarithmic frequency distribution

Interval (μm)	$\Delta \lg D_p$	Frequency (%)	Frequency ($\Delta \lg D_p$)
0–<4	lg4 − lg1 = 0.063	10.4	0.172
4–<6	lg6 − lg4 = 0.176	16.0	0.91
6–<8	lg8 − lg6 = 0.125	16.1	1.29
8–<9	lg9 − lg8 = 0.051	7.5	1.47
9–<10	lg10 − lg9 = 0.046	6.7	1.46
10–<14	lg14 − lg10 = 0.146	18.6	1.27
14–<16	lg16 − lg14 = 0.058	6.1	1.05
16–<20	lg20 − lg16 = 0.097	7.9	0.81
20–<35	lg35 − lg20 = 0.243	10.3	0.42
35–<50	lg50 − lg35 = 0.155	0.4	0.26

2. The normal distribution curve is symmetrical. So it is possible that part of the curve goes through the abscissa zero point and part of particle diameter values is required to be negative, which is absolutely impossible.
3. Due to the right inclination distribution characteristics of the aforementioned particle swarm. If the abscissa of Fig. 1.11 is converted into logarithmic coordinate and the channel frequency distribution method is used, Table 1.5 could be obtained from the data in Table 1.4. In such a way, a curve more symmetrical and closer to the normal distribution will be obtained. This kind of curve is illustrated in Fig. 1.20. This distribution is termed as lognormal distribution.

When the particle size distribution of the before-mentioned oil mist aerosol with bimodal distribution characteristic is plotted on logarithmic graph paper, the main peak is also close to the lognormal distribution as shown in Fig. 1.21.

It should be noted that in the process of drawing frequency distribution curve, the extreme left on the logarithmic scale of the abscissa is not starting at 0 but at the smallest unit of this channel. For example, if the first channel is <0.2 μm, the left side could start at 0.1 μm, which means the value of $\Delta \lg D_p$ is lg0.2 − lg0.1 = 0.301, not lg0.2 − lg0. In some cases other suitable starting point could be considered according to the situation of the instrument. For another example, when the 3030-type electrostatic aerosol analyzer is used to measure the particle size, the particle size channel represents the nominal diameter, so for the first channel 0.0237 μm which includes the range between 0.0178 and 0.0316 μm, the value of $\Delta \lg D_p$ is $\lg \frac{0.0316}{0.0178}$.

When the points from the curve, which is basically in line with the lognormal distribution, are plotted on lognormal probability graph paper (i.e., normal probability graph paper with the logarithmic scale for the abscissa), a straight line could be obtained although no straight line is got at normal probability graph paper as shown in Fig. 1.19. The straight line (3) in Fig. 1.22 is made from Fig. 1.11 (or Table 1.4). This is a simple method to check whether the particle size distribution fits lognormal distribution. Line (2) in Fig. 1.22 is plotted with the data in Table 1.2. Although the data set distances are unequal, the characteristic of lognormal distribution could also be displayed on lognormal probability graph paper.

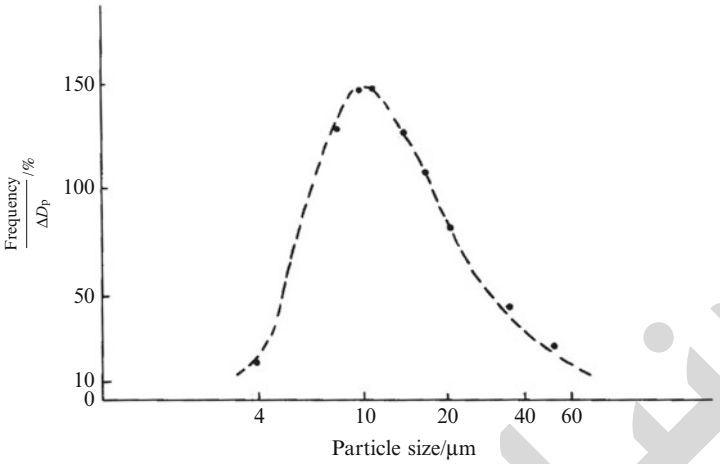

Fig. 1.20 Lognormal distribution

Fig. 1.21 Lognormal distribution of the main peak in the bimodal distribution of oil mist

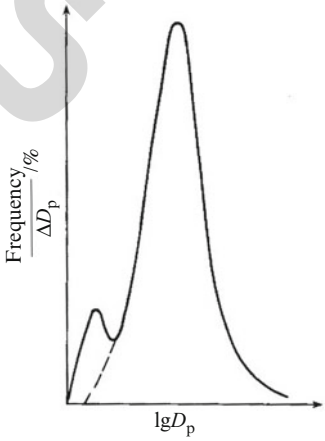

Since sample number (particle group for number counting) is random, a few deviations from straight line are allowable, but it should not deviate too much. Generally speaking, the middle points should get close to the straight line, while points at two extreme edges (especially big particles for dust) could deviate comparatively more from the straight line, such as the points at the 100 % lower cumulative frequency of line (3) (labeled with Δ for particle size >50 μm) made from Table 1.4 and Fig. 1.19. Although they deviate too much from the straight line, it is still reasonable to consider that the data basically fits lognormal distribution. Because both ends of the scale on lognormal probability graph paper are actually amplified, the error range of cumulative frequency at both 5 and 95 % is four times that of 50 %. In addition, grouping and measurement of both ends are generally

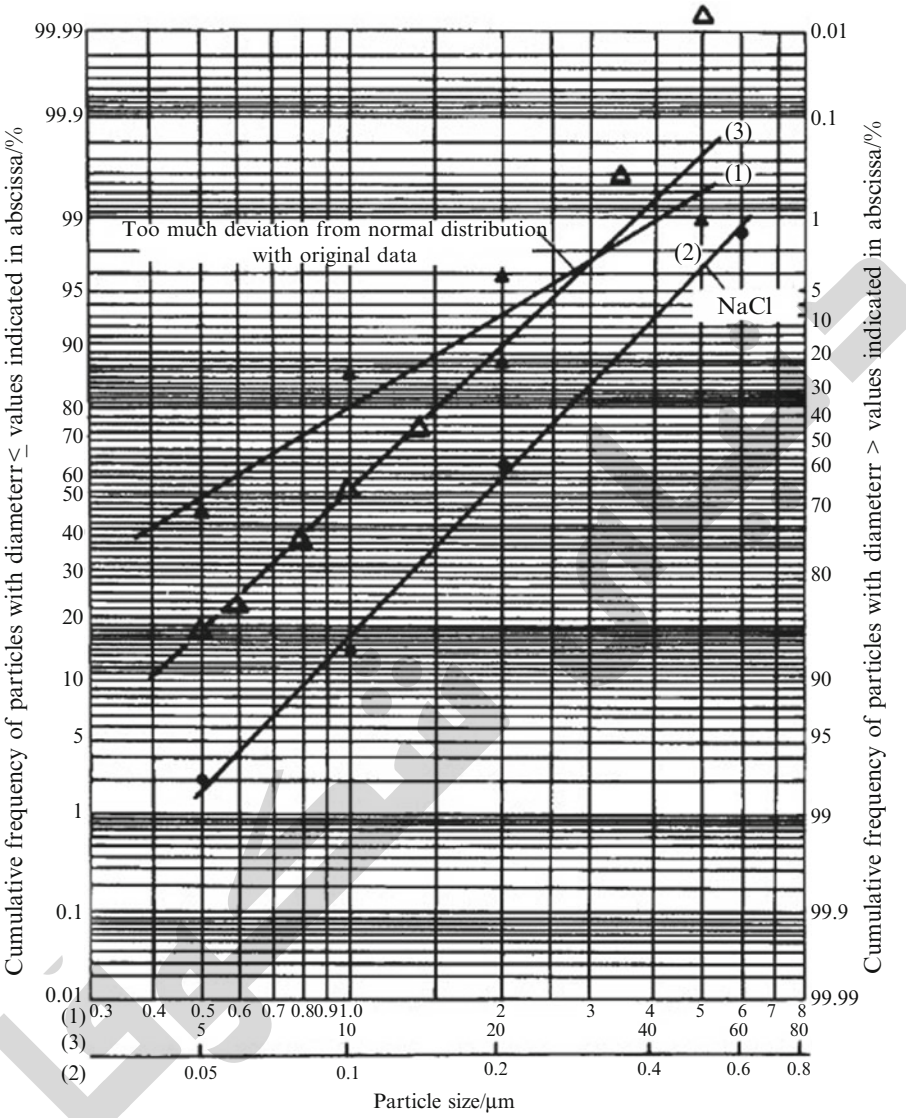

Fig. 1.22 Distribution on lognormal probability graph paper

coarse, so requirement for points with cumulative frequency smaller than 5 % or larger than 95 % is not so stringent, while it is enough to pay attention to the linear feature between 20 and 80 %.

Experiments have shown that particle size distributions of some dispersed aerosol and aggregated aerosol follow lognormal distribution. From the assumption of the characteristic during solid particle rupture process, particle size distribution was found to approach towards lognormal distribution. Although the reason is

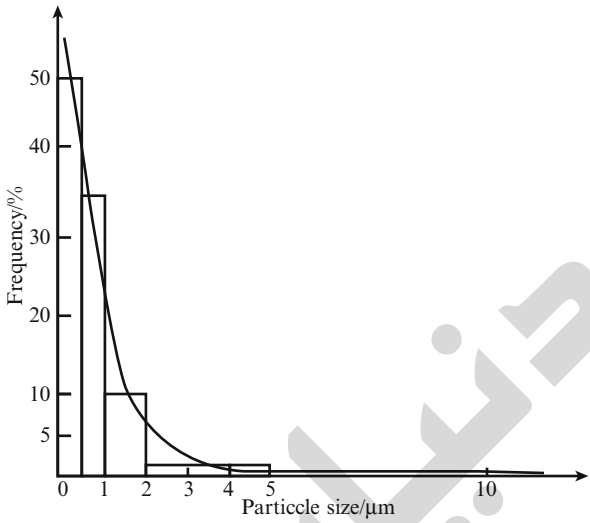

Fig. 1.23 Distribution curve of particle size in the air of a cleanroom

heretofore not clear, lognormal distribution has more theoretical meaning than other distribution [8].

If particle size distribution is quite different from normal distribution, such as an extreme case shown in Fig. 1.23 which represents the sampled particle size distribution curve in the cleanroom air, large deviation could be found when the lognormal probability graph paper is plotted. Line 1 on Fig. 1.22 is the resultant line.

1.3.3 Particle Size Distribution on Log-Log Graph Paper

Experiment has shown that some particle size distribution curves on log-log graph paper are close to be straight and they follow the rule of negative exponent, so they are also termed as negative exponential distribution. For the special case of finer particles, the linear dependence is well presented.

1.3.3.1 Attenuation Distribution Based on Particle Size

Attenuation distribution gives the information about the change of particle number with the change per unit particle size, which is equivalent with the previous frequency distribution when the ordinate means the particle number per unit particle size spectra instead of the frequency per unit particle size spectra. This is often used in the study of atmospheric aerosol, which will be introduced in Chap. 2 in detail.

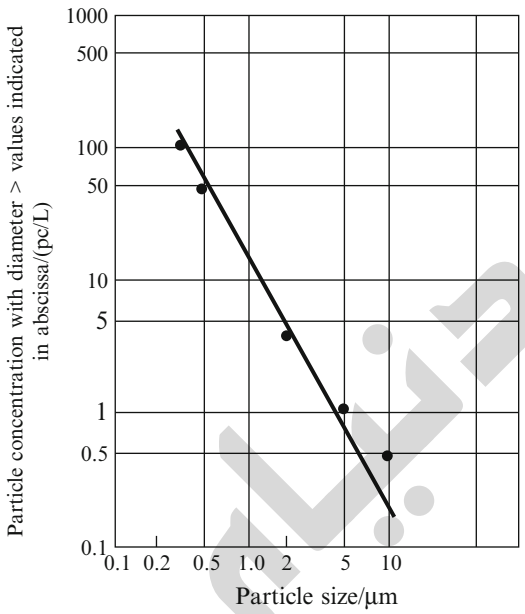

Fig. 1.24 Particle size distribution on log-log graph paper

1.3.3.2 Particle Number Cumulative Distributions Based on Particle Size

This means the change characteristic of particle number for the particle size equals with or larger than a certain value. For airborne particles with various diameters in the air of clean environment, their distribution curves of particle size on log-log graph paper are almost parallel straight lines with quite the same slope (especially those particles with diameter larger than 0.1 μm). Figure 1.24 is an example of a cleanroom which is the same cleanroom shown in Fig. 1.23. The feature of the line in Fig. 1.24 is more obvious than that of Fig. 1.23, so it is more useful for practice use. This is used in the classification of cleanness class, which will be illustrated later.

Atmospheric particles also have this feature, which is usually used in the air cleaning technology. For detailed information, please refer to Chap. 2 about atmospheric particles.

1.3.4 Distribution Based on Density

Particles are not uniformly distributed in terms of density (particle number per unit space or area). For example, when 1 L air is sampled from the cleanroom, the particle number measured by particle counter is 10#. However, particle number is actually not always 10# when 1 L air is sampled. For all that, there is a law existed in the sampled particle number per unit volume of air when particle counter is used.

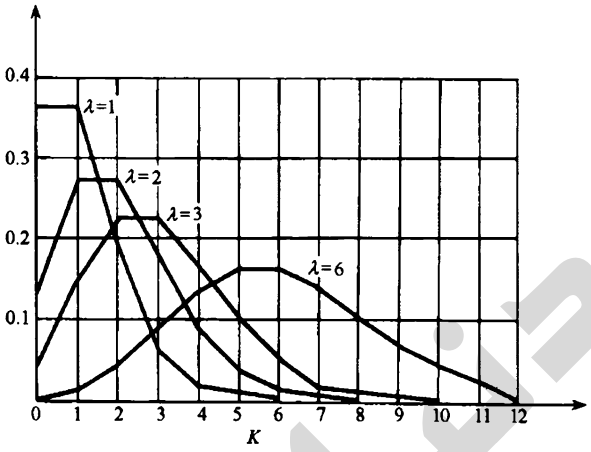

Fig. 1.25 Poisson distribution curve

In general case, the density distribution obeys the law of Poisson distribution. Density data could only be positive integers such as 1, 2, 3, 4, ..., instead of continuous one, so density does not follow normal distribution. Since the most important law for discrete data (counting value) is Poisson distribution, particle density distribution should also accord with Poisson distribution. In addition, four conditions are satisfied for the general cleanroom space, which are also required by Poisson distribution:

1. The measured space is much larger than the sample volume, even 10,000 times (the minimum is 100 times)
2. The probability of single particle appearing in the volume of every sample is very small such as several ten thousandths (the minimum is several hundredths)
3. It is incompatible that particle will fall into the sample volume and not.
4. Since particle concentration in the space is quite low, particle number during each sampling process is a small finite value (e.g., less than 10).

The probability of different particle number with Poisson distribution could be expressed as

$$P(\xi = K) = \frac{\lambda^K}{K!} e^{-\lambda} \tag{1.16}$$

where $P(\xi = K)$ means the probability of K particles where K must be positive integer including 0 and λ means the average time of the appearance of incidence, and it also represents the average concentration – average particle number included in the sampling volume.

Figure 1.25 shows the change of Poisson distribution curve when λ increases. The distribution curve for discrete data could only be polygonal line. When $\lambda > 5$–10, the curve is more symmetric and close to the normal distribution.

Table 1.6 Measured particle number distribution in a cleanroom (with diameter ≥0.5 μm)

	0	1	2	3	4	5	6	7	8	9	10
Measured times	98	125	104	68	28	12	3	1	1*	0	0
Calculated times by Poisson distribution	81.2	137.2	116	65.3	27.6	9.3	2.6	0.6	0.13	0	–

According to the probability theory, the probability for the appearance of more than K particles could be obtained from Eq. (1.15):

$$P(\xi \geq K) = 1 - P(\xi < K) = 1 - P(\xi = 0) - P(\xi = 1) - \cdots - P(\xi = K - 1) \tag{1.17}$$

The probability for the appearance of less than K particles is

$$P(\xi \leq K) = P(\xi = 0) + P(\xi = 1) + \cdots + P(\xi = K) \tag{1.18}$$

People may be afraid that the unidirectional flow in the cleanroom has almost no dilution effect (please refer to the cleanroom principle in Chap. 8), which will change the distribution law of particle size, so the Poisson distribution may not be applicable. But the Poisson distribution does not require uniform distribution of the particles. For example, during the investigation of flaw spots on the cloth and rejecting rate of piles of mechanical parts, they are both not uniformly distributed. But when enough random sampling time is performed, the conclusion of the law will be roughly in line with the actual situation.

Using the measured data from a cleanroom with unidirectional flow, the above conclusion could be validated.

Table 1.6 shows 440 measured data in a cleanroom with unidirectional flow where the original concentration is comparatively high and the efficiency of air filter is low. The sample volume of each test is 0.1 L. The test shows $\lambda = 1.69$.

Table 1.6 also lists the data by theoretical distribution with the value of λ. For example, the probability for the appearance of no particle can be calculated

$$P(K = 0) = \frac{1.69^{\circ}}{0!} e^{-1.69} = \frac{1}{1} \times 0.1845 = 0.1845$$

So the times of appearance are $0.1845 \times 449 = 81.2$. Results show that except for the influence by external interference (data labeled with *), agreement exists between calculation and test. Comparison between them could be clearly seen in Fig. 1.26.

In the following part, several test examples were performed in cleanrooms with unidirectional flow where the initial cleanness is high. Tests were performed at fixed position. Table 1.7 presents cases in China.

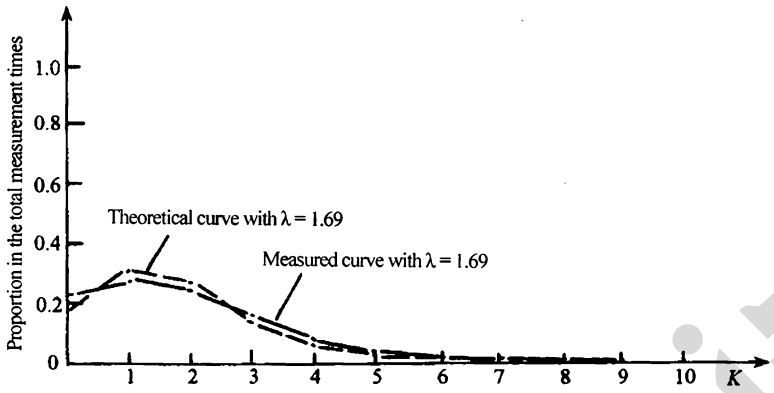

Fig. 1.26 Comparison of curves between test and theory

Table 1.8 presents some test cases in cleanrooms with unidirectional flow where the initial cleanness is high in China overseas. Test positions are at multiple positions.

Data between the examples 2 and 4 from Table 1.8 were collected in three cleanrooms by two particle counters with different types. Both sample flow rates are 0.1 ft^3/min (1 ft = 0.3048 m). The resultant conclusions are consistent.

In the measurement examples both in and outside China, except for the calculated value of nonzero time in the third example of Table 1.7, which is quite different from the measured value, others agree well with measurements. This further proves that Poisson distribution is suitable to describe the particle distribution in terms of particle number density.

Poisson distribution is also valid for the problem of studying the particle deposition number on a surface in cleanroom, which also meets the above four conditions. We have applied this conclusion in the study of the relationship between the yield rate and particle number in air, and agreement was found between calculation and experiment [13]. This conclusion will also be useful for the sample of microorganism particles, and detailed information will be introduced later. Statistical analysis of the measurement data of colony in biological cleanroom also support the above conclusion [14], which is shown in Fig. 1.27.

1.4 Concentration Degree of Particle Size Distribution

In a cluster of particles, it will be called monodisperse when particle sizes approach a single value. Its concentration degree is the maximum. On the contrary, it will be called polydisperse when particle sizes are scattering. Its concentration degree is the minimum. However, particle sizes in practice are not likely to be single value, but may be in the narrow range around the two sides of average diameter. Therefore,

Table 1.7 Particle number distribution in several Chinese cleanrooms with unidirectional flow and high initial cleanness

Test no.	Test times	Frequency with "0"	Particles with diameter more than 0.5 μm		Percentage with non-"0"	λ #/unit sampling volume L	Probability with "0" (%)	Probability with non-"0" (%)	Frequency equivalent with non-"0"	Ref.
			Frequency with "1"	Frequency with "2"						
1	21	18	3	–		0.15	86	14	$0.143 \times 21 = -3$	
2	42	41	1	–		0.03	97	3	$0.03 \times 42 = 1.26$	[9]
3	30	28	2	–		0.02	98	2	$0.02 \times 30 = 0.6$	
4	20	12	7	1		0.45	63.7	36.3	$0.363 \times 20 = 7.26$	
5	20	11	7	2		0.55	57.7	42.3	$0.423 \times 20 = 8.46$	[10]
	20	9	*	*		0.83	43.6	36.4	$0.564 \times 20 = 11.28$	

Note: *means there is no information for the current column in original literature, but the value of λ is given. In the fifth case, two times of measurement data in the same cleanroom are provided

Table 1.8 Particle number distribution in several foreign cleanrooms with unidirectional flow and high initial cleanness

			0.12–0.17 μm								
Test no.	Test times	Frequency with "0"	Frequency with "1"	Frequency with "2"	Frequency with "3"	Percentage with non-"0" (%)	λ #/unit sampling volume L	Probability with "0" (%)	Probability with non-"0" (%)	Frequency equivalent with non-"0"	Ref.
1	16	8	4	2	1		0.69#/3 L	50	50	$0.5 \times 16 = 8$	[11]
2	10	9	1	0	0		0.1#/ft^3	90	100	$0.1 \times 10 = 1$	
3	10	10	0	0	0		0	100	0	$0 \times 10 = 0$	[12]
4	10	8	2	0	0		0.2#/ft^3	82	18	$0.18 \times 10 = 1.8$	

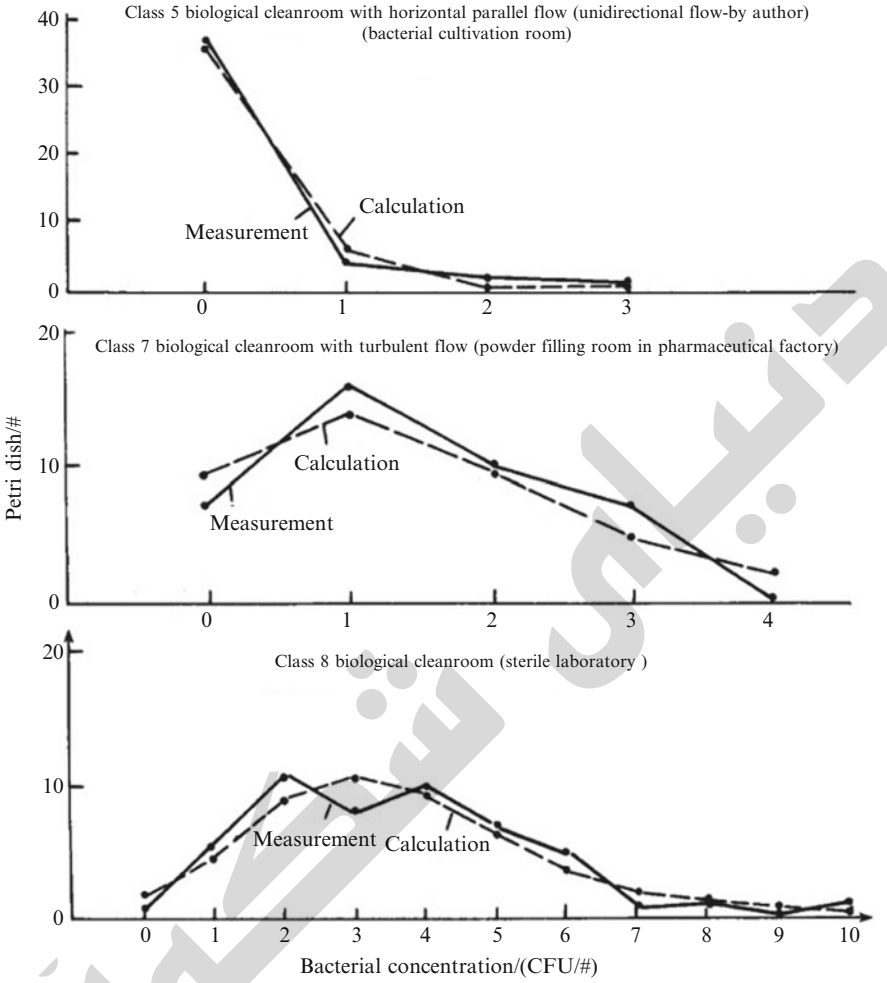

Fig. 1.27 Comparison between measured data and calculated one by the density distribution of microorganism particles

concentration degree of particles is defined as the percentage between particle numbers corresponding to particles with a certain diameter and the whole particle number.

It is obvious that concentration degree of particle sizes is not an antonym of scattering degree of particle sizes introduced in Sect. 1.3. If small particles with one or two kinds of diameters occupy quite a large number of a particle group, e.g., 90 % of the whole particle number, the scattering degree of this particle group is high, while it does not mean the concentration degree is low. On the contrary, since 90 % of particles have diameter concentrated in a small range, the concentration degree is very high.

Table 1.9 Standard of generated particles made by American DOW company (σ of particle sizes)

Standard diameter (μm)	Standard deviation σ
0.365	0.0079
0.557	0.011
0.814	0.0105
0.171	0.013

It is shown in Fig. 1.16 that the value of standard deviation σ represents the degrees of concentration and scattering of particle sizes. So σ could also be used to stand for the concentration degree or monodispersity of particles. We have such experiences that the absolute error for measuring comparatively large things is normally big, and it is small when tiny thing is measured. σ is only an indication of absolute fluctuation of particle size data. Evaluation of the concentration degree and monodispersity of standard latex particles, the standard particles used for calibrating Royco particle counters, made by American DOW chemical company is a good example, which is illustrated in Table 1.9. Error is related to the absolute value of particle size. In order to avoid the influence, it is more reasonable to use the relative fluctuation value to represent the scattering degree of data. Relative standard deviation, also called change coefficient, is usually used to represent the concentration degree of particle sizes.

$$\alpha = \frac{\sigma}{\overline{D}} = \frac{\left\{ \dfrac{\sum_{i}^{n} \left[n_i \left(D_i - \overline{D} \right)^2 \right]}{\sum n_i} \right\}^{\frac{1}{2}}}{\overline{D}} \tag{1.19}$$

However, since particle size distribution is usually close to lognormal distribution, it is more reasonable to use $\lg\sigma_g$ instead of σ. σ_g is called geometrical standard deviation.

When the scattering degree of particle sizes is small and suppose they are near from one certain particle size d_1, we could get the following expression from Table 1.1:

$$\overline{D} \approx \frac{n_1 d_1}{n}$$

$$D_g \approx d_1^{\frac{n_1}{n}}$$

So $\overline{D} \approx D_g$ because $n_1 \to n$.

When $\overline{D}$ is replaced by D_g and the logarithmic coordinate is used, we could get

$$\ln \sigma_g = \left\{ \frac{\sum_i^n \left[n_i \left(\ln D_i - \ln D_g \right)^2 \right]}{\sum n_i} \right\}^{\frac{1}{2}} \tag{1.20}$$

We know $\ln(1+x) \approx x$ when $-1 < x \leq 1$, so we can obtain

$$\ln D_i - \ln D_g = \ln\left(\frac{D_i - D_g + D_g}{D_g} \right) = \ln\left(1 + \frac{D_i - D_g}{D_g} \right) = \frac{D_i - D_g}{D_g}$$

This is why the following expression is obtained [3]:

$$\ln \sigma_g \approx \left\{ \frac{\sum_i^n n_i \left[\frac{\left(D_i - D_g \right)}{D_g} \right]^2}{\sum n_i} \right\}^{\frac{1}{2}} = \left[\frac{\sum_i^n n_i \left(D_i - D_g \right)^2}{D_g^2 \sum n_i} \right]^{\frac{1}{2}} = \frac{\left[\frac{\sum_i^n n_i \left(D_i - \overline{D} \right)^2}{\sum n_i} \right]^{\frac{1}{2}}}{\overline{D}} = \alpha \tag{1.21}$$

So

$$\ln \sigma_g \approx \alpha \tag{1.22}$$

or

$$2.3 \lg \sigma_g \approx \alpha \tag{1.23}$$

Fuchs (Н.А.Фукс) defined monodisperse particle as those particle group with $\alpha \leq 0.2$ (i.e., $\lg \sigma_g \leq 0.087$, or $\sigma_g \leq 1.22$) [15]. This means the proportion of particles within the diameter range $D_1 \pm 0.2\ D_1$ will be 68.3 % where D_1 is the arithmetic diameter of a particle group and $\alpha = 0.2$. For example, TSI Co. Ltd from the USA adopts σ_g as the concentration degree of standard particles which were still manufactured by DOW company. They consider standard particles with $\sigma_g < 1.06$ as monodisperse particles.

In practice, simplified method could also be used, which uses the proportion of particle numbers within certain diameter range to the whole particle number to represent the concentration degree. For example, if particle number of those with diameter 0.3 μm occupies 70 % of whole number, 70 % represents the concentration degree of these particles. It is obviously shown from the above discussion that although the method to determine the concentration degree is simple, it varies with different size range, so it is preferable to judge based on the value of α.

For modern optical particle counter which will be introduced in Chap. 17, the minimum channel is 0.1 μm, and the largest variation of average diameter in this channel is $< 0.2\overline{D}$, which means the ratio between this variation and average diameter is <0.2. The ratio for particles within larger channels will be smaller. Therefore, if we describe the concentration degree with the percentage of particle number in each channel, the ratio will be smaller than 68.3 % mentioned before, and usually it is 60 %. The concentration degree will be higher when it reaches 70–80 %.

1.5 Application of Lognormal Distribution

If particle size distribution follows the lognormal distribution characteristic, logarithmic probability graph could be used to determine the concentration degree of particle sizes and various kinds of average diameter.

1.5.1 Determination of Concentration Degree

If particle size distribution curve on the logarithmic probability graph is a straight line, particle size distribution will follow the lognormal distribution, which is shown in Fig. 1.20. Under this condition, Eq. (1.12) could be expressed as

$$\phi(D) = \frac{1}{\lg \sigma_g \sqrt{2\pi}} \mathrm{e}^{-\frac{\left(\lg D_i - \overline{\lg D_i}\right)^2}{2\lg^2 \sigma_g}} \tag{1.24}$$

From Table 1.1 it is known that $\overline{\lg D_i} = \lg D_g$ where D_g is the geometric average diameter. For the case of normal distribution, $\overline{D} = D_{50}$, so $D_g = D_{50}$ for lognormal distribution, and the above equation could be written as

$$\phi(D) = \frac{1}{\lg \sigma_g \sqrt{2\pi}} \mathrm{e}^{-\frac{\left(\lg D_i - \lg D_{50}\right)^2}{2\lg^2 \sigma_g}} \tag{1.25}$$

This function represents the relative number of particles with diameter D_t. If the total number is 100 %, the percentage of particle number of those with diameter smaller than D_t is

$$y = \frac{100}{\lg \sigma_g \sqrt{2\pi}} \int_0^{D_i} \mathrm{e}^{-\frac{\left(\lg D_i - \lg D_{50}\right)^2}{2\lg^2 \sigma_g}} \mathrm{d}(\lg D_i) \tag{1.26}$$

when

$$\frac{\lg D_i - \lg D_{50}}{\lg \sigma_g} = t \tag{1.27}$$

We know that

$$\lg D_i = t \lg \sigma_g + \lg D_{50}$$

$$\mathrm{d}(\lg D_i) = \lg \sigma_g \mathrm{d}t$$

Since $D_i = 0$–D_t when $t = -\infty$ to t, Eq. (1.26) could be written as [16]

$$y = \frac{100}{\sqrt{2\pi}} \int_{-\infty}^{t} \mathrm{e}^{-\frac{t^2}{2}} \mathrm{d}t \tag{1.28}$$

This is the normal distribution N (0,1) and the standard deviation is 1. From Eq. (1.27) we know

$$t \lg \sigma_g = \lg D_i - \lg D_{50} = \lg\left(\frac{D_i}{D_{50}}\right) \tag{1.29}$$

It is obvious that it is easy to solve $\lg\sigma_g$ when t is supposed to be 1 and $\sigma_g = \frac{D_i}{D_{50}}$. Refer to the normal distribution table and Fig. 1.28, the percentage of particle number with diameter $\leq D_t$ when $t = 1$ is $y \leq 84.13\ \%$ or that of diameter $> D_t$ is $y \geq 15.87\ \%$.

Therefore

$$\sigma_g = \frac{\text{Particle size for } y \leq 84.13\ \%}{\text{Median diameter } D_{50}} = \frac{\text{Particle size for } y \geq 15.87\ \%}{\text{Median diameter } D_{50}} \tag{1.30}$$

In a similar way we could get the following expression for $t = -1$:

$$\sigma_g = \frac{\text{Median diameter } D_{50}}{\text{Particle size for } y \leq 15.87\ \%} = \frac{\text{Median diameter } D_{50}}{\text{Particle size for } y \geq 84.13\ \%} \tag{1.31}$$

The value of calculated $\lg\sigma_g$ could be used to determine the concentration degree of particle group and thus to judge if it is monodisperse.

Suppose the actual particle size distribution measured by electronic microscope on monodisperse PSL spherical particles with claimed diameter 0.8 μm is shown in Table 1.10.

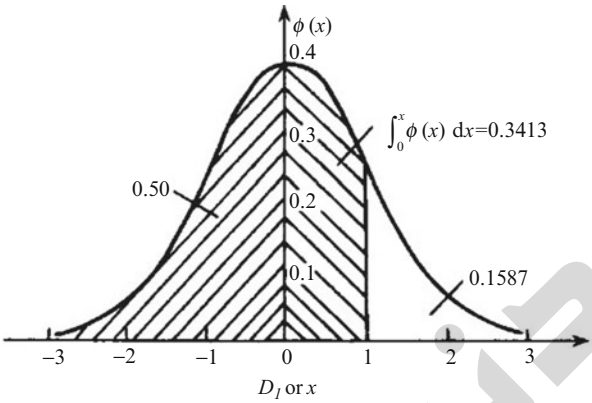

Fig. 1.28 Diagram of normal distribution

Table 1.10 Distribution of 0.8 μm PSL particles

Interval (μm)	Cumulative distribution (%)
≤0.6	1.2
≤0.7	6.1
≤0.8	65.5
≤0.9	88.0
≤1.0	98.5
≤1.2	100.0

Data of Table 1.10 plotted on Fig. 1.29 is a straight line A. We could obtain

$$\sigma_g = \frac{\text{Particle size for } y \le 84.13\%}{\text{Median diameter } D_{50}} = \frac{0.87}{0.78} = 1.115$$

$$\lg \sigma_g = 0.047 < 0.087 \text{ (or } \alpha = 0.108 < 0.2)$$

$$D_1 = 0.784\ \mu\text{m}$$

Therefore it is reasonable to consider this particle group as monodisperse, and 68.3 % of particle diameter will be in the range of $0.784 \pm 0.108 \times 0.784 = 0.784 \pm 0.085$ μm.

1.5.2 Calculation of Average Diameter

As mentioned before, it is quite difficult to calculate the average diameter. But for the case of lognormal distribution, data could be plotted on the lognormal distribution probability graph, and then it is easy to calculate the median diameter D_{50}, geometrical standard deviation σ_g, and various average diameters. Here only the results of various average diameters calculated are shown [16]. Process of data plotting could be referred to Fig. 1.29.

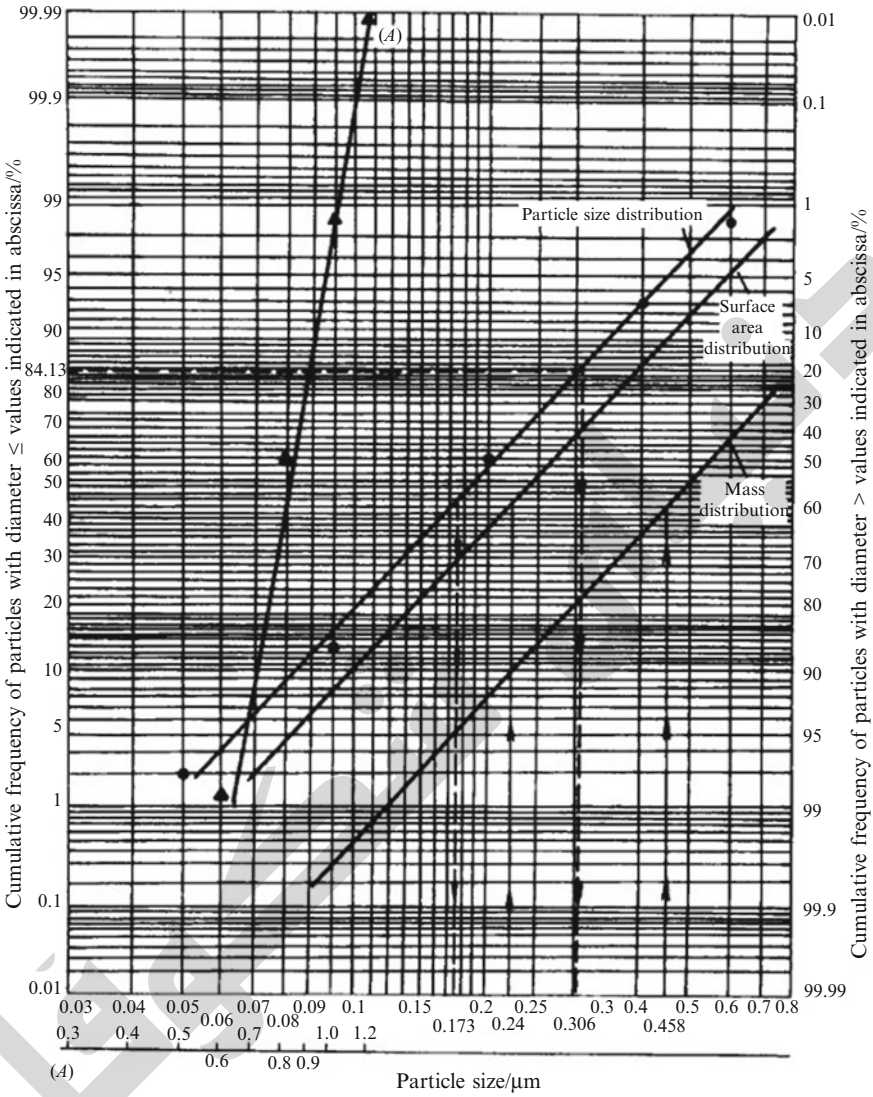

Fig. 1.29 Calculation of σ_g from lognormal distribution probability paper

The calculation expressions between various average diameters and D_{50} are presented below:

Geometric mean diameter

$$D_g = D_{50} \tag{1.32}$$

Arithmetic mean diameter

$$\lg D_1 = \lg D_{50} + 1.151\lg^2\sigma_g \tag{1.33}$$

Specific length diameter

$$\lg D_2 = \lg D_{50} + 3.45\lg^2\sigma_g \tag{1.34}$$

Specific area diameter

$$\lg D_3 = \lg D_{50} + 5.757\lg^2\sigma_g \tag{1.35}$$

Specific mass diameter

$$\lg D_4 = \lg D_{50} + 8.059\lg^2\sigma_g \tag{1.36}$$

Area weighted diameter

$$\lg D_S^2 = \lg D_{50}^2 + 4.605\lg^2\sigma_g \tag{1.37}$$

Volume weighted diameter

$$\lg D_V^3 = \lg D_{50}^3 + 10.362\lg^2\sigma_g \tag{1.38}$$

Various average diameters of the example line (2) on Fig. 1.22 are calculated, which is shown in Fig. 1.29. Since the diameter is $D_{84.13} = 0.306$ μm, which corresponds to 83.13 % on the accumulative distribution curve for geometric average diameter $D_g = D_{50} = 0.173$ μm $\leq D_i$, the geometric standard deviation is

$$\sigma_g = \frac{0.306}{0.173} = 1.769$$

$$D_1 = 0.204\ \mu\text{m} \quad D_2 = 0.282\ \mu\text{m}$$

$$D_3 = 0.39\ \mu\text{m} \quad D_4 = 0.54\ \mu\text{m}$$

$$D_S = 0.24\ \mu\text{m} \quad D_V = 0.282\ \mu\text{m}$$

The above results are close to the calculated results from the data of Table 1.2. The more the linear proportionality on the lognormal probability graph is, the less difference between them it becomes.

1.5.3 Relationship Between Particle Size Distributions

The abovementioned particle size distribution represents the particle number distribution corresponding to the particle size. For particle mass distribution on particle

size, it represents the percentage of particle mass corresponding to certain particle size in the whole mass. For particle area distribution on particle size, it represents the percentage of particle area corresponding to certain particle size in the whole area. They can be derived from the particle size distribution, and measurement on mass or area is not needed. Since each weighted distribution of lognormal distribution is also lognormal, they are parallel straight lines with the same σ_g. Their relationships are

$$\lg D_{50}^{V} = \lg D_{50} + 6.908 \lg^2 \sigma_g \tag{1.39}$$

$$\lg D_{50}^{S} = \lg D_{50} + 2.303 \lg^2 \sigma_g \tag{1.40}$$

where

D_{50}^{V} is the particle size at 50 % in the mass distribution curve, i.e., the mass median diameter; when lognormal distribution is valid, it is called the mass geometric average diameter;

D_{50}^{S} is the particle size at 50 % in the area distribution curve, i.e., the area median diameter; when lognormal distribution is valid, it is called the area geometric average diameter.

From the example of Fig. 1.29, we could know $D_{50}^{V} = 0.458$ μm and $D_{50}^{S} = 0.24$ μm from calculation, and straight lines which represent area distribution and mass distribution and which are parallel to the particle number distribution could be plotted. It should be noted that in order to fit the scale on probability graph paper well, only data group of those "<0.6" is needed at one edge, while those between 0.6 and 1.0 could be considered as data of "≥0.6," which means the proportion of data <0.6 is 98.4 % while that of ≥0.6 is 1.6 %. If more precise data are needed, subdivision of two edges could be made.

As for the case of surface contamination, area distribution is preferred; while for the hygiene problem, mass distribution is used, where mass of particles have direct implications for the problem. When we are dealing with the problem in the cleanroom, particle number distribution with particle size is used.

1.6 Statistic Parameter of Particle Number

Statistic calculation of particle size is needed for the abovementioned particle distributions. It is a basic statistic problem that how many particles should be sampled in the particle group of each sample so that the error of the measured particle size is minimized.

From the principle of statistics, standard deviation of average value equals with the ratio of standard deviation σ to the root of sample number, which is shown in Eq. (1.41):

$$\sigma_{\overline{D}} = \frac{\sigma}{\sqrt{n}} \tag{1.41}$$

where n is the particle number.

The real size of particle under the 95 % confidence level is

$$\overline{\overline{D}} = \overline{D} \pm 2\sigma_{\overline{D}} = \overline{D}\left(1 \pm \frac{2}{\sqrt{n}}\frac{\sigma}{\overline{D}}\right) \tag{1.42}$$

where $\frac{2}{\sqrt{n}}\frac{\sigma}{\overline{D}}$ is the relative error of particle size. When it is set to be ΔC, the following requirement should be met:

$$\frac{2}{\sqrt{n}}\frac{\sigma}{\overline{\overline{D}}} \leq \Delta C$$

So we could get

$$n \geq \left(\frac{2\frac{\sigma}{\overline{\overline{D}}}}{\Delta C}\right)^2 \tag{1.43}$$

The above expression was used in Ref. [17] to obtain the necessary particle number for counting of monodisperse standard particles. According to the definition of monodisperse aerosol, we know

$$\frac{\sigma}{\overline{\overline{D}}} \leq 0.2$$

For calibration of particle counter, the requirement is much stricter, so it could be assumed ≤3 %. With the above data, Eq. (1.43) becomes

$$n \geq \left(\frac{2 \times 0.2}{0.03}\right)^2 = 178$$

During the counting process, the abovementioned problem of relative error exists. When particle number is too less, man-made error will exist because of inadequate randomness. When it is too much, the workload of counting process is heavy. When particle counter is used, to count 178 particles is not difficult, so 300–500 standard PSL particles are needed for calibrating particle counter in the national standard "calibration method of the performance of particle counter," which will result in error smaller than 3 %.

For polydisperse aerosol, σ is unknown, so is $\frac{\sigma}{\overline{D}}$. But for common aerosol particles, the value of σ could be assumed. Now we assume σ in Table 1.2 is 0.13 (in fact it is 0.1287), then we could obtain

$$\frac{\sigma}{\overline{D}} = \frac{0.13}{0.207} = 0.62$$

For the usual test, the relative error of 5 % is acceptable. Therefore the particle counting in Table 1.2 should be

$$n \geq \left(\frac{2 \times 0.62}{0.05}\right)^2 = 615$$

Now we know from the table that $\sum n_i = 823$, which meets the requirement.

Moreover, Ref. [18] presents the guideline to measure the particle number needed. Since it is generally introduced, we will not introduce in the book. For those readers who need the information, please find the original paper.

References

1. Ma GD, Hao JM (2003) Air pollution control engineering, 2nd edn. China Environmental Science Press, Beijing (In Chinese)
2. Lin ZH (1983) Sampling technique and measurement of dispersity of NaCl aerosol. Tsinghua University, Beijing (In Chinese)
3. JACA (1994) Guideline for the generation method of aerosol for pollution control. J Jpn Air Clean Assoc 32(2):60–83 (In Japanese)
4. Hinds WC (1989) Aerosol technology (trans: Sun Yufeng, Chapter 4). Heilongjiang Science and Technology Press, Harbin (In Chinese)
5. Yan HL, Wu HP, Zhang JK (1983) Analysis of the relationship between the average size and the polarizing fault of oil mist aerosol and its dispersity. Institute of HVAC at China Academy of Building Research, People's Liberation Army No. 57605 of the People's Republic of China (In Chinese)
6. Zhao RY, Qian BN, Xu WQ (1987) Characteristic of aerosol generator with Cold DOP aerosol. Tsinghua University, Beijing (In Chinese)
7. Wang JS, Zhu PK, Zhou GH et al (1983) Technical report for the development of JL leakage detection apparatus. Institute of HAVC at China Academy of Building Research, Liaoning Hongbo Radio Factory (In Chinese)
8. Fuchs HA (1960) The mechanics of aerosols (trans: Gu Zhenchao). Science Press, Beijing (In Chinese)
9. Xu ZL, Gu WZ (1980) Calculation of the minimum sampling volume for particle counter in environments with different air cleanliness levels. J HVAC 1:22–25 (In Chinese)
10. Yang YD (1987) Discussion of the deviation phenomena of statistical average value of particle number during measurement. In: Proceedings of the academic conference on air cleaning measurement techniques, Institute of Scientific and Technical Information at Hebei University of Technology (In Chinese)
11. Kamishima K (1984) Performance of ULPA filter in ultra cleanroom. Jpn Air Cond Heat Refrig News 24(1):163–172 (In Japanese)

12. James B (1989) Acceptance inspection of cleanroom with Class 1 (trans: Du Chunlin, Proofread by Chen Changyong). Compiler group for code for construction and acceptance of cleanroom, pp 303–304 (In Chinese)
13. Xu ZL (1981) Relationship between the yield and the air cleanliness level in the clean environment. Mech Eng 3(1):45–49 (In Chinese)
14. Yao GL (1981) Discussion of the bacterial deposition method to measure the air cleanliness level in cleanroom. Tongji University, Shanghai (In Chinese)
15. Sano I (1971) Generation of smoke. J Jpn Air Clean Assoc 9(5):2–11 (In Japanese)
16. Sato E (1971) Introduction to aerosol technology. Build Equip Water Heat Construct 9(8):47–63 (In Japanese)
17. Specification description of "Methods for testing the performance of airborne particle counter" (1983) Institute of HVAC at China Academy of Building Research (In Chinese)
18. Richard D (1981) Aerosol handbook (trans: Zhou Jinqin). Atomic Energy Press, Beijing, pp 131–132 (In Chinese)

Chapter 2
Airborne Particles in Outdoor Air: Atmospheric Dust

Atmospheric dust is the direct treatment object in air purification system. We should understand not only the concept of atmospheric dust in air clean technologies but also its origin, component, concentration, and distribution.

Once the general characteristic of particle size distribution is understood, other characteristics of the airborne particles in outdoor air, i.e., atmospheric dust, are facilitated for further research.

2.1 Concept of Atmospheric Dust

The generalized meaning of atmosphere refers to all the air surrounding the earth. Special atmosphere refers to the outdoor air which person and matter are exposed to, namely, the environmental air.

Atmospheric particles are generally referred to atmospheric aerosol, while they are called atmospheric dust specifically.

Atmospheric dust can also be divided according to the special and the generalized meanings.

At early days, the concept of atmospheric dust refers to the airborne solid particles [1], i.e., the real dust, which is the special meaning of the atmospheric dust. Later someone such as Junge from Germany put forward the concept that the atmospheric dust is the aerosol with coarse diameter [1]. But this concept is not complete [2], because aerosol with high degree of dispersion can be generated using artificial method or natural method occurred in atmosphere. Therefore, the modern concept of atmospheric dust refers to not only the solid dust, but also the polydisperse aerosol containing both solid and liquid particles, which is the generalized concept of atmospheric dust. It means the particles with size (refers to the aerodynamic

Z. Xu, *Fundamentals of Air Cleaning Technology and Its Application in Cleanrooms*,
DOI 10.1007/978-3-642-39374-7_2, © Springer-Verlag Berlin Heidelberg 2014

diameter) less than 10 μm. It is called the floating dust in the environmental protection field, which is different from the deposition dust that deposits onto the floor within a short time. So the concept of the atmospheric dust in the field of air cleaning technology is different from that of the dust in the field of general dust removal technology. The generalized concept of atmospheric dust in the field of air cleaning technology is suitable for the modern technology of particle measurement. Because with the method of photoelectricity, both solid and liquid particles can be detected to obtain the relative concentration or the number concentration of atmospheric dust. Corresponding to this generalized concept of atmospheric dust, particles with diameter less than 10 μm are called "airborne particulate matter" and "environmental aerosol" which were specified in EPA of the USA and special committee from environmental standard related to airborne dust in Japan, respectively. This is the general term for airborne dust and airborne particles [3].

The total suspended particles (TSP) mentioned in Chinese standard "Ambient Air Quality Standard" include both the airborne particles with diameter less than 10 μm and the deposition particles with diameter between 10 and 100 μm. In the past, airborne particles with diameter less than 10 μm were called floating dust, and now they are called inhalable particles (IP) and labeled as PM_{10}. In the field of environmental science, particles with diameter less than 2 μm or 2.5 μm are called fine particles, while others are called coarse particles. In American standard, TSP only includes those with diameter between 0 and 40 μm.

Except for the original particles (from the particle generation source), the concept of atmospheric dust also includes the secondary particles. The secondary particles are generated by condensation of gaseous pollutants discharged from various pollution sources, and complex chemical reaction occurred in atmosphere.

Gaseous pollutants in atmosphere include:

Sulfide – SO_2, H_2S
Nitride – NO, NH_3
Oxycarbide – CO, CO_2
Hydrocarbon – HC
Halogen compound – HF, HCl

The formation of secondary particles is mainly sulfate, nitrate, and semi-volatile organic compounds. Among them, sulfate is very stable while both nitrate and semi-volatile organic compounds transform between gas and particle phase with the temperature. For example, when the temperature is below 15 °C, most nitrates exist in the form of ammonium nitrate particles. That is why the concentration of this kind of particle is much higher in winter when compared with summer.

The aerodynamic diameter of those secondary particles mentioned above are mainly below 2.5 μm, expressed as PM2.5, and it is the frontier of the research about atmospheric dust.

2.2 Source of Atmospheric Dust

2.2.1 Natural Source and Artificial Source

Atmospheric dust comes from natural and artificial sources.

There are many kinds of natural sources. There are sea salt particles which are brought into the air by the effects of sea spray, which can pass through the land for hundreds of kilometers and 90 % of which will be deposited into the sea. There are soil particles blown up by winds. There are plenty of particles released from forest fire and volcanic eruption. There are also meteoric shower in the universe and botanic pollen.

As for the artificial source, atmospheric pollution created by the development of modern industrial technology plays the most important role. Western countries have begun the era of air pollution as they used the coal instead of wood in the fourteenth century, which belongs to the soot type and the first stage in air pollution. Ash component occupies a large proportion of coal as the fuel, and usually it is about more than 20 % by weight, while petroleum has much fewer component of ash. Although soot has became fewer and fewer after petroleum took the place of coal, the generated sulfur dioxide has been converted into sulfuric acid mist through the complex reaction caused by sunlight, when it comes across moisture at high altitude in the air. This kind of fuel oil pollution is the second stage of air pollution. With the further development of fuel oil industry and the increasing amount of motor vehicles, the frequency of photochemical oxidant increases sharply. This is a series of complex reactions between nitrogen oxides and hydrocarbons exhausted from combustion. Ozone, peroxyacyl nitrate, and other substances will be generated. These substances produce a kind of toxic smoke through the radiation of solar ultraviolet. This begins the era of photochemical smog, which is the third stage of air pollution. Although photochemical reaction can be avoided when diesel engine is used and few hydrocarbons are generated, smog is still formed.

It is an important source of evidence that the change of the amount of dust and lead content measured from ice in the Arctic is caused by the industrial development of the modern capitalism. Heavy metal element such as lead is a good tracer material in showing atmospheric transmission path.

Figure 2.1 indicates the change of dust content in ice sample between the early nineteenth century to the 1960s [4]. After 1930, the content of dust in ice sample increased sharply which is consistent with the trend of energy abusing after this period in capitalist countries.

The upper curve of Fig. 2.2 [4] shows the change about the annual yield of the lead refining industry in the Northern Hemisphere. The lower curve shows the change of lead in ice of the Arctic. In 800 B.C., 1 g of ice contained 0.001 μg of lead, but it increased from 200 years ago. The ice sample is taken from the hinterland of Arctic, while most lead refining industry is in the middle latitude of Northern Hemisphere. We can see from the picture that the trend of the two curves is also very consistent.

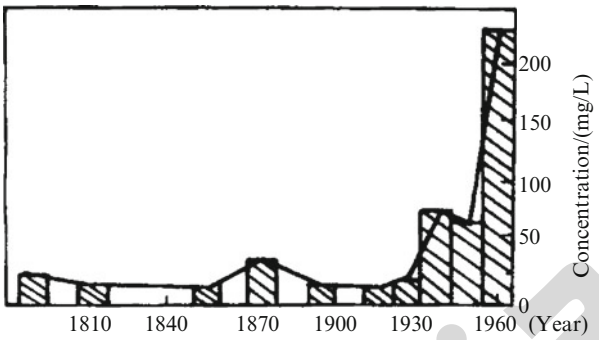

Fig. 2.1 Change of dust content in ice sample

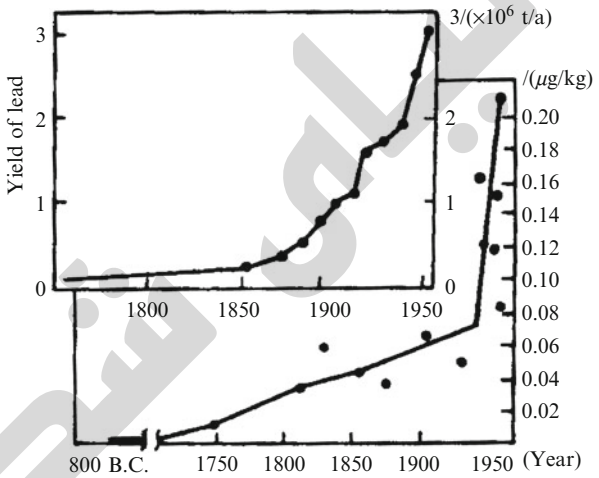

Fig. 2.2 Change of lead content in the ice of Northern Hemisphere

According to the newspaper, Chinese scientists' investigation of lead content in the Arctic Center District shows that pollution has accounted for more than 90 % of the content of lead in Europe, Northern and Western America, and Central Russia and the Far East [5].

In addition to the refining production of lead mentioned above, atmospheric dust sources related to industrial pollution are mainly specified in Table 2.1.

In China, the anthropogenic source of atmospheric dust mainly comes from soot pollution, which can also be seen from Table 2.2 [6]. Coal has been the most important part of energy consumption in China. According to the 2001 China Environment Yearbook (published by the China Environment Yearbook Press), the amounts of coal and oil consumed in the year 2000 are $81{,}188 \times 10^4$ t and $2{,}890 \times 10^4$ t, respectively. What's more, when the scattering effect of solar radiation by the wind and water vapor is excluded, the turbidity factor reflecting the turbidity by atmospheric aerosol can be obtained, which has consistent trend with consumption of coal used in industry as shown in Fig. 2.3 [7]. There is one exception in the year 1965 shown in this figure. Because there were many rainy days that year, so most dust had been cleared.

Table 2.1 Pollution sources of atmospheric dust

Generation apparatus	Dust property
Boiler	Coke button, fly ash, pulverized coal
Cement kiln	Mountain flour, cement
Ore sintering furnace	Metal sulfur oxide, fly ash, mineral flour
Ore furnace	Mineral flour, coke flour, slag
Steelmaking open hearth	Ferric oxide
Kiln	Fly ash, pulverized coal
Converter	Residual
Waste burning furnace	Residual, fly ash, breeze
Vitriol equipment	Sulfurous smog
Ore crushing equipment	Mineral flour

Table 2.2 Primary energy consumption and its constitution in 1989

	World	China	USA	USSR	Federal Republic of Germany	France	UK	Japan
Consumption/ utcD	11,447.1	969.3	2,927.8	2,023.0	383.5	299.4	285.6	630.7
Oil	38.3	17.2	41.9	31.3	40.3	42.8	34.9	57.8
Natural gas	21.3	2.1	24.0	39.6	17.0	12.0	23.6	10.2
Coal	27.8	75.8	23.3	20.9	27.6	9.4	31.6	17.8
Hydroelectricity	7.0	4.9	3.5	6.3	1.4	33.8	2.2	4.7
Nuclear power	6.6		7.0	6.3	12.5	33.8	7.7	9.5
Others			0.3	1.9	1.2	2.3		
In total	100.0	100.0	100.0	100.0	100.0	100.0	100.0	100.0

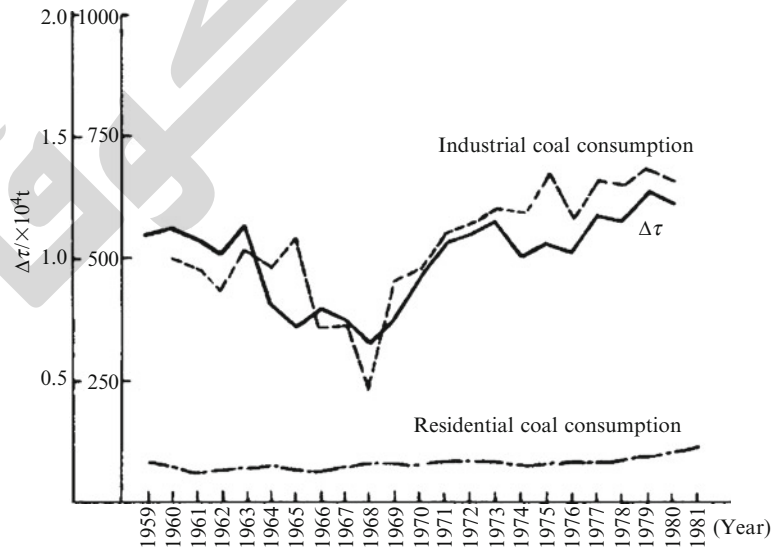

Fig. 2.3 Relationship between the turbidity factor $\Delta\tau$ of atmospheric aerosol and coal consumption for 20 years in one industrial city

Table 2.3 Generation amount of atmospheric dust

Type of dust source			Generation rate (t/d)	Percentage (the maximum)
Natural source	Direct	Sea salt particle	3×10^6	28
		Wind dust	2×10^4–10^6	9.3
		Forest fire	4×10^5	3.8
		Volcanic eruption	10^4	0.09
		Meteoric dust	5×10–5.5×10^2	
	Indirect	Botanic activity (such as pollen release)	5×10^5–3×10^6	28
		Circulation of sulfur and nitrogen	3×10^6	24.1
	Subtotal		10.1×10^6	
Artificial source	Direct	Combustion and industry	1–3×10^5	2.8
		Wind dust (by farming)	10^2–10^3	0.009
	Indirect	From component with aerosol generator	3.7×10^5	3.453
	Subtotal		6.7×10^5	
In total			10.7×10^6	

2.2.2 *Generation Amount of Atmospheric Dust*

Estimation of the generation amount of atmospheric dust from various sources is quite different. For example, estimations of the amount of dust from wind can differ by 10 times. Among the artificial sources, estimations of the amount from coal can also differ by several times. Because at present 3 kg of coal dust will be emitted into the atmosphere during the burning of 1 t coal, however, it will reach 11 kg when incomplete combustion.

Table 2.3 is an estimation for the amount of dust created by different sources. We can see from the table that 70 % of atmospheric dust in the air is produced by wind, while artificial sources only occupies for 6 %. This is because the small value for the amount of industrial pollution is used. Otherwise, given the large proportion of sea aerosol deposition into the sea, atmospheric dust generated by industrial pollution sources will reach up for 25–30 % of the total amount.

According to the report from UNEP, the amount of emissions of total suspended solids between 1982 and 1984 is 1.35×10^8 t per year. Now there are also three hundred million tons of SO_2 and 1.5×10^4 t nitrogen oxides emitted into the atmosphere. Among those emissions, 2.7×10^8 t takes place in the USA [9].

Tables 2.4 and 2.5 show the specific emissions of SO_2, soot, and dust in different industries from different provinces in China in the year 2000 [10].

Figure 2.4 indicates the change of emissions of SO_2, soot, and dust each year according to the data from China Environment Yearbook. Industry emission occupies for 65–85 %. Taking the smoke dust as an example, it decreased after the peak in 1977.

Table 2.4 Situation of exhausted gas emission from different provinces (in 2000), unit: t

Area	Industrial SO_2 emission			Removal of industrial smoke dust	Release of industrial smoke dust	Removal of industrial dust	Release of industrial dust
	Total	From combustion exhaust	From industrial process exhaust				
Beijing	146,431	143,708	2,723	1,357,227	51,842	996,605	93,681
Tianjin	213,709	208,857	4,852	2,312,175	112,234	234,231	37,911
Hebei	1,133,599	960,479	173,120	7,195,272	672,176	2,979,927	812,663
Shanxi	902,681	748,396	154,285	6,416,287	791,100	1,771,044	504,133
Inner Mongolia	506,309	452,201	54,107	4,528,710	303,292	587,030	175,644
Liaoning	705,672	592,624	113,047	8,610,888	547,223	3,087,312	429,231
Jilin	201,688	176,371	25,317	4,544,264	283,006	1,161,732	123,792
Heilongjiang	221,670	208,186	13,484	6,428,612	409,337	502,422	103,853
Shanghai	326,804	319,895	6,910	3,083,548	83,153	2,180,813	26,941
Jiangsu	1,140,991	1,050,967	90,024	7,254,087	374,737	2,104,759	256,790
Zhejiang	561,847	510,230	51,616	4,195,609	247,096	2,049,220	489,627
Anhui	350,625	277,820	72,805	3,362,890	243,493	1,352,453	284,977
Fujian	214,338	191,303	22,134	1,320,414	103,539	1,346,911	187,076
Jiangxi	288,108	216,013	27,099	2,893,533	234,059	1,223,416	343,351
Shandong	1,460,902	1,383,218	77,684	9,027,355	543,067	5,059,711	745,589
Henan	747,384	635,699	111,685	7,182,665	690,618	2,927,880	817,734
Hubei	508,218	406,499	101,719	2,215,959	321,461	2,331,507	410,286
Hunan	626,494	402,091	224,403	2,007,277	381,268	1,737,738	639,667
Guangdong	881,556	805,697	75,859	5,704,256	264,453	2,517,735	579,895
Guangxi	800,485	646,803	153,682	2,435,335	590,999	2,668,408	567,717
Henan	20,178	17,459	2,719	231,497	18,078	121,642	13,470
Chongqing	664,240	640,615	23,625	1,457,313	121,783	446,098	220,127
Sichuan	994,064	865,646	128,417	2,284,428	798,910	1,852,488	559,794

(continued)

Table 2.4 (continued)

Area	Industrial SO_2 emission			Removal of industrial smoke dust	Release of industrial smoke dust	Removal of industrial dust	Release of industrial dust
	Total	From combustion exhaust	From industrial process exhaust				
Guizhou	642,490	576,358	66,132	2,780,444	342,453	480,781	406,234
Yunnan	323,853	258,732	65,123	1,496,724	232,566	1,073,720	122,818
Xizang	756	453	303	613	1,150	14	2,114
Shanxi	553,738	508,220	45,519	2,477,843	371,908	410,829	377,237
Gansu	311,878	148,374	163,504	1,499,372	124,768	820,292	146,347
Qinghai	20,177	14,805	5,372	318,724	63,810	110,119	41,658
Ningxia	174,155	160,773	13,382	1,677,833	125,537	120,093	132,781
Xinjiang	187,689	158,746	28,942	872,389	83,978	538,630	112,574
In total	16,125,100	14,025,509	2,099,594	107,173,542	9,533,292	44,795,560	10,920,000

Table 2.5 Situation of exhausted gas emission from different industries (in 2000), unit: t

Industry	Industrial SO_2 emission			Removal of industrial smoke dust	Release of industrial smoke dust	Removal of industrial dust	Release of industrial dust
	Total	From combustion exhaust	From industrial process exhaust				
Mining	330,828	238,037	92,791	1,655,379	215,467	1,004,377	91,715
Food, tobacco, beverage manufacturing industry	410,355	404,782	5,573	1,255,696	259,855	66,328	14,456
Textile industry	257,114	256,848	266	657,646	119,069	11,884	2,557
Leather, fur, eiderdown manufacturing industry	12,922	12,908	14	18,869	8,503	82	631
Papermaking and manufacturing industry	337,932	334,955	2,977	2,119,467	209,454	24,349	37,298
Printing, recording media copy	5,166	5,141	25	8,874	2,358	726	667
Oil processing and coking industry	378,174	191,165	187,007	1,052,490	247,596	126,832	54,238
Chemical raw material and product industry	822,717	655,390	167,328	3,599,665	42,074	512,574	103,298
Pharmaceutical manufacturing industry	64,502	63,167	1,335	274,577	38,058	623	204
Chemical fiber industry	150,207	147,778	2,429	969,219	55,272	140,859	14,756
Rubber manufacturing industry	46,717	46,706	11	167,590	15,050	2,787	442
Plastic manufacturing industry	14,831	14,208	623	23,496	8,785	3,170	28,217
Nonmetallic mineral industry	2,339,533	1,624,100	714,433	2,479,675	2,423,926	2,916,656	8,241,758
Where: cement manufacturing industry	1,003,428	353,119	650,309	2,123,910	409,552	28,385,848	7,682,081

(continued)

Table 2.5 (continued)

Industry	Industrial SO_2 emission			Removal of industrial smoke dust	Release of industrial smoke dust	Removal of industrial dust	Release of industrial dust
	Total	From combustion exhaust	From industrial process exhaust				
Black metal smelting and rolling industry	755,249	368,504	386,844	2,216,228	289,663	10,811,449	853,460
Nonferrous metal smelting and rolling industry	715,013	212,475	502,538	2,224,449	217,654	2,182,243	115,473
Metal fabricated products	73,126	71,971	1,155	71,627	29,384	6,249	93,952
Mechanical/electrical/electronic equipment	215,051	195,741	19,310	776,460	117,813	252,729	32,857
Other industries	7,199,554	7,186,238	13,316	86,876,648	301,312	211,173	24,577
	1,477,161	1,475,542	1,619	725,486	1,841,447	270,565	55,155

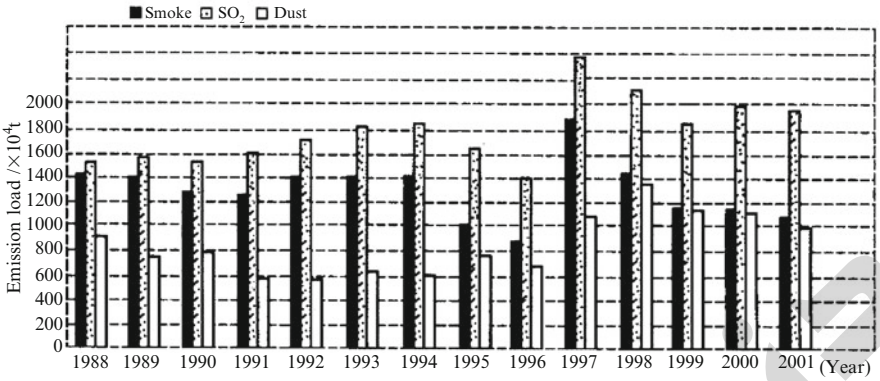

Fig. 2.4 Situation of emission of main pollutants in waste gas between 1988 and 2001

2.3 Composition of Atmospheric Dust

The composition and generation amount of atmospheric dust shown in Table 2.3 is the average value within the scope of the world. But for a specific district, especially the industrial city and its close suburb area, the situation is much complex, since the component and quantity varies a lot with different seasons and places.

2.3.1 Inorganic Nonmetallic Particles

Inorganic particles in atmospheric dust mainly include debris of mineral (including sand), pulverized coal, carbon black, and metal. Figure 2.5 is an electronic microscopic photo of atmospheric dust from a typical industrial city in winter [11]. It is mainly composed of sand, carbon black and crystalline solid material, and a small amount of fiber. In the picture, the silk flocculent particles are coal particles produced by the incomplete combustion of fuels including coal and oil.

For the atmospheric dust in the suburb, silk flocculent particles are very few, because pulverized coal and carbon black particles by incomplete combustion from exhaust gas of the chimney and automobile are few. This can be seen from the comparison between the left and right cases in Fig. 2.6 [12]. Both Figs. 2.7 and 2.8 also reflect the silk flocculent shape of coal or carbon black particles by incomplete combustion [12]. This is an important method to identify whether it is industrial atmospheric dust. These particles usually have diameter between 0.01 and 1 μm. Figure 2.9 is the local amplification of this shape [13].

Characteristic of atmospheric dust is different in the city with serious pollution where smog is usually produced by photochemical reaction. In this situation, particles are big in general and most of them are colloidal substances. With strong

Fig. 2.5 Electronic microscopic photo of atmospheric dust in industrial city. *Upper*: observed in general situation; *Down*: observed by exposure with strong electron beam

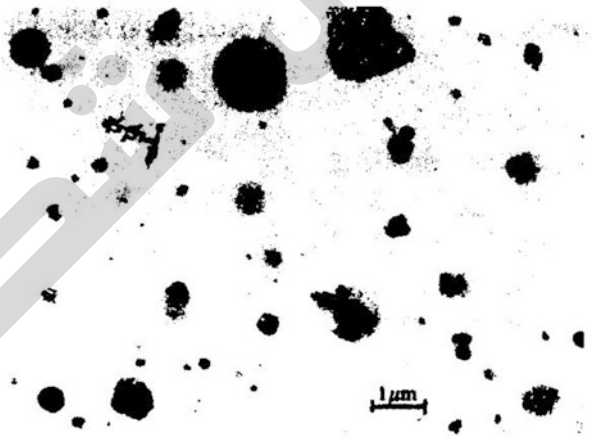

Fig. 2.6 Atmospheric dust in the city (*left*) and suburb (*right*)

irradiation of electron beam, most of them will evaporate and only a small amount of solid particles are left. Figure 2.10 is the photo of this kind of atmospheric dust, which looks quite transparent. This is different from the case where pollution is not serious and there is no photochemical smog. In Fig. 2.5, the difference with and without irradiation by electron beam is not obviously seen.

Chemical particles generated by photochemical reaction are the very harmful ingredient in atmospheric dust, which produces severe erosion effect on the common material. Figure 2.11 shows the extent of erosion effect [11]. In Part (a) of the figure, particles are captured onto the carbon membrane, and the shape of the particulate matter remains spherical, which means there is no effect of erosion by carbon.

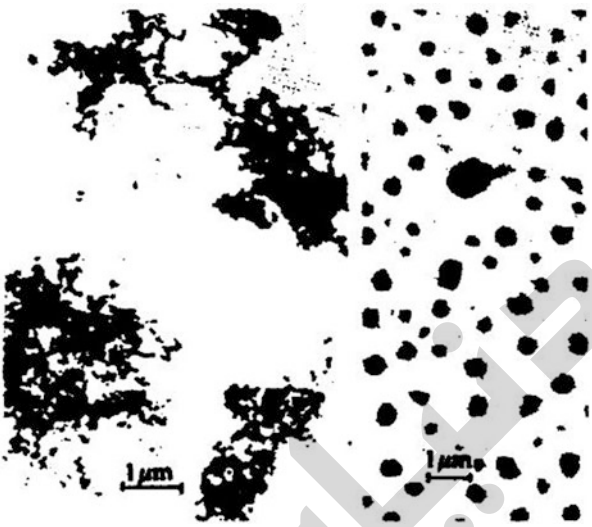

Fig. 2.7 Particles generated by combustion of heavy oil (*Left*: incomplete combustion; *Right*: complete combustion)

Fig. 2.8 Particles emitted from automobile

In Part (b) of the figure, particles are captured onto the copper membrane, and it is shown that the erosion effect on the copper membrane is very strong (the white part surrounding the particles). In Part (c) of the figure, particles are captured onto the iron membrane, the erosion effect only occurs near particles, and the trace of flying droplets can be seen.

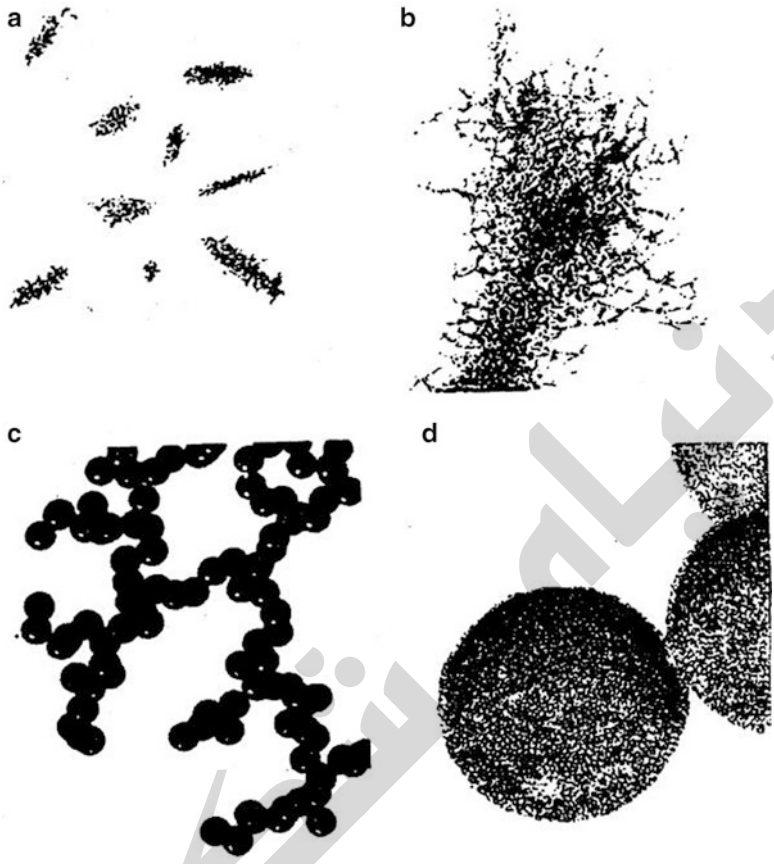

Fig. 2.9 Microscopic photo of pulverized coal particles (0.01–1 μm). (**a**) Coal dust particle (amplification ratio 86). (**b**) Edge of coal dust particle (amplification ratio 860). (**c**) Edge of black carbon particles (amplification ratio 8,600). (**d**) Re-amplification for (**c**) (amplification ratio 860,000)

2.3.2 Metal Particle

The component of metal in atmospheric dust is strongly related to the development of industry. These years, the high content of metal especially heavy metal such as lead, cadmium, beryllium, manganese, and titanium is found in industrial developed countries. In the city where special fuel is used, mercury and arsenic are also found in the atmospheric dust. Near the factories manufacturing Fe and Mn elements, the concentrations of Fe and Mn are very high. In the exhaust gas of automobile, lead smelting factory and lead battery factory, lead and zinc are discharged. Beryllium can be found in the atmospheric dust emitted from smelting plant, electric bulbs factory, and nuclear power plant. Figure 2.12 shows the X-ray

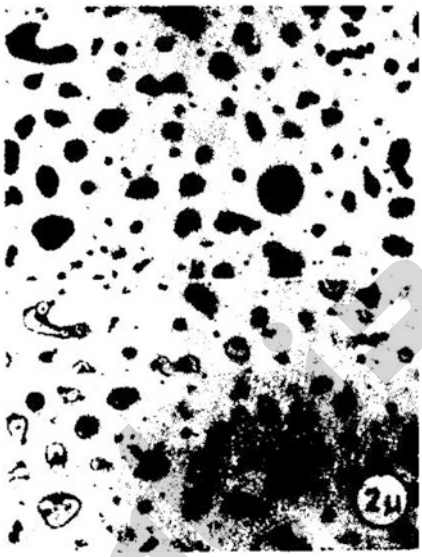

Fig. 2.10 Atmospheric dust by photochemical reaction before (*upper*) and after (*down*) the irradiation of electron beam

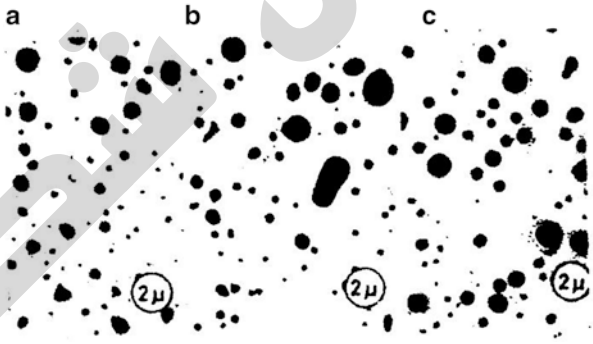

Fig. 2.11 Erosion effect of particles by photochemical reaction. (**a**) Particles captured on carbon membrane. (**b**) Particles captured on copper membrane. (**c**) Particles captured on iron membrane

spectrum of the atmospheric dust in Xinglong district of Hebei Province [14], where various kinds of metal components exist.

Tables 2.6 [13], 2.7 [15], and 2.8 [16] show the data about the metal component in atmospheric dust of large cities. We can see that in the city where the problem of automobile exhaust pollution is serious, the lead content in atmospheric dust is significantly higher than other element.

Table 2.9 is the lead content of particles from one measured data [13].

For industrial products, in addition to the harmful effect like usual particles, the particular harmful effect of atmospheric dust especially metal particles is very large. For example, the light metal element Na is very harmful for the semiconductor device. When the quantity of Na polluted at the silicon wafer surface of the semiconductor device is above 3.6×10^{11} atoms/cm^2, the electrical properties of

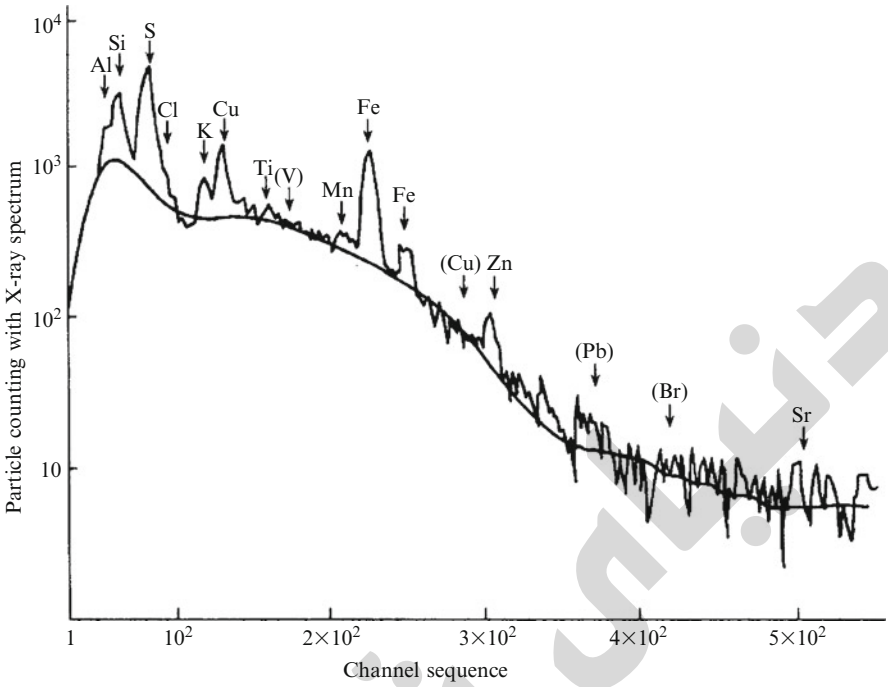

Fig. 2.12 X-ray spectrum of the atmospheric dust

Table 2.6 Metal component of atmospheric dust in Los Angeles, USA

Component	Concentration (μg/m^3)	Component	Concentration (μg/m^3)	Component	Concentration (μg/m^3)
Pb	8.3	Cu	0.45	V	0.034
Mg	8.1	Mn	0.19	As	0.01
Fe	6.2	Ti	0.19	Ag	<0.001
Na	4.2	Sn	0.08	Be	0.0002
K	3.9	Sr	0.09		

the device will be affected. Figure 2.13 shows the extent of influence by Na pollution of the surface on the property of integrated circuit [17]. Curve 2 is a pure silicon, and curve 1 is a silicon wafer contaminated by Na. A 70 μm NaCl particle contains the component which has the harmful effect of a single layer of Na pollution on the entire surface of the silicon wafer [18]. Special attention must be paid during the construction of cleanroom factory near ocean. The contribution of NaCl particles in the atmospheric dust in this kind of area reaches 20 %. For example, in the atmospheric dust of the city Qinhuangdao, the component of NaCl in May reaches 2.48–8.01 % (11.18–24.15 μg/m^3), while in June it is 14.1–18.9 % (27.19–47.62 μg/m^3) [19].

Table 2.7 Metal component of atmospheric dust in Guangzhou

	Concentration (μg/m^3)					
Component	1	2	3	4	5	6
Cu	0.25	0.12	0.18	0.13	0.14	0.17
Zn	0.18	0.26	0.55	0.088	0.87	0.18
Pb	0.16	0.11	0.18	0.16	0.074	0.025
Mg	0.091	0.11	0.075	0.079	0.060	0.17
Sn	0.075	0.0092	0.017	0.018	0.013	0.0076
Mn	0.43	0.018	0.026	0.071	0.015	0.019
Sb	0.0054	0.0026	0.0037	0.0026	0.0031	0.0017
Cd	0.0051	0.0018	0.0031	0.0024	0.0020	<0.0013
Cr	0.0026	0.0014	0.0026	0.0013	0.0010	0.0023
Bi	0.0019	0.0055	0.0075	0.0013	0.0038	0.000042
V	0.0018	0.00067	0.00060	0.0010	0.00038	0.00090
Ag	0.0010	0.00092	0.0011	0.0013	0.0047	0.00012
Be	0.00075	0.00023	0.00027	0.00018	0.00015	0.00013

Table 2.8 Comparison of metal components of atmospheric dust in different cities (μg/m^3)

Element	Shanghai	Beijing	Tianjin	Chongqing	Lanzhou (winter)
Ni	0.0457	0.0097	0.0238	–	–
Mn	0.5614	0.1468	0.1994	0.135	0.3696
Fe	8.7309	4.3008	7.1549	3.51	7.9685
Pb	0.4772	0.2429	0.2436	0.36	0.4731
Cd	0.0159	0.0043	0.0045	–	–
Cr	0.0319	0.1524	0.0259	–	–
Cu	0.2056	0.0295	0.0895	0.075	0.1645
Zn	3.3140	0.3585	0.7098	0.36	1.0168
Na	2.7262	0.6408	0.9964	4.85	–
Al	4.4316	8.5446	–	9.6	8.6762
V	0.0188	0.0665	–	–	0.0284

Table 2.9 Lead content of particles in exhaust gas of automobile

μm	Number	Number percentage (%)	Mass percentage (%)
0–1	724	72.4	6.5
1–2	211	21.1	26.6
2–3	48	4.8	30.4
3–4	12	1.2	22.8
4–5	5	0.5	13.7

Figure 2.14 is one example of mass distribution of NaCl particles in atmospheric dust [20]. It is shown that most of the seal aerosols in atmospheric dust are within the diameter range near 5 μm in terms of mass. Figure 2.15 presents the particle size distribution of NaCl particles which are generated by atomization with artificial sea

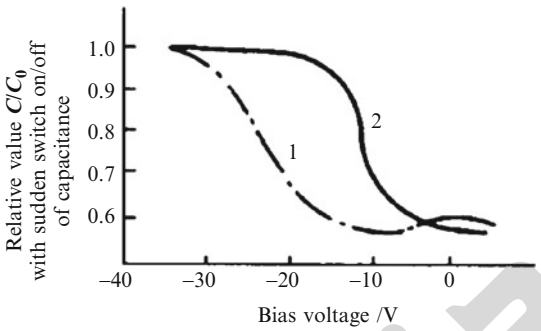

Fig. 2.13 Influence of Na pollution on the C-U property of integrated circuit

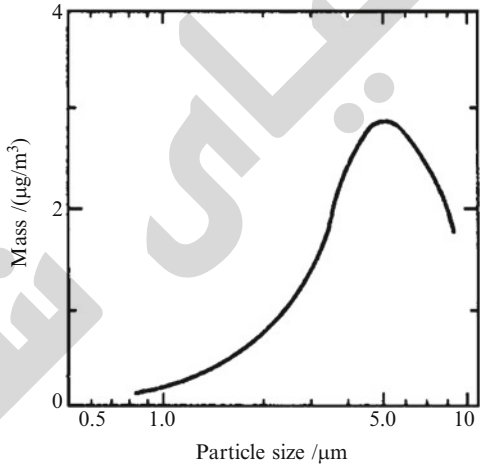

Fig. 2.14 Mass distribution of NaCl particles in atmospheric dust

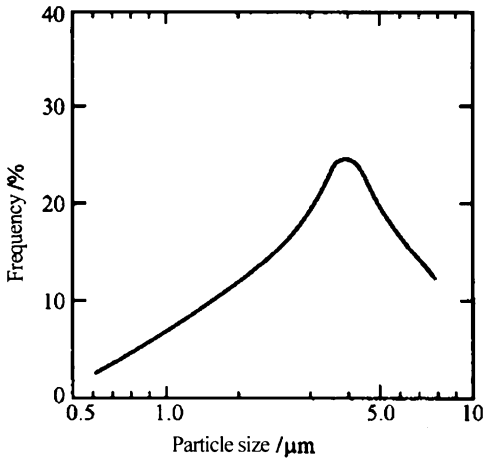

Fig. 2.15 Mass distribution of NaCl particles by artificial atomizing

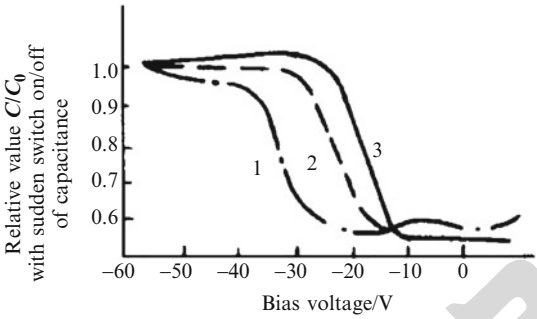

Fig. 2.16 Influence of heavy metal pollution on the C-U property of integrated circuit

water (the mass ratio of NaCl and $MgCl_2$ is 0.82:0.18) under the relative humidity 60 % [20]. The particle diameter is slightly smaller than that of natural particles.

The influence of the heavy metal component in the atmospheric dust is much wider. Taking the wafer on the semiconductor device as an example, when the surface concentrations of iron, copper, and silver increased from 10^{11} to 10^{13} atoms/cm^2, the effective charge value will change by 2–2.5 times, which is shown in Fig. 2.16 [17]. In this figure, curves 1, 2, and 3 represent the situation with surface concentration of heavy metal 10^{13} atoms/cm^2, 10^{11} atoms/cm^2, and 10^4 atoms/cm^2, respectively. Heavy metal is disadvantage for the oscillight of color television. When the fluorescent powder coated on the oscillight is stained by the heavy metal impurities, the light-emitting property of the oscillight will change. This is because the heavy metal penetrating the crystal of the fluorescent powder will become the new energy level center, and it becomes the luminescence center. When the excitation light is located in the range of visible light, the color of fluorescent powder will change. When it is not located in the range of visible light, the brightness will decrease.

Except for the harmful effect for the industrial products, heavy metal particles will cause special hazards for human body. The results are presented in Table 2.10 [21]. Enough attention must be paid on the inorganic particles of the atmospheric dust in city. For example, asbestos are widely used for the materials in the brake, clutch, building materials, and fire insulation, which may cause carcinogenic effect.

2.3.3 Organic Particle

Natural organic particles in atmospheric dust mainly include plant pollen, fiber, animal hair, dander, and excretion. In the area of cotton and textile industry, the concentration of cotton fiber in atmospheric dust is significantly higher than that of other areas. More organic particles are generated by artificial means, including hydrocarbons and tiny plastic particles emitted from various pollution sources.

Table 2.10 Hazards of heavy metal component in atmospheric dust for human body

Element	Damaging parts and disease	Concentrations in common cities of UK and USA ($\mu g/m^3$)
Pb	Nerve, intestines and stomach, anemia	0.2–0.3
Zn	Intestines and stomach, lung, dermatitis	0.004–0.25
Cr	Lung, cancer, dermatitis	0.002–0.02
Co	Lung, heart, dermatitis	0.0007–0.004
Sn	Lung, liver, nerve, dermatitis	0.01–0.03
Ti	Lung, dermatitis	0.01–1.0
Cu	Dermatitis	0.02–0.9
Ni	Nerve, lung, cancer, dermatitis	0.002–0.2
V	Lung, dermatitis	0.001–0.1
As	Lung, nerve, liver, kidney, intestines, skin caner	0.01–0.02
Be	Lung, dermatitis	0.0001–0.001
Mn	Lung, nerve	0.01–0.3
Mo	Nerve, anemia, maldevelopment	0.0005–0.006

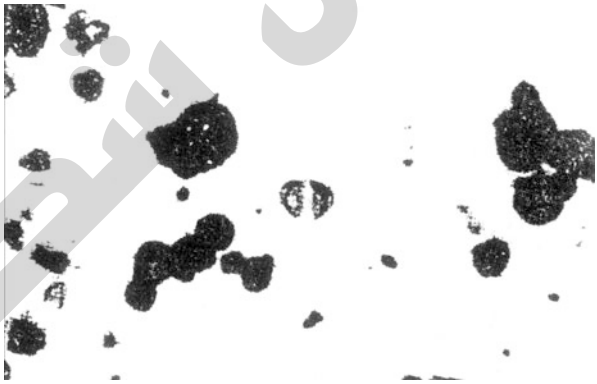

Fig. 2.17 Pollen in the atmospheric dust (the pollen is located in the *middle*)

Here the information about pollen will be emphasized. During the season of pollen outbreak, it will generate many particles between 10 thousands and 1 million. In average it will be several hundreds of thousands. Figure 2.17 shows the situation of atmospheric dust containing the pollen in city [22]. The concentration of pollen in atmospheric dust is related to season. It is shown in Fig. 2.18 that the amount of pollen generated in the period between the spring and summer is the largest [22]. Pollen particles are usually large with semi-monodisperse distribution. Figure 2.19 shows the photo of pollen [22]. Therefore, there is requirement for the variety of tree during the design of afforest scheme for cleanroom factory. These trees with quick effect of afforest, less pollen generation, and no floral production should be chosen.

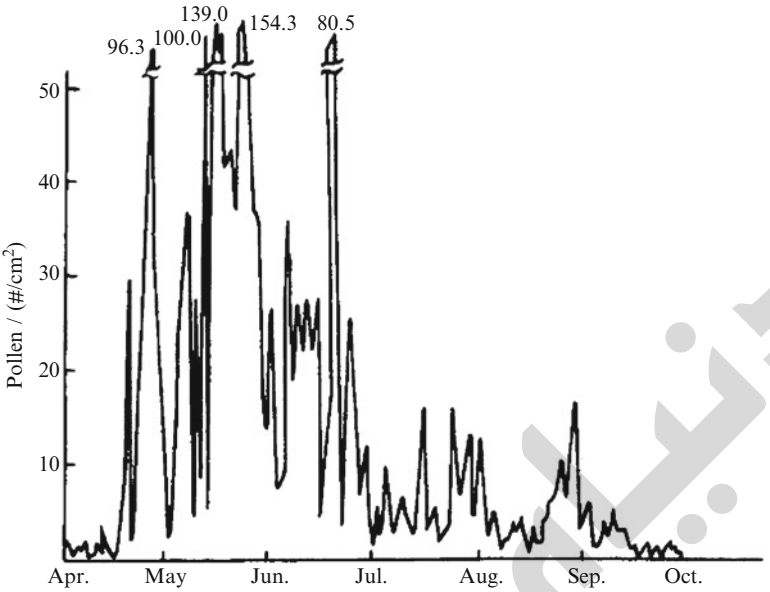

Fig. 2.18 Example of pollen concentration in city

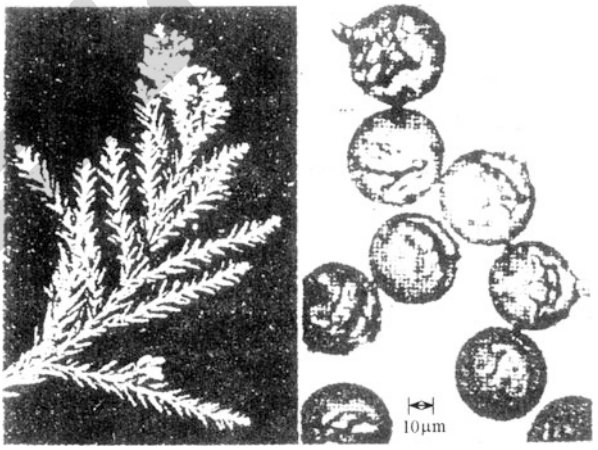

Fig. 2.19 Firry pollen (30 μm)

2.3.4 Vital Particle

In atmospheric dust, there are also a small proportion of vital particles, i.e., microorganism, including protozoa, unicellular algae, fungi, bacteria, rickettsia, and viruses. Among the bacteria, there are also 20 kinds of coccus, 8 kinds of staphylococcus aureus, 37 kinds of tuberculosis, and 7 kinds of blastomycosis. Except for the larger protozoa and unicellular algae, there are other kind of

Table 2.11 Composition of atmospheric dust

Composition	Content (%)
Mineral debris, dross from combustion	10–90
Smoke and pollen	0–20
Plant fiber such as cotton	5–40
Fine particles including coal, charcoal, cement, and concrete	0–40
Decayed plant, scurf	0–10
Metal	0–0.5
Microorganism	Extreme small

microorganisms existing, which has four types of basic state including fungal spores, bacteria bacillus, cenobium (propagant), and virus.

Illustration will be presented later about the features of vital particles.

2.3.5 Composition of Atmospheric Dust

In general, the composition of atmospheric dust in and near city is shown in Table 2.11.

2.4 Concentration of Atmospheric Dust

2.4.1 Methods to Express Concentrations

There are three methods to express the concentrations of atmospheric dust:

1. Particle counting concentration. Particle number in unit volume of air, expressed with pc/L
2. Gravimetric concentration. Particle mass in unit volume of air, expressed with mg/m^3
3. Settlement concentration. Number or mass of particles deposited naturally onto the surface with unit area within unit time, expressed with $pc/(cm^2 \cdot h)$ or $t/(km^2 \cdot month)$

Large variation exists for the concentration of atmospheric dust. In order to determine the concentration of atmospheric dust in a scientific way, we should distinguish the instantaneous (for one time) value from the mean value, or the maximum from minimum value. Or the average, maximum and minimum values should be provided at the same time. As for the average value, the difference between 1 h average, 24 h (1 day) average, and month average must be distinguished. The longer the time is, the smaller the average value is. It is necessary to indicate the continuous average time, such as 1 h mean value with continuous 48 h

Table 2.12 Background value of atmospheric dust concentration (pc/L)

Place	Full size	Above 0.5 μm	Above 0.3 μm	Above 5 μm	Pollen	Virus	Bacterium	Mould	Spore
Ocean	210,000	2,500	7,500	28	–	–	–	–	–
Stratosphere 10 km	35,000	20	55	–	0.1	–	$(0.5–100) \times 10^{-3}$	0.1–10	0–100

sampling, or with 8 h sampling every day, and so on. As for the minimum and maximum value, the information about the time for sampling is also needed, such as the daily maximum (minimum) value.

From the environment and health, industrial hygiene, and general air-conditioning point of view, gravimetric concentration and settlement concentration are used to describe the concentration of atmospheric dust. In the field of air cleaning technology, the particle counting concentration of atmospheric dust is adopted, but the gravimetric concentration also has the value for reference, such as in the calculation process of particle loading in air filters.

2.4.2 Background Value of Atmospheric Dust Concentration

Generally, concentration of atmospheric dust located 2 km above the ground can be regarded as the background value, which is shown in Table 2.12.

2.4.3 Gravimetric Concentration

The determination of gravimetric concentration of atmospheric dust is based on the influence on occupant's health, especially the influence on the respiratory system. The situation of particle penetration and deposition depth in respiratory system is shown in Table 2.13 [23] and Fig. 2.20 [24].

Four principles should be considered to study the influence on human:

2.4.3.1 The Influence Extent on Health

The influence extent of the variation of gravimetric concentration on occupant's health should be determined according to the statistical material, which is the paramount principle.

The death event caused by the famous British London fog shows vividly the relationship between gravimetric concentration of atmospheric dust and mortality rate, which is shown in Fig. 2.21 [13]. It can be seen that when the weigh concentration is above 0.2–0.25 mg/m^3, it is not a general problem, but is related to death apparently.

Table 2.13 The relationship between particle size and deposition depth in respiratory system

Particle size (μm)	Reachable sites
30	Arrive at the trachea of the back, not above the branch part
10	Arrive at terminal bronchi
3	Arrive at alveolar way
1	Most deposit in the alveolar way and alveolar sac (2.6 % exhaled again)
0.3	Most deposit in the alveolar sac (65 % exhaled again)
0.1	Most deposit in the alveolar sac (65 % exhaled again)
0.03	Most deposit in the alveolar way and alveolar sac (34 % exhaled again)

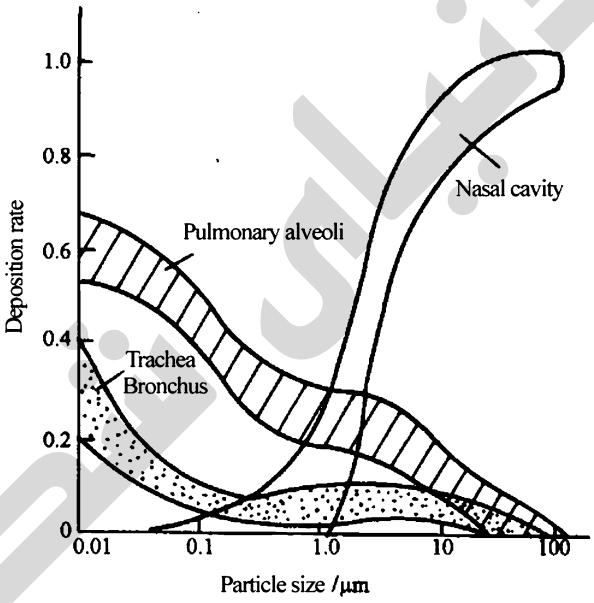

Fig. 2.20 Deposition rate of particles onto human respiratory system with the particle size

Table 2.14 is the trend of influence by the variation of gravimetric concentration of atmospheric dust on human health based on the statistical investigation from some countries. It is shown that when the averaged value is obtained with 24 h every day, the concentration limit of death is 0.15 mg/m^3.

Since the beginning of 1990s, due to the study of epidemic, requirement was put forward for particles with aerodynamic diameter $\leq$2.5 μm (expressed as $PM_{2.5}$). The national Environmental Protection Agency (EPA) of America modified the particle index from the original total suspended particles (TSP) to particles with aerodynamic diameter $\leq$10 μm (expressed as PM_{10}). Later in the revised Ambient Air Quality Standard, the upper limit for $PM_{2.5}$ was specified. According to the definition of the aerodynamic diameter (shown in Eq. (1.1)), the real diameter for particles with density larger than 1 is smaller than 2.5 μm, while it is larger than 2.5 μm for those with density less than 1.

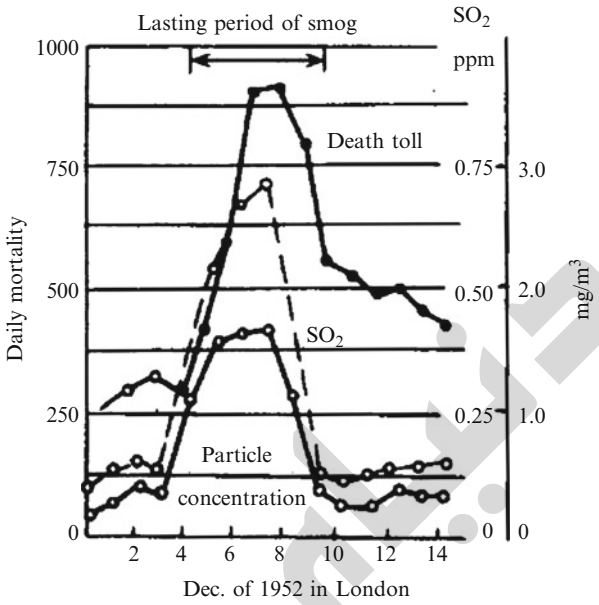

Fig. 2.21 Relationship between atmospheric dust concentration and the mortality rate

Table 2.14 Effect of atmospheric dust on human health

Concentration (μg/m^3)	Influence
100 (24 h average annually)	Diseases such as chronic bronchitis increase, children asthma
150 (24 h average)	Increased death for patients, infirm, old man
300 (1 h average)	Visual distance less than 8 km, with flight difficulties, increased mortality
600 (1 h average)	Visual distance less than 2 km, traffic accident, illness, and increased mortality
From 140 to 60 (average)	The sputum generated will drop accordingly

2.4.3.2 Self-Feeling of Pollution by Occupants

Based on the experimental survey for a certain amount of population, the relationship between the feeling of pollution and the gravimetric concentration is established. One example is shown in Table 2.15 [25]. It is shown that most people will have the feeling for the existence of pollution when the gravimetric concentration is more than 0.15 mg/m^3. This is why many countries set 0.15 mg/m^3 as atmospheric pollution concentration limit for the hygiene standard and design standard.

The World Health Organization (WHO) recommended the annual average concentration of total suspended particulate less than 0.06–0.09 mg/m^3 and the daily average concentration less than 0.15–0.23 mg/m^3, according to statistical data of all countries [8].

Table 2.15 Investigation of the pollution concentration

	Proportion	
Pollution condition	Dust content 0.1–0.15 mg/m^3	Dust content 0.23–0.38 mg/m^3
Feeling the existence of pollution	10 %	90 %
No feeling the existence of pollution	90 %	10 %

2.4.3.3 Degree of No Guarantee

The design standard of gravimetric concentration is determined with the degree of no guarantee (also termed as risk probability) of gravimetric concentration according to the factors including experience and techniques.

In a region, dozens or even hundreds of representative points can be selected. Measurement will be taken at each point every hour. In total 8,760 data will be obtained 1 year. The cumulative distribution curve of gravimetric concentration can be plotted. Then the value of gravimetric concentration with the expected degree of no guarantee can be determined. The so-called degree of no guarantee means how many monthly or daily average concentration in a year surpass this expected gravimetric concentration, which is used as the basis for the design standard. For example, when the degree of no guarantee for residential area of America is set 5 %, the daily average value in a year becomes 0.15 mg/m^3. The degree of no guarantee is dependent on the necessity, economic, and technical conditions. For example, the degree of no guarantee for extreme strict application and allowable economical condition can be 2.5 %. The gravimetric concentration corresponding to the degree of no guarantee should be determined with the actual conditions. For example, in the corresponding concentration with the proposed degree of no guarantee in 1986, Japan was lower by 10–23 % than that of 1975, which is shown in Table 2.16 [26]. This is because the concentration of atmospheric dust generally reduced with the improvement of the environment.

2.4.3.4 Magnitude of Particle Size

The abovementioned atmospheric dust means the total suspended particle (TSP), while particulate matter (PM) is a term in environmental science. Usually particles with aerodynamic diameter between 2.5 and 10 μm are called coarse particles. Those between 0.1 and 2.5 μm are called fine particles. Those less than 0.1 μm are called ultrafine particles. In this book, all of them are called particles.

With the further investigation of epidemic, the standards about gravimetric concentration for atmospheric dust in many countries are more related to the magnitude of particles, which proves the saying “it will be a trend” in the past version of this book.

Table 2.16 Change of suggested gravimetric concentration in Tokyo area

	Measured results in Tokyo (mg/m^3)		The recommended design value (mg/m^3)				
			No assurance 2.5 %		No assurance 5 %		
Grade	No assurance 2.5 %	No assurance 5 %	1975	1986	1975	1986	Corresponding environment
1	−0.13	−0.09	0.16	0.13	0.13	0.10	Suburbs with fresh air
2	0.13–0.15	0.09–0.11	0.19	0.16	0.15	0.12	Suburbs
3	0.15–0.17	0.11–0.13	0.22	0.19	0.17	0.14	Commercial residential
4	0.17–0.19	0.13–0.15	0.25	0.22	0.19	0.16	Commercial street
5	0.19–	0.15–	0.28	0.25	0.21	0.18	Urban with serious air pollution

Ultrafine particles (UF), i.e., particles with diameter smaller than 0.1 μm, have attracted the attention of scientific community. However, the current investigation results of epidemic do not provide enough proof about the relationship between exposure and reaction. This is why the concentration of UF with the expression of particle counting concentration does not become the aim of air quality standard.

Since PM_{10} represents those particles which are able to enter the respiratory tract, it becomes the index of particles for studying the exposure of people in the past time. Therefore, the concentration of PM_{10} is monitored in most common air quality monitoring system.

According to the "Air Quality Guideline" published by WHO in 2006, when the short-term exposure concentration of PM_{10} increases by 10 $\mu g/m^3$ (24 h averaged), the mortality rate will increase by 0.46 % or 0.62 %. When the concentration of PM_{10} reaches 150 $\mu g/m^3$, the mortality rate is expected to increase by 5 %.

In 1987, Environmental Protection Agency (EPA) of the USA adopted PM_{10}, i.e., these particles with aerodynamic diameter $\leq$10 μm, as the index for particles, instead of the total suspension particles (TSP).

In 1982, Chinese national standard "Ambient Air Quality Standard" (GB3095-82) adopted the TSP as the index. In the revised version in 1996 (GB3095), PM_{10} was adopted, and ambient air was defined as the outdoor air exposed by people, plant, animal, and building.

However, study has shown that organic material plays a role in the influence of particles on health. In atmospheric dust, organic material is inclined to exist in fine particles. Fine particles are likely to absorb heavy metal, acid oxidant, and organic pollutants in the air. Table 2.17 shows the absorbed elements [27].

Research results have shown that the lower limit of concentration influencing the survival rate significantly is 10 $\mu g/m^3$, such as American Cancer Society (ACS). Some former studies have also shown the strong correlation between long exposure to $PM_{2.5}$ and the mortality rate. This resulted in the modification of Ambient Air Quality Standard in the USA in 1997, which specified the upper limit of $PM_{2.5}$.

Table 2.17 Distribution of various elements in particles with different sizes

	June			December		
Element	$PM_{2.5}$	$PM_{2.5–10}$	$PM_{10–100}$	$PM_{2.5}$	$PM_{2.5–10}$	$PM_{10–100}$
K	55.22	20.34	24.43	43.39	12.62	43.99
Na	59.27	36.19	4.54	50.01	20.12	29.87
Ag	57.68	36.62	5.70	–	–	–
Al	39.58	44.54	15.88	36.19	32.99	30.82
As	57.70	41.18	1.12	41.77	20.70	37.53
Ba	29.70	34.59	35.72	53.02	29.68	17.30
Ca	28.85	42.71	28.44	34.80	32.98	32.22
Co	56.55	39.35	4.10	79.00	2.86	18.14
Cr	22.52	60.38	17.10	56.10	41.45	2.45
Cu	30.53	23.51	45.96	61.99	36.99	1.02
Fe	32.28	36.62	31.11	41.76	41.11	17.13
Mg	45.90	41.21	12.89	44.34	42.91	12.75
Mn	33.58	17.42	48.99	54.99	21.66	23.35
Ni	86.51	1.08	12.41	80.53	15.43	4.04
P	39.71	26.44	33.86	53.29	21.13	25.58
Pb	62.65	22.73	14.62	54.19	14.93	30.88
S	77.28	13.41	9.31	49.97	14.85	37.18
Se	60.90	26.79	12.31	38.31	16.41	45.28
Sn	91.03	8.18	0.79	44.37	52.07	3.55
Ti	44.16	42.34	13.50	41.18	18.62	40.20
V	62.31	35.71	1.98	42.70	13.67	43.64
Zn	58.50	13.20	28.30	66.73	23.05	10.22
Average	51.47	30.21	18.32	49.38	27.49	23.13

Revisions and drafts have been made for the "Air Quality Guideline" published by WHO in 1987, 1997, and 2005, respectively. After that, it recommended to choose $PM_{2.5}$ as the prior index for particles.

In 2012, the Chinese standard "Ambient Air Quality Standard" was revised, which will be implemented. Both PM_{10} and $PM_{2.5}$ are included in this standard.

Study has shown that when the daily averaged concentration of $PM_{2.5}$ increases by 10 μg/m^3, the total mortality rate will increase by 1.5 % [28]. The mortality rate of stubborn pulmonary disease will increase by 3.3 %, and that of local blood scarce heart disease will increase by 2.1 %. There are other reports showing that the daily total mortality rate will increase by 10 %, the respiratory system disease increased by 3.4 %, cardiovascular disease increased by 1.4 %, asthma increased by 3 %, and lung function decreased by 0.1 % [29]. International Standard Organization (ISO) proposed to consider particles with diameter less than 2.4 μm as the "high-risk particle" to induce the lung disease for children and adult [30], which is equivalent with $PM_{2.5}$.

Study has shown that the poisonous mechanisms of $PM_{2.5}$ mainly include [29]:

1. Immune toxicity. Not only the nonspecific immunity function of macrophagocyte is affected, but also the immune performance of cell with specific immunity function is damaged.

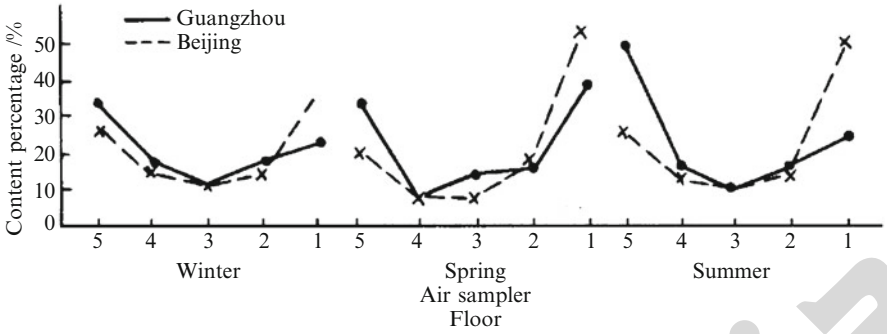

Fig. 2.22 Comparison of mass percentage for particles between Guangzhou and Beijing

2. Oxidation damage toxicity. Except for the radical reactivity itself, particles can also have effect on the epithelial cell and the macrophagocyte. The active oxygen or active nitrogen will be released, and the polyunsaturated fatty acids abundant on the membrane of cell will be oxidized, which will influence the permeability and the mobility of the membrane. The structure of the membrane will be thus damaged.
3. Mutagenicity and potential carcinogenic effect. Toxic heavy metal and PAH (polycyclic aromatic hydrocarbon) absorbed on particles have strong ability of mutagenicity, which can cause the cell division, cultivate the tumor, and have the potential carcinogenic effect.

However, these conclusions have also received accusation from enterprises who believed that it is likely to be overstated. But in other aspect, it is believed that the particles with harmful effect are smaller. For example, the relevant domestic research [31] points out that about 50–70 % of polycyclic aromatic hydrocarbon and 30–50 % of N-alkane are absorbed to particles with diameter $\leq$0.1 μm. It is shown from Fig. 2.20 that this kind of particles has the health significance, which can penetrate through and deposit onto the trachea, bronchus, and especially alveoli. In this sense, the following conclusions can be obtained: since the annual concentration of atmospheric dust for particles with diameter $\leq$0.1 μm (measured with the 6th layer of cascade impactor, i.e., Anderson sampler) in the winter of Guangzhou is 1.6 times than that in Beijing, and in summer the ratio between two cities becomes 1.8 times (shown in Fig. 2.22), the atmosphere with the same concentration of atmospheric dust in Guangzhou is more harmful than that in Beijing.

In the above section, the change of gravimetric concentration standard was discussed. Next the transition of specific standards is presented.

In the "Ambient Air Quality Standard" published in 1982, air quality is classified into three categories:

The first class aims to protect the natural ecology and human health. With the long term of exposure, the air will not cause any risk of harmful effect.

The second class aims to protect the human health, animal, and plant in both urban and rural areas. With the long and short term of exposure, the air will not cause a harmful effect.

The third class aims to protect the human from acute and chronic poisoning and to protect the normal growth of the common animal and plant in city (except the sensitive one).

In this standard, the first class area includes the national specified natural reserves, scenic tourist area, scenic spots and historical resort, and salutarium, where the air with the first class applies. In the revised version of 1996, the salutarium is deleted and replaced by special reserve. The second area includes the city planning specified residential area, the mixed area of commerce, traffic and residence, the cultural area, scenic spots and historical sites, and rural area, where the air with the second class applies. In the revised version of 1996, the general industrial area in the former third class area is classified into the second class area. The third class area includes the city and town with serious air pollution, as well as the industrial area, where the air with the third class applies. In the revised version of 1996, the "urban transportation hub and city" area in the former third class area is deleted. In the revised version of 2012, the third class area is merged into the second class area, and the concentration of $PM_{2.5}$ is required.

It should be noted that there are several kinds of average concentration:

Yearly averaged concentration: The arithmetic average of daily averaged concentrations within any 1 year period.

Quarterly averaged concentration: The arithmetic average of daily averaged concentrations within any one quarter period, which is mainly useful for the lead.

Monthly averaged concentration: The arithmetic average of daily averaged concentrations in 1 month, which is abolished in the 2012 version.

Daily averaged concentration: The average concentration in 1 day, which is abolished in the 2012 version.

24 h averaged concentration: The arithmetic average of hourly averaged concentrations within 24 h of 1 day, which is also called daily averaged concentration (adopted in the 2012 version).

1 h averaged concentration: The arithmetic average of concentrations in 1 h.

Moreover, there are also other kinds which include 8 h averaged concentration and growth season averaged concentration (mainly for fluoride).

Table 2.18 illustrates the change of standards for atmospheric dust concentration in China, and the comparison with American standard is also presented. Table 2.19 shows the target value of WHO.

From the world, the gravimetric concentration of atmospheric dust declines year by year. According to the survey data of 37 countries by the US Environmental Protection Agency, concentration of atmospheric dust in 19 cities declines, that of 12 cities remains the same, and only that of 6 cities increases [8]. The most seriously polluted cities with concentration larger than the recommended value by WHO include Beijing, Calcutta, New Delhi, and Xi'an.

Table 2.18 Ambient Air Quality Standards in China and America

Nationality	Standard development department	Particle concentration ($\mu g/m^3$)						Allowable time with concentration larger than the limit	Remark
			Annual average	Daily average	1 h average	Limit	Average time		
America	National standard for air quality in 1971	Class I		0.260				99.7 % in 1 year	
		Class II		0.150				99.7 % in 1 year	
		Country		0.13				95 % in 1 year	
		Residential district		0.15				95 % in 1 year	
		Industrial area		0.2				95% in 1 year	
	In 1987 (PM_{10})	Class I	0.050	0.150					
	In 1997 ($PM_{2.5}$)		0.015	0.065				Three consecutive years with concentration not less than 98 % of the average daily concentration	
China	National standard "Ambient Air Quality Standard" (GB3095-82) issued in 1982 and the revised edition in 1994	Total suspended particles							
		Level 1	0.10	0.15 (0.15)		(0.30)	(Any time)		Value in () is from the standard in 1982
		Level 2	0.20	0.30 (0.30)		(1.00)	(Any time)		Value in () is from the standard in 1982

(continued)

Table 2.18 (continued)

Nationality	Standard development department	Particle concentration (μg/m^3)					Allowable time with concentration larger than the limit	Remark
			Annual average	Daily average	1 h average	Limit	Average time	
		Level 3	0.30	0.50				
				(0.50)		(1.50)	(Any time)	Value in () is from the standard in 1982
		Inhalable particles						
		Level 1	0.04	0.05				
				(0.05)		(0.15)	(Any time)	Value in () is from the standard in 1982
		Level 2	0.10	0.15				
				(0.15)		(0.50)	(Any time)	Value in () is from the standard in 1982
		Level 3	0.15	0.25				
				(0.25)		(0.70)	(Any time)	Value in () is from the standard in 1982
	Revised standard "Ambient Air Quality Standard" in 2012 (implemented in Jan. of 2016)	PM_{10}						In the standard, the unit has been changed from mg/m^3 into μg/m^3
		Level 1	0.04	0.05				
		Level 2	0.07	0.15				
		$PM_{2.5}$						
		Level 1	0.015	0.035				
		Level 2	0.035	0.075				

Table 2.19 Air Quality Guideline (*AQG*) value in WHO and some countries: annual averaged concentration/24 h concentration

	PM_{10} (μg/m^3)	$PM_{2.5}$ (μg/m^3)
WHO: target during transient period-1(IT-1)	70/50	35/75
Target during transient period-2(IT-2)	50/100	25/50
Target during transient period-3(IT-3)	30/75	15/37.5
Air quality guideline (AQG) value	20/50	10/25
USA (implemented on Dec.17, 2006)		15/35
Japan (issued on Sept. 9, 2009)		15/35
EU (issued on Jan. 1, 2010, implemented on Jan. 1, 2015)		25/None

Table 2.20 Situation of over-standard concentration for atmospheric dust from 1981 to 1990

Overweight situation	Seriously affected area
100 % of particle concentrations in the air of northern cities exceed the standard value, and near 100 % of southern cities are overweight	Hohhot, Taiyuan, Jinan, Shijiazhuang, Lanzhou, Qinhuangdao, Beijing, Tianjin, Chongqing, Shenyang
The pollution of falling dust is very serious regardless of north and south, almost 100 % cities are overweight	Baotou, Benxi, Taiyuan, Shijiazhuang, Anshan, Changchun, Harbin, Shenyang, Urumqi, Jinan

But as for the specific situation in China, the ambient air is seriously polluted, which is shown in Table 2.20 [32]. Table 2.21 is the sorting sequence of atmospheric dust concentrations in several cities in 2000. Table 2.22 is the sorting sequence of particle deposition [32]. It is clear that northern concentration is obviously larger than that of the southern region. However, the atmospheric dust concentration is decreasing, which can be found in Table 2.23 with the sorted data by author according to "China Environment Yearbook." The trendy is also presented in Fig. 2.23, where the data from Taiwan and Japan are also included [26, 33]. The concentration data in China is higher than that of Japan. The good news is that, since 1997, the annual average concentration has been less than the third class, and the trend is continuing to decrease. The peak situation of the dust emission for whole nation shown in Fig. 2.4 is not reflected here. One situation must be noticed that the emission quantity of industrial dust and smoke for the whole nation in 1997 is less than that of 1996, according to the "China Environment Yearbook" published in 1998. The emission quantity in 1997 is far less than that of 1998, which is less than 85 % of the total emission quantity for the whole nation. When other factors are also considered, the total suspended particles are resulted to decrease.

Since 2004, the concentration of TSP by artificial measurement method is no longer reported, and the concentration of PM_{10} by automatic measurement method is adopted. Therefore, the data about TSP is still kept till the end of 2000, but it is impossible to compare these data with the following data. Table 2.24 shows the reported concentration of TSP in some cities for the last time, which is very previous. This is why it is cited here for reference [34].

According to "Environmental Report of China" [35], PM10 concentration distribution in many provinces and cities in 2010 was presented, which is shown in Fig. 2.24. The primary pollutant in Key environmental protection cities is mainly the respirable particles, which occupies 93.5 %. Figure 2.25 shows the situation of key cities with pollution more than 50 days.

Table 2.21 Sorting sequence of annual average concentration of total suspended particles in national monitoring cities in 2000 (mg/m^3)

Northern city	Annual average concentration	Southern city	Annual average concentration
Datong	0.721	Chengdu	0.435
Lanzhou	0.668	Zigong	0.310
Golmud	0.563	Yibin	0.290
Jilin	0.557	Jiujiang	0.268
Yan'an	0.545	Lhasa	0.266
Urumqi	0.501	Nanchong	0.263
Jiaozuo	0.498	Chongqing	0.261
Anyang	0.496	Pingxiang	0.254
Hohhot	0.451	Wuhan	0.253
Xining	0.433	Xiangfan	0.252
Shijiazhuang	0.431	Zhuzhou	0.250
Anshan	0.418	Yichang	0.244
Taiyuan	0.401	Hechi	0.225
Pingdingshan	0.398	Sanming	0.213
Baotou	0.380	Liupanshui	0.211
Shizuishan	0.379	Hengyang	0.201
Baoji	0.365	Guiyang	0.209
Baoding	0.362	Chengdu	0.198
Luoyang	0.354	Guangzhou	0.185
Beijing	0.353	Nanchang	0.180
Tangshan	0.352	Jingdezhen	0.180
Xian	0.351	Changsha	0.179
Yinchuan	0.342	Huaihua	0.172
Hami	0.325	Hefei	0.170
Xuzhou	0.323	Baise	0.167
Kaifeng	0.320	Leshan	0.165
Tianjin	0.304	Nanning	0.162
Zhengzhou	0.291	Gejiu	0.161
Tumen	0.290	Wuzhou	0.161
Qinhuangdao	0.283	Shanghai	0.156
Hegang	0.279	Ningbo	0.154
Qitaihe	0.271	Kunming	0.152
Changchun	0.265	Suzhou	0.152
Shenyang	0.265	Wenzhou	0.149
Siping	0.245	Hangzhou	0.141
Harbin	0.242	Guilin	0.139
Hailar	0.238	Anqing	0.119
Hanzhong	0.238	Zhuhai	0.119
Zibo	0.219	Ganzhou	0.116
Huludao	0.218	Fuzhou	0.113
Yuncheng	0.216	Nantong	0.108
Lianyungang	0.179	Nanjing	0.107
Jinan	0.173	Zhanjiang	0.093
Yichun	0.154	Shenzhen	0.091
Qingdao	0.143	Xiamen	0.084
Ji'an	0.139	Haikou	0.077
Daqing	0.118		
Dalian	0.088		
Average in north	0.336	Average in south	0.186

Table 2.22 Sorting sequence of average annual quantity of dustfalls in national monitoring cities in 2000 (t/(km^2 · month))

Northern city	Dustfall	Southern city	Dustfall
Baoding	38.4	Zhuzhou	27.8
Datong	35.5	Lhasa	20.4
Anshan	35.3	Wuhan	14.1
Yinchuan	35.2	Changsha	13.5
Qitaihe	28.3	Guiyang	13.3
Jiaozuo	28.1	Hangzhou	13.1
Xi'an	27	Xiangfan	11.8
Urumqi	26.9	Nanchong	11.7
Hegang	25.5	Chongqing	11.5
Luoyang	25.4	Chengdu	11.3
Siping	25	Liupanshui	11.1
Jilin	25	Yibin	11
Shijiazhuang	23	Nanjing	10.9
Shizuishan	21.6	Yichang	10.2
Kaifeng	21.4	Jiujiang	9.8
Hailaer	21.4	Nanchang	9.8
Shenyang	21.3	Hengyang	9.7
Lanzhou	21.1	Shanghai	8.9
Xining	19.7	Guilin	8.4
Anyang	19.3	Zigong	8.4
Jinan	18	Wenzhou	8.2
Tangshan	17.7	Anqing	8.2
Zibo	17.3	Nantong	8.1
Dalian	17.2	Kunming	7.4
Qingdao	17.1	Guangzhou	7.3
Harbin	17	Fuzhou	7.1
Zhengzhou	17	Hefei	6.8
Pingdingshan	15.9	Suzhou	6.8
Baoji	15.6	Leshan	6.7
Hami	15.4	Nanning	6.5
Tianjin	15.4	Pingxiang	6.4
Changchun	15.2	Hechi	6
Beijing	15.1	Jingdezhen	5.9
Yan'an	14.8	Ganzhou	5.8
Tumen	13.9	Wuzhou	5.5
Daqing	13.5	Gejiu	5.4
Hohhot	13.4	Ningbo	5.4
Qinghuangdao	13	Xiamen	5.2
Xuzhou	12.1	Huaihua	5.1
Yichun	12	Shenzhen	5
Hanzhong	8.9	Baise	4.5
Huludao	7.3	Zhanjiang	4.4
Lianyungang	7.3	Haikou	3.2
Ji'an	5.6	Zhuhai	2.6
Average in north	19.5	Average in south	8.8

Table 2.23 Comparison between the particulates and the dustfall

		Whole country		Southern cities		Northern cities	
Item	Year	Concentration rage	Annual average	Concentration rage	Annual average	Concentration rage	Annual average
Particle (mg/m^3)	1981	0.160–2.770	0.703	0.160–0.850	0.41	0.370–2.770	0.93
	1982	0.220–1.910	0.729	0.220–0.970	0.47	0.380–1.910	0.95
	1983	0.164–1.358	0.6	0.164–0.540	0.33	0.427–1.358	0.87
	1984	0.190–2.158	0.66	0.190–1.030	0.45	0.370–2.158	0.87
	1985	0.224–1.767	0.59	0.224–0.821	0.444	0.333–1.767	0.74
	1986	0.196–1.575	0.57	0.219–0.627	0.391	0.196–1.575	0.715
	1987	0.154–1.357	0.59	0.154–0.573	0.37	0.439–1.357	0.805
	1988	0.220–1.597	0.58	0.220–0.740	0.44	0.270–1.597	0.674
	1989	0.117–1.043	0.432	0.141–0.916	0.318	0.117–1.043	0.526
	1990	0.064–0.844	0.379	0.064–0.800	0.268	0.138–0.844	0.475
	1991	0.080–1.433	0.324	0.080–0.376	0.225	0.709–1.433	0.429
	1992	0.090–0.063	0.323	0.090–0.474	0.25	0.134–0.663	0.4
	1993	0.108–0.815	0.327	0.108–0.721	0.252	0.142–0.815	0.406
	1994	0.089–0.849	0.316	–	0.25	–	0.407
	1995	0.055–0.732	0.317	–	0.242	–	0.392
	1996	0.079–0.618	0.309	–	0.23	–	0.387
	1997	0.032 ~ 0.741	0.291	–	0.2	–	0.381
	1998	0.011–1.199	0.289	–	0.199	–	0.364
	1999	–	0.266	–	0.179	–	0.346
	2000	–	0.264	–	0.186	–	0.336

Dustfall [t/(km^2 · month)]	1981	10.79–103.75	35.35	10.79–46.50	18.76	21.42–103.75	50.67
	1982	10.83–99.73	32.08	10.83–35.69	16.69	23.73–99.73	48.76
	1983	5.10 ~ 113.90	32	5.10–29.70	16	19.90–113.90	48
	1984	4.048–87.60	27.2	4.48–43.14	16.1	15.30–87.61	38
	1985	7.53–76.50	27.65	7.53–43.69	16.5	16.04–76.50	38.81
	1986	5.96–68.57	25.02	5.96–29.45	13.22	14.82–68.57	32.58
	1987	7.53–73.97	24.41	7.53–26.13	14.09	14.27–73.97	32.79
	1988	7.04–131.25	25	7.04–69.00	13.5	9.90–131.25	35
	1989	3.77–56.70	22.37	3.77–61.92	15.27	6.78–54.61	27.7
	1990	3.22–51.17	19.15	3.71–17.27	10.6	5.91–56.70	26.05
	1991	3.22–51.17	18.1	3.22–49.75	11.05	7.38–51.17	25.46
	1992	3.84–55.75	18.8	3.84–55.75	12.05	9.90–51.08	26.25
	1993	4.03–83.47	18.84	4.03–19.85	10.11	8.50–83.47	26.64
	1994	–	17.6	–	10.57	–	24.76
	1995	–	17.7	–	10.16	–	24.73
	1996	–	16.2	–	9.14	–	23.2
	1997	–	15.3	–	9.29	–	21.48
	1998	–	15.15	–	8.84	–	21.06
	1999	–	14.3	–	8.5	–	20.1
	2000	–	14.15	–	8.8	–	19.5

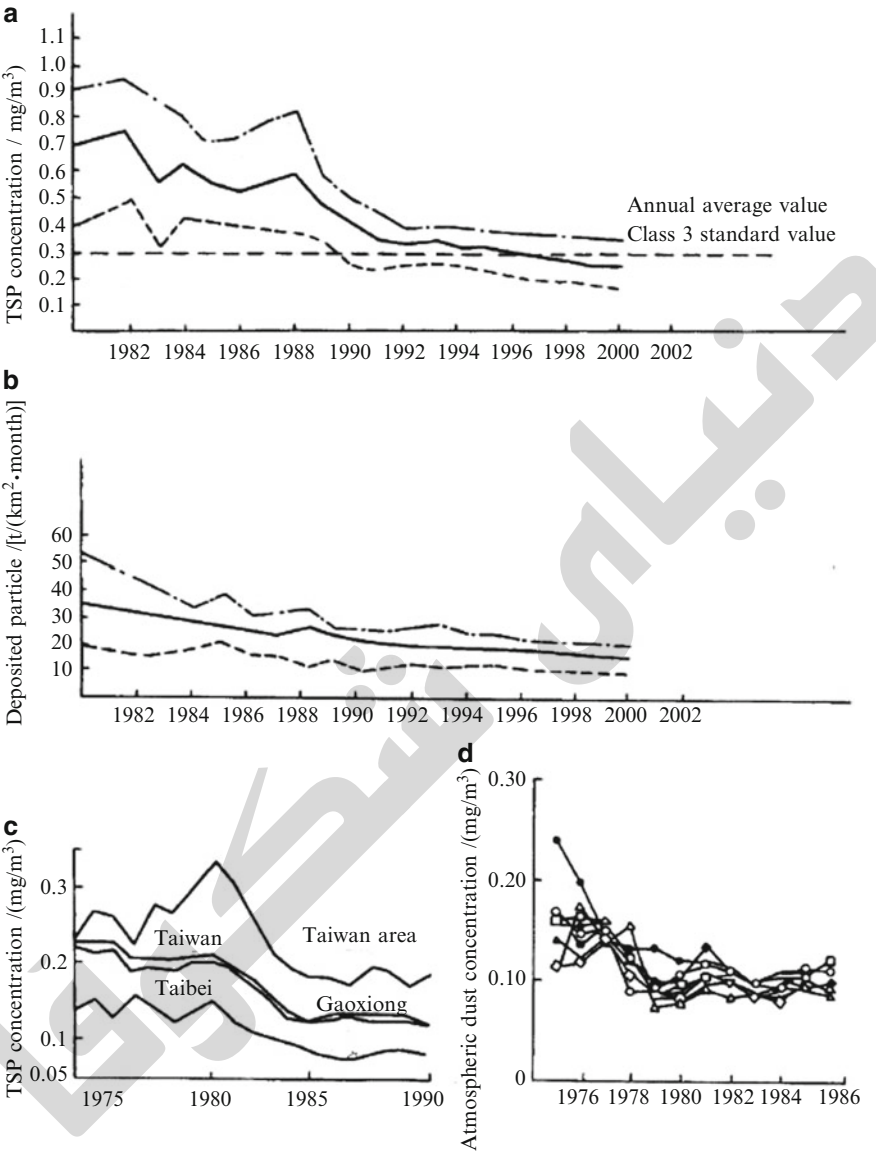

Fig. 2.23 Change of urban atmospheric dust for 10 years at home and abroad. (**a**) Total suspended particulates in China. (**b**) Deposition particulates in China. (**c**) Total suspended particulates in Taiwan. (**d**) Atmospheric dust in Tokyo area of Japan

Table 2.24 Concentration of TSP in some cities in 2004

Northern cities	Annual average	Southern cities	Annual average
Hetian	1.424	Lhasa	0.267
Aksu	0.817	Liuzhou	0.227
Kashgar	0.806	Liupanshui	0.201
Wuhai	0.564	Tongren	0.200
Artux	0.550	Hechi	0.199
Turpan	0.508	Chengdu	0.199
Korla	0.482	Guigang	0.195
Xining	0.472	Hezhou	0.190
Baiyin	0.451	Baise	0.184
Wuzhong	0.449	Xingyi	0.173
Golmud	0.446	Yingtan	0.168
Zhongwei	0.406	Qinzhou	0.157
Hohhot	0.353	Duyun	0.123
Tianshui	0.329	Anshun	0.122
Yining	0.327	Fangchenggang	0.118
Wuwei	0.322	Kaili	0.116
Linxia	0.312	Chishui	0.101
Liaoyuan	0.301	Wuzhishan	0.014
Dingxi	0.297		
Benxi	0.295		
Shangluo	0.292		
Hami	0.291		
Ankang	0.287		
Pingliang	0.285		
Tongliao	0.284		
Jinzhou	0.280		
Anyang	0.279		
Hezuo	0.274		
Zhangye	0.269		
Siping	0.262		
Kuitun	0.261		
Yulin	0.258		
Fushun	0.241		
Ulanqab	0.234		
Qitaihe	0.220		
Bole	0.217		
Shuangyashan	0.210		
Changji	0.209		
Jiuquan	0.207		
Tacheng	0.200		
Liaoyang	0.199		
Chaoyang	0.198		
Changchun	0.185		
Baishan	0.182		
Panjin	0.182		
Ji'an	0.179		

(continued)

Table 2.24 (continued)

Northern cities	Annual average	Southern cities	Annual average
Tumen	0.173		
Qiqihar	0.172		
Yingkou	0.170		
Songyuan	0.167		
Dandong	0.166		
Yichun	0.136		
Baicheng	0.135		
Altay	0.110		

Unit: mg/m^3

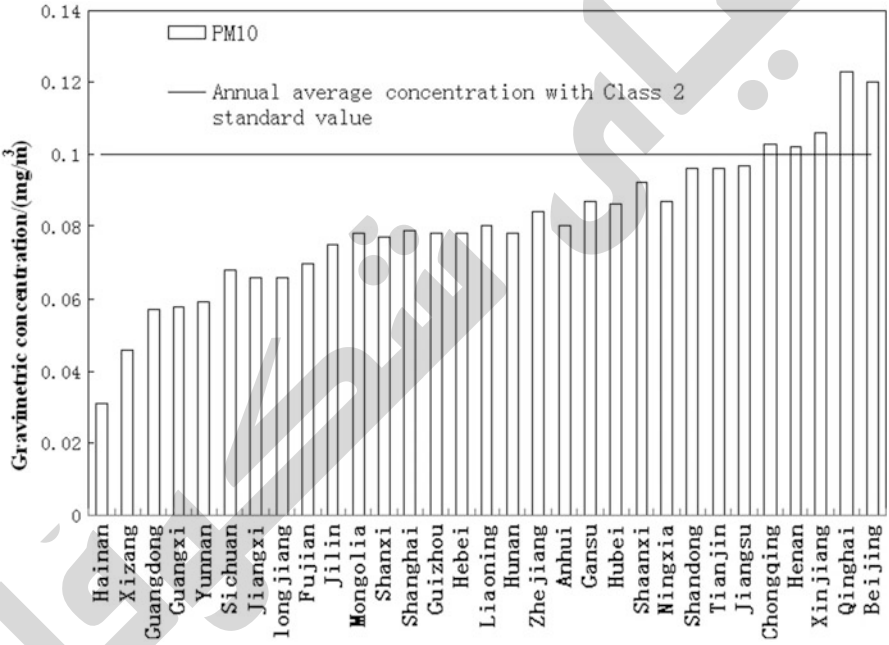

Fig. 2.24 Gravimetric concentration distribution of PM10 in different provinces (autonomous regions and municipalities)

Of course, after the erupt of sand storm, the concentration of PM_{10} may increase by several times. Figure 2.26 is one example from Beijing [35].

Table 2.25 mainly shows the annual average concentration of PM_{10} in cities with the level above the county, but some TSP data are also included for individual cities [35]. They are listed in the corresponding province.

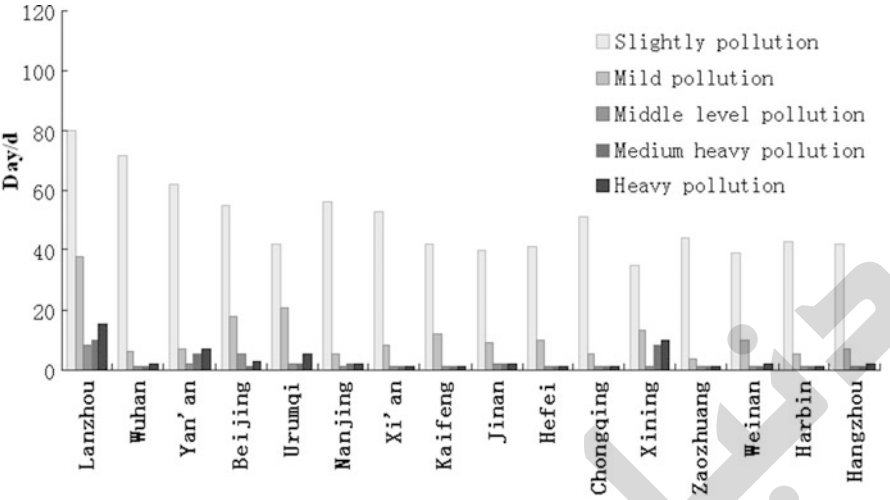

Fig. 2.25 Key cities of environmental protection where the concentration of the primary pollutant PM_{10} overweight for 50 days

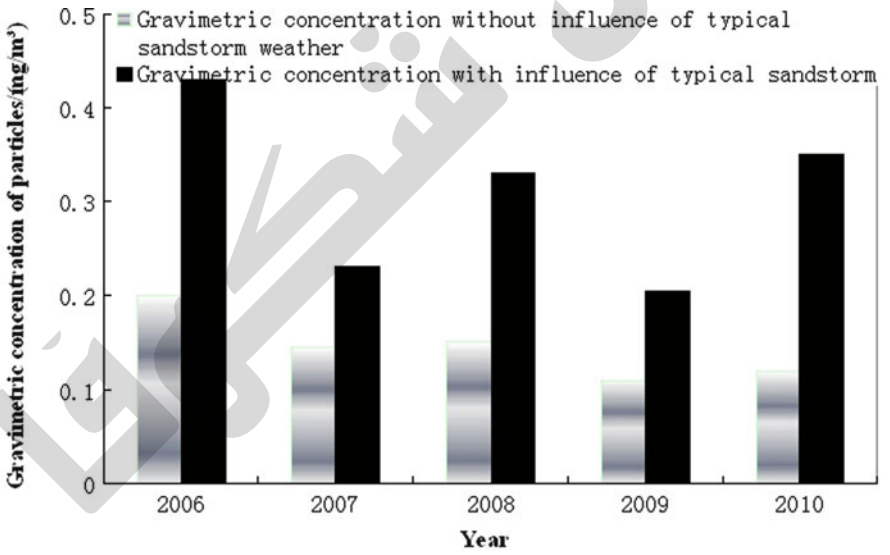

Fig. 2.26 Annual variation of air quality with the influence of the typical sand storm

But in general, among 341 monitoring cities in 2001, air quality reaching or better than the second class of national air quality occupies 33.4 % [36], which is almost the same as the previous year. In 2010, among 655 monitoring cities, this ratio increases to 78.10 %, and the annual average gravimetric concentration of respiratory particles decreases by 16.3 % [35], which is shown in Fig. 2.27. This is

Table 2.25 Annual average concentration of PM_{10} in cities with the level above the county in 2010 (mg/m^3)

Beijing	0.121	Dandong	0.069	Zhenjiang	0.097	Jingdezhen	0.064	Zhoukou	0.106
Tianjin	0.096	Jinzhou	0.079	Taizhou	0.087	Pingxiang	0.066	Zhumadian	0.094
Hebei		Yingkou	0.073	Suqian	0.099	Jiujiang	0.064	*Hubei*	
Shijiazhuang	0.098	Fuxin	0.094	*Zhejiang*		Xinyu	0.077	Wuhan	0.108
Tangshan	0.085	Liaoyang	0.066	Hangzhou	0.098	Yingtan	0.058	Huangshi	0.091
Qinghuangdao	0.064	Panjin	0.074	Ningbo	0.096	Ganzhou	0.059	Shiyan	0.081
Handan	0.09	Tieling	0.078	Wenzhou	0.085	Ji'an	0.072	Yichang	0.086
Xingtai	0.082	Chaoyang	0.083	Jiaxing	0.093	Yichun	0.059	Xiangfan	0.089
Baoding	0.084	Huludao	0.076	Huzhou	0.086	Fuzhou	0.057	Ezhou	0.083
Zhangjiakou	0.07	*Jilin*		Shaoxing	0.095	Shangrao	0.058	Jinmen	0.106
Chengde	0.053	Changchun	0.089	Jinhua	0.067	*Shandong*		Xiaogan	0.101
Cangzhou	0.078	Jilin	0.081	Quzhou	0.065	Jinan	0.117	Jinzhou	0.088
Langfang	0.078	Siping	0.067	Zhoushan	0.061	Qingdao	0.099	Huanggang	0.071
Hengshui	0.074	Liaoyuan	0.067	Taizhou	0.08	Zibo	0.11	Xianning	0.094
Shanxi		Tonghua	0.087	Lishui	0.071	Zaozhuang	0.099	Suizhou	0.086
Taiyuan	0.089	Baishan	0.063	*Anhui*		Dongying	0.089	Enshi	0.077
Datong	0.075	Songyuan	0.06	Hefei	0.115	Yantai	0.081	*Hunan*	
Yangquan	0.078	Baicheng	0.061	Wuhu	0.075	Weifang	0.099	Changsha	0.081
Changzhi	0.083	Yanji	0.069	Bengbu	0.08	Jining	0.116	Zhuzhou	0.095
Jincheng	0.067	*Heilongjiang*		Huainan	0.087	Tai'an	0.097	Xiangtan	0.072
Shuozhou	0.075	Harbin	0.101	Ma'anshan	0.097	Weihai	0.067	Hengyang	0.066
Jinzhong	0.07	Qiqihar	0.078	Huaibei	0.089	Rizhao	0.089	Shaoyang	0.097
Yuncheng	0.075	Jixi	0.066	Tongling	0.095	Laiwu	0.107	Yueyang	0.092
Xinzhou	0.061	Hegang	0.09	Anqing	0.085	Linyi	0.097	Changde	0.071
Linfen	0.084	Shuangyashan	0.08	Huangshan	0.046	Dezhou	0.093	Zhangjiajie	0.077
Lvliang	0.067	Daqing	0.054	Chuzhou	0.09	Liaocheng	0.089	Yiyang	0.065
Inner Mongolia		Yichun	0.045	Fuyang	0.084	Binzhou	0.093	Chenzhou	0.087
Hohhot	0.068	Jiamusi	0.059	Suzhou	0.081	Heze	0.097	Yongzhou	0.069
Baotou	0.102	Qitaihe	0.104	Chaohu	0.079	Zhengzhou	0.111	Huaihua	0.071

Wuhai	0.124	Mudanjiang	0.07	Liu'an	0.067	*Henan*		Loudi	0.061
Chifeng	0.093	Heihe	0.048	Bozhou	0.088	Kaifeng	0.111	Jishou	0.061
Tongliao	0.069	Suihua	0.051	Chizhou	0.045	Luoyang	0.107	*Guangdong*	
Erdos	0.065	Great Khingan	0.057	Xuancheng	0.069	Pingdingshan	0.094	Guangzhou	0.069
Hulunbuir	0.064	*Shanghai*	0.079	*Fujian*		Anyang	0.109	Shaoguan	0.074
Bayannur	0.068	*Jiangsu*		Fuzhou	0.073	Hebi	0.105	Shenzhen	0.057
Ulanqab	0.076	Nanjing	0.114	Xiamen	0.065	Xinxiang	0.089	Zhuhai	0.049
Ulanhot	0.042	Wuxi	0.088	Putian	0.054	Jiaozuo	0.1	Shantou	0.06
Xilinhot	0.061	Xuzhou	0.088	Sanming	0.086	Jiyuan	0.102	Foshan	0.064
Bayanhot	0.056	Changzhou	0.097	Quanzhou	0.068	Puyang	0.103	Jiangmen	0.057
Liaoning		Suzhou	0.09	Zhangzhou	0.078	Xuchang	0.102	Zhanjiang	0.045
Shenyang	0.101	Nantong	0.097	Nanping	0.066	Luohe	0.099	Maoming	0.047
Dalian	0.058	Lianyungang	0.09	Longyan	0.08	Sanmenxia	0.096	Zhaoqing	0.058
Anshan	0.105	Huai'an	0.095	Ningde	0.063	Nanyang	0.099	Huizhou	0.051
Fushun	0.094	Yancheng	0.122	*Jiangxi*		Shangqiu	0.104	Meizhou	0.038
Benxi	0.069	Yangzhou	0.096	Nanchang	0.087	Xinyang	0.091	Shanwei	0.045
Heyuan	0.026	*Sichuan*		Liupanshui	0.047	*Shanxi*		*Ningxia*	
Yangjiang	0.039	Chengdu	0.104	Zunyi	0.087	Xi'an	0.126	Yinchuan	0.093
Qingyuan	0.06	Dujiangyan	0.061	Anshun	0.058	Tongchuan	0.099	Shizuishan	0.088
Dongguan	0.063	Zigong	0.081	Tongren	0.094	Baoji	0.098	Wuzhong	0.064
Zhongshan	0.051	Panzhihua	0.098	Xingyi	0.109	Xianyang	0.094	Guyuan	0.105
Chaozhou	0.072	Luzhou	0.086	Bijie	0.101	Weinan	0.112	Zhongwei	0.101
Jieyang	0.053	Deyang	0.065	Kaili	0.063	Yan'an	0.12	*Xinjiang*	
Yunfu	0.052	Mianyang	0.082	Duyun	0.068	Hanzhong	0.078	Urumqi	0.133
Guangxi		Jiangyou	0.075	*Yunnan*		Yulin	0.095	Karamay	0.051
Nanning	0.069	Guangyuan	0.047	Kunming	0.072	Ankang	0.049	Turpan	0.135/0.44
Liuzhou	0.067	Suining	0.071	Qujing	0.085	Shangluo	0.057	Kumul	0.086
Guilin	0.066	Neijiang	0.052	Yuxi	0.079	Lanzhou	0.155	Changji	0.082/0.28
Wuzhou	0.027	Leshan	0.079	Baoshan	0.051	Jiayuguan	0.097	Fukang	0.072
Beihai	0.058	Emeishan	0.121	Shaotong	0.048	Jinchang	0.088	Bole	0.046/0.167

(continued)

Table 2.25 (continued)

Fangchenggang	0.058	Nancong	0.061	Lijiang	0.043	Baiyin	0.099	Korla	0.137
Qinzhou	0.051	Meishan	0.083	Pu'er	0.105	Tianshui	0.066	Aksu	0.143
Guigang	0.056	Yibin	0.078	Lincang	0.059	Jiuquan	0.089	Artux	0.174/0.592
Yulin	0.049	Guang'an	0.059	Chuxiong	0.041	Zhangye	0.08	Kashgar	0.248/0.799
Baise	0.053	Dazhou	0.069	Mengzi	0.05	Wuwei	0.08	Hetian	0.272/0.988
Hezhou	0.047	Ya'an	0.047	Wenshan	0.054	Dingxi	0.061	Yining	0.08
Hechi	0.061	Bazhong	0.054	Jinghong	0.051	Longnan	0.121/0.32	Kuitun	0.056
Laibin	0.065	Ziyang	0.062	Dali	0.037	Pingliang	0.089	Tacheng	0.036
Congzuo	0.055	Ma'erkang	0.032	Luxi	0.057	Anqing	0.076	Wusu	0.058
Hainan		Kangding	0.027	Liuku	0.038	Linxia	0.121/0.21	Altay	0.039
Haikou	0.04	Xichang	0.041	Shangri-La	0.031	Hezuo	0.107/0.16	Shihezi	0.07
Sanya	0.022	*Guizhou*		*Xizang*		*Qinghai*		Wujiaqu	0.073
Chongqing	0.102	Guiyang	0.075	Lhasa	0.048	Xining	0.124		

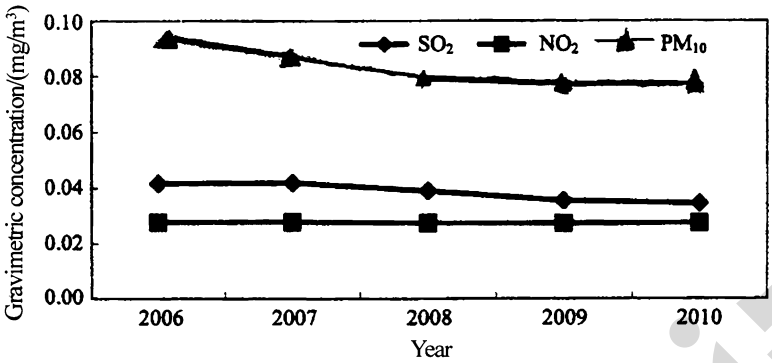

Fig. 2.27 Annual variation of gravimetric concentration of SO_2, NO_2, and PM_{10} between 2006 and 2010

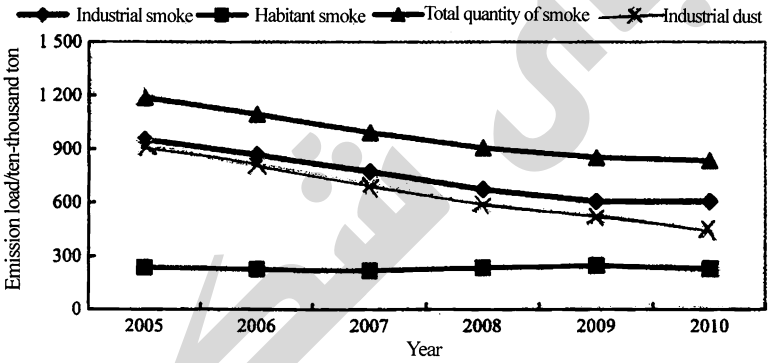

Fig. 2.28 Annual variation of dust emission in the whole country and in industrial field

related to the decrease of dust emission in the whole country these years, which is illustrated in Fig. 2.28 [35].

But it should be noted that the annual average concentration of $PM_{2.5}$ measured in China was higher than that of America by 2.8–9.7 times in 1995 [37].

It should also be mentioned that gravimetric concentration of atmospheric dust is usually used for the design of ventilation and air-conditioning system, while it is not suitable for the design of cleanroom. When it comes to the life time of air filter in air cleaning system, the gravimetric concentration is still used.

2.4.4 Particle Counting Concentration [38]

In the air cleaning technology field, the basis of particle counting concentration is the most commonly used particles with diameter $\geq$0.5 μm. Taking the stratosphere

Table 2.26 Particle counting concentration of typical areas abroad

Area	Particle concentration (≥0.5 μm)/(#/L)	Ref.	Area	Particle concentration (≥0.5 μm)/(#/L)	Ref.
County	3×10^4	[39]	Polluted area	177×10^4	[41]
Metropolis	12.5×10^4		Common area	17.7×10^4	
Industrial center	25×10^4		Clean area	3.5×10^4	
County	10×10^4		For design of cleanroom	17.5×10^4	[42]
Suburb	20×10^4	[40]	Specially clean	0.19×10^4	
Urban	50×10^4		Specially polluted	56×10^4	

(10 km above the land) as an example, the concentration of these particles is about 20 pc/L, while the concentration above the ocean is about 2,500 pc/L. Particle counting concentration near the land differs a lot with locations and period, which is more complex than the parameter such as temperature. Therefore, in order to study the particle counting concentration of typical situations, the method to distinguish between some typical areas is adopted, which is shown in Table 2.26.

In the research report "Cleanroom Calculation" from Institute of HAVC of China Academy of Building Science printed in 1977, three typical areas are used, including "industrial city," "suburb," and "nonindustrial area or rural area." The corresponding atmospheric dust concentrations can be simplified as "city type," "suburb type," and "rural type," which is a rough classification method. The particle counting concentration of "city type" is usually less than 3×10^5 pc/L. That of "suburb type" (the industrial suburb cannot be included) is usually less than 2×10^5 pc/L. That of "nonindustrial area or rural area" is usually less than 1×10^5 pc/L. However, the atmospheric dust concentration of above three types only represents the average level of these areas. Taking the "city type" as an example, the concentration near the corner of area with factories surpasses the above value, and the air is close to the level of air pollution. However, with good weather or after the rainy days, the measured concentration of "city type" may be 10^4 pc/L. But in winter, the concentration may be as large as $(5–6) \times 10^6$ pc/L, or even larger. When outdoor cleaning is performed and weed and leaf piled are burning, the concentration nearby can be as large as 6×10^6 pc/L. The above classification was used as the calculation basis of outdoor concentration for medium-efficiency air cleaning system in "Air Cleaning Technology Measures" by 14 units in 1979.

Three years after 2005, Cui Lei et al. surveyed the atmospheric dust concentration in the whole country [43], and the data from 132 districts were summarized, which is shown in Table 2.27.

Measurement results have shown that there is only one exception that the particle counting concentration for particles ≥0.5 μm is larger than 3×10^5 pc/L, which was thought to be accidental.

Table 2.27 Analysis of measured data

Classification	Results
With area	Northeast 10, north China 40, east China 23, northwest 12, southwest 15, central south 32
With measuring location	Suburb 90, downtown 27, far from city 10, no locations 5
With season	Spring 20, summer 42, autumn 48, winter 22
With time	Morning 12, noon 22, afternoon 44, evening 4, no time 50
With weather condition	Sunshine 84, cloudy 8, sunny days with strong wind 4, overcast 20, Overcast with fog 2, rainy 11, rainy days with strong wind 3

Ten areas with the minimum and maximum concentrations are presented in Tables 2.28 and 2.29.

The particle counting concentration mentioned above is not corresponding to the whole size range. When the whole particle size (mainly particle size below 0.5 μm) is used for calculation, the average concentration in the mixed layer 2 km above the land is 10^5–10^6 pc/L, and that near the land surface is as high as 10^6–10^8 pc/L, where the concentration of particles with heavy metal is about 10^4–10^5 pc/L [44]. In the whole size range, particles with diameter less than 0.1 μm are called condensation nucleus.

Table 2.30 shows the particle counting concentration related to air pollution event in literatures. It is shown that the concentration above 10^6 pc/L only occurs accidentally when smog or photochemical smog is generated. The particle concentration in industrial air recommended by the USA is almost equivalent with the common industrial area in China. Therefore, 3 times of this concentration is used as the particle concentration in seriously polluted air for the outdoor calculation concentration of cleanroom, which was adopted in the monograph "Air Cleaning Technology Measures" (the reason is shown in Chap. 13).

2.4.5 Comparison Between Particle Counting Concentration and Gravimetric Concentration

There is no clear relationship between the particle counting concentration and the gravimetric concentration, because too much influence factors exist. For example, density of atmospheric dust changes with location and season. Mass increases by 10^3 times when particle size increases by 10 times, so the influence of dispersity is very large. In China, the specific comparison of this aspect has not been carried out. Figure 2.29 shows the comparison of measurement at abroad [48], which can be used for reference. It is obvious that the correlation between particle counting concentration and gravimetric concentration is only valid within a range, so two dashed lines are plotted on this figure by author (in the original figure they do not exit).

According to some analysis on data, the relationship among particle counting concentration, gravimetric concentration, and deposition concentration is shown in Table 2.31. In the table, several applications with extreme low particle counting concentration are also listed for comparison.

Table 2.28 The minimum concentrations at ten locations

No.	Particle counting concentration (#/L)						Location	Place	Weather	Tem. (°C)	Relative humidity (%)	Wind force level
	Particle size (μm)											
	0.3	0.5	0.7	1	2	5						
88	2,215	1,193	583	254	85	15	Hohhot (Inner Mongolia)	Far from city	Overcast, rainy, strong wind[a]			4–5
54	3,567	1,683	384	151	57	6	Yizhuang (Beijing)	Suburb	Sunny	31.1	18.30	2–3
125	10,085	4,976	1,958	996	368	151	Lhasa (Xizang)	Suburb	Cloudy			
11	16,599	5,094	1,145	163	28	6	Dali (Yunnan)	Suburb	Sunny	26.4	53.80	
37	10,014	5,309	2,326	979	248	15	Urumqi (Xinjiang)	Suburb	Sunny	29.8	18.10	2–3
113	9,964	5,608	907	281	104	16	Haikou (Hainan)	Far from city	Overcast			
120	22,190	6,234	965	240	16	3	Chengmai (Hainan)	Suburb				
110	12,934	6,688	2,456	517	98	18	Yinchuan ecological preservation area(Ningxia)	Far from city	Cloudy			1–2
124	20,137	8,461	2,238	446	28	6	Chuxiong (Yunnan)	Suburb	Rainy			
95	19,736	9,578	2,110	340	64	7	Baoshan (Yunnan)		Downtown		Sunny	

[a]Refer to the analysis in the Sect. 2.6.1

Table 2.29 The maximum concentrations at ten locations

	Particle counting concentration (#/L)											
	Particle size (μm)											
No.	0.3	0.5	0.7	1	2	5	Location	Place	Weather	Tem. (°C)	Relative humidity (%)	Wind force level
10	184,152	148,917	39,881	3,847	251	10	Shijiazhuang (Beijing)	Suburb	Sunny			
76	182,439	156,967	57,823	8,704	868	37	Shunyi (Beijing)	Suburb	Cloudy			
100	213,561	160,973	60,298	5,636	253	16	Jiaozuo (Henan)	Downtown	Overcast, rainy			
40	230,630	164,485	87,424	11,171	516	33	Chengdu (Sichuan)	Suburb	Sunny	7.9	52.60	1–2
103	221,265	175,637	88,439	43,395	3,500	467	Chongwen district (Beijing)	Downtown	Overcast			
70	238,886	185,804	52,518	7,888	2,044	201	Baoding (Hebei)	Suburb	Sunny			
25	244,145	190,874	54,767	7,865	1,371	126	Pujiang (Chengdu)	Suburb	Overcast	10.9	55.90	1–2
67	245,500	195,517	79,065	7,654	863	95	Rongchang (Chongqing)	Suburb	Sunny	25.2	71.50	
29	258,795	206,473	81,480	8,078	823	81	Qingxu (Taiyuan)	Suburb	Sunny			
97	1,280,998	702,923	203,561	41,220	8,561	1,453	Cangzhou (Hebei)	Downtown	Sunny			

Table 2.30 Particle concentration in polluted air (≥0.5 μm)

Type of polluted air	Concentration (#/L)	Ref.
US industrial air	3.5×10^5	[45]
Pollution	5.6×10^5	[42]
With photochemical smog	10^6	[46]
Seriously polluted	1.75×10^6	[41]
Pollution	10^6	[47]
With smog	2×10^6	[47]
Common industrial air in China	$(2–3) \times 10^5$	Measured in China

Note: Concentration of microorganism in atmospheric dust is between 1 pc/L and thousands pc/L.

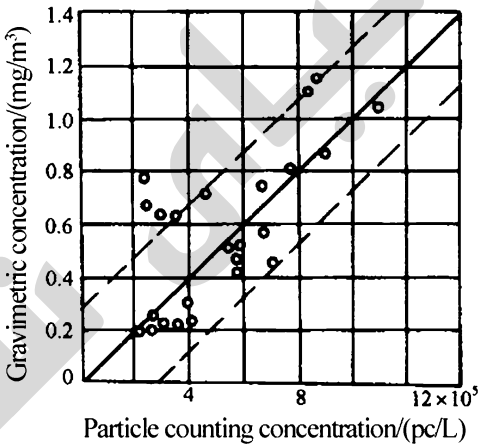

Fig. 2.29 Comparison between particle counting concentration and gravimetric concentration

Table 2.31 Comparison of several kinds of concentrations

Concentration	Industrial city (polluted area)	Suburb of industrial city (intermediate area)	Nonindustrial or rural area (clean area)	Cleanroom for large-scale integrated circuit	For manufacturing passive laser night vision instrument
Particle counting concentration (pc/L)	$\leq 3 \times 10^5$	$\leq 2 \times 10^5$	$\leq 10^5$	≤3	≤0.3
Weighting concentration (mg/m^3)	0.3–1	0.1–0.3	<0.1		
Deposition concentration [t/(km^2 · month)]	>15	<15	<5		

The comparison data are just for reference purpose only. In practice, when it comes to the relationship between concentrations, specific situation must be considered, and the comparison curve between particle counting concentration and gravimetric concentration under specific conditions (such as locations and seasons,) should be obtained.

2.5 Particle Size Distribution of Atmospheric Dust

2.5.1 Full Particle Size Distribution

With the limit of measurement means, it is really difficult to obtain the real particle size distribution of atmospheric dust accurately. Figure 2.30 shows the published data in the early of 1960s [1], which corresponds to the situation of coal smoke. The mass distribution is unimodal, but it maybe not accurate in the range of large diameter. Particle size distribution in the range of small diameter is bimodal. Since the measurement means is not known, we do not know its accuracy. From Fig. 2.31 [49], the abrupt increase of particle number for extreme small particles may occur.

Look at Fig. 2.32 published in the late of 1960s [50]; it is more close to the reality with the advancement of the measurement means. However, we know that:

1. Since the data of particle number distribution in the range of small size is lacking, the detailed information may lose. This is why it is different from the two figures above.
2. When the mass distribution is bimodal, the distribution of atmospheric dust belongs to the photochemical smog. The first peak of mass distribution including small particle size corresponds to the mass medium diameter 0.3 μm and $\sigma_g = 2.05$. The second peak of mass distribution including small particle size corresponds to the mass medium diameter 8 μm and $\sigma_g = 2.3$. There is a trough between 1 and 3 μm for this kind of distribution. The mass of particles with diameter less than 2 μm occupied 1/3–1/2 of the total mass.

In total, when the full particle size distribution of atmospheric dust is considered, the number of so-called large particles with diameter $\geq$0.3 μm is a very small proportion of that of condensation nucleus. The ratio varies from 1:15 to 1:5,000, or even larger [51].

From the practical application of air cleaning technology, particles with diameter larger than 0.3 or 0.5 μm are thought to be 100 %. At this time, the mass of most submicron particles only occupies 2–3 %, which is shown in Table 2.32 [52]. Moreover, submicron particles can almost penetrate air filters with performance lower than that of HEPA filters. So large difference exists when particle number and particle mass are used to evaluate the efficiency. This will be further illustrated in Chap. 4 about the characteristic of air filters.

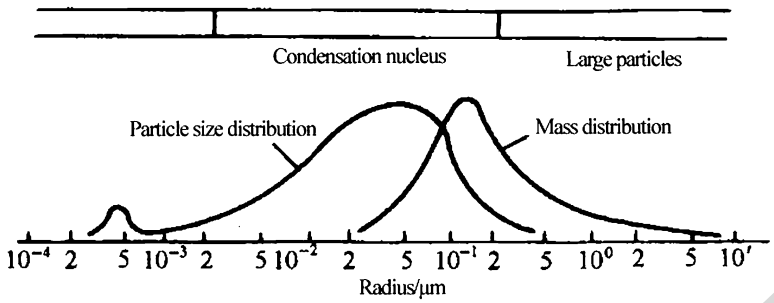

Fig. 2.30 Full particle size distribution of atmospheric dust

Fig. 2.31 Distribution curve of airborne particles under three kinds of conditions: *A* small particle number in atmosphere, *B* near the land, *C* the floating of the maximum value with the increase of pollution, *D* near the ocean, *E* the background value (very clean, and the visibility is good)

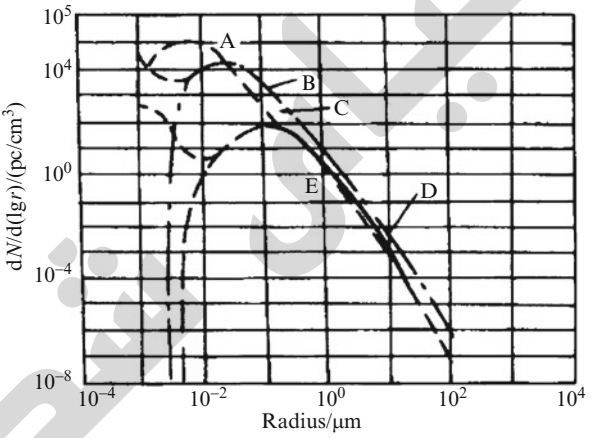

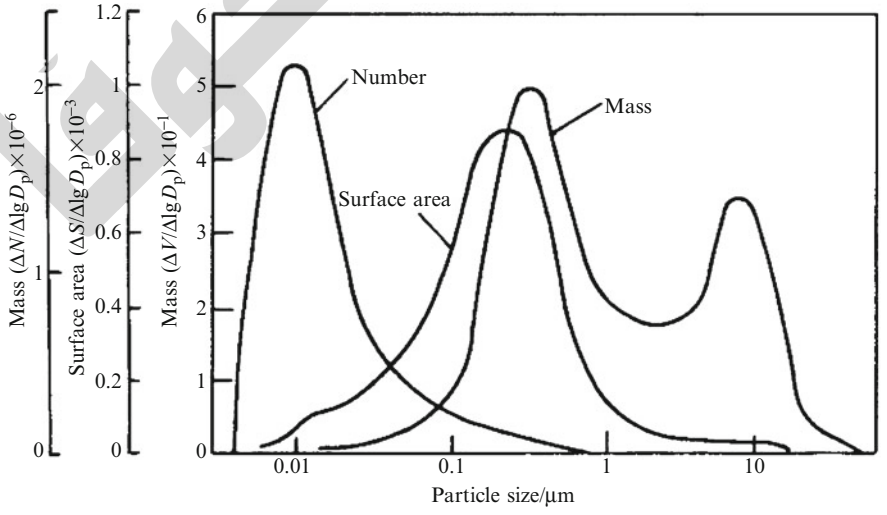

Fig. 2.32 Example of full particle size distribution of atmospheric dust

Table 2.32 Distribution of number and mass of atmospheric dust

Particle size interval (μm)	Average size (μm)	Number (%)		Mass (%)	
		Percentage	More than 0.5 μm are considered as 100	Percentage	More than 0.5 μm are considered as 100
0–0.5	0.25	91.68	–	1	–
0.5–1	0.75	6.78	81.49	2	2.02
1–3	2	1.07	12.86	6	6.06
3–5	4	0.25	3	11	11.11
5–10	7.4	0.17	2	52	52.53
10–30	20	0.05	0.65	28	28.28

2.5.2 *Distribution on Log-Log Probability Paper*

2.5.2.1 Attenuation Distribution with Particle Size

As for the statistical distribution of atmospheric dust, particle number decreases significantly with the increase of particle size, as pointed out by Junge from Germany for the first time [53]. The relationship expression can be simplified as

$$\frac{\mathrm{d}N}{\mathrm{d}\lg D_p} = KD_P^{-\nu+1} \tag{2.1}$$

where

D_p is the particle size;
ν is 4 for clean atmosphere, and 2.5 for smog situation;
K is the coefficient;
dN is the particle number of unit volume in the particle size interval from the size smaller than D_p to D_p.

This kind of distribution is shown in Figs. 2.31, 2.33 [54], and 2.34 [55]. The ordinate is the number of airborne particles within 1 cm^3 air with the change of logarithmic particle radius.

From Figs. 2.32, 2.33, and 2.34, K is obtained to be 2. From Fig. 2.31, the average value of K for B, D, and E situations is about 2.

2.5.2.2 Cumulative Distribution with Particle Size on Log-Log Paper

The so-called distribution on log-log paper means the cumulative distribution of particle number with particle size on log-log paper. Before 1980s, author plotted the particle size distribution on log-log paper according to the measured data at home and abroad, which is shown in Fig. 2.35 [38]. The trend is shown obvious. In the

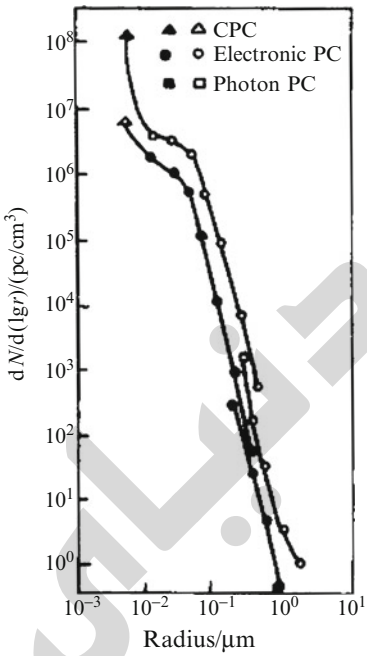

Fig. 2.33 Example of measured data about airborne particle distribution in urban atmosphere

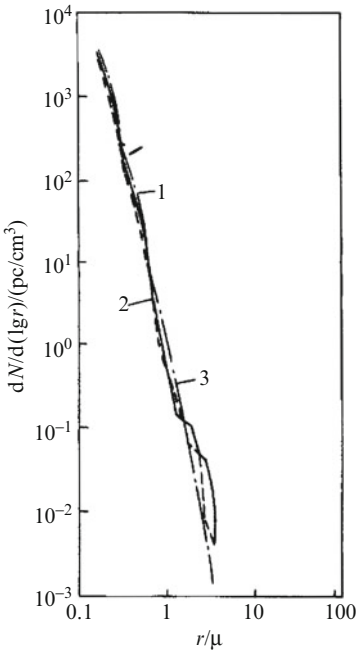

Fig. 2.34 Measured distribution of atmospheric dust near the land: *1* average of 12 samples in the daylight (Aug.1, 1980), *2* average of 12 samples in the evening (from 19:00 of Aug.1, 1980, to 5:00 of Aug. 2, 2980), *3* fitted result with three parameters for the average of evening

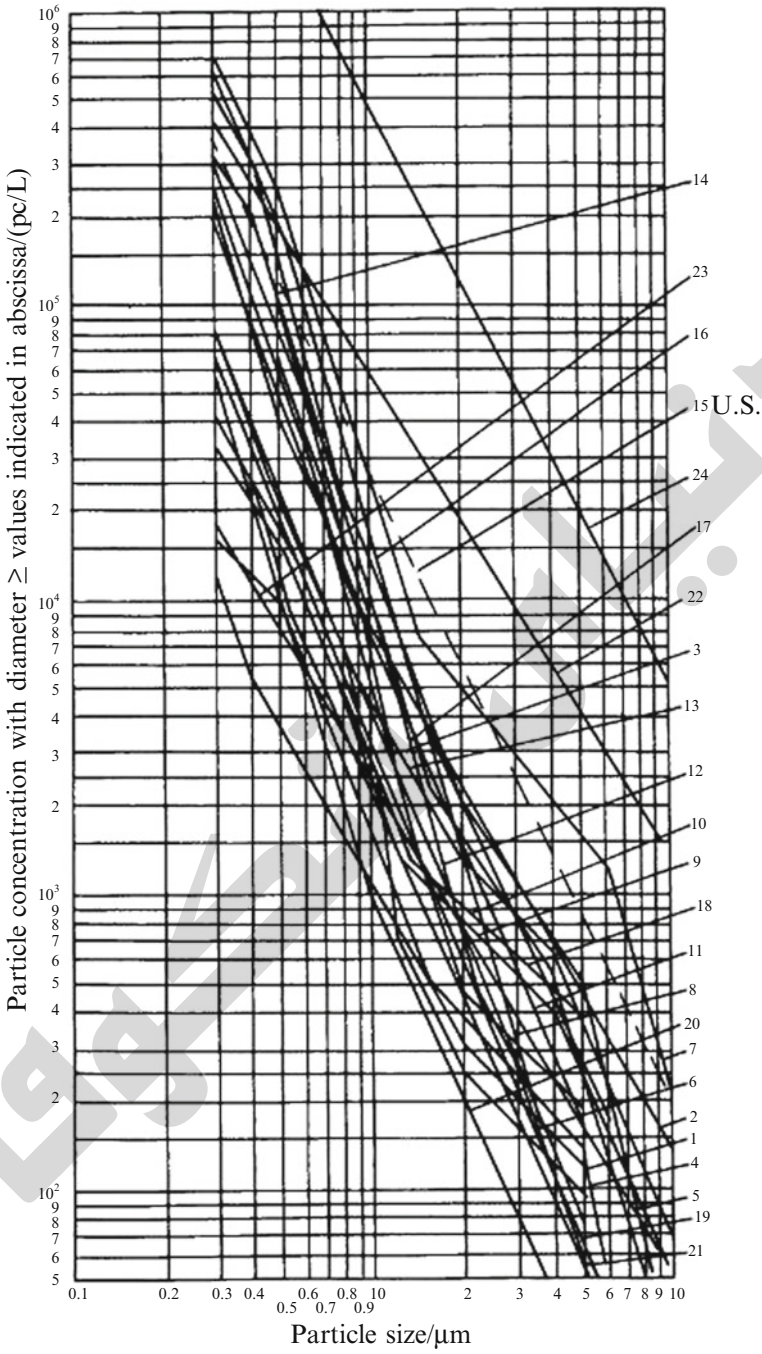

Fig. 2.35 Particle size distribution of atmospheric dust before 1980s. *1* Shahe, Beijing, *2* Lintong, *3* northern suburb, Beijing, *4* Changping, Beijing, *5* Wuxi, *6* Hanzhong, *7* Beijing, *8* Beijing, *9* Beijing, *10* northern suburb, Beijing, *11* Shanghai, *12* Shanghai, *13* Huxian, *14* Tianjin, *15* industrial air of the USA, *16* Shanghai, *17* Tianjin, *18* Ōta special wards of Tokyo, Japan, *19* Hyōgo-ken outskirt, Japan, *20* Nagoya outskirt, Japan, *21* center of Kanagawa, Japan, *22* average polluted area of Tokyo, Japan, *23* clan area of Chiba-ken, Japan, *24* smog period of Tokyo, Japan

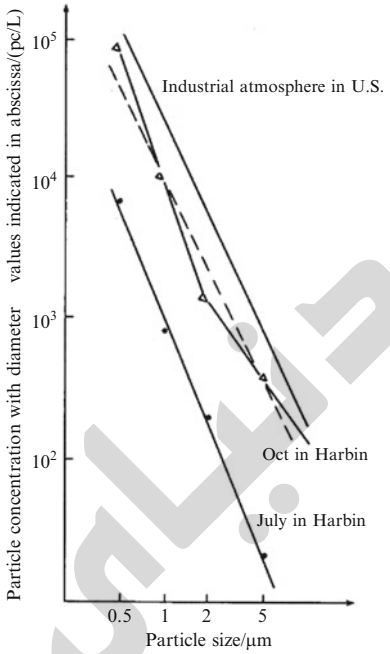

Fig. 2.36 Measured distribution of atmospheric dust in Harbin

figure, the inclination of some curve for particle size between 2 and 5 μm becomes small, which means the proportion of large particles increases. The reason may be related to the sampling. When the sampling height is not high enough, it will be greatly affected by the ground. When particle resuspension from the ground does not occur, the concentration with particles larger than 5 μm will not increase obviously during the sampling process.

This distribution characteristic is also proved by the experiment later. Figure 2.36 is one example [56].

From these curves, the following relationship can be obtained [38]:

$$\frac{N_{d_1}}{N_{d_2}} = \left(\frac{d_1}{d_2}\right)^{-n} \tag{2.1}$$

where

N_{d_1} is the total number of particles with diameter $\geq d_1$ (pc/L);
N_{d_2} is the total number of particles with diameter $\geq d_2$ (pc/L);
n is the exponent of the distribution.

When the proportion of particles with diameter $\geq d_2$ is considered 100 %, N_{d_1}/N_{d_2} means the percentage of particle numbers with diameter $\geq d_1$ among all

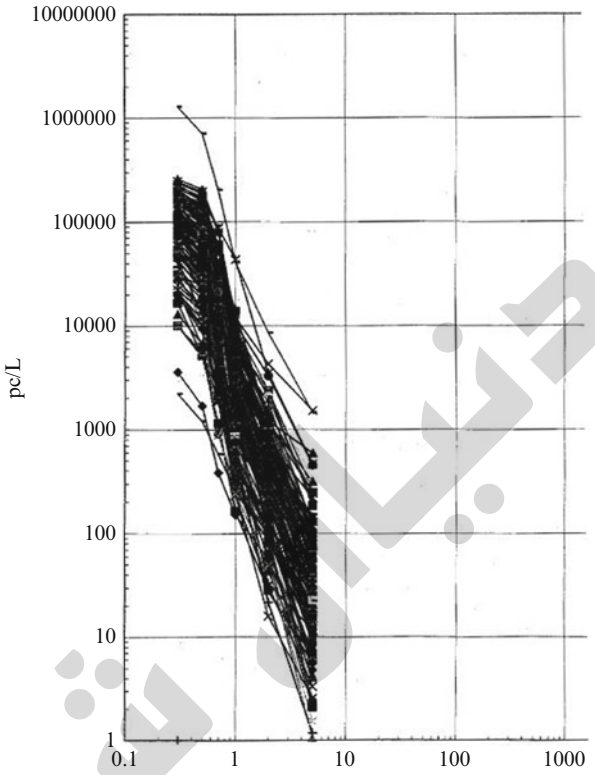

Fig. 2.37 Concentration distribution of atmospheric dust in 132 areas since 2005 in China

particles ($\geq d_2$). The meaning is the same as oversize distribution in the monograph about dust removal. But the usual oversize distribution is based on gravimetric concentration, where the total quantity of particles does not have any limit of particle size. In air cleaning technology, total number of particles is based on the particles with diameter $\geq$0.3 or $\geq$0.5 μm, which depends on the measurement condition and the need. Therefore, Eq. (2.1) can also be written as

$$R_d = \left(\frac{d}{d_0}\right)^{-n} \tag{2.2}$$

where R_d is the percentage of particles with diameter $\geq d$ in the total number of particles with diameter $\geq d_0$. That is the oversize distribution with the basis of d_0 (%);

d is the particle size;

d_0 is the particle size when the percentage of total particles for diameter $\geq d_0$ is 100 %. Usually it is 0.3 μm or 0.5 μm.

The exponent n varies between 2 and 2.3, or sometimes it is larger than 2.3 or 3.

The data of particle size distribution for 132 areas are shown in Fig. 2.37 [43]. The particle size distributions of atmospheric dust for three kinds of areas

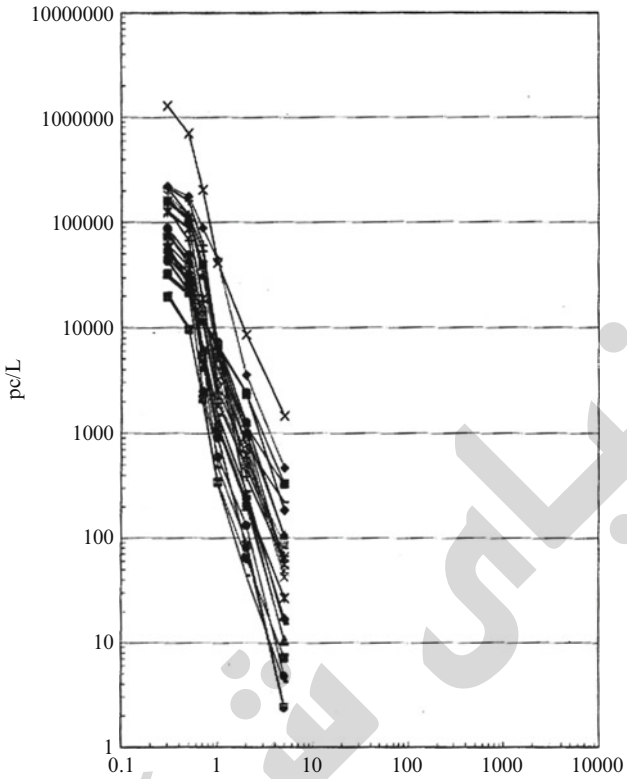

Fig. 2.38 Concentration distribution of atmospheric dust in industrial cities since 2005 in China

are illustrated in Figs. 2.38, 2.39 and 2.40. The average distributions of atmospheric dust in 132 areas are shown in Fig. 2.41 [57].

According to these latest measurement data, the following conclusions can be obtained:

1. The characteristic of particle size distribution of atmospheric dust is similar as that of 30 years ago.

It is known that the value of n obtained from the average distribution curve in Fig. 2.28 remains the same as that of Fig. 2.32.

2. The linear property of particle size distribution of atmospheric dust remains the same on log-log paper.

This kind of linear property is the total distribution characteristic, not the polygonal line from one measurement.

According to the average distribution curve in Fig. 2.38, three conclusions can be reached:

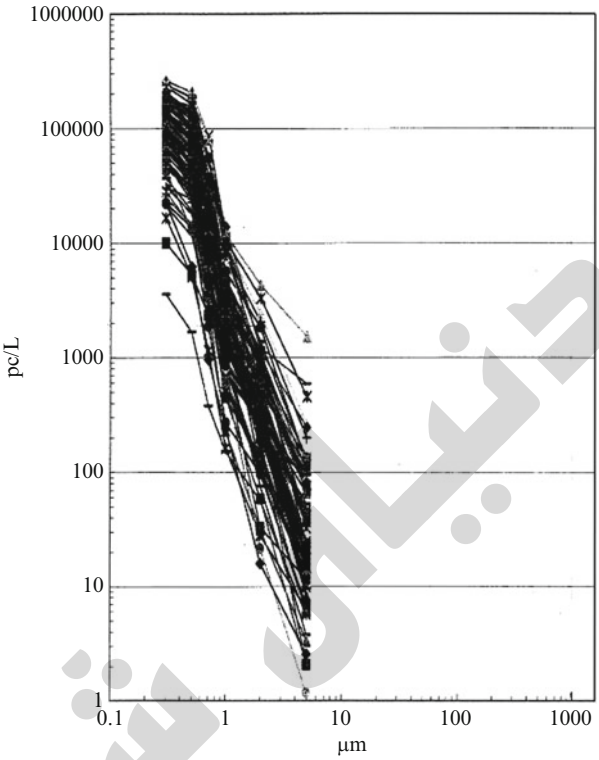

Fig. 2.39 Concentration distribution of atmospheric dust in suburb areas since 2005 in China

1. The inclination of the straight line between 0.5 and 1 μm becomes large, which means the proportion of particles with diameter less than 1 μm increases. This can be used to reflect the fact that with the development of economy these years, the proportion of so-called fine particles increases.
2. The inclination of the straight line between 0.3 and 0.5 μm becomes small. This may caused by the fact that the particle counter used in the experiment was calibrated with 0.5 μm standard particles, and the particle counting efficiency to measure 0.3 μm is very low. Even it reaches the counting efficiency of 0.5 μm, the inclination in this region will not decrease. So in practice, the straight line of 0.5 μm can be extended downstream, which becomes the linear relationship.
3. The particle counting concentration of atmospheric dust decreases by 30–40 % compared with the past concentration.

From Tables 2.37, 2.38 and 2.39, the current average concentrations for three kinds of atmospheric dust can be considered as less than 2×10^5 pc/L, 1×10^5 pc/L, and 0.7×10^5 pc/L, respectively. While in the past they were 3×10^5 pc/L, 2×10^5 pc/L, and 1×10^5 pc/L, respectively.

According to Eqs. (2.1) and (2.2), the statistical distribution of atmospheric dust can be obtained, such as Tables 2.33 and 2.34. The calculation results in Table 2.34 is very close to the measured results in Table 2.32. Therefore, when total number of

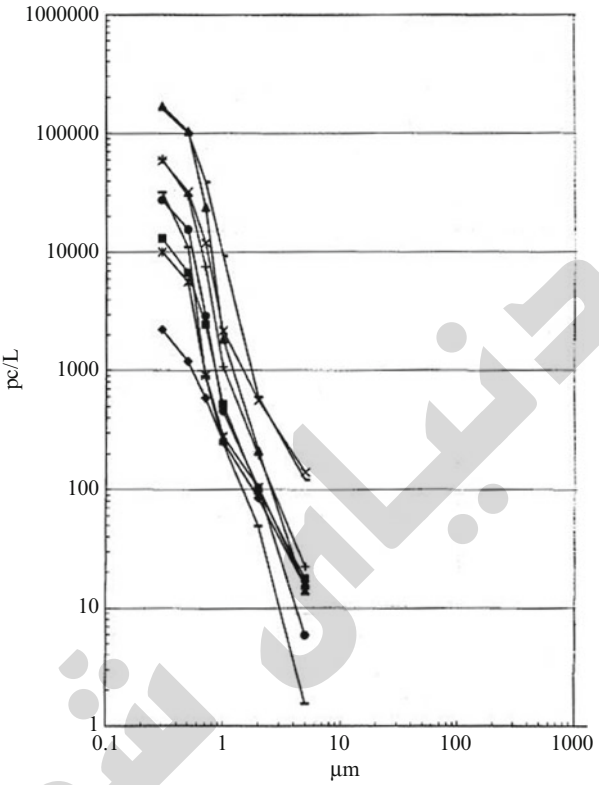

Fig. 2.40 Concentration distribution of atmospheric dust in nonindustrial or rural areas since 2005 in China

particles with diameter $\geq d_0$ is measured, which can be used as the basis, the total number of particles with diameter $\geq d$ can be predicted.

For example, when the concentration of atmospheric dust with diameter $\geq$0.3 μm measured by the particle counter is 3.5×10^5 pc/L, what is the concentration for diameter $\geq$6 μm?

With Eq. (2.1), we know

$$N_6 = 3.5 \times 10^5 \left(\frac{6}{0.3}\right)^{-2.15} = 3.5 \times 10^5 \times 0.0016 = 560 \text{ pc/L}$$

It is shown that Eq. (2.1) obtained by domestic measurement can reflect the statistical distribution relationship, which is completely consistent with the result from abroad [58]. Therefore, the straight line on log-log paper can be parallel with the statistical curve of industrial atmospheric dust in USA, which means the distribution characteristics of atmospheric dust on the earth are fundamentally consistent.

In Fig. 2.42, distributions of atmospheric dust for the above four kinds of typical areas are plotted. Both the land concentration and the background concentration in

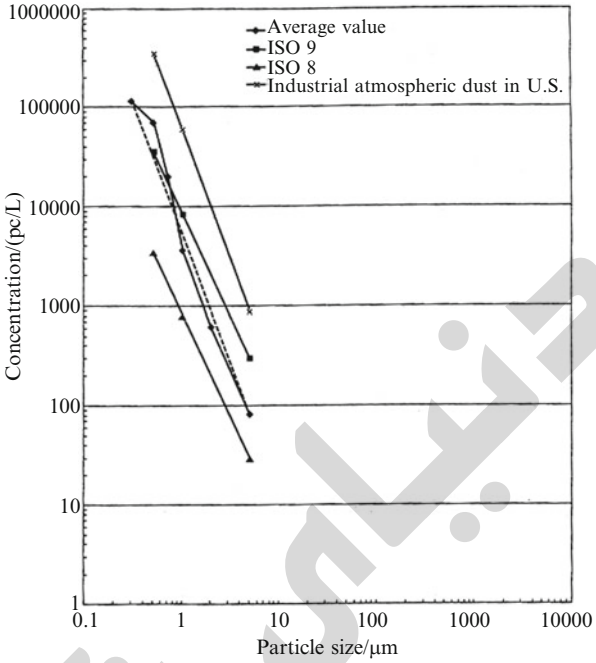

Fig. 2.41 Average concentration distribution of atmospheric dust in 132 areas since 2005 in China

Table 2.33 Statistical distribution of atmospheric dust with diameter (≥0.3 μm)

Particle size (μm)	Relative frequency (%)	Particle size (μm)	Cumulative frequency (%)	Particle size (μm)	Relative frequency (%)	Particle size (μm)	Cumulative frequency (%)
0.3	46	≥0.3	100	1.2	2	≥1.2	5
0.4	20	≥0.4	54	1.5	1	≥1.5	3
0.5	11	≥0.5	34	1.8	1	≥1.8	2
0.6	11	≥0.6	23	2.4	0.7	≥2.4	1
0.8	5	≥0.8	12	4.8	0.3	≥4.8	0.3
1.0	2	≥1.0	7				

Table 2.34 Statistical distribution of atmospheric dust with diameter (≥0.5 μm)

Particle size (μm)	Relative frequency (%)	Particle size (μm)	Cumulative frequency (%)	Particle size (μm)	Relative frequency (%)	Particle size (μm)	Cumulative frequency (%)
0.5	33	≥0.5	100	1.5	3	≥1.5	9
0.6	31	≥0.6	67	1.8	3	≥1.8	6
0.8	15	≥0.8	36	2.4	2	≥2.4	3
1.0	6	≥1.0	21	4.8	1	≥4.8	1
1.2	6	≥1.2	15				

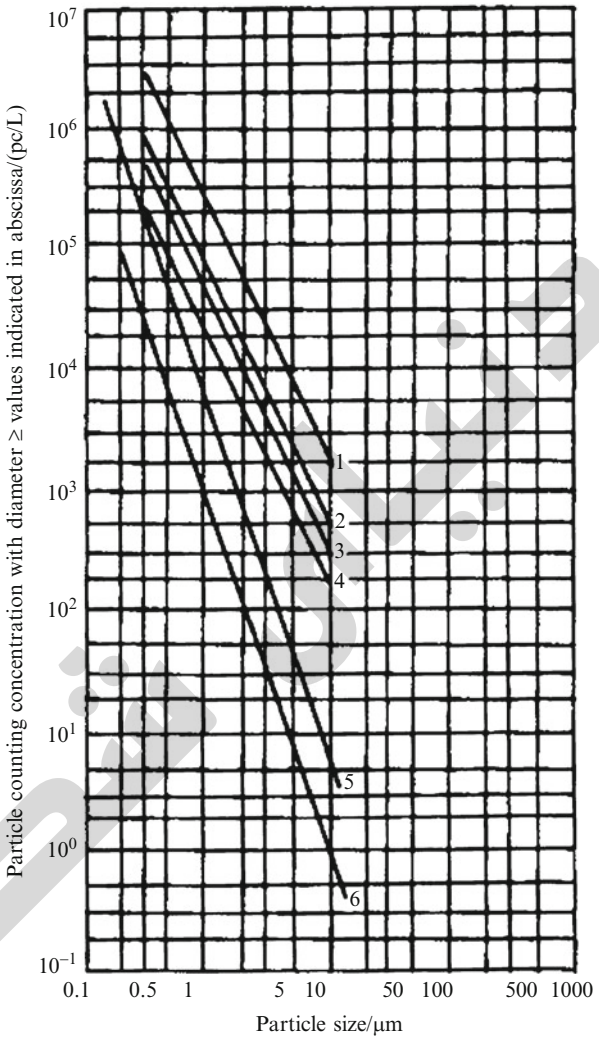

Fig. 2.42 Distribution of atmospheric dust in land condition and background on log-log paper. *1* seriously polluted, *2* industrial city, *3* industrial suburb, *4* nonindustrial or rural, *5* land condition, *6* background

Fig. 2.27 are plotted in this figure after conversion with Table 2.35. When Eq. (2.1) is used to describe these two statuses, the exponent index is approximately −2.7.

Two important points can be found from Fig. 2.42. One is that the distribution of atmospheric dust is linear on log-log paper, which is a general characteristic. Of course this feature is not fit for all the specific situations. The other one is when the concentration of atmospheric dust is very low, such as the clean environment with very low background concentration, this linear characteristic is not suitable for describing particles with diameter less than 0.1 μm. This should be noted for making parallel lines corresponding to the air cleanliness level.

Why does the particle size distribution of atmospheric dust have this kind of characteristic? Someone attempted to investigate the reason in terms of the

Table 2.35 Calculation result with conversion

State		Concentration variation per unit particle size interval $dN/d\lg D_p$ (pc/L)	Concentration variation in the particle size interval dN (pc/L)	Concentration with ≥0.1 μm (pc/L)	Concentration with ≥1 μm (pc/L)	Concentration with ≥10 μm (pc/L)	Concentration with ≥100 μm (pc/L)
B	Increase from 0.01 μm to 0.1 μm	2×10^6	$2 \times 10^6 \times \lg \frac{0.1}{0.01} = 2 \times 10^6$	2.007006×10^6			
	Increase from 0.1 to 1 μm	7×10^3	$7 \times 10^3 \times \lg \frac{1}{0.1} = 7 \times 10^3$		0.007006×10^6		
	Increase from 1 to 10 μm	7×10^0	$7 \times \lg \frac{10}{1} = 7$			0.000007×10^6	
	Increase from 10 to 100 μm	5×10^{-4}	$5 \times 10^{-4} \times \lg \frac{100}{10} = 5 \times 10^{-4}$				Ignored
E	Increase from 0.01 to 0.1 μm	10^5	$10^5 \times \lg \frac{0.1}{0.01} = 10^5$	1.01001×10^5			
	Increase from 0.1 to 1 μm	10^3	$10^3 \times \lg \frac{1}{0.1} = 10^3$		0.01001×10^5		
	Increase from 1 to 10 μm	1	$1 \times \lg \frac{10}{1} = 1$			0.00001×10^5	
	Increase from 10 to 100 μm	10^{-4}	$10^{-4} \times \lg \frac{100}{10} = 10^{-4}$				Ignored

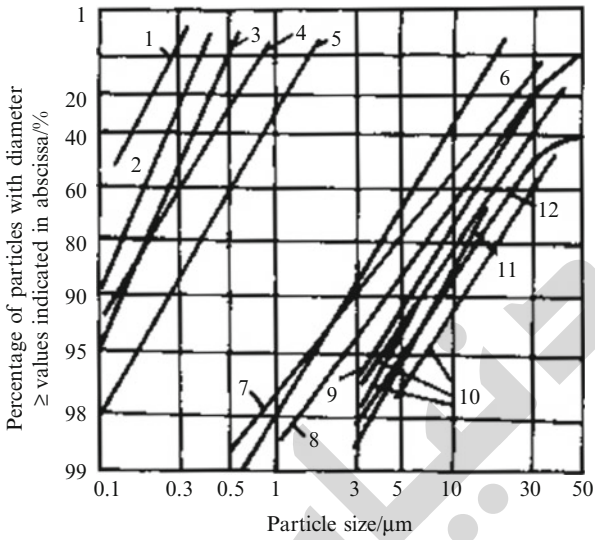

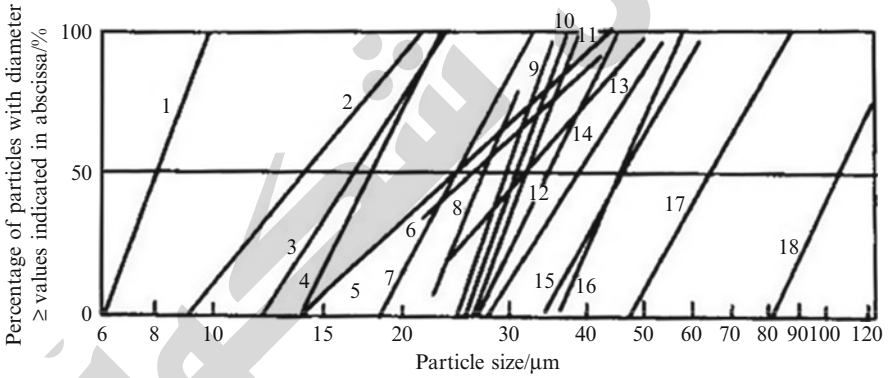

Fig. 2.43 Particle size distribution of some industrial dust. *1* producer gas, *2* converter oxygen steelmaking, *3* open hearth steelmaking, *4* oxygen blowing refining lead, *5* titanium oxide, *6* tin oxide, *7* oil-fired boiler, *8* sintering furnace, *9* cement drying furnace, *10* coal-powder boiler, *11* cement aggregate drying furnace, *12* cupola

Fig. 2.44 Particle size distribution of pollen spore. *1 Mimosa pudica*, *2* primrose, *3* green onion, *4* balsamine, *5* purple *Commelina communis*, *6* pollen typhae, *7 Kalimeris indica*, *8 Lycopodium*, *9* dandelion, *10* phoenix-tail fern, *11* toon, *12* daisy, *13* passion flower, *14 Acacia* grass, *15* tulip, *16* cuckoo, *17* rose moss, *18* hibiscus

formation of some components in atmospheric dust. For example, fine particles of brittle material (such as coal and rock) generated by crush are very consistent in shape and diameter. No matter it is the crush process by mechanical means or ordinary abrasion, all the processes will generate particles with some characteristic of the diameters. This also applied to the particle size distribution of industrial particles, which is shown in Fig. 2.43 [59]. They are almost parallel. Pollen generated naturally has the distribution characteristic like Fig. 2.44 [60].

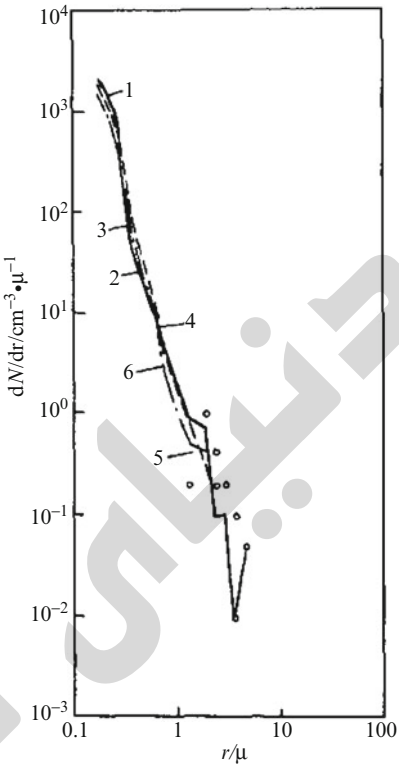

Fig. 2.45 Measured distribution of atmospheric dust with height (20:00–21:06, Aug.1, 1980): *1* 50 m, *2* 100 m, *3* 150 m, *4* 200 m, *5* 250 m, *6* 300 m

Distribution of atmospheric dust is a very important issue. Although there are some regular patterns, it is fickle when it comes to specific distribution of atmospheric dust, which may be far away from the statistical distribution curve. It is related to many factors, which need to be discriminated and investigated specifically.

2.5.3 *Distribution Along Vertical Height*

Figures 2.42 and 2.43 show the distribution near the ground layer. The distribution at the height 50–300 m above the ground is shown in Fig. 2.45 [55]. The distribution of small particles with radius $r_p < 3$ μm is basically linear, which is similar as that near the ground.

According to the solid line representing the relationship between measured concentration and height in Fig. 2.46, the relationship can also be expressed with the dashed line, which is obtained with the least square fit method for the measured data. Therefore, the relationship between the average concentration of atmospheric dust at height Z (N_Z) and the concentration on ground (N_0) is [55]

$$N_Z = N_0 e^{-\frac{Z}{H_P}} \tag{2.3}$$

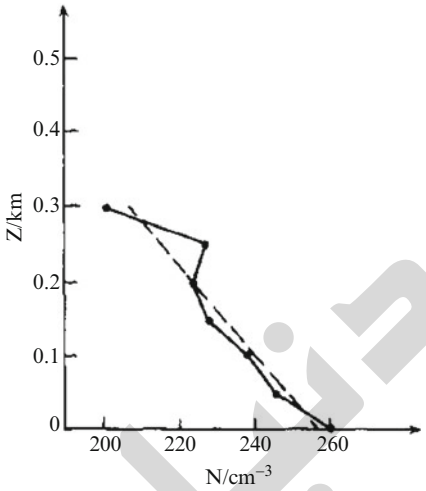

Fig. 2.46 Agreement between fitted vertical distribution and measured distribution

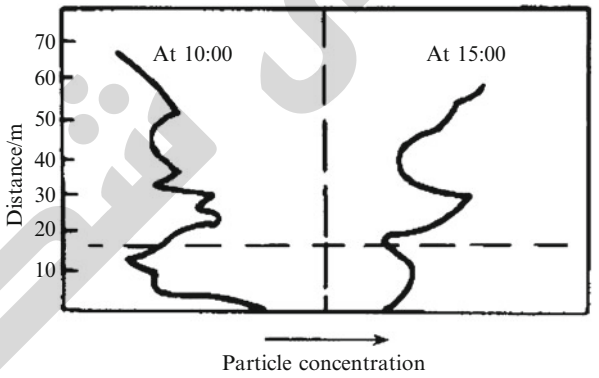

Fig. 2.47 Vertical distribution of atmospheric dust in the center of Leipzig

where a parameter H_p is introduced, which is called the reference height for atmospheric aerosol, $H_p = 1.41$ km, which is equivalent with the reference height under muddy atmospheric condition (the visibility distance in the evening and cloudy days is 5 km).

It is obvious that it is not applicable for describing the atmospheric dust concentration below 50 m with Eq. (2.3). The first reason is that data are lacking in Fig. 2.46 within the height 50 m above the ground. The second reason is that the situation close to the ground is very complex. Figure 2.47 shows one example of atmospheric dust concentration on the vertical direction within 50 m from the ground [51]. It is clear that the concentration becomes the maximum when near the ground and decreases sharply as it becomes higher. The second maximum appears about 22 m above on the ground which is on the roof (it is the chimney that takes particles to the atmosphere). The third one is about 50–60 m high, which

Table 2.36 One example for the vertical distribution of atmospheric dust

	Atmospheric dust concentration (pc/L)	
Height from floor (m)	≥0.5 μm	≥0.5 μm
1	3.19×10^4	49
17	4.33×10^4	29
30	3.98×10^4	28

is the exhaust pollution layer by factory. If the traffic volume is small, the first layer with the maximum concentration appears 20 m above the ground [61], which is shown in Table 2.36.

In short, due to the different environmental conditions, there may be maximum values of first layer, second layer, or even third layer in the vertical distribution of dust concentration. Usually, the dust concentration within the height 5–15 m above the ground is less affected by the ground and so it is more stable. Therefore, the Japan Environmental Agency set the atmospheric dust sampling height to be 5–10 m in the relevant regulations. In China, the "Global Atmospheric Monitoring Work Regulations" laid out by the Environmental Sanitation Monitoring Station under Chinese Academy of Medical Sciences also set the dust sampling height above 3–4 m.

2.6 Influencing Factors for Concentration and Distribution of Atmospheric Dust

2.6.1 Influence of Wind

In modern cities, atmospheric dust is mainly produced from point source (chimney and other emission device), line source (streets that are crowded with cars), and area source (industrial district). The most important means of propagating pollutions are through the wind.

The common impression that people have about wind is that wind always comes with dusts together. But this only shows the case that wind blows up the dusts on the ground. For example, in spring and winter in Beijing, the wind that contains the dusts from the Mongolian Plateau can make the sky dark yellow. In most cases in general, the pollutant concentration in the atmosphere is directly proportional to the total emission amount and inversely proportional to the average wind speed. So if the wind speed increases two times, the leeward pollutant concentration will be reduced by half. This is the common sense in the field of environmental protection. One relevant professional research report abroad mentions that, when the precise particle counter was used carefully to study the properties of atmospheric dust, it can be found that wind is the factor that causes the low atmospheric dust concentration measurable [48, 62]. For example, when the wind changes from 0 to 4 m/s, the variation of dust concentration can be seen on Table 2.37 [51].

Table 2.37 Influence of wind on concentration

Air velocity (m/s)	0	2	4
Concentration (pc/L)	346,000	230,000	84,000

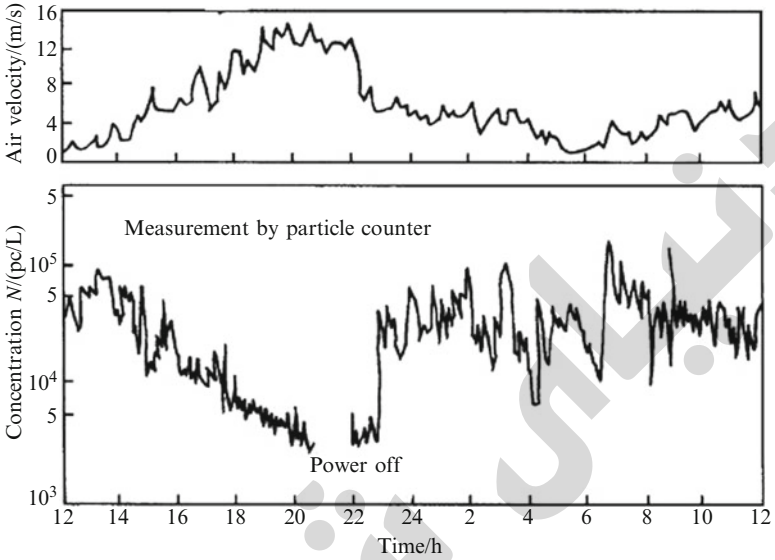

Fig. 2.48 Relationship between wind speed and concentration (Sept. 17, 1965)

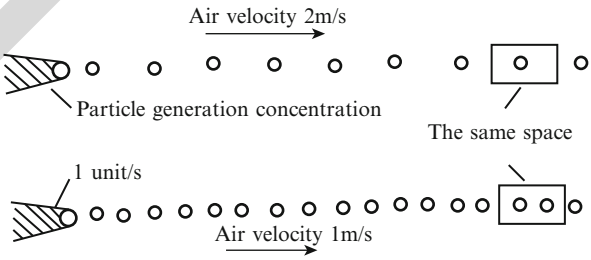

Fig. 2.49 Schematic of the effect of wind

Figure 2.48 is the measured results on a typhoon day [63], and the synchronism between concentration and the wind speed is quite obvious. A small delay can also be seen. The minimum value of the concentration appears just after the maximum speed. It is quite easy to understand the inversely proportional relationship between concentration and wind speed, as shown in Fig. 2.49. Of course, the sand storm is the exception.

As China is located in the eastern coast of Eurasia with the mid or low latitude, the west wind is blocked by the Qinghai-Tibet Plateau and is disturbed by the monsoon. As a result, the northwest wind prevails in winter for most eastern areas from north of the Great Wall to the Hainan Island. The southwest monsoon prevails in the southwest part of China in winter. In spring, the wind changes from northerly winds to southerly winds. And in autumn, the monsoon direction is just opposite as that in spring.

As a result, in the eastern monsoon region, there are two prevailing wind directions. For example:

Shenyang: southerly wind 26 %; northerly wind 17 %
Beijing: northerly wind 26 %; southerly wind 15 %
Jinan: southwest wind 20 %; northeast wind 17 %
Wuhan: northerly wind 21 %; northeast wind 17 %; southeast wind 15 %
Nanjing: northeast wind 21 %; southeast wind 19 %
Guangzhou: northerly wind 17 %; east wind 16 %; southeast wind 14 %

Since there are two prevailing wind directions, in reality the concept is meaningless that pollution can be avoided at the weather side of the prevailing wind direction. The influence of the wind not only depends on the wind frequency, but also depends on the wind speed. When both the frequency and the wind speed are low, the pollution on the lee side may become larger. Therefore, the concept of pollution wind frequency is proposed [64], i.e.,

$$\text{Frequency of polluted wind} = \text{Frequency of directional prevailing wind} \times \frac{\text{Annual average air velocity}}{\text{Average air velocity of directional prevailing wind}}$$

or

$$\text{Frequency of polluted wind} = \text{Frequency of directional prevailing wind} \times \frac{2 \times \text{Annual average air velocity}}{\text{Average air velocity of directional prevailing wind} + \text{Annual average air velocity}}$$

For example, at Fengtai of Beijing, the north wind prevails in winter with wind frequency 17 %. In summer, the frequencies of southwest wind and south wind are 17 % and 14 %, respectively. The wind speed in summer is low. According to the calculation of pollution wind frequency, the southwest wind is the most important prevailing wind in the whole year. One thing to be mentioned here is that "prevailing wind direction" has been replaced by "dominant wind direction" at first and later by "wind frequency direction with the minimum pollution," according to the relevant national regulations.

The pollution wind frequency has important implications for the location of cleanroom. When there is only one main prevailing wind direction, it's better to place the cleanroom and clean area in the weather side of the prevailing wind direction. When there are two prevailing wind directions, they should be built

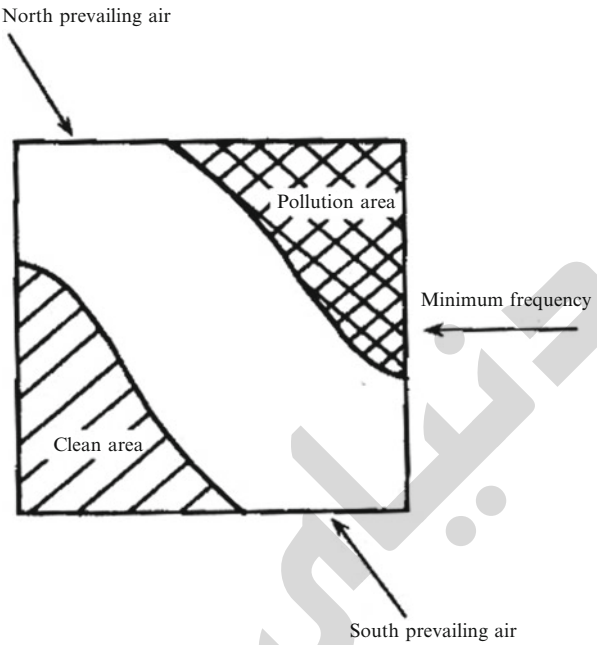

Fig. 2.50 Example I of determining the location for cleanroom with the pollution wind frequency

at one side. In Fig. 2.50, northerly wind is opposite compared with southerly wind. In this condition, cleanroom or clean area should be placed on either left down or right up of the general drawing. The middle is for the general area. The so-called pollution area includes the boiler chamber, the coal site, the building construction site, and the workshop emitting pollution. The so-called general area includes the general workshop and the working facility. Whether the clean area should be placed on left down or right up, the wind frequency on both left and right sides should also be further considered. If the wind frequency at the right side (pollution wind frequency) is the minimum, cleanroom should be placed on the left down corner, and the pollution area should be on the right up side.

In Fig. 2.51, the two prevailing wind directions are intersecting, so the cleanroom or clean area should be placed on the right.

About the pollution wind frequency, readers can refer to author's book "Application of Air Cleaning Technology" (China Building Industry Press, 1989).

2.6.2 Influence of Humidity [65]

2.6.2.1 Basic Process

At the beginning of this chapter, it has pointed out that generally the atmospheric dust contains both solid particles and liquid particles. Particles with diameter between 0.001 and 0.1 μm belong to the range of permanent atmospheric dust, but they are called specially as condensation nucleus.

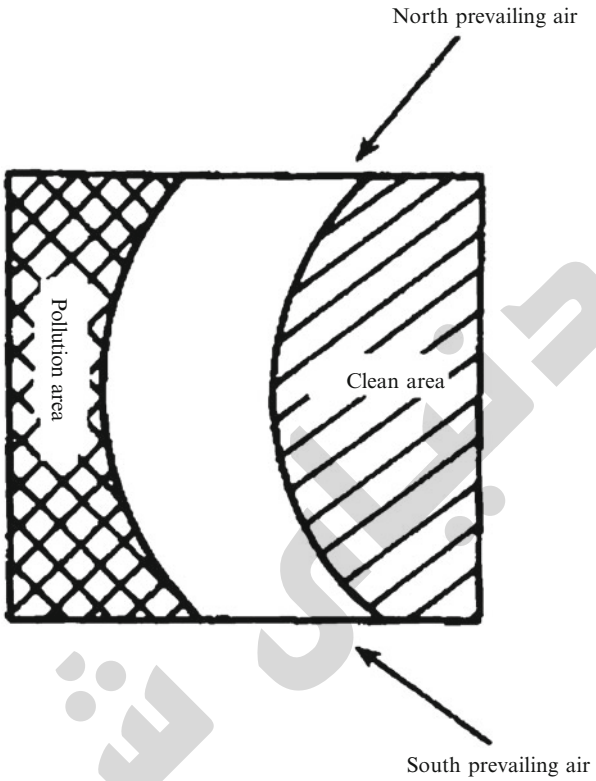

Fig. 2.51 Example II of determining the location for cleanroom with the pollution wind frequency

Condensation nucleus can be divided into two parts. One is easy to absorb water and can be easily dissolved by water, such as NaCl and sulfate, which belongs to soluble condensation nuclei. Another one is not dissolved by water but can be wetted by water like soil particle, ore particle, and soot particle, which are called hygroscopic condensation nuclei.

The generation amount of soluble condensation nuclei such as sulfate is mainly dependent on the amount of sulfuric acid mist formed by the reaction of moisture and SO_2. Therefore, the content of moisture in air, i.e., the absolute humidity, is the important factor for the generation amount of this kind of particles. Soluble condensation nuclei start to become solution after absorbing moisture, which enlarges itself gradually.

For non-soluble condensation nuclei, the process of water vapor condensation depends on the degree of supersaturation $\frac{E_{rm}-E}{E}$ (E_{rm} is the saturation vapor pressure of droplet; E is the saturation vapor pressure of air). When the condensation nuclei are large, the degree of supersaturation on surface needed for condensation is smaller, which means the allowable E is larger and the relative humidity of air can be smaller. On the contrary, with the larger relative humidity, the smaller condensation nuclei can still be wetted to large diameter.

So it is not complete if we hold the view that only relative humidity or absolute humidity is the factor influencing the atmospheric dust concentration. Absolute humidity mainly influences the moisture absorption of soluble condensation nucleus, while further dissolution and enlargement of condensation nucleus (the latter case includes insoluble condensation nucleus) mainly depend on relative humidity.

Someone once gave this idea [1] that when the relative humidity φ reaches 95 %, the radius of particle will be enlarged by 1.3 times, compared with the case $\varphi = 40$ %.

As the particle counter usually has a lower limit of the measurable radius, a large amount of unmeasurable particles will exceed the lower limit and enter to the range that can be measured when condensation nucleus becomes big as it absorbs water vapor. That makes not only the concentration of atmospheric dust count big, but also the proportion of small particles large. If light scattering optical particle counter or photoelectric turbidimeter is usually used to measure the concentration of atmospheric dust, we'll discover that the concentration, especially that of small particles, in the morning is much bigger than others. That is caused by the high humidity in the morning (of course the noise of water vapor molecules may cause overlying influence on the instrument). So do not be surprised when we meet this situation; concentration will reduce after the sunrise. But the concentration is still higher than that in other times.

The following is the specific measurement result.

Figure 2.52a is the measurement result from abroad [48], where the particle counter manufactured in the USA was used. In the figure, the black dot represents the measurement data with relative humidity below 80 %. It is shown with this kind of high relative humidity, most of the measurement data fall in the lower part of the chart, which means the proportion of particle number with diameter larger than 1 μm to that with diameter larger than 0.3 μm reduces. At this time, the number of small particles increases, while that of big particles reduces correspondingly. In summer from mould rainy days to the summit of summer, the humidity is high. The number of small particles measured is very large. Besides, since the humidity varies a lot, the particle size distribution is extremely unstable. This is the reason why the relative humidity limit is set in the fractional efficiency method with atmospheric dust in China, which is used to measure the efficiency of air filter (refer to Chap. 16).

Figure 2.52b illustrates the measurement data with domestic made particle counter, which has the same trend. But due to the lack of the data with small concentrations, it is not so obvious as the above picture.

2.6.2.2 Related Extent

Figures 2.53 and 2.54 show the example of variations of meteorological parameters, including particle counting concentration with atmospheric dust, the relative humidity, and the absolute humidity in "nonindustrial area or rural area" [59]. In the diagram, the ordinate is expressed with the water vapor partial pressure e with the unit mbar. In the range of normal temperature, 1 mbar = 0.75 mm of mercury.

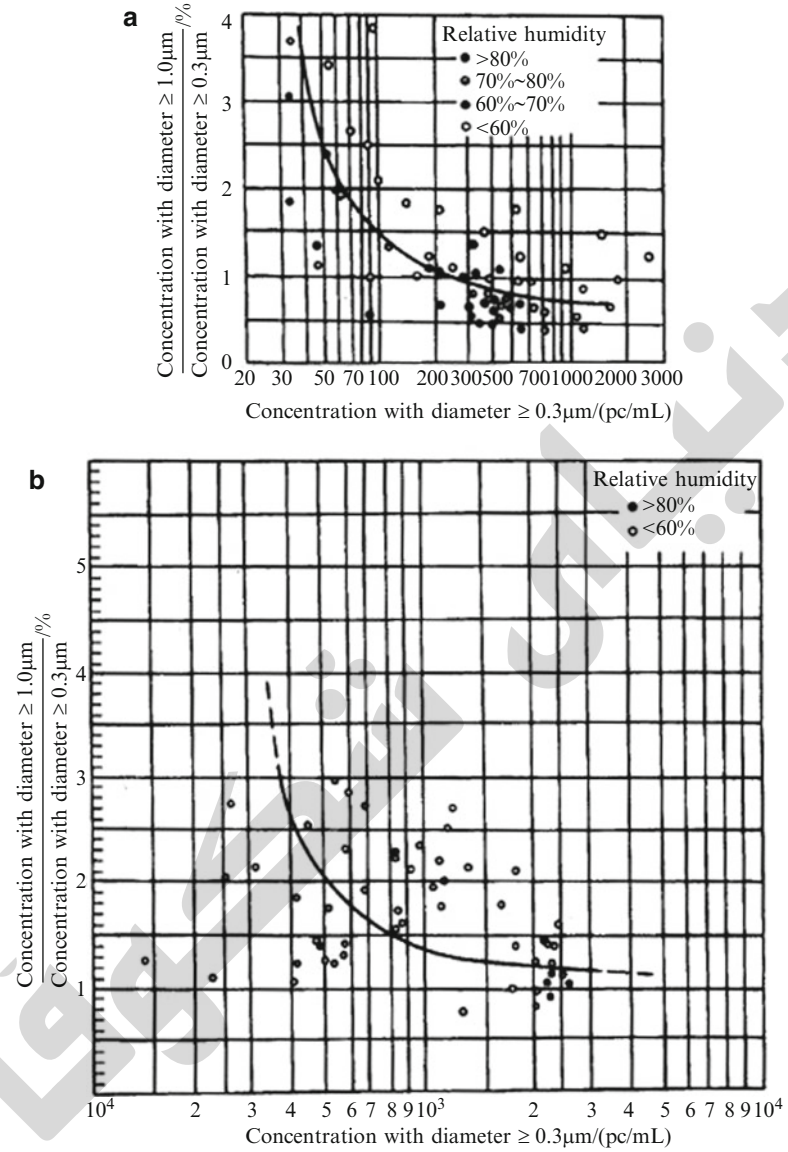

Fig. 2.52 Relationship between relative humidity and the proportion of small particles

From the chart, the variation trend of daily atmospheric dust concentration is basically the same as that of the relative humidity.

Both relative humidity and absolute humidity have influence on atmospheric dust concentration. But there is no solid proof to show which influence is more prominent. But according to the analysis of some measurement result, the relative humidity is

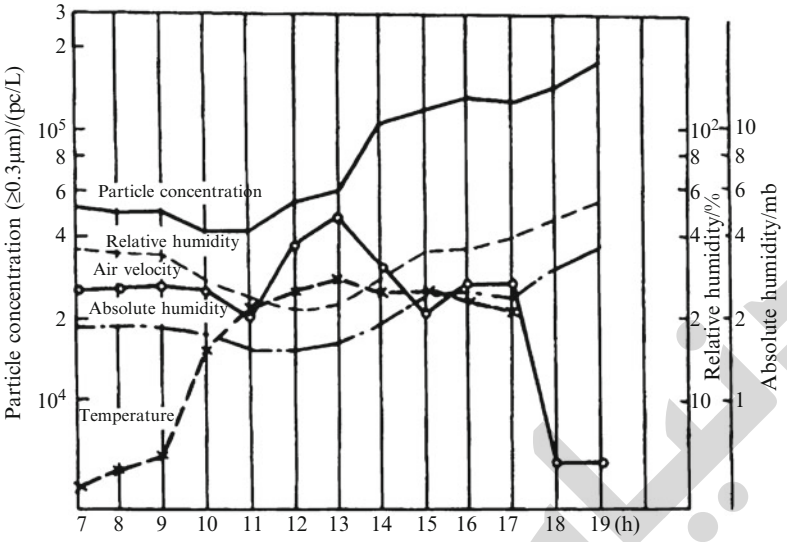

Fig. 2.53 Variation of atmospheric dust in one day at Xinglong of Hebei on March 15, 1980

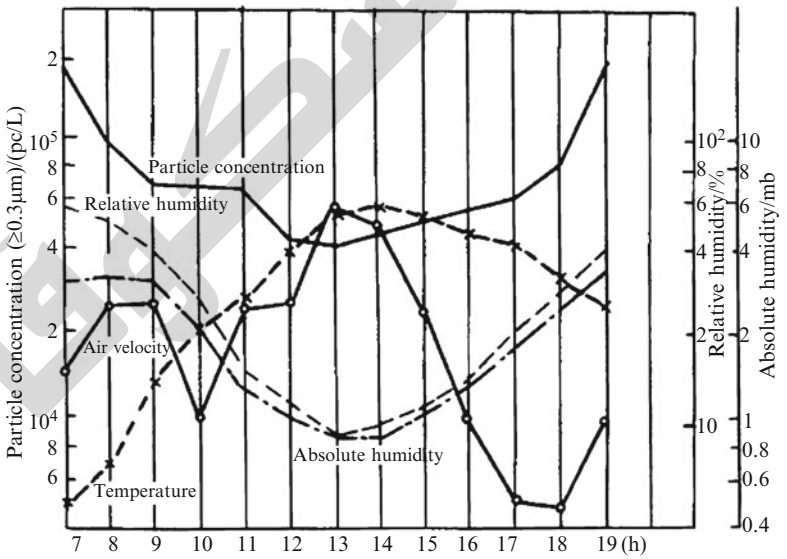

Fig. 2.54 Variation of atmospheric dust in one day at Xinglong of Hebei on March 16, 1980

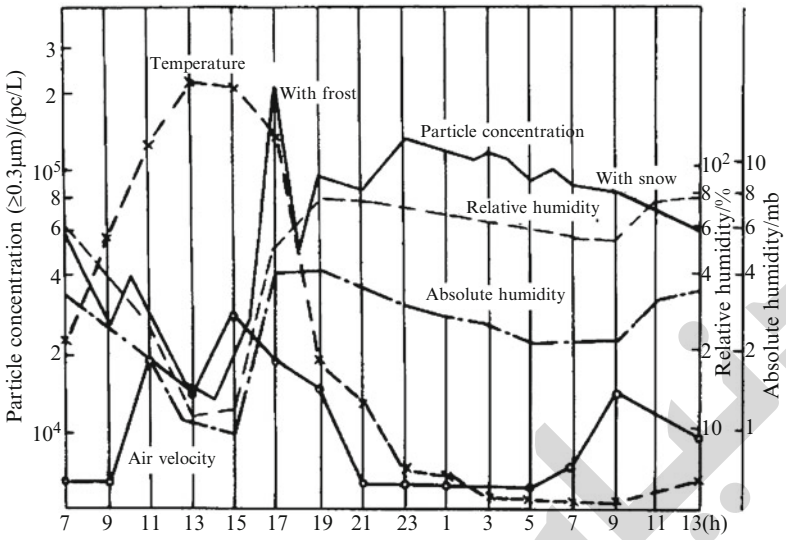

Fig. 2.55 Variation of atmospheric dust in one day at Xinglong of Hebei between March 17 and 18, 1980

thought to have more influence on the atmospheric dust concentration than the absolute humidity. This opinion is possible when the relative humidity has influence on the increase of the condensation nuclei according to the above analysis.

2.6.2.3 Daily Variation Model of Atmospheric Dust

It is really very complicated for the daily variation of atmospheric dust concentration. But the trend can be seen from Figs. 2.53, 2.54, and 2.55. The atmospheric dust concentration generally appears the crest in the morning (7–9 A.M.) and the afternoon (17–19 P.M.), while the trough appears at noon or afternoon.

Figures 2.56, 2.57, and 2.58 show the daily variation of atmospheric dust concentration for the "city type" and "suburban type." Due to the influence factors of urban atmospheric dust concentration are more complex, this can be also seen from these figures. The daily variation of atmospheric dust in city is more complex than that of the rural area. A few small peaks and small wave trough may occur in a day period. However, the peaks in the morning and evening and the troughs around noon are obvious. Figure 2.59 is one example of atmospheric dust concentration measured abroad [58]. The arrow is added by author during quote, where this trend is also shown. Relevant literatures with the trend are also presented, which will not be quoted here one by one.

Therefore, author puts forward a model that can be used to illustrate this trend. It is the W-type model conceived as in Fig. 2.60. The upper part of the figure is mainly

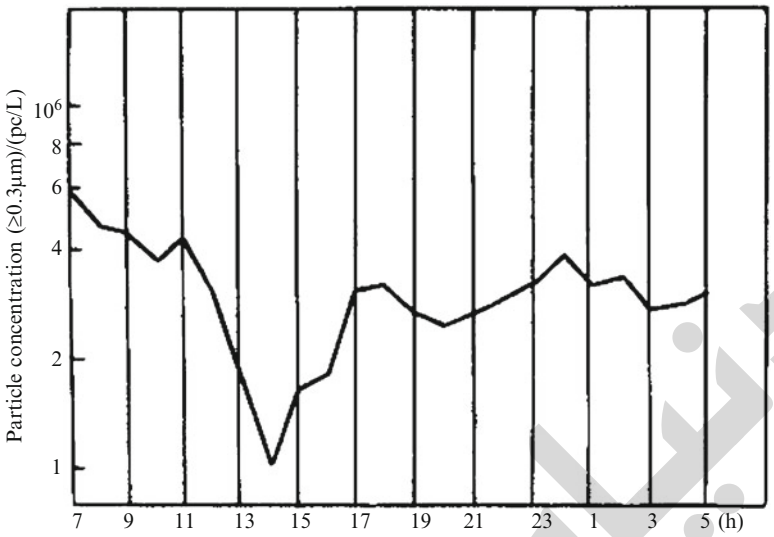

Fig. 2.56 Daily variation of atmospheric dust concentration under the iron tower at Deshengmen of Beijing between August 1 and 2, 1980

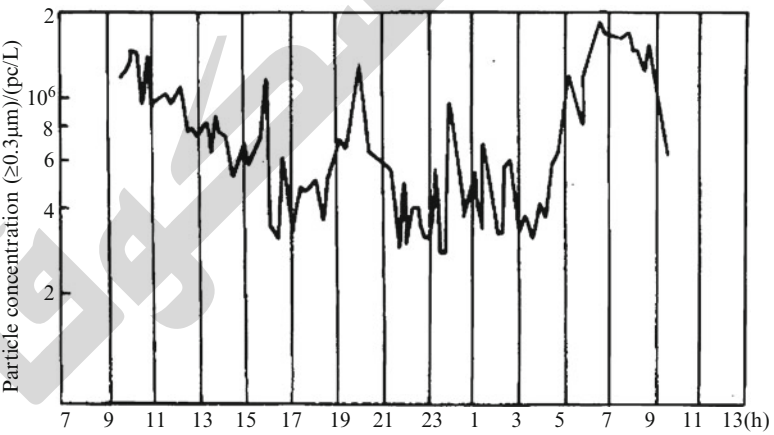

Fig. 2.57 Daily variation of atmospheric dust concentration in Shanghai on Dec. 24, 1975

influenced by the daily variation of humidity, while the lower part is also affected by other factors. The former is the "rural type," and the latter is the "city type." The reason to cause the daily variation of atmospheric dust concentration may be related to the influence factors for the trend of daily variation of the humidity and SO_2.

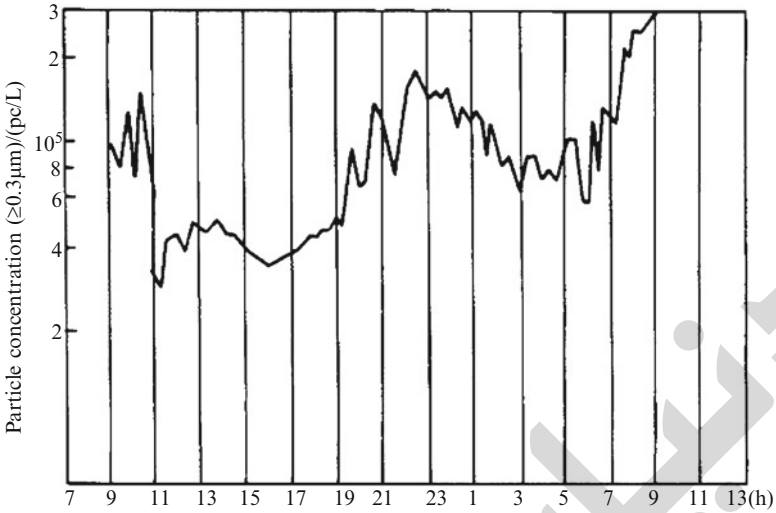

Fig. 2.58 Daily variation of atmospheric dust concentration in northwest region on April 20, 1976

Fig. 2.59 Example of daily variation of atmospheric dust concentration in Japan

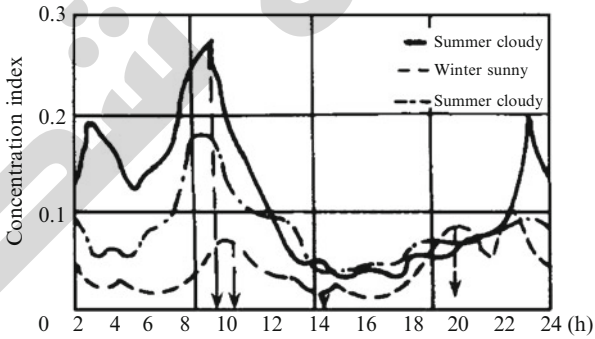

Several measurements have proved that the daily variation of these two parameters also has W type [66, 67].

The above model further needs some measurement proof, and Fig. 2.61 [56] is an example.

2.6.3 Influence of Afforestation

The afforest has a certain effect of reducing the atmospheric dust concentration. Table 2.38 is the comparison of atmospheric dust concentration in open space and afforest area [68].

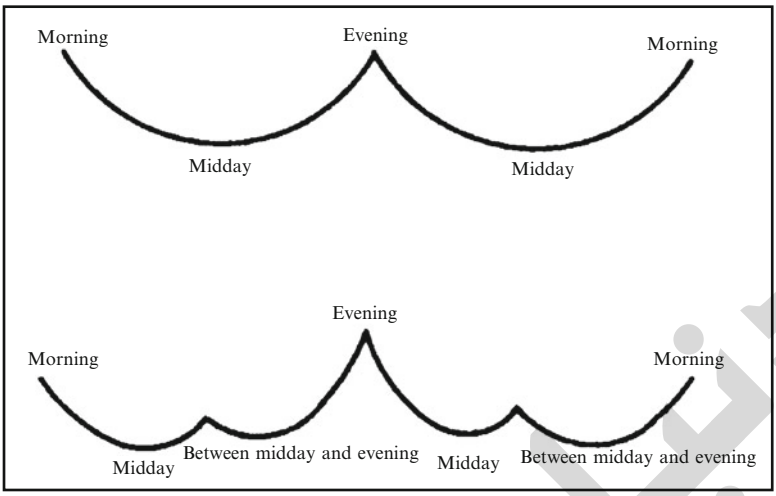

Fig. 2.60 W-type model of atmospheric dust concentration

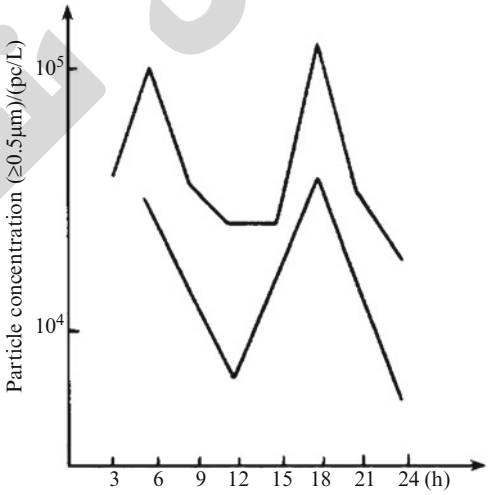

Fig. 2.61 Daily variation of atmospheric dust concentration in Harbin

According to research, when the tree has the following characteristics, the width of leaf is large, the leaf stretches flat and rigidly, the leaf is not easily swayed, the leaf surface is rough and full of fur, and the number of leaves is large, then this kind of tree is conducive to remove dust. For example, the sycamore has a high collection efficiency of dust, which has tall canopy, dense leaves, and large total leaf surface. Table 2.39 has listed the data of dust collection quantity by certain kinds of tree leaves.

Table 2.38 Comparison of atmospheric dust concentrations between open space and afforest area

Distance and direction from the pollution source	Greening states	The atmospheric dust concentration (mg/m^3)	Dust removal rate by greening (%)
Southeast 360 m (located at leeward direction during measurement)	Open space	1.5	53.3
	Under the sycamore forest (canopy density 0.9)	0.7	
Southwest 360 m (located at leeward direction during measurement)	Open space	2.7	37.1
	Behind of the Kalopanax tree	1.4	
East 250 m (located at leeward direction during measurement)	Open space	0.5	60
	Behind the sycamore forest (canopy density <0.9 with height 15 m and width 20 m)	0.2	

Table 2.39 Dust capture rate on certain types of tree leaves with unit area

Tree	Dust capture rate	Tree	Dust capture rate	Tree	Dust capture rate
Elm trees	12.27	*Paper mulberry*	5.87	Cherry tree	2.75
Hackberry	9.37	*Trident maple*	5.52	Wintersweet	2.42
Horizontal tree	8.13	Mulberry	5.39	Canada white cypress	2.06
Magnolia grandiflora	7.10	Oleander	5.28	Western catalpa	2.05
Bischofia polycarpa	6.81	*Euonymus maackii*	4.77	*Osmanthus*	2.02
Privet wood	6.63	*Crape myrtle*	4.42	*Pittosporum*	1.81
Big leaf cortex phellodendri	6.63	Sycamore	3.73	Gardenia tree	1.47
Robinia	6.37	Pomegranate	3.66	*Hydrangea* tree	0.63
Camphor tree	5.89	Maple	3.45		
Ailanthus tree	5.88	*Chinese sapium*	3.39		

2.7 Distribution of Atmospheric Microorganism

2.7.1 Concentration Distribution

To study the atmospheric microorganism, distributions of bacterium and fungus are mainly investigated, which should be measured by the classification sampler such as Anderson sampler. The classification characteristic of standard Anderson sampler is shown in Chap. 16.

There is some research showing that distributions of both bacterium and fungus have certain patterns. Figure 2.62 shows the concentration variation of atmospheric bacteria in the Xidan commercial district in Beijing. Figure 2.63 shows the concentration

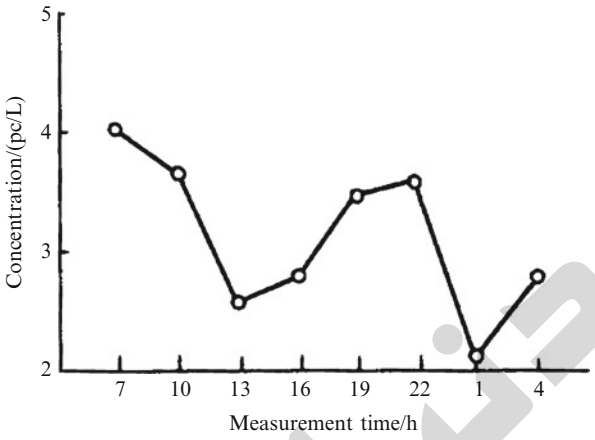

Fig. 2.62 Daily variation of atmospheric bacteria concentration in Xidan

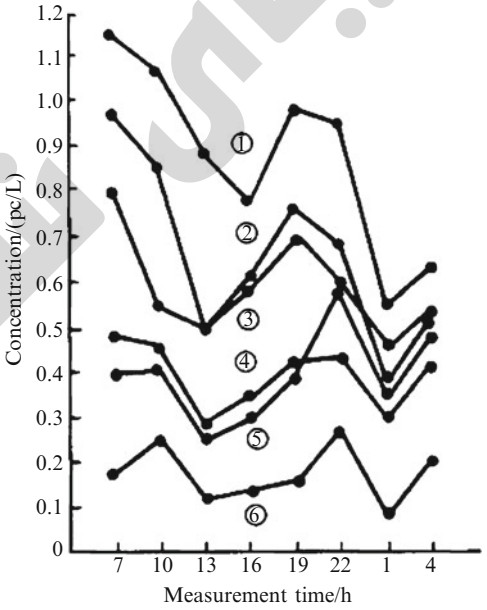

Fig. 2.63 Daily variation of atmospheric bacteria concentration with fractional size in Xidan. *1* the first class, *2* the second class, *3* the third class, *4* the fourth class, *5* the fifth class, *6* the sixth class

variation with fractional size. Figures 2.64 and 2.65 show the data in Fengtai, Beijing [69]. From these measurements, the following conclusions can be obtained:

1. There are two peaks and two wave troughs for the concentration of atmospheric bacteria and fungi within a day.
2. Two peaks appear at about 7:00 A.M. and 22:00 P.M. In the morning, one reason is that both the activity of people and vehicle on the road increases; the other reason is that the atmosphere near the ground is under the steady state with temperature inversion, and the velocity is small that causes the flow rate of

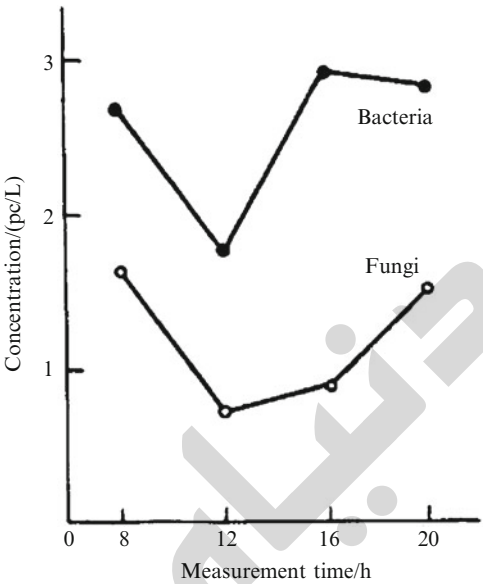

Fig. 2.64 Daily variation of atmospheric bacteria and fungi concentration in Fengtai.

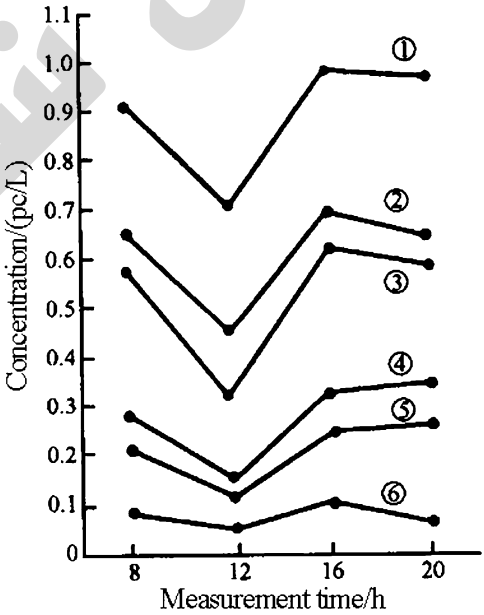

Fig. 2.65 Daily variation of atmospheric bacteria concentration with fractional size in Fengtai (the meanings for the labels from *1* to *6* are the same as that of Fig. 2.62)

atmosphere small, as well as the small radiation intensity. Both of these two reasons result in the first peak. At nightfall, the activity of people and vehicle on the road increases, while the radiation disappears; this has no effect of killing the generated microorganism. So the second peak is formed.

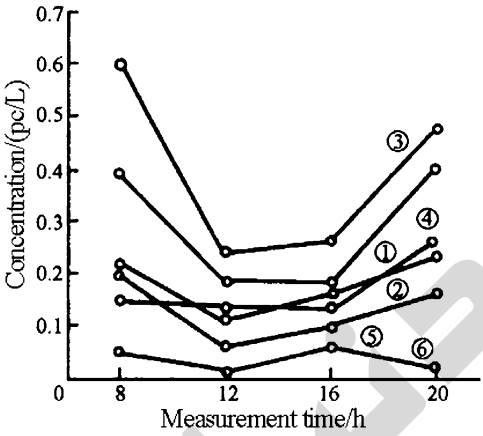

Fig. 2.66 Daily variation of atmospheric fungi concentration with fractional size in Fengtai (The meanings for the labels from *1* to *6* are the same as that of Fig. 2.63)

3. Two troughs appear at about 13:00 P.M. and 1:00 A.M. At noon, the air temperature increases gradually and the wind velocity increases. The steady state of atmosphere is destroyed. The atmospheric dust containing microorganism at the lower layer of atmosphere is taken away to the sky by the dispersion of vertical flow stream, and then diluted [69]. Another reason is that the sterilization effect by solar radiation increases. So the first trough is formed at 13:00 P.M. In the midnight, although there is no solar radiation, the generation amount of bacteria decreases sharply since all the activity on the ground reduces and it is close to be static. This is good for the deposition of big particles. So the second trough is formed.
4. The concentration of atmospheric bacteria is positively correlated with that of atmospheric dust.
5. Concentration is large for the season with the large sandy wind. For example, concentrations between March and May, as well as between September and November, are higher than that of other months in Beijing (Fig. 2.66).

2.7.2 Particle Size Distribution

Figure 2.67 shows the particle size distribution data of atmospheric bacteria and fungi in Xidan district of Beijing [70]. It is shown that the medium diameter of atmospheric bacteria in Xidan approaches the maximum value 8.1 μm at 13:00 P.M. and the minimum value 6.1 μm at 1:00 A.M. That of atmospheric fungi approaches the maximum value 4.5 μm at 13:00 P.M. and the minimum value 3.6 μm at 22:00 P.M. The variation patterns are opposite as that of concentration. It is obvious that the larger the particle size is, the more the deposition is, which will cause the concentration smaller. It should be noted that the particle diameter is not the naked diameter of bacteria, but the carrier diameter (refer to the equivalent diameter introduced in Chap. 9). The particles with larger diameter are likely to be killed by the ultraviolet ray exposure of solar radiation [71].

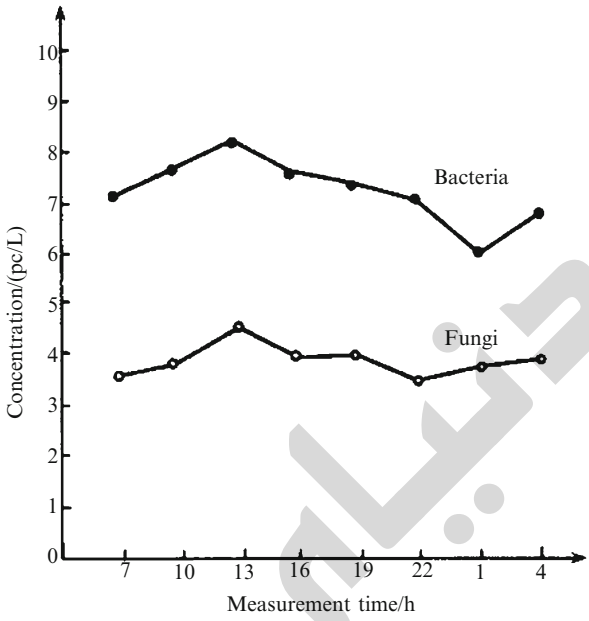

Fig. 2.67 Daily variation of atmospheric bacteria and fungi concentration in Xidan

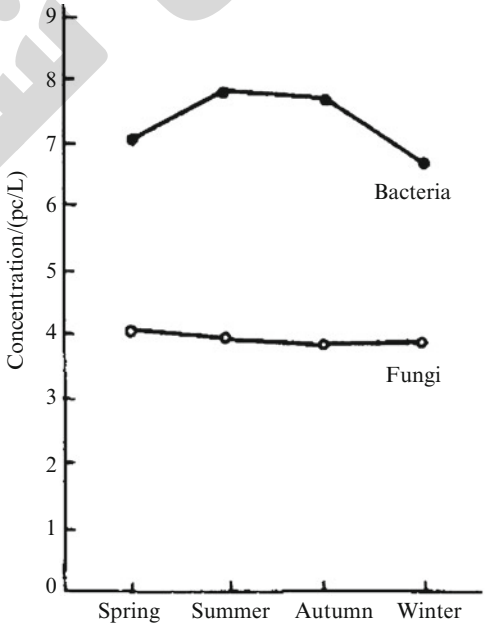

Fig. 2.68 Seasonal variation of atmospheric bacteria and fungi concentration in Xidan

From four season's point of view, the variation of particle diameter for atmospheric bacteria and fungi is small, as shown in Fig. 2.68 [70].

The similar trend is also reflected in the measurement results from other places [72].

References

1. Fett V (1961) Atmospheric dust. Publishing House of Foreign Literature, Moscow (In Russian)
2. Fuchs HA (1960) The mechanics of aerosols (trans: Gu Zhenchao). Science Press, Beijing (In Chinese)
3. Tsziri A (1973) Measurement method of weight and humidity for aerosol. J Jpn Air Clean Assoc 12(4):20–53 (In Japanese)
4. Harada A (1973) Background pollution of atmosphere, Technical reports of the Meteorological Research Institute, Japan (In Japanese)
5. Beijing Evening News (1998) p 15, 4 Apr 1998 (In Chinese)
6. Jin H, Ouyang N, Cheng ZF (1994) Environmental management and technology. China Environmental Science Press, Beijing, p 233 (In Chinese)
7. Jin H, Ouyang N, Cheng ZF (1994) Environmental management and technology. China Environmental Science Press, Beijing, p 190 (In Chinese)
8. UNEP (1993) Urban air pollution (continued). World Environ 2:29–34 (In Chinese)
9. Peng JX (2000) Review and inspiration of global environment and its development during the past century. In: China environment yearbook 2000. China Environmental Science Press, p 580 (In Chinese)
10. Editorial Board of "China Environment Yearbook" (2001) China environment yearbook. China Environmental Science Press, Beijing, p 524 (In Chinese)
11. Katsunori H (1975) Research on the generation of particles by photochemical reaction. J Jpn Air Clean Assoc 12(5):16–25 (In Japanese)
12. Katsunori H (1967) Measurement and monitoring of pollution structure and air cleanliness level indoors. Mag Build Equip 202:39 (In Japanese)
13. Ishibashi T, Nishiwaki J (1966) Department of Public hazard. Hygiene Engineering III (In Japanese)
14. Wang MX, Lv WX, Ren LX, Winchester JW (1981) Sampling and chemical analysis technology of atmospheric aerosol. Tech Equip Environ Pollut Control 2:1–10 (In Chinese)
15. Huang SQ, Kong FC, Jian JS, Xu GP, Luo JH, He RY (1981) Measurement of microelement in airborne particles by emission spectra. Tech Equip Environ Pollut Control 2:24–131 (In Chinese)
16. Zhou BB, Xu JL, Hu GY (1994) Characteristics of metal elements in the atmospheric Particulate of Shanghai. Shanghai Environ Sci 13(9):30 (In Chinese)
17. Ruzyllo J, Hattori T, Opila RL, Novak RE (1978) Cleaning technology in semiconductor device manufacturing. The Electrochemical Society, Inc., Translated by No. 10 Design Institute of the former Fourth Ministry of Machinery and Industry (In Chinese)
18. Control of environment, supply and material in the manufacturing process of integrated circuit (1973) Kejicankao Newspaper (semiconductor) 2 (In Chinese)
19. Zhu T, Bai ZP, Chen W (1995) Source analysis of air particulate in Qinhuangdao city. Res Environ Sci 8(5):49–55 (In Chinese)
20. Lv JM, Takeshi Y (1993) Performance of salt particles by air filter. J Jpn Air Clean Assoc 31 (1):12–19 (In Japanese)
21. Institute of Scientific and Technical Information of China (1973) Atmospheric pollution and control (No. 10 Survey of foreign hazardous matters) (In Chinese)
22. Saito Y (1972) Epidemiology of pollen. J Jpn Air Clean Assoc 9(8):7–14 (In Japanese)
23. Zai I (1975) State of the environment in high-rise buildings observed with the management method. J Jpn Air Clean Assoc 74:27–44 (In Japanese)
24. Katsunori H (1975) Recent development of the measurement method for indoor air pollution. J Jpn Air Clean Assoc 74:13–26 (In Japanese)
25. Motomura K (1976) Study on indoor air pollution. J Jpn Air Clean Assoc 14(4):23–31 (In Japanese)

26. Ishizuki J et al (1988) Statistical study of the atmospheric aerosol concentration as the design load for air cleaning device. Part I: In Tokyo area. Proceedings of the 7th air cleaning and pollution control conference. Japan Air Cleaning Association (In Japanese)
27. Wang SL, Chai FH, Yang TX (2002) Characteristics analysis of elements contained in air suspended particles with different sizes in Beijing. Res Environ Sci 15(4):10–12 (In Chinese)
28. Jiang HM, Wang DY (2001) Research development of inhalable particulate in atmosphere. Environ Sci Trend 1:11–14 (In Chinese)
29. Zhang WL, Xu DQ, Cui JS (2002) The characteristics and toxic mechanism of fine particle pollution (PM2.5) in air. Environ Monit China 18(1):59–62 (In Chinese)
30. Yang FMY, Ma YL, He KB (1991) Research profile of fine atmospheric particulate matter $PM_{2.5}$. World Environ 4:32–340
31. Zhou CY, Ye RQ, Tang GC (1991) Study of organic pollutants in aerosol and its distribution pattern. China Environ Sci 11(5):337–340 (In Chinese)
32. Editorial Board of "China Environment Yearbook" (2001) China environment yearbook. China Environmental Science Press, p 598 (In Chinese)
33. 1993 China environment yearbook. China Environmental Science Press (1993), p 522 (In Chinese)
34. 2005 China environment yearbook. China Environmental Science Press (2005), p 774 (In Chinese)
35. Ministry of Environmental Protection of the People's Republic of China (2011) 2006–2010 environmental report of China. China Environmental Science Press, Beijing, pp 10–35 (In Chinese)
36. Ministry of Environmental Protection of the People's Republic of China (2002) report on the state environment in China. Environ Protect 6:6 (In Chinese)
37. Wei FW, Teng EJ, Wu GP, Wu GP, Wilson WE, Chapman RS (2001) Concentration and elemental components of $PM_{2.5}$, PM10 in ambient air in four large Chinese cities. Environ Monit China 17(7):1–6 (In Chinese)
38. Xu ZL (1980) Particle counting concentration and particle size distribution of atmospheric dust in China 1(4): 20–23 (In Chinese)
39. Нонезов РТ, Знаменский РЕ (1973) Обеспыливание воздушной среди в "Чесмых комнатах". Водоснабжение и Санитарная Техника 3:29–32 (In Russian)
40. Fujisaki H (1971) Actual performance of cleaning device in precision processing factory. Jpn Air Cond Heat Refrig News 11(10):99–108 (In Japanese)
41. Hirasawa K (1973) Planning and design of cleanroom. Jpn Air Cond Heat Refrig News 13 (1):75–88 (In Japanese)
42. Kanai K (1971) Design and operation of cleanroom. J Jpn Air Clean Assoc 8(2):63–83 (In Japanese)
43. Cui L, Xu ZL, Wang R et al (2008) Particle number concentration of atmospheric particles in China. J HV&AC 38(7):1–5 (In Chinese)
44. Motomura K (1974) Measurement method of relative humidity for aerosol. J Jpn Air Clean Assoc 12(4):61–69 (In Japanese)
45. Austin PR, Timmerman SW (1965) Design and operation of clean rooms. Business News Publications, Detroit
46. Hirasawa K (1970) Impact of atmospheric pollution on industrial products and medicine and its countermeasures. Jpn Air Cond Heat Refrig News 10(2):33–40 (In Japanese)
47. Noda K (1970) Cleanroom for precision processing factory. Jpn Air Cond Heat Refrig News 10(10):64–75 (In Japanese)
48. Niitsu Y et al (1967) Study on property of atmospheric aerosol (the 2nd report). J SHASE Jpn 41(4):1–8 (In Japanese)
49. Reeves RG, Anson A, Landen D (1979) Manual of remote sensing, vol I: Theory, instruments and techniques (trans: Tang Dingyuan, Chen Ningqiang). National Defence Industry Press, Beijing (In Chinese)

50. Hinds WC (1989) Aerosol technology: properties, behavior, and measurement of airborne particles (trans: Sun Yufeng, Chapter 14). Heilongjiang Science and Technology Press, Harbin (In Chinese)
51. Kratzer PA (1963) Climate of city (trans: Xie Kekuan). China Industrial Press, Beijing (In Chinese)
52. Fukuyama H (1975) Airborne matter- nature and role. J SHASE Jpn 49(8):57–60 (In Japanese)
53. Junge CE (1953) Die Rolle der Aerosole und der Gasformigen Beimengungen der Luft im Sprenstoffhaushalt der Troposphare, Tellus 1953, 5(1) (cited from Aerosol Handbook, translated by Zhou Jinqin, 1981) (In Chinese)
54. Whitby KT, Liu BYH (1969) Atmospheric aerosol size distributions. Preprint of P,T.S., pp 36–46
55. You RG, Hong ZX, Lv WX et al (1983) Spatial distribution variation of atmospheric aerosol concentration and scale in boundary layer. Chin J Atmos Sci 7(1):88–94 (In Chinese)
56. Wei XM (1987) Analysis of the variation of atmospheric dust. Contam Control Air Condit Technol 3:7–8 (In Chinese)
57. Cui L, Xu ZL, Wang R et al (2008) Characteristic of atmospheric particles in China. J HV&AC 38(5):10–12 (In Chinese)
58. Dorman RG (1974) Dust control and air cleaning. Pergamon Press, Oxford
59. Oono C (1972) Duct collation technology, pollution control measures and technological development. Extra Edition of PPM 7:106–142 (In Japanese)
60. Miyu S et al (1972) Measurement of particle size distribution and density for pollen and spores. J Soc Powder Technol 9(2):102–104 (In Japanese)
61. Uchiyama M (1972) Investigation result on the design and construction of cleanroom. J SHASE Jpn 46(4):19–25 (In Japanese)
62. Senuma I (1960) Variation of airborne particle in outdoor air and its influence on indoor environment. Proc Jpn Build Inst 64:79–85 (In Japanese)
63. Niitsu Y, Yoshikawa S, Tomita H (1966) Study on property of atmospheric aerosol (the 1st report). J SHASE Jpn 40(11):1–13 (In Japanese)
64. Urban geography group at Department of Geology and Geography (1974) Beijing University, Wind and Urban Planning. Environmental Protection 2:16–23 (In Chinese)
65. Xu ZL, Wu ZW (1982) Influence of humidity on particle counting concentration of atmospheric particles. China Environ Sci 6:59–65 (In Chinese)
66. Liu WJ, Zhao GZ (1981) Meteorological field structure and atmospheric concentration in Shenyang. Environ Sci 2(2):26–31 (In Chinese)
67. Wang SF (1981) Mode for air pollution evaluation in suburb of Beijing. China Environ Sci 1:46–53 (In Chinese)
68. Institute of Botany at Jiangsu Province (1978) Effect of air purification with urban greening. Environ Sci 6:49–51 (In Chinese)
69. Hu QX et al (1989) Atmospheric microorganism concentration in Beijing and Tianjin areas. Environ Sci 10(5):31–35 (In Chinese)
70. Hu QX et al (1992) Particle size of atmospheric microorganism in Beijing. China Environ Sci 12(4):296–299 (In Chinese)
71. Che FX (1985) Effect of solar radiation on killing the airborne microbe. Disinfect Steriliz 2 (2):101–105 (In Chinese)
72. Hu QX et al (1994) Study of atmospheric microorganism–median diameter and particle size distribution of atmospheric bacteria 10(6):37–38 (In Chinese)

Chapter 3
Filtration Mechanism of Fine Particle

There are usually four kinds of methods available to separate solids or liquid particles from an aerosol:

1. Mechanical type – gravity dust collector, impinger, and cyclone
2. Electrostatic force – single-stage electrostatic precipitator, double-stage electrostatic precipitator, etc.
3. Washing – spray scrubber, water film precipitator, Venturi dust collector, etc.
4. Filtration – filling-in filter, bag filter, etc.

In the field of air cleaning, the particle concentration is typically very low compared with industrial dust separation applications, and the particle size is small. Hence the reliability of the performance of filters must be assured. Therefore, filtration and separation techniques are often used to remove particles in the airstream and are the focus of this chapter.

3.1 Filtration and Separation

Air filters remove particulate matter via several mechanisms including interception, impaction, and diffusion. According to the position of the capture particles, particulate air filters may be divided into two types: (1) surface filter and (2) depth filter.

Surface filters have many forms including metal wire mesh and perforated plate, where particles are captured on the surface. Chemical porous membrane is made from fibrous ester (nitrocellulose or cellulose acetate), which looks like a piece of white paper, and its characteristic follows that of a surface filter. The thickness of this kind of membrane filtration medium is approximately 50 μm. Circular pores with diameter 0.1–10 μm are uniformly distributed on it; the pore size is controlled during the membrane manufacture process. The average number of pores is about 10^7–10^8 #/cm^2, and the porosity can be as high as 70–80 %. For theoretical purposes the pores are often treated as capillaries. Particles larger than the pore diameter are captured on the surface and the filtration efficiency could be 100 %. It is believed

Z. Xu, *Fundamentals of Air Cleaning Technology and Its Application in Cleanrooms*,
DOI 10.1007/978-3-642-39374-7_3, © Springer-Verlag Berlin Heidelberg 2014

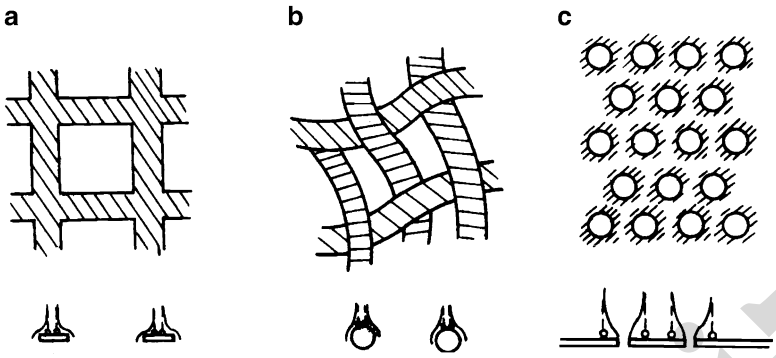

Fig. 3.1 Surface air filters (**a**) Single ribbon model (plate); (**b**) Isolated cylinder model (metal wire mesh); (**c**) Small pore model (perforated plate)

that the minimum size of particles captured by the membrane could be 1/10 to 1/15 of average pore diameter. Figure 3.1 shows the structure of a surface air filter and the schematic of particle capture.

Depth filters can be divided into two with high and low solid fractions (also called low porosity and high porosity). Particles are captured on the surface or inside the medium layer.

The solid fraction α can be expressed as:

$$\alpha = \frac{\text{filter medium density(such as fibrous layer)}}{\text{filter medium material density(such as fiber)}}$$

Depth filters with a high solid fraction ($\alpha > 0.2$) have various forms, such as granular filling layer (gravel layer, activated carbon layer, etc.), porous filter media and thick filter paper. Their structure and a schematic of the particle capture process are shown in Fig. 3.2.

Depth filters with low solid fraction ($\alpha < 0.2$) occur as fibrous filters, high-efficiency air filters with a thin paper medium and foamed material filter, etc. Their structure, together with a schematic of particle capture process, is illustrated in Fig. 3.3.

Although the particle capture mechanism of a surface filter is simple, most of these filters have low efficiency and so are of little practical use. On the contrary, microporous membranes have an extremely high efficiency. With the exception of liquid filtration, they are mainly used for sampling and the final filter for dust-free and aseptic systems where the cleanliness requirement is very high. Moreover, they are more reliable than fibrous filters.

Depth filters, with high solid fraction, have a very complex internal capillary structure, and thus the particle capture mechanism is extremely complex. To date few have performed a theoretical study.

Depth filters, with a low solid fraction, such as fibrous filter (including fiber-filled layer filter, nonwoven filter, and HEPA filters), also have a complex internal fiber distribution. However, since the porosity is large (shown in Figs. 3.4, 3.5, and 3.6),

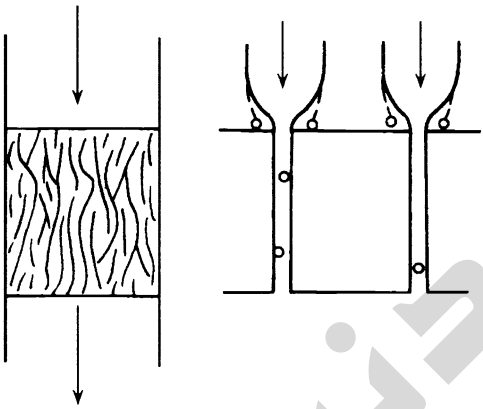

Fig. 3.2 Depth filter with high solid fraction (capillary model)

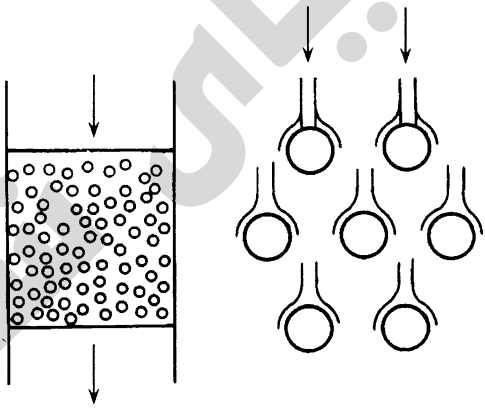

Fig. 3.3 Depth filter with low solid fraction (isolated cylinder model)

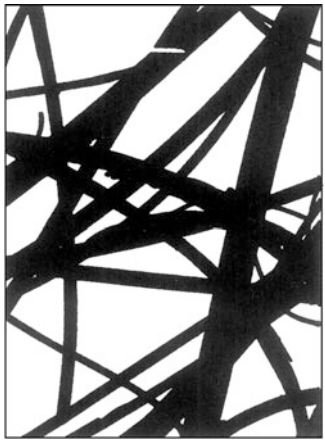

Fig. 3.4 Structure of domestic-made glass fiber filter ($\eta = 99.99999$ % with amplification ratio 10,000)

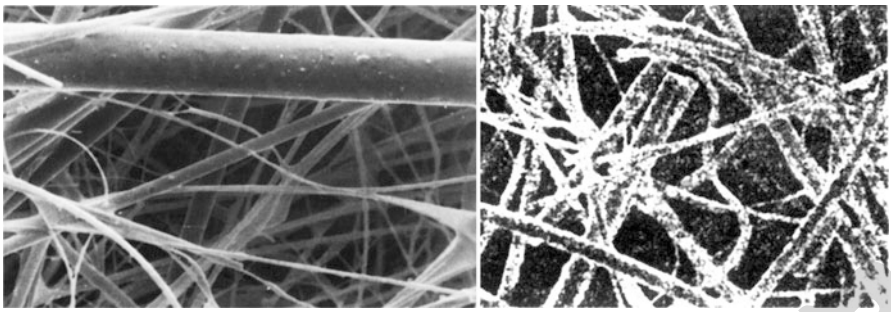

Fig. 3.5 Stereo of fibers from foreign air filter paper made by glass fiber [1, 2]

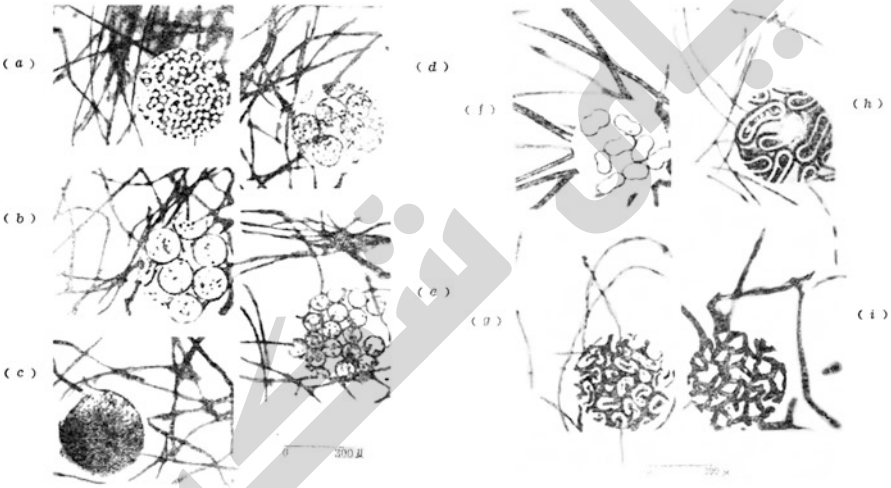

Fig. 3.6 Structure of foreign fibrous media [3] (**a**) glass fiber $\rho = 2.55$ g/cm^3; (**b**) nylon $\rho = 1.14$ g/cm^3; (**c**) polypropylene $\rho = 0.97$ g/cm^3; (**d**) Tacryl fiber $\rho = 1.17$ g/cm^3; (**e**) esterified fiber $\rho = 1.38$ g/cm^3; (**f**) chlorinated alvar $\rho = 1.39$ g/cm^3; (**g**) cotton fiber $\rho = 1.54$ g/cm^3; (**h**) vinylon $\rho = 1.3$ g/cm^3; (**i**) cellulose acetate $\rho = 1.32$ g/cm^3

the interspace is smaller than what is shown in these figures when hundreds of fibrous layers overlap each other. In order to simplify the study, a single fiber of a filter layer is often treated in isolation. The pressure drop of this type of filter is not high, but its efficiency is high, and so has practical significance, especially in the field of air cleaning technology. For investigating the filtration mechanism, a much deeper theory and experimental verification is required. This chapter introduces the particle filtration mechanisms for fibrous filters, while the next chapter will discuss the particle capture mechanism of the electrostatic precipitator.

3.2 Fundamental Filtration Process of Air Filters

The characteristic of captured particle and filter material, as well as their interactions, has extremely important influence on the filtration process. Most researchers are inclined to formulate the filtration process as two stages.

The first stage is called the steady stage, where particle capture efficiency and pressure drop of air filters do not change with time; instead they are determined by the intrinsic geometry of filters, property of particles, and feature of airstream. In this stage, the change of filter thickness is small because of particle deposition. For the case of airstream with low concentration of particles such as indoor air filtration in air cleaning technology, this stage is important for air filters.

The second stage is called nonsteady stage, where the particle capture efficiency and pressure drop change with time and they depend not only on particle property but also on the influence of particle deposition, gas erosion, water vapor, etc. Although this stage is longer than that of the first stage, and it has the decisive significance to the general industrial filters, to some extend it is only meaningful to the filters with efficiency lower than sub-HEPA filters in air cleaning technology, and it is not meaningful to filters with efficiency equal with and higher than sub-HEPA filters.

3.3 Filtration Mechanism of Fibrous Air Filters

It is already known that there are at least five kinds of mechanism, instead of one mechanism, that play roles in the particle capture process during the first stage of air filtration for fibrous filters.

3.3.1 Interception (or Contact/Hook) Effect

Inside the fibrous layer, fibers are located randomly and form numerous meshes. When particles with certain size approach fiber surface when following the streamline, suppose the distance between the streamline (also the centerline of particle) and fiber surface is equal to or smaller than particle radius (shown in Fig. 3.7, $r_1 \leq r_f + r_p$), particles will be intercepted and then deposited on the fiber surface, which is called interception effect. Sieve effect also belongs to the interception effect (shown in Fig. 3.8), and sometimes the interception effect is called filtration effect.

However, interception effect or sieve effect is not the only one or main effect in particle filtration of fibrous filters, so fibrous filters could not be considered as a sieve. Sieve only removes particles whose diameter is larger than the hole, while for

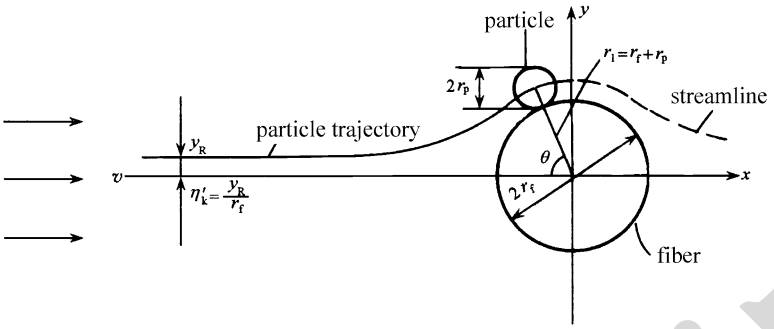

Fig. 3.7 Schematic of interception effect

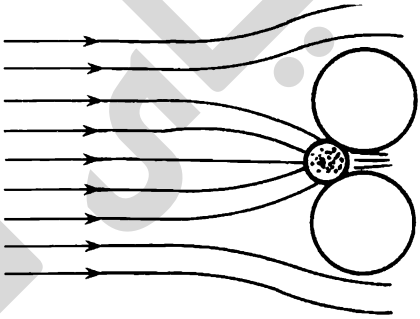

Fig. 3.8 Schematic of sieve effect or filtration effect as one of interception effects

fibrous air filters, not all the particles whose diameter is smaller than mesh size could penetrate, and the most penetrating particle size is located in some range. Particles are not all removed by the surface of fiber layer – deposition. Otherwise, the pressure drop of air filters will increase rapidly when the mesh holes are blocked by particles, which is not true. In fibrous filters, particles will go deeply through fibrous layers, so there are other mechanisms for particle capture process.

3.3.2 Inertial Effect

Because of the complex arrangement of fibers, streamline will change directions frequently and abruptly when air flows through fibrous layers. When the particle mass is large or its velocity (which could be approximated by air velocity) is large, by virtue of its inertia, particle will not follow the streamline when air flows around fibers. Therefore, particles will deviate from the streamline when approaching fibers, then collide with fibers and deposit on it (shown in Fig. 3.9, position A).

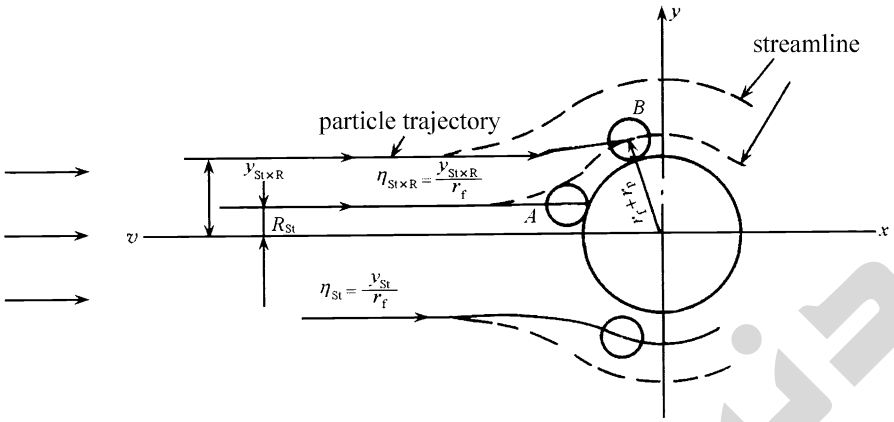

Fig. 3.9 Inertial effect (*A*) and inertial interception effect (*B*)

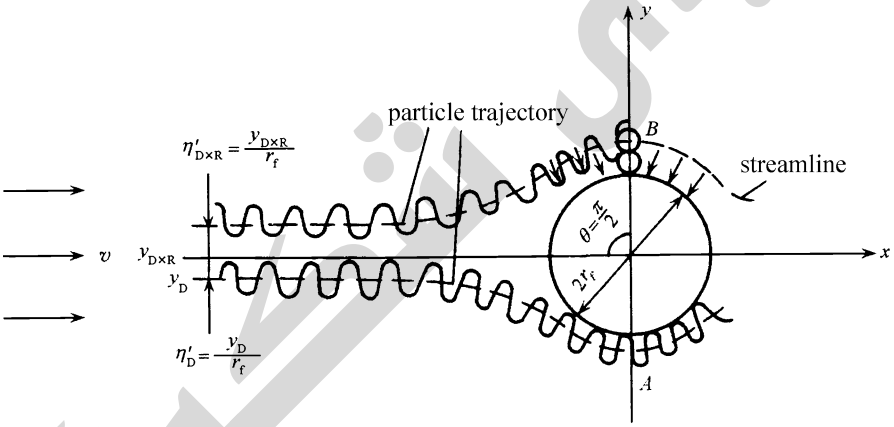

Fig. 3.10 Diffusion effect (*A*) and diffusion interception effect (*B*)

3.3.3 Diffusion Effect

It is much obvious for small particles that show Brownian motion caused by the collision between gas molecules and particles. At normal temperature, the diffusion distance could be 17 μm/s for 0.1 μm particles, which is several times or even dozens of interspace distance between fibers. This results in the larger possibility of particle deposition onto fiber surface (as position A shown in Fig. 3.10). However, the Brownian effect is weaker for particles with diameter larger than 0.3 μm. In this case, particles will not deviate from the streamline and deposit onto fiber surface only by this effect.

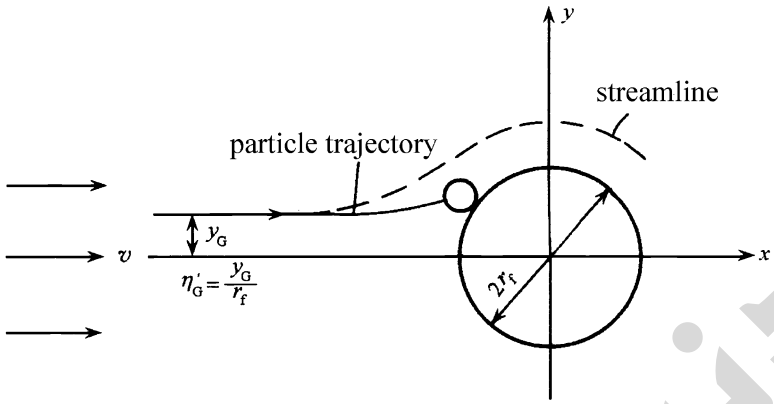

Fig. 3.11 Gravitational effect (gravity is parallel to airstream)

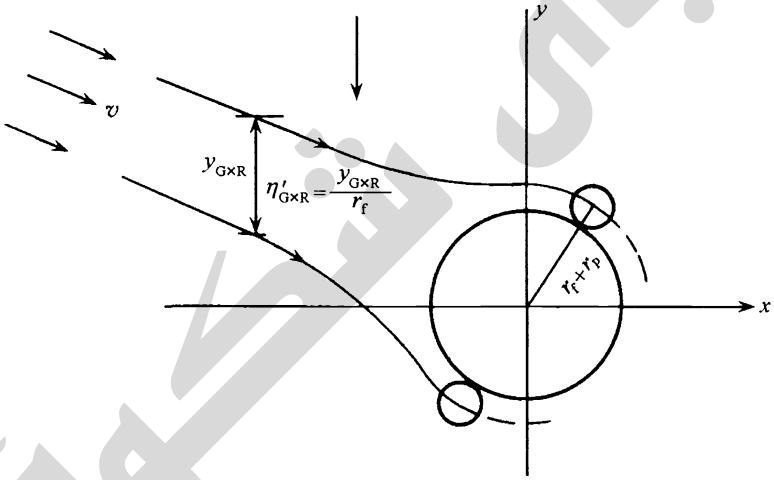

Fig. 3.12 Gravitational interception effect (gravity is perpendicular with airstream)

3.3.4 Gravitational Effect

Particles will deviate from the streamline under the influence of gravity when they pass through fibrous layers, which means they will deposit on fiber surface by gravitational deposition (shown in Figs. 3.11 and 3.12). The time usage for airflows through fibrous air filters, especially paper filters, is far less than 1 s, so particles with diameter smaller than 0.5 μm will pass through fibrous layers without deposition on fiber surfaces. Therefore, it is reasonable to ignore the effect of gravitational deposition.

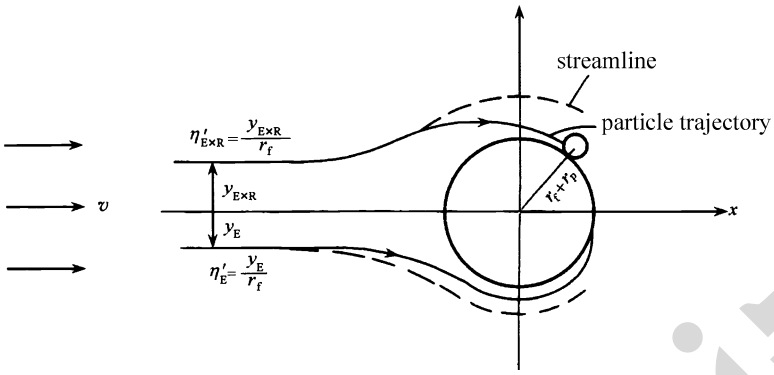

Fig. 3.13 Electrostatic effect and electrostatic interception effect

3.3.5 Electrostatic Effect

By various reasons, charge may exist on both fibers and particles, which will cause electrostatic effect and attract particles (shown in Fig. 3.13). Except for the case of intentional charge on fibers or particles, both fiber charges by friction during the manufacture process and particle charge by charge induction will not exist for a long time. The induced electric field is very weak, and the resulting attractive force is very small. So this kind of electrostatic effect can be neglected.

For the process of particle capture in fibrous filters, all the mechanism or maybe one or some mechanism will take effect, which depends on the particle size, density, fiber thickness, solid fraction, and air velocity.

3.4 Procedures to Calculate Efficiency of Fibrous Air Filters

Although the abovementioned effects exist in the process of particle capture inside the fibrous air filters, it is quite difficult to make description using refined mathematical expressions. Semiempirical formula is obtained based on the reliable experimental data and simplified model. Results from these formulas do not match the experiment completely. So the purpose of performing calculation is to make analysis and comparison qualitatively, not to obtain the accurate data.

For the calculation of fibrous filters with low solid fraction, the theoretical basis is still the isolated cylinder method, which was put forward by Langmuir and had the following assumptions:

1. Filters are made of uniformly distributed isolated circular fibers with the same material.
2. Fibers are perpendicular to the airflow, and they are far enough from each other.
3. Particles are spherical.

4. Filter surface is clean, so only the efficiency of the first stage is considered.
5. Particles attached to the fiber surface will not resuspend.

Based on the theory of isolated fiber, Fuchs et al. developed it theoretically [5]. In the field of HEPA filter, Iinoya et al. performed experimental study. Based on these researches, the following procedures calculate the efficiency of fibrous filters:

1. Determine the main mechanisms among these five effects according to the particle characteristic, filter performance, and condition (usually only the effects of interception, inertia, and diffusion are considered).
2. Determine the individual efficiency η' of corresponding mechanism for isolated single fiber.
3. Determine the total efficiency η_Σ of the combined mechanisms for isolated single fiber.
4. Determine the total efficiency η_Σ of the combined mechanisms for single fiber (not isolated) inside the filter, when the interference influence of adjacent fibers is considered.
5. Determine the total efficiency η of filter from the value of η_Σ according to the lognormal penetration law.

3.5 Particle Capture Efficiency of Isolated Single Fiber: Isolated Cylinder Method

3.5.1 Interception Efficiency

Figure 3.7 illustrates that interception is caused by geometrical effect, which means the particle's capture by direct interception or contact. Since fiber is considered as circular cylinder (as shown in Fig. 3.6, fibers inside glass fibrous filters are regularly circular cylinders), particles will be captured onto these fibers which face towards the incoming airflow stream and all the particles within the airstream with the width d_f (fiber diameter) shown in part (a) of Fig. 3.14. When all these particles are captured, the efficiency is 100 %. But before arriving at the fiber surface, air will flow around the fiber. So particles in the range between $y = r_f$ and $y_1 = r_p + r_f$ are likely to be captured which is shown in part (b) of Fig. 3.14. Here r_p and r_f represent the particle radius and fiber radius, respectively. And y means the distance between any position inside the flow and the cylinder axis.

The width of the airflow is r_p, which is smaller than the width of the previous flow that fiber faces. So the interception efficiency is a probability with the value less than 1, and it equals with the ratio between the particle number per unit time in the range of r_p for a fiber with unit length and the total particle number that flows towards the fiber. When it is assumed uniform for particle concentration, it also equals with the flow rate ratio.

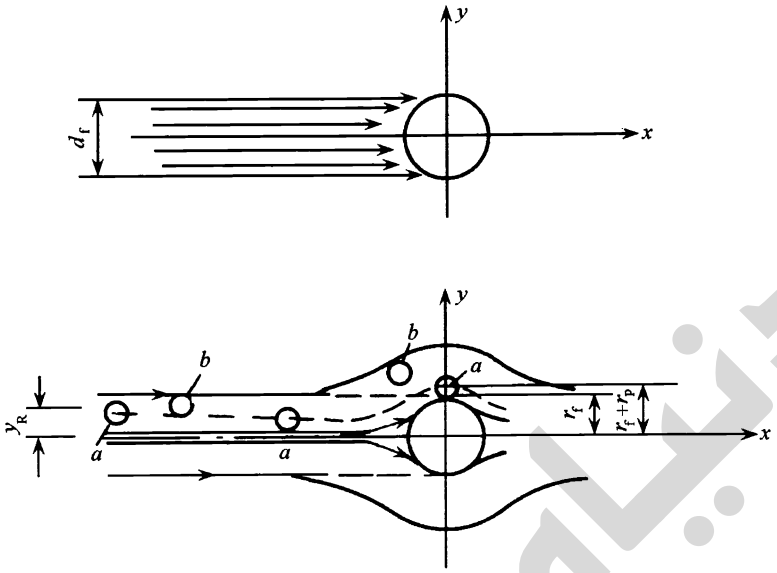

Fig. 3.14 Particle range by interception capture

For a fiber with unit length, the flow rate that passes through the fiber is $r_f v$, the multiplication of fiber radius and air velocity at the far distance. All the captured particles are within the flow between r_f and $r_f + r_p$. The corresponding flow rate can be expressed as $\int_{r_f}^{r_f+r_p} v_{\frac{\pi}{2}} dy$

$$\eta'_R = \frac{\int_{r_f}^{r_f+r_p} v_{\frac{\pi}{2}} dy}{r_f v} \tag{3.1}$$

Since $\frac{\int_{r_f}^{r_f+r_p} v_{\frac{\pi}{2}} dy}{v} = y_R$, it could also be rewritten as

$$\eta'_R = \frac{W_R}{r_f v} = \frac{y_R}{r_f} \tag{3.2}$$

where y_R is the distance between the fiber axis and the effective particle trajectory at the infinite, where particles within this range can be captured due to the interception effect at infinite distance. In practice, the distance far enough is considered as the situation at infinite.

W_R is the flow rate within the width of y_R.

Therefore the particle capture efficiency under certain effect is defined as the ratio between the width of the effective particle trajectory for particle capture and fiber radius.

In fluid dynamics, the velocity distribution around the circular cylinder for the common viscous flow and $Re < 1$ is expressed as [4]:

$$v_y = \frac{v\cos\theta}{2(2-\ln Re)}\left(1-\frac{r_f^2}{y^2}-2\ln\frac{y}{r_f}\right)$$

$$v_\theta = \frac{v\sin\theta}{2(2-\ln Re)}\left(1-\frac{r_f^2}{y^2}+2\ln\frac{y}{r_f}\right)$$

where

v_y and v_θ are radial velocity and tangential velocity near the cylinder, respectively;
v is the velocity at infinite for $\theta = 0$ or $\theta = \pi$;
θ is the angle between radius and horizontal axis;
Re is the particle Reynolds number.

Attention should be paid to the definition of Re number. In the study of air flow, the flow Reynolds number is applied. While in the study of particles, the particle Reynolds number should be used:

$$Re = \frac{\rho v d}{\mu}$$

where both the density ρ and air viscous coefficient μ are used for gas and v and d are determined according to the study object. For the airflow, v is the air velocity, and d is the characteristic size. In the study of airflow inside the pipeline, d is the pipe diameter. For the particles, v is the relative velocity between particles and air, which is the settling velocity of particles, and d is the particle diameter. For the airflow, it is laminar flow for $Re < 2{,}000$ and turbulent flow for $Re > 4{,}000$. For the particles, the flow around the particle is laminar for $Re \leq 1$, while vortex appears downstream of particles for $Re \geq 2$. The number and strength of vertex increase with the increase of Re, which means particles are gradually surrounded by turbulent flow.

The tangential velocity at $\theta = \pi/2$ is:

$$v_{\theta=\frac{\pi}{2}} = \frac{v}{2(2-\ln Re)}\left(1-\frac{r_f^2}{y^2}+2\ln\frac{y}{r_f}\right)$$

Therefore

$$\int_{r_f}^{r_f+r_p} v_{\frac{\pi}{2}}\mathrm{d}y = \frac{v_{rf}}{2(2-\ln Re)}\left[2\left(1+\frac{r_p}{r_f}\right)\ln\left(1+\frac{r_p}{r_f}\right)-\left(1+\frac{r_p}{r_f}\right)+\frac{1}{1+\frac{r_p}{r_f}}\right]$$

$$\eta'_R = \frac{1}{2(2-\ln Re)}\left[2(1+R)\ln(1+R)-(1+R)+\frac{1}{1+R}\right] \tag{3.3}$$

The expression shows that the interception efficiency is a function of Re and $R = r_p/r_f$. R is the interception parameter, and it is used to describe the sedimentation effect under the effect of interception mechanism.

Furthermore, Norio and Iinoya [7] obtained the approximate expression for the velocity distribution inside the boundary layer near cylinder as follows:

$$\eta'_R = \frac{1}{3} R e^{\frac{1}{2}} R^2 \tag{3.4}$$

3.5.2 Inertial Efficiency

Based on the similar definition of Eq. (3.2) and Fig. 3.7, the inertial efficiency could be expressed as follows for the extreme trajectory case:

$$\eta'_{St} = \frac{W_{St}}{r_f v} \tag{3.5}$$

where W_{St} is the flow rate in the width of inertial capture. It is related to the inertial force on the particle and velocity distribution, not only the thickness of the layer r_p. So movement equations must be solved. Given the resistance of airflow, equations could be written for small Re number (usually it is smaller than 1) and curvature movement of particles as follows:

$$\begin{cases} m\frac{\mathrm{d}v_x}{\mathrm{d}t} = -6\pi\mu r_p(u_x - v_x) + F_x \\ m\frac{\mathrm{d}v_y}{\mathrm{d}t} = -6\pi\mu r_p\left(u_y - v_y\right) + F_y \end{cases} \tag{3.6}$$

where

u_x and u_y are x- and y-component of particle velocity, respectively;
v_x and v_y are x- and y-component of air velocity, respectively;
F_x and F_y are x- and y-component of external force, respectively;
μ is the viscous coefficient of air.

But it is difficult to solve this nonlinear partial equation. It is common to use approximation method or semiempirical expression. They have the following form:

$$\eta'_{St} = f(St, Re)$$

Since later calculation will not use η'_{St}, the exact data will not be cited here. We emphasize on the parameter St:

$$St = \frac{1}{9}\frac{{r_p}^2 \rho_p v c}{\mu r_f} \tag{3.7}$$

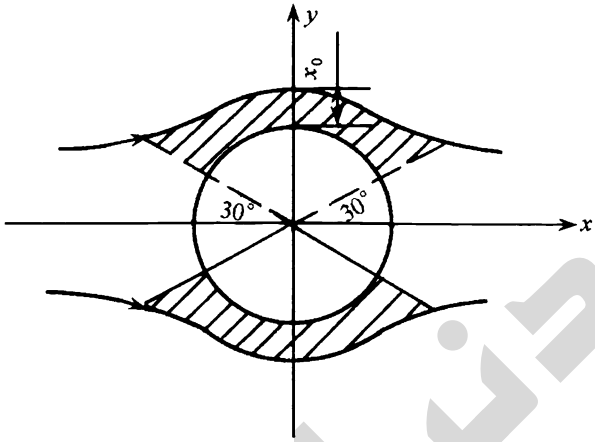

Fig. 3.15 Range of particle diffusion deposition

where

ρ_P is the particle density, kg/m^3;
μ is the viscous coefficient of air, Pa · s;
c is the slip correction factor of particle, shown in Chap. 6.

St is dimensionless and it is termed as inertial parameter or Stokes parameter. It represents the ratio of inertial force and air resistance. When $St \to 0$, inertial force disappears and particle velocity becomes consistent with air velocity. When *St* reaches a small value or a critical value, inertial force on particles cannot offset the attractive force from the airflow; it cannot settle onto the fiber surface. Suppose the value of *St* is less than 0.1, inertial efficiency is very small. Inertial efficiency increases with the increase of *St* number, which corresponds with the increase of air velocity, particle size, and density, as well as the decrease of fiber size.

3.5.3 *Diffusion Efficiency*

Randomized movement of highly dispersed particles makes free displacement in all directions. When an isolated cylinder or fiber is placed in this kind of particle-laden flow, particles will be excluded from the adjacent airflow layer and then deposited onto its surface. The angle range is about $30° \leq \theta \leq 150°$, which is shown in Fig. 3.15.

Suppose the thickness of diffusion layer is x_0 at $\theta = \pi/2$, which is equivalent to the range between r_f and $r_f + r_p$ for interception effect, Langmuir obtained the following expression:

$$\frac{x_0}{r_f} = \left[1.12\frac{(2 - \ln Re)D}{r_f v}\right]^{\frac{1}{3}} \tag{3.8}$$

where D is the air diffusion coefficient.

Based on the similar definition of Eq. (3.2), diffusion efficiency expression could be derived with Eq. (3.3), because it is mainly dependent on the pure geometrical factor: diffusion layer thickness. We obtain the following expression:

$$\eta'_D = \frac{1}{2(2-\ln Re)}\left[2\left(1+\frac{x_0}{r_f}\right)\ln\left(1+\frac{x_0}{r_f}\right)-\left(1+\frac{x_0}{r_f}\right)+\frac{1}{1+\frac{x_0}{r_f}}\right] \tag{3.9}$$

So the expression for diffusion efficiency is obtained by inserting Eq. (3.8) into Eq. (3.9).

In addition, the particle-laden flow rate towards the circular cylinder with unit length is $\pi d_f k$, where k is the mass transfer coefficient, m/s. So the following expression is obtained based on the similar definition of Eq. (3.2):

$$\eta'_D = \frac{\pi r_f k}{r_f v} = \pi\frac{Sh}{Re\ Sc} = \pi\frac{Sh}{Pe} \tag{3.10}$$

where Sh is the Sherwood number ($Sh = \frac{kd_f}{D}$), Sc is the Schmidt number ($Sc = \frac{\mu}{\rho D}$), and Pe is Peclet number ($Pe = \frac{d_f v}{D}$).

3.5.4 Gravitational Efficiency

Efficiency caused by gravitational settling could be written as:

$$\eta'_G = \frac{v_s r_f}{v r_f} = \frac{v_s}{v} \tag{3.11}$$

where v_s is the settling velocity and v is the air velocity.

According to the study performed by Fuchs, additional item related to R should be added to the equation.

When airflow is perpendicular to the fiber surface and goes downwards, it is:

$$\eta'_G = (1+R)\frac{v_s}{v} \tag{3.12}$$

When airflow is perpendicular to the fiber surface and goes upwards, it is:

$$\eta'_G = -(1+R)\frac{v_s}{v} \tag{3.13}$$

When air flows parallel to the fiber surface, it is:

$$\eta'_G = \left(\frac{v_s}{v}\right)^2 \tag{3.14}$$

3.5.5 Electrostatic Efficiency

Expressions for three conditions are presented directly [9].

1. Both fiber and particles are charged:

$$\eta'_{E,Qq} = \frac{4Qq}{3\mu d_p d_f v} \tag{3.15}$$

where Q is the charge on fiber with unit length and q is the charge on particle.

2. Fiber is charged, while particles are not:

$$\eta'_{E,Q0} = \frac{(\varepsilon - 1)4d_p^2 Q^2}{(\varepsilon + 2)3\mu d_f^3 v} \tag{3.16}$$

where ε is the dielectric constant.

3. Fiber is not charged, while particles are:

$$\eta'_{E,0q} = 2\left[\frac{1}{2(2 - \ln Re)}\right]^{\frac{1}{2}}\left[\frac{(\varepsilon - 1)}{(\varepsilon + 2)}\frac{q^2}{12\pi^2\mu d_p d_f^2 v}\right] \tag{3.17}$$

Dimensional constants in the above three equations should have the same unit with the electrostatic charge.

3.5.6 Total Efficiency of Isolated Single Fiber

As mentioned before, gravitational and electrostatic effects could be omitted in the usual case, so the main particle capture mechanisms for fibrous filter include interception, inertial, and diffusion effects. If one mechanism works while others do not, the total efficiency of isolated single fiber with unit length equals with the summation of these three individual efficiencies, i.e.,

$$\eta'_{\Sigma} = \eta'_R + \eta'_{St} + \eta'_D \tag{3.18}$$

However, in fact these mechanisms take effect simultaneously. It is shown in Fig. 3.7 that under the inertial effect only, particles will not be captured when they do not touch fibers; however, it will still be captured by interception effect when the centerline trajectory arrives r_p away from fiber surface. This is called inertial interception effect. This means that the distance between the axis and the trajectory for particle capture at far distance is not y_R for interception effect only, nor y_{St} for inertial effect only, but the enlarged distance $y_{St,R}$ for both effects. For the case of small Re flow (smaller than 1), Davies put forward the following expression [10]:

$$\eta'_{St,R} = 0.16\left[R + (0.25 + 0.4R)St - 0.0263RSt^2\right] \tag{3.19}$$

where parameters *St* and *R* are included, which means this efficiency is related to both inertial and interception effects.

Furthermore, the curve obtained from computer simulation by Susumu can be used for calculation, which is shown in Fig. 3.16 [8]. Naoya also obtained similar result [11].

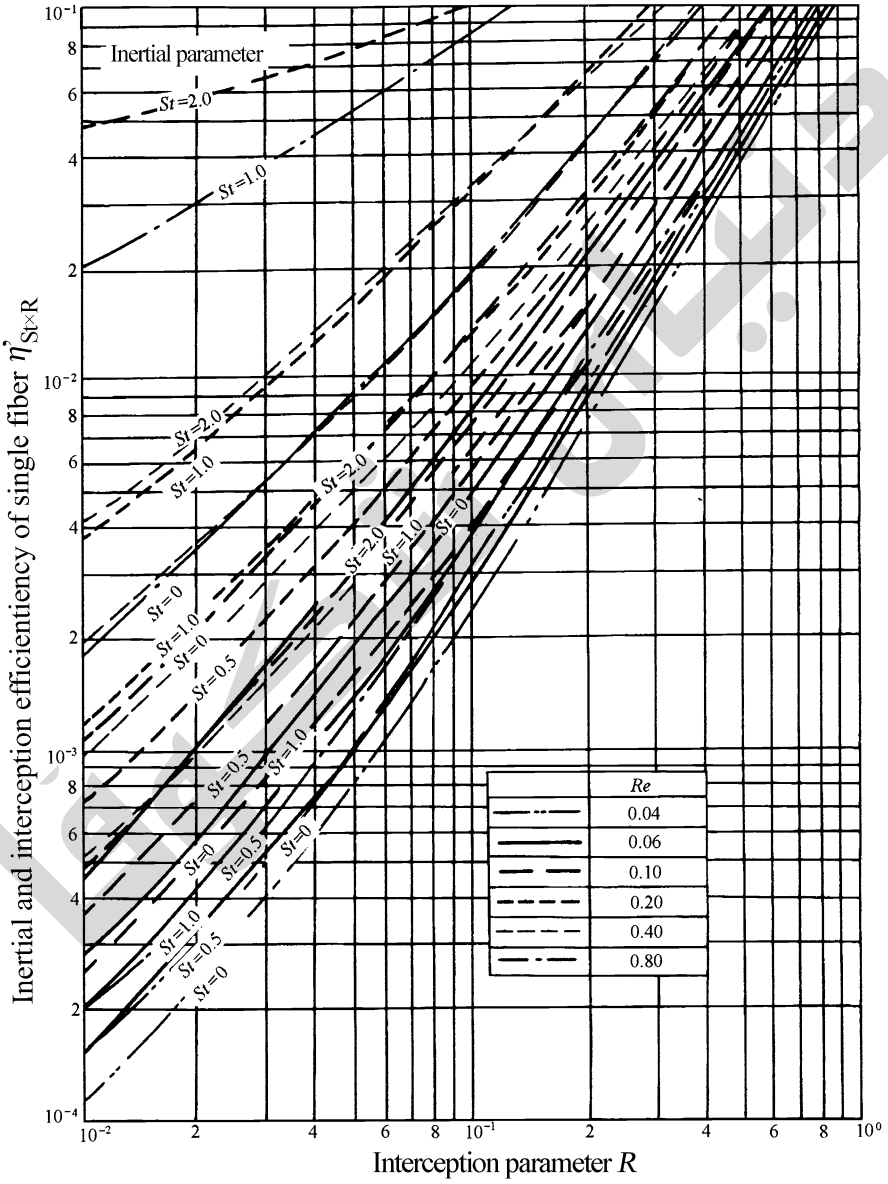

Fig. 3.16 Inertial interception efficiency

It is also shown in Fig. 3.10 that although particles do not arrive at the fiber surface with the diffusion effect only, when it is at r_p away from the surface, it will also be captured by interception effect. This is termed as diffusional interception effect. This means that the distance between the axis and the trajectory for particle capture at far distance is not y_R for interception effect only, nor y_D for diffusion effect only, but the enlarged distance $y_{D,R}$ for both effects. According to the same definition of Eqs. (3.2) and (3.10) is derived:

$$\eta'_{D,R} = \frac{\pi(r_f + r_D)k}{r_f v} = \frac{\pi r_f k}{r_f v} + \frac{\frac{r_p}{r_f}\pi r_f k}{r_f v} = \frac{\pi(1+R)r_f k}{r_f v} = \pi(1+R)\frac{Sh}{Pe} \tag{3.20}$$

So the total efficiency for isolated single fiber is expressed as:

$$\eta'_{\Sigma} = \eta'_{St,R} + \eta'_{D,R} \tag{3.21}$$

3.6 Particle Capture Efficiency of Single Fiber Inside Filter: Influence of Fiber Interference and Correction Method

Mechanism of particle capture for isolated single fiber has been introduced earlier. But the situation inside fiber (fiber filling layer or filter paper) is more complex, because the space distribution of fiber, fiber density, and combination form of fibers are different, and the velocity field around fiber is different from that of isolated fiber. Correction of fiber interference to the efficiency of single fiber is needed. Since the interference effect becomes larger with the increase of solid fraction inside the filter, solid fraction α is included in the correction factor. Three kinds of correction method will be illustrated in the following chapter.

3.6.1 Effective Radius Method

This method was proposed by Davies for small Re flow ($Re < 1$) [4]. Based on Eq. (3.19), the efficiency expression for three simultaneous effects can be written as:

$$\eta'_{\Sigma} = 0.16\left[R + (0.25 + 0.4R)\left(St + \frac{2}{Pe}\right) - 0.0263\left(St + \frac{2}{Pe}\right)^2\right] \tag{3.22}$$

Compared with Eq. (3.19), it has addition item related to $2/Pe$, where Peclet number Pe is a function of diffusion coefficient D and its reciprocal is called as

diffusion parameter and labeled as De. This establishes relationship between η'_{Σ} and three effects.

Given the interference influence of adjacent fiber, the concept of effective fiber method is adopted, and the correction factor including fiber solid fraction α is introduced. The total efficiency of single fiber with unit length is obtained:

$$\eta_{\Sigma} = \eta'_{\Sigma} + \left(10.9\alpha - 17\alpha^2\right) \times \left[R + (0.25 + 0.4R)\left(St + \frac{2}{Pe}\right) - 0.0263\left(St + \frac{2}{Pe}\right)^2\right] \tag{3.23}$$

When $\alpha < 0.02$, real average radius is used for the fiber radius in each parameter. When $\alpha > 0.02$, effective radius $r_{f\alpha}$ is used to replace real average radius. The value of effective radius could be obtained by the experimental data ΔP_{α}:

$$r_{f\alpha}^2 = \frac{17.5\mu v H}{\Delta P_{\alpha}}\alpha^{1.5}\left(1 + 52\alpha^{1.5}\right) \tag{3.24}$$

where H is the thickness of filter layer, m; v is the filtration velocity, m/s; μ is the air viscous coefficient, Pa · s; and ΔP_{α} is the experimental data of filter pressure drop, Pa.

3.6.2 Nonuniform Coefficient Method of Structure

This method was proposed by Fuchs [12], which presented the efficiency expression under various effects for single fiber inside filters:

$$\eta_D = 2.9K_u^{-1/3}Pe^{-2/3} + 0.624Pe^{-1} \tag{3.25}$$

$$\eta_R = (2K_u)^{-1}\left[(1+R)^{-1} - (1+R) + (1+R)\ln(1+R)\right] \tag{3.26}$$

$$\eta_{D,R} = 1.24K_u^{-0.5}Pe^{-0.5}R^{\frac{2}{3}} \tag{3.27}$$

$$\eta_{St,R} = (2K_u)^{-2}ISt \tag{3.28}$$

$$I = \left(296 - 28\alpha^{0.62}\right)R^2 - 2.75R^{2.8} \tag{3.29}$$

where

I is the parameter for combining the influence of interception with inertial effect; Ku is the Kuwabara hydrodynamic factor.

Total efficiency of single fiber is expressed as:

$$\eta_{\Sigma} = \varepsilon\left(\eta_D + \eta_R + \eta_{D,R} + \eta_{St,R}\right) \tag{3.30}$$

where both Ku and ε are parameters when the influence of fiber interference is considered.

$$Ku = -0.5\ln\alpha - 0.65(\text{or} -0.75 - 0.5\ln\alpha + \alpha - 0.25\alpha^2) \tag{3.31}$$

$$\varepsilon = \frac{F_{\mathrm{B}}}{F_{\mathrm{F}}} \tag{3.32}$$

where ε is also called nonuniform coefficient of structure, which represents the ratio of the force acting on fiber with unit length inside the ideal filter to that of real filter.

F_{B} is determined by theoretical equation, i.e.,

$$F_{\mathrm{B}} = \frac{4\pi}{-1.15\lg\alpha - 0.52} \tag{3.33}$$

F_{F} is determined by experimental data of filter pressure drop ΔP_{α}, i.e.,

$$F_{\mathrm{F}} = \frac{\Delta P_{\alpha}\pi d_f^2}{\alpha\mu v H} \tag{3.34}$$

Both F_{B} and F_{F} are dimensionless.

Except for the above correction of filter interference, Fuchs also introduced the slip factor on fiber surface when the fiber size is very small and close to the mean free path of air λ. Since this influence is usually very small, it will not be explained in detail.

This is a complex method for calculation, but it fits well with experiment, which is shown in Fig. 3.17.

3.6.3 *Experimental Coefficient Method*

Chen established the relationship between the efficiency of single fiber inside filter under the fiber interference effect and the efficiency of isolated single fiber [13], i.e.,

$$\eta_{\Sigma} = \eta'_{\Sigma}(1 + 4.5\alpha) \tag{3.35}$$

where η'_{Σ} is calculated by Eq. (3.21). Because this equation is simple and easy for calculation, and it has been validated by experiment, it is frequently used in the literature at present.

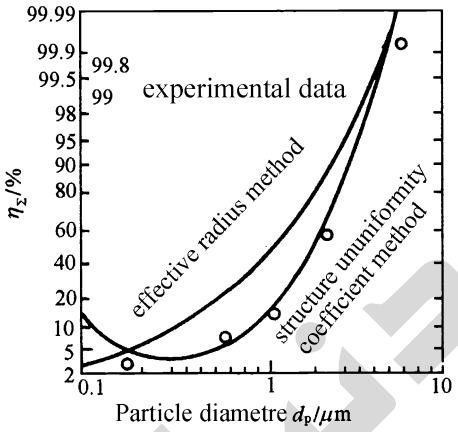

Fig. 3.17 Comparison between calculation and experiment for η_Σ

3.6.4 Semiempirical Equation Method

This method was proposed by Iinoya in 1970 [6], which assumed that paper filter was made by compression on fibrous filter along the width direction. With the method for fibrous filter, data were processed by single fiber efficiency when both diffusion and interception effects were dominant while inertial efficiency was omitted. In the experiment, fiber diameter ranges from 0.92 to 17.7 μm, and solid fraction α is between 0.091 and 0.292. Semiempirical expression for the efficiency of isolated single fiber was obtained:

$$\eta'_\Sigma = 20A_0R^2 \tag{3.36}$$

where A_0 is the theoretical stream function around single fiber when no interference effect was considered.

$$A_0 = \frac{1}{2(2 - \ln Re)} \tag{3.37}$$

At last, the total efficiency of single fiber inside filter was derived:

$$\eta_\Sigma = \eta'_\Sigma\left(1 + 10^6\alpha^6\right) \tag{3.38}$$

Using this method, we could get the monotonic relationship between the increased efficiency and the decreased particle size. However, it cannot reflect the particle size corresponding with the minimum efficiency.

3.7 Logarithmic Penetration Expression for Calculation of Total Efficiency of Fibrous Filter

3.7.1 Logarithmic Penetration Expression

After calculation of single fiber efficiency inside fibrous filter, logarithmic penetration expression is applied to obtain the efficiency of whole filter η.

Take a look at the filtration layer in Fig. 3.18 at first.

Suppose diameters of fibers inside this layer are the same, and all fibers are perpendicular to the airflow. When the initial concentration is N_0 and filtration velocity is v, and concentration after filtration becomes N, then the change or decrease of concentration passing through the filtration layer equals with the number of particles captured inside the filtration layer.

Now let's study the case of unit volume, whose layer has area S and thickness dh. If the change of concentration is dN when air goes through the layer vS in unit time, the number of particles captured is $-vS\mathrm{d}N$.

As mentioned before, the filtration efficiency of single fiber with unit length is η_Σ, so with the efficiency definition in Eq. (3.1), the number of particles captured by fiber with unit length per unit time is $\eta_\Sigma d_f v' N$, where v' is the average velocity across spaces between fibers, i.e.,

$$v' = \frac{v}{1-\alpha} \tag{3.39}$$

$d_f v'$ represents the volumetric flow rate across fibers.

After air flows across this layer vS, the particle concentration decreases by $-vS\mathrm{d}N$. For air with particulate concentration N passing through this layer which

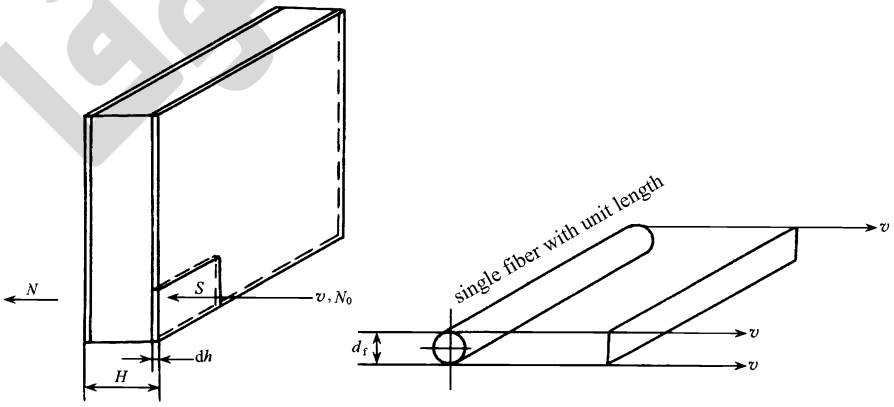

Fig. 3.18 Unit volume inside filter for particle capture

contains the total length of fibers L, the number of particles captured is $\eta_\Sigma d_f v' NL$. These two data should be equal, i.e.,

$$-vS\mathrm{d}N = \eta_\Sigma d_f v' NL$$

where L is the total length of fibers inside the unit layer, i.e.,

$$L = \frac{4\alpha S dh}{\pi d_f^2} \tag{3.40}$$

$$-vS\mathrm{d}N = \eta_\Sigma d_f v \frac{4SN\alpha dh}{(1-\alpha)\pi d_f^2}$$

$$-\frac{\mathrm{d}N}{N} = \frac{4\alpha\eta_\Sigma}{(1-\alpha)\pi d_f} dh$$

After integration, we get:

$$\ln N = -\frac{4\alpha H\eta_\Sigma}{(1-\alpha)\pi d_f} + C \tag{3.41}$$

At the position $H = 0$, all the particles will penetrate, i.e., $N = N_0$.

$$\ln\ N_0 = C$$

Replacing the expression of C into Eq. (3.41), we get:

$$\ln\frac{N}{N_0} = -\frac{4\alpha H\eta_\Sigma}{(1-\alpha)\pi d_f} \tag{3.42}$$

We denote $K' = N/N_0$, and insert it into Eq. (3.42). When the above equation is transformed into logarithmic function ($\lg x = 0.434 \ln x$), we get:

$$\lg K' = -0.55\frac{\alpha H\eta_\Sigma}{(1-\alpha)d_f} \tag{3.43}$$

K' is expressed in decimal. If we denote $K = K' \times 100\ \%$ and it is called penetration of filter, the above equation becomes:

$$\lg K = 2 - 0.55\frac{\alpha H\eta_\Sigma}{(1-\alpha)d_f} \tag{3.44}$$

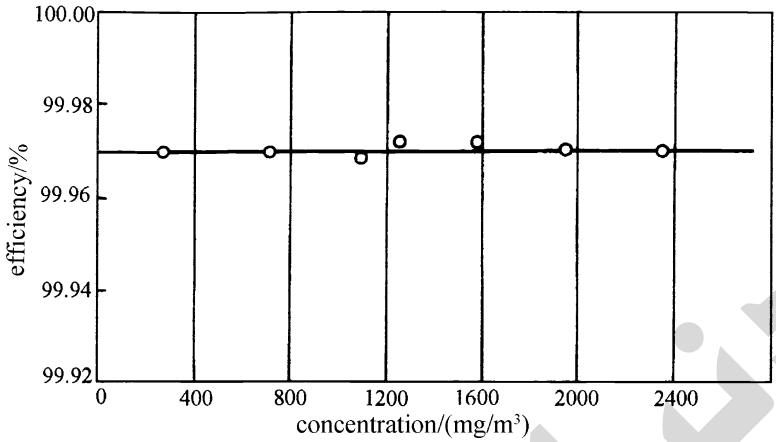

Fig. 3.19 Relationship between penetration and initial concentration

When K is obtained, we get:

$$\eta = \frac{100}{100} - K$$

For example, lg $K = 0.95$, then we get $K = 8.9$ % and $\eta = \frac{100-8.9}{100} = 91.1$ %. When the exponential function is used, Eq. (3.42) becomes:

$$\eta = 1 - \exp\left[-\frac{4\alpha H \eta_\Sigma}{(1-\alpha)\pi d_f}\right] \tag{3.45}$$

Equation (3.44) is called logarithmic penetration expression of filter, which is the fundamental law in the study of filter efficiency [4].

It is shown from Eq. (3.42) that $\frac{N}{N_0}$ is constant. It does not change with the variation of initial concentration N_0. So efficiency of filter will not vary with initial concentration in the airflow. Figure 3.19 is the experimental result of oil mist method for the relationship between efficiency and initial concentration, which is performed by Architectural Research Institute of former Ministry of Metallurgical Industry. The result is consistent with that of logarithmic penetration theory. But recently, results using particle counting method on filters show that change of efficiency at 0.1 μm synchronized with initial concentration [14]. When the latter changes by an order of magnitude, the former changes by about an order of magnitude. At present no explanation has been made for this result.

In this equation, $K = \exp\left[-\frac{4\alpha H \eta_\Sigma}{(1-\alpha)\pi d_f}\right]$. According to Zhou Bin's analysis [15], there is another kind of expression $K = \exp\left[-\frac{4\alpha H \eta_\Sigma}{\pi d_f}\right]$. And the difference between them is given. It should be also noted here that the case with $\alpha = 1$ cannot be explained with the latter expression, because the unreasonable result will be obtained.

Recently results using particle counting method on filters show that change of efficiency at 0.1 μm synchronized with initial concentration [14]. When the latter changes an order of magnitude, the former changes by about an order of magnitude. At present no explanation has been made for this result.

In fact, values of K', H, α, and d_f are usually determined by experiment. Then the total efficiency of single fiber with unit length is derived by Eq. (3.43):

$$\eta_\Sigma = -1.8\frac{(1-\alpha)d_f \lg K'}{H\alpha} \tag{3.46}$$

Then the relationship among η_Σ, η'_Σ, and α is established. The third parameter is calculated when two others are known. This is the common procedure to study the filtration mechanism of fibrous filter.

3.7.2 *Applicability of Logarithmic Penetration Expression*

Filtration layer or fibrous filter consists of multilayers of fiber net. During the derivation process of logarithmic penetration expression, the following conditions must be met:

1. Fibers arrangement is regular.
2. The probability of particle capture for each fibrous layer is the same.
3. No resuspension phenomena occur for particles captured on the fiber surface.

In this way, a linear relationship among penetration, thickness H, and solid fraction α is established, because the item $(1 - \alpha)$ from Eq. (3.42) to Eq. (3.46) is close to 1 for fibrous filter. However, real filters do not meet these requirements. Therefore, it should be clear whether the logarithmic penetration expression is valid.

3.7.2.1 Influence of Thickness

Many experimental results on fibrous filters show that penetration is linearly proportional to layer thickness H, even when the layer thickness arrives at tens of millimeters. Figure 3.20 is the experimental result of the performance of fibrous filter layer with fiber diameter 16 μm for filtering bacterial particles, which was performed by Humphrey and then cited in Ref [16]. It is a good example of this relationship.

Figure 3.21 is the experimental result of the performance of thick fibrous layer with thickness 0.3–15 cm for monodisperse DOP particles, which was done by Norio and Iinoya [7]. It is shown that when the number of nominal layer H/l is less than 500, the logarithmic penetration expression is applicable.

The nominal layer number is the ratio between fibrous layer thickness H and fiber spacing l. Suppose fibers are arranged in such a way shown in Fig. 3.22. Solid fraction α is the percentage of the area occupied by fibers in the area of $l \times l$, i.e.,

$$\alpha = \frac{\frac{\pi d_f^2}{4}}{l^2}$$

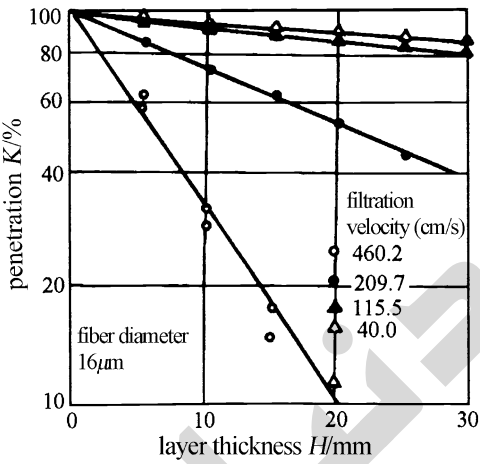

Fig. 3.20 Illustration of logarithmic penetration expression

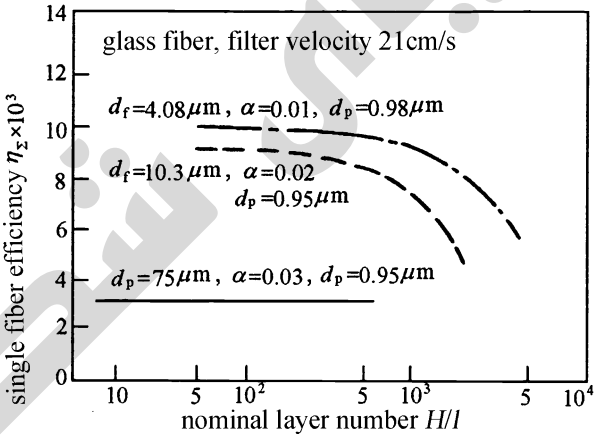

Fig. 3.21 Applicability range of logarithmic penetration theory for fibrous layer

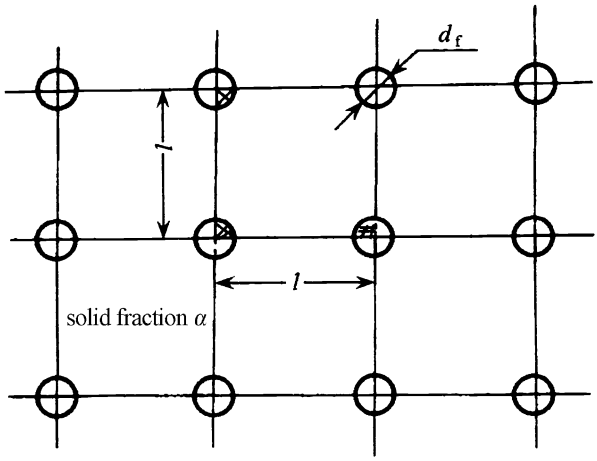

Fig. 3.22 Relationship between solid fraction, fiber size, and fiber spacing

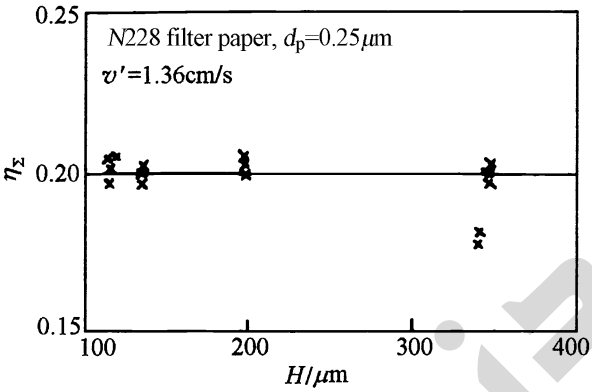

Fig. 3.23 Relationship between single fiber efficiency η_Σ and filter paper thickness H

So we get:

$$l = d_f \sqrt{\frac{\pi}{4\alpha}} \tag{3.47}$$

$$\frac{H}{l} = \frac{H\sqrt{4\alpha}}{d_f\sqrt{\pi}} = \frac{H}{d_f}\sqrt{\frac{4\alpha}{\pi}} \tag{3.48}$$

From Fig. 3.21, the nominal layer becomes thinner for the validity of logarithmic penetration expression with the decrease of fiber diameter.

When different filtration mechanisms are concerned, a linear relationship between K and H exists in the field of diffusion when the penetration $K \geq 60$ % and H is less than 20 mm while a linear relationship between K and H also exists in the field of interception and inertia when H is less than 40 mm and $K \geq$ 20–30 % [3].

For paper filter, the fiber structure could be thought as a fibrous layer filter after compression along the width direction. Several layers of thin papers can be overlapped for test. Different layers of overlapping represent different thickness. Several layers of thin papers can be overlapped for test. During the test, other conditions remain the same. Different layers of overlapping represent different thickness. Figure 3.23 is the result obtained by Iinoya [6]. It is shown that the single fiber efficiency $\eta\Sigma$ keeps the same, no matter how thick the filter paper is. The single fiber efficiency is independent of the thickness H. This means the logarithmic penetration expression is valid and the flow conditions around fibers inside filter paper are unchanged.

3.7.2.2 Influence of Solid Fraction

For fibrous filter with small solid fraction α, many experiments have proved that the relationship between α and efficiency fits the logarithmic penetration expression.

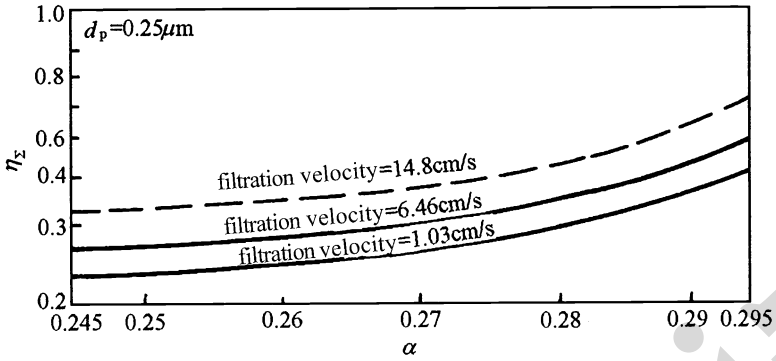

Fig. 3.24 Relationship between single fiber efficiency η_Σ and solid fraction α

For filter paper, the influence of solid fraction α on logarithmic penetration expression is shown in Fig. 3.24 [6]. It is obvious that linear relationship exists between α and η_Σ for $\alpha < 0.25$. When $\alpha > 0.25$, single fiber efficiency η_Σ varies much. So unlike the logarithmic penetration expression, η_Σ varies with α, and the linear relationship between α and lg K does not exist. This means the effect of fiber interference becomes large. Since the solid fractions of most filter papers are less than 0.2, the logarithmic penetration expression is still valid.

3.8 Influencing Factors for Efficiency of Fibrous Filters

Many factors influence the efficiency of fibrous filters, which mainly include particle diameter, fiber size, filtration velocity, and solid fraction. Now their influences are analyzed as follows.

3.8.1 Influence of Particle Size

When particles are polydisperse, under the role of several filtration mechanisms, smaller particles will settle onto fiber surface with diffusion. With the increase of particle size, the effect of diffusion decreases gradually. Larger particles settle onto fiber surface with interception and inertia. With the increase of particle size, both the effects of interception and inertia increase. So there is the lowest point on the efficiency curve related to particle size, which corresponds to the minimum efficiency. Particles with this size are the most difficult to be captured inside filters.

When the derivative is made on the efficiency equation of single fiber, the most penetration K_{max} and the particle size d_{max} corresponding to the minimum efficiency can be obtained.

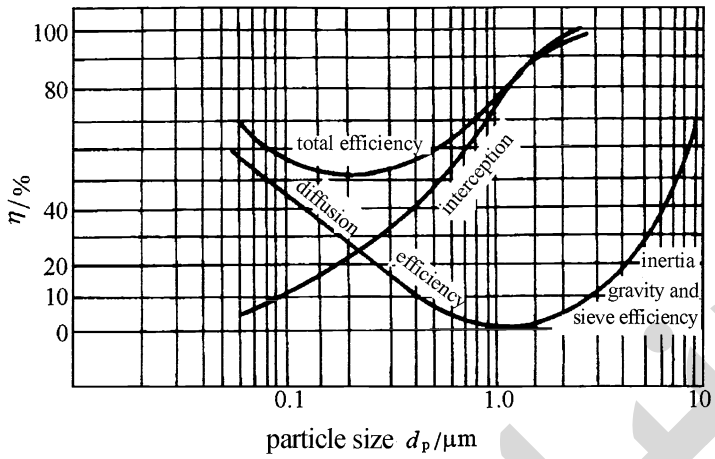

Fig. 3.25 Relationship between efficiency and particle size

It should be noted that d_{max} is not a constant value. In the past it is thought that $d_{max} = 0.3$ μm, so efficiency of HEPA filter is tested using particles with diameter 0.3 μm. But this should be linked with certain conditions. With the development of measurement techniques, many experiments have proved that d_{max} varies with different particles, fibers, and filtration velocities. In most cases, d_{max} for fibrous filters is between 0.1 and 0.4 μm. Figure 3.25 is a typical relationship between particle size and filtration for fibrous filter [17].

Next one example will be provided about the theoretical calculation of d_{max} [18]. When $0.075 < \frac{\lambda}{d_p} < 1.3$, we could get the following result based on Eq. (3.30):

$$d_{max} = 0.885 \frac{Ku}{1-\alpha} \left(\frac{\lambda^{1/2} kT}{\mu} \right) \left(\frac{d_f^2}{v} \right)^{2/9} \tag{3.49}$$

where

λ is the mean free path of air molecular (at normal temperature and pressure it is 0.065 μm);
k is the Boltzmann constant.

The calculated results are presented in Fig. 3.26. Usually fiber diameter of HEPA filter is about 0.4 μm, solid fraction α is about 0.10, and filtration velocity is about 2.5 cm/s. From Fig. 3.26 it is clear that d_{max} is about 0.14 μm. d_{max} decreases with the increase of filtration velocity and with the decrease of fiber diameter.

For $\alpha = 0.03$–0.07 and $d_f = 0.43$–1.68 μm, the following empirical equation could be also used to estimate d_{max} [19], i.e.,

$$d_{max} = 0.2425 v^{-\frac{1}{6}} \tag{3.50}$$

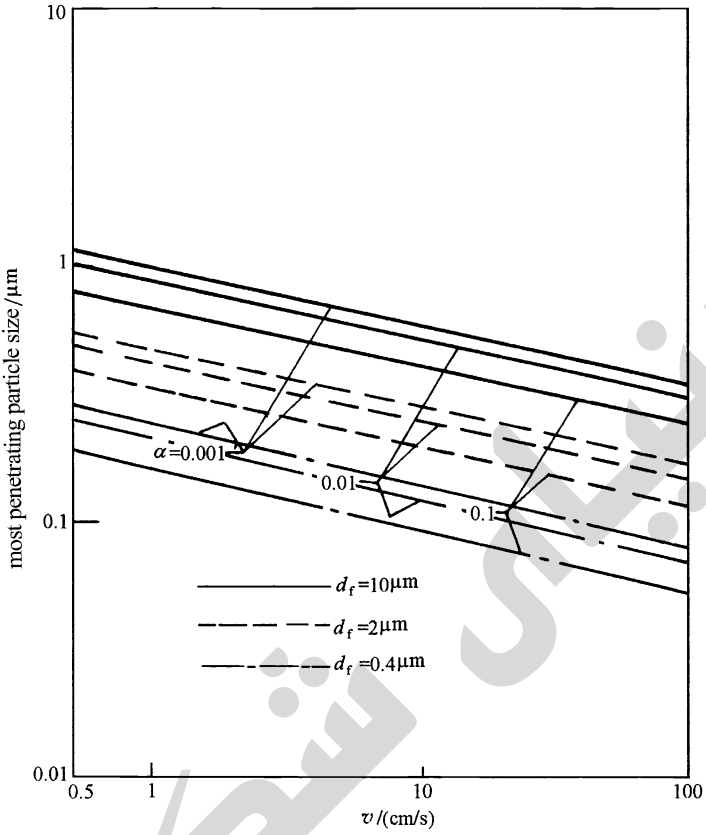

Fig. 3.26 Theoretical calculation of d_{max}

where the units for d_{max} and v are μm and cm/s, respectively.

When $\alpha = 0.07$, $d_f = 1$ μm, and $v = 2.5$ cm/s, we could get $d_{max} = 0.21$ μm. If we look up Fig. 3.26, d_{max} is found between two straight lines and is about 0.2–0.25 μm, which means the estimate equation is useful.

Next take a look at an experiment.

Figure 3.27 illustrates the experimental result of the influence of the filtration velocity on the most penetration for fibrous filters with $d_f = 1.5$ μm [4]. It is obvious that the maximum of penetration moves towards small particle size with the increase of filtration velocity.

For glass fibrous filter, d_{max} is between 0.1 and 0.15 μm with a quite large range of filtration velocity for particles such as NaCl, DOP, and stearic acid. For PSL particles, d_{max} is also not 0.3 μm. Data from related literatures are presented in Fig. 3.28, which clearly illustrates this point. For experimental results are different with atmospheric dust, silver aerosol, and gold aerosol. The efficiency with 0.001–0.1 μm particles is higher than that with 0.3 μm particles, which is believed

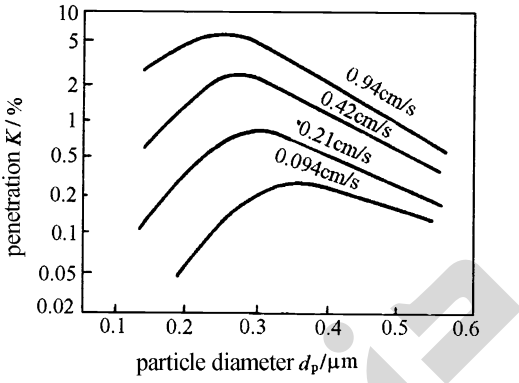

Fig. 3.27 Relationship between penetration and particle size under different filtration velocities

to be caused by the increased diffusional efficiency with these kinds of small particles [20].

However, the most penetrating particle sizes of different fibers are different, which could be verified by the experimental results performed in the USA by the same person and same method [22]. Figure 3.29 is the penetration using DOP for common fibrous filter paper which was made in China. Figure 3.30 is the penetration using DOP for common fibrous filter paper which was made in the USA. Figure 3.31 is the penetration using DOP for ULPA filter paper which was made in China. Figure 3.32 is the penetration using DOP for ULPA filter paper which was made in the USA. It is seen that d_{max} is consistent with that of calculation. Tables 3.1 and 3.2 are experimental results of penetration using DOP for perchlorethylene fiber and polypropylene fiber made in China, respectively. The former d_{max} is about 0.08 μm, while that of the latter is 0.05 μm. According to domestic experiments, d_{max} for polypropylene fiber is 0.085 μm using NaCl aerosol when fiber diameter is 4 μm [23], and some test results even showed that it is 0.55 μm using atmospheric dust when fiber diameter is 6 μm [24]. This may be caused by the electrostatic effect, which will be explained later.

With the increase of the efficiency of filter paper, d_{max} decreases. It is shown in above figures that d_{max} of ULPA filter paper is smaller than that of common HLPA filter. It is about 0.12 μm.

d_{max} is an important parameter, which is termed as the most penetrating particle size. When d_{max} is known and the efficiency corresponding to this particle size is assured, filtration efficiencies of particles with other sizes are guaranteed.

Because of the existing d_{max}, monodisperse particles with this size are needed to the evaluation of filters or polydisperse particles such as NaCl aerosols when the average diameter is close to d_{max}.

With the existence of d_{max}, filtration process of filters has the characteristic of selectivity. When particle-laden flow with polydisperse particles goes through same filters in series, particles penetrate the first filter that has the size of the most penetrating particle size or d_{max}. So the penetration of the second filter is larger than that of the first one. It should be noted that the ability of selectivity for single

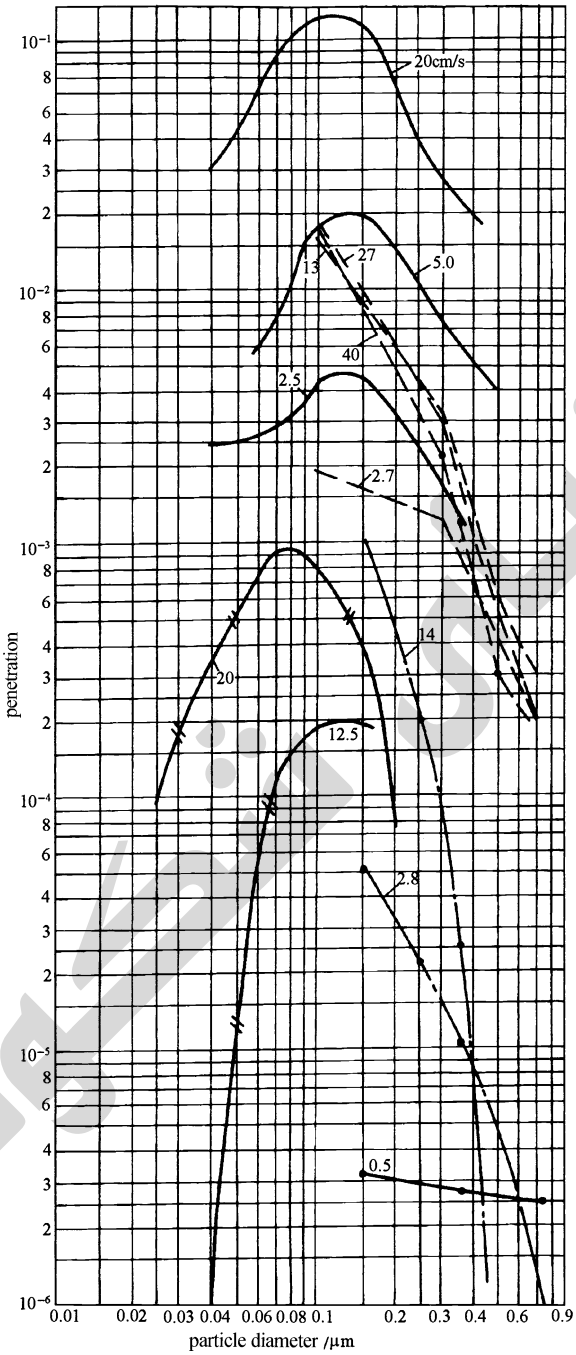

Fig. 3.28 Relationship between filter efficiency and particle size

—— NaCl[20] —•— DOP[20]

—//— No given name[20] — — — stearic acid[21]

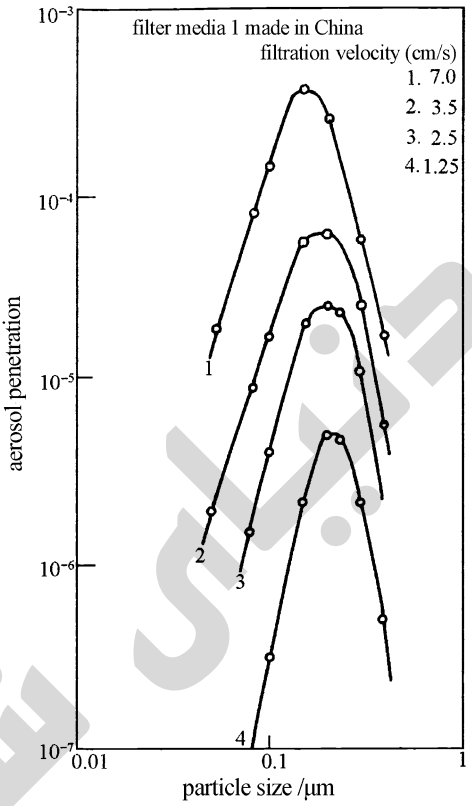

Fig. 3.29 Relationship between particle size and penetration for filter media 1 (common HEPA filter) made in China

fiber with uniformly distributed mass is larger than that of fibers with nonuniform mass inside the fiber layer. For filters with damage on the surface, this ability may disappear completely.

3.8.2 Influence of Particle Type

Even when the particle sizes are the same, different phases have impact on the filtration efficiency. Experiment shows that efficiency for solid particle is higher than that of liquid particle, and constant efficiency is obtained for various filter media using liquid DOP particle [25]. With the increase of filtration velocity, the influence of this phase on efficiency decreases gradually.

In theory it is not clear why efficiency using solid particle is comparatively higher. Usually the following reasons are thought to cause the difference:

1. Coagulation of solid particle is more frequent than liquid one.
2. Influence of charge on solid particle is higher than that on liquid one.
3. Solid particle could significantly increase the load of filter.

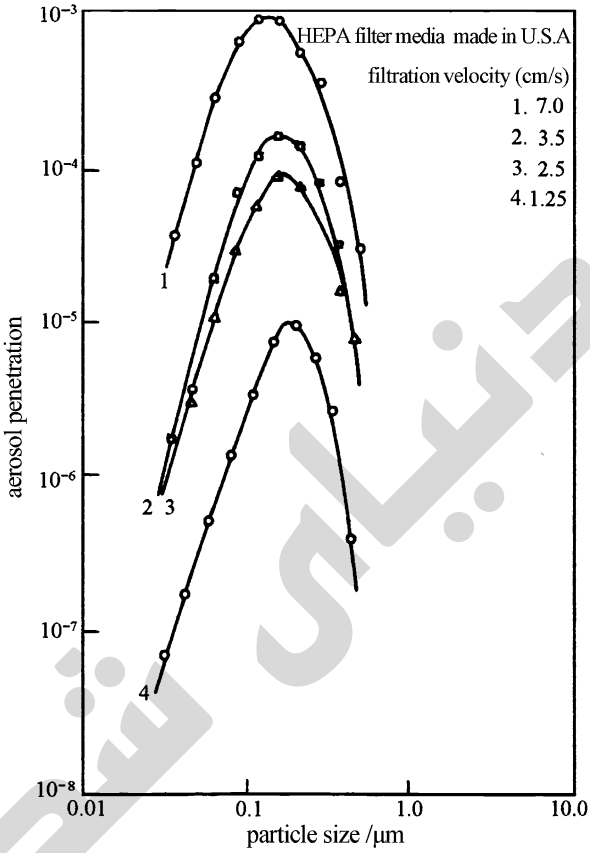

Fig. 3.30 Relationship between particle size and penetration for filter media (common HEPA filter) made in the USA

4. Fibers become damaged after liquid particles are capture on the surface.
5. Error of experimental result is caused by the difference of particle size and density.

So there is some people advocate to test filters using solid particles, which is thought to give real result. However, others prefer to use liquid particle for the test for safety.

3.8.3 Influence of Particle Shape

Particles used for efficiency test of air filters as well as for efficiency calculation are spherical. Contact surface area for spherical particles touching fibers is smaller than that of irregularly shaped particles. So the probability of contact with fibers for irregularly shaped particles is larger, which makes the probability of deposition larger. In fact atmospheric particles are irregular shaped, so the real filtration efficiency is larger than that of calculation and experiment. The largest penetration for spherical particles is safe.

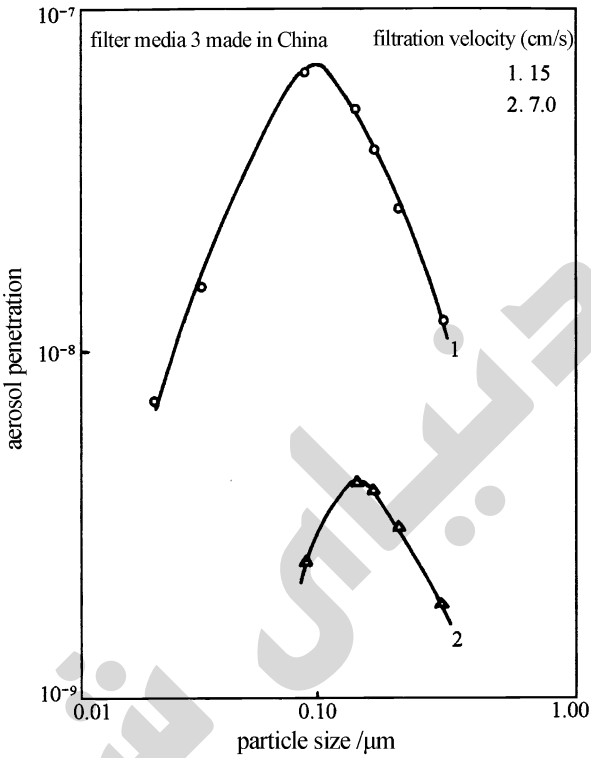

Fig. 3.31 Relationship between particle size and penetration for filter media 3 (ULPA filter) made in China

3.8.4 *Influence of Fiber Size and Cross-Sectional Shape*

According to the aforementioned filtration mechanisms, filtration efficiency increases with the decrease of fiber size. For comparison purpose, results from Figs. 3.29, 3.30, 3.31, and 3.32 are listed in Tables 3.3, 3.4, 3.5, and 3.6 [22]. It is shown that since diameters of fibers in the domestic-made fibrous filter paper are smaller than that made in the USA, the former efficiency is much higher. Therefore, smaller fibers are preferred during the selection of HEPA filter media. Of course the pressure drop of filter will increase with the decrease of fiber size.

Influence of fiber cross-sectional shape on filtration efficiency is not large, which is shown in Fig. 3.6. Although correction factors for shape were proposed by Haya, it is usually ignored because of computational complexity [26].

3.8.5 *Influence of Filtration Velocity*

Like the most penetrating particle size, there is the most penetration filtration velocity for each filter. Qualitative relationship among several filtration mechanisms, filtration velocity, and other parameters is illustrated in Fig. 3.33. The figure illustrates that:

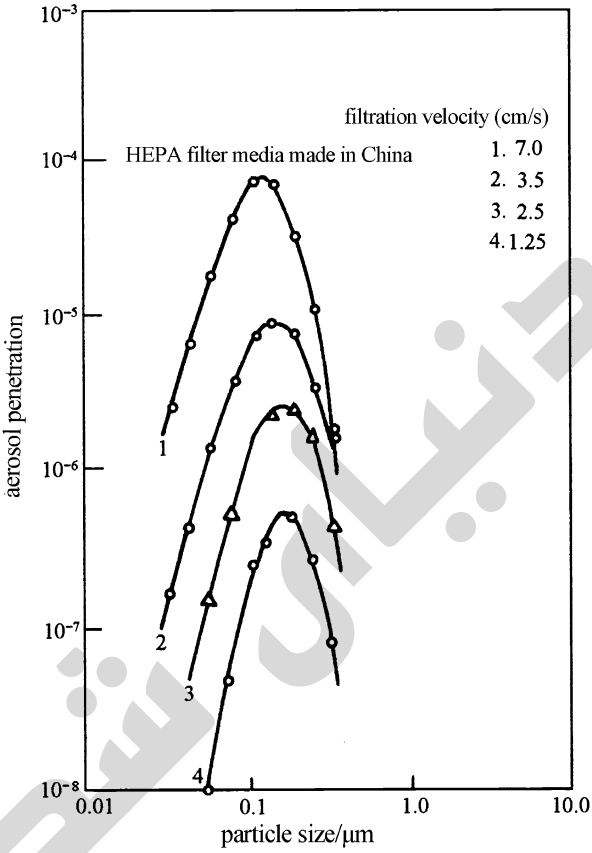

Fig. 3.32 Relationship between particle size and penetration for filter media (ULPA filter) made in the USA

Table 3.1 Efficiency with DOP for domestic-made perchlorethylene fibrous media

△P/Pa	22.9	45.7	63.5	121.9	508.0
v/(cm/s)	1.25	2.5	3.5	7.0	13.4
Particle size/μm	Efficiency/%				
0.5	–	–	–	–	97.60
0.4	99.96	99.78	99.48	98.12	96.27
0.3	99.95	99.71	99.39	97.60	95.72
0.2	99.88	99.52	99.07	97.00	92.29
0.15	99.76	99.11	98.50	96.17	91.70
0.10	99.44	98.01	96.90	93.35	87.72
0.08	99.25	97.56	96.35	93.29	88.08
0.05	99.38	97.87	96.70	93.46	87.81

1. Diffusion efficiency decreases with the increase of filtration velocity.
2. Inertial efficiency increases with the increase of filtration velocity.
3. Interception efficiency increases with the increase of filtration velocity.
4. With the increase of filtration velocity, the total efficiency decreases at first and then increases. So there is a filtration velocity for the minimum efficiency or the maximum penetration.

Table 3.2 Efficiency with DOP for domestic-made polypropylene fibrous media

△P/Pa	20.3	40.6	59.9	116.8	482.6
v/(cm/s)	1.25	2.5	3.5	7.0	13.4
Particle size/μm	Efficiency/%				
0.5		–	–	–	99.83
0.4	99.9994	99.995	99.984	99.83	99.59
0.3	99.9991	99.990	99.970	99.71	99.12
0.2	99.9950	99.970	99.920	99.41	98.37
0.15	99.9600	99.870	99.780	98.48	97.78
0.10	99.8800	99.660	99.370	98.62	96.26
0.08	99.8500	99.560	99.270	96.52	95.39
0.05	99.8400	99.400	99.170	95.54	93.80
0.03	99.9700	99.850	99.710	98.52	–

Table 3.3 Penetration of HEPA filter media 1 made in China and common HEPA filter media made in the USA

	Chinese filter media l		UK filter media	
	Particle size/μm		Particle size/μm	
Filtration velocity/(cm/s)	0.1	0.3	0.1	0.3
1.25	3.25×10^{-7}	2.02×10^{-6}	3.30×10^{-6}	3.20×10^{-6}
2.50	3.64×10^{-6}	1.00×10^{-5}	5.40×10^{-5}	2.50×10^{-5}
3.50	1.53×10^{-5}	2.26×10^{-5}	1.20×10^{-4}	3.80×10^{-5}
7.00	1.41×10^{-4}	5.30×10^{-3}	8.50×10^{-4}	1.50×10^{-4}

Table 3.4 Fiber diameter of HEPA filter media 1 made in China and common HEPA filter media made in the USA

Fiber	Chinese filter media l	UK filter media
The coarsest fiber/μm	4.00	5.60
The finest fiber/μm	0.12	0.20

Table 3.5 Penetration of ULPA filter made in China and the USA

	Chinese filter media		UK filter media	
	Particle size/μm		Particle size/μm	
Filtration velocity/(cm/s)	0.13	0.29	0.13	0.29
7.0	3.27×10^{-9}	1.91×10^{-9}	2.53×10^{-5}	1.32×10^{-5}
1.50	5.1×10^{-8}	1.25×10^{-8}	–	–

Table 3.6 Fiber diameter of ULPA filter media made in China and the USA

Fiber	Chinese filter media	UK filter media
The coarsest fiber/μm	0.73	2.5
The finest fiber/μm	0.04	0.10

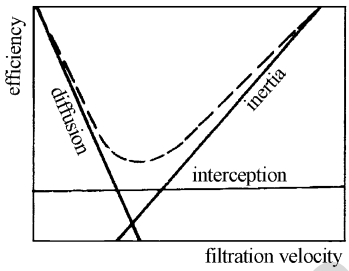

Fig. 3.33 Influence of filtration velocity on various efficiencies

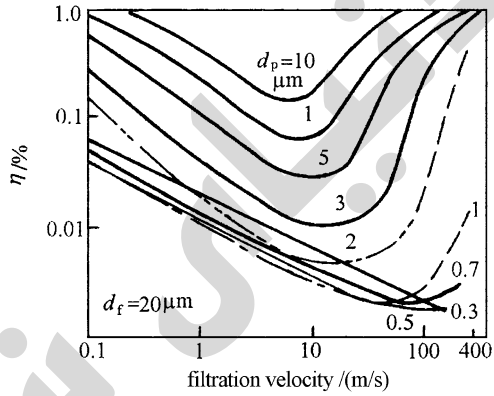

Fig. 3.34 Influence of filtration velocity on singe fiber efficiency

Figure 3.34 illustrates the quantitative relationship between efficiency of single fiber and filtration efficiency [27]. For example, for fiber with diameter 20 μm and particles with diameter 7 μm, the filtration velocity corresponding to the maximum penetration is about 0.8 m/s, while it is 0.2–0.3 m/s for particles with diameter 2 μm. It is advisable to choose suitable filtration velocity during the design of air filters, given the size range of particles captured and fiber diameters.

Figure 3.35 presents the relation curve between filtration efficiency and filtration velocity for two filter papers using methylene blue particles (the mass median diameter is 0.6 μm), which was performed at Institute of HVAC of China Academy of Building Research. It is shown that efficiencies of two filter papers at low filtration velocity (below 0.2 m/s) are quite high, and both efficiencies decrease with the increase of filtration velocity. At filtration velocities 0.7 and 0.9 m/s, filtration efficiencies for synthetic fiber paper and glass fiber paper arrive at the minimum, respectively. When filtration velocities are larger than these respective critical values, both efficiencies of filter papers increase. It is shown from Figs. 3.29, 3.30, 3.31, and 3.32 that efficiency for HELA or ULPA filters will increase by an order of magnitude when filtration velocity decrease from 2.5 cm/s to half. It is not cost-effective to increase the filtration area by two times or reduce half of the flow rate. At present, the practical filtration velocity is mainly 2.5–3 cm/s.

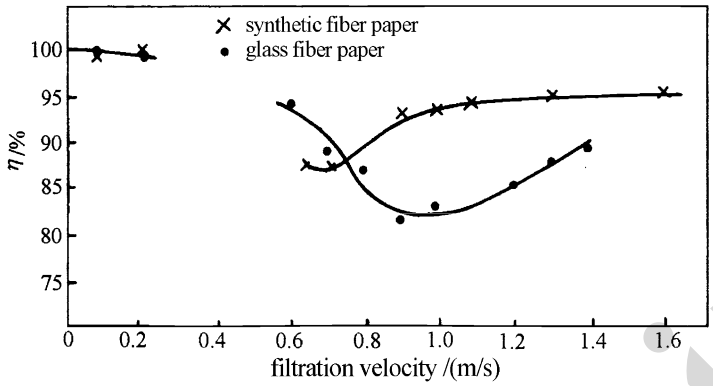

Fig. 3.35 Relationship between efficiency and filtration velocity of two filter papers

Fig. 3.36 Relationship between penetration and filtration velocity for polypropylene media

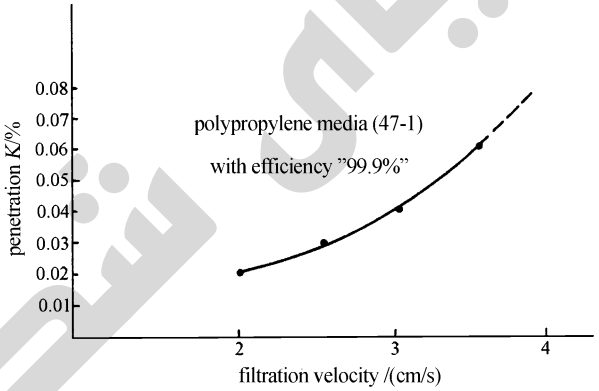

Moreover, it is shown from Fig. 3.34 that for particles with diameter 0.3 μm, the penetration of fiber layer with fiber diameter 20 μm reaches maximum when filtration velocity is larger than 1 m/s. In Fig. 3.27 we could see that for filtering particles with the same diameter, the filtration velocity corresponding to the maximum penetration reduced to 0.2 m/s for fiber layer with fiber diameter 1.5 μm.

So we could see the trend that filtration velocity corresponding to the maximum penetration for the fiber with same diameter increases with the decrease of particle size. For particles with the same diameter, the filtration velocity corresponding to the maximum penetration increases with the increase of fiber diameter.

For filtration velocity below 0.1 m/s, it is common that penetration decreases with the decrease of filtration velocity. However, this law is much obvious for particles with diameter <0.5 μm than that of >0.5 μm. This characteristic is more prominent for smaller particle size [20]. This may be caused by the intense diffusion effect of smaller particles at small filtration velocity.

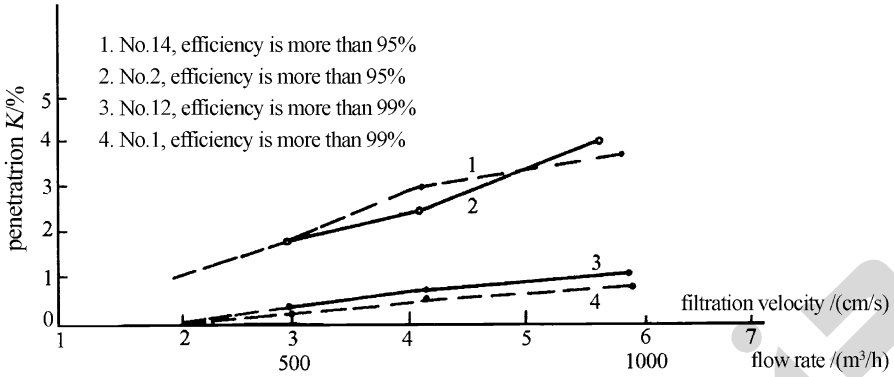

Fig. 3.37 Relationship between penetration and filtration velocity for sub-HEPA filter

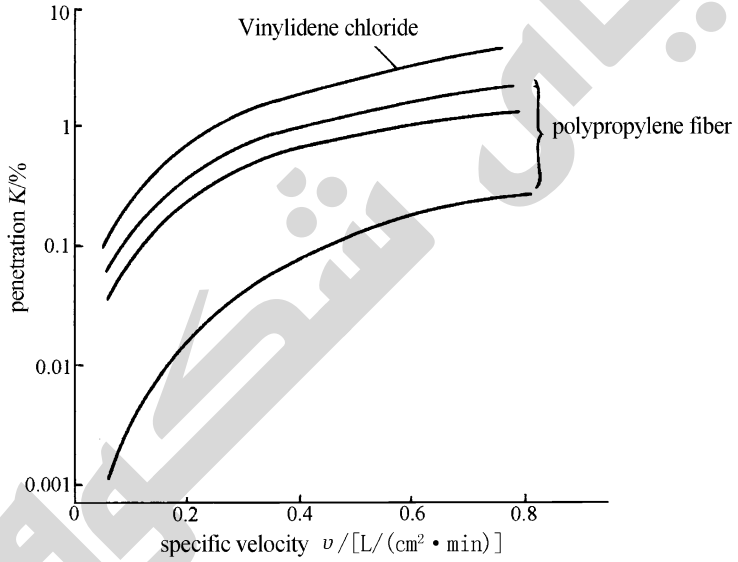

Fig. 3.38 Relationship between penetration and specific velocity (sodium flame method)

For polypropylene fibers, the relationship between penetration and filtration velocity is clear: penetration will increase four times when filtration velocity increases 2 times, which is shown in Fig. 3.36. The relationship could be expressed as $\frac{K_2}{K_1} = \left(\frac{v_2}{v_1}\right)^2$. Filters made of this kind of material have the similar conclusion, which is shown in Fig. 3.37 [28]. This law is also proved by others' experiment [23]: penetration increases by 50–100 times when filtration velocity increases by 10 times. Within the common low filtration velocity range, the change is

comparatively large. While in the range of high filtration velocity, the change is small and gradually goes towards a limit value, which is shown in Fig. 3.38.

3.8.6 Influence of Solid Fraction

Experiments [4] have shown that the relationship between solid fraction and efficiency is:

$$\text{For inertial efficiency} \quad \eta_{St} = \eta'_{St}(1 + 110\alpha) \tag{3.51}$$

$$\text{For interception efficiency} \quad \eta_R = \eta'_R(1 + 30\alpha) \tag{3.52}$$

$$\text{For diffusion efficiency} \quad \eta_D = \eta'_D(1 - 4\alpha) \tag{3.53}$$

Influence of solid fraction on total efficiency of single fiber inside filters is as shown in Eq. (3.35), i.e.,

$$\eta_\Sigma = \eta'_\Sigma(1 + 4.5\alpha)$$

It is shown that fiber layer becomes dense when solid fraction increases, which increases inertial efficiency and interception efficiency. On the contrary, since the filtration velocity inside the space between fibers increases, diffusion efficiency decreases. However, the total efficiency still increases. It should be noted that the increase speed of pressure drop is quicker than that of the total efficiency, so it is not reasonable to increase the total efficiency by increasing the solid fraction α.

3.8.7 Influence of Air Temperature

Diffusion coefficient of particles will increase with the increase of air temperature, which elevates the diffusion efficiency of submicron particles. However, air viscosity will be enlarged by the increase of air temperature, which reduces the deposition efficiency of large particles by gravitational and inertial effects and at the same time increases the pressure drop of filters.

3.8.8 Influence of Air Humidity

Penetration will increase with the increase of air humidity, which decreases the efficiency. For the filter paper made of glass fiber bound with phenol-furfural resin, experiment was performed on it to obtain the performance of bacterial capture efficiency. It is shown that the bacteria can penetrate deeper into the wet filter paper

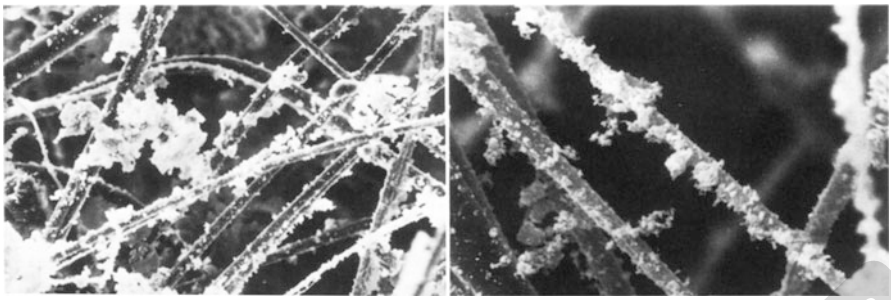

Fig. 3.39 Particle coagulation on filter medium

than into the dry filter paper [29]. When saturated water vapor goes through filters made of glass fiber paper, iron rust carried by vapor can penetrate deeper through several layers of filter papers. While dry air is used, the iron rust is only found on the surface of filter. The reason for efficiency decrease by lower humidity is that electrostatic effect disappears by wet air and Brownian motion is weakened, which makes the air carry away particles to further penetrate.

3.8.9 Influence of Airflow Pressure

The decrease of air pressure will reduce air density and enlarge mean free path of air molecules, which increase the slip correction coefficient. Both diffusion coefficient and inertial parameter will increase, so both diffusion and inertial efficiencies increase. It has little effect on the interception efficiency.

When both air temperature and pressure increase at the same time, inertial efficiency will decrease, because the influence of the increase of pressure on viscosity is larger than that of temperature.

3.8.10 Influence of Dust Holding Capacity

As the deposition process of particles on fiber surface goes on, the dust loaded on filers increases gradually, and the second stage of filtration starts. The shape of deposited particles on fibers is similar as that of deposited snow and ice crystal. They are called dendrite crystal model [30, 31]. Filtration efficiency increases with the increase of particles deposited.

In 1946 the shape of dendrite crystal on single fiber with monodisperse latex particles has been discovered. Thirty years later, the first computer model was set up for modeling two-dimensional dendrite crystal structure on circular cylinder in a microscopic scale, which is a breakthrough progress [32]. Both figures cited from

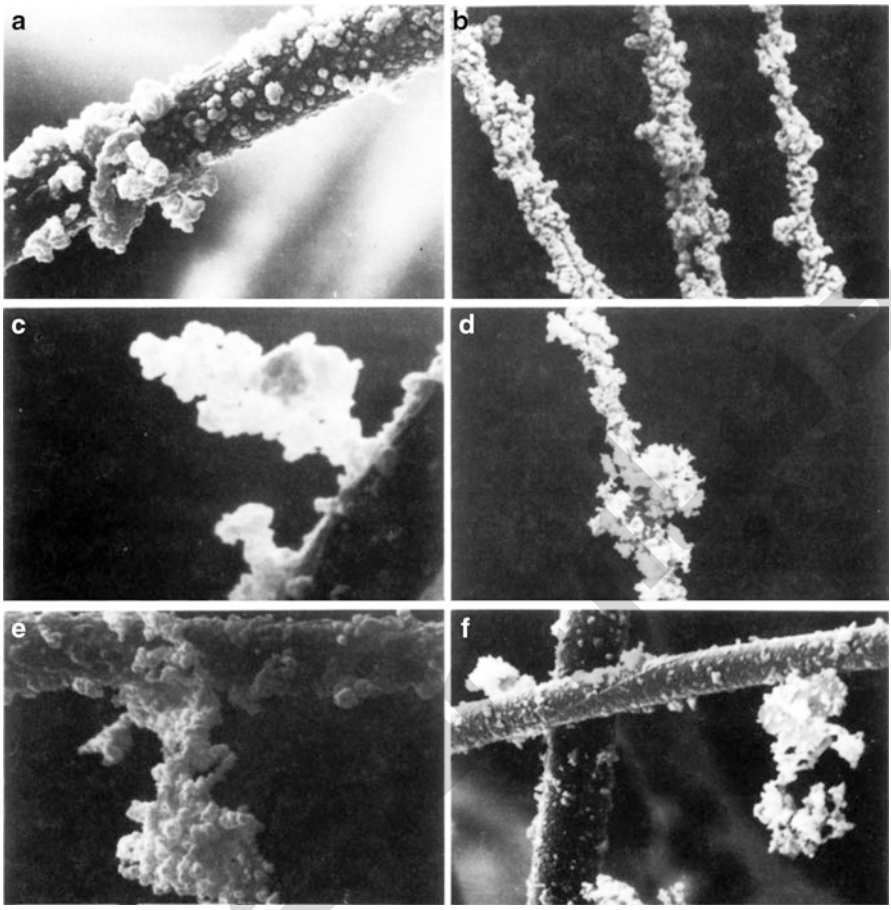

Fig. 3.40 Coagulation of deposited particles on fibers

Ref. [2] and Fig. 3.39 present this kind of dendrite crystal structure vividly for used filters. Generally forming of the dendrite crystal shape is much obvious for comparatively small fiber and comparatively large particle, which are shown in Figs. 3.39 and 3.40c–f (see Ref. [2]). It is difficult to find this kind of structure for large fiber and small particle. They are like the appearance of rough tree rind, which is shown in Fig. 3.40a, b.

If the microscopic photo of coal dust on Fig. 2.9 is understood, the forming of this kind of dendrite crystal structure will not be unimaginable.

Because of the blockage of deposited particles, both efficiency and pressure drop will increase.

But the above dendrite crystal model overestimates the increase of efficiency of used filters, so the lifetime of filters is underestimated. The reasons are as follows:

1. In this model the dendrite structure can only be formed upstream. Fibers are thought rigid, while they can bend in reality. In fact, particles captured will extend in radial direction. So when dendrite is formed along one direction, the flow path will be blocked immediately, which increases both efficiency and pressure drop suddenly and ends the lifetime of filters.
2. Flow field around fibers is assumed constant in this model. This will increase the efficiency unrealistically. Actually flow field near the captured particles will vary or increase with the increase of dust loading.
3. Resuspension of deposited particles from fiber surface is not considered.

Given the above shortcomings, dendrite fiber model was put forward, which could save the computational time [33]. In this new model, particles captured will be thought as the extra fiber added to the filter media. The problem of radial formation of dendrite structure is solved. Computers with high efficiency are used to solve the flow field. So dendrite fiber model is closer to reality than dendrite crystal model, which estimates long lifetime of filters. But the shortcoming of dendrite fiber model is that it cannot provide the figure of single dendrite structure. As for the problem of resuspension, further theoretical study is still needed.

The calculation method of efficiency and pressure drop after dust loading can be referred to Ref [2]. Although efficiency after dust loading increases, most studies of this phenomenon only have theoretical implication. In face efficiency for new filter is used for safety.

3.9 Capillary Model Theory

Fibrous filters have low solid fraction, while membrane filters have high solid fraction. There are two types of membrane filters including porous type and capillary type. Porous membrane and microporous membrane are introduced in Chap. 4. They have pore structure similar as foam plastic, where holes are linked together like network. Their performance is the same as fibrous filter when their thickness and density are the same and effective fiber diameter is slightly less than pore diameter. For example, membrane filter with pore diameter 0.8 μm is equivalent with fibrous filter with effective fiber diameter 0.55 μm. According to calculation, the pressure drop is the same as that of fibrous filter [34].

Another kind of membrane filer is Nuclepore membrane filter which will be described in detail in Chap. 4. Capillary model is more suitable to describe its performance. Pores inside Nuclepore membrane filter are independent from each other, while fibers inside fibrous filters have interference connections. In capillary model, circular parallel pores with diameter d_f are placed equidistantly. They are perpendicular to the membrane surface. The length equals with the membrane thickness. In real situation there is still a small angle between pore axis and normal direction of membrane surface, which is smaller than 15°.

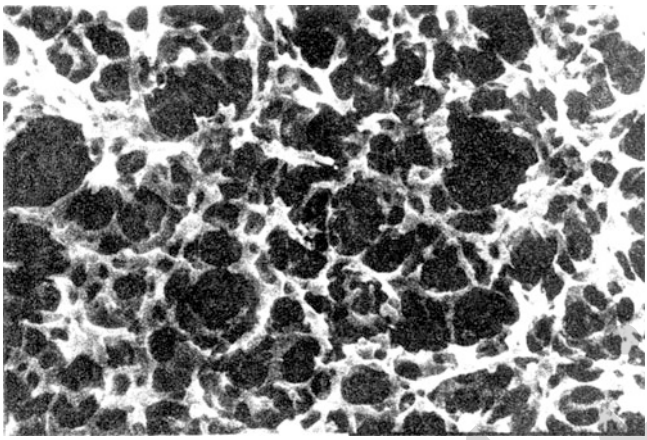

Fig. 3.41 Surface of microporous membrane

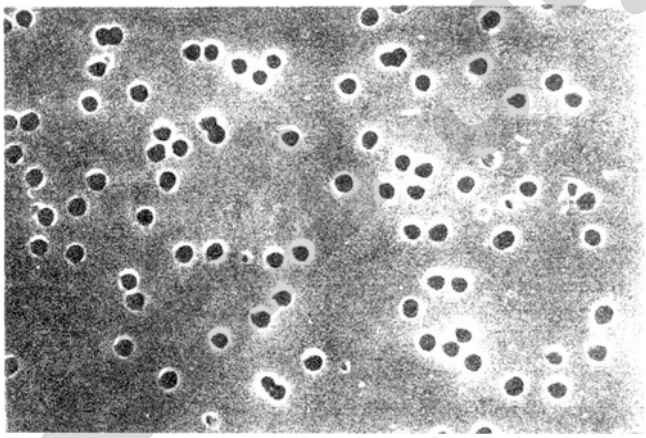

Fig. 3.42 Surface of Nuclepore membrane filter

Figures 3.41 and 3.42 are chemical microporous filter membrane and Nuclepore membrane filter, respectively [35].

Hagen-Poiseuille law is used to describe the continuum flow inside capillary [36], i.e.,

$$\Delta P = \frac{8\mu H v}{\pi r_f^4 n} \tag{3.54}$$

Correction should be considered in the range of small Knudsen number (see Table 6.3), i.e.,

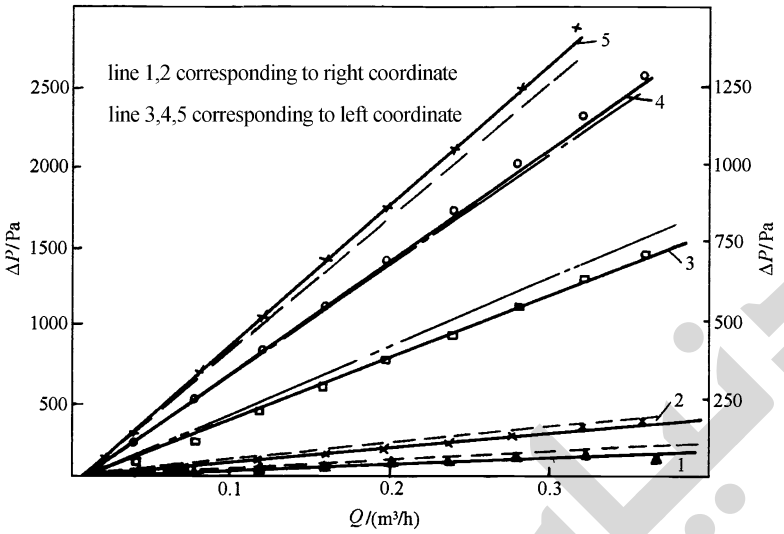

Fig. 3.43 Variation of pressure drop of Nuclepore membrane filter with filtration flow rate

$$\Delta P = \frac{8\mu H v}{\pi r_f^4 n(1 + 3.992K_n)} \tag{3.55}$$

where r_f is the pore radius, n is the pore number, and K_n is the Knudsen number, $K_n = \frac{\lambda}{r_f}$, where λ is the mean free path of air molecule.

Equation (3.55) has the similar form as Eq. (4.15). Pressure drop is proportional to the flow velocity or flow rate. Domestic experiment has shown that linear proportional relationship exists in the range of face velocity $\leq$9 cm/s, which is shown in Fig. 3.43 [37]. Pore radiuses in this figure are: (1) $\overline{r_f} = 1.3257$ μm, (2) $\overline{r_f} = 0.6695$ μm, (3) $\overline{r_f} = 0.4490$ μm, (4) $\overline{r_f} = 0.3990$ μm, and (5) $\overline{r_f} = 0.2515$ μm.

Efficiency expression based on capillary model is [38]:

$$\eta = \eta_{St} + \eta_D + 0.15\eta_R - \eta_{St} \cdot \eta_D - 0.15\eta_{St} \cdot \eta_R \tag{3.56}$$

where

$$\eta_{St} = \frac{2E_1}{1+\beta} - \frac{E_1^2}{(1+\beta)^2} \tag{3.57}$$

$$E_1 = 2St\sqrt{\beta} + 2St^2\beta e^{\left(1-\frac{1}{St\sqrt{\beta}}\right)} - 2St^2 \tag{3.58}$$

$$\beta = \frac{\sqrt{1-\alpha}}{1-\sqrt{1-\alpha}} \tag{3.59}$$

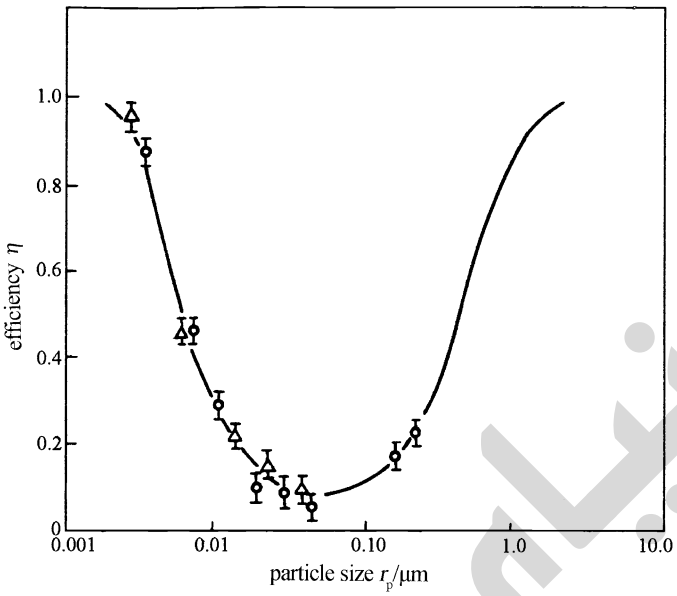

Fig. 3.44 Comparison between efficiencies of theoretical calculation and experimental data on Nuclepore membrane filter (condition: $D_f = 5$ μm, $v = 5$ cm/s)

$$St = \frac{cD_f^2 \rho_P v}{18\mu d_P} \tag{3.60}$$

Expression of St is the same as Eq. (3.7), except that D_f is the pore size, not particle size; and d_p is the particle size, not fiber size.

When dimensionless parameter $N_d = \frac{4HD}{d_P^2 v} < 0.03$,

$$\eta_D = 2.57N_d^{2/3} - 1.2N_d - 0.177N_d^{2/3} \tag{3.61}$$

where H is the pore length and D is the diffusion coefficient of particles.

When $N_d > 0.03$

$$\eta_D = 1 - 0.81904\exp(-3.6568N_d) - 0.09752\exp(-22.3045N_d) - 0.03248\exp(-56.95N_d) - 0.0157\exp(-107.6N_d) \tag{3.62}$$

$$\eta_R = 2N_r - N_r^2 \tag{3.63}$$

where N_r is the interception parameter of capillary

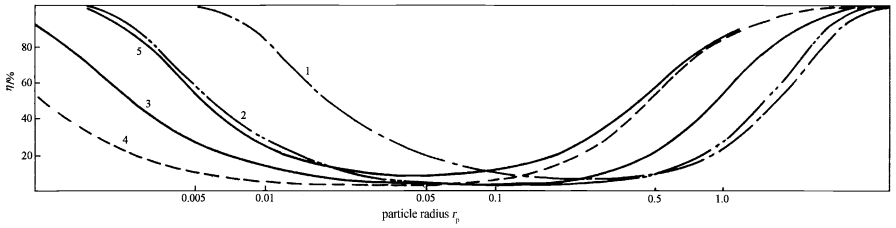

Fig. 3.45 Comparison between the theoretical calculation result from domestic researcher and the result abroad for the efficiency of Nuclepore membrane filter (condition: $D_f = 8$ μm, $\rho_p = 2{,}000$ kg/m^3, porosity is 5 %) *1*. $v = 0.1$ cm/s, *2*. $v = 1.0$ cm/s, *3*. $v = 8.0$ cm/s, *4*. $v = 16.0$ cm/s, *5*. plot with theoretical curve by Fig. 3.44

$$N_r = \frac{D_f}{d_P} \tag{3.64}$$

where D_f and d_p are defined the same as Eq. (3.60). Interception parameter R here is slightly different from the previous mentioned one. In Eq. (3.56), the parameter 0.15 was obtained by measurement with Nuclepore membrane filter. This equation usually underestimates the interception efficiency because only the flow on the pore face is considered.

Figure 3.44 presents the curve of theoretical calculation using the above equation, which fit quite well with experimental data [39]. Figure 3.45 was obtained through theoretical calculation by domestic researcher [40], from which we can see that the curve moves left with the increase of filtration velocity. The reason may be the combined effect of increased collision efficiency with decreased diffusion efficiency. Consistency between the two theoretical calculation results could be found when two curves are plotted together, which is shown in five of the latter figure.

3.10 Efficiency of Granule Air Filter

When granule air filter is used to capture particles in the airflow, the filtration mechanisms are similar as that of fibrous filter. For the convenience of reference, the total efficiency expression is given [41]:

$$\eta = 1 - \exp\left[\frac{-3\alpha L\eta'}{2d_c(1-\alpha)}\right] \tag{3.65}$$

where

η is the total efficiency of granular filling layer;
L is the thickness of granular filling layer;
d_c is the granular diameter;

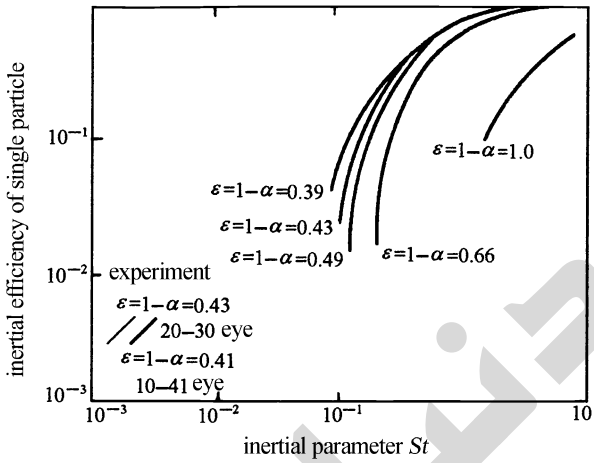

Fig. 3.46 Comparison between theory and experiment for inertial efficiency of granular filter

α is the granular solid fraction:

$$\alpha = \frac{\text{granular filling layer density}}{\text{granular material density}}$$

η' is the efficiency of single granule. The respective effect is introduced below: Diffusion efficiency is:

$$\eta'_{\mathrm{D}} = 5(K'')^{-1/3} Pe^{-2/3} \tag{3.66}$$

$$K'' = \frac{\left(2 - 3\alpha^{1/3} + 3\alpha^{5/3} - 2\alpha^2\right)}{\left(1 - \alpha^{5/3}\right)} \tag{3.67}$$

Direct interception efficiency is:

$$\eta'_R = 3R(K'')^{-1} \tag{3.68}$$

Inertial efficiency η'_{St} is determined with inertial parameter St. Numerical solution to inertial efficiency η'_{St} with St based on layer porosity $(1–\alpha)$ as a parameter is presented in Fig. 3.46. However, the difference between theoretical value and experimental data is still large.

References

1. Takizawa S (1994) Air filter in the pharmaceutical industry. J Jpn Air Clean Assoc 32 (2):28–38 (In Japanese)
2. Cai J (1992) Fibrous filters with non-ideal conditions. The Royal Institute of Technology, Stockholm, p 119
3. Niitsu Y, Yoshikawa S, Kubo T (1972) Study on the filtration of ultrafine particles. J SHASE Jpn 46(9):13–19 (In Japanese)
4. Ужов ВИ, Мягков БИ, Очистка промышленных гаэов фильтрами, Москва (1970) (In Russian)
5. Сгечкина ИБ, Кирш АА, Фукс НА, Исследования В области волокнистых Азрозольных Азрозольных фильтров, Коллоидный журнал (1969), pp 121–126 (In Russian)
6. Kouichi I, Makino K, Inoue O et al (1970) Particle capture performance of filter paper. J Chem Eng Jpn 34(6):632–637 (In Japanese)
7. Kimura N, Koichi I (1965) Particle capture efficiency of single fiber in the filling layer of glass fibrous filter. J Chem Eng Jpn 29(7):538–546 (In Japanese)
8. Yoshikawa S (1978) Air filtration – analysis case of filter structure and its application. J SHASE Jpn 52(5):47–55 (In Japanese)
9. Richard D (1981) Aerosol handbook (trans: Zhou Jinqin), pp 82–83 (In Chinese)
10. Davies CN (1952) The separation of airborne dust and particles. Proc Inst Mech Eng 1B:185
11. Yoshioka N et al (1967) Filtration of fibrous filling layer – collisional efficiency in low *Re* flow. J Chem Eng Jpn 31(32):157–163 (In Japanese)
12. Кирш АА, Стечкина ИБ, Фукс НА, Исследования В области волокнистых Азрозольных Азрозольных фильтров, Коллоидный журнал (1969) pp 227–232 (In Russian)
13. Chen CY (1955) Filtration of aerosol by fibrous media. Chem Rev 55(4):595–623
14. Kamishima K (1981) Air cleanliness level in cleanroom with 0.1μm particles as the study object. Jpn Air Condit Heat Refri News 21(5):91–99 (In Japanese)
15. Zhou B, Zhang XS (2011) Investigation of logarithmic penetration expressions for fibrous media. Build Energy Environ 30(1):63–65 (In Chinese)
16. Yoshikawa S (1978) Air filtration (1) – filter structure. J SHASE Jpn 52(4):69 (In Japanese)
17. Engle PM, Bauder CJ (1964) Characteristics and application of high performance dry filters. ASHRAE J 6(5):72–75
18. Tolliver DL (1993) Handbook of contamination control in microelectronics: principles, applications and technology (trans: Yu Aoyuan et al.), pp 29–30 (In Chinese)
19. Cheng XY, Zhang JK, Shi XC et al (1990) Penetration and the most penetrating particle size. Contamin Control Air-Condit Technol 1:17–26 (In Chinese)
20. Filtration Special Committee of Japan Nuclear Fuel Service (1980) Experimental study of the safety of HEPA filter used in nuclear fuel facilities. J Jpn Air Clean Assoc 18(3/4):2–23 (In Japanese)
21. Ventilation Committee and Subcommittee on Dust Measurement Method (1975) Measurement method of airborne particles in Buildings (2). GA JAPAN 90(1098):849–866 (In Japanese)
22. Liu BYH, Lin B (1987) Performance test of domestic air sampler and high efficiency filter media. Contamin Control Air-Condit Technol 3:9–14 (In Chinese)
23. Zhang JK, Ouyang T, Cheng XY (1986) Performance of polypropylene fibrous filter media. In: Proceedings of the second annual academic conference by Chinese Contamination Control Society, pp 157–161 (In Chinese)
24. Fan CY, Lin ZP (1994) Properties of sub-high efficiency polypropylene filter media. Proceedings of the biennial meeting of China HVAC&R, Zhangjiajie, October 1994 pp 159–162 (In Chinese)
25. Stafford RG, Ettinger HJ (1971) Comparison of filter media against liquid and solid aerosols. Am Ind Hyg Assoc J 32(5):319–326
26. Kimura N, Kouichi I (1969) Particle capture performance of fibrous filling layer filter and influence of fiber cross sectional shape. J Chem Eng Jpn 33(10):1008–1013 (In Japanese)

27. Emi H (1975) Particle capture efficiency of air filter. Chem Ind 19(3):209–215 (In Japanese)
28. Xu ZL, Shen JM (1987) YGG and YGF type low resistance sub-high efficiency air filter. Research report of Building Science, China Academy of Building Science Research, 5–2 (In Chinese)
29. Huang ZL, Hui CR (1979) No. 1 soft leather treatment agent for treating with ultra-fine glass fibrous paper for air filtration. Chin J Antibiot 4(4):15–17
30. Payatakes AC (1976) Model of aerosol particles deposition in fibrous media with dendrite-like pattern-application to pure interception during period of unhindered growth. Filtrat Separat 13 (6):602–608
31. Kanaoka C, Emi H, Myojo T (1978) Simulation of aerosol loading process on fiber surface. Proc Soc Chem Eng Jpn 4(5):535–537 (In Japanese)
32. Cai J (1992) Fibrous filters with non-ideal conditions. The Royal Institute of Technology, Stockholm, 2992, p 137
33. Cai J (1992) Fibrous filters with non-ideal conditions. The Royal Institute of Technology, Stockholm, 2992, pp 195–218
34. Hinds WC (1989) Aerosol technology (trans: Sun Yufeng, Chapter 9). Heilongjiang Science and Technology Press, Harbin (In Chinese)
35. Shi XC (1986) Study of nuclepore membrane filter structure and its filtration performance. Tsinghua University, p 11 (In Chinese)
36. Tolliver DL (1993) Handbook of contamination control in microelectronics: principles, applications and technology (trans: Yu Aoyuan et al.), pp 37–38 (In Chinese)
37. Shi XC (1986) Study of nuclepore membrane filter structure and its filtration performance (Master dissertation). Tsinghua University, p 13 (In Chinese)
38. Tolliver DL (1993) Handbook of contamination control in microelectronics: principles, applications and technology (trans: Yu Aoyuan et al.), China Aerospace Architectural Design Academy, pp 39–40 (In Chinese)
39. Tolliver DL (1993) Handbook of contamination control in microelectronics: principles, applications and technology (trans: Yu Aoyuan et al.), p 41 (In Chinese)
40. Shi XC (1986) Study of nuclepore membrane filter structure and its filtration performance (Master dissertation). Tsinghua University, p 52 (In Chinese)
41. Richard D (1981) Aerosol handbook (trans: Zhou Jinqin). Atomic Energy Press, Beijing, pp 83–84 (In Chinese)

Chapter 4
Characteristics of Air Filters

Air filter is the main equipment in the field of air cleaning technology, and it is an indispensible equipment to create the clean air environment. So it is necessary to know the characteristic of air filters and its design principle so as to use it correctly and effectively.

4.1 Function and Classification of Air Filtration System

In 1992 and 1993, China has issued two national standards "Air Filters" (GB/T 14295-93) and "High-Efficiency Particulate Air Filter" (GB13554-92), respectively. They are revised in 2008.

According to GB/T 14295-2008, air filters could be divided into four types, shown in Table 4.1.

According to GB13554-2008, high-efficiency air filters could be divided into HEPA filter and ULPA filter, which are shown in Tables 4.2 and 4.3.

According to standard, HEPA filter product must pass the leakage test before delivery. The test method and judgment criterion are presented in Table 4.4.

Coarse Air Filter. It is mainly used as prefilter to capture large particles and prevent them from entering the system, especially these airborne particles with diameter larger than 5 μm, settling particles larger than 10 μm and various foreign materials.

Medium-Efficiency Air Filter. Since roughing air filter has been placed to filter large particles, medium-efficiency air filter can be used as the final filter in general ventilation system and prefilter for HEPA filter. It is mainly used to capture airborne particles with diameter between 1 and 10 μm.

High-Efficiency Filter. It is used as final filter for ordinary cleaning ventilation system and as intermediate filter to protect HEPA filter and improve the cleanness of supply air. It is mainly used to capture airborne particles with diameter between 1 and 5 μm.

Z. Xu, *Fundamentals of Air Cleaning Technology and Its Application in Cleanrooms*,
DOI 10.1007/978-3-642-39374-7_4, © Springer-Verlag Berlin Heidelberg 2014

Table 4.1 Efficiency and pressure drop of air filters at nominal airflow rate

	Index					
Type	Label	Face velocity (m/s)	Efficiency with nominal flow rate (E) (%)		Initial resistance with nominal flow rate ($\triangle P_i$) (Pa)	Final resistance with nominal flow rate ($\triangle P_t$) (Pa)
Sub-high efficiency	YG	1.0	Particle size ≥0.5 μm	$99.9 > E \geq 95$	≤120	240
High and medium efficiency	GZ	1.5		$95 > E \geq 70$	≤100	200
Medium efficiency 1	Z1	2.0		$70 > E \geq 60$	≤80	160
Medium efficiency 2	Z2			$60 > E \geq 40$		
Medium efficiency 3	Z3			$40 > E \geq 20$		
Coarse 1	C1	2.5	Particle size ≥2.0μm	$E \geq 50$	≤50	100
Coarse 2	C2			$50 > E \geq 20$		
Coarse 3	C3		Arrestance efficiency with standard artificial dust	$E \geq 50$		
Coarse 4	C4			$50 > E \geq 10$		

Note: When the measured efficiency value meets the requirement for two types at the same time, the higher type is used for assessment

Table 4.2 Performance of HEPA filter

	Efficiency with sodium flame method under nominal flow rate	Efficiency with sodium flame method under 20 % of nominal flow rate	Resistance under nominal flow rate
Type	%	%	Pa
A	$99.99 > E \geq 99.9$	No requirement	≤190
B	$99.999 > E \geq 99.99$	99.99	≤220
C	$E \geq 99.999$	99.999	≤250

Table 4.3 Performance of ULPA filter

	Particle counting efficiency under nominal flow rate	Resistance under nominal flow rate	Comment
Type	%	Pa	
D	99.999	≤250	Scanning leakage detection
E	99.9999	≤250	Scanning leakage detection
F	99.99999	≤250	Scanning leakage detection

Table 4.4 Judgment criterion of unqualified leakage for air filter with qualitative and quantitative tests

Type	Efficiency at nominal flow rate %	Local leakage limit with qualitative test, sampling period	Local leakage limit with quantitative test %
A	99.9 (sodium flame method)	Downstream particle sampling count for diameter ≥0.5 μm is ≥3 pc/min (corresponding upstream concentration must ≥3 × 10^4pc/L)	1
B	99.99 (sodium flame method)		0.1
C	99.999 (sodium flame method)		0.01
D	99.999 (particle counting method, 0.1–0.3 μm)	Downstream particle sampling count for diameter ≥0.1 μm is ≥3 pc/min (corresponding upstream concentration must ≥3 × 10^6pc/L)	0.01
E	99.999 9 (particle counting method, 0.1–0.3 μm)		0.001
F	99.999 99 (particle counting method, 0.1–0.3 μm)		0.0001

Sub-high-Efficiency Particulate Air Filter. It is used as final filter in the cleanroom to obtain a certain class of air cleanness (please refer to Chap. 7), prefilter for HEPA filter to further improve the cleanness of supply air, and final filter of fresh air system to improve the fresh air quality. It is mainly used to capture submicron particles with diameter less than 1 μm, which is similar as that of high-efficiency filter.

HEPA Filter. It is mainly used as final filter in cleanroom. The purpose is to provide various cleanness classes corresponding to 0.5 μm, while its efficiency is usually tested with particle diameter 0.3 μm. If cleanness class corresponding to 0.1 μm is needed, its efficiency should be tested with particle diameter 0.1 μm and it is called ULPA filter. It is usually used as the final filter.

There are several types of roughing air filters and medium-efficiency air filters, such as panel-type air filter, bag air filter, and folded media-type filter. It's better to choose air filters with larger filtration area.

There are several types of high-efficiency filters, such as bag filter, cartridge air filter, and folded media-type filter.

There are several types of sub-high-efficiency particulate air filters, such as cartridge air filter and folded media-type filter. The former is a type of low-pressure drop, which is a patent product of Institute of HVAC of China Academy of Building Research.

There are several types of HEPA filters, such as folded media-type filter which could be classified as separator HEPA filter and no-separator HEPA filter.

Tables 4.5, 4.6, 4.7, and 4.8 are four examples of foreign standards. Related test methods are illustrated in Chap. 17.

Table 4.5 IEST-RP-CC001.4-2005

Test with photometer (test aerosol with mass median diameter 0.3 μm and count median diameter <0.2 μm)	Filtration efficiency	Leakage detection	Test with particle counting method (0.1–0.2/0.2–0.3 μm)
Grade A	≥99.97 %	Leakage detection not needed	Grade H
Grade B		Test efficiency with two flowrates	Grade I
Grade E		Test efficiency with two flowrates for nuclear application	
Grade C	≥99.99 %	Leakage detection needed	Grade J
	≥99.995 %	Leakage detection needed	Grade K
Grade D	≥99.999 %	Leakage detection needed	Grade F
	≥99.9999 %	Leakage detection needed	Grade G (MPPS efficiency)

Table 4.6 Minimum efficiency reporting value (MERV) parameters in US ASHRAE Standard

ASHRAE 52.2 MERV	Composite average particle size efficiency (%) Range 1 0.3–1.0 m	Range 2 1.0–3.0 m	Range 3 3.0–10.0 m	Average arrestance (%), by ASHRAE 52.1–1992	Minimum final resistance (Pa)
1	–	–	$E_3 < 20$	$A_{avg} < 65$	75
2	–	–	$E_3 < 20$	$65 \leq A_{avg} < 70$	75
3	–	–	$E_3 < 20$	$70 \leq A_{avg} < 75$	75
4	–	–	$E_3 < 20$	$75 \leq A_{avg}$	75
5	–	–	$20 \leq E_3 < 35$	–	150
6	–	–	$35 \leq E_3 < 50$	–	150
7	–	–	$50 \leq E_3 < 70$	–	150
8	–	–	$70 \leq E_3$	–	150
9	–	$E_2 < 50$	$85 \leq E_3$	–	250
10	–	$50 \leq E_2 < 65$	$85 \leq E_3$	–	250
11	–	$65 \leq E_2 < 80$	$85 \leq E_3$	–	250
12	–	$80 \leq E_2$	$90 \leq E_3$	–	250
13	$E_1 < 75$	$90 \leq E_2$	$90 \leq E_3$	–	350
14	$75 \leq E_1 < 85$	$90 \leq E_2$	$90 \leq E_3$	–	350
15	$85 \leq E_1 < 95$	$90 \leq E_2$	$90 \leq E_3$	–	350
16	$95 \leq E_1$	$95 \leq E_2$	$95 \leq E_3$	–	350
17	≥99.97 (0.3 μm)	–	–	–	–
18	≥99.99 (0.3 μm)	–	–	–	–
19	≥99.999 (0.3 μm)	–	–	–	–

Table 4.7 Classification of air filters according to European EN779 Standard

Standard	EN779:2002		EN1822-1:2007
Specification	Arrestance (%)	Particle counting efficiency at 0.4 μm (%)	MPPS efficiency (%)
G1	$50 \leq A_m < 65$		
G2	$65 \leq A_m < 80$		
G3	$80 \leq A_m < 90$		
G4	$90 \leq A_m$		
F5		$40 \leq E_m < 60$	
F6		$60 \leq E_m < 80$	
F7		$80 \leq E_m < 90$	
F8		$90 \leq E_m < 95$	
F9		$95 \leq E_m$	
E10			$85 \leq E < 95$
E11			$95 \leq E < 99.5$
E12			$99.5 \leq E < 99.95$
H13			$99.95 \leq E < 99.995$
H14			$99.995 \leq E < 99.999\ 5$
U15			$99.999\ 5 \leq E < 99.999\ 95$
U16			$99.999\ 95 \leq E < 99.999\ 995$
U17			$99.99\ 995 \leq E$

Table 4.8 International standard ISO-29463-2011

Efficiency (%)	Most penetrating particle size method (MPPS)	
99.95	ISO 35(H)	
99.99	ISO 40(H)	ISO 40(U) (leakage detection with scanning method is needed)
99.995	ISO 45(H)	ISO 45(U) (leakage detection with scanning method is needed)
99.999		ISO 50(U) (leakage detection with scanning method is needed)
99.9995		ISO 55(U) (leakage detection with scanning method is needed)
99.9999		ISO 60(U) (leakage detection with scanning method is needed)
99.99995		ISO 65(U) (leakage detection with scanning method is needed)
99.99999		ISO 70(U) (leakage detection with scanning method is needed)
99.999995		ISO 75(U) (leakage detection with scanning method is needed)

Note: *H* and *U* represent HEPA filter and ULPA filter, respectively

Different test methods of air filter efficiency exist in various national standards. For the convenience of comparison, Table 4.9 presents the comparison between air filter standards home and abroad. This kind of comparison is only for information and may not match well, so care should be taken before selection of air filters.

The foreign classification methods for general ventilation air filters are quite confusing, which will not be introduced here [1].

Since 1993, IEST classified HEPA filters into two categories. One is HEPA filter, and the other is ULPA filter. Afterwards these terms are used frequently.

Table 4.9 Comparison of main air filter standards home and abroad

China standard	EUROVENT 4/9	ASHRAE arrestance (%)	ASHRAE dust spot efficiency (%)	USA DOP efficiency (0.3 μm)	EN779	EN1822	DIN 24185	ASHRAE MERV
Coarse filter 4	EU1				G1		A	1
Coarse filter 3	EU1	<65			G1		A	2–4
Coarse filter 2	EU2	65–80			G2		B1	5–6
Coarse filter 1	EU3	80–90			G3		B2	7–8
Medium filter 3	EU4	≥90			G4		B2	9–10
Medium filter 2	EU5		40–60		F5		C1	11–12
Medium filter 1	EU6		60–80	20–55	F6		C1/C2	13
High-efficiency filter	EU7		80–90	55–60	F7		C2	14
High-efficiency filter	EU8		90–95	65–70	F8		C3	15
High-efficiency filter	EU9		≥95	75–80	F9		–	15
Sub-HEPA filter	EU10			>85		H10	Q	16
Sub-HEPA filter	EU11			>98		H11	R	16
HEPA filter A	EU12			>99.9		H12	R/S	17
HEPA filter A	EU13			>99.97		H13	S	17
HEPA filter B	EU14			>99.997		H14	S/T	18–19
HEPA filter C	EU15			>99.999 7		U15	T	19
HEPA filter D	EU16			>99.999 97		U16	U	–
HEPA filter E–F	EU17			>99.999 997		U17	V	–

4.2 Performance Index of Air Filtration

The most important four indexes to evaluate the performance are face velocity (or filtration velocity), efficiency, pressure drop, and dust holding capacity.

There are also other indexes, such as weight, energy consumption, and regeneration feature, which are mainly related to filter media. It is important to choose which kind of filter media is used to make air filters. Except for the impacting factor of filter media, filter structure is also one of the important impacting determinants for the performance of air filters. For example, both the pressure drop and dust holding capacity are different, when the same filter media is used to make panel filter, bag filter, or wedge filter. So it is another important link to find reasonable optimal structure for air filter. These four performance indexes are introduced in the following section.

4.3 Face Velocity and Filtration Velocity

Both face velocity and filtration velocity can be used to describe the ability of airflow through the air filter.

Face velocity is defined as the airflow velocity passing the cross section of air filter (m/s), i.e.,

$$u = \frac{Q}{F \times 3,600} \tag{4.1}$$

where

Q is the flow rate, m^3/h;
F is the cross-sectional area of air filter or frontal area, m^2.

So face velocity represents the passing capacity and installed area of air filter. The larger the face velocity is, the less the occupied area is. Therefore, face velocity is an important parameter to reflect the structural characteristic of air filter.

Filtration velocity is defined as the airflow velocity passing the area of filter media, and it is expressed with the unit $L/(cm^2 \cdot min)$ or cm/s, i.e.,

$$v = \frac{Q \times 10^3}{f \times 10^4 \times 60} = 1.67\frac{Q}{f} \times 10^{-3}\,\mathrm{L}/\left(\mathrm{cm}^2 \cdot \mathrm{min}\right) \tag{4.2}$$

$$v = \frac{Q \times 10^6}{f \times 10^4 \times 3,600} = 0.028\frac{Q}{f}\,\mathrm{cm/s} \tag{4.3}$$

where f is the net area of filter media, i.e., the subtraction of binder area from the total area, m^2.

During the sample test on filter media, the unit of v is $L/(cm^2 \cdot min)$, while it is cm/s for the sample test on air filter. The multiplication of the former value with 16.6 equals with the latter value.

Filtration velocity represents the ability of passing airflow of filter media, especially the filtration performance of filter media. Generally speaking, the smaller the filtration velocity is, the higher the efficiency is. When the allowed filtration velocity of filter is smaller, the pressure drop of filter media is larger.

For given structure of filter, the nominal flow rate can be used to reflect both face velocity and filtration velocity. With the same area of cross section, the larger allowed nominal flow rate is preferred. When the air filter is operated under lower flow rate, the efficiency increases and the pressure drop decreases.

4.4 Efficiency

Filtration performance of air filters can be described with efficiency, penetration, and decontamination factor.

4.4.1 Efficiency

When weight concentration is used to describe the particle concentration in the airflow, performance is evaluated with arrestance. When particle counting concentration is used, performance is evaluated with particle counting efficiency. When other physical parameter is used, performance is evaluated with dust spot efficiency or turbidity efficiency.

1. To describe the efficiency with particle concentrations at both the inlet and outlet airflow, i.e.,

$$\eta = \frac{G_1 - G_2}{G_1} = \frac{Q(N_1 - N_2)}{N_1 Q} = 1 - \frac{N_2}{N_1} \tag{4.4}$$

where

G_1, G_2 refer to particle mass or counting number at inlet and outlet airflow (mg/h or pc/h), respectively;

N_1, N_2 refer to particle concentration at inlet and outlet airflow (mg/m^3 or pc/L), respectively;

Q is the airflow rate passing through air filter (m^3/h or L/h).

This expression is valid for both arrestance and particle counting efficiency.

2. To describe the efficiency with particle concentrations upstream of air filter and particle mass captured on air filter, i.e.,

$$\eta = \frac{G_3}{QN_1} \tag{4.5}$$

where G_3 is the particle mass captured on air filter, mg/h.

This expression is only used for arrestance. The value of η calculated by this method is termed as dust removal efficiency in some countries.

3. To describe the efficiency with particle concentrations downstream of air filter and particle mass captured on air filter, i.e.,

$$\eta = \frac{G_3}{QN_2} \tag{4.6}$$

this expression is also used to describe the arrestance.

4. To describe the efficiency with fractional efficiency corresponding to various particle size channels, i.e.,

$$\eta = \eta_1 n_1 + \cdots + \eta_n n_n \tag{4.7}$$

where

$\eta_1 - \eta_n$ is the fractional efficiency for various particle size, which is expressed in decimal;

$n_1 - n_n$ is the percentage of particles for various particle size in the total particle group, which is expressed in decimal.

It should be emphasized that which kind of method is used to obtain the efficiency when the efficiency value is mentioned. For example, when the arrestance with atmospheric dust is 98 %, it will bring misunderstanding or error when the efficiency is only said to be 98 % or the arrestance is 98 %. This will be explained in detail in Chap. 17.

4.4.2 Penetration

In most cases, people care not only how many particles are captured on air filters but also how many have penetrated through air filters. The concept of penetration (or penetrating coefficient) can be used to represent the extent of the result, although the basic meanings are the same. In the exhaust cleaning system, penetration is used to replace filtration efficiency.

It is customary to label penetration with K, i.e.,

$$K = (1 - \eta) \times 100\ \% \tag{4.8}$$

For cases of $\eta_1 = 0.9999$ and $\eta_2 = 0.9998$, the difference between them is not substantial. When penetration is used, we get $K_1 = 0.01$ % and $K_2 = 0.02$ %, which means K_2 is two times of K_1. When a filter with penetration K_2 is used, the number of particles penetrating through the filter is two times of the filter with penetration K_1. This will attract people's attention.

4.4.3 Decontamination Factor

Decontamination factor K_c is defined as the reciprocal of penetration, i.e.,

$$K_c = \frac{1}{K} \tag{4.9}$$

It means the extent of the decrease of particle concentration when air passes through filters. When $K = 0.01\ \%$,

$$K_c = \frac{100}{0.01} = 10^4$$

This means the difference between upstream and downstream of air filter is ten thousands.

4.5 Pressure Drop

4.5.1 Pressure Drop of Filter Media

Pressure drop of air filter is composed of two components: filter media and structure of air filter. Pressure drop of airflow entering and exiting air filters is usually constant, which is about 5 Pa and could be added as a fixed value. The following part will emphasize on the aforementioned two parts of pressure drop. In some literature and monograph, actually only the pressure drop of filter media layer is mentioned during the introduction of pressure drop of air filter, which will cause misconception to readers.

For fibrous filter, pressure drop of filter media is caused by the frontal resistance during the airflows through fibrous layer. Pressure drop depends on whether the airflow through fibrous layer is laminar or turbulent. Generally speaking, extreme small fiber and low filtration velocity will result in extreme small *Re* number, so airflow is laminar.

For the isolated cylinder with unit length, when its long axis is perpendicular to the airflow, the force acting on its surface is a function of the cross section and dynamic pressure, i.e.,

$$F = C' d_f v^2 \frac{\rho_a}{2} \tag{4.10}$$

where

F is the drag force, N/m;
C' is the drag coefficient;
ρ_a is the gas density, kg/m^3;
v is the filtration velocity, m/s;
d_f is the fiber diameter, m.

The drag force acting on all fibers inside filter media is FL where L is the total length of fibers. The drag force acting on all fibers inside filter media equals with the force that the filter media bears. When it is equally shared to the surface area, the pressure drop is obtained, which is expressed as ΔP and shown in Eq. (3.40).

$$\Delta P = \frac{FL}{S} = \frac{F}{S}\frac{4SH\alpha}{\pi d_f^2} = \frac{4FH\alpha}{\pi d_f^2}\ (Pa) \tag{4.11}$$

where

$4\alpha \Big/ \pi d_f^2$ is the fiber length per unit volume;

H is the thickness of filter layer;
S is the area of filter media, i.e., filtration area.

Inserting Eq. (4.10) into Eq. (4.11), we could get

$$\Delta P = \frac{2Cv^2H\alpha\rho_a}{\pi d_f}\ (\text{Pa}) \tag{4.12}$$

This is the theoretical expression of pressure drop. The problem is how to determine the drag coefficient C'. Because the value of C' is related to the arrangement of fibers, solid fraction and Re number, it is impossible to obtain the relationship between ΔP and every parameter directly. Therefore, experiment needs to be carried on. Results from experiment on the five obvious factors show that [2]:

1. When filtration velocity v varies and other parameters are fixed, the following relationship exist in large range:

$$\Delta P \propto v$$

i.e.,

$$3\ \text{cm/s} < v < 5\ \text{cm/s} \quad \Delta P \propto v^{0.7}$$

$$5\ \text{cm/s} < 19\ \text{cm/s} \quad \Delta P \propto v^{1.0}$$

$$40\text{cm/s} < v < 200\text{cm/s} \quad \Delta P \propto v^{1.2\tilde{}1.3}$$

2. During the measurement of pressure drop of filter media for different thickness, we get

$$\Delta P \propto H$$

3. When solid fraction α varies and both v and H are fixed, we get

$$\Delta P \propto \alpha_2^m$$

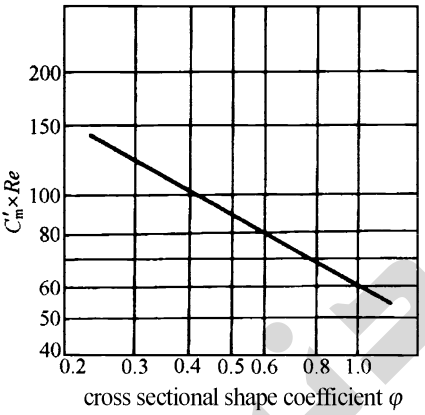

Fig. 4.1 Relationship between cross-sectional shape and drag coefficient

Experiment on fibrous filters shows that

$$m_2 = 1.3 d_f^{-0.05}$$

4. For given cross section, the effect of fiber size on ΔP is

$$\Delta P = d_f^{-2}$$

5. The effect of cross section could be obtained from Eq. (4.12):

$$\pi d_f \Delta P = 2C' v^2 H \alpha^{m_2} \rho_a$$

It is known that $\Delta P \propto \alpha^{m_2}$, so replace α in the above equation with α^{m_2} and C' becomes C'_m, i.e.,

$$\pi d_f \Delta P = 2C'_m v^2 H \alpha^{m_2} \rho_a$$

$$C'_m = \frac{\pi d_f \Delta P}{2 v^2 H \alpha^{m_2} \rho_a} \tag{4.13}$$

With the experiment on fibers with different cross section and different Re number, the relationship shown as the straight line in Fig. 4.1 could be obtained, i.e.,

$$C'_m = \frac{k}{\mathrm{Re}\varphi^{\beta}} \tag{4.14}$$

where

C'_m is the correction factor of pressure drop when influencing factors such as cross-sectional shape are considered while the influence of α is ignored;
$k = 60$;

$\beta = 0.58$;
φ is the cross-sectional shape coefficient of fiber

$$\varphi = \frac{\text{Cross sectional area of fiber}}{\text{Area of circumcircle for the cross section of fiber}}$$

Values of φ for various fibers are:

Cellulose acetate	0.3–0.52 (average 0.42)
Glass fiber	1.0
Chloride vinylon	0.61
Polyamide	1.0
Polypropylene	1.0
Polyester	1.0
Vinylon	0.4
Propylene	1.0

Inserting Eq. (4.14) into Eq. (4.13), we could get:

$$\Delta P = \frac{120\mu v H \alpha^{m_2}}{\pi d_f^2 \varphi^{0.58}} \text{ (Pa)} \tag{4.15}$$

In this equation, the relationship between ΔP and every parameter is consistent with the experimental results. For example, ΔP of filter media is linearly proportional to filtration velocity v, filter layer thickness H, and α^{m_2}, while it is inversely proportional to d_f^2. This means the equation is valid.

According to Eq. (4.15) which is the method of Susumu and other equations by related literatures, pressure drops of three kinds of fibrous layer can be obtained, which is presented in Table 4.10. Substantial difference exists between calculated results by various methods and actual experimental data. Result given by Norio Method has the largest difference. There are many aspects for the difference, of which the accurate determination of every parameter is also important. It is comparatively easy to calculate by Eq. (4.15), while it is complex to use other two methods which will not be introduced in detail here.

4.5.2 Total Pressure Drop of Air Filter

For given air filter, the filter media is chosen, so H, α, d_f, and φ are fixed. Equation (4.15) can be simplified as

$$\Delta P = Av \tag{4.16}$$

This means for given particles, pressure drop is linearly proportional to filtration velocity in quite large range of filtration velocity, where A is a structural coefficient to reflect the structural characteristic of fibrous layer. Figure 4.2 presents the experimental results on several kinds of fibrous filter media about the relationship

Table 4.10 Calculation of pressure drop of fibrous layer

								Calculated ΔP (Pa)			Measured ΔP (Pa)	
Fiber	d_f (μm)	α	m_2	H (m)	v (m/s)	φ	μ at 20 °C/ Pa·s	Eq. (4.15)	Chen method [3]	Norio method [4]	Pa	Tester
Glass fiber	14–18 (average 16)	0.037	1.393	0.02	0.28	1	1.83×10^{-5}	151	95	134	147	Institute of HVAC at China Academy of Building Research
Glass fiber	4	0.0048	1.493	0025	0.50	1	1.83×10^{-5}	188	239	560	261	Institute of HVAC at Tianjin University [5]
	4	0.0048	1.493	0.013	0.50	1	1.83 × 10-5	98	124	291	149	
	4	0.0032	1.493	0.025	0.50	1	1.83×10^{-5}	103	146	372	150	
	4	0.0032	1.493	0.013	0.50	1	1.83×10^{-5}	54	75	194	84	
Polypropylene fiber	5	0.055	1.476	0.015	0.20	1	1.83×10^{-5}	116	93	100	162	

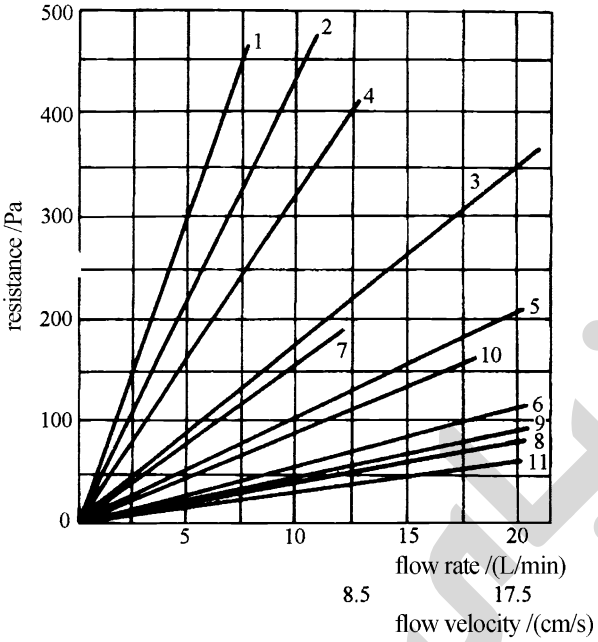

Fig. 4.2 Pressure drops of various filter media: *1* foreign AEC filter medium, *2* 25 wire glass fibrous filter paper, *3* synthetic fibrous filter paper, *4* 20 wire glass fiber filter paper, *5* ФIIII-15 cloth, *6* synthetic fiber No. IV filter paper, *7* eight wire glass fibrous filter paper, *8* synthetic fiber No. 1 filter paper; *9* synthetic fiber No. II filter paper; *10* five wire glass fibrous filter paper, *11* chemical microporous membrane

between pressure drop and filtration velocity, which was done at Institute of HVAC of China Academy of Building Research.

Figures 4.3, 4.4, and 4.5 give experimental results for nonwoven coarse filter media, medium-efficiency air filter media, and sub-high-efficiency particulate air filter media [6].

In these figures there are "front and rear." Fibers near the front side are relatively large. Inside the coarse filter media, fibers are inherently large and spaces between fibers are loose, so difference is small between front and rear. Inside medium-efficiency air filter media, fibers near the rear are relatively dense and they will interference with the airflow. Sub-high-efficiency particulate air filter media used here is not only polypropylene fiber filter paper, but it is composed of prefilter layer, main filter layer, and enhanced gauze. When the enhanced gauze is placed windward and leeward, the function of preventing filter media from stretching and deformation is different, so the resultant pressure drops are different. For common polypropylene fiber filter paper without enhanced gauze, the difference is not obvious.

From above figures, we could see that for high-efficiency filter media, v is below 0.2 m/s; for sub-high-efficiency particulate air filter media, v is below 0.5 m/s; for medium-efficiency air filter media, v is below 0.8 m/s; and for coarse filter media, v is below 1.2 m/s.

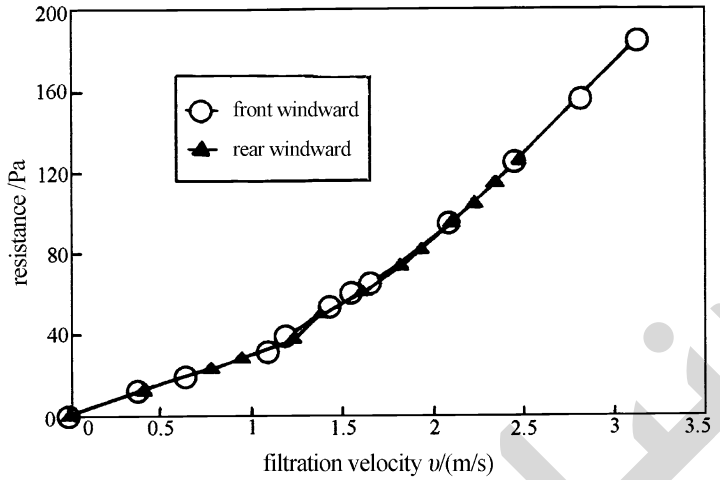

Fig. 4.3 Relationship between pressure drop and filtration velocity for coarse filter media

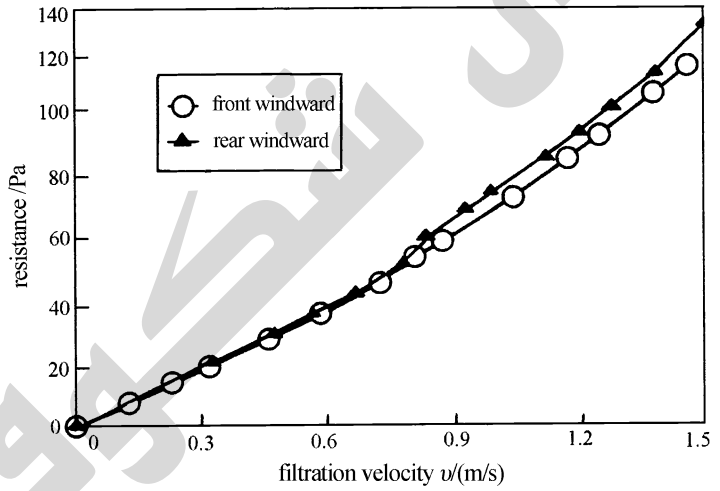

Fig. 4.4 Relationship between pressure drop and filtration velocity for medium-efficiency air filter media

For these four situations, the following approximated relationship is valid, even the filtration velocity is larger than the limit:

$$\Delta P \propto v$$

Except for the pressure drop of filter medium, structural pressure drop of air filter must be added to form the total pressure drop of air filter, where pressure drop of inlet and outlet of airflow occupies very small proportion. There is one view that except for

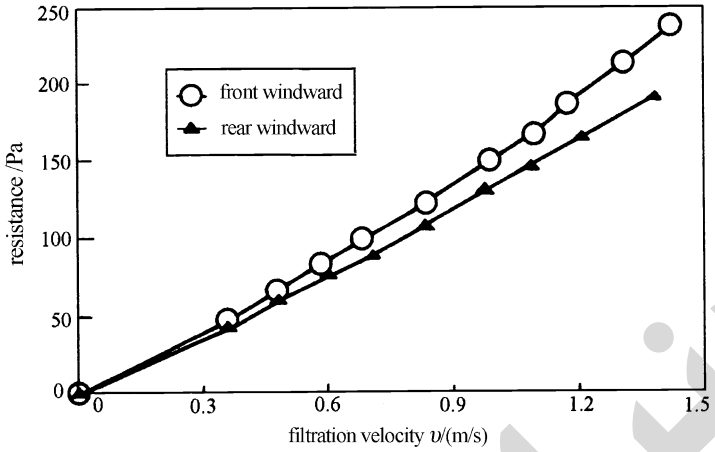

Fig. 4.5 Relationship between pressure drop and filtration velocity for sub-high-efficiency particulate air filter media

the inherent structure of air filter, pressure drop of structure is also affected by filter media performance. The penetrating performance of filter media may influence the flow state passing through air filter; thus, the pressure drop of structure is affected. This view needs further experimental validation. Experiments show that pressure drop of structure is no longer linearly proportional to the airflow velocity. The main reason to nonlinear relationship is that face velocity u is used to describe the airflows through filter frame, which has the magnitude of m/s and is much larger than the filtration velocity passing through filter media layer. The structural size of filter frame is much larger than that of fiber, so inertial force cannot be ignored at large Re number flow (usually $Re > 1$), and the flow is not laminar. In this situation, pressure drop is not linearly proportional to the velocity but is proportional to u^n. Therefore, pressure drop of air filter structure can be expressed as

$$\Delta P_2 = Bu^n \tag{4.17}$$

where B is the drag coefficient of air filter structure. The total pressure drop of air filter is:

$$\Delta P = \Delta P_1 + \Delta P_2 = Av + Bu_n \tag{4.18}$$

It is obvious that values of A and B are different for different air filters. Taking a domestic-made GB-01 HEPA filter for an example, experiment shows that $n = 1.37$.

When expressed with unified filtration velocity v, the total pressure drop can be written as:

$$\Delta P = Cv^m \tag{4.19}$$

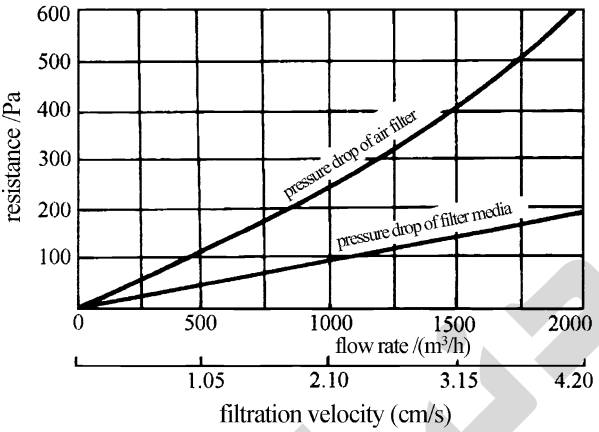

Fig. 4.6 Relationship between pressure drop and flow rate (filtration velocity) for HEPA filter

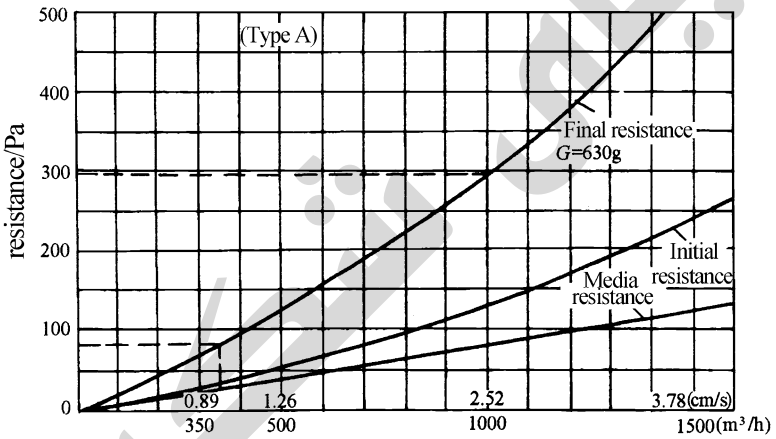

Fig. 4.7 Flow rate (filtration velocity)-pressure drop curve of type A HEPA filter

For domestic-made HEPA filter, C is between 3 and 10 and m is between 1.1 and 1.36. Figure 4.6 shows the experimental curve of pressure drop on domestic-made HEPA filter. Figures 4.7, 4.8, and 4.9 show pressure drop curves of three kinds of HEPA filters [7], from which we can see that for HEPA filter, the value of m is slightly larger than 1 when $v \geq 3$ m/s, i.e., the flow rate is slightly larger than nominal flow rate. So the resultant error will not be big when the relationship between pressure drop and flow rate is considered to be linear. Sub-high-efficiency particulate air filter has similar feature, which will be illustrated in Fig. 4.26.

However, as for coarse filter and medium-efficiency air filter, since their structures differ a lot, the above characteristic is no longer common.

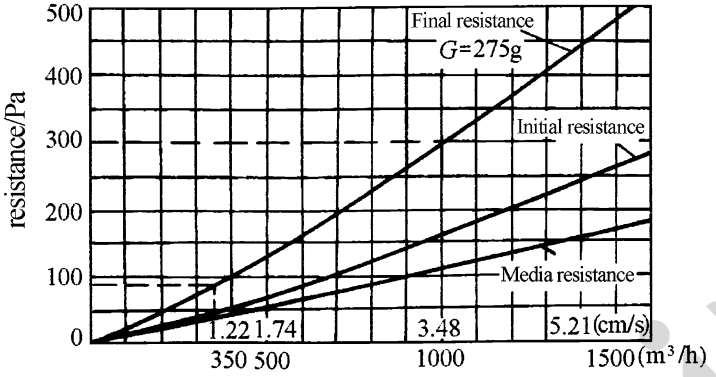

Fig. 4.8 Flow rate (filtration velocity)-pressure drop curve of type C HEPA filter

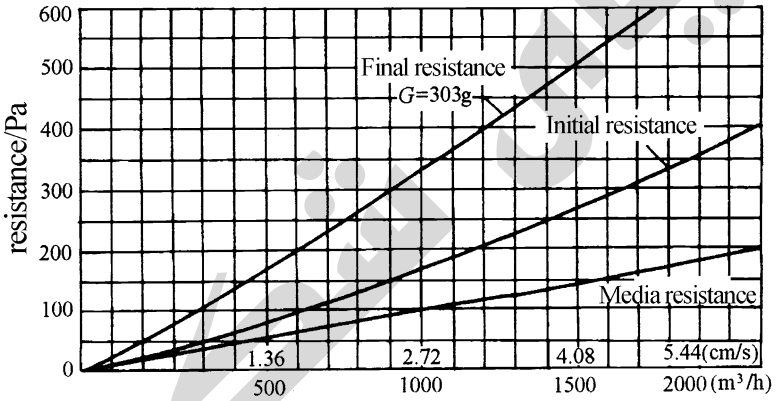

Fig. 4.9 Flow rate (filtration velocity)-pressure drop curve of type K HEPA filter

4.6 Dust Holding Capacity

Dust holding capacity is an index directly related to the lifetime of air filter. When the final pressure drop of air filter at operation is about two times of the initial pressure drop (if two times is too low, other ratio can be set), or when the efficiency becomes less than 85 % of the initial efficiency, the dust weight deposited on air filter is called the standard dust holding capacity of this air filter, which is called dust holding capacity for short.

When the flow rate is 1,000 m^3/h, the dust holding capacity of common folded nonwoven air filter is about 100 g and that of glass fibrous air filter and HEPA filter are 250–300 g and 400–500 g, respectively. Even for the same kind of air filter, dust holding capacities are different for different size.

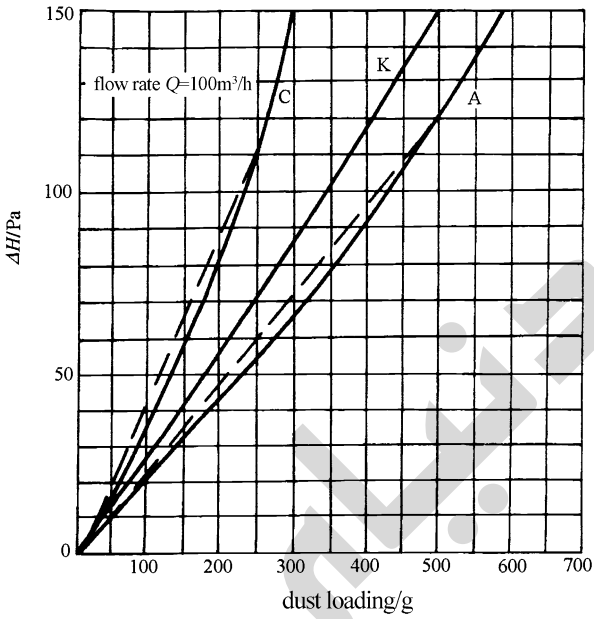

Fig. 4.10 Relationship between deposited dust and pressure drop

As the particle deposition process goes on, the pressure drop of air filter increases. But so far no accurate theoretical calculation expression for the relationship between the dust deposited and pressure drop increase exists. Next several examples are introduced.

Figure 4.10 shows the relationship between pressure drop increase and dust deposited for three kinds of HEPA filters which is mentioned before. Initial pressure drops of these three filters are 150 Pa. Dashed lines are added to the figure by us. It is shown that if the relationship is approximated with straight line, error is not large when it is below the standard dust holding capacity or the pressure drop increase is smaller than two times of initial pressure drop. The maximum difference of pressure drop for these three filters is within 10 Pa. The less the upstream concentration is, the stronger the linear relationship is. So when prefilter especially one with high efficiency is usually placed before HEPA filter, this characteristic appears. If the filtration velocity is larger than ordinary value or dust deposited weighs more than standard dust holding capacity, the pressure drop will increase sharply with the increase of the deposited dust.

The increase of pressure drop is usually linearly proportional to the increase of deposited dust for medium-efficiency air filter.

During the deposition of dust, the efficiency of filters with low efficiency will increase at first and then decrease. This is because the dust deposited is comparatively large for air filters with low efficiency and the filter medium is sparse, which will cause particles to penetrate when pressure drop increases and cause deposited particles to rebound and resuspend. During the operation of HEPA filters, efficiency usually increases with the increase of deposited dust.

4.7 Design Efficiency of Air Filter

Classification of air cleanness at home and abroad is mainly evaluated with particle number of those with diameter ≥0.5 μm per unit volume air, while various kinds of air filters are evaluated with the fractional efficiency corresponding to certain particle size. Therefore, during the design process in air cleaning technology field, efficiency of these certain particle size needs to be converted into these particles with diameter ≥0.5 μm.

Before delivery or during characterization, HEPA filter is evaluated with monodisperse particles with diameter 0.3 μm, which has been introduced in the former chapter. In order to convert into efficiency with particle diameter ≥0.5 μm, the efficiency corresponding to 0.5 μm needs to be known. According to foreign experimental data, an empirical expression has been derived for the relationship between penetration of HEPA filter and particle size [8], i.e.,

$$K_2 = \frac{K_1}{e^{(d/d_{0.3})^2}} \tag{4.20}$$

where

K_1, K_2 refer to penetration of particles with diameter 0.3 μm and certain diameter which is larger than 0.3 μm, respectively;

$d_{0.3}$, d are the particle diameter 0.3 μm and certain diameter which is larger than 0.3 μm, respectively.

The above equation was used to perform calculation on measurement data published abroad [9], which is shown in Table 4.11. In the table, K_2' and K_1 are measurement data and K_2 is the calculated data with Eq. (4.20). From the comparison between the last two columns, we can see that except for the comparatively large difference for the data on the first row, differences of other data are extreme small. This empirical equation is only valid for HEPA filter with 0.3 μm, while it is not useful for HEPA filter with 0.1 μm.

Table 4.11 Relationship of efficiencies between 0.5 and 0.3 μm (when efficiency for 0.3 μm is 0.999)

			Measurement				
d_2 (μm)	d_1 (μm)	$e^{-(d_2/d_1)^2}$	K_2'	K_1	Calculation K_2	η_2' (%)	η_2 (%)
0.5	0.3	0.0622	0.00001	0.00005	0.0000031	0.9999900	0.9999969
0.5	0.3	0.0622	0.000003	0.000025	0.0000016	0.9999970	0.9999984
0.5	0.3	0.0622	0.000001	0.00001	0.0000007	0.9999990	0.9999993
0.5	0.3	0.0622	0.00000013	0.000002	0.00000013	0.9999987	0.9999987
0.5	0.3	0.0622	0.00002	0.0003	0.00002	0.9999980	0.9999980
0.5	0.3	0.0622	0.000007	0.00007	0.0000046	0.9999930	0.9999954
0.5	0.3	0.0622	0.000007	0.000045	0.000003	0.9999930	0.9999970
0.5	0.3	0.0622	0.00000025	0.000004	0.00000026	0.9999975	0.9999974

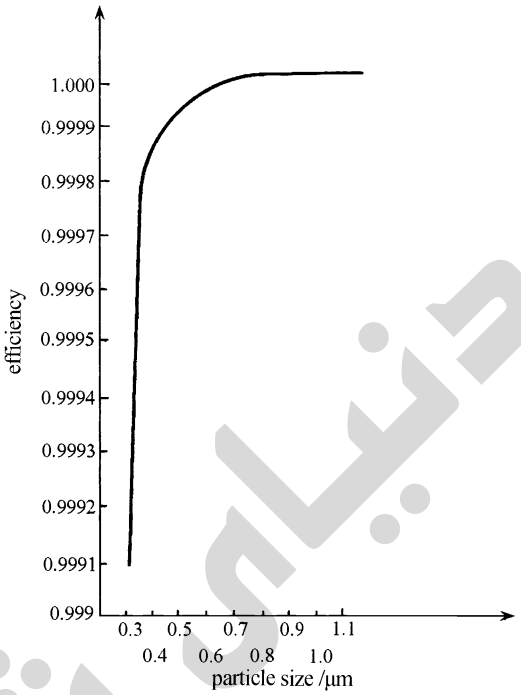

Fig. 4.11 Relationship between efficiency of HEPA filter and particle size

Although the test methods for the efficiency of HEPA filter are different at home and abroad, the results are almost consistent with that of particle counting efficiency with particle diameter 0.3 μm, which is shown in Chap. 17. Efficiency for HEPA filter with particle diameter 0.3 μm is usually considered as the reference baseline, so Eq. (4.20) is used to obtain the relationship of HEPA filter between 0.3 μm and 0.5 μm, which is shown in Fig. 4.11 for reference. Meanwhile, Fig. 4.12 shows the curve in Ref. [10], from which we can see that these results match well with each other. Efficiency η in the figure is represented with decimal.

According to the above curve and the particle diameter distribution of atmospheric dust introduced in Chap. 2, the efficiency with particle diameter $\geq$0.5 μm can be derived, which is shown in Table 4.12.

According to national standard "high-efficiency particulate air filter," filter with efficiency larger than 99.9 % is called HEPA filter. For filter with efficiency equals with 99.9 %, efficiency with particle diameter larger than 0.5 μm becomes 99.9975 %, which is shown in Table 4.12. Since efficiency of common HEPA filter is actually larger than this limit value, it is reasonable to consider efficiency of particle diameter $\geq$0.5 μm to be 99.999 %.

With the above conversion method, we compare the experimental data performed on HEPA filter in the cleaning equipment with calculated data and find they are consistent. There is no literature abroad specially dealing with this problem. In Ref. [11], it is said that "for obtaining Class 100 clean environment with all the fresh air when the particle concentration of outdoor air is about 3×10^5

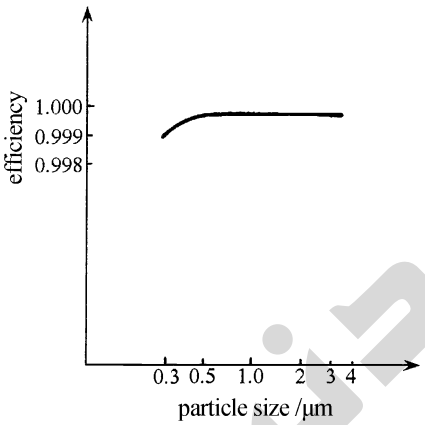

Fig. 4.12 Relationship between efficiency of HEPA filter and particle size [10]

Table 4.12 Calculated efficiency of particle diameter ≥0.5 μm (when efficiency for 0.3 μm is 0.999)

Particle size	η	Occupied proportion	Efficiency with ≥0.5 μm particles
0.5 μm	0.99994	0.33	0.3299802
0.6 μm	0.999982	0.31	0.3099950
0.8 μm	0.9999992	0.15	0.1499998
>1.0 μm	~1	0.21	0.21
			$\eta = 0.999975$

pc/L (≥0.5 μm), it's necessary to set filters with minimum efficiency 99.999 %. So HEPA filter with efficiency larger than 99.95 % is recommended to use as the main filter." Here HEPA filter with efficiency 99.95 % (for 0.3 μm) is thought to have efficiency 99.999 % with particle diameter ≥0.5 μm. For comparison, according to the above conversion method, when particle efficiency is 99.95 % for particle diameter 0.3 μm, its corresponding efficiency for particle diameter 0.5 μm becomes 99.9992 %.

Domestic-made medium-efficiency air filters include glass fibrous medium-efficiency air filter and foam medium-efficiency air filter. At present the most commonly used is nonwoven medium-efficiency air filter, which is actually a kind of fiber felt air filter.

Particle counting efficiency of glass fibrous medium-efficiency air filter ($d_f = 16$ μm, $H = 20$ mm, $\alpha = 0.037$, $v = 0.28$ m/s) with atmospheric dust was performed at Institute of HVAC of China Academy of Building Research, which is shown in Table 4.13. In the table, average efficiency corresponds with the arithmetic average diameter of atmospheric dust, and efficiency is obtained with the theoretical curve of Fig. 4.13 with this average diameter. This theoretical curve is obtained by the method of structural nonuniform coefficient. Since the grouping range of particle diameter is comparatively large, difference between average particle diameter and actual value is large. But it is shown from the table that the efficiency calculated with average particle diameter is close to the actual measured data,

Table 4.13 Particle counting efficiency with atmospheric dust for glass fibrous medium-efficiency air filter

Measurement no.	Group (μm)	Calculated mean size (μm)	Concentration (pc/L)		Efficiency (%)	
			Upstream	Downstream	Measurement	Calculation
1	0.3–1.2	~0.4	468,000	20,296	30.6	40
	1.2–2.4	~1.9	5,310	1,350	74.6	76
	2.4–4.8	~4.2	933	47	95.0	94
2	0.3–1.2	~0.4	495,000	304,300	38.4	40
	1.2–2.4	~1.9	4,550	1,780	74.4	76
	2.4–4.8	~4.2	357	60	98.3	94
3	0.3–1.2	~0.4	665,000	35,700	46.4	40
	1.2–2.4	~1.9	6,170	750	87.8	76
	2.4–4.8	~4.2	308	0	100.0	94
Average	0.3–1.2	~0.4			40.3	40
	1.2–2.4	~1.9			78.9	76
	2.4–4.8	~4.2			97.8	94

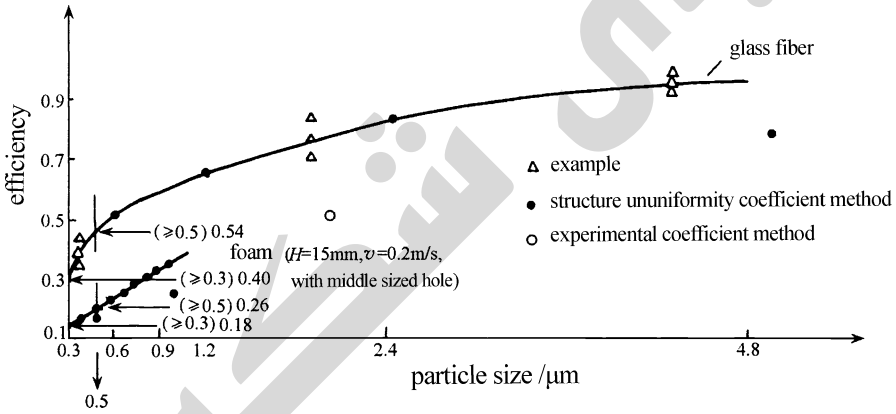

Fig. 4.13 Relationship between efficiency and particle size for medium-efficiency air filter

which is satisfactory. The calculation method has certain reference value. It is also shown from the figure that difference between calculated efficiency and experimental one is comparatively large when experimental coefficient method and the value of η'_{Σ} with Eq. (3.21) are used.

Figure 4.14 shows the experimental data of glass fibrous air filter and foam air filter at home and abroad. It is shown that the difference of efficiency between 0.5 and 0.3 μm is quite small, as well as the difference of efficiency between ≥0.5 and ≥0.3 μm. This is because filtration mechanism for medium-efficiency air filter for small particles has little difference.

From Fig. 4.14, the following approximated relationship exists when $\eta < 0.8$:

$$\begin{cases} \eta_{0.5} = 0.1 + \eta_{0.3} \\ \eta_{\geq 0.5} = 0.1 + \eta_{\geq 0.3} \end{cases} \tag{4.21}$$

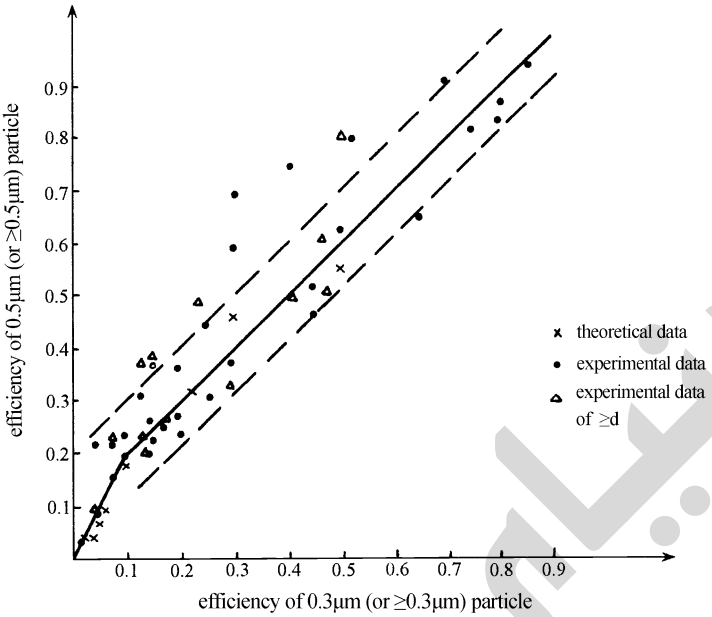

Fig. 4.14 Comparison of experimental efficiency between 0.3 and 0.5 μm (or ≥0.3 and ≥0.5 μm) for glass fiber and foam medium-efficiency air filters

4.8 Efficiency of Air Filters in Series

4.8.1 Efficiency of HEPA Filters in Series

In actual air cleaning system, filters are usually placed in series. Here the efficiency of air filters in series is emphasized.

In filtration theory, for filtering polydisperse aerosol with the same kind of air filter (e.g., they are all fibrous medium-efficiency air filter or HEPA paper filter), the penetration of second air filter should be larger than that of the first one, i.e., the efficiency of second air filter decreases. This is resulted from the selectivity of particles by filter medium, which has been introduced before. In short, mainly because the filtration mechanism for different particles is different, the dispersity of particles after the first air filter varies, which results in the change of total efficiency for the second air filter.

From Eq. (4.7) to derive the efficiency corresponding to various particle diameters, we can see that in order to calculate the efficiency of second air filter, the particle size distribution after the first filter and efficiency of various filers for different particle size must be known. These two problems have been solved, so detailed calculation can be made. Table 4.14 presents the calculation results for two HEPA filters in series (when the atmospheric dust concentration $M = 10^6$ pc/L) [12].

Table 4.14 Efficiency of second HEPA filter

Particle size (μm)	Proportional upstream the first HEPA filter	Calculated efficiency with ≥0.3 μm (the first filter)	Particle size (μm)	Proportional upstream the second HEPA filter	Calculated efficiency with ≥0.3 μm (the second filter)
0.3	0.46	$0.9991 \times 0.46 = 0.459586$	0.3	0.935	$0.9991 \times 0.935 = 0.9341585$
0.4	0.20	$0.99985 \times 0.2 = 0.19997$	0.4	0.0441	$0.99985 \times 00441 = 0.0440934$
0.5	0.11	$0.99994 \times 0.11 = 0.1099984$	0.5	0.0154	$0.99994 \times 0.0154 = 0.0153991$
0.6	0.11	$0.999984 \times 0.11 = 0.1099982$	0.6	0.004	$0.999984 \times 0.004 = 0.0039999$
0.8	0.05	$0.9999992 \times 0.05 = 0.04999996$	≥ 0.8	0.0015	$1 \times 0.0015 = 0.0015$
≥ 1.0	0.07	$1 \times 0.07 = 007$			
		$\eta = 0.99955$			$\eta = 0.99914$

Under normal conditions, atmospheric dust concentration is $M < 10^6$ pc/L. With the decrease of M, the absolute quantity of large particles decreases. So the number of large particles passing through the first air filter is close to zero, which makes the proportion of large particles upstream of the second filter smaller. Efficiency of the second filter for particle diameter $\geq d$ is approaching to that for particle diameter equals with d. This means the penetration of the second air filter is close to be two times of the first filter. Therefore, when the third HEPA filter is placed, its efficiency for particle diameter $\geq d$ is much closer to that for particle diameter equals with d of the first filter. When d is 0.3 μm, efficiency decreases from 0.99955 to 0.9991, or the penetration increases two times from 0.045 to 0.09 % and then reaches stable. If monodisperse aerosol is filtered, the change of efficiency for various stages of air filter is small.

Reports on the problem of efficiency for air filters in series are rare [13]. Both theoretical calculation and experimental data in field have proved that the efficiency of the second filter decreases a lot. There are two reasons: one is that particle concentration becomes extremely small after passing through the second air filter and so on, so data is not accurately measured because of the limit of measurement techniques, and even reverse conclusions are obtained, which has been clearly mentioned in the "Nuclear Air Cleaning Handbook" [14]; the other is that during the field test, particle concentration will increase downstream of air filter in case of sealing problem during installation or even the trivial leakage. Field test data from Japan are listed below [13]:

The first HEPA filter	efficiency 99.99 %
The second HEPA filter	efficiency 99.99 %
The third HEPA filter	efficiency 99.86 %

The increase of penetration between the third HEPA filter and the second one is larger than the calculation result. Tester have pointed out that this is caused by leakage. If there were no leakage made by improper installation, there would be no much difference of efficiency between the third and the second filter. For this aspect, the strict experimental data cited by "Nuclear Air Cleaning Handbook" denied the opinion that the efficiency of air filter in series will decrease.

According to the data from "Nuclear Air Cleaning Handbook," the decontamination factor of the first HEPA filter is 10^4, and that of the second HEPA filter remains the same, while that of the third HEPA filter is 5×10^3.

It is known that $K_c = \frac{1}{K}$, so we can obtain $K_1 = 0.01$ % from $K_{c_1} = 10^4$, and $K_3 = 0.02$ % from $K_{c_3} = 5 \times 10^3$. So K_3 is two times of K_1, which is consistent with the calculated result which increases from 0.045 to 0.09 %.

Therefore, it is suitable to choose HEPA filters with these recommended penetrations for exhaust cleaning system:

$$\text{The first HEPA filter } K_{1(\geq d)}$$

$$\text{The second HEPA filter } K_2 = 2K_{1(\geq d)}$$

$$\text{The third and later HEPA filters } K_{3(d)}$$

$K_{3(d)}$ means the penetration of the third and the following HEPA filters for particle diameter $\geq d$ equals with that for particle diameter d.

In the inlet air cleaning project, efficiency for two HEPA filters in series is quite large, so the influence of the decrease of the efficiency of the second air filter is too small to be neglected. The total efficiency can still be written as:

$$\eta = 1 - (1 - \eta_1)\ (1 - \eta_2) \cdots (1 - \eta_n) \tag{4.22}$$

There are two aspects of meaning to prove the small decrease of efficiency for HEPA filters in series:

1. In the application field of exhaust cleaning system. As pointed out in *Nuclear Air Cleaning Handbook*, the emission permission for radioactive elements concentration (such as plutonium or other super uranium substance) is extreme low, so it is not enough to only install one HEPA filter in the exhaust system. Since the efficiency of air filter in series does not decrease, it is preferred to install two or more filters in series, which is easy to increase the efficiency of the first filter.
2. In the application field of cleanroom for cleanness higher than class 100. When a HEPA filter is installed in series in the fresh air system, the influence of leakage is smaller. Some cleanroom projects in China have adopted this method and the effect is satisfactory.

4.8.2 Efficiency of Medium-Efficiency Air Filters in Series

For two medium-efficiency air filters in series, the efficiency of the second filter almost remains the same. If both filters are glass fibrous filters, in theory $\eta_{\geq 0.3} = 0.4$ and $\eta_{\geq 0.5} = 0.54$. We can obtain that the percentage of particles with diameter ≥ 0.5 μm decreases from 30 to 15 %. The efficiency for particle diameter ≥ 0.3 μm is 0.39 and that of particle diameter ≥ 0.5 μm is 0.54 which remains the same. So the total efficiency of coarse and medium-efficiency air filters in series can be written as:

$$\eta = 1 - (1 - \eta_1)\ (1 - \eta_2) \cdots (1 - \eta_{\mathrm{n}})$$

4.9 Service Life

4.9.1 Lifetime of Air Filter

The weight of dust deposited on air filter can be expressed with the following equation:

$$P = TN_1 \times 10^{-3} Qt\eta \tag{4.23}$$

where

P is the weight of deposited particles on air filter, g;
T is the lifetime of air filter, d;
N_1 is the particle concentration upstream of air filter, mg/m^3;
Q is the flow rate, m^3/h;
t is the operational time per day of air filter, h;
η is the arrestance of air filter.

When air filter is operated under the rated flow Q_0 and the pressure drop increases to several times of initial pressure drop (usually it is two times), the air filter can no longer be used, and the weight of deposited particles is called standard dust holding capacity P_0. The used time of air filter is called lifetime T_0, i.e.,

$$T_0 = \frac{P_0}{N_1 \times 10^{-3} \times Q_0 t\eta} \tag{4.24}$$

where N_1 can be calculated with the method in Chap. 10, i.e.,

$$N_1 = M(1-s)(1-\eta_n) + N_r s(1-\eta_r)$$

where

M is the atmospheric particle concentration, mg/m^3;
s is the recirculation air ratio;
N_r is the return air concentration. For cleanroom with Class 10 000, the concentration is between 0.001 and 0.01 mg/m^3;
η_n is the arrestance of air filter in the fresh air ventilation system;
η_r is the arrestance of air filter in the return air ventilation system.

For different systems with different η_n and η_r, the detailed calculation method will be introduced in Chap. 10. For example, $P_0 = 450$ g for flow rate 1,000 m^3/h, $M = 0.3$ m^3/h, $N_r = 0.005$ m^3/h, $s = 0.7, \eta_n = 0.7, \eta_r = 0.65, t = 24$ h, $\eta \approx 1$ (for HEPA filter), $Q = 1{,}000$ m^3/h, the service life of HEPA filter can be calculated to be 660 day. If the operational time per day is 12 h, T can be prolonged to be 1,320 day, which is 3.5 years. Since particles will also be deposited onto other surfaces, the lifetime of HEPA filters is longer than that of calculation.

Figure 4.15 shows the relationship between operational time and the increase of pressure drop of HEPA filter [15]. In the figure, the dust spot efficiency of prefilter in Curve b is 40–50 %, which is equivalent with the arrestance with atmospheric dust shown in Chap. 17. The service time of air filter is close to the data in the above example. It should be mentioned that there is one opinion that the increase of pressure drop of HEPA filter is faster than that of dust holding capacity, so it is unsafe to calculate the service time with dust holding capacity [16]. Actually it is not clearly pointed out here. Since the concept of dust holding capacity has included the increase of pressure drop, the service time or lifetime calculated with dust holding capacity equals with the operational time needed when the pressure drop becomes two times of the initial pressure drop (or other certain times).

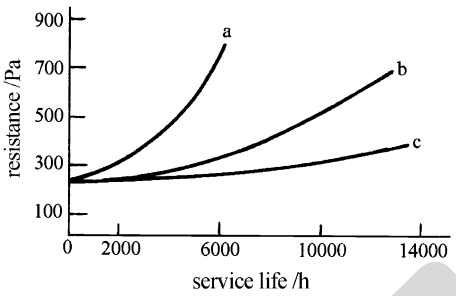

Fig. 4.15 Operational time of HEPA filter (measured with atmospheric dust: *a* without prefilter, *b* with prefilter when dust spot efficiency is 40–50 %, *c* with prefilter when dust spot efficiency is 80–85 %)

4.9.2 Relationship Between Lifetime and Flow Rate

The following relationship is obtained from Eq. (4.24):

$$\frac{T_1}{T_0} = \frac{Q_0}{Q_1} \tag{4.25}$$

It should be noted that T_1 is not the lifetime of air filter under that flow rate Q_1 but is the time needed for the weight of deposited particles on air filter to be P_0 under the flow rate Q_1. For example, if

$$Q_1 < Q_0$$

then

$$T_1 < T_{1,0}$$

$$T_{1,0} > T_0$$

and vice versa. Here $T_{1,0}$ is the lifetime under the flow rate Q_1.

Operational pressure drops are different when $Q_1 \neq Q_0$. Experimental data were given which is given in Fig. 4.16 [17]. It is shown that when $Q_1 = \frac{1}{2}Q_0$, the lifetime is larger than 2 T_0. When we denote $\frac{Q_1}{Q_2} = K$ and the pressure drop H, Tu Guangbei obtained the following equations based on these curves [18]:

$$K = 1.25\,H = 30.45 + 2.0143T + 0.251T^2 \tag{4.26}$$

$$K = 1.0\,H = 28.86 + 1.481T + 0.1555T^2 \tag{4.27}$$

$$K = 0.75\ H = 17.35 + 0.687T + 0.0805T^2 \tag{4.28}$$

$$K = 0.5\ H = 11.08 + 0.2474T + 0.0318T^2 \tag{4.29}$$

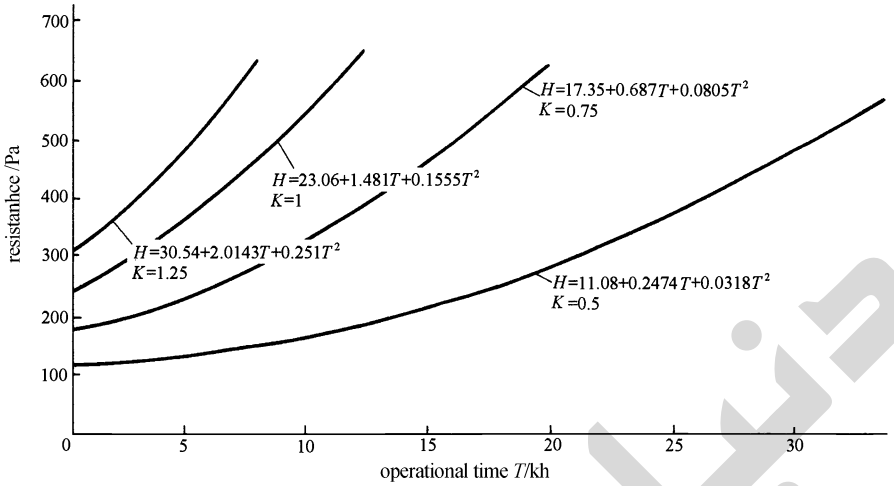

Fig. 4.16 Relationship between the increase of pressure drop and operational time of HEPA filter with prefilter (dust spot efficiency of prefilter is 45 %)

The following comprehensive equation was obtained when log-log plot paper was used with K as the abscissa (Fig. 4.16):

$$H = 23.86K^{1.106} + 1.481K^{2.519}T + 0.1555K^{2.290}T^2 \tag{4.30}$$

It is obvious that the constants in Eqs. (4.26), (4.27), (4.28), and (4.29) are initial pressure drops.

When H is considered constant, T is easily obtained by simplifying Eq. (4.30) [19]:

$$T = \frac{-1.481K^{2.519} \pm \sqrt{(1.481K^{2.519})^2 - 4 \times 0.1555 \times (23.86K^{1.106} - H)}}{2 \times 0.1555} \tag{4.31}$$

When $H = H_0$, T becomes the lifetime T_0. The value of T is only positive.

However, the above expression was obtained from one test case, and it is inconvenient to use it for calculation, which is not obvious to obtain the characteristic at a glance. So it is still unsure whether the relationship between T and K is also universally valid.

From another point of view, author proposed an approximation method for the theoretical analysis of relationship between T and K [19]. When both the operational and rated flow rates are known, the change trend of the lifetime can be calculated.

For example, the increase of pressure drop is ΔH under the rated flow Q_0 when the initial pressure drop is H_0 and standard dust holding capacity is P_0, so the final

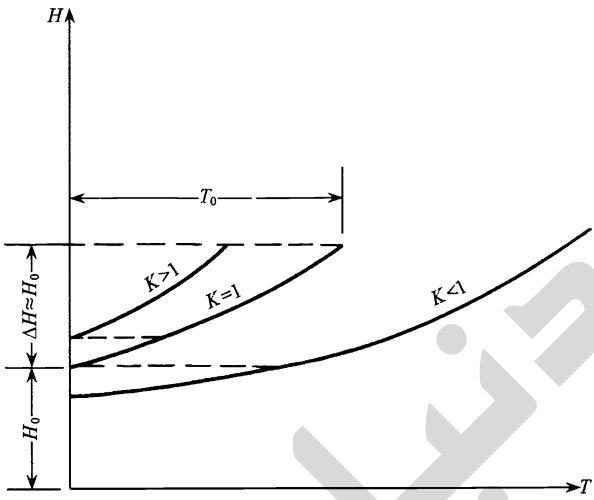

Fig. 4.17 Analysis figure between pressure drop and operational time

pressure drop is $H_0 + \Delta H$ and the operational time or lifetime is T_0. The curve ($K = 1$) is shown in Fig. 4.17.

When the flow rate becomes Q_1 ($<Q_0$), $\frac{Q_1}{Q_0} = K$ ($K < 1$), what is the time $T_{1,0}$ when the pressure drop reaches $H_0 + \Delta H$?

Simplification was made with the assumed condition $\Delta H \approx H_0$. From the aforementioned introduction, we know the increase of pressure drops of HEPA filter and sub-HEPA filter are linearly proportional to the weight of dust deposited under this condition.

1. From Eq. (4.25), it is known that the operational time is reversely proportional to the flow rate, i.e.,

$$T_1 = \frac{Q_0}{Q_1} T_0 = \frac{T_0}{K} \tag{4.32}$$

2. After operation time $\frac{T_0}{K}$ under flow rate Q_1, the weight of deposited particles becomes the standard dust holding capacity P_0, but the finial pressure drop at this time is still far from $H_0 + \Delta H$. From Figs. 4.6, 4.7, 4.8, and 4.9, it is shown that H is approximately linearly proportional to Q (when Q is less than Q_0 or slightly larger than Q_0). Since the final pressure drop is $(1 - K)$ times less, continuous dust loading process is needed to increase the pressure drop. It is known the pressure drop increase is approximately linearly proportional to the weight of deposited particles, and the weight of deposited particles is also linearly proportional to the time, so the time needed for continuous particle loading process or the increased time is:

$$\Delta T_1 = (1 - K) T_0 \tag{4.33}$$

Table 4.15 Relationship between K and T

K	0.5	0.7	0.75	0.8	1.0	1.25
$T_{1,0}$	3.5 T_0	2.15 T_0	1.91 T_0	1.7 T_0	T_0	$\frac{T_0}{1.7} = 0.59T_0$

3. According to the relationship between H and Q, the initial pressure drop decreases to KH_0 under the flow rate Q_1, this is (1 − K) times less. If the operational flow rate is Q_0 and $(1 - K)$ times of original pressure drop is added, the prolonged time needed is $(1 - K)T_0$. Now the operational flow rate is Q_1, so the time should be reversely proportional to Q_0, i.e., the actual prolonged time is

$$\Delta T_2 = \frac{1-K}{K} T_0 \tag{4.34}$$

4. Therefore, for the case $K < 1$, the time needed for the pressure drop to become the final pressure drop with $K = 1$ should be

$$T_{1,0} = T_1 + \Delta T_1 + \Delta T_2 = \frac{T_0}{K} + (1-K)T_0 + \frac{1-K}{K} T_0 \tag{4.35}$$

If $Q_1 > Q_0$, $Q_0 < 1$ when Q_1 is assumed 1, and $\frac{Q_0}{Q_1} = K$ $(K < 1)$. So the reciprocal of prolonged time Q_0/Q_1 is obtained, which is the shortened time.

With the above equations and principles, the relationship between K and $T_{1,0}$ for reaching the final pressure drop with rated airflow, which is shown in Table 4.15. In the table, $K = 1.25$, which is equivalent with $K = \frac{1}{Q_0/Q_1} = \frac{1}{0.8}$. It is equivalent to the reciprocal of its multiple of T_0, which is obtained with the value 0.8.

Taking Fig. 4.16 as an example, the lifetime T_0 of air filters for different K is calculated with the above analysis method, which is illustrated in Table 4.16, together with the measurement value and the calculated result with Eq. (4.31).

From the above comparison, results from three methods are almost consistent. So it is feasible to adopt the analysis estimate method which reflects the general laws. Equation (4.31) is also thought to reflect the general relationship, although it was derived from single case.

One important conclusion from the above analysis is obtained. The operational flow rate of air filter is suggested to be about 70 % of the rated flow, and the lifetime of air filter will be doubled, which is beneficial for both economic operation and energy saving.

In practice, it is impossible to directly estimate how much particles have been deposited onto filters. It is usually to determine whether to change air filters according to the measured pressure drop or the outlet velocity of air filter.

For air filters used in the radioactive exhaust system, except for the index of dust holding capacity or pressure drop, the index of surface contamination is also used to determine the service time. Air filters must be replaced when each index reaches the specified value. The extent of surface contamination of air filter is determined according to the specific situation of usage.

Table 4.16 Comparison of different T_0 obtained with different methods

		T_0 (kh)											
		$K = 0.5$			$K = 0.75$			$K = 1$			$K = 1.25$		
H_0 (Pa)	$H_0 + \triangle H$ (Pa)	Eq. (4.31)	Eq. (4.35)	Measurement [17]	Eq. (4.31)	Eq. (4.35)	Measurement [17]	Eq. (4.31)	Eq. (4.35)	Measurement [17]	Eq. (4.31)	Eq. (4.35)	Measurement [17]
240	480	30.2	30.1	30.0	15.6	16.4	15.9	8.6	8.6	8.6	4.6	5.1	5.0

4.10 Estimate of Arrestance

Arrestance of air filter is used to calculate the service time of air filter in previous section. Experimental data of arrestance can be used if it is available. But in the current national standard the fractional efficiency with atmospheric dust is used to assess the efficiency of air filters in general ventilation. Therefore, the particle counting efficiency should be converted into arrestance.

Here an estimation method is introduced [20].

Taking the data in Table 2.28 as an example, particle size distribution between 0.5 and 1 μm can be divided into the following parts according to the relationship shown in Table 2.30:

0.5 μm	31.64 %	
0.6 μm	29.72 %	In total 81.49 %
0.8 μm	14.28 %	
1.0 μm	5.75 %	

From Table 2.28, when the particle counting efficiency for particles with diameter ≥0.5 μm is 100 %, at least 99 % of particles by weight are filtered. Weight of particles with diameter less than 0.5 μm occupies 1 % of the total weight. Since part of particles with diameter less than 0.5 μm will be captured, the penetration will be less than 1 %. This can be omitted since it is a small value. That is to say, when the particle counting efficiency for particles with diameter ≥0.5 μm is 100 %, the arrestance cannot reach 100 % in theory, but it can be still considered as 100 % because the error is less than 1 %.

From the above analysis, we know when the particle counting efficiency for particles with diameter ≥1 μm is 100 %, at least 97 % of particles by weight and 18.51 % of particles with diameter larger than 0.5 μm will be captured. Since part of particles with diameter between 0.5 and 1 μm will also be captured, the total arrestance will be slightly larger than 97 %. For the convenience of estimation, this excess value can be omitted. Therefore, when the particle counting efficiency for particles with diameter ≥1 μm is 100 %, the corresponding arrestance can be estimated as 97 % or 100 %. When the particle counting efficiency for particles with diameter ≥1 μm is 80 %, 18.51 % × 0.8 = 14.81 % of the total number with particle diameter ≥0.5 μm will be captured, so less particles with diameter between 0.5 μm and 1 μm will be filtered (because efficiency for particles with diameter ≥1 μm is less, the corresponding efficiency for smaller particles is much less, which can be omitted). Therefore, the arrestance corresponding with the particle counting efficiency 14.81 % with particle diameter ≥0.5 μm can be used to express the particle counting efficiency 80 %, i.e., 96.5 %.

But when only the particle counting efficiency with particle diameter ≥5 μm is known without any information about the efficiency with particles diameter between 1 and 5 μm, the above method to estimate the arrestance is not valid since the weight percentage of these particles cannot be omitted.

According to the above analysis, the data in Table 2.28 are used to plot Fig. 4.18. The arrestance found in the figure is an estimation value or the minimum limit value.

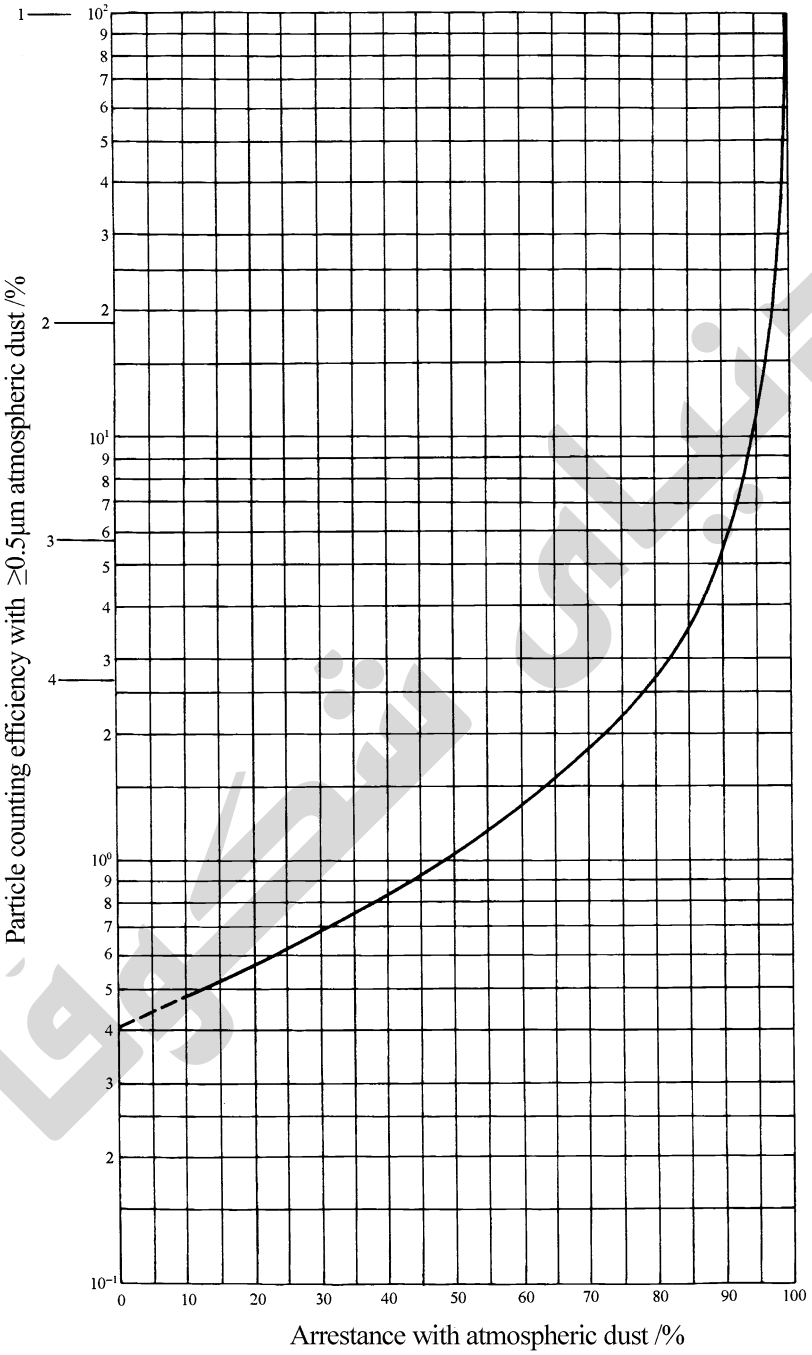

Fig. 4.18 Conversion from particle counting efficiency to arrestance: *1* 100 % efficiency curve for with particle diameter ≥0.5 μm, *2* 100 % efficiency curve for with particle diameter ≥1 μm, *3* 100 % efficiency curve for with particle diameter ≥3 μm, *4* 100 % efficiency curve for with particle diameter ≥5 μm

4.11 Filter-Paper Filter

4.11.1 Folded Filter-Paper Filter

Now the filter-paper HEPA filter is one typical example of folded filter-paper filter, which was developed in the nuclear industry in the Second World War to remove radioactive particles. The main characteristic is its extreme low resistance because the filter paper is thin and filtration area is dozen times of frontal area by the folded structure, which makes the practical use of filter-paper filter possible.

In 1942 the folded filter-paper HEPA filter was first manufactured in the USA and put into the market for sale in 1954. In 1956 HEPA filter was imported into Japan from the USA. Later in 1958 Japanese began to develop their own product, which appeared in the market in 1965 [21]. In 1960s, Chinese began to develop HEPA filter, which passed the identification and began the mass production.

The first filter-paper material used in the air filter of nuclear industry was plant fiber together with blue asbestos fiber. Blue asbestos fiber is very fine with diameter between 0.1 and 1 μm. The yield is very low. It is thought that asbestos fiber will cause cancer, so it is gradually replaced by popular ultrafine glass fiber and glass fiber filter paper, which promotes the application of high-efficiency filter-paper filter and the development of air cleaning technology.

Filter-paper HEPA filters can be classified according to the type of filter media material, and they can also be divided based on whether separator is used; whether the diameter of filtered particle is 0.3 μm (it is called common HEPA filter or 0.3 μm filter) or 0.1 μm (it is called ultrafine air filter or 0.1 μm filter); whether the frame material is board, laminate, plastic plate, aluminum alloy plate, steel plate, or stainless steel plate; whether the structural shape is flat or V type; and whether it is able to endure high pressure, endure high humidity, and endure acid and alkali, high resistance, low resistance, or sterilization.

At present there are three types of structure in filter-paper filter, i.e., with separator, with inclined separator, and without separator. The product of air filters with inclined separator is rare, while the other two types are popular. Structures of these three types are shown in Figs. 4.19, 4.20, and 4.21.

Inside HEPA filters, separator is placed between two sides of folded filter paper to provide the airflow channel, which is the standard practice. So it is called as separator HEPA filter. Separator is also called as corrugated separator. After hot rolling stamp, high-quality kraft paper can be used to make the separator with different crests and pitches. In order to prevent the particle emission from the stretch of separator caused by the cold, hot, dry, or wet conditions, as well as to fix the separator shape, both sides of separator should be immersed into some kind of coating material, which has the disadvantage of abnormal odor. Now chrome papers gluing at two sides are used to make separator. But some practical experience has shown that there is some hidden danger: particles will be released as the pollution source because of its stretch deformation with the variation of temperature and humidity. So aluminum and plastic can also be used to make separator.

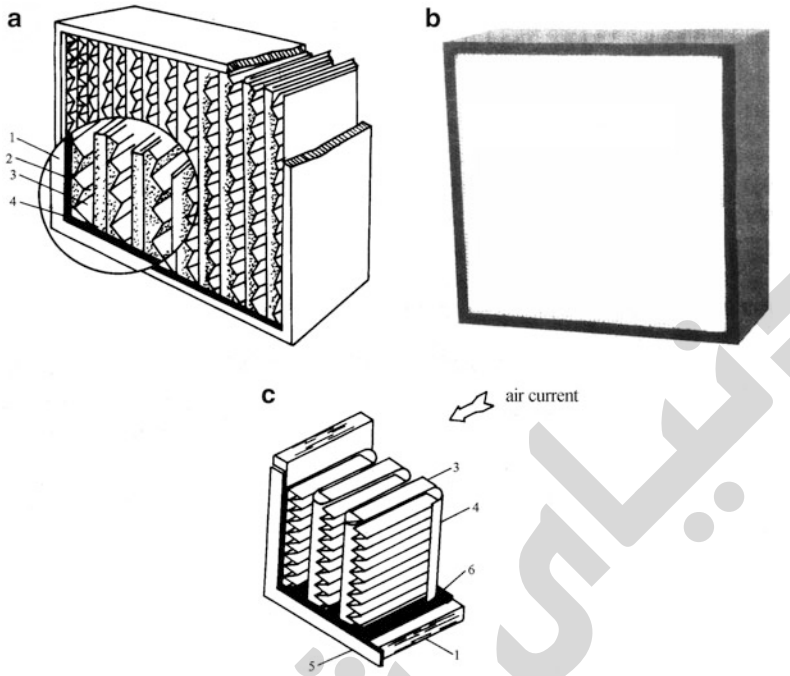

Fig. 4.19 Structure of separator HEPA filter: *1* frame, *2* heat glue, *3* separator, *4* filter paper, *5* gasket, *6* Sealant. (**a**) Wooden frame. (**b**) Iron frame. (**c**) Details of glue separator

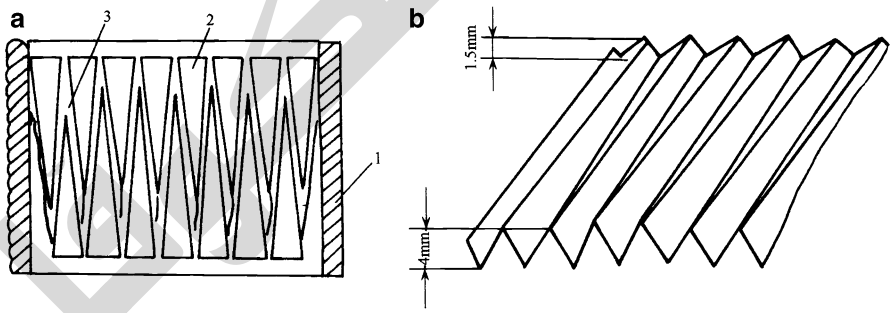

Fig. 4.20 Structure of inclined HEPA filter: *1* frame, *2* separator, *3* filter paper. (**a**) Cross section of inclined separator. (**b**) Peak height of inclined separator

For the separator air filters, corrugation angle is one important parameter, which has great influence on the pressure drop. Practice has shown that 90º corrugation angle is suitable. The influence of cross-sectional area on the pressure drop is not large. With the large cross section and same filtration velocity and thickness along the flow direction, the corrugation height has comparatively large influence on the pressure drop, which will be analyzed in detail later.

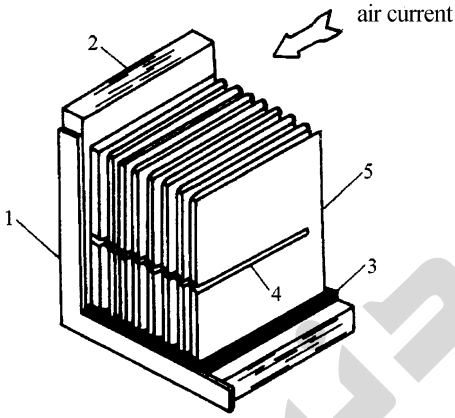

Fig. 4.21 Structure of HEPA filter without separator: *1* sealing gasket, *2* frame, *3* sealing glue, *4* separator, *5* filter paper

The traditional practice to make the separator air filter is to glue at both edges of the corrugation at first, then the endsealing glue is added to the inner side at both two edges of wooden frame painting so as to make the glue sides in order and to prevent leakage. But practice has shown that the endsealing glue has little effect on the leakage prevention, and once there is leakage, it is more difficult to detect the leakage and make repair. Taking the current GB-01 type air filter as an example, the cross-sectional area of filter cartridge is about 0.454 m $\times$ 0.454 m $=$0.206 m^2 and the width of endsealing glue is 1.5 cm. When it was considered as 1 cm, the corresponding cross-sectional area of filter cartridge is about 0.454 m $\times$ 0.434 m $=$0.197 m^2, which means the cross-sectional area without endsealing glue is 5 % larger than that of with endsealing glue. When the net area of filter paper increases, the pressure drop will decrease to some extent. Therefore, the practice to use the endsealing glue on air filter is canceled, which is replaced with potting glue method or inserting glue method.

For traditional separator air filter, the cross-sectional areas of air channel formed by the corrugations on the separator are the same. When the concept of area variable cross sections is applied on air filter, inclined air filter is created, whose projection shape is a right-angled trapezoid when the separator is erected. The cross-sectional area is large when air enters into the channel. As air goes through the filter paper, the air volume near the channel terminal is the minimum, so is the cross-sectional area. In this way, both the length of filter paper around each separator and the number of corrugations increase. According to the product specification abroad, the filtration area will increase by 50 % for inclined separator air filter compared with vertical separator air filter, so the pressure drop under the same flow rate will be much less.

Another method of improvement on traditional HEPA filter is to cancel the separator. It is beneficial for the mechanized production of mini-pleat filter. One case is to cancel the separator, and the filter paper is folded with corrugation matching corrugation and point matching point after corrugation and salient point are pressed on filter paper. The other case is to replace the separator plate with other

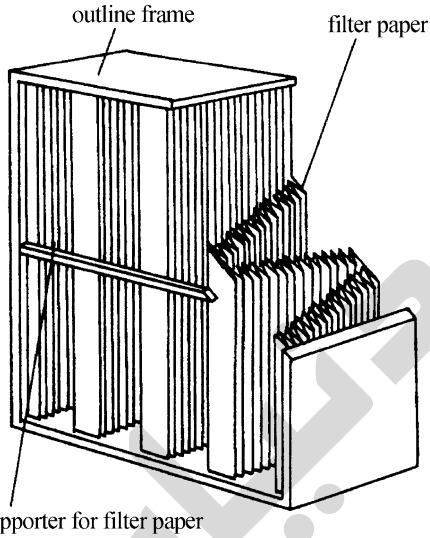

Fig. 4.22 Air filter with double folding structure

separator, such as the streak formed by thermosol on filter paper, the dipping flame retardant silk thread, glass fiber thread, or filter strip pasted on filter paper. During the process of folding filter paper, filter strips are inserted from the two sides of corrugation and they are held with the friction force.

It should also be mentioned that the cross-sectional size of domestic-made HEPA filter includes 484 mm × 484 mm, 630 mm × 630 mm, etc., which are quite irregular. National standard issued in 2008 canceled the specification of maximum overall dimension. It also requires that (1), (2) separator plate is 5–8 mm lower than the frame edge, and (3) the filter element is 3–5 mm lower than the separator edge. The national standard also provides the following specification: (1) The frame width is 15 mm (when the side length is less than or equal to 600 mm) or 20 mm (when the side length is equal to or larger than 600 mm). This is a way to guarantee the quality of air filter, but some manufacturer does not pay attention to it. During the calculation related to air filter, these data should also be considered.

In order to enlarge the filtration area, double folding structure is also adopted. The first folding structure is for filter paper itself, which means a piece of folded filter material is used. The second folding structure is the W type structure inside the frame. The structure is shown in Fig. 4.22.

4.11.2 Cylindrical Filter-Paper Filter

In early times, the former USSR made transversely placed large cylindrical filter with ϕII-15-1.5 filter fabric which is hard to be folded but can be pasted, which is shown in Fig. 4.23. Strictly speaking, that is a kind of equipment, not a single air filter.

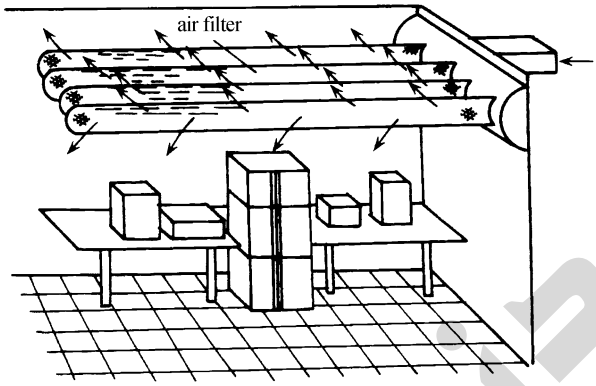

Fig. 4.23 Large cylindrical filter (ϕ200) made in former USSR

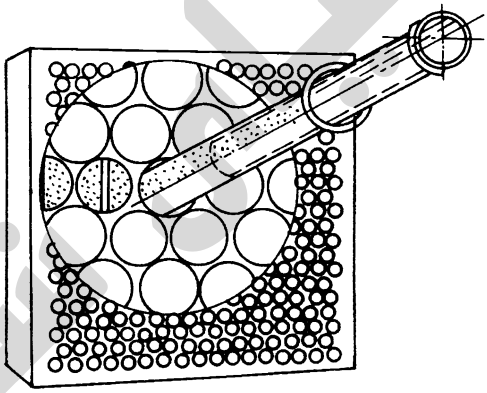

Fig. 4.24 Perspective of low-resistance cylindrical sub-HEPA filter

YCG-type low-resistance sub-HEPA filter is one typical example of filter-paper filter, which was one type of air filters with lower structural resistance innovated firstly in China [23]. Hundreds of filter cylinders are hot welded with polypropylene fiber filter paper. Filter cylinders are plugged onto the panel with the plastic cap stopper with wings. Wings are meant to support the filter cylinders and separator the air channel into two parts.

Figure 4.24 is the perspective of this kind of filter. Figure 4.25 shows the panel plugged with cap stopper, its hole size and details of cap stopper. Figure 4.26 presents the experimental results between this filter and Japanese CP-9A high-efficiency air filter, which was performed on the test rig at Institute of HVAC of China Academy of Building Research. It is shown that efficiency increases by an order of magnitude when the pressure drop is slightly less.

Main features of this kind of air filter include:

1. Low resistance. With the same size of GB-01 HEPA filter (484 mm × 484 mm × 220 mm), the pressure drop is only about 40 Pa under the rated flow 1,000 m^3/h and sodium flame efficiency ≥95 %.

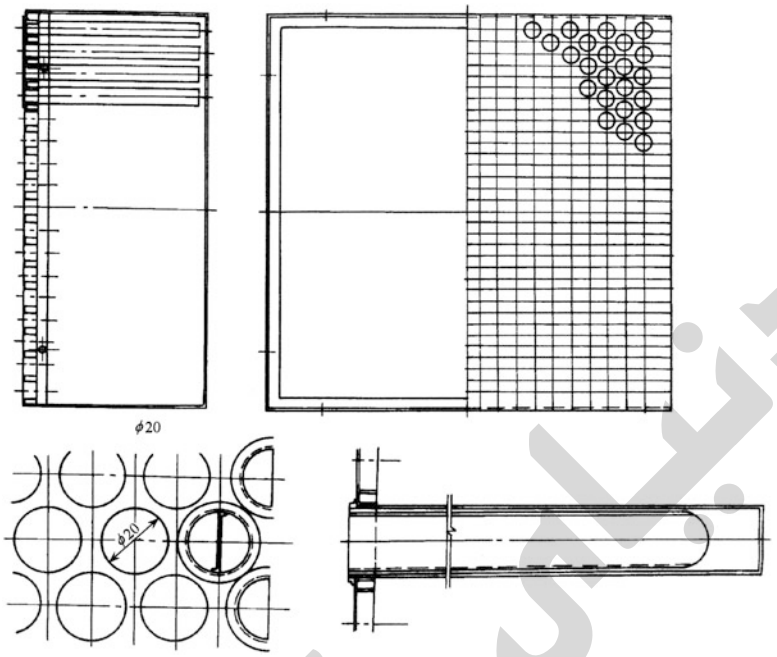

Fig. 4.25 Details of cylindrical filter panel

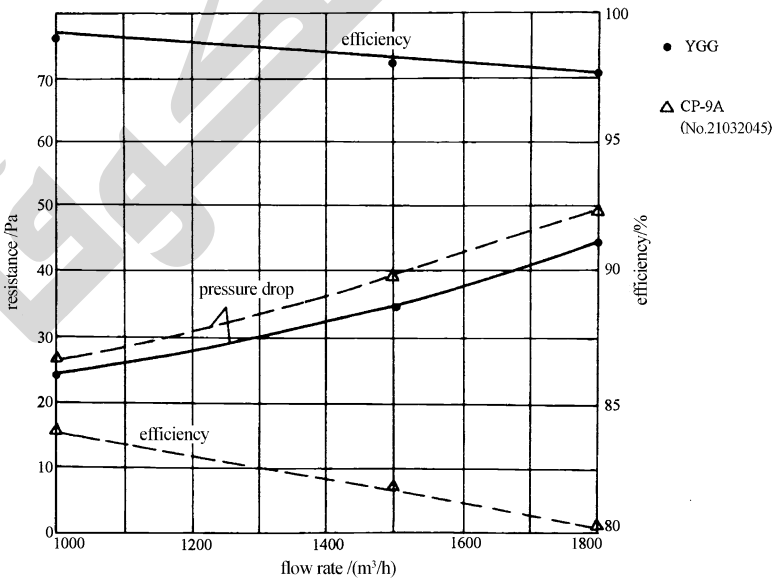

Fig. 4.26 Performance comparison between UGG air filter and Japanese CP-9A filter

Table 4.17 Relationship between efficiency, filtration velocity, and particle size for cellulose fiber filter paper

	Particle size (μm)				
Filtration velocity (cm/s)	0.088	0.188	0.264	0.365	0.557
6	81.5 %	80.7 %	81.4 %	77.7 %	80.6 %
9.5	81.2 %	79.0 %	97.5 %	77.7 %	85.0 %
13	75.2 %	76.9 %	76.6 %	74.1 %	81.9 %
17	78.2 %	75.0 %	80.0 %	78.5 %	86.5 %
27	89.2 %	87.4 %	88.9 %	88.8 %	92.2 %
32.5	91.1 %	87.4 %	90.3 %	92.7 %	93.8 %
38.5	94.0 %	90.0 %	91.7 %	92.6 %	93.4 %
57.5	98.9 %	98.6 %	99.4 %	99.5 %	98.8 %

2. Non-abandon. Old filter cylinders are replaced only with new ones. Others can be used several times for cost saving.
3. Any shape. Diameter of filter cylinder is only 19 mm, so they can be plugged onto the panel with various shapes. Panel is needed while the frame is not, so it is convenient to match with various equipments.
4. No peculiar smell. Unlike the HEPA filter which needs to use glue, it is adhesive-free product, so secondary pollution caused by peculiar smell does not exist, which is suitable for the application with stringent environmental requirement.
5. Light. The weight is only half of the HEPA filter with the same size.

Structural calculation of this kind of air filter will be introduced in Chap. 5.

4.11.3 Filter Paper Used in Filter-Paper Filter

4.11.3.1 Cellulose Filter Paper

It usually means the filter paper made by plant cellulose. Several domestic-made air filters with performance similar as sub-HEPA filter are made of short cotton lint filter paper. The characteristic of this kind of filter paper is that its efficiency is between medium efficiency and sub-high efficiency. The efficiency is small for low filtration velocity. Efficiency increases with the increase of filtration velocity. The performance differs for different kinds of particles.

Table 4.17 shows the filtration efficiency of one cellulose fiber filter paper with PSL [24]. It is shown that for particles with diameter smaller than 0.557 μm, the efficiency is the minimum for filtration velocity 9.5–17 cm/s. Moreover, the minimum efficiency corresponds with smaller particle size with the increase of filtration velocity. The surface dust holding capacity of this kind of filter paper is slightly larger than that of glass fiber filter paper by 60–70 %, but it is smaller than that of membrane filter.

Table 4.18 Relationship between efficiency and composite proportion of glass fiber inside HEPA filter

Efficiency with 0.3 μm DOP particles (%)	Proportion of glass fibers in filter paper (%)
>99.995	>90
>99.97	>60
99	~45

4.11.3.2 Cellulose-Asbestos Fiber Filter Paper

This kind of filter paper has high efficiency and high resistance. Since the surface dust holding capacity is also very high, even higher than that of glass fiber filter paper, it is usually applied in the exhaust treatment system for nuclear facility.

4.11.3.3 Glass Fiber Filter Paper

This kind of filter paper also has high efficiency. Efficiency changes little with the change of particle type and filtration velocity. The relationship between efficiency and composite proportion of glass fiber inside the filter paper is shown in Table 4.18 [25]. The pressure drop is smaller than that of cellulose-asbestos fiber filter paper.

Fiber diameters inside glass fibrous filter paper become smaller. In 1970s diameter of foreign made filter paper reduces to 0.3 μm, and the value of domestic made reduces to 0.5 μm. Figure 4.27 presents statistical analysis of the fiber diameter distribution inside domestic-made filter paper using SEM graph, where all the average diameters are slightly smaller than 0.5 μm. In 1980s the diameter of domestic-made glass fiber was smaller than that of foreign made, which reduced to 0.04 μm. Efficiency increases apparently and that of some filter paper was higher than that made in the USA. However, the most obvious shortcomings of domestic-made filter paper are fiber shedding and the amount of particles deposited by filter media itself is great, which is related to the inaccurate control of manufactory environment and production process. Furthermore, pressure drop of common HEPA filter paper is very high under the usual filtration velocity, and that of most ULPA filters is even much higher [9].

4.11.3.4 Synthetic Fiber (Chemical Fiber) Filter Paper

Since the synthetic fiber has high resistivity and can bring large amount of electrostatic charge, it is an ideal material for making electrostatic material. Perchloroethylene ϕII filter fabric produced in the former USSR in 1950s is one of the kinds of fibrous filter paper. Penetration is 20 % when filtration velocity is 0.1 m/s, while it is 3.2 % when filtration velocity decreases to 0.01 m/s and the corresponding d_{max} is 0.1 μm [22].

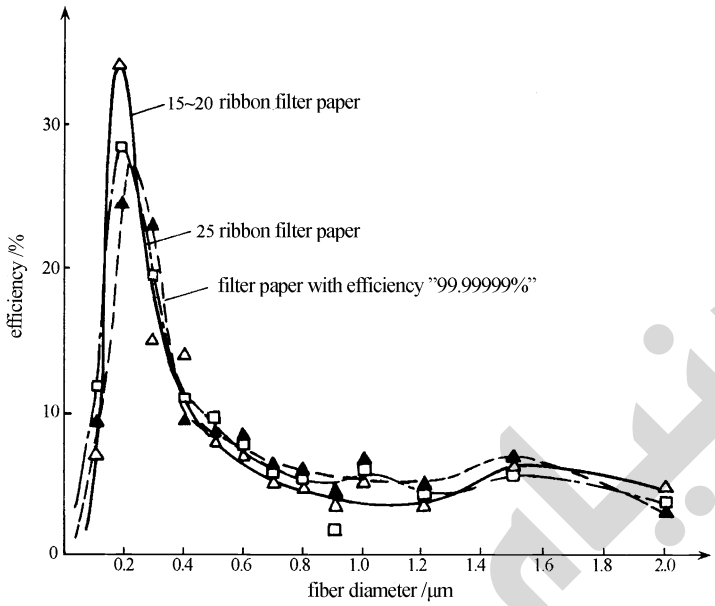

Fig. 4.27 Statistical analysis of fiber diameter distribution inside domestic-made filter paper

Table 4.19 Pressure drop of polypropylene fibrous filter paper

Efficiency with sodium flame method (%)	90	99	99.9	99.99	99.999
Resistance (Pa)	1	3	6	9	12

Polypropylene fibrous filter paper developed in the late 1970s is another example. Its performance is much better than ϕII filter fabric. Polypropylene slice is used to make ultrafine fiber through the meltblown process. Further filtration material is manufactured, which is a soft nonwoven felt. Diameter of single fiber is 2–18 μm (usually it is 4 μm). The sodium flame efficiency with standard specific velocity is 99–99.999 %. It is quite difficult to make the fiber diameter smaller. Fibers are not uniformly distributed inside the filter media. Electrostatic charge on the filter media fades away gradually, so at present it cannot be used to replace glass fibrous HEPA filter. But it is indeed a promising filter media.

Except for the features mentioned in the above chapter and sections in this chapter, polypropylene fibrous filter media has the following characteristics:

1. Pressure Drop. Under the same efficiency range, the pressure drop is only 1/6 that of glass fiber. Table 4.19 presents the pressure drop of several domestic-made polypropylene filter paper when the filtration velocity is 1 cm/s.

   The reason for small pressure drop is that the fiber diameter is comparatively large and particles can penetrate deeper (several hundred micrometer). But particles can only penetrate tens of micrometers from the surface of glass fibrous filter paper.

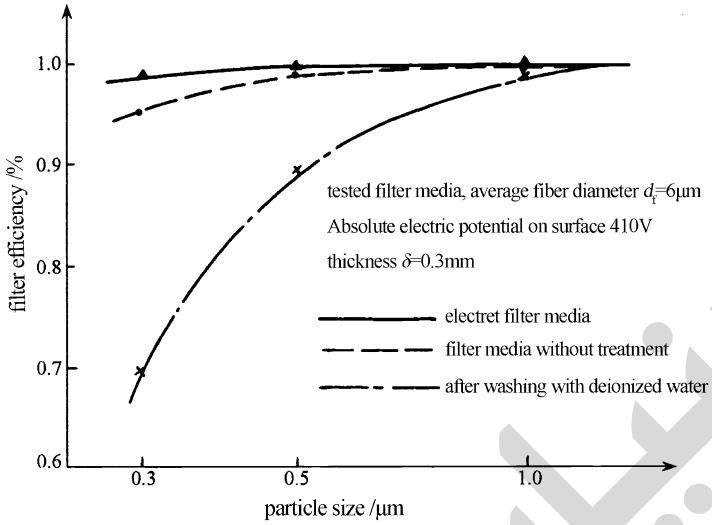

Fig. 4.28 Relationship between efficiency and particle size for polypropylene fibrous filter media with the electrostatic effect

2. Stability of Electrostatic Charge. After passing through the corona discharge, filter media become the electrets which carry large amount of electrostatic charge, and the surface electrostatic potential can reach 1,000 V. With the electrostatic effect, the penetration decreases by 1–2 order of magnitude. After the filter media is immersed into the alcohol and then dried in the vacuum, the electrostatic charge is neutralized and the efficiency decreases a lot, which is shown in Figs. 4.28 [26] and 4.29 [27]. At the same time, it is also found that the electrostatic potential increases by the friction effect when air flows through the filter media, which is shown in Table 4.20. The potential at smooth side is high, so the efficiency using this side as the frontal face is high, while the pressure drops using both sides facing upstream is almost the same (Table 4.19).
3. Dust Loading Performance. Experimental results with NaCl aerosol show that the relative penetration (the ratio of penetration after dust loading K to the initial penetration K_0) of polypropylene fibrous filter media increases firstly then decreases with the time. There is an extreme short transient period where the relative pressure drop (the ratio of pressure drop after dust loading ΔP to the initial pressure drop ΔP_0) increases with the time, which is shown in Figs. 4.30 and 4.31 (Although the unit was not given in the original literature, the qualitative analysis is not influenced).

But experiment was performed on the electrets air filters with polyolefin fiber which concluded that efficiency decreased from 99.9999 to 99.99 % after 2 years' operation without any prefilters. The reason is that the electrostatic effect is shielded by the deposited particles [29].

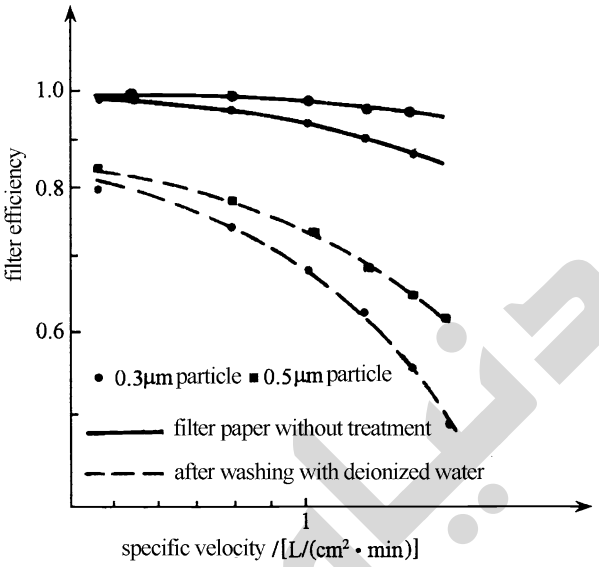

Fig. 4.29 Relationship between efficiency and filtration velocity for polypropylene fibrous filter media with the electrostatic effect

Table 4.20 Influence of airflow on the electrostatic charge (unit: V)

Front and back of filter media	Condition			
	Without any treatment	Blow with hair drier for 2 min (normal temperature)	Dry with vacuum oven after immersed in alcohol for 5 min	Dry with vacuum oven after immersed in alcohol for 5 min, and then blow with hair drier
Glaze surface	−1434	−1601	+12	−204
Rough surface	+916	+1280	+4	−80

1. Hydrophobicity. Polypropylene fibrous filter media are hydrophobic. The hygroscopicity is only 0.01–0.1 %. Under the wet condition, the strength is almost unchanged. When it is placed in the environment with relative humidity 80 %, no obvious influence is made on both the efficiency and pressure drop [28].
2. Temperature Characteristic. The operating temperature is −40 to +110 °C. When it is baked under the temperature 50 °C for 4 h, no obvious change appears in both efficiency and pressure drop [26]. But efficiency decreases when the operating temperature is above 120 °C. The melting point is 164–174 °C.
3. Density. It is 0.91 g/cm^2. The solid fraction is 0.12 with measurement [26].
4. Characteristic of Acid and Alkaline Resistance. Except chlorosulfuric acid, concentrated nitric acid, and some oxidants, it has good performance of resisting acid, alkaline, and organic solvent.

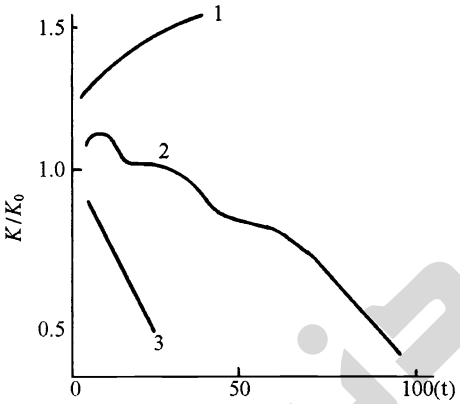

Fig. 4.30 Relationship between relative penetration and time: *1* perchlorethylene, *2* polypropylene, *3* glass fiber

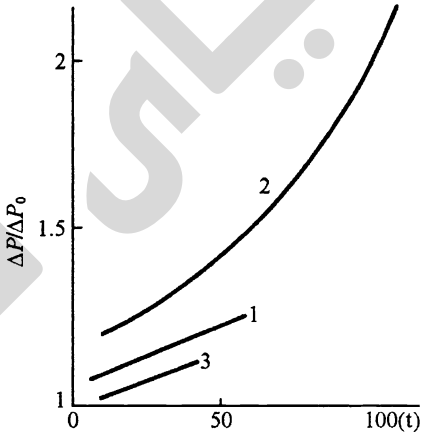

Fig. 4.31 Relationship between relative pressure drop and time: *1* perchlorethylene, *2* polypropylene, *3* glass fiber

5. Strength. The transverse tensile strength is larger than 500 g/100 × 15 cm, and the longitudinal tensile strength is larger than 1,000 g/100 × 15 cm. The strength is more than two times of glass fibrous filter paper. It is fold resistant.
6. Environmental Property. Nontoxic, odorless, no borer, and it can be disposed by combustion.
7. Ability to Absorb Oil. It can absorb oil with weight equals with 14–15 times of self weight.
8. Bonding Characteristic. It is difficult to bond with the glue, but it's easy to bond with iron.

4.11.3.5 Membrane Filter Paper

The gel type microporous filter membrane is the main form, which is made of the nitrocellulose. The gel is the mixture of the ether alcohol with the fibers of nitrate

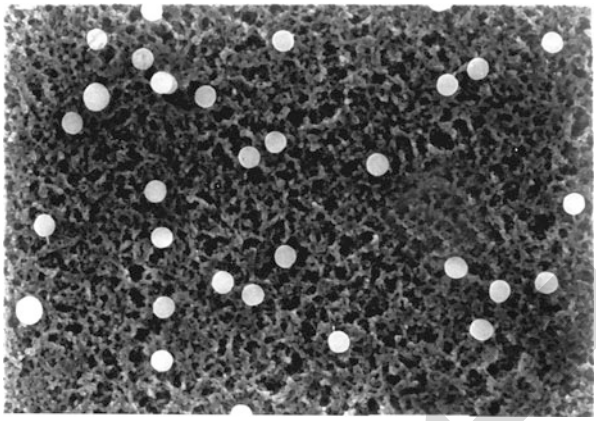

Fig. 4.32 SEM figure of microporous membrane surface (particle diameter is 2.20 μm)

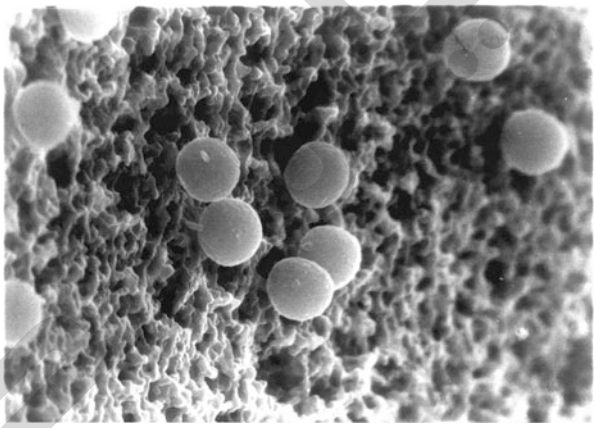

Fig. 4.33 Microporous membrane surface when the SEM figure inclines 60º

ester, and it is also called celloidin. When the celloidin is diluted with the acetone and the pentanol, the gel used for make the membrane is formed. This kind of filtration membrane has very high efficiency and surface particle deposition rate, so it is usually used to act as a standard filter paper to measure the efficiency of other filter papers. It is also used to capture radioactive particles, but it is not convenient to use since the pressure drop is high and the tensile strength is low.

Pores on the surface of microporous membrane are irregular, which is similar as that of foam. Their SEM figures are shown in Figs. 4.32 and 4.33 [30], where the spheres are methylene blue particles.

Nuclear microporous membrane is also one kind of membrane filter paper. It is called nuclear track microporous membrane, which is developed in the late 1960s. Thermal neutron during the nuclear reaction is used to bombard the heavy element such as ^{235}U. Then the fission fragment from ^{235}U is used to bombard the plastic film such as polycarbonate film or polyester film, or the heavy element such as K_r and X_e accelerated by the accelerator is used to bombard these films, so track injury

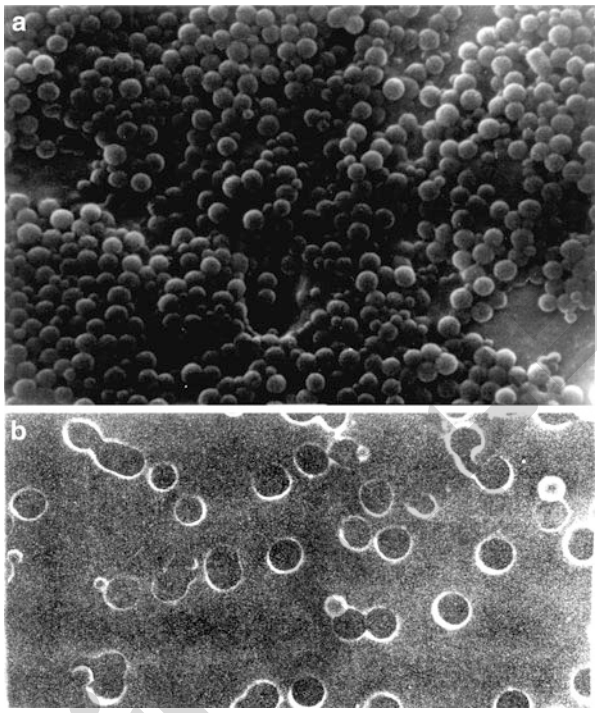

Fig. 4.34 SEM figure of both frontal and rear faces when nuclear microporous membrane is clogged. (**a**) Frontal face. (**b**) Rear face

is left. Afterwards, they are etched with chemical reagent, and pores appear on the surface. Its strength is good. It is fold resistant and can bear high temperature 140–170 °C. Pore density can be controlled when both the bombardment intensity and time are monitored. Pore size can be controlled when the reagent concentration, temperature, and etching time are controlled. The thickness of nuclear microporous membrane is usually between several micrometer and dozens of micrometer. The thickness of domestic-made nuclear microporous membrane is 11 μm. Diameter of pore size is between 30 Å and tens of micrometer, and it is usually about 1 μm. The porosity is about 20 %. The monodisperse of pore size is better than chemical microporous membrane. Since the surface is quite smooth, it is suitable for qualitative analysis of aerosol sampling and study of bacteria filtration. The pressure drop of nuclear microporous membrane is large, so it is not suitable for common air filter, but it is very useful for special filtration (for the application field where particles with diameter larger than certain value are not allowed to penetrate). It is shown from Fig. 4.34 that almost no particles appear on the rear face when the frontal surface is already clogged. It is widely used in the medical applications. As for the filtration mechanisms of nuclear microporous membrane, domestic scholars have already made detailed investigation [31], which will not be introduced here.

Except for the above five kinds of filter paper, there is also plastic fibrous filter paper, which is not illustrated here.

4.11.4 General Features of Filter Paper

Special attention should be paid on the representative features during the selection of filter paper, which is presented in Table 4.21. It is hoped that the larger tensile strength and smaller fiber are preferred. While larger thickness and larger solid fraction will result in high efficiency, but the pressure drop will increase dramatically at the same time.

The content of metal component is one important feature for filter paper. When the content of metal component in the captured particles is investigated, the background value in the filter paper itself is needed. There is little study in this aspect home and abroad. For reference purpose, Table 4.22 presents the contents of several metal components inside the common glass fibrous filter paper according to the literatures home and abroad.

It is shown in Table 4.21 that the largest shortcoming of this kind of glass fibrous filter paper is the weak tensile strength. The ability to bear the shock press is extreme low. During the manufacturing process, it is too fragile to be damaged if it is not careful enough. Experiment of the compressive strength of HEPA filter was performed using the shock tube. Protection device was developed to increase the ability to bear high shock force. Common HEPA filter with tensile strength of filter paper no less than 230 g and other air filters were used in the test. Different conditions were compared when no baffle was placed and different baffles were set 5 cm upstream of the air filter. The test results for common HEPA filters are shown in Table 4.23. Both Figs. 4.35 and 4.36 show the damaged filters, where the white part means the damaged part of filter paper which turned outwards [32]. Moreover, the stiffness and rigidity of filter paper have decisive influence on the height of corrugation and pressure drop.

From the test results shown above, the pressure for damaging domestic-made glass fibrous filter paper (or 6901 filter paper) used in common HEPA filters is less than 0.16 kg/cm^2. According to American Air Force Design Manual (AD295408, TDR-62-138 Report), the pressure to cause damage on AEC filter from US Atomic Energy Commission is only 0.14 kg/cm^2. Therefore, when glass fibrous filter is installed on the pipeline with shock press, the protection device must be installed, and the most common measurement is to place the baffle plate.

The tensile strength of glass fibrous filter paper is very small, and it decreases a lot under the high wet environment, so it is easy to be blown through. If special treatment is made on filter paper, its tensile strength can be improved. Domestic researchers have proved that when the filter paper is treated by spraying with “soft No. 1” leather treatment agent, the tensile strength can be increased by ten times, while the pressure drop does not increase too much and the efficiency remains the same [33]. Experimental results are summarized in Table 4.24.

Table 4.24 is the experimental result of pressure drop with high filtration velocity 0.16 m/s. Pressure drop data for low filtration velocity are not available. With low filtration velocity, the rise velocity of pressure drop is slower than that of high filtration velocity.

Table 4.21 Characteristic of filter paper

Item	Thickness (mm)	Average mass per unit area (g/m^2)	Solid fraction of fiber	Fiber size (μm)	Pore size (μm)	Tensile strength[a] (g)	Combustion content (%)	Metal content (μm/g)
Common range	0.15–0.4	Depend on material	HEPA: 0.1–0.25 Medium efficiency: <10	HEPA: <0.1 Medium efficiency: ~10	<1 (filter membrane)	250–450	Requirement for fire-proof filter: <5	Depend on material
Example								
Glass fibrous filter paper with 99.99999 %	0.4 ± 0.03	130–140	0.118	0.5		≥645		
Glass fibrous filter paper with 99.9999 %	0.36 ± 0.02	110	0.113	0.5		>400		
Glass fibrous filter paper used in clean bench	0.20 ± 0.03	60–70	0.12	0.4		200		
Glass fibrous filter paper used as general HEPA filter (such as 6901 paper)	0.23 ± 0.02	70–80	0.12	0.4		>230		
Japan GB-100 glass fibrous filter paper	0.41	148	0.138	0.3				
Japan No.228 glass fibrous filter paper	0.275	76	0.102	0.92				
No. 3 asbestos filter paper	0.5	170	0.09			~300		

[a]According to domestic requirement, the tensile strength is the reading value at fracture when one side of filter paper with width 15 mm and length 180 mm is fixed and the other side is stretched with the spring balance

Table 4.22 Common range of content of metal component in glass fibrous filter paper (atomic extinction analysis)

Metal	Content (μg/g)	Metal	Content (μg/g)	Metal	Content (μg/g)
Cd	<1	Pb	5–90	K	400–1,800
Cu	1.5–3	Sb	20–60	Ca	300–6,000
Ni	1–15	Zn	10–50,000	Na	4,000–40,000
Mn	2–30	Fe	60–500		
Cr	2.5–10	Mg	300–1,600		

Table 4.23 Ability of common HEPA filter to bear shock press

Inlet pressure (kg/cm^2)	Bypass flow baffle	Damage situation
0.16–0.18	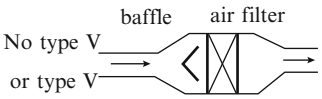 ϕ200 circular plates. No perforation within ϕ60. Perforations with ϕ4 and distance 8 mm are made in the left area of the plates	Damage occurs in the center of the air outlet face
0.23	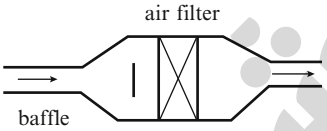 ϕ200 circular plates. No perforation within ϕ60. Perforations with ϕ4 and distance 8 mm are made in the left area of the plates	No damage occurs in the center. Damage occurs at both sides

The filter paper is still undamaged when it is treated with "soft No. 1" leather treatment agent and then with steam. This means it can bear high temperature environment of steam for sterilization, so it is useful for pharmaceutical and biological clean rooms.

It is dependent on the application and performance to choose what kind of components including filter paper, frame, and separator (corrugation) for making air filter, especially HEPA filters. For information, Table 4.25 shows the general performance of air filter made by components with different materials.

Because the filter paper is too fragile to be damaged during the manufacturing process, the efficiency of filter-paper air filter is usually smaller than that of small filter-paper sample by "half 9," and the poorest performance difference could be less than "one 9." Therefore, for making HEPA filter with efficiency for particle diameter 0.3 μm to be above "three 9" (i.e., 99.9 %), filter paper with efficiency "four 9" must be used.

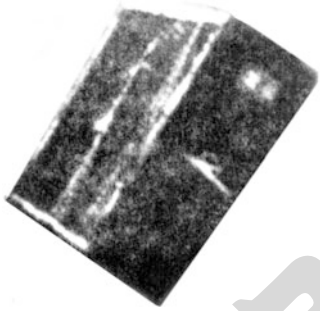

Fig. 4.35 The damaged situation of the most lateral side and middle part in paper filter

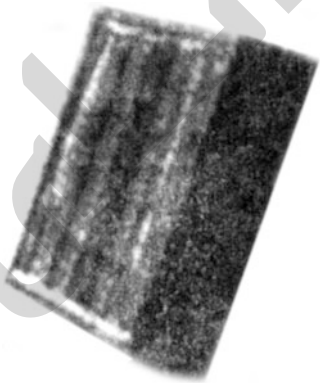

Fig. 4.36 The damaged situation of both sides in paper filter

4.11.5 Development of Filter-Paper Air Filter

With the development of science, technology and manufacturing process, both the standard and test methods for HEPA filters in many countries are developing, which will not be introduced here [34]. More stringent requirement for filter-paper air filter will be put forward. There are following requirements [35]:

1. Efficiency for particle diameter 0.1 μm should get close to 99.99999 %, or for particle diameter 0.01 μm should get close to "eight 9," which is called ULPA filter and shown in Fig. 4.37.
2. It is more stringent to make requirement on the chemical pollution of filter paper.

At present, most of HEPA filter is composed of filter media with ultrafine glass fiber which is made from silicon boric acid. 58 % of its component is SiO_2.

In 1980s the requirement of silicon pollution was proposed. Silicon particles volatilize and emit from the hydrophobia material, which cause harmful effect on the production of hard disk drive.

In 1990s the problem of phosphorus pollution was put forward. Phosphorus pollution comes from the seal glue of air filter, which may cause pollution to the wafer.

Table 4.24 Performance of glass fibrous filter paper before and after treatment

No.	Handling method	Tensile strength[a] (g)	Tenacity[b]	Resistance (filtration velocity 0.15 m/s) (Pa)	Efficiency (%)
1	No treatment	163	Break after 0.57 s	1,360	99.99–99.999
2	Spray or coat with 5 % 2124 phenolic resin	275	Break immediately at start	1,460	
3	Spray or coat with mixture of 5 % organic silicon and 2.5 % phenolic resin	300	Break immediately at start	1,570	
4	Uniform spray with 5 % emulsion by dilution of "No. 1 soft" leather agent by either times of water. The spray for filter paper with thickness 0.25 mm is 0.06 mL/cm^2. Then dry it naturally.	1,625	Break after 2.8 s	1,660	99.9978
5	Treat with "No. 1 soft" leather agent, then bake for 24 h with the environment 120 °C			1,580	
6	Treat with "No. 1 soft" leather agent, then immerse it into the water, then bake for 16 h with the environment 100–120 °C			1,510	

[a]Test filter paper: width 7.5 mm, length 70 mm
[b]The time of filter paper with width 7.5 mm and length 25 mm having fractures during the repeated process of stretching and folding, when its one side is fixed and the other side is connected with an eccentric wheel which has an eccentricity 7 mm and speed 1,390 r/min

In the late twentieth century, the problem of boron pollution was put forward, since about 11 % of the component in the filter media is B_2O_3. Except for the boron pollution of atmospheric air as the main source, air filter is also one important source. Under high-humid environment, hydrofluoric acid will make corrosion on glass fiber and produce gaseous boric acid if hydrofluoric acid exits, which will pollute the wafer.

1. The pressure drop with rated flow is smaller than 50 Pa.
2. The deposited particles are unlikely to reenter into the flow.
3. No crack exits inside the structure of air filter, so no seal material is needed and no leakage appears on it. Leakage test before delivery is not needed.
4. The lifetime is more than 5 years.
5. It is easy to handle after usage.

In the late of twentieth century, PTFE filter with filter media made by microporous PTFE membrane appeared in the market. The average diameter of the pores

Table 4.25 Performance of air filters

Frame material	Filter material	DOP efficiency (%)	Separator	Glue	Maximum temperature (°C)	Heat resistance	Moisture resistance (relative humidity) (%)	Acid-base resistance property	Organic solvent resistance
Laminated board or board	Glass fiber	99.97	Kraft paper	Fire resistant neoprene	104	Combustible	85	Poor	Poor
			Chrome paper						
			Aluminum				100		
			Polyvinyl chloride					Good	
	Asbestos fiber	99.5	Kraft paper				85	Rare	
			Chrome paper						
Fire resistant laminated board	Glass fiber	99.97	Aluminum			Fire resistant	100	Poor	
			Asbestos						
Galvanized iron			Aluminum	Glass ceramic	287				Good
Stainless steel			Asbestos		427				
Galvanized iron			Aluminum	Neoprene	121				Poor
				Silicon resin	260				
				Neoprene	104	Combustible		Good	

Epoxy resin coated copper plate			Polyvinyl chloride					
Galvanized iron			Aluminum	Glass ceramic	287	Noninflammable	Poor	Good
Stainless steel			Waterproof asbestos		427	Fire resistant		
Galvanized iron			Aluminum	Neoprene	121			Poor
				Silicon resin	260	Noninflammable		
				Glass ceramic	287			Good
Epoxy resin coated copper plate			Polyvinyl chloride	Neoprene	104	Combustible	Good	Poor
Ceramic	Ceramic fiber	80	Ceramic	Ceramic	870	Noninflammable	Resist other acid and base except strong and middle alkali	Good

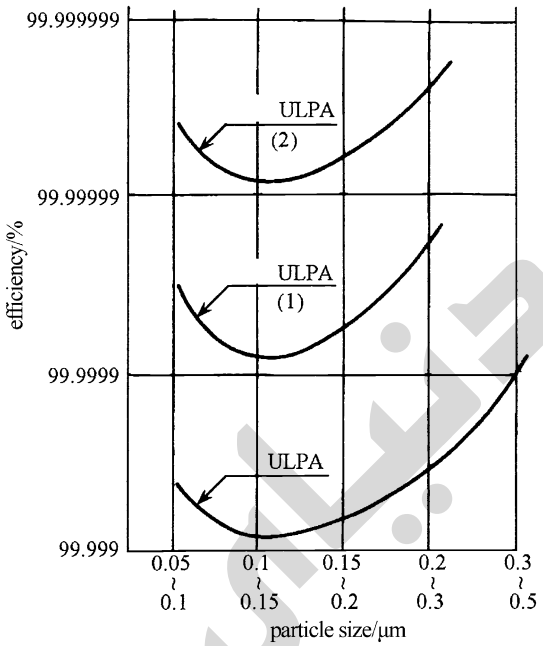

Fig. 4.37 Efficiency of ULPA filter

within the filter media is about 0.3 μm. Fiber diameter is between 0.05 and 0.2 μm, which is only a fraction of that of glass fiber and shown in Fig. 4.38 [36].

The main characteristics of PTFE filter is:

It has strong ability to anticorrosion including acid and alkali.

The volatile amount of chemical substance is extremely low. For example, the volatile amount of boron and sodium is only 1/400 to 1/200 of that from glass fiber filter.

The pressure drop is very small, which is less than common HEPA filter by 2040 %.

At present the price of PTFE filter is comparatively high and the dust holding capacity is a little small.

As for the structure of nonleakage air filter with the requirement as item (5) mentioned above, it has been replaced by author's invention patent of zero leakage air supply outlet. When common air filter is installed in this air outlet, no leakage into the room can be realized.

4.12 Fibrous Layer Filter

Fibrous layer filter is mainly composed of a fibrous filling layer. The fiber used can be divided into three categories: one is natural fiber such as wool and cotton fiber, another is chemical fiber which is made with chemical method to modify the characteristic of raw material, and the third is artificial fiber which is separated

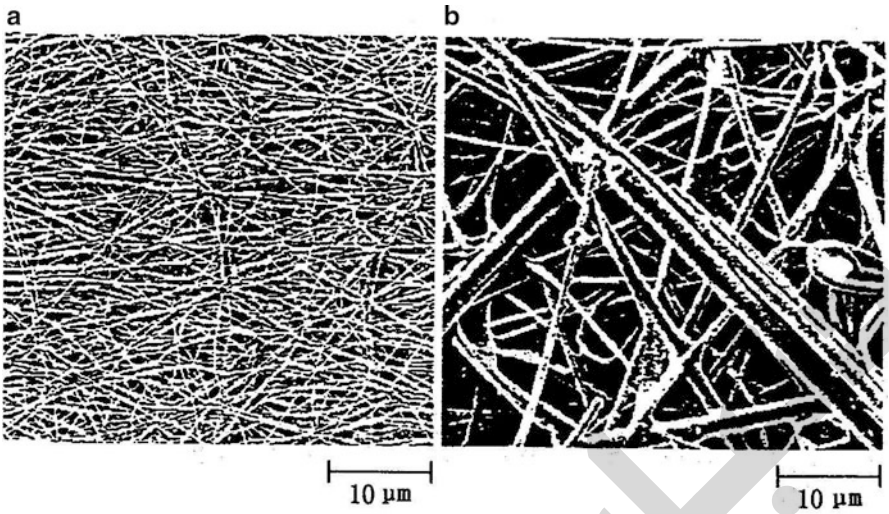

Fig. 4.38 Comparison of filter media. (**a**) PTFE media. (**b**) Glass fibrous media

from the raw material with fibrous shape by physical method or formed to be fibers from raw material. For the second type, the chemical feature of fiber is totally different from that of raw material. For the third type, the chemical feature before and after fiber formation remains the same, such as spinning after the melt of glass.

The surface feature of fiber has great influence on the filtration effect. Taking natural fiber including wool and cotton as an example, the particle capture efficiency is higher than that of smooth plastic fiber because of the scale shape and fibrous shape. The efficiency of glass fiber improves after treatment with hydrofluoric acid [37].

In order to prevent the fiber abscission during operation, binder is sprayed onto fibers. Fibers with different diameter can be chosen to make packed bed with different solid fraction. Particles with large diameter are captured by crude fiber layer. Posterior fine fiber layer is used to filter small particles. In this way, the needed filtration efficiency and dust holding capacity are guaranteed, and the resultant pressure drop is not too high.

Fibrous layer made by nonwoven manufacturing process can also be used to make air filter. Figure 4.39 shows the nonwoven bag filter. The common techniques include needle injection sticking method and hot melt method.

Fibers with different diameters are used as raw material. It forms the web shape after loose carding and folding. Movement of thousands of needles on the needle board of the needle machine makes fibers move along the perpendicular direction. After going forward and backwards, certain numbers of fibers entangle together on the fiber web because of this movement. The glue is sprayed on the surface and then dried. This is called the needle injection sticking method.

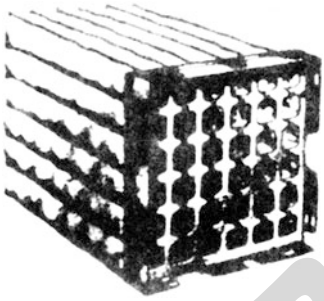

Fig. 4.39 Nonwoven bag filter

If fibers with low melting point such as polypropylene are added into fibers such as polyester, the fiber web formed by folding is placed into the hot melt equipment and heated to certain temperature, then fibers with low melting point are melted and binding other fibers to form the filter media. This is called the hot melt method. Nonwoven fabric made by this kind of method is in the range of coarse efficiency, which is suitable for making rolling filter material. In terms of nonwoven fabric shape, it is one kind of felt fibrous layer. The thickness of this fibrous layer is between less than 1 mm and dozens of micrometer. The efficiency range is so large to cover the coarse efficiency and sub-high-efficiency ranges. Taking one kind of domestic-made polypropylene nonwoven fabric PP-K_2 for an example, its thickness is 1 mm and the pressure drop is about 8 Pa with the filtration velocity 0.06 L/($cm^2 \cdot$ min). The particle counting efficiency with atmospheric dust is 94 % when particle counter is used. It is comparatively cheap and is only several Yuan for each meter squared.

Table 4.26 presents the characteristic of several fibers, which could be used for reference during selection of filter material [38].

Fibrous layer air filter has small solid fraction, so its pressure drop is very low. It is especially suitable for the application of HVAC air cleaning system as medium-efficiency air filter.

There are two principles during the design and selection of fibrous layer air filter. One is based on a single index. It is the priority to consider the requirement of efficiency during the design of air filter. So with the same filtration efficiency, the optimum of certain index is expected. For example, the minimum pressure drop is expected, when requirements of other indexes should follow this requirement of pressure drop. This is a simple case. The other is based on the comprehensive index. With the same filtration velocity, the optimum comprehensive index is expected. When this comprehensive index is labeled with E, Chen proposed to use the ratio of efficiency and pressure drop [3], i.e.,

$$E = \frac{-\ln(1-\eta)}{\Delta P} \tag{4.36}$$

It is obvious that this index is only related to the technical performance of air filter, while its economic performance is not included. If the cost of filter material

was considered, the comprehensive index reflecting the usage of filter material should be used [5]. When this index is denoted with J, we get,

$$J = \frac{W_f}{E} \tag{4.37}$$

where W_f is the usage amount of filter in the filter layer per each meter squared.

It is shown from the above two expressions that E is larger when the efficiency is larger or the pressure drop is smaller. J is smaller when E is larger or the usage amount of filter material W_f is more. Therefore, the smaller value of J is preferred when the efficiency of air filter is given.

Moreover, comprehensive analysis with the fuzzy method was performed [6]. It is comprehensive, but it is not easy for visual understanding because of so many influencing factors. The weight of each factor is determined subjectively by the interest of referee. The comparability of this index is weakened.

Whatever evaluation method is adopted, the filtration efficiency requirement is of the priority, and then other comprehensive indexes are considered. The following items should be noted during the design of air filter:

First of all, filter material with suitable fiber diameter should be selected. It is known from filtration theory that efficiency decreases with the increase of fiber diameter, but the decrease velocity is slower than the decrease velocity of pressure drop caused by the increase of fiber diameter. Meanwhile, for the given filtration velocity and solid fraction of fibrous layer, thicker fibrous layer is needed for large fiber diameter in order to obtain the same efficiency. Although the usage amount of filter material is obviously much for thicker fibrous layer, the pressure drop still decreases compared with that of small fiber diameter. Therefore, suitable fiber diameter should be determined according to the design requirement.

Secondly, the fibrous layer thickness should be determined. This index depends on the structure and operation condition of air filter.

Thirdly, it should be remembered to keep the structure from being too close or too loose. It seems that the corrugation number could be increased, but this will cause two unreasonable consequences. One is that air does not flow thoroughly near the corrugation edge and stagnant airflow space is formed, so the effective filtration area reduces. At the same time, the corresponding support for filter material increases, so part of filtration area reduces by 7–20 % since the filter material is sheltered by the support. The other is that distance of filter material in each corrugation is very close when the corrugation number increases. Under the airflow pressure, the soft filter material between two corrugations squeezed together, which increases the pressure drop. In order to obtain the maximum effective filtration area, comprehensive consideration of various factors including filter thickness, ridge distance, ridge angle, and filter material thickness. Take bag-type air filter with frame of fixed volume, for example. When bag number increases from two to four, the filter material area increases and the pressure drop of filter material decreases. But the pressure drop of structure will increase because the flow channel is narrowed to increase the pressure drop of structure. When the number of bags is not large, the pressure drop decreases with the increase of the number of bags. On the contrary, when the number

Table 4.26 Properties of several fibers

	Natural fiber		Chemical fiber			
Chemical name			Polyvinyl chloride	Poval	Polyamine	Polyamine (aromatic)
Product name	Wool	Cotton	Polyvinyl chloride fiber	Vinylon	Polyamide	
Density (g/cm^3)	1.32	1.47–1.5	1.39–1.44	1.3	1.13–1.15	1.38–1.41
Tensile strength (expressed with breaking length)[a] (mm)	9–15.3	22.5–36	24.3–35		40.5–55	
Ratio between wet strength and dry strength (%)	85	110	100		90	
Extension ratio at breakage (%)	25–35	7–10	12–25		25–45	
Hygroscopic capacity at 20 °C and 65 % (%)	10–15	8–9	0	3.4	4.0–45	4.5–5
Expansion ratio (%)	50–70	50–80	Max. 1		10–14	
Acid resistance property	Good under low temperature and concentration	Poor	Good under various concentrations	Satisfying	Good under low concentration, poor at high temperature	Insufficien
Alkaline resistance property	Poor	Good	Good for almost all the alkali	Extreme good	Stable	Good
Insect and bacterial resistant property	Resist without treatment	Resist without treatment	Absolute to resist			
Thermal resistant: normal temperature (°C)	80–90	75–85	40–50	115	75–85	220
Thermal resistant: maximum temperature (°C)	100	95	65	180	95	260
Price factor (the value in 1971 is used as the standard)	3.5	1	2.7			13

[a]The weight of the fiber with this length is equivalent with the breakage load

									Artificial fiber
Pure polyacrylonitrile		Polyacrylonitrile		Polyester	Polyester compound	Polypropylene	Polyethylene	PTFE	Glass
Acrylic fiber		Acrylic fiber		Terylene		Polypropylene fiber			Glass fiber
1.17	1.14–1.16	1.14–1.16	1.14	1.38	1.23	0.9–0.91	0.95–0.96	2.3	2.54
25–30	27–31.5	23–30	36–45	40–49				45–80	56–62
90–95	90–95	90	90	93–97				100	
30–40	15–30	24–30	18–22	40–55				10–25	3–4
1.3	2	1	1	0.4	0.4	0.01–0.1	0.01–0.1	0	0
~7	~7	~13	~13	3–4				0	0
Good	Good	Good	Good	Good for almost all the acid	Good	Extreme good	Extreme good	Very good	Poor for some acid
Have enough resistance to weak base				Good under small concentration and room temperature	Satisfying	Extreme good	Extreme good	Very good	Poor under high concentration
Extreme good	Extreme good	Extreme good	Extreme good					non corrosion	non corrosion
125—135	125–135	110–130	110–130	140–160	180	95	60	220–250	250–300
150	150			Resistance to dry heat	200	120	100		350
2.7	2.7	2.7	2.7	2.7	2.7	1.7	2	25	3

of bags is comparatively large, the pressure drop increases. The decrease of pressure drop of filter material cannot offset the increase of pressure drop of structure. Meanwhile, when the number of bags is large or they are too long, the two walls of neighboring bags almost contact each other under the effect of airflow. So it is meant to increase the filtration area by increasing the bag number, but the result is different. It can be improved by setting formed line inside the bag or setting frame outside the bag. With the formed line, walls of bags will be tightened and bags will not be stretched outside. With the frame, walls are kept from stretching outside. For the filtration velocity between 0.2 and 0.5 m/s, the pressure drop can decrease by 30–50 %. There are similarities between folded air filters and the bag filter.

If no frame is placed, with the same total filtration area, the more the number of bag is (or the smaller the bag is), the narrower the airflow channel is, and the larger the structural pressure drop is. Since the pressure drop of filter material is the same, the total pressure drop increases. This is consistent between experiment and theoretical analysis [6].

4.13 Foam Air Filter

Foam air filter is a combination of individual pin hole. Membrane between pin holes is melted with the chemical treatment, so that air can flow through it. It is then used as filter material. Foam plastic filter is one example. It is composed of three dimensional net skeletal frames, whose cross section is not circular. The size of this skeletal frame differs a lot. When the skeletal frame is considered to be fibers inside the filling layer, the filtration efficiency can be derived with the application of fibrous filtration mechanism [39]. Figure 4.40 is the calculation plot for efficiency. In the figure, the number of pores is counted with microscopic after the surface of foam plastic is dyed.

The usage of foam plastic filter is rare.

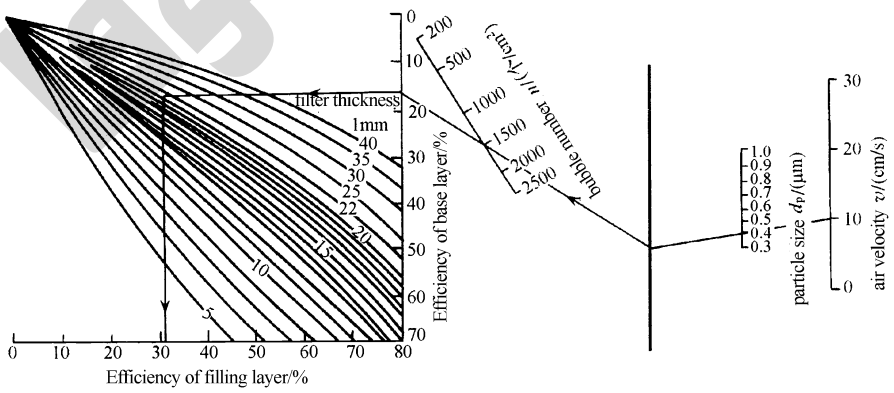

Fig. 4.40 Calculation plot for efficiency of foam plastic air filter

4.14 Electrostatic Cleaner

In this section, the mechanism and device of electrostatic precipitation will not be introduced comprehensively. Only one kind of popular electrostatic precipitation equipments – electrostatic cleaner is presented.

4.14.1 Application of Electrostatic Cleaner

In the turbulent cleanroom, eddy current forms near the four corners of rooms because of the limit of air supply mode, where the cleanness cannot be improved by air distribution. Because of the eddy current and the dust source, the cleanness of the room will be greatly influenced. In order to reduce the particle concentration in these regions, local cleaning equipment can be used.

Air is cleaned when the local air goes through the air cleaner repeatedly. The pressure drop of electrostatic cleaner is very small, and it is usually only 10–20 Pa. The axial fan can be used and the noise level is low. Besides it has the advantage of flexibility and convenience to use. So it is especially suitable for self-purification of indoor air. In the past, the electrostatic cleaner was called electrostatic self-purifiers in China.

If a layer of activated carbon filter is added into the electrostatic cleaner, it also has the effect of gas and carbon dioxide adsorption. Now this kind of electrostatic cleaner can be used as self-purification in rooms where the air cleanness is required. For example, it can be applied in meeting room, guest room, and living room. Test has shown that when an electrostatic cleaner with two-stage ionization and efficiency of 95 % operates in room with area 25 m^2 for 1.5 h, the dust concentration reduces to 1/8 of the original value, and the colony count becomes 1/6 of the original value.

In cleanrooms, electrostatic cleaner should not be used as final filter, which has already specified in related standards. This is because the air delivery rate is very small. Moreover, particle resuspension caused by power failure, shutdown of the device, and discharge will cause unexpected result. It efficiency is less than that of sub-HEPA filter and HEPA filter. It is mainly used in the air handling system of fresh air.

4.14.2 Working Principle of Electrostatic Cleaner

It is shown in the expression that for given particle group, u_e is proportional to $\frac{n}{d_p}$ when other conditions remain the same. However, as mentioned before, for particles with diameter less than 1 μm, $\frac{n}{d_p}$ is stable. So u_e will approach stable and do not decrease. When it is noticed that the slip correction coefficient C will increase with the decrease of particle size (introduced in Chap. 6), the separation velocity will be a little larger. That means the decrease of u_e becomes stable. Therefore, compared with

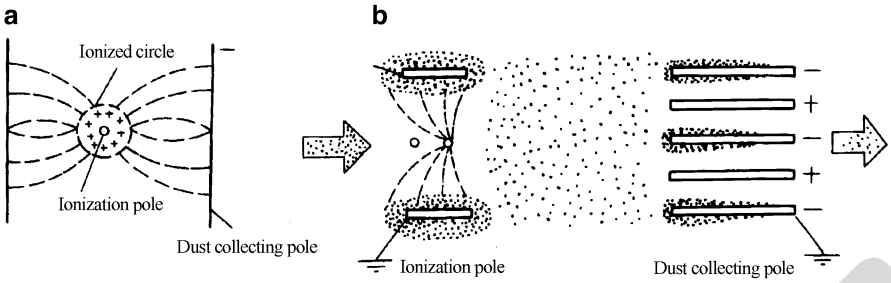

Fig. 4.41 Types of electric field. (**a**) Single area type. (**b**) Double area type

other kinds of air filters, electrostatic cleaner is more suitable for capture of fine particles. When particle diameter is larger than 1 μm, u_e is proportional to d_p because $\frac{n}{d_p}$ is proportional to d_p (because n is proportional to d_p^2).

4.14.2.1 Charge on Airborne Particles

Inside the electrostatic cleaner, the electric field usually has two forms: single zone and double zones, which are shown in Fig. 4.41.

For the case of electric field with double zones, ionization electrode and dust collecting electrode are separate. In this way, the voltage of ionization electrode can be reduced from tens of thousands of voltage, which is used in single zone, to ten thousands voltage. Several dust collectors can be used to increase the collecting area. The distance between collecting plates reduces so that the voltage can be as low as several thousands, which is much safer. Therefore, the electrostatic cleaner with double zones is applied in the field of air-conditioning and cleaning system.

The main difference between electrostatic cleaner used in air-conditioning and cleaning system and electrostatic precipitator used in industrial application is the discharge by positive corona instead of negative corona. For positive corona, it is easy to convert from corona discharge into spark discharge. So only lower charge voltage can be exerted, which reduces the generated ozone. For the occupied space, the concentration of ozone generated is limited.

When positive corona is used, high enough DC positive voltage is exerted on the metal wire of ionization electrode, and two sides of polar plates are grounded. In this way, nonuniform electric field is formed near the ionization electrode. A few free electrons in the air obtain energy from the electric field. They collide with air molecules fiercely, which generates collision ionization, and incomplete discharge appears, which is called corona discharge. Around the ionization electrode, a ring of light blue halo could be seen, which is termed as corona. So ionization electrode abounds with positive ions and electrons. Electrons move towards metal wire and neutralize on it, while positive ions move regularly under the effect of electric field, and they attached onto neutral particles when they encounter each other. In this

way, particles become positive, which is the first kind of charge mechanism, i.e., electric field charge. Secondly, except for the movement under the effect of electric field, ions have thermal motion. Ions attach onto particles during the process of thermal movement, which makes particles positive. This is called the second kind of charge mechanism, i.e., diffusion charge.

According to the electrostatic theory, electric field charge mainly has influence on the particles with diameter larger than 1 μm. The maximum charge particles can obtain is

$$q = ne = \frac{kE_1 d_p^2}{4} \tag{4.38}$$

where

E_1 is the electric field intensity in the space of ionization electrode, e.s.u. (300 V/cm = 1 e.s.u.);
n is the number of charge;
e is the unit charge, 4.8×10^{-10} e.s.u.;
d_p is the particle diameter, cm;
k is the coefficient, $k = \frac{3\varepsilon}{\varepsilon+2}$; the average is between 1.5 and 1.8;
ε is the dielectric constant; the average value is 2–3.

Diffusion charge has the main influence for particles with diameter less than 1 μm, especially less than 0.2 μm. However, no simplified expression has been obtained for the maximum diffusion charge so far. It is known from Eq. (4.38) that the charge on particles with diameter larger than 1 μm is proportional to the square of particle diameter. But with the effect of diffusion charge, the charge on particles with diameter equal to or less than 1 μm is larger than that obtained by Eq. (4.38). So the ratio of charge and its particle size $\frac{n}{d_p}$ keeps stable. It will not decrease inversely proportional to the square of particle size.

4.14.2.2 Capture of Charged Particles

Charged particles enter into the space composed of parallel thin aluminum plates. Since aluminum plates are placed by staggered rivets with one aluminum plate positive and the other grounded, an uniform electric field is formed in the space.

With the Coulomb force in the electric field, charged particles obtain repellent force from the positive plate, and they settle down onto the grounded plate. The repellent force can be expressed as

$$F_e = QE_2 = neE_2 \tag{4.39}$$

where

F_e is the Coulomb force;
Q is the charge on particle (e.s.u.).

For the flow with small Re (usually less than 1), the pressure drop of spherical particles is obtained by Eq. (6.5). When the pressure drop is balanced with the Coulomb force, i.e., $3\pi\mu d_{\mathrm{p}}v = neE_2$, the motion velocity u_e of particles in the electric field is obtained when the slip correction is considered, which is also called separation velocity or migration velocity. It can be expressed as

$$u_e = C\frac{neE_2}{3\pi\mu d_P} = Ck\frac{E_1E_2d_P}{12\pi\mu}\ (\mathrm{cm/s}) \tag{4.40}$$

where μ has the cgs unit (shown in Chap. 6), and other symbols have already been explained.

It is shown in the expression that for a given particle group, u_e is proportional to $\frac{n}{d_p}$ when other conditions remain the same. However, as mentioned before, for particles with diameter less than 1 μm, $\frac{n}{d_p}$ is stable. So u_e will approach stable and does not decrease. When it is noticed that the slip correction coefficient C will increase with the decrease of particle size (introduced in Chap. 6), the separation velocity will be a little larger. That means the decrease of u_e becomes stable. Therefore, compared with other kinds of air filters, electrostatic cleaner is more suitable for capture of fine particles. When particle diameter is larger than 1 μm, u_e is proportional to d_p because $\frac{n}{d_p}$ is proportional to d_p (because n is proportional to d_p^2).

4.14.3 Structure of Electrostatic Cleaner

Electrostatic cleaner is composed of box, power supply, fan, dust collecting electrode, ionization electrode, activated carbon filter, and prefilter. Figure 4.42 shows the structure of domestic JZQ-II electrostatic self-purifier [7]. The box is made by single layer of thin steel plate. With the requirement of air tightness, the box gates are connected with circlip, which is used for the convenience of maintenance.

The ionization electrode is a nickel chrome silk with diameter 0.5 mm. Dust collecting electrode is composed of rigid aluminum alloy plates with thickness 1 mm and inter-plate spacing 6 mm (between opposite plates). Each polar is made of 46 pieces of plates with area of each plate 0.2 m × 0.23 m. The surface of these plates has been electropolished to get rid of the burr and sharp corner, so the phenomena of spark discharge will not occur and the voltage between plates will be decreased. Figure 4.43 presents the structure of JZQ-1 electrostatic self-purifier with one time ionization method.

The height of JZQ electrostatic self-purifier is 0.8 m and the net cross-sectional area is 0.34 m × 0.34 m.

During the design of structure, the leakage inside the structure is usually neglected, which will greatly reduce the dust capture efficiency. There are mainly two reasons: one is caused by the electric wire when it goes through holes (such as the separator between layers); the other is the leakage between frame of each layer and box.

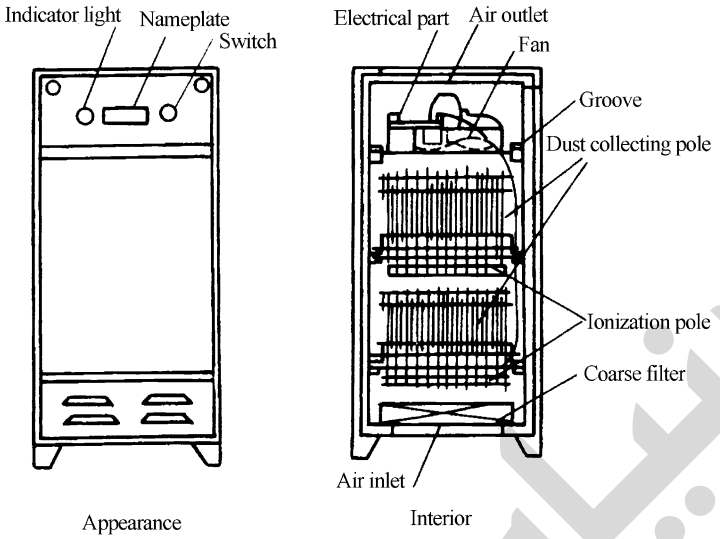

Fig. 4.42 JZQ-II electrostatic self-purifier

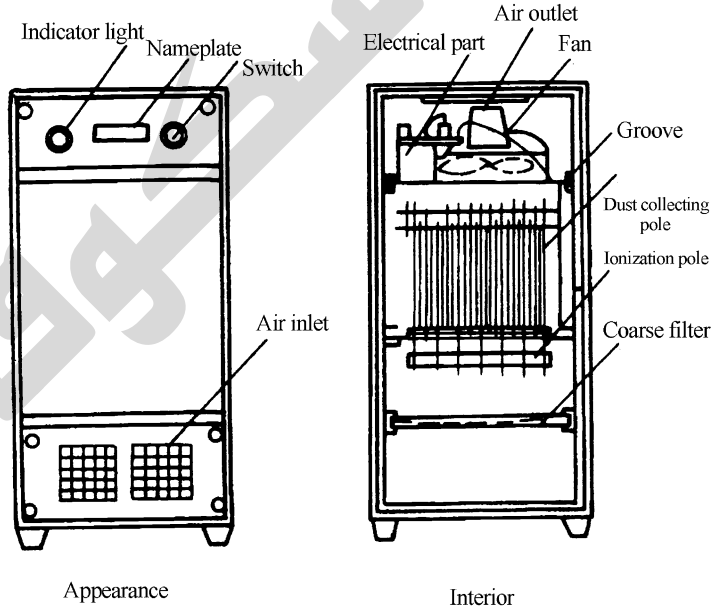

Fig. 4.43 JZQ-I electrostatic cleaner

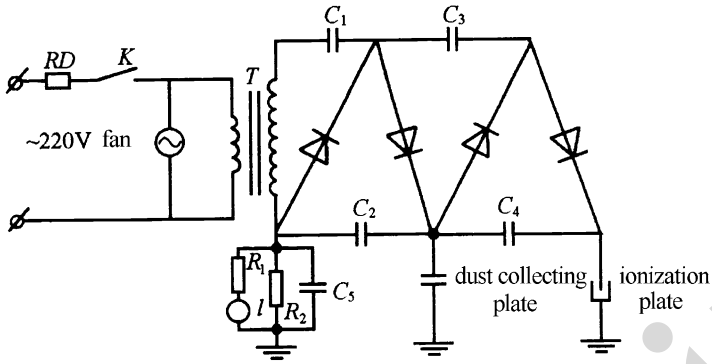

Fig. 4.44 Circuit of JZQ-II electrostatic cleaner

It should be noted during the design of structure that two grounded plates must be added at both sides of ionization electrode (metal wire) and dust collecting electrode (metal plate). If both the ionization wire and the electrode plate near the edge are only connected with the power and without being grounded, both the airflow and particles will not be easily ionized and particles will not deposit readily, which will lower the total efficiency.

Since the volume of electrostatic cleaner is small, silicon rectified circuit is used for the power supply. In order to reduce the output voltage of transmitter so as to insulate, four times voltage circuit is usually adopted. Figure 4.44 shows the circuit of JZQ-II electrostatic cleaner. When too much dust has been deposited on the dust collecting plate, the indicator light will turn dark. The plate should be taken out for clean in time so that the dust collecting efficiency will not be affected.

4.14.4 Efficiency of Electrostatic Cleaner

4.14.4.1 Efficiency Expression

The following steps can be used to derive the dust collecting efficiency of electrostatic cleaner when the dust collecting electrode is plate.

Suppose the concentration at x distance from the inlet of dust collecting plate is N_x, the airflow velocity between plates is v, the total flow rate through the dust collecting plate is Q, the total effective area of dust collecting plate is F, and the length of plate is L. During the time dt, the decrease of dust along the dust collecting plate (perpendicular to the flow) equals with the number of deposited particles at this section of dust collecting plate, i.e.,

$$-\mathrm{d}N = N_x \frac{u_c F \mathrm{d}t}{\frac{Q}{v} L}$$

Since

$$\mathrm{d}x = v\mathrm{d}t$$

We get

$$\frac{\mathrm{d}N}{N_x} = -\frac{Fu_c}{QL}\mathrm{d}x \tag{4.41}$$

When the concentration at $x = L$, i.e., the outlet concentration, is N_L, and the concentration at $x = 0$, i.e., the inlet concentration, is N_0, integration is performed on the above equation and the following expression is obtained:

$$N_L = N_0 \mathrm{e}^{-\frac{Fu_e}{Q}} \tag{4.42}$$

Then the dust collecting efficiency is

$$\eta = 1 - \frac{N_L}{N_0} = 1 - \mathrm{e}^{-\frac{Fu_e}{Q}} \tag{4.43}$$

4.14.4.2 Separation Velocity

It is obvious that η increases with the increase of the separation velocity u_e. For given particles, u_e mainly depends on the voltage between the ionization electrode and the dust collecting plate.

When the voltage of the dust collecting plate increases, the electric strength in the space between dust collecting plates also increases, which will increase the separation velocity. However, when the electric strength between dust collecting plates is too high, the phenomena of electrode discharge are likely to appear. Even through the electropolishing, the surface of plates will inevitably unsmooth, especially burr exists near the edge. Even through the surface is very smooth, discharge will occur when a large dust especially fiber deposits on the surface, which will decrease the electric strength rapidly. During the process of discharging, sounds with cracking will be heard. For common manufacturing level, the electric voltage of the dust collecting plate can be increased to 7,000–8,000 V, which is equivalent to the electric strength about 1 kV/mm.

When the voltage of the ionization plate is elevated, particles will be charged more, which increases the separation velocity u_e. But the extent of voltage increase is limited by the manufacturing precise. Too much voltage will cause electric discharge. So the voltage is usually less than 15,000 V.

The separation velocity u_e calculated from Eq. (4.40) is only a theoretic value. In practice there are many influencing factors which are not included in this equation. These influences include: distribution of air and airborne particles at the cross section between plates, movement characteristic of air in the channel, coagulation of particles, and re-entrainment of particles deposited on plates. Therefore,

the actual separation velocity is much less than theoretical value. Research performed on industrial electrostatic cleaner shows that the actual velocity is half of the theoretical value. But the situation is better for electrostatic cleaner used in air cleaning system, because the distance between dust collector plates is small, and velocity is small so that the flow is laminar. The particle size distribution at inlet is comparatively uniform. So the disturbance extent on u_e is small. Therefore, the actual separation velocity of electrostatic cleaner is a little higher than that of industrial electrostatic cleaner.

4.14.4.3 Effective Length of Dust Collector Plate

For the given height (width), the larger the effective area is, which corresponds to the larger length, the higher the efficiency derived by Eq. (4.43) is. The effective area of plate mentioned in literature means the area which is effectively used in structure. According to the expression of efficiency, efficiency will reach 100 % when the area is large and the plate is lengthy. But in reality not all the area of the plate along its length can collect dust efficiently. Test on JZQ-I electrostatic cleaner with length 30 cm shows that only 2/3 of the area along the length collect dust. If all the particles are deposited on the plate along this 2/3 length, the efficiency of this electrostatic cleaner approaches 100 %, while in fact it is only 70–80 % which can been seen from the comparison table about efficiencies. This is not caused by the length of plate which is not long enough so that particles do not have time to deposit but by part of particles which is not charged or whose electric charge is not enough. For particles whose charge is not enough and u_e is small, it is effective to prolong the length of dust collector plate. However, for particles which are not charged at all, they will not be deposited on plate even when its length is prolonged. Since particles without charge do exist, a concept "effective length of dust collector plate" is proposed. It means that under certain electric field, only certain part of the plate has effect on dust collecting. When it is longer than this length, the efficiency of the left part of the plate cannot be described by Eq. (4.43), which implies that no more particles can be captured or not all the particles can be collected.

Why do some particles carry very few charges or no charges? According to the theory of electric corona discharge, there are mainly two reasons:

1. Since the electric ionization polar is a metal wire, the electric field with high electric strength only appears near the small distance around it, while the electric strength far from it is very weak. For the latter situation, the movement velocity of ions is very slow and the air in that region is not ionized (If all the air between plates is ionized, the electric field will be penetrated when spark discharge appears and short electric circuit is formed, thus the electrostatic cleaner stops).
2. As mentioned before, with certain voltage of electric ionization polar, the ionization strength for air is fixed and the charge amount is determined. If the dust concentration of air entering electrostatic cleaner is high, charge on every particle is not enough or some particle cannot be charged at all.

It is obvious that the former reason is mainly for electrostatic cleaner.

From the above analysis, if the effective length of dust collector is measured, the actual separation velocity can be derived from the dust collector efficiency.

4.14.4.4 Flow Rate

It is obvious that the less the flow rate of electrostatic cleaner, the higher the efficiency is. But for particles without charge, efficiency will become stable when the flow rate is less than a certain value.

4.14.5 Electrostatic Cleaner with Two-Stage Ionization

According to the above analysis, in order to increase the efficiency of electrostatic cleaner with one-stage ionization, the extent of particle charge must be increased. So author proposed a scheme "two-stage ionization" which put two electric fields in series. With this method, air molecules not ionized in the first electric field will be likely to be ionized in the second electric field. In the late of 1960s, Institute of HVAC at China Academy of Building Science and the former Tianjin Medical Equipment Factory invented and manufactured JZQ-II electrostatic cleaner together, which adopted this method.

It is meaningless if the height of the equipment with two-stage ionization is two times that of the original equipment. According to the above analysis, the effective dust collector length under the given conditions is about 0.2 m. So the length of dust collector of JZQ-II electrostatic cleaner is 0.2 m under the condition of compact structure, which is the same as that of the one-stage ionization.

With the scheme of two-stage ionization, the predicted effect of electrostatic cleaner is realized. Related experimental data are presented in the following tables.

Table 4.27 is the experimental data about the relationship between efficiency and voltage of dust collector.

Table 4.28 is the experimental data about the relationship between efficiency and velocity between plates of dust collector.

Table 4.29 is the experimental data about the relationship between efficiency and capacity of capacitor in the rectifying circuit.

The influence of capacity of capacitor in the rectifying circuit on efficiency is large. When the capacity is small, the decrease of voltage on each octave band pressure level will be large, which reduces the particle capture efficiency, while increasing the capacity will smooth the wave profile after rectifying and the effective voltage approaches the summit value. But it is not safe if the capacity of capacitor was too big. For JZQ-II electrostatic cleaner, it is feasible to choose 8,800μμF as the capacity of capacitor.

According to Eqs. (4.38) and (4.40) with the cgs unit and 1 e.s.u. of E_1 and E_2, the separation velocity for the condition with $c = 1$, $k = 2$ (for oil mist from the

Table 4.27 Experimental data about the relationship between efficiency and voltage of dust collector

Air velocity between dust collector plates (m/s)	Capacitor capacitance (μμF)	Transformer output voltage (V)	Voltage of dust collector (V)	Turbidity efficiency (%)
1.3	8,800	4,200	7,250	96.9
1.3	8,800	3,860	7,000	96.5
1.3	8,800	3,410	6,600	95.8
1.3	8,800	2,950	6,250	93.7

Table 4.28 Experimental data about the relationship between efficiency and velocity between plates of dust collector

Transformer output voltage (V)	Capacitor capacitance (μμF)	Air volume (m^3/h)	Air velocity between dust collector plates (m/s)	Turbidity efficiency (%)
4,200	8,800	240	0.66	99.3
4,200	8,800	440	1.2	99.1
4,200	8,800	500	1.4	96.9
4,200	8,800	710	2	91.4

Table 4.29 Experimental data about the relationship between efficiency and capacity of capacitor in the rectifying circuit

Air velocity between dust collector plates (m/s)	Transformer output voltage (V)	Capacitor capacitance (μμF)	Turbidity efficiency (%)
1.4	3,860	8,800	96.5
1.4	3,860	4,400	93.3
1.4	3,860	1,100	86.8

transformer, $k = 1.5$; for marble particles, $k = 2.4$), and both E_1 and E_2 are 1 e.s.u. becomes

$$u_e = \frac{2d^2E_1E_2}{12\pi \times 1.8 \times 10^{-4}d} \approx 0.03E_1E_2d \times 10^4 \text{ cm/s}$$

When $d = 0.5 \times 10^{-4}$ cm, $c = 1.3$, $E_1 = 14{,}000$ V ≈ 46.5 e.s.u., and $E_2 = 7{,}000$ V ≈ 23.3 e.s.u., the derived separation velocity is $u_c = 21$ cm/s (which is equivalent with the calculation result based on average particle size of atmospheric dust).

According to Eq. (4.40), the relationship between $\frac{Fu_e}{Q}$ and η is

η (%)	60	70	80	90	95	99
$\frac{Fu_e}{Q} = \frac{\frac{E}{s}u_e}{v} = B$	0.9	1.21	1.6	2.3	3.0	4.6

Table 4.30 Comparison of separation velocity

Air velocity (m/s)	Actual separation velocity (m/s)	Theoretical separation velocity (m/s)
0.66	0.09	
1.2	0.14	
1.4	0.12	0.21
2	0.12	

Suppose the effective cross-sectional area of the cleaner is S and the velocity at the cross section (the velocity between dust collecting plates) is v, we could get:

$$\frac{Fu_e}{Q} = \frac{\frac{F}{S}u_e}{v} = B$$

So

$$u_e = \frac{Bv}{\frac{F}{S}} \tag{4.44}$$

For JZQ-II electrostatic cleaner, we know

$$\frac{F}{S} = \frac{(46-2) \times 0.2 \times 0.23}{0.1} = 20$$

where 46 is the number of dust collecting surfaces. Each dust collecting plate has two surfaces. Since the most outer two sides do not play a role, they are not included and the total number of dust collecting surfaces is 44. So the actual separation velocity of each section for given efficiency can be calculated, which is shown in Table 4.23.

From Table 4.30, the average of actual separation velocity is 0.12 m/s, which is slightly higher than half of theoretical separation velocity. It is consistent with the aforementioned analysis.

For JZQ-II electrostatic cleaner with two-stage ionization method, the comparison of its turbidity efficiency measured by photoelectric turbidimeter with the foreign similar products is shown in Table 4.31.

In terms of efficiency, results obtained by the turbidimetry method are usually smaller than that of dust spot method and weighing method. So the performance of JZQ-II electrostatic cleaner is better than that presented in Table 4.31.

For simplifying the structure, cylindrical electrostatic cleaner appears in the market. Thin metal plate is used to make the cylinder with circular or hexagonal cross section. It acts as the grounding plate. Circular electrode with cusp is placed in the center of cylinder, where high-voltage electrostatic is applied. It becomes the high-voltage discharging electrode in the electrostatic field, which is shown in Fig. 4.45.

But the efficiency of this kind of cylindrical electrostatic cleaner is very low. Table 4.32 shows the test data from Mao Huaxiong [40].

Table 4.31 Comparison of efficiency for the same kind of electrostatic cleaner

Country	Air velocity (m/s)	Measurement method	Efficiency (%)	Remark
JZQ-I type in China (with once ionization)	0.51	Particle counting method	72.0	Measured with the same instrument
		Turbidity method	80.6	
China JZQ-II type (with twice ionization)	0.66	Turbidity method	99.3	
	1.20	Turbidity method	99.1	
	1.40	Turbidity method	96.9	
	2.00	Turbidity method	91.4	
UK (with once ionization)	0.50	Turbidity method	75–80	
Japan (with once ionization)	1.25	Turbidity method	72.8	
	2.00	Turbidity method	69.7	
	2.00	Turbidity method	85	Data from the same sample product
		Dust spot method	90	
Former Soviet Union (with once ionization)	2.00	Turbidity method	80–85	Data from the same product in literature
		Gravimetric method	98.5	
Former Federal Germany (with once ionization)	1.70	Gravimetric method	99	Data from the same sample product
		Dust spot method	90	
	2.00	Dust spot method	83	
UK (with once ionization)	1.70	Dust spot method	90	Data from the same sample product
	2.20	Dust spot method	80	

4.15 Special Air Filters

4.15.1 Activated Carbon Filter

More attention has been paid on the influence of chemical pollution inside cleanrooms (please refer to Chap. 7), so people starts to care about activated carbon filter.

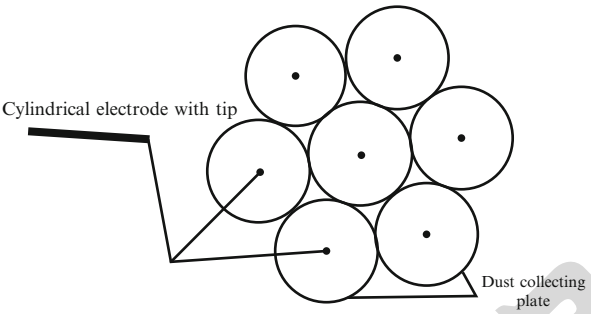

Fig. 4.45 Electrostatic field with circular cylinder (cusp discharging)

Table 4.32 Fractional efficiency of cylindrical electrostatic cleaner with atmospheric dust (%)

Flow rate (m^3/h)	Face velocity (m/s)	≥0.3 μm	≥0.5 μm	≥0.7 μm	≥1.0 μm	≥2.0 μm	≥5.0 μm
800	0.8	19.8	22.6	35.9	41.2	53.0	84.7
1,000	1.2	14.1	16.1	23.7	29.3	50.0	69.4
1,800	1.8	7.6	9.0	15.8	21.0	37.5	58.2
2,500	2.5	4.8	6.8	11.0	14.7	28.8	54.1
3,000	3.0	3.9	5.7	9.9	21.5	36.8	38.2
3,600	3.6	3.6	5.6	10.7	22.6	28.4	37.1

Activated carbon filter has functions of both physical adsorption and chemical adsorption, so in fact it is an adsorber.

The adsorption ability of activated carbon has selectivity. For these chemical substances which cannot be removed by physical adsorption mechanism, different chemical agents must be used as adsorbent during the process of impregnation. With the chemical reaction between adsorbent and adsorbate, the property of adsorbate is modified and it becomes nontoxic and harmless.

Many monographs and literatures have introduced the general application of activated carbon filters, which will not be mentioned in this section. Only several aspects are emphasized here:

1. At present there are three kinds of activated air filters. One is the activated carbon particulate filter where the size of particle varies from small to large. The second is activated carbon particles with diameter 0.5 mm pasted on multiply layers of porous polyurethane foam material. Since the air permeability of foam material is good, its pressure drop is smaller than that of the former kind and the corresponding adsorption efficiency reduces. The third is activated carbon fibrous filter by carbonization of fibrous media. It is thin, and both the pressure drop and adsorption efficiency are comparatively small.
2. The problem of invalid layer exists in the activated carbon filters. Invalid layer is meant to adsorb a certain amount of chemical pollutants. The larger the activated carbon particle is, the thicker this layer is. This problem is usually ignored.

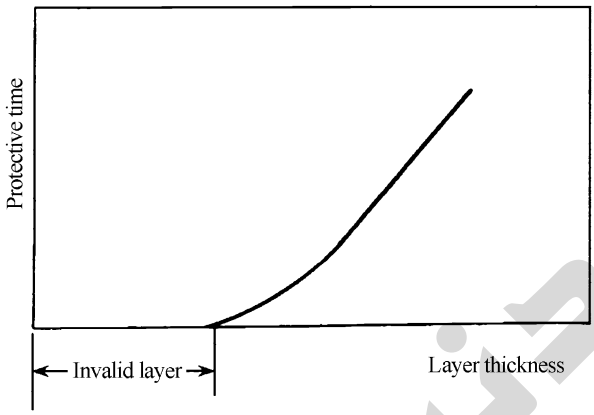

Fig. 4.46 Theoretical curve of invalid layer

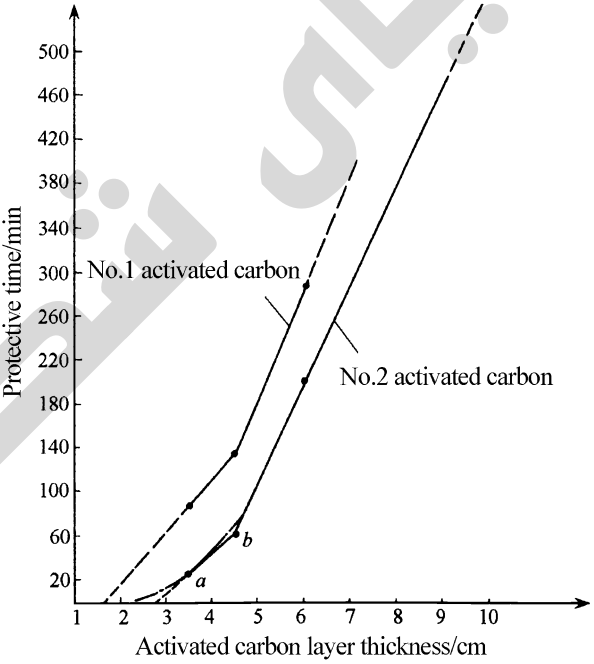

Fig. 4.47 Experimental curve of invalid layer

Figure 4.46 shows the theoretical relationship between the invalid layer thickness and the amount of pollutant adsorbed. When the amount does not reach a certain value, it is called the non-protective time. Figure 4.47 is the result performed with cyan chloride [41].

The existing of this invalid layer is related to the adsorption mechanism of chemical pollutant by activated carbon. When polluted airflows through activated carbon, the pollutant diffuses towards the whole surface of activated carbon particles.

Then it goes towards to the pore interior surface of the particles and the surface of pores. So chemical reactions occur inside the particle interior surface to decompose the pollutant by adsorption of pollutant molecules and between adsorbed chemical pollutant and chemical agent (catalyst) dipped with activated carbon or between adsorbed oxygen and water. If several adsorption mechanisms inside a layer with certain thickness do not have enough time to play a role, for example, pollutant only diffuses onto the particle surface while they do not have time to diffuse towards the interior surface of pores and then adsorbed and decomposed, but it has already penetrated this layer, the pollutant concentration cannot be reduced to allowable value or has no time to be reduced at all, this layer is called invalid layer. If the activated carbon is within the invalid layer, there is no effect of adsorption.

With certain physical and chemical property of activated carbon and temperature/humidity conditions, the thickness of invalid layer is only related to the specific velocity and pollutant concentration. When both the specific velocity and concentration are fixed, the thickness is constant, which is not related to the thickness of whole activated carbon layer.

3. Since the pressure drop of activated carbon filter filled with particulate activate carbon is very large, the allowable specific velocity cannot be very large. Therefore, it is necessary to understand the specific velocity-pressure drop characteristic of this kind of activated carbon filter.
4. When the activated carbon filter is designed to be circular cylinder, it has been proved by the author that the performance is better when the polluted air flows from outer towards inside, which improves the amount of adsorption [40].

4.15.2 Antibacterial Filter

Since the risk of microorganism becomes higher, antibacterial filters develop in the USA and Japan. This kind of filter is made by adding bactericidal substance in the filter media. However, doubt about its effectiveness exists.

One kind is only to spray the additive onto the surface of filter media, so not all the filter layer have the ability to kill bacteria. The second kind is only to add bacteriostatic agent, which cannot kill the bacteria and instead may cultivate the ability of drug resistance of the bacteria. The third kind may generate some gaseous substance or odor which is harmful for people.

It should be emphasized, which will also be introduced in Chap. 9, that it is difficult for the bacteria captured on the windward side of the HEPA filter made by inorganic material to reproduce and even penetrate. Only with the suitable conditions of temperature and humidity, they are likely to survive. So the final conclusion of the necessity to use the antibacterial filter has not been reached. ASHRAE has warned as for this issue and suggests using antibacterial product in HVAC system cautiously, so as not to produce any chemical pollution and new harm to the indoor environment and people.

References

1. Xu ZL, Shen JM (1989) Application of air cleaning technology. China Architecture & Building Press, Beijing, pp 145–172 (In Chinese)
2. Yoshikawa S (1978) Air filtration (3). J SHASE Jpn 52(6):57–63 (In Japanese)
3. Chen CY (1955) Filtration of aerosols by fibrous media. Chem Rev 55(4):595–623
4. Kimura N, Kouichi I (1969) Particle capture performance of fibrous filling layer filter and influence of fiber cross sectional shape. J Chem Eng Jpn 33(10):1008–1013 (In Japanese)
5. Institute of HVAC at Tianjin University (Tu Guangbei) (1980) Fibrous filter media and air filter, Science and technology information reference room at Tianjin University, pp 52–56 (In Chinese)
6. Ye H (1996) Study of influencing factors for the performance of air filters [D]. Harbin University of Civil Engineering and Architecture (In Chinese)
7. Institute of HVAC of China Academy of Building Research (1973) Assembly cleanroom (In Chinese)
8. Xu ZL (1976) Calculation of cleanroom. Inst HVAC China Acad Build Res 58:59 (In Chinese)
9. Liu BYH, Lin B (1987) Performance test of domestic air sampler and high efficiency filter media. Contam Control Air Cond Technol 3:9–14 (In Chinese)
10. Sato E (1976) Status of industrial cleanroom. J Jpn Air Clean Assoc 13(8):32–41 (In Japanese)
11. Hirasawa K (1973) Planning and design of cleanroom. Jpn Air Cond Heat Refrig News 13 (1):75–88 (In Japanese)
12. Xu ZL (1981) Calculation and verification of in-series efficiency of HEPA filters. J HV&AC 2:64–67 (In Chinese)
13. Filtration Special Committee of Japan Nuclear Fuel Service (1980) Experimental study of the safety of HEPA filter used in nuclear fuel facilities. J Jpn Air Clean Assoc 18(3/4):2–23 (In Japanese)
14. Burchsted CA (1981) Air cleaning handbook (trans: Shi Youren et al). Atomic Energy Press, Beijing (In Chinese)
15. Japan Refrigeration and Air Conditioning Industry Association (1971) Handbook of refrigeration and air conditioning (application). Bunshodo Printing Co. Ltd. (In Japanese)
16. Hayakawa K et al (1974) Air conditioning and air cleaning (In Japanese)
17. Onobori I (1968) Absolute filter of Cambridge Filter Corporation. J Air Cond Heat Refrig News 8(1):5–13 (In Japanese)
18. Tu GB (1987) Discussion of standard flow rate for HEPA filter. J Contam Control Air Cond Technol 2:31–34 (In Chinese)
19. Xu ZL, Zhang YZ, Zhang TG et al (1997) Influence of non rated flow volume on the life time of HEPA filter. J Contam Control Air Cond Technol 1:6–8 (In Chinese)
20. Xu ZL (1995) Conversion method between the particle counting efficiency and the arrestance with atmospheric dust. J Contam Control Air Cond Technol 1:16–20
21. Hirasawa K, Oshige K (1989) The latest filter. Build Equip Water Heat Constr 27(6):70–82 (In Japanese)
22. Kupriyanov TM (1982) Cleanroom technology (trans: Yu Zhaoji). China Architecture & Building Press, Beijing, p 115 (In Chinese)
23. Xu ZL, Shen JM (1987) TGG and YGF low resistance and sub-high efficiency air filter. Report from China Academy of Building Research, No.5-2 (In Chinese)
24. Yoshida Y, Ikezawa Y (1972) Characteristic of filter paper used for collection of radioactive particles. J Jpn Air Clean Assoc 10(2):41–48 (In Japanese)
25. Otake N (1971) Recent development of particulate capture system. J Jpn Air Clean Assoc 8 (7):32–35 (In Japanese)
26. Xu P (1995) Evaluation and performance study of air cleaner [D]. Tongji University (In Chinese)
27. Lin Zhongping (1993) Optimization design of corrugated sub-high efficiency air filter without separator [D]. Tongji University (In Chinese)

28. Zhang JiK et al (1986) Performance of polypropylene fibrous media. In: Proceedings of the Second Academic Conference of Chinese Contamination Control Society, 2986, pp 157–161 (In Chinese)
29. Tani Y, Takase S (1993) Performance evaluation of electret HEPA filter. J Jpn Air Clean Assoc 31(2):13–19 (In Japanese)
30. Gu WZ et al (1983) Monodisperse aerosol generator, Institute of HVAC at China Academy of Building Research (In Chinese)
31. Shi XC (1986) Study of nuclepore membrane filter structure and its filtration performance [D]. Tsinghua University (In Chinese)
32. Institute of HVAC at China Academy of Building Research (1975) Two kinds of 300 type protective air filter. J HV&AC 1:23–35 (In Chinese)
33. Huang ZL, Hui CR (1979) No. 1 soft leather treatment agent for treating with ultra-fine glass fibrous paper for air filtration. Chin J Antibiot 4(4):15–17
34. Feng X (2013) Introduction to Chinese current standardization system on high efficiency particulate air filter. Standard Inspect HVAC 49(3):36–38 (In Chinese)
35. Suzuki M (1993) Performance and prospect of HEPA filter used in cleanroom. J Jpn Air Clean Assoc 31(3):29–36 (In Japanese)
36. Sample brochure from Japan DAIKIN Co Ltd. and AAF company from Suzhou, China (In Chinese)
37. Fuchs HA (1960) The mechanics of aerosols (trans: Gu Zhenchao). Science Press, Beijing (In Chinese)
38. Batel W (1973) Development status and trends in the filtration dust. Dust Pollut Air 9:359–367 (In German)
39. Niitsu Y et al (1967) Study on the filtration of ultrafine particles. J SHASE Jpn 41(8):1–8 (In Japanese)
40. Mao HX (2008) Study of the application of electrostatic air cleaner for improving IAQ [D]. Tongji University (In Chinese)
41. Institute of HVAC at China Academy of Building Research (1974) Two kinds of 300 type protective air filter (In Chinese)

Chapter 5
Structural Design of HEPA Filter

With a certain amount of filtration efficiency with rated flow, the structural design of HEPA filter at present is how to obtain the minimum pressure drop with the corrugation angle (for the type with isolator), the corrugation height (for the type with isolator) or the line height (for the type without isolator), and the passage depth (for both types).

5.1 Flow State in the Passage of HEPA Filter

For the flow state in the passage (inlet and outlet) of ideal HEPA filter with isolator as shown in Fig. 5.1, Cheng Daiyun obtained the calculation result about the flow distribution in the passage on the basis of Bernoulli equation and modified momentum conservation equation, which is shown in Fig. 5.2 and Table 5.1 [1].

The conclusion obtained is that under the condition of low initial velocity, high corrugation, and high pressure drop, the flow in the passage is close to laminar flow with linear distribution of velocity ($Re < 2{,}000$), i.e.,

$$v_1 \approx v_0\left(1 - \frac{x}{L}\right) \tag{5.1}$$

$$v_2 \approx v_0 \frac{x}{L} \tag{5.2}$$

Otherwise, the nonlinear distribution will be obvious.

Experiment with Laser Doppler velocimeter has proved the above conclusion, which is shown in Fig. 5.3 [1]. In terms of outlet passage, the linear correlation coefficient of velocity distribution is more than 0.99.

Z. Xu, *Fundamentals of Air Cleaning Technology and Its Application in Cleanrooms*,
DOI 10.1007/978-3-642-39374-7_5, © Springer-Verlag Berlin Heidelberg 2014

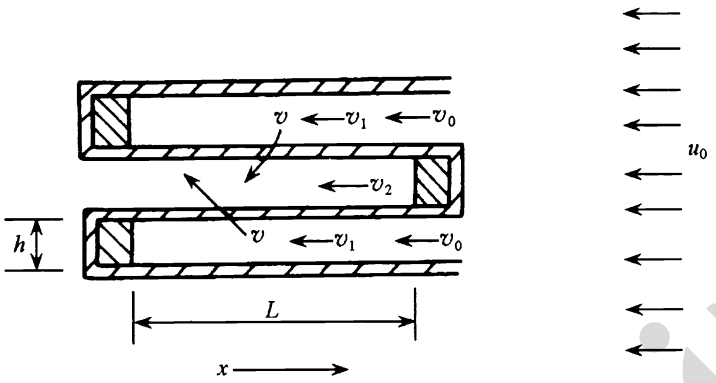

Fig. 5.1 Model for passage of air filter

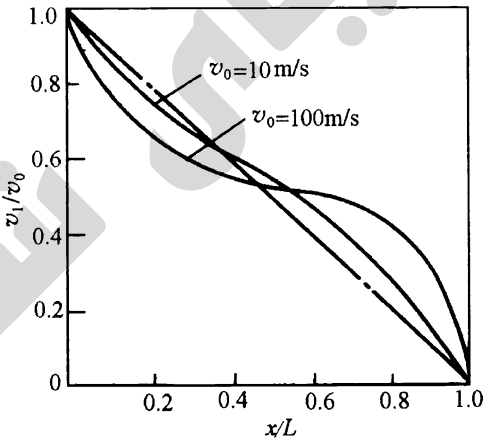

Fig. 5.2 Relationship between the velocity and distance in the passage

Table 5.1 Calculation result about the velocity distribution in passage of air filter with low initial velocity (m/s) and high corrugation (several millimeters)

x/L	v_1/v_0
0.1	0.899
0.2	0.800
0.3	0.701
0.4	0.603
0.5	0.505
0.6	0.407
0.7	0.308
0.8	0.207
0.9	0.105

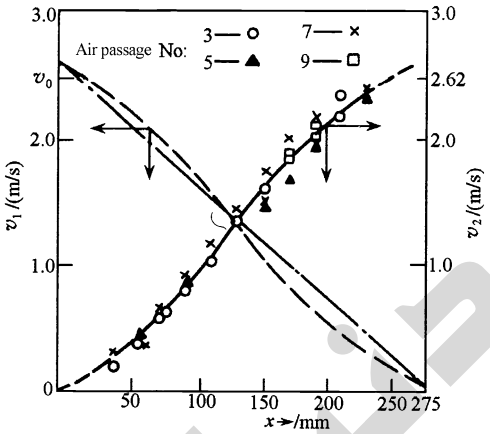

Fig. 5.3 Measured axial distribution of velocity along the outlet passage

5.2 Total Pressure Drop of HEPA Filter

According to Chap. 4, the total pressure drop of air filter can be expressed as:

$$\begin{aligned} \Delta P =& \Delta P_1 + \Delta P_{2(1)} + \Delta P_{2(2)} + C \\ C =& \Delta P_3 + \Delta P_4 \end{aligned} \tag{5.3}$$

where

ΔP_1 is the pressure drop of filter media;
$\Delta P_{2(1)}$ is the frictional resistance of inlet passage;
$\Delta P_{2(2)}$ is the frictional resistance of outlet passage;
C is the local resistance of both inlet and outlet passages;
ΔP_3 is the local resistance of inlet passage;
ΔP_4 is the local resistance of outlet passage.

The core purpose of structural design is to calculate the pressure drop. Foreign scholar has proposed other kind of the expression for the total pressure drop [2]. It did not reflect the influence of the flow rate, so the meaning is not clear. But in Chap. 4 we know that ΔP_2 is related to the n power of the velocity, where the exponent n should be determined by experiment. It reflects the property, but it is not convenient for calculation. From the above theoretical and experimental analysis for the flow state in the air passage, the flow velocity is approximately linear. This finding provides the condition for obtaining the more accurate expression of the pressure drop in the passage, i.e., the frictional resistance in the structural resistance, with various structural parameters.

Cheng Daiyun investigated the flow state in the air passage, and obtained the pressure drop of filter material in filters with separator, as well as the frictional resistance. Then the derivation with some parameters was performed. On this basis, various kinds of pressure drop expressions with the actual process conditions of HEAP filters are derived.

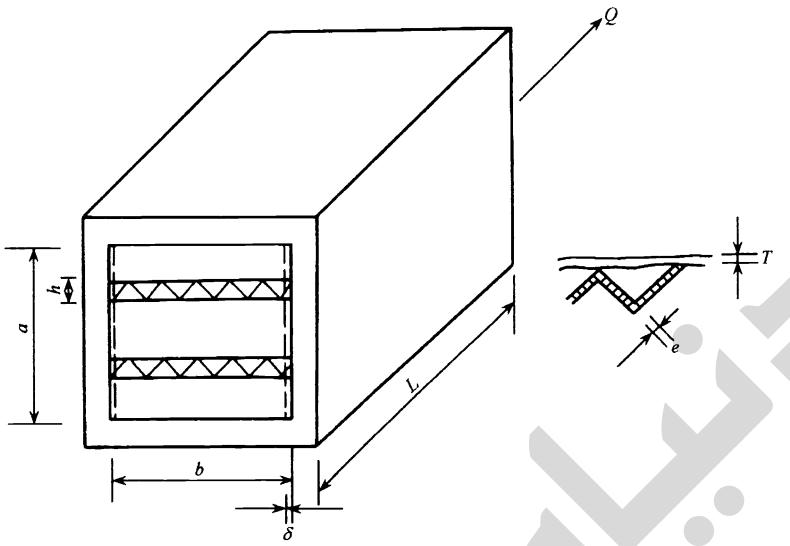

Fig. 5.4 Calculation dimension for HEPA filter

5.2.1 *Pressure Drop of Filter Media* ΔP_1

From Chap. 4, we know

$$\Delta P_1 = Av$$

where A is the structural coefficient or the drag coefficient. It is equivalent with the pressure drop of filter media under the filtration velocity $v = 1$ m/s, (Pa·s/m).

The number of corrugation is $(\frac{a}{h+T} + 1)$ for filter media. According to the manufacturing process of air filter, the two corrugations near the frame are pasted to it. So the total area of filter media is $\Sigma f - 2f$.

From Fig. 5.4, we know:

$$\Delta P_1 = A\frac{Q}{\Sigma f} = A\frac{Q}{\left(\frac{a}{h+T} + 1 - 2\right)(b-2\delta)L} = A\frac{Q}{\left[\frac{a-(h+T)}{h+T}\right](b-2\delta)L} \tag{5.4}$$

where

Q is the flow rate per second through air filter;
a and b are the side length of air filter and the net length after the frame thickness is subtracted;
L is the depth of air passage, i.e., the length of corrugation line on the separator;
f is the area of filter media on each corrugation;
T is the thickness of filter media;
δ is the depth of adhesive at two ends of filters (including the altitude of glue on filter media) or the height of head glue.

For wooden frame, the depth of adhesive with new process can be as less as 5 mm. For iron frame, the surface of adhesive is within the thickness of frame. For both cases, there is no head glue. The height of glue can be thought to be 5 mm (it can be larger than this value for poor process). For the old process of gluing, the thickness of the head glue can be 15 mm or even more.

When labels a' and b' are introduced with the following expressions:

$$a' = a - (h + T)$$

$$b' = b - 2\delta$$

then the above expression can be written as:

$$\Delta P_1 = A\frac{Q(h+T)}{a'b'L} \tag{5.5}$$

According to the detail investigation on air filter [3], the part of filter media near the top of the corrugation does not play a role in filtration. The effective filtration area reduces to 92 %. So ΔP_1 should be enlarged by $(1/0.92) = 1.087$ times. Then the above expression is rewritten as:

$$\Delta P_1 = \frac{jAQ(h+T)}{a'b'L}\ (\text{Pa}) \tag{5.6}$$

where $j = 1.087$.

5.2.2 *Frictional Resistance of Air Passage* ΔP_2

From the Ref. [1], the flow inside the air passage is laminar. According to the fluid dynamics, the frictional resistance can be expressed as:

$$\Delta P_{2(1)} = \frac{64}{\text{Re}}\frac{L}{D_\text{p}}\frac{\rho v^2}{2}\ (\text{Pa}) \tag{5.7}$$

where

$\Delta P_{2(1)}$ is the frictional resistance of inlet passage;
L is the depth of air filter (m);
D_p is the equivalent diameter of air passage (refer to the next section about corrugation angel) (m);
v is the velocity in the air passage (m/s);
ρ is the air density, 1.2 kg/m^3.

Suppose the corrugation height is h (m), and the corrugation angle is 90°, we can obtain the following expression:

$$D_{\mathrm{p}} = \frac{4 \times \left(\frac{2h^2}{2}\right)}{2\sqrt{h^2 + h^2} + 2h} = 0.83h \tag{5.8}$$

Suppose the nominal effective size of the cross section for air filter is $a \times b(\mathrm{m}^2)$, where in practice b is replaced by b'. The total number of air passage is $a/(T+h)$. The net height of passage is h. The total net height of all air passages is $(a/(T+h))h$. In all the air passage, one half of the area is inlet, and the other half is outlet. The passage area F' for real inlet is:

$$F' = \frac{b'\Sigma h}{2} = \frac{b'\frac{a}{T+h}h}{2} \tag{5.9}$$

On the other hand, there are hundreds of separators in a filter. The space they occupied in air passage cannot be neglected. So the actual value of a is that when the total thickness of all separators are subtracted. Since the separator is tortuous and its length is $\sqrt{2}$ times more than the side length of air filter, the total thickness is $1.414e\frac{a}{T+h}$. So the value of a is $a^n = a - 1.414e\frac{a}{T+h}$. The inlet velocity becomes:

$$\begin{aligned} v_0 = \frac{Q}{F'} &= \frac{Q}{\frac{b'(a''/(T+h))h}{2}} = 2 \times \frac{Q}{a''b'} \times \frac{T+h}{h} \\ &= 2 \times \frac{Q}{\left(a - 1.414\, e\frac{a}{T+h}\right)b'} \times \frac{T+h}{h} \end{aligned} \tag{5.10}$$

When we set $(a'/a'') = i$, we know:

$$v_0 = 2 \times \frac{Q}{a'\frac{a''}{a'}b'} \times \frac{T+h}{h} = 2 \times \frac{Qi}{a'b'} \times \frac{T+h}{h} \tag{5.11}$$

Differential is performed on Eq. (5.7). When $Re = \frac{D_{\mathrm{p}}v}{\mu}\rho$ and $v = v_0\frac{L-x}{L}$ are inserted, we obtain:

$$\mathrm{d}\left(\Delta P_{2(1)}\right) = \frac{32\mu}{D_{\mathrm{p}}^2} v_0 \left(\frac{L-x}{L}\right) \mathrm{d}x$$

and

$$\Delta P_{2(1)} = \int_0^L \mathrm{d}\left(\Delta P_{2(1)}\right) = \frac{16\mu v_0}{D_{\mathrm{p}}^2} L \tag{5.12}$$

It is obvious that frictional resistance of inlet passage is equal with that of outlet passage, i.e.,

$$\Delta P_{2(1)} = \Delta P_{2(2)}$$

So

$$\Delta P_2 = 2\Delta P_{2(1)} = \frac{32\mu v_0 L}{D_p^2} \tag{5.13}$$

When the expressions of v_0 and D_p are inserted, we can get the following expression:

$$\Delta P_2 = \frac{32\mu \frac{2iQ}{a'b'} \frac{(T+h)}{h}}{(0.83h)^2} L = 93\mu \frac{iQ}{a'b'} \frac{(T+h)}{h^3} L \tag{5.14}$$

5.2.3 *Local Resistance of Both Inlet and Outlet* C

The local resistance of inlet passage ΔP_3 can be thought as the abrupt contraction resistance.

$$\Delta P_3 = \xi_1 \frac{v_0^2 \rho}{2} \text{ (Pa)} \tag{5.15}$$

Where ξ_1 is the inlet drag coefficient, which can be found with the following value:

$$\frac{\text{Net cross sectional area of the passage}}{\text{The windward cross sectional area of air filter}} = \frac{a''b'/2}{ab} = \frac{a''b'}{2ab}$$

the inlet drag coefficient ξ_1 can be found with the above value.

The local resistance of outlet passage ΔP_4 can be thought as the abrupt expansion resistance.

$$\Delta P_4 = \xi_2 \frac{v_0^2 \rho}{2} \text{ (Pa)} \tag{5.16}$$

The outlet drag coefficient ξ_2 can be found with the value of $a''b'/2ab$.

$$C = \Delta P_3 + \Delta P_4 \tag{5.17}$$

5.2.4 *Total Pressure Drop* ΔP

$$\begin{aligned} \Delta P &= \Delta P_1 + \Delta P_2 + \Delta P_3 + \Delta P_4 \\ &= jA \frac{Q}{a'b'} \frac{(T+h)}{L} + 93i\mu \frac{Q}{a'b'} \frac{(T+h)}{h^3} L + C \end{aligned} \tag{5.18}$$

5.3 Optimal Height of Corrugation

When the crest is lower, the number of corrugation becomes large, which will cause the pressure drop of filter media lower, but the pressure drop of structure will increase. The conclusion of the case for higher crest is the opposite. Therefore, there is an optimal height of corrugation crest, which corresponds to the minimum pressure drop.

According to the common mathematic method, the first order and second order of the partial derivative of Eq. (5.18) can be performed with certain values of Q and cross-sectional area, i.e.,

$$\frac{\partial(\Delta P)}{\partial h} = \frac{Q}{a'b'}\left[\frac{jA}{L} + 93i\mu L\frac{h^3 - 3(T+h)h^2}{h^6}\right] \tag{5.19}$$

$$\frac{\partial^2(\Delta P)}{\partial h^2} = \frac{93i\mu LQ}{a'b'}\left(\frac{12T+6h}{h^5}\right) \tag{5.20}$$

Since $h > 0$, we know $\frac{\partial^2(\Delta P)}{\partial h^2} > 0$. So when $\frac{\partial(\Delta P)}{\partial h} = 0$, there is a limit value for ΔP, which is the minimum value. At the same time, the optimal height of h is h_0, i.e.,

$$\frac{Q}{a'b'}\left[\frac{jA}{L} + 93i\mu L\frac{h_0^3 - 3(T+h_0)h_0^2}{h_0^6}\right] = 0 \tag{5.21}$$

When both sides of the equation are multiplies with $\frac{a'b'}{Q}$, it can be simplified to:

$$\frac{jA}{L} + 93i\mu L\frac{h_0 - 3(T+h_0)}{h_0^4} = 0$$

$$\frac{h_0^4 jA + 93i\mu L^2[h_0 - 3(T+h_0)]}{h_0^4 L} = 0$$

$$h_0^4 jA + 93i\mu L^2 h_0 - 279i\mu TL^2 - 279i\mu L^2 h_0 = 0$$

$$h_0^4 - 186i\frac{\mu L^2}{jA}h_0 - 279i\frac{\mu L^2}{jA}T = 0 \tag{5.22}$$

Then the value of h_0 can calculated with the trial method.

Now with the structural sizes and related parameters of A, C, and K type filters (the thickness of filter media is 0.25 mm), the parameters needed in the equation can be calculated. Then various pressure drops can be obtained, which is shown in Table 5.2. The optimal heights h_0 of corrugation crest can be derived, which are 3.3, 3.3, and 4.6 mm, respectively. The total pressure drops calculated with these data are indeed smaller than that with the original corrugation crest height.

Table 5.2 Calculation result of resistance and corrugation crest height

Type		Known parameters									Calculation result												Measured value		
		Q (m^3/s)	a (m)	b (m)	L (m)	h (m)	T (m)	e (m)	μ (Pa·s)	A (Pa·s/m)	a' (m)	a'' (m)	b' (m)	i	j	v_0 (m/s)	ξ_1	ξ_2	ΔP_1 (Pa)	ΔP_2 (Pa)	C (Pa)	ΔP (Pa)	ΔP_1 (Pa)	ΔP_2 + C (Pa)	ΔP (Pa)
To obtain the optimal corrugation crest height	A	0.2778	0.55	0.52	0.18	0.003	0.00025	0.0002	1.83×10^{-5}	3.3×10^3	0.5468	0.502	0.49	1.082	1.087	2.40	0.28	0.31	68	41	2	111	76	54	130
	C	0.2778	0.55	0.52	0.18	0.005	0.00025	0.0002	1.83×10^{-5}	3.3×10^3	0.5468	0.52	0.49	1.038	1.087	2.30	0.28	0.31	110	14	2	126	105	53	158
	K	0.2778	0.37	0.52	0.30	0.005	0.00025	0.0002	1.83×10^{-5}	3.3×10^3	0.3648	0.35	0.49	1.027	1.087	3.43	0.28	0.31	96	35	4	135	93	59	152
						h_0																			
	A					0.0033					0.543	0.508	0.49						74	34	2	110			
	C					0.0033					0.543	0.506	0.49						74	34	2	110			
	K					0.00455					0.36	0.348	0.49						88	42	4	134			

Table 5.3 Optimal corrugation crest height h_0 of GB-01 HEPA filter (484 × 484 × 220, 1,000 m^3/h, with the head glue)

A (Pa·s/m)	T (m)	e (m)	h_0 (m)	$\Delta P_1 + \Delta P_2$ (Pa)
3.3×10^3	0.00028	0.00017	0.0037	101.9 + 45.4 = 147.3
4.0×10^3	0.00028	0.00017	0.0036	111.2 + 50.3 = 161.5
4.5×10^3	0.00028	0.00017	0.0034	121.2 + 53.2 = 174.4
5.0×10^3	0.00028	0.00017	0.0033	130.7 + 56.9 = 187.6

Now taking the GB-01 HEPA filter as an example, the optimal corrugation crest heights with different drag coefficients of filter media can be calculated, which are shown in Table 5.3.

From the above calculation results, it is found that they are very close to the measured values. The key is that if some parameters in these examples are accurate. Taking the drag coefficient as an example, two different values can be calculated with the data shown in literatures. This is the important reason for the difference above.

Another reason is the error of measurement. For example, except that the corrugation crest height of C type filter is much larger than that of A type filter, other parameters are all the same; the structural pressure drop of C type should be much higher than that of A type, but in measurement the difference between them is only 1 Pa, which is not correct obviously. At present, the value of A is about 4.7×10^3 for filter media with efficiency "four 9," and the total pressure drop of filer can reach 190 Pa (including that of inlet and outlet), which is very close to the actual situation.

Secondly, it can be seen that the crest height varies in a small range. For example, for conventional filters, this value is only between 3 and 4 mm.

Thirdly, the following derivation can be performed. Suppose $T = xh_0$, both sides of Eq. (5.21) can be multiplied with $(T + h_0)$, so that it can be simplified as:

$$\frac{Q}{a'b'}\left[\frac{jA}{L} + 93i\mu L\frac{-(3x+2)}{h_0^3}\right] = 0 \tag{5.23}$$

$$(T+h_0)\frac{Q}{a'b'}\frac{jA}{L} = (3x+2)93iQ\mu\frac{T+h_0}{a'b'h_0^3}L \tag{5.24}$$

The left is the pressure drop of filter media ΔP_1, and the right side means $(3x + 2)$ times of frictional resistance ΔP_2. So it can be rewritten as:

$$\Delta P_1 = (3x+2)\Delta P_2 \tag{5.25}$$

The above calculation shows that if $T = 0.1\ h_0$, then $\Delta P_1 = 2.3\Delta P_2$. Therefore, for the conventional HEPA filter, when the structural resistance is smaller than half of the filter media resistance, the total resistance reaches the minimum. The crest height of this type is the optimal height with the condition of L. From Table 5.3, it can be seen that the conclusion is correct. So the opinion that the total pressure drop reaches the minimum when the resistance of filter media equals to that of structural is wrong.

5.4 Optimal Depth

With the fixed value of crest height, the increase of passage depth of filter can increase the filtration area, which reduces the resistance of filter media. But at the same time the structural resistance along the air passage increases, so there is a smallest depth L_0 corresponding to the total resistance.

The first-order and second-order derivative of L are performed for Eq. (5.18), i.e.,

$$\frac{\partial(\Delta P)}{\partial L} = \frac{Q}{a'b'}\left[93i\mu\frac{(T+h)}{h^3} - jA\frac{(T+h)}{L^2}\right] \tag{5.26}$$

$$\frac{\partial^2(\Delta P)}{\partial L^2} = \frac{2jAQ(T+h)}{a'b'}\frac{1}{L^3} \tag{5.27}$$

Since $\partial^2(\Delta P)/\partial L^2 > 0$, ΔP is the minimum for the condition of $\partial(\Delta P)/\partial L = 0$, i.e.,

$$\frac{Q}{a'b'}\left[93i\mu\frac{(T+h)}{h^3} - jA\frac{(T+h)}{L^2}\right] = 0 \tag{5.28}$$

$L = L_0$.

$$jA\frac{(T+h)}{L_0^2} = 93i\mu\frac{(T+h)}{h^3} \tag{5.29}$$

So we know

$$L_0 = \sqrt{\frac{jAh^3}{93i\mu}} \tag{5.30}$$

Values of L_0 for three kinds of filters in Table 5.2 can be obtained, which is illustrated in Table 5.4. It is shown that the structural resistance with L_0 is smaller than that with h_0. This also applies for the total resistance.

It is found that compared with Eqs. (5.6) and (5.14), both sides of Eq. (5.29) do not have the item $\frac{Q}{a'b'}L_0$. When both sides of Eq. (5.29) are multiplied this item, the following expression can be obtained:

$$\frac{Q}{a'b'}jA\frac{(T+h)}{L_0} = \frac{Q}{a'b'}93i\mu\frac{(T+h)}{h^3}L_0 \tag{5.31}$$

It means that left and right sides represent the filter media resistance and structural resistance with the optimal depth.

Table 5.4 Optimal calculated depth L_0 of air passage

Filter type	h (m)	Original L (m)	ΔP with L (Pa)	L_0 (m)	$\Delta P = \Delta P_1 + \Delta P_2$ with L_0 (Pa)
A	0.003	0.18	109	0.23	53 + 63 = 106
C	0.005	0.18	124	0.51	38.8 + 39.7 = 78.5
K	0.005	0.3	131	0.51	56.5 + 59.5 = 116

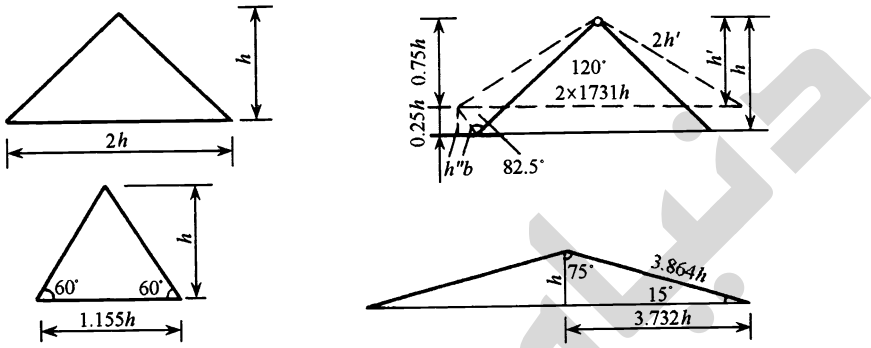

Fig. 5.5 Schematic for calculation of corrugation angle

Conclusions can be obtained by the above calculation.

First of all, for the general HEPA filter its depth may increase.

Secondly, due to the extreme small resistance at inlet and outlet, as long as the filter media resistance equals to the structural resistance, the depth of this filter under the condition of h is optimal. It should be noted, the optimal values of L_0 and h_0 are calculated when h or L is fixed.

5.5 Corrugation Crest Angle

From the expression of the frictional resistance, with the fixed velocity and length, the influence of the equivalent diameter is the largest among all the influencing factors. When the corrugation crest height is required to be fixed, the corrugation angle will influence the equivalent diameter.

The traditional corrugation angle is 90°. The influence of angle can be expressed as (refer to Fig. 5.5) [4]:

With the corrugation angle 90°, the equivalent diameter $d = \dfrac{4F}{S} = \dfrac{4 \times h/2 \times 2h}{2\sqrt{2}h + 2h} = 0.83h.$

With the corrugation angle 60°, the equivalent diameter $d = \dfrac{4 \times h/2 \times 1.155h}{3 \times 1.155h} = 0.67h$

where

F is the cross-sectional area of air passage;
S is the perimeter of air passage.

For the separator plate with poor quality, during the folding process the corrugation is lowered by the exerted force (this happens frequently) and the angle becomes 120°, the new corrugation height becomes $h' = 0.75\ h$, which is less than the original height by $h' = 0.25\ h$. At this time, the equivalent diameter is:

$$d = \frac{4 \times 0.75h \times 1.732 \times 0.75h}{2 \times 2 \times 0.75 + 2 \times 1.732 \times 0.75h} = 0.7h$$

The equivalent diameter for the corrugation crest angle 120° and the same corrugation height h is:

$$d = \frac{4 \times h/2 \times 2\sqrt{3}h}{2 \times 2h \times 2\sqrt{3}h} = \frac{6.928h}{7.454} = 0.928h$$

The equivalent diameter for the corrugation crest angle 150° and the same corrugation height h is:

$$d = \frac{4 \times h/2 \times 2 \times 3.732h}{2 \times 3.864h + 2 \times 3.732h} = \frac{14.928h}{15.192} = 0.983h$$

The structural resistance is inversely proportional to d_2 according to Eq. (5.13). When the corrugation angle is 60° and 90°, the structural resistance is mainly dependent on the frictional resistance, i.e.,

$$\frac{\Delta P_{2,60^\circ}}{\Delta P_{2,90^\circ}} = \frac{0.83^2}{0.67^2} = 1.53$$

Similarly, the ratio of structural resistance between the case of corrugation crest angle 120° with less corrugation height h' to the above case with corrugation crest angle is 90° is:

$$\frac{\Delta P_{2,120^\circ}}{\Delta P_{2,90^\circ}} = \frac{0.83^2}{0.7^2} = 1.41$$

The ratio of structural resistance between the case of corrugation crest angle 120° with the same corrugation height h and the above case with corrugation crest angle is 90° is:

$$\frac{\Delta P_{2,120^\circ(h)}}{\Delta P_{2,90^\circ}} = \frac{0.83^2}{0.928^2} = 0.8$$

The ratio of structural resistance between the case of corrugation crest angle 150° with the same corrugation height h and the above case with corrugation crest angle is 90° is:

$$\frac{\Delta P_{2,150^\circ(h)}}{\Delta P_{2,90^\circ}} = \frac{0.83^2}{0.983^2} = 0.713$$

The following conclusions can be reached with the above analysis:

1. With the constant corrugation height, the larger the corrugation crest angle is, the smaller the structural resistance is.
2. When the corrugation crest angle increases to 150°, the equivalent diameter of the air passage is near the crest height. So it has little effect on increase of crest angle.
3. For the widely used partition board at present, which is not dipped with glue (gluing or adhesive spraying only happens on the surface or even one side of the surface), the texture is very soft and is not rigid. With very little pressure, the crest angle becomes larger and crest height decreases, which increases the structural resistance.
4. If the production process of separator improves, which means neither the past dipping method with serious pollution nor the chrome paper coated with glue will be used, instead one fixed process of crest height is adopted, the crest angle can increase from the traditional 90° to about 150°, which can reduce the structural resistance by about 30 %.

5.6 Structural Parameters for Filters Without Separator

For the filter without separator, suppose the partition (line) height is h and partition interval is B, the equivalent diameter of air passage is:

$$d = \frac{4hB}{2(h+B)}$$

Because the magnitude of B is centimeter and $B \gg h$, so:

$$d \approx \frac{4Bh}{2B} = 2h \tag{5.32}$$

Since the linewidth occupies a very small proportion of the effective area, j can be neglected in the above process of derivation. Since the corrugation number for filters without separators is more than that with separator, the filter media pasted onto the two ends can be neglected. So the value of i can also be neglected. The total resistance can be obtained with Eqs. (5.14), (5.18), and (5.32) as follows:

$$\Delta P = \frac{AQ}{ab}\frac{(T+h)}{L} + 16\mu\frac{Q}{ab}\frac{(T+h)}{h^3}L + C \tag{5.33}$$

The expression to calculate the optimal crest height is:

$$h_0^4 - 32\frac{\mu L^2}{A}h_0 - 48\frac{\mu L^2}{A}L = 0 \tag{5.34}$$

The expression of optimal depth is:

$$L_0 = \sqrt{\frac{Ah^3}{16\mu}} \tag{5.35}$$

The conclusion about the optimal match between the filter media resistance and the structural resistance is also valid for the filter without separator.

Let $A = 3.5 \times 10^3$ Pa·s/m, the depth of common filter without separator $L = 0.08$ m, and the thickness of filter material 0.0003 m, we can obtain the following expression:

$$h_0^4 = \frac{32 \times 1.83 \times 10^{-5} \times 0.08^2}{3.5 \times 10^3}h_0 - \frac{48 \times 1.83 \times 10^{-5} \times 0.08^2}{3.5 \times 10^3} \times 0.0003 = 0$$

$$h_0^4 - 1.07 \times 10^{-9}h_0 = 0.48 \times 10^{-12}$$

With the trial method, we get $h_0 = 1.14$ mm. Insert it into the above equation, we obtain:

$$1.69 \times 10^{-12} - 1.22 \times 10^{-12} = 0.47 \times 10^{-12} \approx 0.48 \times 10^{-12}$$

Suppose the dimension of filter is 484 mm × 484 mm × 80 mm and the flow rate is 1,000 m^3/h (the side width is 15 mm), the filter material resistance and structural resistance with $h_0 = 1.14$ mm can be calculated with Eq. (5.33) (the third item about inlet and outlet resistances is neglected):

$$\Delta P_1 = \frac{3.5 \times 10^3 \times 0.2778}{0.454^2} \times \frac{(0.00114 + 0.0003)}{0.08} = 84.9 \text{ Pa}$$

$$\Delta P_2 = 16 \times 1.83 \times 10^{-5} \times \frac{0.2778}{0.454^2} \times \frac{(0.00114 + 0.0003)}{(1.14 \times 10^{-3})^3} \times 0.08 = 30.7 \text{ Pa}$$

$$\Delta P_1 + \Delta P_2 = 115.6 \text{ Pa}$$

According to Sect. 5.3, we know:

$$x = \frac{T}{h} = \frac{0.0003}{0.00114} = 0.263$$

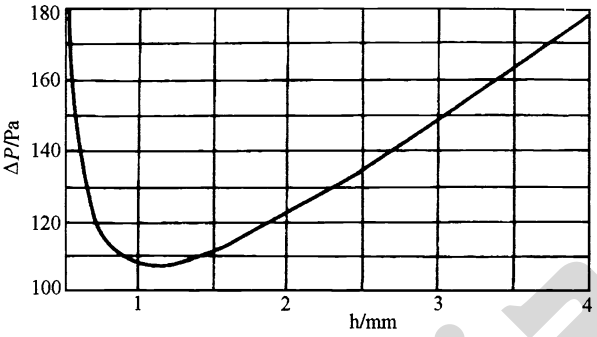

Fig. 5.6 Relationship between ΔP and h for HEPA filter without separator ($L = 0.08$ m, $A = 3.5 \times 10^3$)

So with Eq. (5.25), we know:

$$\Delta P_1 = (3 \times 0.263 + 2)\Delta P_2 = 2.79\Delta P_2$$

and

$$2.79 \times 30.7 = 85.6 \text{ Pa}$$

It is reasonable to consider that there is no difference between this value and 84.9 Pa obtained beforehand. It proves that the resistance of filter media should match with the frictional resistance.

Because of the process that aims to reduce the installation height of filter, the thickness of filter without separator at present is usually less than 80 mm. The relationship between ΔP and h can be calculated, which is shown in Fig. 5.6 ($A = 3.5 \times 10^3$).

But now the height of partition line (the height for the adhesion of two lines) is 1.5 mm, instead of 1.14 mm. Other parameters are almost the same as before mentioned values. We can get:

$$\Delta P_1 = 106 \text{ Pa}$$

$$\Delta P_2 = 17 \text{ Pa}$$

$$\Delta P_1 + \Delta P_2 = 123 \text{ Pa}$$

For the common products, A is about 5×10^3. The theoretical total resistance is about 180 Pa, while the actual resistance of the product is higher than this value by 20 %. Except for the uncertainty of the calculated parameters, there is also space for the discussion in theory.

But 80 mm is not the optimal depth for the case $h = 1.5$ mm. According to Eq. (5.35), the optimal depth for the case $h = 0.0015$ mm should be:

$$L_0 = \sqrt{\frac{3.5 \times 10^3 \times (1.5 \times 10^{-3})^3}{16 \times 1.83 \times 10^{-5}}} = 0.2 \text{ m}$$

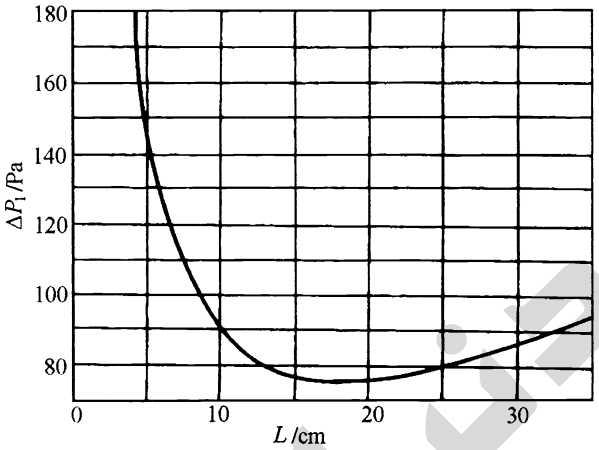

Fig. 5.7 Relationship between ΔP and L for filter without separator ($h = 0.0015$ mm, $A = 3.5 \times 10^3$)

After calculation, $\Delta P = 84.9$ Pa, which is smaller than the case $L = 0.08$ m by 38 Pa. Figure 5.7 shows the relationship between ΔP and L for this kind of filter ($A = 3.5 \times 10^3$).

From the technical and economic point of view, it is still appropriate to choose the depth 0.08 m.

For the corrugated air filter without separator which is made of polypropylene fiber, $A = 0.3 \times 10^3$ while other parameters remain the same, we know:

$h = 0.0015$ m	$L_0 = 0.06$ m	$\Delta P = 24.6$ Pa
$h = 0.001$ m	$L_0 = 0.032$ m	$\Delta P = 32.6$ Pa

Figure 5.8 illustrates the relationship between ΔP and L ($A = 3.5 \times 10^3$). It shows that $L = 0.06$ m is indeed the optimal value for $h = 0.0015$ mm.

For the sub-HEPA filter without separator when $L = 0.08$ m, the optimal crest height can be thought as $h_0 = 2.2$ m from Fig. 5.9 ($A = 3.5 \times 10^3$). When in practice $h = 1.5$ mm, the resistance is higher than that with optimal crest height by 4 Pa, where the difference is very small.

5.7 Calculation of Tubular Filter

If the resistance of filter is required to be lower, one method is to choose filter material with less resistance and the other one is to reduce the structural resistance. The tubular structure may meet the requirement of the second method. Now analysis for the structure of tubular sub-HEPA filter is performed as Chap. 4.

The frictional resistance of inlet passage is supposed to be equal to that of outlet passage, i.e.,

$$\Delta P_{2(1)} = \Delta P_{2(2)}$$

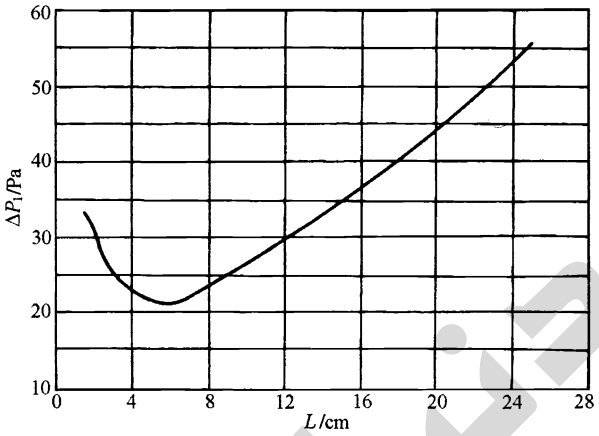

Fig. 5.8 Relationship between ΔP and L for sub-HEPA filter without separator ($h = 0.0015$ mm, $A = 3.5 \times 10^3$)

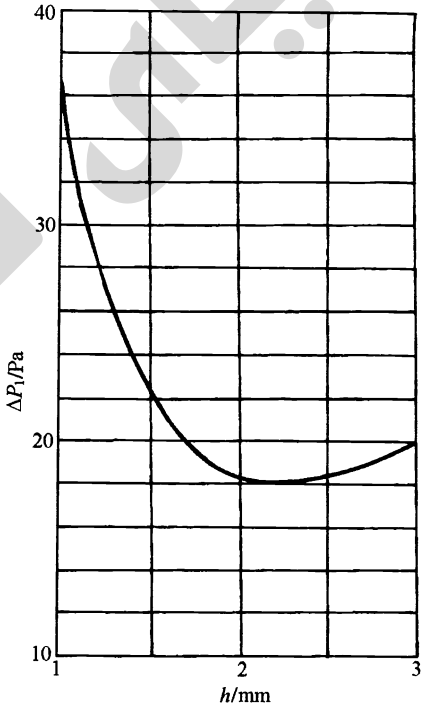

Fig. 5.9 Relationship between ΔP and h for sub-HEPA filter without separator ($h = 0.08$ mm)

From the process point of view, the tubular diameter which is easy for process is determined at first. The appropriate number of tubes within the area $a \times b$ is chosen. Then the total resistance can be calculated with the following expression (refer to Fig. 5.10):

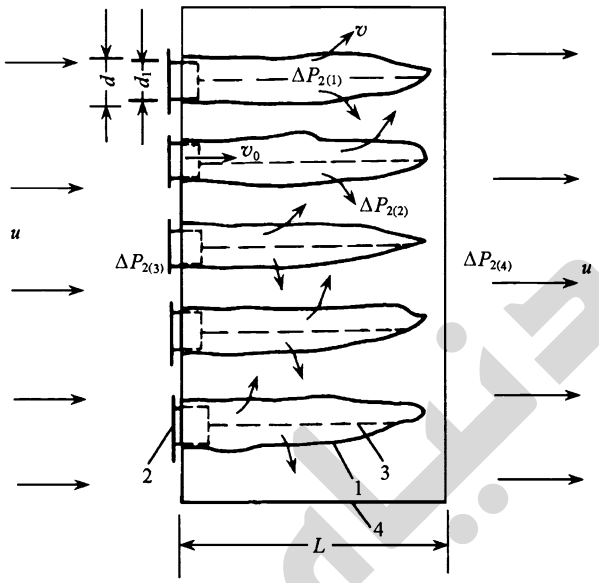

Fig. 5.10 Calculation parameters of tubular filter. *1* filtration tube, *2* plug head, *3* vane, *4* frame

$$\Delta P = \Delta P_1 + 2\Delta P_{2(1)} + \Delta P_{2(3)} + \Delta P_{2(4)} \tag{5.36}$$

where ΔP_1 is the filter media resistance (Pa)

$$\Delta P_1 = A\frac{Q}{n\pi d} = Av \tag{5.37}$$

$\Delta P_{2(1)}$ is the frictional resistance of inlet passage (Pa), which can be obtained with the method for corrugated filter

$$\Delta P_{2(1)} + \Delta P_{2(2)} = 2\Delta P_{2(1)} = \frac{32\mu v_0}{d'^2}L = \frac{86\mu v_0}{d^2}L$$

$\Delta P_{2(3)}$ is the resistance of inlet perforated plate (Pa)

$$\Delta P_{2(3)} = \zeta_1 \frac{u^2\rho}{2} \tag{5.38}$$

$\Delta P_{2(4)}$ is the resistance of outlet (Pa).

In the above items, n is the number of tubes;

d is the diameter of tube, m;

v is the filtration velocity, m/s;

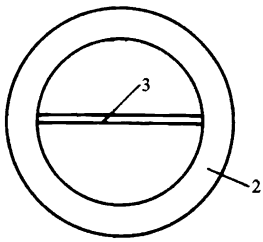

Fig. 5.11 Filtration tube with space divided into two parts: *2* plug head, *3* vane

v_0 is the inlet velocity of tube, m/s;
d' is the equivalent diameter of air passage. For the case in Fig. 5.11, the vane is placed in the middle of the tube, where the tubular space is divided into two parts. For half circle, $d' = 0.61d$;
u is the velocity at the weather side, m/s;
ζ_1 is the inlet drag coefficient

$$\zeta_1 = \frac{1 - c^2S^2}{c^2S^2} \tag{5.39}$$

where c is the contraction coefficient of the pore where air passes through. Usually it is 0.9. When the tubular diameter is as small as 15 mm, filter paper will become corrugated at the throat where the plug is placed. The air passage becomes narrower or even half when c is 0.5.

S is the porosity

$$S = \frac{\text{Net total area of the pores}}{\text{Area of windward surface}} = \frac{F_1}{F_2} \tag{5.40}$$

where

F_1 is the net total area of pores, which is equivalent to the subtraction of the cross-sectional area of vane $0.001d_1$ from the total area (which is dependent on the plug diameter d_1 (m), $d_1 = d - 0.002$ m).

F_2 is the area at the weather side, which is assumed the same as that of corrugated HEPA filter, i.e., 0.484×0.484 m^2.

Since the outlet of filtration tube is flat, the actual outlet cross-sectional area is very close to that of air filter and it is gradually changed. $\Delta P_{2(4)}$ can be neglected.

Taking the parameters of YGG low-resistance sub-HEPA filter introduced in Chap. 4 as an example, various resistances are calculated with the above method, which is shown in Table 5.5. From this table, the calculated result is very close to the experimental value, which means the calculation method is feasible. It is also shown that with the same dimension and flow rate, the structural resistance of tubular filter is much smaller than that of corrugated filter. At present, due to other reasons, the tubular HEPA filter made of polypropylene fiber has not appeared in the market.

Table 5.5 Calculation example of tubular filter

Filtration tube (m)	Number of filtration tubes (#)	Tube lengt (h/m)	Opening area (m^2)	Filtration velocity v (m/s)	Face velocity u (m/s)	Velocity v_0 in tube (m/s)	A (Pa·s/m)	C	ζ_1	S	Calculation result (Pa)				Measured result (Pa)	
											ΔP_1	$2\Delta P_{2(1)}$	$\Delta P_{2(3)}$	ΔP	ΔP	ΔP_2
0.019	330	0.215	0.0692	0.066	1.35	4.01	5.5×10^2	0.9	10	0.336	36.3	3.7	10.9	50.9	50	13.7
0.019	330	0.215	0.0692	0.066	1.35	4.01	7×10^2	0.9	10	0.336	46.2	3.7	10.9	60.8	60	13.8
0.019	347	0.215	0.0728	0.0624	1.35	3.81	7.5×10^2	0.9	9	0.353	46.8	3.5	9.8	60.1	60	13.2
0.019	347	0.215	0.0728	0.0624	1.35	3.81	5.6×10^2	0.9	9	0.353	34.9	3.5	9.8	48.2	50	15.1
0.019	347	0.215	0.0728	0.0624	1.35	3.81	7.8×10^2	0.9	9	0.353	48.6	3.5	9.8	61.9	60	11.4
0.015	630	0.215	0.0753	0.044	1.35	3.69	7×10^2	0.9	29.3	0.336	31	5.5	31.9	68.4	75	44

References

1. Cheng DY (1983) Fluid dynamics model of air filter. Mech Eng 1:34–37 (In Chinese)
2. Пречистенский СА (1961) Радиоактивные выбросы в атмосферу, Москва: Госатом издат, p 36 (In Russian)
3. Institute of HVAC of China Academy of Building Research (1973) Assembly cleanroom (In Chinese)
4. Xu ZL (1991) Discussion of enlarging the corrugation crest angle of the separator on HEPA filter. J HV&AC 6:26–28 (In Chinese)

Chapter 6
Movement of Indoor Fine Particle

Only when indoor airborne particles move towards the nearby of the precision product and then deposit onto the sensitive area, damage may be caused for the product. So it is important to understand the mechanism of particle movement and deposition for the control of environment.

6.1 Force Acting on Particles

It is the force that changes the state of movement. Forces acting on particles can be roughly divided into five categories.

1. *Mass force*. This refers to the force which is proportional to the particle mass, including the gravity, the inertia force, and the inertial centrifugal force.
2. *Molecular force*. This is the force which pushes particles to move by the motion of gas molecules, including the diffusional force with the Brownian movement, the turbulence force by the fluctuation of gas molecules, and the force by acoustic wave.
3. *Field force*. It is the forces expect the gravity, including the electric field force, the magnetic field force, and the forces formed in the concentration field, the temperature field, and the light. With the effect of these forces, the movement phenomena are formed, such as electrophoresis, magnetophoresis, diffusiophoresis, temperature-phoresis, and photophoresis.
4. *The attraction force between particles*.
5. *Airflow force*. It is the force caused by supply airflow, return airflow, heat convection airflow, airflow caused by artificial agitation, and other airflows with certain velocity.

For the pollution control of cleanroom, the airflow force is the most important force among the above forces, but it is too complex to be investigated. Secondly, the gravity, the inertia force, and the molecular diffusional force are important, while other kinds of forces are not important for the movement of indoor particles in

Z. Xu, *Fundamentals of Air Cleaning Technology and Its Application in Cleanrooms*, DOI 10.1007/978-3-642-39374-7_6, © Springer-Verlag Berlin Heidelberg 2014

cleanroom comparatively. As for the movement of particles in the electric field, it has been introduced in the chapter about air filter, so both the electrostatic force and other kinds of forces with little significance are not discussed in this chapter.

6.2 Gravitational Sedimentation of Particles

For the airborne particle shown in Fig. 6.1, it will be influenced by the gravity F_1, the buoyancy F_2, and the resistance F_3 by the medium.

For spherical particles, the gravity is:

$$F_1 = m_p g = \frac{\pi}{6} d_p^3 \rho_p g \tag{6.1}$$

The buoyancy is equal to the weight of the medium with the same volume, i.e.,

$$F_2 = m_a g = \frac{\pi}{6} d_p^3 \rho_a g \tag{6.2}$$

The resistance equals to the multiplication of the relative velocity between the particle and the airflow, the projected area of particles, and the drag coefficient, i.e.,

$$F_3 = \psi \frac{\pi}{4} d_p^2 \frac{v^2}{2} \rho_a = \psi \frac{\pi d_p^2 \rho_a v^2}{8} \tag{6.3}$$

where

m_p and m_a are mass of particle and air, respectively (kg);
ρ_p and ρ_a are density of particle and air, respectively (kg/m^3);
v is the relative velocity of particle (m/s);
d_p is the particle diameter (m);
ψ is the drag coefficient.
The unit of various kinds of force is N.

When forces are acting on the particle, it deposits simultaneously. The settling velocity increases during the deposition process. When the resistance, the buoyancy, and the gravity are balanced, i.e., $F_1 - F_2 = F_3$, it becomes the uniform settlement.

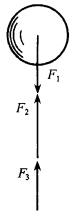

Fig. 6.1 Forces acting on the spherical particle during the deposition process

Then, the speed is $v = v_s$, which is called the settling velocity or Stokes velocity. It can be calculated with the following expression:

$$v_s = 3.62\sqrt{\frac{d_p(\rho_p - \rho_a)}{\psi\rho_a}}(m/s) \tag{6.4}$$

The drag coefficient ψ depends on the flow state where particle is suspended, i.e., the laminar flow or the turbulent flow. It is also dependent on the shape of particle. The flow state is decided by the Reynolds number Re of the particle with the relative movement.

$$Re = \frac{d_p v \rho_a}{\mu}$$

where μ is the gas viscous coefficient, Pa · s. It is also called dynamic viscous coefficient, which is different from the kinematic viscous coefficient $\upsilon, \upsilon = \frac{\mu}{\rho_a}$. With the legal unit, for air with temperature 20 °C, $\mu = 1.83 \times 10^{-5}$ Pa · s and $\rho_a = 1.2$ kg/m^3.

For the movement of particle, Re is usually less than 1. When Re is smaller than 1 especially smaller than 0.5, the resistance for spherical particle can be calculated with the following formula:

$$F_3 = 3\pi\mu d_p v \tag{6.5}$$

This is the famous Stokes formula, where the resistance has the opposite direction to the movement. 1/3 of this resistance is the component of shape resistance for the particle, and 2/3 is the component of the frictional resistance for the particle. With Eq. (6.3), the drag coefficient can be derived:

$$\psi = \frac{24}{Re} \tag{6.6}$$

Therefore, the resistance is strictly related with the particle velocity. For the flow with larger Re, the value of ψ is shown in Table 6.1 [1, 2].

For nonspherical particle, the drag coefficient should be multiplied by a correction coefficient β. This means the drag coefficient for nonspherical particle is $\psi' = \beta\psi$. Value of β is shown in Table 6.2.

When Eq. (6.6) is substituted into Eq. (6.4), and let $\rho_p - \rho_a \approx \rho_p$, then the settling velocity is:

$$v_s = 3.62\sqrt{\frac{d_p\rho_p v_s d_a \rho_z}{24\rho_a}}$$

Table 6.1 Value of ψ for $Re > 1$

Re	ψ	Re	Ψ	Re	ψ	Re	ψ
1.0	26.5	10.0	4.1	100.0	1.07	1,000	0.46
2.0	14.4	20.0	2.55	200.0	0.77	10^3–2×10^5	0.4–0.5
3.0	10.4	30.0	2.00	300.0	0.65	$>10^5$	≈ 0.22
5.0	6.9	50.0	1.5	500.0	0.55		
7.0	5.4	70.0	1.27	700.0	0.50		

Table 6.2 Correction coefficient β of the drag coefficient

Particle shape	β
Equivalent spherical particles	1.0
Circular particle with rough surface	2.42
Oval particle	3.08
Slice particle	4.97
Irregular shape particles	2.75–3.5

When square is performed on both sides, it becomes:

$$\upsilon_s = 0.54 \frac{d_p^2 \rho_p}{\mu} (m/s) \tag{6.7}$$

Two points should be paid attention to during the application of this equation:

1. In the field of aerosol technology, particle density is generally assumed $\rho_p = 1{,}000$ kg/m^3, while for atmospheric dust, particle density is generally assumed $\rho_p = 2{,}000$ kg/m^3.
2. The unit of μ is very confusing. In some literature, when the wrong unit is used, the calculated result can differ by ten times, where complete opposite conclusion can be obtained (for detailed information, please refer to the later chapter about isokinematic sampling). In this book, the legal system with international unit is adopted. The difference between this kind of unit and the engineering unit in the past is shown as follows:

	International unit (legal)	cgs unit	Engineering unit	KMS unit
Unit	N · s/m^2 or Pa · s	P or dyn · s/cm^2	kgf · s/m^2	kg/m · h
Difference	1	10	0.102	3,600
	0.1	1	1.02×10^{-2}	360
	9.807	98.07	1	3.53×10^4
	2.778×10^{-4}	2.778×10^{-3}	2.833×10^{-5}	1

When the found value of μ is based on cgs unit, the corresponding value with legal unit is the found value divided by 10. When the found value is based on the engineering unit, the corresponding value with legal unit is the found value multiplied by 9.81. When the found value of μ is based on KMS unit, the corresponding value with legal unit is the found value divided by 3,600.

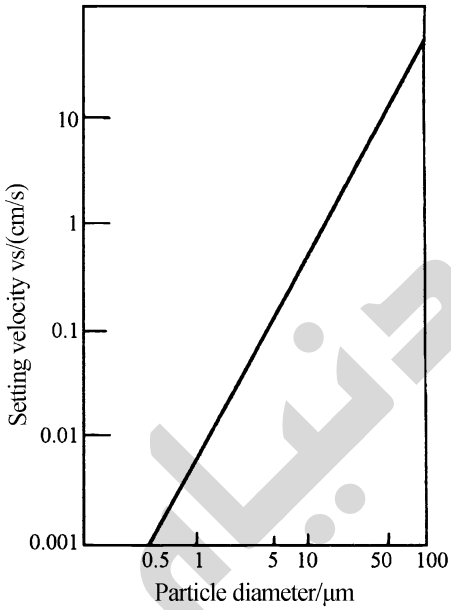

Fig. 6.2 Relationship between the settling velocity and the particle diameter

So, for atmospheric dust, the relationship between the settling velocity (m/s) and particle diameter with normal temperature 20° can be obtained with Eq. (6.7):

$$v_s \approx 0.54 \frac{2,000 \times \left(d_P \times 10^{-6}\right)^2}{1.83 \times 10^{-5}} (\mathrm{m/s}) = 590 \times 10^{-7} \times 10^2 d_P^2 (\mathrm{cm/s})$$

or

$$v_s \approx 0.6 \times 10^{-2} d_P^2 (\mathrm{cm/s}) \tag{6.8}$$

The calculation result is also shown in Fig. 6.2. It is shown that for particles with diameter 1 μm, v_s is only 0.006 cm/s. That means it only takes 4 h for the deposition of particles from the working area (0.8 m above the floor) to the floor. But for particles with diameter less than 0.5 μm, the diffusional distance is even larger than the settling distance, and this is why it is not easily deposited.

It should be noted that slip correction should be considered for particles with diameter less than 1 μm. According to the aerosol mechanics, Stokes formula is derived with the continuous flow condition, which assumes that there is no velocity jump on particle surface. That is to say, there is no relative velocity between the flow particles and the infinite thin medium layer attached to the surface, or there is a boundary layer on particle surface without relative velocity. For small particles, when the radius is close to the mean free path of gas molecule or the gas pressure is comparatively small, the movement of particle has the characteristic of molecular. Particles will be so small that they will "slide" between gas molecules, namely, the

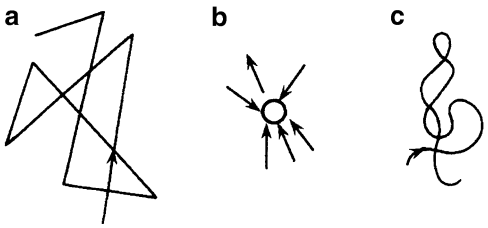

Fig. 6.3 Diffusional movement of molecules and particles. (**a**) Trajectory of gas molecule with Brownian motion. (**b**) Nonequilibrium condition of particles with the impact of air molecules. (**c**) Trajectory of particle with Brownian motion

Table 6.3 Particle size range with *Kn* number

Particle size system	*Kn*	d_p (μm)
Continuous flow	≤0.001	>130
Slip flow	0.001–0.3	130–0.43
Transition flow	0.3–10	0.43–0.013
Free molecular flow	>10	<0.013

existence and movement of particle will neither influence the gas velocity distribution nor cause any airflow in gas medium. So the abovementioned boundary layer with zero velocity does not exist. Conversely, there is a speed jump layer on the particle surface, namely, air slippage phenomena occur on the surface of the moving particle. Obviously, the resistance caused by medium should be reduced, which is favorable for the Stokes settling velocity. This is the reason to consider the slip correction for small particles.

The decisive parameter for the flow in the slip flow range or others is called Knudsen number:

$$Kn = \frac{2\lambda}{d_P} \tag{6.9}$$

The specific division of flow range is shown in Fig. 6.3 (Table 6.3).

Let C the slip correction coefficient, which is also called Cunningham correction coefficient, the settling velocity after correction becomes:

$$v'_s = Cv_s \tag{6.10}$$

$$C = 1 + \frac{2\lambda}{d_P}\left(1.257 + 0.4e^{-1.1\frac{d_P}{2\lambda}}\right) \tag{6.11}$$

Table 6.4 shows the value of C with normal temperature and normal pressure by Eq. (6.11). It is found that for particles with diameter 1 μm, the corrected settling velocity will be faster by that without correction by 16 %.

Table 6.4 Slip correction coefficient C

d_p (μm)	0.003	0.01	0.03	0.1	0.3	1.0	3.0	10.0
C	90	24.5	7.9	2.9	1.57	1.16	1.03	1

6.3 Movement of Particles Under the Action of Inertia Force

The movement of particles under the action of inertia force means particle moves with inertia with initial velocity after the external force disappears. For example, particles on human body and equipment are affected by the mechanical force because of the activity of people and the movement of equipment. Suppose initial horizontal velocity is obtained after particles leave the human body or equipment, the applied force disappear (now the airflow force and gravity are neglected), then particles decelerate with the inertia.

According to the Newton's law, the movement of particles with initial horizontal velocity v_0 can be described with the following equation:

$$m\frac{\mathrm{d}v}{\mathrm{d}t} = F - F_3 \tag{6.12}$$

where

F is the external force. When only inertia force exists, $F = 0$.
F_3 is the resistance.

Here the slip correction should be considered. The expression of F_3 with Stokes equation becomes

$$F_3 = \frac{3\pi\mu d_P v}{C} \tag{6.13}$$

Then, Eq. (6.12) becomes:

$$\frac{\mathrm{d}v}{\mathrm{d}t} = -\frac{v}{\dfrac{Cm}{3\pi\mu d_P}}$$

Assuming $\dfrac{Cm}{3\pi\mu d_P} = C\tau$, i.e., $\tau = \dfrac{d_P^2\rho_P}{18\mu}$, then

$$\frac{\mathrm{d}v}{v} = -\frac{\mathrm{d}t}{C\tau}$$

Table 6.5 Horizontal distance of movement for particles (ρ_p = 2 g/cm ^{3}) with inertia force at 20 °C

Particle size (μm)	τ (s)	S_R (cm)	
		v_0 = 100 cm/s	v_0 = 1,000 cm/s
10	6×10^{-4}	0.06	0.6
5	1.6×10^{-4}	0.16	0.16
1	7×10^{-6}	0.0007	0.007

After integration, we get:

$$v = v_0 e^{-\frac{t}{C\tau}} \tag{6.14}$$

The distance of movement in time t is:

$$S_t = \int_0^t v dt = \int_0^t v_0 e^{-\frac{t}{C\tau}} dt = C\tau v_0 \left(1 - e^{-\frac{t}{C\tau}}\right) \tag{6.15}$$

When t tends to infinity, the movement of particles becomes stable. The distance of inertia movement, expressed as S_R, can be calculated with the following expression:

$$S_R = C\tau v_0 \tag{6.16}$$

Inserting the expression of τ into Eq. (6.16), the calculation results are listed in Table 6.5. It is shown that τ has the dimension of time, and it is called the "relaxation time" in aerosol dynamics. It is an important parameter to describe the movement of particles, and it is also termed as the characteristic time. It is the time needed for the transition from initial stable state to another stable state. For example, it is known from Eq. (6.16) that after the force is removed, the velocity of particle with diameter 1 μm will reach 1/3 of the initial velocity within the time $t = \tau$. So when $t > \tau$, the movement status of particles will change a little.

From Table 6.5, because of the rapid decline of velocity, the horizontal movement distance of a particle with initial velocity 1,000 cm/s is very short. It is impossible to be suspended with this mechanical force.

6.4 Diffusional Movement of Particles

Due to the impact of air molecules with Brownian motion, significant uneven displacement of airborne particles will occur, and the disorderly movement will be shown, which is shown in Fig. 6.3.

After the collision, the movement direction and speed of molecules change suddenly. The trajectory is composed of many segments of straight lines. Because the mass of particle is much larger than that of the air molecule, after the impact

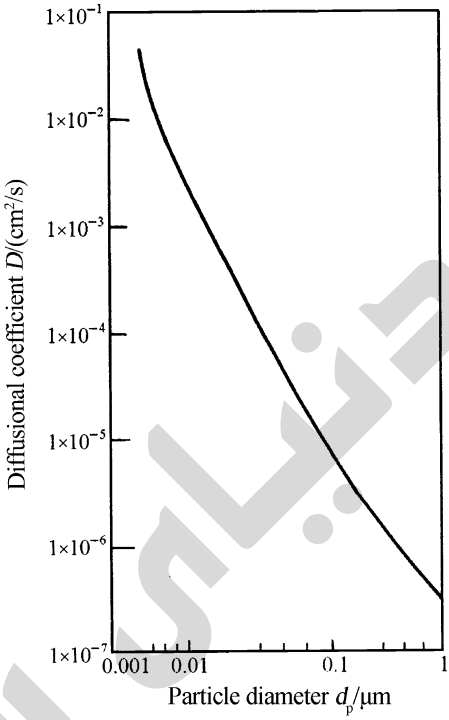

Fig. 6.4 Relationship between diffusional coefficient and particle size

with air molecules, the velocity of particle can be reduced to be small enough to ignore. Only after several times of impact, the direction and velocity of particle will change significantly. So the trajectory of particle is almost smooth curve. This kind of phenomena about disorderly movement for particle is called diffusional movement.

Although the displacement of particle in all direction with diffusional movement is random, pure linear displacement will occur when $t >> \tau$ and $t = 1$ s is enough. So the absolute value of average displacement during 1 s in the given direction can be obtained with the following expression [3]:

$$S_D = \sqrt{\frac{4Dt}{\pi}} \tag{6.17}$$

where

t is time (s);
D is the diffusional coefficient of particle (cm^2/s).

Figure 6.4 gives the relations between D and particle size. Table 6.6 gives the diffusional movement distance with different sizes. From the table, the movement distance of particle with diffusion is insignificant.

Table 6.6 Diffusional movement distance of particles during $t = 1$ s

Particle size (μm)	S_D (cm)
10	1.23×10^{-4}
5	1.74×10^{-4}
2	2.78×10^{-4}
1	4.02×10^{-4}
0.5	5.90×10^{-4}
0.1	1.68×10^{-3}

6.5 Deposition of Particles on Surface

6.5.1 Diffusional Deposition of Particles on Vertical Surface of Room Without Air Supply

Inertia deposition of particles onto flat vertical surface can be completely ignored. Usually it is thought that only diffusional deposition exists. This kind of diffusional deposition includes molecular diffusion and convection diffusion. For the room without air supply, indoor air will not keep stagnant because of the existence of convection. With the effect of convective diffusion, particles approach to the surface gradually at first and then deposit onto the surface with the molecular diffusion within a very thin layer near the surface, which is shown in Fig. 6.5.

For the particle with a certain particle size, the molecular diffusion coefficient D is known, while the convective diffusion coefficient is unknown. Fuchs solved this problem with a simplified method [4].

In any deposition mechanism, the concentration variation of particles because of deposition is linearly proportional to the particle concentration N, i.e.,

$$\frac{\mathrm{d}N}{\mathrm{d}t} = -\beta N \tag{6.18}$$

The negative sign represents the decrease of concentration. After integration, the above expression becomes

$$\ln\left(\frac{N_0}{N}\right) = \beta t \tag{6.19}$$

where

N_0 is the original concentration (pc/cm^3);
N is the concentration at the moment t after deposition (pc/cm^3).

Then, the problem is attributed to find out the value of β related to the diffusional deposition mechanism.

There is convection in the room without air supply. It means outside of the molecular diffusion layer, concentration becomes uniform with the effect of convection.

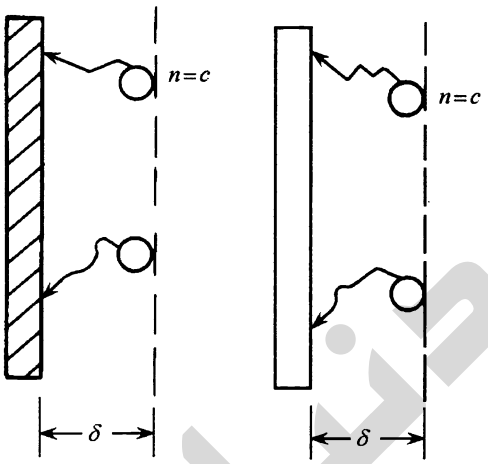

Fig. 6.5 Schematic diagram for the diffusional deposition of particles onto the surface

And the concentration decreases continuously with time (with air supply, N is a constant). Therefore, the particle number deposited onto the vertical surface with unit area within unit time is

$$I = v_{\mathrm{d}} N = \frac{DN}{\delta} \tag{6.20}$$

where

v_{d} is the velocity of diffusion deposition (m/s);
N is the concentration which decreases continuously;
I is the deposition rate [pc/(cm^2·s)];
δ is the thickness of molecular diffusion layer. Although it is difficult to specify the value, it is about 20 μm on the order of magnitude according to the experimental results [1].

So the variation of particle number in the space because of diffusion deposition within time dt is

$$-V\mathrm{d}N = sI\mathrm{d}t$$

$$\frac{\mathrm{d}N}{\mathrm{d}t} = -\frac{sI}{V} \tag{6.21}$$

where

V is the space volume (cm^3);
s is the area of vertical surface (cm^2).

Inserting Eq. (6.21) into Eq. (6.18), we obtain:

$$\frac{sI}{V} = \beta N$$

So we know:

$$\beta = \frac{sI}{VN} = \frac{sD}{V\delta} \tag{6.22}$$

When it is inserted into Eq. (6.19) and simplification is made, the number of particles deposited on vertical surface with unit area by diffusional deposition is:

$$N_g = \frac{V}{s}(N_0 - N) = \frac{V}{s}\left(1 - e^{-\frac{sDt}{V\delta}}\right)N_0\left(\mathrm{pc}/\mathrm{cm}^2\right) \tag{6.23}$$

In order to have an idea about the value of N, an example is made as follows:

Assume $\frac{s}{V} = \frac{1}{4{,}000}\mathrm{cm}^{-1}$, $t = 3.6 \times 10^3$ s, $D = 6.2 \times 10^{-7}$ cm^2/s (for particle with diameter 0.5 μm), and the number of these particles is $N_0 = 1$ pc/cm^2, so:

$$N_g = 4{,}000 \times \left(1 - e^{-0.00028}\right) \times 1 = 4{,}000 \times 0.00028 \times 1 = 1.12\left(\mathrm{pc}/\mathrm{cm}^2\right)$$

6.5.2 Deposition of Particles on Undersurface of Room Without Air Supply

Deposition of particles on undersurface includes the settlement and the diffusion. And diffusion also includes the molecular diffusion and the convective diffusion. In Fuchs' opinion, the convective diffusion coefficient is close to 0, because the convective velocity approaches zero when it is near the undersurface. It is only the molecular diffusion that plays a role in the very small distance from the undersurface, which will influence the particle concentration distribution near the bottom, but will not influence the total deposition rate. Therefore, the number of particles settled down onto the bottom with area 1 cm^2 within time t is:

$$N_g = \int_0^r v_s N \, \mathrm{d}t \ \left(\mathrm{pc}/\mathrm{cm}^2\right) \tag{6.24}$$

As mentioned before, although concentration keeps uniform in the space of the room without air supply, it varies with time t. The reduction of particle number in the air column with height H is consistent with the number of deposited particles, which can be express as:

$$-H\,\mathrm{d}N = v_s N\,\mathrm{d}t$$

So

$$N = N_0 \mathrm{e}^{-\frac{v_s t}{H}}$$

When it is inserted into Eq. (6.24), we know:

$$N_g = N_0 H\left(1 - \mathrm{e}^{-\frac{v_s t}{H}}\right)\left(\mathrm{pc}/\mathrm{cm}^2\right) \tag{6.25}$$

With the same data of the example in previous section (for particles with diameter 0.5 μm, $v_s = 0.0015$ cm/s, and assume $H = 200$ cm),

$$N_g = 1 \times 200 \times \left(1 - \mathrm{e}^{-\frac{0.0015 \times 3.6 \times 10^3}{200}}\right) = 200 \times \left(1 - \mathrm{e}^{-0.027}\right)$$
$$= 200 \times (1 - 0.973) = 200 \times 0.027 = 5.4\left(\mathrm{pc}/\mathrm{cm}^2\right)$$

6.5.3 Deposition of Particles on Interior Surface of Room with Air Supply

Fumiko and Susumi proposed the expression for the deposition of particles on the interior surface in the room with air supply [5, 6]:

$$N_g = N v_s f t\left(1 - \mathrm{e}^{-\frac{n h_s}{v_s} \times \frac{h}{h_s}}\right) \tag{6.26}$$

where

f is the sedimentary area;
t is the settling time;
h_s is the room height;
h is the distance between the settling plane and the ceiling;
n is the air change rate.

Since $\frac{n h_s}{v_s}$ is far greater than 1 for 0.5 min^{-1}, the above expression can be simplified as

$$N_g = N v_s f t \tag{6.27}$$

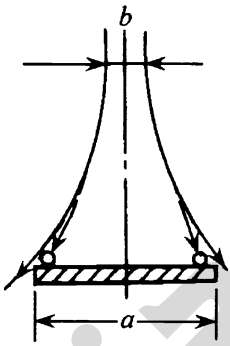

Fig. 6.6 Inertial deposition of particles on the plane

It should be noted that Eq. (6.27) is valid for the extreme case with room height $h_s \to \infty$ for the room without air supply. Only when the height is infinite ideally, the indoor particle concentration can be considered without variation because of deposition and considered as a constant. But there is no practical significance for the condition $h_s \to \infty$. In other words, this equation is not valid for the room without air supply.

Although Eq. (6.26) is derived for the room with air supply, author thought it is not comprehensive to consider the particle deposition only, especially for the local plane. In the room with air supply, there are several ways for the deposition of particles onto plane, so the method to estimate the deposition efficiency for these ways is given.

6.5.3.1 Inertial Deposition

Inertial deposition of particles on the plane is shown in Fig. 6.6. The inertial deposition efficiency is:

$$\eta_{St} = \frac{b}{a} = f(St) \tag{6.28}$$

Figure 6.7 shows the relationship between η_{St} and St [8]. St is the inertial parameter, which has been introduced in Chap. 3. Table 6.7 presents the exact value of η_{St}. In the table, u is the air velocity and d_p is the particle diameter.

6.5.3.2 Interception Deposition

Interception deposition of particles on the plane is shown in Fig. 6.8. For the condition with large Reynolds number (equivalent with the situation of cleanroom) with unknown *Re* value, only the upper limit of interception deposition efficiency can be calculated, namely,

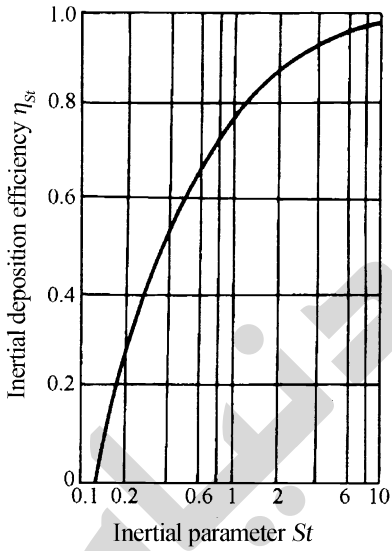

Fig. 6.7 Relationship between η_{St} and St

Table 6.7 Value of η_{St}

d_p (μm)	1		5	
a (cm)	10^{-3}	3	10^{-3}	3
u (m/s)	0.3	0.3	0.3	0.3
St	$\sim 2 \times 10^{-1}$	$\sim 10^{-4}$	4.8	$\sim 3 \times 10^{-3}$
η_{St}	0.27	~0	$\sim 9.5 \times 10^{-1}$	~0

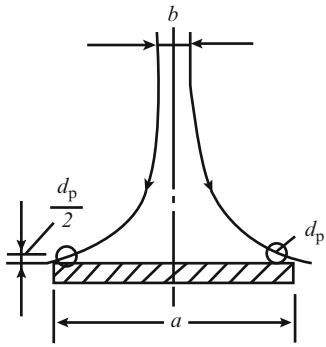

Fig. 6.8 Interception deposition of particles on the plane

$$\eta_R < (1+R) - \frac{1}{(1+R)} \tag{6.29}$$

Table 6.8 gives the value of η_R. R is the interception parameter, which has been introduced in Chap. 3.

Table 6.8 Value of η_R

a (cm)	3 – ≥30	
d_p (μm)	1	5
η_R	$<6 \times 10^{-5}$ to 0	$<3 \times 10^{-4}$ to 0

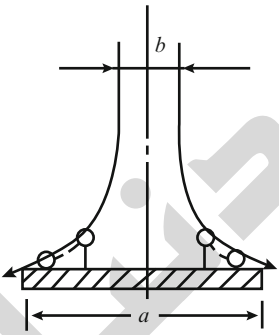

Fig. 6.9 Inertial deposition of particles on the plane

Table 6.9 Value of η_G

a (cm)	0.3		
d_p (μm)	0.07	1	5
η_G	10^{-4}	2×10^{-4}	5×10^{-3}

6.5.3.3 Sedimentation Deposition

Sedimentation deposition of particles on the plane is shown in Fig. 6.9. The sedimentation deposition efficiency is

$$\eta_G = \frac{v_s}{u} \tag{6.30}$$

where

v_s is the sedimentation speed;
u is the air velocity.

Table 6.9 gives the value of η_G for the general circumstance.

6.5.3.4 Diffusion Deposition

For horizontal plane, there is a very thin layer close to it, where the height and the temperature gradient are extreme small. Its vertical component of convective velocity is much less than the vertical component to the plane. It tends to zero, which means the convective flux is approaching zero. So the corresponding molecular diffusion flux towards the plane is greatly reduced. When the dispersity of particles is larger, the number of particles deposited on the vertical plane with

diffusion deposition is larger, while that on the horizontal plane is less. This means the diffusion deposition efficiency on horizontal plane is less than that on vertical plane, or the maximum number of deposited particles can be considered with vertical plane.

When $n = 1$ pc/cm^3 and the diffusional coefficient for particles with diameter 1 μm is $D = 3 \times 10^{-7}$ cm^2/s, we can obtain the value of I is 0.54 pc/cm^2 within 1 h according to Eq. (6.20).

So the diffusion deposition efficiency for the velocity 0.3 m/s is [5]

$$\eta_D = \frac{0.54(\mathrm{pc}/\mathrm{cm}^2) \times 1\ \mathrm{cm}^2}{1\ \mathrm{cm}^2 \times 30\ \mathrm{cm/s} \times 3,600\ \mathrm{s} \times 1(\mathrm{pc}/\mathrm{cm}^3)} \approx 5.4 \times 10^{-6}$$

For particles with diameter 5 μm, $\eta_D = 5 \times 10^{-7}$.

Of course, the value of η_D for horizontal plane should be smaller than the above calculation result, or the maximum value can be determined with vertical plane.

6.5.3.5 Electrostatic Deposition

Usually it could be ignored.

6.5.3.6 Total Deposition Efficiency

When the circular monocrystalline silicon wafers with diameter 3 and 30 cm which is used for the production of integrated circuit are made as an example, the above deposition efficiency can be listed as follows:

For particles with diameter 1 μm

On the plane with diameter 3 cm	On the plane with diameter 30 cm
$\left.\begin{array}{l}\eta_G = 2 \times 10^{-4} \\ \eta_R \sim 6 \times 10^{-5} \\ \eta_D \sim 5.4 \times 10^{-6} \\ \eta_{St} \sim 0\end{array}\right\} \sum \eta \approx 1.3 \times (2 \times 10^{-4})$	$\left.\begin{array}{l}\eta_G = 2 \times 10^{-4} \\ \eta_R \sim 0 \\ \eta_D \sim 0 \\ \eta_{St} \sim 0\end{array}\right\} \sum \eta \approx 1 \times (2 \times 10^{-4})$

For particles with diameter 5 μm

On the plane with diameter 3 cm	On the plane with diameter 30 cm
$\left.\begin{array}{l}\eta_G = 5 \times 10^{-3} \\ \eta_R < 3 \times 10^{-4} \\ \eta_D = 5 \times 10^{-7} \\ \eta_{St} \sim 0\end{array}\right\} \sum \eta \approx 1.06 \times (5 \times 10^{-3})$	$\left.\begin{array}{l}\eta_G = 5 \times 10^{-3} \\ \eta_R \sim 0 \\ \eta_D \sim 5 \times 10^{-7} \\ \eta_{St} \sim 0\end{array}\right\} \sum \eta \approx 1 \times (5 \times 10^{-3})$

Table 6.10 Value of α (for plane with diameter $\geq$30 cm)

d_p (μm)	1	0.7	0.4	0.3	0.25	0.18	0.1
α	1	1.25	1.5	2.3	4.5	9	10

From the above sequence, the probability of sedimentation deposition is the largest in the room with air supply. Others should also be considered appropriately. But the larger the plane area is (such as the example with diameter 30 cm), the lower the efficiency of both the interception deposition and the inertial deposition is (for the plane with diameter 30 cm, $\eta_R \approx 0$ for particles with diameter 1 μm, and $\eta_R < 3 \times 10^{-5}$ for particles with diameter 5 μm). Therefore, in order to make the estimation simple, the sedimentation deposition can only be considered with a deposition correction factor α. From the above sequence of efficiencies, it is known that for the circular silicon wafer with diameter 3 cm, α can be 1.3 for particle with diameter 1 μm, and it can be 1.1 for particle with diameter 5 μm, while it can be about 1 for particle with diameter 7.5–10 μm. For the circular silicon wafer with diameter 30 cm, α can be 1 for particle with diameter larger than 1 μm.

With the above method, the value of α for particles with diameter $\leq$1 μm when the plane diameter $\geq$30 cm is shown in Table 6.10.

For particles with the same diameter, values of α are different if the air velocity is different. The above data correspond to the air velocity 0.3 m/s. If the air velocity becomes 0.6 and 0.15 m/s, values of α are 1.6 and 1.15, respectively, for particles with diameter 1 μm on the plane with diameter 3 cm. That means when the benchmark is based on the air velocity 0.3 m/s, the deposition rate will increase by 1.23 times in the room with the same particle concentration, if the air velocity increases to two times. When the air velocity decreases by half, the deposition rate can also be reduced to 88 % of the original value.

So we have the following correction formula:

$$N_g = \alpha v_s f t N \tag{6.31}$$

Except for α, the influence factors of settlement amount include air velocity, particle settling resistance, particle density, and equivalent diameter. Further correction can be made for the above express so that it can reflect the real situation well [9]. The formula can be rewritten as:

$$N_g = \alpha\omega \frac{1}{\sqrt{\beta}} \frac{\rho'_P}{\rho} v_s f t N \tag{6.32}$$

Where α is the deposition correction coefficient;

ω is the air velocity correction coefficient, which considers the correction of α by air velocity. (The previous calculation is based on the air velocity 0.3 m/s in cleanroom. When the air velocity differs, the value of α will change. So $\omega = 1$ for the air velocity 0.3 m/s. When the air velocity increases to two times, the value of α will increase by 1.23 times, so $\omega = 1.23$. In the room without air distribution,

there is still flow movement, so the corresponding air velocity can be 0.15 m/s. Meanwhile, the value of α will decrease to 88 % of the original value, so $\omega = 0.88$.)

$(1/\sqrt{\beta})$ is the settlement resistance correction coefficient, which considers the influence of particle shape on the settling velocity during the natural sedimentation process. It is obtained by Eq. 6.4. (Generally v_s is calculated with spherical particle. But in reality dust particles are not completely spherical, and their surfaces are irregular. So the correction coefficient β considering the particle shape should be used. v_s is linear proportional to the root of correction coefficient. For irregular particles, β is 2.75–3.35, and generally it is 2.75. Correction is not needed for the unnatural sedimentation process.)

(ρ'_P/ρ) is the density correction coefficient. It can be obtained with Eq. (6.7). (As mentioned before, the density for atmospheric dust is usually $\rho_P = 2$. But in the place where people density, activity, and dust are a lot, the particle density ρ'_P may be 2–2.5. In some experiment such as the liquid droplet, $\rho'_P = 1$. So this kind of correction is not needed for the general situation.)

It is easy to determine the value of v_s in Eq. (6.32) when particles are monodisperse. When airborne particles are polydisperse, it should be calculated with some kind of average diameter. The amount of deposited particles is dependent on the frontal resistance, which is related to the cross-sectional area. So the area weighted diameter should be adopted to describe the average diameter of whole particles, which is used to estimate the deposition amount.

When the particle concentration of cleanroom is $N = 1{,}000$ pc/L $= 1$ pc/cm^3, the area weighted diameter for airborne particles with diameter larger than 0.5 μm is $D_s = 0.98$ μm [9]. That means the deposition amount for particles with diameter ≥ 0.5 μm can be considered as the deposition amount with particle diameter 1 μm.

So the total deposition amount of particles on the surface with area 1 cm^2 per hour can be obtained in the cleanroom, where the airborne particle concentration is 1,000 pc/L and the air velocity is 0.3 m/s. It is also called the unit deposition rate, which is the deposition concentration mentioned in Chap. 2.

$$N_g = 1.3 \times 0.006 \text{ cm/s} \times 3{,}600 \text{ s} \times 1\left(\text{pc}/\text{cm}^3\right) = 28 \text{ pc}/\text{cm}^2$$

As mentioned before, the calculated result only represents the possibility of the deposition amount of particles. It may be possible for the resuspension after deposition or no deposition because of the disturbance on the ground. The above data can only show the maximum probability of deposition, which is related to the surface exposure time and the actual dispersity of specific particles.

Table 6.11 shows the comparison of measured data and calculated data about the deposition amount of particles on the surface with unit area in the room with air supply. The experimental data are from the report of Tan Dade from Institute of HAVC at Chinese Academy of Building Science. It was obtained with the microscope, when the total number of particle with diameter ≥5 μm is counted on the steel disk.

Table 6.11 Comparison of measured and calculated data about deposition amount of particles on the surface with unit area in the room

	Average particle concentration (pc/L)		Measured deposition concentration [pc/(cm^2·h)]	Calculated deposition concentration [pc/(cm^2·h)]
Room	In total	≥5 μm	≥5 μm	≥5 μm
104	18,382	72	39	70.8
106	18,180	65	42	63.0
113	11,604	44	81	43.8
121	12,358	53	77	52.0
122	20,799	66	46	63.9
123	17,606	29	52	29.2
127	4,813	23	11	22.8
Average		50.3	50	49.4

In the table, the calculated deposition rate was obtained with the standard particle size distribution for particle diameter 5–10 μm. The particle size distribution is as follows:

5 μm	0.415
6 μm	0.246
7 μm	0.108
8 μm	0.077
9 μm	0.077
10 μm	0.077

From this particle size distribution, it can be obtained that $D_s = 6.59$ μm [7].

With the above value of α, $\alpha = 1.05$.

With Eq. (6.8), $v_s = 0.26$ m/s.

Taking the room No.104 from Table 6.11 as an example, we can perform the calculation with Eq. (6.31) and obtain:

$$N_g = 1.05 \times 0.26 \times 3,600 \times 0.072 = 70.8 \text{ pc}/\left(\text{cm}^2 \cdot \text{h}\right)$$

Other rooms are omitted.

This result is much closer to reality compared with the calculation result with the average diameter as the equivalent diameter performed by author [7].

With the calculation results in previous sections, the ratio of particle deposition amount on the vertical surface to that on the undersurface is very small. So it is unnecessary to use the material such as the advanced stainless steel for the wall in the cleanroom, and the requirement for the hygienic cleaning of the vertical wall is lower than that of the floor.

6.6 Influence of Airflow on Particle Movement

6.6.1 Influence Factors of Indoor Particle Distribution

From the discussions in previous sections, with the effect of gravity, inertia force (mechanical force), and diffusional force, the velocity and the distance are very small. For particles with diameter 1 μm, the movement distances are 0.006, 0.006, and 0.0004 cm, respectively. The indoor air velocity (including the air velocity with heat convection) is usually more than 0.1 m/s. In the flowing air, small particles will follow the movement of airflow with the same velocity [10]. Semiempirical equation can be used to calculate the flow in circular pipe, and the calculation result is well agreed with the experimental data.

For the single spherical particle with diameter d_p and density ρ_P in the flowing air with density ρ_P, when it follows the airflow completely, the force acting on the particle equals with that on the fluid whose volume is occupied by the particle, i.e.,

$$\frac{d}{dt}\left(\frac{\pi}{6}d_p^3\rho_a u_a\right)$$

where

u_a is the velocity of the fluid in the space which is occupied by the particle;
t is the time.

In fact, particles will not completely follow the airflow. The force exerted on the particle equals with the force component F_r by the relative movement between particles and the fluid subtracted from the above force. So the governing equation for the movement of the particle is

$$\frac{d}{dt}\left(\frac{\pi}{6}d_p^3\rho_a v_p\right) = \frac{d}{dt}\left(\frac{\pi}{6}d_p^3\rho_a u_a\right) - F_\tau \tag{6.33}$$

where

v_p is the particle velocity;
F_r is equivalent to the resistance on the particle with velocity $v_p - u_a$ in the still viscous flow.

The solution process of this equation is so complex that it will not be cited here. The study result is given:

$$\frac{v_p}{u_a} = \frac{\left(a + C\sqrt{(\pi\omega/2)}\right)^2 + \left(b\omega + C\sqrt{(\pi\omega/2)}\right)^2}{\left(a + C\sqrt{(\pi\omega/2)}\right)^2 + \left(\omega + C\sqrt{(\pi\omega/2)}\right)^2} \tag{6.34}$$

where

$$\begin{cases} a = \dfrac{36\mu}{(2\rho_{\mathrm{p}} + \rho_{\mathrm{a}})d_{\mathrm{p}}^2} \\ b = \dfrac{3\rho_{\mathrm{a}}}{2\rho_{\mathrm{p}} + \rho_{\mathrm{a}}} \\ c = \dfrac{18}{(2\rho_{\mathrm{p}} + \rho_{\mathrm{a}})d_{\mathrm{p}}} \sqrt{\dfrac{\rho_{\mathrm{a}}\mu}{\pi}}. \end{cases} \tag{6.35}$$

ω is the fluctuation frequency of turbulent flow (kHz). Except the semiempirical equation for the flow in circular pipe where both the calculation and the experimental results agree well with each other, so far there is no good result in this aspect for the cleanroom. But compared with the calculation result in circular pipe, the order of ω is only thousands Hz in the cleanroom. So particles with diameter $d_{\mathrm{p}} = 5$ μm and $\rho_{\mathrm{p}} = 1$ g/cm^3, $\frac{v_{\mathrm{p}}}{u_{\mathrm{a}}} \approx 0.9$; for $d_{\mathrm{p}} = 1$ μm, $\frac{v_{\mathrm{p}}}{u_{\mathrm{a}}} \approx 0.999$; for $d_{\mathrm{p}} < 1$ μm, $\frac{v_{\mathrm{p}}}{u_{\mathrm{a}}} = 1$. This means the relative difference between the velocity of particle following the airflow when the diameter $d_{\mathrm{p}} = 1$ μm and the air velocity is less than 10^{-3}. This can be further verified by the research about the particle trajectory and the streamline trajectory at the control site (such as the bench) which was performed by Shuji et al. [11]. The obstacle at the control site will cause influence on the particle and generate the energy by the turbulent flow. This influence is larger than that at other places. These influences include the inertial force, the diffusional force, the buoyant force, and the electrostatic force. Only when the gravity was considered, the x- and y-components of the velocity were calculated with the movement equation of the particle by Fujii [11]. The change rate was obtained with the integration in the small time ΔT (1×10^{-5} s), and the movement coordinates of the particle is then calculated.

Figure 6.10 shows the calculation result about the particle trajectory. The initial condition of calculation is that the particle velocity is the same as the air velocity. The calculation terminates at the height with ordinate -0.05 above the control site. The particle sizes used were 0.621 and 1.004 μm. It is shown from the figure that ΔM_X and ΔM_Y are the difference between the particle trajectory and the streamline trajectory in X- and Y-directions. The values are shown in Table 6.12. It is shown in the table that for particle with diameter 1.004 μm, when u_{a} is less than 0.3 m/s, the relative deviation between the particle trajectory and the streamline trajectory is not possible to be larger than 10^{-3}, which agrees with the above velocity. So the conclusion of this research was that the particle trajectory at the control site is approximately the streamline trajectory. So in other places of the cleanroom, it is reasonable to consider that particle moves with the airflow together.

From the above result, it can be thought that even for the case $\frac{v_{\mathrm{p}}}{u_{\mathrm{a}}} < 0.9$, the air velocity is much larger than that caused by settlement, diffusion, and inertia of particles. So the following velocity of particle is still the main factor that influences the distribution of particles, but there is a lag of time for the airflow. It will not cause any problem for the investigation, and it should be considered only for the study of laser Doppler velocimetry.

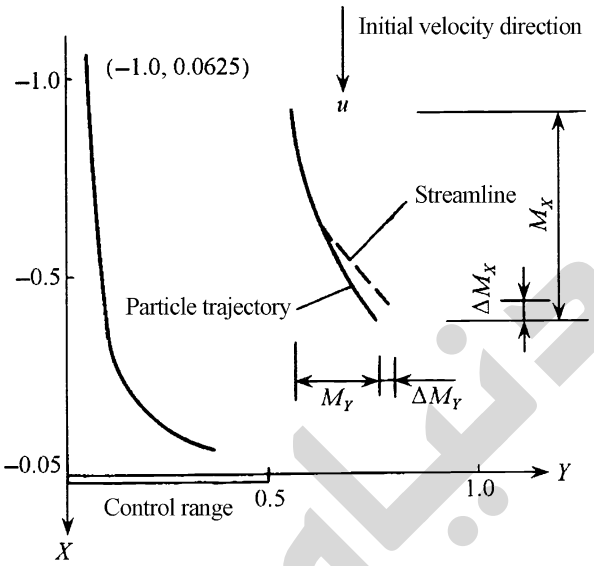

Fig. 6.10 Particle trajectory

Table 6.12 Difference between the particle trajectory and the streamline

		Air velocity (m/s)		
Particle diameter (μm)		0.5	0.4	0.3
0.621	$\Delta M_X/M_X$	5.086×10^{-5}	9.543×10^{-5}	16.065×10^{-5}
	$\Delta M_Y/M_Y$	1.916×10^{-5}	2.505×10^{-5}	3.453×10^{-5}
1.004	$\Delta M_X/M_X$	11.454×10^{-5}	21.318×10^{-5}	35.637×10^{-5}
	$\Delta M_Y/M_Y$	4.284×10^{-5}	5.611×10^{-5}	7.695×10^{-5}

Therefore, it is the air distribution that mainly influences the airborne particle distribution. Indoor particles will be affected by the airflow from air supply (including the primary air and the secondary air), the flow caused by occupant's walk, and the flow by heat convection. Except for the primary air from the supplied air, the influence of other kinds of flow will be introduced in this section.

6.6.2 Migration of Particles

It is a concern for the people that under what kind of situation, resuspension of particles by the airflow will occur, after they deposit onto the surface. Because resuspended particles may be taken away by vortex and then cause damage. This is the migration effect of airflow.

When particles are assumed spherical, the force to suspend particles with the effect of horizontal airflow is a function of the weather area of the particle, i.e.,

$$F = \varphi \frac{\pi}{4} d_p^2 \frac{\rho_a}{2} u_c^2 \tag{6.36}$$

where

u_c is the surface velocity, namely, the air velocity flowing along the surface of the particle (m/s);
φ is the suspension coefficient.

When the suspension force is larger than the particle weight, it can be expressed as:

$$\varphi \frac{\pi}{4} d_p^2 \frac{\rho_a}{2} u_c^2 > \frac{\pi}{6} d_p^3 g(\rho_p - \rho_a)$$

So

$$u_c > \sqrt{\frac{4 d_p g(\rho_p - \rho_a)}{3\varphi\rho_a}} \tag{6.37}$$

The suspension coefficient is an experimental value, which is difficult to determine. But for spherical particles, the suspension coefficient is approximately same as the resistance coefficient. So when $Re < 1$, $\varphi = \frac{24}{Re}$ can be inserted into Eq. (6.36). When ρ_a is ignored, we can obtain

$$u_c > \frac{d_p^2 \rho_p g}{18\mu} \tag{6.38}$$

There is a boundary layer when air flows along the surface. The air velocity above the boundary layer is much larger than that within the boundary layer, and usually it reaches more than three times. So the air velocity to suspend particles should be

$$u > 3u_c = \frac{d_p^2 \rho_p g}{6\mu} (\mathrm{m/s}) \tag{6.39}$$

When the air velocity reaches u, the migration of particles is formed in the following way. As shown in Fig. 6.11, with the effect of gravity, particles in the airflow will deposit on the bottom gradually and rotate forward and slide with the frontal airflow. When air passes through the rotating particles, vortex will be formed at the bottom and the side of the particle, which increases the pressure relatively. The pressure at the top of the particle reduces by the airflow. With the difference of the pressure between the top and the bottom, particles are suspended. When particles suspend to the height where the air velocity at the top is the same as that at the bottom, particles begin to deposit again with the gravity. Particles near the surface undergone the migration process of deposition-rotation-suspension with the enough intensity of the horizontal airflow, and it repeats continuously.

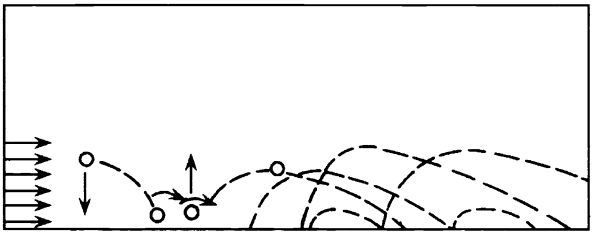

Fig. 6.11 Migration process of particles

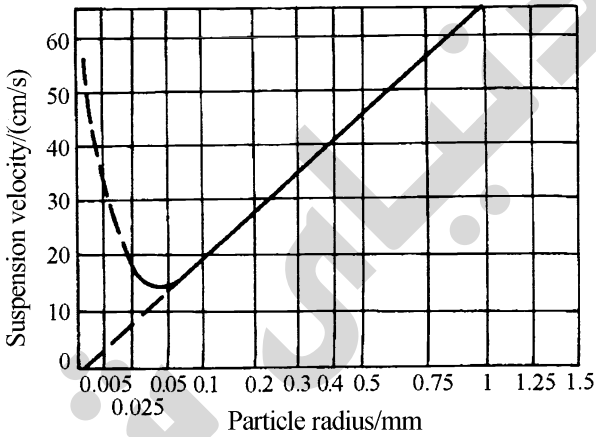

Fig. 6.12 Experimental result for the air velocity needed for particle suspension

The migration velocity calculated with Eq. (6.36) is very small. But experiment has shown that it is not easy for the very small particle on the plate to be blown away by the airflow, and the reason is that the molecular force of the interaction between the particle and the wall surface, as well as between particles, is not considered. It is shown in Eq. (6.36) that the velocity u_c needed for the suspension of the particle will be large when this kind of molecular force is added. But detailed experimental data in this aspect are very rare, and it is very difficult to determine the magnitude of this molecular force. However, the influence of the molecular force can be estimated from the experimental curve in Fig. 6.12 [12]. In the figure, the abscissa represents the particle radius. The curve shows that the air velocity needed to suspend particles with radius less than 50 μm will increase. The solid line in the figure is the experimental data, and the dashed line for extrapolation is added by author. After suspended by the airflow, particles with diameter larger than 10 μm will deposit soon. While for particles with diameter less than 10 μm, the air velocity needed to suspend them is bigger, namely, these particles are difficult to be suspended. Therefore, when air velocity should be controlled that particles will not be suspended, the control diameter can be 10 μm. In the experiment, the grit was used. For the grit with diameter 10 μm, u is about 32 cm/s. If particles with the density which is 2/3 of the grit, u can be 20 cm/s. This means the air velocity along the surface (mainly the floor) in the cleanroom should not be larger than 20 cm/s (it is not limited

for the horizontally unidirectional flow air cleanroom). For example, the backflow velocity for the side air supply mode should be determined with this consideration.

From the analysis above about the particle deposition and suspension, for the deposited particles on the horizontal plane such as the floor in the cleanroom, big particles are more likely to suspend and migrate, which generate the secondary float. This is opposite with the common opinion that the smaller particles are likely to be blown away from the floor. For cleanroom, one large particle is more hazardous than one small particle. On the other hand, large particles are likely to deposit, and the number of deposited particles on the floor is large. So the cleaning work on the horizontal surface in the cleanroom cannot be neglected. Surface cleaning treatment must be performed for the object entering the room, since the air velocity along the surface is much larger and particles on the surface are more likely to suspend than that on the floor.

6.6.3 Influence of Heat Convection Airflow

Since particles follow the airflow almost with the same velocity of the air, except for the supply air, other local airflows will also have influence on the movement and distribution of particles. Heat convection airflow is one kind of important factors. For example, the buoyant flow near the shadowless lamp can be 0.6 m/s [13], but its influence on the particle distribution in the cleanroom has not been noticed and investigated.

There are three kinds of situations for the buoyant flow generated by heat convection airflow. The following part will introduce the method to determine the velocity for this kind of the airflow.

6.6.3.1 Vertical Heat Wall

The surface temperature of the heat wall is higher than that of the ambient air. Convection will be generated near the wall surface because of the temperature difference. After the rise of the air, it will stretch out, which will promote the dispersion of particle pollution [14].

Author has ever observed the fluorescent lamp with 40 W vertically installed on the wall (the bottom of the lamp was 0.62 m above the floor) as shown in Fig. 6.13 [15]; the buoyant flow in a certain range of two ends was measured with thermometer velocimetry when no air supply was provided. At the top, the air velocity at the place 2 cm from the lamp surface reached 0.22 m/s, and the thickness of the layer with obvious air velocity reached 20 cm. When smoke was released to observe along the whole length of the lamp surface with 15 cm away, the buoyant flow appeared. Outside the layer of this buoyant flow and until about 1 m away, backflow appeared with both the method of the silk thread and the smoke release. So it is advisable to consider the airflow within 15 cm away from the surface turbulent, and

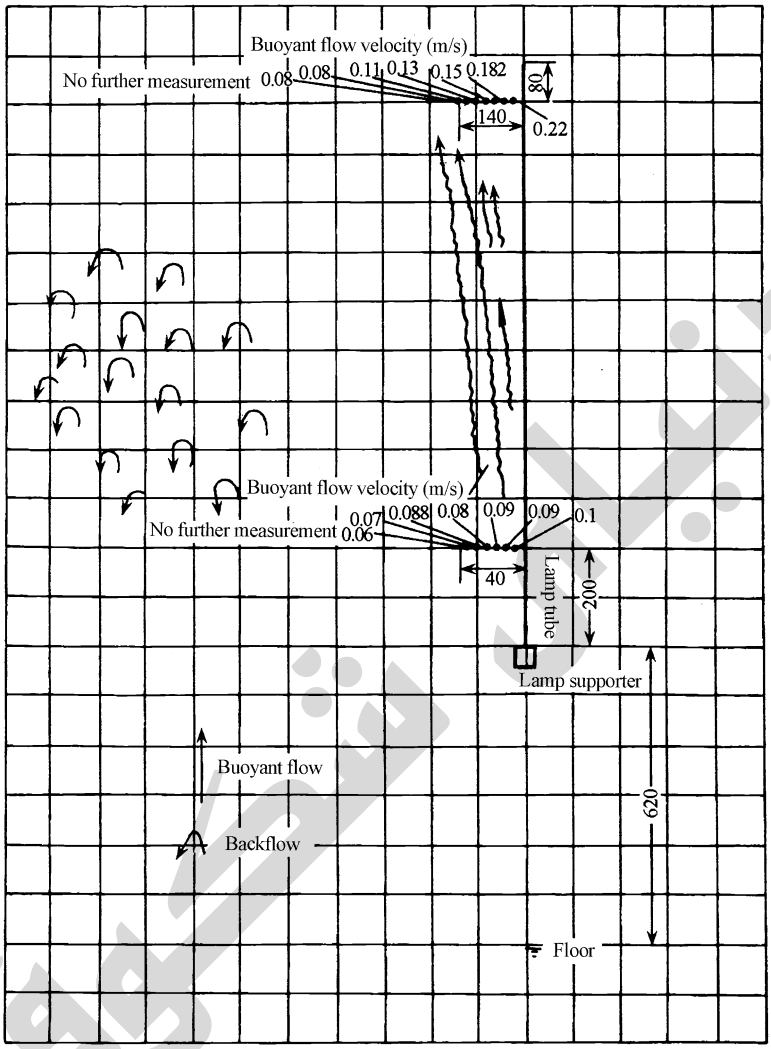

Fig. 6.13 Airflow near the lamp in the room without air supply (unit: mm)

that in the range between 15 cm and 1 m is eddy with uncertain direction. In Ref. [16], it is also pointed out that there is usually three layers of airflow in the direction perpendicular to the vertical heat wall. Except for the above two layers, the most inner layer is laminar flow with very thin thickness, which is difficult to distinguish. The combined thickness of laminar and turbulent flow is much thinner than the third layer.

Figure 6.14 shows the situation of parallel flow with air supply velocity 0.25 m/s. The two flow patterns observed in the above experiment near the fluorescent lamp

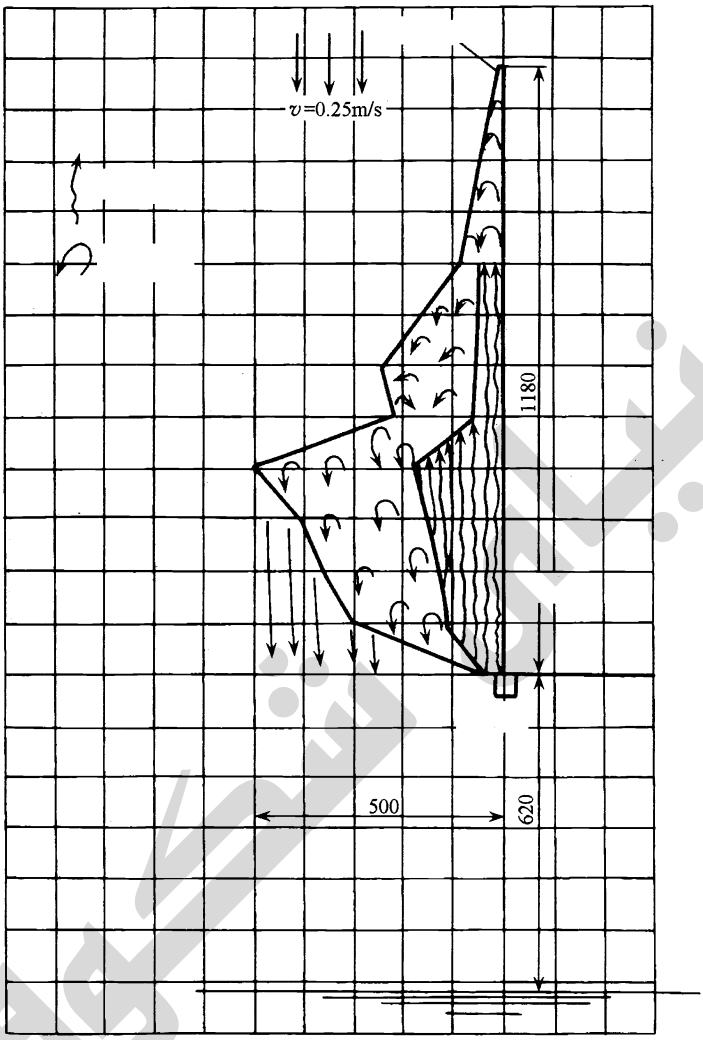

Fig. 6.14 Airflow near the lamp in the room with air supply (unit: mm)

still exist, and only the range along the horizontal and vertical directions reduces. Below the backflow, the air turns to downwards with the influence of return air.

The above observed phenomena show that:

1. The buoyant flow near the vertical heat wall such as vertically installed fluorescent lamp is very strong, and the influence range is very large.
2. Under the situation of air supply with a certain velocity, the influence will be limited. When the particle source is 0.5 m outside of the lamp surface, the particle distribution will not be affected by this buoyant flow. Experiment with the particle source located in the room center where is 1.5 m away from the lamp

surface shows that even though the air supply velocity is as small as 0.105 m/s, particles released from the source will appear in the range 1 m below the lamp. Ref. [10] also pointed out that if the pollution source is in the stagnant region of the lee side of the object, its influence is much larger than that in the backflow region. If there is also no pollution source in the backflow region, no influence will be generated. This is consistent with the above observed case when pollution source is far from the backflow region.

Since it is difficult to install the lamp at the ceiling of the unidirectional flow cleanroom and it also occupies the air supply area, someone has ever proposed to install the lamp on the vertical wall. From the above analysis, when there is air supply with a certain speed in the room where the indoor area is very small, the buoyant flow generated will cause very large influence, when the fluorescent lamp was installed at a relative high position of the vertical wall (such as above 1.5 m).

Fuchs gave the equation to calculate the buoyant flow velocity along the heat wall [17], (Table 6.13):

$$u = 0.55\sqrt{gl\beta(T_s - T_a)} \tag{6.40}$$

where

l is the height from the bottom of the heat wall (m);
T_s and T_a are the surface temperature of the wall and air temperature, respectively (K);
β is the air expansion coefficient, which equals with $1/T_a$;
g is the gravitational acceleration (m/s^2).

But according to the experimental data provided by Батурин[18], Eq. (6.40) should be modified to:

$$u = 0.36\sqrt{gl\beta(T_s - T_a)} \tag{6.41}$$

In the environment with normal temperature 23 °C, the surface temperature of the fluorescent lamp with 40W was measured to be about 40 °C, namely, the temperature difference is 17 °C. Table 6.14 shows the calculated velocity of the buoyant flow with Eq. (6.39) and the measured velocity. They are close to each other. So it is appropriate to use Eq. (6.41) to calculate the buoyant flow velocity near the heat wall. The velocity of the buoyant flow on the heat surface reaches the maximum at 1–2 cm above the surface [16].

In author's opinion, human body can be treated as the vertical heat wall approximately [15]. The relationship between surface temperature of the human body and the room temperature is shown in Fig. 6.15 [19]. When the temperature difference is 5 and 7 °C, the calculated value of u with Eq. (6.40) is 0.18 and 0.22 m/s, respectively. According to the measurement abroad [13], the velocity of the buoyant flow near the surface of human body reaches 0.2 m/s, which is consistent with the calculated result. It is clearly shown in Fig. 6.16 that even with the down supply of

Table 6.13 Velocity of the buoyant flow along the vertical heat wall (m/s) (wall height 2.74 m, $t_s = 59$ °C, $t_a = 20$ °C)

Horizontal distance from the hot wall (cm)	Vertical distance from the bottom of the hot wall (cm)																				
	11	22	33	44	55	66	77	88	99	110	121	132	143	154	165	176	187	198	209	220	274
1	0.15	0.26	0.38	0.44	0.45	0.46	0.48	0.50	0.47	0.49	0.52	0.49	0.47	0.49	0.55	0.53	0.60	0.53	0.55	0.57	0.55
2		0.12	0.19	0.23	0.31	0.38	0.42	0.44	0.46	0.47	0.50	0.50	0.51	0.55	0.57	0.57	0.58	0.60	0.60	0.65	0.60

Table 6.14 Velocity of the buoyant flow near the fluorescent lamp (m/s)

Ascending velocity	0.1 m apart from the bottom of the lamp tube	1 m apart from the bottom of the lamp tube
Calculated value	0.083	0.25
Measured value	0.08–0.1	0.22

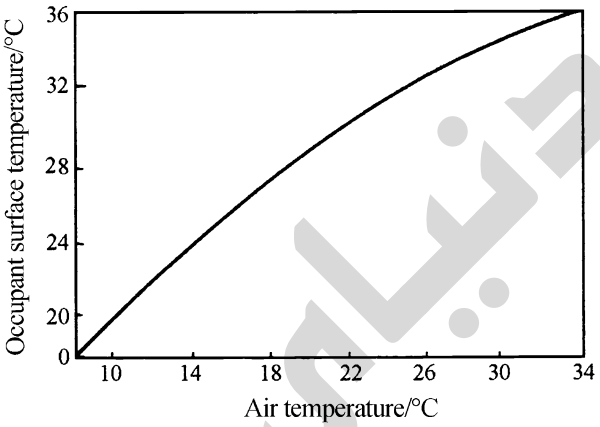

Fig. 6.15 Relationship between surface temperature of human body and the room temperature

Fig. 6.16 Influence of the buoyant flow near human body on the air distribution. Human body located at two both sides with the *white color*. The *white part* in the *middle* represents the airflow. The *white part below* means the operating table

parallel flow, backflow will appear near the surface of human body [20] (of course the surface of human body is uneven). This explains the influence of the buoyant flow on the air distribution.

As for the buoyant flow along the wall in the room with air-conditioning system in summer, the temperature difference between room and inner wall is about 2 °C, so the buoyant flow along the wall is weaker than that along the human body.

6.6.3.2 Heat Object with a Certain Volume

Лыков gave the equation to calculate the velocity of the buoyant flow along the heat object with a certain volume [14]:

$$u = 0.71\sqrt{gl\beta(T_s - T_a)} \tag{6.42}$$

where l is the characteristic length, i.e., the length of the airflow around a body (m).

For example, $l = l'$ (l' is the thickness of the plate) for the plate, $l = (\pi d/2)$ for sphere, and $l = h$ for the cube where its height is h.

It is obvious that compared with the pure vertical heat wall, the velocity of the buoyant flow along the heat object with the same height is much larger, which can be explained by the fact that the coefficient in Eq. (6.24) is much larger than that in Eq. (6.41).

Figure 6.17 shows the electric furnace with two pipes. The velocities of the buoyant flow at the intervals of 20 cm above the shell were measured, and the measuring positions are shown in the figure. The velocity of the buoyant flow increases and reaches the maximum (0.75 m/s) at about 1.2 m above the shell and then reduces gradually. It is not easy to choose the value of the parameter in Eq. (6.42) when it is used for calculation. Since the value of l is only several centimeters (when the porcelain tube is concerned) and the temperature difference is several hundreds, the order of magnitude for the calculated result is equivalent with that of measurement.

6.6.3.3 Plane Heat Source and Heat Surface with Small Thickness

It is obvious that Eq. (6.42) is not suitable to describe this problem. Эльтерман has performed experimental study [18], and Куница derived the theoretical expression which agrees well with experiment [21]:

$$u_Z = 0.06\Delta t^{4/9} Z^{1/3}\left\{1 - \exp\left[-9.4\left(\frac{R_y}{Z}\right)^2\right]\right\} \tag{6.43}$$

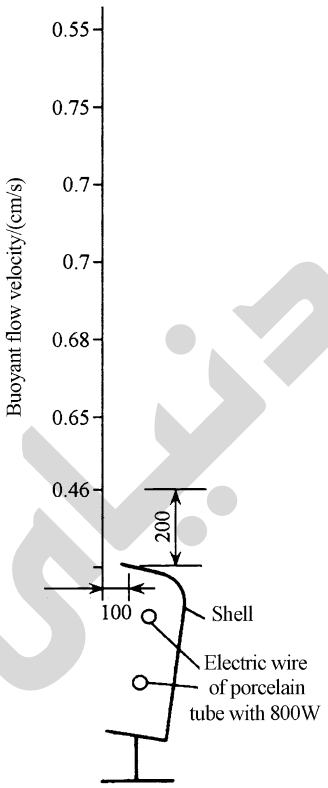

Fig. 6.17 Velocity of the buoyant flow near the vertical electric furnace

where

Z is the vertical height from the heat source surface (m);
u_Z is the air velocity at Z (m/s);
Δt is the temperature difference between surface and ambient medium (°C);
R_y is the equivalent radius of planar heat source (m).

For rectangular heat source

$$R_y = b\sqrt{\frac{k}{\pi}}(\text{m})$$
$$k = \frac{a}{b}$$

where

a is the length of long side on the rectangle (m);
b is the length of short side on the rectangle (m).

For circular heat source

$$R_y = R(\text{m})$$

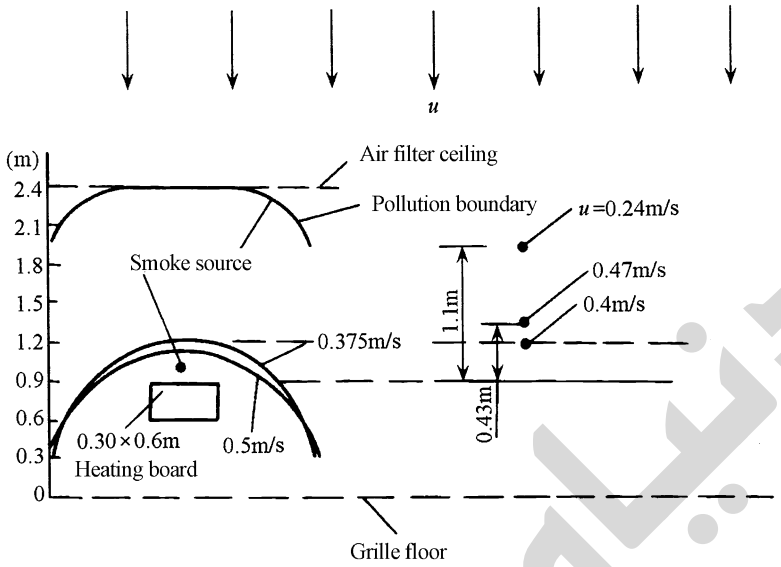

Fig. 6.18 Air velocity above the plane heat source with surface temperature 200 °C

When $Z \approx 1.8R_y$, the above equation can be simplified as

$$u_Z = 0.06\Delta t^{4/9} Z^{1/3} \tag{6.44}$$

The above equation shows that the velocity of the buoyant flow above the heat source increases from zero to the maximum which is at about $Z \approx 0.43$ m and then reduces gradually when it is further above the heat source.

Figure 6.18 shows the curve by experiment abroad [22]. It represents the boundary of the pollution (namely, the boundary of the particle distribution). The larger the air supply velocity is, the lower the height of the pollution boundary is. Data on the right are the data added by author with the above equation. When the temperature of hot surface reaches 200 °C in the room without air supply, the maximum velocity of the buoyant flow is 0.47 m/s, which appears at $Z = 0.43$ m. At the height of 1.2 m, the measured velocity is 0.375 m/s, while the calculated value is 0.4 m/s. So the calculated result is close to the measure value.

6.6.4 *Influence of Secondary Airflow by Movement of Occupant*

In the common references, people in cleanroom should not walk too fast. Usually it is about 3.6 km/h (1 m/s), because the secondary flow caused by people's walk will drive particles to move together. But there is no study about how much is the

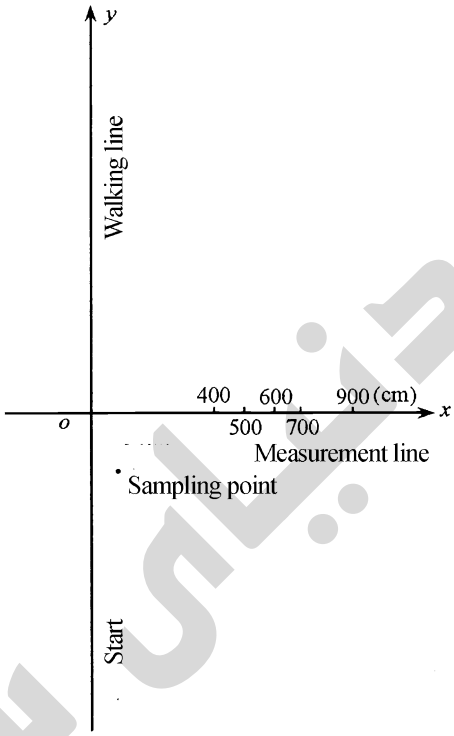

Fig. 6.19 Route of people's walk

velocity of secondary flow caused by people's walk. Experiment was performed with the walk route shown in Fig. 6.19, and the following conclusions were obtained:

1. The maximum velocity of secondary flow. This value was not obtained with the velocity sampling at some place when people pass by (the intersection place "o" in the figure) but was the measured velocity at the place where people stop (a certain distance from the sampling place). Meanwhile, the closer the distance from the human body is, the larger the velocity of secondary flow is.
2. The relationship between the maximum velocity of secondary flow and the speed of people's walk. Figure 6.20 shows the measured velocities along x- and y-directions. Although the relationship between the maximum velocity v_{max} of secondary flow and the speed v of people's walk is not apparent, the boundary for the maximum value can be estimated with the following equation:

$$v_{max} = 0.21 + 0.13v \tag{6.45}$$

where v is the speed of people's walk.

The maximum velocity of the secondary flow can be calculated with the above equation about the speed of people's walk. For example, if $v = 1$ m/s, $v_{max} = 0.34$ m/s; if $v = 2$ m/s, $v_{max} = 0.48$ m/s. This means the velocity of

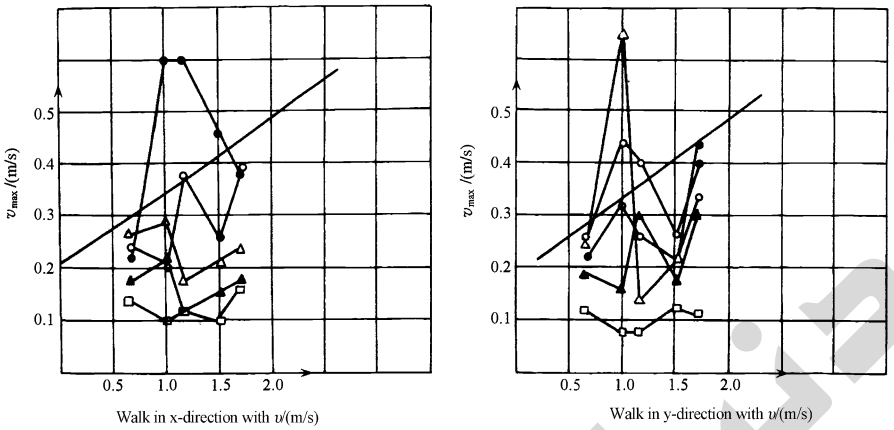

Fig. 6.20 Relationship between the maximum velocity of secondary flow and the speed of people's walk. Vertical distance along the route. ● 400 mm, ○ 500 mm, △ 600 mm, ▲ 700 mm, □ 900 mm

secondary flow caused by people's walk is less than the speed of people's walk. Usually $\frac{v_{max}}{v}$ is in the range of 0.2–0.4.

3. Direction of the secondary flow. Experiment has shown that secondary flow has two obvious components along x- and y-directions, and they are equal with each other.

The above measurement and analysis of the secondary flow caused by people's walk can be the basis to determine the lower limit of air velocity in horizontally unidirectional flow cleanroom. This will be discussed in Chap. 8.

6.7 Coagulation of Particles in Airflow

Airborne particles will become big particle because of the mutual collision and adhesion during the relative movement process (that caused by Brownian motion, gravity, or aerodynamic force). This phenomenon is called coagulation of particles. With particle coagulation, particle size will become large, which is good for observation, measurement, and removal. The coagulation process can be classified as thermal coagulation and movement coagulation (the movement resulted from airflow movement and acoustic vibration).

Next the phenomenon of thermal coagulation will be briefly introduced.

According to Fuchs' derivation [23], the average time interval between two collisions is $\frac{1}{4\pi D d_p N}$. The relative dispersion coefficient of two contacting particles equals with the summation of dispersion coefficients of two particles. When two particles have the same size, it becomes $2D$. So the number of particles which contact with one particle per unit volume in the time period $t = 1$ s is

$$\frac{1}{\frac{1}{4\pi 2Dd_pN}} = 8\pi Dd_pN$$

Because there are N particles in total per unit volume, the time of collisions will be $\frac{1}{2}N8\pi Dd_pN$. The coefficient 1/2 was introduced because two particles will coagulate and become one particle when they collide with each other. The collision rate (dN/dt) will be negative with the following expression:

$$\frac{dN}{dt} = -4\pi Dd_pN^2 \tag{6.46}$$

Since d_pD can be approximately constant, the change rate of particle concentration will become

$$\frac{dN}{dt} = -K_0N^2 \tag{6.47}$$

where K_0 is called coagulation coefficient. It can be calculated with the following expression:

$$K_0 = 4\pi Dd_p \tag{6.48}$$

When integration is performed on Eq. (6.47), we obtain:

$$\int_{N_0}^{N_t} \frac{dN}{N^t} = \int_0^t -K_0 dt$$

So we get:

$$\frac{1}{N_t} - \frac{1}{N_0} = K_0t \tag{6.49}$$

where N_0 is the initial concentration;

N_t is the concentration at the moment t, which can be obtained with the following expression:

$$N_t = \frac{N_0}{1 + N_0K_0t} \tag{6.50}$$

Table 6.15 shows the value of K_0 under standard condition. Table 6.16 shows the variation of concentration during the thermal coagulation process for monodisperse particles when $K_0 = 5 \times 10^{-10}$ cm^3/s [24].

From the above data, when initial concentration is less than 10^6 pc/cm^3, the influence of coagulation can be neglected during measurement with time period

Table 6.15 Value of K_0 under standard condition

d_p (μm)	$K_0 \times 10^{-10}$ (cm^3/s)
0.01	67
0.1	8.6
1.0	3.5
10	3.0

Table 6.16 Time needed to double particle size with coagulation and to reduce half of concentration

Initial concentration N_0 (1/cm^3)	Time needed when concentration becomes 0.5 N_0	Time needed when particle size doubles ($N = 0.125\ N_0$)
10^{14}	20 μs	140 μs
10^{12}	2 ms	14 ms
10^{10}	0.2 s	1.4 s
10^{8}	20 s	140 s
10^{6}	33 min	4 h
10^{4}	55 h	16 day
10^{2}	231 day	4 × 365 day

10 min. If the measurement time is 2 days, the concentration should be less than 10^3 pc/cm^3 so that the coagulation effect can be ignored. This aspect should be noticed during the experimental study, leakage detection of air filter, and self-purification time with smoke release.

6.8 Enclosure Line of Point Pollution in Parallel Flow

The above sections have discussed various movement situations of single particle and the influence generated by local airflow. Now the further study is presented about the particle distribution with particles released by the source in the flow field. The simplest case is the particle distribution with the point source in the parallel flow field. The specific aim is to determine the boundary of particle distribution, namely, the range of pollution. Here it is called the enclosure line of pollution. In practice, there is the particle source which can be treated as point source, such as the spray of the leakage hole in one direction or several directions or the release of the leakage from the unsealed equipment. These particle sources exist in clean environment, and their size is very small; otherwise, they are not allowed to be inside the room. The meaning to study this problem is to find the basis for the air velocity which can be used to control pollution from various directions. This will also be discussed in Chap. 8 about the lower limit of air velocity in unidirectional flow cleanroom.

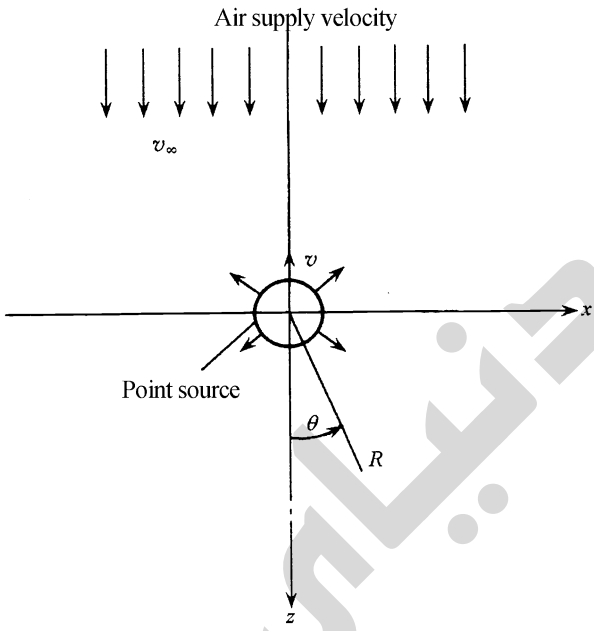

Fig. 6.21 Point pollution source in parallel flow (i.e., unidirectional flow)

6.8.1 Enclosure Line of Point Pollution

Figure 6.21 shows the case with point pollution source in parallel supply air. The flow field in the room is the combination of the parallel supply air and the flow field by point pollution source. Now the spherical coordinate is adopted. R is the radial distance from point pollution source. θ is the intersection angle between R and z axis, and the anticlockwise direction is positive.

The stream function of parallel flow field is:

$$\varphi_1 = \frac{1}{2} v_\infty R^2 \sin^2\theta \tag{6.51}$$

The stream function of point source flow field is:

$$\varphi_2 = -\frac{Q}{4\pi} \cos\theta \tag{6.52}$$

The stream function of the stack flow field is:

$$\varphi = \varphi_1 + \varphi_2 = \frac{1}{2} v_\infty R^2 \sin^2\theta - \frac{Q}{4\pi} \cos\theta \tag{6.53}$$

where v_∞ is the air velocity of parallel supply air (m/s);

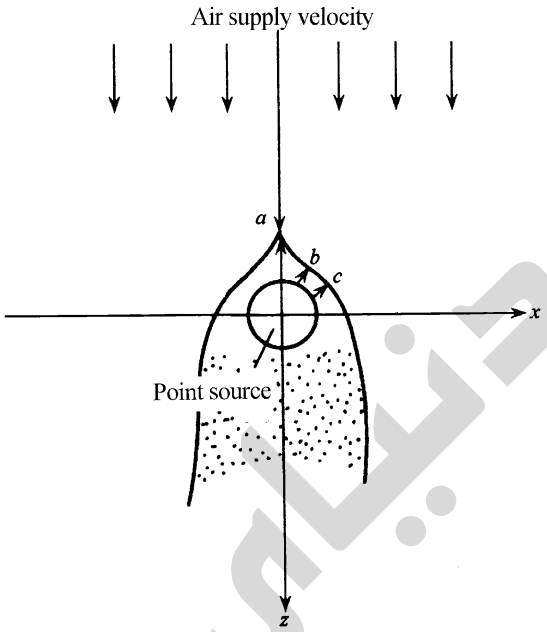

Fig. 6.22 Enclosure Line of Point Pollution

Q is the source strength, which is equal to the flow rate of polluted flow (m^3/h).

When the air velocity equals with the velocity of polluted air, the polluted air along z axis direction is restrained at the position a (shown in Fig. 6.22), which can be called the stagnation point. Polluted air in other directions will be restrained at positions b and c. When the supplied air arrives at position a, it begins to turn round and moves forward when passing positions b and c (it is the same for other directions). This means when the polluted air flows through the lines a, b, and c, the component of velocity along z direction disappears. When the influence of molecular dispersion is not considered and that of flow fluctuation is very small, the polluted air cannot pass through this line and is strained under this line. Therefore, this line can be called the enclosure line of pollution [15].

So the enclosure line of pollution is the line passing through points a, b, and c. For position a, $\theta = 180°$, so the stream function is:

$$\varphi_{180} = \frac{Q}{4\pi} \tag{6.54}$$

When the above two equations are combined, we obtain:

$$\frac{Q}{4\pi} = \frac{1}{2} v_\infty R^2 \sin^2\theta - \frac{Q}{4\pi} \cos\theta \tag{6.55}$$

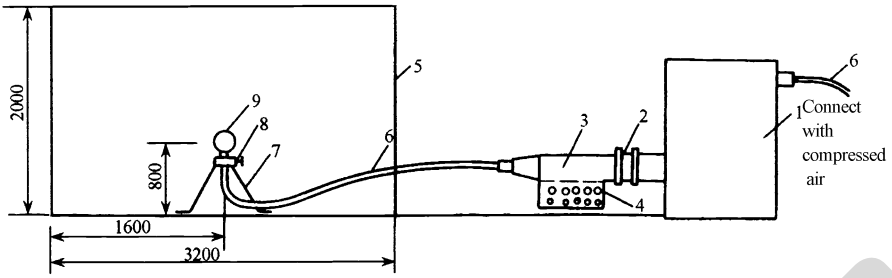

Fig. 6.23 Schematic of the test rig for point pollution source (unit: mm). *1* buffer box, *2* Valve, *3* smoke chamber, *4* smoke release hole, *5* Cleanroom, *6* rubber hose, *7* Lampstand, *8* Jackscrew, *9* dust release ball

Table 6.17 Average pollution concentration releasing into the room (pc/min)

	Polluted air velocity (m/s)[a]			
Item		1.27(9)	2.5(17.8)	2.7(19.4)
One Balan cigarette was lighted indoors	7.8×10^8	6.18×10^8	7.36×10^8	9.53×10^8
Five cigarettes were lighted inside the cigarette box and smoke was released as point source indoors				

[a]The data in the bracket is the flow rate (L/min)

In fact, pollution source is not a geometrical point; instead, it should have a certain volume. Suppose the radius is r and the velocity on the spherical surface with radius r is v ($Q = 4\pi r^2 v$), the above expression can be simplified as

$$R = 1.414\, r\sqrt{\frac{v}{v_\infty(1-\cos\theta)}} \tag{6.56}$$

This is the trajectory equation for the enclosure line of pollution which passes through points a, b, and c.

6.8.2 Actual Particle Distribution of Pollution Source

Now take the actual distribution of particles released by point pollution source simulated in parallel flow as an example, the test rig is shown in Fig. 6.23 [15]. The pollution source was the table tennis with radius $r = 2$ cm and many perforation on it. Compressed air was used to spray the smoke from five cigarettes. The average pollution concentration supplied into the room is shown in Table 6.17. Particle counter was used to measure the cross-sectional concentration in the center of the room at the working area height 0.8 m above the floor, when different conditions

with parallel air velocity and particle generation rate were provided. Figures 6.24, 6.25, 6.26, 6.27, and 6.28 are several cases. In the figure, the abscissa represents the sampling position. The measured concentrations by particle counter were labeled. The sampling position without data means the measured value is zero. This means the average concentration in these positions is extremely low, so these places are not polluted.

It is observed in the experiment that for pollution flow with velocity $v = 1.27$ m/s from the pollution source, it disappears once leaving the hole. From the figure of concentration field, pollution can barely be measured at the same height of the pollution source. For pollution source with velocity 2.5 m/s, the elevated height of the polluted buoyant flow was observed only several centimeters. From the figure of concentration field, pollution can only be detected at the height of the pollution source. For pollution source with velocity 2.7 m/s, the increase of pollution concentration becomes larger. The elevated height of the buoyant flow was observed 10 cm. It is shown from the figure of concentration field that pollution was detected at the height 10 cm above the pollution source. In short, when the ratio of the polluted air velocity to the supply air velocity is less than 20, the elevated height of the polluted flow is within 20 cm (in the figure of concentration field, there is not sampling point at 10 cm below).

Experiment has also shown the situation of the buoyant thermal flow from the fluorescent lamp on the wall. The left of the concentration field is the situation when the lamp is turned on. Since the downwards supply air velocity above the lamp is between 0.16 and 0.3 m/s and the dust source is 1.5 m away, polluted particles are not detected near the region above the lamp. The right of the figure shows that the downwards supply air velocity above the lamp is less than 0.1 m/s. Three rows of measured data at 0.5 m away from the lamp show the obvious increase of pollution when the lamp is turned on. The pollution height reaches 1.5 m (shown in Fig. 6.25). This is consistent with the previous case about the buoyant flow near the wall.

6.8.3 Calculation of Enclosure Line of Pollution

Difference is large between the calculated enclosure line with Eq. (6.54) and the boundary of particle distribution by experiment. The range of the former case is relative narrow, while that of the latter case is much spacious. It can be found with the analysis of experimental concentration field that:

1. Although the decrease rate of pollution flow is very fast, it is still slower than the calculated result with spherical coordinate.
2. The crosswise stretching range of polluted air is much larger than the range in the enclosure line.

As for the first conclusion, the main reason is that the actual pollution source is not a uniform spherical dispersion source, and it has the characteristic of jet flow

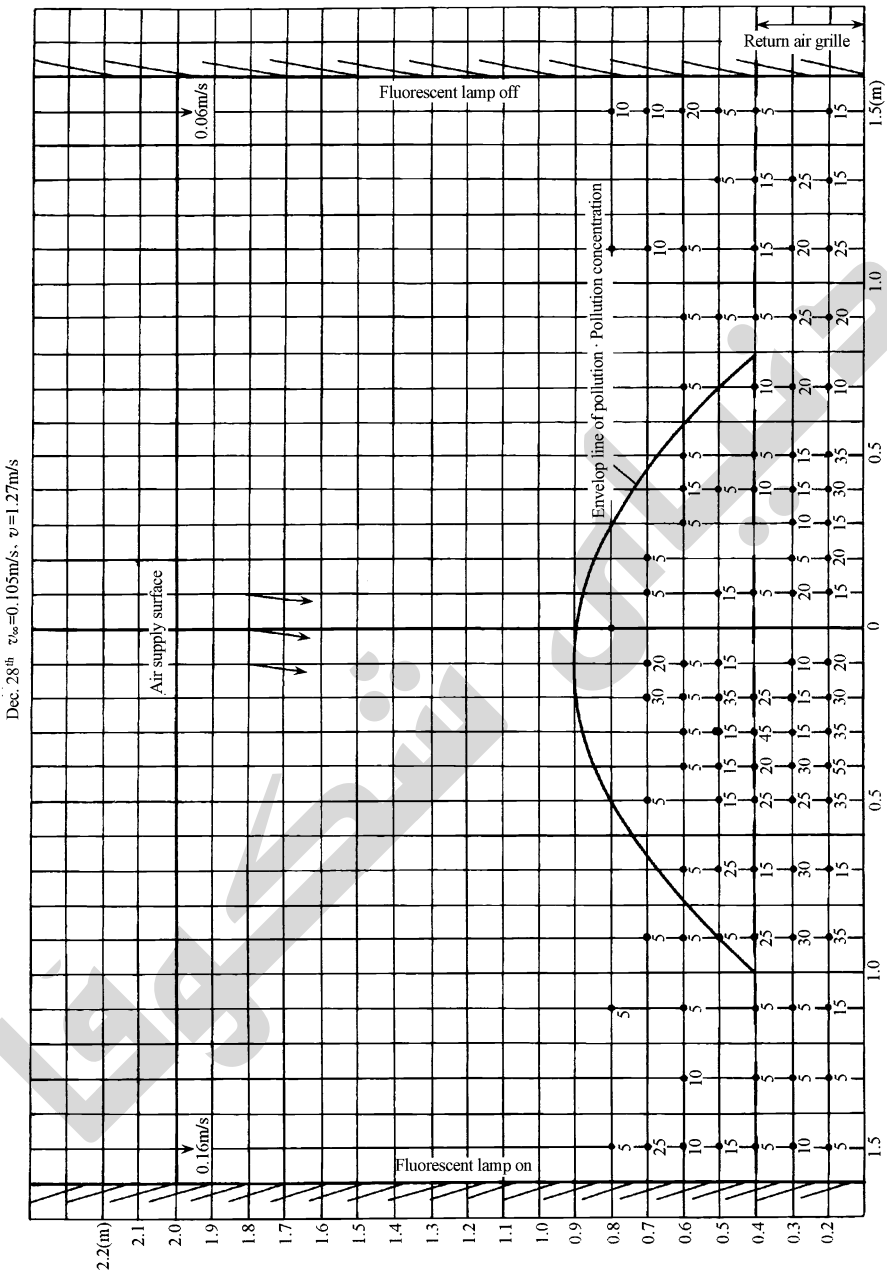

Fig. 6.24 Actual measured pollution range with point pollution source (1)

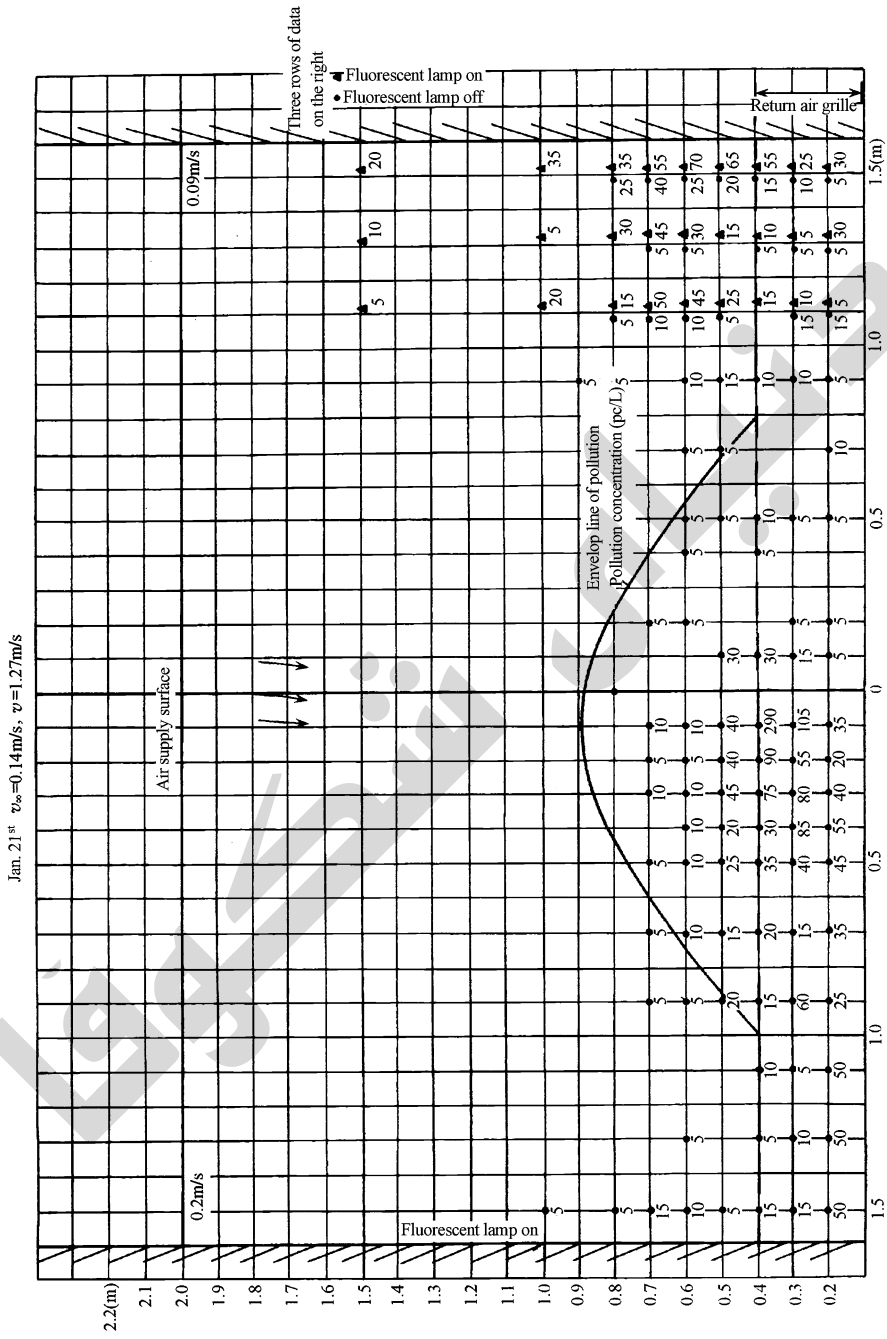

Fig. 6.25 Actual measured pollution range with point pollution source (2)

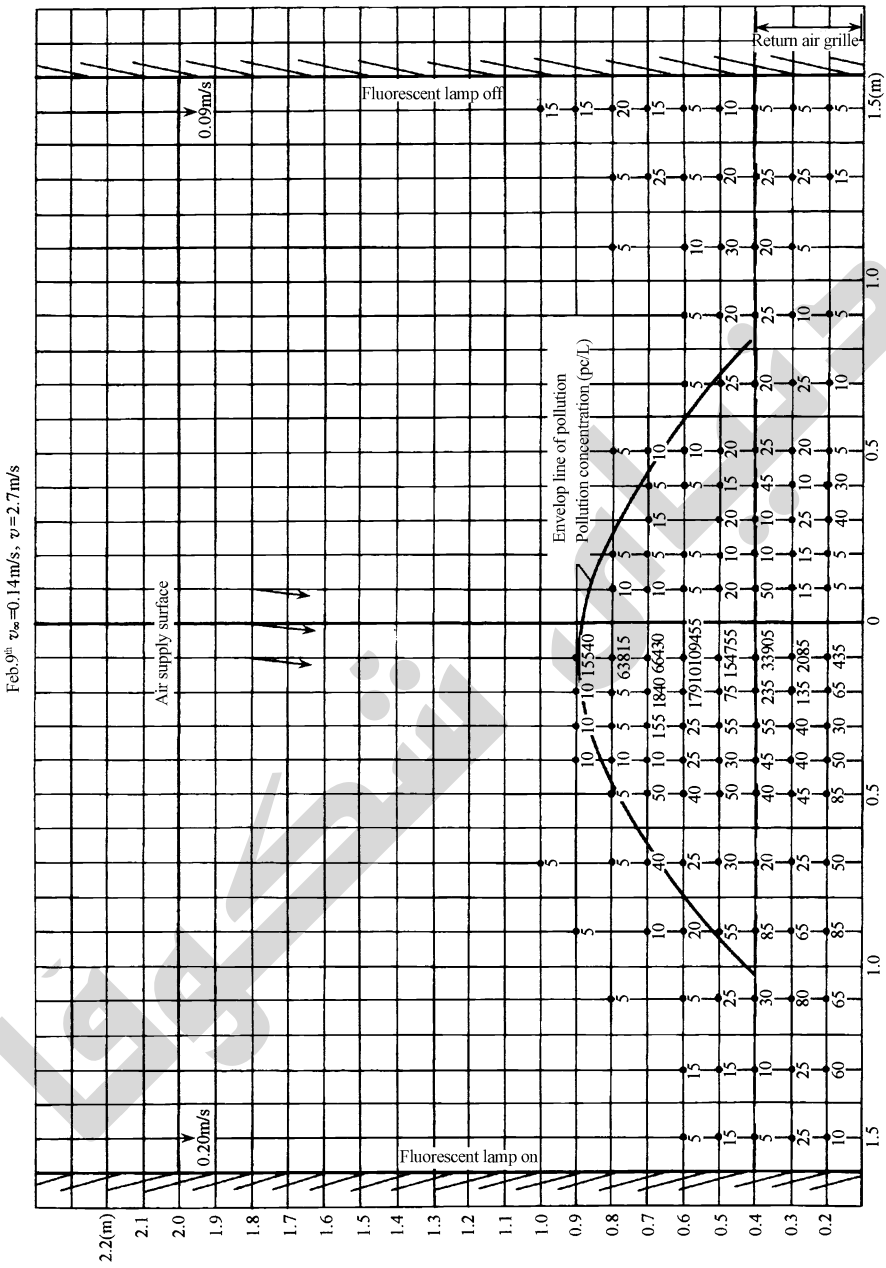

Fig. 6.26 Actual measured pollution range with point pollution source (3)

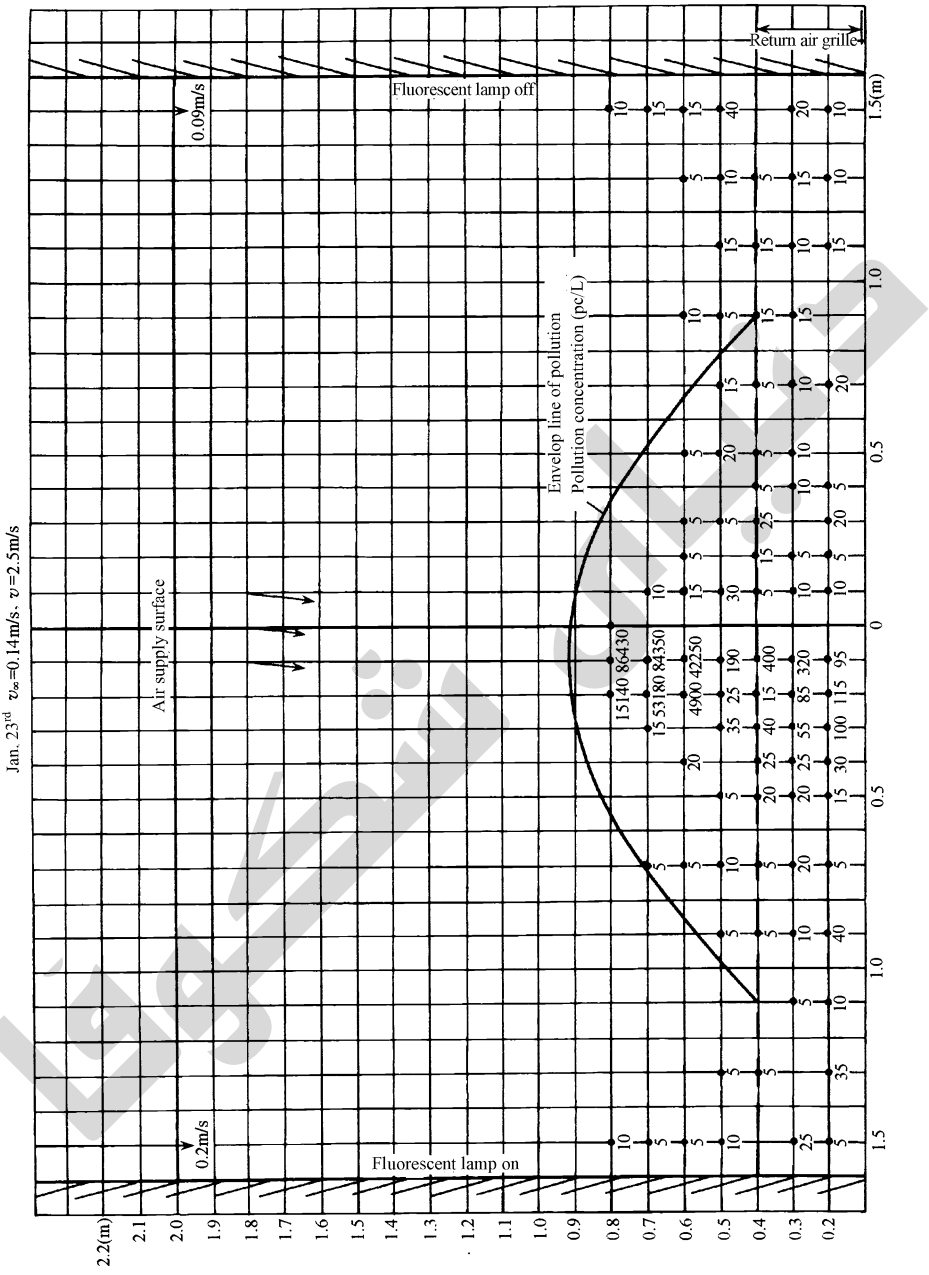

Fig. 6.27 Actual measured pollution range with point pollution source (4)

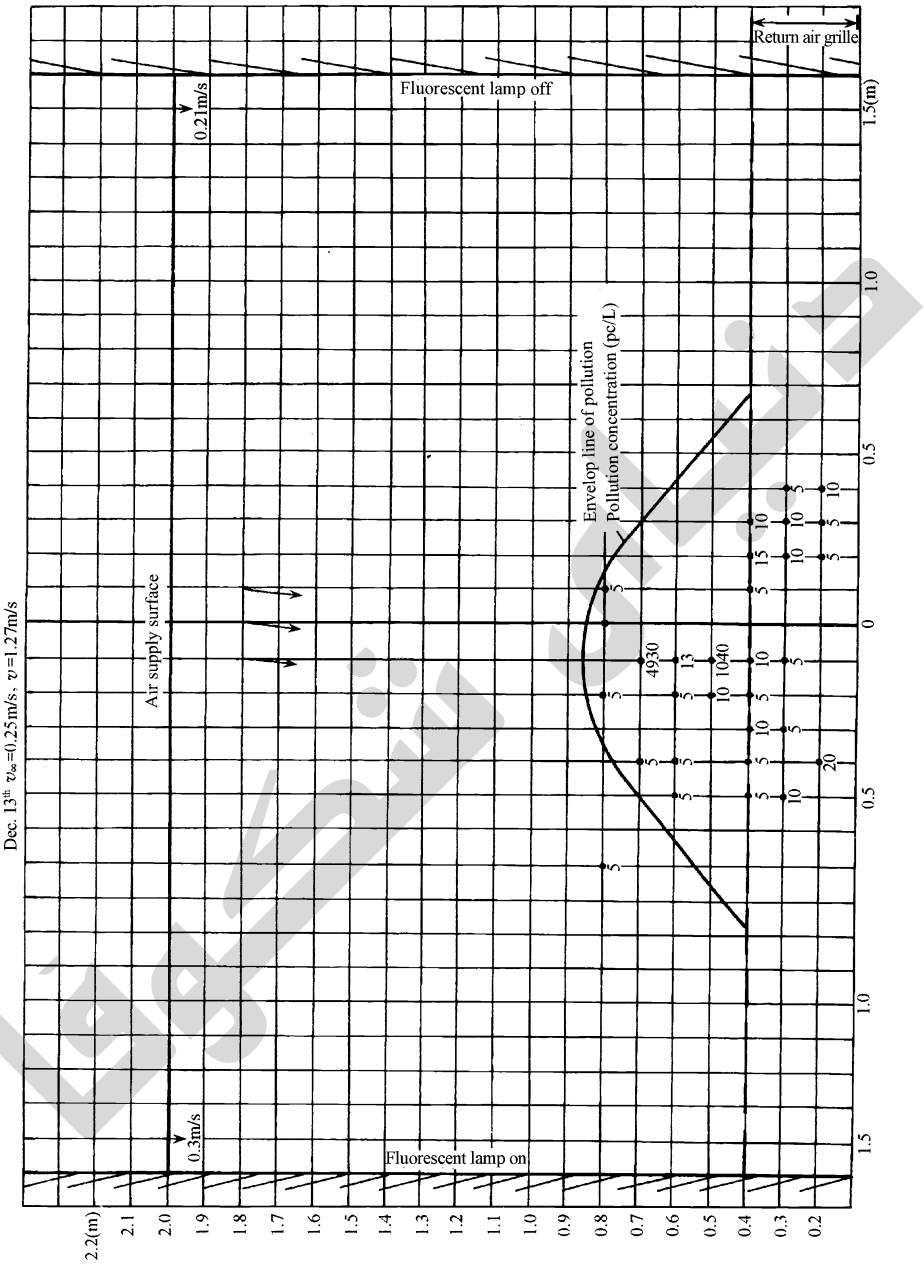

Fig. 6.28 Actual measured pollution range with point pollution source (5)

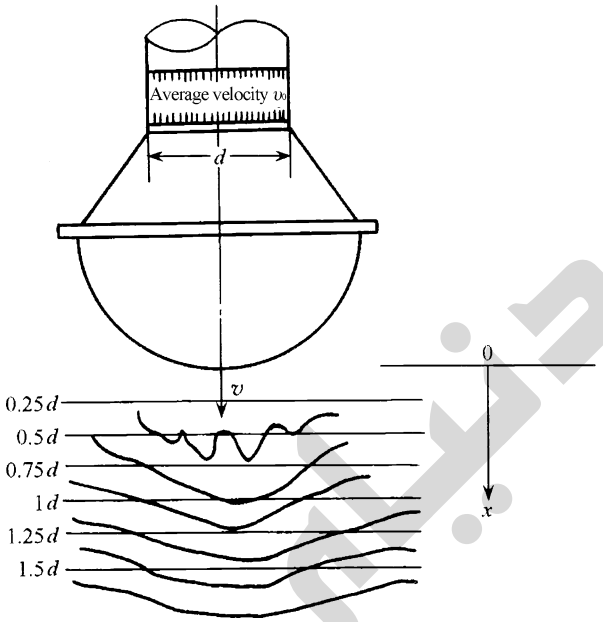

Fig. 6.29 Velocity decline of perforated spherical air supplier

Table 6.18 Decline of axial velocity v from spherical air supplier

x/d	0	1	2	3	4	5	6
v/v_0	0.35	0.98	0.97	0.95	0.88	0.8	0.7

from small pore. The decline of velocity is very slow. After a certain distance, it declines like the spherical surface. As for this problem, there is no special investigation, and the data of perforated spherical air supplier performed by Baturin can be referred [17], which is shown in Fig. 6.29 and Table 6.18.

As for the second conclusion, it has also been shown in the experiment performed by Baturin, which was specially pointed out in Fig. 6.29. This kind of velocity field in different directions with θ is not uniform, and the crosswise stretch is much faster. The feature of the velocity field with the perforated spherical air supplier should be investigated further. A correction coefficient related to θ should be added for Eq. (6.56). According to the in-site tested concentration field, the value of this correction coefficient can be $(1-\cos\theta)^{-1.5}$. So Eq. (6.56) becomes the following semiempirical equation:

$$R = 5.7(1-\cos\theta)^{-1.5} r \sqrt{\frac{v}{v_\infty(1-\cos\theta)}} \tag{6.57}$$

where R is called pollution radius.

Curves in Figs. 6.24, 6.25, 6.26, 6.27, and 6.28 are the enclosure line calculated with this equation.

As mentioned before, with the influence of thermal convection caused by the fluorescent lamp and the influence of the eddy caused by the frame between air filter and side wall (refer to Chap. 8 about the unidirectional flow cleanroom), the buoyant flow along the wall will drive the polluted flow towards two sides, so the two end of the pollution region from experiment is wider than the width of the calculated envelope line. It is also the case under the height of the return air grille. But compared with the calculated envelope line, it is still consistent for the pollution region above the return air grille. Particles released from the pollution source are within the range of the envelope line. Only when $\frac{v_{\infty}}{v}$ is larger than 20, some particles will go outside of the envelop line. It can be estimated that the theoretical result will match well with practice for the standard parallel line by full return air on the floor.

The further discussion about Eq. (6.57) will be performed in Chap. 8 about the lower limit of air velocity.

References

1. Fuchs HA (1960) The mechanics of aerosols (trans: Gu Zhenchao). Science Press, Beijing, p 43 (In Chinese)
2. Li XJ, Li JY (1977) Dust removal in the crush and sieve workshop. Metallurgy Industrial Press, Beijing (In Chinese)
3. Fuchs HA (1960) The mechanics of aerosols (trans: Gu Zhenchao). Science Press, Beijing, p 186 (In Chinese)
4. Fuchs HA (1960) The mechanics of aerosols (trans: Gu Zhenchao). Science Press, Beijing, Chapter 4 (in Chinese)
5. Sugawara F (1972) Abstracts of the academic lectures by Japan Building Institute (Kanto), pp 25–26 (In Japanese)
6. Yoshizawa S (1977) Measurement of sterile environment. J SHASE (Soc Heat Air Cond Sanit Eng) Jpn 51(1):15–21
7. Xu ZL (1981) Relationship between the yield and the air cleanliness level of the environment. Mech Eng 3(1):45–49 (in Chinese)
8. Ranz WE, Wong GB (1952) Impaction of dust and small particles on surface and body collectors. Ind Eng Chem 44:1371–1381
9. Xu ZL (1993) Exploration of the relationship between the deposition bacterial method and the airborne bacterial method. China Public Health 9(4):160–162 (In Chinese)
10. Shu W (1979) Following characteristic of discrete particles in turbulent flow. Science and Technology Information from Tianjin University (In Chinese)
11. Fujii S et al (1982) Investigation on the design of laminar flow cleanroom. Abstracts of the academic lectures by Japan Building Institute (Tohoku), p 277 (In Japanese)
12. Fuchs HA (1960) The mechanics of aerosols (trans: Gu Zhenchao). Science Press, Beijing, p 343 (in Chinese)
13. Sano T (1876) Influence of obstacle and thermal plume in laminar flow room. J Jpn Air Clean Assoc 17(1):37–42 (In Japanese)
14. Fyodortsov AB (1965) Theoretical basis of building thermal physics (trans: Ren Xingji, Zhang Zhiqing). Science Press, Beijing (In Chinese)

15. Xu ZL, Qian ZM, Shen JM et al (1983) Lower limit of air velocity in parallel flow cleanroom. Research report from Building Science, p 11 (In Chinese)
16. Serebryakov (1979) Indoor air dynamics (trans: Zhou Moren). Acad J Chongqin Build Constr Coll 1 (In Chinese)
17. Fuchs HA (1960) The mechanics of aerosols (trans: Gu Zhenchao). Science Press, Beijing, p 238 (In Chinese)
18. Baturin BB (1965) Industrial ventilation principle (trans: Liu Yongnian). China Industrial Press, Beijing (In Chinese)
19. Колпаков ГВ (1951) Вопросы лучистого отопления (In Russian)
20. Furuhashi M et al (1977) Fundamental and clinical study of vertical flow device in cleanroom. J SHASE (Soc Heat Air Cond Sanit Eng) Jpn 51(1):27–32 (In Japanese)
21. Куница ВИ (1977) Конвективные струи над нагретыми поверхностями. Водоснабжение и Санитарная Техника 8:19–20 (In Russian)
22. Morrison Phylip W (1973) Environmental control in electronic manufacturing
23. Fuchs HA (1960) The mechanics of aerosols (trans: Gu Zhenchao). Science Press, Beijing, p 383 (In Chinese)
24. Hinds WC (1989) Aerosol technology (trans: Sun Yufeng, Chapter 12). Heilongjiang Science and Technology Press, Harbin (In Chinese)

Chapter 7
Classification of Air Cleanliness

With the fast development of semiconductor industry, pharmaceutical, food, and other industries, attention has been shifted from the particulate pollution in the past to the chemical pollution recently. For the control object related to the air cleanliness, it has been shifted from single object, i.e., particles in the past, to two objects which also include airborne molecular contaminant (AMC). In fact standard related to air cleanliness and classification of air cleanliness has contained both the particle concentration level (customarily it is still called air cleanliness level) and the AMC concentration level. However, the air cleanliness specifically related to particle concentration level is still the core index to evaluate the air cleanliness of the environment.

7.1 Development of Air Cleanliness Standards (Classification)

The development process of national standards in different countries will not be introduced here, but it can be seen in the course of the development of air cleanliness standards (classification):

1. Due to the limit of the means to sample the dust and the limit of the depth of understanding of air cleaning technology in early times, either the particle counting concentration or the particle weight concentration has been used to describe the air cleanliness. For example, the former Soviet Union had made the following specification in national standards: particle concentration for level I is 0.00036 mg/m^3, for level II is 0.5 mg/m^3, and for level III is 0.8 mg/m^3.
2. Because the characteristic of particle distribution in air was unknown in early times, it was confused even though the air cleanliness was classified with the particle counting concentration. For example, in the Technology Regulations T.O.00-25-203 published in the March of 1961 by US Air Force, particle concentration for level I is 8,834 pc/L (250,000 pc/ft^3) for all the countable

Z. Xu, *Fundamentals of Air Cleaning Technology and Its Application in Cleanrooms*, DOI 10.1007/978-3-642-39374-7_7, © Springer-Verlag Berlin Heidelberg 2014

particles, for level II is 3,004 pc/L (0.3–10 μm) (85,000 pc/ft^3), for level III is 1,237 pc/L (0.3–10 μm) (35,000 pc/ft^3), and for level IV is 353 pc/L (0.3–10 μm) (10,000 pc/ft^3).

3. Due to the understanding of the characteristic of particle distribution on log-log paper, parallel lines on this kind of paper were used to distinguish between different places for the first time in the USA – levels of cleanliness for atmosphere, control area, standard cleanroom (equivalent to Class 8), and laminar flow devices (equivalent to Class 5). This was the revised air force technical order 203 published in July 1963. Even if it may be inspired by the distribution characteristic of atmospheric dust, it can be still considered as the first cornerstone of cleanroom technology.
4. Because "laminar" cleanroom (namely, unidirectional flow now) appears, air cleanliness can be classified into several classes according to the concentration level reached by unidirectional cleanroom and general cleanroom (namely, turbulent flow cleanroom or non-unidirectional flow cleanroom). This forms the classification or standard for air cleanliness, which will be introduced in the principle of cleanroom in Chap. 8. The class of air cleanliness is based on the corresponding measures of air cleaning technology. So the first scientific classification of air cleanliness standard was born, which was the US Federal Standard 209 published at the end of 1963. The concept of "laminar flow" cleanroom is the second cornerstone of cleanroom technology.
5. Due to the expansion of cleanroom applications, biological cleanroom standard appears which encompasses the control of inanimate particles and life particles. This is the standard published in August 1967 by US Aeronautics and Space Administration (in the past "the National Aeronautics and Space Administration") (NASA) (it is customary to mention as aerospace standard for abbreviation, which is shown in Table 7.1). But later in the revised version of this standard US Federal Standard 209B amended in 1973, no requirement has been made for controlling the life particles. It is only mentioned that microorganism suspended in air is natural in the world, so they are included in the total number of particles in the air cleanliness classes. In 1978, the Fourth International Pollution Control Association has formally proposed the international standards (draft) including the control of life particles (see Table 7.2), but subsequently it was not implemented.

   However, in US Federal Standard from 209C to 209E, it is clearly illustrated that the relationship between air cleanliness levels and biological particles has not been established. All these standards did not provide the specification of biological particle number corresponding to the number of particles.
6. For the need of production, a higher level than Class 100 appears since the outset of 209C, such as Class 10 and Class 1 for 0.5 μm or Class 10 and Class 1 for 0.1 μm.
7. Following with Europe, China, and Japan, the USA started to introduce the international system of units since 209E, but the British units still exist. The development process is shown in Figs. 7.1, and 7.2, Table 7.3.

Table 7.1 Classification of air clean cleanliness in American Aerospace Standard

	Particles			Organism particles			
		Maximum		Maximum of airborne		Deposition	
Air cleanliness level	Particle size (μm)	pc/ft^3	pc/L	pc/ft^3	pc/L	pc/ (ft^3 · week)	pc/ (m^2 · week)
100	≥0.5	100	3.5	0.1	0.0035	1,200	12,900
10,000	≥0.5	10,000	350	0.5	0.0176	6,000	64,600
	≥5.0	65	2.5				
100,000	≥0.5	100,000	3,500	2.5	0.0884	30,000	323,000
	≥5.0	700	25				

Table 7.2 International standard draft for air cleanliness in 1978

	Total number of airborne biological and nonbiological particles		Airborne biological particles		Surface biological particles	
			Maximum number of airborne vital forming colony per unit volume air			
Air cleanliness level	Maximum number of ≥0.5 μm particles				Maximum number of deposition bacteria	
	ft^3	L	ft^3	L	pc/(ft^2 · d)	pc/(m^2 · week)
1	Not controlled		Not controlled		Not controlled	
2	100,000	3,500	2.5	0.0884	200	323,000
3	10,000	350	0.5	0.0176	40	64,600
4	100	3.5	0.1	0.0035	8	12,900
5	10	0.35	0.04	0.0014	3	5,200

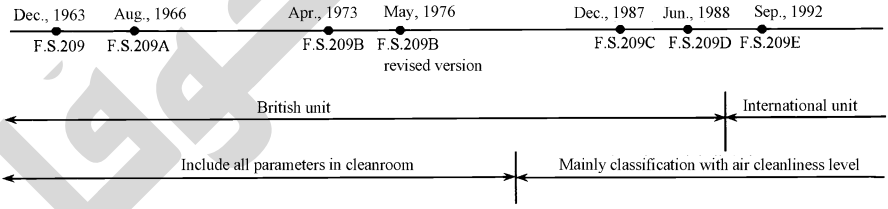

Fig. 7.1 Development of US Federal Standard 209

As for the difference between 209E and its previous versions and as well as its specific application, please refer to other books [1].

8. In nature there is no difference between standards in other countries. The main difference is the expression of dust concentration: some adopts the metric system, while others used the approximated integer. For example, in the monograph "Air cleaning technology" published in 1979, the statistic results about the actual air cleanliness levels reached by the technical measures at that time were issued,

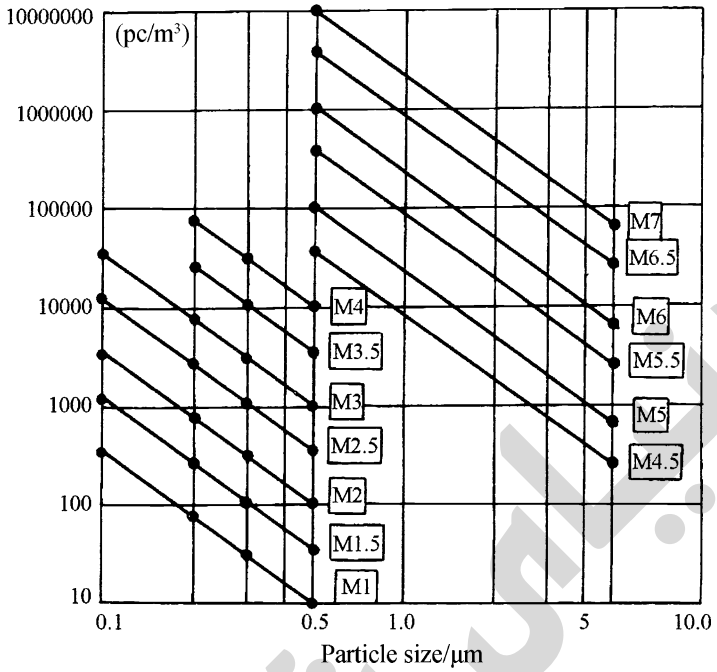

Fig. 7.2 209E

which was carried out by 14 units including the former State Construction Committee Research Institute of Building Science. It forms the "3 series" air cleanliness levels. The first level is called Class 3 (equivalent to Class 100), the second level is called Class 30, and so on. In 1984 the national standard "Code for Design of Clean Room" (GBJ73-84) formally put forward Chinese classification of air cleanliness, which adopted the name from 209 with the international system of units in the content.

Other innovative classification of air cleanliness in cleanroom is the Japanese standard published in 1989, which is shown in Table 7.4. Since then, the European standard also provides a different method to classify the air cleanliness levels, which is presented in Table 7.5 [2].

It should be noted that the particle number in Tables 7.3, 7.4, and 7.5 means the sum of particle number whose diameter is equal to and larger than the corresponding size.

9. Little difference exists among standards about air cleanliness classification in different countries. Their expression for particle size 0.5 μm is consistent with US Federal Standard. So it is the trend to develop unified international standard. Therefore, International Confederation of Contamination Control Societies (ICCCS) organized a Standards Committee (ISO/TC 209) called "cleanroom and associated controlled environments" in 1993. ICCCS is composed of air cleaning technical societies (or associations) from 16 countries. There were

Table 7.3 US Federal Standard 209E

Air cleanliness level		Upper limit of the corresponding concentration									
		0.1 μm		0.2 μm		0.3 μm		0.5 μm		5 μm	
		Per unit volume		Per unit volume		Per unit volume		Per unit volume		Per unit volume	
International unit	British unit	m^3	ft^3	m^3	ft^3	m^3	ft^3	m^3	ft^3	m^3	ft^3
M1		350	9.91	75.7	2.14	30.9	0.875	10.0	0.283	–	–
M1.5	1	1,240	35.0	265	7.50	106	3.00	35.3	1.00	–	–
M2		3,500	99.1	757	21.4	309	8.75	100	2.83	–	–
M2.5	10	12,400	350	2,650	75.0	1,060	30.0	353	10.0	–	–
M3		35,000	991	7,570	214	3,090	87.5	1,000	28.3	–	–
M3.5	100	–	–	26,500	750	10,600	300	3,530	100	–	–
M4		–	–	75,700	2,140	30,900	875	10,000	283	–	–
M4.5	1,000	–	–	–	–	–	–	35,300	1,000	247	7.00
M5		–	–	–	–	–	–	100,000	2,830	618	17.5
M5.5	10,000	–	–	–	–	–	–	353,000	10,000	2,470	70.0
M6		–	–	–	–	–	–	1,000,000	28,300	6,180	175
M6.5	100,000	–	–	–	–	–	–	3,530,000	100,000	24,700	700
M7		–	–	–	–	–	–	10,000,000	283,000	61,800	1,750

Table 7.4 Classification of air cleanliness in Japan (JIS B-9920)

	pc/m^3							
Particle size (μm)	Class 1	Class 2	Class 3	Class 4	Class 5	Class 6	Class 7	Class 8
0.1	10^1	10^2	10^3	10^4	10^5	(10^6)	(10^7)	(10^8)
0.2	2	24	236	2,360	23,600	–	–	–
0.3	1	10	101	1,010	10,100	101,000	1,010,000	10,100,000
0.5	(0.35)	(3.5)	35	350	3,500	35,000	350,000	3,500,000
5.0	–	–	–	–	29	290	2,900	29,000
Size range/μm	0.1–0.3		0.1–0.5		0.1–5.0		0.3–5.0	

Table 7.5 Draft classification of air cleanliness in Europe CEN/TC243

	pc/m^3						
Air cleanliness level	0.1 μm	0.2 μm	0.3 μm	0.5 μm	1.0 μm	5.0 μm	10 μm
0	20	6	–	(1)	–	–	–
1	250	63	28	10	–	–	–
2	2,500	625	278	100	25	–	–
3	25,000	6,250	2,778	1,000	250	10	–
4	–	62,500	27,778	10,000	2,500	100	25
5	–	–	–	100,000	25,000	1,000	250
6	–	–	–	1,000,000	250,000	10,000	2,500
7	–	–	–	(10,000,000)	2,500,000	100,000	25,000

Note: the value in the *bracket* is for the purpose of reference only

29 countries attending ISO/TC 209. After the formulation, the standard becomes one of the technical ISO standards. It was published on May 1, 1999, with the standard number ISO14644-1, which is shown in Table 7.6.

Compared with Japanese standard, ISO 14644-1 includes the particle size 1 μm and Class 9 which equivalents with Class 1000000. There is little difference about the particle number between them.

Now, the revised Code for Design of Clean Room in China (GB50073-2001) also adopts the same air cleanliness classification with ISO14644-1 [3].

7.2 Mathematical Expression of Air Cleanliness Levels

As for the particle number mentioned in the classification of air cleanliness in the abovementioned countries, particle counting concentration in the cleanroom is approximated to be parallel lines on log-log paper. When the reference size of controlled particle is known, straight line parallel to the lines of atmospheric dust concentration can be obtained, and then the allowable particle number corresponding

Table 7.6 Air cleanliness classification in ISO 14644-1 and GB50073-2001

	Corresponding limit value					
	0.1 μm	0.2 μm	0.3 μm	0.5 μm	1.0 μm	5.0 μm
Air cleanliness level	m^3	m^3	m^3	m^3	m^3	m^3
1	10	2				
2	100	24	10	4		
3	1,000	237	102	35	8	
4	10,000	2,370	1,020	352	83	
5	100,000	23,700	10,200	3,520	832	29
6	1,000,000	237,000	102,000	35,200	8,320	293
7				352,000	83,200	2,930
8				3,520,000	832,000	29,300
9				35,200,000	8,320,000	293,000

to other sizes can be determined (the rounding correction of integer is made). Formula can be used as follows:

$$\frac{N_D}{N_d} = \left(\frac{D}{d}\right)^{-n} \tag{7.1}$$

where d is the reference size, D is other size, N_d is the particle number for size d (i.e., $\geq d$), N_D is the particle number for size D (i.e., $\geq D$), and n is the exponential which is slightly different in various national standards.

It is obvious that this expression is exactly the same as Eq. (2.1).

Because of the rounding correction of integer, the value obtained by Eq. (7.1) is not exactly the same as that in classification table. Take Japanese standard as an example, 0.1 μm is the size of controlled particle. The particle number with size 0.1 μm in Class 3 is 10^3 pc/m^3 where 3 is the exponential.

So how much is the number of particles with size ≥0.3 μm in Class 3?

With Eq. (7.1), the value of n in JIS, and the particle number of controlled size 0.1 μm $N_{0.1}$ in Class 3, it can be written as:

$$N_{0.3} = N_{0.1} \times \left(\frac{0.3}{0.1}\right)^{-2.08} = N_{0.1} \times \left(\frac{0.1}{0.3}\right)^{2.08}$$
$$= 10^3 \times 0.10176 \text{ pc}/\text{m}^3 \left(\text{set } 101 \text{ pc}/\text{m}^3\right)$$

It is clear that this result is exactly the same as that in Table 7.4 for particle size 0.3 μm in Class 3.

But 0.1 μm can also be used as the control size for Class 3 in ISO14644-1. $N_{0.3} = 102$ pc/m^3. It is obvious that the calculated value of 0.10176 is approximated into 0.102. The difference between them by this rounding is little.

For another example,

Class 100 in 209E → 100 pc/ft^3 = 3,530 pc/m^3 ≈ $10^{3.548}$ pc/m^3 ≈ $10^{3.5}$ pc/m^3

This is the integer rounding in the value of class. When another expression of class in 209E is used, the following equation can be obtained:

$$N_M = 10^M \left(\frac{0.5}{D}\right)^{2.2} \text{pc/m}^3 \tag{7.2}$$

The particle number for particle size D (such as 0.2 μm) in Class 3.5 is:

$$N_M = 10^{3.5} \left(\frac{0.5}{0.2}\right)^{2.2} = 23,739 \text{ pc/m}^3$$

So it is smaller than the value 26,500 in Table 7.3.

If the value of class without integer rounding is inserted into the expression to calculate the particle number corresponding to the control size, then:

$$N_M = 10^{3.548} \times \left(\frac{0.5}{0.2}\right)^{2.2} = 3,530 \times \left(\frac{0.5}{0.2}\right)^{2.2} = 26,500 \text{ pc/m}^3$$

It is exactly the same as that in the table.

So 209E explains that the approximated particle number for various sizes can only be obtained by Eq. (7.2).

The only difference among various expressions for air cleanliness classification in various standards is the change of exponent n. $n = 2.2$ in 209E, $n = 2.08$ in JIS B9920 and ISO14644-1, and $n = 2$ in CEN/TC243. However, the value of n is not directly given in the US 209 ~ 209B and GBJ73-84, but we can know that $n = 2.15$ by using the back calculation method (or based on the parallel characteristic to the standard distribution of atmospheric dust).

When the concentration for particle with size 0.5 μm is 1 pc/m^3, the corresponding concentration for particle with size 0.1 μm can be calculated by Eq. (7.1):

For 209E

$$N_{0.1} = N_{0.5} \left(\frac{0.5}{0.1}\right)^{2.2} = 1 \times \left(\frac{0.5}{0.1}\right)^{2.2} = 34.49 \text{ pc/m}^3$$

For the Japanese standard

$$\frac{N_{0.5}}{N_{0.1}} = \left(\frac{0.1}{0.5}\right)^{2.08}$$

$$N_{0.1} = \frac{N_{0.5}}{\left(\frac{0.1}{0.5}\right)^{2.08}} = \frac{1}{\left(\frac{0.1}{0.5}\right)^{2.08}} = 28.43 \text{ pc/m}^3$$

For European standards

$$N_{0.1} = N_{0.5} \left(\frac{0.5}{0.1}\right)^{2} = 1 \times \left(\frac{0.5}{0.1}\right)^{2} = 25 \text{ pc/m}^3$$

The calculated results about the influence of n on particle concentration are plotted on Fig. 7.3, which shows that the difference is not big.

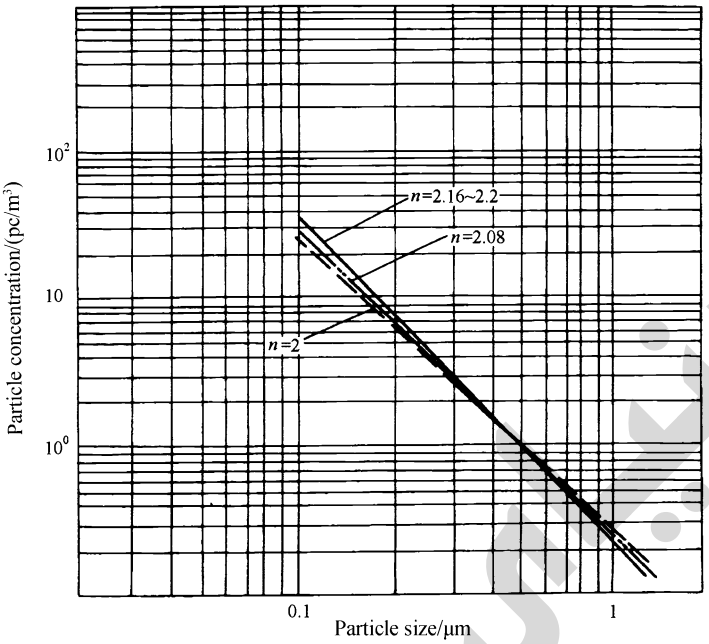

Fig. 7.3 Influence of n on concentration

7.3 Conversion Relationship of Particle Number for Different Sizes

According to the calculation equation ($n = 2.08$) in ISO 14644-1, the conversion coefficient for particle number is presented in Table 7.7.

The value ϕ of particle with diameter 0.1–0.007 μm is cited from Ref. [4] (it is based on the calculated result by Kazuya).

7.4 Parallel Lines for Air Cleanliness Levels

It is known from Fig. 7.3 that parallel lines representing in air cleanliness levels in various national standards have both the characteristic of particle distribution in cleanroom and the artificial factor. For example, according to US Federal Standard 209, the lines for $n = 2.15$ are plotted in order to be consistent with the distribution of atmospheric dust. While in Japanese and European standards, particle numbers of two particle sizes are considered (such as 0.1 and 0.5 μm or 0.5 and 5 μm). Therefore, it is not right to consider the parallel lines representing cleanliness levels as the characteristic of particle distribution in cleanroom directly. There is difference between the value of n in the actual indoor distribution and the value of n in

Table 7.7 Conversion coefficient of particle number for different sizes

Particle size (μm)	0.5	0.3	0.2	0.18	0.15	0.12	0.1	0.09	0.08	0.07	0.06
Conversion coefficient of particle number	1	2.85	6.8	8.4	19	19.5	28.6	34	44.9	56.3	57.1
Particle size (μm)	0.05	0.04	0.035	0.03	0.025	0.02	0.018	0.015	0.013	0.01	0.007
Conversion coefficient of particle number	76.3	89.1	91.1	93.1	95.7	98.3	98.6	98.9	99.4	100	100.3

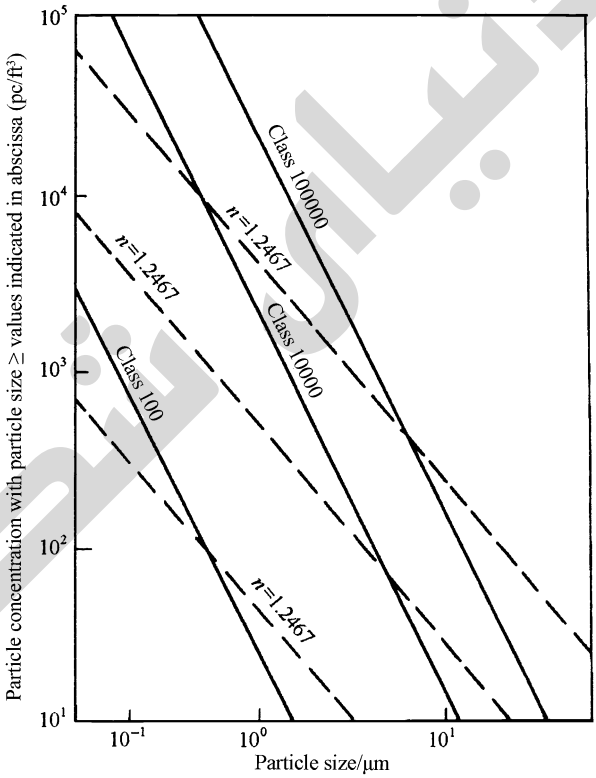

Fig. 7.4 Distribution of particle concentration in cleanroom on log-log paper (example 1)

parallel lines for corresponding class. It is only reasonable to state that the particle distribution in cleanroom is approximately straight in log-log paper. But the actual particle distribution for specific cleanroom is not exactly the same as that of parallel lines for corresponding class, and large difference may exist, which is similar as the relationship between the distribution feature of atmospheric dust and the measured data of atmospheric dust. Besides, there is artificial factor as mentioned before.

For example, some actually measured data shows that the distribution of the particle concentration in cleanroom has the characteristic of inclination and slow change, as shown in Figs. 1.24 and 7.4 [5]. For the latter case, $n = 1.2467$ for the

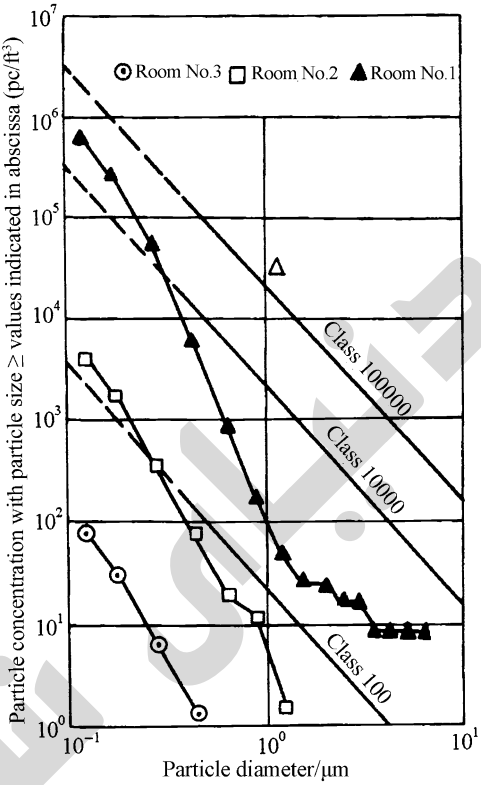

Fig. 7.5 Distribution of particle concentration in cleanroom on log-log paper (example 2)

average value of all the measured data. Obviously, if more measurement was performed, the average value is no longer 1.2467. Even for the unidirectional and non-unidirectional flow in the same measurement, the value of n is different. In the above figure, $n = 1.1089$ for unidirectional flow and $n = 1.1778$ for non-unidirectional flow. However, there is other measurement that shows the different trend which has the characteristic of steeper inclination, which is shown in Fig. 7.5 [6]. But anyway it is a common feature that the particle distribution in cleanroom is approximately parallel straight lines on log-log paper.

Why this feature remains for the particles inside the cleanroom when they go through air filters? It is obvious that without particle generation inside the cleanroom, particle distribution through air filter is close to monodisperse or it has the feature of steep and short straight line (or polyline). It is because particles with larger diameter are captured by air filter. This can be proved by the measurement from high-grade as-built cleanroom without occupants. But there is particle generation in the operational cleanroom, and human is the main source. The particle distribution generated from human is straight on log-log paper and is very similar as that of typical atmospheric dust.

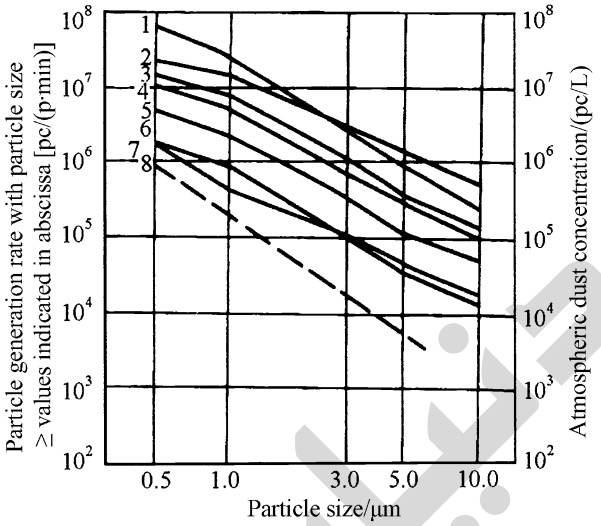

Fig. 7.6 Particle emission characteristic of work clothes made of different materials. *1–3* non-woven, *4* new cotton, *5* half-new cotton, *6* Polyester, *7* cotton underwear for surgery, *8* atmospheric dust

Polylines 1 to 7 in Fig. 7.6 show the particle generation characteristic from work clothes made of different materials [7]. Dashed line 8 shows the typical distribution of atmospheric dust. It is obvious that the trend between them is very similar.

Figure 7.7 is the measured data by author and others labeled with various symbols [8]. They are on behalf of the different amounts of particle generation with various activities. The amount of dust generated is approximately within the range sandwiched by the two straight lines. The dotted line is a typical distribution of atmospheric dust. It is clear that their trends are very close.

The above material shows that the particle distribution features in the operational cleanroom should be similar as that of particles generated by occupant (other kind of particles generated should also be included), which means it is similar as that of atmospheric dust. This can also been seen from the comparison among Figs. 7.8 [6], 2.28, and 2.29. The approximated linearity is mainly valid for particles with diameter larger than 0.1 μm. Therefore, another group of oblique lines parallel to that of atmospheric dust can be used to indicate different levels of air cleanliness. Of course, the smaller the amount of particles generated is, the higher the air cleanliness is, and the steeper the oblique line is. It should be noted that these parallel straight lines are obtained by statistical analysis. For one specific cleanroom, the distribution of particle concentration with size may deviate from this result.

7.5 Controlled Object for Corresponding Air Cleanliness

Two main objects are needed for air cleanliness. One is the minimum particle diameter in the air which may cause damage. The other is the particle counting number in the air which may also cause damage.

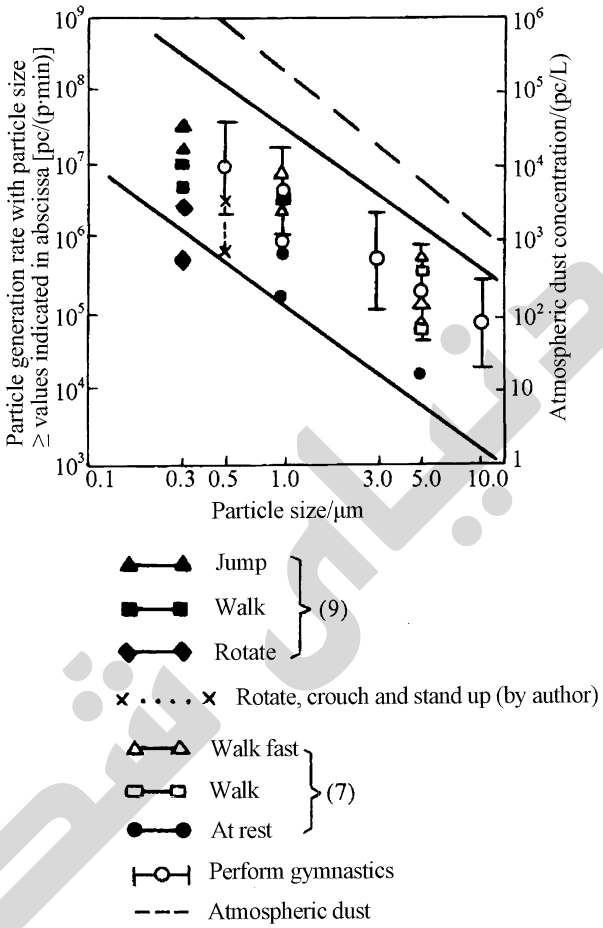

Fig. 7.7 Particle generation feature with different occupational activities

7.5.1 Minimum Controlled Size

In the past, the requirement for minimum particle size was put forward to meet the need of precision machinery, especially from the aspect of mechanics such as blockage and abrasion which cause damage to the product. This minimum size should be less than certain geometric distance on the product – tolerance, gap, line spacing, line width between the components, and so on. Since it is possible that small particles could coagulate to be large particles or several small particles fell to the critical position of the product at the same time, the minimum controlled particle size is usually set to be between half and 1/3 of this geometric distance [9]. Since this kind of geometric distance can be as small as 1, 0.5 μm becomes the minimum controlled particle size in the air cleaning technology for a long time. In addition, when optical particle counter with light scattering is used to perform the measurement, only particles with diameter larger than 0.3 μm is in the area

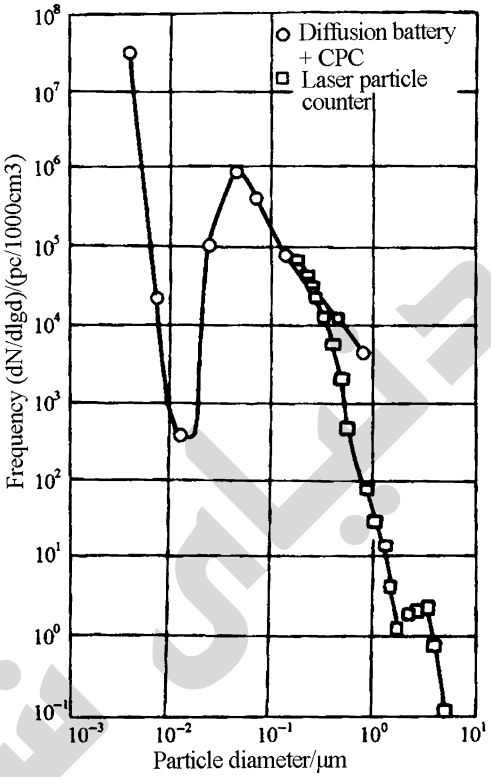

Fig. 7.8 Particle distribution example in the cleanroom (Test instrument will be introduced in Chap. 17)

suitable for light scattering detection. But the sampling efficiency for 0.3 μm is lower than that for 0.5 μm (refer to Chap. 17); the minimum controlled particle size is limited, which is usually 0.5 μm.

However, due to the development of integrated circuits, higher requirement was needed for the minimum controlled particle size. From one hand, the geometric distance on integrated circuits becomes smaller. For example, the thickness of the coating or mask is only a few tenths even a few percent of microns. Before the appearance of VLSI, the distance between the conductive lines on the element, or the width of the metal line connecting elements (it is called the basic graphic size), or the characteristic size has reached to 1 μm, but now it has been reduced to be less than 0.1 μm. From the other hand, the minimum controlled particle size should be determined not only from a mechanical point of view but also from a physicochemical point of view. Even when a particle settles down within a certain geometric distance such as the thickness of a coating, pinhole and impurities source surface may be formed to destroy the product performance. Therefore, the minimum controlled particle size is further required to be between 1/10 and 1/3 or even less [10].

Table 7.8 shows a comprehensive literature survey on the relationship between the linewidth and the development trend of integrated circuits. It can be seen from the table that since 1970, the integration density has increased by four times every 3 years.

Table 7.8 Development of integrated circuit

Year	Representative product DRAM	Silicon diameter/mm	Chip area (mm^2)	Finest optically carved linewidth (μm)	Element number (#)
1970	1 K			10	2×10^4
1975	16 K			5	
1980	64 K	75		3	
1983	256 K	100	40	2	5×10^5
1986	1 M	125	50	1	2×10^6
1989	4 M	150	90	0.8	8×10^6
1992	16 M	200	130	0.5	$107–10^9$
1995	64 M	200	200	0.3	$107–10^8$
1998	256 M	200	300	0.2	$107–10^9$
2001	1 KM(G)	300	700	0.18	$107–10^9$
2004	4 KM(G)	300	1,000	0.113	Possible 2×10^9
2007	16 KM(G)			0.10	
2010	64 KM(G)			0.07	

Table 7.9 Requirement of integrated circuit on the controlled particle size

Year	Integration degree	Controlled minimum size (μm)	Processing times β	Air cleanliness level (50 % yield)	Pure gas/water
1970	1 K	2	<100	100	~10^3 ppb
1975	16 K	0.4–1.3	<100	100	~10^3 ppb
1980	64 K	0.25–0.8	100	100	10^3 ppb
1983	256 K	0.12–0.4	140–160	100	10^3 ppb
1986	1 M	0.08–0.26	160–200	10	500 ppb
1989	4 M	0.05–0.17	200–300	1	100 ppb
1992	16 M	0.05	300–400	0.1 or 10(0.1 μm)	50 ppb
1995	64 M	0.035	400–500	10(0.1 μm)	5 ppb
1998	256 M	0.025	500–600	10(0.1 μm)	1 ppb
2001	1 G	0.018	530–700	1(0.1 μm)	0.1 ppb
2004	4 G	0.013	600–700	0.1(0.1 μm)	0.01 ppb
2007	16 G	0.01			
2010	64 G	0.007			

Table 7.9 shows the influence of the development of the integrated circuit in the literature on the requirement of controlled particle size and related contaminant control [11].

Except the integrated circuit, there is no requirement for such a small controlled particle size so far. Usually the limit is 0.5 μm. For example, the minimum controlled particle size is still 0.5 μm in pharmaceutical manufacturing cleanrooms and hospitals cleanrooms at home and abroad.

7.5.2 Number of Controlled Particles

Different processes have different requirement for the number of controlled particles ($\geq$ controlled particle size). It will be very complicated if the standard of air cleanliness was made with these quantities. For example, the maximum allowable particle number per liter air for one process is 110 pc, while for another process it is 130pc, so little difference exists in the measures of air cleaning for these two cases, and it is not necessary to set different levels of air cleanliness. Therefore, the following principles should be followed during the development of controlled particle number in air cleanliness standards (level):

1. It can be achieved by current existing measures.
2. Economic difference is significant.
3. It is convenient for use. For example, it's easy to keep in memory, which requires these controlled numbers are regular and integer.

It should be noted that in addition to "Air Clean Technology Measures" in China in the past, no other domestic and foreign standards set the requirement for the equivalent Class 1000000 in ISO/TC209. The above 209E and European air cleanliness level lists the minimum level whose particle concentration is 10,000 pc/L, which is equivalent to Class 300000. Now Chinese "Good Manufacture Practice" (GMP) has included Class 300000. Both "Implementation Details of Drug Packaging Materials, Container Manufacturing Practices" and "Architectural Technical Code for Hospital Clean Operating Department" include Class 300000, which is the base for the design of quasi-clean areas. It is sound to do so. Because with the expansion of service object by air cleaning technology, air cleanliness of many places need to be slightly lower than Class 100000. For example, in "Design Code for Electronic Computer Room" (GB50174-93), the particle concentration of the host room at-rest should be less than 18,000/L, which is equivalent to Class 500000. Some applications for transition to high-level cleanliness will need the so-called "quasi-clean" state. So it is necessary to set the appropriate level of cleanliness, and it is good for energy conservation and will promote the application of air cleaning measures in more departments. In order to meet this kind of need, the international standard IS014644-1 has formally set out Class 9 which is equivalent to Class 1000000.

7.6 Specific Conditions for Controlled Particle Concentration

When the controlled particle concentration corresponding to the air cleanliness level is considered, the following specific conditions must be also taken into account:

1. Which state is it under which the particle concentration is obtained?

In US Federal Standard 209, the particle concentration is measured during the working time near the working place.

In Chinese standard, the particle concentration is also determined during the normal operation. This is called operational level, which is adopted by many countries before 209C.

It is found that the test result is affected by many actual conditions when the operational particle concentration is used to evaluate the air cleanliness level. It is difficult to accurately measure the concentration. It cannot reflect the problem of the project itself accurately and in time. So the air cleanliness level and state are separated since 209C, where only the particle number itself is mentioned.

In the last chapter about test technologies, the concept of operational, at-rest and as-built will be introduced.

2. Which area is it for measuring the concentration?

For the environment of a cleanroom, various standards have different specifications. Whether the particle concentrations in each area and every position meet the requirement or only the particle concentration in certain area meet the requirement. But practice has proved that the former is impossible, but also not necessary, especially in the past when the air cleanliness level is linked with operational state. Because in the vortex flow area, particle concentration is high near the particle source, but people is mainly concerned about the working area. In order to meet the cleanliness requirement and save energy, the particle concentration in the working area should be controlled. Therefore, air cleanliness levels in current standards are determined by the particle concentration in the working area.

The regional technical regulation for acceptance of Class 100 cleanroom has pointed out that the working area means the room space which is 3 ft (about 90 cm) below the ceiling and 30 in (about 76 cm) above the floor. In this region, "the measurement at any height must meet the requirements."

In the past, when operational level is specified, the workspace or dust source is not included in this working area. It is the region near but outside the working position. In the abovementioned technical regulation, this concentration is measured at any place which is in the distance 24 in (about 61 cm) away from any pollution source. This specification is very scientific. Because near the dust source such as the lacquering machine, the grinding head, and the powder filling, the particle concentration must be very high. But this kind of high concentration does not make sense for the object itself which is spinned, grinded, and filled. So it is also unnecessary to keep high air cleanliness at the dust source for operational state.

In China's "Air Clean Technology Measures," the working area is defined as the region which is 0.8–1.5 m high from the floor, except the special requirement of some process. For the cleanroom with horizontal unidirectional flow, the first workspace is used as a representative which is a certain distance (usually it is 0.5 m) away from the outlet of the air filter.

To 209E, cleanroom is a "room" which includes one or more clean areas, and clean area means a certain space within which the air cleanliness with specific airborne particle is controlled. This means that the cleanroom includes many clean areas with different cleanliness. So "cleanroom with certain cleanliness" means the

main region of the cleanroom should reach this cleanliness level, and not all the cleanroom should control the particle concentration.

3. How is the particle concentration obtained including sampling times and sampling volume? These will be introduced in detail in the section about test techniques.
4. Is it the average, maximum, or other value of particle concentration?

Before 209C, the maximum particle concentration is generally used to assess the air cleanliness level, or the average is adopted but with some provisions at the same time (such as Chinese relevant standards). From 209C, the combination of statistical value and one maximum value is used, which will also be analyzed in the section about test techniques.

7.7 Theoretical Method to Determine the Yield by Air Cleanliness

7.7.1 Influence of Air Cleanliness on Yield

It is a very complex issue to determine what kind of cleaning environment is needed for the production of each precision product. It is determined by many factors such as methods, tools, equipment, pure water, pure air, chemical reagents, processing times, and personnel who presides the process comprehensively. Traditional particle pollution should be controlled, and more attention has been paid on the influence of AMC on critical surface. Especially for the integrated circuit over 256M, the air component in the production workshop has almost become the monitoring object with the same importance of particles.

AMC include both the metal components at molecular level such as Na, K, Zn, Al, and Fe but also the gas-phase chemical contamination. Since in most countries there is no standard related to AMC, it is still the most basic problem for controlling the influence of particles in the cleanroom. In this section, only the influence of particle concentration on the yield is discussed. The probability of a product to be flawed by particle settling reduces with the decrease of the particle concentration, exposure area, and time. Of course, only these particles which can contact the product surface have the direct effect. Therefore, the following items must be investigated:

1. Which approach does the particle in air take to contact the product surface? How much is the probability for particles to deposit on surface? And how many particles?
2. What is the relationship between the deposition density onto the surface and the probability to cause the flow?

The first question has been discussed in Chap. 6 and will be discussed continuously in Chap. 9. Here the second problem will be discussed in detail.

Since particles are randomly distributed in air and their deposition is also random, the amount of particles deposited onto a surface with certain area is limited for a given time period, when the airborne particle concentration is known. For example, the number of particles deposited on the surface with area 1 m^2 during 1 h is 100 thousands, the average deposition density is 10 pc/($cm^2 \cdot$ h). This does not mean the number of particles deposited onto each surface with area 1 cm^2 is 10 pc. Some is more, but other has less.

When particles are randomly distributed, the probability of a particle deposited onto a surface with a given area is fixed. Although the probability for the case of two particles is different from that of one particle, it is also fixed. It is the same for the case of n particles. The probability for the deposition of different number of particles follows the binomial distribution. As mentioned in Chap. 1, when the area of deposited surface is very small and the number of particles in this space is not large, the deposition density is very small. The probability of particle deposition can be approximated with Poisson distribution.

Taking the integrated circuit as an example, there are many graphics on the silicon chip with diameter 3 cm. The area of each graphic is termed as the area of chip. Figure 7.8 illustrates the chip areas and element number. With the increase of the chip diameter, the number of integrated elements is larger. Now the chip diameter increases from 30 cm towards 40 cm, so the chip area will further be increased. The chip area of ULSI (ultra large-scale integrated circuit) increases to several hundreds or thousands square millimeters from the initial 40–50 mm^2.

Metal wires are used to connect the elements on the integrated circuit. The whole circuit is made of complex electric net by multiply layers of these wires. Figure 7.9 is an enlarged figure of this kind of connected wires [12]. This kind of multiply layers is shown in Fig. 7.10, where the above is alumina wire, down the molybdenum wire and between isolated. Therefore, as long as one particle deposits on this complex wire net or any place on the element, break or shortcut of the electric circuit is formed, which makes the graphic flawed. This destroys the function of whole electric circuit, and thus this piece of chip is abolished.

Figure 7.11 is one example of the distribution of flawed chips on the silicon crystal wafer[13]. In the figure, the area with inclined lines represents the flawed chips by shortcut of the circuit. The graphic flaws on the observed chip are expressed by "●".

Figure 7.12 shows the number of particles deposited onto a silicon crystal wafer with diameter 150 mm in a Class 1 level cleanroom for 0.1 μm particles. The data was obtained by placing the silicon wafer vertically with 1 m distance up from the roof for one week and people walk with 30 cm away from it. The value means the total particle number with diameter $\geq$ the indicated particle size at the abscissa [13]. It is obvious that diffusional deposition is important for small particles. Before the measurement, the background number on the clean silicon wafer has been taken into account.

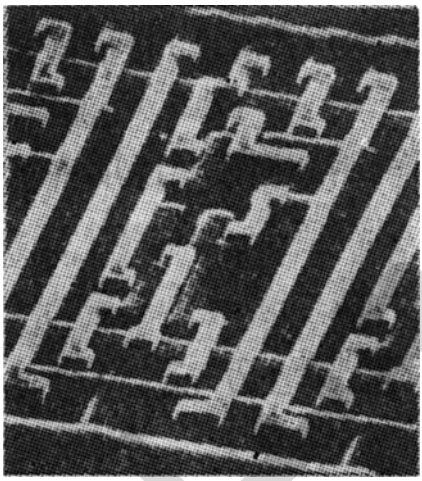

Fig. 7.9 Alumina connection wire with width 0.1 μm

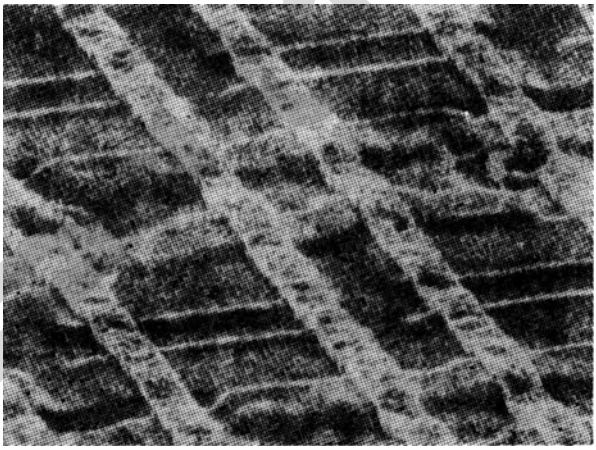

Fig. 7.10 Structure of multiply layers of wires

It is obvious that the higher the integrated intensity is and the larger the chip area is, the higher the probability of the damage caused by one particle deposition. Since the chip area is larger than any particle and the geometrical distance on the circuit (such as layer thickness and wire distance) is equivalent with the diameter of very tiny particle, the surface deposition density, which means the number of particles deposited, is much more meaningful than particle size for integrated circuit especially ULSI circuit. Normally this density has the similar implication as air cleanliness level, which is used to describe the particles with diameter $\geq$0.5 μm. The minimum diameter to cause damage on the manufacturing process can be adopted as the particle size for defining the deposition density.

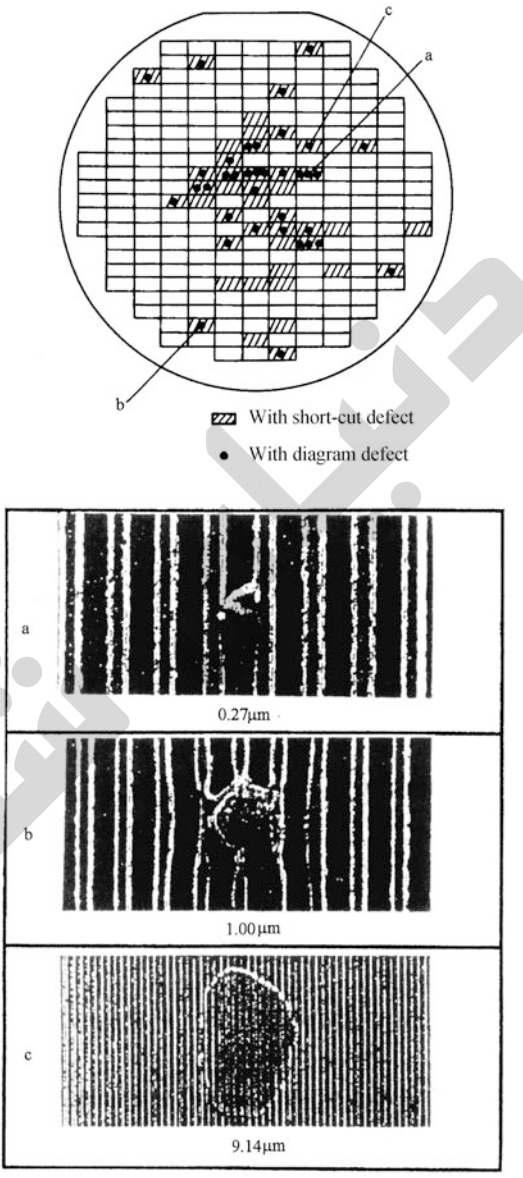

Fig. 7.11 One example of damaged chip on the silicon circular wafer with 0.25 μm graphic size

7.7.2 Theoretical Expression for Yield

7.7.2.1 Yield of Single End Product

When an end product is not assembled by several parts, it can be considered as single manufacturing procedure, no matter how many steps it takes to manufacture.

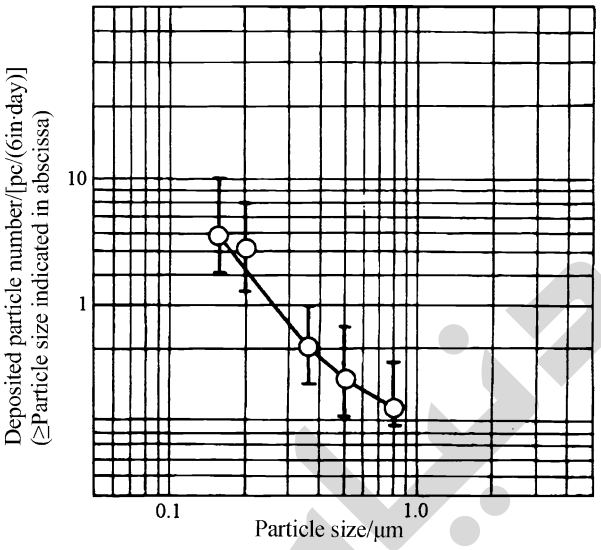

Fig. 7.12 Number of particles deposited on silicon circular wafer with diameter 150 mm which is vertically placed in the Class 1 level cleanroom for 0.1 μm particle

It is the total exposure time that influences the yield. A typical example is the integrated circuit chip.

In order to get rid of the flaw caused by the deposition of particles on chips and to reduce the probability less than 10 % or even 1 %, the probability of the deposition of one and more than one particles onto the chip within the area of each graph is required to be 0.1 or 0.01.

Poisson distribution can be used to correlate the probability of particle deposition on the surface and the deposition density on this surface, i.e.,

$$P(\xi \geq 1) = 1 - P(\xi = 0) = 1 - \frac{n_s^0}{0!} e^{-n_s} \tag{7.3}$$

where n_s is the surface deposition density on the chip.

The probability without particle deposition is the minimum yield, i.e.,

$$P' = P(\xi = 0) = e^{-n_s} \tag{7.4}$$

Of course, the deposited particles may be removed by cleaning. But as mentioned before, there are other reasons to cause flaw except for the particles. In abroad, the total flaw number or flaw density D was proposed, where particles only cause partial flaw number βD [14]. But it is difficult to determine the value. So it is useful for comparison between two situations, while it is difficult to make calculation alone. Furthermore, as analyzed before, one flaw may be caused by the deposition of one particle, as well as the deposition of multiply particles, which makes it difficult to define the flaw number caused by particle deposition. In this book, only the reason of air cleanliness is considered for the minimum yield, which

is appropriate from the safety point of view. This concept is applied in the following explanation of yield.

When the yield of the chip is known, the maximum deposition density n_s can be calculated, i.e.,

$$n_s \leq 0.01 \text{ for yield } 99\ \%$$

$$n_s \leq 0.1 \text{ for yield } 90\ \%$$

The value of n_s is obtained for the whole expose time t of the chip. With the known chip area (deposition area) and t, n_s can be converted into the unit deposition density. At last, with the aforementioned method, the particle concentration in the air can be calculated. In the former two versions of this book, the graph for calculation was given while the equation was not presented. Here the derivation equation for big silicon circular chip with high degree of integration is presented.

As for the deposition quantity of particles onto the surface, although development has been made from some research report abroad, the deposition expression is still Eq. (6.27) without correction in Chap. 6, which does not include other deposition factors. As mentioned before, for particles with diameter less than 0.1 μm which are controlled in ULSI, diffusional deposition plays an important role in the deposition quantity. The deposition density of particles with diameter 0.08 and 0.05 μm onto the chip is 2–5 times for particles with diameter 0.1 μm [13].

As introduced in Chap. 6 that Eq. (6.31) should be used to calculate the deposition quantity on surface with unit area in the room with ventilation. Since the unidirectional flow velocity in the cleanroom is about 0.3 m/s, the velocity correction proposed in Chap. 9 can be omitted.

Therefore, the total deposition quantity n_s onto one chip is:

$$n_s = \alpha v_s t N f \ (\text{pc}) \tag{7.5}$$

The particle concentration (for the controlled size) in the air is:

$$N = \frac{n_s}{\alpha v_s t f} \ \left(\text{pc}/\text{cm}^3\right) \tag{7.6}$$

With Eq. (7.4), the minimum yield η which is the minimum probability P' that caused by particles (may be non-full deposition, washed out after deposition, or with the effect of coagulated deposition) can be expressed with decimal:

$$\eta = P' = e^{-n_s} = e^{-\alpha v_s t f N} \tag{7.7}$$

$$N = \frac{-\ln \eta \times 1{,}000}{\alpha_D v_{s,D} t f} \ (\text{pc/L}) \tag{7.8}$$

where

α_D is found in Chap. 6 with the average area-weighted diameter D_s for particles with diameter $\geq$ controlled size. While for vital particles, the equivalent diameter is used instead of the average area-weighted diameter. It is the same hereinafter;
$v_{s,D}$ is the deposition velocity for particles with the average area-weighted diameter D_s for particles with diameter $\geq$ controlled size, cm/s;
f is the chip area, cm^2;
t is the exposure time, s.

The relationship between D_s and v_s is presented below:

Controlled particle size (μm)	D_s (the percentage above the controlled particle size is assumed 100 %) (μm)	v_s (cm/s)
0.007	0.132	0.0001
0.035	0.14	0.0001
0.05	0.16	0.00015
0.07	0.194	0.0002
0.1	0.24	0.00035
0.12	0.3	0.00054
0.18	0.4	0.001
0.5	1	0.006

There are two methods to calculate the exposure time:

1. There is linear proportional relationship between the manufacturing times and the exposure time for chip. When the known exposure time for certain integrated circuit is set 1, the exposure time for other integrated circuit with known manufacturing times can be obtained by multiplying the time coefficient with the known exposure time.

   The time coefficient l_t is shown in Table 7.9.

256 K	$l_t = 1$
1 M	1.2
4 M	1.66
16 M	2.3
64 M	3
256 M	3.7
1 G	4.06
4 G	4.3

   For the exposure time of former integrated circuit before 256 K, the value used by author was 8 h [15].
2. The exposure time is directly adopted from the actual value. According to the report these years [16], among the exposure time of former 1 h in the cleanroom environment during 1/10 of the whole manufacturing times, such as the waiting time during the cleaning procedure, the chip is exposed in the environment, so the average waiting time can be set 1 h. With this estimation method, when the minimum manufacturing steps were 140 times for the 256 K integrated circuit, so 1/10 of the steps is 14 times, and the exposure time becomes 14 h.

For the same integrated circuit with certain integration level, the manufacturing times among different factories are different. Take the integrated circuit 64 M–1G DRAM as an example, the manufacturing steps usually arrives 500–600 times. Since the time limit for 64 M is about 2 months, the time for each procedure or each manufacturing step is about 2.5–3 h [13].

When the second method to calculate the exposure time is used, the equation to calculate the air cleanliness level based on the yield can be derived:

$$N_{0.1} = \frac{-\ln \eta \times 1,000 \times 28.3}{\alpha_D v_{s,D} f \times 0.1\beta \times 3,600} \times \frac{\phi_{0.1}}{\phi_{1/10}} \left(\text{pc}/\text{ft}^3\right) \tag{7.9}$$

where

α_D is the value of α based on D_s;
$v_{s,\,D}$ is the value of v_s based on D_s;
$\phi_{0.1}$ is the value of ϕ for 0.1 μm;
$\phi_{1/10}$ is the value of ϕ for the controlled particle size which is equivalent with 1/10 of the linewidth.

The calculation procedures are as follows:

1. Determine the controlled particle size.
2. Calculate D_s with the controlled particle size.
3. Calculate α_D and $v_{s,\,D}$ with D_s.
4. Determine the manufacturing times β with the integration level, and 0.1β is used.
5. Multiply the concentration pc/L with 28.3, and the concentration pc/ft^3 is obtained. $N_{0.5}$ (pc/ft^3) is then obtained by dividing it with $\phi_{1/10}$. The particle concentration (pc/ft^3) for 0.1 μm, which means the air cleanliness level corresponding to 0.1 μm, is obtained by multiplication between it and $\phi_{0.1}$. The value with metric unit system can be obtained when it is multiplied with 1,000 instead of 28.3. For the convenience of comparison with results in the literature, the English system is still used.

Table 7.10 shows the summary of two calculation results for the yields 50 and 80 %. In the table, the controlled particle size is 1/10 of the linewidth. But recently the controlled particle size tends to be enlarged. For example, the Semiconductor Industry Association (SIA) adopted 1/5 of the linewidth as the controlled particle size in 1993, while 1/3 of the linewidth was proposed in 1994 [13].

Take 256 K with the yield 50 % in the table as an example, the particle concentration with the controlled particle size 0.18 μm is calculated as follows:

$$N = \frac{-\ln\ 0.5 \times 1,000}{\alpha_D v_{s,D} f \times 0.1\beta \times 3,600} = \frac{0.69 \times 1,000}{1.5 \times 0.001 \times 0.4 \times 14 \times 3,600} = 22.8\ (\text{pc}/\text{L})$$
$$= 645\ \left(\text{pc}/\text{ft}^3\right)$$

Table 7.10 Air cleanliness level (pc/ft^3 for particles with diameter $\geq$ certain value)

Integration degree of DRAM		256 K	1 M	4 M	16 M	64 M	256 M	1 G	4 G
Chip area/cm^2		0.4	0.5	0.9	1.3	2	3	7	10
Controlled size (choose 1/10 of the linewidth)		0.18	0.12	0.08	0.05	0.035	0.025	0.018	0.01
Processing times β		140–160	160–200	200–300	300–400	400–500	500–600	530–700	600–700
Time coefficient l_1		1	1.2	1.66	2.3	3	3.7	4.06	4.3
Minimum yield ($\eta = 50$ %)	Controlled size level	645	415	165	88	80	46	17	12
		1,129	727	289	155	141	81	30	21
	0.5 μm level	77	21	3.7	1.1	–	–	–	–
		134	37	6.5	2				
			(28.6)	(4.7)					
	0.1 μm level	–	–	–	33	25	14	5	3.4
					58	44	24	8.8	6
					(28)	(21)	(11)	(4)	(2.6)
Minimum yield ($\eta = 80$ %)	Controlled size level	206	132	52	28	26	15	5.5	3.8
		360	232	92	49	45	25.8	9.6	6.7
	0.5 μm level	25	6.8	1.2	0.3	–	–	–	–
		13	12	2.1	0.6				
			(9.1)	(1.5)					
	0.1 μm level	–	–	–	9.8	8	4.4	1.6	1.1
					17.2	14	7.7	2.8	1.9
					(16)	(6.5)	(3.8)	(1.4)	(0.83)

When the air cleanliness level with 0.5 μm is needed, the particle concentration should be divided with the conversion coefficient ϕ_D for the controlled particle size of 256 K, which is shown in Table 7.7:

$$N_{0.5} = \frac{645}{\phi_D} = \frac{645}{8.4} = 77 \text{ pc}/\text{ft}^3$$

The equation to calculate the yield was given in the literature [13], i.e.,

$$\eta = \left(\frac{1 - e^{-fD}}{fD}\right)^2 \tag{7.10}$$

where

f is the chip area, cm^2;
D is the allowable concentration of the total flaw density (caused not only by particles), pc/cm^2, where the part caused by particles is defined as βD and β is unknown.

Since it is difficult to determine the value of D and there's no factor of time in the equation, it is not convenient to be used for calculation directly. With the condition that the actual yield arrives at 50 % for 256 K in the Class 100 environment, the value of D can be obtained. When the exposure time is assumed to be linearly proportional to the manufacturing times, both the value of D and the yield or the air cleanliness needed can be derived with the relative relationship. It is shown in the bracket of row 3 in the air cleanliness part of Table 7.10, but the information about 256 K is missing in the original table.

In the table, row 2 in the air cleanliness part is obtained firstly for 256 K with 8 h exposure time. Air cleanliness level for other integration levels is calculated by multiplying the time coefficient with the basic value for 256 K. Row 1 is based on 14 h exposure time.

Literature [14] presents the estimation value of the yield for 4–256 M DRAM in Class 1 level cleanroom with 0.1 μm particles. It is the particle number deposited on the silicon wafer which was vertically placed in Class 1 level cleanroom for 0.1 μm particles after the 40 day(960 h) exposure time. The estimated controlled particle sizes chosen were 1/1, 1/2, and 1/3 of the graphic size. The detailed information of estimation method and parameters were not given. Figure 7.13 shows two estimation curves.

Calculation was performed with author's method, when the controlled particle sizes were set 1/2 and 1/3 of the graphic size. Results are presented in Tables 7.11 and 7.12 and plotted in Fig. 7.13.

From Tables 7.10, 7.11, and 7.12, the following conclusions can be reached:

1. In China, the theoretical method to determine the air cleanliness level corresponding to the minimum yield was proposed in 1981. When further correction was made on this method, the result agrees well with that of the calculation result abroad.

   Figure 7.14 shows the calculation curve with author's method. From the comparison of the methods between home and abroad, it is known that the accuracy of the curve is good, and author's method is convenient to use.

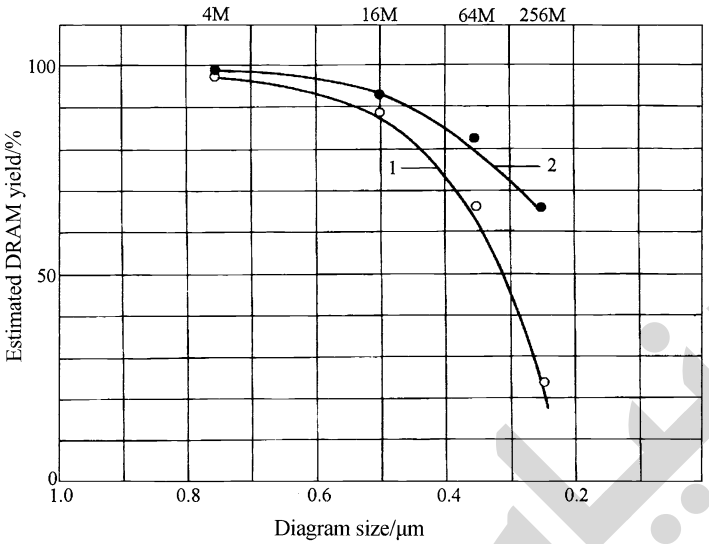

Fig. 7.13 Estimated yield of silicon integrated circuit in Class 1 level cleanroom for 0.1 μm particles after 40 day exposure time. *1* Estimation curve in literature for controlled particle size equivalent with 1/3 of graphic size, *2* Estimation curve in literature for controlled particle size equivalent with 1/2 of graphic size, ●○ represents the calculation results by author

2. The minimum air cleanliness for 0.5 μm is Class 134 (it is temporarily called with the number) for 256 K integration level and 8 h exposure time, when the yield can be reached 50 %. It is not surprised that the yield reached 50 % in Class 100 cleanroom for 0.5 μm in the early report. While the exposure time becomes 14 h, the air cleanliness level needed should be Class 77. Since the actual air cleanliness level is far lower than the cleanliness upper limit, it is natural that the yield reaches 50 % in Class 100 level cleanroom corresponding to 0.5 μm.
3. Even for 256 K, Class 268 is needed for exposure time 4 h, and Class 67 is needed for exposure time 16 h. But the cleanroom for manufacturing process should still be designed with Class 100 level (the yield is 50 %).
4. For 256 M, Class 14 level is needed corresponding to 0.1 μm, and it is obvious that the environment with air cleanliness Class 10 corresponding to 0.1 μm should be provided. For 1G, Class 5 corresponding to 0.1 μm is needed, so it is unsafe to provide the environment with air cleanliness Class 10 corresponding to 0.1 μm. It is only practical to design the environment with air cleanliness Class 1 corresponding to 0.1 μm (the yield is 50 %).
5. When the yield is 97 % for 4 M and 20 % for 256 M, Class 1 corresponding to 0.1 μm is needed when the exposure time is assumed to be 960 h. When the actual exposure time is used and 1/3 of the graphic size is considered, Class 50 for 0.1 μm or Class 1 for 0.5 μm is enough.
6. Taking the integrated circuit as an example, the air cleanliness improves by ten times every 10 years.

Table 7.11 Calculation results with controlled particle size equivalent with 1/3 of the graphic size

Integration degree	Graphic size (μm)	Controlled size (μm)	D_s (μm)	v_s (cm/s)	α	f (cm^2)	η (%)	1/10 of the processing steps exposed with 1 h for each step	0.1 μm level	Entire exposure with 40 (day/h)	0.1 μm level
256 M	0.25	0.25/3= 0.08	0.194	0.0002	8	3	20	55	30.5	960	1.7
64 M	0.35	0.35/3= 0.12	0.3	0.00054	2.3	2	65	45	44.4	960	2.1
16 M	0.5	0.5/3 = 0.17	0.4	0.001	1.5	1.3	88	35	35.1	960	1.3
4 M	0.8	0.8/3 = 0.27	0.55	0.0018	1.3	0.9	97	25	33.7	960	0.9

Table 7.12 Calculation results with controlled particle size equivalent with 1/2 of the graphic size

Integration degree	Graphic size (μm)	Controlled size (μm)	D_s (μm)	v_s (cm/s)	α	f (cm^2)	η (%)	1/10 of the processing steps exposed with 1 h for each step	0.1 μm level	Entire exposure with 40 (day/h)	0.1 μm level
256 M	0.25	0.25/2 = 0.125	0.31	0.0006	2.3	3	65	–	–	960	1.3
64 M	0.35	0.35/2 = 0.18	0.4	0.001	1.5	2	80	–	–	960	2.1
16 M	0.5	0.5/2 = 0.25	0.53	0.0017	1.4	1.3	93	–	–	960	1.1
4 M	0.8	0.8/2 = 0.4	0.8	0.0038	1.1	0.9	98.5	–	–	960	0.5

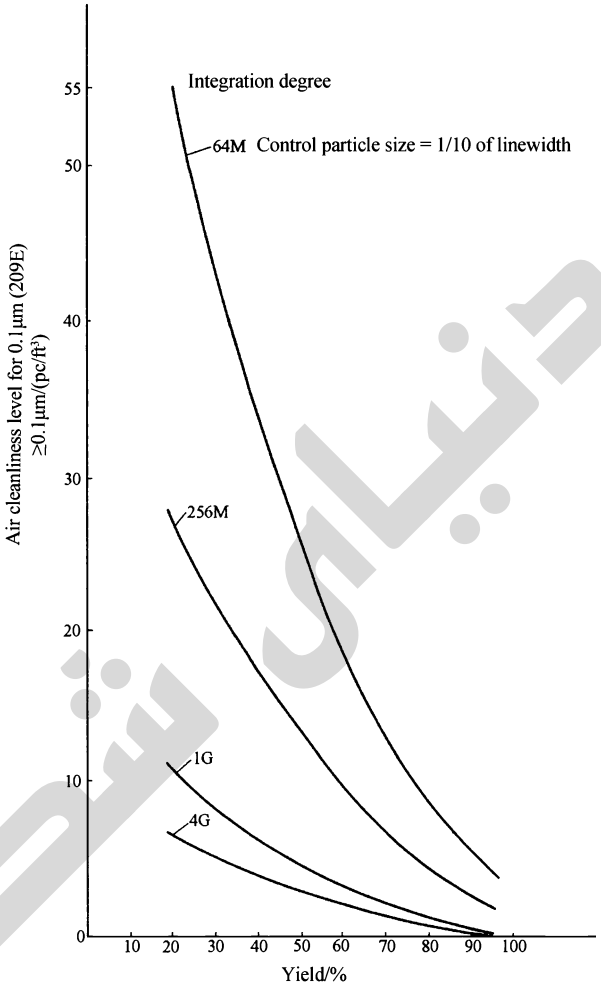

Fig. 7.14 Air cleanliness curve calculated based on the yield of integrated circuit

1960s–1970s	Small- and middle-scale integrated circuits	Class 100 for 0.5 μm
Late 1970s	Large-scale integrated circuit	Class 10 for 0.5 μm
Late 1980s	ULSI	Class 1 and Class 0.1 for 0.5 μm (or Class 10 for 0.1 μm)
Late 1990s	ULSI	Class 0.1 for 0.5 μm or Class 1–Class 10 for 0.1 μm
Beginning of this century	ULSI	Class 0.1–Class 1 for 0.1 μm
The first decade of this century	ULSI	Class 0.1 for 0.1 μm

Since the cleanrooms with air cleanliness Class 10 and Class 1 for 0.1 μm have been available for many years, it is very like to build a cleanroom (clean space) with air cleanliness Class 0.1 for 0.1 μm. In this way, the manufacturing requirement for 64G DRAM will be met in 2010.

7.7.2.2 Yield for Composite End Product

Although there are hundreds of procedures to manufacture the integrated circuit chip, they are completed on the same chip. But the process is less for the drug filling and potting. And it is completed on different objects. Such as the cleaning of penicillin bottle, waste product may be generated when pollution leaves inside it without complete cleaning. When the environmental air cleanliness in the process of bottle filling and potting is not good enough, it will be polluted during this process, which will also cause waste product. When the plug for bottle potting is not completely disinfected, it will contact the medicine and cause waste product. The end product of this kind is called composite end product, which will be made through many individual procedures.

Now taking the bottle filling and potting of sterile powder medicine (which cannot be disinfected at last) as an example, the bottle of the medicine will be discarded if one bacterium drops into during the process, which cannot be disinfected. This is similar as the waste product resulted from the deposition of one particle onto the chip.

After being cleaned and disinfected, the penicillin bottle will be open and delivered to the production line of bottle filling and potting. Let's assume the open area of exposure $f = 1$ cm^2. It usually takes about 20 s to arrive at this production line for bottle filling and potting. The whole process of bottle filling and potting takes about 12 s. Therefore, the exposure time during the whole process of bottle filling and potting can be assumed to be 30 s.

The difference between medicine and chip is that for medicine, it should not be infected with bacteria absolutely. It is not a problem of economical benefit affected by the yield but a safety problem of 100 % for the patient. It is obvious from the expression to calculate N that if the yield is required to be $\eta = 100\,\%$, the number of particles which carry bacteria should be $N = 0$. In practice this is impossible. Therefore, we need to consider the situation when the deposition probability is extremely low.

Usually the output of the penicillin bottles can reach more than 10,000 bottle/(turn · people). If the probability of the deposition of particles carrying bacteria is as small as 1/10,000 for bottles delivered to the bottle potting after cleaning (e.g., the number of bottles on the turntable is only 200), which means the contamination of one bottle is likely to happen if the exposed bottles increase by 50 times, the number of particles carrying bacteria deposited under the original manufacturing situation is regarded as "0."

Suppose there are n procedures during the process of manufacture and the qualified ratio of the semifinished products for each procedure is $P_1, P_2, \ldots, P_n$, so the qualified ratio, i.e., the yield of the end product is η_Σ, can be obtained.

Since the incidence of the waste product in each procedure is independent from each other, "the product is qualified" (η_Σ) means "the first procedure is qualified" (P_1), "the second procedure is qualified" (P_2)... until "the n procedure is qualified" (P_n). With the multiplication law of probability, we can obtain the yield from many individual procedures:

$$\eta_\Sigma = E\prod_{i=1}^{n} P_i \tag{7.11}$$

When all the semifinished products are qualified, the final qualified ratio, i.e., the yield, will be decreased during the influence of reliability of whole manufacturing process. This can be reflected with a coefficient E in the above equation, where E is between 0.1 and 1.0. Since this is also one kind of probability concepts, one more procedure may be added for the convenience of discussion. Therefore, the above equation is converted into

$$\eta_\Sigma = \prod_{i=1}^{n+1} P_i$$

For the assumed values of n and P_i, the results (the yield η_Σ of composite product) can be obtained which are shown in Table 7.13.

It is shown from Table 7.13 that:

1. When there are many procedures, the final yield is also very low even though the yield of each procedure is high.
2. When there are many procedures, the final yield is greatly affected even if only the yield of one procedure is very low. Therefore, not only the air cleanliness level for critical procedure should be guaranteed but also that of the ordinary procedure must be guaranteed.
3. The yield of composite product with few procedures can be easily improved.

Taking the bottle filling and potting of sterile medicine as an example, three procedures including cleaning, canning, and potting are necessary. The composite yield of these three procedures should be 0.9999 (the defect rate is 1/1,000), which means with the above equation the yield of each procedure is 0.99997. Therefore, the concentration of airborne bacteria is

$$N = \frac{-\ln\ 0.99997 \times 1,000}{1.2 \times 0.09 \times 30 \times 1} \approx 0.01\ \text{pc/L}$$

where

1.2 is the value of α_D obtained with the equivalent diameter 3.9 μm of the bacteria, which is shown in Chap. 9.

0.09 is the value of $v_{S,\,D}$.

Table 7.13 Yield η_Σ of composite product

	$n+1$						
P_i	10	9	8	11	6	5	4
0.8	0.107	0.134	0.168	0.21	0.262	0.328	0.41
0.9	0.349	0.387	0.43	0.478	0.531	0.59	0.656
0.95	0.599	0.63	0.663	0.699	0.735	0.774	0.815
0.99	0.904	0.914	0.923	0.93	0.94	0.95	0.96
0.999	0.99	0.991	0.992	0.993	0.994	0.995	0.996
0.9999	0.999	0.9991	0.9992	0.9993	0.9994	0.9995	0.9996

From the bacteria concentration required for bottle filling and potting of sterile product in Table 7.14, the following conclusions can be reached:

1. Because with unidirectional flow, the standard for dynamic state should be 2–3 times higher than static state (please refer to Sect. 17.5.2). So when the bottle filling and potting process of sterile powder is carried out in the class 5 environment with Chinese GMP standard published in 1998, the airborne bacteria concentration with dynamic state for GMP class 5 space should be 0.005* (2∼3) = 0.01–0.015 pc/L, which is slightly higher than that of the needed value 0.01 pc/L. So it is basically feasible. If the defect rate was increased to 1/1,000, namely the comprehensive yield increases to 0.99999, the yield for each procedure should be increased by 10 times, which is 0.999997. In this case, N should reach 0.001 pc/L, i.e. 1 pc/m3. The current GMP specifies the environmental bacteria concentration for sterile bottle filling process to be less than 1 CFU/m3, which meets this requirement. If the defect rate of each procedure increased to 1/1,000,000, N should be reduced to 0.3 pc/L.
2. If measures can be taken to reduce the number of exposed bottles for filling and potting, such as shorten the route, reduce the turntable area, and use the clean tunnel on the turntable or the conveying line like in the manufacture of integrated circuit, the requirement on the air cleanliness level can be reduced, which reduces the investment of cleanroom accordingly.

7.8 Level of AMC in Clean Environment

Airborne molecular compound (AMC) includes the following kinds:

1. Acid gas, such as HF, NO_x, SO_2, SO_3, H_2S, Cl_2, and HCl
2. Alkaline gas, such as NH_3
3. Condensation organic compound, such as HCHO and HMDS($C_6H_{19}Si$)
4. Mixture compound, such as BF_3 and $B(OH)_3$
5. High volatile organic compound ($VVOC_s$), such as NHHC
6. Molecular metal, such as Fe, Na, K, Ca, Zn, and Al

These contaminants do not only come from the manufacture process itself but also from the building decoration material in the cleanroom. For the former case, the representative includes the disinfection agent from solvent vapor, phenol, and

Table 7.14 The airborne bacteria concentration required for bottle filling and potting of sterile product

Standard	Airborne bacterial concentration with air cleanliness level Class 8 (CFU/L)	Airborne bacterial concentration with air cleanliness level Class 7 (CFU/L)	Airborne bacterial concentration with air cleanliness level Class 5 (CFU/L)	Airborne bacterial concentration with air cleanliness level Class 4 (0.5 μm) (CFU/L)
US NASA	0.0884	0.0176	0.0035	0.0014
EU GMP (operational state)	0.1	0.01	0.001	–
China GMP(1998) (at-rest state)	0.5	0.1	0.005	–
China GMP (2010) (operational state)	0.1	0.01	0.001	–
China Standard: architectural technical code for hospital clean operating department (at-rest state)	0.15	0.05	0.005	–

ether from anesthetic. For the latter case, the representative includes NH_3 and Ca from the concrete; siloxane from the aquaseal, PH_3, PF_3, Na, Ca, and Fe from the anti-static material; metal ion, toluene, and dimethylbenzene from the painting; NO_x, SO_x, Na, and Cl from the fresh air; B, DOP, Na, and Cl from the interior of cleaning air-conditioning system such as HEPA filter; and NH_3, Na, Cl, and various organic materials from people, costume, and cosmetic.

As for the TVOC (total volatile organic compound) from building decoration material only, the concentration measured was 3,500 μg/m^3 in a newly decorated cleanroom performed by Osaka University from Japan. After operation for 1 month, it reduced to 500 μg/m^3, while it kept at 200 μg/m^3 stably after operation for 4 months [17].

It is increasingly important to control AMC in cleanroom. This has already become an essential condition especially for ULSI.

Table 7.15 lists the source of AMC during the manufacture of ULSI [18].

In 1995, International Association of Semiconductor Equipment and Material proposed the classification standard for AMC in clean environment: SEMI F21-95.

Table 7.15 Source of AMC during the manufacture of ULSI

Pollutant	Existing matter	Process	Resultant default
C	CO_2, CH_4, CCl_4, $CClF_3$, CF_4, DOP, resin, oscillight liquid, skin, fiber	Photoetching, dry corrosion, passivation, organic cleaning, dry	Leakage of electricity, poor contact by membrane
Cl	HCl, $SiCl_4$, $SiHCl_3$, SiH_2Cl_2, NaCl, oscillight light, clamp, pipe	Epitaxy, dry corrosion, wet corrosion	Leakage of electricity, corrosion
Fe, Cr	Stainless steel, steel, chroming material, impurity in the medicine liquid	Photoetching, cleaning	Leakage of electricity, reduced lifetime
B	Glass, BN, B_2H_6, BBr_3, BF_3, BCl_3	Ion injection, diffusion, single crystal mixing, doping in epitaxial layer, dry corrosion	Nonuniform electrical resistivity
F	Fluorine acid, NH_4F, dry corrosive gas (BF_3, CF_4, SF_6, CHF_3, etc.), PTFE, clamp, container	Cleaning, silicon corroded by oxidation film	corrosion
O	Air, water, O_2, H_2O_2, H_2SO_4, HPO_3, etc.	Natural oxidization, thermal oxidization, CVD SiO_2, dry corrosion, ion injection	Deficient, irregular corrosion shape
P	P_2O_5, PH_3, H_3PO_4	Diffusion, epitaxy, CVD, wet corrosion, ion injection	Leakage of electricity, corrosion
Cu	Container, sputtering target, impurity in the medicine liquid	Sputtering, cleaning, display	Consume material, difficult for cleaning

Table 7.16 Classification for AMC in SEMI F21-95

	Air cleanliness level				
	1 pptM	10 pptM	100 pptM	1,000 pptM	10,000 pptM
Acid	MA-1	MA-10	MA-100	MA-1000	MA-10000
Alkali	MB-1	MB-10	MB-100	MB-1000	MB-10000
Coagulative organic matter	MC-1	MC-10	MC-100	MC-1000	MC-10000
Dopant	MD-1	MD-10	MD-100	MD-1000	MD-10000

The maximum allowable concentrations for four kinds of contaminants were given in this standard, which is shown in Table 7.16. The magnitude of pptM in the table means 1×10^{-12}.

In 2000, Air Cleaning Association of Japan proposed the draft "Label and test method for air cleaning level about AMC in cleanrooms and related controlled environment" [19], which proposed the expression method for the AMC cleanliness level, i.e.,

$$N = \lg(1/C_{\mathrm{AMC}}) \tag{7.12}$$

Table 7.17 Classification of air cleanliness for AMC (Japan)

Pollutant	Volumetric concentration ($\times 10^{-N}$ g/m^3)	Surface concentration ($\times 10^{-N}$g/cm^2)
Acid gas (expressed with A)	$N = 9 \cdots 2$	$N = 11 \cdots 5$
Alkali gas (expressed with B)	$N = 9 \cdots 2$	
Coagulative organic matter (expressed with C)	$N = 9 \cdots 2$	
Dopant (expressed with D)	$N = 9 \cdots 2$	
High volatile organic compound (expressed with V)	$N = 9 \cdots 2$	

where C_{AMC} is the allowable upper limit of concentration for specific AMC and its derivation. The unit for volumetric concentration is g/m^3, while for surface concentration g/cm^3. It is shown in Table 7.17.

Compared with the standard SEMI, the item about high volatile organic material is added, but not metal content is included.

This standard specified to use the following method to make the label, which starts from X:

$$Xa(b;c);[d;e]$$

where

a is the symbol representing the contaminant in Table 7.17. For example, HCl is expressed with A;
b is the specific name of the contaminant, such as DOP and HCl;
c is the air cleanliness level *N*[−], such as the value shown in Table 7.17;
d is the test method;
e is the exposure time (when the surface concentration is used).

Furthermore, the operational state and related parameters (such as temperature, humidity, and pressure drop) should be recorded.

References

1. Xu ZL (1994) Design of cleanroom. Seismological Press, Beijing (In Chinese)
2. Kawamata T (1993) Specifications of air cleanliness level in US, Japan and Europe. J Jpn Air Clean Assoc 31(4):74–85 (In Japanese)
3. GB50073-2001 (2001) Code for design of clean room. China Planning Press, Beijing (In Chinese)
4. Wang YB, Wang WG (1998) Prediction of particle concentration in ambient air for VLSI production. Contam Control Air Cond Technol 3:10–13 (In Chinese)
5. Tang HP, Fan CY (1987) Discussion of particle size distribution characteristics inside cleanroom. Department of Science and Technology Information at Tongji University (In Chinese)

6. Lv JM (1984) Measurement of ultrafine particles in cleanroom. J Jpn Air Clean Assoc 21(4):36–46 (In Japanese)
7. Hayakawa K (1980) Air conditioning in comprehensive hospital. Jpn Air Cond Heat Refrig News 20(8):51–59 (In Japanese)
8. Xu ZL, Qian ZM, Shen JM (1983) Lower limit of air velocity in parallel flow cleanroom. Research report of Building Science, p 4 (In Chinese)
9. Austin PR, Timmerman SW (1965) Design and operation of clean rooms. Business News Publishing Company, Detroit, USA
10. Kawamura A (1981) Design planning and measurement of high performance cleanroom. Jpn Air Cond Heat Refrig News 21(5):69–75 (In Japanese)
11. Morrison PW (1973) Environmental control in electronic manufacturing. Van Nostrand Reinhold Company, New York, USA, pp 278–292
12. Ohara S (1982) Prospect of super LSI high performance computer. Jpn Refrig Air Cond Technol 33(383):2–24 (In Japanese)
13. Wang WG, Wang YB (1996) Prediction of air cleanliness level. Contam Control Air Cond Technol 1:2–4 (In Chinese)
14. Kitajima Y, Sasaki K (1997) Influence of particle diameter on the yield of semiconductor. J Jpn Air Clean Assoc 35(2):20–29 (In Japanese)
15. Xu ZL (1981) Relationship between the yield and the air cleanliness level of the environment. Mech Eng 3(1):45–49 (In Chinese)
16. Kitajima H, Shiramizu Y (1997) Requirements for contamination control in gigabit era. IEEE Trans Semicond Manuf 10(2):267
17. Fan CY, Xu WH, Lin ZP (2001) Certain progress of air cleaning technology in microelectronics industry. J HV&AC 31(5):30–38 (In Chinese)
18. Wang WG (2000) Chemical pollution and its control for the environment of VLSI production. Contam Control Air Cond Technol 1:20–23 (In Chinese)
19. Fujii S (2000) Cleanrooms and associated controlled environments – classification method and guideline of measurement for airborne molecular contamination. J Jpn Air Clean Assoc 37(6):31–34 (In Japanese)

Chapter 8
Principle of Cleanroom

Cleanroom is the most important and most representative measure to create the clean microenvironment with air cleaning technology. The principle of cleanroom is the theoretical base for the design, operation, and maintenance of the cleanroom well.

8.1 Approach to Control Contaminants

In terms of the controlled objects, cleanroom can be divided into two kinds: industrial cleanroom and biological cleanroom.

The main task of industrial cleanroom is to control the pollution of nonbiological particles, while that of biological cleanroom is to control the biological particles.

However, no matter it is nonbiological or biological particles, non-vital or vital particles, they are considered to be particles in the air cleaning technology field, which has the feature of particles. Therefore, no matter what kind of cleanroom it is, the approach to control particular pollution is the same. These methods have the following features:

1. Prevent the outdoor pollution from entering indoors (or effectively prevent indoor pollution from emission outdoors). This is the main approach to control the pollution in the cleanroom, which mainly includes the method of air cleaning and indoor pressurization, etc.
2. Exhaust the pollution that occurs indoors effectively, which mainly includes the indoor air distribution. This represents the key function of cleanroom.
3. Control the pollution source and reduce the generation of pollution, which mainly includes the method to place and manage the equipment which generates pollution, as well as the cleaning of people and objects entering into the cleanroom. The former belongs to the process problem, which will not be discussed. The latter will be introduced later.

The above three items will be illustrated in this chapter and later.

Z. Xu, *Fundamentals of Air Cleaning Technology and Its Application in Cleanrooms*, DOI 10.1007/978-3-642-39374-7_8, © Springer-Verlag Berlin Heidelberg 2014

8.2 Flow State

8.2.1 Several Fundamental Fluid States

In order to illustrate the principle of cleaning function by cleanroom from the airflow aspects, the following concepts of fluid dynamics are emphasized.

8.2.1.1 Steady-State Flow and Unsteady-State Flow

Various parameters of fluid particles (such as velocity, acceleration speed, density, and stress including the pressure, tension, shear force, and viscous force) differ with position of fluid particles, but remain the same with the time t. This kind of fluid is called steady-state flow. If various airflow parameters are function of both position (x, y, z) and time (t), it is called unsteady-state flow.

8.2.1.2 Gradually Varied Flow and Mutation Flow

When the flow has the following characteristics, it is called gradually varied flow, which is shown in Fig. 8.1.

1. The angle β between flow lines is very small, which means the distance between flow lines is almost equidistant.
2. The radius of curvature R is very large, which means the flow line is close to be straight (combined with the above item, the flow lines are almost parallel). So the inertial force can be neglected.

If the flow does not have the above two features, it belongs to the mutation flow.

8.2.1.3 Uniform Flow and Nonuniform Flow

When the flow of the gradually varied flow has the following features, it is termed as uniform flow:

1. The shape and scale of the flow at any cross section are the same along the flow stream.
2. The velocities at any two positions along the same flow line are the same.

It is clear that uniform flow is the limit case for gradually varied flow.

As long as any condition is missing, it is nonuniform flow. The example of the nonuniform flow is shown in Fig. 8.2a which does not have either features. Figure 8.2b shows the example which does not have the second feature at the inlet section. Figure 8.2c shows the example which has both features.

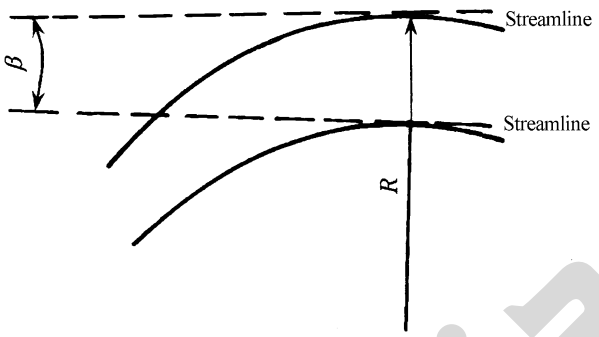

Fig. 8.1 Gradually varied flow

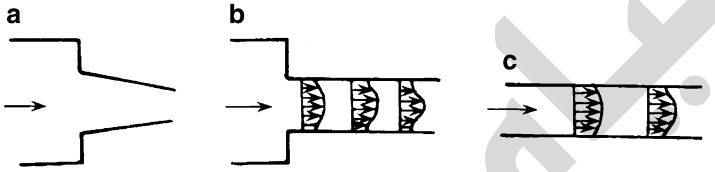

Fig. 8.2 Uniform flow and nonuniform flow

8.2.1.4 Laminar Flow and Turbulent Flow

When there is no exchange of fluid particles between fluid layers, it is called the laminar flow, and vice versa, it is the turbulent flow.

For pipeline flow, it is laminar flow when *Re* number decreases to be less than 2,400. When *Re* number increases to about 13,800, it becomes the turbulent flow. But the critical value of *Re* number is usually not fixed. In some cases the flow keeps laminar even if *Re* number increases to 10^5. The critical value of *Re* number for the transition of flow mainly depends on the stability of the incoming flow.

With the state of turbulent flow, fluid particles mix randomly, which differs with the time *t*. So in fact the turbulent flow is not one type of steady flow.

When a longer time period *T* is chosen, the average velocity (also called time averaged velocity) can be obtained:

$$\overline{u_x} = \frac{1}{T}\int_T u_x \mathrm{d}t$$

If the condition of incoming flow remains the same (such as the flow rate or disturbance condition), the time averaged velocity can also be unchanged even for turbulent flow, so it is still called steady flow. This means although the transient flow line cannot be plotted for this kind of turbulent flow, the time averaged flow

line can be obtained. On the contrary, if the time averaged velocity is unchanged, it is obviously not the steady flow. The field we investigated belongs to the former case.

In cleanrooms, it is turbulent flow in terms of the *Re* number.

Based on the above analysis, the flow situations can be divided into the following groups:

- Whether the airflow movement is time dependent
  - Steady-state flow
  - Unsteady-state flow
- Classify according to streamline shape
  - Gradually varied flow
    - Uniform flow
    - Nonuniform flow
  - Suddenly varied flow
- Whether mass particle exchanges
  - Laminar flow
  - Turbulent flow

8.2.2 *Physical State of Turbulent Flow*

The flow state in cleanroom belongs to the turbulent flow. The physical state of turbulent flow is the fundamental concept of fluid dynamics, which has been introduced in many monographs about fluid dynamics. Here the following two points are emphasized.

8.2.2.1 Formation Process of Turbulent Flow

1. Formation of Eddy
   (a) Viscous Property. In the flow field with relative movement, the shear stress forms between fluid layers because of the viscous property. For one side of fluid layer, the effect of shear stress on it by the fluid layer with relative high velocity is following the flow direction, while that by the fluid layer with relative low velocity is against the flow direction. Therefore, the moment of force and eddy are likely to be formed on this fluid layer.
   (b) Fluctuation Property. If the fluctuation perpendicular to the flow direction occurs by certain reasons, the velocity increases at the convex side since the cross-sectional area reduces by fluid squeezing, while the velocity decreases at the concave side. The difference of velocity at both sides further forms the eddy. Figure 8.3 shows the schematic for the process of eddy formation, where the situation between the fluid line with ordinary turbulence and eddy is presented.

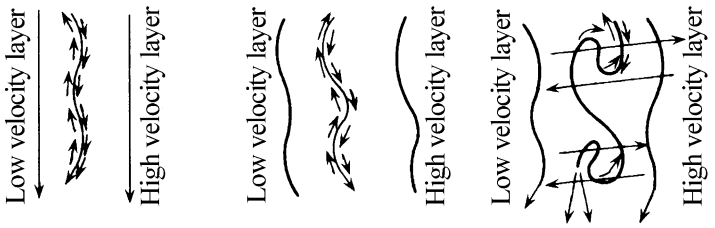

Fig. 8.3 Eddy formation

2. Once the eddy is formed, it detaches from the original fluid layer and enters into the adjacent fluid layer.

Once the eddy is formed, the flow direction of fluid layer with higher velocity is consistent with the rotation direction of eddy, and it is opposite for the flow direction of fluid layer with lower velocity. So the velocity of fluid layer with higher velocity becomes larger and that of fluid layer with lower velocity becomes smaller. The pressure reduces at the place where the velocity increases, and the pressure increases at the place where the velocity decreases. So the pressure difference perpendicular to the flow direction is formed. When the force of this pressure difference is larger than that of resistance, the eddy is forced to detach from the original fluid layer and enters into the adjacent fluid layer.

As long as these two conditions exist, which includes the formation of eddy and the entering of eddy into adjacent fluid layer, the exchange of eddy and mutual supply between fluid layers can occur because of the continuity of the flow. The chaos formed will influence the further fluid layer. If many initial eddies are formed, the whole fluid state will change completely.

8.2.2.2 Properties of Turbulent Flow

With the analysis of physical state about the formation process of turbulent flow, the following conclusions about the feature can be obtained:

1. Large *Re* number.
2. Irregular.
3. Diffusional.
4. Eddy flow at three dimensions.
5. Energy dissipates quickly because of viscosity.

Except for the above features, the turbulent flow is also dependent on the incoming flow condition. If the incoming flow is not uniform, tiny fluctuation can be generated and thus the eddy is formed. This explains the reason why there is no fix upper critical value of *Re* number.

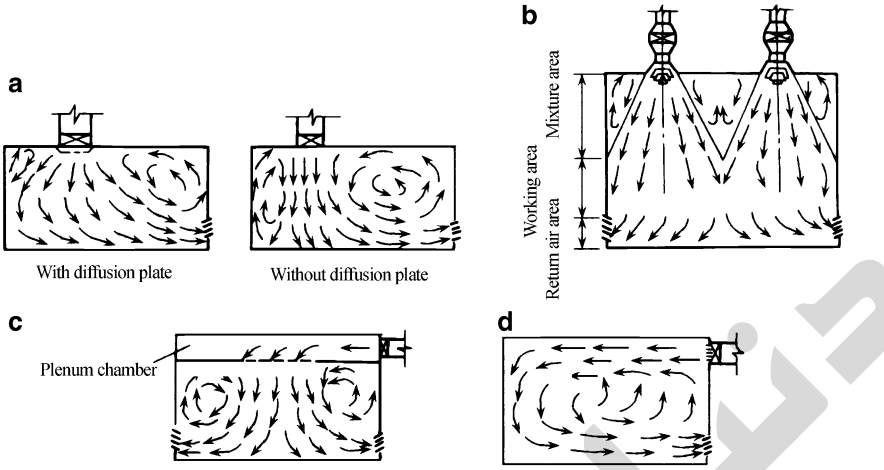

Fig. 8.4 Air supply form of mixed flow cleanroom. (**a**) Air supply through HEPA filter ceiling. (**b**) Air supply through concentrated streamlined diffuser ceiling. (**c**) Air supply through local perforated plated ceiling. (**d**) Side air supply

8.3 Principle of Cleanroom with Mixed Flow

8.3.1 Principle of Cleanroom with Mixed Flow

According to the flow state, cleanrooms can be classified as cleanroom with mixed flow (non-unidirectional flow), cleanroom with unidirectional flow, and cleanroom with radial flow (also called vector flow). In this section, the cleanroom with turbulent flow is introduced. As mentioned before, the flow in any kind of cleanroom is turbulent. So why not all of them are called turbulent flow cleanroom?

The term "mixed flow cleanroom" was referred to the Japanese language. In Japanese language, the meaning of mixed flow is the same as the turbulent flow in hydrodynamic field, while it differs in the monograph "Air cleaning technical measures" in China. At present, this kind of cleanroom is customarily called non-unidirectional cleanroom.

There are various kinds of air supply for mixed flow cleanrooms:

1. Ceiling supply air with HEPA filter (with or without diffuser plate), shown in Fig. 8.4a
2. Ceiling supply air with streamlined diffuser, shown in Fig. 8.4b
3. Ceiling supply air with local perforated plate, shown in Fig. 8.4c
4. Sidewall supply, shown in Fig. 8.4d

When the flow type is determined on the *Re* number, it is obvious that all these cleanrooms have the turbulent flow. But it is inappropriate to call them turbulent

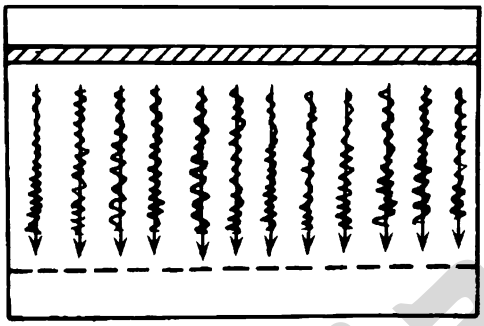

Fig. 8.5 Unidirectional flow of turbulent flow

flow cleanroom. Take the type in Fig. 8.5 as an example, when air is supplied from all the ceiling with the velocity more than 0.25 m/s, it is also turbulent. But it will be illustrated later that although both two kinds of air supply cause turbulent flow in the room, their principles to clean indoor air are different, because for the latter case, the principle of cleanroom with unidirectional flow or parallel flow applies. Therefore when the former case is called turbulent flow cleanroom, the latter case should also be included.

It is shown in Fig. 8.4 that the main feature of mixed flow cleanroom is that the cross-sectional area changes along the flow stream from the incoming flow towards the outlet flow (from air supply inlet to return air grille). Since the cross-sectional area of cleanroom is larger than that of air supply inlet, uniform flow cannot be formed at the whole cross section or at the cross section of working area. The streamlines after leaving the air supply inlet will have a large included angle which will become larger and larger. The radius of curvature is very small, so air cannot flow unidirectionally in the room, and steamlines will impact on each other, which generates the backflow and vortex. This results in the essence of flow state in the mixed flow cleanroom: mutation flow and nonuniform flow.

It is more accurate and comprehensive to describe the cleanroom with the mixed flow instead of with turbulent flow. Turbulent flow is mainly dependent on *Re* number, which is mainly influenced by the velocity. If the ceiling supply air with HEPA filter was used, the above consequences will occur even for extreme low velocity, because it is mutation flow and nonuniform flow. Therefore in this case, the mixture occurs between fluid layers not only because of turbulent flow but also because of the backflow and vortex in the whole room.

To summarize, the principle of mixed flow cleanroom is that when a certain amount of clean air is supplied into the room, it will disperse and mix with the surrounding air, and at the same time the same amount of air is exhausted from the return air grille. The clean air dilutes the indoor polluted air, which reduces the indoor pollution concentration from original state and arrives at the equilibrium state. Therefore, the faster and the more uniform the air diffuses, the better the effect of dilution it is.

So the principle of mixed flow cleanroom is the effect of dilution. Figure 8.6 shows the general situation of this principle.

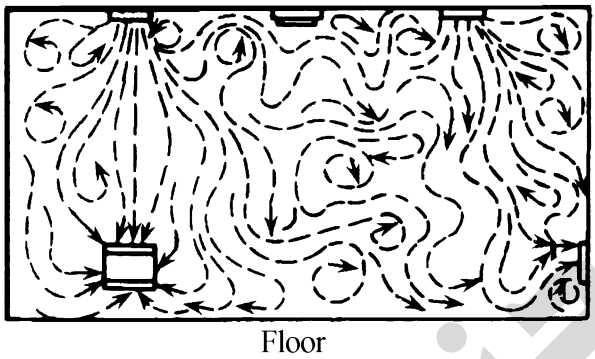

Fig. 8.6 Schematic for the principle of mixed flow cleanroom

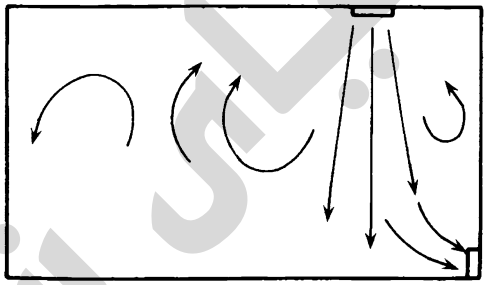

Fig. 8.7 Air distribution with poor performance of dilution

8.3.2 Air Inlet in Mixed Flow Cleanroom

8.3.2.1 Air Supply Outlet

According to the principle of mixed flow cleanroom, if low particle concentration in the whole room, instead of only the region below the air inlet, is needed, the clean air should play the role of dilution sufficiently after leaving the air inlet, and more space before the working area is diluted. So this kind of air inlet should have the enough capability of dilution. If the air inlet has high velocity and small diffusion angle as shown in Fig. 8.7, the proportion of clean air is likely to be exhausted from the return air grille directly, and its capability of dilution in other space is not shown.

Usually the air supply inlet with HEPA filter has the diffusion angle of tens degrees, which are shown in Figs. 8.8 and 8.9. However, when the perforated diffusion plate with the thickness of 65 mm is added, the diffusion angle can be as large as 45° or even larger according to the air flow test abroad, which is shown in Fig. 8.10. In this case, the velocity near the air supply inlet is more uniform than that without diffusion plate.

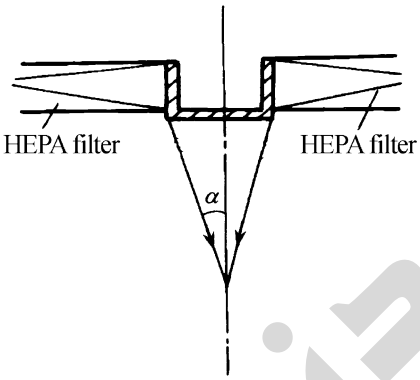

Fig. 8.8 Dispersion angle of supplied air through HEPA filter

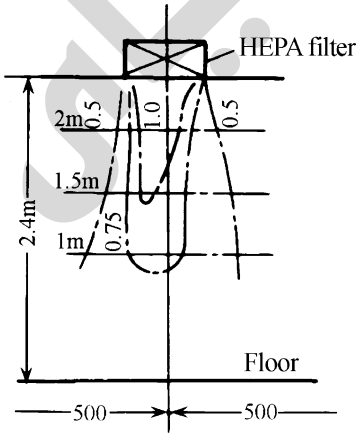

Fig. 8.9 Velocity field with HEPA filter air supply outlet without diffusion plate

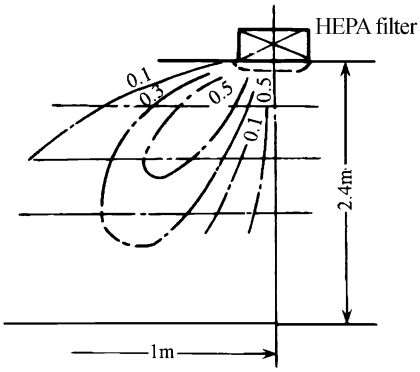

Fig. 8.10 Velocity field with HEPA filter air supply outlet with diffusion plate

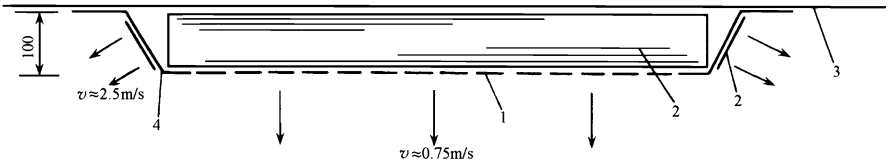

Fig. 8.11 Diffuser outlet with slot and orifice: *1* orifice, *2* slot outlet, *3* ceiling, *4* side (inclined or vertical)

According to the experiment performed by No. 10 Design Institute of the former Fourth Ministry of Machinery and Industry, under the same air change rate, the ratio of average particle concentration in the working area of the cleanroom and the concentration at the return air grille, for the case with the HEPA filter air supply inlet and nonuniformly perforated diffusion plate, is 20 % less than that without this kind of diffusion plate. It means the air inlet with this kind of diffusion plate can dilute the whole room air very well, which makes the indoor particle concentration more uniform and the average concentration much lower. Since this kind of diffusion plate has nonuniform perforation, it is much difficult to manufacture, so it is less popular compared with the diffusion plate with uniform perforation.

However, because of the attenuation effect of hole, the velocity at the four sides of diffuser outlet becomes small. So the region below the ceiling between two air supply outlets is likely to be stagnant, which is not good for the dilution of mixed flow. Therefore one kind of air supply outlet appears as shown in Fig. 8.11. Except for the orifice below the outlet, slot outlets are placed at four sides. The upper velocity is 3 times more than the middle velocity, so that the clean air can arrive at the corner of cleanroom and the air stagnant region is eliminated.

8.3.2.2 Return Air Grille

In order to remove indoor particles rapidly and effectively, return air grilles should be placed at the underpart of the room, so that the flow direction is consistent with that of particle deposition. As mentioned in Chap. 6 that the difference between particle velocity and flow velocity is very small, so particles can be removed towards the return air grille easily because of the consistence between flow direction and particle deposition direction. Therefore, the upper supply and bottom return mode is usually used in cleanroom, which is a fundamental principle of cleanroom.

The upper side of return air grille at the underpart of the room should not be too high from the floor. Since the working area starts from 0.7 m above the floor, so the upper side of return air grille should be lower than this level, and the minimum safety distance should be 0.2 m. Otherwise, except for the air above the working table flows through it, air from other places will also pass through, and the working table will be polluted. The related experimental analysis will be presented in Sect. 8.8 in this chapter.

If the return air grille is placed on the upper side of the room, i.e., the upper supply and upper return mode, the following three phenomena will occur at least:

1. At a certain height such as the respiratory height, big particles with diameter 5 μm are popular. So it is qualified up to the standard in terms of 0.5 μm, while it is not qualified in terms of 5 μm.
2. For application with local cleanliness of Class 100, the velocity at the working area is usually very small, so it is difficult to be qualified.
3. The self-purification period is very long. Experiment has shown that it is two times longer. (the self-purification period will be introduced in the latter chapters).

Therefore, although the designed air cleanliness level can be reached for the as-built test with the upper supply and upper return mode, it is very unfavorable to remove pollutant in the operational status. It is not recommended to adopt this mode for the following reasons:

1. With the upper supply and upper return mode, the air of a certain region at the certain height is likely to be stagnant. When the buoyant force of the particle is balanced with the gravitational force, large particles (mainly particles with diameter 5 μm) are apt to stay in this space, which is not good for particle removal, and the velocity at the working area is not guaranteed (for local Class 100 cleanroom).
2. The shortcut of airflow is easily formed. Part of the clean air and fresh air will not be efficiently used in the room, so the cleaning and hygiene effect is reduced.
3. Pollutant particles are likely to pass through the working place during the process of removal. According to the item 17.25 of GMP by WHO, "the airflow in the cleanroom should be verified that no pollution risk exists, for example, particles generated by occupant, operation and machine should not disperse into the high risk region close to the product." However, there is the risk for this upper supply and upper return mode. For the clean corridor, there is no working place, so there's no risk of this kind for upper supply and upper return mode. When there is no special cross contamination between the rooms at two sides, it is permissible to use the upper supply and upper return mode.

8.3.3 Effect of Mixed Flow Cleanroom

According to the principle of mixed flow cleanroom, the corresponding limit for air cleanliness level has been calculated. As proved by practice, the highest level of air cleanliness is Class 1000. In order to obtain Class 100 or even higher, only unidirectional flow cleanroom should be used. In the related chapters about cleanroom calculation, this will be discussed in detail.

8.4 Principle of Cleanroom with Unidirectional Flow

The unidirectional (parallel) flow cleanroom appeared in the USA in 1961 at the earliest, which was called laminar flow cleanroom. The appearance of this kind of cleanroom is an important milestone in air cleaning technology field. It makes the creation of extreme clean environment possible.

8.4.1 Classification of Unidirectional Flow Cleanrooms

Unidirectional flow cleanroom can be divided into two main categories:

8.4.1.1 Vertically Unidirectional Flow Cleanroom

HEPA Filter Air Supply Outlet Fully Placed at the Ceiling and Return Air Grille Fully Placed at the Floor

This is the typical type of vertically unidirectional flow cleanroom, which is shown in Fig. 8.12.

The feature of this kind cleanroom is that uniform parallel unidirectional air flowing downwards can be obtained. The self-purification ability is very good. The highest cleanliness level can be achieved. The processing equipments can be arranged in any place. The facility to clean the occupant can be simplified. For example, the airshower is not necessary and workers can wear long smock. But the ceiling structure is complex, and the construction and maintenance costs are very high. It is difficult to prevent the leakage on HEPA filter. Figure 8.13 is the scenograph of this kind of cleanroom.

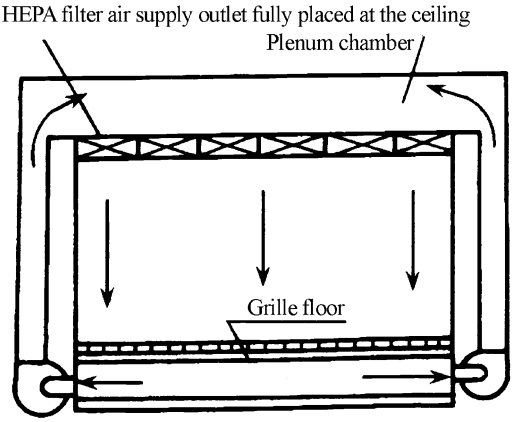

Fig. 8.12 Vertically unidirectional flow cleanroom with HEPA filter air supply outlet fully placed at the ceiling

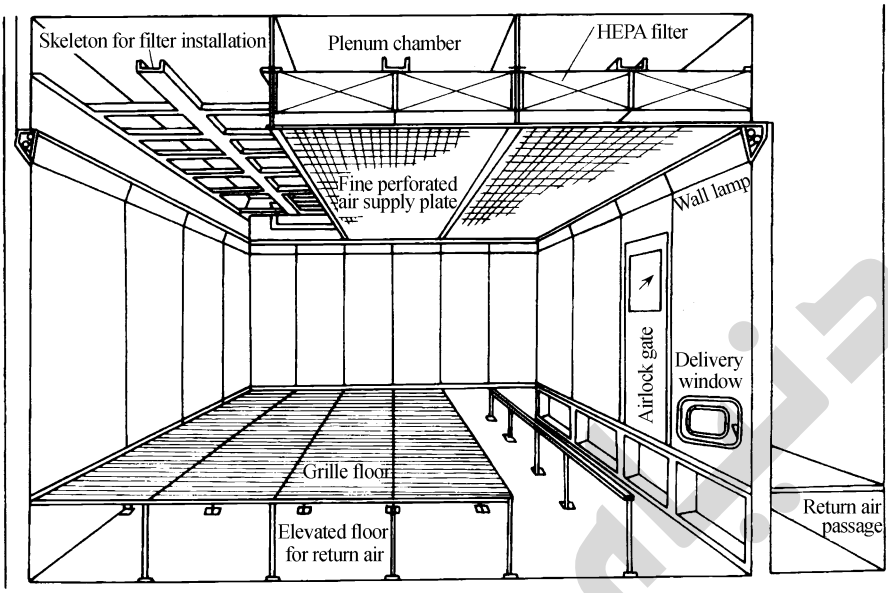

Fig. 8.13 Scenograph of vertically unidirectional flow cleanroom

Leakage-Preventing Layer Air Supply at the Ceiling with HEPA Filter Installed at the Side and Return Air Grille Fully Placed at the Floor

The main shortcoming of vertically unidirectional flow cleanroom is the high construction cost. One of the main reasons is that HEPA filters are placed fully at the ceiling. The role of HEPA filters is to distribution air and filter particles. In order to further make the airflow uniform and the ceiling artistic, the leakage-preventing layer with grille and orifice is placed below the HEPA filter. If the cleanroom area is very small, the airflow rate is not large, and the room width is not large, HEPA filters can be installed at the side as recommended by AACC CS-6T, which is shown in Fig. 8.14. However, it is not easy to meet the requirement of flow rate for the area of HEPA filters installed at the side, especially when the flow rate should not be larger than 80 % of the rated flow.

When HEPA filters are placed at the side, the metal orifice plate plays the role of distributing the air. This orifice plate is termed as "leakage-preventing layer." The leakage-preventing layer should also guarantee the uniformity of parallel unidirectional flow, so the aperture ratio should be larger than 60 % (it will be illustrated in detail later). In the same technical requirement of Class 100 unidirectional cleanroom by the USA was given [2].

Materials which contain particles itself cannot be used as the leakage-preventing layer, such as the nonwoven cloth. Except for the metal pore plate, other materials with good air permeability such as the nylon yarn can be used. For example, nylon yarn is fastened to the frame which is placed onto the ceiling skeleton [3].

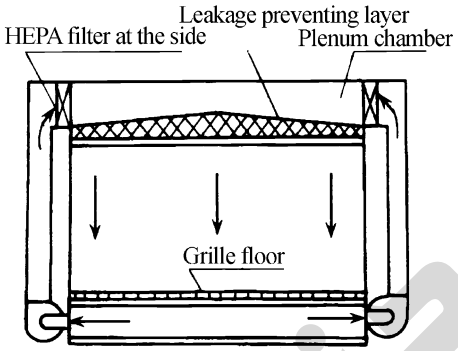

Fig. 8.14 Leakage-preventing layer air supply at the ceiling with HEPA filter installed at the side

The skeleton is made of light metal material, so it is easy to install and uninstall. The pressure drop for this kind of nylon yarn (diagonal grain or twill) and nylon screen (pore size $\geq$ 100 μm $\times$ 100 μm) at the velocity 0.01 m/s is about 2–3 Pa. Because of the small pressure drop for these materials, the space between itself and HEPA filter is not closed. There is a great disadvantage that particles will inevitably deposit on the interior surface of this space.

HEPA Filter Air Supply Outlet Placed at the Ceiling and at the Side and Return Air Grille Fully Placed at the Floor

This kind of vertically unidirectional flow cleanroom is the comprehensive of two air supply and return modes [1, 4]. This kind of vertically unidirectional flow cleanroom was firstly adopted in the USA for cleaning the container filled with moon rocks. The purpose is not only to obtain high cleanliness but also to reduce the frequency of changing HEPA filters at the ceiling. The ceiling can be regarded as the semipermanent ceiling. Figure 8.15 shows the schematic of the cleanroom designed in China. It is obvious that it will not be used under usual condition.

HEPA Filter Air Supply Outlet Fully Placed at the Ceiling and Return Air Grille at Both Sides

The other reason of high construction cost for vertically unidirectional flow cleanroom is to use grille floor. Usually this kind of floor is made of cast aluminum, plastic, and steel. Figure 8.16 shows the photo of grille floor with cast aluminum in the first fabricated cleanroom in China. People do not feel comfortable by vision, since both walking and placing objects seem unstable and tiny objects are likely to fall down underground. Therefore, this kind of floor is not good for promotion of vertically unidirectional flow cleanroom. To improve the air return mode by this kind of grille floor, the mode with HEPA filter air supply outlet fully placed at the ceiling and return air grille at both sides appears, which is shown in Fig. 8.17.

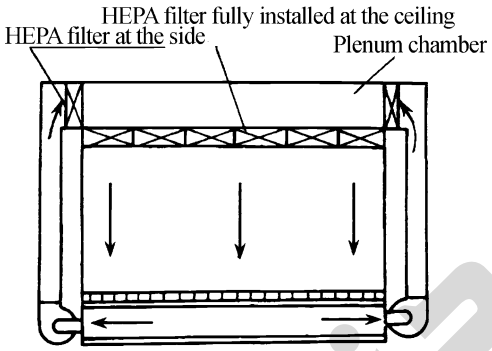

Fig. 8.15 Vertically unidirectional flow cleanroom with HEPA filters placed at both sides

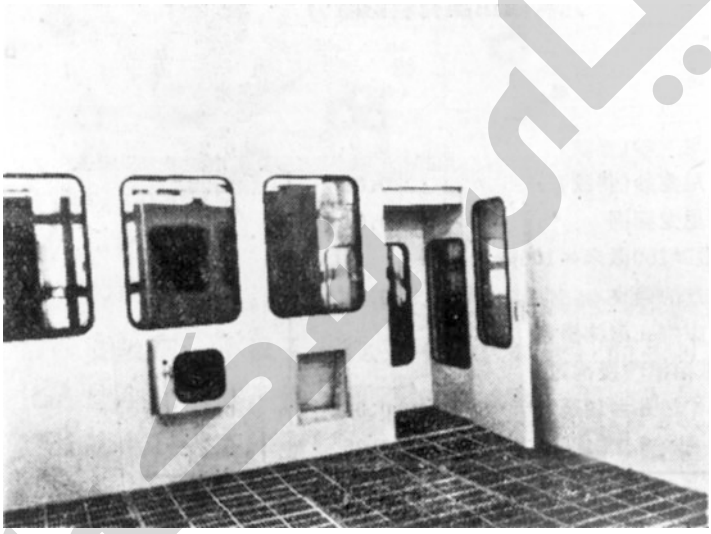

Fig. 8.16 Grille floor with cast aluminum

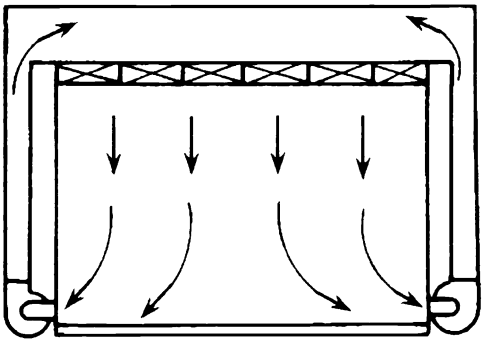

Fig. 8.17 Cleanroom with return air grille at two sides

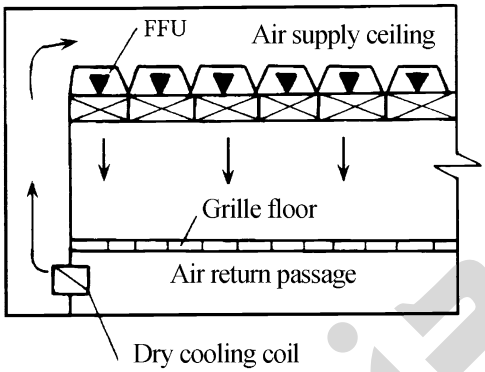

Fig. 8.18 FFU fully placed at the ceiling

Abroad, it is called quasi-laminar flow cleanroom. It is thought to be able to provide the environment with air cleanliness Class 100 when the width is only 3.6 m (USA) [2]. It is also believed to provide the environment with air cleanliness Class 1000 (former Soviet) [6]. Studies at home evaluated this kind of cleanroom comprehensively from theory, experiment, and actual application for the first time [7]. It is concluded that when the distance between two return air grilles is within 6 m, unidirectional flow with cleanliness Class 100 can be obtained (illustrated later in detail).

HEPA Filter Air Supply Unit Fully Placed at the Ceiling and Return Air Grille at the Floor or Both Bottom Sides

The way of air supply in this kind of cleanroom is different from that of common HEPA filter air supply. Instead, HEPA filter air supply unit is used, which can be divided into two types:

(a) Fan filter unit – abbreviation form is FFU.
The unit is composed of one fan and one filter. Several FFUs are placed at the ceiling as the air supply outlets. The feature is that air supply and return pipelines are not needed, and most air needed in cleanroom is circulated by FFU. Fresh air is treated for temperature and humidity control in a central way. When the load is not enough, additional dry cold coil can be placed at the return air passage, which is shown in Fig. 8.18. The shortcoming is that the failure rate is large because of so many fans. Since both fan and filter are placed in a box, the air cleanliness will be affected during the maintenance of fans, and it is a little difficult to maintain it in the ceiling.

(b) Fan module unit – abbreviation form is FMU.
One fan corresponds to several air filters, and the fan chamber is separated from the air filter chamber. Also supply and return pipelines are not needed. But the

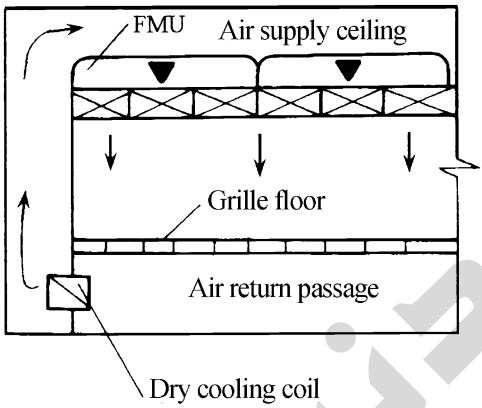

Fig. 8.19 FMU fully placed at the ceiling

shortcoming of FFU does not appear here. Its energy consumption is lower than that of FFU. It is easy to maintain. It is shown in Fig. 8.19.

Leakage-Preventing Layer Air Supply Outlet Fully Placed at the Ceiling and Return Air Grille on the Floor or at Both Bottom Sides

It is an air supply mode to get rid of the shortcomings by the terminals with HEPA filters. It is abbreviated with "clean air supply ceiling with leakage-preventing layer," which will be introduced in Chap. 15.

8.4.1.2 Horizontally Unidirectional Flow Cleanroom

Horizontal Air Supply with HEPA Filters Fully Placed at the Side Wall and Return Air Fully Placed at the Side Wall

This is a typical type of horizontally unidirectional flow cleanrooms, which is shown in Fig. 8.20. Fine air filters are usually installed at the return air wall in the cleanroom. But for the cleanrooms with certain purpose, such as cleanrooms for pharmaceutical production and bacteria cultivation, HEPA filters are installed on the wall for return air and fine air filters on the wall for supply air under the full circulation situation, so that pollutant particles generated from the operation indoors will not influence the pipeline system and these particles can be collected for centralized process.

The characteristic of this kind of cleanroom is that the environment with highest cleanliness can only be obtained in the first working area (the concept of first working area will be introduced in Chap. 17). When air flows to other side, the particle concentration increases gradually, which is suitable for the application of multiple air cleanliness levels. It is obvious that the construction cost is lower than vertically unidirectional flow cleanroom.

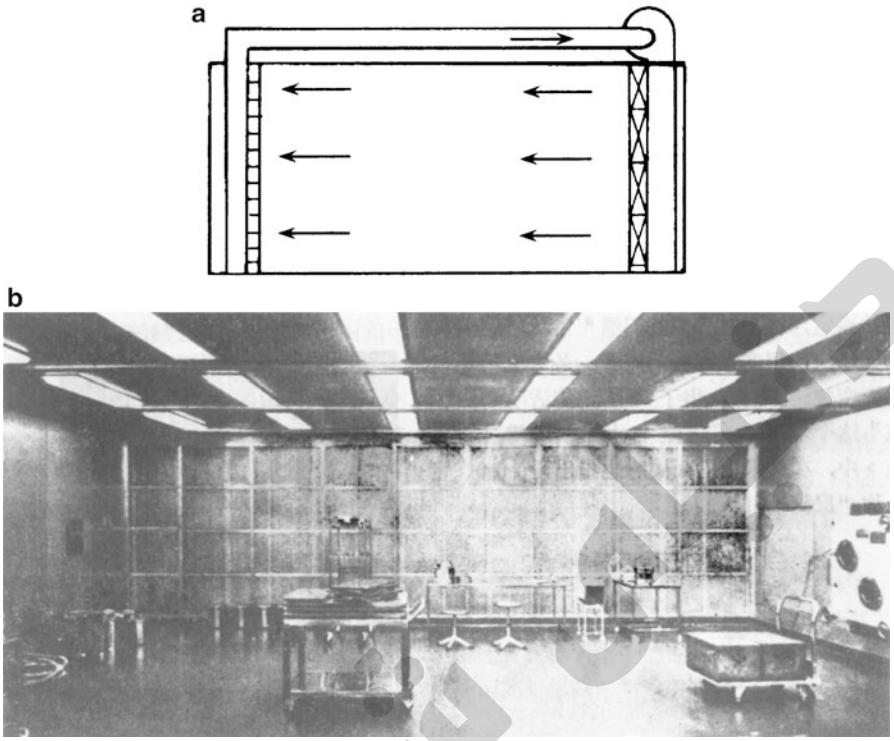

Fig. 8.20 Horizontally unidirectional flow cleanroom. (**a**) Typical structure. (**b**) Scenograph

"Tunnel" Unidirectional Flow Cleanroom

This kind of cleanroom is shown in Fig. 8.21. The difference with the above kind is as follows:

(a) On the opposite wall of the supply air wall which installs HEPA filters, there is no return air wall. It is open to the outside.
(b) There is no circulation air, and indoor air is exhausted to the surrounding environment.
(c) For this kind of cleanroom, it is not the elevated pressure that prevents the pollution from surrounding environment; instead, it is the air velocity that prevents the invasion of pollution.
(d) The temperature and humidity indoors should be the same as that of the surrounding environment.

It is customary to call it the "tunnel" unidirectional flow mode, which is the cheapest of unidirectional flow cleanrooms and is portable. It is especially useful for the assembly of large-scale equipment and temporary maintenance.

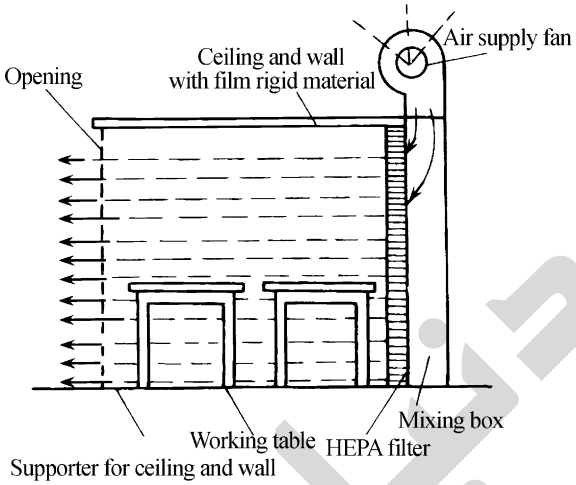

Fig. 8.21 "Tunnel" unidirectional flow cleanroom

8.4.2 Principle of Unidirectional Flow Cleanrooms

8.4.2.1 Fundamental Principle

According to various kinds of unidirectional flow cleanrooms mentioned above, the cross-sectional area almost remains the same along the flow passage from the air supply outlet and return air grille in the cleanroom. Besides, with the uniform effect by the plenum chamber and HEPA filter, velocity at the cross section is comparatively uniform. At least in the working area, the streamlines are parallel and unidirectional, and vortex does not exist. These are the three characteristics of unidirectional flow cleanrooms. That the streamlines are parallel and unidirectional means the time averaged streamlines are parallel with each other and the direction is unique, which are shown in Figs. 8.22 and 8.23.

As mentioned in the previous section, the flow in unidirectional flow cleanroom is turbulent in terms of *Re* number. So the concept of "laminar flow" in the so-called laminar flow cleanroom is completely different from that of fluid dynamics. Therefore, it is inappropriate to use the name "laminar flow cleanroom." This has also been pointed out in some standards and papers abroad. For example, British Standard BS-5295 defines the "laminar flow cleanroom" as "unidirectional flow cleanroom," where the laminar flow is marked in the bracket to take account of the habit. The former German Federal Standard VDI-2083 adopts the term "nonturbulent replacement flow," where the concept of laminar flow is used to distinguish from the mixed flow cleanroom which appeared before. The exact meaning of "laminar flow" is not stratified flow but is the replacement flow of turbulent flow. It is the gradually varied flow of turbulent flow in this chapter. In German Standard DIN1946-4 published in Dec. of 2008, the laminar flow region is divided into "laminar flow" and "low turbidity flow" (LTF). In the field of hydrodynamics, it is also termed as parallel

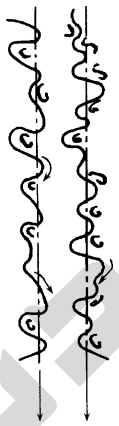

Fig. 8.22 Schematic diagram of time averaged parallel flow

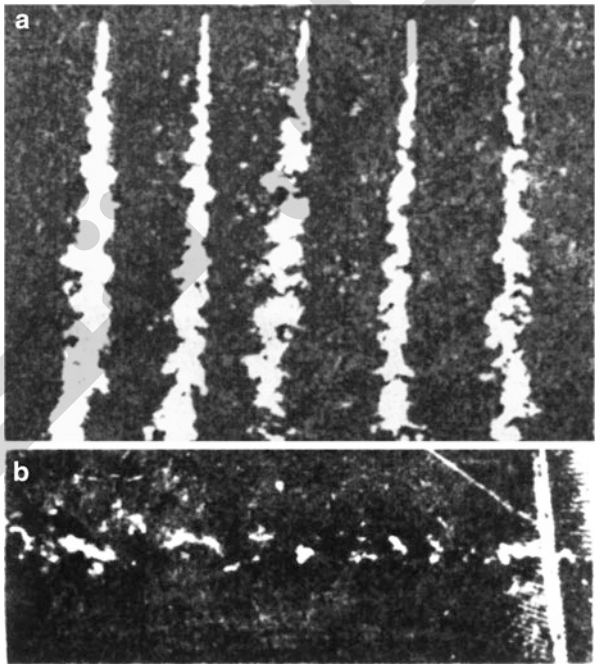

Fig. 8.23 Actual photo of the time averaged flow in unidirectional flow cleanroom. (**a**) Vertical unidirectional flow. (**b**) Horizontal unidirectional flow

flow or unidirectional flow. In 1977 the term "parallel flow" was adopted in the monograph "measures of air cleaning technology," where the customary term "laminar flow" was also mentioned. In Sweden Standard "Mikrobiologisk renheti operationsrum" published in 2011 also adopted the concept of "parallel flow," which is defined as the air flows in a certain (same) direction.

In unidirectional flow cleanroom, the cross section of whole room is full of the clean air. So it is not the mixed dilution effect of clean air on the polluted air indoors but the pushing effect of the clean air which exhausts the polluted air indoors towards

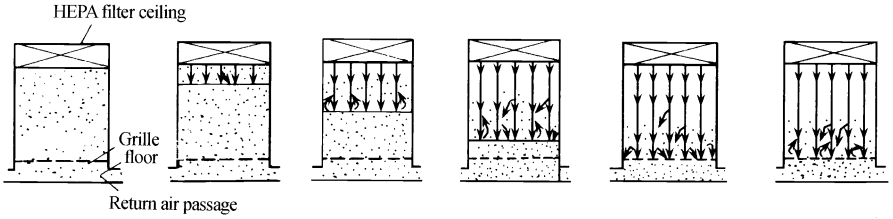

Fig. 8.24 Schematic diagram of the principle for unidirectional flow cleanroom

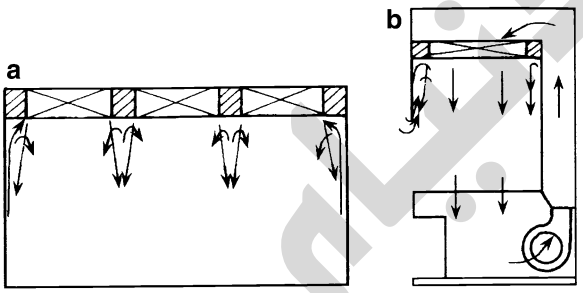

Fig. 8.25 Locally reversed flow. (**a**) Cleanroom. (**b**) Clean working bench

outdoors, so that the indoor air is cleaned. Therefore, the flow in unidirectional flow cleanroom was called "piston flow" and "pushing flow" in the former Federal Germany [8]. In the former Soviet, it was called "jet of squeezed air" [9]. Clean air is similar as an air piston, which pushes forward along the room as the cylinder. Particles are forced to move forward, and the air with high particle concentration is squeezed out of the room. The process of the squeeze is shown in Fig. 8.24.

In the unidirectional flow cleanroom and equipment, the reversed flow appears along the wall and the region under the connection of two filters. This kind of flow brings the pollution from downwards to upwards, which damages the status of "piston flow" and is very harmful. For the locally cleaning equipment with open outdoors, such as the cleaning bench, this kind of flow will induce the polluted air outdoors, which is shown in Fig. 8.25. Therefore, the noneffective area occupied by the filter frame must be reduced during the design, and the wall should be as close as possible to the effective air supply cross section of air filters.

According to the above analysis, two preliminary conditions should be met to guarantee the feature of unidirectional flow cleanroom (high level of air cleanliness and fast self-purification ability): (1) the air cleanliness level of incoming flow and (2) the status of piston flow from incoming flow.

As for the air cleanliness level of incoming flow, it is not a problem for the unidirectional flow cleanroom when HEPA filter air supply unit is used. But as for the status of piston flow from incoming flow, further analysis is needed.

According to the principle of fluid dynamics, the status of incoming flow will have important influence on the future flow directly. Air from the air supply outlet is the incoming flow of the working area.

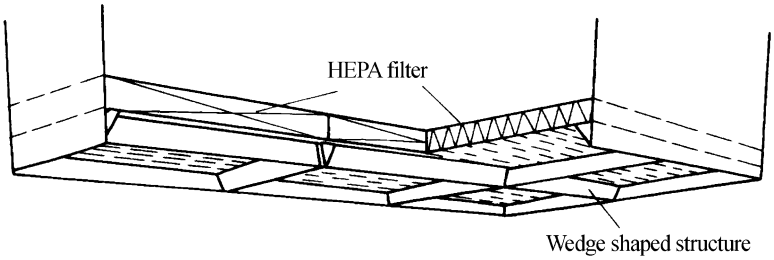

Fig. 8.26 Wedge installed under the frame of filters

When the turbulent fluctuation of the incoming flow is large, it will influence the characteristic of unidirectional flow in the future. When the cross section is not filled with the incoming flow, it will affect the formation of "piston flow" and the speed of formation. That the cross section is not full of the incoming flow is also one factor of the turbulent fluctuation for the incoming flow. Therefore, when HEPA filters are installed, the essential condition for keeping the characteristic of unidirectional flow cleanroom is "piston flow." The essential condition of "piston flow" is that the cross section is full of the incoming flow. However, compared with the pipeline, it is impractical to make the cross section full of the flow from the air supply outlet to the air exhaust grille for the whole room.

At first, it was thought that parallel unidirectional flow should fill in the whole cross section of cleanroom, which is not unfavorable from the technical and economic point of view. With the development of understanding, this kind of unidirectional flow was believed to mean all the air in a certain limited region flows parallel with a constant velocity, which could be used to restrain the generation of vortex. The room where the characteristic of unidirectional flow with clean air in the whole space is dominant can also be called "unidirectional flow cleanroom" [10]. This means that it is not required that the whole room is full of parallel unidirectional flow with uniform velocity and without vortex, but it is only required that the characteristic of unidirectional flow is dominant in the room. For example, when the flow in the space of working area is unidirectional, the room is a unidirectional flow cleanroom. The high level of air cleanliness, which is for unidirectional flow cleanroom mentioned before in related standard and measures at home and abroad, means the air cleanliness level achieved in the working area. Therefore, the measures to install streamlined diffuser intensively and full orifice supply at the ceiling are also considered to be the way to realize the vertically unidirectional flow.

In the space navigation auxiliary building for the Mars Explorer built in Feb. of 1971, the height of the room is 15 m, and streamlined diffusers were installed intensively. Unidirectional flow becomes dominant at 1.93 m distance below the air supply outlet, which provides the air cleanliness level with Class 100 [12].

In order to improve the airflow situation under the frame of air filters, wedge can be placed under the frame of filters. The angle of the wedge is about 20°, which is shown in Fig. 8.26 [11]. Special attention should be paid on these palaces during the test. If high concentration appears locally, the above reasons should be considered.

8.4.2.2 Main Features

Understanding of the above concepts is beneficial for the development of unidirectional flow cleanrooms. But two main features should also be emphasized:

1. In the past, parallel flow was emphasized in unidirectional flow cleanrooms, while the parallel of time averaged flow lines was not pointed out. Since the flow in unidirectional flow cleanrooms is still turbulent in nature, it is impossible for the instant flow lines to be parallel as the laminar flow in the fluid dynamics. It is only required that polluted air can be exhausted at the same time along all cross sections in this kind of cleanroom, so time averaged parallel flow lines are enough.
2. In the past, unidirectional flow was emphasized in unidirectional flow cleanrooms, so that the secondary contamination caused by backflow can be avoided. However, since the actual cleanroom is not empty, the flow cannot be unidirectional absolutely. In order to avoid backflow and vortex generation, the radius of curvature should be small and the angles between flow lines should be small, which means the gradually varied flow can meet the requirement of this kind of cleanroom. Therefore, the gradually varied flow is the actual status existing in unidirectional flow cleanrooms.

Therefore, when the dominant flow in cleanrooms is uniform flow or gradually varied flow, it can be called unidirectional flow cleanroom. This means when the working area (the space between 0.7 and 1.5 m above the floor) is full of unidirectional flow, this cleanroom can be treated as unidirectional flow cleanroom.

In order to obtain this effect, the area of HEPA filters horizontally placed in the plenum chamber at the ceiling should occupy a certain proportion of the total area. The ratio is defined as "ratio of blowing area"

$$\text{Ratio of blowing area} = \frac{\text{Net area of final filter}}{\text{Total area of the cross section where final filters are placed}}$$

Under usual situation (when only the frame between filters and wall is subtracted), the "ratio of blowing area" $\not<80\ \%$.

The minimum value (when a certain amount of air filter is still installed):

For vertically unidirectional flow, the "ratio of blowing area" $\not<60\ \%$.
For horizontally unidirectional flow, the "ratio of blowing area" $\not<40\ \%$.

For the decoration layer parallel to the air filter, or the so-called damping layer, its pressure drop is extreme low and it is close to the air filter, so the space between it and the air filter cannot be similar as the plenum chamber. If the "ratio of blowing area" for air filter is very small and at the same time the permeability area ratio of the damping layer (which means the ratio of clean air passage area to the whole cross-sectional area) is large, i.e., the "ratio of blowing area" for the clean air is larger than that of the air filter, clean air flow lines will connect with each other at the lower position, which is not helpful for the formation of "piston flow" in advance, which is shown in Fig. 8.27.

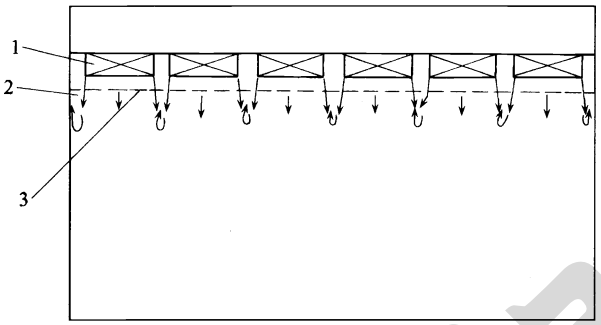

Fig. 8.27 The situation which is not helpful for the formation of "piston flow" in advance. *1* HEPA filter, *2* dead zone by damping layer, *3* decoration damping layer with small resistance

On the contrary, if the "ratio of blowing area" for the clean air is smaller than that of the air filter, air filter cannot play its role properly. But when the damping layer is the orifice plate whose porosity cannot be very large, there is a problem of jet flow lapping after the jet leaves the pore. The allowable porosity should be larger than 60 %.

There must be a certain amount of height for the combination of the plenum chamber and air filter. For HEPA filter with isolator, the height reaches 800 mm. For HEPA filter without isolator, the height reaches more than 600 mm. When the height for installation is not enough, HEPA filters were reported to be installed at the side instead of being installed horizontally. In most cases, HEPA filters cannot be installed properly at the side, and the airflow rate and the pressure drop have to be increased. Moreover, since the pressure drop of the decoration layer, i.e., the damping layer, is very small, the airflow inside the plenum chamber is very turbulent because of the side arrangement of air filters, although the "ratio of blowing area" for the clean air may be large. The turbulent incoming flow will influence the characteristic of unidirectional flow downstream greatly. Even for this case, the "ratio of blowing area" for air filters is expected to be more than 80 % with this installation mode (corresponding to the side cross-sectional area). Otherwise, the incoming flow will be more turbulent, which may cause backflow.

When HEPA filters are installed outside of the plenum chamber and the leakage-preventing layer is used at the surface of air supply outlet, the leakage-preventing layer has a certain value of pressure drop and good performance of comprehensive permeability and filtration of submicron particles (shown in Chap. 15), so the continuous clean space between HEPA filter and leakage-preventing layer is formed, and it is a closed system before the air supply outlet. Therefore, the damping layer is actually the extension of the HEPA filter terminals. The area of air permeability of the damping layer can be treated equal with that of air filters. The "ratio of blowing area" can be expressed as:

$$\text{Ratio of blowing area} = \frac{\text{Flow area of the clean area through the air supply outlet}}{\text{Total area of the cross sections on the air supply surface}}$$

8.5 Three Characteristic Indexes for Unidirectional Flow Cleanroom

The feature of unidirectional flow has never been completely and quantitatively described. Until the later twentieth century, ISO 14644-3 only generally points out that unidirectional flow is defined as "the controlled flow is parallel at the whole cross section of the cleanroom, and the velocity is stable." Three characteristic indexes describing the performance of unidirectional flow are proposed in the Chinese version of "Principle of Air Cleaning Technology" published in 1983, including the parallel degree of flow lines, the turbidity, and the lower-limit velocity. In order to realize the purpose of the unidirectional flow cleanroom, these three indexes must be satisfied.

8.5.1 Parallel Degree of Flow Lines

It is not easy for the flow lines to be unidirectional and parallel with each other completely for the unidirectional flow cleanroom. As mentioned before, the gradually varied flow can meet the requirement. The problem is that what the allowable extent of the streamline inclination angle is.

The purpose of the parallel flow lines is to prevent the particles from dispersion in the direction which is perpendicular to the flow direction. If this kind of dispersion is within the allowable range, the slight inclination of the flow lines is also allowable. Therefore, for the unidirectional flow cleanroom, there is a problem about the allowable parallel degree for the flow lines.

At first, take a look at the specification of the working area in the cleanroom at home and abroad, which is shown in Table 8.1.

It is shown from the table that the height of the unidirectional flow cleanroom should not be less than 2.7 m, which means the clear height of the working area in the American specification is comparatively large. The working area is the region where the main process occurs. So the air cleanliness level is expressed with the particle concentration in the working area. However, some auxiliary operations may occur in the place where it is above the working area, for example, opening the valve or screwing the component. Given the common height of the cleanroom and the convenience of the occupant operation, the height of these auxiliary operations and the equipment is usually less than the occupant height, which is about 1.8 m.

The lower limit of the working area specified in "Air Cleaning Technology Measures" was 0.8 m. Here the more stringent value 0.75 m is used (the height of the working table can be lower than this value).

When the staff stands up to operate, particles are released at the height of 1.8 m above the floor. It is expected that when these particles fall to the height of 0.75 m above the floor, they will not enter the region of adjacent staff which is outside of

Table 8.1 Specification for the range of the working area

Country	Above floor (cm)	Below ceiling (cm)	Working height (cm)	Remark
USA	76	92	102	Minimum room height
China	80–150		70	2.7 m

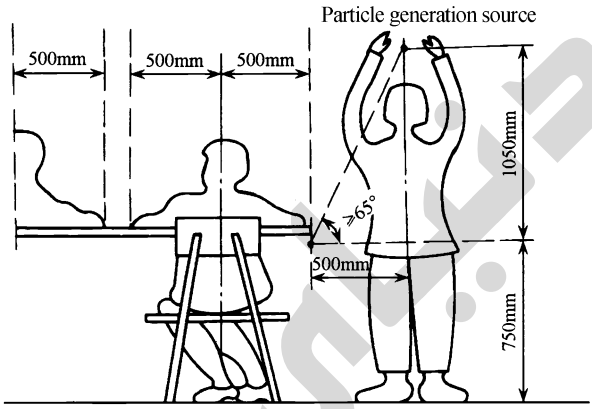

Fig. 8.28 Crosswise pollution distance for vertically unidirectional cleanroom

the working area of this staff, which will cause pollution. From Fig. 8.28, it is shown that the maximum distance between the people and the two sides is about 50 cm, when the operational area of the staff is in the middle of the table. If particles, released at the place where it is 1.05 m above the table, are still within the operational area during its fall down to the height of the table when people stand up to operate, the adjacent area will not be polluted. In this case, when the flow is inclined straight lines, the inclination angle between the flow line and the horizontal should be larger than $\text{arth}\frac{1.05}{0.5} = 65°$. For horizontally unidirectional flow cleanroom, the above value of 1.05 m can meet the requirement of the length for the first working table. So this angle of inclination can also be valid for horizontally unidirectional flow cleanroom.

If the flow lines are the profile of gradually varied flow, the angle between it and the lower-limit surface of the working area, as well as between it and the connection line with the upper-limit surface at the height 1.05 m, should be larger than 65°, which is shown in Fig. 8.29.

In the specification of acceptance check for Class 100 unidirectional flow cleanroom in the USA [2], the requirement for the parallel degree of flow lines is as follows: For the region where is 92 cm below the ceiling and 76 cm above the floor, the horizontal component of velocity should not be so large that the distance of particle dispersion is larger than 60 cm. But there's no reason to explain about this specification. Since the height of cleanroom is 2.7 m, the inclination angle of the flow lines can be obtained. It is about 61°, which is 4° smaller than the

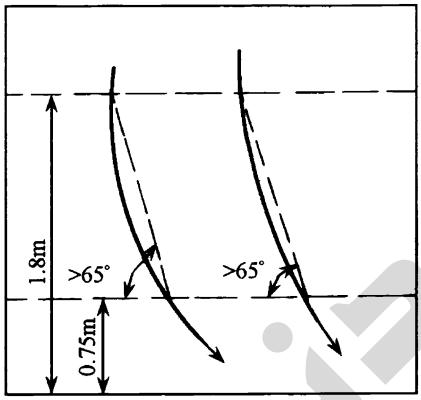

Fig. 8.29 The inclination angle of the gradually varied flow lines

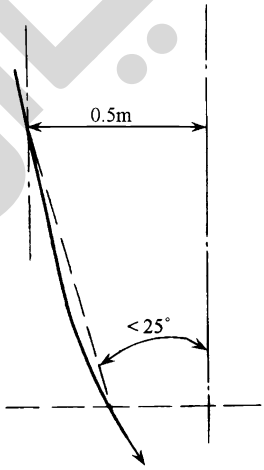

Fig. 8.30 Angle of flow lines

calculation result above. It is obvious that the requirement based on the above calculation is much higher.

According to the requirement of the parallel degree and angle, the inclination angle of each flow line should be larger than 65°, and the angle between two adjacent flow lines should be as small as possible. For example, when the angle between two closing flow lines changes from 65° to almost 90°, the flow status will change intensively and thus the vortex will be generated. In the extreme case, the angle of two flow lines is (90°–65°) = 25°. According to the illustration about the horizontal dispersion distance, the distance should not be less than 0.5 m, which is shown in Fig. 8.30. Therefore, there are two aspects for the requirement of the parallel degree: (1) the minimum of the inclination angle is about 65° and (2) flow lines incline gradually from the vertical position, and the extent of the inclination that equals to the increase of the angle per unit centimeter distance is less than 0.5°.

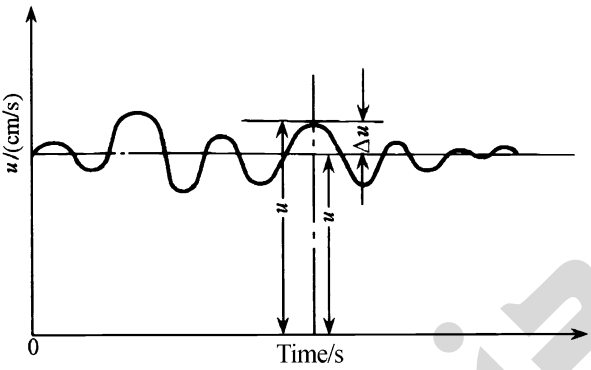

Fig. 8.31 Fluctuation of velocity field

8.5.2 Turbulence Intensity

As mentioned before, it is required for the indoor air to be uniform flow based on the essence of unidirectional flow cleanroom. Since various cross-sectional areas are the same along the streamline for uniform flow, the flow fields at each cross section are uniform. It is extremely important for the flow field to be uniform in the uniform flow cleanroom. Nonuniform flow field will increase the fluctuation of velocity, which promotes the mixture of fluid particles between fluid lines. If the flow field is nonuniform, obviously, the difference between the maximum and the minimum velocities will be large, which will generate large vortex indoors.

8.5.2.1 Fluctuation Velocity

The air velocity at a certain place indoors is not constant. When accurate velocimetry is used, the change of velocity with time can be measured, which is shown in Fig. 8.31. At any time t, the velocity u can be thought to be composed of two parts, i.e.,

$$u = \overline{u} + \Delta u \tag{8.1}$$

where

$\overline{u}$ is a positive constant value;

Δu changes with time t. It may be positive or negative, large or small. For a longer time, the time averaged value $\Delta\overline{u}$ is zero.

u is called the transient velocity, $\overline{u}$ is called time averaged velocity, Δu is called fluctuation velocity. When the velocimetry with needle is used, only the time averaged velocity can be obtained.

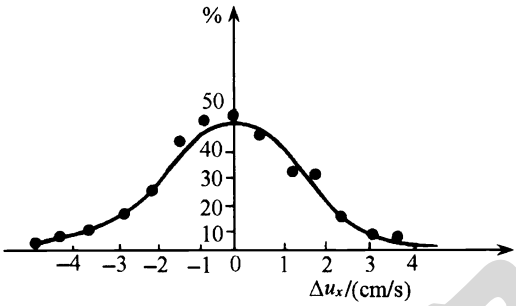

Fig. 8.32 Change characteristic of fluctuation velocity

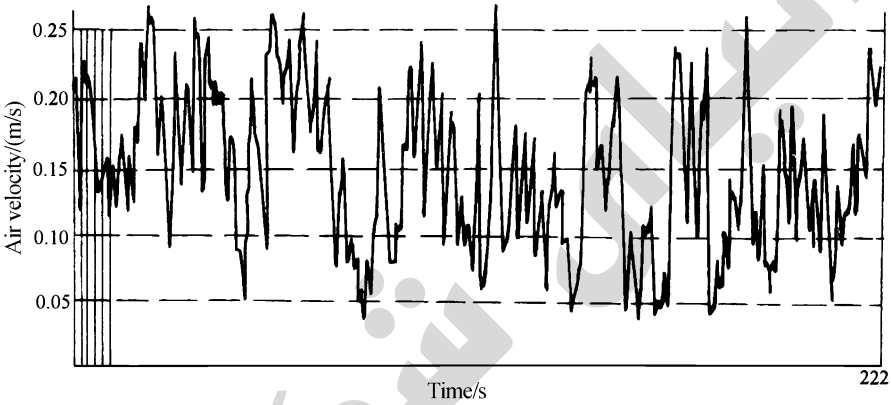

Fig. 8.33 Experimental data of the velocity

Although the fluctuation velocity may be positive and negative from time to time, the frequency of the fluctuation velocity with the smaller absolute values is large, and that with the larger absolute values is small. Normal distribution can be used to describe the variation pattern of time averaged velocity [13], which is shown in Fig. 8.32.

The normal distribution feature of the fluctuation velocity also results in the normal distribution of transient velocity. The fluctuation of velocity field in the room with air-conditioning system was measured and presented in Fig. 8.33 [14]. The abscissa is the time. The former five data are corresponding to 1 s. The total sampling time is 222 s. The ordinate is the flow velocity. The time averaged velocity of this flow field is $\overline{u} = 0.148$ m/s, and the maximum fluctuation velocity is $\Delta u_{\max} \approx 0.1$ m/s.

With the total number of 222 s, the proportion of each time period with this total number can be calculated, which can be plotted with the statistical data of velocities on the normal probability paper in Fig. 8.34. It is shown from the approximated linear line that the characteristic of the velocity meets the normal distribution.

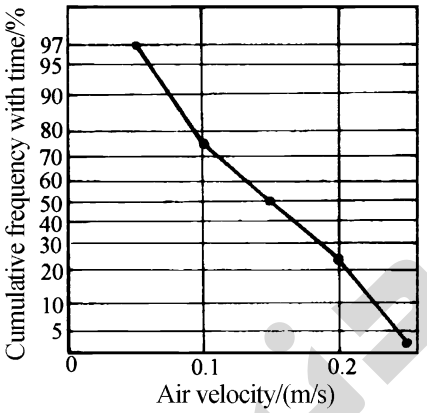

Fig. 8.34 Characteristic of the velocity change with time

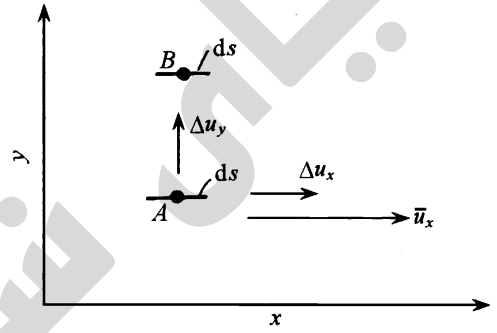

Fig. 8.35 Influence of the fluctuation velocity

There are many reasons for the fluctuation of indoor air velocity. Both the characteristic of air supply outlet and the air distribution will pose influence, and the supplied air itself is also one factor. For example, the periodic change of the gap between the fan blades will also play a role in the fluctuation of airflow.

Next the influence of the fluctuation velocity will be investigated. Suppose the time averaged velocity at the place A in the flow field is $\overline{u_x}$, which is shown in Fig. 8.35. The fluctuation velocities at the x- and y-directions are Δu_x and Δu_y, respectively. According to fluid dynamics, for the tiny area ds with the center located at A, the fluid transport mass per unit time from layer A to the adjacent layer B is $\rho\Delta u_y \mathrm{d}s$. Since there is the fluctuation velocity along x-direction, the momentum in this direction is $\rho\Delta u_y \mathrm{d}s\Delta u_x$. The force exerted on the place B by this momentum in this direction is $\rho\Delta u_x\Delta u_y \mathrm{d}s$. Therefore, the shear stress generated by the fluctuation velocity is:

$$\tau_A = -\frac{\rho\Delta u_x\Delta u_y ds}{ds} = -\rho\Delta u_x\Delta u_y \tag{8.2}$$

The time averaged value is:

$$\overline{\tau_A} = -\rho\overline{\Delta u_x\Delta u_y} \tag{8.3}$$

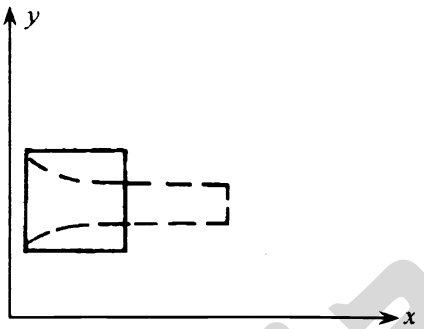

Fig. 8.36 Deformation along x- and y-directions

This is a kind of attached shear stress. The real shear stress for the velocity with fluctuation can be obtained when the pure viscous shear stress is added [15]:

$$\tau = \mu \frac{d\overline{u_x}}{dy} - \rho \overline{\Delta u_x \Delta u_y} \tag{8.4}$$

Because of the continuity of the fluid, when the fluctuation velocity Δu_x is positive for one controlled volume, there will be the extension deformation along x-direction, which will result in the shortened deformation along y-direction (Fig. 8.36). So for two-dimensional case, Δu_y will be negative, which means the sign of Δu_x and Δu_y will be opposite and that of $\Delta u_x \Delta u_y$ is negative. So according to Eq. (8.4), the shear stress τ with the fluctuation velocity will be larger than that without the fluctuation velocity. This means the friction force of the former is larger than that of the latter, which further drives the airflow to be turbulent.

8.5.2.2 Turbulence Intensity

Although the magnitude of the fluctuation velocity can be used to describe the strength of the exchange of the fluid particles between layers for indoor air, it is not easy to measure the fluctuation velocity. So it is not convenient to evaluate the turbulent flow with this index. It is hoped that it can be linked with the time averaged velocity.

According to the general monograph about the fluid dynamics, the fluctuation velocity is greatly influenced by the velocity gradient between layers. When the velocity difference between adjacent layers is very large, i.e., $\frac{\mathrm{d}\overline{u_x}}{\mathrm{d}y}$ is large, the driven effect on the current layer is strong, and Δu_x is much larger.

It is supposed that

$$\Delta u_x = \pm l_1 \frac{\mathrm{d}\overline{u_x}}{\mathrm{d}y}$$

$$\Delta u_y = +l_2 \frac{\mathrm{d}\overline{u_x}}{\mathrm{d}y}$$

When they are inserted into Eq. (8.4), the following equation can be obtained:

$$\tau = \mu \frac{d\overline{u_x}}{dy} + \rho l^2 \left(\frac{d\overline{u_x}}{dy}\right)^2 \tag{8.5}$$

The item $\mu \frac{\mathrm{d}\overline{u_x}}{\mathrm{d}y}$ in the above expression is much smaller. When it is omitted, the above equation can be simplified as [15]

$$\tau = \rho l^2 \left(\frac{d\overline{u_x}}{dy}\right)^2 \tag{8.6}$$

$$l = l_1 l_2$$

Where l_1, l_2, and l are proportional coefficients which have the dimensions of length. They are also called the mixture lengths. It is a parameter which is proportional to the actual average mixture distance and is also related to the velocity gradient.

It is shown that when the nonuniform extent of the velocity field indoors is reduced, i.e., the velocity gradient between layers is reduced, the fluctuation velocity and fluid particle exchange between layers will be smaller. This is why it is required that the uniform flow in the unidirectional flow cleanroom must be the gradually varied flow at least.

The meaning of the uniform extent of the velocity field is similar as that of the concentration degree of the particle sizes. Therefore, the similar expression can be used, i.e.,

$$\beta_u = \frac{\sqrt{\frac{\sum (u_i - \overline{u})^2}{n}}}{\overline{u}} \tag{8.7}$$

where u_i is the measured velocity at each sampling position. n is the sampling number; when it is less than 30, it can be treated as small sample, so Bessel correction should be made, namely, n is replaced by $n - 1$. $\overline{u}$ is the average velocity.

β_u can be termed as the turbulibity (or turbidity, nonuniformity of velocity). For unidirectional flow cleanroom, it should not be larger than 0.2, and meanwhile the measured self-purification time is less than 1 min. But practice has shown that it is quite difficult to fulfill this aim. In terms of the self-purification ability, it cannot be larger than 0.25 or even 0.3. If it is too large, the performance of this unidirectional flow cleanroom is rather poor. Other factors should also be referred to evaluate, which will be analyzed in detail in Chap. 10.

In the appendix of American Federal Standard 209B, the uniformity of the velocity field is specified that the local nonuniformity without disturbance should be less than ±20 %. This means all the velocities at every sampling position must be within the range of ±20 % compared with the specified velocity. It is obvious that for the empty room during the acceptance check, there is no disturbance, so the velocity at every place should be within the range of ±20 % compared with the specified velocity. Suppose all the velocities are close to the average velocity except one velocity is larger by 20 %, this velocity field is not qualified according to this specification. It is obvious that the uniformity of the whole velocity field is not considered while only one larger value is considered. In fact, this case will not pose great influence on the usage effect. When the turbulivity is calculated, the value of β_u may be smaller than 0.2 or even smaller. It means the flow field is quite uniform. It is shown that it is more appropriate to use the turbulivity at the cross section to evaluate the flow in the unidirectional flow cleanroom. The condition for the comparison of uniformity between velocity fields is also given.

In German Standard DIN 1946-4 published in 2008, one kind of more detailed division method for medical cleanroom was proposed. At the height 1.2 m above the floor, when the turbidity for every sampling point is < 5 % (Comparison is performed with 100 samples taken during 100s when probes are placed horizontally and vertically, respectively.), it is designated as "laminar flow". The case with the turbidity between 5 % and 20 % is thought as "low turbidity flow". The case with the turbidity > 20 % is thought as "turbulent flow". In fact, in German Standard it corresponds to the airflow turbidity at every sampling position (The difference of air velocity at each sampling position within the planar velocity field cannot be reflected). While in this book it means the airflow turbidity of the planar velocity field in the working area (The difference of air velocity at each sampling position within the planar velocity field can be reflected). They are different from each other. In our opinion, it is inappropriate to define the "laminar flow" in the room with the German classification method.

8.5.3 Lower-Limit Velocity [16]

8.5.3.1 Effect of Flow Velocity in Unidirectional Flow Cleanroom

There are three main reasons for the large construction cost of unidirectional flow cleanroom. Two reasons have been introduced before. The third reason is the large flow rate. As for the flow rate of the unidirectional flow cleanroom, the air change rate reached 400–500 h-1 in early times. The large flow rate is caused by the large velocity at the cross section.

In some standards, the specified velocity is large for the unidirectional flow cleanroom (e.g., in 209B, it is 0.45 m/s), and there's no difference for the different applications. Some only specifies a value for the velocity, and others suggest a value of the velocity for each kind of cleanroom. This is not convenient for the usage. For example, although the requirement of the air cleanliness for some application is extremely high, when the indoor air is not disturbed since few staff enter in or out according to the process (such as the atom clock in the metering department, which is

an equipment with very low heat generation and is placed quietly in the room), or high velocity is not allowed because of the process (e.g., the biological cleanroom for bacterial cultivation and breeding, cleanroom in hospitals), it is inappropriate to design with high velocity. In order to investigate the relationship between the velocity change and air cleanliness in unidirectional flow cleanroom, as well as the allowable lower limit of the velocity, the effect of flow velocity in this kind of cleanroom will be used. Part of the content has been introduced in Chap. 6.

There are mainly four aspects about the effect of flow velocity in unidirectional flow cleanroom:

1. When polluted air flows in all the directions, the supplied air should control not only the pollution area effectively but also the elevation height and the dispersion distance in the crosswise direction.
2. When the pollution air flows in the same direction as the supplied air, the supplied air should effectively control the polluted air towards the downstream of the dispersion area.
3. When the pollution air flows in the opposite direction as the supplied air, the supplied air should control the elevation or advance distance of the polluted air.
4. When the whole room is polluted, it should take reasonable time for the quick self purification of the room.

When the above four requirements are met, the so-called lower-limit velocity can be obtained.

8.5.3.2 Pollution Control in All Directions

Pollution in all directions means particles generated from holes emit in all directions, or particles generated from occupant's movement disperse all around.

The Encompassing Profile of Pollution to Control the Particle Source

The experimental and theoretical analysis has been performed for the encompassing profile of the pollution source in Chap. 6. The semiempirical equation has been obtained. According to the result mentioned in the previous part of this chapter, the pollution at the working height cannot disperse into the region where it is more than 0.5 m from the pollution source. With Eq. (6.50), the relationship between the ratio of the velocity v of the pollution air to that of the supplied air v_∞ and the radius of the pollution source can be obtained. For the case of $\theta = 90°$, we know:

$$R \leq 50 \text{ cm}$$

So we can get:

$$\frac{v}{v_\infty} = \frac{2,500}{32.5r^2} \tag{8.8}$$

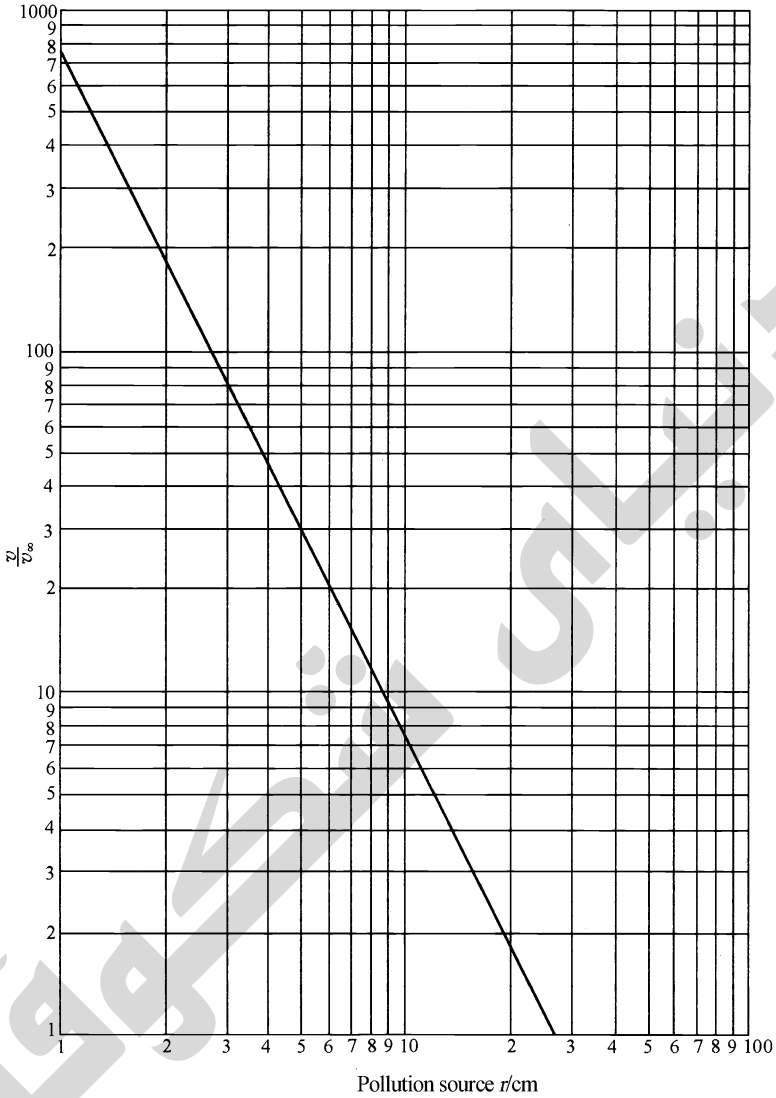

Fig. 8.37 Relationship between the scale of pollution source r and v/v_∞

Therefore the relationship between r and v/v_∞ can be plotted as shown in Fig. 8.37.

From the above equation and figure, the trend can be seen that:

1. The influence of the scale of pollution source on the pollution radius is more than that of the air velocity emitted from the pollution source. So it is the priority to control the scale of pollution source at first during the pollution control process.

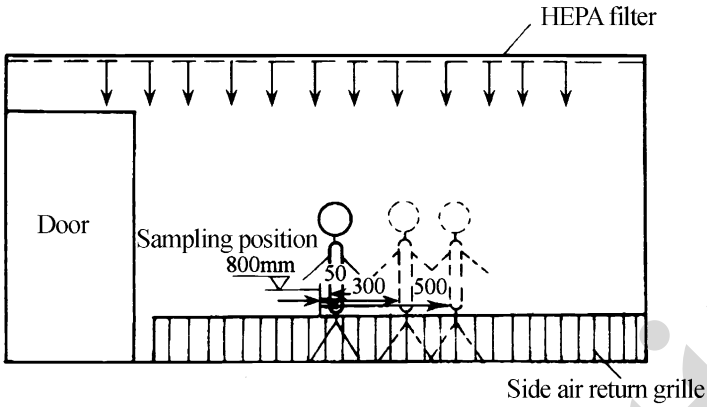

Fig. 8.38 Influencing radius of particle generation from occupant

2. When the radius of the pollution source reaches the magnitude of 10 cm, the air velocity which is larger than the polluted air velocity must be adopted. In other words, when the velocity of polluted air is smaller than that of the indoor air, the allowable radius of the pollution source should be larger than 10 cm.
3. With the same scale of the pollution source, the range of the crosswise pollution mainly depends on v/v_∞. When $v_\infty \geq 0.25$ m/s, the radius r of the pollution source can reach 3 cm. The pollution source in all directions with v/v_∞ equals 8.5 is very large.

Influencing Radius of Particle Generation from Occupant

Since occupant's activities are versatile, which becomes a complex pollution source, it is difficult to find the pollution profile through theoretical analysis and experimental investigation. For the cleanroom, the influencing radius of particle generation from occupant is the concern, which means how far the distance is from the occupant for the pollution to disappear under the supplied air velocity. According to Fig. 8.38, the experiment of this topic was performed [16]. Experimental results are plotted in Fig. 8.39. Squat stand and rotation are the types with the most energy-consumption activities. The particle generation for one activity was measured with 10 times of squatting and standing up or rotation. The particle generation quantity was presented in Table 8.2. Comparison with foreign data was also given. It is shown that the particle generation quantity is large. From the table, when the velocity reaches 0.22 m/s, the pollution concentration at 30 cm from the human body reduces to 1 pc/L, which is much lower than the upper limit of concentration for Class 100 cleanroom.

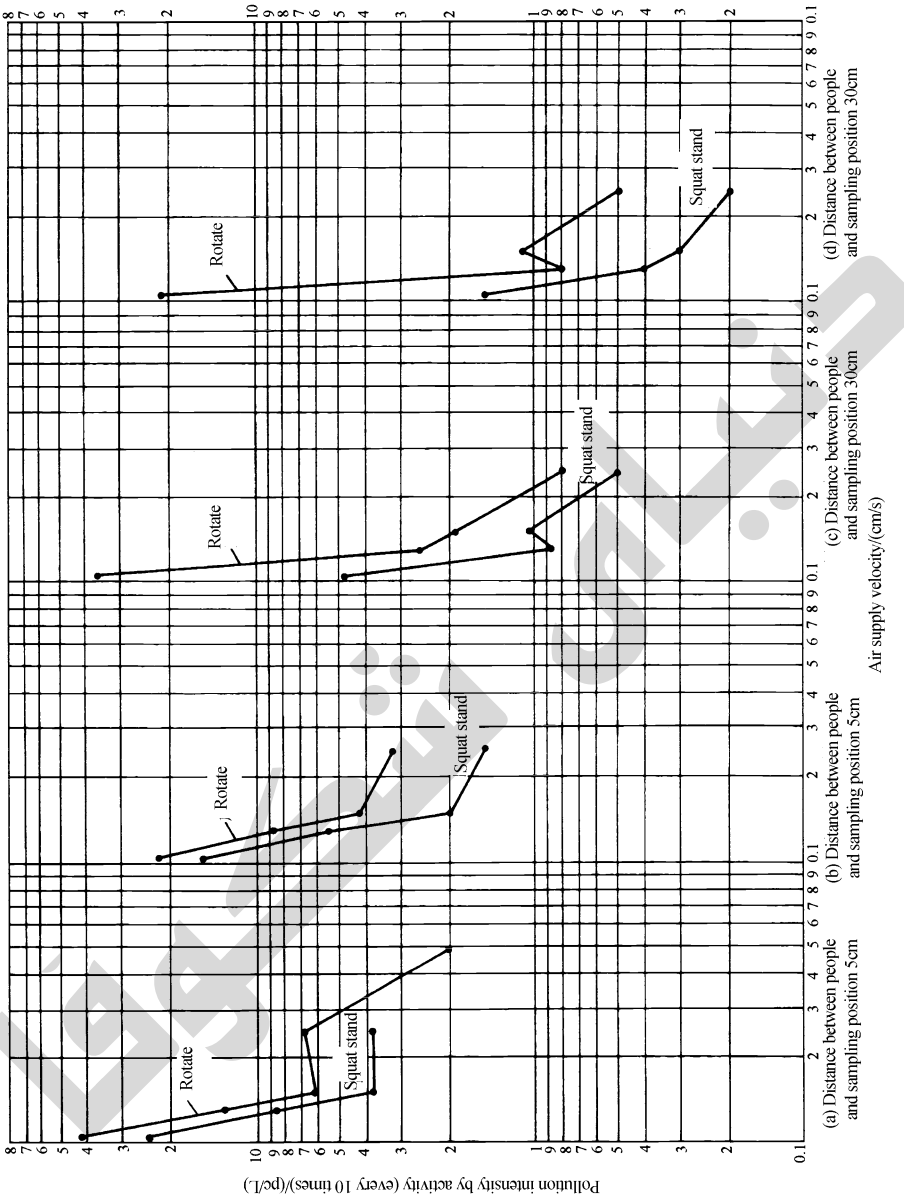

Fig. 8.39 Influencing radius of particle generation with different types of activities

8.5.3.3 Pollution Control with the Same Direction

Air should be supplied with enough velocity, so that the pollution upstream can be driven to the downstream quickly, which will not disperse outside of the

Table 8.2 Particle generation for different activities

Particle size (μm)	Particle number [pc/(p · mm)]	Working cloth	Activity intensity	Ref.
≥0.5	2×10^6–3×10^7		Perform gymnastic activity	[17]
	0.63×10^6		Head move around	
	0.85×10^6		Upper body movement	
	2.7×10^6	Clean working garment	Bend body	[18]
	2.8×10^6		March on the spot	
	$(0.25–0.5) \times 10^6$		Walk with average velocity 0.8 m/s	[19]
	0.27×10^6		Walk with velocity 110 steps/min	[20]
	2.6×10^6	Fabric working garment	Walk with velocity 110 steps/min	
	$(0.7–3) \times 10^6$	Clean working garment	Squat, stand, or rotate	[16]
≥0.3	5×10^6		Walk with velocity: 3.6 km/h	
	7.5×10^6	Clean working garment	5.6 km/h	[21]
	10×10^6		8.8 km/h	

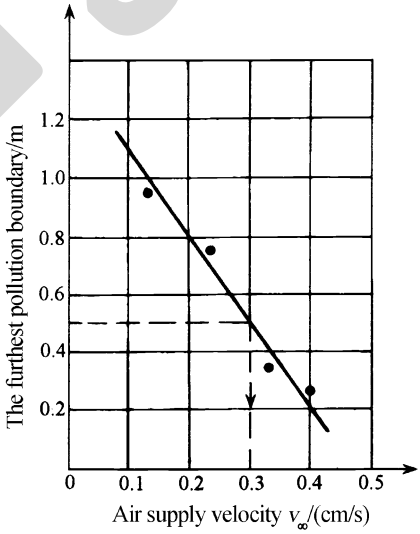

Fig. 8.40 Relationship between the crosswise pollution distance downstream and velocity

allowable range. Figure 8.40 shows the experimental results [16]. As proposed in the section about the parallel degree of fluid lines, the requirement of the crosswise distance of the fluid lines downstream is that pollution generated at the height of 1.8 m disappears at the downstream height of 0.75 m. The relationship between the distance from the projected position of the pollution source and the air velocity is given. This distance is termed as the furthest pollution boundary. The distance of

Table 8.3 Relationship between velocity and parameters of heat source

	Air supply velocity (m/s)											
	0.2		0.25		0.3		0.35		0.4		0.5	
$\triangle t$ (°C)	l (m)	R_y (m)	l (m)	R_y (m)	l (m)	R_y (m)	l (m)	R_y (m)	l (m)	R_y (m)	l (m)	R_y (m)
10	0.24	1	0.38	2	0.54	3.4	0.735	5.4	0.96	8.1	1.5	11.5
30	0.08	0.23	0.125	0.46	0.18	0.78	0.245	1.25	0.32	1.87	0.5	2.7
50	0.05	0.11	0.08	0.23	0.113	0.4	0.153	0.63	0.2	0.95	0.313	1.3
70	0.035	0.08	0.055	0.15	0.079	0.27	0.107	0.40	0.14	0.60	0.22	0.86
100	0.024	0.05	0.04	0.1	0.054	0.16	0.073	0.25	0.096	0.40	0.15	0.53
150	0.017	0.03	0.027	0.06	0.037	0.1	0.05	0.15	0.067	0.22	0.104	0.37
200	0.012	0.02	0.019	0.04	0.027	0.07	0.037	0.10	0.048	0.15	0.075	0.21

0.5 m is called the limit pollution boundary. It is shown that when the furthest pollution boundary is located in the limit pollution boundary, the air supply velocity should not be less than 0.3 m/s.

8.5.3.4 Pollution Control with the Opposite Directions

For Vertically Unidirectional Flow Cleanroom

The main pollution with opposite directions in vertically unidirectional flow cleanroom is the flow aroused from the heat source. As illustrated in Chap. 6, for the vertically unidirectional flow cleanroom with heat source inside, the necessary air supply velocity should be determined with the parameters of heat source. Or the parameters of heat source should be limited with the given air supply velocity. Or strict measures should be adopted to isolate the heat. Table 8.3 presents the relationship between velocity and parameters of heat source. In the table, l is the characteristic length of the heat object, and R_y is the equivalent radius of the planar heat source.

For Horizontally Unidirectional Flow Cleanroom

The main pollution flow with opposite directions of the horizontally unidirectional flow cleanroom is the secondary flow caused by occupant's walk. As for the magnitude of the secondary flow, it has been illustrated in detail in Chap. 6, which will not be repeated again.

8.5.3.5 Reasonable Self-Purification Time

When all the room is polluted, indoor air should be self-purified rapidly within a reasonable time period, which is greatly related to the air velocity in the cleanroom. With the increased flow velocity, the self-purification ability is stronger and the

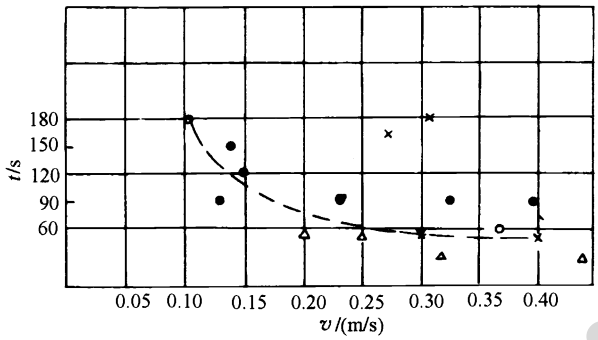

Fig. 8.41 Relationship between self-purification time and velocity: Δ vertically unidirectional flow cleanroom with grille floor [6], × measured data of the cleanroom. ○ domestic assembled vertically unidirectional flow cleanroom with full air supply at the ceiling and air return at both *bottom* sides (authenticated data), ● vertically unidirectional flow cleanroom with full air supply at the ceiling and air return at one *bottom* side

self-purification time is short, but it is not economical. Therefore, the lower limit of velocity should be determined, with which the shortest self-purification time can be guaranteed. Figure 8.41 presents the relationship between the self-purification time and velocity performed abroad and by the author.

It is shown that when the velocity is larger than 0.25 m/s, the self-purification time almost remains the same, which is about 1 min. The effect of increased velocity on shortening the self-purification time is not obvious. Therefore, it is advisable to choose the lower limit of velocity 0.25 m/s corresponding to the shortest self-purification time. As for the self-purification time of the cleanroom, it will be illustrated in detail in Chap. 10.

8.5.3.6 Comprehensive Analysis

The difference of the velocity needed to consider the above four aspects is small, which are listed in Table 8.4. According to the comprehensive conditions and the abovementioned viewpoint, it is suitable to divide the lower limit of velocity into three categories for vertically and horizontally unidirectional flow cleanroom, which are listed in Table 8.5.

It is clear that the lower limit of velocity means the minimum velocity that cleanroom should always keep. During the design process, the increased pressure drop caused by air filter should be considered. The flow rate will be reduced. So this will be used to determine the initial velocity, and it should be adjustable for the flow rate.

It should be mentioned that the data in the middle is usually fit for most cleanrooms. When there is not occupant or activity, the lower limit of velocity can be used, such as

Table 8.4 Velocity needed to control pollution [15]

Pollution control type	Air velocity (m/s) and situation
Pollution from multiple directions	
Envelope line of pollution generation	≥0.25 (this is common for ordinary pollution source)
Radius of pollution generation from people	≥0.22
Pollution from the same direction	≥0.3
Pollution from opposite directions	
1. For vertical unidirectional flow cleanroom	
Heat source	Generally determined by the size and the temperature of heat source (e.g., it is 0.64 for the heat plane with surface temperature 200 °C and size 0.3 m × 0.6 m)
Thermal plume from people	0.18–0.22
2. For horizontal unidirectional flow cleanroom	≥0.34 (the ordinary walk velocity is 1 m/s, and the maximum velocity of secondary air is considered)
	≥0.28 (the ordinary walk velocity is 1 m/s, and the average velocity of secondary air is considered)
	≥0.4 (the walk velocity is about 1.5 m/s)
	≥0.5 (the walk velocity is about 2 m/s)
Self-cleaning ability	≥0.25

Table 8.5 Suggested lower limit of velocity [16]

Cleanroom	Lower limit of air velocity (m/s)	Condition
Vertical unidirectional flow	0.12	No occupant during ordinary times or rare pass in and out, no obvious heat source
	0.3	With the general condition without obvious heat source
	≯0.5	With occupant inside and obvious heat source. If it is still not feasible to set 0.5, the size of the heat source should be controlled, and isolation measures should be taken
Horizontal unidirectional flow	0.3	No occupant during ordinary times or rare pass in and out
	0.35	General condition
	≯0.5	With higher requirement or frequent pass in and out

the night situation of ward and the equipment monitoring room without entering in and out. Experiment has been performed in the control room of the atom clock, it was found that with the velocity 0.11 m/s, the requirement is met when twice and three times of instrument check every day is done. The upper bound of the lower limit of velocity should be 0.5 m/s; otherwise, the draught effect will be felt.

The average velocity suggested for unidirectional flow cleanroom in ISO14644-4 in 2000 is: 0.2–0.5 m/s for Class 5 (equivalent with Class 100) and 0.3–0.5 m/s for

higher than Class 5. This is the first breakthrough of the specification $\not<0.45$ m/s in American Federal Standard 209. But the exact condition for choosing the value is not given. They are all within the theoretical range of lower limit of velocity shown in Tables 8.4 and 8.5.

8.6 Principle of Radial Flow Cleanroom

8.6.1 Type of Radial Flow Cleanroom

Radial flow cleanroom appeared later than turbulent flow cleanroom and unidirectional flow cleanroom. It is a novel type of cleanroom with the significance of energy saving. It has application abroad, but it is almost blank in China.

This kind of cleanroom was ever termed as "arrow flow cleanroom." However, the concept of "arrow" cannot completely represent the meaning of the radial streamline. Since any streamline can be called "arrow," author calls it as "radial flow cleanroom" [22].

The type of radial flow cleanroom is shown in Fig. 8.42, where fan-shaped, semispherical, or semicylinder air supplier combined with corresponding type of HEPA filter is used to supply air at the top side of the room and air is returned at the opposite bottom side (Fig. 8.43).

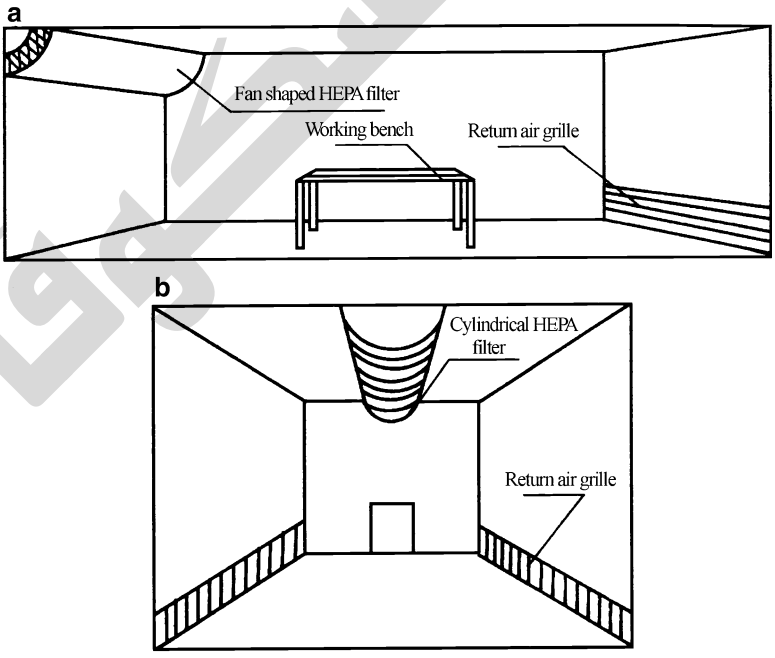

Fig. 8.42 Schematic of radial flow cleanroom. (**a**) Fan shaped air supply outlet. (**b**) Cylindrical air supply outlet

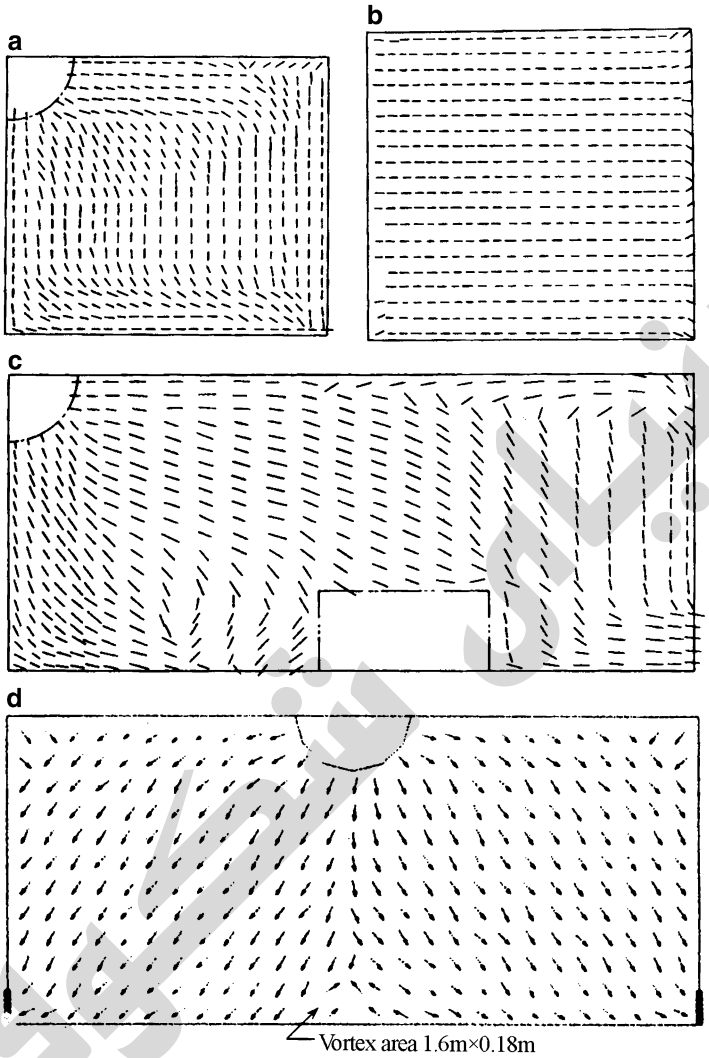

Fig. 8.43 Calculated flow field of radial flow cleanroom. (**a**) Profile of as-built room. (**b**) Horizontal profile of as-built room. (**c**) Profile of at rest room (with fan shaped air supply outlet). (**d**) Profile of as-built room (with fan shaped air supply outlet)

8.6.2 Principle of Radial Flow Cleanroom

8.6.2.1 Fundamental Principle

The principle of radial flow cleanroom is different from the mixture and dilution effect of turbulent flow cleanroom and also different from the "piston" flow of unidirectional flow cleanroom. The streamlines are neither unidirectional nor

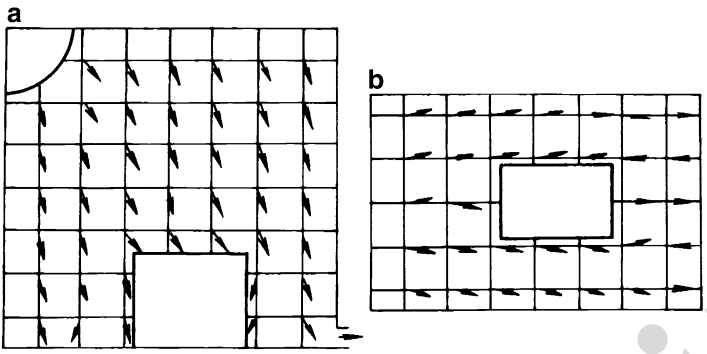

Fig. 8.44 Experimental flow field of radial flow cleanroom with fan-shaped air supplier. (**a**) Profile of at rest room. (**b**) Vertical profile of at rest room

parallel. This is the same as the turbulent flow cleanroom. But the difference with the turbulent flow cleanroom is that streamlines do not intersect. So it is not the mixture effect, but the squeezing effect with "inclined push" instead of "flat push" that works in this kind of cleanroom.

8.6.2.2 Feature of the Flow Field

A study about this kind of cleanroom has been reported in China [23–25]. Calculated and experimental flow fields in the above literatures are presented in Figs. 8.34 and 8.44.

8.6.2.3 Feature of the Concentration Field

With the method of smoke release ball at the working area, the experimental data about the concentration field in radial flow cleanroom with fan-shaped air supplier were obtained, which is shown in Fig. 8.45 [24]. The air change rate with circulated air in cleanroom is $\frac{785\text{m}^3/\text{h}}{1.5\times1.5\times1} = 349\ \text{h}^{-1}$. The velocity of polluted air $v = 1.5$ m/s. The flow rate is 16 L/min. The pollution source is a Balan cigarette.

The numerical simulation of the concentration field is presented in Fig. 8.46 [24]. In the figure, "1" presents the concentration of particles with diameter $\geq$0.5 μm less than 1 pc/L. "2" represents the concentration less than 3.5 pc/L. "3" represents the concentration $\geq$3.5 pc/L. The trend of concentration distribution is almost consistent with experimental result.

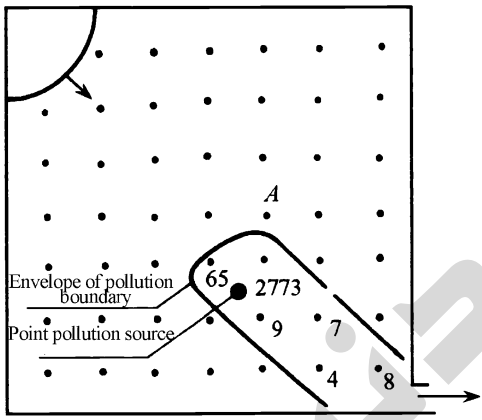

Fig. 8.45 Measured concentration field in as-built radial cleanroom

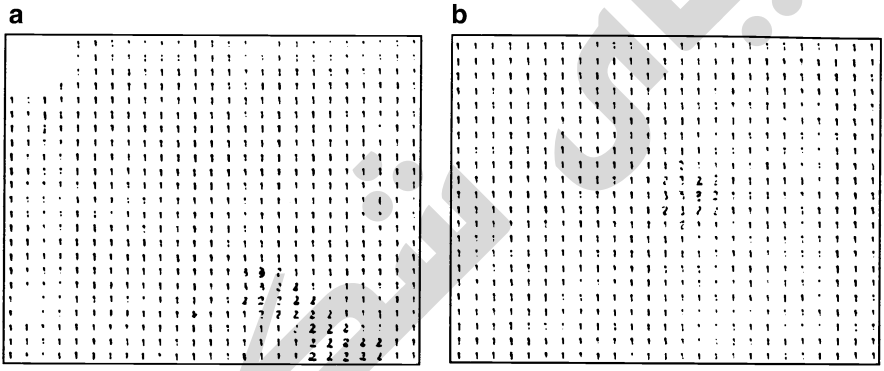

Fig. 8.46 Calculated concentration field in radial flow cleanroom. (**a**) Profile of as-built room. (**b**) Horizontal profile of as-built room

8.6.2.4 Basic Features

From the comparison between calculated and experimental result in the above literature, the radial cleanroom is thought to have the following features:

1. The streamlines do not intersect in the as-built situation. The lateral diffusion between streamlines is very weak. At the upper corner of the downwind side, there is a very weak backflow, which will not influence the exhaust of polluted flow to downwind. Although the detention time of pollution is longer than that of unidirectional flow cleanroom, it is shorter than the self-purification time of turbulent flow cleanroom, which meets the requirement for the feature of cleanroom which can exhaust the polluted flow in a comparatively short or even the shortest route.

2. In the status of at-rest, eddy appears on the downwind side or two sides of the obstacle. So in this kind of cleanroom, obstacles should be avoided along the streamline. For example, the bottom of the table shown in Fig. 8.44 should be perforated.
3. In the cleanroom with fan-shaped air supplier, the influence of return air grille on the flow field and concentration field is very small. In the cleanroom with semicylinder air supplier, return air grille installed at low position is good for pollution control. The height of return air grille is usually 0.3 m.
4. The appropriate design parameters for radial flow cleanroom were proposed by experimental result:

   For fan-shaped air supplier,

$$\frac{\text{Room height}}{\text{Room length}} = 0.5 - 1$$

   For semicylinder air supplier,

$$\frac{\text{Room height}}{\text{Room length}} = 0.25 - 0.5 \text{ (room width should be between 6 and 12 m)}$$

$$\text{Area off an shaped air supplier} \approx \frac{1}{3} \times \text{Area of the side wall where air supplier is placed}$$

$$\text{Cylinder radius of semicylinder air supplier} \approx 0.5\text{m}$$

$$\text{Area of return air openings whenfanshaped air supplier is used} \approx \left(\frac{1}{5} - \frac{1}{6}\right) \times \text{Area of air suppliers}$$

$$\text{Height of return air grille when semicylinder air supplier} \approx 0.3\text{m}$$

$$\text{Air supply velocity with fan} - \text{shaped air supplier} = 0.45 - 0.55\text{m/s}$$

$$\text{Air supply velocity with semicylinder air supplier} = 0.45 - 0.6\text{m/s}$$

In short, although the air distribution in radial flow cleanroom is not uniform as that in unidirectional flow cleanroom, both air supplier and air filter are much complex than the common case, and eddy is easily formed in the status which is not as-built. The construction cost is much lower than that of unidirectional flow cleanroom. The surface cleanliness level can reach Class 100. So this is one kind of cleanroom worthwhile for attention.

8.7 Pressure of Cleanroom

In order to prevent the cleanliness of cleanroom from the contamination by adjacent room, the pressure of the cleanroom is maintained to a value which is higher or lower than adjacent room. This is the important feature of cleanroom which is different from ordinary air-conditioning room. This is also the important component for the principle of cleanroom. It is usual to set a positive differential pressure (abbreviated as "positive pressure" in the following section) between cleanroom and the adjacent environment, which is the situation for industrial cleanroom and ordinary biological cleanroom. Negative differential pressure is only maintained in special biological cleanroom (abbreviated as "negative pressure" in the following section).

8.7.1 Physical Meaning of Differential Pressure

When doors, windows, and any kinds of pore exist between cleanroom and adjacent space, a relative positive pressure should be kept between them when these doors, windows, and pores are closed. The value of differential pressure corresponds to the resistance of the air flowing through the closed aperture with a certain amount of flow rate. So the differential pressure reflects the resistance characteristic of the aperture.

Suppose pressures at both sides the aperture are P_1 and P_2, respectively. The differential pressure according to the hydrodynamics theory is:

$$\Delta P = P_1 - P_2 = (\xi_1 + \xi_2)\frac{v_c^2 \rho}{2} + h_w \text{ (Pa)} \tag{8.9}$$

where

h_w is the frictional resistance for air flowing through the aperture. Since the aperture is very short, and v_c is usually smaller than 4 m/s with the usual differential pressure in the cleanroom, h_w can be neglected.

ξ_1 is the local resistance of abrupt contraction. Since the cross-sectional area of the aperture is extreme small, $\xi_1 \approx 0.5$.

ξ_2 is the local resistance of abrupt expansion. With the same reason, $\xi_2 \approx 1$.

Therefore

$$v_c = \frac{1}{\sqrt{\xi_1 + \xi_2}}\sqrt{\frac{2\Delta P}{\rho}} = \varphi\sqrt{\frac{2\Delta P}{\rho}}(\text{m/s}) \tag{8.10}$$

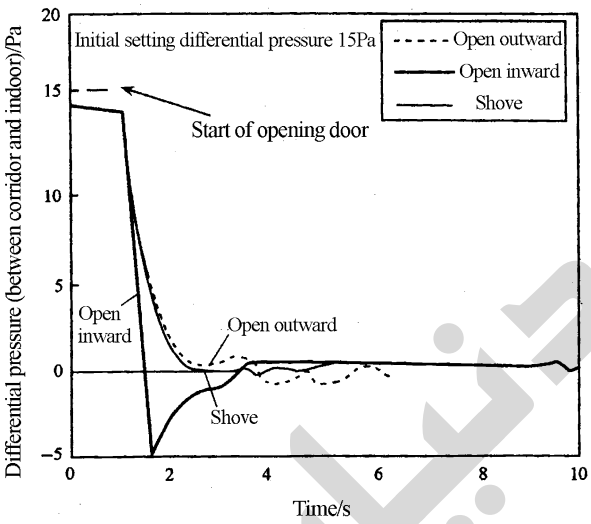

Fig. 8.47 Variation of differential pressure with time during opening of door

$$\varphi = \frac{1}{\sqrt{\xi_1 + \xi_2}} = 0.82 \quad \text{(called flow velocity coefficient)}$$

A study by author has shown the actual value of φ is usually between 0.2 and 0.5 [26].

The relationship between the flow rate and the resistance through the aperture is:

$$Q = \varepsilon F \varphi \sqrt{\frac{2\Delta P}{\rho}} = \mu F \sqrt{\frac{2\Delta P}{\rho}} \tag{8.11}$$

where

ε is the contraction coefficient;
μ is the flow rate coefficient, and it is usually 0.3–0.5.

If the aperture structure is very complex, the above proportional relationship between Q and the square of ΔP is no longer valid; instead, Q is linearly proportional to 1–1/2 order of ΔP. But the above calculation expression can also be used for the aperture of cleanroom since the surface is very flat and the aperture is not complex.

Since the differential pressure reflects the resistance feature of aperture relative to the region outside of the room, the resistance will disappear when the aperture is open, so the differential pressure will disappear accordingly. So the differential pressure appears and plays its role only when the door is closed.

Figure 8.47 shows the time characteristic of the differential pressure [37].

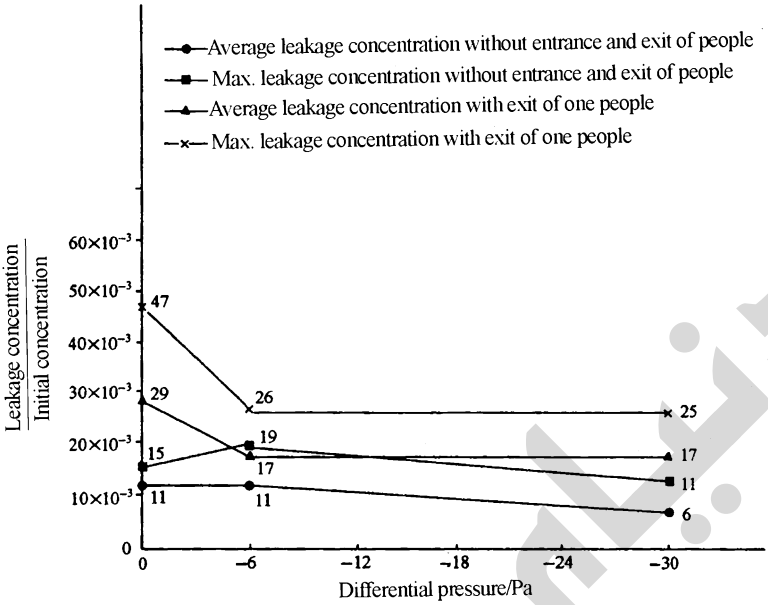

Fig. 8.48 Relationship between the concentration of leakage and the differential pressure

8.7.2 Function of Differential Pressure

The general function of differential pressure has been introduced in the beginning of this section. From the theoretical point of view, there are two functions for differential pressure:

(1) With the closed door and window, it can prevent the infiltration of pollution outside of the cleanroom into the room.
(2) At the moment of opening the door, it can provide enough air flowing outwards. The amount of airflow entering the room by the opening of door and the entering of the occupant should be reduced as much as possible. When the door is open, the direction of airflow should be guaranteed to be outwards, so that the pollution generated can be minimized.

As for item (1), it does not mean the larger the differential pressure is, the stronger the ability to prevent the pollution infiltration is. It is known from Eq. (8.10) that in theory the differential pressure 0.22 Pa is enough, which can generate the air velocity 0.5 m/s at the aperture. A study performed by author has shown that the variation of blockage effect is relatively large when the differential pressure changes from 0 to 6 Pa while it is relatively small when the differential pressure varies from 6 to 30 Pa, which is shown in Fig. 8.48.

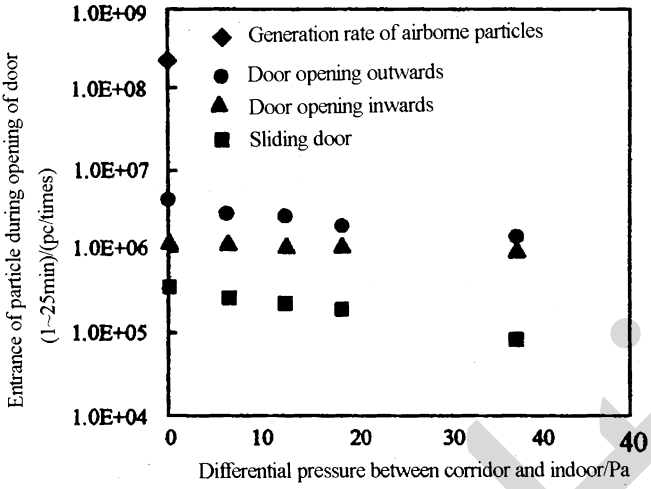

Fig. 8.49 Number of particles entering into the negative pressure cleanroom with the closed door

Figure 8.49 presents the data from Japan [27]. When the differential pressure increases from 0 to 6 Pa, the dispersion amount of particles reduces by about 40 %. But it only reduces by 60 % when the differential pressure increases from 0 to 30 Pa.

The above results are basically consistent.

As for item (2), in the initial standard about cleanroom, i.e., American Air Force Design Manual (AD295408, TDR-62-138 Report) and US Federal Standard 209A, only the second item was mentioned. From the calculation introduced later, we can see that it is difficult to realize the second item. Therefore, since the beginning of 209B, the first item was made as the compulsory one, while the second item was optional and used for guidance. It is the same for NASA NHB 5340-2. In British Standard BS5295(I), only the first item was mentioned. Experiment has shown that the second item is very important for the cleanroom with cleanliness Class 100 or higher. So in the standard "Test and Acceptance Evaluation of Industrial Cleanroom" (AACC CS-6 T) published by American Association of Contamination Control and other standards published by some companies, except for the requirement of differential pressure between inside and outside of the cleanroom when the door is closed, the upper limit of particle concentration at 60 cm away from the door in the cleanroom with air cleanliness Class 5 or lower was specified. It is aimed to prove that the invasion flow from outside of the room is extreme small and the invasion flow is resisted by the external flow. The requirement of this item is not so strict in Chinese Industrial Standard GB50591-2010 *Code for construction and acceptance of cleanroom*. This is the compulsory standard for cleanroom with air cleanliness Class 5 or higher. The effect of differential pressure is not clearly presented in related standards and regulations in China before this standard. But in national standard GB 50591 implemented since 2010, this is required for cleanroom with air cleanliness Class 5 or higher.

8.7.3 Determination of Differential Pressure to Prevent Leakage from Gap Between Cleanroom and Adjacent Room

From Eq. (8.10), the velocity can be 1.06 m/s when the positive pressure between cleanroom and the adjacent room is $\Delta P = 1$ Pa. This air velocity with this magnitude can prevent the infiltration of air flowing through the aperture. Of course 1 Pa is an extreme small value and not stable. For two rooms connecting with each other, their pressures will vary with waxing and waning effect for the differential pressure with 1 Pa. When the fresh air varies with the volume corresponding to the need of one people, i.e., dozens cubic per hour, the change of differential pressure will be larger than 2 Pa. This easily occurs because of the untimely adjustment of air filter and valve. So the differential pressure needed for the room should be a little larger. In those countries (such as China and Japan) where the metric system was used in the past, mmHg was used to express the differential pressure. So the minimum unit, namely, the half of 1 mm H_2O (5 Pa), is the minimum readable value. It is 5 times larger than 1. So 5 Pa is habitually used as the necessary value of differential pressure. In those countries (such as the UK and USA) where the imperial system of unit was used, inch H_2O was used to express the differential pressure. So the minimum unit, namely, the half of 0.1 in. H_2O (1.27 mm H_2O, 12.4 Pa), is the minimum readable value. So 0.05 in. H_2O is habitually used as the necessary value of differential pressure.

8.7.4 Determination of Differential Pressure to Prevent Leakage from Gap Between Cleanroom and Outdoor (or the Room Open to the Atmosphere)

Among all kinds of the apertures and pores connected to atmosphere, apertures, doors, and windows are the most common. Even for the sealed windows, infiltration will occur under the effect of wind pressure if the indoor pressure is negative. When air flow is perpendicular to the building envelop, positive pressure will be formed at the weather side and negative pressure at the lee side, which is shown in Fig. 8.50. The pressure at the weather side is:

$$p = C\frac{u^2\rho}{2} \text{ (Pa)} \tag{8.12}$$

where

u is the calculated infiltration velocity at the weather side (m/s);
ρ is the air density, and at normal temperature it is 1.2 kg/m^3;
C is the wind pressure coefficient, which can be set 0.9 on average.

Calculated infiltration velocity at the weather side is related to many factors, including air velocity at the weather side, building shape, layer height, orientation,

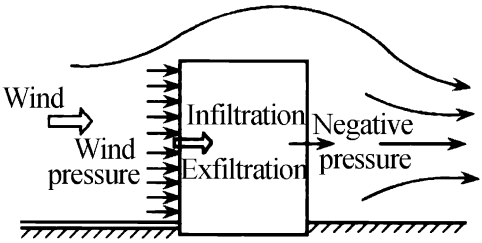

Fig. 8.50 Pressure on the wall by wind

Table 8.6 Calculated air velocity at various orientations in ten Chinese cities

City	N	NW	W	SW	S	SE	E	NE	Partition of air velocity regions
Urumqi	1.0	0.9	0.3	0.3	0.6	0.3	0.3	0.3	I, weak
Xi'an	0.8	0.3	0.3	0.7	0.7	0.3	0.3	1.0	
Hohhot	1.8	2.8	1.1	0.3	0.3	0.3	0.3	0.3	II, intermediate
Shenyang	3.6	2.5	0.3	0.3	1.5	0.3	0.3	2.0	
Tianjin	3.8	3.8	1.5	0.3	0.3	0.3	0.3	1.8	
Zhangjiakou	4.0	4.0	1.2	0.3	0.3	0.3	0.3	1.4	
Beijing	4.5	4.2	1.4	0.3	0.3	0.3	0.3	2.7	
Harbin	2.2	4.1	4.7	5.2	4.9	2.5	0.3	0.3	
Dalian	6.6	5.6	3.0	3.4	3.4	0.9	0.3	5.0	III, strong
Qingdao	7.0	7.0	4.5	2.9	3.6	3.4	2.0	4.7	

and temperature difference. If the assurance rate is set larger than 90 %, it can be calculated by equation. Table 8.6 shows the calculated air velocity at various orientations in ten Chinese cities [28]. The trend is that it is the strongest in the region near the ocean. It is in the middle for cities in eastern area. It is weak in cities like Xian and Urumqi.

If the middle zone is selected, the maximum air velocity can be set 5 m/s, so ΔP =14 Pa, which is larger than the value 10 Pa specified in current standard by 40 %. If it is much stricter, 6 m/s can be used as the calculation basis, so ΔP = 20 Pa. Of course, this is not the strictest situation.

8.7.5 Determination of Differential Pressure to Prevent Air Pollution During the Open of Door in Turbulent Flow Cleanroom

When people enter Cleanroom B from Cleanroom A (shown in Fig. 8.51), it was measured that at the moment people enter the room along the direction of door, the air velocity generated at the entrance is within the range 0.14–0.2 m/s.

At the moment people enter the room against the direction of door, the air velocity generated at the entrance is within the range 0.08–0.15 m/s, which is

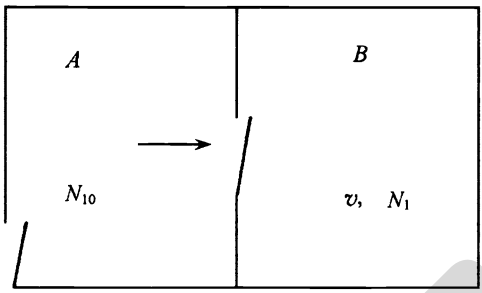

Fig. 8.51 Situation of occupant's entrance into cleanroom with the open door

smaller than the previous situation. From measurement, it is found that only when people enter the room and the door is open, the air velocity reaches the maximum, and it lasted for 2 s.

The flow rate by the entrance of people into the room is:

$$\Delta V = \text{human body area} \times 0.2\ \text{m/s} \times 2\ \text{s} = 1.7 \times 0.4 \times 0.4 = 0.27\ \text{m}^3$$

Next two situations will be discussed:

1. When the particle concentration of the entrance flow is 10 times higher than N which is inside the room, namely, it corresponds to the air cleanliness lower by 1 level, and the unfavorable volume V of the cleanroom is assumed 25 m^3 (the less it is, the more disadvantage it will be).

Suppose two people enter the room, the increased ratio of indoor particle concentration by the entrance flow is (here the particle generation from people is not considered, which is needed for the design of cleanroom; transient self-purification of indoor air circulation is also not considered):

$$\frac{2\Delta V \times 10N + (V - 2\Delta V)N}{VN} = \frac{0.27 \times 2 \times 10N + (25 - 0.27 \times 2)N}{25N} = \frac{29.86}{25} = 1.19$$

This means the indoor particle concentration increases by 1.19 times instantaneously because of the entrance of two people. Since normal concentration indoors N should be less than the upper limit of concentration corresponding to the related air cleanliness, 1/3–1/2 of this value is used during the design process (refer to Chap. 13 about the design calculation). The cleanroom is operated in the limit of 2/3, i.e., 0.7 N, for most of the time. So there is an ascensional range for the allowable concentration less than N. It is appropriate to set this range 0.2 N, which means the increase of instantaneous value can be not larger than 1.2 N. The larger the cleanroom volume is, the less the increase of the ascensional range will be.

So when people enter room B from room A, where the air cleanliness of Room A is one class lower than that of Room B, the disturbance of entrance does not pose any threat for the air cleanliness of Room B, and self-purification will complete within several minutes. The detailed information is shown in Sect. 10.8.

2. When the particle concentration of the entrance flow is 100 times higher than N which is inside the room, namely, it corresponds to the air cleanliness lower by 2 levels, and the volume V of the cleanroom is assumed 25 m^3, so we know:

$$\frac{2\Delta V \times 100N + (V - 2\Delta V)N}{VN} = \frac{0.27 \times 2 \times 100N + (25 - 0.27 \times 2)N}{25N} = \frac{78.5}{25} = 3.14$$

This means the indoor particle concentration increases by 3.14 times instantaneously at most.

If the limit to surpass the corresponding concentration is set 1.2 N, the following expression can be written:

$$\frac{2\Delta V \times 100N + (V - 2\Delta V)N}{VN} \leq 1.2$$

$$V \geq \frac{198\Delta V}{0.2}$$

When $\Delta V = 0.27$ is inserted, we can obtain $V \geq 267$ m^3.

This means when the volume of the cleanroom is larger than 270 m^3, the concentration can be increased instantaneously by 1.2 times at most when two people enter in.

Let $V = 25$ m^3, the allowable air velocity intruding into the cleanroom can be obtained as follows:

$$\Delta V = 1.7 \times 0.4 \times v = \frac{0.2 \times 25}{198}$$

So

$$v = \frac{0.2 \times 25}{0.68 \times 198} = 0.04 \text{ m/s}$$

So the squeezing velocity from the cleanroom is:

$$u = 0.2 - v = 0.16 \text{ m/s}$$

Table 8.7 Leakage flow rate through non-seal door

Differential pressure (Pa)	4.9	9.8	14.7	19.6	24.5	29.4	34.3	39.2	44.1	49
q [$m^3/(h \cdot m)$]	17	24	30	36	40	44	48	52	55	60

When it is the single-leaf door, and the open area is 1.5 m^2, the flow rate of positive pressure needed is:

$$1.5 \times 0.16 \times 3{,}600 = 864 \text{ m}^3/\text{h}$$

It is quite difficult for the small room with volume 25 m^3. So other measures are needed, which is shown in Sect. 8.8 about the buffer chamber.

If $\Delta V = 75$ m^3, we can obtain $n = 0.08$ m/s, which corresponds to the flow rate with positive pressure 432 m^3/h.

The flow rate Q with positive pressure can be calculated with the following expression:

$$Q = \alpha_1 \alpha_2 \sum (ql) \tag{8.13}$$

where

α_1 is the safety coefficient and the suggested value is 1.2;
α_2 is the coefficient when both the door aperture and other apertures, and the suggested value is 1.2;
q is the leakage flow rate per unit length through non-seal door [$m^3/(h \cdot m)$], and it can be found in Table 8.7 [29];
l is the aperture length of non-seal door (m). For single-leaf door, it is 6 m.

It is calculated that only when the differential pressure is 39.2 Pa (4 mm H_2O), the flow rate with positive pressure can be 449 m^3/h. When the requirement of 432 m^3/h is satisfied, the air change rate of the flow rate with positive pressure is equivalent to 6 h^{-1}, which is the flow rate of fresh air (this value is usually not surpassed for other applications for the requirement of the fresh air).

If the aperture is very small, with the requirement of relative large flow rate during the process of opening the door, the differential pressure needed should be above 40 Pa, which will influence the process of opening the door and generate noise easily. So in terms of this aspect, except the strict requirement for the sealing of other places, the requirement for the door is not necessarily strict. For example, there is a certain aperture between the door and the floor, which is easy for the manufacture and open of the door but also for prevention of the particle generation because of the friction by the sealing strip. It can also adapt to the comparatively large flow rate with positive pressure under the specified differential pressure, so that part of the invasion flow can be offset. If the calculated flow rate with positive pressure through the aperture is not enough, the flow rate can be increased and the excess pressure damper can be installed. The excess pressure damper is used to

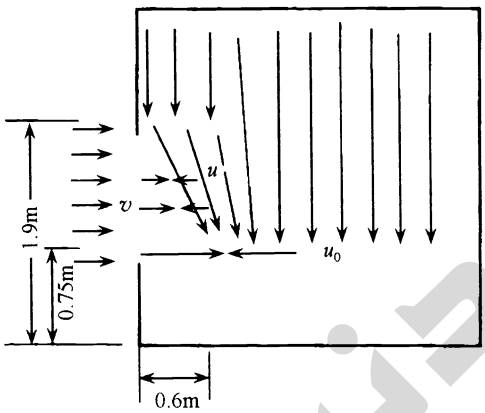

Fig. 8.52 Allowable depth of invasion flow through the door hole

exhaust the superfluous flow rate. The room pressure decreases once the door is open, then the excess pressure damper turns small automatically. The pressurized air flows outwards with the required velocity to offset the invasion-polluted flow rate.

There is another opinion for this aspect, which requires the door to be very sealed (actually it is hard to be realized). The method of constant exhaust system is adopted. Most flow rate of the positively pressurized air is exhausted when the door is closed. When the door is open, most positively pressurized air is still exhausted, and the available flow rate outwards is extreme less, which cannot meet the requirement of the second item about the differential pressure. So this method cannot completely solve the pollution problem from outside (suppose this pollution exists). If necessary, the buffer chamber should be placed, which will be analyzed in detail later. If it is not allows for the indoor air flowing outwards, the cleanroom should be designed as negative pressurized.

8.7.6 Determination of Differential Pressure to Prevent Air Pollution During the Open of Door in Unidirectional Flow Cleanroom

The ability of anti-disturbance is extremely strong for the unidirectional flow cleanroom, since the self-purification time is extremely short (analyzed in detail later). The pollution brought by the invasion flow during the opening of the door will be exhausted by the unidirectional flow quickly, and it is impossible to exchange the air transversely. So this problem should not be considered during the determination of the differential pressure.

But according to the requirement of *Code for construction and acceptance of cleanroom* (GB 50591-2010) for cleanroom with air cleanliness Class 5 or higher, the indoor air cleanliness level at 0.6 m from the door during the opening of the door should not be lower than the corresponding air cleanliness level with the negative pressure. This means the pressurized air should prevent the instantaneous invasion flow from entering into the place 0.6 m from the door, which is shown in Fig. 8.52.

Table 8.8 Recommended differential pressure

Purpose		Difference between turbulent flow cleanroom and the adjacent room with air cleanliness level lower by one Class level (Pa)	The same as the left condition but with air cleanliness level lower by more than one Class level (Pa)	Difference between unidirectional flow cleanroom and the adjacent communicating room (Pa)	Difference between cleanroom and outdoors (or the space communicating with outdoor air)
General	To prevent infiltration through gap	5	5–10	5–10	15
Strict	To prevent entrance of pollution during door opening	5	40 or it is 5 relative to buffer chamber	10 or it is 5 relative to buffer chamber	It is 10 relative to buffer chamber
	Sterile cleanroom	5	It is 5 relative to buffer chamber	It is 5 relative to buffer chamber	It is 10 relative to buffer chamber

When the lower velocity 0.3 m/s is set for the indoor air velocity u_0, and the door height is assume 1.9 m, we can get:

$$\frac{0.3}{v} = \frac{1.9 - 0.75}{0.6}$$

So we obtain:

$$v = 0.16 \text{ m/s}$$

This means the allowable air velocity of invasion flow should be less than 0.16 m/s. When the air velocity caused by the entrance of people is assumed 0.2 m/s as mentioned before, the air velocity needed to push outwards should be:

$$u = 0.2 - v = 0.04 \text{ m/s}$$

With the same parameters as the above case, the pressurized flow rate should be larger than 216 m^3/h, and ΔP should be larger than 10 Pa.

8.7.7 Recommended Differential Pressure

Combined with the analysis in above sections, the recommended differential pressure is proposed, which is shown in Table 8.8.

The detailed information about the calculation method for the fresh air and exhaust airflow rates with the requirement of positive and negative pressure is illustrated in other monograph [22].

8.8 Buffer and Isolation

The purpose of the pressure kept in the cleanroom is to prevent the entrance of pollution into the cleanroom. But sometimes it is too large to be realized. The auxiliary measures should be taken, including setting the buffer chamber, the airlock chamber, the air curtain chamber, and the airshower chamber. All these measures aim to reduce the entrance of the pollution into the room or reduce the generation of pollution indoors.

8.8.1 Airlock Chamber

It is the Technology Regulations T.O.00-25-203 published by US Air Force that first proposed the airlock chamber which has the buffer effect. "Airlock chamber is the small room at the entrance of the cleanroom. There are several doors in the airlock chamber, and only one door can be open at the same time. The purpose is to prevent the external pollution from entering into the cleanroom and to play the role of sealing." Other standards in America later and the Good Manufacture Practice (GMP) from WHO have the same definition.

WHO proposed that "the airlock chamber means the sealed space with two doors, which is placed between two or several rooms, such as the rooms with different air cleanliness levels. The purpose is to control the air flow between rooms with airlock chamber when people enter in or out of these rooms. The airlock chamber should be designed for people or goods." It is obvious that the airlock chamber is only the room where doors are interlocked and cannot be opened at the same time. Although the air change rate was required in some literatures, for example, in NASA NHB5340-2 it was proposed that "enough ventilation and air exchange should be provided in the airlock chamber"; the supplied air was required to be clean in some literatures, the air cleanliness level is not clearly presented. The room without supplying clean air can act as the buffer at most. However, this kind of buffer cannot effectively prevent the invasion of outside pollutants. Because when people enter this airlock chamber, the dirty air from ambient enters into the chamber. When the other door is opened, the already polluted air in the chamber will enter the cleanroom. This has been illustrated in the previous sections.

In the literature from Japan [30], the airlock chamber was also translated into the antechamber, which has the implication of preparation room and is shown in Fig. 8.53. Although the air cleanliness level is not specified, it is suggested to supply clean air. It should be negatively pressurized relative to the cleanroom and positively pressurized relative to the ambient.

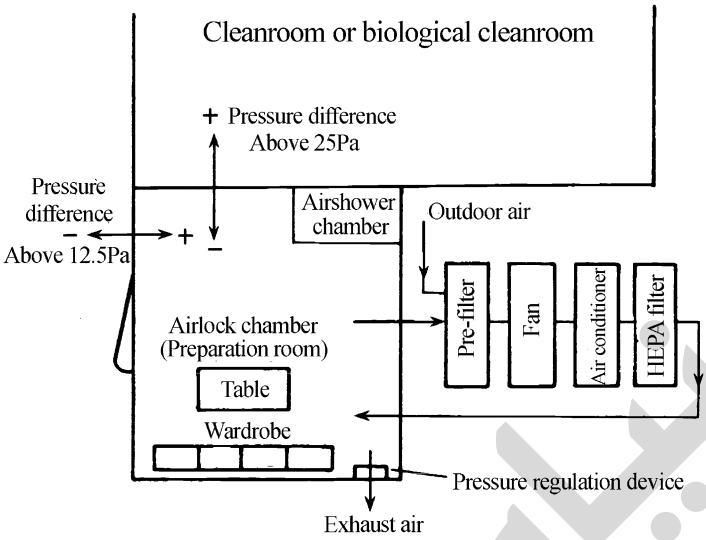

Fig. 8.53 Setting of the airlock chamber in Japan

British Standard BS5295 I has also pointed out that "airlock chamber can be used as the antechamber."

The implication of airlock chamber is inconsistent in China. One adopted the definition from the Technology Regulations T.O.00-25-203 published by US Air Force. The other considered the airlock chamber as the small room with air curtain at the entrance of the cleanroom, which is illustrated in Fig. 8.54.

The above airlock chamber with air curtain is called air curtain equipment. Doors in this kind of air curtain chamber do not need to be interlocked. It is the air curtain that seals the door hole. There can be one air curtain or two air curtains, which is shown in Fig. 8.55.

At present, the term of airlock chamber used in America is not appropriate. But since it has been popular, it is not good to change the term. The airlock chamber with air curtain in domestic area can be called airlock chamber with air curtain, while the air curtain equipment without door interlock in Japan can be called air curtain chamber. This will help people distinguish between the two situations.

8.8.2 Buffer Chamber with Positive Pressure

From the analysis in the above section, only when the volume of the cleanroom is less than 270 m^3, the buffer chamber should be installed at the entrance, so that the pollution caused by the entrance and exit of the people can be controlled. When polluted particles are the same kind and it is allowable for the self-purification time larger than 2 min, the buffer chamber is not needed. But when cross infection occurs

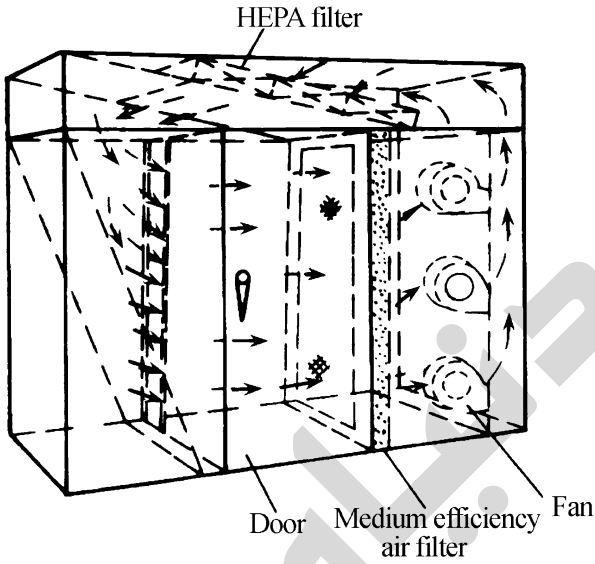

Fig. 8.54 Airlock chamber with air curtain

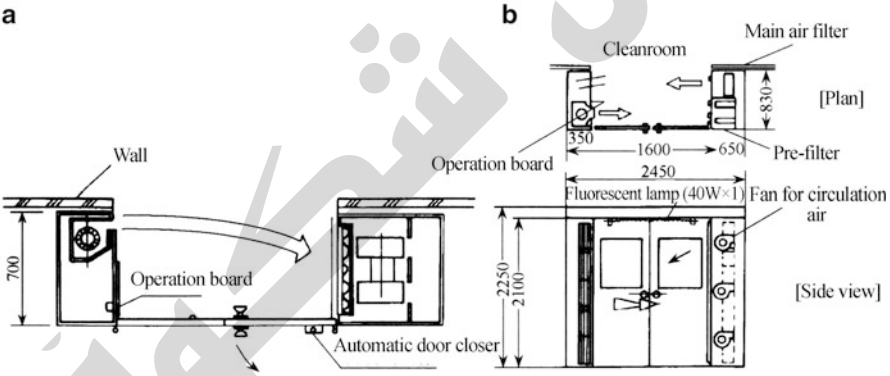

Fig. 8.55 Air curtain equipment in Japan. (**a**) One air curtain. (**b**) Two air curtains

and the damage caused is very serious, it should be placed even for two adjacent cleanrooms with the same air cleanliness level.

It is shown in Fig. 8.56 that when a buffer chamber is placed between two cleanrooms with two levels of air cleanliness difference (N_1 and N_{100}), its air cleanliness level should be the same as that of the higher level (N_1).

Suppose only when the concentration of the buffer chamber increases to x times, the increase of the concentration in the cleanroom with higher air cleanliness level will be less than 1.2 times because of the entrance of the air from the buffer chamber

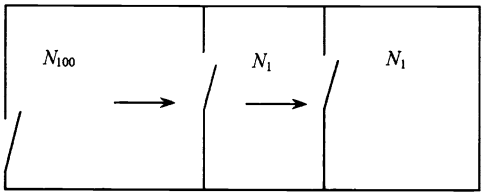

Fig. 8.56 Design of buffer chamber

to the cleanroom with higher air cleanliness level (every time two people enter and the cleanroom has the most unfavorable volume). We can obtain:

$$\frac{0.27 \times 2xN_1 + (25 - 0.27 \times 2)N_1}{25} = 1.2N_1$$

So

$$x = 10.3$$

If the increase of the concentration in the buffer chamber is less than 10.3 times, the volume should be calculated as follows:

$$\frac{0.27 \times 2 \times 100N_1 + (Y - 0.27 \times 2)N_1}{25} = 10.3N_1$$

So

$$Y = \frac{53.46}{9.3} = 5.75\,\mathrm{m}^3$$

This means the volume of the buffer chamber should be $\geq$6 m^3.

The above calculation is valid for turbulent flow cleanroom. For unidirectional flow cleanroom, the difference between its air cleanliness and Class 8 is 1,000 times. Because the ability of anti-disturbance is extremely strong, pollution entering the cleanroom will be exhausted quickly by unidirectional flow, which will not influence the indoor distribution. So the buffer chamber is not needed for this case. Moreover, in Technology Regulations T.O.00-25-203 published by US Air Force and Federal Standard 209, airlock chamber and airshower chamber are not needed at the entrance of this kind of cleanroom. Only the aerospace standard specifies that airlock chamber should be considered to set for unidirectional flow cleanroom for the situations of product and people. This also applies for the buffer chamber. If buffer chamber is set for the cleanroom with Class 5, its cleanliness level can be Class 6, given the strong ability to anti-disturbance.

Buffer chamber plays the role of preventing pollution from entering the room and offsetting the differential pressure.

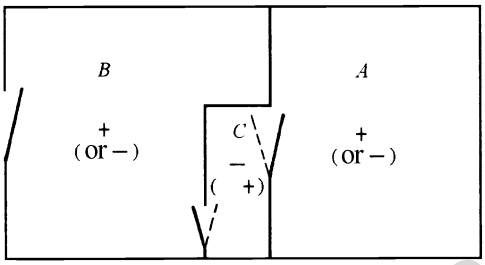

Fig. 8.57 Buffer chamber with the function of offsetting the differential pressure

Two cleanrooms *A* and *B* are shown in Fig. 8.57. When positive pressure should be kept in Room A relative to Room B in the design process, where the volume of Room *A* or the door aperture is very large (such as the tall workshop for the assembly of satellite), a large amount of positively pressurized flow rate is needed to maintain this differential pressure. This means it is quite difficult to realize and maintain this status.

In this case, a buffer chamber is placed at the gate of Room *A*, where negative pressure is kept in Room *C* relative to Room *A*. Since the volume of Room *C* is very small, it is easy to maintain this negative pressure. This means positive differential pressure is maintained between Room *A* and Room *C*. Of course, Room *C* is also negatively pressurized relative to Room *B*.

This also applies for the case when Room *A* should be negatively pressurized relative to Room *B*. Buffer chamber *C* can also be placed, where positive pressure should be maintained in Room *C* relative to both Room *A* and Room *B*. The purpose of the original design is obtained.

8.8.3 *Buffer Chamber with Negative Pressure*

In order to design the isolation ward with negative pressure, the calculation formula for the isolation coefficient of the negatively pressurized buffer chamber was proposed by author [31]. The isolation coefficient means the increased ratio of the protection ability with buffer chamber to that without buffer chamber, which is expressed with β.

Figure 8.58 shows the so-called "three rooms with one buffer chamber" mode, where $\beta_{3,1} = 42.9$.

Figure 8.59 shows the so-called "five rooms with two buffer chambers" mode, where $\beta_{5,2} = 2042$.

According to investigation result, the effect with air supply through HEPA filter in negatively pressurized buffer chamber is better by two times than that without air supply. The air change rate of exhaust air is better to be 60 h^{-1} (actual flow rate is very small). Even when it increases to 120 h^{-1}, the effect only increases by 100 %.

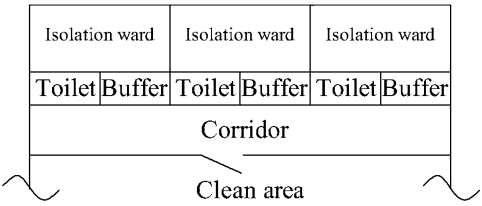

Fig. 8.58 Three rooms with one buffer chamber

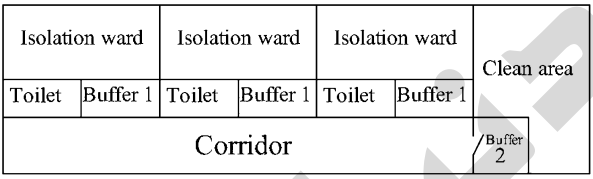

Fig. 8.59 Five rooms with two buffer chambers

8.8.4 Airshower Chamber

Since it was found that the indoor pollution concentration in cleanroom is related to the activity of the personnel, the number of occupants in the cleanroom should be limited, and the capture of particles on the surface of cloth which will generate particles during the activity should be reduced. For the latter reason, the measures to use airshower chamber was proposed in the Technology Regulations T.O.00-25-203 published by US Air Force in 1961.

The schematic of airshower chamber is shown in Fig. 8.60. But when the captured particles on the cloth surface need to be removed, vibration must be made on cloth.

According to the hydrodynamics theory, the boundary layer is formed near the surface when air flows around an object, which is very thin. The flow inside the boundary layer is laminar. Since the laminar streamlines are parallel and the velocity is uniform, it cannot generate vibration on cloth, so the attached particles are difficult to be blown away. Only when the laminar flow in this boundary layer becomes turbulent, the movement trajectory of fluid particles is extremely irregular. The displacement occurs not only along the flow direction but also perpendicular to the movement direction. This may vibrate the cloth.

The condition for the conversion from laminar flow to turbulent flow is that Re number reaches a critical value, which is usually 1×10^5–5×10^5.

Austin made the following calculation for $Re = 5 \times 10^5$ according this principle in this monograph [32]:

$$Re = \frac{V_m D \rho}{\mu}$$

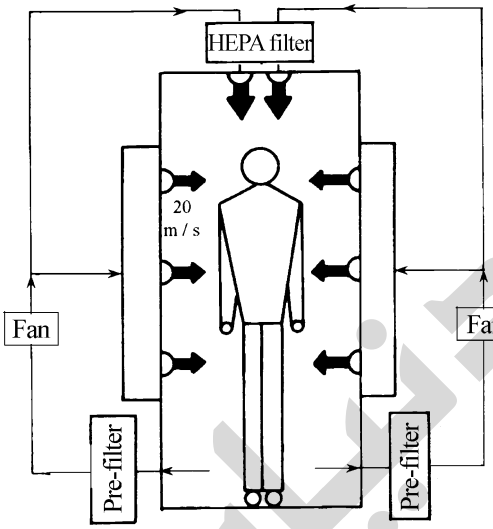

Fig. 8.60 Schematic of airshower chamber

where

V_m is the critical airshower velocity (m/s);
ρ is the air density. At normal temperature it is 1.2 kg/m^3;
μ is the dynamic viscosity of air (Pa · s). At normal temperature it is 1.83×10^{-5};
D is the object diameter (m).

Austin assumes the human body as circular cylinder with $D = 40.6$ cm, and it was obtained $V_m = 18$ m/s (with the above parameters it should be 18.8 m/s), which is shown in Fig. 8.61. But it is not close to the real situation when the human body is considered as circular cylinder, compared with rectangle. This assumption was made during the design of slot scanning airshower chamber [33]. Given the thickness of cloth, all is based on the upper part of the cloth. Let the long side length of rectangle be $b = 55$ cm and the short length $a = 30$ cm; the equivalent diameter D' of human body is:

$$D' = \frac{2ab}{(a+b)} = 0.39 \text{ m}$$

When average value of Re number is 3×10^5,

$$V_m = \frac{3 \times 10^5 \times 1.83 \times 10^{-5}}{0.39 \times 1.2} = 11.7 \text{ m/s}$$

If Re number is 5×10^5, $V_m = 19.6$ m/s.

Airshower velocity does not necessarily mean the air supply velocity at the nozzle. It depends on the distance between the human body surface and the nozzle.

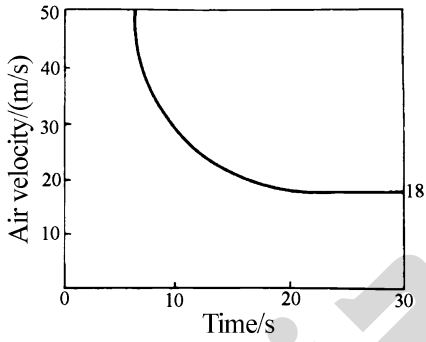

Fig. 8.61 Relationship between airshower velocity and time

The net width of airshower chamber with spherical nozzle is 750–800 mm. When the length of the extruded part for both sides of the nozzles is $80 \times 2 = 160$ mm, which should be subtracted, the average distance between human body surface and nozzle is 108 mm. Nozzles are placed at four corners in airshower chamber with slot nozzle. The distance between the two slots is 0.9 m, so the average distance between human body surface and nozzle is 158 mm. According to hydrodynamics [34], air exiting the nozzle is the jet with circular cross section with the following core length S_n at the beginning section:

$$S_n = 0.672 \frac{d_0}{2a} \tag{8.14}$$

Air exiting the slot nozzle is the planar jet with the following core length S_n at the beginning section:

$$S_n = 1.03 \frac{b_0}{a} \tag{8.15}$$

where

d_0 is the diameter of spherical nozzle;
b_0 is the half width of slot nozzle;
a is the turbulent coefficient of nozzle. It is 0.07 for spherical nozzle and 0.11 for slot nozzle.

Let $d_0 = 38$ mm and $b_0 = 4$ mm, we can obtain:

$$\text{For spherical nozzle,} \quad S_n = 0.18\text{m}$$
$$\text{For slot nozzle,} \quad S_n = 0.075\text{m}$$

This means the distance between human body surface and nozzle is within the beginning section in airshower chamber with spherical nozzle. Since the velocity at the beginning section is the same as the air supply velocity, the axial velocity

Table 8.9 Exit velocity from nozzle

Nozzle	Air supply outlet velocity V_0 (m/s)	
Spherical	11.7	19.6
Slot	21.3	35.6

Table 8.10 Effect of airshower on strip fabric

Sampling state	Airshower time (s)	Efficiency for single row of nozzles with $V_0 > 28$ m/s (%)	Efficiency for double rows of nozzles with $V_0 > 24$ m/s (%)
No vibration	30	~68	~71
	60		~71
	120	~71	~76
Vibration	30	94–100	86–96
	60		96–113

arriving at human body surface is the exit velocity from nozzle, i.e., $V_0 = V_n$. While in airshower chamber with slot nozzle, the distance between human body surface and nozzle is out of the beginning section. In this case, the axial velocity should be calculated with the main section instead of the beginning section for slot nozzle:

$$\frac{V_n}{V_0} = \frac{1.2}{\left(\frac{as}{b_0} + 0.41\right)^{1/2}} \tag{8.16}$$

Where V_0 is the exit velocity from nozzle, which is also called the velocity blowing towards the human body by free jet. The calculated results are shown in Table 8.9.

It is shown from Table 8.8 that when *Re* number is considered, the exit velocity from spherical nozzle should not be less than 20 m/s. When the safety coefficient is considered, it should be not less than 25 m/s.

Experiment for slot nozzle [35] has proved that the shear force with its scanning activity is larger than that of the spherical nozzle by one time. The effect of the airshower chamber with velocity 25 m/s is apparently better than that with spherical nozzle. So the exit velocity from nozzle can be 25–30 m/s.

There are different opinions about the effect of airshower chamber. First of all, the airshower chamber is effective in our opinion. Take a look at the experimental data in China [36]. The effect on "strip fabric" was tested at first. Particles attached were observed with microscope (with magnification ratio 150) before and after airshower. Results are shown in Table 8.10. Efficiency with 113 % appears in the table, which means airshower under the vibration condition can blow away the background particles on the original blank sample.

The second step is to paste the sample on various positions of the human body. The airshower time is 30 s. Results are shown in Table 8.11.

Since it was measured using the microscope with the magnification ratio 150, submicron particles may not be seen. The actual efficiency may be a little higher.

Table 8.11 Effect of airshower on various positions of human body

Position	Efficiency for single row of nozzles with $V_0 > 28$ m/s (%)	Efficiency for double rows of nozzles with $V_0 > 24$ m/s (%)
Top of head	31.8	72.8
Chest	52.0	72.0
Below armpit	30.8	72.0
Knee	41.8	55.8
Foot	17.9	34.3

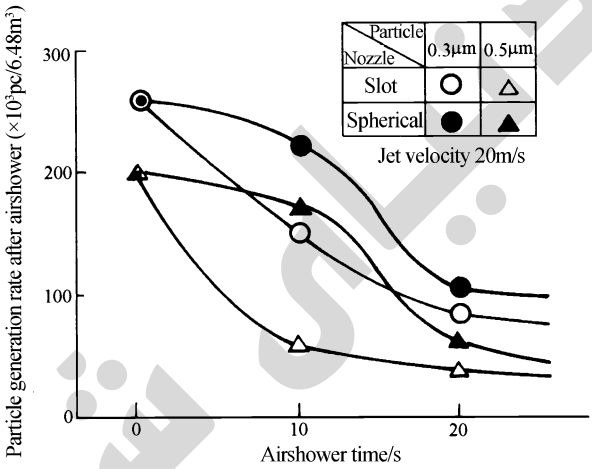

Fig. 8.62 Reduce of particle generation from cloth after airshower

Next take a look at the data about particle generation after airshower with different time period in Japan [35], which is shown in Fig. 8.62. It is shown from the figure that the particle generation of particles with diameter ≥0.5 μm after 30 s of airshower in the airshower chamber with spherical nozzle reduces to about 1/6 of that before airshower, while it reduces to about 1/10 in the airshower chamber with slot nozzle.

From the above data, we can see that the domestic effect is lower than the foreign effect, which may be related to the measurement observed by microscope.

The effect of airshower can also be evaluated from the falling particles, which is also Japanese experiment.

In the experiment, people enter the airshower chamber with the clean cloth. In the chamber the velocity is 20 m/s and the variation of particle concentration in the chamber was measured. Results in Fig. 8.63 show that the concentration (≥0.5 μm) in the airshower chamber increases by 80 times after 20 s of airshower. With the longer time, the increase of effect becomes slow.

Secondly, the actual effect of airshower chamber is not so good as the theoretical and experimental effects. The reasons are as follows:

1. Some operators overestimate the function of airshower chamber which prevents large amount of particles from entering the cleanroom.

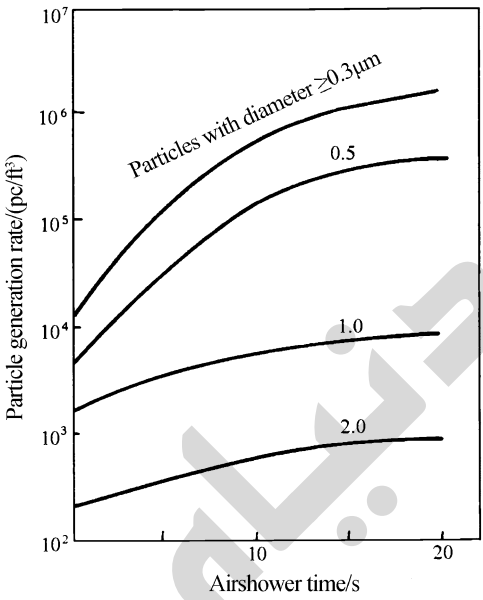

Fig. 8.63 Relationship between falling particle number and airshower time

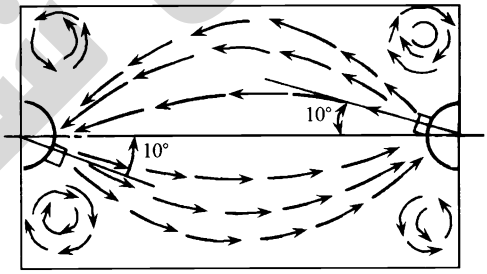

Fig. 8.64 Direction of nozzles

2. The airshower chamber is designed improperly. The number of nozzles can be different by more than one time. Some chamber has no nozzle at the ceiling. Some only set a row of nozzle, while it is shown from the previous data that the effect with two rows is better than one row, because of the enlarged exposed area on human body to the airflow. Some only place nozzle at one side.
3. The airshower velocity is too small. According to some measurements, the velocity at the nozzle exit is usually 10 m/s or even lower.
4. During usage, people usually try to avoid the airflow, or open the door with shortened time (doors are not interlocked).
5. The flow direction should be inclined to, instead of perpendicular to, the cloth surface. This means the angle of nozzle should be adjusted not to face people directly. The opposite nozzles should not be face-to-face. It is recommended to install as shown in Fig. 8.64 [34].
6. People in the airshower chamber do not cooperate to rotate or vibrate the cloth.

Table 8.12 Influence with no airshower process

Air cleanliness level	Average particle concentration (pc/L)	Air change rate (h^{-1})	Particle generation rate (pc/h)	Increase of particle concentration for each liter of air (pc)	Increase of particle concentration (%)	Variation of air cleanliness level
100,000	2000	15	5.4×10^7	144	7.2	100,000
10,000	200	25	5.4×10^7	86.4	43.2	10,000
1,000	20	50	5.4×10^7	43.2	216	10,000
100	2	450	5.4×10^7	–	–	–

It should be emphasized that given the interlock relations between two doors in the airshower chamber, the airshower chamber can be considered as the airlock chamber which can be used to perform the airshower process. The Technology Regulations T.O.00-25-203 published by US Air Force has ever pointed out that "the entrance and exit doors can be interlocked with the combination of airshower chamber and airlock chamber" and "the standing airshower chamber in the cabinet should be placed in the middle of the airlock chamber."

In the monograph of Austin [32], "airshower process is usually placed in the airlock chamber," and "after the entrance of personnel and the close of the door, air with high speed flows towards the cloth. After the airshower process is complete, people can enter the working area with higher requirement."

There is certain efficiency for airshower chamber, but it does not mean airshower chamber must be placed for any cleanroom.

Suppose the occupant density is 0.2 p/m^2, namely, there are two people in the space 25 m^3 (10 m^2). If people do not pass through the airshower chamber, the average particle generation during activity is 0.45×10^6 pc/(min · p) (with white nylon clean working garment). The influence on various air cleanliness levels is shown in Table 8.12.

The design concentration of cleanrooms with various air cleanliness levels cannot be the upper limit of the corresponding concentration, which is usually 1/3–1/2 of the upper limit. Now assume the average concentration between the upper and lower limits is used. It is known from the above result that for cleanroom with air cleanliness Class 8, the concentration will increase by 144 pc/L when no airshower chamber is used, but it will not influence the designed air cleanliness level. For cleanroom with air cleanliness level Class 7, the air cleanliness level will not be affected with the above assumptions, but it will be influenced when the average concentration is 300 pc/L. So for cleanroom with air cleanliness level Class 7, the airshower chamber is usually not necessary. But if the requirement is higher, it should be considered. The airshower chamber should be placed for cleanroom with Class 6. For cleanroom with Class 5, it should not be considered with the above principles. Because the flow in cleanroom with Class 5 is unidirectional, the generated particles from occupant will not mix with the room air; instead, they will be exhausted away by unidirectional flow. Transverse exchange will not be considered. This is the reason why the anti-disturbance ability is strong in unidirectional

flow cleanroom, and it is not necessary to install airshower chamber. In both the Technology Regulations T.O.00-25-203 published by US Air Force and the Federal Standard 209A and 209B, it is specified that "airlock chamber and airshower chamber are usually not necessary for this kind of cleanroom." For unidirectional flow cleanroom with special purpose, NASA NHB 5340-2 specified that "airlock chamber and airshower chamber should be applied according to the purpose of product and personnel." This means these two kinds of chambers should be considered to install for unidirectional flow cleanroom, or sometimes it may be not necessary. But from another point of view, airshower chamber is placed even when it is not necessary, which aims to strength the impression and generate the psychological effect. The inner side of airshower chamber is already the clean area! This has already been noticed in the foreign literatures.

There are some applications where the airshower chamber cannot be installed. In some place the airflow with high speed is not allowed. For example, at the entrance of the operating room or some intensive care unit, patient cannot bear the airshower with high speed. The entrance process will be affected because the floor of the airshower chamber is higher than the outside. The airshower chamber will not operate properly when the object is too long or too wide, which is larger than that of the airshower chamber. The time to pass through is very long and continuous that the airshower chamber cannot operate. There are too many personnel that it takes a lot of time to pass through the airshower chamber.

Someone may be afraid that after the airshower process, will particles and bacteria falling down from the human body enter the cleanroom?

As long as it is properly designed, the door will be opened only when the airshower process is completed. In this way, particles will not leave from the chamber. The airshower chamber should be negatively pressurized. According to the Technology Regulations T.O.00-25-203 published by US Air Force, the airshower chamber should be positively pressurized relative the outside, so that no problem will appear. But this has not been realized for the current chamber. Only zero pressure is realized. According to the foreign report, the influence of the opening of the door after the airshower process is meaningful only for cleanroom with air cleanliness level higher than Class 5.

8.9 Feature of Cleanroom with Full-Ceiling Air Supply and Two-Bottom-Side Air Return

The technological and economic meaning of the cleanroom with full-ceiling air supply and two-bottom-side air return mode has been understood from the previous introduction about the classification of unidirectional flow cleanroom. But what is the characteristic of this kind of cleanroom? Can it replace the vertical flow cleanroom with the standard air return on the grille floor? What is the maximum width? If it is too wide, it is natural to worry about whether unidirectional flow can be formed in the working area, or whether the above index can be satisfied. A foreign study has put forward that when the width of the cleanroom of this kind is less than

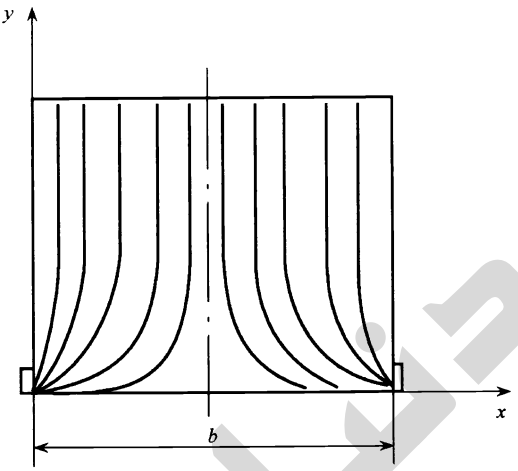

Fig. 8.65 Flow field along x- and y-directions with two-bottom-side air return

3.6 m, the air cleanliness level can reach Class 5 in American Federal Standard [5]. But results of further study were not provided. Since 1970s, the comprehensive investigation from line sink theory, experiment, and field test was initiated in China [7]. The allowable width of this kind of cleanroom and many features of the flow field were obtained, which provides the basis for the promotion of the cleanroom. It is easy to obtain the flow field of this kind of cleanroom with computational simulation. But it is much easier for understanding the physical meaning by the line sink theory. The derivation of this theory will be introduced below.

8.9.1 Line Sink Model

8.9.1.1 Flow Pattern of the Line Sink

Figure 8.65 shows the flow pattern along x- and y-directions for the cleanroom with full-ceiling air supply and two-bottom-side air return. Along the z-direction which is perpendicular to the paper, the flow properties (such as velocity and pressure) are the same. This properties (mainly the velocity) are only related to x and y, while it is not related to z. This kind of flow pattern is the special case of the flow field, namely, planar flow, and there is no eddy in the flow field.

For ideal planar flow without eddy, there exists a function $\psi(x, y)$:

$$\mathrm{d}\psi = u_x \mathrm{d}_y - u_y \mathrm{d}_x$$

where u_x and u_y are the components of the velocities along x- and y-directions, respectively. ψ is the stream function.

According to the physical meaning of ψ, ψ is a function for the planar position (x, y). One value of ψ will be given for every position (x, y). Let

$$\psi(x, y) = \text{constant}$$

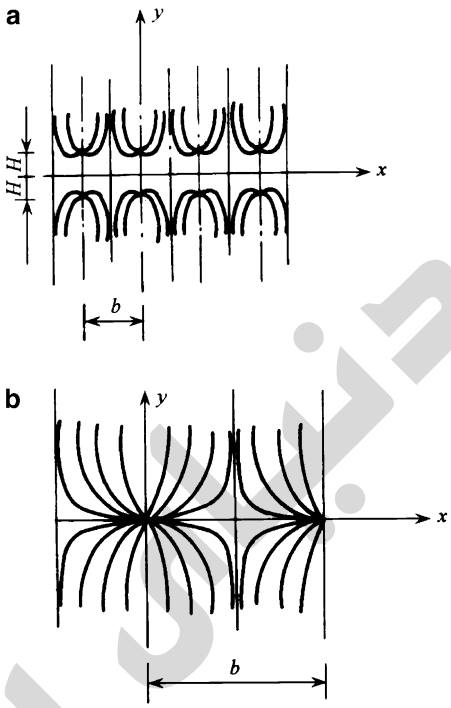

Fig. 8.66 Flow field with two rows of line sinks

We obtain:

$$\mathrm{d}\psi = 0$$

i.e.,

$$u_x \mathrm{d}_y - u_y \mathrm{d}_x = 0$$

This is the streamline function. When the positions with the same value of ψ are linked together, the streamlines are generated. The problem is how to obtain the value of ψ.

According to the hydrodynamics, there is a complex potential for planar flow without eddy. This complex potential is composed of stream function and potential function, where the imaginary part is the stream function.

$$W(Z) = \varphi(x, y) + \psi(x, y) \tag{8.17}$$

If the complex potential $W(Z)$ of the flow field can be found and decomposed into the real and imaginary parts, the stream function can be found.

It is shown in Fig. 8.66 that two rows of infinite sinks, i.e., line sinks, with interval distance b have the similar flow pattern as shown in Fig. 8.65.

8.9.1.2 Stream Function

If there is a pair of sinks parallel to the y-axis and the distance from x-axis approaches zero (which is equivalent to the situation when the return air grille is at the floor, the bottom of Fig. 8.66), the flow pattern is as shown in Fig. 8.65. So when the condition of the problem is the same as that in Fig. 8.66, the corresponding stream function and complex potential are that in Fig. 8.65.

The conditions to form the sink flow as in Fig. 8.66 include the following items:

1. The streamlines along y-direction are parallel, and they bend with the effect of sink.
2. Flow properties do not vary along z-direction.
3. x-axis, y-axis, and the longitudinal axis are streamlines. If the partition wall is placed along these axes, the shape of streamlines will not be affected.

The actual flow field shown in Fig. 8.65 meets the above three conditions.

1. Since the height of the room has a certain value. After air passes through HEPA filter or the damping layer at the ceiling, the streamlines are almost parallel, which meets the first condition.
2. It is planar flow and the flow properties are independent of z-axis, which meets the second condition.
3. The side wall and the floor are equivalent with y-axis and x-axis in Fig. 8.61, respectively. So other streamlines are not affected by these walls. There is an invisible wall at the position $b/2$, which separates the room into two parts. It meets the third condition.

Except for the above three aspects of similarities, the most difference is that the return air grille is not a line sink since it has a certain amount of height. So it is approximated when the sink model is used. This should be investigated through experiment.

The complex potential in Fig. 8.66 is known [37]:

$$W(z) = -\frac{Q_0}{\pi} \ln \sin \frac{\pi}{b} z \tag{8.18}$$

where Q_0 is the flow rate of return air at each side and b is the interval between two rows of sinks, namely, the width of the cleanroom:

$$z = x + \mathrm{i}y$$

From Eq. (8.18), we know

$$W(Z) = -\frac{2Q_0}{2\pi} (\ln \sin \frac{\pi}{b} Z) = -\frac{Q_0}{2\pi} (\ln \sin \frac{2\pi}{b} Z) \tag{8.19}$$

Since we know

$$\sin\frac{\pi}{b}Z = \frac{\left(e^{\mathrm{i}\frac{\pi}{b}Z} - e^{-\mathrm{i}\frac{\pi}{b}Z}\right)}{2\mathrm{i}}$$

$$\cos\frac{\pi}{b}Z = \frac{\left(e^{\mathrm{i}\frac{\pi}{b}Z} + e^{-\mathrm{i}\frac{\pi}{b}Z}\right)}{2}$$

Let $P = \sin^2\frac{\pi}{b}Z$, so we obtain

$$P = \sin^2\frac{\pi}{b}Z = \left(\frac{e^{\mathrm{i}\frac{\pi}{b}Z} - e^{-\mathrm{i}\frac{\pi}{b}Z}}{2\mathrm{i}}\right)^2 = \frac{1-\cos\frac{2\pi x}{b}ch\frac{2\pi y}{b}}{2} + \frac{\mathrm{i}\sin\frac{2\pi x}{b}sh\frac{2\pi y}{b}}{2} \tag{8.20}$$

The derivation process is omitted.

According to the definition of complex number, the magnitude of $P = U + \mathrm{i}V$ is:

$$\begin{aligned}\rho &= \sqrt{U^2 + V^2} \\ &= \sqrt{\frac{\left(1-\cos\frac{2\pi x}{b}ch\frac{2\pi y}{b}\right)^2}{4} + \frac{\left(\sin\frac{2\pi x}{b}sh\frac{2\pi y}{b}\right)^2}{4}} \\ &= \frac{1}{2}\sqrt{\left(1-\cos\frac{2\pi x}{b}ch\frac{2\pi y}{b}\right)^2 + \sin^2\frac{2\pi x}{b}sh^2\frac{2\pi y}{b}}\end{aligned} \tag{8.21}$$

And the angle is:

$$\theta = arctg\frac{V}{U} = arctg\frac{\sin\frac{2\pi x}{b}sh\frac{2\pi y}{b}}{1-\cos\frac{2\pi x}{b}ch\frac{2\pi y}{b}} \tag{8.22}$$

Because we know

$$p = \rho e^{\mathrm{i}\theta}$$

With Eqs. (8.19) and (8.20), we obtain

$$\begin{aligned}W(Z) &= -\frac{Q_0}{2\pi}\ln p \\ &= -\frac{Q_0}{2\pi}\left\{\ln\sqrt{\left(1-\cos\frac{2\pi x}{b}ch\frac{2\pi y}{b}\right)^2 + \sin^2\frac{2\pi x}{b}sh^2\frac{2\pi y}{b}}\right. \\ &\quad \left. -\ln 2 + \mathrm{i}\,arctg\frac{\sin\frac{2\pi x}{b}sh\frac{2\pi y}{b}}{1-\cos\frac{2\pi x}{b}ch\frac{2\pi y}{b}}\right\}\end{aligned} \tag{8.23}$$

The stream function can be obtained with Eqs. (8.17) and (8.23):

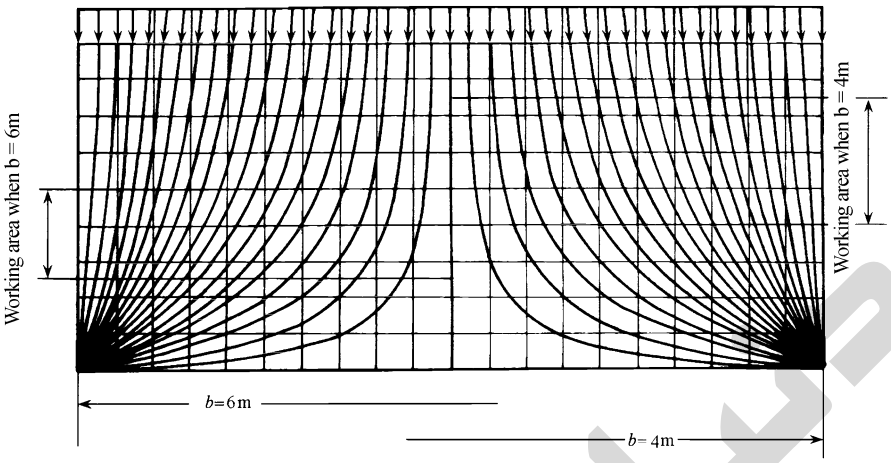

Fig. 8.67 Theoretical flow field of cleanroom with full-ceiling air supply and two-bottom-side air return

$$\psi(x,y) = -\frac{Q_0}{2\pi} arctg \frac{\sin\frac{2\pi x}{b} sh\frac{2\pi y}{b}}{1-\cos\frac{2\pi x}{b} ch\frac{2\pi y}{b}} \tag{8.24}$$

Since positions with the same value of stream function are located in the same streamline, we obtain the following expression for every streamline:

$$\frac{\sin\frac{2\pi x}{b} sh\frac{2\pi y}{b}}{1-\cos\frac{2\pi x}{b} ch\frac{2\pi y}{b}} = cons. \tag{8.25}$$

With the value of each constant, the corresponding values of x and y can be obtained. The streamlines can thus be obtained. Figure 8.67 shows the plotted flow field. It fits well with the measured results by water model with 1/40, 1/30, 1/20, and 1/10 scales, as well as the field test results.

Figure 8.68 shows the schematic of water model. Figure 8.69 shows the cleanroom model made with organic glass.

In the model experiment, water with common temperature was used as the working medium in the model. Colorful liquid was injected into the water, so that the streamline is visible and it is easy for observation and photograph. The scale of test equipment can be reduced when water is used as the working medium, because the dynamic viscosity of water with common temperature is much smaller than that of air with common temperature and the ratio is 1/15. When the geometric size of the model is fixed, the proportional scales of velocity and flow rate with the ratio of 15 were obtained. When the streamline at the position $\frac{1}{4}b$ is used as the reference (the reason will be shown later), the measured and theoretical streamlines of four models will be plotted on Fig. 8.70. It is shown that various streamlines are similar when Re is above 6,000.

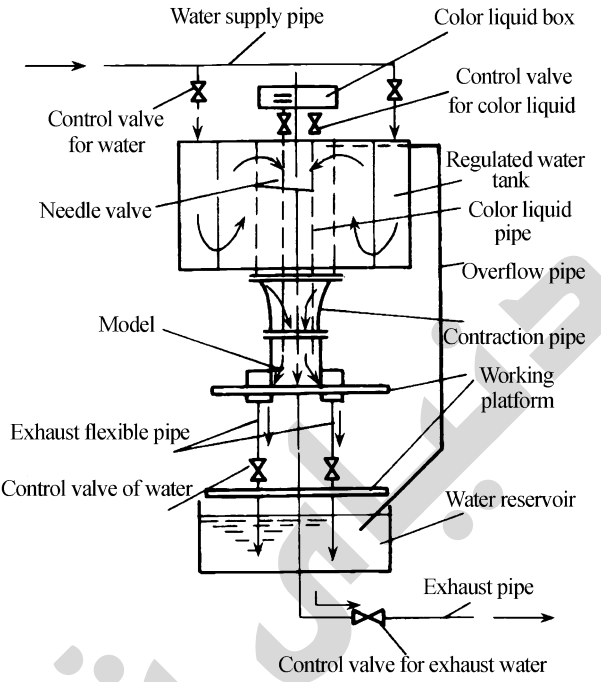

Fig. 8.68 Schematic of water model system

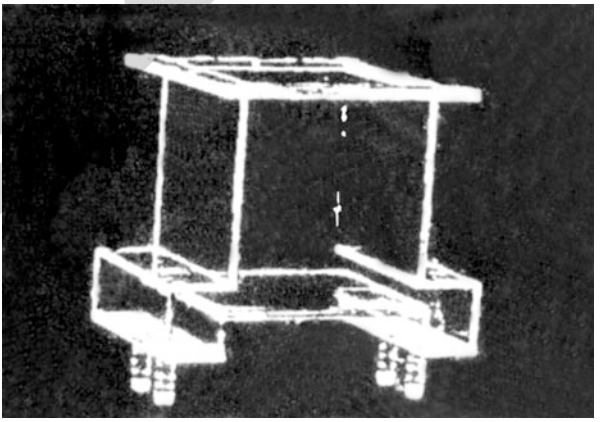

Fig. 8.69 1/30 cleanroom model. The black line represents the streamline of the colored liquid, i.e. the airflow streamline.

When the theoretical model with extrapolated sink point was used for calculation, the difference between the ordinates of the theoretical and measured streamlines at the position $\frac{1}{4}b$ is about $\frac{1}{70}b$~$\frac{1}{50}b$. The inclination degree is almost seldom changed, which is shown in Figs. 8.71 and 8.72.

The actual return air grille has a certain amount of height itself, and its bottom side is also a certain distance away from the floor. This is equivalent with the case when there is a distance between sink and floor, which is assumed to be H. The stream function can be derived:

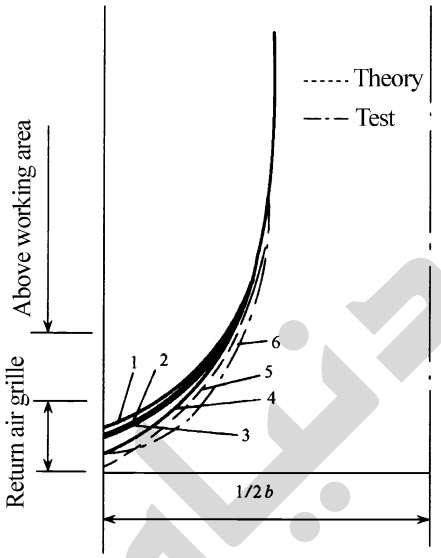

Fig. 8.70 Streamlines at the position $b/4$ of four models ($Re > 6{,}000$). *1* 1/30 model, $Re = 8{,}500$, 1/40 model, $Re = 6{,}000$; *2*, *3* 1/10 and 1/20 models, $Re = 6{,}800$–$20{,}000$; *4* 1/40 model, $Re = 5{,}000$ and height of return air grille $= b/13$; *5* theoretical streamline; *6* 1/10 model, $Re < 2{,}000$

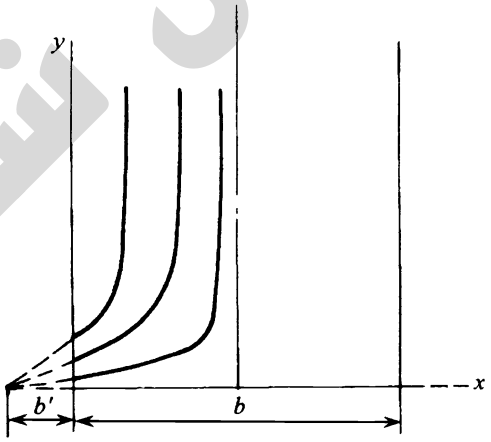

Fig. 8.71 Situations with extrapolated sink point

$$\psi(x,y) = -\frac{Q_0}{2\pi} arctg \frac{\sin\frac{2\pi x}{b} sh\frac{2\pi y}{b}}{ch\frac{2\pi H}{b} - \cos\frac{2\pi x}{b} ch\frac{2\pi y}{b}} \tag{8.26}$$

H is usually very small, and it is less than $0.05b$. So $ch\frac{2\pi H}{b} \leq 1.04$, which is a little larger than the value "1" in Eq. (8.24). This has small influence on calculated results. Streamlines bend downwards slightly near the sink position and then upwards, which is shown in Fig. 8.80 in the next section.

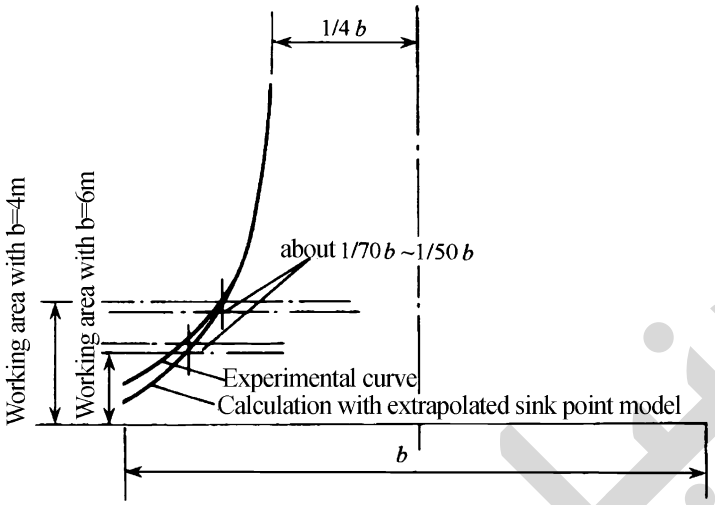

Fig. 8.72 Deviation of calculated curves

8.9.2 Feature of Flow

8.9.2.1 Basic Feature

1. Two streamlines at two sides and in the middle (including these near the floor) are straight lines. Curved streamlines appear firstly at the position of 1/4 width (i.e., *b*/4). The streamlines become straighter when it goes towards two sides. This is completely opposite with the opinion that the farther it is from the return air grille, the much curved the streamline is. Theoretical, experimental fields (Fig. 8.73) and field tested flow field (Figs. 8.74 and 8.75, both are cited from the test report from Institute of HVAC at Chinese Academy of Building Science) all show the same trend, which can be used to provide the proof.
2. It is shown from the theory of sink that the flow field is already determined when the value of *b* is fixed. The flow field will be contracted with smaller *b*, when the streamlines tend to move downwards.
3. In the middle bottom region, the velocity gradient between streamlines becomes larger when it approaches to the center, and the curvature of the streamline gets larger. The triangular region appears which is opposite from the definition of unidirectional flow. This kind of triangular region appears in both experimental and field test, and the scale of the latter is relatively small. In experiment, since colorful liquid is used, the scale of the triangular region is larger. When the velocity increases a little, it will appear. The height is about 0.15*b*, especially 0.1*b*, away from the bottom, which is shown in Fig. 8.76.

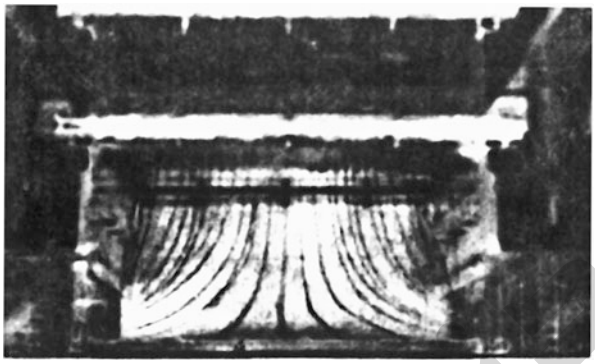

Fig. 8.73 Photograph of flow field measured with water model (1/10 model) with the height of return air grille $\frac{1.5}{10}b$. The black line represents the streamline of the colored liquid, i.e. the airflow streamline.

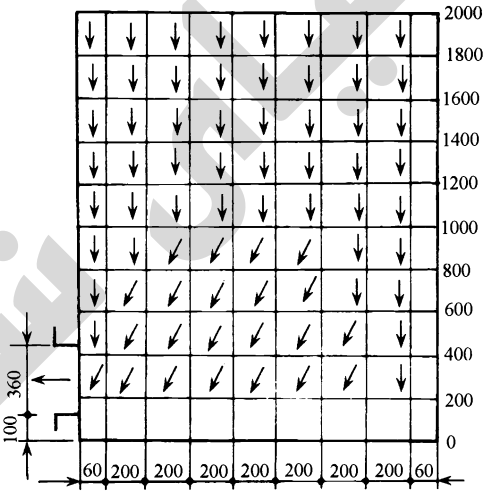

Fig. 8.74 Measured flow field in the cleanroom with bottom return air at one side

The triangular region in the experiment was not obvious, which can be found in the flow field figure shown above. The possible reasons include: (1) The widths of two examples were both narrow. It was only 1.52 m in the latter case (one side). (2) Thread method was adopted to measure the streamlines. Since the weight itself caused influence, the streamlines measured in experiment show straighter. But when particles were generated in the triangular region, the self-purification process was quite difficult, which means the flow in this place is different from unidirectional flow. Although the theoretical calculation above did not provide the basis for the existence of eddy in this triangular region, the recent computational simulation also presents the same conclusion (shown in Fig. 8.77 [38]). So it is not certain that there must be an eddy flow in the center of cleanroom. Even though the triangular region exists, the turbidity will not influence the flow field in the working area. But it is clear that the streamlines in this triangular region is different from unidirectional flow without a doubt. In this aspect, this kind of triangular region with

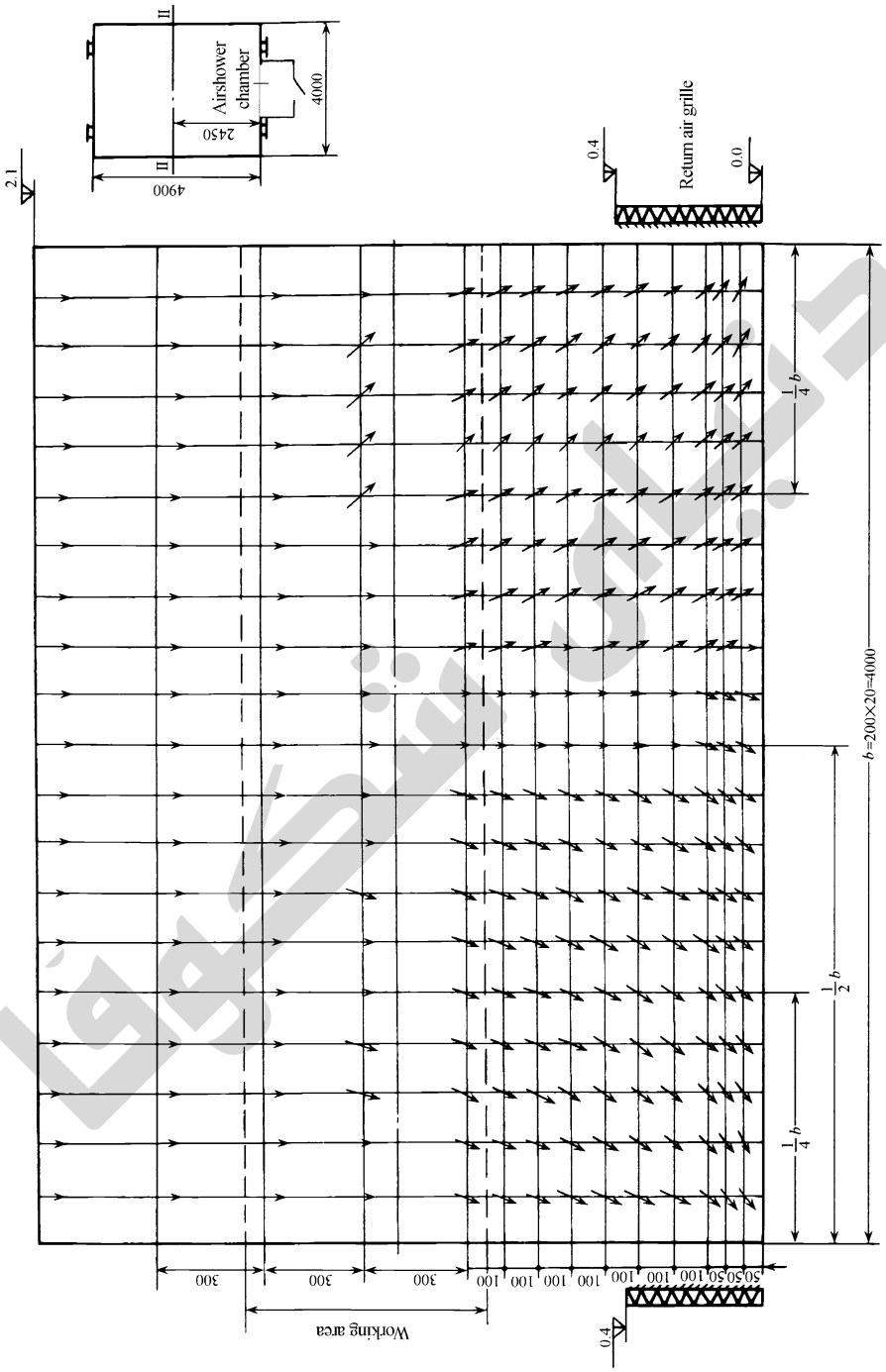

Fig. 8.75 Measured flow field in JJS20 type assembly cleanroom with two-bottom-side air return

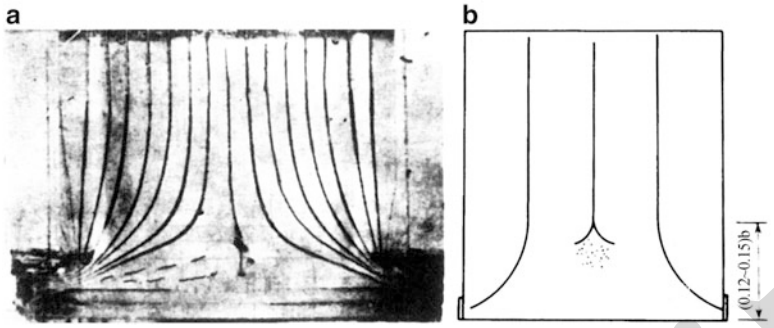

Fig. 8.76 Situation of triangular region at the central bottom place. (**a**) Photo. (**b**) Visual inspection record (1/40 model, $Re = 50{,}000$)

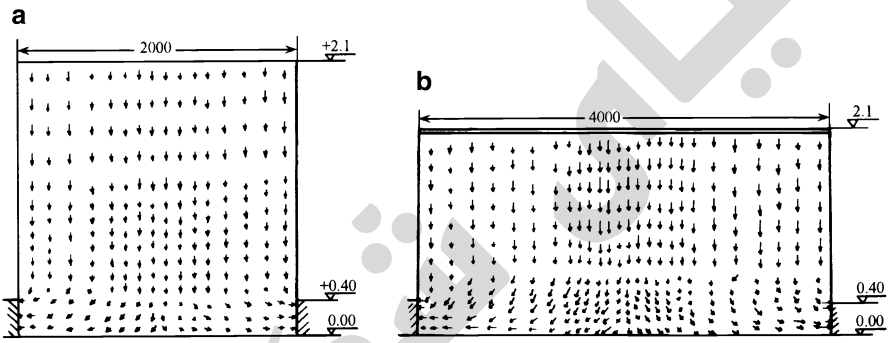

Fig. 8.77 Simulated flow fields. (**a**) Room width 2 m. (**b**) Room width 4 m

obvious curved bifurcation of streamlines is not allowed to exist in the working area of cleanroom with full-ceiling air supply and two-bottom-side air return mode, where the flow field in this kind of cleanroom is thought as unidirectional. So the height of the triangular region is an important feature to evaluate the unidirectional flow property of this kind of cleanroom. Therefore it is necessary to limit the width of this kind of cleanroom. It should be mentioned that since the boundary conditions cannot be given precisely, it is very difficult to simulate the turbulent flow and eddy with computer.

8.9.2.2 Influence of Return Air Grille

Influence of the Resistance of Return Air Grille

The resistance of return air grille has significant influence on the turbidity of the streamlines. For the return air grille with complete opening, streamlines will vibrate even for very low velocity according to experiment. When perforated plate is

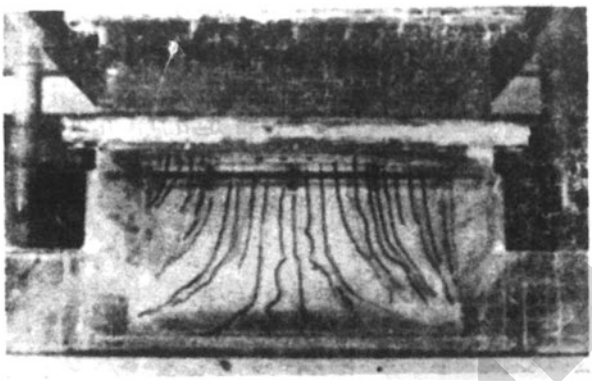

Fig. 8.78 Streamlines when return air grille is opened (1/10 model) (height of return air grille = $b/10$)

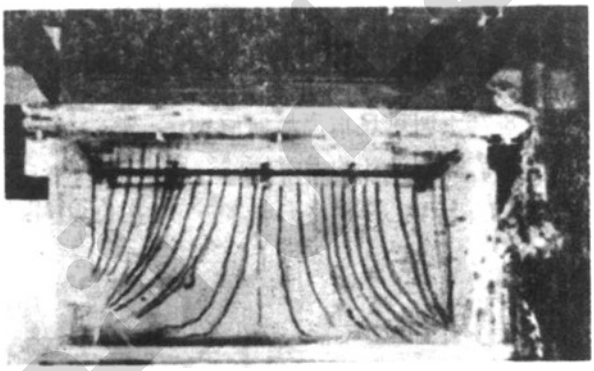

Fig. 8.79 Streamlines when perforated plate is added on return air grille (1/10 model) (height of return air grille = $b/10$)

added, no vibration will occur in streamlines even when the velocity is much larger. Figures 8.78 and 8.79 show the streamline photo with the same velocity, which proves this point. The reason may be that the resistance of return air grille is uniformly distributed with perforated plate, so that each pore on the perforated plate is equivalent with the sink with the same intensity, which is beneficial for the uniformities of velocity field and streamlines. Therefore, during the actual design process, it is not enough to place net and grille on return air opening. When the resistance is allowed, coarse and medium air filters should also be installed, which is the requirement of cleanroom itself.

Influence of the Height of Return Air Grille

The variation of opening height of return air grille itself has little influence on the streamline trajectory. But with simulated results, it is shown that the less the height is, the smaller the inclination degree of the streamlines above the working area is. So this means the streamlines are straightened [38].

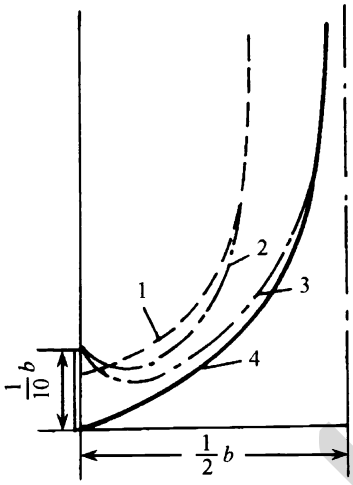

Fig. 8.80 Streamlines with different distances between the bottom of return air grille and the floor; *1* experimental streamlines when height of return air grille is *b*/10, and distance from the floor is *b*/20; *2* experimental streamlines when height of return air grille is *b*/20, and distance from the floor is *b*/10; *3* experimental streamlines when height of return air grille is *b*/10, and distance from the floor is *b*/10; *4* Experimental streamlines when height of return air grille is *b*/10, and the bottom is on the floor

Influence of the Distance Between the Bottom of Return Air Grille and the Floor

Figure 8.80 shows the experimental and calculated results of the streamlines with different distances between the bottom of return air grille and the floor. It is shown in the experiment that when the bottom is elevated, the trend of the streamlines does not change, except that streamlines bend slightly downwards near the return air grille. When the elevated distance is very small, it is hard to observe the shape of curvature (such as curve 1). Moreover, when it is elevated more, streamlines tend to be close to the center. At the same time, the curved streamline may reach the floor, which will blow particles on the floor easily. These results are consistent with the theoretical law.

This means for whatever kinds of cleanroom, it's better not to elevate the return air grille on the side wall; otherwise particles on the floor will be blown away, and pollution range will be expanded. It is shown in Fig. 8.81.

Influence of Number of Slot Return Air Grille

Slot air return grilles are usually placed at the bottom of side wall in cleanroom with two-bottom-side air return model and can also be placed on the floor. Figures 8.82 and 8.83 present the experimental streamline photo when return air grille with three

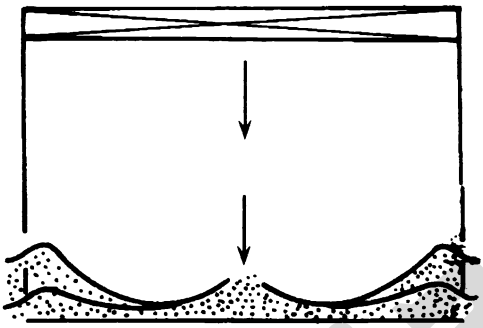

Fig. 8.81 Schematic of the expanded pollution range when the return air grille is elevated

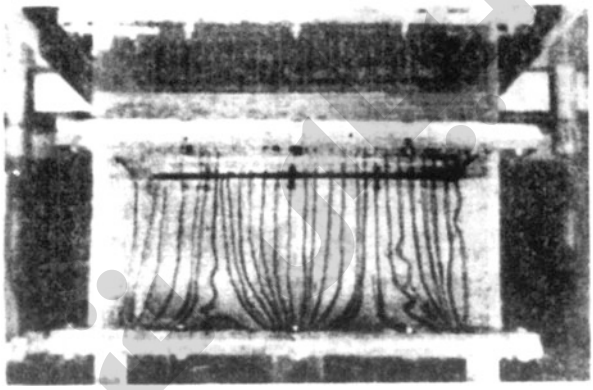

Fig. 8.82 Air return grille with three slots on the floor (the total area of return air grille is 20 % of the floor)

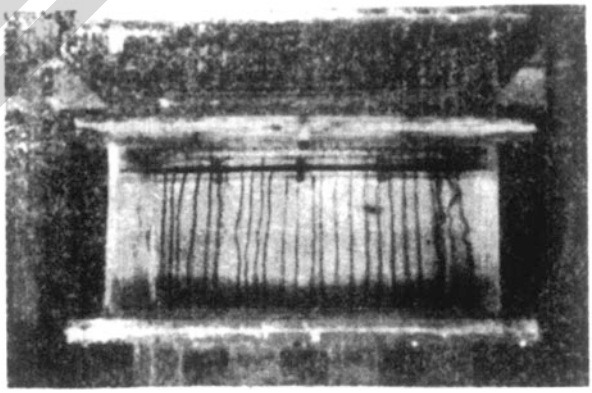

Fig. 8.83 Air return grille with four slots on the floor (the total area of return air grille is 40 % of the floor)

slots and four slots is placed on the floor respectively. It is shown that streamlines with four slots are straighter than three slots. This is because the case with three slots is equivalent with the room width $b/2$, while the case with four slots is equivalent with the room width $b/3$. With the theoretical calculation, streamlines are much straighter. It can be conceived that for the cleanroom with large width, return air channel with multiply slots on the floor can be used, as long as the suitable unit length b is kept, which is shown in Fig. 8.66.

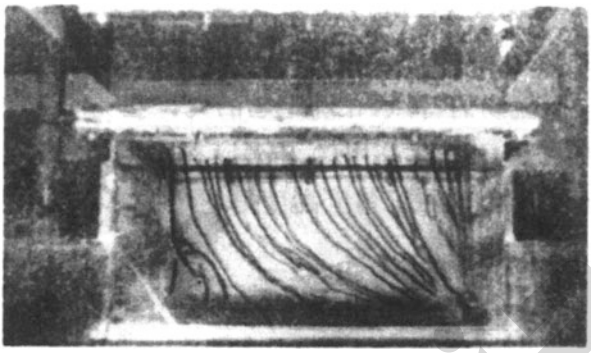

Fig. 8.84 One-side air return mode

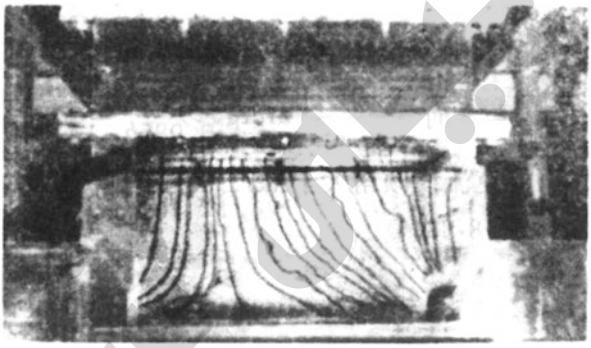

Fig. 8.85 Nonequivalent return air at two sides

Influence of Return Air at One Side and Nonequivalent Return Air at Two Sides

Figure 8.84 is the experimental streamline photo for return air at one side, which is equivalent with the doubled room width. It is shown that streamlines are more inclined compared with two-side air return mode. The triangular region originally located in the central bottom of the cleanroom moves to the left corner.

It is imaginable that when appropriate air return is provided at the left corner, the flow condition will be ameliorated. Results are shown in Fig. 8.85. When return air with a few amount of flow rate is added on the left corner (which means flow rates at left and right sides are different), the streamlines' condition is improved. The triangular region is reduced and the position also changes.

The above introduction shows that nonequivalent return air at two sides (when the room width is small, return air with small amount of flow rate can be placed) can be used, if two-side air return mode is not possible, because of the allocation of process or the narrow room width. It also applies for the case when larger triangular region may appear with one-side air return mode for relatively large room width, or it is hoped to remove the triangular region since the process should be placed in the center of the room. For example, there is one cleanroom with width 3 m, one-side air return mode is used, and an opening with many holes is placed at the other side, so that air is exhausted here with the positively pressurized air. It is not organized

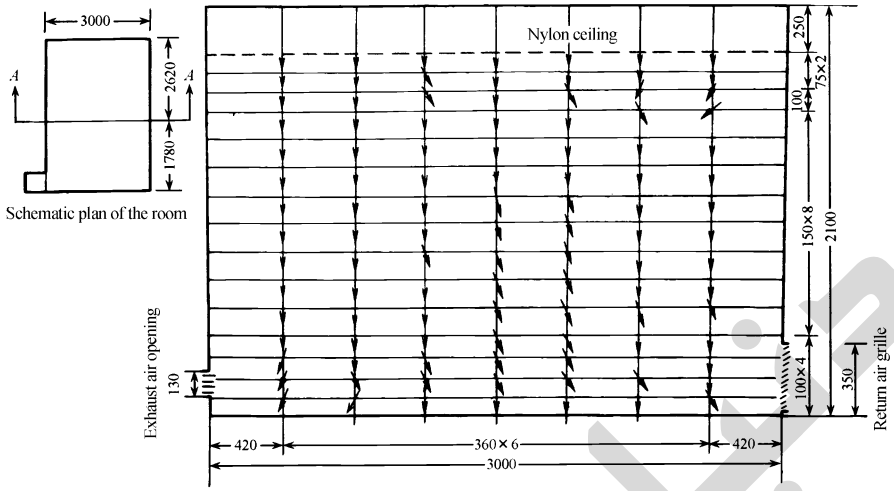

Fig. 8.86 Flow field in one cleanroom with one-side air return and one-side air exhaust mode

return air, but the flow field condition is also ameliorated. The triangular region is too small at one side to be measurable, which is shown in Fig. 8.86. All these methods make it flexible to apply the two-bottom-side air return mode.

8.9.3 Allowable Room Width

With above features of the flow field in the cleanroom, two aspects are mainly considered for determination of the allowable room width.

1. With the allowable room width, the working area (0.8 m above the floor) should be above the height of the triangular region.

   It is shown from the above water models that the average height of this triangular region can be $0.125b$. When the height of working area is assumed 0.8 m, b can be a little larger than 6 m.

2. With the allowable room width, the inclination angle of streamlines in the specified region should be larger than 65°.

From the flow field figure obtained by theoretical calculation, the streamlines are used as reference at the place $b/4$ where curve first appears. The inclination angle in the region between 0.75 and 1.8 m above the floor can be obtained:

$$\text{For } b = 4,\ arctg\frac{0.26b}{0.075b} = 73.9^\circ$$

$$\text{For } b = 6,\ arctg\frac{0.175b}{0.085b} = 64.1^\circ$$

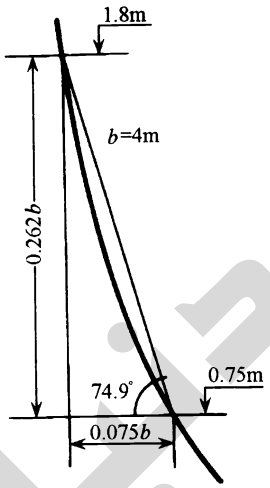

Fig. 8.87 Inclination angle of streamline when $b = 4$ m

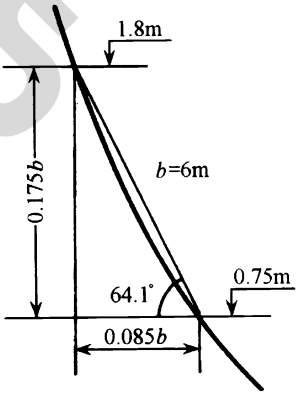

Fig. 8.88 Inclination angle of streamline when $b = 6$ m

So when b is slightly less than 6 m, the inclination angle of the streamline can be larger than 65°.

The above results are shown in Figs. 8.87 and 8.88.

From the above two aspects of analysis, when the width of cleanroom with full-ceiling air supply and two-bottom-side air return mode is not larger than 6 m, it can be thought as the unidirectional flow cleanroom. When the room width is less than 5 m and the limit is supposed 5 m, it is much stricter and the corresponding inclination angle is 69°. This is why it is recommended so in "Design guideline of cleanroom factory" published in 1984 (GBJ 73-84). According to field test, the air cleanliness level can reach Class 5. For the above two examples with field test, the indoor particle concentrations under as-built status are 0.026 pc/L (≥0.5 μm) and 0.24 pc/L (≥0.5 μm), respectively.

References

1. NASA SP-5076 (1969) Contamination control handbook, Sandia National Laboratories
2. Morrison PW (1973) Environmental control in electronic manufacturing. Van Nostrand Reinhold Company, New York, USA
3. Institute of HVAC of China Academy of Building Research (1973) Assembly thermostatic cleanroom, pp 6–7 (In Chinese)
4. Sato E (1976) Status of industrial cleanroom. J Jpn Air Clean Assoc 13(8):32–41 (In Japanese)
5. Meckler M (1970) Packaged units provide clean room conditions in moon rock. Heat Pip Air Cond 42(7):71–76
6. Кочерин ИД (1978) Air cleaning technology in production of semiconductor and integrated circuits (trans: 10th design research institute of the former fourth machinery industry department) (In Chinese)
7. Xu ZL, Shi NS, Lu Y (1981) Research of airflow characteristic in cleanroom with air supply fully at the ceiling and air return at two bottom sides. Research at Institute of HVAC of China Academy of Building Research, p 11 (In Chinese)
8. Fitzner K (1976) Luftstromungen in raumen mittlerer Hohe Bei Verschiedenen arten von Luftauslassen. Gesundheits Ingenieur 12:293–300 (In German)
9. Карпис ЕЕ (1975) Кондиционирование Воздуха В Чистых Помещениях. Холодилъная техника 1:54–58 (In Russian)
10. Kikuchi I (1969) Design of dust-free sterile environment. Jpn Air Cond Heat Refrig News 9(1):91–96 (In Japanese)
11. Naoi T (1979) “Eye curtain” by the combination of vertical laminar flow and air curtain. J Jpn Air Clean Assoc 17(1):47–49 (In Japanese)
12. Rivenburg H (1973) Environmental control for high big clean room. Heat Pip Air Cond 45(3):57–64
13. Wuhan Institute of Hydraulic and Electric Engineering (1960) Hydrodynamics. Water Conservancy and Electric Power Press, Beijing (In Chinese)
14. Finkelstein W, Ritzner R, Moog W (1975) Measurement of room air velocities within air conditioned buildings. Heat Ventilat Eng J Air Condit (Part 2) 49(575):6–11
15. Department of HVAC, Water Supply & Exhaust at Xi’an Metallurgy College (1961) Fluid dynamics. China Industrial Press, Beijing (In Chinese)
16. Xu ZL, Qian ZM, Shen JM et al (1983) Lower limit of air velocity in parallel flow cleanroom. Research at Institute of HVAC of China Academy of Building Research, p 11 (In Chinese)
17. Hayakawa K (1980) Air conditioning in comprehensive hospital. Jpn Air Cond Heat Refrig News 20(8):51–59 (In Japanese)
18. Kato S (1971) Selection method of air cleaning devices for different application. Jpn Air Cond Heat Refrig News 11(9):103–110 (In Japanese)
19. Kawamoto S et al (1971) Design planning of cleanroom for industrial facilities (No.1), Jpn Air Cond Heat Refrig News 11(9):91–100 (In Japanese)
20. Nishi T, Sakamura T (1980) Actual situation of cleanroom design in recent comprehensive hospitals. Jpn Air Cond Heat Refrig News 20(8):81–85 (In Japanese)
21. T.O.00-25-203 (1972) Contamination control of aerospace facilities. Technology Regulations of U.S. Air Force
22. Xu ZL (1994) Design of cleanroom. Seismological Press, Beijing (In Chinese)
23. Zhang WG (1992) Experimental study of radial flow cleanroom model. Master dissertation of Harbin Building Engineering College (In Chinese)
24. Wei XM, Fan HM, Zhang WG (1994) Numerical simulation and experimental assessment of radial flow cleanroom. In: Proceedings of the annual national conference on HVAC&R, pp 232–235 (In Chinese)
25. Wei XM, Sha L (2001) Numerical simulation of one cleanroom with new type of air supply and return modes. Contam Control Air Cond Technol 3:13–17 (In Chinese)

26. Xu ZL (2006) Design principle isolation ward. Science Press, Beijing, p 39 (In Chinese)
27. Kita J, Isono K, Morikawa K (2004) Dynamic characteristics of opening and closing of door in cleanroom for solid dosage workshop and related study on migration of airborne particles. J Soc Heat Air Cond Sanit Eng Jpn 95:63 (In Japanese)
28. Zhao HZ, Zhai HL (1994) Infiltration air velocity calculated with the safety probability method in China. J HV&AC 24(1):16–20 (In Chinese)
29. Xu ZL, Shen JM (1989) Application of air cleaning technology. China Architecture & Building Press, Beijing, p 222 (In Chinese)
30. Japan Air Cleaning Association (1981) Handbook of air cleaning. OHM Press, Japan, p 450 (In Japanese)
31. Xu ZL (2005) The application of surge chamber of negative pressure isolating room. Build Sci 21:52 (In Chinese)
32. Austin PR, Timmerman SW (1965) Design and operation of clean rooms. Business News Publ, Detroit
33. Editorial Department of Chinese Contamination Control Society (1989) Development report of HG-8801 slot scanning airshower chamber (In Chinese)
34. Moren Z (1979) Fluid dynamics-pump and fan. China Architecture & Building Press, Beijing, p 236 (In Chinese)
35. Fukao H (1985) Chapter 5: Evaluation experiment on airshower. In: Evaluation study of cleanroom performance (exchanged paper) (In Japanese)
36. Institute of HVAC of China Academy of Building Research (1973) Assembly thermostatic cleanroom, pp 62–69 (In Chinese)
37. Талиев ВН (1963) Азродинамнка Вентнляции (In Russian)
38. Li BT, Wei XM (1997) Study of the characteristic of cleanroom with air supply outlet fully placed at the ceiling and return air grille on both side walls. J Harbin Build Coll 30(3):59–62 (In Chinese)

Chapter 9
Theory of Biological Cleanroom

Modern biological cleanroom was developed on the basis of the industrial cleanroom. Except for the common principles of the cleanroom, the specific principles for the control of biological particles should also be complied with. This chapter will illustrate on these particularities.

9.1 Application of Biological Cleanrooms

The first biological cleanroom was built in the USA in Jan. 1996 as the operating room in hospital.

Now, biological cleanroom has been widely used in astronavigation, medical science, pharmacy, microbiology, biological experiments, genetic engineering, instrument industry, and so on.

In medical science, one of the applications of biological cleanroom is mainly the operating rooms for joint replacement, organ transplantation, cerebral surgery, and thoracic surgery. This effect is obvious. Table 9.1 is the statistical result of the infection rate after the operation of hip joint replacement [1]. Table 9.2 is the result with the culture on the wound smears directly in general operating room [2]. In clean operating room, the main pathogenic bacterium disappears near the wound area, which decreased the postoperative infection rate from 9 to 0.5 %.

Yu Xihua emphasized that air cleaning is the main measure to remove airborne bacteria with the following examples [3]:

Charnley et al. from the UK performed study for 15 years. When laminar flow cleanroom was used to replace the common operating room, the infection rate among more than 5,000 surgery cases decreased from 7.7 to 1.5 %. When the whole body suction suit was used, the infection rate among more than 6,000 surgery cases decreased further to 0.6 % [4]. During the study, the antibiotic was not used.

Medical Research Committee of the UK (MRC) performed comparison researches for more than 8,000 surgical cases of hip joint replacement in 19 hospitals. The

Z. Xu, *Fundamentals of Air Cleaning Technology and Its Application in Cleanrooms*,
DOI 10.1007/978-3-642-39374-7_9, © Springer-Verlag Berlin Heidelberg 2014

Table 9.1 Postoperative infection rate of hip replacement

Air-conditioning methods in operation room	Time (year)	Air change rate (h^{-1})	CFU (#/h)	Operation number	Postoperative infection rate (%)
General form: exhaust	1961	–	80–90	190	8.9
I type closed electric dust collector	1962	10	25	108	3.7
II type closed electric dust collector	1963–1965	80	18	1,079	2.2
Vertical unidirectional flow cleanroom	1966–1968	300	0	1,929	1.5
Vertical unidirectional flow cleanroom (improved operating cloth)	1969–1970	300	0	2,152	0.5

Table 9.2 Comparison of results on the wound smears

Operating room	Number of smear	Polluted number	Percentage (%)	Results with culture
General	84	24	28.5	*Staphylococcus albus*, *Staphylococcus aureus*, *Bacillus, Sarcina*, *Streptococcus viridans*, Coliform bacteria, Fungi
Horizontal unidirectional flow	83	12	14.5	*Staphylococcus albus*, Coliform bacteria, Fungi

infection rate during 1–4 years was 0.6 %, while it is 1.5 % when the same operations were performed in common operating room by the same doctors.

The application effect of clean operating room was usually reported from abroad in the past. At present, some Chinese examples can also be presented.

At the beginning of 1980s in China, with the application of two clean operating room in the burn surgery, not only the postoperative infection rate for the general operation was generally declined, but also the infectious rate of two-degree burnt patients with more than 70 % of large area burnt was significantly reduced, and the healing process on the burnt face went on well and quickly [5]. Among 9,337 cases with I class operation performed in the clean operating room at Shanghai Changzheng Hospital during 1989–1990, no infection case appeared. There was no infection accident among 16,427 cases with I class operation performed in the clean operating room at 301 Hospital during 1995–1996. Of course there were other factors.

According to the report by Wang Fang at the 2011 National Hospital Building Forum, investigation about the postoperative infectious rate with 1,808 cases of operation was performed between June and Nov. of 2000 at attached hospital of Xuzhou Medical College. It was found that with clean operating room, the postoperative infectious rate decreases from 6.41 % with traditional general operating room to 0.93 %.

Table 9.3 shows the statistical result about the postoperative infectious rate with 2,328 cases of operation in one educational medical hospital when different methods of disinfection were used in the operating room, which was investigated

Table 9.3 Infectious rate with different disinfection methods in operating room (%)

	Surgery site infection			Nonsurgery site infection		
Group	Case number	Infection number	Infectious ratio	Case number	Infection number	Infectious ratio
Laminar flow	332	3	0.90	332	6	1.81
Air cleaner	928	28	2.02	928	19	2.05
Ultraviolet sterilizer	1068	68	6.37	1068	22	2.06

by Xu Qinghua et al. [6]. The conclusion is that the risk of postoperative infectious rate with ultraviolet sterilizer is 7.08 times of the laminar flow cleanroom, which is 2.11 times of the indoor air cleaner. The performance with laminar flow operating room is significant.

Xia Muya reported the change of surgery site infection with Class I cut before and after the clean operation room was applied in No.1 attached hospital of Suzhou University. Although the original infectious rate is not high, it reduces by half when the clean operating room was used. In 2000 it was 0.74 %, and in 2001 it was 0.35 %, then in 2002 it was 0.32 %, and in 2003 it was 0.31 %. It is almost stable afterwards [7].

With the application of the clean operating room, less or no antibiotics can be used. In the past due to the abuse of antibiotics, the drug resistance ability of bacteria was greatly increased. When bacteria are exposed to antibiotics during the growth period, due to the effect of selection pressure, its metabolic pathway or the fine structure is forced to change. For example, bacteria can produce inactivated enzyme to destroy the structure of antibiotics, which deprives the competence of the antibiotics. Bacteria can modify the structure and quantity of the target protein which antibiotics act on, so that the bacteria are no longer sensitive to antibiotics. With the effect of the barrier by outer membrane and the efflux pump, the amount of antibiotics entering in the bacteria is reduced, and the ability of pump out antibiotic is increased, which reduces the antibiotic concentrations in the bacterial body. In this way, the bacteria do successfully escape being destroyed by the antibiotics and survive. In the long run, the application of large amount of antibiotic results in the reduced autoimmune ability of patients.

It should be emphasized that the reduction of infectious rate in clean operating room is obviously related to the type of operation cut. The decrease of infectious rate for Class I clean cut should be more obvious than that for Class II clean-polluted cut. The infectious rate for Class III and Class IV infection cuts is greatly reduced, because the possible infectious rate generated for this kind of cut can reach more than 20 %.

In the *Design and management guideline of hospital air conditioning equipment* published by Japanese Association of Medical Equipment in 2004 [8], the infectious rate of 8,052 cases of hip joint and knee joint replacement operations was given under the conditions of ultra-clean air (it is defined as the bacterial concentration less than 10#/m^3) and precautious anti-poison drug, which is shown in Table 9.4.

It is obvious that the use of antibiotics can kill the bacteria in the body (including the surgery site) with the higher efficiency than the measures to prevent the deposition of bacteria onto the surgery site. But as mentioned before, in order to

Table 9.4 Relationship between the surgery site infection and the conditions of ultra-clean air and precautious anti-poison medicine

Treatment condition	Surgery site infection (SSI) at the deep layer of cut (%)
No measures	3.4
Only use ultra-clean air	1.6
Only use precautious anti-poison medicine	0.8
Use ultra-clean air and precautious anti-poison medicine at the same time	0.7

prevent the increase of antidrug ability of bacteria and the generation of super bacteria, the appeal to use less antibiotics or no antibiotics is increasing strong at present. It does not mean the effect of biological cleanroom should be questioned in the Japanese example; instead it means that compared with nonbiological cleanroom "without any measures," it is relative efficient with biological cleanroom, since the infectious rate can reduce by more than a half. The value of 1.6 % is almost the same the value of 1.5 % by Charnley in previous chapter. Although the infectious rate with only ultra-clean air is one time higher than that only with antibiotics, it is an important goal not to use antibiotics. At present some detailed measures have been issued in some region. For example, it specifies that medicine is given 30 min before operation for one time. Therefore, the cleanroom technology, where antibiotics are not needed and at the same time the postoperative infectious rate is greatly reduced, is the goal people have paid attention to.

Just as the Sweden *Fundamental requirement and guideline for cleaning in biological cleanroom* (SIS-TR 39 *Vägledning och grundläggande krav för mikrobiologisk renhet I operationsrum*) issued in 2011, it pointed out that: "Precautious antibiotics have individual effect on the infectious rate. But the anti-drug ability of bacteria will be correspondingly increased, which will reduce the effect of precautious antibiotics."

It should be noted that in addition to burn surgery, good performance was obtained with the application of biological cleanroom for special treatment of asthma and leukemia. Especially for patients with leukemia, most of leukocytes in patient are naive cells, which have lost the defense ability against infection severely. In order to provide the time gap for the preparation of implantation growth for hematopoietic stem cell, which means the existing leukemia cells must be removed and patients' immune function must be inhibited so that hematopoietic stem cells mismatched with the tissue can be implanted, patients used to take high-dose immune inhibitors and radiation therapy before operation, which will reduce the number of leukocytes to "0" in seven days. Therefore, lethal infections of leukemia patients are the major causes of death with the mortality of 50–60 %. So during the treatment, it is especially important to prevent infection from bacteria including Gram-negative bacteria, Candida, and Aspergillums, but this can only be achieved in biological cleanrooms. For the morbidity of leukemia in China is about 3/100,000 [9], more and more importance has been attached for the development of biological cleanroom which is used for the treatment of leukemia.

Table 9.5 Performance for treatment of leukemia with three groups of patients

Group	Patient number	Ward	No chemical therapy	Number of four fatal infection	Death rate (%)	Survival ratio in 100 days (%)
A	26	Unidirectional flow biological cleanroom	Use antibiotics simultaneously	3	5	91
B	32	General ward	Use antibiotics simultaneously	17	24	66
C	28	General ward	Use a variety of chemical therapy	16	25	61

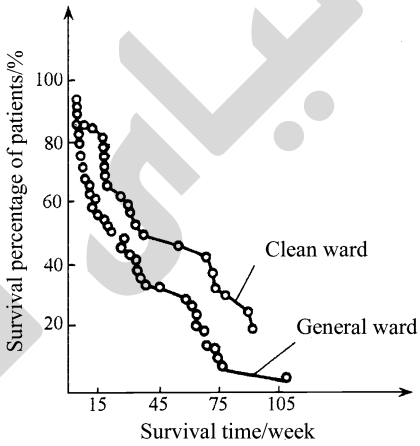

Fig. 9.1 Comparison of survival condition for leukemia patients

According to the report from National Institutes of Health in the USA in recent 10 years [10], the performance of the treatment of leukemia is remarkable with antibiotics, when it was performed in biological cleanroom aseptic conditions, which can extend the patient's life in this condition. Table 9.5 shows the comparison of the performance with a contrast group.

With the data about the survival percentage of patients shown in Fig. 9.1 [11], the life of leukemia patients treated in the isolation unit of biological cleanroom will be prolonged by about one time than that in the general ward. Studies have also shown that, in biological cleanrooms, the ratio of leukemia patients who can completely recover can reach 33 %, while in general wards, it is 19.6 % [12].

Since the later period of 1970s, biological cleanroom has been constructed for the therapy of leukemia in China, which has made gratifying achievements. There are reported cases with successful operations at Shanghai Xinhua Hospital and Institute of Hematology from Beijing Medical College. For example, it was the first time for Xinhua Hospital to perform marrow transplantation on leukemia patient in cleanroom in Oct. of 1980, which obtained a success. With the severe condition of leukocyte less than 400, the patient had a fever only for several days in the

cleanroom, and afterwards there was no fever again, which means the infection has been successfully prevented. During the period of more than 1 year after leaving the hospital, the patient was still in good health condition. In the late of 1990s, the number of hospitals with clean blood ward in China was at least more than 30. The largest one in Asia is Beijing 307 Hospital where 10 hematology wards with Class 100 were newly built. The air cleanliness level in its internal corridor was Class 1000. At the end of 1994 when it was put into service, the index under its as-built state was: average cross-sectional velocity was 0.21 m/s for 10 rooms (in Chinese military standard implemented in 1996, the value specified was 0.18–0.25 m/s), average noise was 49.8 dB(A), the maximum of mean particle concentration (for particles with diameter $\geq$0.5 μm, when particle counter with sampling flow rate 28.3 L/min was used for detection) was 0.55#/L, statistic average concentration indoors was 0.66#/L, and average settlement of bacteria was 0.15 CFU (with the sampling vessel ϕ 90 for 0.5 h). The performance was quite good during several years of operation. It went without infection for the treatment of 110 patients during 1994–1997. Until 2009, there were 4 million leukemia patients in China. The healing rate of the leukemia by acute lymph cell reached more than 95 %. The possibility of healing without recurrence also reached 70 % and 80 % in the five continuous years. When different types of leukemia were considered comprehensively, the healing rate should be about 60 % (according to the report of Beijing Evening Newspaper on the 7th page on Feb. 22, 2009). Now, there is no doubt that biological cleanroom (device) is an indispensable guarantee condition for the treatment for leukemia.

In the development field of medical biological cleanroom, the USA was ever on the top of the world. In the late of 1970s, there were already 288 biological cleanrooms, of which 240 was operating room and 48 wards. Except the USA, in the late of 1970s, there were already 127 cleanrooms of this kind in Japan, which was several times of Germany, France, England, Switzerland, and other European countries. In clean operating room, artificial joint replacement operation takes the most proportion, while in cleanroom, acute leukemia ward is of the majority [14].

With the development of economy and construction in China, the *Code of designing and building the clean operating department in military hospitals* has already been implemented in 1996, the *Building standard for the clean nursing ward in army hospitals* implemented in 1997, the national standard *Clean operation Department in hospital construction standard* implemented in 2000, and the national standard *Architectural code for Clean Operating Room in Hospital* implemented in 2002. *Architectural design code for comprehensive hospital building* has been drafted. Various kinds of cleanrooms (rooms with clean environment) have been applied in various departments of hospital. According to incomplete statistical investigation, there are already ten thousands of cleanrooms built.

It should be emphasized here that although the infectious rate on the operating site through indoor air is far less than that through direct contact, with the great advancement of the operating technique itself, operating apparatus, instrument and

equipment, medical care technique, and building techniques, the control of air pollution becomes the most important role because only the air quality lags behind. Air cleaning technology is only one of the routes for disinfection and sterilization of air in cleanroom, but it is the only route which can be controlled from the whole process and can be controlled comprehensively and at critical positions, which was believed to be the fundamental elements for quality control of modern products [13]. But there are also cases where cleanrooms were poorly built and managed, which results in poor performance.

In the pharmaceutical field, the requirement becomes increasingly demanding for the purity of drugs, especially for intravenous, intramuscular, and ophthalmic purpose, where more drugs must be manufactured in a clean environment. Experiments show that the entrance of a certain number of particles into the circulatory system will cause a variety of deleterious symptoms, and if the injection or infusion medicament contains any bacteria, polysaccharide it produced can cause the patient to the pyrogen reaction [15]. So biological cleanrooms with different classes are widely applied in advanced pharmaceutical industry, especially for the filling of injection, packaging process and quality inspection, testing, and other processes. Since the middle of 1980s, the system *Good Manufacturing Practice for pharmaceutical production* (GMP), which begins from 1960s internationally, has been widespread. And it specifies that the standard should be followed for the construction of clean workshop for the production of human medicine, veterinary medicine, equipment, and packaging supplies, which has received satisfied results. In addition, biological cleanroom technology has also been applied in food and cosmetics industry. In 2011, the national standard *Architectural technique code for food industrial cleanroom* was implemented.

In the asepsis test, biological cleanroom has been successfully applied to departments including tissue culture, cancer cell culture, vaccine culture, the production of antibiotics, etc. It usually takes more than one year to produce live cancer cells outside the human body, and all the previous efforts will be wasted once it is slightly contaminated. In the production process of antibiotics, tons of nutritional raw materials will be wasted by inadvertent contamination. There is also a notable asepsis test, that is, the breeding of sterile animals. Animals used for biological, chemical, and pharmaceutical test are called "sterile animal," which means there is no pathogenic microorganisms in vivo.

Animals without specific pathogenes or only with known or specified bacterial, that is, SPF (Specific Pathogene-Free animal) animal, are also used. When these animals are used for experiment, the influence of impurity bacteria contained in the animal itself can be eliminated, and the real results can be obtained quickly. The sterile animal or SPF animal must be breed from generation to generation in biological cleanroom, which removes the possibility of bacterial infections since it's born, so that the purity can be ensured.

Aseptic animal is the highest level, that is, the fourth level, in the experimental animals. In 1992, China also issued the classification standard for experimental animal [16]. In the *Architectural technique code for experimental animal* implemented

in 2008, it specifies that for the second-level animals, except for that there is no specified microorganism for this class or when it is need, the microorganisms specified for the first class must not exist or when it is needed. It applies for the following classes. The detailed information is presented in Tables 9.6, 9.7, and 9.8. National or local environmental standards have also been issued on the experimental animal.

In the space navigation field, it was the Lunar Lander that first has the application of biological cleanroom [17]. Biological cleanrooms must be used for the manufacture of the Lunar Lander, the container used to retrieve a moon rock and for the test of recaptured rock. Because if any organic matter from the earth was taken into another star of the universe or if the organic matter from the earth during the assay was mistaken as the inherent planet organics as the recaptured material, a false research conclusion and extremely serious consequences will be made.

9.2 Main Characteristics of Microbe

For the control of microbial contamination, understanding of microbial characteristics is necessary. Because algae and protozoa are larger, they can be not mentioned. According to the relevant microbiology works, the main characteristics of several other microorganisms will be listed, which is shown in Table 9.9.

For bacteria, there is an important characteristic, that is, the growth characteristics. It can be described by the growth curve, which is useful to understand the bacteriological feature in biological cleanroom. In later section, the phenomenon for the explosion of the bacterial concentration when air-conditioning equipment is started will be introduced. The knowledge for the filtration treatment of fresh air needs to be updated. All these are related to this characteristic.

According to the conventional practice of bacteriology, the bacterial growth curve can be obtained, which shows the change of living bacteria number with time, when the living bacteria number is counted after the bacteria are cultured on the substrate. The curve is shown in Fig. 9.2. Several bacterial growth stages are apparently shown on this curve.

9.2.1 Preparation Period or Delayed Period

After the inoculation of some bacteria onto the culture medium, they need time to adapt to new environment. They usually don't divide and develop immediately. Bacterial number almost does not increase, even some will die, and the number reduces when they don't adapt to new environment.

Table 9.6 Classification standard for virus detection on experimental animal

Grade of Animals				Virus	Animal type				
					Mouse	Rat	Guinea pig	Hamster	Rabbit
IV: Aseptic animal	III: Non-special pathogene animal	II: Clean animal	I: Ordinary animal	Lymphocytic Chor Lomegltls Virus (LCM)	○		○	○	
				Eplzootlc Hemorrhaglc Fever Virus (EHFV)	○	○			
				Eorromella Virus (poxvirus of Milce)	○				
				Rabbit Hemorrhaglc Dlseasc Virus					○
				Mouse Hapatltis Virus (MHV)	○				
				Sendal Virus	○	○		○	
				Slmian Virus (SV5)			○	○	
				Pneumonla Virus of Mice (PVM)	○	●	○	●	
				Reovirus Type 3 (Reo-3)	●	●	○	○	
				Mouse Enceptalomyelltls Virus (GdDN)	○	●	○	○	
				Mouse Adenovirus (MAd)	●				
				K Virus (KV)	●				
				Minute Virus of Mice (MVM)	○				
				Polyoma Virus	○				
				Rotavirus					●
				Toolan's Virus (H-1)		○			
				Kllharm' Rat Virus (KRV)		○			
				Rat Corona Virus (RCV)		○			
				Slalodacryoadenitls Virus (SDAV)		○			
				Eplzootic Diarrbea of infat Mice (EDIM)	●				
				Lactic Dehydrogenase Virus (LDV)	●				
				Mouse Cytomegalo Virus (MCMV)	●				
				No detectable virus					

Note: ○ means there is no requirement, ● means it should be checked when needed

Table 9.7 Classification standard for pathogenic bacteria detection on experimental animal

Grade of Animals				Pathogenic bacteria	Animal type					
					Mouse	Rat	Guinea pig	Hamster	Rabbit	Dog
IV: Aseptic animal	III: Non-special pathogene animal	II: Clean animal	I: Ordinary animal	Salmonella Sp	○	○	○	○	○	○
				Listeria Monocytogenes	●	●	●	●	●	
				Yersinia Pseudotuberculosis	●	●	●	●	●	
				Brucella						○
				Pasteurella Multocida	○	○	○	○	○	○
				Bordetella Bronchiseptica	○	○	○	○	○	○
				StreptobacIllus MonIliformis	●	●	●	●	●	●
				Yesinia Enterocoliltica	●	●	●	●	●	●
				Mycoplasma Pulmonis	○	○				
				Mycoplasma Neurolyticum	●					
				Mycoplasme Arthrilidis		●				
				Corynebacterium Kutscherl	○	○				
				Bacillus Piliformis	○	○	○	○	○	
				Escherlchia Coll 0115aC: k(B)	●					
				Pasteurella Pneumotropica	○	○	○	○	○	
				Klebsiella Pneumoniae	○	○	○	○	○	
				Staphylococcus Aureus	○	○	○	○	○	
				Streptococcus Pneumoniae	○	○	○	○	○	
				β-hemolytic Streptococcus	○	○	○	○	○	
				Pseudomonas Aeruginosa	○	○	○	○	○	
				No detectable virus	○	○	○	○	○	

Note: ○ means there is no requirement, ● means it should be checked when needed

Table 9.8 Classification standard for parasite monitoring on experimental animal

Grade of Animals				Parasite	Animal type					
					Mouse	Rat	Guinea pig	Hamster	Rabbit	Dog
IV: Aseptic animal	III: Non-special pathogene animal	II: Clean animal	I: Ordinary animal	Ectoparaslte	○	○	○	○	○	○
				Encephalitizoon Cunlculi	●	●	●	●	○	
				Entamoeba Sp	○	○	○	○	●	●
				Eimeria Sp	●	●	○	●	○	
				Taenia Sp	○	○		○	○	●
				Hymenolepis Nana	○	○		○		
				Hymenolepis Diminuta	○	○		○		
				Spirometra Mansonl						●
				Clonorchis Sinensis						●
				Opisthorechis Felineus						●
				Paragonlmus Westermanl						●
				Ancylostoma Caninum						○
				Toxocara Sp						○
				Syphacia Sp	○	○		○		
				Aspiculurls Tetraptera	○	○		○		
				Thelazia Callipaeda						●
				Gnathostoma Spinigerum						●
				Dirorilaria Immitis						○
				Dioctophyma Renale						●
				Trihosomoides crasslcauda	○	○		○		
				Capillaria hepallca	○	○		○		
				Passalurus Sp.			○		○	
				Pneumocystis Carinii	○	○		○		
				Trichomonas Sb	○	○		○		
				Giardia Muris	○	○		○		
				Spironucleus Muris	○	○		○		

Note: ○ means there is no requirement, ● means it should be checked when needed

Table 9.9 Main microbial characteristics

Microorganism	Colony characteristics	Individual form	Physiological characteristics	Reproduction mode
Virus	No colony form	No structure of cell, rod, sphere, poly-angle, tadpole shape	Parasitize on animal, plant, bacteria, and human body	Self-reproduce of nucleoprotein in host cell
Rickettsia	No colony form	Pleomorphic	Parasitize on insect and human body	Reproduce in host cell
Bacteria	Humid, smooth, glossy, semi-transparent, or opaque	Single cell; cell structure is imperfect; with shapes of rod, sphere, or arc	Usually with the phagocytosis of phage; live in neutral and alkalescence environment	Fissiparity reproduction
Actinomycetes	Dry, rigid, wrinkled	Mycelium is tenuous; no partition; nucleus structure is imperfect; when the spore is dry, it usually appears hanging state	Grow slower than bacteria and mould in the neutral and alkalescence environment	Spore is formed by split of fibrillae
Yeast	Similar as bacteria, large	Single cell; cell structure is perfect; circular or oval shape	Live in slight acid environment	Gemmation, and some is zoogamy
Fungi and mould	Lint shape, colorful, big	Mycelium has horizontal septates or no septates; cell structure is perfect	With the ability of acid resistant	Various types including conidia, sporangium, and zoogamy

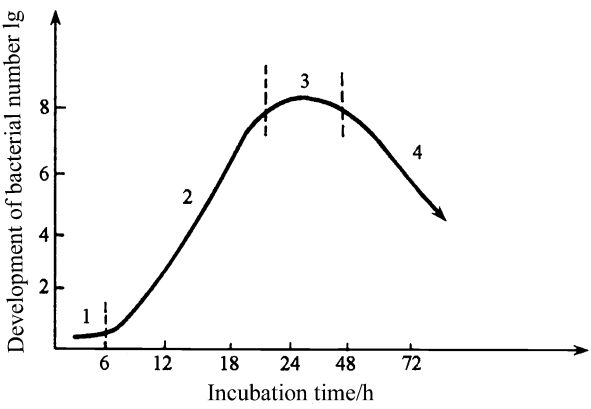

Fig. 9.2 Bacterial growth curve. *1* preparation period (or delayed period), *2* logarithmic growth period, *3* stable period (or quiescent period), *4* decay period

9.2.2 Logarithmic Growth Period

It can be seen that the curve in this stage can be approximated as straight line, during which bacterial number increases according to the geometric series approach, that is, $2^0 \rightarrow 2^1 \rightarrow 2^2 \rightarrow 2^3 \rightarrow 2^4 \cdots \rightarrow 2^n$. The time needed between this split and the next split time is different for different kinds of bacteria. For example,

Intestinal bacteria ~20 min
Staphylococcus 30–40 min
Mycobacterium tuberculosis 18–24 h

Taking the Staphylococcus as an example, 2 divisions occurred in 1 h, so 16 divisions will occur in 8 h, through which bacterial number increases from the 1 to 65,536, and after 12 h, it reaches 1.6777×10^7. The logarithmic growth period generally lasted a day. The reproduction rate of virus is much faster. A virus within living cells can reproduce 100 thousands of subsets of virus.

9.2.3 Stable Period or Quiescent Period

In a specified volume of culture medium, bacteria cannot be increased unrestrictedly with the rate in logarithmic growth period. Because the nutritional deficiency in culture medium and accumulation of harmful metabolites, the bacterial growth rate in late of logarithmic growth period decreased gradually, and the death rate gradually increased. When it reaches the balance state, the living bacterial number is stabilized, just as the bacteria have stop breeding. This stage lasts about 1 day in length. So it is appropriate to set 24–28 h as the culture time in the Petri dish.

9.2.4 Decay Period

After culture continues after the stable period, the bacterial mortality rate exceeds the growth rate, so decay period begins with the decreasing number of living bacteria.

9.3 Microbial Pollution Routes

In order to control the microbial contamination, it is also necessary to understand the pathways of microbial contamination, which mainly includes the bacterial and viral contamination.

Microbial pollution usually has four ways:

1. Self-pollution, which is caused by bacteria carried on the own body of patients or staffs

2. Exposure to pollution, which is caused as a result of contact with an incomplete sterile utensils, equipment, or human
3. Air pollution, which is because of the settlement, attachment, or inhalation of bacteria suspended in air
4. Other pollution, which is caused by insects and other factors

For cleanroom, there are variety of pollution pathways since air is added as the transmission medium of air pollution. It can be shown as follows [18].

In the same room:

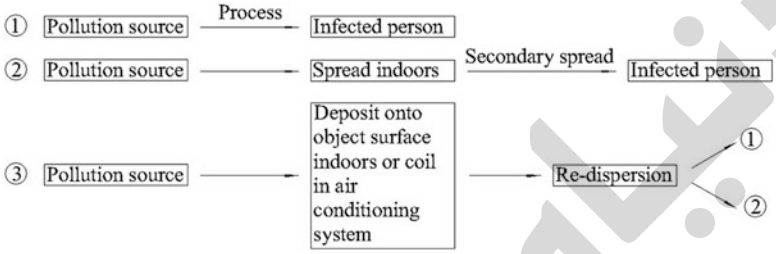

Effects of other rooms:

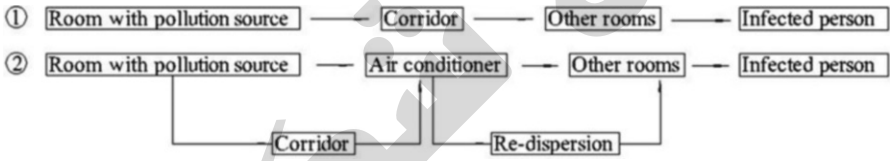

So the difference between the biological cleanroom and the industrial cleanroom is that not only air filtration method needs to be used so that the number of the biotic and abiotic particles entering indoors can be strictly controlled, but also various surfaces including indoor personnel, apparatus, panel, and others must be sterilized. So the internal materials in biological cleanroom should be able to withstand the erosion from a variety of sterilizing agents. Therefore, in foreign literatures, one explanation of the biological cleanroom is that it is the industrial cleanroom with the structure and material allowed for sterilization.

Therefore, there are two major technical problems for biological cleanroom, which are the filtration of airborne microorganism especially the bacteria and the sterilization treatment on various surfaces.

9.4 Equivalent Diameter of Biological Particles

9.4.1 Size of Microorganism

Microorganism is also one kind of solid particles. The biological particles include the following microorganism, which will be shown in Table 9.10 together with their sizes [19–21].

Table 9.10 Size of microorganism (μm)

Algae	3–100	Virus	0.008–0.3
Protozoa		Poliovirus	0.008–0.03
Fungi		Epidemic type B encephalitis virus	0.015–0.03
Bacteria		Rhinovirus	0.015–0.03
Staphylococcus albus and *Staphylococcus aureus*	0.3–1.2	Hepatitis virus	0.02–0.04
Bacillus anthracis	0.46–0.56	SARS virus	0.06–0.2
Common Bacillus pyogenes	0.7–1.3	Adenovirus	0.07
Enterococcus	1–3	Respiratory syncytial virus	0.09–0.12
Bacillus typhi	1–3	Mumps virus	0.09–0.19
Coliform	1–5	Parainfluenza virus	0.1–0.2
Diphtheria bacillus	1–6	Measles virus	0.12–0.18
Lactobacillus	1–7	Hydrophobin	0.125
Silicosis bacillus	1.1–7	Smallpox virus	0.2–0.3
Tubercle bacillus	1.5–4	Enterovirus	0.3
Clostridium tetani	2–4	Rickettsia	0.25–0.6
Bacillus oedematis	5 – 10		

9.4.2 Equivalent Diameter of Biological Particles

Is it difficult to filter bacteria than particles in the biological cleanroom? It is people's intuition that bacteria are so small. Actually this is not the case. In this book, this related concept is presented, which is the equivalent diameter of biological particle.

Microorganisms including bacteria, spirochetes, rickettsia, and virus cannot exist alone in the air, which are often found on the surface of dust particle which is several times larger than themselves [22]. They do not exist as monomer; instead, they appear with the form of bacterial clump or spore. Because air lacks nourishments and they are subject to the irradiation of sunlight especially ultraviolet, only those bacteria and fungi which produces spores and pigment, as well as fungi with strong ability to resist sunlight and dry environment, can survive in the air. So for most airborne bacteria in the air, it doesn't make much sense for the nude size, while what makes sense is the equivalent diameter.

Equivalent diameter can have three meanings:

1. When safety is taken into consideration, let the equivalent diameter equal to the most penetrating particle size, which means it is the lower limit of diameter (the minimum diameter) for the carrier particle penetrating through filters. It can be termed as the penetration equivalent diameter of particles with microorganism.
2. In terms of the filtration performance, the particle size corresponding to the filtration efficiency of the bacterial group can be called as the efficiency equivalent diameter.

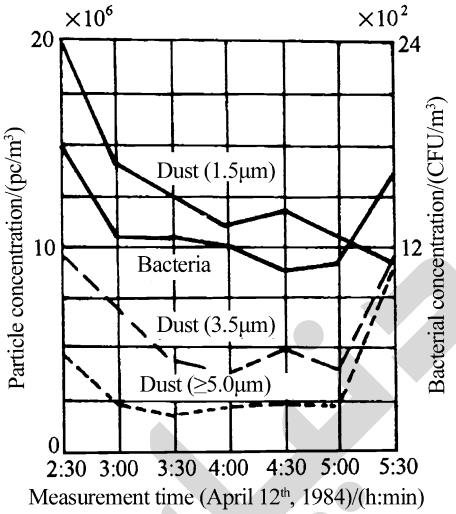

Fig. 9.3 Bacterial and dust concentration variations in hospital air

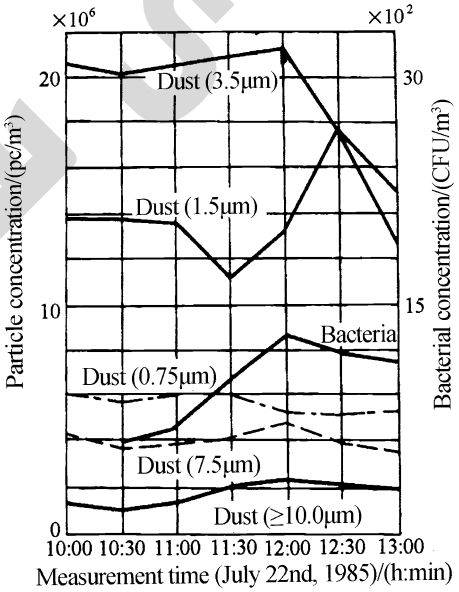

Fig. 9.4 Bacteria and dust concentration variations in office

Li Hengye concluded that there is a certain correlation between the airborne bacteria concentration and the 3.5 μm particle concentration according to the measured data [23], which will be shown in Figs. 9.3, 9.4, and 9.5. It was believed that the filtration efficiency of several fibrous filter materials with atmospheric bacteria is equal to that with 4–5 μm particles. But Tu Guangbei found out that the filtration efficiency of fibrous filter materials with atmospheric bacteria has quite good linear correlation with the particle counting efficiency with ≥5 μm atmospheric dust [24], which is shown in Fig. 9.6. So the filtration efficiency with

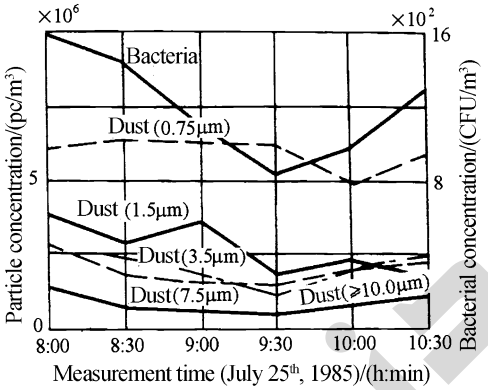

Fig. 9.5 Atmospheric dust concentration curve of bacteria

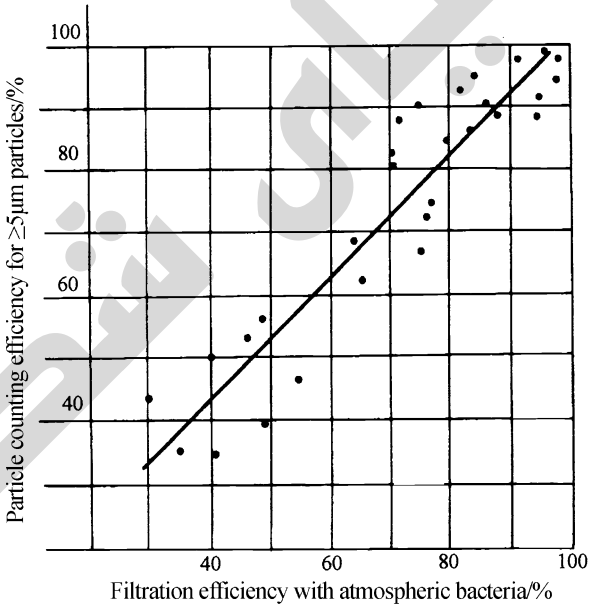

Fig. 9.6 Relationship of bacteria efficiency and dust efficiency

atmospheric bacteria can be approximated as the particle counting efficiency with diameter ≥5 μm, or the following formula can be used:

$$\eta_b = 1.07\eta_d - 5.02 \tag{9.1}$$

where

η_b is the filtration efficiency with atmospheric airborne bacteria;
η_d is the particle counting efficiency for atmospheric dust with diameter ≥5 μm.

That is to say, the efficiency equivalent diameter of atmospheric bacteria is about 7 μm. Because only the efficiency with 7 μm is equivalent to that with diameter ≥5 μm.

Note: (1) Particle concentration with diameter 1.5 μm can be obtained with 10 times of the ordinate value multiplied.

(2) Particle concentration with diameter 0.75 μm can be obtained with a 100 times of the ordinate value multiplied.

Note: (1) Particle concentration with diameter 3.5 μm can be obtained with 10 times of the ordinate value multiplied.

(2) Particle concentration with diameter 0.75 μm and 1.5 μm can be obtained with a 100 times of the ordinate value multiplied (refer to Page 171 from the cleaning association paper in 1986).

(3) When the settlement velocity is taken into consideration, let it be equivalent to the particle diameter with the same settlement quantity, that is, the same sedimentation velocity, of the bacterial group. It is called as the settlement equivalent diameter.

Equation (6.8) reflecting the relationship between v_s and d_p was derived with the particle density 2 kg/m^3. In relative clean place, most of the carriers for biological particle are organic, where the density may be considered as less than 2 and greater than 1. So corrections must be made with Eq. (6.8) to obtain the value of d_p for any ρ:

$$d_p = \left(\frac{v_s}{0.6 \times 10^{-2} \frac{\rho}{2}} \right)^{\frac{1}{2}} \tag{9.2}$$

where the settlement velocity v_s can be obtained by Eq. (6.27) with the following expression:

$$v_s = \frac{N_g}{NfT} \text{ (cm/s)} \tag{9.3}$$

If this formula is used to obtain the value the value of d_p through the measured data, the implications of each parameter in the formula are: N_g is the bacterial settlement quantity, #; N is the airborne microbe concentration, #/cm^3; f is the sampling area, i.e., the area of sedimentation, or the planar utensil area, m^2; and T is the sampling time, i.e., the settling time, s.

In this book, the quantities of the sedimentation bacteria and airborne bacteria are used with "#," which are obtained with the sampling method, either the sedimentation method or the suction method, following by culture. They are expressed with bacterial colony. One bacterial colony contains tens of thousands of bacteria, but it represents one bacterium sampled from the air (or by the sedimentation method). In some literature, the bacterial colony is used to be expressed as CFU (colony-forming units).

As for the settlement equivalent diameter with particle density $\rho = 1$ according to the measured data [25], it is between 6 and 9 μm in the general operating room without air purifying, and the average is 7.36 μm; it is between 3 and 8 μm in the operating room with air purifying, and the average is 5.5 μm. If ρ is assumed as 1.5,

the average settlement equivalent diameters are 5.2 μm and 3.9 μm, respectively. So attention must be paid to the particle density during the calculation of equivalent diameter.

The three kinds of equivalent diameters above are certainly not equivalent. To determine what equivalent diameter should be adopted depends on the purpose. For example, when it comes to the filtration efficiency of bacteria, of course the efficiency equivalent diameter should be used. When the bacterial settlement is involved, the settlement equivalent diameter should be chosen. But when it comes to the bacterial equivalent diameter, unless it is specified, all are the settlement equivalent diameter, which is 1–5 μm for clean place, 6–8 μm for the general place, 8–12 μm general situation outdoors, and up to 10–20 μm where human activities are intensive with much dirty places [26].

Although virus diameter is only 0.01–0.1 μm, the above principle about the equivalent diameter is also suitable. Wang Yuming et al. collected the virus phage from bacterial sampled in the six main monosodium glutamate factories in China; they deposited mainly on the III and IV sections of Anderson sampler [27], which means the main size is 2–5 μm (see Sect. 15.7) and the average value is 3 μm.

This is because although bacteria and virus are small, they need to attach to the carrier. This kind of carrier contains nutritious material for microorganism, which is released into the air by the human activity and mechanical force. So the size of virus entering into the air is not related to the size itself of the virus, instead it is dependent on the mechanical force of the spray or the biological acting force. For example, when cascade liquid impactor was used to sample the Foot-and-mouth disease virus particles naturally suspended in air, the result showed that 65–71 % of particles are larger than 6 μm, 19–24 % of particles between 3 and 6 μm, and 10–11 % of particles smaller than 3 μm, although the real size itself is only 25–30 nm [28].

9.5 Biological Particle Standard

Although standard about the biological particle in cleanroom has been given by US Aerospace Standard and the international standard draft proposed at the Fourth International Pollution Control Association in 1978 with the same provisions, the explanation of the standard compilation has not been given. With the methods mentioned in previous sections, how to determine the standard for biological particles will be discussed in this section.

9.5.1 Microbial Concentration

Microbial concentration is expressed as the microbial quantity in unit volume of air, which is the main control target in biological cleanroom.

According to related report, 53 % of the apparatus used in cleanroom are polluted by airborne bacteria in the operating room [3]. This means the contact infection is greatly related to the airborne bacteria concentration. The infectious rate of joint repair operation is related to the airborne bacteria concentration in the space 30 cm from the wound. For example, 30 % of the bacteria found on the cut of the hip joint are from the settlement from air, and 68 % come from other indirect routes.

Based on the research result by two American scholars Blwer and Wallace (cited from the July of 1968 Issue of ASHRAE Journal), WHO proposed that when total number of airborne bacteria reaches 700–1,800#/m^3, air will have the apparent risk of infection through air transmission. When the total number of bacteria is less than 180#/m^3, this kind of infectious risk seems very little [29]. Therefore, it is the minimum bacterial number when bacterial concentration is less than 16#/m^3. It is low bacterial number when bacterial concentration is less than 200#/m^3. It is general bacterial number when bacterial concentration is between 200 and 500#/m^3. They also pointed out that among the whole bacteria with risk, the proportion of Staphylococcus aureus with obvious pathogenic effect can reach 5 %. Under this situation, septicemia is easily induced.

Swedish scholar has obtained the correlation between the morbidity of septicemia in knee reshaping and transplanting operations and the indoor microbial concentration [30], which is shown as follows:

$$\text{Septicemia morbidity} = 0.84 \times 0.18\sqrt{A} \tag{9.4}$$

where A is the airborne microbial concentration.

After the relation between the clinical microbe and the infectious rate was analyzed, Zhong Xiuling described this relation vividly with the following equation [31]:

$$\text{SSI risk} = \frac{\text{Bacterial number} \times \text{bacterial toxicity} \times \text{foreign matter}}{\text{Resistance of human body}} \tag{9.5}$$

This indicates that both the bacterial concentration and the foreign matter are factors to cause surgery site infection. Sterile foreign matter will cause adhesion and granuloma, which will make the risk of all operations as high as 50–100 %, and even next operation is needed. It is obvious that the above equation can be used for calculation quantitatively. It is only vividly illustrated that the larger the factors on the numerator is, the higher the infectious risk is. The larger the factor on the denominator is, the less the infectious risk is. The risk mentioned here does not mean the specific index.

So far the direct relationship between the total particle number and the microbial concentration has not been found, but a lot of tests performed at home and abroad all prove the fact that “the microbial concentration in Class 100 cleanroom is much less than that in Class 10000 and Class 100000 cleanrooms” and “microbe are

rarely found in Class 100 cleanroom" [32]. (The air cleanliness levels mentioned in these sentences are based on 209E standard.)

The higher the air cleanliness level is, the lower the microbial concentration is. The lower the microbial concentration is, the smaller the pollution and infectious risk will be (when other conditions are the same). This should be a fundamental principle.

9.5.2 *Airborne Bacteria Number and Standard*

The microorganism in the biological cleanroom mentioned in the following section mainly refers to bacteria. Although virus cannot be cultured to be visible colony by usual methods, there is a certain relationship between bacteria and dust. But the exact correlation between them has not been given so far with the related studies, which is required to develop the standard for airborne bacteria. Two solid lines on Fig. 9.8 are the related range of the relationship between the airborne bacteria and the particles in biological cleanroom found in literatures [33]. It can be seen that the difference of airborne bacteria is large for the same dust concentration. But the correlation range on this figure can be used to determine the maximum value of airborne bacteria concentration corresponding to a certain dust concentration. The following formula can be used to approximate the relation:

$$N_b = \frac{\sqrt{N}}{100} \tag{9.6}$$

where

N_b is the airborne bacteria concentration, #/ft^3;
N is the dust concentration.

If the unit was changed to "L," it can be rewritten as

$$N_b = \frac{\sqrt{N}}{530} \tag{9.7}$$

Or the approximated expression can be used for calculation:

$$N_b \approx \frac{\sqrt{N}}{500} \tag{9.8}$$

The dashed lines on Fig. 9.8 are the maximum airborne bacterial concentration calculated with Eq. (9.6).

According to the bacterial size introduced in the section about microorganism and Fig. 1.1, the largest bacterial diameter can be considered as 10 μm (not including individual larger one). Accordingly, with the known value of N_{ob}, the value of N_{gb} can be calculated, and the results are shown in Table 9.11.

Table 9.11 Settlement quantity of bacteria on the surface per square meter per week

Airborne bacteria concentration N_{ob} for 0.5 μm in US Aerospace Standard		Bacterial number (#)		
		Calculated value N_{gb}		
		1 μm	10 μm	US Aerospace Standard
Grade 10	0.00142#/L(0.004#/ft^3)	67	5,153	5,200
Grade 100	0.00354#/L(0.5#/ft^3)	169	12,846	12,900
Grade 10000	0.0177#/L(0.5#/ft^3)	835	64,230	64,600
Grade 100000	0.0884#/L(2.5#/ft^3)	4,170	320,785	323,000

Table 9.12 Settlement quantity on each culture plate within half an hour

		Airborne bacteria concentration (#/L)			
Culture plate size	Bacterial size (μm)	0.00142	0.00354	0.0177	0.0884
Φ100	1	0.0013	0.0033	0.0165	0.0825
Φ90		0.0011	0.0027	0.0135	0.0675
Φ100	10	0.11	0.28	1.4	7
Φ90		0.09	0.23	0.15	5.7

With the calculated results in Table 9.11, author has found that the standard about settlement bacteria in both the US Aerospace Standard and the international standard (draft) is given with the largest settlement quantity, which serves the safety considerations for a standard.

If Sugawara Fumiko's formula, i.e., Eq. (6.26) in Chap. 6, is used to calculate the settlement quantity of bacteria, the calculated result will be smaller than that with Eq. (6.31). On the contrary, when the airborne bacteria concentration is calculated with the settlement quantity, the result will become larger. For example, the difference for particles with diameter 5 μm will reach 20 %. Moreover, as mentioned in Chap. 6, Sugawara Fumiko's formula is not valid for the room with limited height and without air supply. Because if the culture plate (abbreviate as flat vessel) is taken to be open for time period $T = 3$ h, which is about 10^4 s, the deposition distance of particles with diameter 5 μm will be 15 m, which is much more than the room height. It means that all indoor particles with diameter 5 μm have been settled down. In other words, the airborne bacteria concentration during the settlement time of the sampling is not constant, so Sugawara Fumiko's formula is not valid.

The bacterial settlement numbers above were obtained for the area of one square meter per week. They can be converted to be the settlement quantity in half an hour on one culture plate (In U.S. standard the recommended diameter is 100 mm, while Chinese standard uses 90 mm). The results are specified in Table 9.12.

It is apparent from Fig. 9.8 that the values of 0.1, 0.5, and 2.5 correspond to the airborne bacteria concentrations (#/ft^3) for Class 100, Class 10000, and Class

100000 in Aerospace Standard, respectively. The airborne bacterial concentrations for these three classes are not on the same straight line. The airborne bacteria concentrations with 2.5#/ft^3 and 0.5#/ft^3 are equivalent with the average value of associated range of upper and lower limits in the corresponding classes, respectively. But the third value is neither the average value of these two values nor the value 0.02 on the extended line; instead it is the upper limit 0.1 of the related range. According to "NASA Standard Procedures for the Microbial Examination of Space Hardware" (NASA NHB5340-1) by National Aeronautics and Space Administration, it is specified for the microbial measurement that the sampling flow rate should be 28.3 L/min (1 ft^3/min) and the sampling period should be less than 15 min. Since the sampling period is too long, the status of the sampled object may be varied. This is not a problem for continuous sampling or simultaneous sampling at multiple positions. The minimum sampled bacteria can only be one (a decimal value may not appear) in the sampling period less than 15 min (usually 10 min), which corresponds with the least number of airborne bacteria 0.0025–0.0035#/L (0.07–0.1#/ft^3). Since the sampling time may be shorter than 15 min, the possible measurable minimum value should be set at 0.0035 #/L (1#/ft^3), which is the upper limit of the related range. If this value was set very low, such as 0.0007#/L, no bacteria will be sampled even when the equipment with sampling flow rate 28.3 L/min was used for 15 min, and it is unlikely to increase sampling rate with the technology at that time. So in the international draft standard, the airborne bacteria concentration for the dust concentration for 0.35#/L was only proposed to be the upper limit of the range, i.e., 0.0014#/L (0.04#/ft^3). It is shown from Fig. 9.7 that it is just near the connection line with the values corresponding to previous two grades. If Eq. (9.4) is used for calculation, it becomes 0.0011 #/L(0.032#/ft^3).

To conclude, the related links in the standard about the suspended biological particles can be found. Author thinks that interpolation is not suitable with the numerical values in this standard, which is inconvenient for use. Regardless of the accuracy of the relevant range between these bacteria and the particle, these values in current standard are close to the upper limit of related range, while only one value deviates a little further, so it is more reasonable to replace the values in the standard with the upper limit of relevant range, that is determined with Eq. (9.6) (the long dashed line in Fig. 9.8). In this way, various grades can be connected, and interpolation can be made between different grades.

9.5.3 Number of Sedimentation Bacteria and Related Standard

Sedimentation number of bacteria depends on the amount of airborne bacteria. The calculation method for the settlement quantity is the same as the method for sedimentation of general particles introduced in Chap. 6.

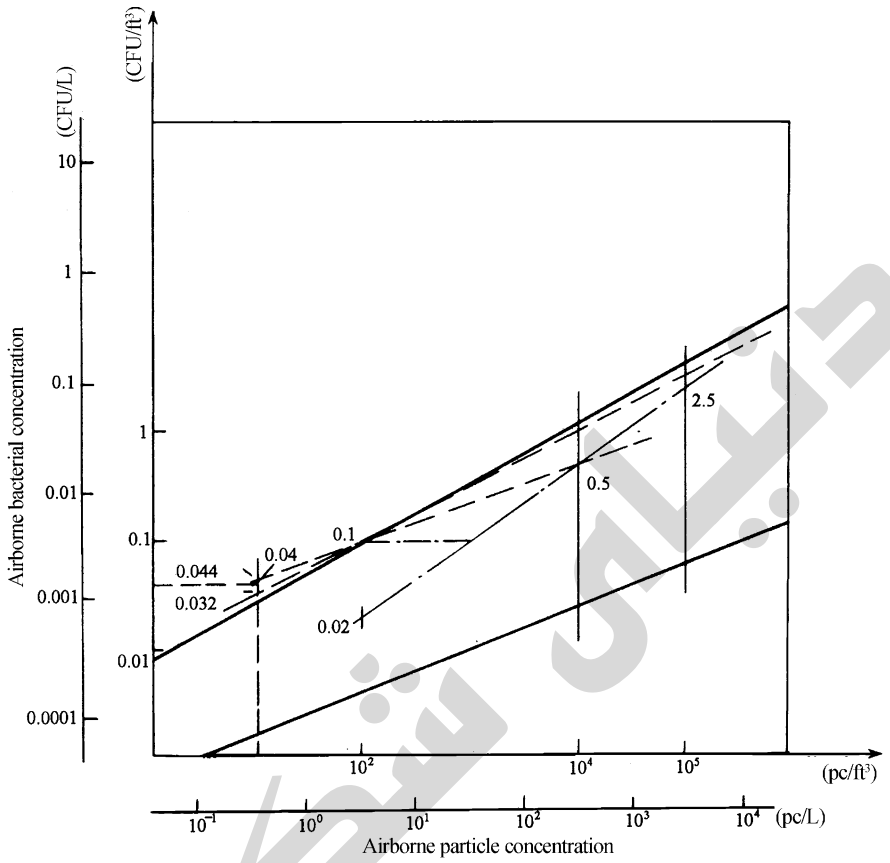

Fig. 9.7 Relationship between the airborne bacteria concentration and the dust concentration

When the airborne concentration per cubic meter of air is assumed as N_{0b}, the settlement quantity of bacteria on the surface per square meter per week is N_{gb}; we can obtain the following expression according to Eq. (6.31):

$$N_{gb} = \alpha v_s N_{0b} \times 3{,}600 \times 24 \times 7 \tag{9.9}$$

During the application of this formula, the main problem is how to determine the particle size of airborne bacteria, which will thereby determine the coefficient α. As for airborne particles, the distribution in air is certain, where the settlement quantity can be calculated according to the average particle size. But sizes of airborne bacteria may be very different in different cases. If all of them are large, they are prone to deposit. Obviously, since the settlement quantity of bacteria is used in the standard, the maximum settlement quantity should be used as the basis for determining the

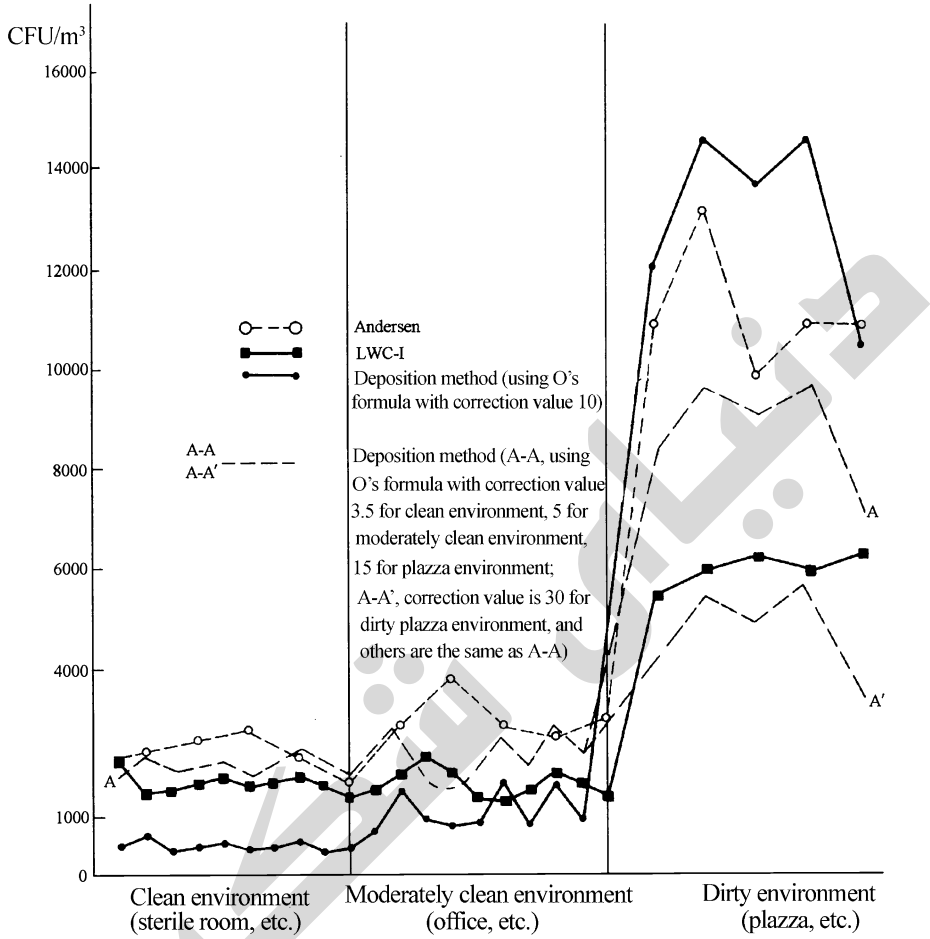

Fig. 9.8 Comparison of three sampling methods under three kinds of environments

value in standard, which means that the settlement quantity of airborne bacteria corresponds with the largest diameter. In fact, the actual settlement quantity should not be larger than this value, otherwise the airborne bacteria concentration exceeds the value in standard.

By the above comparison, it is feasible to obtain the relationship between the airborne bacteria and the settlement bacteria with Eq. (6.31). It is simple to use the correlation between bacteria and particle with Eq. (9.6) as the concentration standard for the airborne bacteria. Therefore, author has ever proposed to set Table 9.13 as the reference for biological particle standard of cleanroom with air cleanliness level "3" series and "3.5" series.

Table 9.13 Reference value for biological particle standard

Maximum concentration of particle (#/L)	Maximum concentration of airborne bacteria (#/L)	Allowable maximum settlement quantity of bacteria (#/(week · m^2))	Maximum settlement quantity during 0.5 h sampling time with Φ90 Petri dishes (#)
0.3	0.001	3,629	0.068
0.35	0.0011	3,992	0.075
3	0.0033	11,976	0.225
3.5	0.0035	12,700	0.239
30	0.01	36,290	0.682
35	0.011	39,920	0.75
300	0.033	119,760	2.25
350	0.035	127,000	2.39
3,000	0.1	362,900	6.82
3,500	0.11	399,200	7.5
30,000	0.33	1,197,600	22.5
35,000	0.35	1,270,000	23.9

In Table 9.13, with the low dust concentration, the colony settlement quantity in each Petri dish is very small. It is apparent that accurate detection with one or even several Petri dishes is not attainable. But at least how many Petri dishes should be used, which will be discussed in the Chap. 16.

9.6 Relationship Between Settlement Bacteria and Airborne Bacteria

There are criteria for both settlement bacteria and airborne bacteria for biological particles in biologic cleanroom standards, such as EU GMP promulgated in 1997, China's GMP implemented in 1998, China's veterinary GMP implemented in 2002, China's newly issued GMP implemented in 2011, as well as the previously mentioned standards and specifications about the clean operating department. So attention should be paid on the relationship between them.

Because we know that:

1. It is the most classical approach to measure the biological particles with settlement method, which has the most obvious feature of simplicity and practicability.
2. There are a lot of data about settlement bacteria concentration in the past. The conversion relationship between settlement bacteria concentration and airborne bacteria concentration should be known when necessary.
3. When in some applications it is impossible to measure the airborne bacteria concentration, the conversion relationship between settlement bacteria concentration and airborne bacteria concentration is needed.
4. Because the index of surface deposition has attracted more and more attention, the settlement method to measure biological particles still has its applications.

Therefore, it is necessary to set criteria for both the settlement bacteria concentration and the airborne bacteria concentration, respectively. Of course, we also need to investigate the conversion relationship.

9.6.1 *Proof of Омелянский Equation*

Омелянский (referred to as O's) equation from the former Soviets has been widely adopted for the conversion between the settlement bacteria and the airborne bacteria in China. This equation shows that the bacterial number settled on the 100 cm^2 of culture medium within 5 min is the same as the airborne bacteria number in the air with volume 10 L. The volume of 10 L is a correction value. It can be expressed with the following formula:

$$N_g = 10N_L \tag{9.10}$$

where

N_L is the bacteria concentration (#/L);
N_g is the colony number on 100 cm^2 of culture medium within 5 min of deposition (#).

However, it is generally reflected that this formulation is not accurate. Somebody puts forward the actual test argument [34, 35]. Author thinks the main reason for inaccuracy is that suitable application conditions are not specified and it is used without consideration of occasions.

Since the literature about O's formula is not founded, it will be proved with the principle in Chap. 6.

Now Eq. (6.27) is rewritten as follows:

$$N_g = v_s f T N \tag{9.11}$$

It should be noted that the unit of N is "#/cm^3."

Based on the discussion about equivalent diameter, the diameter is 5–20 μm in the general environment, and in most cases, it can be 5–10 μm. If the average of the rage is used with $d_p = 7.5$ μm and $\rho_p = 2$, we obtain $v_s = 0.33$ cm/s. When they are put into the formula above, the amount of settlement bacteria on 100 cm^2 within 5 min (300 s) is obtained:

$$N_g = 0.33 \times 100 \times 300 \times N = 10\ (1{,}000)N = 10N_L$$

where 10 is a correction value (L).

This is the proof of O's formula, i.e., Eq. (9.10) [36].

Table 9.14 Examples of correction values

No.	Place	Example	Instrument type	Condition	Average correction values with measured data (L)	Ref.
1	Asepsis room in hospital and pharmaceutical factory	11	SS-1	Static	3.1	[25]
2	Ordinary lab and office	5	LWC-1	Only three staffs with less activity	3.5	[35]
3	Warehouse, ward, disposal room	6	LWC-1	More activities	13.4	[35]
4	Outdoor	1	LWC-1	In spring, drizzle, and sunny days	16	[35]
5	Outdoor	1	LWC-1	2–3 grade wind outdoors, more pollution	22.4	[35]
6	Outdoor	1	LWC-1	3–4 grade wind outdoors, more pollution	47.6	[35]
7	Operating room	23	LWC-1	Not cleanroom, in preoperative, operation, and postoperative status	5	[37]
8	Classroom, shopping malls, theaters, waiting hall		LWC-1	Natural wind with speed 0.1–0.4 m/s	32.48	[34]
9	Laboratory	1	LWC-1	Artificial bacteria spray, area-weighted diameter is 9.6 μm, wind speed 0.1–0.4 m/s	13.28	[38]
10			Kroto cascade impactor		3	[38]

9.6.2 Correction of Settlement Formula [36]

According to some measured data, the correction values are obtained with the above formula, which are shown in Table 9.14.

We can see from the table that the correction value is not equal to 10. The general rule is that the correction value is small in a clean place, which is only 3–5. It is larger in the place where more activities occur or at general outdoor environment, which is about 15–20. In places with a lot of activities (such as waiting hall, shopping malls in the table), the correction value exceeds 30. This means that for the same settlement

Table 9.15 Calculated correction values

No.	α	$\frac{1}{\sqrt{\beta}}$	$\frac{\rho'_p}{\rho_p}$	ω	d_p	v_s	N_g	Calculated correction values (L)	Calculated correction values / Measured correction values
1	1.2	1	1	1	3.9	0.15	$3.3N_L$	3.24	1.05
2	1.16	0.61	1	0.88	6	0.216	$4.03N_L$	4.03	1.15
3	1	0.61	1.1	0.88	10	0.6	$10.62\ N_L$	10.62	0.79
4	1	0.61	1.1	1.1	10	0.6	$13.3N_L$	13.3	0.83
5	1	0.61	1.35	1.2	12	0.864	$27.32\ N_L$	27.32	1.22
6	1	0.61	1.35	1.4	15	1.35	$46.67\ N_L$	46.67	0.98
	1	0.61	1.35	1.8	15	1.35	$59.93\ N_L$	59.93	1.26
7	1.16	0.61	1	0.88	6	0.216	$4.04\ N_L$	4.04	0.81
8	1	0.61	1.25	0.95	15	1.35	$29.4\ N_L$	29.4	0.91
	1	0.61	1.25	0.95	17	1.73	$37.6\ N_L$	37.6	1.16
9	1	1	0.5	0.95	9.6	0.55	$7.85\ N_L$	7.85	0.60
								Average	0.98

quantity, large particles are more in the dirty place with a lot of people, and large particles are easy to settle, so the correction value is large. The settlement quantity can be reached when the airborne particle concentration is not large.

Different correction values will be found, because Eq. (6.27) for the settlement quantity is used, which is the general formula without any correction.

As proved in Chap. 6, Eq. (6.32) with polynomial corrosion should be used. Various correction coefficients in this equation can be calculated with the condition shown in Table 9.14, which are summarized in Table 9.15.

For the first situation in Tables 9.14 and 9.15, the air velocity in the asepsis room can be considered as 0.3 m/s. It is 0.15 m/s with the situations No. 2, 3, and 7, and $\omega = 0.88$. It is about 0.25 m/s with the situations No. 8 and 9, and $\omega = 0.95$. There are several kinds of air velocities with the situations No. 4, 5, and 6. It is the outdoor situation in spring with No. 4, the air velocity can be regarded as slightly larger than the indoor velocity 0.3 m/s, and the coefficient ω is 1.1. There is wind with grade 2–3 in situation No. 5, and ω is 1.2. There is wind with grade 4–5 in situation No. 6, and result with $\omega = 1.8$ is better close to the measured data since both values of 1.4 and 1.8 are used for trial. Little data exist for No. 10, so it is not checked.

The situation No. 9 corresponds with spraying experiment, so ρ'_p is 1, while for others it is 2–2.5.

The impact is the biggest for the equivalent diameter. Three times of difference can result in nearly 10 times of difference for the correction value. According to the previous principle and the condition set in Table 9.14, it is 3.9 μm for condition No. 1, and it is larger than 5 μm for condition No. 2 and 7. For condition No. 9, it should be calculated with real values. For other conditions, it is larger than 10 μm. So the value of α for condition No. 1 is 1.2, for conditions No. 2 and 7 are 1.16, and for the remaining conditions are 1.

The condition No. 1 is unnatural sedimentation. No. 9 is spherical drip. For both cases, $\frac{1}{\sqrt{\beta}} = 1$. While for other conditions, the correction item with β is considered.

Therefore, when one correction value of O's formula is adopted, it is not appropriate, so it is inevitable that the result is not accurate. If the coefficient is

Table 9.16 Suggested coefficients

α	$\frac{1}{\sqrt{\beta}}$		$\frac{\rho_p'}{\rho_p}$		ω		
Clean → dirty	Natural sedimentation	Lab spray and nonnatural sedimentation	Clean → dirty	Lab spray	Without air supply	Cleanroom	Outdoor wind
1–1.2	0.61	1	1–1.16	0.707	0.88	1	1.2–1.6

not determined one by one according to the specific conditions, for the convenience of calculation, it is suggested to use the coefficient listed in the Table 9.16.

Calculated values with the coefficient in Table 9.16 are close to the measured values. If calculation is not performed, the correction values in Table 9.17 for reference can also be used directly.

When the Petri dish is used for measuring the settlement bacteria, the following derivation process should be performed:

$$\begin{aligned} N_m &= 1,000/X \times C \times 100/A \times 5/T \\ &= 5 \times 10^5/X \times C/AT \end{aligned} \tag{9.12}$$

where

N_m is the airborne bacteria concentration (#/m^3);
C is the average colony on ϕ 90 Petri dish (#);
X is the correction value;
A is the area of the settlement plate expressed with square centimeter (based with ϕ 90 Petri dish);
T is the settling time (min).

After settlement of 30 min, we obtain

$$N_m = 262/X \times C_{(30)} \tag{9.13}$$

With O's formula, $X = 10$. With Eq. (9.12), we can obtain

$$\text{Deposition of } 30\,\text{min}, \frac{N_\text{m}}{C_{(30)}} = 26.2$$

$$\text{Deposition of } 5\,\text{min}, \frac{N_m}{C_{(5)}} = 157.2$$

Example 9.1. There are five ϕ 90 Petri dishes placed in the cleanroom. After settlement of 30 min, there is one colony after the culture process. How much is the equivalent microbial concentration?

Solution. According to the passage, $C_{(30)} = 0.2$. Because of the cleanroom, the correction value in Table 9.17 is $X = 5$. So

$$N_m = \frac{262C}{5} = 52.4 \times 0.2 = 10.5\ \#/\text{m}^3$$

Table 9.17 Correction values for reference

Environment	Correction value (L)
Cleanroom and cleanroom with fewer people	5
General outdoor and indoor environments	10
Public places with many people and many activity	30
Outdoor environment with large wind and pollution source	50

Table 9.18 Values of $N_m/C_{(5)}$

Country	The former Soviet Union	USA	Japan			China	
Name	Омелянский	NASA NHB5340.2	Shiniohiro	Yamagata	Hashimoto	Wang Lai Tu Guangbei	Xu Zhonglin
$N_m/C_{(5)}$	157. 2	86.0	30–50	130	98–600 (349 ± 251)	286	262 × 6/correction value

From the above expression, it is visible that the ratio $N_m/C_{(5)}$ is a constant value of 157.2 in O's formula. While in the other methods, it is also a fixed value, and the specific number is different. Although there is a range for application, conditions are not specific [38], which is shown in Table 9.18. In addition to the data from author, others in the table are cited from literatures [38]. Of course it is not appropriate to use fixed value regardless of the circumstances. In author's method, it is varied. In Eq. (9.13), it is different with different values of X, which is more consistent with the actual situation.

9.6.3 Application of Settlement Bacteria and Airborne Bacteria Methods in Cleanroom

1. The airborne bacteria method should be an ideal microbiological sampling method due to the randomness of sampling, faster sampling, and less affected by sampling conditions, which could theoretically capture any carrier particles in the space.

But there are many kinds of principles for the airborne bacteria method. Each kind of principle corresponds with many methods, and each method may have a variety of models of the instruments. The measuring results with these instruments can vary a lot. In their respective most appropriate sampling range (diameter), there is a problem of sampling efficiency, which is difficult to compare with each other, and even conflicting [33].

Moreover, the pumped air in the airborne bacteria method is not from a certain position, so it is unfavorable for the analysis of microbial concentration field.

2. When bacteria and virus are regarded as particles, the motion in the cleanroom with air supply is mainly controlled by the flow field. Wherever air can reach, the carrier particles can also arrive quickly. As long as the air can reach to the surface of the culture medium, carrier particles can also quickly contact the medium surface. There is the misunderstanding opinion that the settlement quantity is too little, and the settlement velocity is too slow, and it is even believed not suitable for

cleanrooms, because the concept of "natural sedimentation" is still used when the settlement method is applied in cleanroom. The characteristic of particles following the airflow is ignored, so it is thought that it takes dozens of hours for the settlement. However, this is right for the naked bacteria particles only in absolute stationary windless place. In places with air supply, it is secondary for natural sedimentation. Of course, if the Petri dish is placed in the vortex area, the opportunity of contact with the Petri dish (base) is reduced by turbulent airflow and backflow. Therefore, a Petri dish should be put in the place where air can reach and where it is not vortex area.

3. The settlement method has the characteristics such as the most simple and direct and can realistically reflect the natural pollution extent on the object surface (especially the control site). The monitoring data with the settlement method in the control site can reflect the site pollution feature more truly. If there is no pollution source along the upstream of the streamline (such as the filter leakage), the result with the settlement method is certainly not as high, although there may be pollution near the incoming flow at the same time (such as leakage). If the airborne bacteria method is adopted, it may suck the polluted airflow into the equipment, and judgment can be made that the bacterial concentration at this point is below standard which does not reflect the real situation. Of course, in order to reflect the concentration field realistically, enough Petri dishes need to be placed.
4. Although with the conversion method close to reality, the data with the settlement method can be converted into the airborne bacteria concentration, accurate determination of some parameters during calculation is not easy. Different opinions about the recognition of results may be caused, especially when O's formula with only one correction value is used.

Figure 9.8 shows the comparison of the sampled results with two kinds of airborne bacteria samplers in different occasions and the calculated results by O's formula with one correction value based on the settlement method [33]. It shows that in clean environment, the sampled result with the settlement method is the least, while in dirty environment, the sampled result with the settlement method is the most.

If the settlement quantity under different circumstances is calculated with the correction form of O's formula based on the above results, the polyline 4 is obtained and shown in the figure. For every environment, it is between the results with two airborne bacteria method.

Therefore, it is better not to evaluate the result with the settlement method through conversion but with the value in the microbial standard directly.

9.7 Bacterial Remove with Filter

Dust particles are often the carrier of bacteria. So in this sense, the more the airborne dust particles are, the more the opportunities of contact between bacteria and dust are, which means the opportunity of attachment of bacteria onto dust particles increases. So it is mainly dependent on air filtration to remove bacteria in biological cleanroom.

As for filters used for biological cleanroom, there are three problems which have attracted more attention. It will be discussed as follows.

Table 9.19 Filtration efficiency of HEPA filter for bacteria

Year	Bacterial size used (μm)	Efficiency (%)	Filtration velocity (m/s)
1960	0.01–0.012	99.999	0.1
1966	>1	99.999	0.2
1966	0.094–0.17	99.97	0.3
1966	1	99.9993	0.3
1968	0.05–0.45	99.97	0.5
1977	0.5–1.0	99.97–99.95	0.1
1977	1	100	0.13

Table 9.20 Efficiency of various air filters for viscid Serratia bacteria (concentration of spray bacterial liquid 1.1×10^7#/L)

Filter types	Number of tests	Efficiency (%)	Filtration velocity (m/s)
DOP99.97	20	99.9999	0.05
DOP99.97	19	99.9994 ± 0.0007	0.025
DOP99.97	20	99.996 ± 0.0024	0.025
DOP95	17	99.989 ± 0.0024	0.025
DOP75	20	99.88 ± 0.0179	0.05
NBS95	20	99.85 ± 0.0157	0.09
NBS85	18	99.51 ± 0.061	0.09
DOP60	20	97.2 ± 0.291	0.05
NBS75	19	93.6 ± 0.298	0.09
DOP40	20	83.8 ± 1.006	0.05
DOP20~30	18	54.5 ± 4.903	0.2

9.7.1 Filtration Efficiency of HEPA Filter for Microorganism

Since the equivalent diameter of bacteria is much more than 0.5 μm, the filtration efficiency of HEPA filter for bacteria is nearly 100 %, so the outlet concentration of bacteria can be considered as "0." When solution spray containing bacteria was used for test, since the size of the droplet solution is greater than bacteria itself, the efficiency obtained was quite high. For the commonly used HEPA filter, when it was exposed to air with bacterial concentration 8.2×10^2 to 6×10^4#/L, the filtration efficiency for different size of bacteria and different filtration velocities was obtained, which is shown in Table 9.19 [39]. It can be seen from the table that the filtration efficiency for bacteria with their own size 0.1–0.5 μm is the same with the efficiency of the 0.3 μm DOP particles. Table 9.20 shows the efficiency of various air filters for viscid Serratia bacteria [40]. In the table, "DOP" represents the efficiency of 0.3 μm DOP particles, and "NBS" indicates the efficiency with the dust spot method, which will also be illustrated in later chapters.

Since for HEPA filter, the resistance is big and it is expensive, so it is not appropriate to use it for all the general biology cleanrooms with low requirement. From the above bacterial equivalent diameter, it is feasible to use sub-HEPA filter and even fine air filter. This view is also found in some research report overseas.

Table 9.21 Comparison of air filter penetrations

HEPA filter	Flow rate (m^3/h)	Resistance (Pa)	Penetration (%)				Ref.
			Phage T_1 (0.1 μm)	Virus (0.3 μm)	Foot-and-mouth disease virus (0.01–0.012 μm)	DOP (0.3 μm)	
A	42.5	264	0.0039			0.011	
B	42.5	175	0.00085			0.02	[37]
C	42.5	135	0.00085			0.006	
D	–	–	0.003	0.0036	0.001	0.01	[39]

For example, it has been reported that in the turbulent flow cleanroom with sub-high-efficiency air filter as the final air filter whose dust spot efficiency is equivalent to 90 %, where the air change rate was only 17 ~24 h^{-1}, the average microorganism concentration in operation period of 30 years was only slightly higher than 0. 35#/L [41]. Experimental results of middle-efficiency air filter in China also prove that the filtration efficiency for bacteria reached over 80 % [42]. Author performed experiment on the sub-high-efficiency air filter and found that the filtration efficiency for *Escherichia coli* was up to 99.9 % [43].

As for virus, it is much smaller than bacteria. However, we can know from Table 9.9 that virus has no complete enzyme system. Compared with bacteria, it can even neither metabolize independently nor grow on inanimate medium. Instead, it can reproduce only in living host cells. Therefore, it also has carrier in the air, and it can be considered as a form of group. So it is unnecessary to worry about that HEPA filter can't filter virus. Only when the carrier is small, the filtration efficiency may be lower. Test introduced in Sect. 9.4.2 has proved that the penetration of HEPA filter for the phage or virus which is smaller than 0.1 μm is also much less than the rated penetration of filter (for 0.3 μm DOP), which is shown in Table 9.21. This means that the efficiency of HEPA filter for virus is far outweigh the efficiency for 0.3 μm particles. This also explains that the equivalent diameter of virus is larger than 0.3 μm on the other hand.

Moreover, it is known from Fig. 9.9 [44] that it is not necessarily the case that all the efficiency for bacteria is large while that for virus is small.

In conclusion, there are following features for filtration of air filters with bacteria and virus:

1. No matter for bacteria or virus, filter efficiency will improve. This is of great significance to choose which kind of filter in biological cleanroom and to popularize its application.
2. Dust particles and bacteria are removed at the same time, which is easy for application.
3. When both dust particles and bacteria are kept outside of both the system and the cleanroom, the active pollution control is realized [45]. If bacteria are killed with disinfection method after they enter in, the corpse and the secretion left over by bacteria are still toxic.
4. Side effect and harmful substance will not be generated.
5. It is possible to control pollution in overall process when people are present.
6. It has a certain amount of resistance. It is more meaningful to develop low-resistance products.

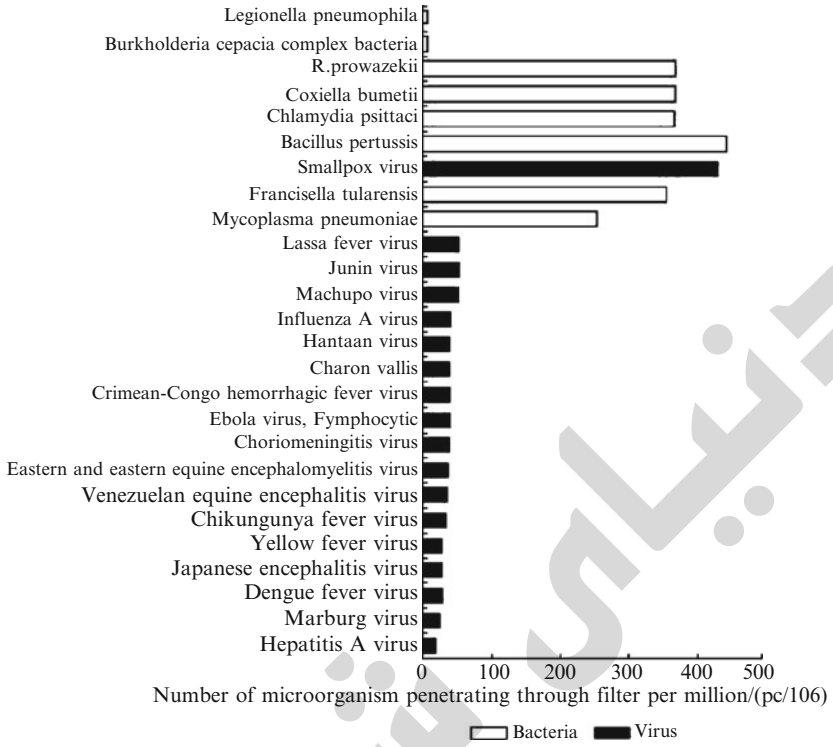

Fig. 9.9 Penetration of air filter for various kinds of microorganism

Table 9.22 Experimental results for the adhesion of bacteria on HEPA filter material surface

Filter material position	Sampling at the upper part of filter	Sampling in the middle of filter
Windward surface	17 CFU	4 CFU
Leeward surface	0	0

9.7.2 Penetration of Filter Medium for Bacteria

For people lack of knowledge about the characteristic of bacteria and filter material, they always worry about if the "live" bacteria can go through the filter material. Someone took part of the filter material from a used HEPA filter and put it onto the medium and perform the culture process [46]. The result is shown in Table 9.22. It shows bacteria were not found on the back of the filter medium. So the bacteria passing throughout problem is rejected. In addition, the culture result also shows that the bacteria attached on the windward face of the prefilter accounts for 90 % of the bacteria in whole flow, while it only accounted for 10 % on the windward face of HEPA filter. This also means that due to the large bacteria equivalent diameter, most are already filtered by the prefilter.

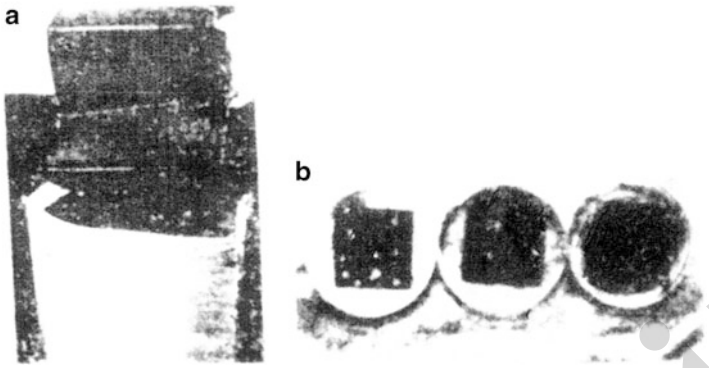

Fig. 9.10 Growth situations of bacteria on filter. (**a**) Windward surface of HEPA filter after operation of 13,000 h in the operating room. The color of windward surface of air filter after operation is *black*. The *white* part represents the cross section of air filter media. (**b**) Bacterial growth on windward surface. Results for conditions (1), (2), and (3) are shown from *left* to *right*, respectively. The white part represents the CFU. The larger the area of white part is, the more the CFU is. The left one contains the most CFU

9.7.3 Reproduction of Microorganisms on Filter Material

This is the problem that both technical personnel and medical personnel are concerned about. Appropriate temperature, humidity, and nutrition are needed for the reproduction of bacteria. For filter material made of inorganic material, due to the lack of necessary nutrition, it is very difficult for bacteria to survive (although it has been found that there is almost nothing that bacteria do not "eat"). Someone took the filter material sample on the HEPA filter which has been used for 13,000 h in the operating room, and treatment was performed according to the following three kinds of conditions:

(1) Put the dust collecting surface of filter material close on the medium.
(2) According to method (1), sterile distilled water was dripped onto the filter material, which fully soaked the material.
(3) According to method (1), the relative humidity is kept 90 %.

Result with culture is:

With the condition (1), the colony of hay bacteria and fungi formed on the filter material is (2–3 #/cm^2). With condition (2), only mould colony was formed. With the high humidity condition (3), it is thought that the bacteria are unable to develop completely.

These results are shown in Fig. 9.10.

The test results show that after the capture of most bacteria on filter, due to inappropriate conditions of humidity and nutrition (temperature effect is not mentioned here), they approach to natural death, or only part of colony with the form of

spore or fungus survives. If there is no nutrition source even in high humidity condition, bacteria also cannot survive. On the other hand, as long as there is nutrition source, bacteria are able to survive and develop even in the general environment. Distilled water itself is of no nutrition, but it may help the dissolution of nutrition particles contained in the filter material, and this is likely to be more beneficial for bacteria than high humidity.

9.8 Disinfection and Sterilization

9.8.1 Concept

It should not be deemed that when air entering into the biological cleanroom is sterile, all kinds of surface indoors will not be polluted by bacteria. If there is nutrition source in these places, the possibility for the reproduction of bacteria exists.

In biological cleanroom, human body is one of the main bacteria source. There is about $1–10^4$ bacteria for every 6–7 cm^2 skin, about 1 % of which are pathogenic. Bacteria will be released during the breath and talk of people. In biological cleanroom, not only ordinary mask should be used, sometimes mask made of high-efficiency filter paper is needed, which can reduce 4/5 of the bacterial quantity released than the former situation. Even the doctor must wear a set head-type gown with expiratory suction device, which has a better effect. So sterilization on surfaces in biological cleanroom is still an important measure.

But, sterilization and disinfection should be two different concepts.

Sterilization refers to the complete extinction of bacteria and virus, which has the absolute meaning. While the narrow meaning of disinfection is that in the process bacteria or virus will not be destroyed (traditionally bacterial spore is not included) due to the resistance to thermal effect or drug efficacy, which has relative meaning. For example, disinfection liquid wiped on surface is one example of disinfection.

9.8.2 Main Disinfection Methods

9.8.2.1 Dry Heating Method

This method is based on the principle that in the dry air with the heating treatment, microorganism is destroyed with the oxidation effect by intensive heating process. In general the temperature needed should be above 160 °C, and the time needed can reach 1–2 h.

9.8.2.2 Humid Heating Method

This is a sterilization method with high-temperature humidity steam (usually it is a saturated steam). It is based on the principle that protein will be solidified under the hot and humid environment. In general the temperature needed is lower than that of dry heating method, and the time is also short, for example, 12 min is needed for temperature 121 °C, or 2 min is needed for temperature 134 °C.

9.8.2.3 Drug Method

It is fumigated or scrubbed by a gas or agent. Its effect is related to the drug types and bacteria's sensitivity to the drug. But designers must understand that some materials may adsorb some drugs to have erosion effect. For example, the common ethylene oxide is a kind of very good sterilizing agent. Although it cannot permeate the solid material, it can be absorbed by plastic, rubber, and so on, and it is toxic. So proper materials should be selected according to the object used in biological cleanroom.

9.8.2.4 Electromagnetic Radiation Method

It is based on the principle that bacterial protein and nucleic acid (deoxyribonucleic acid is DNA) are damaged, as well as the thermal effect after absorption.

Here it should be pointed out that although ultraviolet radiation sterilization is one of the sterilization methods, it is specified in the Article 17.34 of the GMP published in 1992 by World Health Organization (WHO): "because of the limited effect of ultraviolet, it cannot be used to replace the chemical disinfection." It is also explicitly pointed out in Article 17.65 that: "ultraviolet radiation cannot be used as the final sterilization method." These are also specified in the later version of GMPs in EU and China.

However, because in the special condition of air circulation, ultraviolet radiation sterilization still have a certain effect, which will be discussed in detail in the next section.

Among the above several sterilization methods, do not use a single method for a long time. It should be changed regularly in order to prevent the generation of drug-resistant bacteria.

9.8.3 Disinfection and Sterilization with Ultraviolet

9.8.3.1 Disinfection Sterilization Effect

Before the appearance of biological cleanroom, ultraviolet disinfection is an indispensible method for disinfection.

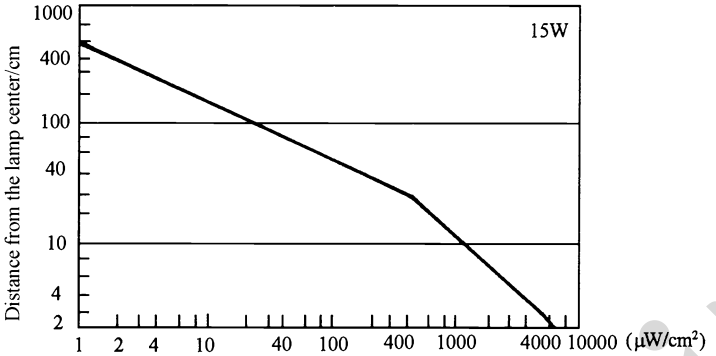

Fig. 9.11 Relationship between distance and exposure intensity

The optimal wavelength characteristic of ultraviolet disinfection corresponding with the best disinfection effect is in the range of 2,500–2,600 Å. The wavelength of market ultraviolet lamp is about 2,537 Å.

Here are some factors that influence ultraviolet disinfection sterilization effect:

1. The opening time of tube. The rated output of tubes generally refers to the value after operation of 100 h. The initial output is 25 % higher than this value, and it decreases gradually between 100 and 3,000 h, which is only about 85 % of the rated value.
2. Ambient temperature. Output is the largest at 20 °C, while it remains only 60 % at 0 °C.
3. Ambient relative humidity. Most view is that the sterilization effect is best for the relative humidity between 40 and 60 %. When it is larger than 60–70 %, the rate of killing microorganisms will fall. Activation effect may appear for the relative humidity more than 80 %. But experiment also proves that the influence of humidity is conditional. At the beginning of the exposure, the effect is obvious. After 10–15 mins, this kind of influence is not very obvious [47]. Some research has proved that in the extreme high-humid environment, the sterilization rate will decrease. This is because that the adsorption of water on the virus surface may protect DNA and RNA from the damage by ultraviolet.
4. Irradiation distance. In the distance within range of 500 mm from the light tube center, irradiation intensity is in inversely proportional with the distance. But for the distance larger than 500 mm, irradiation intensity is in inversely proportional to the distance squared [48]. Figure 9.11 shows one example for the relationship between the irradiation intensity and the distance for a 15 W ultraviolet lamp. We can see from the picture that when the irradiation intensity with the distance 100 mm is about 1,200 $\mu W/cm^2$, it reduced to less than 600 $\mu W/cm^2$ for the distance 200 mm, and it drops to 260 $\mu W/cm^2$ for the distance 400 mm; the irradiation intensity is about 120 $\mu W/cm^2$ for the distance 500 mm, and it reduced to one-fourth of the former value, i.e., 30 $\mu W/cm^2$ for the distance 1,000 mm; it drops to one-fourth of the value for distance 1,000 mm, that is, 8 $\mu W/cm^2$ for the distance 2,000 mm.

Table 9.23 Comparison of ULV radiation dose in gas phase and on the medium with the sterilization rate 90 %

Bacteria	Irradiation dose $E_{0(A)}$ in gas phase (mW · s/cm^2)	Irradiation dose $E_{0(A)}$ on agar medium (mW · s/cm^2)	$E_{0(A)}/E_{0(B)}$
Serratia marcescens	1.03	2.96	0.35
Escherichia coli	1.00	3.60	0.28
Gambogic Sarcina	4.93	18.4	0.27
Bacillus subtilis (spore)	11.5	40.3	0.29

5. Bacteria type. Ultraviolet sterilization takes effect with the reason that pyrimidine polymers are formed on the DNA, which produces damage on DNA. But the sterilizing rate is different between different types of bacteria under this situation. This is because of the physical phenomena that since the membrane structure and shape of bacteria are different, the amount of ultraviolet radiation reaching to DNA is different [49].

   If the exposure dose is defined as the product of the exposure intensity and the irradiation time, when the dose required for *Escherichia coli* is 1, the needed dose is about 1–3 for *Staphylococcus*, *Mycobacterium tuberculosis*, and so on; it is about 4–8 for hay bacteria and its spore and yeast and so on; it is about 2–50 for mould fungi. Compared with the negative coli such as *Bacillus coli* and *Escherichia coli*, the sterilization rate for the positive coccal gambogic Sarcina is only 1/5–1/6, and the sterilization rate for positive Bacillus such as the hay bacteria is only 1/11–1/14.
6. Whether it is in the gas phase or on the culture medium. Table 9.23 gives the comparison of ultraviolet irradiation dose needed for the sterilization rate 90 % with various bacteria in the gas phase and on agar medium [49]. We can see that the sterilizing rate in gas phase is higher than that on the culture medium. The possible reason believed is that due to the surface tension, bacteria cover the water content of the culture medium, which reflects the ultraviolet ray and reduces the amount of ultraviolet ray arrived at the bacterial body. In addition, on the culture medium, there is only one direction for the ultraviolet irradiation, while in gas phase, the irradiation comes from various directions with the light-directed emitted from the germicidal lamp and reflected on the interior surface of the equipment. This is also one reason of high sterilization rate in the gas phase.

   But it also can be considered that the ratio of necessary ultraviolet irradiation dose between the gas phase and the agar medium with sterilization rate 90 % is almost is a fixed value 0.3 (0.27–0.35) for four kinds of bacteria.
7. Shelter. The penetration ability of UV ray is very low. Its function is limited to the exposed objects.
8. "Light recovery." Bacterial DNA is damaged with the exposure to ultraviolet radiation. But it can be repaired again by exposure to irradiation of visible light. The shortest recovery time is only 2 min, and the slowest recovery time is 1 h. That is the so-called "recovery" phenomenon. In practical applications, this phenomenon should be taken into account.

It is shown from the above influencing factors of sterilization effect:

1. A long time is needed for the sterilization of UV irradiation on the exposed object. When the sterilization rate needs to reach 99 % for general bacterial, the irradiation dose should be approximately 10,000–30,000 μW/cm^2. According to Fig. 9.11, when one 75 W UV lamp is placed at the height 2 m above the ground, the irradiation intensity is about 8 μW/cm^2, so the irradiation time needed should be at least 1 h. During the 1 h (in fact it is often several hours) of irradiation, people cannot enter into the irradiation space, otherwise the skin cells will also be destroyed, which have the carcinogenic effects. So in biological cleanroom, the UV lamp has effect for the sterilization of surfaces including the ground. But for the indoor air with the relative convention status, the sterilization effect is very small, and the expected sterilizing effect is unstable. But even for the ground, it is difficult that all the irradiation rays arrived at the surface, so it is not more convenient than the sterilization with liquid medicine wiped on the surface.
2. Although there is a certain effect of sterilization for indoor air, once the irradiation is stopped and human activities restored, in particular when outdoor air continues to enter the room, the original sterilization effect soon vanished.
3. Usually ozone with large concentration is generated during the usage of UV lamp. When the irradiation stops, it even takes a long time for the dilution of ozone flavor before people enter, which affects the use effect.
4. The most concern is that after exposure to the UV irradiation, bacteria have the antidrug ability. When *Aerobacter cloacae* and surface *Staphylococcus* are exposed to the UV irradiation, the former has the antidrug ability for five kinds of antibiotics including cephalosporin, and the later has the antidrug ability for three kinds of antibiotics. And both the survival periods are prolonged [55].

So the opinions shown in recent literatures are as follows [50–54]:

The sterilization method with UV irradiation should not be considered as the substitute of ventilation technology and HEPA filter, instead it is only an auxiliary measure. In clean operating room with air change rate larger than 4–6 h^{-1} or other rooms which are well designed, it seems that UV irradiation has little effect. Therefore, investigator from NIH, USA, recommended to use laminar flow technology as the available optional for infectious control. CDC from the USA does not recommend to use the sterilization method with UV irradiation as the precautious measure for SSI. In short, it is believed that "the mature status of this technology has not arrived yet." When HEPA filters are used together, a certain effect will appear under special circumstances.

In brief, in the biological cleanroom with flowing air, ultraviolet has lost its position in air sterilization field. Air cleaning technology has completely replaced it. The reason to discuss it here is the interest of the sterilization with circulation air, which will have a role in the spaces where the air cleaning technology cannot be used but the sterilization is needed.

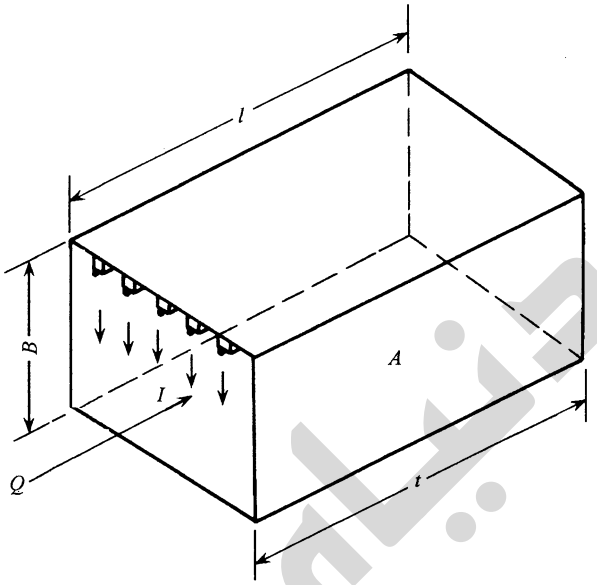

Fig. 9.12 Rectangular container model for sterilization with circulated airflow

9.8.3.2 Sterilization with Air Circulation

Role

If air can be circulated through the effective irradiation area of the UV lamp, the UV-irradiation time on air will be increased. If the hurt by the leakage of UV light can be prevented and ozone is not generated, the sterilization effect on air by ultraviolet will be greatly improved. The UV lamp (light) can be turned on continuously. This is the idea of the sterilization by circulating air with ultraviolet.

This kind of air sterilization system with UV was used in a newly built hospital with 60 beds as early as in 1964 [56]. "Sterile" air (note: dust is not removed) was supplied to the operating room, delivery room, and so on, During 2 years of operation, the infection rate among 3,791 surgical cases by 90 doctors was only 0.2 %, while in another hospital, it was 0.19 %. In other two hospitals without application of such sterilization systems, the infection rates reached up to 1.3 %. In this sterilization system, the UV lamp was installed in the air duct. If the lamp is mounted within a device which is placed indoors, it will be more flexible and effective. This sterilization device has been produced successfully in China, which does not generate ozone.

Theoretical Formula of Rectangular Sterilizer

For a rectangular container as shown in Fig. 9.12, B is the height of airflow cross section, and A is one side exposure area of the container along direction of flow.

Table 9.24 Comparison of the ultraviolet doze needed for sterilization efficiency 90 % with bacterium prodigious under different experimental velocities

Velocity (m/s)	Ultraviolet doze (mW·s/cm^2)	Correlation coefficient	Experimental no.
0.37	1.06	0.96	5
0.66	0.95	0.95	6
0.76	0.97	0.84	10
Average	1.03	0.88	-

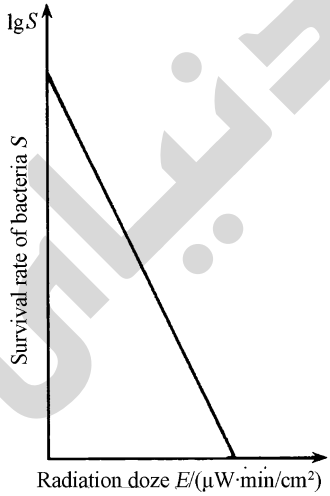

Fig. 9.13 Relationship between the survival rate of bacteria and the radiation doze

Because it is a rectangular container, the exposed areas along the irradiation ray for the height B of the container are the same.

When the airflow rate is Q (m^3/min), the time that air is exposed under the irradiation within the container is

$$T = \frac{AB}{Q} \tag{9.14}$$

where units of both A and B are "m."

The greater the flow rate within the container is, the shorter the irradiation time is. But experiments have showed that when air velocity is between 0.37 and 0.76 m/s, there is no difference for the UV-irradiation intensity needed when the sterilization rate is required to be 90 % which is shown in Table 9.24 [49].

For the irradiation intensity I (μW/cm^2), the linear proportional relationship between the survival rate of bacteria and the radiation doze on single logarithmic paper was obtained by experiment [49], which is shown in Fig. 9.14. It can be expressed with the following expression:

$$\lg S = -\frac{It}{E_0} \tag{9.15}$$

or

$$It = -E_0 \lg S \tag{9.16}$$

where S is the bacterial survival rate;

E_0 is the necessary radiation dose (μW·min/cm^2 or μW·s/cm^2) when $S = 10^{-1}$, and its values are shown in Table 9.23.

When Eq. (9.16) is rewritten, it is found that there is negative exponential relationship between the survival rate and the radiation dose, namely,

$$S = 10^{-\frac{It}{E_0}} \tag{9.17}$$

With Eqs. (9.14) and (9.16), the following expressions can be obtained:

$$\lg S = \frac{-IAB}{E_0 Q} \tag{9.18}$$

Therefore, we get

$$\mathrm{IA} = \frac{-E_0 Q}{B} \lg S \tag{9.19}$$

where IA is the product of the UV intensity and the radiation area, which is the output (W) needed for the UV lamp.

In Eq. (9.19), except I and S, other variables are constant. So when the radiation intensity increases by one time, the survival rate S will reduce by an order of magnitude. For example, the necessary radiation dose for *Escherichia coli* is $E_0 = 1{,}000$ μW · s/cm^2 when the survival rate is $S = 0.1$. So if it is required $S = 0.01$, the radiation doze needed should be $\mathrm{IA} = 2E_0 = 2{,}000$ μW · s/cm^2. When it is required $S = 0.0001$, the radiation doze needed should be $\mathrm{IA} = 4E_0 = 4{,}000$ μW · s/cm^2.

If the value of E_0 for the case $S = 0.1$ is used as the basis, we can obtain the radiation doze needed for the case $S = 10^{-\mathrm{m}}$:

$$\mathrm{IA} = -E_0 \frac{Q}{B} \lg S = mE_0 \frac{Q}{B} \tag{9.20}$$

When the needed output is equal as the practical output, i.e.,

$$\mathrm{IA} = W_t' \varphi n \tag{9.21}$$

where

W_t' is the ultraviolet output of each UV lamp (w);

φ is the utilization factor of ultraviolet;

n is the UV lamp number.

So

$$n = \frac{mE_0Q}{BW_i'\varphi} \tag{9.22}$$

If the sterilization efficiency for the *E. coli* is required to be 99 % (i.e., $S = 0.01$), the output needed of UV lamp can be obtained with Eq. (9.20) (note the following conversion of unit should be performed: m^2 into cm^2, s into min, and μW into W):

$$\begin{aligned} IA &= -\frac{1,000}{60}\left(\mu W \cdot \min/cm^2\right)\frac{Q(m^3/\min)}{B(m)} \times 10^4 \times \lg 10^{-2} \times 10^{-6} \\ &= 33.4 \times 10^{-2}\frac{Q}{B} = 0.334\frac{Q}{B}(W) \end{aligned}$$

According Japanese data [49], the average rated output of ultraviolet for the general UV lamp with 15 W is 2.5 W. Usually the lowest utilization efficiency of ultraviolet generated by UV lamp can be considered as 50 %, which depends on the installation method of UV lamp, position and dead corner, etc. It is obvious that this is a safe value. With Eq. (9.22), we obtain:

$$n = \frac{IA}{W_i'\varphi} = \frac{0.334}{2.5 \times 0.5} \times \frac{Q}{B} = 0.27\frac{Q}{B} \tag{9.23}$$

If it is required that $S = 0.1$, we get:

$$IA = 0.17\frac{Q}{B}$$

$$n = 0.13\frac{Q}{B} \tag{9.24}$$

According to the same literature, the number of UV lamps needed for the case $S = 10^{-2}$ can be calculated in the rectangular air chamber, when it is under the condition of $E_0 = 11.5$ μW · min/cm^2 (for relative dry air). It is the following expression:

$$n = 0.18\frac{Q}{B} \tag{9.25}$$

It is obvious that this expression cannot be applied to the circular air chamber. Besides, there are the limit conditions for rectangular container, where it is not appropriate to use any parameters for calculation. Therefore, it has significant limitations compared with Eq. (9.22).

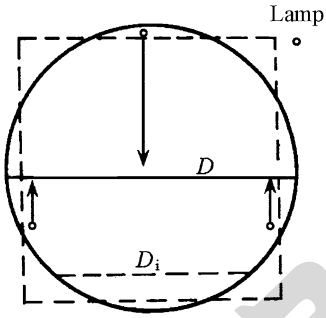

Fig. 9.14 One example of UV lamp layer in cylindrical container

Theoretical Formula for Cylindrical Sterilization Equipment

From the practical point of view, the cylindrical structure is better than the rectangular one. Based on the cylindrical structure with length l as shown in Fig. 9.14, author has derived the formula for cylindrical structure [57]. Since the UV lamps are placed all around, cylindrical air is exposed to the UV radiation on the wall with different areas, $A_i = D_i l$. In order to simplify the derivation process, the circular area can be considered as many squares with equal area (where the volumetric flow rate is constant). It can be approximated with $\overline{D_i} = B$ (B is the side length of the square). So the average cross-sectional area of exposure can be approximated as $A = Bl$. Because we know

$$B^2 = \frac{\pi}{4} D^2$$

So

$$A = 0.886 Dl$$

If the radiation intensity on the surface is used as the basis, the following expression can be obtained for cylindrical container from Eq. (9.18):

$$\lg S = \frac{-I \frac{\pi}{4} D^2 l}{E_0 Q} \tag{9.26}$$

The value of I can be obtained. When it is multiplied by the average exposure area A, the average ultraviolet output exposed on the surface of cylindrical structure is calculated, i.e.,

$$\mathrm{IA} = I \times 0.886 Dl = \frac{-E_0 Q \lg S}{\frac{\pi}{4} D^2 l} \times 0.886 Dl = \frac{-1.13 E_0 Q \times 10^{-2}}{D} \lg S \tag{9.27}$$

The UV output needed for the *E. coli* when $S = 0.01$ is:

$$IA = 0.38 \frac{Q}{D}$$

The number of UV lamps can be obtained with Eq. (9.21), i.e.,

$$n = 0.3\frac{Q}{D} \tag{9.28}$$

When $S = 0.1$, we obtain:

$$\mathrm{IA} = 0.19\frac{Q}{D}$$

$$n = 0.15\frac{Q}{D} \tag{9.29}$$

It is seen from the above formula that in the same air volume, the larger the cylindrical container is, the less the number of UV lamps is. The flow rate can be between 1.5 and 2.5 m/s.

When $D = B$, it is shown from the comparison between Eqs. (9.20) and (9.27) that the number of UV lamps in cylindrical container is 1.13 times of the square container. Although it is a slightly more, the cylindrical shape has the advantages of both the structure and the appearance.

With the unit conversion on Eq. (9.22), the sterilization efficiency of cylindrical ultraviolet sterilization equipment can be obtained by Eq. (9.20), i.e.,

$$1.25n = mE_0\frac{1.13Q}{D} \times 10^{-2}$$

So

$$m \times \frac{1.1nD}{E_0Q \times 10^{-2}} \tag{9.30}$$

or the number of 75w UV lamps is:

$$n = \frac{mE_0Q \times 10^{-2}}{1.1D} \tag{9.31}$$

When the sterilization efficiency is P, then:

$$P = 1 - S = 1 - 10^{-\mathrm{m}} \tag{9.32}$$

When the above equations are used to reexamine the design of actual cylindrical ultraviolet sterilization equipment [49, 56–59], the results are shown in Table 9.25.

Table 9.26 presents the sterilization effect in the same experimental room with domestic-made XK-1 screen-type cylindrical UV sterilization equipment with circulated air [47, 56, 57]. In the room, the original bacteria environment was

Table 9.25 Calculated number of UV lamps in cylindrical UV sterilization equipment

Cylinder diameter D (m)	Actual flow rate Q (m^3/min)	Experimental Bacillus E_0 ($\mu W \cdot min/cm^2$)	Actual tube number n/n × W	Calculated value of m	Theoretical disinfection rate with actual tube number (%)	Theoretical disinfection rate with 99 % of actual tube number/n × W
0.264	5.33	17.1	3 × 30 (consideration with 6 × 15)	1.91	98.8	7 × 15

Table 9.26 Sterilization effect of the cylindrical sterilization equipment in the laboratory

		Bacterial removal rate (%)					
Time (min)	Level	1	2	3	4	5	Average
15	Low	92.73	91.41	92.41	94.30	92.09	92.59
	Middle	92.86	90.04	93.53	93.26	93.21	92.58
	High	92.43	92.54	91.90	92.85	91.25	92.19
30	Low	97.02	95.82	96.09	97.04	95.21	96.23
	Middle	95.77	95.98	97.25	96.21	95.04	96.05
	High	95.55	96.44	94.91	96.67	96.35	95.98
60	Low	97.84	97.51	97.35	98.09	97.44	97.65
	Middle	98.24	97.67	97.90	98.22	97.59	97.92
	High	97.91	98.09	97.87	97.87	97.70	97.89
120	Low	94.38	95.81	92.89	89.92	89.81	92.56
	Middle	93.69	91.98	94.62	91.70	91.38	92.67
	High	93.94	93.63	91.12	91.77	90.25	92.14

created with the spray of the bacterium prodigiosum liquid, where it was 1.16×10^7 pc/m^3. The air change rate was 11.6 h^{-1}. The temperature was 16.5 °C, and the relative humidity was 14 %. After the sterilization equipment was turned on, the sterilization effect at different time and at different height is presented in the table.

In the start period of 15 min, the sterilization efficiency did not reach the maximum. When the sterilization equipment works properly, the sterilization efficiency should be the maximum, which is the theoretical sterilization efficiency. The average efficiency at the time 60 min is 97.82 %, which is almost consistent with the calculated value 98.8 %. After 60 min, the total bacterial concentration indoors decreased gradually. The corresponding bacterial concentration before the UV equipment also decreased. So the sterilization efficiency maybe reduced.

In a cleanroom with area 11.6 m^2 in a pharmaceutical factory, where any mechanical ventilation and air-conditioning equipment were not installed, one XK-1 sterilization equipment and one fresh air unit operated simultaneously. Since the fresh air unit has three stages of air filtration, including coarse, medium, and sub-high-efficiency air filters, the supplied outdoor air can be considered free of bacteria. It is reasonable to consider that the sterilization equipment plays the role

of sterilizing the bacteria with circulated indoor air. With the measured data before and after the startup of the equipment, the actual sterilization efficiency is 93 %, which is slightly less than theoretical value. This is because the situation of actual cleanroom is much complex than the laboratory with circulated air only, which created more opportunity of bacterial pollution.

It should be also mentioned that although UV sterilization with circulation air has effect, air filter should be installed in the equipment in order to prevent the malfunction of UV lamp by the cover of dust particles. So for places where ventilation and air-conditioning systems are used, it is much simple to install filters with efficiency larger than fine filters. Meanwhile, it must be emphasized that UV light with circulation air still may cause the mutation of microorganism, so enough attention should be paid.

9.9 General Biological Cleanroom

According to the latest development of biological cleanroom technology, biological cleanroom can be divided into two categories, including the general biological cleanroom and the isolated biological cleanroom. The latter is also habitually called biosafety cleanroom (it is also termed as the biological cleanroom with biological risk).

In the general biological cleanroom, abbreviated as the biological cleanroom later, it is aimed to prevent the biological pollution from the working personnel. For example, the purpose of clean operating room is to prevent the bacterial infection of the operating site on the patient. For the working personnel himself, there is usually not risk. Similar as the industrial cleanroom, the positive pressurized environment should be kept indoors.

9.9.1 Type

Air pollution control mechanism in clean space is realized by the supply of clean air through HEPA filter placed at the air supply terminal, which is the largest difference for the concept between the cleaning air conditioner and the general air conditioner.

There is no basic difference between the general biological cleanroom and the industrial cleanroom. The former is guaranteed with the condition of air cleanliness. As for the biological cleanroom used in the hospital, especially the clean operating room, there is still the debate about the question whether vertical unidirectional flow cleanroom is superior than the horizontal one or vice versa. From the situations of the USA and Japan, in early times, the horizontal unidirectional flow cleanroom was much popular than the vertical one, because the number of newly built cleanroom was not much, or because the height of some renovated room was too low to make any fitment, where it is relative easy at the horizontal level. Later the type of local clean area was developed. At present, the type of local vertical unidirectional flow is more widely applied.

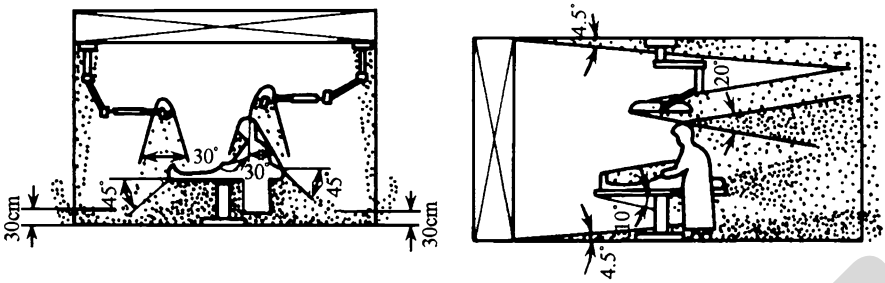

Fig. 9.15 Pollution models of vertical and horizontal unidirectional flow clean operating rooms

Table 9.27 Comparison of types adopted in biological cleanroom of hospitals

Comparison items	Vertical unidirectional flow cleanroom	Horizontal unidirectional flow cleanroom
Air cleanliness level	The highest	Poorer, but it should reach Class 3 at the first working area.
Surgery and assistant	Attention should be paid for the movement of head and hand	No special attention should be paid. However, people must stand at the downstream side of the surgery site
Nurse	Attention should be paid for the movement of head and hand	People must stand at the downstream side of the surgery site
Operation appliance	Allocation position is not limited. Attention should be paid when it is taken	Placed and taken at downstream side
Shadowless lamp	Multihead type should be used	Ordinary shadowless lamp can be used
People entering from outside and playing activity indoors	Degree of freedom for activity is big	Movement at upstream locations is not allowed
Occupied area needed	No	Yes
Setup in existing house	Difficult	Easy
Construction cost	High	Low

Figure 9.15 shows the pollution model of two kinds of clean operating room under usual circumstance. According to this model, the comparison between two kinds of clean operating rooms is performed, which is shown in Table 9.27.

If many turbulent flow air supply outlets are concentrated, the mainstream area will be enlarged and the effect will be better. The detailed information will be presented in Chap. 15.

It is Germany that started the method to place the air supply outlets concentratedly above the operating table in the clean operating room. It is aimed to protect the critical area of the operating table. This is different from the development of model in the industrial cleanroom at that time. And this kind of clean operating room is called the sterilized operating room in Germany. It promotes the development of this cleanroom.

After the check by National Identification Committee is passed, the concepts of "overall cleaning" and "local cleaning" were put forward in 1979, which was also introduced in the officially published monograph "Measures of Air Cleaning Technique" in July of 1977 [60].

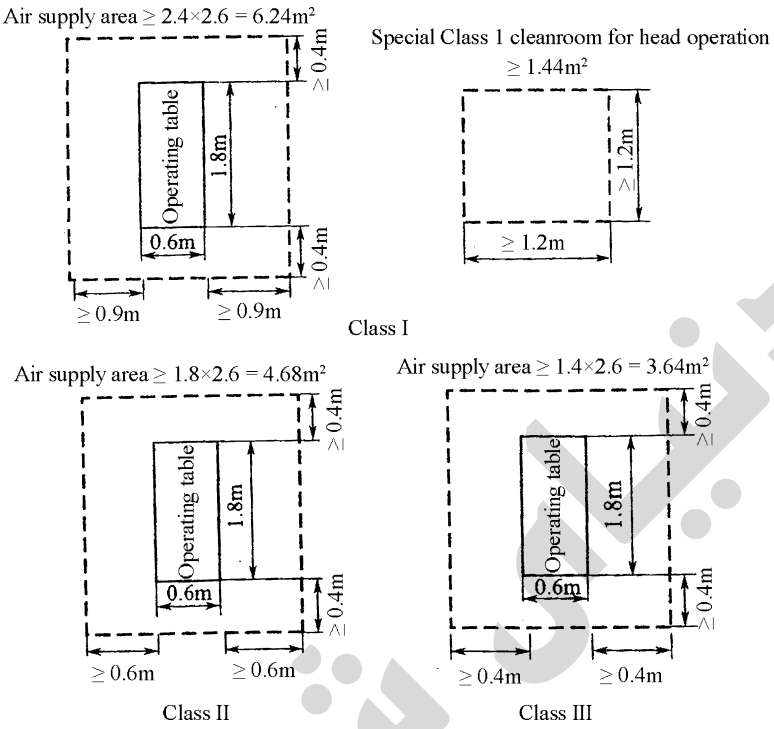

Fig. 9.16 Size of concentrated air supply outlets

"It is called the overall cleaning that the whole indoor working area becomes the clean environment with the air cleaning and other comprehensive measures." "It is called the local cleaning that the local indoor working area or specific local region becomes the clean environment." "When the condition required by the process is satisfied, the local cleaning method should be adopted as much as possible." Of course, this kind of local cleaning method will also have cleaning effect for the whole room.

It begins in China where the theoretical explanation for the effect of this concentrated air supply method was provided. The detailed specification was also provided, and the standard to distinguish the operating area from the surrounding area was developed [61]. With this method, the air change rate for Class 6 can be used to realize the air cleanliness Class 5 in the central cleaning area and Class 6 in surround area. The air change rate for Class 7 can be used to realize the air cleanliness Class 6 in the central cleaning area and Class 7 in surround area. The air change rate for Class 8 can be used to realize the air cleanliness Class 7 in the central cleaning area and Class 8 in surround area. So the energy-saving effect is obvious.

Figure 9.16 shows the division of concentrated air supply area in clean operating room in China [61].

In 2006, Russian Federal Standard GOST R52539 also adopted the classification method, where the air cleanliness in central area is Class 5 and in surrounding area Class 6.

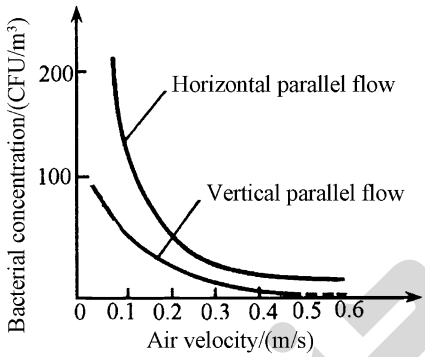

Fig. 9.17 Relationship between the bacterial concentration and the indoor air velocity

9.9.2 Air Velocity

The air velocity to be discussed here refers to the value in the biological cleanroom with unidirectional flow field. For the cross-sectional air velocity in this kind of cleanroom, the recommended lower limit of air velocity for classification mentioned before should be referred. Because they are not only the reasons mentioned during the discussion of the lower limit velocity but also the following points in biological cleanroom of the hospital:

1. From the above discussion about the relationship between the bacteria and the particle concentrations, when the supplied air velocity in unidirectional flow biological cleanroom is not 0.5 m/s, it has no influence on the indoor bacterial concentration. One experiment tested in the UK is cited here [62]. Among 16 cases of operating in vertical unidirectional flow cleanroom (10 cases for hip joint operation, 4 for antisternum operation, and 2 for knee joint operation), the relationship between the bacterial concentration and the indoor air velocity was obtained, where the bacterial concentration was sampled below the cut center on the patient body with the most direct release of bacteria. It is shown in Fig. 9.17. It is shown that the indoor bacterial concentration has almost reached stable, when the supplied air velocity reaches more than 0.3 m/s in vertical unidirectional flow cleanroom, or more than 0.35 m/s in horizontal unidirectional flow cleanroom. The improvement of air velocity on the indoor bacterial concentration is trivial. This conclusion completely coincides with the recommended lower limit of air velocity for the middle classification. It is also shown in this experiment that compared with the case in turbulent flow cleanroom when the supplied air velocity is 0.3 m/s, the bacterial concentration of vertical unidirectional flow cleanroom is less by 97 % and that of horizontal unidirectional flow cleanroom is less by 90 %.

   There are also similar results by numerical simulation. When the combined effect of airflow and the buoyancy plumes is considered, Ling Jihong obtained the results shown in Fig. 9.18 [63]. It is demonstrated that when the air velocity is less than 0.3 m/s, the bacterial concentration near the cut area increases dramatically. But there is also another opinion that with larger air velocity, the

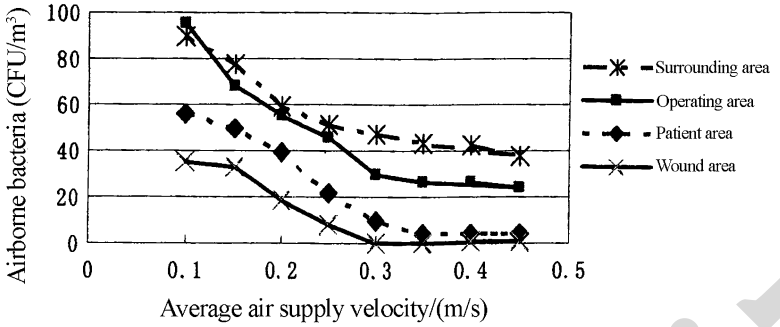

Fig. 9.18 Bacterial concentration distribution in various areas with different air velocities

Table 9.28 Comparison of the percentage of dissatisfied for patients in the isolation ward with six positions of air supply outlets

	Air supply from single-side ceiling and air return at the opposite side				High-efficiency air cleaner	
Evaluation index	Single deflection grille	Double deflection grille	Square diffuser	Low velocity perforated ceiling air supply	Air supply and air return at ceiling (US CDC)	Ceiling air supply and air return at two sides (US CDC)
Surface air velocity (m/s)	0.05	0.05	0.09	0.05	0.03	0.13
Percentage of dissatisfaction by draught (%)	0	0	4.5	0	0	6.8

bacteria brought out by buoyancy plume from the cut area will be pressed back. But so far there is no test about this idea. Moreover, it is also not supported with the fact that the air velocity approaches "0" in the "triangular area" of the airflow center, which has been introduced in Chap. 8.

2. Even in the clean operating room with temperature 26 °C, the patient on the operating table is easily to suffer from lacking of water under the supplied air velocity 0.5 m/s [64]. It is very disadvantageous for the patient with the lacking of water on the tissue near the cut. With this reason and others including the thermal comfort of the surgeon, the air velocity near the operating table is expected to be less than 0.25 m/s.
3. In the cleaning ward or the cleaning cabin, the air velocity larger than 0.2 m/s is usually not needed. One reason is that there is not any disturbance, and the other is that the patient does not prefer any high air velocity. Deng Weipeng obtained the percentage of dissatisfied with six positions of air supply outlets [65]. Table 9.28 shows the results.

Table 9.29 Relationship between the air velocities at the air supply outlet and near the face

Air change rate (h^{-1})	Air supply outlet number	Air supply velocity (m/s)	Air velocity at height 0.8 m above the floor (m/s)
10	1	0.5	0.11
10	2	0.5	0.055
15	2	0.75	0.095
25	3	0.40	0.109
25	4	0.40	0.073

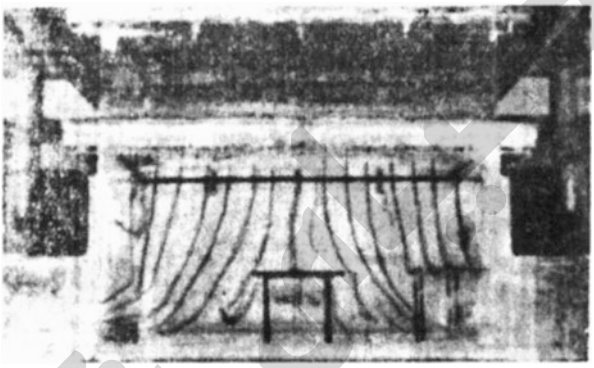

Fig. 9.19 Pollutants accumulated under the working table. The *black line* represents the streamline of the colored liquid, i.e. the airflow streamline

It is shown from Table 9.28 that if the percentage of dissatisfied for patients should be less than 5 %, the air velocity at the face should be less than 0.1 m/s. Usually the air velocity at the face is required to be less than 0.12 m/s in comfortable air conditioning.

When the air supply outlet is not right above the human face, the relationship between the air velocities at the height 0.8 m and at the air supply outlet is obtained, which is shown in Table 9.29 [66].

9.9.3 Local Airflow

Here the several problems of local airflow in biological cleanroom ant its improvement methods will be emphasized.

1. In the cleanroom where biological experiments are performed, including the plant cultivation and microorganism cultivation, a multilayer stand similar as the bookshelf is usually used. Every layer is full of various containers (even open containers) including the utensils, bottle, and jar. If vertical unidirectional flow was used, air can not only pass through the outside of the stand but also form the turbulent flow inside the stand. Therefore, it's better to use horizontal unidirectional flow in this kind of cleanroom.
2. In vertical unidirectional flow cleanroom, air flows downwards, so eddy maybe formed below the working table, where it is not easy to exhaust the polluted air from this region. Figure 9.19 is the experimental results with the water model [67]. When the air velocity is small, pollutants will accumulate below the table

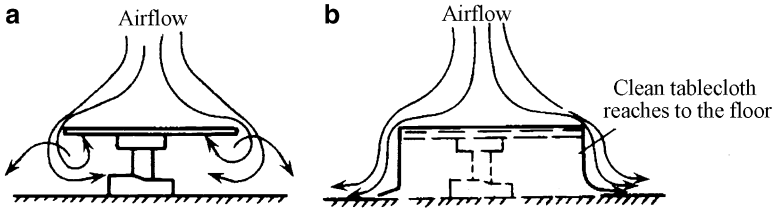

Fig. 9.20 Method to prevent the appearance of eddy beneath the working table. (**a**) Situation with appearance of vortex flow below table. (**b**) Situation with cover of tablecloth

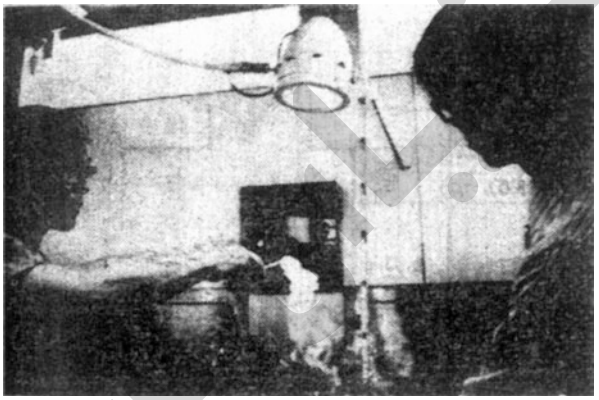

Fig. 9.21 Airflow below the shadowless lamp. The ellipse in the *upper middle* is the streamlined shadowless lamp. The *black* parts at *both sides* represent the head of occupant. In the *middle*, the *white* part means the smog released by experimenter.

quickly, which is not easily removed. But when common air velocity is used, this kind of pollution can be removed quickly. The problem is that surgeons stand around the operating table in the clean operating room, which will weaken the air velocity passing through the table. Therefore, pollutants generated by occupants' activity area easily accumulated under the table. With the occasional fierce activity, the airflow generated will disperse these pollutants outside of the table, which may cause risk for the patient on operation. This problem has also been noticed by some researchers abroad. They proposed a method to prevent the appearance of turbulent flow below the operating table and the apparatus table. For vertical airflow, the clean table cloth is used to cover the table until the floor, which will reduce the exchange between the air below the table and the clean air. Figure 9.20 shows the schematic of this proposal [1]. On the contrary, table cloth should not be used to cover the table until the floor for the horizontal flow cleanroom, so that air can pass through the region beneath the table. There are also different conclusions by calculation [63]. However, both of them are validated by experiment.

3. The shadowless lamp usually used in the operation has very great influence on the air cleanliness; since it is too big to prevent, the airflow and the buoyant plume will be generated. At present, one kind of streamlined shadowless lamp is applied abroad. It is used to replace the big shadowless lamp, and several small shadowless lamps are used. With the streamlined shape, the influence on the airflow is greatly reduced. Figure 9.21 shows the situation of airflow below the shadowless lamp [68]. It is shown that airflow recovers to parallel flow under the distance of 35 cm

Table 9.30 Comparison of two kinds of shadowless lamps

Measurement location (x represents the sampling position)		Particle concentration (pc/L) ≥0.5 μm	≥0.3 μm	Sampled bacterial concentration with gap method (CFU/L)
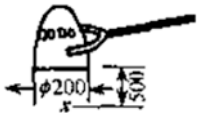	Streamlined lamp	0	0	0
		0	0.7	
	Shadowless lamp	0	0	
		0	0	
	Ordinary lamp	30	37	0
		14	18	
	Shadowless lamp	11	10	
		29	50	

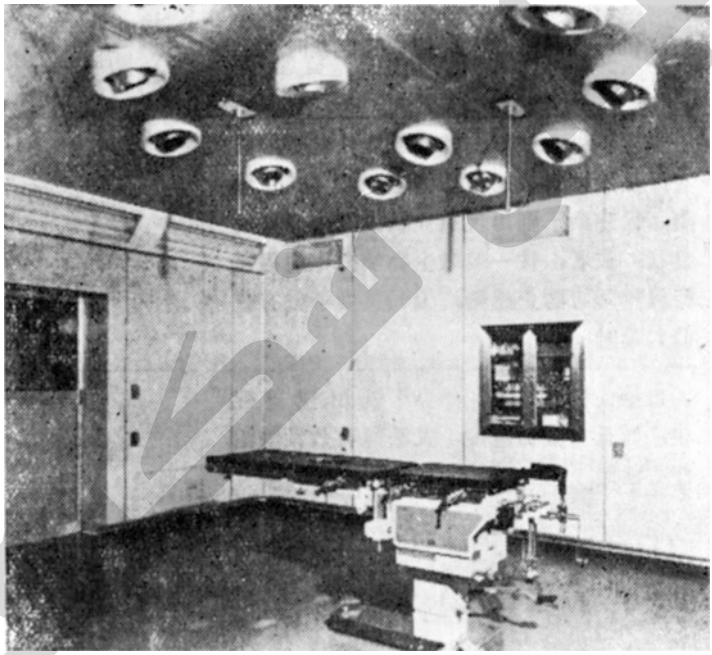

Fig. 9.22 Shadowless lamps inlayed in the ceiling

below the lamp. Table 9.30 shows the comparison of these two kinds of shadowless lamps. Particles with diameter ≥0.5 μm are not detected below the streamlined shadowless lamp, while there are a lot of these particles under the usual shadowless lamp. Although bacteria are not detected for both cases, the probability of the existence of airborne bacteria will be large when particles are too much. In order to weaken the influence of turbulent flow below the shadowless lamp, it was proposed to supply clean air from the lamp body [69], but there is still no real product in the market. Moreover, there are many shadowless lamps inlayed in the ceiling, which is shown in Fig. 9.22.

9.10 Isolated Biological Cleanroom

Compared with the general biological cleanroom, the difference of the isolated biological cleanroom is that it is aimed to prevent the escape of microbial contamination. Therefore, it has not requirement for the air cleanliness itself, where HEPA filter is not needed in the air supply system. But one or two HEPA filters must be installed before the exhaust of air to the ambient, and isolation is needed. Isolated biological cleanroom is also called the biological cleanroom with biological risk, or abbreviated as the hazardous biological cleanroom, such as biosafety laboratory and negative pressurized isolation ward.

9.10.1 Biological Risk Standard

The class of biosafety laboratory, which belongs to the isolated biological cleanroom, is determined by the risk extent of the microorganism isolated. Some foreign authoritative research agencies have published their own independent risk criteria.

In the early of 1990s, our country ever made the risk standard of microorganism. In 2004, the National Council published "Management Regulation of the Biosafety Laboratory with Pathogenic Microorganism." Later in 2005 and in 2006, the Department of Agriculture and Department of Health issued the classification of pathogenic microorganism in animal and human, which is shown in Table 9.31.

It is shown that pathogene microorganisms for the risk degree above Class 2 include Class 1 and Class 2, which are relative large hazardous and the most hazardous. But it should be pointed out that in Chinese standard, the risk degree increases from 4 to 1, while in foreign standard, it increases from 1 to 4, which is shown in Table 9.32.

The risk levels in each column of Table 9.32 are the same. For example, the risk level of Class P_3 in the USA is the equivalent to Class 3 in Japan and Class 2 in China.

9.10.2 Isolation Methods

The concept of isolation includes the first isolation and the second isolation. The first isolation refers to the isolation between staff and pathogenic. The second isolation means the isolation between the laboratory or the work area and the outside ambient. For high-biological-risk level, not only the first isolation measures but also the second isolation measures are needed. At present, the main method of the first isolation abroad is to use the biosafety cabinets or biosafety working table, which acts as a screen to prevent the escape of microorganism. With the second isolation, negative pressurized environment is created in the working area, where airlock chamber or even the buffer chamber should be set in the passage for occupant and sterilizer apparatus with high pressure should be placed for the

Table 9.31 Classification of pathogenic microorganism

Class	Harmful degree	Representative pathogenic microorganism
I	Highly harmful microorganism, which may cause serious diseases to human or animals, and some microorganisms have not been found or some announced elimination	Virus infecting in people: *Alastrim virus, Crimean/Congo hemorrhagic fever virus (Xinjiang hemorrhagic fever virus), Eastern equine encephalitis virus, Ebola virus, Flexal virus, Guanarito virus, Hanzalova virus, Hendra virus, simian herpesvirus, Hypr virus, Junin virus, Kumlinge virus, Kyasanur forest disease virus, Lassa fever virus, Louping-ill virus, Ma Qiubo virus, Marburg virus, Monkeypox virus, Mopeia virus (and other Tavaribe virus), Nipah virus, Omsk hemorrhagic fever virus, Sabia virus, Saint Louis encephalitis virus, Tacaribe virus, Variola virus, Venezuelan equine encephalitis virus, Western equine encephalitis virus, Yellow fever virus, Tick-borne encephalitis* Virus infecting in animals: *Foot-and-mouth disease virus, Highly pathogenic avian influenza virus, swine vesicular disease virus, African swine fever virus, African horse sickness virus, Rinderpest virus, Peste-des-petits-ruminants virus, contagious bovine pleuropneumonia/Mycoplasma mycoides, Bovine spongiform encephalopathy agent, scrapie agent*
II	Moderately harmful microorganism, which may cause serious diseases to human or animals, easy to spread in people and in animals directly or indirectly	Virus infecting in people: *Bunyamwera virus, California virus, Chikungunya virus, Dhori virus, Everglades virus, Foot-and-mouth disease virus, Garba virus, Germiston virus, Getah virus, Gordil virus, Hantaviruses, others. Hantaviruses cause pulmonary syndrome. Hantaviruses cause hemorrhagic fever with renal syndrome. Herpesvirus saimiri, High pathogenic avian influenza virus, Human immunodeficiency virus(HIV) (type 1 and 2 virus), Inhangapi virus, Inini virus, Issyk-Kul virus, Itaituba virus, Japanese encephalitis virus, Khasan virus, Kyzylagach virus, Lymphocytic choriomeningitis (neurotropic) virus, Mayaro virus, Middelburg virus, Milker's nodule virus, Mucambo virus, Murray valley encephalitis virus (Australia encephalitis virus), Nairobi sheep disease virus, Ndumu virus, Negishi virus, Newcastle*

		disease virus, *Orf virus*, *Oropouche virus*, *other pathogenic orthopoxviruses not in BL 1*, *3*, *or 4*, *Paramushir virus*, *Poliovirus*, *Powassan virus*, *Rabbitpox virus (vaccinia variant)*, *Rabies virus (street virus)*, *Razdan virus*, *Rift valley fever virus*, *Rochambeau virus*, *Rocio virus*, *Sagiyama virus*, *SARS-associated coronavirus (SARS-CoV)*, *Sepik virus*, *Simian immunodeficiency virus (SIV)*, *Tamdy virus*, *West Nile virus* Pathogenes infecting in people: *Bacillus anthracis*, *Brucella*, *Burkholderia mallei*, *Coxiella burnetii*, *Francisella tularensis*, *Mycobacterium bovis*, *Mycobacterium tuberculosis*, *Rickettsia*, *Vibrio cholerae*, *Yersinia pestis* Fungus infecting in people: *Coccidioides immitis*, *Histoplasma farciminosum*, *Paracoccidioides brasiliensis* Virus infecting in animals: *Hog cholera virus*, *Newcastle disease virus*, *Rabies virus*, *Sheep pox/goat pox virus*, *bluetongue virus*, *Rabbit hemorrhagic disease virus*, *Bacillus anthracis*, *Bacterium burgeri*
III	Lightly harmful microorganism, which may cause diseases to human or animals but do no serious harm to them and the environment, while they have limited risk of transmission and low probability of causing serious diseases and can be treated and prevented effectively	Acute hemorrhagic conjunctivitis virus, Adenovirus, Adeno-associated virus, Alphaviruses, Astrovirus, Barmah Forest virus, Bebaru virus, Buffalopox virus: 2 viruses (1 a vaccinia variant), Bunyavirus, Calicivirus, Camelpox virus, Coltivirus, Coronavirus, Cowpox virus, Coxsackievirus, Cytomegalovirus, Dengue virus, ECHO virus, Enterovirus,Enterovirus 71, Epstein-Barr virus, Flanders virus, Flaviviruses known to be pathogenic, others, Guaratuba virus, Hart Park virus, Hazara virus, Hepatitis A virus, Hepatitis B virus, Hepatitis C virus, Hepatitis D virus, Hepatitis E virus, Herpes simplex virus, Human herpesvirus 6, Human herpesvirus 7, Human herpesvirus 8, Human T- lymphotropic virus, Influenza virus, Kunjin virus, La Crosse virus, Langat virus, Lentivirus, except HIV, Lymphocytic choriomeningitis virus, Measles virus, Metapneumovirus, Molluscum contagiosum virus, Mumps virus, O'nyong-nyong virus, Oncogenic RNA virus B, Oncogenic RNA virus C, except HTLV I and II, other

(continued)

Table 9.31 (continued)

Class	Harmful degree	Representative pathogenic microorganism
		Bunyaviridae known to be pathogenic, Papillomavirus (human), Parainfluenza virus, Paravaccinia virus, Parvovirus B19, Polyoma virus, BK and JC viruses, Rabies virus (fixed virus), Respiratory syncytial virus, Rhinovirus, Ross river virus, Rotavirus, Rubivirus (Rubella), Saumarez Reef virus, Sandfly fever virus, Semliki Forest virus, Sendai virus (murine parainfluenza virus type 1), Simian virus 40, Sindbis virus, Tanapox virus, Tensaw virus, Turlock virus, Vaccinia virus, Varicella-zoster virus, Vesicular stomatitis virus, Yellow fever virus, (vaccine strain,17D)
		Pathogenes infecting in people:
		Acinetobacter lwoffii, *Acinetobacter baumannii*, *Mycobacterium chelonae*, *Actinobacillus actinomycetemcomitans*, *Actinomadura madurae*, *Actinomadura pelletieri*, *Actinomyces bovis*, *Actinomyces gerencseriae*, *Actinomyces israelii*, *Actinomyces naeslundii*, *Actinomyces pyogenes*, *Aeromonas hydrophila*, *Aeromonas punctata*, *Afipia* spp., *Amycolata autotrophica*, *Arachnia propionica*, *Arcanobacterium equi*, *Arcanobacterium haemolyticum*, *Bacillus cereus*, *Bacteroides fragilis*, *Bartonella bacilliformis*, *Bartonella elizabethae*, *Bartonella henselae*, *Bartonella quintana*, *Bartonella vinsonii*, *Bordetella bronchiseptica*, *Bordetella parapertussis*, *Bordetella pertussis*, *Borrelia burgdorferi*, *Borrelia duttonii*, *Borrelia recurrentis*, *Borrelia vincenti*, *Calymmatobacterium granulomatis*, *Campylobacter jejuni*, *Campylobacter sputorum*, *Campylobacter fetus*, *Campylobacter coli*, *Chlamydia pneumoniae*, *Chlamydia psittaci*, *Chlamydia trachomatis*, *Clostridium botulinum*, *Clostridium difficile*, *Clostridium equi*, *Clostridium haemolyticum*, *Clostridium histolyticum*, *Clostridium novyi*, *Clostridium perfringens*, *Clostridium sordellii*, *Clostridium tetani*, *Corynebacterium bovis*, *Corynebacterium diphtheriae*, *Corynebacterium minutissimum*, *Corynebacterium pseudotuberculosis*, *Corynebacterium ulcerans*, *Dermatophilus congolensis*, *Edwardsiella tarda*, *Eikenella corrodens*,

Enterobacter aerogenes/cloacae, *Enterobacter* spp., *Ehrlichia sennetsu*, *Erysipelothrix rhusiopathiae*, *Erysipelothrix* spp., *Pathogenic Escherichia coli*, *Flavobacterium meningosepticum*, *Fluoribacter bozemanae*, *Francisella novicida*, *Fusobacterium necrophorum*, *Gardnerella vaginalis*, *Haemophilus ducreyi*, *Haemophilus influenzae*, *Helicobacter pylori*, *Kingella kingae*, *Klebsiella oxytoca*, *Klebsiella pneumoniae*, *Legionella pneumophila*, *Listeria ivanovii*, *Listeria monocytogenes*, *Leptospira interrogans*, *Mima polymorpha*, *Morganella morganii*, *Mycobacterium africanum*, *Mycobacterium asiaticum*, *Mycobacterium avium-chester*, *Mycobacterium fortuitum*, *Mycobacterium hominis*, *Mycobacterium kansasii*, *Mycobacterium leprae*, *Mycobacterium malmoense*, *Mycobacterium microti*, *Mycobacterium paratuberculosis*, *Mycobacterium scrofulaceum*, *Mycobacterium simiae*, *Mycobacterium szulgai*, *Mycobacterium ulcerans*, *Mycobacterium xenopi*, *Mycoplasma pneumoniae*, *Neisseria gonorrhoeae*, *Neisseria meningitides*, *Nocardia asteroids*, *Nocardia brasiliensis*, *Nocardia carnea*, *Nocardia farcinica*, *Nocardia nova*, *Nocardia otitidiscaviarum*, *Nocardia transvalensis*, *Pasteurella multocida*, *Pasteurella pneumotropica*, *Peptostreptococcus anaerobius*, *Plesiomonas shigelloides*, *Prevotella* spp., *Proteus mirabilis*, *Proteus penneri*, *Proteus vulgaris*, *Providencia alcalifaciens*, *Providencia rettgeri*, *Pseudomonas aeruginosa*, *Rhodococcus equi*, *Salmonella arizonae*, *Salmonella choleraesuis*, *Salmonella enterica*, *Salmonella meleagridis*, *Salmonella paratyphi A,B,C*, *Salmonella typhi*, *Salmonella typhimurium*, *Serpulina* spp., *Serratia liquefaciens*, *Serratia marcescens*, *Shigella* spp., *Staphylococcus aureus*, *Staphylococcus epidermidis*, *Streptobacillus moniliformis*, *Streptococcus pneumoniae*, *Streptococcus pyogenes*, *Streptococcus* spp., *Streptococcus suis*, *Treponema carateum*, *Treponema pallidum*, *Treponema pertenue*, *Treponema vincentii*, *Ureaplasma urealyticum*, *Vibrio vulnificus*, *Yersinia enterocolitica*, *Yersinia pseudotuberculosis*, *Human granulocytic ehrlichia*, *Ehrlichia chaffeensis*, *EC*

(continued)

Table 9.31 (continued)

Class	Harmful degree	Representative pathogenic microorganism
		Fungus infecting in people:
		Absidia corymbifera, *Alternaria*, *Arthrinium*, *Aspergillus flavus*, *Aspergillus fumigatus*, *Aspergillus nidulans*, *Aspergillus ochraceus*, *Aspergillus parasiticus*, *Blastomyces dermatitidis*, *Candida albicans*, *Cephalosporium*, *Cladosporium carrionii*, *Cladosporium trichoides*, *Cryptococcus neoformans*, *Dactylaria gallopava*, *Dermatophilus congolensis*, *Emmonsia parva*, *Epidermophyton floccosum*, *Exophiala dermatitidis*, *Fonsecaea compacta*, *Fonsecaea pedrosoi*, *Fusarium equiseti*, *Fusarium graminearum*, *Fusarium moniliforme*, *Fusarium nivale*, *Fusarium oxysporum*, *Fusarium poae*, *Fusarium solani*, *Fusarium sporotrichioides*, *Fusarium tricinctum*, *Geotrichum*.spp., *Loboa loboi*, *Madurella grisea*, *Madurella mycetomatis*, *Microsporum*. spp., *Mucor*.spp., *Penicillium citreoviride*, *Penicillium citrinum*, *Penicillium cyclopium*, *Penicillium islandicum*, *Penicillium marneffei*, *Penicillium patulum*, *Penicillium purpurogenum*, *Penicillium rugulosum*, *Penicillium versicolor*, *Penicillium viridicatum*, *Pneumocystis carinii*, *Rhizopus cohnii*, *Rhizopus microsporus*, *Sporothrix schenckii*, *Stachybotrys*, *Trichoderma*, *Trichophyton rubrum*, *Trichothecium*, *Xylohypha bantiana*
		Virus infecting in animals:
		Pathogenic microorganism of a common disease in various animals: *Low pathogenic influenza virus*, *Pseudorabies virus*, *Clostridium tetani*, *Clostridium chauvoei*, *Mycobacterium tuberculosis*, *Mycobacterium paratuberculosis*, *enteropathogenic Escherichia coli*, *Salmonella*, *Pasteurella*, *Pathogenic Streptococcus*, *Listeria monocytogene*, *Clostridium perfringens*, *Aeromonas hydrophila*, *Clostridium botulinum*, *Clostridium putrificum and other pathogenic clostridia*, *Chlamydia psittaci*, *Actinomycete*, *Leptospira*
		The cattle disease pathogenes: *Malignant catarrh virus*, *Bovine leukemia virus*, *Bovine ephemeral fever virus*, *Infectious bovine rhinotracheitis*

virus, *Bovine viral diarrhea virus*, *Bovine viral diarrhea-mucosal disease virus*, *Bovine genital campylobacteriosis*, *Schistosoma japonicum*

Sheep and goat pathogenic microorganisms: *Caprine arthritis/encephalomyelitis virus*, *Maedi-Visna virus*, *Contagious pustular dermatitis virus*

Swine pathogenic microorganisms: *Japanese encephalitis virus*, *Porcine reproductive and respiratory syndrome virus*, *Porcine parvovirus*, *Porcine circovirus*, *Porcine epidemic diarrhea virus*, *Transmissible gastroenteritis virus*, *Bacillus rhusiopathiae suis*, *Swine Bordetella bronchiseptica*, *Actinobacillus pleuropneumoniae*, *Haemophilus parasuis*, *Mycoplasma hyopneumoniae*, *Treponema hyodysenteriae*

Equine pathogenic microorganisms: *Equine infectious anemia virus*, *Equine arteritis virus*, *Equine abortion virus*, *Equine rhinitis virus*, *Pseudomonas mallei*, *Pseudomonas pseudomallei*, *Histoplasma farciminosum*, *Ulcerative lymphangitis*, *Corynebacterium pseudotuberculosis*

Avian pathogenic microorganisms: *Duck plague virus*, *Duck hepatitis virus*, *Gosling plague virus*, *Infectious bursal disease virus*, *Marek's disease virus*, *Avian leucosis/sarcoma virus*, *Avian reticuloendotheliosis virus*, *Avian infectious anemia virus*, *Avian infectious laryngotracheitis virus*, *Avian infectious bronchitis virus*, *Avian egg drop syndrome virus*, *Avian molluscum roup virus*, *Avian viral arthritis virus*, *Avian infectious encephalomyelitis virus*, *Haemophilus paragallinarum*, *Mycoplasma gallisepticam*, *Avian coccidiosis*

Rabbit pathogenic microorganism: *Myxomatosis virus*, *Francisella tularensis*, *Bordetella bronchiseptica in rabbit*, *Rabbit coccidia*

Aquatic animal pathogenic microorganism: *Infectious hematopoietic necrosis virus*, *Epizootic hematopoietic necrosis virus*, *Infectious haematopoietic necrosis virus*, *Oncorhynchus masou virus*, *Viral hemorrhagic septicemia virus*, *Koi herpesvirus*, *Channel catfish virus*, *Viral encephalopathy and retinopathy virus*, *Infectious pancreatic necrosis virus*, *Red sea bream iridovirus*, *White sturgeon iridovirus*,

(continued)

Table 9.31 (continued)

Class	Harmful degree	Representative pathogenic microorganism
		Baculoviral midgut gland necrosis virus, *Infectious hypodermal and hematopoietic necrosis virus*, *Nuclear polyhedrosis virus*, *Shrimp spawning mortality syndrome virus*, *turtle gill adenitis virus*, *Taura syndrome virus*, *Shrimp white spot syndrome virus*, *Shrimp yellowhead virus*, *Grass carp hemorrhagic virus*, *Spring viraemia of carp virus*, *Abalone spherical virus*, *Infectious salmon anaemia virus*
		Honeybee pathogenic microorganism: *Paenibacillus larvae causing American foulbrood disease*, *Melissococcus pluton causing European foulbrood disease*, *Ascosphaera apis causing bee chalkbrood disease*, *Nosema apis*, *Tarsonemid mite*, *Varroa jacobsoni*
		Other animal pathogenic microorganism: *Canine distemper virus*, *Canine parvovirus*, *Canine adenovirus*, *Canine coronavirus*, *Canine parainfluenza virus*, *Feline panleukopenia virus*, *Aleutian mink disease parvovirus*, *Mink enteritis virus*
IV	Lightly harmful microorganism, including veterinary bio-products which is lowly dangerous and pathogenic, with less infection opportunities in laboratory, and attenuated pathogenic microorganism used for producing vaccine and low-toxic pathogenic microorganism not included in Classes 1, 2, and 3	Virus infecting in people: *Guinea pig herpesvirus*, *Hamster leukemia virus*, *Herpesvirus saimiri*, *Monkey disease*, *Murine leukemia virus*, *Mouse mammary tumor virus*, *Rat leukemia virus*
		Virus infecting in animals: Veterinary bio-products which is lowly dangerous and pathogenic, with less infection opportunities in laboratory, and attenuated pathogenic microorganism used for producing vaccine and low-toxic pathogenic microorganism not included in Classes 1, 2, and 3

Table 9.32 Biological risk criteria

Organization	Object	~Low		Risk level A		High~	
Centers for Disease Control and Prevention, USA (CDC)	Pathogenic microorganism	1	2	3		4	5 6
National Cancer Institute, USA (NCI)	Cancer virus		Low	Medium		High	
National Institutes of Health, USA (NIH)	Combination of genetic gene	P_1	P_2	P_3		P_4	
National Institute of Health Sciences, Japan (NIHS)	Microbial virus		2_a	2_b	3_a 3_b	4_a	4_b
China	Microbial virus	4	3	2		1	

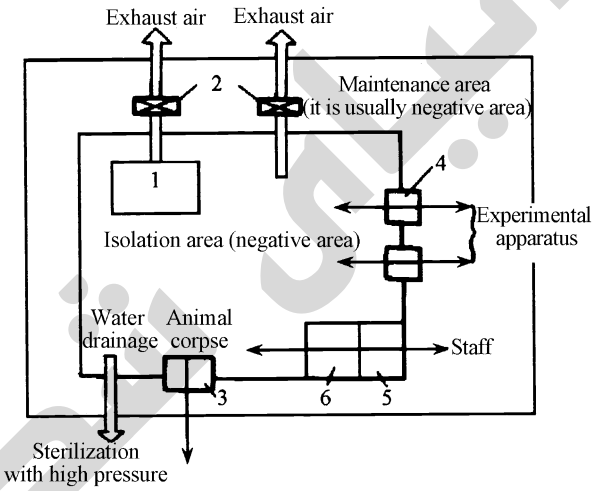

Fig. 9.23 Isolated biological cleanroom. *1* biosafety cabinet, *2* HEPA filter, *3* sterilizer container with high pressure, *4* pass-by window, *5* shower and cloth replacement chamber, *6* airlock chamber

delivery of goods into or out of the room. Figure 9.23 is such kind of this isolation method [70], which is called biosafety laboratory.

It is important to note the requirement for coming out is stricter than entering in for the occupants' cloth requirement in isolated biological cleanroom. People must not only replace clothes but also pass through the shower and drying treatment, after which all the clothes must be disinfected and then cleaned.

9.10.3 Biosafety Cabinet

This is the first isolation means in the isolated biological cleanroom, which is similar to the negatively pressurized clean bench but has stricter requirements. Table 9.33 shows three kinds of specifications which are common in the world. The requirement of structure is shown in Fig. 9.24 [71–74].

Table 9.34 shows the classification of biosafety cabinet according Chinese standard "Biosafety Cabinet" (JG170-2005).

Figure 9.25 illustrates the structure of domestic-made II-A biosafety cabinet.

Table 9.33 Level of biosafety cabinet

Safety cabinet level	Isolation properties	Air-sealing requirement	Opening surface velocity (m/s)	Application of biological risk level	Protection object
1	Partial isolation	Specific requirements	0.38	Can reach Class 2	User
2 Type A	Partial isolation	The leakage rate $<1 \times 10^{-5}$ L/s when the shell is under the positive pressure 510 Pa	0.38	Up to Class 3 (by HEPA filter, exhaust air can enter the room)	Users and products
Type B	Partial isolation	No soap bubble with the soap liquid examination when the shell is under positive pressure 510 Pa	0.51	Reach Class 3 (cannot exhaust indoors)	Users and products
3	Complete isolation	The leakage rate $<1 \times 10^{-9}$ L/s when the shell is under the positive pressure 510 Pa	–	Up to 4 class (object should pass through the disinfection liquid tank before entering)	User first, sometimes also includes the product

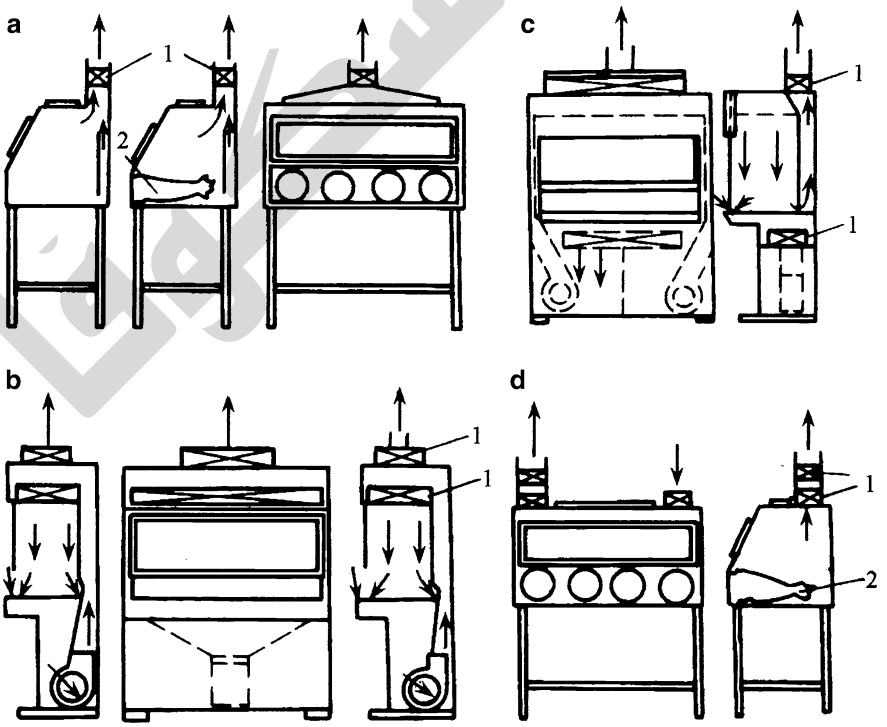

Fig. 9.24 Structure of biosafety cabinet. (**a**) Class 1. (**b**) Class 2 Type B. (**c**) Class 2 Type A. (**d**) Class 3. *1* HEPA filter, *2* safety glove

Table 9.34 Classification of biosafety cabinet

Class	Type	Exhaust	Circulation air ratio (%)	Airflow in cabinet	Average velocity at the entrance of working window (m/s)	Protected object
I	–	Can exhaust indoors	0	Turbulent flow	≥0.40	User and environment
II	A1	Can exhaust indoors	70	Unidirectional flow	≥0.40	User, test sample, and environment
	A2	Can exhaust indoors	70	Unidirectional flow	≥0.50	
	B1	Cannot exhaust indoors	30	Unidirectional flow	≥0.50	
	B2	Cannot exhaust indoors	0	Unidirectional flow	≥0.50	
		Cannot exhaust indoors	0	Unidirectional flow or turbulent flow	No air supply from working window. When one glove is taken down, air velocity at the glove opening ≥0.7	Mainly user and environment. Sometimes test sample is also considered

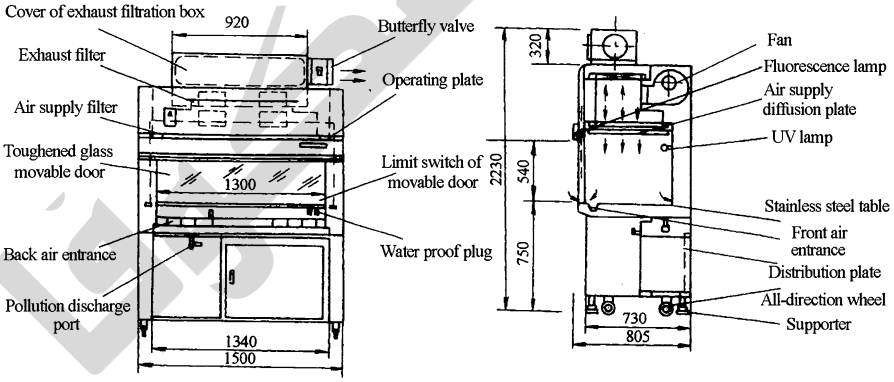

Fig. 9.25 Structure of domestic-made II-A biosafety cabinet

Here it should be pointed out that, according to the general provisions, if there is rotating machinery in the safety cabinet, other activities are not allowed indoors during the period when the rotating machinery is in use, which increases the possibility of the escape of pollutants out of the cabinet. When the operation in the safety cabinet is finished, the safety cabinet is not allowed to immediately stop; instead it should continue to run for several minutes before stop.

Detailed information about biosafety cleanroom and biosafety cabinet will be presented in Ref. [75].

Table 9.35 Laboratory type and risk categories formulated by WHO

Risk category	Lab classification	Laboratory example	Microbial example
I Very low risk for individual and the public	Basics	Basic teaching	Bacillus subtilis *Escherichia coli* K
II Slight risk for individual and limited risk for public	Basics (if necessary, biosafety cabinet or other suitable personal protection equipment or closed equipment should be equipped with)	Primary health unit; primary hospital; doctor office; diagnostic laboratories; university teaching unit; public health laboratories	*Salmonella typhi* Hepatitis B virus Mycobacterium tuberculosis Lymph cell vein meningitis virus
III Higher risk for individual and low risk for public	Sealed	Special diagnostic laboratory	Brucella Lassa fever virus Histoplasmosis
IV Higher risk for both individual and public	Highly sealed	Dangerous pathogenes unit	Ebola-Marburg virus Foot-and-mouth disease virus

9.10.4 Classification of Biosafety Laboratory

In 1983, World Health Organization (WHO) published "Laboratory Biosecurity Handbook," and China's Ministry of Health was authorized to publish it in our country in 1985 [70], where the explanation of four kinds of risk classes was described. It is shown in Table 9.35.

Table 9.36 shows the classification in Japan [71].

The classification of biosafety laboratory in China by national standards "General requirement of biosafety laboratory" (GB19489-2004) issued in 2004 and "Building technical specification of biosafety laboratory" (GB50346-2004) is consistent with international standards. There are four levels from 1 to 4 with the increasing requirements. In the revised version of GB50346 in 2011, there are three categories, which are shown in Tables 9.37 and 9.38.

For biosafety laboratories with Class 3 and Class 4 in China, air cleanliness levels are required, where air filter at the air supply terminal should be HEPA filter.

9.10.5 Negatively Pressurized Isolation Ward

As for one of the important applications of isolated biological cleanroom, great attention has been paid on the negatively pressurized isolation ward in hospital since

Table 9.36 Classification of cleanroom with risk level in Japan

When it is impossible for infection in most cases	For the grade 1	No special provisions are specified for the isolation of the experimentation area
When it is impossible for infection in most cases, and morbidity is unlikely to appear even when infection occurs	For the grade 2_a	No special provisions are specified for the isolation of the experimentation area, and the personnel are prohibited to enter
Infection can be prevented when the general microbiology procedures are followed, and morbidity is unlikely to appear even when infection occurs	For the grade 2_b	Only the experimentation area needs the first isolation. During experiment, non-staffs are prohibited to enter
When the opportunity of infection is large, the symptom is very milder after infection. Or infection is rare due to the immunity of a adult, but the symptom is heavy once infection occurs	For the grade 3_a	Two isolation steps are needed. Seam is not allowed on the ground material, and sealing should be made on the joint gap. Usually non-staffs are also prohibited to enter. Circulating air and exhaust air should pass through HEPA filters. Indoor negative pressure should be maintained
When the opportunity of infection is large, the symptom is very heavy after infection. Or although infection is rare due to the effective precaution measures, the symptom is heavy or the symptom unusual in China appears once infection occurs	For the grade 3_b	Except for the same requirement as grade 3_a, unidirectional flow is needed for air distribution
When the opportunity of infection is large, the symptom is very heavy after infection, and it is deadly, which cannot be cured by effective precaution measures	For the grade 4	Building should standalone. Two isolation steps are needed in the building. Airlock door should be interlocked automatically. The interior surface should be decorated with the whole material. Usually non-staffs are prohibited to enter. Unidirectional flow and full fresh air are needed. Exhaust air from the safety cabinet and indoor should pass through HEPA filters. Supply air should be interlocked with exhaust air. Before the stop of exhaust air, the supply air system must be stopped. The negative pressure indoors should be more than −15 Pa

the outbreak of SARS. The design concept is represented by "high negative pressure, seal door, and full fresh air." This concept was called "static isolation" by author, which has poor performance, very expensive cost, and no benefit for promotion.

The novel theory of negative pressurized ward proposed by author is "dynamic isolation" [66, 76–79]. Low value of negative pressure (−5 Pa) is used to replace

Table 9.37 Classification of biosafety laboratory

Classification	Risk extent	Object
Class 1	Low risk for both individual and group	Risk is low for human body, environment, animal, and plant. Pathogenic factors for healthy adult, animal, and plant do not exist
Class 2	Medium risk for individual and limited risk for group	Risk is medium for human body, environment, animal, and plant, and potential pathogenic factors exist. No severe damage will be caused for healthy adult, environment, animal, and plant. There are effective precaution and treatment measures
Class 3	High risk for individual and low risk for group	Risk is high for human body, environment, animal, and plant. Severe or pathogenic disease will be infected by direct contact or inhalation of aerosol. Potential pathogenic factors with high risk exist for environment, animal, and plant. There are precaution and treatment measures
Class 4	High risk for individual and high risk for group	Risk is high for human body, environment, animal, and plant. It is transmitted by aerosol or unknown approach. Unknown pathogenic factors with high risk exist. There are no precaution and treatment measures

Table 9.38 Classification of biosafety laboratory

Type	Feature
A	The laboratory where the pathogenic biological factors without the transmission of air passage during the operation
b1	The laboratory where the safety isolation equipment (such as biosafety cabinet) can be effectively used during the operation
b2	The laboratory where the safety isolation equipment cannot be effectively used during the operation

the high value. Buffer chamber used for negative pressurized cleanroom and common non-wooden door are used to replace the seal door. Dual air supply outlets, circulated air, and negative pressurized high-efficiency exhaust equipment sealed with dynamic air are used to replace the full fresh air.

Figure 9.26 shows the pressure distribution in negative pressurized isolation ward with planned pressure gradient 5 Pa [80].

Because both the ward and its toilet are polluted area, exhaust air system is set in the toilet, where air must pass from the ward towards the toilet. From the theory of dynamic isolation, there is no requirement of the differential pressure between the ward and the toilet, instead it is only required that directional flow should pass from the ward towards the toilet. Exhausted air is adjusted in the toilet so that its negative pressure is slightly higher than the ward. Louver is set on the door of the toilet.

There is no requirement for the air cleanliness level in negative pressurized isolation ward. It is enough that air filters with medium efficiency or above should be placed in the air supply system. When part of the exhaust air will be used as circulated air and the other part exhausted with any influence on the ambient, HEPA filters must be installed.

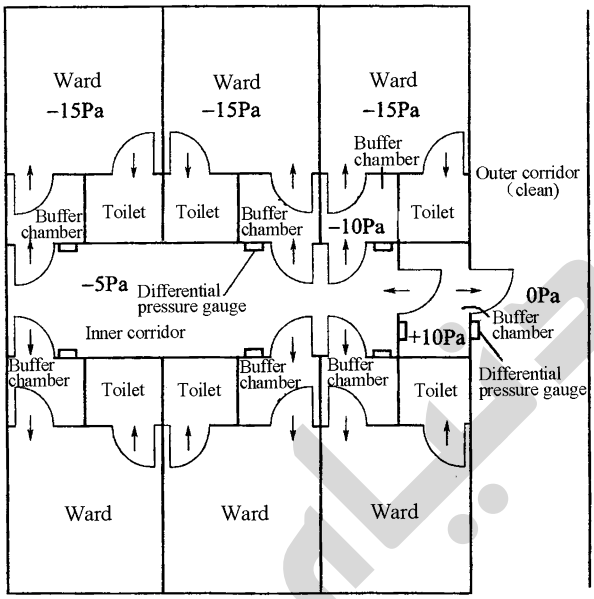

Fig. 9.26 Requirement of differential pressure

9.10.6 Safety of Exhaust Air from Isolated Biological Cleanroom

9.10.6.1 Requirement of Zero Leakage Air Exhaust

Pathogenic microbe with risk may exist in the exhausted air from the isolated biological cleanroom. Not only the blockage effect of HEPA filters (even two filters) is needed, but also leakage is not allowed on the whole exhaust equipment.

Since the air outlet surface of the return air (or return air) is placed inside the wall, it is very difficult to detect and block the leakage. Therefore, it is necessary to invent air exhaust equipment without leakage in theory.

Negative pressurized high-efficiency air exhaust equipment with dynamic air sealing was developed by author and others [81], which belongs to the above kind of equipment. During the installation of HEPA filters in field, in-site detection apparatus (ancillary facility) must be installed at first to detect the leakage. Before installation, it should prove that there is no leakage. The main leakage position is near the frame, where leakage will not occur with dynamic airflow sealing technique.

Figure 9.27 shows the situation when this kind of air exhaust equipment is placed indoors.

In this equipment, the surrounding of HEPA filter is positive pressurized cavity, which is connected with the air supply pipeline with the flexible pipe. It is shown by

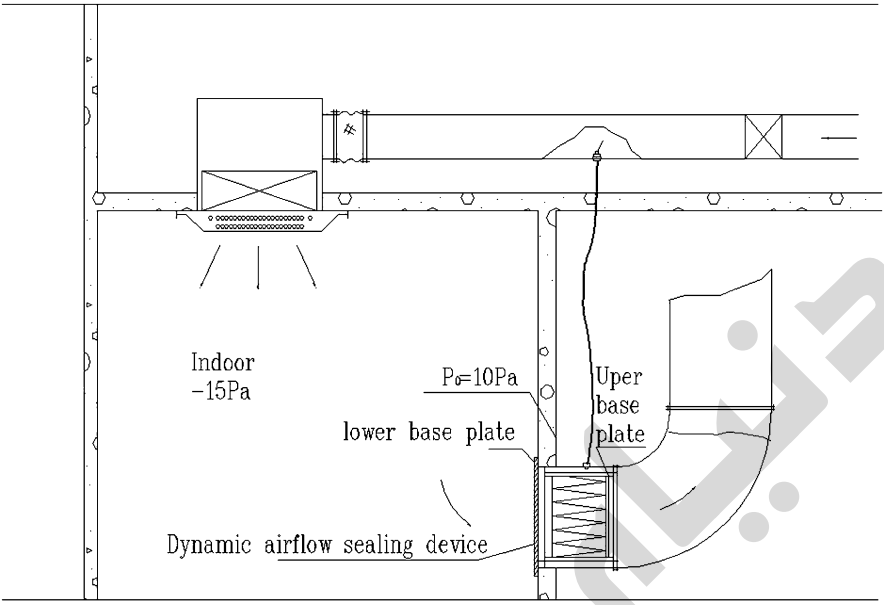

Fig. 9.27 Installation of air exhaust equipment with dynamic airflow sealing device

experiment that when the pressure in the positive pressurized cavity is 1 Pa, indoor aerosols will not be drawn towards the exhaust outlet through the leakage gap. In practice, the positive pressure in this cavity can be required to be 10 Pa, which will be displayed on the meter of the equipment.

This equipment is suitable for the application where in-site leakage detection is needed, such as the negative pressurized isolation ward.

9.10.6.2 Requirement of Air Exhaust with In-Site Leakage Detection

In-site leakage requirement is needed for the biosafety laboratory of Class 3 or even Class 4.

There are usual following features for the in-site leakage detection equipment:

1. Manual leakage detection. During the leakage detection process, the probe should be inserted through the guide hole sealed onto the plastic glove into the box, where the detection support and speed of probe should be controlled.
2. Automatic leakage detection. When the complex movement assembly is placed inside the box, it is easily polluted and difficult to maintain.
3. The scanning trajectory does not overlap.
4. It is line scanning instead of point scanning.
5. The equipment is huge, which can only be installed on the technical interlayer sometimes.

6. Disinfection can be performed at the original place.
7. Differential pressure can be measured across air filter.

There are usual following features for the complete in-site leakage detection equipment:

1. Both automatic and manual leakage detection can be performed.
2. It is not leakage detection at fixed position (to measure the penetration). It is point scanning leakage detection, instead of the line scanning leakage detection.
3. The scanning leakage detection trajectory overlaps.
4. The mechanical component is placed outside of the equipment.
5. The equipment is integrated with the monitoring system of the laboratory, which realized the long distance integrated control.
6. Disinfection can be performed at the original place.
7. Differential pressure can be measured across air filter in the equipment.

The international invention patented by author has the above features.

9.10.6.3 Requirement of the Safety Distance for Exhaust Air System

Although the requirement is high for the zero leakage of exhaust air and the long distance leakage detection, a certain value of safety distance is still required between the exhaust air outlet in some special applications and the public buildings nearby. This is because leakage may occur on air filters occasionally.

At first, in order to perform the safety assessment of safety distance for exhaust air, the limit of the safety value and dangerous value must be known, and the most unfavorable conditions should be used.

How much is the safety concentration of the microbe in the exhaust air? How much is the risky bacterial concentration in the environment? The results are different for different kinds of microorganism, but a reference can also be found.

Taking the Japanese standard (1983) as an example, it is stricter than the American standard. Table 9.39 shows the safety cabinets with Classes I and II applied in BSL-3 and lower-grade biosafety laboratories [82].

It is shown from Table 9.39 that:

1. The safety airborne bacteria concentration near the working area is $5 \times 1{,}000/28.3 \times 10 = 17.7$ CFU/m^3. This can also be considered as the safety concentration in the environment.
2. The simulated accidental bacteria concentration in the cabinet is 10^8–10×10^8/(volume of cabinet 0.5 m^3) = (2–20) $\times$ 10^8/m^3.
3. For the safety test, the sprayed bacteria concentration reaches the magnitude of 10^8. In practice, the aerosol generated will not be so high, where aerosols are generated by spurting instead of spraying. The bacterial concentration can be considered as the maximum value in usual situation, i.e., 10^8–10×10^8/2.5 mL = (0.4–4) $\times$ 10^8#/mL.

Table 9.39 Limit of safety and dangerous concentration

Performance			
Name	Item	Standard	Method
Safety for operational staff	Gap sampling method	Two air samplers with flow rate 28.3 L/min is used near the working area with sampling period 10 min. The colony-forming units (CFU) sampled in each sampler ≤ 5	The volume of sprayed bacterium culture liquid is 2.5 mL which is less than half of the total volume of 5 mL within 5 min in the cabinet. The total sprayed Bacillus subtilis is 1×10^8–10×10^8
Indoor pollution with high concentration	Petri dish method	Petri dishes are full of the working table in the safety cabinet. The total CFU ≤ 5	The total sprayed Bacillus subtilis is 5×10^6–10×10^8 outside of the safety cabinet. The volume of sprayed bacterium culture liquid is 2.5 mL which is less than half of the total volume of 5 mL within 5 min

4. The total amount of microbial aerosol indoors $\geq 5 \times 10^6$ CFU is considered as the upper limit of pollution in the room, which is used to test whether the samples in the cabinet will be affected by pollution.

Secondly, it is quite difficult to know the aerosol generation quantity during various operations. Table 9.40 shows part of the abstract about the fly-off coefficients of microbe during various kinds of experimental operations performed in Fort Detrick, USA [83].

It can be expressed with the following expression: $\beta \times$ average concentration of microorganism (#/mL) = sprayed microbial aerosol number (#).

It is shown from Table 9.40 that the maximum value of β is corresponding to the case when suction pipe is used for mixture (with blowout), which is 1×10^{-4}. When the above bacterial concentration (0.4–4) $\times 10^8$#/mL is used as the maximum value, the maximum quantity of microbial aerosol generated with different volume of bacterial liquid is shown as follow: (0.4–4) $\times 10^4$# for dealing with 1 mL, (0.4–4) $\times 10^5$# for dealing with 10 mL, (2–20) $\times 10^5$# for dealing with 100 mL, and (0.4–4) $\times 10^6$# for dealing with 100 mL. For example, the aerosol generated by the spray of bacterial liquid on the ground, when the bottle is smashed, is different from that by the operation of suction pipe.

Suppose this improper operation occurs near the exhaust air outlet within the room space of 1 m^3, and the flow rate of exhaust air from one safety cabinet placed in the laboratory is usually 1,300 m^3/h. During the improper operation, the air supply system will not stop, so the exhaust airflow rate will neither change. After mixed with the large volume exhaust air along the long exhaust pipeline, the

Table 9.40 Fly-off coefficients of aerosol during some operations

Operation	Fly-off coefficient
Ultrasonic treatment	5×10^{-7}–9×10^{-5}
Liquid dripping	2×10^{-6} (at the height 90 cm)
Mixture with suction pipe	2×10^{-6} (without blowout)–10^{-6} (with blowout)
Spray with the centrifugal effect	2×10^{-6}
For the triturator, the cap is screwed when the machine is in operation and then opened when stopped for 1 min	2×10^{-6}

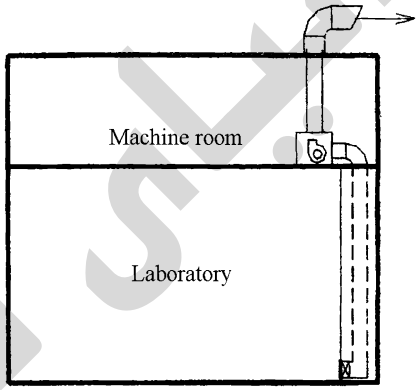

Fig. 9.28 Horizontal exhaust air outlet

leakage at the exit can be considered as uniform. When the number of leakage holes suddenly appeared on air filter is assumed to reach 10 and the diameter is assume 1 mm, the leakage flow rate of 10 leakage holes with diameter $\Phi 1$ under the differential pressure 400 Pa is about 0.36 m^3/h [84]. The concentration at the exhaust outlet with the volume of bacterial liquid 100 mL is

$$\left[(0.4-4)\times 10^6 \#/m^3 \times 0.36\, m^3/h\right]/1{,}300\, m^3/h \approx (0.001-0.01)\times 10^5 \#/m^3$$

If vertical exhaust method can be used for the dilution of the air from exhaust outlet, which is similar as the chimney, the safety distance from the surrounding environment can be shortened. The difference between the exhaust outlet and the chimney is that the cowl-like hat is needed for the exhaust outlet, which will influence the dispersion of airflow and may drive the airflow downwards. Therefore, for safety reason, the following calculation and analysis are performed with the common horizontal side exhaust outlet (Fig. 9.28).

The flow formed by the air jet from the orifice of this kind of exhaust outlet is one submerged jet flow, which is abbreviated as jet flow. Since the outdoor environment of the exhausted air completely follows the condition of infinite space jet flow, the theory of jet flow can be applied. When the most unfavorable

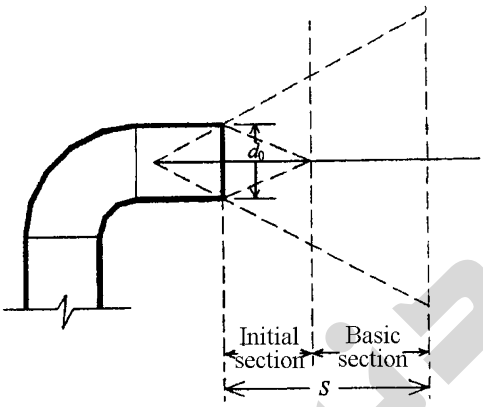

Fig. 9.29 Theory of jet flow

windless condition is assumed with the circular tube jet flow (the equivalent diameter is used for noncircular tube) [85], the axial concentration difference can be expressed with the following equation according to the theory of jet flow as shown in Fig. 9.29 and the concentration difference equation for jet flow:

$$\frac{\Delta X_m}{\Delta X_0} = \frac{0.35}{\left(\frac{\alpha s}{d_0} + 0.147\right)} \tag{9.33}$$

where

ΔX_m is the difference between the axial concentration and the ambient concentration;

ΔX_0 is the difference between the outlet concentration and the ambient concentration.

Since the ambient concentration (test microbe) can be considered 0, $\Delta X_m/\Delta X_0$ can represent the ratio of the concentration at the cross section S and that at the outlet.

From the above calculation, we know the maximum concentration at the outlet should be 0.01×10^5#/m^3 for treating with the 100 mL bacterial liquid. When the safety value for environment is required 17.7#/m^3, we can obtain $\Delta X_m = 17.7$#/m^3 and $\Delta X_0 = 0.01 \times 10^5$#/m^3.

For the bend nozzle with diameter d_0, the turbulent flow coefficient of the air outlet can be $\alpha = 0.2$. Then we get:

$$\frac{0.35}{\frac{0.2s}{d_0} + 0.147} = \frac{17.7}{0.01 \times 10^5}$$

So $S = 98.14\ d_0$. We know $d_0 = 0.0188\sqrt{\frac{Q}{v}}$, where Q is the exhaust flow rate, m^3/h; and v is the exhaust air velocity, m/s. In consideration of the noise generated at the outlet, v should be less than 8 m/s. We can get $d_0 = 0.28$ m.

$$S = 1.84\sqrt{\frac{Q}{v}}$$

When $Q = 1{,}300\ \mathrm{m}^3/\mathrm{h}$ (which is equivalent with the situation of a safety cabinet in a laboratory with area 15 m^2) and $v = 6$ m/s, we get $S = 27.1$ m. When the volume of bacterial liquid treated is 50 mL, $S = 13.6$ m.

The jet flow velocity can be as small as 0.25 m/s [86], and less than this value, the dispersion effect will be very small. So the ratio between the axial velocity v_m and the outlet velocity v_0 should be verified. According to experiment [86], the relative range of the wind S/d_0 can reach 95, which is also one condition for verification. With the above two conditions, we obtain:

$$\frac{v_m}{v_0} = \frac{0.48}{\left(\frac{\alpha s}{d_0} + 0.147\right)}$$

When $S = 27$ m, we obtain $v_m = 0.15$ m/s. When $S = (27.1 + 13.6)/2 = 20$ m, we obtain $v_m = 0.25$ m/s.

When $S = 20$ m, we obtain $S/d_0 = 20/0.28 = 71.4$.

It is shown that the result with $S = 20$ m is within the applicable range.

With the downwind condition, dispersion will be increased and safety probability will also be increased. For the safety reason, the influence of the air with downwind direction is not considered, and the windless condition is used for calculation of jet range.

In Ref. [87], it was mentioned that the above safety distance is the minimum value, which did not consider the psychological factor and safety coefficient.

In the revised version of national standard GB50346 in 2011, it specifies that the minimum distance between the exhaust air outlet from the biosafety laboratory containing biosafety cabinet and the public building is 20 m.

References

1. Inoue U (1974) Air conditioning technology in hospital. Build Equip Water Heat Constr 12(11):35–43 (In Japanese)
2. Fukuyama H (1979) Experience from one year operation of horizontal laminar flow system in cleanroom. J Jpn Air Clean Assoc 17(1):32–36 (In Japanese)
3. Yu XH (2011) Air cleaning: the major measure for removing microbial aerosol particles. J HV&AC 41(2):32–37 (In Chinese)
4. Charnley J, Eftekhar N (1969) Postoperative infection in total prosthetic replacement arthroplasty of the hip-joint with special reference to the bacterial content of the air of the operating room. Br J Surg 56(9):641–649
5. Wei XM (1980) Sterile cleanroom. J HV&AC 2:14–16 (In Chinese)
6. Xu QH, He WS, Ni JF (2002) Comparison of air disinfection methods in operating rooms. Chin J Nosocomiol 12(8):604–605 (In Chinese)

7. Xia MH (2011) Development and effect of the construction of clean operating department in a hospital. Chin J Public Health Eng 2:44–47 (In Chinese)
8. Healthcare Engineering Association of Japan (2004) Guidelines for design and operation of hospital HVAC systems, HEAS-02-2004 (Standards), Tokyo, Japan (In Japanese)
9. Wang WP (1994) Application of biological clean ward in the treatment of blood diseases and management of total environmental protection. People's Liberation Army 307 Hospital (In Chinese)
10. Sato E (1977) The 3rd international symposium on contamination control. J Jpn Air Clean Assoc 14(7):17–22 (In Japanese)
11. Tanaka S (1979) Laminar flow cleanroom for Leukemia patient. J Jpn Air Clean Assoc 17(4):1–4 (In Japanese)
12. Ueda K (1977) Sterile ward in Paul-Brousse Hospital (Paris). J Jpn Air Clean Assoc 14(7):59–62 (In Japanese)
13. Xu ZL, Pan HH, Cao GQ, Shen JM (2013) Revision of the code for clean operating room from the point of view of quality control of modern products: Part 1 of the series of research practice of the revision task group of the architectural code for clean operating room. J HV&AC 43 (3):7–9 (In Chinese)
14. Xu ZL (1980) The state-of-the-art of the biological clean room. J HV&AC 2:44–45 (In Chinese)
15. Xie HM, Sun DR (1975) Injection knowledge. People's Medical Publishing House, Beijing (In Chinese)
16. State Pharmaceutical Administration (1992) Implementation details for management of laboratory animal (draft), Beijing, China (In Chinese)
17. Meckler M (1970) Packaged units provide clean room conditions in moon rock. Heat Pip Air Cond 42(7):71–76
18. Inoue U (1977) Biological cleanroom in hospital. J SHASE Jpn 51(1):1–4 (In Japanese)
19. China Center for Disease Control and Prevention (2003) Q&A for prevention and control of SARS. Peking Union Medical College Press, Beijing (In Chinese)
20. Hirasawa K (1970) Impact of atmospheric pollution on industrial products and medicine and its countermeasures. Jpn Air Cond Heat Refrig News 10(2):33–40 (In Japanese)
21. Shanghai First Medical College (1973) Practical internal medicine. People's Medical Publishing House, Beijing (In Chinese)
22. Intag CE, Wiebe HA, Partain CL (1975) An investigation of the importance of air flow in control post-operative infections. ASHRAE J 2:27–33
23. Li HG (1988) The research on the equivalent diameter of microbial particles in air. J Tianjin Univ 1:57–61 (In Chinese)
24. Tu GB, Zhang SF (1990) Relationship between the filtration efficiency of microbe and particle for fibrous filter media. Contam Control Air Cond Technol 2:20–21 (In Chinese)
25. Yao GL, Fan CY (1981) Determination of the air cleanliness level in sterile room with the bacterial deposition method. Science and Technology Information Station at Tongji University, Shanghai (In Chinese)
26. Xu ZL, Shen JM (1989) Application of air cleaning technology. China Architecture & Building Press, Beijing, p 272 (In Chinese)
27. Yu XH, Che FX (1998) Modern air microbiology and sampling detection and identification techniques. Military Medical Science Press, Beijing, p 82 (In Chinese)
28. Sellers RF, Parker J (1969) Airborne excretion of foot-and-mouth disease virus. J Hyg 67:671–677
29. Parker MT (1978) Hospital-acquired infections: guidelines to laboratory methods. WHO Regional Publications European Series No.4, Copenhagen
30. Zhong XL (2010) Main hazards and countermeasures in management for prevention and control of infection in operating room in China. In: The 19th national conference on nosocomial infection of Chinese and the 6th Shanghai International Forum of Infection Control (SIFIC), Shanghai, China (In Chinese)

31. Feng X, Xu ZL (2013) Necessity of particulate pollutant control in clean operating environment: Part 2 of the series of research practice of the revision task group of the *Architectural technical code for hospital clean operating department*. J HV&AC 43(4):1–5 (In Chinese)
32. YFB001-1995 (1995) Technical standard for construction of cleaning operation room in Military Army Hospital, Ministry of Health of P.R.China, Beijing, China, 7 (In Chinese)
33. Xu ZL (1999) Discussion of the question whether the sedimentation method can be used to determined the bacterial concentration in cleanroom. Chin J Public Health 15(9):777–780 (In Chinese)
34. Zhang LH, Lu WZ, Yang XP et al (1989) Quantitative conversion relationship (correction value) of two sampling methods and comparison with obtained particle size distribution. Chin J Public Health 8(5):315–317 (In Chinese)
35. Shi NS, Zhu PK, Wu ZY (1986) Development of LWC1 type centrifugal air microbial sampler. Institute of HVAC of China Academy of Building Science Research, p 13 (In Chinese)
36. Xu ZL (1993) Relationship between the results with the precipitating bacterial method and the planktonic bacterial method. Chin J Public Health 9(4):150–162 (In Chinese)
37. Research group of air conditioning system in hospital at Tongji University (written by Fan Cunyang) (1982) Principle and application of biological cleaning technology. Science and Technology Information Station at Tongji University (In Chinese)
38. Wang L, Tu GB (1990) Relationship between the measured concentration by Koch method and the airborne bacterial concentration. Contam Control Air Cond Technol 1:27–30 (In Chinese)
39. Huruhashi M (1978) Study on bacterial filtration performance of HEPA filter. J Jpn Air Clean Assoc 15(7):1–10 (In Japanese)
40. Huruhashi M (1980) Usage problem of biological cleanroom. J Jpn Air Clean Assoc 17 (7):19–25 (In Japanese)
41. Gaulin RP (1966) Design of hospital ventilation systems in respect to surgery. AACC Proceedings
42. Li HY (1984) Study of middle efficiency air cleaning system in biological clean operating room. Master dissertation at Tianjin University (In Chinese)
43. Xu ZL, Shen JM (1987) YGG and YGF type low resistance sub-high efficiency air filter. Research report of Building Science. China Academy of Building Science Research, pp 5–2 (In Chinese)
44. Yan H (2009) Cleaning technology by UVGI and the combination of air filter and UVGI. Mech Elect Inform 29:8 (In Chinese)
45. Xu ZL (2007) Solution for the pollution control in the duct of centralized air cleaning system (I). Clean Technol 18 (In Chinese)
46. Yamayoshi T et al (1978) Study on bacteria in sterile environment. J Jpn Air Clean Assoc 16 (6):1–6 (In Japanese)
47. Xu LD, Wang JQ, Lin B, Wang JQ, Wang YB (1993) Design of shielded circulating air UV disinfection device and its performance. Chin J Public Health Eng 3:8–9 (In Chinese)
48. Huruhashi M (1990) Current study status of ultraviolet sterilization irradiation. Jpn J Medical Equip 6(7):315–326 (In Japanese)
49. Adachi S et al (1989) Microbicidal effects of ultraviolet radiation on environmental microorganisms. Jpn J Antibiot 17(1):15–21 (In Japanese)
50. Yu XH (2010) Characteristics of ultraviolet germicidal irradiation and application analysis. J HV&AC 40(7):58–62 (In Chinese)
51. First MW, Nardell EA, Chaisson W, Riley R (1999) Guidelines for the application of upper-room ultraviolet germicidal irradiation for preventing transmission of airborne contagion. Part II: design and operation guidance. ASHRAE Trans 105:77–88
52. ASHRAE (2008) Chapter 16: Ultraviolet lamp systems. In: ASHRAE handbook: HVAC systems and equipment. ASHRAE, Atlanta
53. Centers for Disease Control and Prevention and Healthcare Infection Control Practices Advisory Committee (2003) Guidelines for environmental infection control in healthcare

facilities: recommendations of CDC and the Healthcare Infection Control Practices Advisory Committee (HICPAC). Morb Mortal Recomm Rep 52(RR-10):1–42
54. Memarzadeh F, Olmsted RN, Bartley JM (2010) Applications of ultraviolet germicidal irradiation disinfection in healthcare facilities: effective adjunct, but not stand-alone technology. Am J Infect Control 38(suppl 1):S13–24
55. Sun RG, Wang MY, Gao H (2009) The effect of ultraviolet irradiation on the two different types of bacteria. Chin J Disinfect 26:2 (In Chinese)
56. Chen CY, Xu ZL, Lin B, Xu LD (1993) Comprehensive report on the development of shielded circulating air UV disinfection device (material from appraisal meeting) (In Chinese)
57. Xu ZL, Chen CY, Shen JM (1998) Calculating method for the necessary lamps and sterile rate in a tube shaped ultraviolet air washer. J Hyg Res 3:213–216 (In Chinese)
58. Shen JM, He SP, Sun GQ (1993) Structural design of circulating air UV disinfection device. J Shanghai Urban Constr Coll 4:50–55 (In Chinese)
59. Xu ZL, Chen CY (1993) Development of shielded circulating air UV disinfection device (material from appraisal meeting) (In Chinese)
60. Preparation Group for Air Cleaning Technology Measures (1979) Air cleaning technology measures. China Architecture & Building Press, Beijing (In Chinese)
61. GB50333–2002 (2002) Architectural technical code for hospital clean operating department. China Planning Press, Beijing (In Chinese)
62. Field AA (1973) Operating theater air conditioning. Heat Pip Air Cond 45(11):91–93
63. Ling JH (2005) Study on air cleaning effect in operating room. Tianjin University, Tianjin (In Chinese)
64. Inoue U (1971) New air conditioning method in operating room. Heat Pip Air Cond 9(7):41–52 (In Japanese)
65. Deng WP (2005) Comprehensive measures to prevent spread and infection of SARS virus in the hospital building and countermeasures. Tongji University, Shanghai (In Chinese)
66. Xu ZL (2006) Design principle of isolation ward. Science Press, Beijing, p 127 (In Chinese)
67. Xu ZL, Shi NS, Lu Y (1981) Characteristic study of air flow in cleanroom with air supply fully on the ceiling and air return at two bottom sides. Research Report of Building Science. China Academy of Building Science Research, p 11 (In Chinese)
68. Akiyama Y et al (1977) Experience from laminar flow sterile operating room. J SHASE Jpn 51 (1):33–43 (In Japanese)
69. Sano T (1876) Influence of obstacle and thermal plume in laminar flow room. J Jpn Air Clean Assoc 17(1):37–42 (In Japanese)
70. WHO (1985) Laboratory biosafety manual, 1983 (trans: Ma Yuanshan and Li Shengtian). People's Medical Publishing House, Beijing (In Chinese)
71. Tanaka M et al (1979) Biological risk facilities by NIH. J Jpn Air Clean Assoc 16(7):46–55 (In Japanese)
72. Yamauchi K (1980) Basic viewpoints of biological hazards measures and isolation facilities. J Jpn Air Clean Assoc 17(7):1–11 (In Japanese)
73. Editorial Department of Science (1980) History of 10 years of genetic engineering. Scientist Press Co., Ltd., Japan (In Japanese)
74. ASHRAE (1978) Chapter 15. In: ASHRAE Handbook-HVAC applications, Atlanta, U.S.A.
75. Xu ZL, Wang QQ (2004) Biosafety laboratory and biological safety cabinets. China Architecture & Building Press, Beijing (In Chinese)
76. Xu ZL, Zhang YZ et al (2006) Study on isolation effects of isolation wards (1). J HV&AC 1:1 (In Chinese)
77. Xu ZL, Zhang YZ et al (2006) Study on isolation effects of isolation wards (3). J HV&AC 4:1 (In Chinese)
78. Xu ZL, Zhang YZ et al (2006) Study on isolation effects of isolation wards (1). J HV&AC 1:1 (In Chinese)
79. Xu ZL, Zhang YZ et al (2006) Study on isolation effects of isolation wards (2). J HV&AC 3:1 (In Chinese)

80. Xu ZL, Wu YH (2010) Requirements of the basic configuration for isolation ward building. China Architecture & Building Press, Beijing (In Chinese)
81. Xu ZL, Zhang YZ et al (2005) Study on the dynamic airflow sealing negative pressure exhaust device (Invention patent). Build Sci 57 (In Chinese)
82. Japan Air Cleaning Association (1981) Standard for Class II biological safety cabinets. JIS (Japanese Industrial Standard), Tokyo, Japan (In Japanese)
83. Ootani M (1981) Countermeasure manual for biohazard. Kindai Press, Japan (In Japanese)
84. Xu ZL (2004) Bio-safety laboratory, Bio-safety seminars by Chinese Contamination Control Society, p 236 (In Chinese)
85. Zhou MR (1979) Hydromechanics – pump and fan. China Architecture & Building Press, Beijing, p 240 (In Chinese)
86. No. 10 Design & Research Institute from Ministry of Machinery and Electronics Industry of China (1995) Design manual of air conditioner, 2nd edn. China Architecture & Building Press, Beijing, p 249 (In Chinese)
87. Xu ZL, Wang QQ et al (2004) The safe distance of a biosafety lab considered form the angle of exhaust air diffusion. Build Sci 4:46 (In Chinese)

Chapter 10
Calculation Theory of Uniform Distribution in Cleanroom

Calculation of the dust concentration is the core of the design calculation for cleanroom. The theoretical calculation in this chapter is based on the assumption that particles are uniformly distributed in cleanroom.

10.1 Three-Stage Filtration System in Cleanroom

Three-stage filtration system is usually installed for cleanroom, which includes coarse, fine, and HEPA filters (or called primary, intermediate, and final stages). In the system, fine filter is installed in the positively pressurized section downwards of the fan. HEPA filter is installed at the air supply terminal. Fine or coarse filter is installed at return air terminal. It is called high-efficiency air cleaning system when the final stage filter is a HEPA filter, and it is called medium-efficiency air cleaning system when the final stage filter is a fine filter. Figure 10.1 shows the schematic diagram of turbulent flow cleanroom system.

The meanings of each symbol are as follows:

N_t is the indoor particle concentration at time t (min) (#/L);
N is the indoor steady-state particle concentration (#/L);
N_0 is the indoor original particle concentration, which is the particle concentration at time $t = 0$ (#/L);
V is the cleanroom volume (m^3);
n is the air change rate (h^{-1});
G is the particle generation rate per unit volume [#/(m^3·min)];
M is the atmospheric particle concentration (#/L);
S is the ratio of return air rate to the supply air rate;
η_1 is the efficiency of primary filter (or combined with fresh air filter), (particle number concentration, expressed with decimal, this applies for the following symbols);
η_2 is the efficiency of intermediate filter;
η_3 is the efficiency of final filter.

Z. Xu, *Fundamentals of Air Cleaning Technology and Its Application in Cleanrooms*,
DOI 10.1007/978-3-642-39374-7_10,

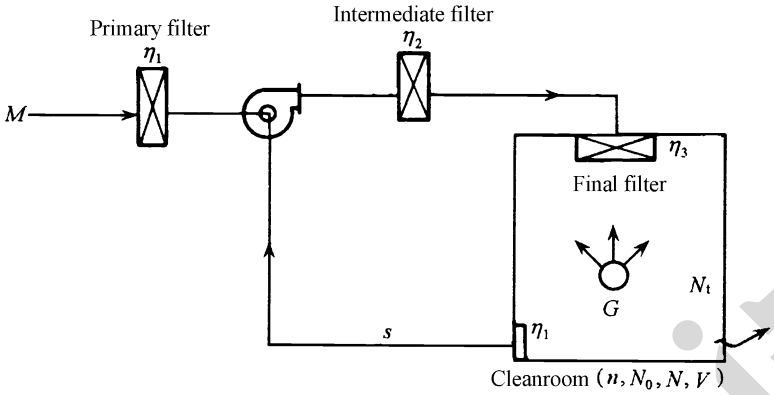

Fig. 10.1 Schematic diagram of turbulent flow cleanroom system

In practice, coarse filter is usually placed for filtration of fresh air in the three-stage filtration system. It has been proved that it is the time to update the concept. In 1994 author formally put forward this view [1], and argument was performed on the general air-conditioning system, special air-conditioning system, and air cleaning conditioning systems, respectively [2, 3].

This problem was put forward with the reason that when air-conditioning system is started, both the indoor bacteria concentration and the foul smell increase, which is also reported in foreign country recently [4]. The condensation water left on heat exchange coil, fin, valve, and its surrounding area will provide the high humidity condition near the coil, because water will evaporate slowly with the increase of temperature during the stop of the system. This is suitable for the breeding microorganism, especially for fungi reproduction. During the startup of the system, a lot of gas will be released suddenly, which is generated by the breeding and becomes the source of foul smell. It is believed that microorganisms are brought in with large amount of dust in fresh air and they settle in these places, and nutritious condition indispensable for microbial growth is provided. The main reason for the generation of foul smell is the reproduction of fungi (for general air-conditioning system, the role of return air is larger).

The efficiency of coarse filter for filtration of fresh air is too low. The atmospheric dust concentration in China is too high (see Chap. 2). So the problem mentioned above will be more serious. The consequences are that not only the fresh air quality declines, but also the high atmospheric dust concentration entering into the system will clog the system components soon, which will greatly reduce the fresh air rate and the indoor oxygen proportion, and result in a vicious circle.

So the new concept of three-stage filtration system should include: three-stage filters for fresh air (coarse, fine and HEPA filters), intermediate preliminary filter (preliminary filter for terminal filter), and terminal HEPA (or sub-high efficiency) filter.

10.2 Instantaneous Particle Concentration in Turbulent Flow Cleanroom

In order to calculate the indoor particle concentration of turbulence cleanroom and the air change rate, we must determine the particle distribution in the cleanroom. Generally there are two types including the uniform distribution and the uneven distribution. In this chapter the calculation theory and method under uniform distribution condition will be discussed (the main content from this chapter to Chap. 13 has been published in the report "Calculation of cleanroom" by HVAC instituted in 1977). In the next chapter, the calculation theory and method for the uneven distribution will be discussed.

For uniform distribution, it is assumed that indoor particles are evenly distributed. If there is any particle source, particles generated will reach the equilibrium state quickly in the room with the diffusional effect of particles and driven force and dilution of air flow.

In order to simplify the calculation, we also need further assumptions: Ventilator flow rate is stable; Particles generated are constant; Atmospheric dust concentration is constant; The influence of particle density both indoors and outdoors and its dispersity variation on the influence of filter efficiency is ignored; Particles by infiltration and the possibility of particle generation by pipeline are ignored; Settlement of particles both inside the pipe and in the room is ignored.

In addition, the total efficiency of filter on the fresh air passage is η_n. The total efficiency of filter on the return air passage is η_r. With Fig. 10.1, we obtain that:

$$\eta_n = 1 - (1 - \eta_1)(1 - \eta_2)(1 - \eta_3)$$

or

$$(1 - \eta_n) = (1 - \eta_1)(1 - \eta_2)(1 - \eta_3) \tag{10.1}$$

$$\eta_r = 1 - (1 - \eta_1)(1 - \eta_2)(1 - \eta_3)$$

or

$$(1 - \eta_r) = (1 - \eta_1)(1 - \eta_2)(1 - \eta_3) \tag{10.2}$$

For the combination of fresh air filters, we know

$$\eta_1 = 1 - (1 - \eta_{10})(1 - \eta_{20})(1 - \eta_{30}) \tag{10.3}$$

η_{10}, η_{20}, and η_{30} are the efficiency of combined coarse, fine, and HEPA filters, respectively.

According to the front schematic diagram and the above hypothesis, it is visible that:

1. Indoor dust particle consists of three parts.
   (a) Particles brought in by return air. The flow rate of return air per unit time is $\frac{snV\times10^3}{60}$ (L/min). With the air filters (air filter at the return air grille, intermediate filter and final filter) on the return air passage, particles number entering indoors per unit time is $\frac{snV\times10^3}{60}N_t(1-\eta_r)$ (#/min). Therefore, during Δt time period, increase of particle number per liter air indoors by return air is $\frac{snN_t}{60}(1-\eta_r)\Delta t$ (#/min).
   (b) Particles brought in by fresh air. The flow rate of fresh air is $\frac{nV\times10^3}{60}(1-s)$ (L/min). After passing through air filters on the fresh air passage, including primary, intermediate, and final stage filters, particle number per unit time entering indoors is $\frac{MnV\times10^3}{60}(1-s)(1-\eta_n)$ (#/min). Therefore, during Δt time period, increase of particle number per liter air indoors by fresh air is $\frac{Mn(1-s)(1-\eta_n)}{60}\Delta t$ (#/min).
   (c) During Δt time period, increase of particle number per liter air by particle generation source indoors is $G\times10^{-3}\Delta t$ (#/min).
2. Particles exhausted from indoors include particles exhausted by organized return air (sometimes exhaust air is included) and particles by disorderly exhaust (discharge) air.

The ventilation rate per unit time is $\frac{nV\times10^3}{60}$ (L/min), So during Δt time period, particle number per liter air exhausted by ventilation system is $\frac{nN_t}{60}\Delta t$ (#/min).

According to above analysis about the particle number in and out of cleanroom, it is known that the variation of particle concentration in the cleanroom during time period Δt is

$$\begin{aligned}\Delta N_r &= (\text{Particle concentration into the room}) - (\text{Particle concentration discharged from room})\\ &= \left[\frac{N_t ns(1-\eta_r)\Delta t}{60}+\frac{Mn(1-s)(1-\eta_n)\Delta t}{60}+G\times10^{-3}\Delta t\right]-\frac{N_t n}{60}\Delta t\end{aligned}$$

When some items are moved and $\frac{\mathrm{d}N_t}{\mathrm{d}t}$ is used to replace $\frac{\Delta N_t}{\Delta t}$, we know that

$$\begin{aligned}\frac{\mathrm{d}N_t}{\mathrm{d}t} &= \frac{60G\times10^{-3}+Mn(1-s)(1-\eta_n)}{60}\\ &\quad\times\left\{1-\frac{N_t n[1-s(1-\eta_\tau)]}{60G\times10^{-3}+Mn(1-s)(1-\eta_n)}\right\}\end{aligned}$$

After integration is performed on the above expression when variables are separated, we obtain:

$$-\frac{60G\times10^{-3}+Mn(1-s)(1-\eta_n)}{n[1-s(1-\eta_\tau)]}\ln\left\{1-\frac{N_t n[1-s(1-\eta_\tau)]}{60G\times10^{-3}+Mn(1-s)(1-\eta_n)}\right\}$$
$$=\frac{60G\times10^{-3}+Mn(1-s)(1-\eta_n)}{60}t+C$$

where C is an integral constant, which is determined with the initial condition. When $t=0$, there are three kinds of situations:

(a) Calculation starts since the startup of the system; indoor particle concentration at time $t=0$ is the instantaneous particle concentration before the operation of cleanroom. This particle concentration is relatively large due to factors such as leakage.
(b) After a certain period of operation for the system, calculation starts at any time when particle concentration reaches stable. So the indoor particle concentration at the moment $t=0$ means the steady-state particle concentration. For cleanroom with different cleanliness levels, the values of the concentration are also different.
(c) When calculation starts from any moment during the operation of the system, the indoor particle concentration at the moment $t=0$ means the indoor particle concentration when the system operates until this moment.

In a word, we can call the particle concentration at the moment $t=0$ as the original particle concentration, which is expressed with N_0:

$$t=0 \quad N=N_0$$

The value of C can be calculated by substituting it into the above formula. The original formula can be rewritten as:

$$\frac{1-\dfrac{N_t n[1-s(1-\eta_r)]}{60\times G\times10^{-3}+Mn(1-s)(1-\eta_n)}}{1-\dfrac{N_0 n[1-s(1-\eta_r)]}{60\times G\times10^{-3}+Mn(1-s)(1-\eta_n)}}=\mathrm{e}^{-\frac{nt[1-s(1-\eta_r)]}{60}} \tag{10.4}$$

So the instantaneous particle concentration in the cleanroom is:

$$N_t=\frac{60G\times10^{-3}+Mn(1-s)(1-\eta_n)}{n[1-s(1-\eta_r)]}$$
$$\times\left\{1-\left[1-\frac{N_0 n[1-s(1-\eta_r)]}{60\times G\times10^{-3}+Mn(1-s)(1-\eta_n)}\right]\mathrm{e}^{-\frac{nt[1-s(1-\eta_r)]}{60}}\right\} \tag{10.5}$$

10.3 Steady-State Particle Concentration in Turbulent Flow Cleanroom

10.3.1 Steady-State Expression for Single Room

In a stable ventilation condition, although particle source exists in cleanroom, which constantly releases particles, after a certain period of time, it will tend to be stable theoretically when $t \to \infty$. At this time, Eq. (10.5) can be rewritten as

$$N = \frac{60G \times 10^{-3} + Mn(1-s)(1-\eta_n)}{n[1-s(1-\eta_r)]} \tag{10.6}$$

When Eq. (10.6) is applied, the stable expression for one ventilation system can be easily obtained when it is clear which is the combination efficiency of filters η_n and which is η_r. Taking Fig.10.2a as an example, we can write:

$$N = \frac{60G \times 10^{-3} + Mn(1-s)(1-\eta_1)(1-\eta_2)(1-\eta_3)}{n[1-s(1-\eta_2)(1-\eta_3)]}$$

It is the same for the rest categories.

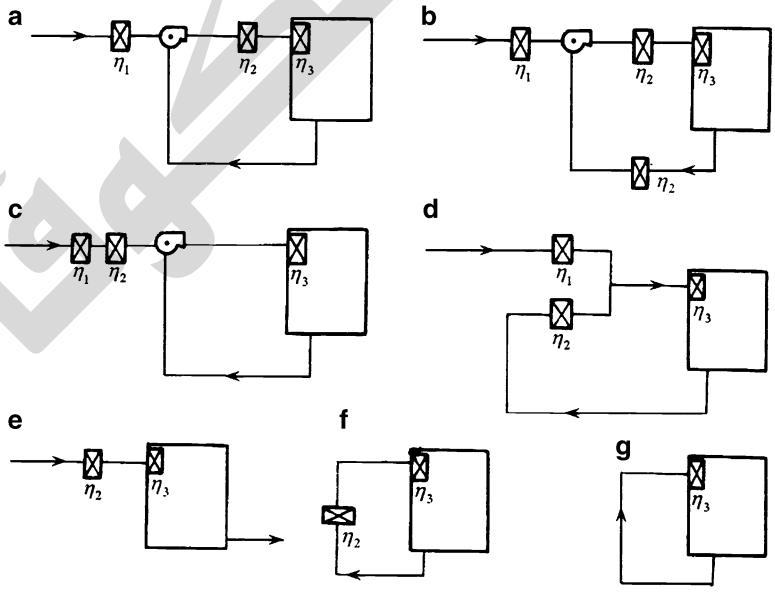

Fig. 10.2 Systems with different arrangement of filters

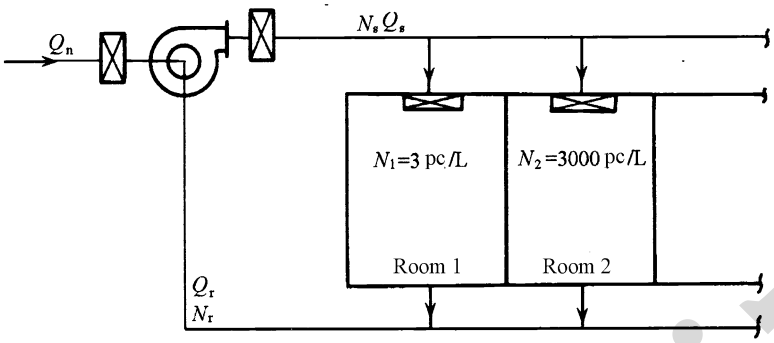

Fig. 10.3 Multiroom system in parallel

10.3.2 Steady-State Expression for Multiroom

The actual air cleaning systems are parallel between multirooms. The steady-state expression for multiroom is different from that of single room. Although foreign literatures [5] have given the steady-state expression, the calculation method for actual multiroom system was not explained. The relationship between two kinds of steady-state expressions was also not given. The parallel case with multirooms shown in Fig. 10.3 will be analyzed. With this parallel condition, calculation becomes very complicated for the particle concentration of each cleanroom.

First, the following expressions can be obtained with the method for single-room steady-state particle concentration:

$$N_1 = \frac{60G_1 \times 10^{-3} + N_s n_1 (1 - \eta_3)}{n_1} \tag{10.7}$$

$$N_2 = \frac{60G_2 \times 10^{-3} + N_s n_2 (1 - \eta_3)}{n_2} \tag{10.8}$$

where N_s means the particle concentration of the mixture air after passing through the intermediate filter (#/L):

$$N_s = \frac{MQ_n(1 - \eta_1)(1 - \eta_2) + Q_r N_r (1 - \eta_2)}{Q_s} \tag{10.9}$$

Where

Q_n is the flow rate of fresh air (L/h);
Q_r is the flow rate of the overall return air (L/h);
Q_s is the flow rate of the overall supply air (L/h);
N_r is the particle concentration of the overall return air (#/L):

$$N_r = \frac{s_1 N_1 n_1 V_1 + s_2 N_2 n_2 V_2 + \cdots}{Q_r} \tag{10.10}$$

where V_1 and V_2 are the volumes of every room. It is obvious this calculation method is complicated.

The cleanroom shown in Fig. 10.3 will be analyzed. One cleanroom with particle concentration $N_1 = 3$ #/L is connected in parallel with another cleanroom where the particle concentration is $N_2 = 3{,}000$ #/L. The particle concentration of the return air from multiroom system must be higher than 3 #/L. If the steady-state expression for single room was used to obtain the particle concentration of Room 1, it is lower for Room 1, which is unsafe. If the unsafe coefficient is too large, the steady-state expression for multiroom must be used to calculate the particle concentration of Room 1. Now how big the difference is will be analyzed.

The particle concentration of the overall return air for the multiroom system is no more than that of the dirtiest cleanroom. In Fig. 10.3, it is less than N_2, namely, 3,000 #/L. Provided that the particle concentration of the overall return air is 3,000 #/L, it is 1,000 times higher than 3 #/L. So for Room 1 in the multiroom, it is operated under the extreme condition that the particle concentration of the return air for single room is 1,000 times higher.

Under this circumstance, the balance equation of the steady-state particle concentration is:

$$\frac{10^3 N_1 nS(1-\eta_r)}{60} + \frac{Mn(1-s)(1-\eta_n)}{60} + G \times 10^3 = \frac{N_1 n}{60}$$

So

$$N_1 = \frac{60G \times 10^{-3} + Mn(1-\eta_n)}{n[1 - 10^3 \times s(1-\eta_r)]} \tag{10.11}$$

where N_1 means the particle concentration of Room 1 in multiroom system (#/L).

Because HEPA filter is installed in return air passage, its efficiency for particles with diameter $\geq$0.5 μm reaches 0.99999 (see Chap. 4), then we know:

$$(1-\eta_r) = 0.00001$$

$$\left[1 - 10^3 \times s \times (1-\eta_r)\right] \approx [1 - s \times (1-\eta_r)] \approx 1$$

So

$$N_1 \approx N$$

where N means the particle concentration of Room 1 in single-room system.

It has shown that for those air cleaning systems with HEPA filter as the final stage filter, the steady-state expression for single-room system can be utilized to calculate the steady-state particle concentration of each room in multiroom system, no matter what system is (multiroom system or single-room system), which makes the calculation more simple.

In the above assumption, $N_1 = 3$ #/L and $N_2 = 3{,}000$ #/L, which can be regarded as the connection of cleanrooms with difference of three classes in parallel. If the difference is less than three classes, there is no problem. If the highest class cleanroom of the high-efficiency air cleaning system and the cleanroom of the medium-efficiency air cleaning system are in parallel, the difference of the concentration indoors is about 10,000 times; then we get:

$$1 - 10^4 \times s \times (1 - \eta_r) = 0.9\text{-}1$$

The less the fresh air is, the bigger the error is. But it wouldn't be more than 10 %. Apparently, if two medium-efficiency cleanrooms are connected in parallel, where filters and recirculation ratio s are the same, the difference of indoor particle concentration would not be more than one time with different values of G. In this case, the error would be about 10 % when the single-room system is used to calculate the situation in multiroom system. But if the difference of filter efficiencies between two cleanrooms is too big, and so is the values of s, the error would be much bigger.

10.4 Steady-State Particle Concentration with Local Air Cleaning Equipment

In the turbulent cleanroom, it is common that local cleaning equipment is installed at the same time. Clean bench and self-purifier are used most frequently. For local cleaning equipment working intermittently, although its operation is beneficial for improving the indoor air cleanliness, we do not calculate it separately. Only for local cleaning equipment which operates stably and regularly, the indoor steady-state particle concentration can be calculated for the system including the local cleaning equipment when it is necessary.

Now it is unnecessary to derive as the process for the instantaneous expression above. From the schematic diagram as shown in Fig. 10.4, just like Eq. (10.11), the following equation for the steady-state particle concentration can be obtained directly:

$$\frac{Nn}{60}[s(1-\eta_r) + s'(1-\eta')] + \frac{Mn(1-s)(1-\eta_n)}{60} + G \times 10^{-3} = \frac{Nn}{60}(1+s')$$

So

$$Nn[(1+s') - s(1-\eta_r) - s'(1-\eta')] = 60G \times 10^{-3} + Mn(1-s)(1-\eta_n)$$

where s' means the ratio of the circulation flow rate through the local cleaning equipment, which is the self-circulation flow rate, to the total flow rate for the whole system;

η' means the total efficiency of each filter in the local cleaning equipment;

Other symbols have the same meanings as Fig. 10.1.

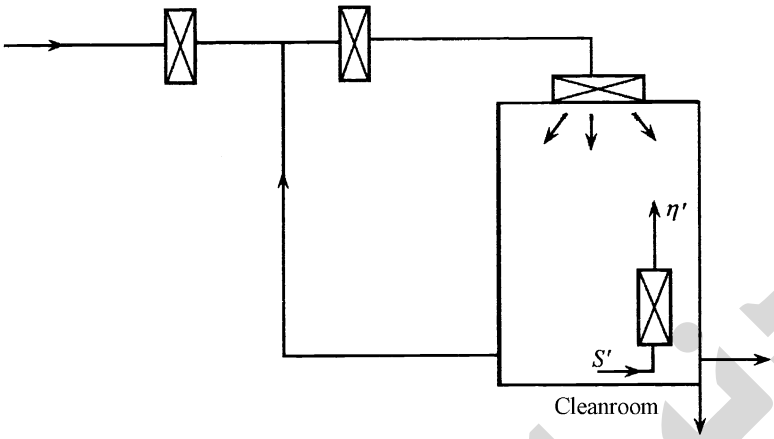

Fig. 10.4 Schematic diagram with local cleaning equipment

Therefore, the indoor particle concentration can be obtained:

$$N = \frac{60G \times 10^{-3} + Mn(1-s)(1-\eta_n)}{n[(1+\eta' s') - s(1-\eta_r)]} \tag{10.12}$$

Because HEPA filter must be installed in the local cleaning equipment which is used in cleanroom, $\eta' \approx 1$, Eq. (10.12) can also be rewritten as:

$$N = \frac{60G \times 10^{-3} + Mn(1-s)(1-\eta_n)}{n[(1+s') - s(1-\eta_r)]} \tag{10.13}$$

The difference between this equation and Eq. (10.6) is the denominator, where it changes from "1" to "$1 + s'$." This means that with the local cleaning equipment, the air change rate increases compared with original room.

Since $s(1 - \eta_r)$ is much smaller than 1, Eq. (10.13) can be simplified as:

$$N = \frac{60G \times 10^{-3} + Mn(1-s)(1-\eta_n)}{n(1+s')} \tag{10.14}$$

Therefore, the influence of local cleaning equipment on the particle concentration can be clearly seen.

10.5 Physical Meaning of Instantaneous and Steady-State Expressions

From Eqs. (10.5) and (10.6), the instantaneous and steady-state equations of the particle concentration in turbulent flow cleanroom, it is clear that the latter is included in the brace of the former. When the steady-state expression is inserted into Eq. (10.5), we can obtain:

$$N_t = N + (N_0 - N)\mathrm{e}^{-\frac{nt[1-s(1-\eta_r)]}{60}} \tag{10.15}$$

If $N_0 > N$, we get

$$N_t = N + \Delta N\mathrm{e}^{-\frac{nt[1-s(1-\eta_r)]}{60}} \tag{10.16}$$

If $N_0 < N$, we get

$$N_t = N - \Delta N\mathrm{e}^{-\frac{nt[1-s(1-\eta_r)]}{60}} \tag{10.17}$$

If $N_0 = 0$, we get

$$N_t = N\left\{1 - \mathrm{e}^{-\frac{nt[1-s(1-\eta_r)]}{60}}\right\} \tag{10.18}$$

Since the case when $N_0 = 0$ can also be included in the situation when $N_0 < N$, the above expression can be simplified as:

$$N_t = N \pm |\Delta N|\mathrm{e}^{-\frac{nt[1-s(1-\eta_r)]}{60}} \tag{10.19}$$

where ΔN means the difference between the original and the steady-state particle concentrations. "+" represents the positive number and "−" the negative number.

From Eq. (10.19), the physical meaning of instantaneous expression is very obvious. For $+\Delta N$, it means that the original particle concentration N_0 is higher than the steady-state concentration N, which is the decrease process of particle concentration, namely, the cleaning process. It is the decline curve a in Fig. 10.5. Obviously, the particle concentration N_t at any time is higher than N, and the differential between N and N_t is a fixed value correlated with ΔN.

For $-\Delta N$, it means the original particle concentration N_0 is lower than the steady-state concentration N. It is an increasing process of the particle concentration, namely, the polluting process. That is the ascending curve b in Fig.10.5. Obviously, the particle concentration N_t at any time is lower than N, and the differential is also a certain fixed times of ΔN.

If $N_0 = 0$, the particle concentration varies as the ascending curve c in Fig.10.5. The difference between curve c and curve b is that curve c goes through the zero position of axis.

It also could be deduced from the instantaneous and the steady-state expressions that the instantaneous concentration is relevant to the original concentration N_0, while the steady-state concentration has nothing to do with N_0, which is only relevant to the characteristic of air cleaning system. It only depends on the balance of the amount of particles in and out of the cleanroom under the steady-state situation. This is an important characteristic of the steady-state particle concentration.

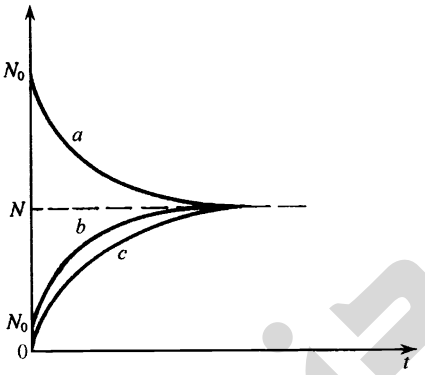

Fig. 10.5 Physical meaning of instantaneous expression

10.6 Other Calculation Methods for Turbulent Flow Cleanroom

Except for the instantaneous and steady-state expressions of particle concentration based on the above three-stage filtration system proposed by author in 1976, both American Air Force Technology Regulation T.O. 00-25-203 (at that time it was mentioned as Austin from the USA; in fact it was Austin who cited this regulation [6]) and Kayatawa [7] from Japan deduced following equations from simplified schematic diagram (Figs. 10.6 and 10.7).

Instantaneous expression in Regulation 203:

$$N_t = \frac{60G}{\eta n V}\left(1 - \mathrm{e}^{\frac{-\eta n t}{60}}\right) \tag{10.20}$$

Steady-state expression in Regulation 203:

$$N = \frac{60G}{\eta n V} \tag{10.21}$$

The unit of G in the above two expressions is #/min. It is different from the particle generation rate per unit volume, where V is the room volume. Obviously, Eq. (10.20) is the special case of the previous derivation expression when $N_0 = 0$ and $s = 1$. However, $N_0 = 0$ is impossible in real world, and for most cases $s \neq 1$. So the limitation of this expression is big.

Instantaneous expression by Kayatawa:

$$N_t = N + (N_0 - N)\mathrm{e}^{-\frac{nt[1 - s(1-\eta)]}{60}} \tag{10.22}$$

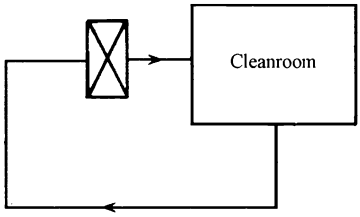

Fig. 10.6 Schematic diagram cited by Austin

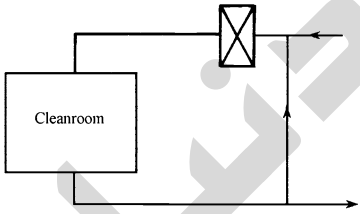

Fig. 10.7 Schematic diagram from Kayatawa

For the convenience of comparison, unified symbols are used in this chapter. The steady-state expression similar as Eq. (10.6) can also be deduced. But because the filtration efficiency η is the so-called main filtration efficiency according to the single-stage filter, it cannot be used in other circumstances. In other literatures, different steady-state expressions will be deduced from different specific systems, which is also inconvenient for use.

Additionally, in the instantaneous expression of the indoor particle sedimentation proposed by Morrison from the USA, consider the sedimentation rate is uncertain, which makes the expression too complex to be applied. Also some people assume that various kinds of particles were captured when passing through HEPA filter, and then the simplified diagram was made [13]. The error caused is bigger, so it is disadvantageous for the investigation of the characteristic. And also some people proposed to use the method that the particle concentration at air supply outlet was calculated first and then the ventilation rate is calculated [14]. All of them are not systematic calculation and derivation, which will not been introduced in detail here.

Except for the accuracy of expression itself, the agreement between theoretic calculation and practical result also depends on the accurate determination of various parameters. A more practical calculation can be acquired when using the equation in this chapter and the parameter suggested in Chap. 13. The result will be presented in Chap. 13.

10.7 Calculation of Dust Concentration in Unidirectional Flow Cleanroom

Since the air cleanliness of unidirectional flow cleanroom can be higher than Class 100, it will mislead people that there is no need of calculation. But the equation of turbulent flow cleanroom mentioned above cannot be used in unidirectional flow

cleanroom. But as the appearance of the unidirectional flow cleanroom with air cleanliness higher than Class 100, and with the need of energy conservation, it is hoped that air cleanliness can still reach Class 100 by decreasing the number of filters originally placed full on the ceiling. Therefore, the calculation of the particle concentration is still necessary for unidirectional flow cleanroom. Author presented oversimplified calculation method based on uniform distribution model in 1976. Fukuda [8] also proposed the similar calculation theory and method based on the assumption that the dust released by people will not disperse in the crosswise direction. This is the first time that foreign countries presented the calculation method of unidirectional flow cleanroom. Fukudan equation ignores the particle generated by filter surface, but takes the particle brought in by return air into account (N_r). It can be written as:

$$N = N_s + N_r$$

where N_s is the particle concentration at the air supply outlet.

Actually, N_r is much smaller than N_s, and the amount of the dust generation on the surface is also much smaller, which can be ignored. If this is the case, N is just equal to N_s, which is much different from the practical situation.

In order to better calculate the particle concentration of unidirectional flow cleanroom, only the calculation theory of uneven distribution can be used, which will be introduced in detail in the next chapter.

10.8 Calculation of Self-Purification Time and Pollution Time in Turbulent Flow Cleanroom

10.8.1 Concept

After the startup of air cleaning system, the indoor particle concentration of the cleanroom decreases from a high value to a certain stable value (which is measured in the working area or the first working plane in horizontal flow cleanroom), and the time needed is called the self-purification time. The shorter it is, the better the condition is. If the indoor particle concentration increases from a low stable value back to a high one because of pollution, the time needed is the pollution time. The difference is, if the pollution is caused by the halt of the cleanroom, the longer the time is, the better the system and the strictness of the building are. If the indoor particle concentration increases to a new value due to the increase of the particle generation source and the particle generation rate in the operation process of the cleanroom, the time needed is the particle pollution time. And the shorter the time is, the better it is, which means that the clean air current can dilute the pollution quickly. This chapter focuses on the calculation of self-purification time and

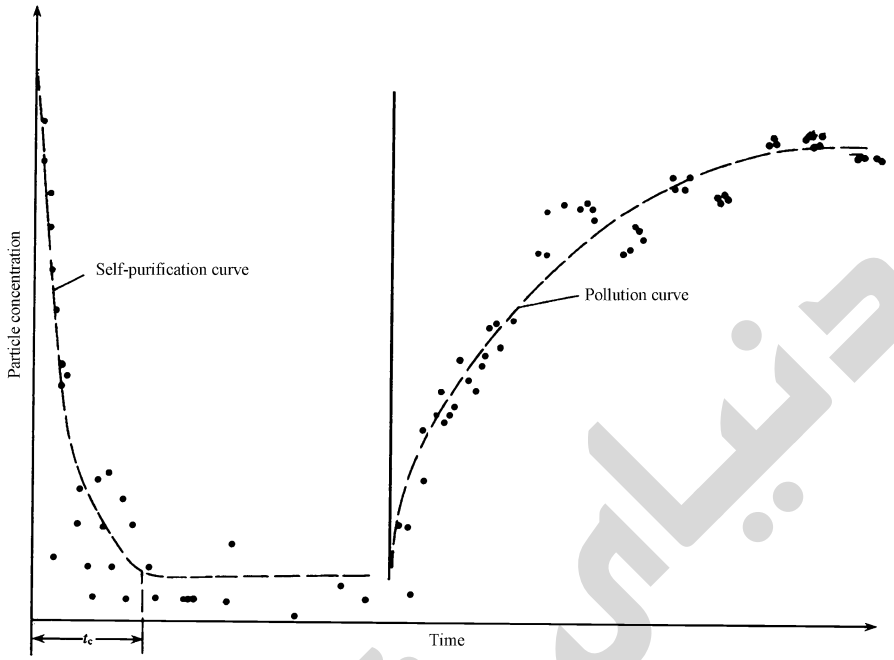

Fig. 10.8 Instance of self-purification curve and pollution curve

particle pollution time. Because the pollution time by halt of cleanroom is influenced by both the system and the building, it is too complicated to be calculated.

Figure 10.8 is an example of self-purification curve during the startup of cleanroom and the pollution curve during the halt of the cleanroom in actual situation.

High-efficiency air cleaning system owns the conception of self-purification time and pollution time. The indoor particle concentration with medium-efficiency air cleaning system will change with the change of atmospheric dust concentration (see Chap. 12), so there is no self-purification time and pollution time in this situation.

10.8.2 Calculation of Self-Purification Time

From the instantaneous expression of particle concentration in turbulent flow cleanroom, the particle concentration N_t at any time and time t are unknown, so the self-purification time or the pollution time cannot be solved directly. Author has put forward the following simplified method.

In Eq. (10.5), the item outside of the bracket { } is a steady-state expression, so it can be written as:

$$N_t = N\left\{1 - \mathrm{e}^{-\frac{nt[1-s(1-\eta_r)]}{60}}\right\} + N_0\mathrm{e}^{-\frac{nt[1-s(1-\eta_r)]}{60}}$$

$$\frac{N_t}{N} = 1 + \left(\frac{N_0}{N} - 1\right)\mathrm{e}^{-\frac{nt[1-s(1-\eta_r)]}{60}} \tag{10.23}$$

For cleanroom with high-efficiency air cleaning system, we know $\eta_t > 0.99$. While for the case of $s \leq 1$, $[1 - s\,(1 - \eta_t)] \approx 1$, so Eq. (10.23) can be simplified as:

$$\frac{N_t}{N} = 1 + \left(\frac{N_0}{N} - 1\right)\mathrm{e}^{-\frac{nt}{60}} \tag{10.24}$$

Further simplification can be made for Eq. (10.24). Let $\frac{N_t}{N}$ is a number a little bigger than 1 (such as 1.01, 1.03, shown in Fig. 10.9), the particle concentration is thought to reach stable, so we can obtain the following expression with Eq. (10.24):

$$1.01 - 1 = \left(\frac{N_0}{N} - 1\right)\mathrm{e}^{-\frac{nt}{60}}$$

So we get:

$$nt = 60\left[\ln\left(\frac{N_0}{N} - 1\right) - \ln 0.01\right] \tag{10.25}$$

This formula will become a straight line in the single-logarithmic paper, which is shown in Fig. 10.10. Because usually $N_0/N >> 1$, so the value of 1 can be omitted during calculation.

In order to obtain the self-purification time, N_0/N must be calculated first. N_0 is the original particle concentration in the cleanroom. It should be determined if it is not known in advance. It is shown from practice that, when the system has stopped for several hours just before startup, no matter what system it is in cleanroom, the value of N_0 at last tends to outdoor atmospheric dust concentration M. It can be seen from Table 10.1 that for cleanroom with the general building envelope, N_0 approximately reaches up to 80 % of M. Because difference of N_0 is not large, and its influence on self-cleaning time is also not large, in order to facilitate the calculation, let $N_0 = M$.

The value of M can be determined according to the principle introduced in Chap. 2.

N is the stable particle concentration in cleanroom, which should be determined based on the requirements or calculation. The specific method will be introduced in Chap. 13.

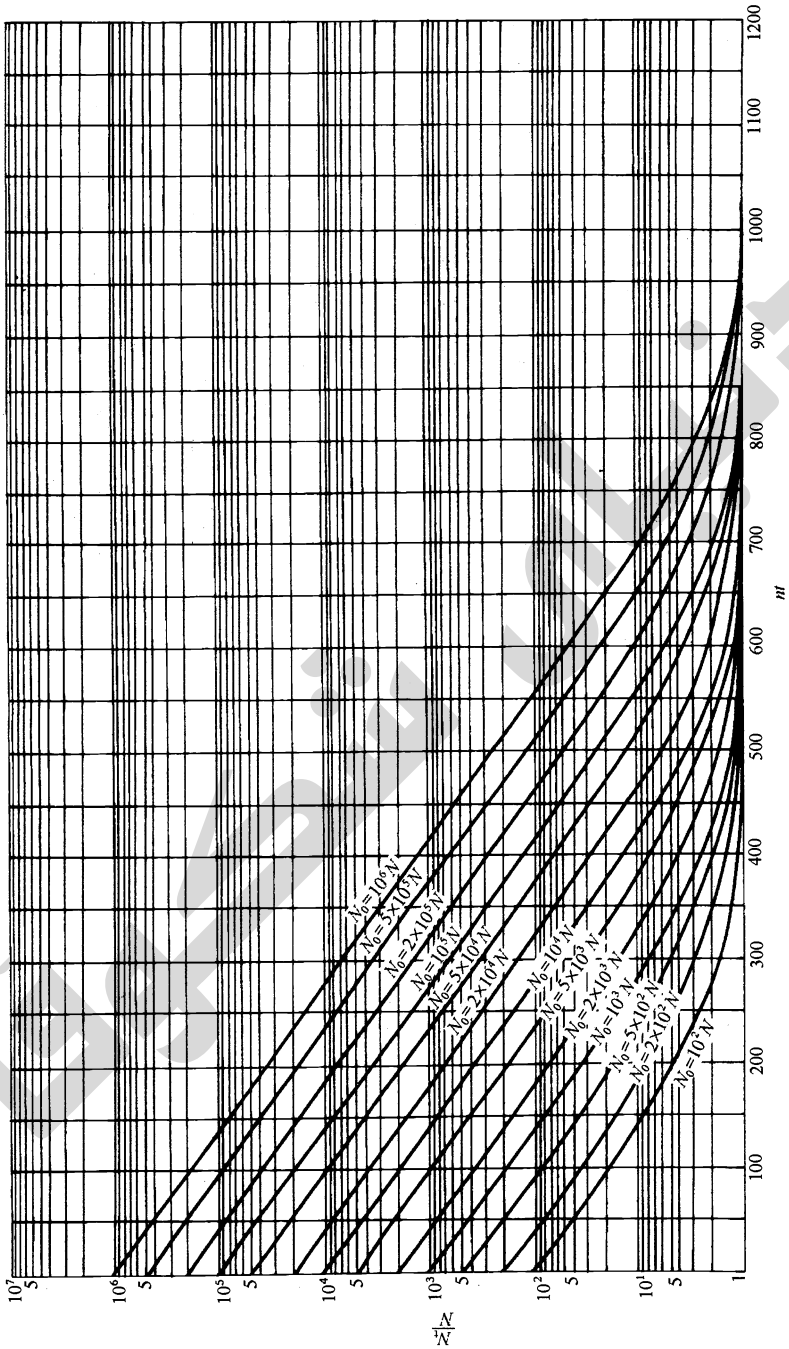

Fig. 10.9 Decline of particle concentration in cleanroom

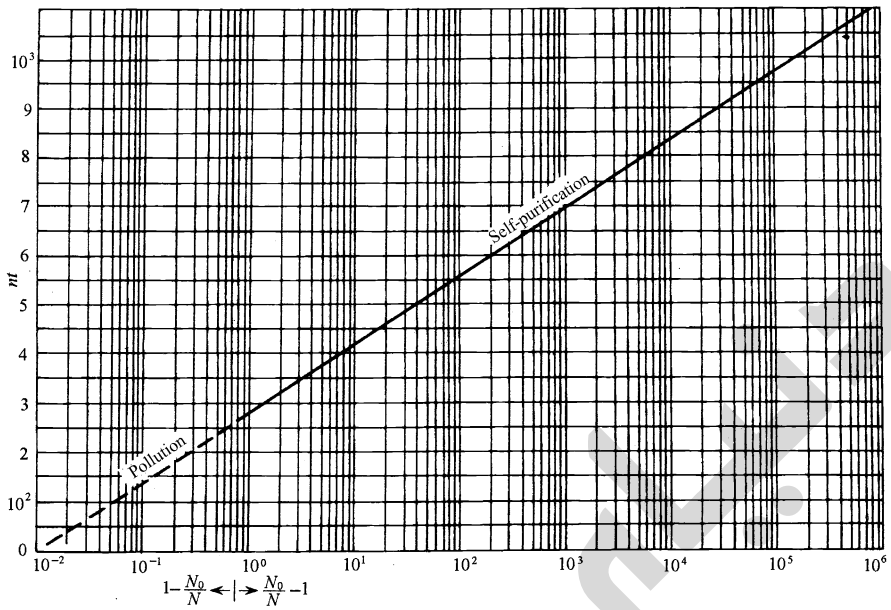

Fig. 10.10 Self-purification time and pollution time

According to N_0/N, the value of nt can be obtained from Fig. 10.10, so we get

$$t = \frac{nt}{n}$$

As explained in Sect. 10.1, the unit of t is "min."

Table 10.2 lists comparison of self-purification time during the startup of the system in 18 cases between the calculation value and the measured value. It is shown that they are closer.

Figure 10.11 is plotted with the foreign experimental data [9]. Because experiment was performed in the same cleanroom with different air change rates, the relationship between the air change and the self-purification time is single, which is more convincing.

Now the self-purification time needed to remove the pollution brought in by the opening of the door introduced in Chap. 8 will be calculated.

It is known that because of the door opening, the indoor concentration ratio increases to $N_0/N = 3.14$. The self-purification time should be calculated when $N_t/N = 1.2$.

According to Eq. (10.24), we know

$$nt = 60\left[\ln\left(\frac{N_0}{N} - 1\right) - \ln\left(\frac{N_t}{N} - 1\right)\right] = 60\left(\ln\frac{2.14}{0.2}\right) = 60 \times 2.37 = 142.2$$

Table 10.1 Indoor particle concentration after stop of the system

Cleanroom	Stable particle concentration after shutdown N_0 (#/L)	Atmospheric dust concentration at the same time M(#/L)	N_0/M
The envelop structure is the welded steel plate, sealed doors, pipes, seams, plus welding	1.4×10^4	2.5×10^4	0.56
General civil engineering clean room	12×10^4	17×10^4	0.70
General assembly clean room	9.8×10^4	10.5×10^4	0.93

Table 10.2 Comparison of self-purification time between the calculation value and the measured value

No.	n (h^{-1})	N_0 (test value) (#/L)	N (calculated value) (#/L)	$\frac{N_0}{N}$	nt	t(calculated value) min	t(test value) min
1	28.1	2.6×10^4	22	1.18×10^3	765	27	26
2	29	1×10^4	16	6.3×10^2	670	23	24
3	67	5.4×10^4	14	3.85×10^3	775	12	18~20
4	59	4.5×10^4	16	2.8×10^3	750	13	15~27
5	21	2×10^4	22	9×10^2	680	33	33~38
6	21	6×10^3	22	270	620	30	30~35
7	70	9×10^4	9.5	9.5×10^3	830	12	8~15
8	185	5.8×10^4	3.8	1.5×10^4	850	4.6	19
9	36	7×10^4	28	2.5×10^3	748	21	14
10	72	7×10^4	14	5×10^3	780	11	11.5
11	120	7×10^4	9.8	7.2×10^3	810	6.7	6.5
12	150	7×10^4	8	8.7×10^3	820	5.5	5.5
13	180	7×10^4	6.8	1.1×10^4	830	4.7	3
14	230	7×10^4	5.4	1.3×10^4	850	3.6	3
15	25	1.1×10^3	10	1.1×10^2	560	22	16
16	50	8.5×10^2	10	0.85×10^2	540	11	10
17	40	10^5	200	5×10^2	650	16	30
18	29	1.06×10^5	15	7×10^3	810	28	30

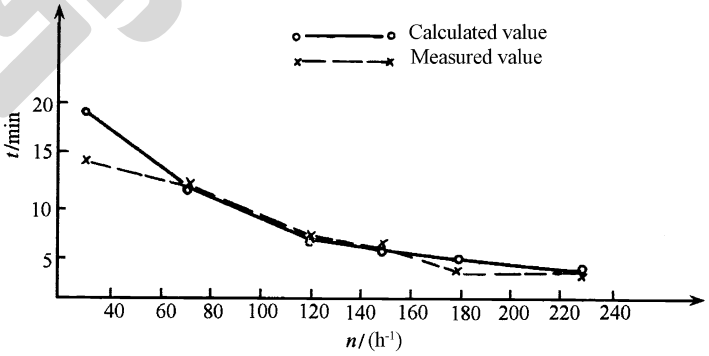

Fig. 10.11 Relationship between self-purification time and the air change rate

If the air cleanliness of cleanroom is Class 1,000, and n is 60 h^{-1}, we can get the following expression from the above expression:

$$t = \frac{142.2}{60} = 2.37\,\text{min}$$

The pollution brought in not only increases the particle concentration but also brings in the foreign particles (such as different bacteria, dust sources with opposite natures). The self-purification time is expected to be within 2 min. Since it is less than 2 min for general unidirectional flow, the limit is set with 2 min. So the results above show that the pollution by opening of the door is dangerous. In this case, the buffer room should be set, as already discussed in Chap. 8.

From a series of calculation above, it is clear that the particle concentration in turbulent flow cleanroom reaches to a stable state in very short time. Under the extreme serious pollution condition after the stop of the system, namely, $N_0 \rightarrow 10^6 \times N$ and $nt \rightarrow 1{,}100$, when the air change rate reaches 20 h^{-1}, the self-purification time after the startup of the system does not exceed 1 h. When the air change rate reaches 30 h^{-1}, it is less than 40 min. When the air change rate reaches 50 h^{-1}, it is less than 22 min. But such a serious pollution is extremely rare, and usually $N_0 \approx 10{,}000N$. According to the above air change rates, the self-purification times correspond to 41, 28, and 17 min. In the past there was no measurement on system; the effect of turbulent flow cleanroom was underestimated. So regardless of the ratio between the indoor original particle concentration and the stable concentration, as well as the air change rate, it was generally put forward that the self-purification time needed for turbulent flow cleanroom should be 1 h [10], and the duty fan must be set. Now it has been proved from both theory and practice that the self-purification time for turbulent flow cleanroom is not long. This means that, unless the product cannot be collected to avoid pollution after the stop of the system, usually the duty fan could not be set, as long as the system starts up half an hour before the operation of the cleanroom.

10.8.3 Calculation of Pollution Time

With particle generation pollution, the stable concentration before pollution becomes the original concentration N_0, and the new stable concentration is N after pollution. So $N_0/N < 1$. Equation (10.23) can be rewritten into:

$$1 - \frac{N_t}{N} = \left(1 - \frac{N_0}{N}\right) e^{-\frac{nt[1 - s(1 - \eta_r)]}{60}} \approx \left(1 - \frac{N_0}{N}\right) e^{-\frac{nt}{60}} \tag{10.26}$$

N_t/N can be assumed slightly less than 1, such as 0.99 (or 0.98). The particle concentration at this time can be regarded as stable. With Eq. (10.26), we know:

$$nt = 60\left[\ln\left(1 - \frac{N_0}{N}\right) - \ln 0.01\right] \tag{10.27}$$

It is also a linear line on a single-logarithmic paper with this expression. It is equivalent to the extension of the line for self-purification, but with the abscissa N_0/N changes into $1 - N_0/N$.

10.9 Calculation of Self-Purification Time in Unidirectional Flow Cleanroom

The self-purification time in unidirectional flow cleanroom is extremely short. In principle, according to the piston flow theory, the ideal of self-purification time should be obtained with the room height divided with the velocity at the cross section. However, due to the uneven distribution of indoor particulate matter (see Chap. 11), the airflow in unidirectional flow cleanroom is actually the gradually varied flow, and reverse flow appears near the wall and overlap of airflow occurs beneath the air filters (see Fig. 8.23). Therefore, some particles cannot be discharged along with air for one time. They may be discharged after two times or even more than two times of circulation. This kind of circulation may also occur in local area with only a very small distance. This prolongs the self-purification time of the cleanroom. Therefore, the self-purification time in unidirectional flow cleanroom from practical measurement is generally longer than 30 s, and for vertical unidirectional flow cleanroom it is about 1 min, and for horizontal unidirectional flow cleanroom it is slightly longer, up to 2 min. This number is very important. If it is claimed that the self-purification time in unidirectional flow cleanroom reaches up to 5 min or even up to 10 min, the indoor velocity field may be not uniform. The turbidity of airflow will be greater, and the risk of leakage may be present, which lost the due function of unidirectional flow cleanroom.

Author thinks that, because the particle concentration in unidirectional flow cleanroom is very low, and the difference of measured results may be large (e.g., difference between 0.3 and 0.5 #/L is 70 %), it is inappropriate to judge the extent of unidirectional flow only with the particle concentration value. Since the self-purification time is closely related to the uniformity of velocity and the parallelization of streamline, it is much convenient and intuitive to judge with the characteristics of the flow field. Based on this view, author has collected some test cases with complete data of the velocity field in vertical unidirectional flow cleanroom, and the deviation of average velocity and the turbidity were calculated, which are listed in Table 10.3. From the table it is visible that: (a) except No. 7, with the increase of the turbidity and the average deviation of average velocity, the self-purification time is also lengthened;

Table 10.3 Relationship between the self-purification time and the velocity field in vertical flow cleanroom

No.	Average velocity (m/s)	Maximum deviation with average velocity			Turbidity (β_u)	Actual self-purification time	Ratio between actual and ideal self-purification times	Investigator
		+	−	Avg.				
1	0.44	9.1	6.8	8	0.045	28	4.4	Kamishima Ya [11] (These are measurement data in China. The largest value 0.76 m/s in Case No. 11 was omitted)
2	0.4	32	42	37	0.17	50	8	
3	0.295	59	52	56	0.227	52	6	
4	0.329	73	51	62	0.31	90	15	
5	0.234	84	66	75	0.34	90	10.6	
6	0.398	81	52	67	0.34	90	18	
7	0.37	62	67	65	0.356	50	9	
8	0.313	92	68	80	0.36	180	22.5	
9	0.274	57	64	60	0.374	160	17.4	
10	0.1	90	83	87	0.412	300	49	
11	0.274	177	64	120	0.449	160	17.4	

(b) from the functional requirement of unidirectional flow cleanroom, the self-purification time is hoped to be less than 1 min. This is also suggested in the accep tance measurement about cleanroom in foreign country [12], and β_u is about less than 0.25; and (c) if β_u is between 0.25 and 0.35, and the self-purification time is not more than 2 min, which is 10 times less than the ideal self-purification time, it is feasible to regard it as the unidirectional flow cleanroom, and of course its performance was slightly worse.

For horizontal unidirectional flow cleanroom, the actual cases are rare which are consistent between the measuring point for the self-purification time and the measured velocity field plane, so it is not analyzed above. But the relationship between the self-purification time and the velocity field should also be the case.

References

1. Xu ZL (1994) Design of cleanroom. Seismological Press, Beijing (In Chinese)
2. Xu ZL (1996) Essential measures to insure cleanliness in computer rooms. J HVAC 26(6):65–69 (In Chinese)
3. Xu ZL, Zhang YZ (1997) Three stage filtration in fresh air handling for better IAQ. J HVAC 1:5–9 (In Chinese)
4. Wada E (1991) Anti-bacterial fan coil unit. Mag Build Equip 42(5):41–44 (In Japanese)
5. Practical handbook of air conditioning technology, 1974 (In Japanese)
6. Austin PA, Timmerman SW (1965) Design and operation of clean rooms. Business News Publishing Co, Detroit, USA
7. Kazuya H et al (1972) Study of cleanroom (1). J SHASE Jpn 46(9):1–12 (In Japanese)
8. Fukuda M et al (1978) Design method of biological cleanroom. Jpn Air Cond Heat Refrig News 18(2):44–48 (In Japanese)

9. Oshitari Laboratories, Inc. (1974) Test report of cleanroom for experiment (In Japanese)
10. Bringold W (1972) Reine Raüme und Reine Werklänke. Schweiz Bläther Heiz Lüft 39:3 (In German)
11. Kamishima K (1981) Air cleanliness level in cleanroom with 0.1 μm particles as the study object. Jpn Air Cond Heat Refrig News 21(5):91–99 (In Japanese)
12. Morrison PW (1973) Environmental control in electronic manufacturing. Van Nostrand Reinhold Company, New York, USA, pp 278–292
13. Schichr HH (1973) Clean room technology-principles and applications. Sulzer Techn Rev 1:3–15
14. Нонезов РТ, Знаменский РЕ (1973) Обеспыливание воздушной среди в"Чесмых комнатах". Водоснабжение и Санитарная Техника 3:29–32 (In Russian)

Chapter 11
Calculation Theory of Nonuniform Distribution in Cleanroom

Due to the nonuniform distributions of airflow and dust particles, particles in cleanroom are actually not evenly distributed. This chapter will focus on the calculation theory of three-zone nonuniform distribution.

11.1 Influence of Nonuniform Distribution

Because of the nonuniform distribution of particles in cleanroom, deviation is inevitable when results are based on the calculation theory of uniform distribution. In general, the larger the nonuniform distributions of indoor airflow and dust particles are, the larger the difference between the measured values and the calculated values according to the uniform distribution theory will be.

For the nonuniform distribution discussed here, it is assumed that the generation of particles is uniform and stable, but the dust particle distribution is not uniform. Even for this nonuniform distribution, it does not mean the nonuniform distribution at every place, but the regional nonuniform distribution. There is regional concentration difference.

In the following sections, we will discuss the factors affecting the nonuniform distribution of indoor particle concentration separately.

11.1.1 Impact of Air Distribution (Including Air Supply Outlet and Its Position)

Different air distribution patterns have an effect on the uniformity of indoor particle concentration field. In general, the difference of existing airflow patterns in this respect is not very significant. The measured results show that the measured particle concentration with side supply mode is generally higher than the calculated value

Z. Xu, *Fundamentals of Air Cleaning Technology and Its Application in Cleanrooms*,
DOI 10.1007/978-3-642-39374-7_11, © Springer-Verlag Berlin Heidelberg 2014

Table 11.1 Indoor particle concentration with different number of air supply outlet (#/L)

Experimental group	Measured and calculated results	Air change rate (h^{-1})								
		18	18	40	60	70	80	120	140	200
1	Measured value with four air supply outlets	90	55		23		16	10		7
	Measured value with eight air supply outlets	70	40	–	20	–	13	8	–	6
	Calculated value	70	48		22		16	10		7
2	Measured value with eight air supply outlets	120		110		50		35	26	21
	Measured value with 12 air supply outlets	150	–	80	–	30	–	27	19	15
	Calculated value	210		110		60		36	28	22

according to the uniform distribution calculation method. The measured value will be higher than the calculated value only when the airflow distribution is not uniform, which weakens the dilution effect. Both positive and negative deviations exist between the measured value and the calculated value for local perforated plate, top supply, and diffuser, which indicates that they are slightly better than the side supply mode in terms of uniformity. For the full perforated plate, all the measured values are almost lower than the calculated values, which mean the uniformity may be better.

The effect of the position of air supply outlet is more obvious. For example, for the top air supply outlet with larger air supply velocity, if they are placed on the ceiling where is concentrated at one side of the room, the indoor airflow will become extremely uneven, where several vortex may appear. In this case, the measured particle concentration is much higher than the calculated value, which has been introduced in Chap. 8.

11.1.2 Impact of the Number of Air Supply Outlet

The air inlet quantity has significant effect on the uniformity of air distribution. Table 11.1 is based on the experimental results of Kayatawa [1].

It can be seen from Table 11.1 that with the same filters and air change rate, the lesser the number of air supply outlet is, the higher the average indoor particle concentration is, when it is compared with the calculated value by the uniform distribution method. Because when the number of air supply outlets is small, the proportion of turbulent flow and the eddy area become large, and the uniformity becomes poor. When the number of air supply outlets is more, the average particle concentration is gradually lower than the calculated value. Because when the eddy current area becomes small, the velocity field becomes more uniform, and the turbidity is reduced. Moreover, with more air supply outlets, the extrusion effect of airflow increases. In addition, it has been mentioned in the Chap. 6 that with the

same air change rate, when the number of air supply outlets increases, the air velocity reduces, which is helpful to reduce the deposition of particles on the surface of the workpiece.

11.1.3 Impact of the Air Change Rate

The air change rate has great impact on the uniform distribution of indoor airflow and particle concentration. In order to make the airflow and particle concentration fields uniform, there must be sufficient air flow rate to dilute, and the dilution area should be as large as possible, until the whole room. When the air change rate becomes less, the flow rate becomes insufficient, and the corresponding number of air supply outlets would become less, which is likely to cause more big vortex area. Therefore the measured particle concentration is generally bigger than the calculated value, because in fact the effect of uniform dilution is not achieved at all. But when the air change rate is more than 10 h^{-1}, the differences are generally not obvious. With the increase of the air change rate, more uniform field will be achieved in full chamber with dilution. The measured value will approach to the calculated value gradually. When the air change rate is about 70 h^{-1}, both of them are roughly the same (this will be explained later). When the air change rate continues to increase, opposite situation will occur, where the measured value is generally lower than the calculated value. This is because not only the full uniform dilution has been reached, but also the extrusion effect of the airflow increases because of the increase of the flow rate and the number of air supply outlets (if the number of air supply outlets does not increase, the flow rate of one air supply outlet will be too large, which then causes the opposite result). In this case, the actual particle concentration is still lower than that calculated by uniform dilution method. In conclusion, there are two main aspects for the influence of the air change rate. For a small number of air change rate, the measured particle concentration is higher than the calculated value. For a large number of air change rate, the measured particle concentration is lower than calculated value. Of course, this is only the general rule, which may not be absolutely true.

11.1.4 Impact of the Type of Air Supply Outlet

Different forms of air supply outlets have obvious effect in the turbulent flow cleanroom. Several main types of air supply outlets are listed in Fig. 11.1.

The following conclusions can be reached with the experiment [3]:

1. Self-purification times area different for various kinds of air supply outlets. Type C with the extrusion airflow is the best, which is slightly better than the theoretical value with the uniform distribution method. Type B with actively mixing

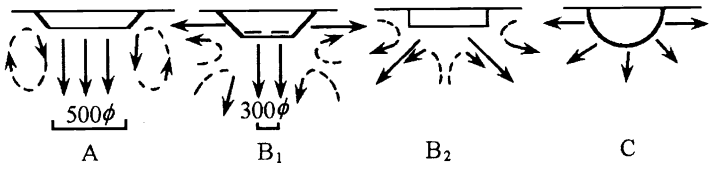

Fig. 11.1 Four kinds of air supply outlets: Type *A*: normal diffusion plate, mainly for direct downward current. Type B_1: diffusion plate with outlet at peripheral sides [2], mainly for direct downward current and horizontal current. Type B_2: diffuser, mainly for diagonal flow. Type *C*: hemispherical outlet with the isotropic radial flow

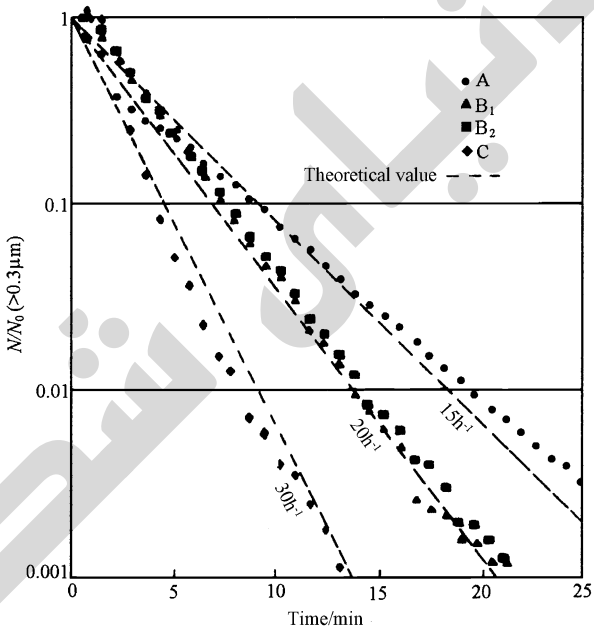

Fig. 11.2 Comparison of the self-purification capacity between four kinds of air supply outlets

flow is the next, which is close to theoretical value. Type A with common airflow is the worst, which is worse than the theoretical value, which is shown in Fig. 11.2.

2. When there is indoor dust generation source, the indoor particle concentration with Type C is very small.
3. For Type B with actively mixing flow, due to the induction effect of suction, the dust generation near the head may have effect on the top of the table.
4. For the general Type C, the diffusion performance near the head and foot is good. But since the current near the room end is weak and there is updraft, high concentration is prone to appear when particle is generated indoors.
5. When interferences occur when people are walking around, no matter what kind of air supply outlet is, the difference is not large. When the external disturbance is small, the advantage with Type C appears.

To sum up, in order to overcome the problem of deviation of calculated result with assumed uniform distribution method, and to deeply research the characteristic of cleanroom, it becomes an important topic to study the nonuniform distribution calculation method in cleanroom. In 1974, dual zone model was proposed by Kayatawa [1] who tried to solve this problem, but the specific calculation method was not available.

11.2 Three-Zone Nonuniform Distribution Model

The three-zone nonuniform distribution model is shown in Fig. 11.3 [4], which is divided into the mainstream area, the vortex area, and the return air area. The starting point is as follows:

1. In the mainstream area, because there is a certain air velocity above the working area, particles will not be dispersed into the whole mainstream area continuously and uniformly against the airflow by the dust source G_a. As illustrated in front chapters, the probability of particle dispersion into the whole room with the effect of dispersion, deposition, and mechanical force is very small. They distributed mainly along the airflow. So it is more appropriate to term it as "distribution" instead of "diffusion." This is why all this book "uniform distribution" and "nonuniform distribution" are used, instead of "uniform diffusion" and "nonuniform diffusion." Moreover, it is easy to wrongly consider the term "diffusion" as pure molecular dispersion diffusion movement.

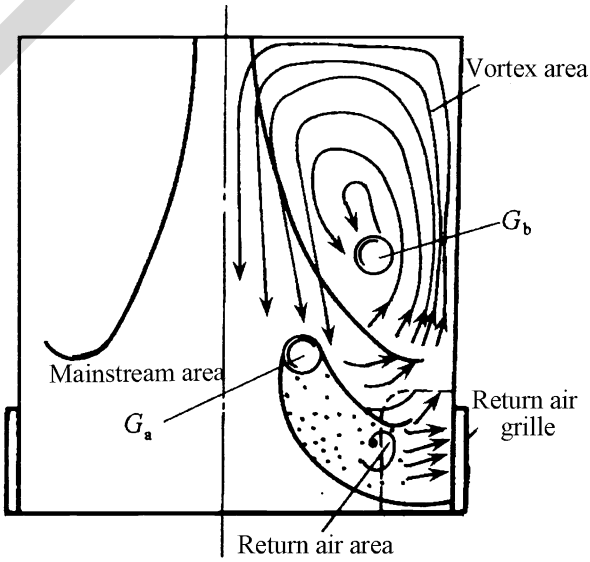

Fig. 11.3 Three-zone nonuniform distribution model

2. For particles generated from the dust source in the mainstream area, a part of them is uniformly driven into the boundary layer of the airflow along the eddy upwards and then downwards. According to the simple experiment, when there is a dust source in the air supply flow with enough width, it is unlikely to distribute crosswise to the whole cross section of the flow. When air velocity is 0.5 m/s, the expansion angle behind the dust source is only 5–6° [5]. It has been clear when the lower limit of air velocity was introduced that it is enough to control the lateral spread of pollution with the release velocity of 2 m/s, when the air supply velocity is 0.25 m/s. For pollution with smaller release velocity (such particle generation by occupant), it is less likely for particles to disperse against the airflow. According to the jet flow principle, the cross section of airflow expands, and the flow rate increases, which is mainly from the supplement of side eddy air. Therefore, for particles generated in the mainstream area, they will move along the airstream direction with only slightly extension, and then enter the return air area, where a certain degree of mixture occurs. Part of them is exhausted through the return air grille, and others return to the vortex area. In the vortex area, particles spread out and then go through the whole mainstream area uniformly with the airflow induced by the mainstream area. According to this mechanism, the unidirectional flow and the turbulent flow cleanrooms can be linked together. For the vertical unidirectional flow cleanroom, return outlets are placed on the floor, so the airflow in the entire cross section of the working area is the mainstream, and there is no eddy current area. So below the working area, there is no back vortex in the flow, where basically particle cannot be brought back upwards and then "disperse" again. If there is no eddy current in the upper part of the room, it is the ideal unidirectional flow. Even if dust source exists in the upper part, dust particles will not spread into the entire mainstream area because no eddy current exists in this region. This situation is the basis for the analysis of particle concentration in unidirectional flow cleanroom which is discussed in the previous uniform distribution method. If eddy area exists in the upper part, such as the situation when filters are placed with intervals, the amount of particles entering into the eddy area then the mainstream area will be dependent on the ratio of blowing area, the eddy size, and the size of upper dust source. Generally for the unidirectional flow cleanroom, the upper eddy area is very small, and dust source is also rare. So particles scattered in the mainstream area are few. Therefore, in the unidirectional flow cleanroom, the influence of dust source on the particle concentration is very small. With the increase of eddy area, the particle concentration may be affected when the eddy area increases to a certain extent. In this case, it becomes the turbulent flow cleanroom.
3. There is a return air area where particle concentration is different from that in the mainstream and eddy areas. The actual test has showed [6] that, for a unidirectional flow cleanroom with hundreds of air change rate and air return below both sides, the particle concentration of the working area in the mainstream area is equivalent to about 70 % of the average concentration in the return air area (the height of return air outlet is about 0.4 m). The detailed data are shown in Table 11.2.

Table 11.2 Ratio of particle concentrations between the working area and the return air area

Height above ground (m)	0.4	0.8	0.9	1
Total particle counting concentration for particles ≥0.5 um (#/L)	87	64	61	59
Ratio of concentration at the height 0.4 m (%)	–	74	70	67
Total particle counting concentration for particles 0.5 um (#/L)	41	32	29	28
Ratio of concentration at the height 0.4 m (%)	–	78	70	68

According to the measurement by No. 10 Design Institute of the former Fourth Ministry of Machinery and Industry, the air change rate in turbulent flow cleanroom reached 128 h^{-1}. The particle concentration at the height between 0.9 and 1 m is about 66 % of the average concentration at the return air area. This is consistent with the results shown in the table above. The measured results also show that, for small value of air change rate, the average ratio is 0.8. From the front analysis, particles generated in the mainstream area are concentrated in the return air area, and this is the important reason why the concentration at the return air area is higher than that in the mainstream area. But the concentrated area of particles should be very small.

The above three points are the main content for three-zone nonuniform distribution model.

11.3 Mathematical Model for Three-Zone Nonuniform Distribution

According to the three-zone model, particle concentration N_c at the return air area is composed of two parts: one is the concentration of the mainstream area, and the other is the concentration of the return air area where particles released from dust source G_a are mixed with the total air volume $(Q + Q')$, that is,

$$N_c = \frac{N_a + G_a}{(Q + Q')} \tag{11.1}$$

Particle concentrations in other two areas should be calculated with the differential equations.

Let

$$D = \frac{d}{dt}$$

We know

$$DN_a = \frac{N_a Q}{V_a} + \frac{N_b Q'}{V_b} - \frac{N_a (Q + Q')}{V_a} \tag{11.2}$$

$$DN_b = \frac{G_b}{V_b} + \frac{N_b Q'}{V_b} + \frac{G_a Q'}{V_b (Q + Q')} - \frac{N_b Q'}{V_b} \tag{11.3}$$

where

N_a is the concentration of the mainstream area (#/L);
N_s is the concentration at the air supply outlet (#/L);
N_b is the concentration of the eddy area (#/L);
G_a is the particle release rate in the mainstream area (#/min);
G_b is the particle release rate in the eddy area (#/min);
Q is the air supply flow rate (L/min);
Q' is the induced flow rate by the mainstream area (L/min);
V is the room volume (L);
V_a is the volume of the mainstream area (L);
V_b is the volume of the eddy area (L).

Let

$$\beta = \frac{G_a}{G_0}$$

$$\frac{\beta G_0}{Q + Q'} = \frac{G_a}{Q + Q'} = G_a{}'$$

$$\frac{(1 - \beta) G_0}{Q'} = \frac{G_b}{Q'} = G_b{}'$$

$$G_0 = G_a + G_b$$

For Eq. (11.3), we know:

$$D^2 N_b = \frac{Q'}{V_b} \left\{ \frac{Q}{V_a} N_s + \frac{Q'}{V_a} N_b - \frac{Q + Q'}{V_a} \frac{V_b}{Q'} \left[DN_b - \frac{G_a{}' Q'}{V_b} - \frac{G_b{}' Q'}{V_b} + \frac{Q'}{V_b} N_b \right] \right\} - \frac{Q'}{V_b} DN_b$$

After reorganization, we know:

$$\left[D^2 + \left(\frac{Q + Q'}{V_a} + \frac{Q'}{V_b} \right) D + \left(\frac{Q + Q'}{V_a} \frac{Q'}{V_b} - \frac{Q'^2}{V_a V_b} \right) \right] N_b = \frac{Q Q'}{V_a V_b} N_s + \frac{Q' (Q + Q') (G_a{}' + G_b{}')}{V_a V_b} \tag{11.4}$$

So the differential equation can be rewritten as:

$$\alpha_1 = \frac{-\left(\frac{Q+Q'}{V_a}+\frac{Q'}{V_b}\right)-\sqrt{\left(\frac{Q+Q'}{V_a}+\frac{Q'}{V_b}\right)^2-4\frac{QQ'}{V_aV_b}}}{2} \tag{11.5}$$

$$\alpha_2 = \frac{-\left(\frac{Q+Q'}{V_a}+\frac{Q'}{V_b}\right)+\sqrt{\left(\frac{Q+Q'}{V_a}+\frac{Q'}{V_b}\right)^2-4\frac{QQ'}{V_aV_b}}}{2} \tag{11.6}$$

Let

$$\frac{QQ'}{V_aV_b}A = \frac{QQ'}{V_aV_b}N_s + \frac{Q'(Q+Q')(G_a{}' + G_b{}')}{V_aV_b}$$

so

$$A = \frac{N_sQ + Q'(G_a{}' + G_b{}')}{Q} + G_a{}' + G_b{}' \tag{11.7}$$

We obtain:

$$N_{bt} = K_1 e^{\alpha_1 t} + K_2 e^{\alpha_2 t} + \frac{N_sQ + Q'(G_a{}' + G_b{}')}{Q} + G_a{}' + G_b{}' \tag{11.8}$$

Similarly we can get:

$$N_{at} = K_1{}' e^{\alpha_1 t} + K_2{}' e^{\alpha_2 t} + \frac{N_sQ + Q'(G_a{}' + G_b{}')}{Q} \tag{11.9}$$

The coefficients of K_1, K_2, $K_1{}'$ and $K_2{}'$ in above expressions are determined with the initial conditions.

When $t \to \infty$, we know:

$$N_b = \frac{N_sQ + Q'(G_a{}' + G_b{}')}{Q} + G_a{}' + G_b{}' \tag{11.10}$$

$$N_a = \frac{N_sQ + Q'(G_a{}' + G_b{}')}{Q} \tag{11.11}$$

Since the range of return air area is smaller, its volume can be ignored. The average concentration of the mainstream area and the eddy area is approximately the average room concentration, that is,

$$N = N_a \frac{V_a}{V} + N_b \frac{V_b}{V} = N_s + (G_a{}' + G_b{}') \left(\frac{Q'}{Q} + \frac{V_b}{V} \right) \tag{11.12}$$

Let

$$Q' = \varphi Q$$

$$Q' + Q = \varphi Q + Q = Q(1 + \varphi)$$

$$Q = \frac{nV}{60}$$

When they are inserted into the expressions of $G_a{}'$ and $G_b{}'$, and let $\frac{G_0}{V}. = G$ [#/(m^3·min)], Eq. (11.12) can be rewritten as:

$$N = N_s + \frac{60G \times 10^{-3}}{n} \left(\frac{1}{\varphi} - \frac{\beta}{\varphi} + \frac{\beta}{1 + \varphi} \right) \left(\varphi + \frac{V_b}{V} \right) \tag{11.13}$$

Equation (11.13) can be called the *N*–*n* general formula for cleanroom.

11.4 Physical Meaning of *N*–*n* General Formula

1. Obviously, under the condition of uniform distribution:

$$N = N_s + \frac{60G \times 10^{-3}}{n} \tag{11.14}$$

Let the coefficient at the right of Eq. (11.13):

$$\left(\frac{1}{\varphi} - \frac{\beta}{\varphi} + \frac{\beta}{1 + \varphi} \right) \left(\varphi + \frac{V_b}{V} \right) = \psi \tag{11.15}$$

It can be used to express the difference of the particle concentration between uniform and nonuniform distribution conditions.

For the conventional cleanroom with air cleanliness level below Class 100 for particles ≥0.5 μm, since the efficiency of HEPA filter can reach above 0.99999(for ≥0.5 μm), N_s is usually about 0.1–0.3 #/L when circulating air system is used. When full fresh air system is used and M is about 10^5 #/L, N_s is less than 0.7 #/L.

For the cleanroom with air cleanliness level higher than Class 10 for particles ≥0.1 μm, since the efficiency of HEPA filter can reach above 0.999999

(for ≥0.1 μm) and the efficiency of prefilter is also required to be about 0.9, N_s is usually below 0.06 #/L when circulating air system is used.

It is clear that N_s in air cleaning system is very small, which can be approximated as:

$$N_v \approx \psi N \tag{11.6}$$

Where

N is the particle concentration with the uniform distribution calculation method;
N_v is the particle concentration with the nonuniform distribution calculation method;
ψ is the uniformity coefficient.

But for the cleanroom with air cleanliness level Class 100 for particles ≥0.5 μm when the full fresh air system is used, the maximum result of N_v can be added with 1.

2. Equation (11.13) is an *N*–*n* general formula for describing both the turbulent flow cleanroom and the unidirectional flow cleanroom. That means no matter it is turbulent flow cleanroom or unidirectional flow cleanroom, when different air supply modes are used in turbulent flow cleanroom or filters are placed fully or partially on the ceiling of the unidirectional flow cleanroom, the *N*–*n* general formula can be used to reflect the influence of the number of staff:

   (a) For unidirectional flow cleanroom with the ratio of blowing area 100 % of filters (there is no border for filter), unidirectional parallel flow exists along the entire height and the cross section in the room, where eddy flow does not exist, so we get:

$$V_b = 0$$

$$Q_s = 0$$

$$\psi = 0$$

   So in Eq. (11.13), we know:

$$\left(\varphi + \frac{V_b}{V}\right) = 0$$

   Therefore, we obtain:

$$N_v = N_s$$

This is like the situation in the test pipeline for air filter, where the downstream concentration of filter depends only on the inlet concentration. Of course, this is only the ideal situation.

(b) If filters are not fully placed on the ceiling, and there is a certain value of the ratio of blowing area, eddy area will exit. With the decrease of this ratio, both ψ and V_b will increase, and β will reduce, so N_v will also increase. This means the particle concentrations are different for the unidirectional flow cleanroom with different values of the ratio of blowing area. Equation (11.13) can be used for calculation. Similarly, the particle concentrations are different for the unidirectional flow cleanroom with different occupational densities. Therefore, the number of occupants in the unidirectional flow cleanroom should be controlled appropriately.

(c) For different turbulent flow cleanrooms, the size of the mainstream area, the size of the eddy area, and the volume of induced airflow are different.

Table 11.3 Comparison of calculated results with both the uniform distribution calculation method and the nonuniform distribution calculation method

		Particle concentration (pc/L)		
No.	Air supply mode	$\bar{N}$	N	N_v
1	Side supply	26	21	23
2	1/3 local perforated plate	13	10	12
3	2/3 local perforated plate	26	22	26
4	Ceiling supply	5	14	6
5	Ceiling supply	30	26	32
6	Ceiling supply (Japan Oshitari Lab)	1	7	2.3
7	Ceiling supply with air diffuser plate	30	26	29
8	Air diffuser	19	25	21.5
9	Full perforated plate	1	3.8	1.6 (with mainstream area)
10	Full perforated plate	2.8	8.4	3.6(with mainstream area)
11	Full perforated plate	8.3	12	5(with mainstream area)
12	Air supply with filters fully placed on the ceiling (the ratio of blowing area 80 %), air return with grid-type floor	0.25 (room average) 0.14(mainstream area)	0.042	0.23 0.16(with mainstream area)
13	Two HEPA filters are placed. Air supply with filters fully placed on the ceiling (the ratio of blowing area 80 %), air return on single bottom side	0.026	0.05	0.042(with mainstream area)
14	Two HEPA filters are placed. Air supply with filters fully placed on the ceiling (the ratio of blowing area 80 %), air return on both bottom sides	0.033	0.04	0.044(with mainstream area)

For example, the diffusion angle of diffuser is a little larger than HEPA filter air supply outlet, so V_b is smaller and ψ is larger. So the difference of particle concentrations in different turbulent flow cleanrooms is shown.

11.5 Comparison Between Uniform Distribution and Nonuniform Distribution

In Table 11.3, results with different air supply modes are shown. In the table, $\overline{N}$ represents the mean value of measured concentration. N is the calculated results according to the uniform distribution theory. N_v is the calculated value according to the nonuniform distribution theory. It is shown that compared with the calculated results with uniform distribution theory, the calculated results with nonuniform distribution theory are generally closer to the actual value. The final three examples in table correspond to the unidirectional flow cleanroom. Although the difference of the calculated results is not large in the final two cases between the uniform distribution calculation method and the nonuniform distribution method, the calculated results are only related to the air change rate, which has been illustrated in the uniform distribution calculation method for unidirectional flow in Chap. 10. Other factors are not reflected in these two cases. So the calculated results among the final three cases are basically the same. But it is obvious that in the 12th case, the calculated result is much different from the actual value. Although in general the calculated results with the nonuniform distribution calculation method are more accurate than the uniform distribution calculation method, in some circumstances, opposite results may appear, which will be illustrated later.

References

1. Hayakawa K, Aoki H (1974) Study of cleanroom (2). J SHASE Jpn 48(2):13–88 (In Japanese)
2. Xu ZL, Shen JM (1989) Application of air cleaning technology. China Architecture & Building Press, Beijing, p 99 (In Chinese)
3. Suzuki K (1988) Study of characteristics of air supply outlet in conventional cleanroom. In Proceeding of the 7th international symposium on contamination control, Paris, France, pp 97–102 (In Japanese)
4. Xu ZL (1979) Calculation method for the non-uniform distribution in cleanroom. J HV&AC 4:15–21 (In Chinese)
5. Hayakawa K et al (1974) Air conditioning and air cleaning. Soft Science Co. Ltd., Tokyo, Japan (In Japanese)
6. Кочерин ИД (1978) Air cleaning technology in production of semiconductor and integrated circuits. Translated by the 10th Design Research Institute of the Former Fourth Machinery Industry Department (In Chinese)

Chapter 12
Characteristics of Cleanroom

Cleanroom shows different characteristics when it is in at-rest and operational states respectively, which is the reflection of its own laws. By further analysis, curve can be drawn with the expression of its particle concentration, through which the influence of every parameter on the air cleanliness level can be shown intuitively. Furthermore, the curve will reveal the law of cleanroom.

12.1 Characteristic of At-Rest State

Figure 12.1, 12.2, 12.3, 12.4, 12.5, and 12.6 can be obtained with the analysis of the steady-state formula when particle concentration is uniformly distributed. During the plot of the curve, suppose $1 - S = 0.3$, according to the test data at home and abroad. Prefilters, placed before the final filter, contain primary filter (often the coarse filter, the efficiency for particles with diameter $\geq$0.5 μm is taken as 0.15) and intermediate filter (often the medium-efficiency filter, the efficiency for particles with diameter $\geq$0.5 μm is taken as 0.4). Its overall efficiency is about 0.5, which can be calculated through $1-(1-0.15)(1-0.4) = 0.49$.

These curves are called as the characteristic curves of turbulence flow cleanroom with uniform particle distribution. These characteristics are called at-rest state characteristics, because it helps people to understand many important characteristics when the particle concentration reaches stable. It has the following characteristics:

(1) In a wide range, i.e., $M \leq 10^6$ #/L, the influence of the fluctuation of the atmospheric particle concentration is small on the cleanroom with air cleanliness level equal to or lower than Class 100 where HEPA filters are installed as the final filters (the situation of cleanroom with air cleanliness level higher than Class 100 will be analyzed in the last chapter), which can be negligible.

It is observed that the characteristic curve is quite flat at the range of $M = 10^6$ to 2×10^6 #/L, when the efficiency of the final filter whose efficiency is $\eta_3 = 0.99999$, regardless of the orders of magnitude of the particle generation rate G per unit volume.

Z. Xu, *Fundamentals of Air Cleaning Technology and Its Application in Cleanrooms*,
DOI 10.1007/978-3-642-39374-7_12, © Springer-Verlag Berlin Heidelberg 2014

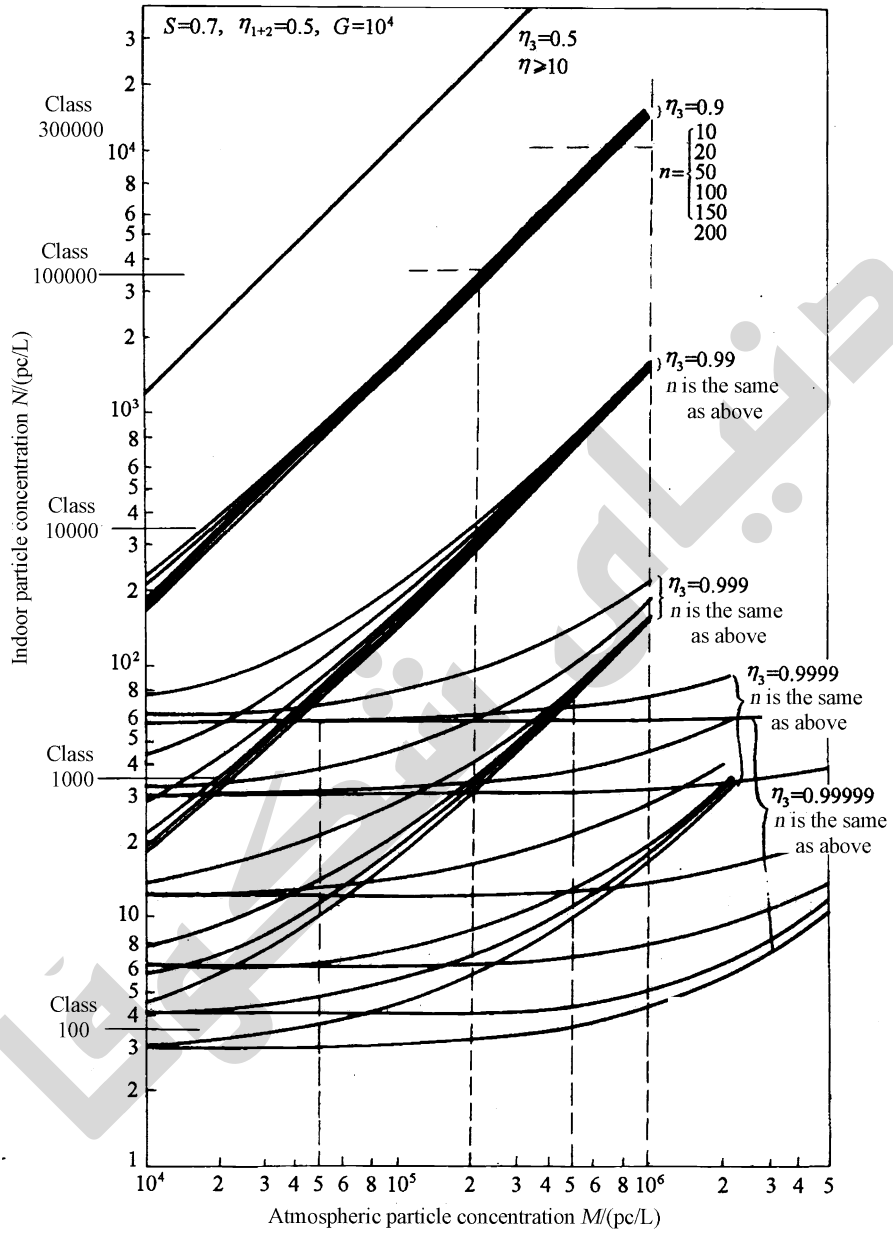

Fig. 12.1 The curve of at-rest state characteristic in cleanroom (1)

It is known from Chap. 2 that the value of 10^6 #/L corresponds to the seriously polluted atmospheric particle concentration, which is two times of that is in general industry. Thus, it is acceptable to consider that the present particle concentration in the cleanroom is free of the influence by atmospheric dust concentration.

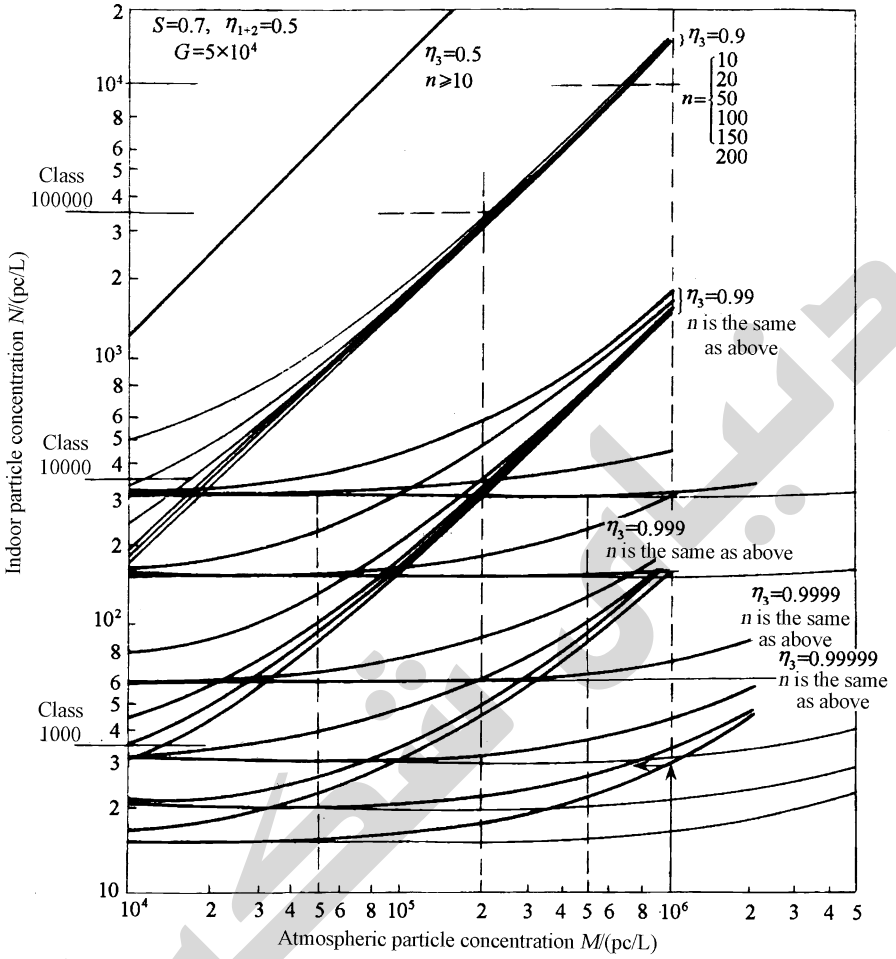

Fig. 12.2 The curve of at-rest state characteristic in cleanroom (2)

(2) For the cleanroom with medium-efficiency filter as the final filter, the indoor particle concentration fluctuates with the atmospheric particle concentration.

It is observed that the characteristic curve is already straight when $\eta_3 \leq 0.9$. For the room with general particle generation rate, namely, $G = 10^4$ to 10^5 #/(m^3·min), M_2/M_1:$N_2/N_1 \approx 1$:1. Only when G is larger, N_2/N_1 will decrease.

The effect of M on N is also in between when η_3 is between the values of high- and medium-efficiency filters.

These characteristics have been completely proved by experiments. For example, for a cleanroom with a medium-efficiency air purification system, when the atmospheric particle concentration M changes from 1.7×10^5 to 2.5×10^5 #/L by the increase rate 50 %, the indoor particle concentration N changes from 1.4×10^4 to 2.1×10^4 #/L, correspondingly, which also increases approximately by 50 %.

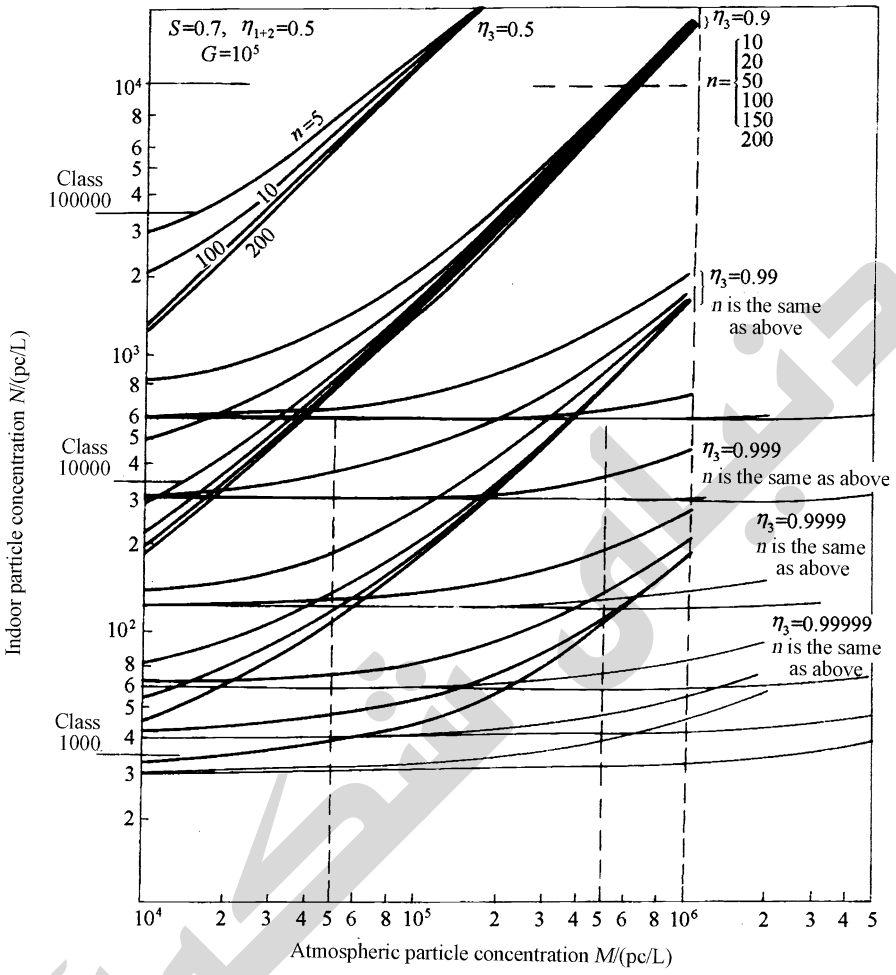

Fig. 12.3 The curve of at-rest state characteristic in cleanroom (3)

Conversely, when the atmospheric particle concentration M changes from 5.3×10^4 to 3×10^4 #/L, decreasing by 40 %, the indoor particle concentration N changes from 0.63×10^4 to 0.46×10^4 #/L, correspondingly, also decreasing approximately by 40 %. The change of the indoor particle concentration in the room with this kind of system is simultaneous with that of the atmospheric particle concentration, as shown in Fig. 12.7.

(3) When the indoor particle generation rate G per unit volume changes, it will influence the particle concentration of the cleanroom. The larger the efficiency of the final filter is, the bigger the influence is. For example, when $\eta_3 = 0.5$–0.9 and G increases by 10 times, N only increases by tens of percents. When $\eta_3 > 0.999$, however, N also increases by one time approximately as G increases by one time.

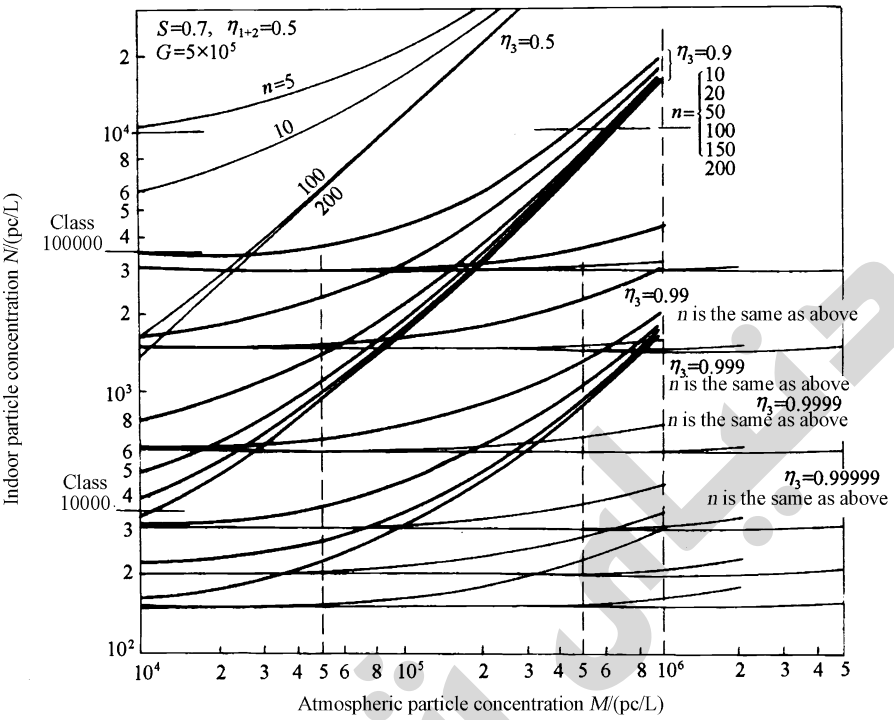

Fig. 12.4 The curve of at-rest state characteristic in cleanroom (4)

This shows that for cleanroom with high-efficiency air purification system, indoor particle generation rate per unit volume is a significant factor to the indoor particle concentration, which has a greater impact than the atmospheric particle concentration. In this sense, interior management is more important than outdoor environment for this kind of cleanroom.

(4) It is not necessary to install final filter with $\eta_3 \geq 0.99999$ in all cases. When the efficiency of final filter reaches a certain level, the function to increase the air cleanliness level becomes significantly less for cleanroom with air cleanliness level equal to or lower than Class 100. From the perspective of increasing the cleanroom's air cleanliness level, it has little sense to further increase the efficiency $\eta_3 \geq 0.99999$. In this case, it is much important to solve the leakage problem. From the characteristic curve, final filter that is less efficient but also with lower resistance and lower price will be suitable for the cleanroom where the requirement of the air cleanliness is not high enough, such as sub-HEPA filter. It is beneficial to the development of air cleaning technology. However, for cleanrooms where air cleanliness should be higher than Class 100, it is not enough to install the normal HEPA filter with the efficiency 0.99999 (i.e., 0.3 μm filter); 0.1 μm filter must be used.

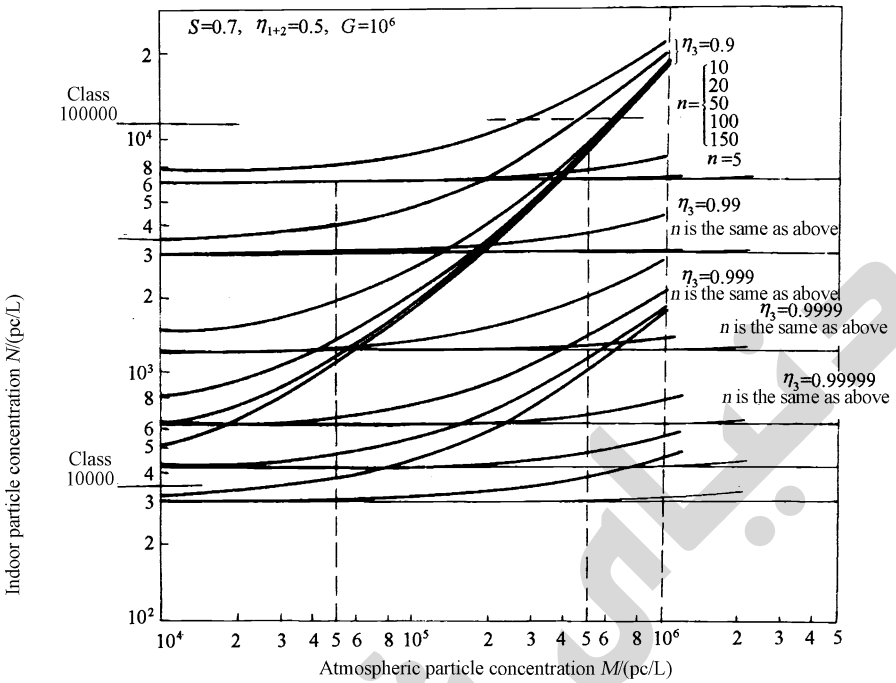

Fig. 12.5 The curve of at-rest state characteristic in cleanroom (5)

(5) The influence of air change rate n on the particle concentration N:

(a) In accordance with the theory of uniform distribution, it is a linear relationship between the air change rate n and the particle concentration N. It can be observed from the characteristic curves above. However, as indicated in last chapter about the influence of nonuniform distribution, with large air change rate, N changes faster than n (this will be introduced in detail later). This should be paid attention to during the analysis of the at-rest characteristic curve.

(b) The larger the value η_3 is, the greater the influence of n will be. Because when the supplied air is clearer, the dilution effect is more efficient. If the air supply volume is larger, the dilution effect will be more efficient.

It should be pointed out that there is a general misconception. It seems that the lower the filter efficiency is and the higher the local atmospheric particle concentration is, it is more likely to increase the air change rate to offset these shortcomings and to increase the air clean effect. But this is not the case. When the value of η_3 is smaller and the value of M is bigger, the curves with different air change rates n are almost approaching to a line. Because of the small value of η_3, the particle concentration of the supply air is the equivalent to the indoor particle concentration by the generation source, which has little effect on diluting the indoor particle concentration. So the value of n has little effect on the cleanroom where medium-efficiency filters are installed as the final filters. On contrary, the larger the value of η_3 is, which reaches up to 0.9999–0.99999, for example, the larger the effect of n will be.

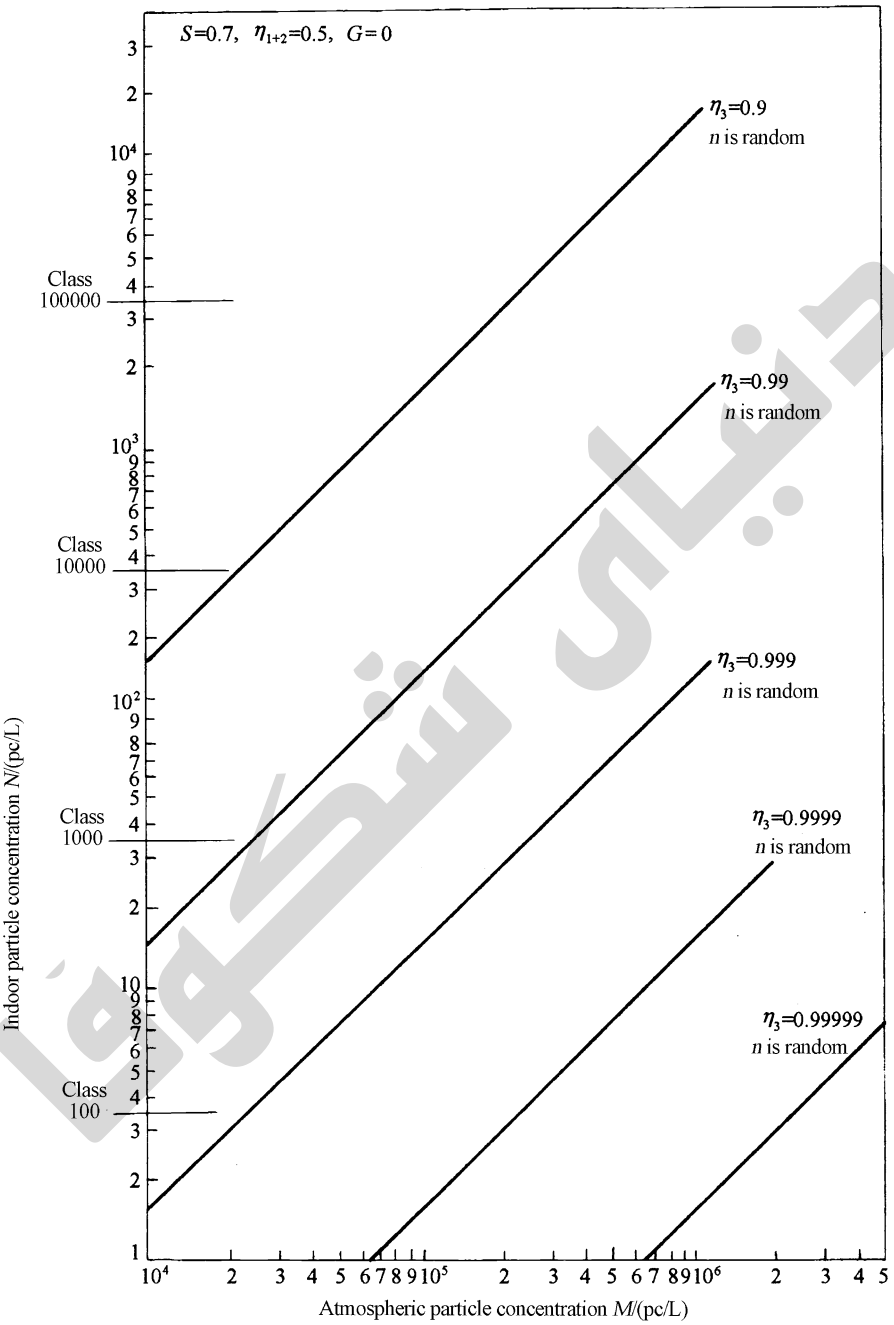

Fig. 12.6 The curve of at-rest state characteristic in cleanroom (6)

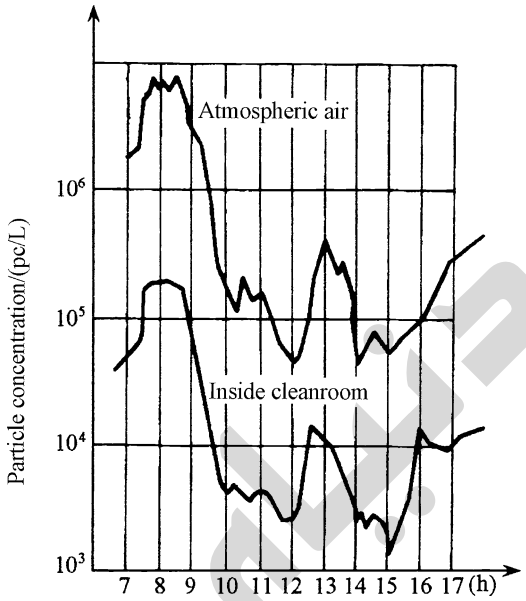

Fig. 12.7 Relationship between the indoor particle concentration and the atmospheric particle concentration in cleanroom with medium-efficiency air purification systems

(c) The effect of n increases with the increase of G, which means the effect of n will be bigger when the particle generation rate in the cleanroom is large.

(d) For the generation situation, the indoor particle generation rate is $G = 10^4$–10^5 #/(m^3·min). If the value of M is not too small (more than 10^5 #/L), the curves with $n = 10$–$200\ h^{-1}$ are quite close to each other for medium-efficiency air purification systems. This means in general conditions, the effect of the change of n on N is negligible when $n \geq 10\ h^{-1}$ for medium-efficiency air purification systems. In other words, $n = 10\ h^{-1}$ will be practicable for medium-efficiency air purification systems.

In short, it is inappropriate to have the opinion that the larger the value of n is, the better it is, regardless of what situation it is.

Here again, the relationship between the air velocity and the deposit density mentioned in Chap. 6 is emphasized again. If the air velocity above the workpieces increases too much by the increase of the air change rate, especially when the air supply concentration is also large, the consequence is that the probability of contamination on the workpieces will be larger, which is the opposite to the expectation of improving the dilution effect.

(6) For turbulence flow cleanroom with high-efficiency air purification system, the normal air change rate is $\leq 100\ h^{-1}$, and the indoor particle generation rate can be considered as 5×10^4 #/(m^3·min) (introduced in detail in Chap. 13). From Fig. 12.2, the particle concentration N can reach 50#/L at most when $M = 10^6$, which is equivalent to the circumstance of no-people condition (see Fig. 12.1). When the actual condition with $M = 10^5$ is used, N is also between 6 and 10 #/L. When the air change rate is as large as $150\ h^{-1}$ (it is unlikely to increase in the

turbulent flow cleanroom), N is close to 100. So generally speaking, it is impossible to reach Class 100 for a turbulent flow cleanroom. It is appropriate to distinguish the unidirectional flow and the turbulent flow with Class 100. The method of unidirectional flow must be taken in cleanroom with air cleanliness level Class 100 or higher. The method of turbulent flow can be used in cleanroom with air cleanliness level lower than Class 100. But according to the theory of nonuniform distribution (Fig. 12.27 and the calculation about the nonuniform distribution in next chapter), if the measuring points are located in the mainstream of the cleanroom with large air change rate, it is possible to obtain the concentration equivalent with Class 100. Of course, this is entirely different from the effect of the Class 100 unidirectional flow. They are not rate interchangeable with each other. So it is not reasonable to replace the unidirectional flow cleanroom with turbulent flow cleanroom with large air change.

In the turbulent flow cleanroom with medium-efficiency air purification system where $\eta_3 = 0.9$, air cleanliness level can reach Class 1,000,000 under the premise of $M = 10^6$#/L. Class 1,000,000 can be realized under the premise of $M < 3 \times 10^5$ #/L when $\eta_3 = 0.5$.

12.2 Dynamic Characteristic

The variation process of particle concentration in the cleanroom before the steady state is regular, which includes the "rising curve" and the "decline curve." The main reason for the variation of the particle concentration is the change of indoor particle generation rate. It can be divided into the following two kinds of circumstances:

12.2.1 To Increase the Particle Generation Rate After Steady State Is Reached by Self-Cleaning Process

This is the major situation. For example, since the system is booted in advance, the indoor particle concentration has reached a lower stable value at the beginning of working time. With the start of the work, people enter in, which increases the particle generation rate. This is the situation:

(1) Particles generate stably (e.g., people stay inside until the end of the working day)

Before working time, point b in Fig. 12.8 represents the indoor condition. Particle generation rate increases as people enter in (increase from G_1 to G_2), which disturbs the original stable state. As the indoor particle concentration rises, a new stable state appears. Point b becomes the beginning of a new process. The steady-state concentration N_1 of the previous process becomes the initial concentration of the

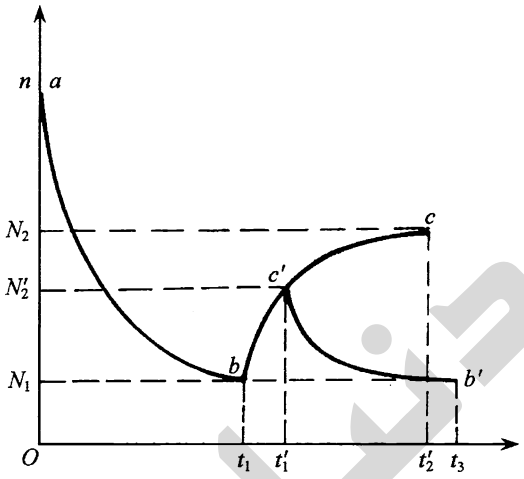

Fig. 12.8 Variation process of particle concentration (1)

following progress. Since the steady-state concentration of the new progress $N_2 > N_1$, the variation of particle concentration can be written as Eq. (10.12):

$$N_{2t} = N_2 - (N_2 - N_1)\mathrm{e}^{-\frac{nt[1 - s(1 - \eta_r)]}{60}}$$

where N_{2t} is the instantaneous particle concentration of the second process. This is a rising progress, as shown the curve *bc* in Fig. 12.8.

(2) The increased particle generation source disappears at a certain time (e.g., people who enter in will leave the room again midway).

In Fig. 12.8, the indoor particle generation rate increases from the moment of t_1. But it disappears suddenly at the moment t'_1 (point c' in the figure). Then the indoor particle concentration changes from b to c', and the indoor particle generation rate decreases from G_2 to G_1. After that, the variation progress of the particle concentration is the same as the previous self-purification process, which decreases along with the curve $c'b'$ (at the moment people leave the room, the particle generation rate increases suddenly because of the activity of people. Otherwise, there is a lag time for the decrease). The particle concentration N'_2 at point c' is also the initial concentration of the third progress. Since the increase of the particle generation rate disappears suddenly, the steady-state concentration of this progress should be the original particle concentration N_1, and $N_1 < N'_2$. The formula to describe this process can be written as

$$N_{3t} = N_1 + (N'_2 - N_1)\mathrm{e}^{-\frac{nt[1 - s(1 - \eta_r)]}{60}}$$

where N_{3t} is the instantaneous particle concentration of the third process.

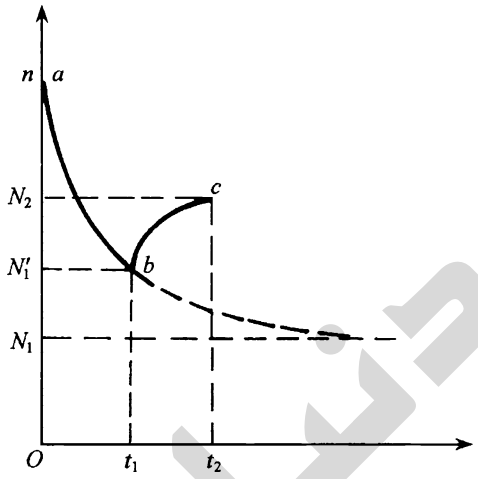

Fig. 12.9 Variation process of particle concentration (2)

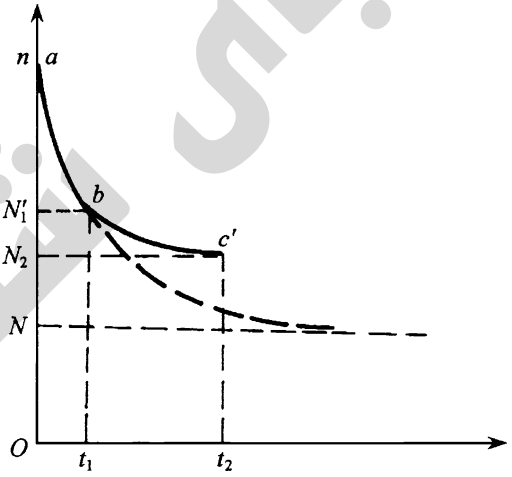

Fig. 12.10 Variation process of particle concentration (3)

12.2.2 *Increase the Particle Generation Rate Before the Steady State of Self-Cleaning Process*

(1) Generate particles continuously and stably

In Fig. 12.9, at the moment of t_1, the indoor particle concentration at point b increases. Thus, the new process starts from this point with the initial concentration N'_1. Assume the steady-state concentration of this new progress is N_2. If the increase of the particle generation rate is big enough, it is likely that $N_2 < N_1'$, which is represented by the rising curve bc. If the increase of the particle generation rate is too small to change the downturn trend of original process, it can just slow down the trend and it will be $N_2 < N_1'$. But it is apparent that $N_2 > N_1$. The process is represented by the declining curve bc' (as shown in Fig. 12.10).

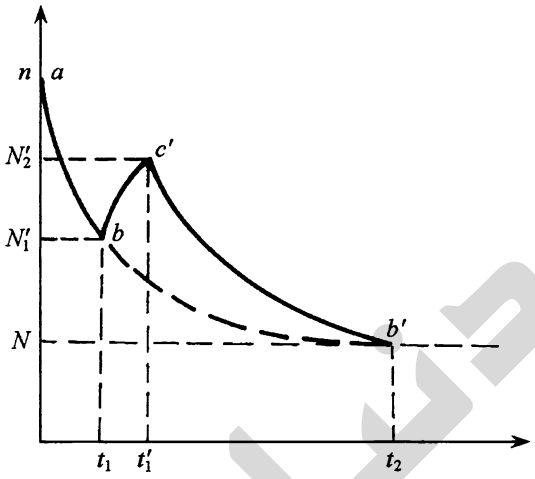

Fig. 12.11 Variation process of particle concentration (4)

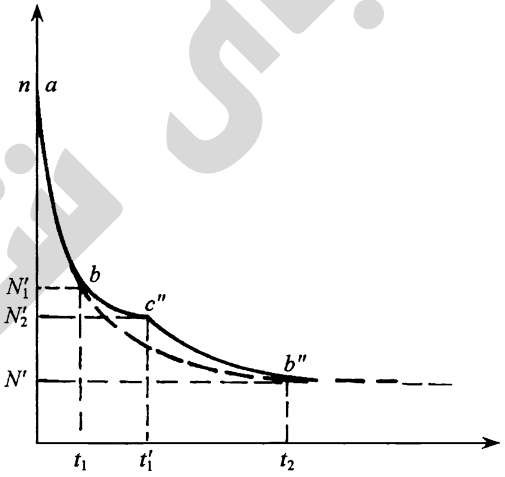

Fig. 12.12 Variation process of particle concentration (5)

(2) Sudden disappearance of the increased particle generation rate

As shown in Fig. 12.11, the new increased particle generation rate will increase the indoor particle concentration to point c', and then it disappears. If its original curve is a rising curve bc' (its mathematical expression is the same as the former expression of curve bc), the following new process will begin with N_2' as its initial concentration, and N is the steady-state concentration of $c'b'$. If the original curve is the decline curve cb'' (as shown in Fig. 12.12), the following new process will begin with N_2' at point c'' as its initial concentration, and N is the steady-state concentration of $c''b''$. The mathematical expressions of these processes won't be repeated here.

Through the analysis above, it is known that the variation progress of the particle concentration in cleanroom can be separated into two basic processes according to the practical measurement. One is the pollution process with indoor particle generation source, which is represented by the rising curve. The other is the

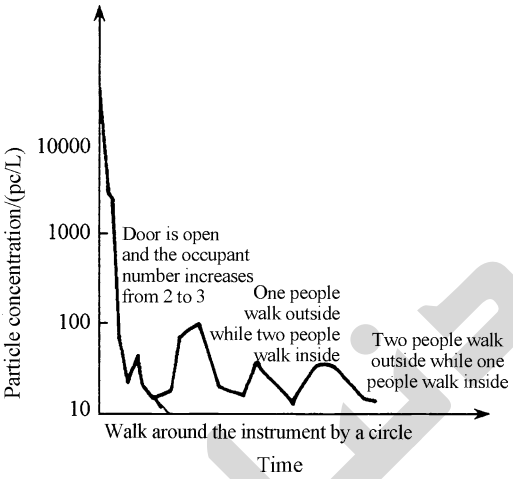

Fig. 12.13 Variation of measured particle concentration

self-purification process, which is represented by the decline curve. This is also the dynamic characteristic of the cleanroom. Figure 12.13 shows the variation of the particle concentration by measurement in cleanroom. It is clearly proved that the above conclusion is suitable for the reality.

According to the characteristic of the variation of particle concentration, the method to plot the curves was proposed by author.

With the instantaneous particle concentration, we obtain:

$$N_t = N \pm \Delta N\, \mathrm{e}^{-\frac{nt[1-s(1-\eta_r)]}{60}} \approx N \pm \Delta N\, \mathrm{e}^{-\frac{nt}{60}}$$

So we obtain

$$\text{If } nt = 60, \quad then \quad \mathrm{e}^{-\frac{nt}{60}} = \frac{1}{\mathrm{e}} = 0.362$$

$$\text{If } nt = 120, \quad then \quad \mathrm{e}^{-\frac{nt}{60}} = \frac{1}{\mathrm{e}^2} = 0.135$$

$$\text{If } nt = 180, \quad then \quad \mathrm{e}^{-\frac{nt}{60}} = \frac{1}{\mathrm{e}^3} = 0.050$$

$$\text{If } nt = 240, \quad then \quad \mathrm{e}^{-\frac{nt}{60}} = \frac{1}{\mathrm{e}^4} = 0.018$$

$$\text{If } nt = 300, \quad then \quad \mathrm{e}^{-\frac{nt}{60}} = \frac{1}{\mathrm{e}^5} = 0.008$$

and so on.

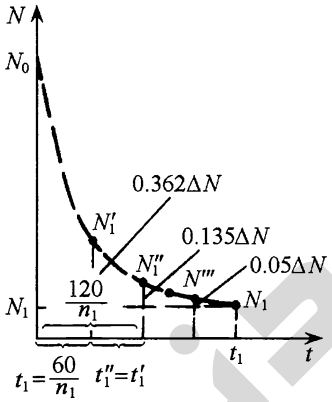

Fig. 12.14 Plot of the curve for the self-purification process

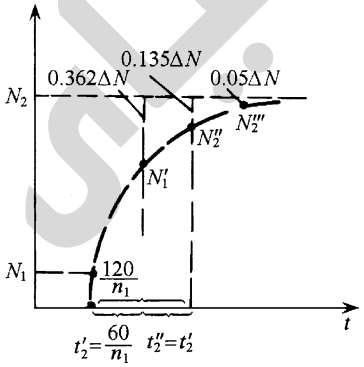

Fig. 12.15 Plot of the curve for the pollution process

Then the curve of the variation of the particle concentration can be drawn on the coordinate paper, as shown in Fig. 12.14. Firstly, the self-purification time t and the steady-state particle concentration N_2 should be calculated. Secondly, interception $\frac{60}{n_1} . = t_1'$ is made on the abscissa and interception $\Delta N \times 1/\mathrm{e} = 0.362\Delta N$ is made on the ordinate from N_1 (the original concentration N_0 is known). Their intersection point should be the point $N_1{}'$ on the variation curve of particle concentration. Similarly, interception of $120/n_1$ is made or the abscissa of $t_1{}'$ is directly prolonged by one time, namely, $t_1{}' = t_1{}''$, and the intersection point with the $0.135\triangle N$ is $N_1{}''$ and so on. Then, when points $N_0, N_1{}', N_1{}'', N_1{}'''$, and N_1 are connected, the variation curve of particle concentration can be obtained. Of course, with the curve connecting points N_0, $N_1{}'$, $N_1{}''$, and $N_1{}'''$, the line parallel with the abscissa and tangential to this curve at point N_1 can be plotted, so that the self-purification time t_1 can be obtained in turn.

If the indoor particle generation rate increases from G_1 to G_2 after the particle concentration reaches stable, the new steady-state particle concentration can also be obtained with the known value of G_2. So the curve of pollution process can also be drawn, as shown in Fig. 12.15. Unlike the curve of self-purification, the points $N_1{}'$ and $N_1{}''$ are obtained with the interception downwards from point N_2. When points N_1, $N_2{}'$, $N_2{}''$, $N_2{}'''$, and N_2 are connected, the curve of pollution process can be obtained.

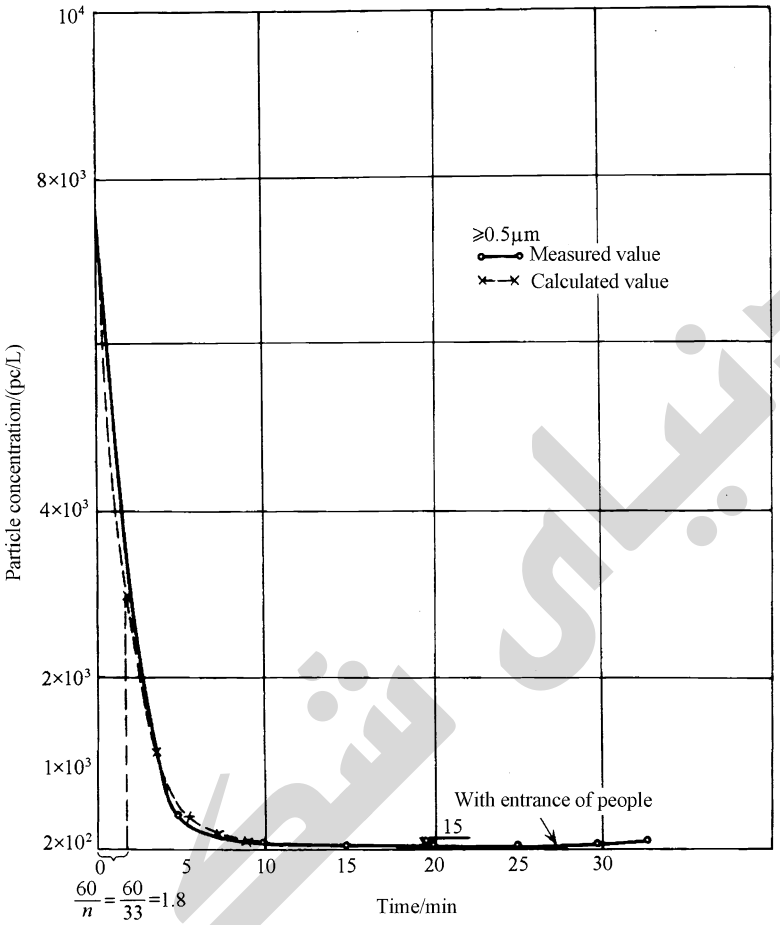

Fig. 12.16 Comparison between the theoretical process and the actual process (1)

The theoretical calculation results accord well with the actual measurement results. Comparison between the theoretical process and the actual process is shown in Figs. 12.16 and 12.17.

12.3 Characteristic Curve of Nonuniform Distribution

A series of curves can be obtained with Eq. (11.15), as shown in the Figs. 12.18, 12.19, 12.20, 12.21, 12.22, 12.23, 12.24, 12.25, and 12.26. They can reflect the relationship between the nonuniformity coefficient and several characteristic parameters of the cleanroom. They are called as the characteristic curve of the nonuniform distribution in cleanroom [1].

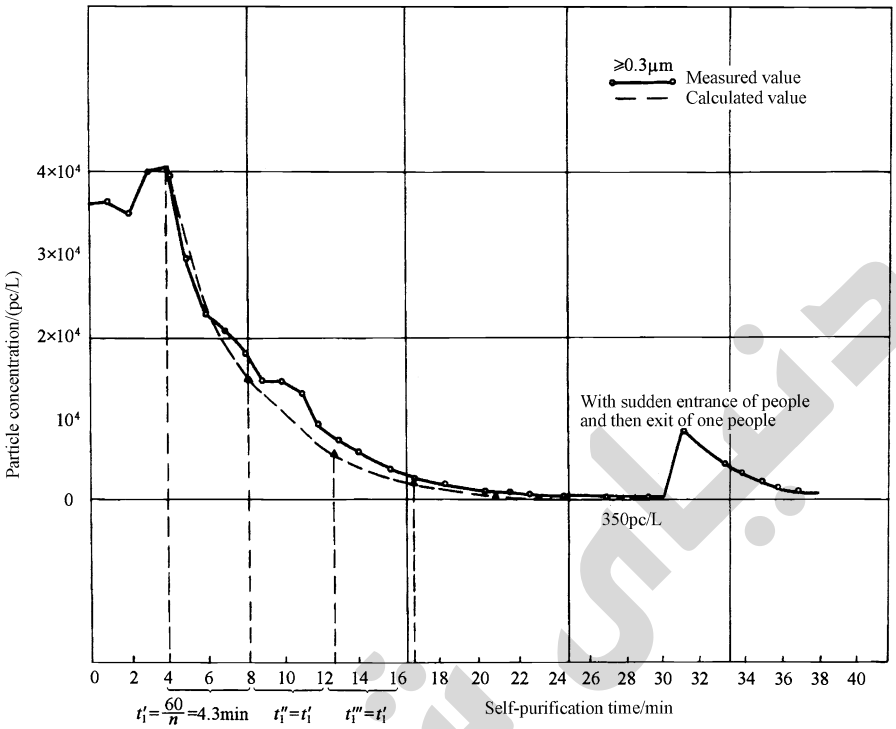

Fig. 12.17 Comparison between the theoretical process and the actual process (2)

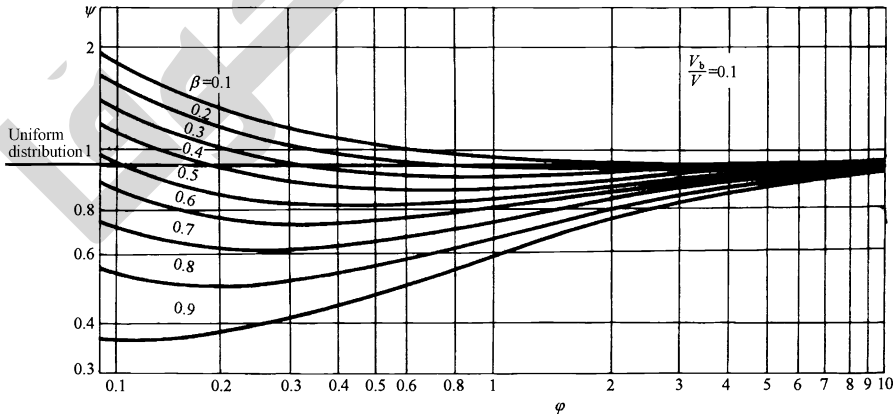

Fig. 12.18 Characteristic curve of nonuniform distribution (1)

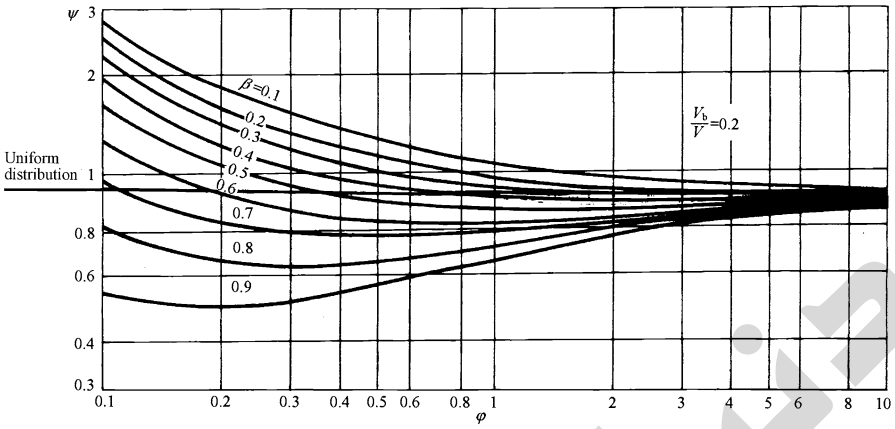

Fig. 12.19 Characteristic curve of nonuniform distribution (2)

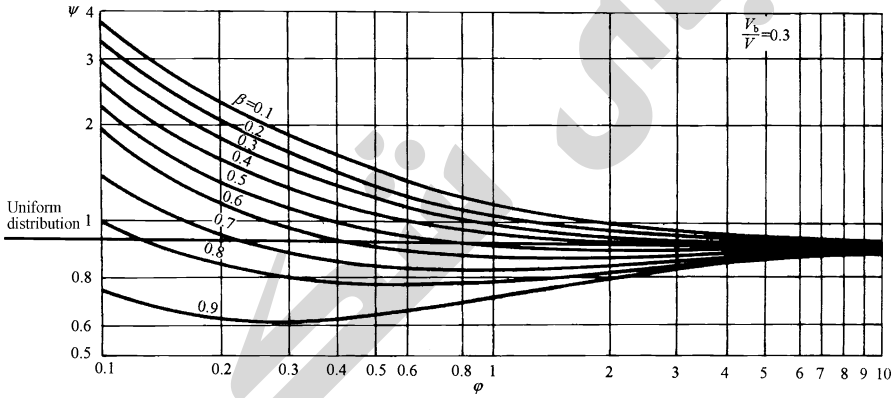

Fig. 12.20 Characteristic curve of nonuniform distribution (3)

It can be observed from these characteristic curves:

1. In all conditions, the bigger the value of β is, the smaller the nonuniformity coefficient ψ is. That means if the particle generation source can be placed in the mainstream area as possible, the average particle concentration indoors will be smaller.
2. For the turbulent flow cleanroom, V_b/V is usually larger than 0.5. So the bigger the value of φ is, the smaller the uniformity coefficient ψ will be, and ψ is approaching 1. This means the air supply outlet with large induction ratio should be installed in the turbulent flow cleanroom, so that the airflow indoors will be well mixed, and uniform dilution effect can be realized as much as possible. Thus the particle concentration is closer to the calculated result with the expression of uniform distribution.

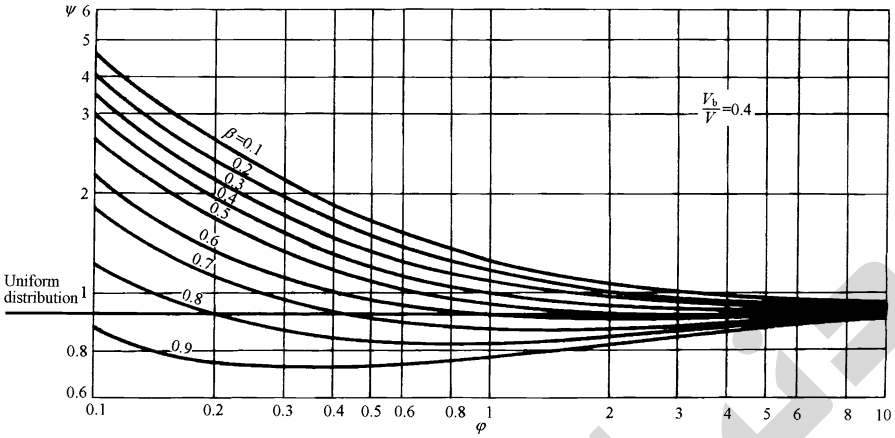

Fig. 12.21 Characteristic curve of nonuniform distribution (4)

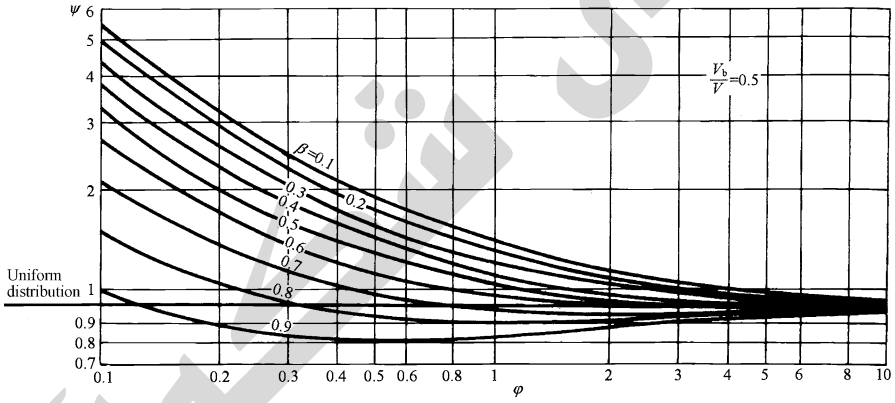

Fig. 12.22 Characteristic curve of nonuniform distribution (5)

3. For the unidirectional flow cleanroom, $V_b/V < 0.1$. The smaller the value of φ is, the lesser the uniformity coefficient ψ will be, which is smaller than 1. This means airflows are already parallel in the unidirectional flow cleanroom; the inducted airflow is expected not to be large, which disturbs the unidirectional parallel flow. On contrary, the smaller the induced airflow is, the more stable the unidirectional parallel flow will be, and the lower the particle concentration will be.
4. For the cleanroom when V_b/V is between the two above values (usually it is the cleanroom with high air cleanliness level), the value of φ should be an intermediate value, so that the uniformity coefficient ψ can be minimum.

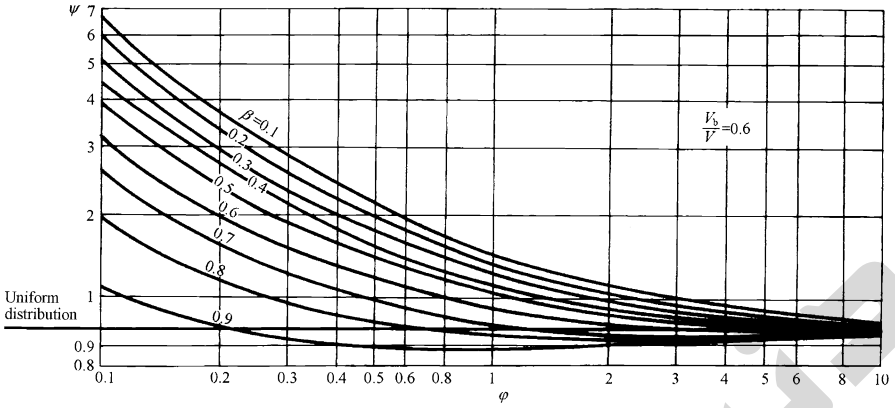

Fig. 12.23 Characteristic curve of nonuniform distribution (6)

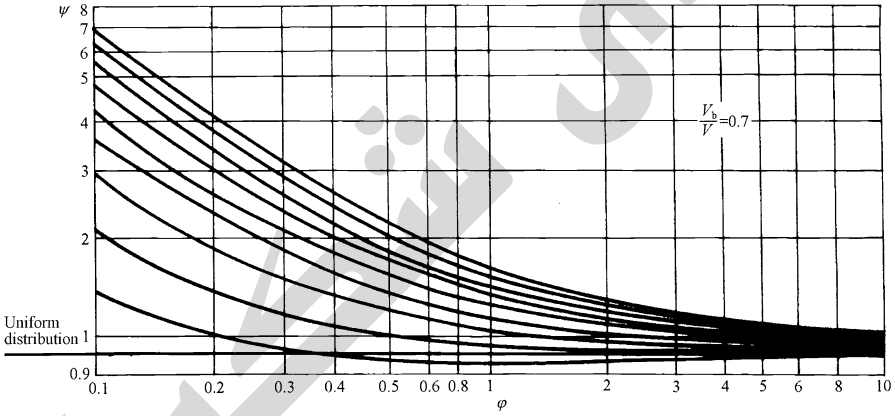

Fig. 12.24 Characteristic curve of nonuniform distribution (7)

12.4 Inhomogeneity of Concentration Field

12.4.1 Concentration Ratio Between the Mainstream Area and the Return Air Area:

$$\frac{N_c}{N_a} = \frac{N_a + \frac{G_a}{(Q+Q')}}{N_a} = 1 + \frac{G_a}{\frac{(Q+Q')}{\frac{N_s Q + Q'(G_a{}' + G_b{}')}{Q}}}$$

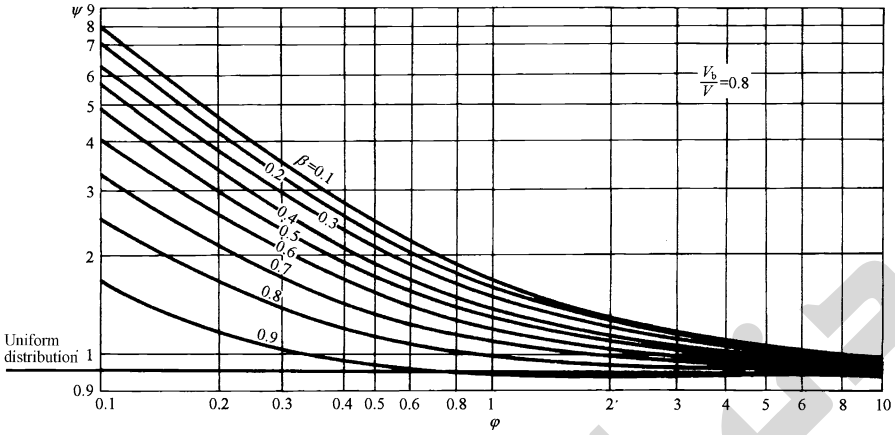

Fig. 12.25 Characteristic curve of nonuniform distribution (8)

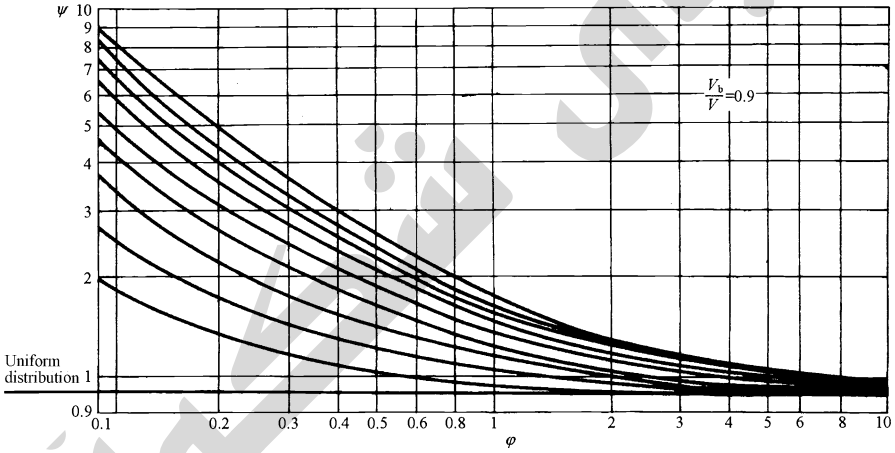

Fig. 12.26 Characteristic curve of nonuniform distribution (9)

When the concentration of supplied air N_s is omitted, then:

$$\frac{N_c}{N_a} \approx 1 + \frac{\frac{G_a}{Q+Q'}Q}{Q'(G_a{}' + G_b{}')} = 1 + \frac{\frac{G_a}{1+\varphi}}{\frac{G_a Q'}{Q(1+\varphi)} + G_b}$$

$$= 1 + \frac{G_a}{1+\varphi}\frac{Q(1+\varphi)}{Q[G_a\varphi + G_b(1+\varphi)]}$$

$$= 1 + \frac{\beta G_0}{G_0(1-\beta)(1+\varphi) + G_0\varphi\beta}$$

$$= 1 + \frac{\beta}{(1-\beta)(1+\varphi) + \beta\varphi}$$

$$= \frac{1+\varphi}{1+\varphi-\beta}$$

So,

$$\frac{N_a}{N_c} \approx 1 - \frac{\beta}{1+\varphi} \tag{12.1}$$

It is clear that for different values of β and φ, N_a/N_c is different. But for the turbulent flow cleanroom where the air change rate is not too big, on average $\varphi = 1$–2 and β will be about 0.5 (see details in Chap. 13). Inserting them into the equation above obtains:

$$\frac{N_a}{N_c} = \frac{1.5}{2} \sim \frac{1.5}{3} \approx 0.8$$

For cleanroom with large air change rate and several air supply outlets, on average $\beta = 0.6$–0.7 and $\varphi = 0.7$–1. Inserting them into the equation above obtains:

$$\frac{N_a}{N_c} = 0.6 - 0.65$$

The result is consistent with the measurement data by relevant units mentioned in Chap. 11.

12.4.2 Concentration Ratio Between the Mainstream Area and the Vortex Area:

$$\frac{N_b}{N_a} = \frac{N_a + G_a{}' + G_b{}'}{N_a} = 1 + \frac{G_a{}' + G_b{}'}{N_a}$$

When the concentration of supplied air N_s is also omitted, then:

$$\frac{N_b}{N_a} \approx 1 + \frac{Q}{\varphi Q} = 1 + \frac{1}{\varphi} \tag{12.2}$$

For common turbulent flow cleanroom, $\varphi = 1$–2. Inserting them into the equation above obtains:

$$\frac{N_b}{N_a} = 1.5 - 2$$

If the number of air supply outlets increases, take $\varphi = 0.7$, so we obtain:

$$\frac{N_b}{N_a} = 2.44$$

In the actual measurement, the measuring points are usually placed in the mainstream area and the vortex area, so N_b/N_a can reflect the extent of the maximum deviation of the measured concentration field caused by the nonuniform distribution. In the measurement process, it is found that if the measuring points for the working area are placed in the vortex area or on the edge of the mainstream flow region, it is easily influenced by the vortex pulsation. The ratio of the measured concentrations of different measuring points or the values of the same measuring point will be different from about 1.5 times, or even two times as the maximum. For more air supply outlets, it will be more than two times, which is roughly equivalent to the above calculated value of N_b/N_a.

From the above analysis, for a turbulent flow cleanroom, the difference of measured concentrations will be within one time because of the influence of the inherent characteristic of nonuniform distribution, which is allowed. There are also studies abroad [2] that according to the difference of the measured data, the concentration field is nonuniform, and it is suggested that the measurement should be performed at multipoints and multiple times.

12.4.3 Concentration Ratio Between the Vortex Area and the Mainstream Area:

$$\frac{N_b}{N_c} = \frac{N_a + G_a{}' + G_b{}'}{N_a + G_a{}'} = 1 + \frac{G_b{}'}{N_a + G_a{}'} \approx 1 + \frac{1-\beta}{\varphi}$$

The expression shows that $N_b > N_c$. By substituting specific data, it is easy to find that N_b is larger than N_c by 60 % or even 100 %.

12.4.4 Concentration Ratio Between Uniform Distribution and Nonuniform Distribution

The nonuniformity coefficient ψ is defined as the ratio of the particle concentration between the uniform distribution and the nonuniform distribution. For the turbulent flow cleanroom, ψ is usually within ± 0.5, which is shown in Table 13.16. So it is acceptable if the difference between the results calculated by the uniform distribution method and experimentally measured concentration is within a half time, because they are still in the fluctuation range of nonuniform distribution. This is not necessarily the problem of calculation.

It is known from Eq. (11.1) that:

$$\begin{aligned} N_c &= N_a + \frac{G_a}{Q + Q'} \\ &= \frac{\varphi G_a}{Q(1+\varphi)} + \frac{G_b}{Q} + \frac{G_a}{Q(1+\varphi)} + N_s \\ &= \frac{1}{Q}(G_a + G_b) + N_s = \frac{G_0}{Q} + N_s \end{aligned} \tag{12.4}$$

It is shown that the concentration in the return air area is the average concentration with uniform distribution. However, the real average concentration, i.e., the average concentration with nonuniform distribution, can be larger than that with uniform distribution ($\varphi > 1$) or smaller than it ($\varphi < 1$). So the real average concentration can be both bigger and smaller than that in the return air area.

Many actual measurements also show that the indoor average concentration measured in cleanrooms with relatively uniform airflow or multiple air supply outlets is often lower than the concentration in the return air area. In cleanroom with poor air distribution, the measured average concentration is often higher than that in the return air area. This indicates that, the correction coefficient of the calculated results on uniform distribution can be smaller or bigger than 1. When correction is made along the single direction based on the calculated results of uniform distribution will result in the conclusion far from reality.

It can be observed from Fig. 12.27 that line A is the calculated results with as-built and at-rest states with the theory of uniform distribution. Polyline B corresponds with the measured values with as-built and at-rest states. Polyline C is an example of the calculated particle concentration with the theory of nonuniform distribution in a common cleanroom. In this kind of cleanroom, when the air change rate exceeds 120 h^{-1}, the number of air supply outlets should be increased correspondingly. The mainstream area will extend to the whole working area, so the indoor average concentration can be calculated with the concentration of the mainstream area. The calculated concentrations can be plotted as the polyline D, which is closer to the actual measurement. It is worthy to point out that the turning points exit in the measured data in the studies at home and abroad [3]. And the air change rates at the turning point are close to each other, which has not been paid attention to and analyzed. This phenomenon that appeared in the actual measurement has not been explained and proved by theory. Now with the above analysis and theoretical calculation, the turning point on the calculated polyline is close to that of the measured polyline, so it has been illustrated from theory.

It is indicated that in the real circumstance, which is under the nonuniform distribution condition, there is a polyline relationship between the particle concentration in the working area and the air change rate of the cleanroom. It is not an ideal linear relationship with the uniform distribution condition. This *N*–*n* polyline relationship has been the basic rule of the cleanroom.

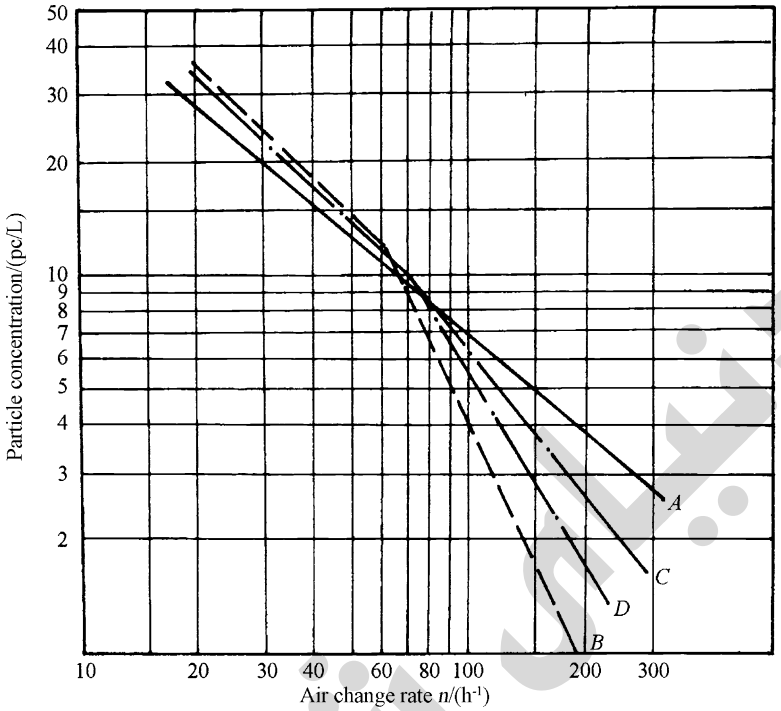

Fig. 12.27 Comparison of the calculated concentration by two distributions with the actual measurement

12.5 Particle Load Characteristic of Fresh Air

According to the concept of three-stage air filtration on the fresh air passage, the particle load characteristic of fresh air should be understood for further application of this concept.

12.5.1 Effect of Three-Stage Air Filtration for Fresh Air

For places with HEPA filter as the final filter, it can be observed from Fig. 12.2 that when three-stage air filtration is used for fresh air so that the comprehensive efficiency can be increased by an order of magnitude, it is equivalent to the condition that the atmospheric particle concentration will be lowered by an order of magnitude. In this case, its influence on the indoor particle concentration can be ignored. In other words, for a common cleanroom, the feature of three-stage air filtration is not to reduce the indoor particle concentration.

For places with sub-HEPA filter as the final filter, it can be shown from curves 2–3 in the figure that, when the comprehensive efficiency can be increased by an order of magnitude, it is equivalent to the condition that the atmospheric particle concentration will be lowered by an order of magnitude. In this case, the indoor particle concentration can be lowered by an order of magnitude.

For places with medium-efficiency filter as the final filter such as $0 < \eta_3 < 0.5$, the indoor particle concentration will reduce inversely by more than one order of magnitude after three-stage air filtration for fresh air is used.

The above conclusion is shown with the following examples. Table 12.1 shows an example of a cleaning air-conditioning system.

Table 12.2 is an example of a common air-conditioning system, as shown in Fig. 12.28.

The results indicate that, in order to reduce the particle concentration by a half in a room with a common air-conditioning system, where final filter is not installed, air filter with efficiency $\eta_3 = 0.3$ should be installed at every air supply outlet. In this specific system, there are ten air filters with the same airflow rates. If air filters are not installed at the air supply outlets and combined filters are only installed for fresh air (e.g., one coarse filter and one medium-efficiency filter, or one coarse filter and one high- and medium-efficiency filter, are combined in the air handling unit of fresh air) with the comprehensive efficiency $\eta_0 = 0.62$, the effect of lowering the indoor particle concentration will be the same as the measures to install air filters on every air supply outlet, but the ratio of the number (assuming the rated air volumes are the same) of filters is 2:10. Meanwhile, the efficiency of bacterial filtration is about 80–90 %. If three-stage air filtration with sub-HEPA filter is used, $\eta_0 = 0.97$. Not only the indoor particle concentration can decrease to 1/10, but also the efficiency of bacterial filtration can reach up to 99.9 %.

12.5.2 Particle Load Ratio of Fresh Air

In order to quantitatively study the economic effects of three-stage filtration of fresh air, the concept of "particle load ratio of fresh air" is proposed [4]. It can be expressed with α, then we obtain:

$$\alpha = \frac{\text{Particles deposited on various components brought by fresh air}}{\text{Total quantity of particles deposited on various components}} \tag{12.5}$$

For the system shown in Fig. 12.29, coarse filter is installed on the return air passage (in some cases, return air does not go through the coarse filter, as shown with the dotted line in Fig. 12.28). The following calculation is performed ($\eta_0{}'$ in the picture is neglected first):

The atmospheric dust weighing method is used during calculation. In the figure, M' is the weighing concentration of atmospheric dust, mg/m^3; η_1' denotes the

Table 12.1 Relationship between the indoor particle concentration (#/L) and the concentration of fresh air for the cleaning air-conditioning system under different conditions

	$S = 0.7$				$S = 0.85$			
	$M = 10^6$		$M = 3 \times 10^5$		$M = 10^6$		$M = 3 \times 10^5$	
Condition	Operational state ($G_m = 0.65 \times 10^5$)	At-rest state ($G_m = 0.17 \times 10^5$)	Operational state, as left	At-rest state, as left	Operational state, as left	At-rest state, as left	Operational state, as left	At-rest state, as left
Final HEPA filter	157	42	–	–	156	42	–	–
Final sub-HEPA filter ($\eta = 0.97$)	5,384	4,398	1,714	1,599	2,753	2,637	935	689
Final sub-HEPA filter ($\eta = 0.97$)	384	268	225	109	270	155	191	75
Three-stage filters for fresh air, comprehensive efficiency 0.97								

Table 12.2 Relationship between the particle concentration and the concentration of fresh air in common air-conditioning system

Combined scheme	η_0	η_1	η_2	η_3	η_n	η_r	N (#/L)
1	0	0.05	0.2	0	0.24	0.24	77,430
2	0	0.05	0.2	0.3	0.47	0.47	33,900
3	0.62	0.05	0.2	0	0.72	0.24	31,956
4	0.97	0.05	0.2	0	0.97	0.24	8,127

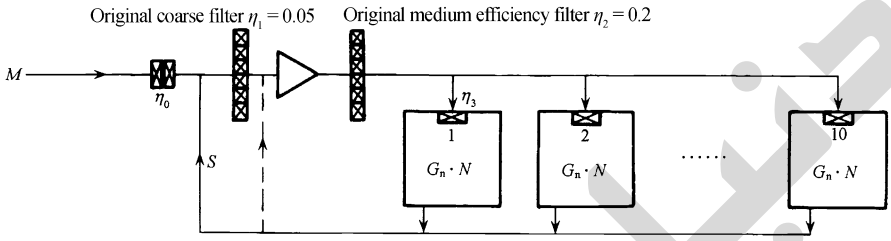

Fig. 12.28 One calculation example of the common air-conditioning system

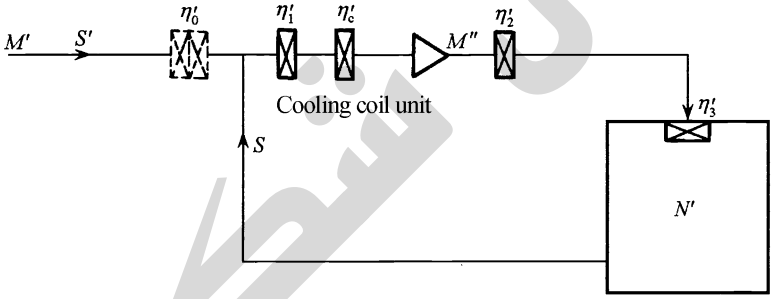

Fig. 12.29 General mode of cleaning air-conditioning system

arrestance of the first-stage coarse filter; $\eta_c{}'$ represents the "arrestance" of the cooler in air-conditioning system (If there are four rows of coils in the cooler or heater in air-conditioning system, the resistance can reach 100 Pa, which is even higher than that of a medium-efficiency filter. The particle deposition rate is large. This is why it is easily blocked as mentioned before. So we assume that it also has certain "arrestance" for the deposited particles.); $\eta_2{}'$ denotes the arrestance of the medium-efficiency filter; $\eta_3{}'$ refers to the arrestance of HEPA filter; S and S' denote the proportions of the return air volume and the fresh air volume in the total air volume, respectively, and $S' = 1-S$; and N' indicates the weighing concentration of indoor particles.

The particle load ratio in fresh air through the first-stage coarse filter is:

$$\alpha_1 = \frac{M'S'\eta_1{}'}{M'S'\eta_1{}' + N'S\eta_1{}'} = \frac{M'S'}{M'S' + N'S}$$

Table 12.3 Particle load ratio α of fresh air in air-conditioning systems

		N' (mg/m^3)			
S'	M' (mg/m^3)	0.1	0.15	0.20	0.25
0.1	0.2	0.18	0.13	0.10	0.08
0.1	0.3	0.25	0.18	0.14	0.12
0.1	0.4	0.31	0.23	0.18	0.15
0.1	0.5	0.36	0.27	0.22	0.18
0.1	0.6	0.40	0.31	0.25	0.21

Table 12.4 Particle load ratio α of fresh air in air-conditioning systems

	M' (mg/m^3)							
S'	1.0	0.9	0.8	0.7	0.6	0.5	0.4	0.3
0.2	0.962	0.957	0.952	0.946	0.938	0.926	0.910	0.882
0.3	0.977	0.975	0.972	0.968	0.963	0.955	0.945	0.928

For the particle load ratio through the cooler, since the upstream concentration changes from M' to $M'(1-\eta_1{}')$ and from N' to $N'(1-\eta_1{}')$, so we can obtain

$$\alpha_c = \frac{M'S'}{M'S' + N'S}$$

Likewise, for other medium-efficiency filters and HEPA filters:

$$\alpha_2 = \alpha_3 = \alpha_1 = \alpha_c = \alpha = \frac{M'S'}{M'S' + N'S} \tag{12.6}$$

Final filters are rarely used in simple air-conditioning systems, but the value of α does not changed.

This means the proportions of particles brought in by fresh are the same in the total amount of deposited particles on various components. Specific values are shown in Table 12.3. It can be seen that since the particle concentration of return air is relatively high, the value of α is relatively lower, which is about 0.3. Therefore, filtration should be strengthened not only for fresh air, but also for return air.

Since the value of N' in a cleaning air-conditioning system ranges from 0.01 to 0.00001 mg/m^3, it can be assumed 0.001 mg/m^3 and the calculated results are shown in Table 12.4. It is obvious that in cleaning air-conditioning systems, α is more than 0.9, namely, more than 90 % of the deposited particles on various components come from fresh air. In all, apparent technological and economic effects will be generated in any systems when α is lowered.

12.5.3 Relationship Between Particle Load Ratio of Fresh Air and Lifetime of Component

When the efficiency of air filters for fresh air increases, the indoor particle concentration can be lowered, and the lifetime of all components in the system can be prolonged.

With the particle load ratio α, the relative change of components' lifetime (time period to reach the standard dust holding capacity) can be calculated quantitatively. Suppose the change rate of the particle concentration in fresh air is denoted by β, which is

$$\beta = \frac{\Delta K}{K} \tag{12.7}$$

where K is the original penetration of the components;

ΔK is absolute value of the increment or decrement of the penetration.

If the original particle load ratio is α, and the decrement rate of fresh air is β, the decrease of particle deposition by fresh air is $\beta\alpha$. The total quantity of deposited particles on the component during the original lifetime period decreases to $1 - \beta\alpha$. If particles continue to deposit by $\beta\alpha$, under the fixed air volume when the standard dust holding capacity reaches 100 %, the ratio between the prolonged time and the original lifetime is $\Delta t = \beta\alpha/(1 - \beta\alpha)$. So the lifetime can be prolonged by $t = (1 + \Delta t)$ times. Also, suppose the particle concentration in fresh air increases by β, then the quantity of deposited particles by fresh air increases by $\beta\alpha$, and the total quantity of deposited particles during the original lifetime period increases to $1 + \beta\alpha$. When the standard dust holding capacity achieves 100 %, the quantity of deposited particles will decrease by $\beta\alpha$. Accordingly, if particles continue to deposit by $\beta\alpha$, the ratio between the extended time and the original lifetime is $\Delta t = \beta\alpha/(1 + \beta\alpha)$, and the lifetime will be reduced by $t = (1-\Delta t)$ times.

For an air-conditioning system, suppose the standard dust holding capacity is 100 g, 30 g of which are brought by fresh air; then $\alpha = 0.30$. If the particle concentration of fresh air reduces by half, which means $\beta = 0.5$, the deposited particles brought by fresh air during the period of original lifetime are only 15 g, and the total quantity of deposited particles becomes: 70 g (dust from return air) + 15 g (dust from fresh air) = 85 g. Since there can be 15 g more dust deposited within the lifetime, it is equivalent with the time 15/85 = 0.176 of the original lifetime. We can obtain:

$$\Delta t = \frac{\beta\alpha}{1 - \beta\alpha} = \frac{0.5 \times 0.3}{1 - 0.5 \times 0.3} = \frac{0.15}{0.85} = 0.176$$

So, the prolonged lifetime is 1.176 times of the original lifetime ($t = 1 + \Delta t = 1 + 0.176 = 1.176$).

As it is calculated above, the standard dust holding capacity is 85 g, 15 g of which is brought by fresh air, and $\alpha = 0.176$. When the change rate of the particle concentration increases by 100 %, $\beta = 1$ (change from 15 to 30 g), there will be 100 g particles deposited during the original lifetime. However, if the lifetime is calculated with the standard dust holding capacity, the deposited particles will be less by 15 g, which occupies 15 % of the original value 100 g, so the lifetime will also be reduced by 15 %.

With the above expression, we obtain:

$$\Delta t = \frac{\beta\alpha}{1+\beta\alpha} = \frac{1 \times 0.176}{1 + 1 \times 0.176} = \frac{0.176}{1.176} = 0.15$$

Therefore, the shortened lifetime is 0.85 times of the original one ($t = 1 - \Delta t = 1 - 0.15 = 0.85$).

For the system mentioned above, if combined filters with arrestance 0.99 are installed (its particle counting efficiency is more than 70 %) at the entrance of fresh air opening, the particle concentration in the fresh air will decrease by $\beta = 1 - 0.01/1 = 0.99/1$ for each original component, as shown Fig. 12.29 with the dot line. Thus, the prolonged lifetime of the original components, including the coarse filter at the mixing section of the fresh air and return air, air cooler, and medium-efficiency filter, becomes:

$$\Delta t = \frac{\frac{0.99}{1} \times 0.3}{1 - \frac{0.99}{1} \times 0.3} = \frac{0.297}{0.703} = 0.42$$

It means that the lifetime becomes 1.42 times of the original one (1 + 0.42 = 1.42), which is rather remarkable.

For the air cleaning system, it is known from the first row of Table 12.4 that $\alpha_2 = \alpha_3 = \overline{\alpha} = 0.934$, and from the next row that $\overline{\alpha} = 0.96$. If air filter with efficiency $\eta_0{}'$ is not installed in the system, instead the efficiency $\eta_1{}'$ of the original fresh air filter increases from 0.7 to 0.99, the prolonged lifetime for air cooler, medium-efficiency filter, and HEPA filter will be:

$$\Delta t = \frac{\frac{0.3 - 0.01}{0.3} \times 0.934}{1 - \frac{0.3 - 0.01}{0.3} \times 0.934} = 9.3$$

$$\Delta t = \frac{\frac{0.3 - 0.01}{0.3} \times 0.96}{1 - \frac{0.3 - 0.01}{0.3} \times 0.96} = 12.9$$

That means the lifetimes are extended to 10.3 times and 13.9 times of the original value, respectively.

By economic comparison [4], the scheme of three-stage filtration is cost-saving (cost of installation and operation) and energy-saving compared with the scheme where the efficiency of air filters at the air supply outlet increases only.

With the combined scheme in Table 12.2 as an example, the result is as follows (see details from Ref. [4]):

$$\frac{\text{Expense of scheme 4}}{\text{Expense of scheme 2}} = 0.78 - 0.85$$

$$\frac{\text{Electrical energy consumption of scheme 4}}{\text{Electrical energy consumption of scheme 2}} = 0.83$$

References

1. Xu ZL (1979) Calculation method for the non-uniform distribution in cleanroom. J HV&AC 4:15–21 (In Chinese)
2. Sato E (1976) Status of industrial cleanroom. J Jpn Air Clean Assoc 13(8):32–41 (In Japanese)
3. Hayakawa K, Aoki H (1974) Study of cleanroom (2). J SHASE Jpn 48(2):13–88 (In Japanese)
4. Xu ZL, Zhang YZ (1997) Three stage filtration in fresh air handling for better IAQ. J HV&AC 1:5–9 (In Chinese)

Chapter 13
Design Calculation of Cleanroom

Both the uniform and nonuniform distribution theories of cleanroom have been introduced. In order to meet the need of practical application, the method and procedure of specific analysis calculation will be given in this chapter.

13.1 Determination of Indoor and Outdoor Parameters for Calculation

13.1.1 Atmospheric Dust Concentration

Through the discussion about atmospheric dust in Chap. 2 and the at-rest state characteristics of the cleanroom in Chap. 12, the following two points should be clear:

1. Generally, the corresponding atmospheric dust concentrations for three typical areas at present are 0.75×10^5 #/L, 10^5 #/L, and 2×10^5 #/L, respectively. The highest is about 10^6 #/L, which is the concentration with the situation of most severe pollution. Since the beginning of this century, the concentration reduces about one third.
2. For the cleanroom with air cleanliness level equal to or lower than Class 100, when the atmospheric dust concentration is under 10^6 #/L, the effect of the variation of this concentration on the particle concentration in the cleanroom can be ignored.

Therefore, the atmospheric dust concentration for design of cleanroom can be determined as follows:

(1) For HEPA cleaning system with air cleanliness level equal to and higher than Class 5, in order to ensure the safety of the cleanroom in whatever outdoor situations (except the situation with extremely severe pollution), the design value of atmospheric dust concentration ought to be $M = 10^6$ #/L. When three-stage

Z. Xu, *Fundamentals of Air Cleaning Technology and Its Application in Cleanrooms*,
DOI 10.1007/978-3-642-39374-7_13, © Springer-Verlag Berlin Heidelberg 2014

filtration systems are placed on the passage of fresh air (see Chap. 12), the local specific atmospheric dust concentration can be used for calculation.

As for the atmospheric dust concentration for HEPA cleaning system, there is no single value given explicitly in foreign literatures, and it was pointed out that the variation results in the inconvenience of the design process. However, the single value 10^6 was suggested in the past by author (see the research report "Calculation of cleanroom" printed in 1977 at Institute of HVAC, China Academy of Building Research), which brings convenience for design calculation and also has high safety coefficient. When the explicit single value of atmospheric dust concentration is given for the HEPA cleaning system, there is no need to search for the data in this aspect.

(2) For a non-HEPA cleaning system, it is not economic to use $M = 10^6$ #/L for design since the atmospheric dust concentration affects the concentration of cleanroom a lot. It is better to choose the actual concentration. Of course, filtration of fresh air should be strengthened.

This chapter will not repeat discussing other problems about atmospheric dust.

13.1.2 Particle Generation Rate per Unit Volume of Indoor Air

13.1.2.1 Indoor Particle Source

The main generation sources of indoor particles include humans and building surfaces, equipment surface, and process. But practice has shown that particles are mainly released from human. The particle concentration in the cleanroom can be doubled or more when there is some action from people or when people enter in and out of the cleanroom. Rotating equipment is a particular example which generates a lot of particles. Electromotor (especially the one with carbon brushes), rotating components of gear, components of servo machine, hydraulic and pneumatic starter switch, and manual-controlled equipments will produce particles because of the friction between moving (turning) surfaces. An electromotor (less than 300 W) can produce particles about 2×10^5 to 5×10^5 # [1] for diameter 0.5 μm or bigger in one minute, which equals to the particles generated from an acting human. According to the measurements from Institute of HVAC at China Academy of Building Research, a furnace for phosphorus diffusion used in semiconductor process will increase the indoor particle concentration by six times or more. However, except the special cases, the particle generation rate from process equipment is considered less than that from people. Because in principle the process equipments acting as the particle generation source are not allowed to be placed in the cleanroom, or they only operate under the hood or near the return air opening. But special attention should be paid on the papers, especially the crumpled papers, because they will generate a lot of particles. So in the cleanroom, the usage of paper and the type of paper should be limited. Table 13.1 is the data of the generation rate of papers from foreign study [1]. Table 13.2 is the measured data from domestic study.

Table 13.1 One example of particle generation rate by paper [#/(min · paper)]

Condition / Particle size / Type	Move up and down	Tear	Knead broken
	>0.5 μm	>0.5 μm	>0.5 μm
Art paper	0	216,800	269,500
Sulfuric paper	0	75,600	15,400
Graph paper	15,400	491,400	1,193,500
Kraft paper	15,400	216,800	541,000
Copying paper	0	124,740	693,000
Newsprint paper	15,400	604,800	3,965,00
Winding paper	3,850	143,600	616,000

Table 13.2 Another example of particle generation rate from paper [#/(min · L)][a]

Species	Tore half a minute (≥0.3 μm)	Knead half a minute (≥0.3 μm)
Plain paper	4,410	10,220
Sulfuric paper	1,837	523

[a]It is measured at the distance of 0.5 cm from the center of particle generation source

Generally, indoor particles in the cleanroom mainly come from people, which accounts for 80–90 %. The second largest particle generation source is building, which accounts for 10–15 %. The proportion from supplied air is much less.

13.1.2.2 Calculation of Indoor Particle Generation Rate Per Unit Volume of Air

Next we will discuss two situations for people in static state (or almost static) and an acting static, respectively.

Situation for People in a Static State (or Basically)

The particle generation rate from people varies a lot with different actions. But it is easy to measure accurately when people are in a static state. After analyzing a large amount of data measured at home and abroad, it appropriate to use 10^5 #/(min·person) as the particle generation rate for people in static state. It is shown from the measured data in Table 13.3 [2] that data during the states of "standing" and "sitting" are similar.

Table 13.3 One example of particle generation from people

Action	#/(min · people) (≥0.5 μm)		
		Clean working cloth	
	Ordinary working clothes	General nylon suit	Full set of nylon suit covering from head to foot
Stand	3.39×10^5	1.13×10^5	5.58×10^4
Sit down	3.02×10^5	1.12×10^5	7.42×10^3
Wrist move up and down	2.98×10^6	2.98×10^5	1.86×10^4
Upper body anteflexion	2.24×10^6	5.38×10^5	2.42×10^4
Wrist free movement	2.24×10^6	2.98×10^5	2.06×10^4
Head move around	6.31×10^5	1.51×10^5	1.10×10^4
Twisting motion of upper body	8.50×10^5	2.66×10^5	1.49×10^4
Body bend	3.12×10^6	6.05×10^5	3.74×10^4
Foot movement	2.80×10^6	8.61×10^5	4.46×10^4
Walk	2.92×10^6	1.01×10^6	5.60×10^4

Particle generation rate from building surface is tenth of that from human. According to the analysis between the measurement data and literature references, it is recommended that the particle generation rate from indoor surface represented by 8 m^2 floor is equivalent with that of a person in static state. In other words, the particle generation rate of every static-state person corresponds with eight times of that released from unit area of floor. According to dozens of measurement cases, it has been validated by author that the difference between the calculated indoor particle concentration with the above method and the measured concentration is very small. Deviations in most cases are smaller than that with nonuniform distribution method (see Ref. [3]).

The authors have validated tens of results and consider the gap between the dust concentrations measured actually and using the values above is the narrowest. Most examples have a smaller deflection than the inherent deviation of a nonuniform distribution (see details from the author's book [3]). With the development of processing of materials, the particle generation rate from the envelope structure is much smaller. Calculation with the above principle is much safer.

In order to facilitate the calculation process, the concept of particle generation rate per unit volume is put forward.

First of all, when the occupant density is only one person per unit square of floor and occupant is the only source of particles, what is the particle generation rate per unit volume of air? Assume the room height is 2.5 m, the particle generation rate per unit volume is:

$$\frac{1 \times 10^5}{2.5 \times 1} = 0.4 \times 10^5 \ \#/\left(\mathrm{m}^3 \cdot \mathrm{min}\right)$$

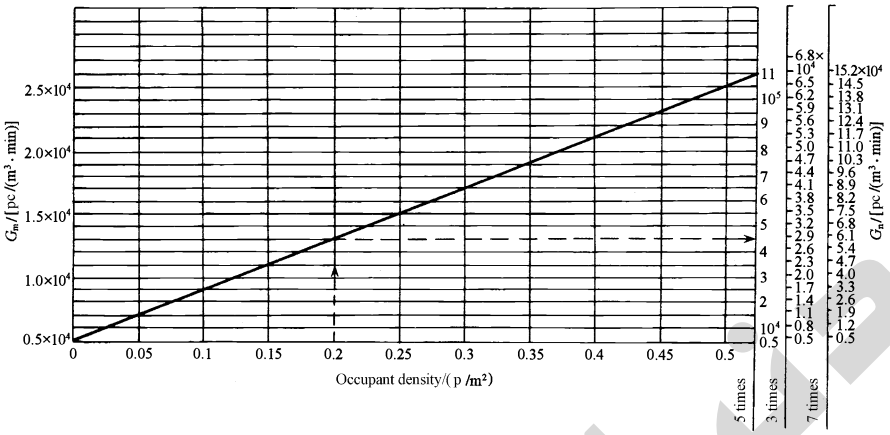

Fig. 13.1 Calculation charter of particle generation rate per unit volume in cleanroom

Second, convert the particle generation rate from surfaces into that from people. This means the particle generation rate from the indoor surface with the floor area β m^2 can be considered as that from one people. The whole surface can be thought as a certain number of people. Assuming P as the number of people and F as the area of cleanroom, then the equivalent occupant density is:

$$q' = \frac{\frac{F}{\beta} + P}{F}$$

This means the occupant density per square meter of floor is assumed q'. Since the particle generation rate per unit volume of air when the occupant density is one people per square meter is known, the particle generation rate per unit volume for people at static state when the occupant density is q' is

$$G_m = 0.4 \times 10^5 \times q' = 0.4 \times 10^5 \left(\frac{1}{\beta} + \frac{P}{F}\right) \tag{13.1}$$

where P/F is the actual occupant density, which can be indicated by q.

The calculation above is under the condition that the room height is 2.5 m. If the real room height is higher than 2.5 m, the uniform distribution of particles between the upper and lower spaces would be worse. Usually the concentration in the upper space is smaller. So it is unsafe to make correction simply with the inverse relationship between the concentration and the height. If calculating is still performed with the assumed room height 2.5 m, the particle generation rate per unit volume will be larger than the actual value, which is much safer. Although it is a little unsafe when calculation is performed with the assume room height 2.5 m although the actual height is less than 2.5 m, the conditions of room height less than 2.5 m are rare in practice.

According to Eq. (13.1), the straight line can be plotted as shown in Fig. 13.1, so that the value of G_m can be obtained directly with the occupant density q.

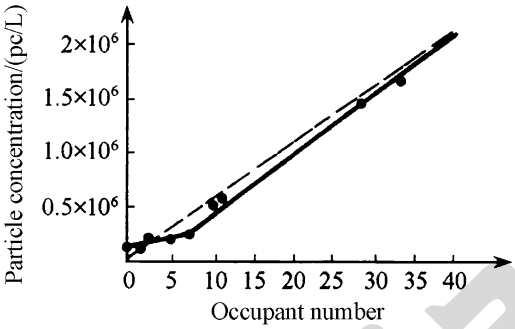

Fig. 13.2 One example for relationship between the particle concentration and the number of people

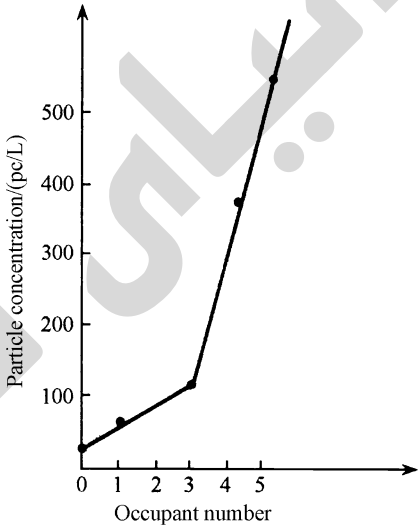

Fig. 13.3 Another example for relationship between the particle concentration and the number of people

From the figure, when $q = 0$, G_m is equal to the particle generation rate from indoor surface. G_m increases with the increase of q by different ratios, so the indoor particle concentration will increase with the increase of the number of people in a different rate (see details in Chap. 12). When the number of occupants is relatively small and q is relatively small, the increase rate between G_m and q will be small because the particle generation rate from indoor surface as a base (namely, the intercept in the figure) occupies a larger proportion. For example, when q changes from 0.01 to 0.04, which increases four times, G_m only changes from 0.55 to 0.65, which increases less than 20 %. When q changes from 0.4 to 0.6, which increases 50 %, G_m only changes from 2.1 to 2.9, which increases about 40 %. The increase rates between two parameters are very close. For HEPA cleaning system, the relationship between G_m and q can be considered similar as that between N and q. This is visible from Figs. 13.2 and 13.3. One figure is from foreign literature (Fig. 13.2 [4]). The dotted line is original. But according to the data points, polygonal line should be plotted (solid line). Figure 13.3 also shows the polygonal line plotted by author with the measured data by No. 10 Design Institute of the

former Fourth Ministry of Machinery and Industry. It means that for HEPA cleaning system with few/many persons, the relationship between N and q should be the case mentioned above.

Table 13.4 lists the particle generation rate recommended by this book and other related literatures.

According to various numbers of particle generation rates in Table 13.4, the particle concentrations at rest in 46 cases of various cleanrooms were calculated by author (G_m is considered as 1/5 of G_n in operational state) with the theory of uniform distribution. Here the specific number will not be presented and only list the comparison result is shown in Table 13.5.

From the above comparison, the particle generation rate for people at rest can be chosen as 10^5 #/(min·person), and the particle generation rate from surfaces represented by each square meter of floor is assumed 1.25×10^4 #/min, which are suitable for the current management and technical levels in cleanroom. It goes without doubt that the particle generation rate from people is greatly relevant to the types of clothes, and it is even influenced by the ways to treat clothes such as washing and blowing. According to the actual usage and measurement, the particle generation rate from nylon taffeta working clothes is the least. The particle generation rate from both cotton polyester and electro spinning clean working cloth is larger than that from nylon taffeta. And the electro spinning cloth should not be used only. If cotton polyester working cloth is added inside the nylon taffeta cloth, the particle generation rate from nylon taffeta cloth will be further reduced. From the aspect of clothing form, the particle generation rate from the connecting body clean working cloth is much smaller than the split-type clean working cloth. But it is not convenience to wear the connecting body clean working cloth as the split type. Moreover, the type with zipper will generate fewer particles than that with nylon hasp. The clean working cloth should not be kneaded during washing process, and it should be dried in the clean environment after washing.

With the improvement of the management level in cleanroom, the property (such as abrasion resistance and electrostatic elimination) of various materials improves further. In this case, the particle generation rates from people and surface mentioned above will be further reduced, and the above statistical values are not constant.

Situation When People Move

The mechanism of particle generation during the action of people is quite complex. But after analyzing various statistic data (such as Table 13.1), the ratio of particle generation rate between the intense activity state and the static state (or basically) is about ten times. In fact, not all indoor activities are intense. If the average value of all the actions is taken, the particle generation rate for the people with activity is considered to be five times the value of the static state (or basically). Then Eq. (13.1) will be changed correspondingly into

$$G_n = 2 \times 10^5 \left(\frac{1}{\beta} + \frac{P}{F} \right) \tag{13.2}$$

Table 13.4 Recommended particle generation rate

No.		1	2	3	4	5	6
Particle generation rate/[#/(min · people)]	During activity	10^6	10^6	10^6	3.3×10^6	10^5	5×10^5
	At rest (or basically)	–	–	–	–	–	10^5
Particle generation rate from surface/[#/(min · people)]		4.5×10^5	4.5×10^5	Not considered	Not considered	Not considered	1.25×10^4
Source		Ref. [5] and forum material from Japan electronic industry and measuring instrument exhibition in 1,975	Thematic information about integrated circuit factories in Japan through investigation by No. 10 Design Institute of the former Fourth Ministry of Machinery and Industry	Ref. [6]	Ref. [7]	Ref. [8]	This book

Table 13.5 Comparison of calculated results about several kinds of particle generation rates

No. of particle generation rate (same as Table 13.4)		Ratio between calculated and measured values (%)					
		1	2	3	4	5	6
Calculated value deviating from the measured value	$\leq \pm 30$	Deviation is too big, so comparison result is not given					56
	$\leq \pm 50$		7	50	28	10	71
	$\leq \pm 100$		22	74			85
	$\leq \pm 200$		50	74			

where $\beta = 40$. This expression is still represented by a straight line similar as that in Fig. 13.1, and the only difference is the vertical axis, which is shown in the right side of the figure. In this way, the value of G_n can be found with q.

When the particle generation rate for the people with activity is five times the value for people at rest, it is 5×10^5 #/(person·min). According to the measurement performed by No. 10 Design Institute of the former Fourth Ministry of Machinery and Industry, when people wear four types of common clean working clothes, the particle generation rates with common actions are 8.57×10^5 #/(person·min), 3.63×10^5 #/(person·min), 3.23×10^5 #/(person·min), and 1.83×10^5 #/(person·min), respectively. The average value is 4.3×10^5 #/(person·min), which is equivalent to the common particle generation rate in electronic industry. It is also close to the value which is five times the value for people at rest. It is of course that five times is considered by average. The magnification ratio will be different with different property of process and the intensity of occupant activity. The two extreme cases for lowest (the intensity of activity is extremely low, or people operate when sitting down and seldom stand up) and highest (the intensity of activity is higher than the ordinary level, or the activity is relative frequent) values are three times and seven times of the particle generation rate during at-rest state, respectively. The corresponding values are 3×10^5 #/(person·min) and 7×10^5 #/(person·min), which can be used for calculation. The relationships with three times and seven times of G_n can also be found in Fig. 13.1.

13.1.3 Fresh Air Ratio

The function of fresh air in air cleaning system is to meet the hygiene requirement, maintain the positive pressure, supply the local exhaust air volume, and make up the leakage air volume of the system.

From the aspect of sanitation, fresh air is often used to dilute the toxic gas and smell in air. The quantity of diluted air volume in the states of equilibrium is:

$$Q = \frac{L}{(C - C_0) \times 10^{-3}} \tag{13.3}$$

Table 13.6 Influence of CO_2 contents on human beings

CO_2 content/%	Influence on occupant
0.04	Normal air
0.5	Long-term safety limit
1.5	Physiological limit (metabolic disturbance with Ca and P). Work must be stopped
2.0	Deep breath is needed. The inspiratory airflow increases by 30 %
3.0	Work is worsened. Physiological function varies. Respiratory rate increases by 2 times
4.0	Breath becomes deeper and faster
5.0	Strong gasp. When it lasts for 30 min continuously, poisoning symptom will appear
7–9	The allowable tolerant limit. When it lasts for 15 min, people will be unconscious
10–11	People can adjust normally. When it lasts for 10 min, people will be unconscious
15–20	People can survive for more than 1 h
25–30	Breath will disappear. Blood pressure reduces. Coma occurs. Reflection and feeling disappear. People die within hours

Where

L is the harmful gas generated indoors (m^3/h);
C_0 is the concentration of harmful gas in the atmosphere (L/m^3);
C is the controlled concentration of toxic gas (L/m^3).

For cleanrooms where harmful gases are often generated with a large amount, the air volume of fresh air should be determined with the hygienic standard. For the common cleanroom, it should be determined mainly based on CO_2. The USA also specifies the adjustment of fresh air on the basis of CO_2 for air-conditioning system after 1980 [9].

According to the research by scholars from the former Soviet Union [10], in the closed room with artificial ventilation system, the oxygen content in air is often lower than normal value, which fluctuates between 17.4 and 20.5 %. It reaches its minimum value at dusk. CO_2 content exceeds 1–2 times of the standard value (0.06–0.09 %). It reaches to 0.15 % at dusk.

Tables 13.6, 13.7, and 13.8 show the influence of CO_2, O_2, and CO contents on human beings. Table 13.9 gives the exhaled carbon dioxide produced by people [11].

In terms of CO_2, the value of C_0 in Eq. (13.3) is usually taken as 0.3 L/m^3, but the data measured in city is often bigger than this value. C is usually taken as 1 L/m^3, which is specified in Japanese environmental control standard.

When the value of L is taken in the condition of light labor strength, the essential fresh air per person is:

$$Q = \frac{0.022}{0.0007} \approx 30 \text{ m}^3/\text{h}$$

This value was specified as the lower limit of fresh air volume in both the hygienic standard and the design specification for air-conditioning system. When

Table 13.7 Influence of O_2 contents on human beings

O_2 content/%	Influence on occupant
21	Normal
17	Long-term safety limit
15	Feeling of fatigue
10	Dizzy with short of breath
7	Unconsciousness, memory judgment malfunction
5	The lowest limit to maintain life
2–3	People die within several minutes

Table 13.8 Influence of CO contents on human beings

CO content		
%	ppm	Influence on occupant
0.0002	2	Normal
0.0025	25	Visual disorder
0.005	50	Long-term safety limit
0.01	100	With influence when exposed for 6 h
0.02	200	Headache occurs during 2–3 h. Insomnia by longer time
0.04	400	Deep breath and visual disorder. Headache during 1–2 h. Death by longer time
0.08	800	Headache, nausea, and dizzy during 45 min. Unconsciousness during 2 h. Die after 4 h
0.64	6,400	Headache during 1–2 min. Die after 10–15 min
1.28	12,800	Die after 1–3 min

Table 13.9 Relationship between the male labor intensity and the exhaled CO_2 quantity

Labor intensity	CO_2 exhalation volume/[m^3/(p·h)]	Exhalation volume for calculation/[m^3/(p·h)]
Quiet	0.0132	0.013
Extreme light labor	0.0132–0.0242	0.022
Light labor	0.0242–0.0352	0.03
Middle labor	0.0352–0.0572	0.046
Heavy labor	0.0572–0.0902	0.074

people's operation is taken into consideration, $L = 0.03$ m^3/(person·h) under the light labor strength, then $Q = 43$ m^3/h. In both the "Code for Design of Clean Room" and the former Soviet Union's standards for airtight workshop, the fresh air volume per person is set 40 m^3/h [10]. The value is set as 42.5 m^3/h in British relevant regulations, and 51 m^3/h in US Federal Standard 209. There are even specified 72–85 m^3/h in some standards [11].

As for the standard of fresh air volume, different opinions exist for a long time. Some people consider the fresh air volume as the only factor that influences the

indoor sanitary conditions. Although it is surely harmful for people's health with lack of fresh air, it is not appropriate to attribute the discomforts such as headache, eye ache, fatigue, dizziness, and general debility that appear in the closed workplaces to high concentration levels of CO_2 or insufficiency of fresh air by researches at home and abroad. According to the research [10], the possibility may increase for men to suffer from vegetative nervous disorder symptom and instability of blood pressure when they work in closed workplaces without windows. And there are several possible factors.

1. With special conditions with no windows, specific affect is posed on staff's body organisms, which causes unfavorably subjective sensations and psychological abnormality when people is isolated from outside, and decreases the general tension intensity of body organisms and immunologic functions. The total incidence is thus increased.
2. No natural light and lack of fresh air.
3. Negative ion content in the air is insufficient.
4. Trace of other kind of toxic gas is present.
5. Due to the filter media material, the manufacturing process, and the experimentation procedure, filters will have a special smell which emits into the air continuously.
6. Temperature and relative humidity are higher. Especially when the relative humidity increases, people may feel uncomfortable and may fall on the floor in the cleanroom.

Therefore, the conclusion about the issue of fresh air volume can be obtained only when comprehensive study is performed from several aspects.

From the aspect of relative risk for the occurrence of the sick building syndrome, the fresh air volume through experiment is obtained, which is shown in Fig. 13.4 [12]. It is clear that increasing the fresh air volume is beneficial to human health. The effect is obvious and stable only when it reaches more than 90 m^3/h (25 L/s) for each person.

Although this conclusion is not based on the cleanroom, it can be still used as the reference for the closed cleanroom. Because the pollutions in the cleanroom are similar as that in the sick buildings, they come from two aspects including people and indoor gaseous pollutants (not only CO_2).

For the convenience of use, especially when the precise number of people is unknown, fresh air volume can be considered as a percentage of the total air volume. The percentages are different according to the ventilation rate and occupational density, which are listed in Table 13.10 (round-off numbers are taken and the story height is taken as 2.5 m).

For general cleanroom, Japanese have claimed that it is acceptable to use 0.25 as the fresh air ratio, but it should be a little higher in view of hygienic standard [13]. However, the revised version of the standard "Code for Design of Clean Room" (GB50073-2001) in China did not present the values of fresh air ratios.

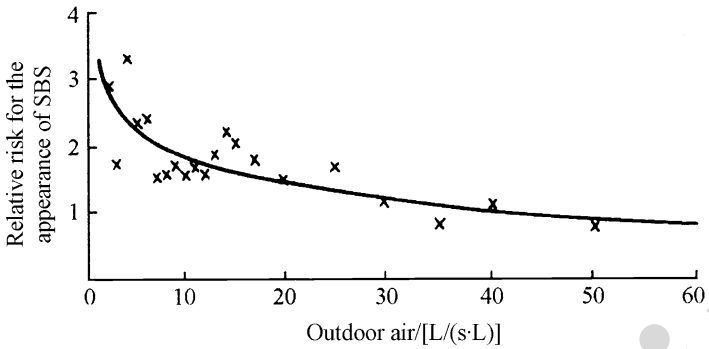

Fig. 13.4 Risk of the sick building syndrome expressed as the function of ventilation rate in 160 buildings in Sweden

Table 13.10 Relationship between the percentages of fresh air ratio (%) and the air change rate

Fresh air volume per person (m^3/h)	Occupant density (p/m^2)	Air change rate (h^{-1})									
		10	20	30	40	50	60	70	80	200	400
30	0.1	12	6	4	3	3	2	2	2	1	1
	0.2	24	12	8	6	5	4	4	3	2	1
	0.3	36	18	12	9	8	6	6	5	2	1
	0.4	48	24	16	12	10	8	7	6	3	2
40	0.1	16	8	6	4	4	3	3	2	1	1
	0.2	32	16	11	8	7	6	5	4	2	1
	0.3	48	24	16	12	10	8	7	6	3	2
	0.4	64	32	24	16	13	11	10	8	4	2
50	0.1	20	10	7	5	4	4	3	3	1	1
	0.2	40	20	14	10	8	7	6	5	2	1
	0.3	60	30	20	15	12	10	9	8	3	2
	0.4	80	40	28	20	16	14	12	10	4	2

The calculation of the fresh air volume in terms of positive pressure has been introduced in detail in the monograph "Design for the cleanroom" [3], which will not be discussed further here.

The method to determine the calculation parameters inside and outside of the room has been discussed. In Chap. 4, the filtration efficiency of air filter has been introduced in detail, which will not be repeated here.

13.2 Calculation of HEPA Cleaning System

This chapter will introduce the specific calculation procedures with the theory of nonuniform distribution theory mentioned in Chap. 11.

13.2.1 Calculation of the Value N

Here Eqs. (11.12) and (11.13) are listed again. With the condition of uniform distribution, we obtain:

$$N = N_s + \frac{60G \times 10^{-3}}{n}$$

With the circumstance of nonuniform distribution, we obtain:

$$N_v = N_s + \psi \frac{60G \times 10^{-3}}{n}$$

$$N_s = \frac{N_r ns(1-\eta_r) + Mn(1-s)(1-\eta_n)}{n} \tag{13.4}$$

where N_r is much smaller than M, so in the numerator of the above equation, the left item is much less than the right one. Thus, it can be considered that

$$N_s \approx M(1-s)(1-\eta_n) \tag{13.5}$$

where the meanings of each symbols and their determination methods can be referred to previous related chapter.

During the design calculation process, if N_s should be calculated based on parameters such as s, η_1 and η_2 which are unknown or cannot be fixed (e.g., when a practical project is not measured), a simplified method can be used with the equivalent concentration $M = 2 \times 10^5$–10^6 #/L.

For unidirectional flow cleanroom [$(1 - \eta_1)(1 - \eta_2)$ can be assumed as 0.5, and $(1 - \eta_3) = 0.00001$], we can obtain:

$$N_s = 0.02 \sim 0.1\ \#/\mathrm{L} \quad \text{when} \quad (1-s) = 0.02$$

$$N_s = 0.04 - 0.2\ \#/\mathrm{L} \quad \text{when} \quad (1-s) = 0.04$$

For turbulent flow cleanroom [$(1 - \eta_1)(1 - \eta_2)$ can be assumed as 0.5, and $(1 - \eta_3) = 0.00001$], we can obtain:

$$N_s = 0.2 - 1\ \#/\mathrm{L} \quad \text{when} \quad (1-s) = 0.2$$

$$N_s = 0.5 - 2.5\ \#/\mathrm{L} \quad \text{when} \quad (1-s) = 0.5$$

$$N_s = 5 - 5\ \#/\mathrm{L} \quad \text{when} \quad (1-s) = 1.0$$

From these numbers, we can consider that in Eq. (11.14) N_r is much smaller than the right item, so Eq. (11.13) can be approximately written as

$$N_v \approx \psi\left(N_s + \frac{60G \times 10^{-3}}{n}\right) = \psi N \tag{13.6}$$

which is the same form as Eq. (11.15). For high-efficiency air cleaning systems, if certain parameters are unknown, Fig. 13.4 can be used to find the common range of these parameters. The range given by the figure is wide, and the deviation between the valued found in the figure and the calculated value is around 10 %.

13.2.2 Calculation of the Value n

During the calculation of the air change rate with the given indoor particle concentration, the result with nonuniform distribution theory obtained by Eq. (13.4) can be expressed as the following expression, where n is replaced by n_v:

$$n_v = \psi\frac{60G \times 10^{-3}}{N_v - N_s} = \psi n \tag{13.7}$$

where

N_v is the indoor average particle concentration with nonuniform distribution theory required in the cleanroom;
n is the air change rate calculated by the uniform distribution theory;
n_v is the air change rate calculated by the nonuniform distribution theory.

Similarly, n can be found from Fig. 13.5 during simplified calculation process.

It should be illustrated that when the air cleanliness level is used to represent the requirement for the design, such as when air cleanroom with air cleanliness level Class 7 is designed, the value of N_v cannot be the maximum particle concentration. The particle concentrations for the cleanroom with a certain air cleanliness level are within a range. For example, it is between 35 and 350 #/L for air cleanliness level Class 7. It is obvious that it is hard to meet the requirement when the value 350 #/L is used. Furthermore, as the reason mentioned for the dynamic-to-static ratio in Chap. 15, the design value of the particle concentration ought to be 1/2–1/3 of the maximum value.

For unidirectional flow cleanroom, no matter what kind of air distribution theories are, n is determined by the air velocity at the cross section of the cleanroom. The air velocity at the cross section should be referred to the section about the lower limit of air velocity.

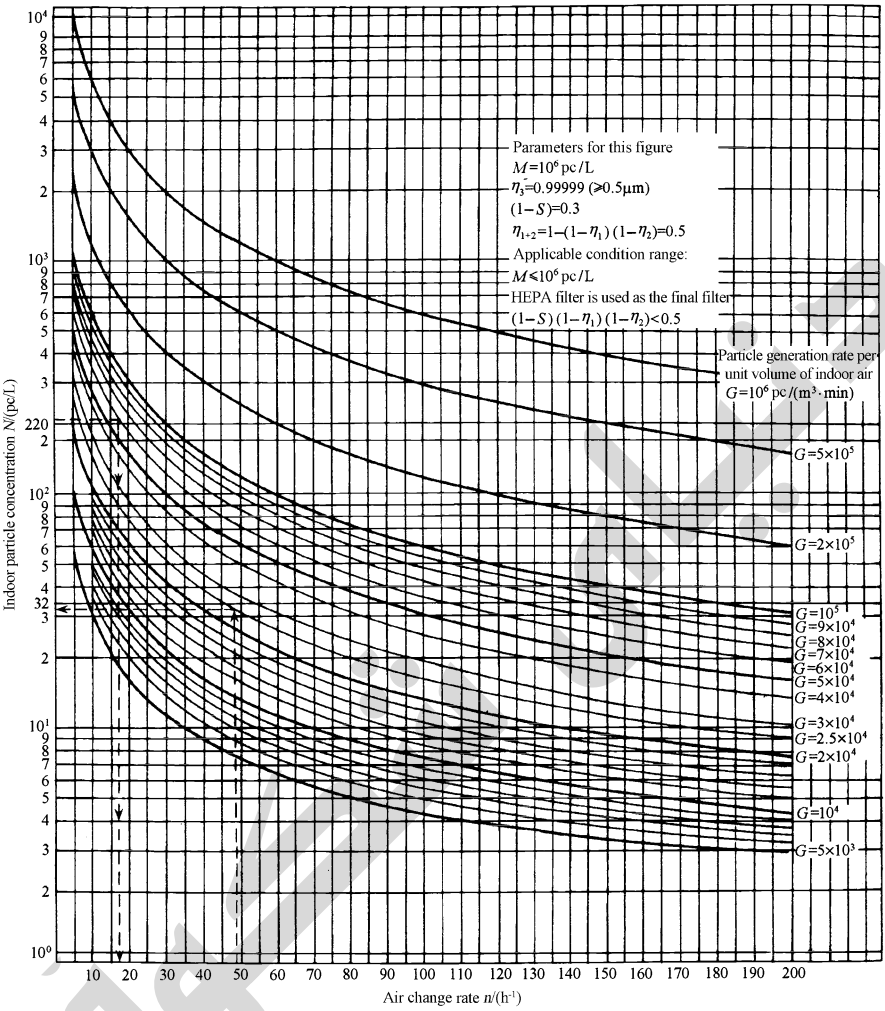

Fig. 13.5 Calculation graph of N–n in high-efficiency air cleaning cleanroom

13.2.3 Calculation of the Value Ψ

In order to calculate the uniformity coefficient ψ, the property curves in Figs. 12.18–12.26 can be used. When these curves are used, values of β, ψ, and V_b/V are needed. Although it is impossible to determine these coefficients precisely, a reference value can be given.

Table 13.11 Values of β

Area corresponding with one filter on the ceiling (larger value could be used if air supply outlet is not in the middle /m^2)		In unidirectional flow cleanroom, air is supplied with air supply outlets fully on the ceiling and air is returned at two lower bottom sides	0.97
≥15	0.3	In unidirectional flow cleanroom, filters are placed fully (the ratio of blowing area ≥ 80 %)	0.99
>10	0.4	Side supply and side return mode	0.5–0.7 (small value can be used when the distance between air supply outlets is more than 3 m)
>5	0.5–0.7		
>2	0.7–0.8	Orifice plate: when placed in the middle with area ≤ 1/2 of the ceiling area;	0.4
>1	0.8–0.9	when placed at both sides with area ≤ 2/3 of the ceiling area	
In unidirectional flow cleanroom, filters are placed in between (the ratio of blowing area ranges from 40 to 80 %)	0.9–0.99	Placed fully at the ceiling	0.9–0.95

13.2.3.1 β

This is proportion between the particle generation rate in mainstream area and the total particle generation rate. In practice it is a variable, so it is impossible to propose a fixed value.

If the location of particle generation source cannot be determined, the average method can be used. Let $\beta = 0.5$, or let $\beta < 5$ to ensure the safety, which means that the particle source is considered to be in the mainstream area.

It can also be considered from the aspect of the height covered by airflow. This is related to the area corresponded with filter. According to the flow boundary and the height overlapped with wall, values of β are listed in Table 13.11.

13.2.3.2 ψ

This is the ratio between the induced airflow rate from the vortex area to the mainstream area and the total air supply volume. For air supply outlet at the side, the equation used in the design manual of air conditioning can be referred to:

Table 13.12 Values of ψ

Area corresponding with one filter on the ceiling (larger value could be used if air supply outlet is not in the middle /m^2)		In unidirectional flow cleanroom, filters are placed in between (the ratio of blowing area is 60 %)	0.05
≥7	1.5	In unidirectional flow cleanroom, filters are placed fully (the ratio of blowing area ≥ 80 %)	0.02
5–7	1.4	Orifice plate: placed locally	1
3–5	1.3	placed fully	0.65
2.5–3	0.65	Diffuser	Value (ceiling supply mode) × (1.3–1.4)
2–2.5	0.3		
1–2	0.2	HEPA filter air supply with diffuser on ceiling: Good diffusion	Value (ceiling supply mode) × (1.3–1.4)
In unidirectional flow cleanroom, filters are placed in between (the ratio of blowing area is 40 %)	0.1	Poor diffusion	Value (ceiling supply mode) × (1.1)

$$\psi = 0.5\frac{\sqrt{F}}{d} - 1 \tag{13.8}$$

Where

F is the room's cross-sectional area corresponding with each air supply outlet (perpendicular to the flow)(m^2);
d is the equivalent diameter of the air supply outlet (m).

$$d = 1.13\sqrt{L_1 \times L_2} \tag{13.9}$$

where L_1 and L_2 are two side lengths of the air supply outlet (m).

For HEPA filter air supply outlet at the ceiling, due to the low height of room, the problem of overlapping also exists for flows between neighboring filters. It will be not suitable to use the equation of side air supply mode. Values of ψ are listed in Table 13.12 when the experimental data about the induction flow rate ratio at different distances from the air supply outlet under the air supply velocity 0.51 m/s, as well as the correction to the perforation ratio on the orifice plate, is referred to [14].

The data in the above table are obtained based on the diffuser air supply outlet with 484 mm × 484 mm HEPA filter, which is about 0.3 m^2.

The data above are also obtained according to the experimental curves for air supply velocity more than 0.51 m/s. If air velocity is below 0.5 m/s, which is

Table 13.13 Relationship between the air change rate (less than 10 h^{-1}) and the particle concentration

Air change rate (h^{-1})	12	10	8	6	4	3	2	1
Measured value (N)	1	1	1	2.5	7	15	25	70
Calculated value (N)	1	1.2	1.5	2	3	4	6	12

Table 13.14 Value of V_a (m^3)

	Number of top air supply outlets									
Room volume (m^3)	1	2	3	4	5	6	7	8	9	10
<5	3									
5	4									
10	5	8	9							
20	7	10	13	16	18					
30	8	12	15	18	20	24	26			
40	9	14	18	20	24	27	28	32	32	35
50	9	15	18	20	25	28	32	32	36	40
60	9	16	21	22	25	30	32	36	36	42
70	10	17	21	22	28	30	35	38	40	45
80	10	17	23	28	30	33	35	40	44	46
90	10	17	23	28	34	36	38	40	45	48
100	10	17	25	30	35	36	40	44	45	50
120	10	17	25	30	35	40	42	48	50	52

equivalent to the air change rate 10 h^{-1} for ordinary condition, the measured particle concentration has an apparent trend of increase compared with the calculated value based on uniform distribution theory. Table 13.13 is the comparison between the two values according to the measured data rearranged by author [15].

If the number of air supply outlets increases although the air supply velocity is very low, several coefficients influencing ψ will vary and opposite results may be obtained, namely, the particle concentration will be decreased greatly.

13.2.3.3 V_b/V

This is the ratio between the volume of vortex area and the room volume.

The value for top air supply outlet can be obtained with the value of V_a in Table 13.14 (if air supply outlet is not placed in the middle, V_b/V can be multiplied by the coefficient about 1.2).

The performance of top air supply outlets with diffuser plate varies a lot from each other due to the difference of diffusion angle. The value of V_b/V for a good diffusion plate is 0.6 times of the one without diffusion plate, while the value for the poorest one is 0.9 times.

The value of V_b/V for the diffuser can also be considered as 0.6 times of the top air supply outlet without diffuser plate.

Table 13.15 Value of V_b/V for orifice plate

	Airflow overlap height (m)				
	0.1	0.2	0.3	0.4	0.5
Full orifice plate	0.96	0.92	0.88	0.84	0.8
1/2 orifice plate	0.58	0.56	0.54	0.52	0.5
1/3 orifice plate	0.46	0.45	0.43	0.42	0.41
1/4 orifice plate	0.42	0.41	0.40	0.39	0.38

Table 13.16 Value of ψ (top air supply outlet)

	Turbulent flow	Unidirectional flow		
Air change rate (484 mm × 484 mm air filter in the air supply outlet has rated airflow 1,000 $m^3/h)/h^{-1}$	1 2 5 10 20 40 60 80 100 120 140 160 180 200	Air supply and return openings fully placed	Two lower bottom side air return	Two lower bottom side air return with nonuniform and unequal area
When air supply outlets are uniformly placed	>6 4.2 2 1.5 1.22 1.16 1.06 0.99 0.9 0.86 0.81 0.77 0.73 0.64	0.03	0.05	0.15–0.2
When $n \geq 120\ h^{-1}$ and air supply outlets are placed centralized, the mainstream area theory can be used for calculation	0.65 0.51 0.51 0.43 0.43			

For side air supply outlet, it is acceptable to assume $V_b/V = 0.7$–0.5 (Big value can be used when the distance between two vent outlets is larger than 3 m).

For orifice plate, it can be considered with Table 13.15.

For unidirectional flow cleanrooms, let $V_b/V = 0.02$ when filters are fully placed, and let $V_b/V = 0.06$ when the ratio of blowing area is 60 %, and let $V_b/V = 0.12$ when the ratio of blowing area is 40 %.

One thing should be point out that the vortex zone here is caused only by airflow, while equipments and occupants can also form the vortex zone, which is difficult to estimate. So the amount of equipments and occupants need to be controlled.

The determination method of parameters β, ψ, and V_b/V has been introduced above. In case they are not easy to be determined, the coefficient of nonuniformity ψ cannot be calculated. For general situation, the value of ψ can be roughly determined according to the air change rate with Table 13.16 (it is applicable only to top air supply outlet). For example, if the flow rate is 10,000 m^3/h for the air change rate 100 h^{-1}, ten air supply outlets should be placed, which has the dimension of 484 mm × 484 mm and the rated airflow 1,000 m^3/h. In this case, the value of ψ is shown in the table.

13.2.4 Three Principles of Design Calculation

Although it is more realistic to perform calculation on the basis of the nonuniform distribution theory, it needs to point out that there is still considerable discrepancy between the calculated results and the actual values. This is because it is quite difficult to determine the relevant coefficients which change constantly. Taking the parameter β as an example, it changes frequently during the movement of people. When it is assume $\beta = 0.8$ during calculation, but in fact or during measurement the particle generation source moves so that the main particle source is located in the vortex area, the calculated results will obviously different, which maybe deviate further from the one obtained based on the uniform distribution theory. Regarding these facts, different principles can be used during the design calculation process for three kinds of situations.

(1) Calculation according to the average indoor concentration, that is, with Eq. (11.13) or Eq. (11.16).

(2) According to the specific condition, when it can be ensured that the mainstream area is relatively larger, or when the operation is conducted within the mainstream area, calculation can be performed with the particle concentration in the mainstream area. With Eqs. (12.1) and (12.4), we can obtain:

$$N_a \approx \left(1 - \frac{\beta}{1+\varphi}\right)\left(N_s + \frac{60G \times 10^{-3}}{n}\right) \tag{13.10}$$

In brackets on the right side of the above formula, the value N is calculated with uniform distribution theory, which can also be approximately found out according to Fig. 13.4.

(3) For cleanroom with strict requirement of air cleanliness or for the workpiece with frequent movement indoors, which should be prevented from pollution, or for cleanroom with large space or for operation with fixed location within the vortex zone, the particle concentration in the vortex area can be used for calculation. With Eqs. (12.3) and (12.4), we can obtain:

$$N_b \approx \left(1 + \frac{1-\beta}{\varphi}\right)\left(N_s + \frac{60G \times 10^{-3}}{n}\right) \tag{13.11}$$

13.2.5 Examples

Example 13.1. There is a turbulent flow cleanroom with a high-efficiency air cleaning system. This cleanroom is 28 m^2 in area (5.6 m in width and 5 m in length), and 2.5 m in height. It is equipped with two side air supply outlets with the size 0.3 m $\times$ 0.2 m. The air change rate is 28 h^{-1}. The fresh air ratio is 25 %. When

there are three people working inside, please calculate how much is the particle concentration inside the cleanroom.

Ans:
∵ Occupant density is:

$$q = \frac{3}{28} = 0.104 \text{ people/m}^2$$

According to Fig. 13.1 (using the vertical axis with five times, which is the same below), $G_n = 2.7 \times 10^4$ #/(m^3·min). With the values of G_n and n in Fig. 13.4, we can get that $N = 60$ #/L.

∵ Distance between the two side air supply outlets approximates 3 m.
∴ We can have $\beta = 0.6$, and $V_b/V = 0.6$.
∴ According to Eq. (13.8), we can obtain:

$$\varphi = 0.5\frac{\sqrt{5.5 \times 2.5/2}}{1.13\sqrt{0.3 \times 0.2}} - 1 = 4.6 - 1 = 3.6$$

According to Eq. (11.15), we know:

$$\psi = 1.013$$

$$N_v = \psi N = 1.013 \times 60 = 61 \text{ \#/L}$$

Example 13.2. The condition is the same as Example 13.1. When the indoor particle concentration is required to be 61 #/L, what is the required air change rate?

Ans:
With 61 #/L and $G_n = 2.7 \times 10^4$ #/(m^3·min), the air change rate can be found from Fig. 13.4 that $n = 26$ h^{-1}.

With the same method above, $\psi = 1.013$. According to Eq. (13.7), we can obtain
$n_v = \psi n = 1.013 \times 26 = 26.3$ h^{-1} (approximately 27 h^{-1})

Example 13.3. There is a turbulent flow cleanroom with a high-efficiency air cleaning system. This cleanroom is 14 m^2 in area and 2.5 m in height. It is equipped with one top air supply outlet. There are two people working in the room. When the indoor particle concentration is required to be less than or equal to 84 #/L, what is the required air change rate?

Ans:
∵ Occupant density is:

$$q = \frac{2}{14} = 0.144 \text{ people/m}^2$$

According to Fig. 13.1, $G_n = 3.3 \times 10^4$ #/(m^3·min). With G_n and 84 #/L, the air change rate for uniform distribution can be found from Fig. 13.4 that $n = 24\ \text{h}^{-1}$. Since the area corresponding with one air supply outlet is larger than 10 m^2, we can get $\beta = 0.6$ and $\psi = 1.5$.

∵Volume of the cleanroom is $V = 35\ \text{m}^3$; according to Table 13.14, we get $V_b = 8\ \text{m}^3$.

∴ $V_b/V = 0.73$ and then $\psi = 1.24$.

∴According to Eq. (13.7), we get:

$$n_v = \psi n = 1.24 \times 24 = 30\ \text{h}^{-1}$$

If the above calculation is not performed and instead Table 13.16 is used, we can obtain $\psi \approx 1.21$, so $n_v \approx 1.21 \times 24 = 29\ \text{h}^{-1}$. So the discrepancy is acceptable.

Example 13.4. The condition is the same as Example 13.3. When the air change rate is 30 h^{-1}, what is the indoor particle concentration?

Ans:
According to Fig. 13.4 with the given values of 30 h^{-1} and G_n, we can get $N = 67$ #/L. With the same method above, we get $\psi = 1.24$, then:

$$N_v = \psi N = 1.24 \times 67 = 83\ \#/\text{L}$$

Example 13.5. There is a cleanroom with a high-efficiency cleaning system. When the particle generation rate G_m at static state is 2×10^4 #/(m^3·min), and the fresh air ratio is 0.5, what is the required air change rate for air cleanliness level Class 7?

Ans:
∵ The fresh air ratio = 0.5. According to the data given before, we can get:

$$N_s = 2.5\ \#/\text{L}$$

Assume for Class 7 it is designed with the concentration of 100 #/L. According to Eq. (13.7), we can obtain the value of n:

$$n = \frac{60 \times 2 \times 10^4 \times 10^{-3}}{100 - 2.5} = 12.3\ \text{h}^{-1}$$

From Table 13.16 with the value of n, we can interpolate and obtain $\psi = 1.4$. Then we get:

$$n_v = 1.4 \times 12.3 = 17.2$$

∴ $n_v = 18\ \text{h}^{-1}$.

Example 13.6. With the same condition as the former example, when the air change rate is 18 h^{-1}, and the fresh air ratio is 0.25, which air cleanliness level can be reached in the at-rest state?

Ans:
∵ Fresh air ratio = 0.25. According to Fig. 13.4 with the air change rate 18 h^{-1} and $G_m = 2 \times 10^4$ #/L, we can obtain $N = 68$#/L.

According to Table 13.6, we can obtain $\psi = 1.27$ with the air change rate is 18 h^{-1}. With Eq. (13.6), we can obtain:

$$N_v = 1.27 \times 68 = 86.4\ \#/\mathrm{L}$$

∴ Air cleanliness level Class 7 can be reached during at-rest state. If the air cleanliness level at operational state should be estimated, the dynamic-to-static ratio should be assumed.

If the dynamic-to-static ratio is set to be 3, then:

$$N_v \approx 260\ \#/\mathrm{L}$$

It's still Class 7.

If the dynamic-to-static ratio is set to be 5, then:

$$N_v \approx 432\ \#/\mathrm{L}$$

It's beyond the range of Class 7. Only when the air change rate is increased, the particle concentration can be lowered.

Example 13.7. There is a turbulent flow cleanroom with a high-efficiency air cleaning system. This cleanroom is 7 m^2 in area and 2.5 m in height. It is equipped with five top air supply outlets placed on one side. The fresh air ratio is 20 % and there is one person working in the room. Because the area is small, and the number of air supply outlets is large, the workspace is almost within the mainstream area, and it can be designed with the particle concentration in the mainstream area. When the indoor particle concentration is 7 #/L, what is the required air change rate?

Ans:
∵ Occupant density is:

$$q = 17 = 0.14\ \mathrm{persons}/\mathrm{m}^2$$

According to Fig. 13.1 when the dynamic-to-static ratio is assumed to be 5, $G_n = 3.3 \times 10^4$ #/(m^3·min), which is beyond the available range of Fig. 13.4.
So Eq. (13.7) can be used for calculation. As $(1 - s) = 0.2$, $N_s = 1$ #/L. Then we can obtain:

$$n = \frac{60G \times 10^{-3}}{N - N_s} = \frac{60 \times 3.3 \times 10}{7 - 1} = \frac{1980}{6} = 330\ \mathrm{h}^{-1}$$

Because one air supply outlet corresponds with the area larger than 1 m^2, and the air supply outlets are located on one side, with Table 13.11 we can get $\beta = 0.8$–0.9, and $\psi = 0.2$.

$\therefore$ According to Eq. (13.10), we can obtain the following expression when the particle concentration in the mainstream area is used:

$$\psi = 1 - \frac{\beta}{1 + \varphi} = 1 - \frac{0.8 \sim 0.9}{1 + 0.2} = 0.25 \sim 0.33$$

$\therefore n_v = \psi n = 0.33 \times 330 = 108\ \mathrm{h}^{-1}$, or $n = 0.25 \times 330 = 82.5\ \mathrm{h}^{-1}$.

When the dynamic-to-static ratio is assumed to be 3, we can obtain $n = 210\ \mathrm{h}^{-1}$ and $n_v = 52.5$–$69.3\ \mathrm{h}^{-1}$.

Example 13.8. There is a cleanroom with air supply outlets mounted at the whole ceiling and return air openings on two lower sides. One HEPA filter has been installed in series in the fresh air passage. The cleanroom is 20 m^2 in area, and the air change rate is 617 h^{-1}. When there are two people for measurement, what is the particle concentration under at-rest state?

Ans:

$\because$ We know

$$N_v = N_s + \psi \frac{60G_m \times 10^{-3}}{n}$$

During calculation with the mainstream theory

$$\psi = 1 - \frac{\beta}{1 + \varphi}$$

$\because$ HEPA filter has been installed in series in the fresh air passage.

$\therefore N_s \approx 0$.

Because air supply outlets are mounted on the whole ceiling, we get $\varphi = 0.02$. Because return air openings are installed on two lower sides, we get $\beta = 0.97$. So $\psi = 0.05$. Because the occupant density is $q = 0.1$ people/m^2, we get:

$$G_m = 0.9 \times 10^4\ \#/\left(\mathrm{m}^3 \cdot \mathrm{min}\right)$$

$\therefore$The particle concentration is obtained:

$$N_v = 0.05 \times \frac{60 \times 0.9 \times 10^4 \times 10^{-3}}{617} = 0.044\ \#/L$$

The measured results showed that among 84 times of measurement, the average concentration is 0.033 #/L. Because of the insufficient measuring points and measuring times, the measurement result can be relatively lower. (Refer to the section about cleanroom in Chap. 17.)

Example 13.9. There is a cleanroom with air supply outlet mounted on the ceiling (covering slightly over 80 % of the whole ceiling area) and return air openings are placed on one lower side. One HEPA filter has been installed in series in the fresh air passage. The cleanroom is 5.5 m^2 in area, and the air change rate is 500 h^{-1}. When there is one person for measurement, what is the particle concentration under the at-rest state?

Ans:
As the former example, we know $N_s \approx 0$ and $\varphi = 0.02$. Since the ratio of blowing area is slightly larger than 80 %, we can choose $\beta = 0.99$. Since $q = 0.1$ people/m^2, we get:

$$G_m = 0.9 \times 10^4 \ \#/(m^3 \cdot \min)$$

On the basis of mainstream area theory, we can get $\psi = 0.03$.

Since $n = 500\ h^{-1}$, we get:

$$N_v = 0.03 \times \frac{60 \times 0.9 \times 10^4 \times 10^{-3}}{500} = 0.042\ \#/L$$

The measured results showed that the average concentration is 0.026 #/L. Because of the insufficient measuring points and measuring times, the measurement result can be relatively lower.

13.3 Calculation for Applications with Local Filtration Device

In some applications such as computer rooms or program-controlled rooms, special air-conditioning systems are always used due to special requirements for the parameters, in order to circulate and clean indoor air. These special air-conditioning systems are equipped with filters. This is equivalent with the case where local air cleaning equipment is used. Under these circumstances, filtration measures are usually supplemented for fresh air, whose efficiency is equivalent to that of medium-efficiency air cleaning system. For example, in large- and medium-scale computer rooms, it is required that the concentration should be $\leq$18,000 #/L for particles with diameter $\geq$0.5 μm, which is even lower than the lowest air cleanliness level Class 9. But even so, the requirements can be met only with feasible calculation. Taking the computer rooms as an example, calculations will be performed with different types [16].

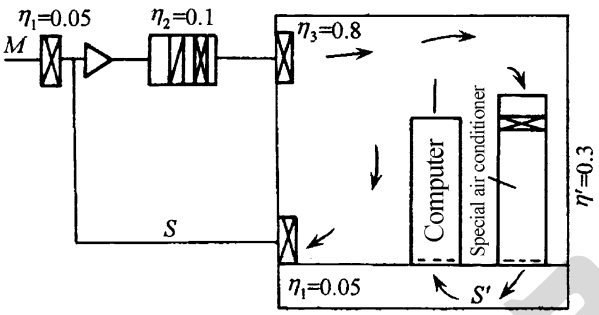

Fig. 13.6 Computer room with both central air-conditioning system and special air conditioner

13.3.1 *Computer Room with Both Central Air-Conditioning System and Special Air Conditioner*

The use of special air conditioner is equivalent to installing local air cleaning equipment in the cleanroom, as shown in Fig. 13.6.

Central air-conditioning system is usually targeted for thermal comfort indoors. However, places with large amount of computers will generate a lot of heat, which needs the dedicated air conditioner to solve this problem. In this case, the indoor particle concentration should be calculated with Eq. (10.10) when local air cleaning equipment is used, i.e.,

$$N = \frac{60G \times 10^{-3} + Mn(1-S)(1-\eta_n)}{n[(1+\eta' S') - S(1-\eta_r)]}$$

where η' is the filtration efficiency of the local air cleaning equipment. Here it is the efficiency of filters in the special air conditioner, which is generally equivalent to 0.3;

S' is the ration between the circulation airflow rate and the total air volume through the local air cleaning equipment.

Other parameters are shown as follows: assuming $q = 0.1$ preson/m^2, then $G_n = 1.07 \times 10^5$ #/(m^3·min); let $M = 3 \times 10^5$ #/L; n is the air change rate of the computer room, which can be considered 10 h^{-1} as a normal air-conditioning room; S is the ratio of the circulated airflow, which can be chosen as $S = 0$ when the air change rate for positive pressure indoors is considered and the fresh air flow rate can be assumed 2 h^{-1} at least; η_n is the overall efficiency of the filters in the fresh air passage (for particles with diameter ≥ 0.5 μm) and $\eta_n = 0.829$; η_r is the overall efficiency of the filters along the return air passage (for particles with diameter ≥ 0.5 μm), and from Fig. 13.6 we know $\eta_r = \eta_n = 0.829$.

According to the "Design Code for Electronic Computer Room" (GB50174-93), the large- and medium-scale computer rooms are those with area larger than 140 m^2. When the story height is 3 m, the room volume is 420 m^3, where one or two special air conditioners can be usually placed. When one air conditioner is used, the airflow rate is 10,000 m^3/h. When two air conditioners are used, the

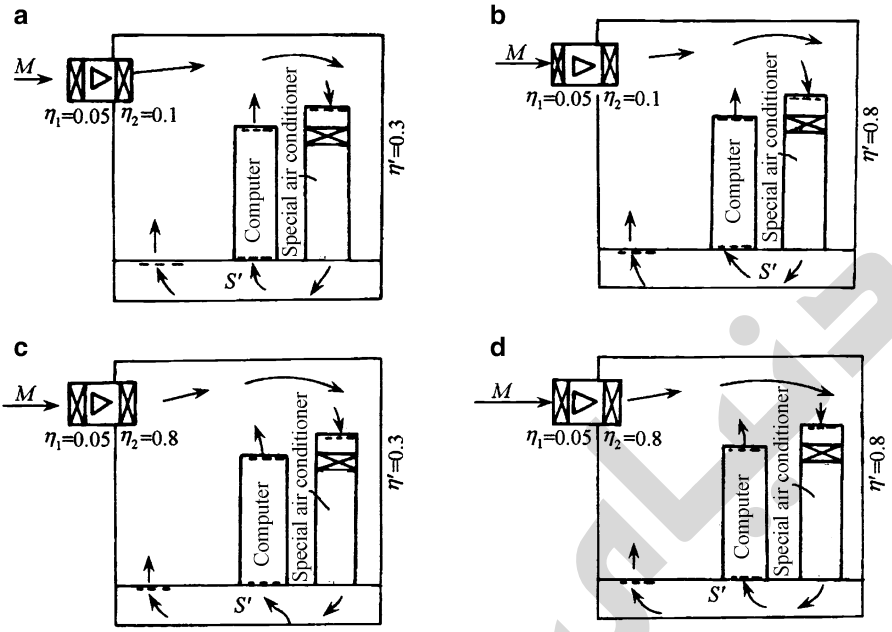

Fig. 13.7 Computer room with installation of special air conditioner and fresh air handling unit

airflow rate is 20,000 m^3/h. This means the air change rate of self circulation indoors is 25–50 h^{-1}, which is 2.5–5 times as that of the central air-conditioning system (10 h^{-1}). It means S' is equivalent to 250–500 %. Suppose 400 % is used as an average, which is four times, we can obtain that $N = 5{,}285$ #/L.

13.3.2 Computer Room with Special Air Conditioner and Air Handling Unit for Fresh Air

At present, central air-conditioning systems are not installed in most of the existing computer rooms, and it is aimed to solve the problem of heat generation from computers. The special air conditioner is used to deliver the cold air into the plenum box. On part of the cold air enter the computer from bottom to up, and the other part is sent indoors from the floor air supply outlets. In order to meet the hygienic standard, another fresh air supply outlet is set in another place inside the computer room, so that the treated outdoor air is sent into the room, as shown in Fig. 13.7.

There are several situations:

(1) At present, the most commonly used computer room is that equipped with special air conditioner and fresh air handling unit with medium-high-efficiency filters (Fig. 13.7a).

Since there is no air supply system, it is equivalent to the straight flow system. So the total airflow rate is the same as the fresh airflow rate. The circulation ratio is $S = 0$.

It is not allowed for a special air conditioner to have a large proportion of fresh air, which is usually about 5 %. That means for the air conditioner, the fresh air ratio is $(1 - S) = 0.05$. So the proportion of circulating airflow rate of the special air conditioner to the indoor total airflow rate is $S' = 1/0.05 = 20$.

According to Fig. 13.7a, the efficiency of the combined filters is:

$$\eta_n = 1 - (1 - 0.05)(1 - 0.1) = 0.145$$

The filter efficiency in special air conditioner η' is equivalent to 0.3 (for particles with diameter $\geq$0.5 μm). It is known from the above introduction that the chosen value of n has little effect on the indoor particle concentration N. If $n = 50$, we can obtain $N = 36{,}661$ #/L according to the equation above. So the requirement can hardly be met in this kind of the computer room, where special air conditioner is commonly used and fresh air handling unit with medium-high-efficiency filters are installed.

(2) When the efficiency of filter installed in the special air conditioner is increased to 0.8 (for particles with diameter $\geq$0.5 μm) (Fig. 13.7b), and substitute $\eta' = 0.8$ to the above equation, we can obtain $N = 15{,}096$ #/L. It only basically meets the requirements since the number is quite close to the upper limit of the specified concentration.

(3) In the computer room where the efficiency of filter installed in the fresh air passage is increased to 0.8 (for particles with diameter $\geq$0.5 μm) (Fig. 13.7c).

Because $\eta_n = 1 - (1 - 0.05)(1 - 0.8) = 0.81$, we can obtain $N = 8{,}161$ #/L.

It is obvious that this method can meet the requirement.

(4) In the computer room where the efficiencies of both filters used for fresh air and special air conditioner are increased to 80 % (Fig. 13.7d).

We can get $\eta_n = 0.81$. When other conditions are the same, we can obtain $N = 3{,}360$ #/L.

It is obvious that this method can not only meet the requirement but can also reach the upper limit of air cleanliness level Class 8.

References

1. Shigeharu H (1967) Local dust collection for the environment in clean sterile workshop. Mag Building Equip 2:46–57 (In Japanese)
2. Shiobin K (1971) Selection method of air cleaning devices for different application. Jpn Air Cond Heat Refrig News 11(9):103–110 (In Japanese)
3. Xu ZL (1994) Design of cleanroom. Seismological Press, Beijing, pp 12–125 (In Chinese)
4. Schütz H, Raüme R (1969) Staubfreie Arbeitsplätze für die Feiwerktechnik. Feinwerktechnik, Oktober, pp 444–449 (In German)

5. Kosuke H (1973) Planning and design of cleanroom. Jpn Air Cond Heat Refrig News 13(1):75–88 (In Japanese)
6. Humikura A (1967) Design and construction of cleanroom. Jpn Air Cond Heat Refrig News 13(17):20–29 (In Japanese)
7. Нонезов РТ, Знаменский РЕ (1973) Обеспыливание воздушной среди в"Чесмых комнатах". Водоснабжение и Санитарная Техника 3:29–32 (In Russian)
8. Schichr HH (1973) Clean room technology-principles and applications. Sulzer Techn Rev 1:3–15
9. Wang SG (1997) Fresh air and control of fresh air systems. J HV&AC 1:23–28 (In Chinese)
10. Кокорев НП (1972) Гигиени ческая оценка без оконых и бесфонарных промышленных зданий. Гигиена и Санитария 6:25–28 (In Russian)
11. Kanzi S, Keiji K (1979) Design basis of air cleaning system indoors. Jpn Air Cond Heat Refrig News 19(9):68–76 (In Japanese)
12. Fanger PO (2000) IAQ in the 21st century: search for excellence (trans: Yu Xiaoming). J HV&AC 30(3):32–35. (In Chinese)
13. Kazuya H et al. (1974) Air conditioning and air cleaning. (In Japanese)
14. Tuve GL (1953) Air velocity in ventilating jets (Heating, Piping and Air Conditioning, No.6360). Special Science and Technology Information Collection (HVAC). (In Chinese)
15. Shunzou B, Tora B (1973) Design of cleanroom. Jpn Air Cond Heat Refrig News 13(1):89–95 (In Japanese)
16. Xu ZL (1996) Essential measures to insure cleanliness in computer rooms. J HV&AC 26(6):65–69 (In Chinese)

Chapter 14
Local Clean Area

It is called the comprehensive cleaning method when the environment in whole working area indoors is clean by the air cleaning and other comprehensive treatment measures. It is called the local cleaning method when the environment in local working area indoors or the particular local space is clean only by the local air cleaning measures. For the application where local cleaning method can be used, the comprehensive cleaning method should be avoided as much as possible.

14.1 Application of Mainstream Area Concept

There are three main development circumstances for the air cleaning methods: application in cleanroom alone, application as the local air cleaning device (such as the cleaning bench) alone, and application both in cleanroom and as the local cleaning device, namely, both the overall and the local cleaning methods are used.

But since a long term, because the understanding of the pollution control technology is not enough, the so-called pigeon cage type construction is usually adopted in the cleanroom, where the environment with the requirement of air cleaning is divided into smaller spaces. Although it is helpful to control the pollution, the disadvantage is also increasingly apparent:

1. The building plane is complex, and the cost increases with an excessive use of enclosure structure.
2. With the development of new process and new technology, the working procedures are often changed to form the new production line, which needs different air cleanliness level or methods. But it cannot be adapt to the requirement of this change.
3. For the production line where partition and obstruction are not allowed, and the application where people will enter in or out frequently, it is not easy for use.

Z. Xu, *Fundamentals of Air Cleaning Technology and Its Application in Cleanrooms*,
DOI 10.1007/978-3-642-39374-7_14, © Springer-Verlag Berlin Heidelberg 2014

Table 14.1 Values of (N_v/N) and (N_a/N)

		Turbulent flow cleanroom with small air change rate	Turbulent flow cleanroom with large air change rate (120 h^{-1} or above)	HEPA filters installed on the ceiling (or wall) with 40 % area	Filters installed fully
Calculation with room average concentration	$\frac{N_v}{N}$	1–1.2	0.64–0.86	0.4	–
Calculation with concentration in mainstream area	$\frac{N_a}{N}$	0.75–0.84	0.43–0.65	0.2	0.1

Note: N and N_v are the room average particle concentrations calculated with the uniform and the nonuniform distribution theories, respectively. N_a is the particle concentration in the mainstream area calculated with the nonuniform distribution theory

4. When the core zone with small area but high air cleanliness requirement is needed, and the surrounding area with low air cleanliness requirement is also essential, it is not feasible to enclose the core zone.

It is clear that the above disadvantage can be avoided with the comprehensive cleaning method for large area space, but it is economically unreasonable. If the comprehensive cleaning method for large area space with low air cleanliness requirement is used (e.g., the air cleanliness level is Class 100000 for the whole workshop), and local cleaning device is used to achieve the air cleanliness level Class 100, this is economically better than the comprehensive cleaning method with higher air cleanliness level, but the above shortcomings are still not completely avoided. For example, sometimes the rotation magnitude of the component in the process equipment is so large that it cannot be covered inside the workbench (such as the lifting and displacement of the bell jar for vacuum coating machine).

With the above situation, the concept of "mainstream area" was proposed in theory in 1978, which was introduced in Chaps. 11, and 12. When the process is placed in the mainstream area, the particle concentration can be smaller than the room average concentration by 30 % or a half, which is shown in Table 14.1. This means when the particle concentration in the mainstream area is designed with the room average concentration, the air change rate will be reduced by 30–50 %. It has been improved with practice that the effect of these schemes was quite good. Figure 14.1 shows the layout of the cleanroom by a foreign company, where HEPA filters were placed fully on two sides of the ceiling so that mainstream area with air cleanliness level Class 100 was achieved below. The clean air concentrated towards the room center. With the further effect of air supply outlet with a few HEPA filters placed in the center of the ceiling, the air cleanliness level in the middle space can reach Class 1000. For the application where the processes are mainly placed at two sides, this method is much economical compared with the method to achieve the air cleanliness level Class 100 by placing air filters fully on the ceiling.

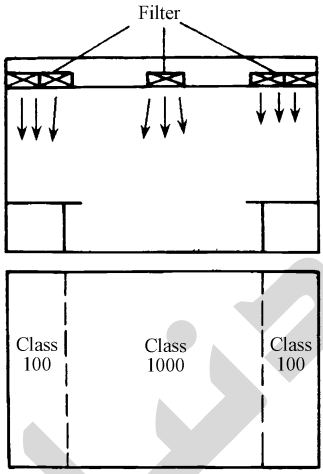

Fig. 14.1 One application example of mainstream area

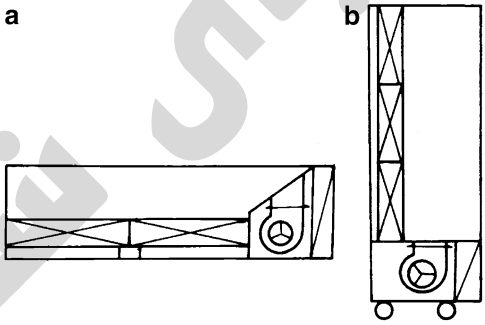

Fig. 14.2 Unit to form the air supply mode with mainstream area. (**a**) Ceiling unit for vertical air supply; (**b**) horizontal unit when it lay down

As for the air supply mode when the mainstream area concept is used, the concentrated air supply can be replaced by an independent unit. For vertical air supply mode, the ceiling unit can be used; while for horizontal air supply mode, the horizontal unit can be used. The same unit can be hung on the ceiling or placed on the ground so that horizontal airflow can be supplied. It is used according to the specific need, which is shown in Fig. 14.2.

By the application of the above mainstream area concept for local clean area, ideal effect was obtained in the operating room of the hospital [1]. Figure 14.3 is an example. The right part of this figure shows that the mainstream areas are 20 cm inside both sides of the edges. The tested particle concentrations are shown in Table 14.2.

From the table, the air cleanliness in the mainstream area can reach up to Class 100 in 5 min, and it only takes 7 min for the air cleanliness in the vortex area to reach Class 100. The effect is quite good. From Fig. 14.3, it is related to the ratio which reached 45 % between the air filter area and the ceiling area.

It should be emphasized that it is not reasonable to think that unidirectional flow with air cleanliness Class 100 can be reached with the ratio of blowing area 45 %.

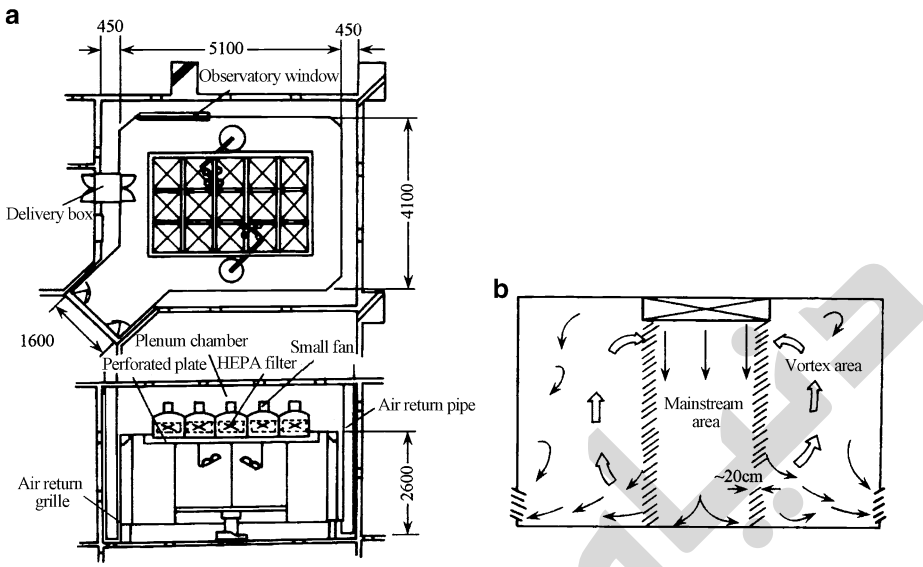

Fig. 14.3 Local clean area with Class 100 in operating room of the hospital. (**a**) Plana and profile (**b**) Schematic of streamline

Table 14.2 Particle concentration in local clean area of the operating room (0.4 m above the floor)

		Particle concentration with diameter ≥0.5 μm (pc/L)	
		Mainstream area	Vortex region
Before starting up		4,350	4,200
After starting up/min	1	2,750	4,260
	2	225	4,060
	3	76	1,840
	4	20	480
	5	0.4	98
	6	0.035	6.2
	7	0	1.7
	8	0	0.25
	9	0	0.12
	10	0	0.035
	11	0	0.07
	12	0	0

Although the air cleanliness level in the vortex area can also reach Class 100, the self-cleaning time after 7 min is much larger than that of the unidirectional flow cleanroom. In terms of anti-disturbance ability and other properties, this kind of

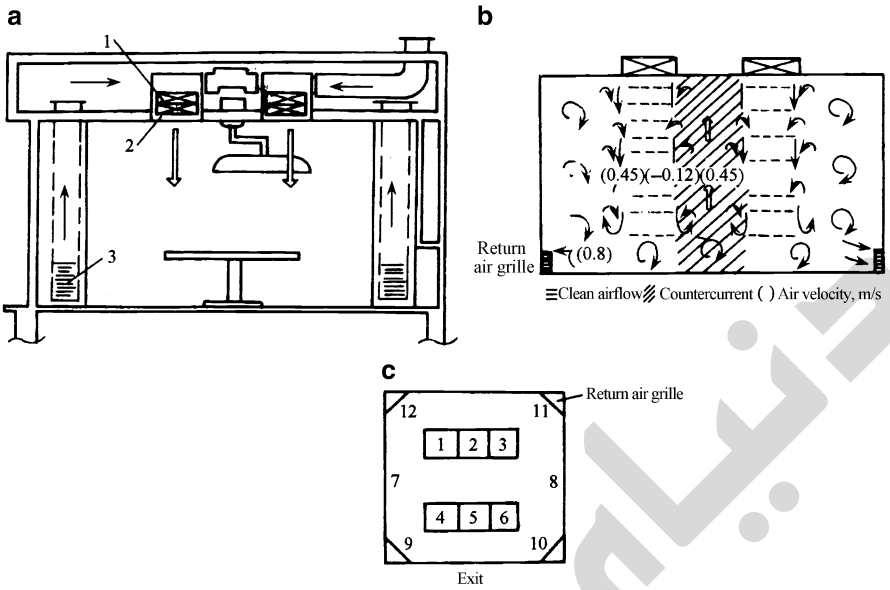

Fig. 14.4 Local clean area in the operating room. (**a**) Profile, *1* Prefilter, *2* HEPA filter, *3* return air opening. (**b**) Schematic of streamline. (**c**) Layout of the sampling points

Table 14.3 Particle concentration in local clean area of the operating room

		On the ceiling		0.9 m above the floor	
	Sampling position	Particle concentration with diameter ≥0.5 μm (pc/L)	Particle concentration with diameter ≥5 μm (pc/L)	Particle concentration with diameter ≥0.5 μm (pc/L)	Particle concentration with diameter ≥5 μm (pc/L)
Before starting up		31,500	60	31,500	60
20 min after starting up (without surgery operation)	1	0	0	3.5	0
	3	0	0	3.2	0
	5	0	0	5	0.6
	7	16	2.5	7	0.6
	8	16	1.4	5.3	0
	At the return air grille				
	10	9.5	0.6		
	12	11	0.9		

cleanroom is comparable with the room with filters placed fully on the ceiling. There is local Class 100 for this kind of cleanroom.

Figure 14.4 shows one form of a local clean area which is much smaller. Table 14.3 shows the measured particle concentrations. Although the effect is poorer than the above local clean area which is much larger, the air cleanliness level in the working area is close to Class 100. Since the complete aseptic operation

is performed, the average particle concentration during the operating process is about 1,000 #/L, and the average bacterial concentration is only 0.0016#/L, which is within the range of Class 100 [1].

There are three points which should attract attention for cleanroom with local air cleanliness level Class 100:

1. The area of local clean area with Class 100 should be larger than that of the working area. At least it should be bigger by 15–20 cm for each side.
2. The ratio of blowing area is also a problem. When the air supply area for local Class 100 is used as the total area, its relationship with the air filter area should meet the definition of the ratio of blowing area introduced in Chap. 8.
3. In order to guarantee the Class 100 effect in the working area and the certain cross-sectional air velocity (such as the lower limit of air velocity), especially when the area of the local Class 100 area is relatively small, there should be enough air supply velocity and the partition wall with curtain should be added. The detailed information will be given in the next section.

14.2 Characteristics of Mainstream Area

14.2.1 Air Distribution Characteristic

In order to make full use of the mainstream area and the expanded mainstream area, the characteristics of the air distribution should be understood.

The supplied air in the mainstream area can be considered as a weak jet flow from the overall filter. Compared with normal jet, it is vulnerable to be affected by factors such as the type, shape, and location of air supply outlet, the ratio between the air supply outlet area and the effective area of the whole room, the air supply velocity, the location of return air opening, and the envelope structure of the room.

The boundary of this weak jet flow also expands outwardly, as shown with the outer dotted lines in Fig. 14.5. The triangular region surrounded by two dotted lines is equivalent to the boundary layer. Because the external airflow is induced, the particle concentration will be higher than that of the supplied air in the mainstream area. The isoconcentration line with the concentration ratio between outside and inside $N/N_0 = 1$ % can be calculated, which starts from two ends of the air supply outlet and has an inclination angle 10.7° from the plumb line [2, 3]. The observed expansion angle by domestic study showed it is smaller than 10° [4]. The concentration variation in the mainstream area from place *B* to *A* can be expressed with the curve in the figure. This conclusion is valid in the region which is about four times of the air supply outlet size below the air supply outlet (except the region near the floor). Obviously, the clean area formed with this kind of air supply mode is relative narrow. When the air supply diffuser plate is 2.4 m above the floor, at the height of 0.8 m above the floor, each side of the airstream boundary border in the mainstream

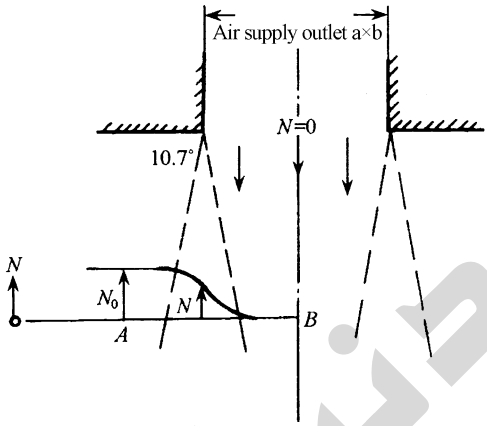

Fig. 14.5 Concentration variation in the mainstream area and its boundary

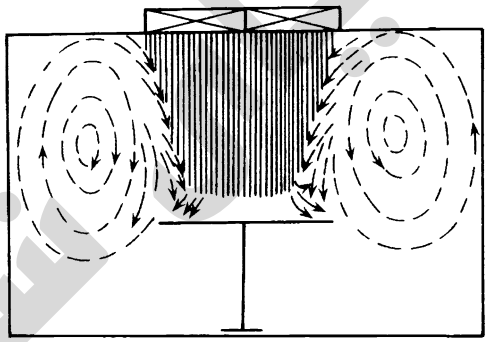

Fig. 14.6 Interference on the boundary of the mainstream area

area will contract (2.4–0.8) × tg 10.7° ≈ 0.3 m. So the working area is vulnerable to the external interference, as shown in Fig. 14.6.

According to streamline displayed with the bubbles [5], when the air supply velocity is not less than 0.31 m/s for this kind of air supply mode, the bubbles are suppressed at the air supply outlet once they are generated, until to the region near the floor. But the cross-sectional air velocity in the working area is much less than 0.25 m/s.

The characteristic of air distribution in the mainstream is also influenced by the induction coefficient φ by different types of air supply outlets, which thus influences the turbidity of the airflow below. From Chap. 13, the values of φ for diffuser air supply outlet and the ceiling air supply outlet with perforated diffuser plate are larger than that of the air supply outlet with filter by 1.3–1.4 times. Curves can be plotted with the calculated values in Table 13.12, which is shown in Fig. 14.7 [4].

With the increase of φ, more airflow outside of the mainstream area will be induced into the mainstream area, which will inevitably increase the concentration in the mainstream area. Therefore, perforated plate should not be used as the air supply surface in the mainstream area. The performance of mesh damping layer is better than the perforated plate. The leakage prevention layer introduced later with larger resistance and better filtration effect is most suitable for the air supply in the mainstream area.

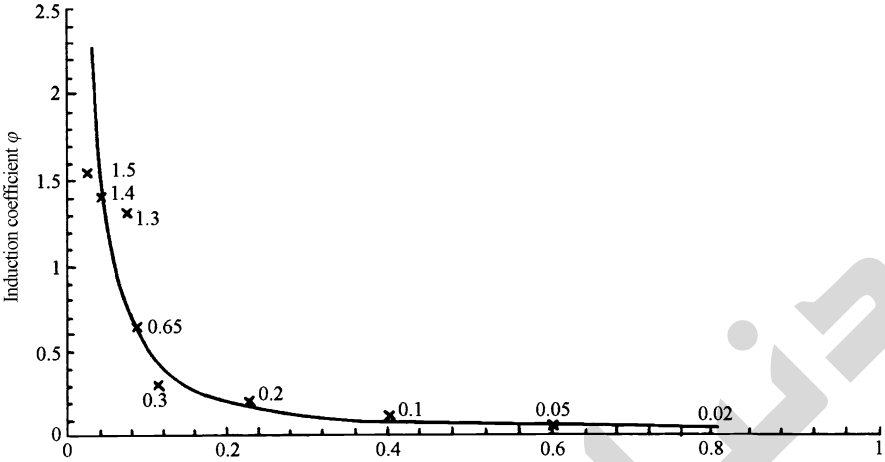

Fig. 14.7 Relationship between the effective area ratio (the ratio between the air supply area and the ceiling area) and φ

14.2.2 Velocity Decay Characteristic

With the influence of a weak jet and the surrounding induced airflow, the air velocity below the air supply surface decays, but it is much smaller than the decay speed for the jet flow.

Liu Hua obtained the relationship between the number of air supply outlets, i.e., the air supply area of the mainstream area, and the relative decay rate of velocity v/v_0 by experiment, which is shown in Fig. 14.8 [4]. In the figure, v is the average velocity at the cross section of the working area, v_0 is the average velocity at the air supply outlet, x/r is the dimensionless distance from the edge of the air supply outlet, r is the equivalent radius of the air supply surface [$r = (\text{length} \times \text{width})/(L + W)$], and x is the vertical distance from the air supply surface. In the figure, the solid line is the regression result on the experimental data. The expression for the maximum decay rate λ is:

$$\lambda = 1 - \frac{v}{v_0} = 0.093\frac{x}{r} \tag{14.1}$$

The above fitted result is compared with the 16 cases of engineering measurement data which contain the parameter about the size of air supply surface [4]. There are no differences.

$$1 - v/v_0(\text{experimental average value}) = 81\ \%$$

$$1 - v/v_0(\text{fitted average value}) = 81.4\ \%$$

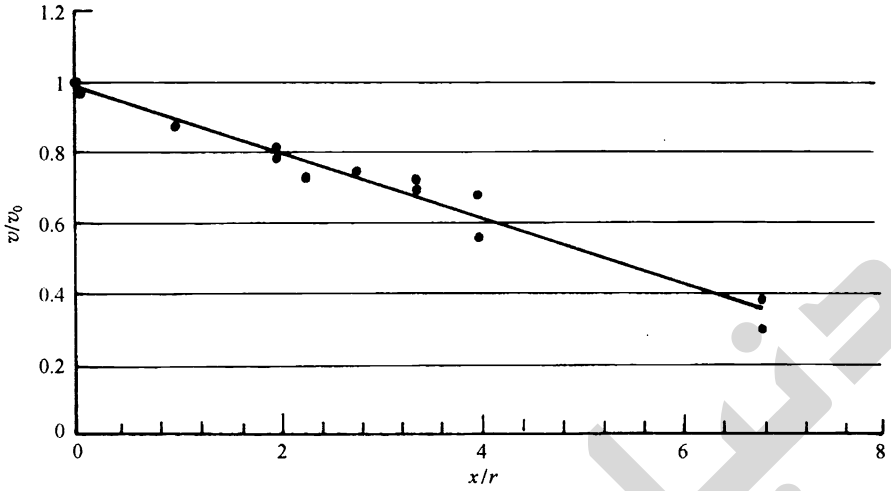

Fig. 14.8 Experimental data and fitted results of the velocity decay in different places of the mainstream area

Table 14.4 Comparison between the experimental and the calculated velocity decay rates

换气次数 (次/h)	Number of air suppliers (0.5 m × 0.5 m)	Air velocity on the outlet surface (2.46 m) (m/s)	Air velocity on the working surface (0.8 m) (m/s)	Measured decay rate of velocity	Calculated decay rate with Eq. (14.1)	Average decay rate		
						Test	Simulated flow field	With Eq. (14.1)
15	1	0.54	0.32	0.41	0.61	0.43	0.48	0.53
	2	0.27	0.15	0.44	0.46			
25	1	1.02	0.55	0.46	0.61	0.45	0.44	0.4
	2	0.50	0.28	0.44	0.46			
	3	0.34	0.20	0.41	0.41			
	4	0.25	0.13	0.48	0.38			

With another group of experimental data [6], the calculated results by Eq. (14.1) can be obtained, which are shown in Table 14.4. It is clear that the calculated results are very close to the experimental data and simulated velocity field.

However, the relationship between the air supply velocity and the velocity decay rate is not obviously seen from the experiments and measured results. The simulated velocity field showed that with the increase of the air change rate, which corresponds with the increase of the air supply velocity or the reduction of the number of air supply outlet under the same air change rate, the velocity decay rate reduces accordingly, which is shown in Fig. 14.9 [7].

There are a lot of factors that affect the velocity decay rate, and the effect is very complex. The applicable range of x/r is 1–4, and for safety reason, it should be considered with 3–4. So the resultant velocity decay rate is in the range 0.28–0.37. According to the experimental results by Niu Weile [8], the maximum velocity decay rate reached 0.35. It is recommended that this range can be used as the basis

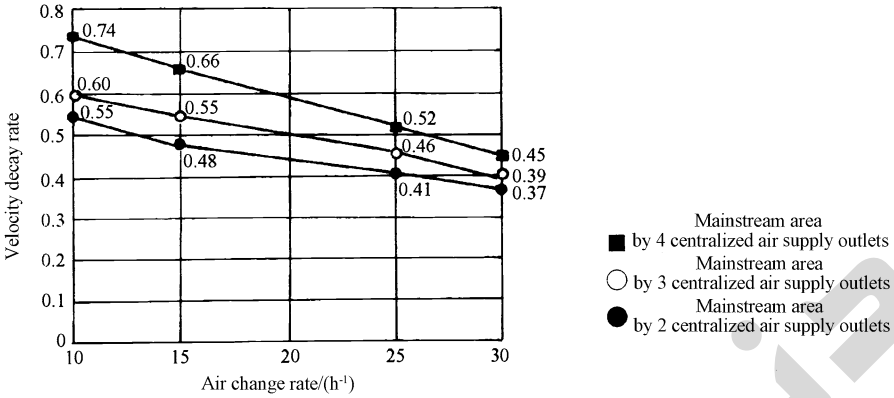

Fig. 14.9 Relationship between the air supply velocity (influenced by the number of air supply outlets and the air change rate) and the velocity decay rate

for the design air supply velocity in the local clean area (mainstream area). It can also be expressed in another way. Let λ' be the amplification magnitude between the air velocity at the working area and the air supply velocity. When $\lambda = 0.36$, $\lambda' = 1 - (1 - 0.36) = 1.56$.

14.2.3 Particle Concentration Characteristic

When the air supply mode to form the mainstream area with concentrated placed air supply outlets is used in the finite space which is not very large, the average particle concentrations in both this space and the mainstream area can be calculated with the method introduced in Chap. 13. Moreover, this kind of air supply mode can be approximated as the air supply outlets in Fig. 14.5. Its specific concentration field can be expressed with the analytical expression, which has already been verified by experiment [2, 3].

When the number of centralized placed air supply outlets increases, the area of the mainstream area also increases, whenever the air supply volume increases or not. The particle concentration in the mainstream area at this time does not rise but appears a declining trend, which is the expect result of engineering applications. Simulation results show that the particle concentration in the mainstream area with two air supply outlets is the lowest when the air supply volume is less than 15 h^{-1}, which has the best effect, while the particle concentration in the mainstream area with three or four air supply outlets is the lowest when the air supply volume is larger than 25 h^{-1}. When the number of air supply outlets increases, the particle concentration in both cases increases. The data with the air change rates 15 and 25 h^{-1} are shown in Table 14.5.

Table 14.5 Simulated particle concentration in the working area without artificial particle generation

Air change rate/ (h^{-1})	Number of air supply outlets	Relative concentration in the mainstream area (the concentration at one air supply outlet is assumed 1)	Relative concentration in the surrounding area (the concentration at one air supply outlet is assumed 1)
		Ratio of particle generation rates among ceiling, wall, and floor	Ratio of particle generation rates between surfaces
		1:5:100	1:5:100
10	1		
	2		
	3		
	4		
15	1	1	1
	2	0.65	0.70
	3	0.85	0.86
	4	1.65	1.01
25	1	1	1
	2	0.58	0.8
	3	0.48	0.74
	4	0.50	0.80
30	1		
	2		
	3		
	4		

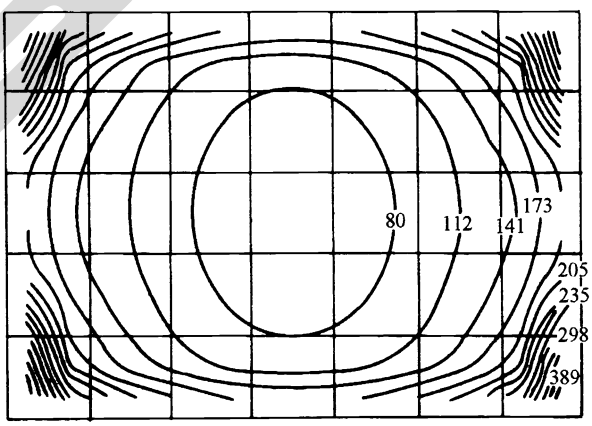

Fig. 14.10 Planar concentration field in the mainstream area formed by one air supply outlet and the air change rate 15 h^{-1}

Figures 14.10, 14.11, 14.12, 14.13, 14.14, 14.15, 14.16, and 14.17 are the calculated particle concentration by Zhang Yanguo [7]. There are 1–4 air supply outlets in the mainstream area. The air change rates are 15 and 25 h^{-1}, respectively.

The analysis of related experimental data will be performed in the next section.

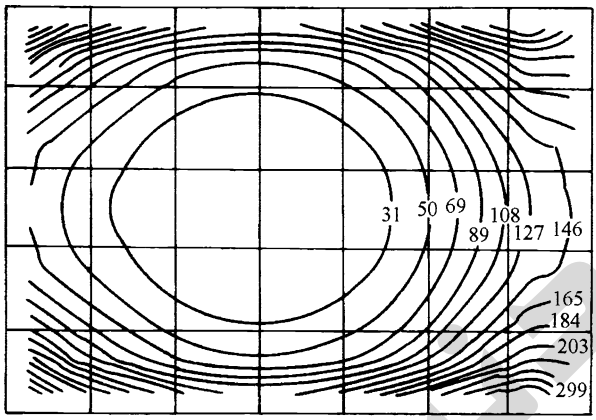

Fig. 14.11 Planar concentration field in the mainstream area formed by two air supply outlets and the air change rate 15 h^{-1}

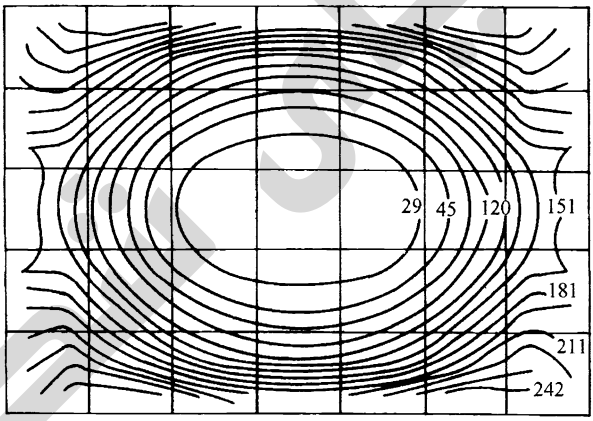

Fig. 14.12 Planar concentration field in the mainstream area formed by three air supply outlets and the air change rate 15 h^{-1}

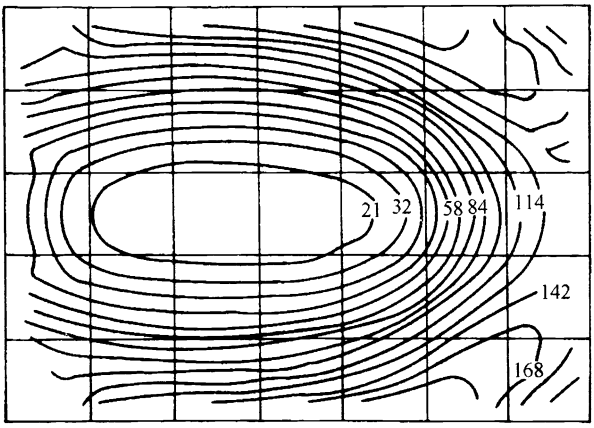

Fig. 14.13 Planar concentration field in the mainstream area formed by four air supply outlets and the air change rate 15 h^{-1}

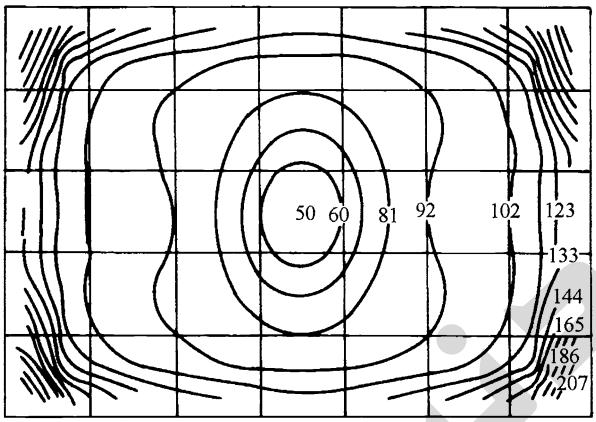

Fig. 14.14 Planar concentration field in the mainstream area formed by one air supply outlet and the air change rate 25 h^{-1}

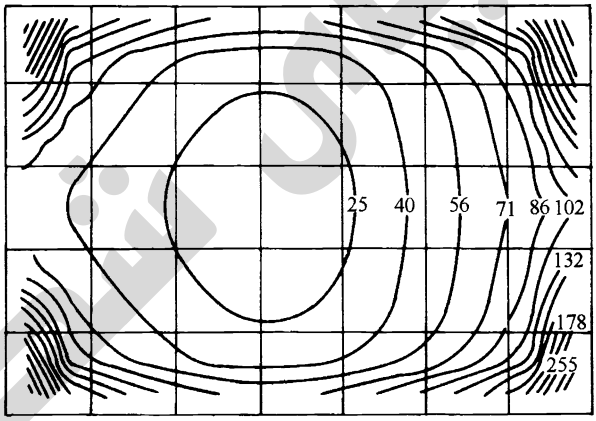

Fig. 14.15 Planar concentration field in the mainstream area formed by two air supply outlets and the air change rate 25 h^{-1}

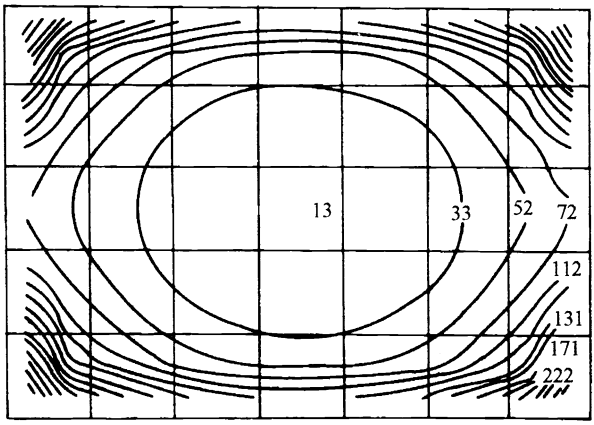

Fig. 14.16 Planar concentration field in the mainstream area formed by three air supply outlets and the air change rate 25 h^{-1}

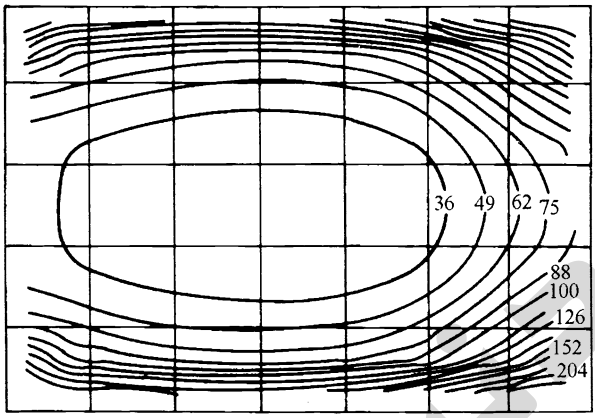

Fig. 14.17 Planar concentration field in the mainstream area formed by four air supply outlets and the air change rate 25 h^{-1}

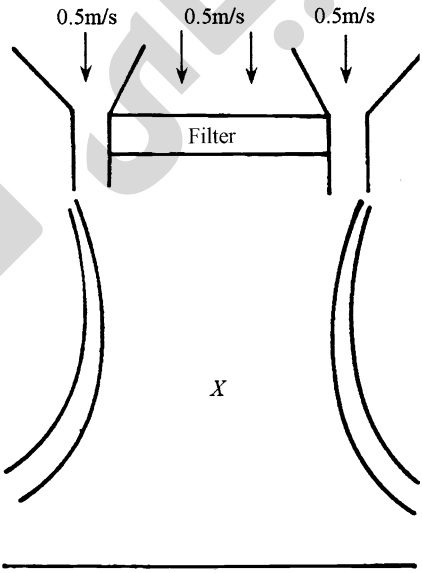

Fig. 14.18 Particle concentration field when the air supply velocity is 0.5 m/s (*X* represents the measuring height (1 m). The concentration ratios of the three regions from the mainstream area towards outside are below 1 %, 1–10 %, and above 10 %)

As for the optimal number of air supply outlets which are centralized placed in the mainstream area (namely, the size of the mainstream area), when the area of air supply outlets increases to a certain extent that the velocity reduces by a half, and the air supply velocity reduces to 0.13 m/s which is the lower limit, the effect will be lower if the air supply velocity decreases further [6].

In German standard DIN4799, the minimum air flow rate in the operating room is specified to be 417 $m^3/(h \cdot m^2)$, i.e., 0.12 m/s, which seems that it is not coincident.

It is of course good to improve the air supply velocity for the mainstream area. Figure 14.18 shows the particle concentration field for air supply mode when the air supply velocity is 0.5 m/s and air curtain with velocity 0.5 m/s is also placed at two sides [9]. The size of the clean area below is much larger.

14.2.4 Contamination Degree in Mainstream Area

With the concept and characteristic of the mainstream area introduced before, the air cleanliness level in the mainstream area is higher than other area. The evaluation method of this characteristic will be discussed below.

It is known from Eq. (11.16) that

$$N_v \approx \psi N$$

It is also known from Eq. (12.4) that the concentration at the return air opening is the room average concentration. So we can get:

$$\text{The concentration in the mainstream area} \quad N_a = \psi_a N \tag{14.2}$$

$$\text{The concentration in the vortex area} \quad N_b = \psi_b N \tag{14.3}$$

$$\text{The concentration at the return air opening} \quad N_c = \psi_c N = N \tag{14.4}$$

where N_v is the room average concentration with nonuniform distribution. N is the room average concentration with uniform distribution. ψ_a, ψ_b, and ψ_c are nonuniform distribution coefficients in various areas. We know that:

$$\psi_a = 1 - \frac{\beta}{1+\varphi} \tag{14.5}$$

$$\psi_b = \frac{1+\varphi-\beta}{\varphi} \tag{14.6}$$

$$\psi_c = 1 \tag{14.7}$$

The advantage of the air supply mode with the mainstream area formed by centralized placed air supply outlets compared with the conventional scattered placed air supply outlets can be expressed with the following methods:

1. Expressed with ψ_a/ψ. This expression has some inadequacy, because the average concentration of the mainstream area is included in the room average concentration. So the lower the concentration of the mainstream area is, the less the room average concentration will be. The value of this ratio will not reduce too much, so the superiority of the mainstream area is not shown. At the same time, when the mainstream area is formed by centralized placed air supply outlets, the opinions of the room average concentration will be different. Because it is quite difficult to determine the number of the measuring points in the mainstream area, as well as their respective weighting coefficients, it is not easily applicable.

2. Expressed with ψ_a/ψ_c. This is also expressed with ψ_a. This expression way has certain of operability, since the concentration at the return air opening can be measured. But it also has some shortcomings. The working position cannot be arranged in the return air area, because they are not the most concerned area. The contamination degree in the aforementioned German concept is such a ratio. It cannot answer the question that when air supply outlets area centralized arranged, how about the situation in the surrounding area without air supply outlets? How much difference exists in these two areas? Therefore, the practical implication is quite poor. In addition, although the concentration in the return air area can be measured, concentrations are obviously different with the return air opening at different positions. All of the concentrations at the return air opening should be measured so that the error caused is not too big.
3. Expressed with ψ_a/ψ_b. This can be used for clear description of the phenomena. As stated earlier, the vortex area means the turbulent flow area containing vortex at both sides of the mainstream area. Its concentration represents the concentration in other main regions outside of the mainstream area and the return air area, which is also the concentration in the surrounding areas of the mainstream area. So ψ_a/ψ_b can be used to reflect the concentration difference between the working area and the nonworking areas. At the same time, the concentrations of these two areas can be measured with the setting of samplers in different areas. The size of the mainstream area at the height of the working area can be considered slightly larger than the projected area of the air supply outlet, according to the experiment and numerical simulations (detailed information will be given below). During the actual test in the cleanroom, measurement is performed with the classification of areas, and the projected area is used.

So the contamination degree in the mainstream area is the relative particle concentrations between the mainstream area and the surrounding area, which is also the nonuniform distribution coefficients between two areas. If the contamination degree in the mainstream area is defined as B, we can get:

$$B = \frac{\psi_a}{\psi_b} \tag{14.8}$$

Generally speaking, the bacteria concentration is proportional to the particle concentration, so the value of B is also suitable for the evaluation of the bacteria concentration in the mainstream area.

In 1977, Prof. Esdorn from Berlin University of Technology in Germany proposed the contamination degree for the bacteria concentration in the operating room [10], which was

$$u_s = \frac{K_s}{K_r} \tag{14.9}$$

where u_s is the contamination degree, K_s is the bacteria concentration in the working area, and K_r is the room average bacteria concentration (equivalent to that of return air opening). When the air change rate was 20 h^{-1} and the mainstream

Table 14.6 Calculated parameters in the mainstream area with different number of centralized placed air supply outlets (25 h^{-1})

Particle generation type	Number of air supply outlets	Ratio of area between air supply outlet and the ceiling	ψ	$\psi_a = \psi_a/\psi_c$	ψ_b	ψ_a/ψ	ψ_a/ψ_b
No artificial particle generation	1	0.03	1.16	0.80	1.33	0.70	0.60
	2	0.06	1.05	0.65	1.14	0.62	0.57
	3	0.09	0.98	0.55	1.10	0.56	050
	4	0.12	1.0	0.41	1.78	0.41	0.23
Average				0.60		0.57	0.48

area was formed by centralized placed air supply outlets above the operating table, the bacteria concentration in the mainstream area is only a half of the room average bacteria concentration, which means $u_s = 0.5$. This is the difference of the performance with the mainstream area formed by centralized placed filters and the conventionally placed filters.

From the above introduction, the contamination degree in Germany is only limited to the bacteria concentration. If the nonuniform distribution coefficient is used, it can be expressed as:

$$u_s = \frac{\psi_a}{\psi_c} \tag{14.10}$$

It is obvious that u_s is different from B. In the original literature, u_s was only obtained through experiment. Here both u_s and B can be obtained through calculation. For example, the calculated parameters in the mainstream area with different number of centralized placed air supply outlets are shown in Table 14.6 [6, 7]. The above method was also used for the classification of the clean operating rooms in China, which is shown in Table 14.7 [6].

The air change rates are different for the same air cleanliness level, which is much prominent in engineering projects. When the air supply area is larger, the value of β is larger, so the calculated nonuniform distribution coefficient is not large. Therefore, for the same air cleanliness level, ψ_a/ψ_b will be apparently different by experiment, calculation and field test. When these results are used for plot as shown in Fig. 14.19, the variation characteristics of the contamination degree in mainstream area are consistent. The range between two lines corresponds with the most frequently appeared contamination degree in the mainstream area.

If the value of B which is used to describe the particle concentration is more than 1, the possibility of leakage on air filter should be checked. If the value of B which is used to describe the bacteria concentration is more than 1, there will be leakage on air filter. For example, there is one measurement in engineering project where $B = 2.92$ for description of particle concentration and $B = 2.1$ for description of bacteria concentration, which belongs to this kind of situation. This is not included in the statistical investigation as shown in Fig. 14.19.

Table 14.7 Air supply area in the clean operating room with the contamination degree in the mainstream area

Type	Design condition	Centralized air supply area	Ratio of air supply area	$\psi_a = \psi_a/\psi_c$	ψ_a/ψ	ψ_a/ψ_b	Surgery area (as-built)	Surrounding area (as-built)
Ordinary clean operating room	15 h^{-1}, Class 100000	1 m^2	0.05	0.76	0.69	0.57	Class 10000	Class 10000
Ordinary clean operating room	20 h^{-1}, Class 100000	2.8 m^2	0.09	0.48	0.44	0.29	Class 1000	Close to Class 1000
Clean operating room	30 h^{-1}, Class 10000	5.4 m^2	0.18	0.37	0.44	0.21	Class 1000	Class 1000
Special clean operating room	Local Class 100	7.2 m^2	0.19	0.27	0.44	0.17	Class 100	Close to Class 100

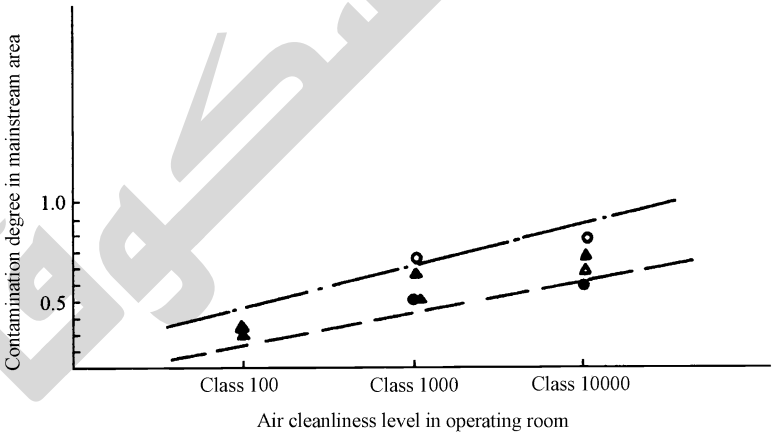

Fig. 14.19 Comprehensive comparison of the contamination degree in the mainstream area. ▲ Measured average value in engineering project (There are 14 cleanrooms with air cleanliness Class 100 in 8 hospital, 37 cleanrooms with air cleanliness Class 1000 in 9 hospital, 38 cleanrooms with air cleanliness Class 10000 in 11 hospital), Δ Theoretical calculated average value, ● Simulated average value (the ratio of particle generation among ceiling, wall and floor is 1:5:100), — Calculation, -·-·-Measurement, ○ Measured average value in lab (22 h^{-1}, no particle generation)

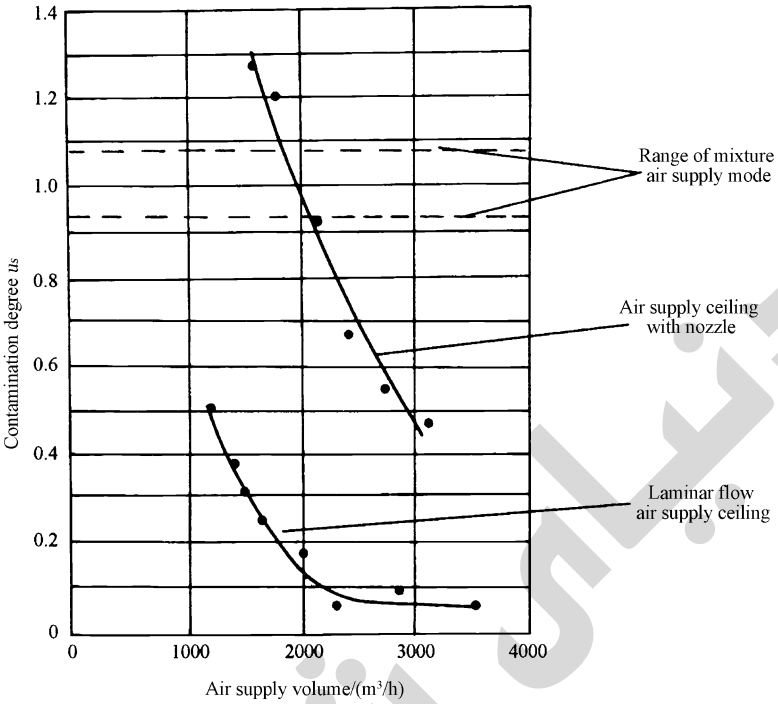

Fig. 14.20 Relationship between the contamination degree and the flow rate (From Germany)

Figure 14.20 shows the measured value of u_s from Germany [11], which was between 0.08 and 1.3. When the ratio of blowing area of the air supply surface is very large in the cleanroom with return air grilles fully placed at both sides, which reached 0.95, we obtain $\psi_a = 0.095$ and $u_s = 0.095$. It is close to the measured value 0.08. So the measured data from Germany are in the theoretical calculation range. It can be seen from Fig. 14.19.

14.2.5 Concept of Expanded Mainstream Area

In 2000, author proposed the concept of expanded mainstream area (refer to Sect. 14.2.3) [6]. In the clean operating room in China, air supply outlets were placed centralized above the operating table. The air cleanliness level in this area is higher than that of the surrounding area by one magnitude. This is the concept of the mainstream area, especially the expanded mainstream area, because the area of air filter is less than the centralized air supply area.

It has been proved with the calculation theory of uniform distribution that the air cleanliness level Class 5 cannot be realized in turbulent flow cleanroom with scattered placed air supply outlets (the flow rate through each air filter in the air

supply outlet is close to the rated flow volume), or when the air change rate is above 200 h^{-1}, the particle concentration can reach 3#/L (see Fig. 13.5 where the ratio of fresh air is 0.3 and $N_s = 1.5$ #/L), while according to traditional knowledge, the air cleanliness level Class 5 and higher is realized in unidirectional flow cleanroom.

However, when the calculation theory of nonuniform distribution and the expanded mainstream area are combined, the air cleanliness level Class 5 can be realized in turbulent flow cleanroom when the air change rate is not very large. Of course, the requirements of several conditions in unidirectional flow cleanroom are not satisfied in this kind of air cleanliness level Class 5, and only the value is reached. In the monograph "Design, Operation and GMP Certification of Cleanroom in Pharmaceutical Factory" (the second version) [12], this research finding was introduced. From the theoretical point of view, it is possible to create the at-rest air cleanliness level Class 5 for the background environment B zone (non-unidirectional flow) of the aseptic core zone A zone (unidirectional flow), which has already been verified by practice.

For the concept of expanded mainstream area, the flow rate of each air supply outlet is much less than the rated flow volume. So for the given design flow rate, the number of the air supply outlets will increase. According to Table 13.16, when the norminal rated flow volume with the increased number of air supply outlets is used to calculate the air change rate, which can be further used to find the value of ψ, we can find that the value of ψ reduces accordingly.

This can be proved from the parameters in Tables 13.11, 13.12, and 13.14. For example, when the number of the air supply outlets increases, which equivalent to the situation that 0.3 m^2 of the air filter (the perforated plated area of air filter with dimension 484 mm × 484 mm and rated flow volume 1,000 m^3/h) is responsible for the room area <2.5 m^2, φ <0.3–0.65. For the operational status, $\beta \approx 0.8$. When the norminal rated flow volume of air filter is equivalent with the air change rate 120 h^{-1} or larger, it can be calculated with the mainstream area as mentioned before, so $\psi = 1 - \frac{\beta}{1+\varphi}$. When φ is set 0.6 since we know $\varphi < 0.65$, for the condition of so many air supply outlets and the condition of at-rest status without any particle generation from occupant and equipment, it is equivalent with the condition that particles generated will be removed by the streamline in the mainstream area, so $\beta \approx 1$ and $\psi = 0.375$.

For the special case of the non-production B zone under the at-rest status and without occupant, it is specified in GMP that, when the self-purification time from Class 7 to Class 5 should be less than 20 min, the air change rate is less than 46 h^{-1} when the air cleanliness level reached Class 5 in turbulent flow cleanroom (the detailed calculation can be seen in the monograph "Design, Operation and GMP Certification of Cleanroom in Pharmaceutical Factory" (the second version), Tongji University Press, 2010).

The above results are based on the assumption that each air filter with dimension 484 mm × 484 mm is responsible for the room area <2.5 m^2 (In the room with area 30 m^2, there should be 12 air filters of this dimension). The actual flow rate through the air filter is obtained through the air change rate above (46 h^{-1}). The actual flow rate is only about 1/3 of the rated flow volume.

This theoretical finding has already been validated by several practical projects (papers will be published soon).

14.3 Clean Area with Partial Wall

In order to make full use of the clean air below the HEPA filter, the USA had proposed the air supply device with curtain in the 1960s [13], which is shown in Fig. 14.21. This device is slightly different from the cleanroom with curtain later. It is just a local device, and the curtain is not the substitute of wall. It just reached above the workspace. The aim is to guarantee that the unidirectional parallel airflow can reach the working table. It is apparent that it is not convenient to use the nonstationary curtain. Therefore, later someone tested the situation when the partial wall was placed along the flow direction (it can be rigid board or soft curtain) [3, 14]. This device can be called the clean area with partial partition wall. This is equivalent with the increase of the air supply outlet size or the decrease of the distance between the air supply outlets to the working area. This kind of partial wall can be perpendicular to the air supply surface. It can also be inclined with the air supply surface by an angle, or even an orifice plated can be added below, which are shown in Figs. 14.22, and 14.23.

In the former Federal Germany, vertical unidirectional flow cleanroom with partial wall was designed, which was used for the filling and packaging processes of the medicine in pharmaceutical industry with requirements of high air cleanliness level, as shown in Figs. 14.24 and 14.25 [15]. They were also applied in the continuous production line, as shown in Fig. 14.26 [16]. They were application examples which attracted attention.

It is especially suitable to design the horizontal air supply mode for the clean area with partial wall. The cleanrooms in Heilongjiang People's Hospital introduced in Chap. 9 adopted this kind of design, which is shown in Fig. 14.27. The partial wall can be bilateral or unilateral. It can be fixed or mobile. Figure 14.28 shows several types of cleanrooms in hospital [17]. Practical operation shows that the airborne bacterial concentration is only 1/40 of the normal operating room, and the depth infection rate is only 1/5.

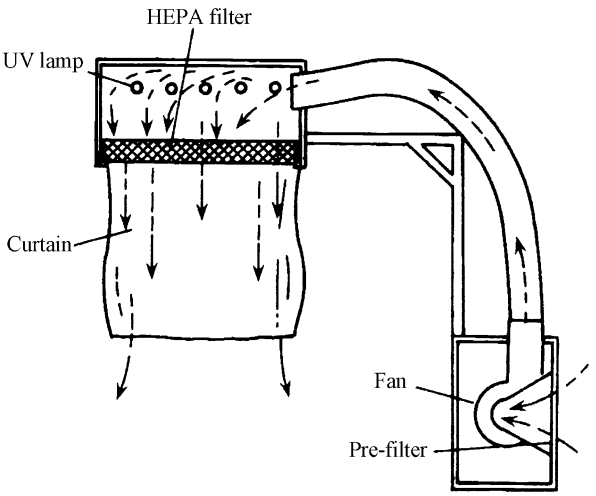

Fig. 14.21 Air supply device with curtain in the USA (For medical applications)

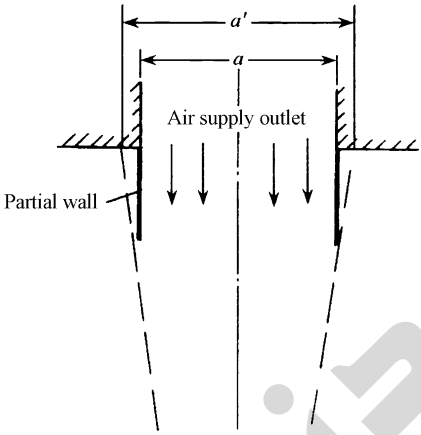

Fig. 14.22 Air supply outlet with partial vertical wall

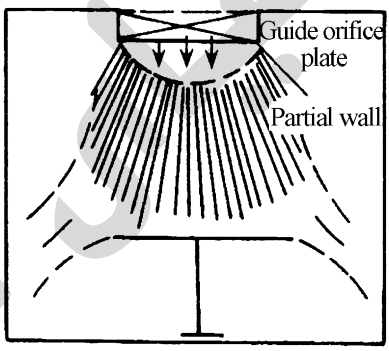

Fig. 14.23 Air supply outlet with inclined partial wall

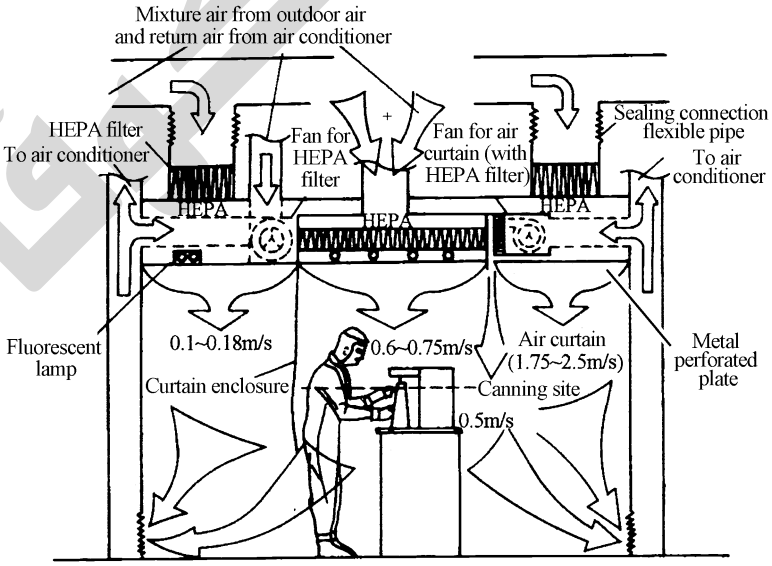

Fig. 14.24 Local clean area with curtain (HEPA means high-efficiency particulate filter)

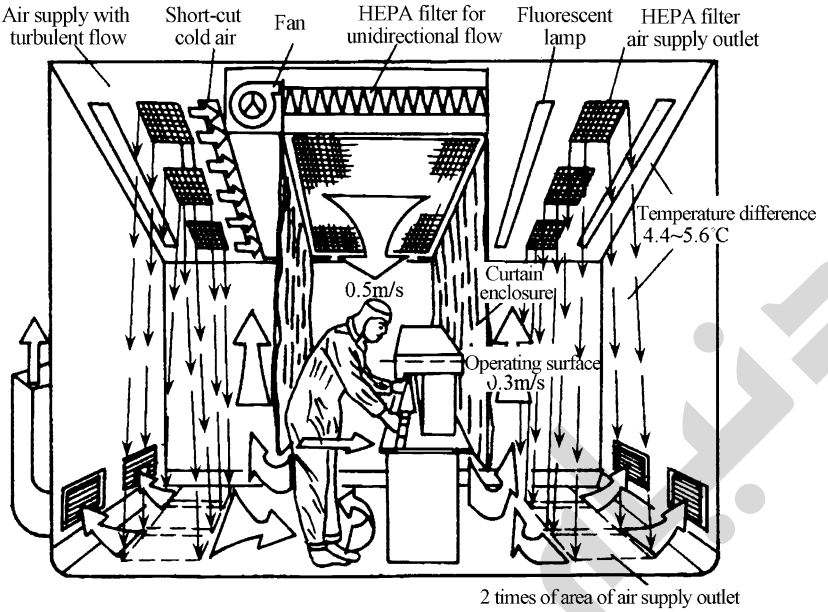

Fig. 14.25 Unidirectional flow clean area with curtains at both sides based on the improved scheme of the above method

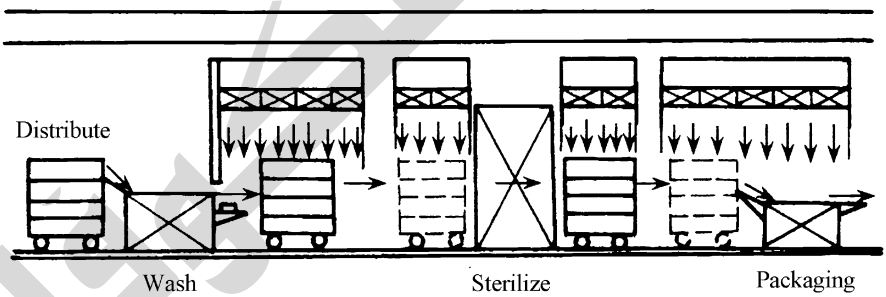

Fig. 14.26 Application of the local clean area with partial wall in the production line of pharmaceutical manufacturing company

14.4 Air Curtain Cleaning Booth

14.4.1 Application

Although the performance of the clean area with partial wall is improved compared with that without partial wall, there is limit because this kind of partial wall cannot be too long. Although the anti-disturbance ability improves with the increase of the

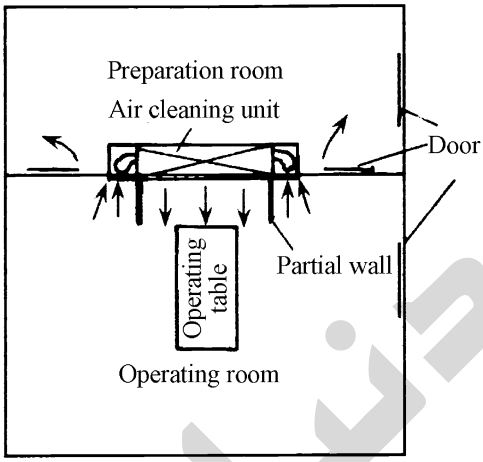

Fig. 14.27 Schematic diagram of the clean area with partial wall for the horizontal air supply mode in operating room

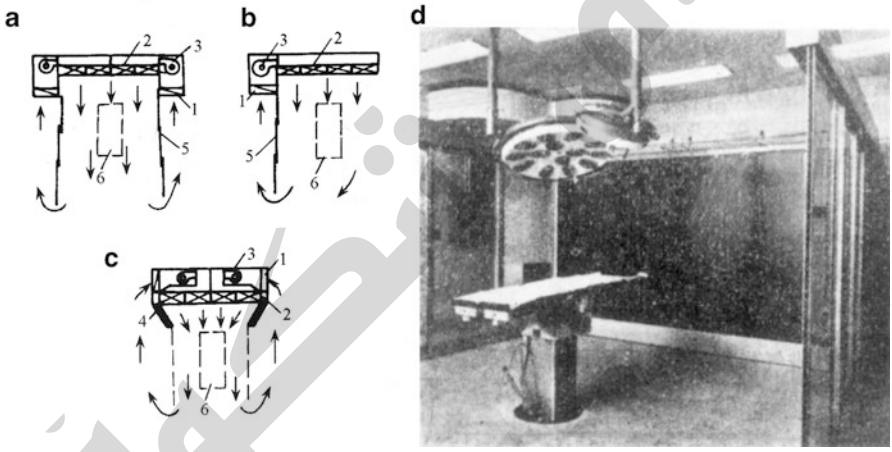

Fig. 14.28 Several types of partial walls. (**a**) Horizontal unidirectional flow, partial wall placed at both sides. (**b**) Horizontal unidirectional flow, partial wall placed at one side. (**c**) Horizontal unidirectional flow, partial wall placed with inclination. *1* Prefilter, *2* HEPA filter, *3* Fan, *4* partial wall, *5* partial wall with sliding glass, *6* operating table. (**d**) Application of partial wall in opening room

air supply velocity on the whole cross section, it is not economic. In this case, people began to think the scheme with elevated surrounding air velocity to protect the central mainstream area, which is the combination of surrounding air curtain and the vertical unidirectional flow. It can be called the air curtain cleaning booth.

In the early 1960s, the USA first made improvement on the air supply device with curtain, and the air curtain cleaning booth was manufactured, which was applied to the inspection and assembly of huge rocket components [13]. In order to protect the

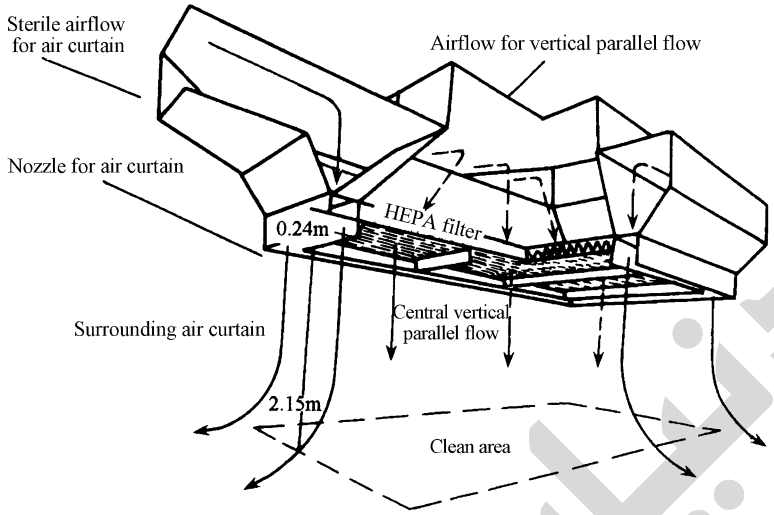

Fig. 14.29 Experiment device of the air curtain cleaning booth in the UK

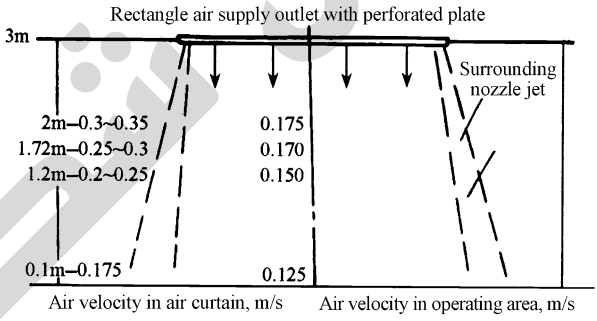

Fig. 14.30 Air curtain cleaning booth applied in a hospital in Switzerland (air supply outlet with perforated plate)

component from the influence of external flow during the stop of the air supply, the curtains around are pulled to the ground. Later, this device was also been applied successfully in the 150 m long automatic production line of color TV set.

The UK established the experiment device for air curtain cleaning booth [9]. The device was hung on the ceiling, with the distance 2.15 m above the floor and the size of the mainstream area 1.26 m $\times$ 2.34 m, which is shown in Fig. 14.29.

In a hospital in Switzerland, the combination of the surrounding air curtain and the central rectangular air supply perforated plate was used with success. The area of perforated plate is 2.4 m $\times$ 3.3 m. When the air change rate in the mainstream area is 130 h^{-1}, the size of the clean area available can be 3.6 m $\times$ 4.5 m, which is shown in Fig. 14.30 [18]. It is worthy noticed that the air velocities in both the air curtain and the center of the device are not large, and the decay of velocity field is also not fast. But particles are easily deposited on the perforated plate, which is difficult to clean, so the appearance is rather poor.

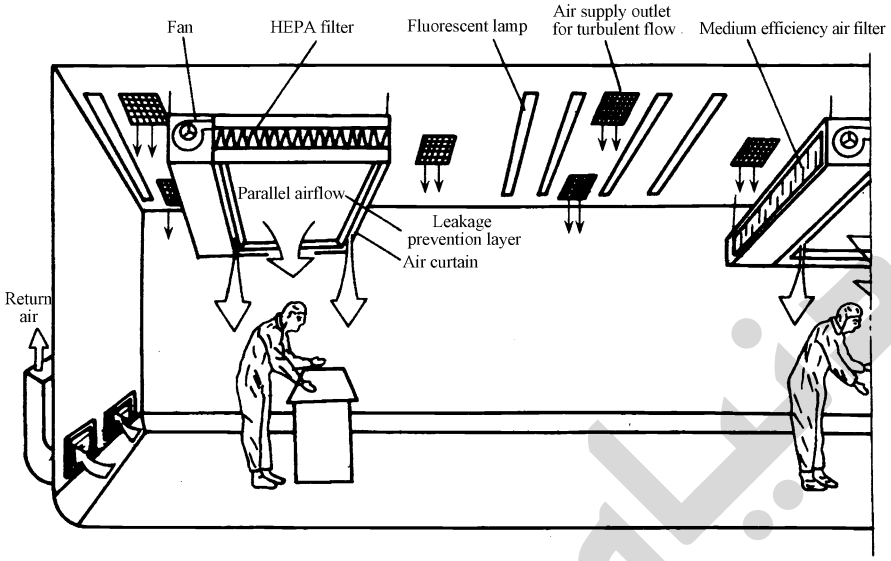

Fig. 14.31 Proposed scheme for the application of air curtain cleaning booth in large space workshop

These devices with air curtain belong to the centralized placed air supply mode, and they are not local purification equipments. Neither the design data nor the theoretical analysis is provided. Shen Jinming developed this combination form into local purification equipment, and theoretical study was performed [19]. The quantitative indicators for the isolation performance of air curtain were obtained. The idea for application in large space was proposed, which was shown in Fig. 14.31. This can be used to overcome the shortcomings that cleanroom was divided into small rooms as mentioned in Section one of this chapter. Figure 14.32 is one form of the device (for vacuum coating machine).

14.4.2 Isolation Effect of Air Curtain

Only when the air curtain reaches the floor, its isolation function can be realized which is shown in Fig. 14.33 [20]. In this case, air curtain is used to completely separate the pollution area from the clean area (or the dust-free area). When the air velocity from the air curtain increases above a certain value but the isolation effect is not improved, the air supply velocity of the air curtain is called the shield velocity under this condition. From the performance of linear air curtain shown in Fig. 14.34 [20], the corresponding shield velocity can be obtained.

The above study shows that for the surrounding air curtains with fixed nozzle width and air velocity, the isolation effect under steady state is the same, no matter

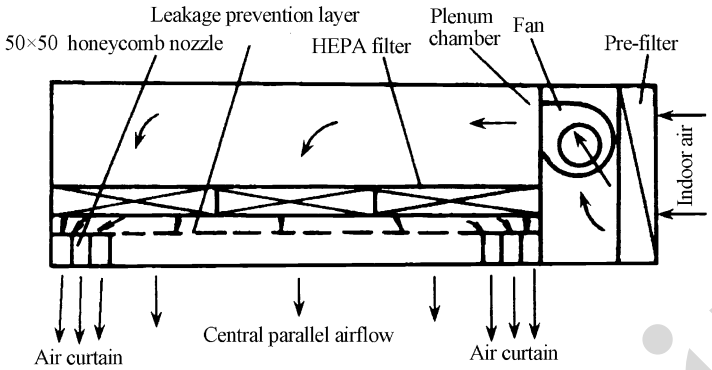

Fig. 14.32 One form of air curtain cleaning booth for the application of vacuum coating machine

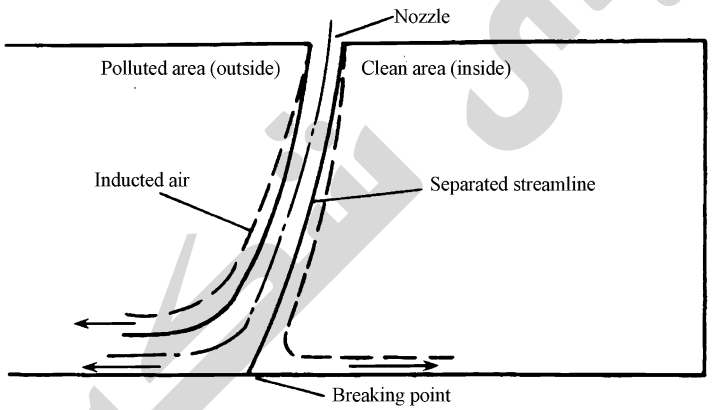

Fig. 14.33 Theoretical cross section of linear air curtain

whether clean air is supplied beforehand in the central area. Therefore, the isolation effect of air curtain is realized with the continuous induction of air at both sides, which is unlike the prevention of particle penetration by solid wall. Dirty air is continuously diluted and removed (because clean air is supplied from the nozzle of the air curtain), so that particles cannot penetrate the air curtain. Only a few particles may enter the central area because of the lateral fluctuation of airflow. Therefore, with the same amount of flow rate, the larger the nozzle width is, the less the induction flow rate is, and the less the penetrated particles are. It is more difficult for particles to penetrate when the lateral distance is larger. At this time, the isolation effect is much better (Fig. 14.34).

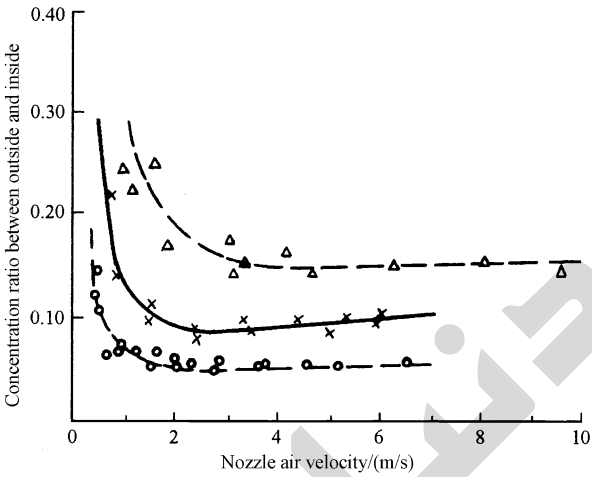

Fig. 14.34 Shield effect of air curtains with different nozzle widths (outlet width of air curtains, Δ means 0.085 m, × means 0.15 m, ○ means 0.23 m)

14.4.3 Theoretical Analysis of the Isolation Effect by Air Curtain Cleaning Booth

Under the steady state situation, three-zone mathematical models can also be proposed for the air curtain cleaning booth, which is shown in Fig. 14.35 [19].

In the finite space, we know

$$\frac{dN_a}{dt} = \frac{(Q_a - Q')N_a + Q'N_d - (Q_a + Q' - Q')N_a}{V_a}$$

$$\frac{dN_d}{dt} = \frac{Q_dN_d + Q'N_a + Q''N_b - (Q' + Q'' + Q_d)N_d}{V_d}$$

$$\frac{dN_b}{dt} = \frac{G_b + \frac{G_aQ_a}{Q_a - Q' + Q'}} + (Q'' + Q_d)N_d + Q_aN_a - (Q'' + Q_a + Q_d)N_b}{V_b}$$

where

N_a is the particle concentration in the mainstream area, #/L;
N_d is the particle concentration in the air curtain area, #/L;
N_b is the particle concentration in the vortex area, #/L;
N_s is the average particle concentration in the mainstream area and the air curtain area, #/L;
G_a is the particle generation rate in the mainstream area, #/L;
G_b is the particle generation rate in the vortex area, #/L;
Q_a is the air supply volume in the mainstream area, L/min;
Q_d is the air supply volume in the air curtain area, L/min;
Q' is the induced air volume between the air curtain area and the mainstream area, L/min;

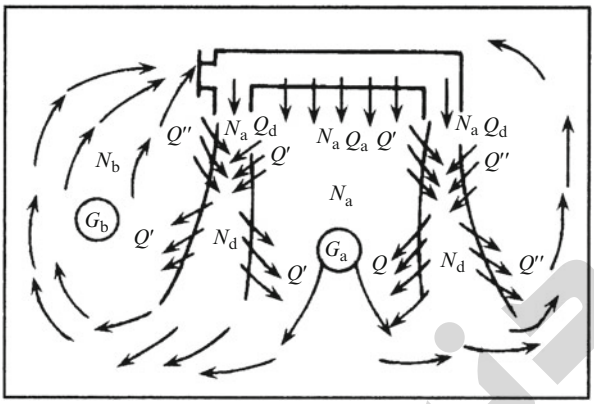

Fig. 14.35 Airflow model of the air curtain cleaning booth

Q'' is the induced air volume between the air curtain area and the vortex area, L/min;
V_a is the volume of the mainstream area, L;
V_d is the volume of the air curtain area, L;
V_b is the volume of the vortex area, L.

Let φ_1 be the induction coefficient of the air curtain for the mainstream area, so $\varphi_1 = \frac{Q'}{Q_d}$. Let φ_2 be the induction coefficient of the air curtain for the vortex area, so $\varphi_2 = \frac{Q''}{Q_d}$. Let α be the ratio of the air supply volume between the air curtain area and the mainstream area, so $\alpha = \frac{Q_d}{Q_s}$. Let V be the total volume of the finite space (L). Let G be the particle generation rate per unit volume [#/(m^3 · min)].

So we obtain:

$$Q_a + Q_d = \frac{nV}{60}$$

$$\frac{G_a + G_b}{V} = G \times 10^{-3}$$

When $t \to \infty$, the particle concentrations in three zones can be expressed as:

$$N_b = N_s + 0.06\frac{G}{n} \tag{14.11}$$

$$N_d = \frac{(1+\varphi_1)N_s + \varphi_2 N_b}{1+\varphi_1+\varphi_2} \tag{14.12}$$

$$N_a = (1-\alpha\varphi_1)N_s + \alpha\varphi_1 N_d \tag{14.13}$$

Then we obtain:

$$\frac{N_a}{N_b} = \left(1 - \frac{\alpha\varphi_1\varphi_2}{1+\varphi_1+\varphi_2}\right)\frac{N_S}{N_b} + \frac{\alpha\varphi_1\varphi_2}{1+\varphi_1+\varphi_2} = (1-f)\frac{N_S}{N_b} + f \tag{14.14}$$

$$f = \frac{\alpha\varphi_1\varphi_2}{1+\varphi_1+\varphi_2} = \text{const.} \tag{14.15}$$

The less the value of N_a/N_b is, the better the isolation effect of the air curtain is. It is obvious that the actual isolation effect of the air curtain cleaning booth is different under different environment. When N_b is very large, such as $N_b > 2{,}000$#/L, the particle concentration N_s at the air supply outlet through HEPA filter is usually 0.1 ~ 0.2#/L. So $N_s/N_b \approx 10^{-4}$, and

$$(1-f)\frac{N_s}{N_b} \ll f$$

So we obtain:

$$\frac{N_a}{N_b} \approx f \tag{14.16}$$

Therefore, f is considered as the intrinsic property of the isolation effect by the air curtain cleaning booth. This means, when the environmental particle concentration is very large, the measured value of N_a/N_b can reflect the isolation effect, which is the value of f. It is the best isolation effect with this kind of device. It should be noted that when the isolation effect reaches the maximum, the particle concentration in the mainstream area is not the minimum. When the environmental particle concentration is large, the particle concentration in the mainstream area will be correspondingly large, but the isolation effect is large.

The item $(1-f)\frac{N_s}{N_b}$ in Eq. (14.14) shows the influence of the environmental concentration N_b. It is called the environmental additional item of the isolation effect.

Since it is quite difficult to determine the coefficients of φ_1 and φ_2, it is not easy to calculate the value of f. In Eq. (14.15), both φ_1 and φ_2 will not be less than 10^{-1}, and α will also be larger than 10^{-1} for this device, so f is usually not be less than 10^{-2}. This means the isolation ratio of the air curtain cleaning booth will not be lower than 0.01. This is the reason why the measured value of the isolation ratio (corresponding to the clean area with practical implication), namely, the particle concentration ratio between the inside and the outside of this device, is not be less than 0.01 so far from literatures at home and abroad.

It is shown from Eq. (14.15) that the induction ratio of the flow rate can be reduced by the air curtain with low velocity and large width, which can decrease the value of f. So the better isolation effect can be obtained, which is also the case for the application where the space is large and the particle generation rate is large.

Table 14.8 Suitable air velocity at the outlet of the air curtain from the cleaning booth

Width of air curtain (mm)	75	100	150	200	225
Suitable air velocity (m/s)	146–1.75	1.26–1.52	1.03–1.24	0.89–1.07	0.84–1.01
Necessary average flow rate for unit length of air curtain (m^3/h)	434	500	612	707	749

In the application where space is small and the particle generation rate is small, the advantage of the air curtain with large width is not realized, but better effect may be achieved by the air curtain with narrow width. In the past, it was thought that the isolation effect of the air curtain with large velocity was better, but this is not true according to the above analysis.

14.4.4 Performance of Air Curtain Cleaning Booth

The experimental study of the air curtain cleaning booth above was carried out in an equipment with two air supply systems provided for the central area and the air curtain area (for the convenience of adjustment during test). Indoor air enters the plenum chamber of the central area and the air curtain, respectively. Air is supplied into the room after passing through fine air filter and HEPA filter.

14.4.4.1 Proper Air Velocity at the Outlet of the Air Curtain

In the central area surrounded by the air curtain, vertical unidirectional flow was supplied, which increased the interior pressure. It will inevitably expand outwards. A lateral force will be exerted on the air curtain, which makes the air curtain flow outwards and enlarges the size of the central mainstream area. Moreover, flow is induced by the air curtain. The resultant velocity field in the central mainstream area will decay quickly, which is very detrimental for the steady of the large clean area. It is shown that this situation can be ameliorated by application of suitable nozzles and air supply velocity at the outlet of air curtain (i.e., the partition velocity). For this kind of nozzle, vertical partition plates were used (which is equivalent with the case that one nozzle is separated into many small nozzles) and the outer plate was not used. Airflow is supplied when it is attached to the inner surface of steel plate. The suitable air velocity of the air curtain was obtained through experiment, which is shown in Table 14.8.

14.4.4.2 Concentration Field

Various curves can be plotted as shown in Fig. 14.36 for the particle concentration generated by the air curtain cleaning booth with different widths, when the particle concentration ratio between the central area and the environment (non-clean area)

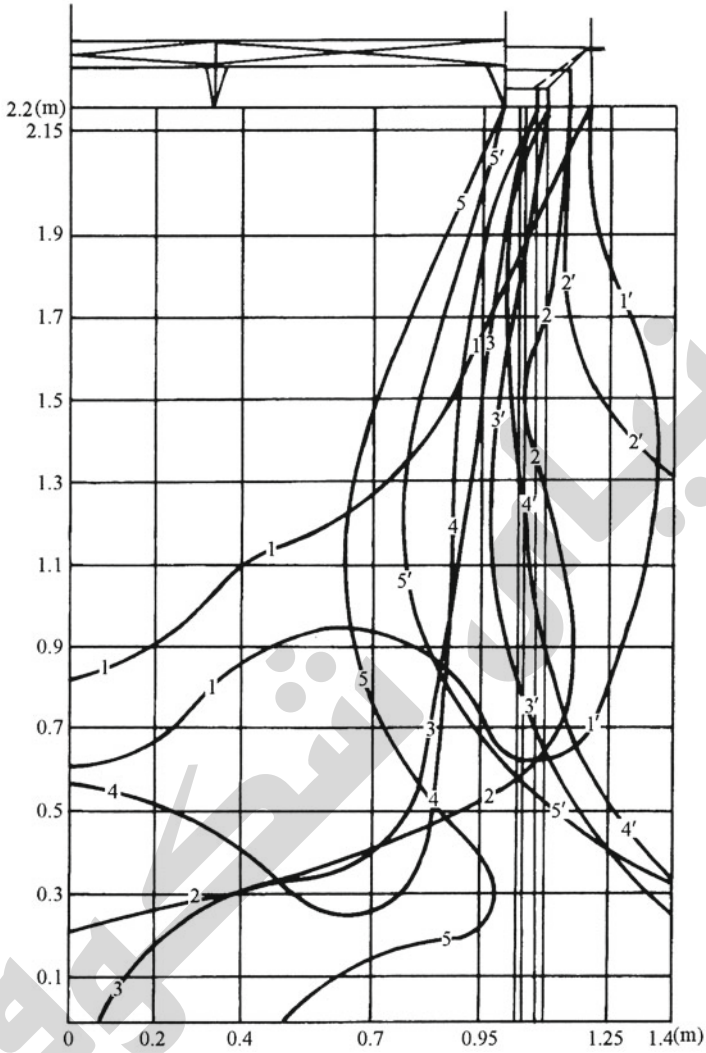

The operational conditions of each curve in the figure are

No.	Air curtain width (mm)	Air supply velocity (m/s)	Exit velocity at the air curtain outlet(m/s)	Total flow rate (m^3/h)	$\frac{N_a}{N_b}$ <1 %	1 % < $\frac{Na}{Nb}$ < 10 %
1	200	0.31	0.69	8,743	-1-	-1'-
2	150	0.31	0.92	8,743	-2-	-2'-
3	100	0.31	1.37	8,743	-3-	-3'-
4	75	0.31	1.94	8,743	-4-	-4'-
5	Without air curtain	0.31	0	4,397	-5-	-5'-

Fig. 14.36 Concentration field of the air curtain cleaning booth with different widths (profile)

Table 14.9 Comparison of the size of clean area when $N_a/N_b < 1$ %

No.	Condition	Air supply velocity in clean area (m/s)	Total flow rate/(m^3/h)	Ratio of the minimum side length of the cross section in clean area at the working height to the side length of the air supply cross section (%)	The minimum cross-sectional area in the clean area at the working height (m^2)	Ref.
1	150 mm air curtain	0.31	8,743	105	2.1 × 2.1	[19]
2	100 mm air curtain	0.31	8,743	85	1.7 × 1.7	
3	75 mm air curtain	0.31	8,743	85	1.7 × 1.7	
4	225 mm air curtain	0.3	11,529	131	Convert with square: 2.4 × 2.4	
5	75 mm air curtain	0.3	6,561	60	Convert with square: 1.51 × 1.51	[9]
6	Vertical uni-directional flow without air curtain	0.31	4,397	64	1.28 × 1.28	[19]
7	Vertical uni-directional flow without air curtain	0.5	7,200	78.7	Convert with square: 1.64 × 1.64	[9]

(namely, the particle concentration ratio between the mainstream and the vortex area in the non-clean environment) N_a/N_b reached 1 and 10 %.

It is shown that the performance of the air curtain with low velocity and large width is better than that of the air curtain with high velocity and narrow width. The concentration field of the air curtain with width 150 mm is better than other kinds of air curtain in terms of the width and the extent to approach the floor (the air velocity of air curtain with width 150 mm is slightly less).

14.4.4.3 Size of Clean Area

The sizes of clean area formed by the air curtain cleaning booth with different widths of air curtains are different. Table 14.9 presents the comparison between the measured data and foreign data.

It is shown from Table 14.9 that when the total flow rate is not too large, the performance of air curtain cleaning booth with the width 150 mm of the air curtain is the best.

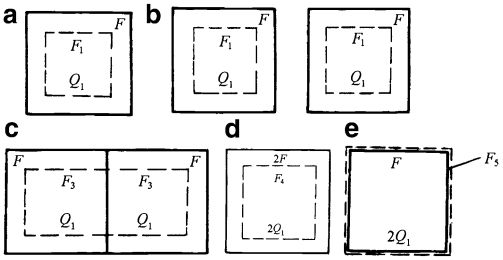

Fig. 14.37 Comparison of the size of clean areas formed between the air curtain cleaning booth and the unidirectional flow supply mode without air curtain. (**a**) Air supply device for vertical unidirectional flow air curtain $F = 4\ m^2$, $F_1 = 1.63\ m^2$. (**b**) Two air devices for vertical unidirectional flow without air curtain $F_1 + F_1 = 3.28\ m^2$. (**c**) Two air devices for vertical unidirectional flow without air curtain $F_3 + F_3 = 3.28\ m^2$. (**d**) Air supply devices for vertical unidirectional flow without air curtain when the air supply area in enlarged by one from that in (**a**) $F_4 = 4.35$ m. (**e**) Air curtain cleaning booth $F_5 = 4.41$ m. ☐ Cross section of air supply outlet, ⬚ min. cross-sectional area of clean area ($N_d/N_b < 1$ %). F air supply area, F_i min. cross-sectional area of clean area in corresponding i), Q_1 the flow rate of air supply device for vertical unidirectional flow with air curtain

According to Table 14.9, the sizes of clean area for the unidirectional flow supply mode before and after the air curtain is used were compared by author, which is shown in Fig. 14.37. For the former case, energy consumption is not wasted because of air curtain. With the same total flow rate (the flow rate through the air curtain is included when the air curtain is used) and the same air supply area (i.e., the area of air filter), the size of clean area is the smallest at the working height where is 0.8–1.5 m above the floor, which is the largest when air curtain cleaning booth is used. Although the narrowest size of clean area with unidirectional flow supply equipment when air curtain is not used, which means the air supply areas are combined, is almost the same as that with air curtain cleaning booth, it is too large to be installed with convenience, so it is not suitable to be used as mobile equipment. It has the disadvantage of no protection from air curtain and being likely to be disturbed for the central mainstream area, so the air curtain cleaning booth is still superior, which can be energy saving.

It is shown from Table 14.9 that, although the size of clean working area provided by air curtain cleaning booth with width 225 mm was larger than that with width 150 mm based on the foreign experiment, the superiority of technical and economical indexes cannot be reflected since this was performed under the condition of artificial high concentration. For the former case, the total flow rate is much larger when the width of the air curtain is larger, so the energy consumption becomes larger and both the structure and the weight are correspondingly enlarged, which is not practical. Therefore, from the practical point of view, the air curtain with width 150 mm under usual particle concentration is relative appropriate.

It should be emphasized that from the development of the technology, semi-centralized air cleaning system is the trend proposed both at home and abroad. Only

fresh air with certain parameters is supplied through central air supply system, and local clean area with high air cleanliness is generated with "terminal device" such as the air curtain cleaning booth. The self-circulation ability of this device is extreme strong, which can reduce the particle concentration greatly. In this way, the system is simplified and the cross-sectional area of air pipeline is reduced, but the resultant noise may be larger.

This kind of air curtain cleaning booth has the above features. It is suitable to be suspended and mobile because of the simple structure, the small volume and the light weight. So it provides the possibility for the application in large area workshop where the production process is variable.

14.5 Partition Curtain Cleaning Booth

14.5.1 Application

Partition curtain cleaning booth is popular, since it is a kind of local cleaning equipment with less investment, fast implementation, high performance, and low energy consumption.

This kind of transversely placed tubular filter dates back to the former Soviet Union in 1950s [21]. At that time, the folded HEPA filter made of glass fibrous filter paper was not available. The main filter medium was vinylidene chloride, namely, ФП filter cloth. When the filtration velocity was 0.01 m/s, the penetration was 3.2 %. It was equivalent with the performance of sub-HEPA filter in China. Since this kind of filter medium was thick, it was not easily folded but could be pasted. So flexible pipe with diameter 400 mm was made with ФП-15-17 filter cloth. It was applied in the cleanroom in the late of 1960s. They were uniformly placed on the ceiling to form the transversely placed air supply surface. Air was supplied into the cleanroom through the flexible pipe and the perforated ceiling below made of organic glass (it was not cleaning booth, but in essence it was the same). Air was returned through both bottom sides. Return air was delivered to the air conditioner placed outside of the cleanroom.

The above air filter and cleanroom are shown in Fig. 14.38.

The similar cleaning booth appeared in 1990s in China. Filter tubes made of polypropylene fibrous filter paper were transversely placed to form the air supply surface. The difference is that the plastic curtains were placed around in the common room. Filter tubes were transversely placed sub-HEPA filters. When complete self-circulation was used, the air cleanliness in the booth could only reach Class 100 [22]. Similar as Fig. 14.38, air was supplied from one side.

As for the double filter tubes and one side air supply mode, theoretical analysis was performed for a new type of cleaning booth with air curtain. The following innovation items were adopted in the structure [23].

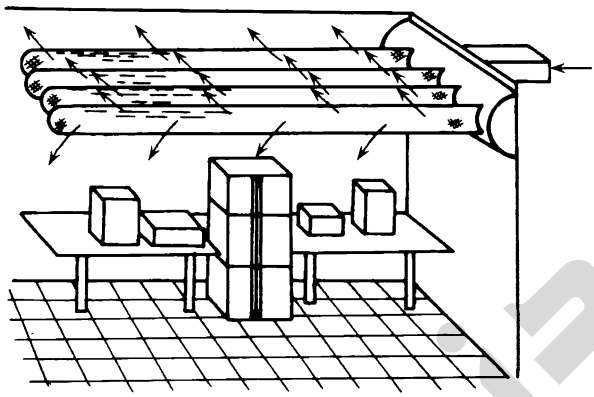

Fig. 14.38 Transversely placed air filter in former Soviet Union (Φ200)

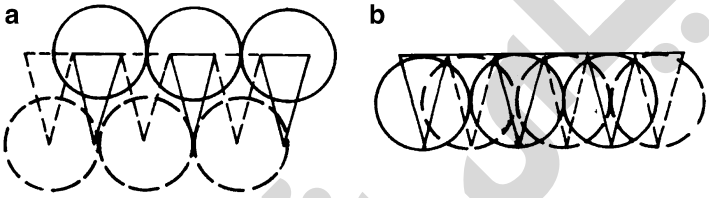

Fig. 14.39 Schematic diagram of change from circular tube to wedge tube. (**a**) Two rows of circular tubes are changed into single row of wedge tube. (**b**) Two rows of circular tubes back and forth are changed into single row of wedge tube

1. Multiple filtrations were simplified into one filtration. The important design principle for this new type of cleaning booth was that when circulation mode was used, only sub-HEPA tubular filter was needed according to theoretical analysis, while the previous prefilter can be omitted.
2. One side air supply mode is changed into bilateral air supply mode. Since the diameter of filter tube cannot be very large, the static pressure inside the tube cannot be stable and the filtration velocity along the whole filter tube cannot be very uniform. It also means that it is impossible to improve the uniformity of the air velocity inside the filter tube. Another way is that although there is nonuniformity in the tube, the whole flow field becomes uniform with the overlap of the uniform flow from single filter tube, when half of the filter tube supply air from one side and the other half of the filter tube supply air from the other side.
3. The circular filter tube becomes the wedge filter tube. It is known that for a certain area, the edge length of circle is the minimum, and the effective filtration area is only the low half of the circumference. For the given cross-sectional area, when the filtration area should be increased, and both the internal space of filter tube and the resistance of the airflow after filtration are required to be reduced, the best way is to change the circular filter tube into wedge filter tube, which is

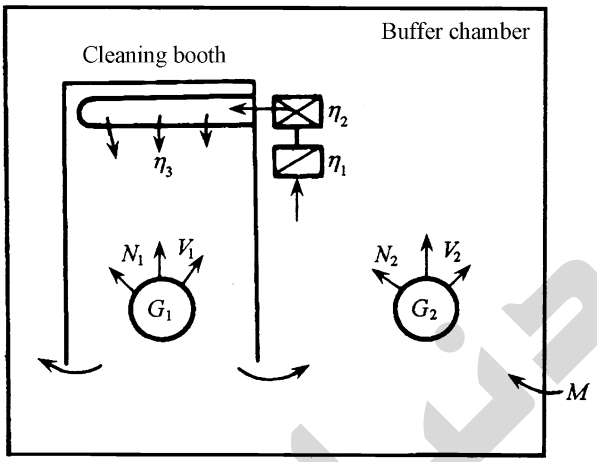

Fig. 14.40 Mathematical model

shown in Fig. 14.39. The key factors are how to determine appropriate height and bottom side length.

4. Partition support is used to fix the filter tube. In order to avoid the collision between filter tubes, the partition supports are used to separate and fix each filter tube. They can be placed one by one, which increases the filtration area and avoids the high air velocity between tubes. The other important purpose is to change circular tubes into wedge tubes.
5. When multiple rows of filter tubes are combined to one row, the partition support can provide a good solution to this problem.
6. The ceiling height where air filters are installed can be further reduced. When two rows are combined to one row, the height only reduces to 250 mm, which is only half of the height of the device abroad.

14.5.2 Theoretical Analysis of Cleaning Effect

Whether the air cleanliness level Class 100 can be achieved with the cleaning booth when sub-HEPA filters are used as the final filters? What kind of conditions should it be so that the air cleanliness level can reach Class 100? What kind of conditions should it be so that the air cleanliness level cannot reach Class 100? The conclusion cannot be made with measurement by only one or two devices. The relationship between indoor air cleanliness, the air change rate, the filter efficiency, the indoor particle generation rate, and the fresh air flow rate should be considered through theoretical analysis. The regular conclusion should be found out [24, 25]. The typical example can be simplified as the mathematical model shown in Fig. 14.40.

1. Particles entering the cleaning booth of unit volume per unit time at equilibrium state

   (a) Due to the leakage of doors and windows, and because of entering in and out, particles enter into the buffer, then supplied into the cleaning booth through the air cleaning system of the cleaning booth.

$$\frac{Mn_3\varepsilon}{60}(1-\eta_n)=\frac{Man_1\varepsilon}{60}(1-\eta_n)$$
$$\eta_n=1-(1-\eta_1)(1-\eta_2)(1-\eta_3)$$
$$a=\frac{n_2}{n_1}$$
$$\varepsilon=\frac{n_3}{n_2}$$

   where

   M is atmospheric particle dust concentration (#/L);
   n_1 is the air change rate of self-circulation through the cleaning booth;
   n_2 is the equivalent air change rate of the buffer chamber from the self-circulation flow rate through the cleaning booth;
   n_3 is the equivalent air change rate of the buffer chamber from the total leakage flow rate;
   η_n is the total efficiency of the cleaning system for the cleaning booth.

   (b) Particles generated in the buffer chamber and then enter the cleaning booth can be expressed as

$$G_2\times10^{-3}(1-\eta_n)=bG_1\times10^{-3}(1-\eta_n)$$
$$b=\frac{G_2}{G_1}$$

   where

   G_1 is the particle generation rate in unit volume of the cleaning booth [#/(min · m^3)];
   G_2 is the particle generation rate in unit volume of the buffer chamber [#/(min · m^3)].

   (c) Particles enter the cleaning booth by the return air can be expressed as

$$\frac{s_1n_1N_1}{60}(1-\eta_n)$$

   where

   N_1 is the average particle concentration in the cleaning booth, which can be considered as the concentration of the return air (#/L);
   s_1 is the ratio of return air. It is one for complete circulation.

   (d) The particle generation rate inside the cleaning booth is $G_1\times10^{-3}$.

2. At equilibrium state, particles exhausted from the unit volume of the cleaning booth per unit time can be expressed as $n_1N_1/60$.
3. The balance of particles in and out can be expressed as:

$$\left(\frac{Man_1\varepsilon}{60} + bG_1 \times 10^{-3}\right)(1-\eta_n) + G_1 \times 10^{-3} = \frac{n_1N_1}{60} - \frac{s_1n_1N_1(1-\eta_n)}{60}$$

When $s = 1$, we can obtain:

$$N_1 = \frac{60G_1 \times 10^{-3}[1 + b(1-\eta_n)] + Man_1\varepsilon(1-\eta_n)}{n_1\eta_n} \tag{14.17}$$

If nonuniform distribution theory is used for calculation, when the nonuniform distribution coefficient is ψ and the average particle concentration inside the cleaning booth is N_v, we obtain:

$$N_v = \psi N_1$$

In order to calculate N_1, the following parameters need to be determined.

(a) At the as-built state, $G_1 = 0.5 \times 10^4$. When there is one person at rest, the dynamic-to-static ratio can be assumed 3. The occupants' density can be the average value between 1/2 and 1/4, namely, 0.375. At this time, $G_1 = 5 \times 10^4$. When the dynamic-to-static ratio is 7, $G_1 = 11 \times 10^4$.
(b) a – when areas between inside and outside are equivalent, $a = 1$; when the outside room is large, n_2 is small and $a < 1$; when the outside room is small, n_2 is big and $a > 1$.
(c) b – according to Eq. (14.17), the effect of b is not large due to the influence of $1 - \eta_n$. Because the outside room is the buffer chamber, the occupant's activity is very large, it is assumed $b = 10$ for safety consideration.
(d) ε – in the buffer chamber, there are usually one non-closed door and a single layer stationary airtight window. Since the pressure inside the buffer chamber is "0," the influence of wind pressure from outside ambient can be taken into account, which is the intermittent pressure 5–10 Pa. When the slot length is assume 11 m, according to the data about the leakage flow rate for this kind of door and windows [26], the total leakage flow rate is:

$$L = 11 \times \left[\frac{(17+24) + (1+0.7)}{2}\right] = 234.9 \text{ m}^3/\text{h}$$

Since the wind pressure is intermittent, the leakage flow rate can be assumed half, i.e., 118 m^3/h.

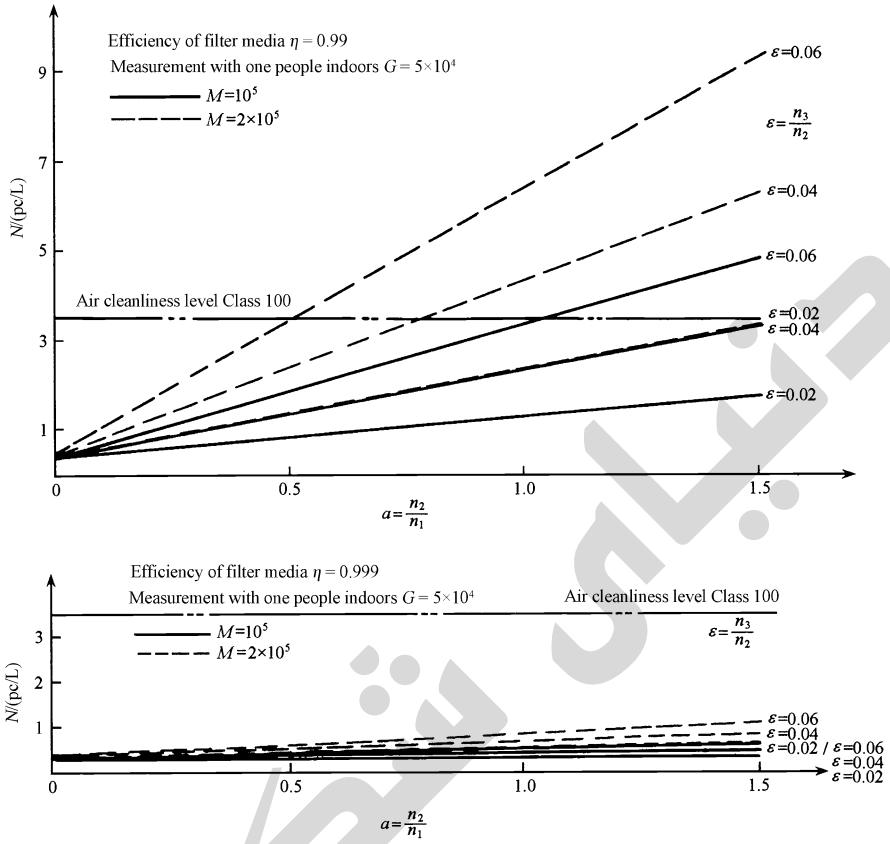

Fig. 14.41 Various factors influencing the particle concentration inside the cleaning booth

According to the area of the cleaning booth, the air velocity on the cross section is usually 2,000–2,500 m^3/h. Although n_2 varies with the size of the buffer chamber, the air leakage flow rate is fixed, namely,

$$\frac{118}{2,000-2,500} = 0.059\text{~}0.047$$

In the table, $\varepsilon = 0.02$, 0.04, and 0.06, respectively.

(e) n is usually about 500 h^{-1}.

(f) ψ – from Table 13.16, it is 0.05 for return air at both bottom sides. In the cleaning booth, air is returned at four bottom sides, so the flow uniformity is poorer than the situation when air is returned on both bottom sides. But because the chamber width is small, it can be still calculated with the situation when air is returned on both bottom sides.

Figure 14.41 shows the calculation results.

Table 14.10 Particle concentration in the buffer chamber (#/L)

M	a	G_1	ε	b	n_1	N_v	N_2
2×10^5	1.0	11×10^4	0.04	10	500	3.5	5,344
1×10^5	0.5	11×10^4	0.02	10	500	3.5	2,016

4. Particle concentration in the buffer chamber

Let N_2 the particle concentration in the buffer chamber. According to the balance of particle concentration, the equilibrium expression can be made:

$$\frac{n_2 N_2}{60} = G_2 \times 10^{-3} + \frac{Sn_1 N_v}{60} + \frac{Mn_2 \varepsilon}{60} \tag{14.18}$$

Because $n_2 = an_1$, $S = 1$, and $G_2 = bG_1$, we can obtain

$$\begin{aligned} an_1 N_2 &= 60bG_1 \times 10^{-3} + n_1 N_v + Man_1 \varepsilon \\ N_2 &= \frac{60bG_1 \times 10^{-3} + n_1 N_v + Man_1 \varepsilon}{an_1} \end{aligned} \tag{14.19}$$

where the implications of each symbols are the same as before. Under the most unfavorable situation, the calculated results are shown in Table 14.10.

Through the above analysis and calculation, the cleaning booth with transversely placed filter tubes has the following features in performance:

1. When M is not more than 10^5 and the filter efficiency η_n is only 0.99 (the penetration K is less than 1 %), the air cleanliness level can reach Class 100 under the condition of self-circulation (except several individual cases). When η_n is close to 0.999, the air cleanliness level can reach Class 100 as long as M is less than 2×10^5.

The filtration velocity inside the filter tube is generally 3–5 cm/s, which is 3–5 times larger than the standard specific velocity 1 cm/s of the filter media. When the specific velocity is assumed to increase by four times, according to Chap. 4 the penetration will increase about 20–40 times, which can be considered 30 times.

According to the above requirements, for particles with diameter ≥0.5 μm we know:

$$K \times 30 = 1\ \%$$

$$\begin{aligned} K &= \frac{1}{100 \times 30} = 0.00033 = 0.033\ \% \\ \eta_n &= 1 - K = 1 - 0.033\ \% = 99.96\ \% \end{aligned}$$

It shows that the filtration velocity should be less than 5 cm/s for the air supply surface with transversely placed filter tubes made of polypropylene fibrous filter material whose efficiency is 99.99 %, so that the cleaning booth with air cleanliness level Class 100 can be manufactured, where coarse and medium

efficiency air filters are not used. With self-circulation, the particle concentration in the buffer chamber is lower than the required value for Class 200000, where the gravimetric concentration is much less than 0.1 mg/m^3.

When the gravimetric concentration is assumed 0.05 mg/m^3, the dust holding capacity of filter media 40 g/m^2, the total filtration area of cleaning booth 20 m^2, and the filtration efficiency 0.99, the service life can be obtained when it operates continuously everyday under the flow rate 2,000 m^3/h:

$$T = \frac{20 \times 40 \times 10^3}{2,000 \times 24 \times 0.05 \times 0.999} = 334$$

It is shown that when only a sub-HEPA filter is used, the service life can also maintain nearly one year or longer. Not only the application requirements are met but also the device structure is simplified and the cost is reduced.

2. Because self-circulation is very important for the device, the leakage rate should be reduced as much as possible. The leakage rate is almost proportional to the particle concentration N_v. This also applies for the situation when $\eta_n = 0.99$.

   So if fresh air is supplied into this device, sub-HEPA filter must be placed along the passage of fresh air. If fresh air is supplied into the buffer chamber to maintain the positive pressure, $\varepsilon = 0$, and the air cleanliness level in the cleaning booth will be greatly improved. It is better to use this device together with the fresh air handling unit containing sub-HEPA filter.
3. The larger the buffer chamber is, the smaller the particle generation rate G_2 per unit volume is. When equilibrium state is reached, it will contribute to the air cleanliness. From Fig. 14.30, when $a = 0.5$, namely, the area of the buffer chamber is larger than that of the cleaning booth by one time, the particle concentration inside the cleaning booth reduces by half, and the volume of the buffer chamber is inversely proportional to the particle concentration in the cleaning booth. When more outdoor fresh air infiltrates into the buffer room, G_2 becomes larger and the particle concentration inside the cleaning booth increases faster.
4. If the airflow in the cleaning booth can be approximated as unidirectional flow, when the particle generation rate G per unit volume of air increases by 22 times, the increase of particle concentration is still less. In the condition $\eta_n = 0.999$, it increases only by 1/10 to 1/3. When $\eta_n = 0.99$, it increases by 1–3 times. When the airflow is much closer to the unidirectional flow, the performance is much better.

14.5.3 Experimental Effect

Table 14.11 shows the experimental data after the system operated for half an hour in the cleaning booth where are two testing people inside. The cleaning booth was placed inside the ordinary room.

From the measurement result, when sub-HEPA filter tube was used, the particle concentration was sensitive to the inlet particle concentration. Even so, when the cleaning booth operates with self-circulation mode in the buffer chamber

Table 14.11 Summary of particle concentration measurement in cleaning booth (≥0.5 μm, #/2.83L)

Item / Condition	Initial concentration in buffer chamber before measurement	During operation of cleaning booth	Concentration in buffer chamber after operation	Concentration in cleaning booth
Air supply system in buffer chamber operates	5×10^3(Class 100000)	0.5 h	~130	1.8
Air supply system in buffer chamber is stopped	~5×10^4	0.5 h	~1,000	5.4
Both inner and outer doors are open in buffer chamber	~5×10^4	0.5 h	~5×10^4	317

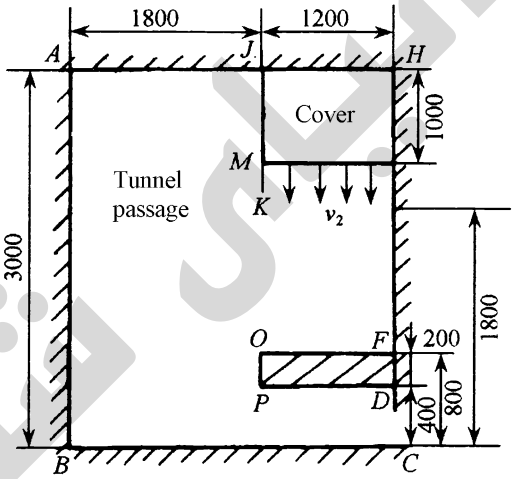

Fig. 14.42 Laminar hood in the cleaning tunnel (no auxiliary air supply at the operating surface and only partition board is placed (mm))

with concentration 50,000 #/L, the air cleanliness level inside the buffer chamber can reach Class 10000 and that inside the cleaning booth can reach Class 1000000. If the initial concentration corresponds with Class 100000, the air cleanliness inside the buffer chamber can also reach Class several thousands.

14.6 Laminar Flow Hood for Cleaning Tunnel

14.6.1 Requirement of Anti-disturbance

Basically the conventional cleaning tunnel can be divided into two sections, namely, the process area assembled with the laminar flow hood and the operation channel area for transportation and passage. In the process area, comprehensive unidirectional flow is supplied from laminar flow hood. In the operation channel area, turbulent air is supplied. Partition board is usually used to separate the process area from the operation channel area (Fig. 14.42). Since the production line with air

cleanliness level Class 100, especially Class 10 or higher, is extremely sensitive to the disturbance of pollution. The clean area in the process area with this kind of conventional cleaning tunnel reduces, so it is difficult to reach the prescribed air cleanliness level. This is because when turbulent flow is supplied in the operation channel, vortex circulation is easily formed by the airflow between the ceiling and the partition board in front of the hood. Pollution, especially the pollutants generated at the head of the operational personnel, will retain for a long term. Airflow will be easily induced below the partition board and vortex will be produced, which increases the risk of the pollutant invasion from the operation channel into the cleaning area. During operation, hands will be swing back and forth, which will cause disturbance and reduce the air cleanliness inside the hood.

Therefore, the following three requirements are proposed for the anti-disturbance ability of the laminar flow hood applied in the cleaning tunnel.

1. Remove the vortex area at the above corner of the laminar flow hood in the process area. Get rid of the possibility of the pollution induction into the laminar flow hood from the bottom of the partition board.
2. If particle generation source exists near the laminar flow hood, it should be removed as soon as possible, so that it will not cause risk for the clean area inside the laminar flow hood.
3. Improve the anti-disturbance ability by the activity in front of the hood (namely, the disturbance with a certain lateral velocity).

14.6.2 Effect of Auxiliary Air Supply at the Working Surface

In order to realize the above three purposes, Wang Jie [27] proposed the measures of auxiliary air supply hood placed at the working surface of the laminar flow hood. Through experiment and theoretical study, the effect obtained was quite good.

In Figs. 14.43 and 14.44, hood with inclination angle 30° or 60° was placed at the working surface, or the hood with inclination angle 45° and regulating board was added.

14.6.2.1 Effect of the Hood Shape

1. In terms of the total effect, the performance of the hood with inclination angle 30° is better than that with partition board only and without hood. The hood with inclination angle 60° is better than that with inclination angle 30°. The hood with inclination angle 45° and regulating board is better than that with inclination angle 60°.

   Curves *a*, *b*, and *c* in Fig. 14.45 show the theoretical boundaries under the above three situations with air cleanliness Class 100. It is shown that the range of

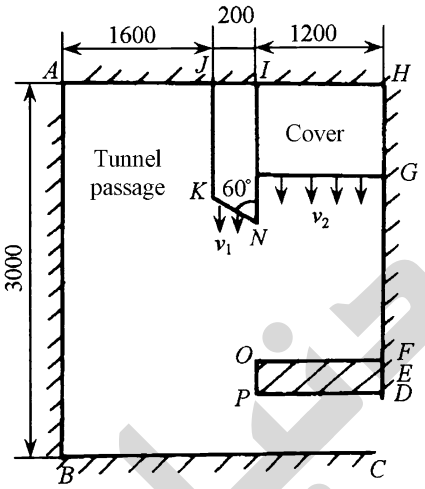

Fig. 14.43 Auxiliary air supply hood placed at the working surface (with inclination angle 60° (mm))

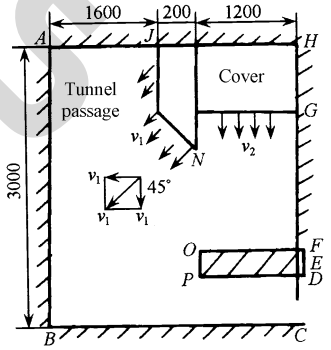

Fig. 14.44 Auxiliary air supply hood placed at the working surface (with inclination angle 45° and regulating board (mm))

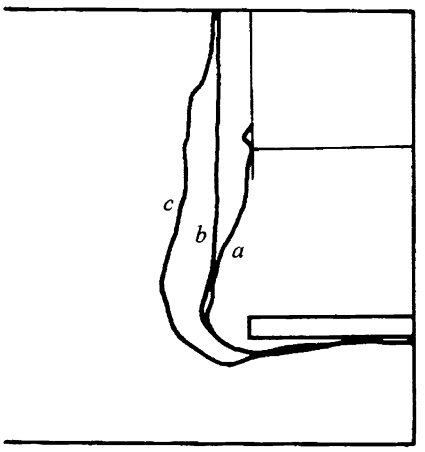

Fig. 14.45 Theoretical boundary of region with air cleanliness Class 100 for three kinds of laminar flow hoods

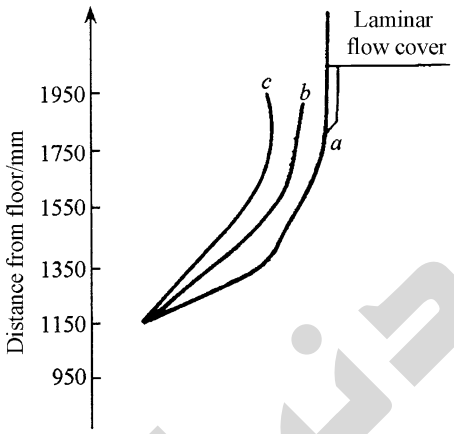

Fig. 14.46 Experimental clean area boundaries for three kinds of laminar flow hoods

Curve *c* is the largest. Fig. 14.46 shows the boundary of clean area (better than air cleanliness level Class 100000) obtained by experiment with the same total flow rate.

2. In terms of anti-disturbance from the lateral (horizontal) velocity, when lateral air pollution (simulated with hair dryer) exists at the working height where is 730 mm from the operation surface, the hood with inclination angle 30° and 60° can completely resistant the intrusion of disturbance, and their performances are not different from each other. When no hood is placed, the polluted air will invade to a certain range.
3. From the pollution near the front partition board, particles can be removed quickly when the hood is placed in front. When there is no hood, vortex area will be formed near the partition board and induction could be found inside the hood.

14.6.2.2 Effect of the Air Velocity Ratio

The air velocity ratio means the ratio between the exit velocity v_1 of the auxiliary air supply and the exit velocity v_2 of the laminar flow hood. Experiment has shown that it is better not to increase the value of this ratio only. For example, when v_1/v_2 increases from 0.57 to 0.86, although the flow rate only increases by 4 %, the range of the region with air cleanliness level Class 100 is obviously enlarged. If it increases from 0.86 to 1.43, although the flow rate only increases by 8 %, the range of the region with air cleanliness level Class 100 is almost unchanged. Experiment shows that the suitable air velocity ratio should be 0.77, when the cross-sectional area of the clean area is slightly larger than that with 0.86 and the invasion range by lateral velocity disturbance is also the minimum.

References

1. Akiyama Y, Shimizu A, Wei GX (1977) Experience from laminar flow sterile cleanroom. J SHASE (Soc Heat Air Cond Sanit Eng) Jpn 51(1):33–43 (In Japanese)
2. Niitsu Y, Katou T (1960) Study on performance and design of cleanroom (4): infiltration of inhomogeneous gas through the jet flow onto the isothermal plane. J Jpn Pub Health Assoc 34 (12):883–890 (In Japanese)
3. Tanaka M (1979) BBL business division of Becton, Dickinson and Company. J Jpn Air Clean Assoc 16(7):43–45 (In Japanese)
4. Liu H (2000) Study of the factors influencing the velocity field in the working area of the cleanroom with local air cleanliness level Class 100. Master dissertation at China Academy of Building Science Research (In Chinese)
5. Shen JM (1982) Discussion of the airflow visualization with bubble. Contam Contr Air Cond Technol 3:57–61 (In Chinese)
6. Xu ZL, Zhang YZ, Zhang YG, Mei ZL, Shen JM, Guo DR, Jiang PC, Liu H (2000) Mechanism and performance of an air distribution pattern in clean spaces. J HV&AC 30(3):1–7 (In Chinese)
7. Zhang YG, Xu ZL, Zhang YZ, Mei ZL, Shen JM, Guo DR, Jiang PC (1999) Numerical simulation analysis on concentration field in clean room with different air supply areas. Build Sci 15(6):6–11 (In Chinese)
8. Niu WL (2002) Study on air flow uniformity and anti-jamming capability of local Class 100 air supply mode with the leakage preventing layer. Master dissertation at Institute of HVAC of China Academy of Building Science Research (In Chinese)
9. Naoi T (1979) "Eye curtain" by the combination of vertical laminar flow and air curtain. J Jpn Air Clean Assoc 17(1):47–49 (In Japanese)
10. Esdorn H, Nouri Z (1977) Vergleichsuntersuchungen Ueber Luftfuehrungssysteme mit Mischstroemung in Operationsraeument, HLH, 4, p 28 (In German)
11. Scheer FA (1996) Lamnar-Flow-Decken in Opeationstraumen. MLH 47(7):41 (In German)
12. Xu ZL (2011) Design, operation and GMP certification of cleanroom in pharmaceutical factory. Tongji University Press, Shanghai, pp 90–94 (In Chinese)
13. Austin PR, Timmerman SW (1965) Design and operation of clean rooms. Business News Publication, Detroit
14. Takeno A (1979) Assessment of vertical laminar flow wall. J Jpn Air Clean Assoc 17(1):43–46 (In Japanese)
15. Tanaka M (1979) Design method of sterile filling equipment. J Jpn Air Clean Assoc 17(4):9–13 (In Japanese)
16. Inoue U (1979) Comprehensive technology of laminar flow in cleanroom of pharmaceutical industrial field. J Jpn Air Clean Assoc 17(4):5–6 (In Japanese)
17. Inoue U (1977) Biological cleanroom in hospital. J SHASE (Soc Heat Air Cond Sanit Eng) Jpn 51(1):1–4 (In Japanese)
18. Field AA (1973) Operating theater air conditioning. Heat Piping Air Cond 45(11):91–93
19. Shen JM (1981) Study on the characteristic of air curtain cleaning booth. Master dissertation at Institute of HVAC of China Academy of Building Science Research (In Chinese)
20. Kamishima K (1979) Laminar air curtain for the barrier of particles. J Jpn Air Clean Assoc 17 (1):50–51 (In Japanese)
21. Куприянов ИП (1982) Cleanroom technology (trans: Yu Zhaoji). China Architecture & Building Press, Beijing (In Chinese)
22. Li ZL, Cheng H, Yang YM (1990) Development of SMU-1 type screen unit, Academic exchange information on HVAC, thermal, power and energy-saving by related provinces and cities in east China (In Chinese)
23. Shen JM, Xu ZL (1994) Tube form filter series. In: Proceedings of the 12th ISCC conference, Yohohams

24. Shen JM, Xu ZL (1995) Research report on the air curtain cleaning booth system. Institute of HVAC of China Academy of Building Science (In Chinese)
25. Xu ZL, Shen JM (1998) Air clean screen supply system. J HV&AC 28(2):21–26 (In Chinese)
26. Xu ZL, Shen JM (1989) Application of air cleaning technology. China Architecture & Building Press, Beijing, pp 250–251 (In Chinese)
27. Wang J, Xu ZL (1995) Study on the anti-disturbance capability of clean tunnel laminar flow hood. J HV&AC 25(5):34–38 (In Chinese)

Chapter 15
Theory of Leakage Preventing Layer

It is a brand new concept for leakage prevention layer. The practice to place HEPA filter at the terminal is improved when the theory of leakage prevention layer applies, which becomes the core of novel air distribution method in cleanroom.

15.1 Overview

Air pollution control mechanism in clean space is realized by the supply of clean air through HEPA filter placed at the air supply terminal, which is the largest difference for the concept between the cleaning air conditioner and the general air conditioner.

However, it is inevitable that minor apertures and cracks invisible to the naked eyes may be generated during manufacturing, delivering, and installation processes. Therefore, the problem of leakage cannot be effectively solved only with sealing and leakage stoppage. In practice, the incidence of the abrupt increase of particle concentration or bacteria concentration in some region occurs more than one time. After careful and repeat check, the leakage pore is found on the air supply surface of HEPA filter. But it is still unknown whether the leakage pore is produced by filter media with poor quality, formed by scrape during installation, or generated gradually with the supplied air with the former two reasons. The leakage phenomena are much more along the frame. It will not attract people's attention when the air cleanliness level of turbulent flow cleanroom is not affected by these leakages. But whenever leakage occurs at the terminal, the safeguard system is not guaranteed. Severe or un-retrieved consequences may be generated, especially for unidirectional flow cleanroom with high level of air cleanliness.

As for the leakage problem on air filter, there are various methods to seal. But it cannot seal all the leakage passages through ceiling frame, air filter frame, head glue, and filter paper. Therefore, the concept of leakage prevention layer is proposed [1].

The purpose of leakage prevention layer is to decouple three functions including leakage stoppage, filtration, and flow equalization [2]. Leakage stoppage is realized

Z. Xu, *Fundamentals of Air Cleaning Technology and Its Application in Cleanrooms*,
DOI 10.1007/978-3-642-39374-7_15,

with HEPA filter at the terminal. Filtration should have certain efficiency. Flow equalization is equivalent with high value for the ratio of air distribution area. Leakage prevention layer can disperse, dilute and filter the penetrated air flow. The possible local leakage is converted into the complete integral un-leakage. The closed property of the system upstream of the air supplier is not modified.

The concept of leakage prevention layer is completely different from that of sealing the frame of air filter. The latter only aims to remove the leakage near the frame. The former aims to convert the problem of possible leakage at the last defense line or along other leakage passages into the integral un-leakage, which is equivalent with stopping the leakage.

The concept of leakage prevention layer is also completely different from that of the damping layer. The latter only plays the role of limited flow equalization and has certain decoration effect (when perforated plate is used, particles will be deposited instead). The former can have substantial effect to improve the cleaning performance with several mechanisms (introduced later).

When the concept of leakage prevention layer is combined with that of expanding mainstream area, new air distribution type will be formed, namely, the terminal air distribution with leakage prevention layer. The traditional model that HEPA filters must be placed at terminal is changed from both theoretical and practical point of view. The quality of air distribution and the ability of leakage stoppage are further improved.

15.2 Leakage Equation

Leakage equation is used to estimate the quantity of leakage.

Leakage is a kind of jet flow, since it is the phenomenon of high speed outflow through the hole. Because the cross-sectional area of leakage hole is much smaller than that of air filter, it can be omitted, so the related principle of free jet flow is valid to describe the leakage jet flow.

The influence of polluted flow through the leakage jet flow is the maximum for unidirectional flow. The local particle concentration near the working area will be elevated, which will bring particles to the object directly. If there are too many leakage positions, the polluted flow will overlap, which will increase the particle concentration on certain surface of the working area. The resultant average concentration in the whole room will be influenced, which is shown in Fig. 15.1.

For the common HEPA filter air supply inlet with diffusion plate with partial leakage as shown in Fig. 15.2, the concentration of air supply should be:

$$N_1 = K_1 N_0 \tag{15.1}$$

where

N_0 is the upstream concentration of air filter;

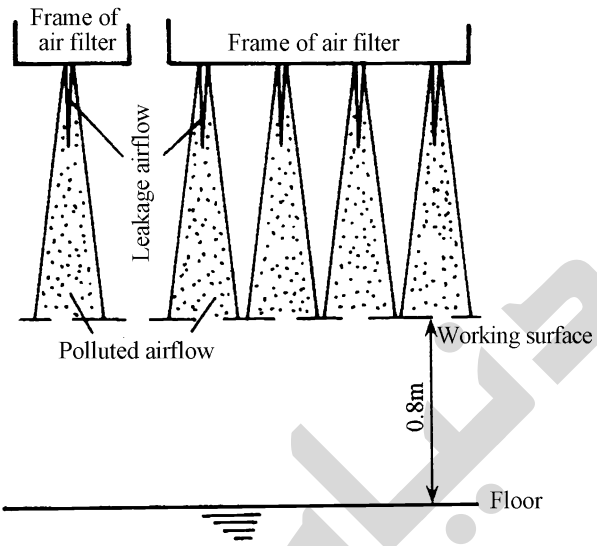

Fig. 15.1 Influence of leakage flow on the working area

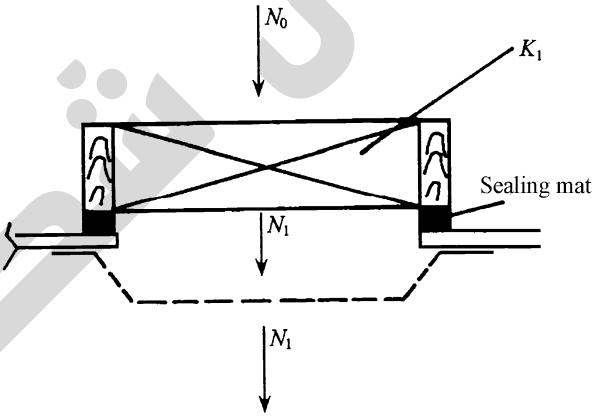

Fig. 15.2 HEPA filter air supply inlet with diffusion plate

N_1 is the downstream concentration of air filter, which is the concentration of air supply mentioned here;
K_1 is the penetration of air filter.

For the air supply inlet with leakage hole as shown in Fig. 15.3, the particle concentration of polluted flow constitutes of the following two parts, when Q_{m1} is the flow rate of leakage through the hole, Q_M is the total flow rate through air filter, Q_{s1} is the flow rate of polluted flow when the leakage jet flow is mixed, α_1 is the leakage coefficient with $\alpha_1 = \frac{Q_{m1}}{Q_M}$, and a_1 is the mixture coefficient with $a_1 = \frac{Q_{s1}}{Q_M}$.

1. In the unit volume of polluted flow, the particles brought in by leakage jet flow are $\frac{N_0\alpha_1}{a_1}$.

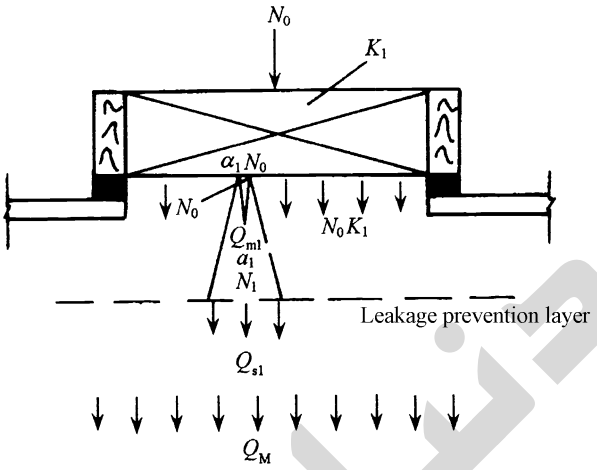

Fig. 15.3 Air supply inlet with leakage hole

2. In the unit volume of polluted flow, the particles brought in by the proportion of original flow before mixture are $\frac{N_0 K_1 (a_1 - \alpha_1)}{a_1}$.

So the particle concentration in the unit volume of polluted flow, i.e., the average concentration N'_1, is made of the summation of above two items, namely,

$$N'_1 = \frac{N_0\alpha_1 + N_0 K_1 (a_1 - \alpha_1)}{a_1} = N_0 \left[K_1 + \frac{\alpha_1}{a_1}(1 - K_1) \right] = N_0 (K_1 + \Delta K_1)$$
$$= N_0 K'_1 \tag{15.2}$$

With the comparison between Eqs. (15.1) and (15.2), the penetration of air filter with leakage for polluted flow increases from K_1 to $(K_1 + \Delta K_1)$. $K_1 + \Delta K_1 = K'_1$ is called the penetration with leakage.

There are two kinds of mixture of leakage jet flow with supplied air. One is the mixture during the process of jet flow. The other is the mixture with ambient flow, namely, mixed with the turbulent flow near the air supply inlet. When unidirectional flow, which is greatly affected by the leakage, is taken into account, the second kind of mixture is not considered here.

For the mixture during the process of jet flow, we obtain:

$$\frac{\alpha_1}{a_1} = \frac{Q_{m1}/Q_M}{Q_{s1}/Q_M} = \frac{Q_{m1}}{Q_{s1}} \tag{15.3}$$

When Eq. (15.2) is expanded, it is converted into:

$$N'_1 = N_0 K_1 + N_0 \frac{\alpha_1}{a_1} - N_0 K_1 \frac{\alpha_1}{a_1} \tag{15.4}$$

where N_0K_1 is the outlet concentration of filter, which is also the ambient concentration near the exit of the leakage jet. Let it be N_e, i.e.,

$$N'_1 - N_e = (N_0 - N_e)\frac{\alpha_1}{a_1} \tag{15.5}$$

Substituting it into the Eq. (15.3) gives:

$$\frac{N'_1 - N_e}{N_0 - N_e} = \frac{Q_{m1}}{Q_{s1}} \tag{15.6}$$

According to Г.Н. Абрамович (referred to as the A's), the law of concentration difference in jet flow derived before the 1960s is the following equation[3], where the concentration is inversely proportional to the flow rate and is proportional to the change of the speed:

$$\frac{\Delta N_1}{\Delta N_0} = \frac{Q_0}{Q} \tag{15.7}$$

where

ΔN_1 is the difference of mass average concentrations between the cross section of jet flow and the environment, i.e., $N'_1 - N_e$ in Eq. (15.5) (in order to keep the symbols in the book consistent, we change the subscript in A's formula from 2 to 1);
ΔN_0 is the difference of mass average concentrations between the jet flow outlet and the environment, i.e., $N_0 - N_e$ in Eq. (15.5);
Q is the flow rate at the cross section after mixture, i.e., Q_{s1};
Q_0 is the leakage flow rate, i.e., Q_{m1}.

Therefore,

$$\frac{Q_0}{Q} = \frac{Q_{m1}}{Q_{s1}} \tag{15.8}$$

Equation (15.7) also becomes:

$$\frac{\Delta N_1}{\Delta N_0} = \frac{N'_1 - N_e}{N_0 - N_e} = \frac{Q_{m1}}{Q_{s1}} \tag{15.9}$$

From Eqs. (15.5) and (15.9), we can see that the leakage equation is derived from the principle of cleanroom, which is exactly the same as the concentration difference formula of jet flow derived with the principle of jet flow structure by A's. This means the jet flow theory is valid to describe the pinhole leakage phenomenon.

But since 1960s, A's amended his formula and then obtained

$$\frac{\Delta N_1}{\Delta N_0} = \frac{Q_{m1}}{Q_{s1}}\sqrt{\frac{N_e}{N_0}} \tag{15.10}$$

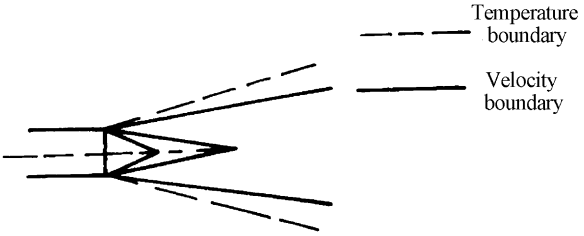

Fig. 15.4 Boundary layer of jet flow

Compared with Eq. (15.9), a factor is multiplied in Eq. (15.10), that is, $\sqrt{\frac{N_c}{N_0}}$. If this formula is applied for the leakage jet flow, the value of $\Delta N_1/\Delta N_0$ will be smaller than that with the original formula by several hundreds, because N_0 is larger than N_c by about 10 thousands of times. In other words, the jet flow diffuses faster, which is correct to describe the temperature change. In A's opinion, the heat diffusion is faster than the momentum diffusion, so the development of temperature boundary layer is faster, which is thicker, than the velocity boundary layer. It is shown in Fig. 15.4 [4]. From the foregoing derivation process about leakage equation, Eq. (15.9) is correct. It is inappropriate to use Eq. (15.10) for describing the concentration difference of jet flow or leakage jet flow, because it does not fully comply with the fact. It should be considered that the concentration diffusion cannot fully apply the law of temperature diffusion, especially for the diffusion with low concentration in the air cleaning technology.

As pointed out in the derivation process of Eq. (15.2), there are two parts of particles brought in by the polluted flow. But in theory the amount of particles by diffusion should be considered. Since the concentration of leakage jet flow is greater than the ambient concentration, particles are mainly taken outside. Given to the fact that diffusional movement of particles is mainly influenced by the Brownian motion of the gas, the diffusion coefficient of the particles is much smaller than the diffusion coefficient of the gas molecules, which is about 100,000 of the latter value. Result will never reduce by hundreds times even if it is taken into consideration. This has been proved by both experience and experiment.

According to the principle of pinhole leakage and round hole jet flow, the relationship between the axial velocity of round hole leakage jet flow and the exit velocity is

$$\frac{v_1}{v_0} = \frac{0.48}{\frac{\alpha S_1}{d_0} + 0.147} \tag{15.11}$$

where

v_1 is the axial velocity of leakage jet flow, and it is 0.3 m/s;
v_0 is the exit velocity of round hole;
S_1 is the distance from the mouth of the round hole when the velocity is v_1 (m or mm);

Table 15.1 Value of v_0

ΔP (Pa)	20	40	60	80	160	200	300	400
v_0 (m/s)	4.75	6.69	8.20	9.46	10.58	14.96	18.33	21.77

d_0 is the diameter of the leakage aperture (m or mm);
α is the turbulence coefficient, and it is 0.08 for round hole.

The relationship between the flow rates is:

$$\frac{Q_{m1}}{Q_{s1}} = \frac{1}{4.4\left(\frac{\alpha S_1}{d_0} + 0.147\right)} \tag{15.12}$$

So

$$\frac{S_1}{d_0} = \frac{0.48v_0 - 0.147v_1}{\alpha v_1} \tag{15.13}$$

The relationship between the exit velocity v_0 of the leakage aperture and the differential pressure ΔP (Pa) across two sides is

$$v_0 = \varphi\sqrt{\frac{2\Delta P}{\rho}} \tag{15.14}$$

where

φ is the flow velocity coefficient, and it is defined as the ratio of actual flow velocity to the ideal value. Given the resistance of the leakage aperture, it is obtained that $\varphi = 0.82$;
ρ is the gas density 1.2 kg/m^3. The value is shown in Table 15.1.

The initial operating condition during leakage detection and the vertical leakage aperture are used as the basis. The differential pressure ΔP is set 200 Pa. Then the following expression is obtained:

$$\frac{S_1}{d_0} = 297.4$$

It is shown that when the differential pressure ΔP and the axial velocity v_1 are fixed, and S_1/d_0 is constant since $\frac{\alpha_1}{a_1} = \frac{Q_{m1}}{Q_{s1}}$, we obtain the following expression:

$$\frac{\alpha_1}{a_1} = \frac{1}{4.4(0.08 \times 297.4 + 0.147)} = 0.0095$$

If $d_0 = 1$ mm, $S_1 \approx 300$ mm. When this distance is reachable, namely, α_1/a_1 is not more than 0.0095, d_0 must be larger. So for the predetermined distance 300 mm,

α_1/a_1 will be greater than 0.0095, which means the leakage extent is more serious. Otherwise, structure should be improved to increase S_1.

In Eq. (15.2), the larger the value of α_1/a_1 is, the larger the concentration by leakage pollution is. It is also shown from Eq. (15.12) that the farther it is from the leakage aperture (i.e., the larger S_1) and the less the pinhole is (i.e., the smaller d_0), the smaller the value of α_1/a_1 is, which means the polluted concentration is reduced. However, the value of S_1 cannot be infinite, namely, the jet cannot diffuse and dilute unlimitedly. The leakage jet flow mentioned here is not in the stationary space but in the surrounding flow along the same direction with the same velocity (or velocity component). According to the jet flow theory, jet flow will not disperse when the axial velocity of the leakage jet flow is equivalent with that of the surrounding flow. It will move forward with the surrounding flow and become part of the surrounding flow.

For full placed HEPA filter air suppliers, the surrounding flow velocity is essentially the same, so the velocity of unidirectional flow can be considered 0.3 m/s. Since the velocity below the air supply inlet in the turbulent flow cleanroom is relative large, the velocity in the mainstream just below the air supply inlet can also decay to 0.3 m/s. When it is smaller, the turbidity will be large. Moreover, when the velocity decay to 0.25 m/s, the pollution concentration obtained finally will be slightly less than the case with 0.3 m/s. From the safety aspect, it is only extended to 0.3 m/s.

In Eq. (15.2), $(1 - K_1) \approx 1$. From Chap. 4, it is known the penetration K_1 of HEPA filter should reach 0.00002 (for particles with diameter ≥ 0.5 μm)

$$N'_1 \approx N_0(K_1 + 475K_1) = K_1N_0 + 475K_1N_0 \tag{15.15}$$

This means when leakage occurs without installation of leakage prevention layer, the concentration N'_1 of polluted air flow by leakage will be larger than the normal concentration K_1N_0 in the supplied air by 475 times, when the above velocity decays to the proximity of supplied velocity. So leakage is the most important factor affecting the air cleanliness with HEPA filter. Leakage prevention layer is the most important measures to improve the cleanliness.

Therefore, Eq. (15.2) can reflect the extent of leakage, which is termed as leakage equation.

15.3 Equation for Leakage Prevention

In this chapter, leakage prevention layer is proposed, where the air distributor with a certain value of penetration and resistance is placed below the HEPA filter. It is shown in Fig. 15.5.

When the penetration of leakage prevention layer is also the same value, i.e., $K_2 = K_1$, it is equivalent with the condition when two HEPA filters are installed.

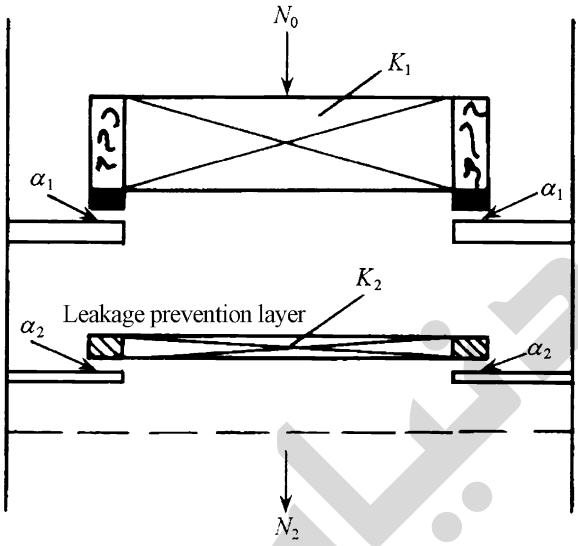

Fig. 15.5 HEPA filter air supply inlet with leakage prevention layer

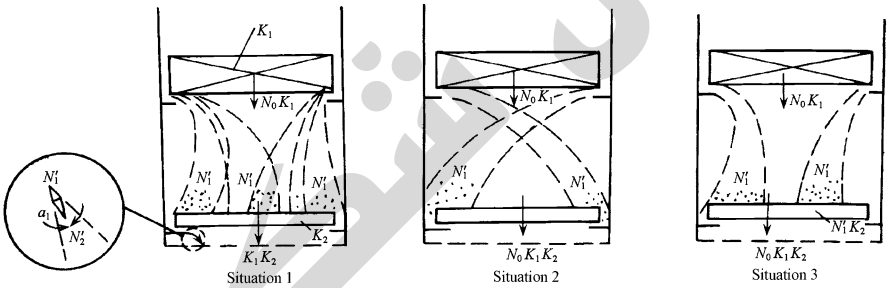

Fig. 15.6 Situation of the polluted flow passing through leakage prevention layer

If the method to seal the frame of HEPA filter is adopted to threat the frame of the leakage prevention layer, it is impractical since this is not within the scope of leakage prevention. For the leakage prevention layer mentioned here, special sealing is basically not considered for the connection between it and the frame. There may be three situations when polluted flow, caused by the leakage through the frame of air filter, passes through this kind of leakage prevention layer. It is shown in Fig. 15.6.

1. Polluted airflow directly reach and cover the entire aperture and the surface of the leakage prevention layer, which makes the concentration of this flow through the leakage prevention layer N'_1K_2. The polluted flow through the aperture of leakage prevention layer will not be mixed with the clean air whose concentration is N_0K_1. This is the worst situation. But it is impossible to happen, because part of the clean air not through the leakage may pass through the leakage prevention layer.

The derivation process of the polluted flow after the leakage prevention layer is similar as that of N'_1. It is also composed of two parts, i.e.,

$$N'_2 = \frac{N'_1\alpha_2 + N'_1K_2(a_2 - \alpha_2)}{a_2} = N'_1\left[K_2 + \frac{\alpha_2}{a_2}(1 - K_2)\right]$$
$$= N_0\left[K_1 + \frac{\alpha_1}{a_1}(1 - K_1)\right]\left[K_2 + \frac{\alpha_2}{a_2}(1 - K_2)\right] \tag{15.16}$$

or

$$N'_2 = K'_1K'_2N_0$$

where the meanings of α_2, a_2, K_2 and N'_2 are the same as that of α_1, a_1, K_1, and N'_1, respectively. They are parameters for the second layer, i.e., the leakage prevention layer.

2. All the polluted airflow goes through the aperture of the frame on the leakage prevention layer. The leakage concentration N'_1 after passing the leakage prevention layer becomes $N_0K_1K_2$. In this case, the polluted air through leakage will be mixed with the most clean air through the leakage prevention layer. This is the best situation, but it is also impossible to happen. At this time, it is

$$N'_2 = \frac{N'_1\alpha_2}{a_2} + \frac{N_0K_1K_2(a_2 - \alpha_2)}{a_2} \tag{15.17}$$

Inserting the expression of N_0K_1 in Eq. (15.2) into (15.17) gives

$$N'_2 = N_0\left[K_1 + \frac{\alpha_1}{a_1}(1 - K_1)\right]\left[K_2 + \frac{\alpha_2}{a_2}(1 - K_2)\right]$$
$$- N_0\frac{\alpha_1}{a_1}\left(1 - \frac{\alpha_2}{a_2}\right)K_2(1 - K_1) \tag{15.18}$$

It is known from the later calculation that both $\frac{\alpha_2}{a_2}$ and K_1 are $<< 0.1$. So both $\left(1 - \frac{\alpha_2}{a_2}\right)$ and $(1 - K_1)$ can be considered approximately 1. Equation (15.18) can be simplified as:

$$N'_2 = N_0\left[K_1 + \frac{\alpha_1}{a_1}(1 - K_1)\right]\left[K_2 + \frac{\alpha_2}{a_2}(1 - K_2)\right] - N_0\frac{\alpha_1}{a_1}K_2 \tag{15.19}$$

or

$$N'_2 = K'_1K'_2 - K_2\frac{\alpha_1}{a_1}N_0 \tag{15.20}$$

3. One part of the polluted airflow goes through the frame aperture of the leakage prevention layer, which has the concentration of N'_1. The other part of the polluted airflow goes through the leakage prevention layer. So the leakage airflow through the aperture of the leakage prevention layer will be mixed with the air which is neither clean nor dirty (the mixed flow by the combination of $N_0K_1K_2$ and $N'_1K'_2$). It is the condition between the above two situations. In this case, the proportion of the polluted air flows through the aperture of the leakage prevention layer and its surface is unknown, so it is difficult to determine the value of N'_2. When the averaged value of the first and second situations is used, the value of N'_2 can be obtained:

$$N'_2 = N_0\left[K_1 + \frac{\alpha_1}{a_1}(1 - K_1)\right]\left[K_2 + \frac{\alpha_2}{a_2}(1 - K_2)\right] - N_0\frac{K_2\alpha_1}{2a_1} \tag{15.21}$$

or

$$N'_2 = \left(K'_1K'_2 - \frac{K_2\alpha_1}{2a_1}\right)N_0 \tag{15.22}$$

Under the common situation, the concentration of polluted air formed by the leakage jet flow after passing through the leakage prevention layer is less than that of the worst situation by $N_0\frac{K_2\alpha_1}{2a_1}$. The multiplication of the first and second items in Eq. (15.21) is N'_1.

Both Eqs. (15.21) and (15.22) can reflect the effect of leakage prevention, which are the leakage prevention equations.

15.4 Leakage Prevention Effect

If there is no special seal between the leakage prevention layer and the frame, and it is not tightly pressed, apertures through the longitudinal sealing pad will exist. From the side view, they look like the holes, so it should still be applicable to describe it with the round hole jet flow.

Assuming that the differential pressure across the leakage prevention layer is $\Delta P = 120$ Pa, and the exit velocity of the leakage jet flow through the leakage prevention layer is $v_0 = 9.5$ m/s, and the axial velocity of the leakage jet flow decays to 0.3 m/s, it is then obtained $S_2/d_0 = 230$. So we get $\alpha_2/a_2 = 0.0122$.

Now a simple analysis will be presented to show what range of K_2 should be selected. From Eq. (15.16) which corresponds to the most unfavorable situation with the minimal effect of the leakage prevention, it is known that the less the value of $K_2 + \alpha_2/a_2(1 - K_2)$ is, the better it is. And it seems it is better if K_2 is as small as possible. But if K_2 is so small that it is near the value of filter media with high efficiency, which is only below one tenths of α_2/a_2, the contribution appears trivial

Table 15.2 Calculated value of N'_2

K_2	0.05	0.01	0.001
K'_2	0.0616	0.022	0.0132
$\frac{K_2\alpha_1}{2\alpha_1}$	0.0002375	0.0000475	0.00000475
N'_2 Eq. (15.21)	$0.0366N'_1$	$0.017N'_1$	$0.0127N'_1$
N'_2 Eq. (15.22)	0.000349 N_0	0.000162 N_0	0.000121 N_0

on the leakage prevention effect. At this time, the leakage prevention effect mainly depends on α_2/a_2, so only the resistance and the cost will increase when K_2 is reduced.

From Eq. (15.16), it is better K_2 and α_2/a_2 are comparable, namely, it is most appropriate that K_2 corresponds to the efficiency 95–99 % for sub-HEPA filter media. In this case, it not only has good performance of both leakage prevention effect and prevention of the air pollution by backflow but also simplifies the requirement on the filtration and sealing performance of the leakage prevention layer, which has practical meaning.

The influence of K_2 on the leakage prevention effect can be calculated with the following steps.

It is known

$$\alpha_2/a_2 = 0.0095$$
$$\alpha_2/a_2 = 0.0122$$

For particles with diameter ≥0.5 μm, we have

$$K_1 = 0.00002$$

$$K'_1 = K_1 + \frac{\alpha_1}{a_1}(1 - K_1) = 0.00952$$

The concentration N'_2 of leakage polluted air through the leakage prevention layer is shown in Table 15.2. It is shown when K_2 decreases from 0.01 to 0.001, N'_2 does not change very much. So corresponding to the sealing condition with $\alpha_2/a_2 = 0.0122$, the effect of reducing the polluted concentration is little with high-efficiency leakage prevention layer $K_2 = 0.001$, which means it is unnecessary to chose high performance materials as the leakage prevention layer. When sub-HEPA leakage prevention layer is chosen and the most unfavorable condition without the mixture of turbulent flow is taken into consideration, the polluted air concentration at the downstream of the leakage prevention layer which has leakage aperture can be reduced to below 0.04 of that without the leakage prevention layer. Because there is mixture of turbulent flow in actual applications, it would be much less than this value.

Table 15.3 shows the test results before and after the leakage prevention layer is installed, where the size of test chamber is 3.4 m × 2.4 m [4, 5].

1. With the leakage prevention layer, the indoor particle concentration is much lower than that without the leakage prevention layer.

Table 15.3 Comparison of the situations with full leakage prevention layer and without leakage prevention layer

Leakage prevention layer	Total flow rate (m^3/h)	Fresh air volume (m^3/h)	Upstream concentration of HEPA filter (≥0.5 μm) (pc/L)	Additional leakage position	Indoor concentration (≥0.5 μm) (pc/L)		Remark
					Ave.	Max.	
With	9,500	201	2,119	Without	1.98	3.30	Leakage exists on filter frame, which has been stopped by measures
Without	9,500	201	2,119	Without	0.36	0.80	
					0.33	0.60	
		Closed	457	Without	0.46	0.60	Ave. 0.07
					0.37	0.80	
		201	2,119	With	0.33	0.70	
		Closed	457	With	0.36	0.70	
					0.29	0.50	Ave. 0.68
					0.50	0.80	

2. With the leakage prevention layer, the influence of the existence of both leakage and fresh air is not obvious on the indoor particle concentration, which means the leakage prevention layer has played its role properly.
3. When the artificial leakage source is added, where the leakage flow rate of 12 pipes is 0.74 m^3/h, the total amount of particles injected into the upstream of HEPA filter is 1.57×10^6 pc/h, and the indoor concentration can be increased by 0.17 pc/L. But due to the leakage prevention layer, this effect is not prominent.

15.5 Mechanism of Leakage Prevention Layer

15.5.1 Leakage Prevention with Dilution Effect

1. Mixed dilution with jet flow. From the above calculations, we can know that due to the mixture of jet flow, the concentration of leakage polluted jet flow can be diluted to 1/100 of the original level, when the conditions are that there must be long enough for the expansion of jet flow from the leakage position to the leakage prevention layer. With the previous calculation for $S_1/d_0 = 297.4$, when the leakage aperture diameter is $d_0 = 1$ mm, the length needed will be 300 mm. When the leakage prevention layer is separately placed from the filter, the air filter is used for filtration only and the leakage prevention layer is used to distribute airflow only, which is shown in Fig. 15.7. The terminal HEPA filter is designed in the filter box placed in the technical interlayer, which is connected to the leakage prevention layer for air distribution through a short pipe. Since the

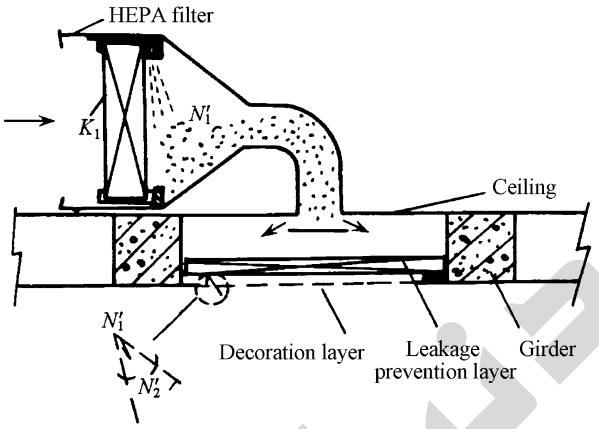

Fig. 15.7 Separate installation of air filter and leakage prevention layer

distance between the leakage position and the leakage prevention layer is much larger than the above value S_1, it is beneficial for the complete dilution of polluted jet flow, which will reduce both α_1/a_1 and K'_1.

2. The dilution with turbulent flow. If the polluted concentration should be further reduced, the turbulent mixture of airflow must be used for dilution. With the definition of α_1, the value of α_1/a_1 will be the smallest if the polluted air is full of the whole supplied air, i.e., $Q_{s1} = Q_M$ and $a_1 = 1$. As shown in Fig. 15.7, the mixture dilution is intensified because the unidirectional flow streamlines are destroyed and the velocity increases after air passes through the contracting part and the elbow. Moreover, the baffle board is placed at the entrance of the plenum chamber, which further increases the mixing effect, the value of a_1 in this situation is much larger than the situation when these measures are not taken. The filtration area of HEPA filter in the filter box is much smaller than that of the leakage prevention layer, which not only saves the material for air filter, but also makes the sealing convenient. During the sealing process, the area for sealing is much smaller, and it is operated outside of the plenum chamber.

Experiment and calculation have proved that it is quite difficult to increase the value of a_1. Usually it is already very good when a_1 becomes 0.1–0.3. In this case, the penetration only increases by about 3 times on average.

The influence of a_1 on the mixing effect of airflow is shown in Table 15.4.

15.5.2 Leakage Prevention with Filter

It is shown from Eq. (15.2) that the leakage prevention effect of the leakage prevention layer is related to the filtration effect of this layer. When there is no leakage prevention layer, the concentration of supplied air is:

$$N'_1 = N_0 K_2$$

Table 15.4 Effect of increased mixture by airflow

Condition		Assumed α_1	α_1/a_1	N'_2 Eq. (15.22)
There is no sealing for the leakage prevention layer. Only needle hole exists for leakage. Jet flow mixture appears with $\alpha_2/a_2 = 0.0122$	For the first air filter, there are only needle hole leakage and jet flow mixture	No mixture by turbulent flow	0.0095	$18K_1N_0$
$K = 0.00002$; $K_2 = 0.05$. Air flow is 800 m^3/h	The first air filter is connected with the sealing by a closed sponge. The leakage flow rate is 0.3 m^3/h when $P = 200$ Pa. The side length is 2 m (the calculated leakage flow rate is shown in Table 15.5). $\alpha_1 = 0.000375$. There are mixtures of turbulent flow with different extents	0.1	0.00375	$6.9K_1N_0$
		0.3	0.00125	$2.35K_1N_0$
		0.7	0.000536	$1.04K_1N_0$
		1.0	0.000375	$0.75K_1N_0$

When the leakage prevention layer is installed, the concentration of supplied air is

$$N'_2 = N'_1K'_2 = N_0K'_1K'_2$$

where K'_2 contains the information reflecting the filtration effect K_2 of the leakage prevention layer. K'_2 will be smaller if K_2 is smaller. As explained earlier, K_2 does not need to be too small, because too small value of K_2 will increase the resistance, where the meaning of the leakage prevention layer is lost. Even if it is only one tenth or two tenths of the value α_2/a_2, namely, the filtration efficiency is equivalent to more than 99.5 %, its effect is almost offset by α_2/a_2.

But the appropriate value of K_2 for the leakage prevention layer will further play its role in reducing the concentration N'_2 of supplied air. As analyzed before, when there is no obvious requirement for the sealing measures taken for the leakage prevention layer, it's better to have the filtration effect of sub-HEPA filter.

15.5.3 Leakage Prevention with Reduced Differential Pressure

The leakage flow rate through the aperture depends on the differential pressure, which is clearly shown in Table 15.5 about the leakage formula. The final resistance

Table 15.5 Experimental parameters for the leakage flow rate equation for various apertures [6,7]

Aperture structure	Sealing method	Leakage intensity sequence	Leakage flow rate of the aperture per unit meter				
			A	n	$P = 10$	$P = 20$	$P = 4$
Open aperture with thickness 1.5 mm	No	1	20.2	2	127.8	90.4	28.6
Open aperture with thickness 1.0 mm	No	2	18.6	2	117.6	83.2	26.3
Open aperture with thickness 0.5 mm	No	3	7.3	1.6	73.2	51.8	16.4
Connected with steel angle flange	Filling with common rubber	4	0.24	1.6	2.4	1.7	0.57
Connected with steel angle flange	Filling with 850 rubber strip	5	0.024	1.3	0.41	0.29	0.07
Connected with steel angle flange	Filling with KS-5 K sealing rubber	6	0.021	1.3	0.36	0.25	0.06
		7	0.021	1.3	0.21	0.15	0.035
Connected with steel angle flange	Filling with a closed sponge rubber strip ($\delta = 3$), groove connection	7					
Connected with steel angle flange	Double-loop sealing strip	8	2.2×10^{-3}	1.1	0.0006	0.0004	0.00008
Ten holes with $d = 1$ mm					0.36	0.25	0.114
Ten holes with $d = 0.5$ mm					0.09	0.61	0.29

of HEPA filter under the (0.5–1) times of the rated air flow can reach up to 200–400 Pa. When the leakage prevention layer is placed and the low resistance and sub-high-efficiency material is used as the leakage prevention layer, the differential pressure across the planar leakage prevention layer can be reduced to 100–120 Pa. The smaller the differential pressure is, the less the leakage flow rate is. In this case, more airflow will pass through the leakage prevention layer, so more air will be subjected to the second filtration process. With the reduced differential pressure, the condition for the sealing of the frame can be simplified, which has practical implication. When the differential pressure reduces, v_0 decreased, and thus v_2 will reduce. But it will reflect the change of the particle concentration in unit volume of air, so there is no direct reflection in both the leakage equation and the leakage prevention equation.

From Table 15.5, it is shown that when the differential pressure is reduced by one half, the leakage flow rate will be reduced by 30 %.

15.5.4 Barrier Leakage Prevention

Even though only hard contact exists between the frame of the leakage prevention layer and the frame, there is still resistance for the leakage airflow, namely, there is still the

barrier effect. In this case, there is still a certain sealing effect, which plays the role of reducing a_2. When there is still considerable sealing effect if no obvious measure of sealing was adopted for the leakage prevention layer, the value of a_2 for the leakage prevention layer will be further reduced, so as the value of α_2/a_2. For example, the soft material is attached on the frame, which can avoid the hard contact. When appropriate value of K_2 is adopted, the value of K'_2 will be reduced further, which will improve the leakage prevention effect. But as mentioned before, if the leakage prevention layer with sub-high-efficiency is used, the value of α_2/a_2 should not be much smaller than K_2.

15.6 Air Supply Terminal with Leakage Prevention Layer

15.6.1 Overview

In Sect. 15.1 of this chapter, it has pointed out that the mechanism of air pollution control in cleanroom is that HEPA filter placed at the end of air supply terminal supply the clean air into the cleanroom. But different air cleanliness levels will appear with different air distributions, including the dilution distribution of turbulent flow, the piston-type extrusion distribution with unidirectional flow, and with different forms with leakage in the terminals. The change of conventional air distribution modes in the quantity and quality is accompanied by the number of HEPA filters proportionally, namely, the number of HEPA air supply inlets will increase with the increase of the expanded supply area. So it is of little practical significance, and the influence of occasional leakage of the air terminal on the property of clean space cannot be ruled out.

The meaning of mainstream area has been clarified in Chap. 14. So the new air distribution mode by air supply terminal with the leakage prevention layer is put forward, when the leakage prevention layer is combined with the expanded mainstream area.

15.6.2 Structure of Air Supply Terminal with Leakage Prevention Layer

The air supply terminal with the leakage prevention layer has been patented, which is also called the leakage prevention type clean air supply ceiling. There are two forms:

15.6.2.1 Made of Single Leakage Prevention Layer

The equipment made of single leakage prevention layer shown in Fig. 15.8 can also be termined as the air supply inlet with the leakage prevention layer. Filters can be placed inside the air supply inlet (Fig. 15.8a) and can also be outside the air supply inlet (Fig. 15.8b). For the latter case, it is installed in the filter box.

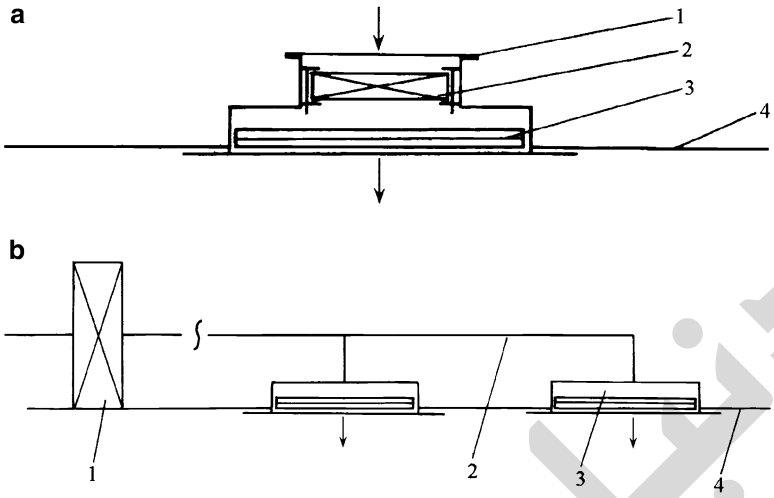

Fig. 15.8 Air supply inlet with leakage prevention layer. (**a**) *1* Air supply with leakage prevention layer, *2* HEPA filter (air supply area *F*), *3* leakage prevention layer (air supply area 2 *F*), *4* ceiling. (**b**) *1* Sealed filter box with zero differential pressure (or the common filter box), *2* Pipeline, *3* air supply inlet with leakage prevention layer and without air filter, *4* ceiling

The equipment of this form can be directly connected with the large system. Since the area of the leakage prevention layer can be larger than the cross-sectional area of the filter, the mainstream area will be expanded, which is suitable for turbulent flow cleanroom. With the same number of filters, the area of air supply outlet can be enlarged by one time, which increases the clean area and strengthen the unidirectional flow property in the mainstream area.

15.6.2.2 Made of Multiple Leakage Prevention Layers

With multiple leakage prevention layers, Class 100 locally or in the whole room can be achieved when the room area is relative large.

The above two forms include the following parts:

(a) Filter Box

(b) Thin Plenum Chamber

The thickness of each plenum chamber is only 250–350 mm.

There is device for promotion of mixing inside the plenum chamber. According to the principle of leakage prevention layer, the mixing coefficient can be improved to more than 0.3.

The inlet velocity of plenum chamber should not be too big, and baffle should be placed [8]. Otherwise, negative pressure will be formed at the inlet, and the exit velocity at the remote end will increase, which is shown in Fig. 15.9 [9].

(c) Terminal of Leakage Prevention Layer

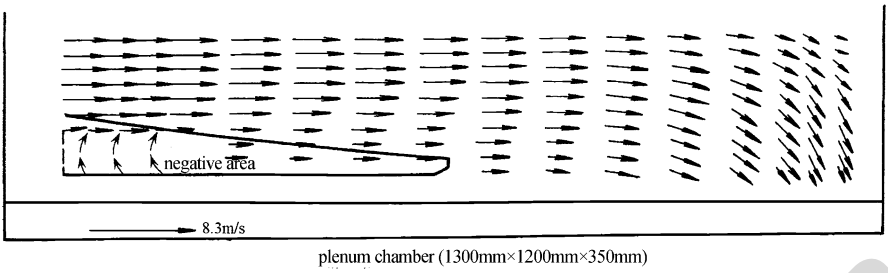

Fig. 15.9 Negative pressure zone in plenum chamber with numerical simulation

It is very convenient for installation because the special sealing means is not needed. Especially when the ratio of blowing area with clean air is about 95 %, its considerable resistance makes the airflow in the plenum chamber stable and uniform easily.

(d) Short Jointed Plumbing

The air supply terminal of leakage prevention layer has four main features including: preventing leakage, expanding the mainstream area, reducing the story height, and easy replacement and maintenance of air filter and decoration layer outside of room. So it is widely used in engineering projects.

15.6.3 Property of Air Supply Terminal of Leakage Prevention Layer

15.6.3.1 Decay of Air Supply Velocity

Experimental study has been performed by Niu Weile for the property of air supply terminal of leakage prevention layer. The study of anti-disturbance property of mainstream area with concentrated air supply mode has valuable for practical work. Data cited here are all from the result of this study [9]. Table 15.6 shows the experimental results.

The conclusions can be reached from the above table:

1. As mentioned before, the relationship between decay rate of supply velocity and the magnitude of supply velocity is not very obvious. But it is shown that the larger the supply velocity is, the smaller the decay rate is.
2. When the velocity v on the working surface is between 0.2 and 0.25 m/s (which is required in clean operating room at home and abroad), the air supply velocity v_0 may be between 0.35 and 0.40 m/s, which has the significance of energy saving (for status 1).
3. When the temperature difference is only 1.4 °C, the decay rate increases, which means larger air supply velocity v_0 is needed for the same velocity required on the working surface. When the temperature of hot air supply is reached, air may

Table 15.6 Property of air velocity, decay rate, and frequency

Frequency (Hz)		44	45	46	47	48	49	50
Temperature difference of supplied air, 0 °C	v_0	0.396	0.414	0.424	0.431	0.443	0.452	0.462
	v	0.250	0.264	0.270	0.272	0.281	0.300	0.322
	λ	0.369	0.362	0.363	0.369	0.366	0.336	0.303
Temperature difference of supplied air, +1.4 °C	v_0	0.394	0.407	0.424	0.431	0.444	0.464	0.497
	v	0.212	0.226	0.229	0.241	0.251	0.268	0.280
	λ	0.462	0.445	0.441	0.444	0.445	0.422	0.437

Table 15.7 Property of turbidity and frequency

Frequency (Hz)		44	45	46	47	48	49	50
Status 1	Face turbidity of supplied air	0.096	0.093	0.093	0.089	0.089	0.084	0.080
	Face turbidity of working area	0.266	0.245	0.232	0.227	0.208	0.199	0.202
Status 2	Face turbidity of supplied air	0.099	0.104	0.092	0.094	0.094	0.087	0.081
	Face turbidity of working area	0.361	0.342	0.346	0.354	0.344	0.301	0.296

not come down. This is why in both German and Chinese standards the required air supply temperature in the cleanroom should be smaller than room temperature. When cold air is supplied, the precool effect becomes better.

15.6.3.2 Turbidity

Table 15.7 shows the experimental results.

The conclusions can be reached from the above table:

1. The difference of turbidity under two statuses is very small, because the face velocity of supplied air was measured at 5 cm below the air supply outlet and the difference of statuses is not obviously shown.
2. The turbidity at the working area (0.8 m above the floor) reduces when the temperature difference of supplied air changes from "+" to "0." It can be expected that it will reduce further when the temperature difference changes from "0" to "−."
3. The larger the supplied air velocity is, the less the turbidity is. With the elevated working height, the turbidity may reduce, but the influence of return air grille should be considered.

15.6.3.3 Anti-disturbance

1. Anti-disturbance of the Activity from people in the Surrounding Area around Mainstream Area

   Sampling positions are shown in Fig. 15.10. Three minutes after particle concentrations are stable, one person without wearing clean cloth began to walk with velocity 1 m/s in the surround area of mainstream area. After the

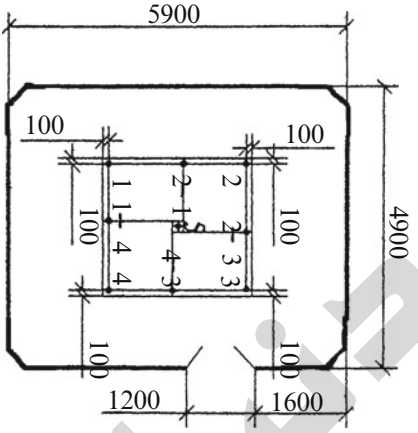

Fig. 15.10 Sampling points for the anti-disturbance study in mainstream area

Table 15.8 Concentration variation of anti-disturbance sampling points in mainstream area

Time (min)			1	2	3	4	5	6	7	8	9
Particle concentration, pc (2.83 L)	1	≥0.5 μm	0	0	0	1	5	1	0	0	0
		≥5.0 μm	0	0	0	0	0	0	0	0	0
	1-2	≥0.5 μm	0	0	0	0	0	0	0	0	0
		≥5.0 μm	0	0	0	0	0	0	0	0	0
	2	≥0.5 μm	0	0	0	4	9	14	1	0	0
		≥5.0 μm	0	0	0	0	0	0	0	0	0
	2-3	≥0.5 μm	0	0	0	1	0	0	0	0	0
		≥5.0 μm	0	0	0	0	0	0	0	0	0
	3	≥0.5 μm	0	0	0	3	4	8	1	0	0
		≥5.0 μm	0	0	0	0	0	0	0	0	0
	3-4	≥0.5 μm	0	0	0	5	15	21	2	0	0
		≥5.0 μm	0	0	0	0	1	0	0	0	0
	4	≥0.5 μm	0	0	0	2	5	10	0	1	0
		≥5.0 μm	0	0	0	0	0	0	0	0	0
	4-1	≥0.5 μm	0	0	0	0	4	2	0	0	0
		≥5.0 μm	0	0	0	0	0	0	0	0	0

walk for three minutes, concentration variation was monitored since the fourth minute. When the person stops, the concentration variation was continuously recorded for 3 min. Table 15.8 shows the experimental result.

The conclusions can be reached from the above table:

(a) The influence of walk in the surround area is small for the particle concentration in mainstream area. There are only three positions in eight positions, where small particle concentration slightly exceed the value suggested in standard. Particle concentrations in other positions are within the range suggested in standard.

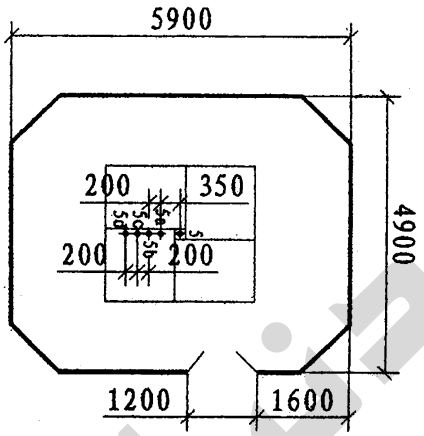

Fig. 15.11 Sampling points for the anti-disturbance study in mainstream area

Table 15.9 Particle concentration variation for the anti-disturbance study in mainstream area

Time (min)			1	2	3	4	5
Particle concentration, pc (2.83 L)	5a	≥0.5 μm	36	17	8	7	7
		≥5.0 μm	4	2	0	0	0
	5b	≥0.5 μm	28	31	29	22	28
		≥5.0 μm	4	2	5	2	5
	5c	≥0.5 μm	16	4	21	11	13
		≥5.0 μm	1	0	1	2	1
	5d	≥0.5 μm	5	4	2	3	2
		≥5.0 μm	0	0	0	0	0

(b) The influence vanishes immediately when the person stops walking.

2. Anti-disturbance of the Activity from people in Mainstream Area

As shown in Fig. 15.11, the person stands in the center and waves the front arms continuously from the first and fifth minutes.

Table 15.9 shows the experimental result.

The conclusions can be reached from the above table:

(a) With the increase of the distance between the sampling positions and mainstream area, the particle concentration first increases and then decreases. The maximum arrives at 550 mm from the center, where it is the boundary of occupant activity.

(b) The increased concentration is less than three times of upper limit concentration (for Class 5), which meets the required ratio between dynamic and static statuses for unidirectional flow cleanroom (refer to Chap. 17).

3. Anti-disturbance of Door Opening

The distance between the door and the center of mainstream area is only 2.3 m, and it is only 1.1 m between the door and the boundary of mainstream

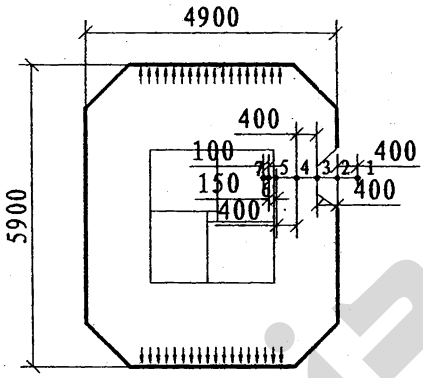

Fig. 15.12 Layout of sampling positions between door and mainstream

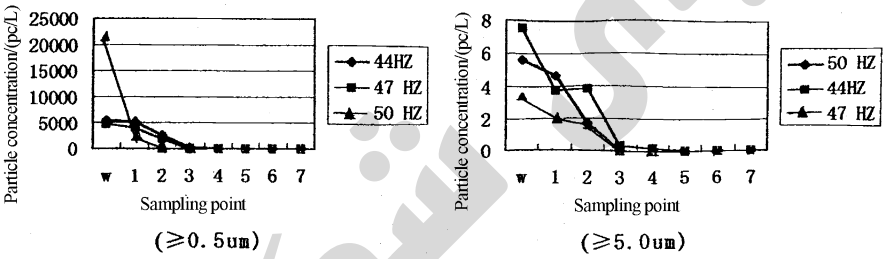

Fig. 15.13 Concentrations at sampling positions between the door and mainstream

area. There are seven sampling positions in total, which is shown in Fig. 15.12. The period of opening door is more than 2 h.

Experimental results are plotted on Fig. 15.13.
The conclusions can be reached from the above figures:

(a) The air cleanliness level outside of the door can be considered as Class 8.
(b) Particle concentration decreases from the outside of the door to the mainstream. The larger the air supplied velocity is, the faster the decline of velocity is.
(c) Particle concentration at the fourth sampling position, i.e., 800 mm from the door, reaches the level of Class 6. It is between 1.83 pc/L (with minimum air supplied velocity) and 0.35 pc/L (with maximum air supplied velocity) at the fifth sampling position, i.e., the boundary of the mainstream area. This means the ability to anti-disturbance of the mainstream area for the incoming flow from the door with concentrated air supply mode is extreme strong. In reality, door is open for temporary period, so the influence is much less.

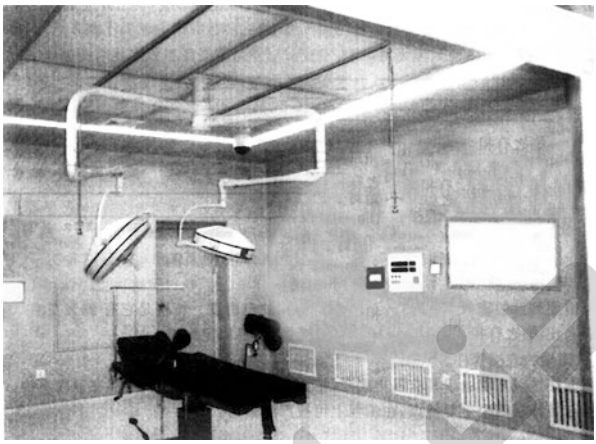

Fig. 15.14 Application of air supply terminal with leakage prevention layer in cleanroom with local unidirectional flow (interior scene of clean operating room with Class 1 in Longyan No.1 Hospital)

15.6.4 Application of Air Supply Terminal of Leakage Prevention Layer

15.6.4.1 Application in Cleanroom with Local Unidirectional Flow Cleanroom

It is No.301 Hospital built in 1994 where air supply terminal of leakage prevention layer was first applied in cleanroom with local unidirectional flow. The difficulty of low story height was overcome. It provided the guarantee that the terminal is without a leak. During 8 years of operation, the effect is very good.

The official application of patented product starts in the cleanroom with Class 1 in Longyan No.1 Hospital in Fujian Province, which was built in 2002. It is shown in Fig. 15.14.

In "Building standard of hospital clean operating department" and "Building technical specification of hospital clean operating department," it specified for the concentrated air supply area above the operating table in clean operating room with Class 1, where the local air supply area with Class 100 should be 2.6 m × 2.4 m = 6.24 m^2. The area of room served should be no more than 1.2 times of that of large-scale cleanroom (45 m^2), which is 54 m^2.

According to the usually practical method, dozens blocks of perforated plates or decoration layers should be placed at the bottom of the plenum chamber. But when the air supply terminal of the leakage prevention layer, i.e., clean air supply ceiling with leakage prevention type, is used, only four blocks are needed, where a small square in the middle is prepared to be empty in advance which is equivalent with the size of the square externally connected with the rod of shadowless lamp. The bottom view of the air supply ceiling is shown in Fig. 15.15, where two tracks are used for guiding the transfusion.

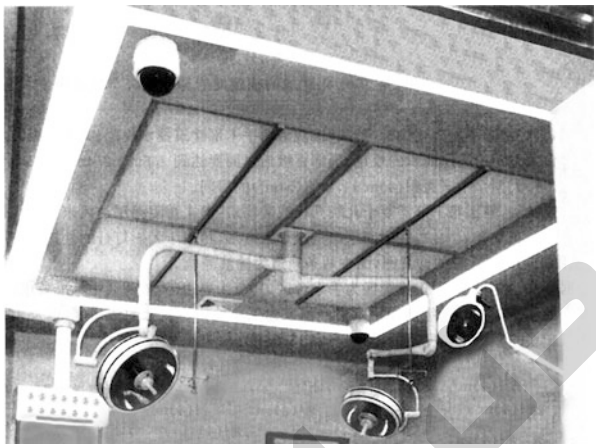

Fig. 15.15 Bottom view of clean air supply ceiling with leakage prevention type in cleanroom with Class 1 (with guide rail)

Table 15.10 Basic performance of Class 1 type air supply ceiling with leakage prevention type

Class I operating room	Air supply ceiling			Clean air supply ceiling with leakage prevention layer				In-field test with common air supply modes
				Standard	Measured by experiment	In-field test 1	In-field test 2	
Basic property	Air supply velocity (m/s)				0.46	0.35	0.45	0.4–0.5
	Air velocity at the working area (m/s)			0.25–0.3	0.30	0.30	0.32	0.25–0.3
	Particle concentration in operating area (pc/L)	≥0.5 μm	Max.	≤3.5	0.06	0.05	0.05	0.35–2
			Min.	≤3.5	0.07	0.05	0.05	0.35–2
		≥5 μm	Max.	0	0	0	0	0
			Min.	0	0	0	0	0
	Particle concentration in surrounding area (pc/L)	≥0.5 μm	Max.	≤35	0.59	0.8	0.2	3.5–35
			Min.	≤35	0.27	0.5	0.2	3.5–35
		≥5 μm	Max.	≤0.3	0	0	0	0–1
			Min.	≤0.3	0	0	0	0–1
	Self-cleaning time/min			<15	2			

According to standard, the projected area of the concentrated air supply ceiling is the area of operating table, and other area is the surrounding area. The air cleanliness levels which is specified in standard, measured in the field test in laboratory, measured in two clean operating rooms with Class 1 by the State Inspection Center of Construction Engineering are shown in Table 15.10, as well as the measured air cleanliness range with most common air supply methods.

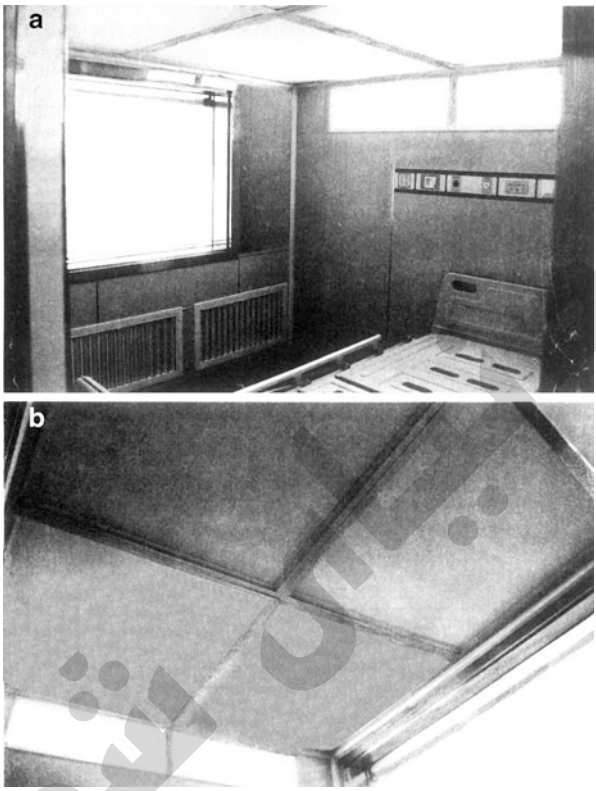

Fig. 15.16 Clean air supply ceiling with leakage prevention mode installed in blood ward with area 7 m^2. (**a**) Interior scene. (**b**) Ceiling consisting of four leakage prevention clean air supply models

15.6.4.2 Applied to the Whole Room Unidirectional Flow Cleanroom

When the area especially the width of cleanroom is not large, ceiling supply surface constituting of the plenum chamber with two leakage prevention layers can be used, where air is supplied into the plenum chamber from the side. At present, the maximum size of the plenum chamber with single leakage prevention chamber is 1.2 m × 1.3 m. It is not convenient to use larger product.

Figure 15.16 shows the photo of clean air supply ceiling with leakage prevention mode which was installed in three blood wards, each of which is 7 m^2, at Shenzhen Hospital of Peking University.

When the area of the cleanroom is large, two or more clean air supply ceilings with leakage prevention mode should be installed. And air should be supplied into the plenum chamber from the top. Since there is no ceiling frame, hoisting method can be adopted. The installation process of cleanroom with Class 100 for larger area can be simplified, so that good quality can be ensured.

15.6.4.3 Applied to Turbulent Flow Cleanroom

Dispersed Air Inlets

As shown in Fig. 15.8a, the leakage prevention layer is used to replace the dispersion plate on the common air inlet, or the area of the leakage prevention layer increases to two times of the original area of air inlet. For the latter situation, the effect of increasing the mainstream area is realized (refer to Chap. 14). Since the air supplied velocity is reduced and air filters can be uninstalled exterior of cleanroom (such as the technical layer), it is especially suitable for the application where low and uniform velocity is needed and cross infection is not allowed, such as sterile animal raising room. According to the operational result in animal raising room, the performance is very good. This method is also applicable for the clean operating room where indoor pollution should not be increased, as well as the blood ward.

Concentrated Air Inlets

Air inlets can also be allocated concentratedly in turbulent flow cleanroom, where the flow rate and number of air filter area unchanged. A larger mainstream area is thus formed. Since the air supply velocity is smaller than that of unidirectional flow, the property of quasi-unidirectional flow appears below the air inlet. Patented products were developed for clean operating room with Class II and III, including clean air supply ceiling with leakage prevention mode, which is shown in Figs. 15.17 and 15.18. For the former case, air is supplied with concentrated air inlets with air change rate corresponding to Class 10000 so that the air cleanliness level in operating area is Class 1000 while it is Class 10000 in surrounding area. For the latter case, air is supplied with concentrated air inlets with air change rate corresponding to Class 100000, so that the air cleanliness level in operating area is Class 10000, while it is Class 100000 in surrounding area. The actual performance is far better than these values, which is shown in Table 15.11.

15.6.5 Comparison of Several Air Supply Terminals

Comparisons of the air supply terminal with leakage prevention layer and common air supply terminals are shown in Table 15.12.

Appearance comparisons between the common air supply ceiling with perforated plate and without guide rail and the clean air supply ceiling with leakage prevention mode are shown in Figs. 15.19 and 15.20 shows the foreign air supply ceiling consisting of many blocks of screen or perforated plates[10].

Fig. 15.17 Upward view of clean air supply ceiling with leakage prevention mode used in clean operating room with Class II

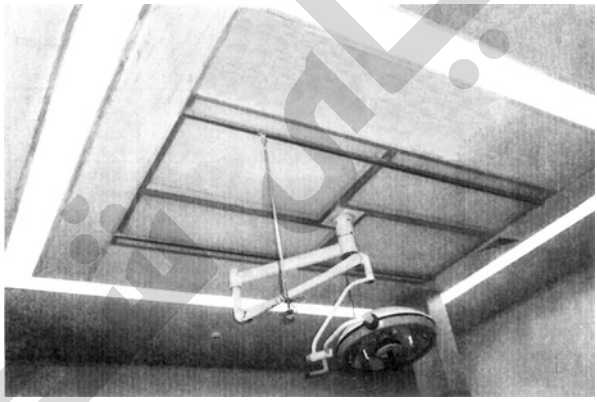

Fig. 15.18 Upward view of clean air supply ceiling with leakage prevention mode used in clean operating room with Class III

Table 15.11 Basic performance of clean air supply ceiling with leakage prevention mode for Classes II and III

Operating room	Air supply ceiling			Clean air supply ceiling with leakage prevention mode			
				Project			
Basic	performance (3 rooms)	Air supply velocity (m/s)			Class II (3 rooms)		Class III
	Standard				Measured	Standard	Measured
	≥30				36	≥20	25.7–26.6
	≤43	≤29					
	Turbidity			–		–	
	Particle concentration in operating area (pc/L)	≥0.5 μm	Max.	≤35	0.1–0.5	≤350	2.5–4.9
			Statistical	≤35	0.2–0.6	≤350	2.9–5.5
		≥5 μm	Max.	≤0.3	0	≤3	0
			Statistical	≤0.3	0	≤3	0
	Particle concentration in surrounding area (pc/L)	≥0.5 μm	Max.	≤350	0.9–1.6	≤3,500	4.9–7.9
			Statistical	≤350	0.6–1.3	≤3,500	4.8–7.8
		≥5 μm	Max.	≤3	0	≤30	0–0.5
Statistical			≤3	0	≤30	0–1.2	

Table 15.12 Comparison of several air supply terminals

Item	Leakage prevention mode	Common nylon net	Common perforated plate
Principle	The concept of leakage prevention layer is used	The traditional concept of air supplier with air filter is used	
Property	Decoupling of three functions including filtration, flow equalization, and leakage stoppage	Integration of three functions including filtration, flow equalization, and leakage stoppage	
Flow	Unidirectional flow with good uniformity of air velocities at the cross section. The streamlines are intensive and parallel. The anti-disturbance ability is good	The uniformity of streamlines is relative poor. Air is likely to disperse. The anti-disturbance ability is poor	
Possibility of leakage	No	Yes	Yes
Air distribution ratio	Extreme large	Maybe large	Small
Number of HEPA filters	A few and the condition that the flow rate should be less than 80 % of the nominal value is satisfied	Many for planar layout; a few for installation at two sides, but the condition that the flow rate should be less than 80 % of the nominal value is not easily satisfied	Many for planar layout; a few for installation at two sides, but the condition that the flow rate should be less than 80 % of the nominal value is not easily satisfied
Turbidity	Relative small	Higher	The highest
Reverse ash blowing	Yes	It is possible when air filter is placed with planar allocation; it is impossible when air filter is placed with side allocation	It is possible when air filter is placed with planar allocation; it is impossible when air filter is placed with side allocation
Installation	Easy and can be installed in site	Difficult and part is manufactured in site, which causes large error	Difficult and part is manufactured in site, which causes large error
Appearance	Consistence in module and specification	The randomness degree is large, which depends on the workers' skill	The randomness degree is large, which depends on the workers' skill
Leakage detection and stoppage	No	Yes	Yes
Maintenance indoors	No	Needed	Needed
Life time	Semi-eternal	Relative long	Frequent cleaning is needed, and corrosion may occur

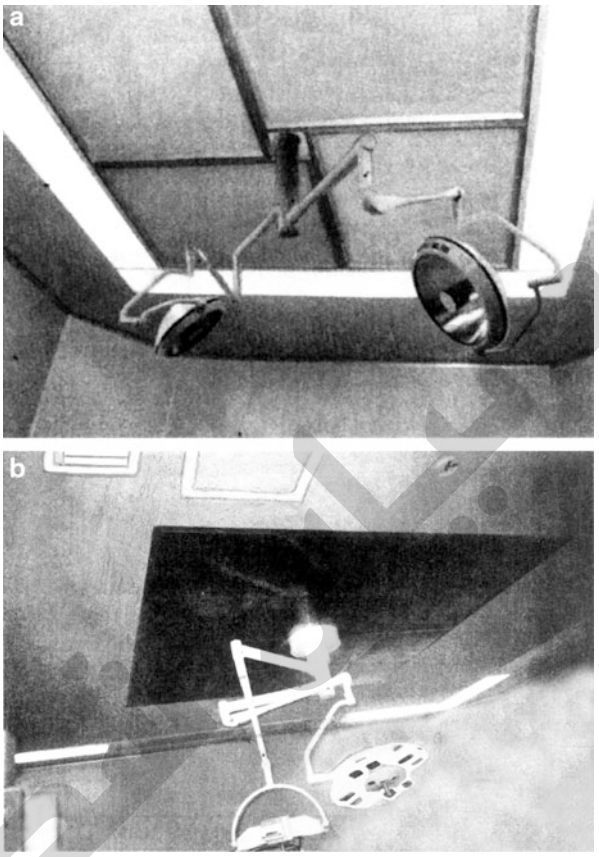

Fig. 15.19 Comparison of appearance for air supply ceiling. (**a**) Leakage prevention mode (consisting of four blocks). (**b**) Common perforated plates (consisting of 15 blocks)

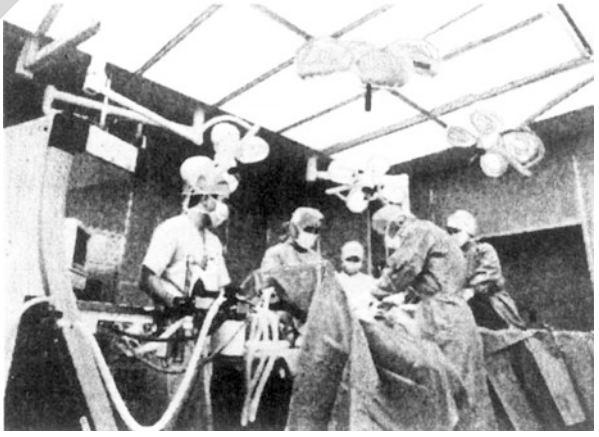

Fig. 15.20 Common air supply ceiling in clean operating room in Japan

References

1. Xu ZL, Zhang YZ, Zhang YG, Mei ZL, Shen JM, Guo DR, Jiang PC (1999) A new type of terminal air distributing unit in clean space. The theory of damping leakage layer. Build Sci 2:1–10 (In Chinese)
2. Shen JM, Xu ZL (1998) A new idea of terminal distributing unit in airclear system. Build Sci 14(2):3–8 (In Chinese)
3. Zhou MR (1979) Fluid dynamics-pump and fan. China Architecture & Building Press, Beijing, p 236 (In Chinese)
4. Xu ZL, Zhang YZ, Zhang YG et al (2000) Mechanism and performance of an air distribution pattern in clean spaces. J HV&AC 30(3):1–7 (In Chinese)
5. Zhang YZ, Xu ZL, Zhang YG et al (2000) Design of multi-purpose clean laboratory. Build Sci 16(1):46–49 (In Chinese)
6. Xu ZL (1990) Experimental study of the bicyclic sealing system with the combination of sealing and leading methods. In: Proceeding of the third annual academic conference by Chinese Contamination Control Society, Beijing, China (In Chinese)
7. Peng R (1992) Experimental study and discussion about the reduction of air leakage flowrate in ventilation and air conditioning system. J HV&AC 1:21–24 (In Chinese)
8. Xu ZL, Shen JM (1989) Application of air cleaning technology. China Architecture & Building Press, Beijing, p 117 (In Chinese)
9. Niu WL (2002) Study on air flow uniformity and anti-jamming capability of local Class 100 air supply mode with the leakage preventing layer. Master dissertation at Institute of HVAC of China Academy of Building Science Research, 2002 (In Chinese)
10. Yasushi M (1999) Cleaning air conditioning equipment in hospital. J Jpn Air Clean Assoc 37 (3):41–49 (In Japanese)

Chapter 16
Sampling Theory

In order to ensure the reliability of the measurement results of particle concentration, except for the reasonable detecting method and the sophisticated detection equipment, the correct sampling principle to minimize the sampling errors must be followed, which requires that people who carry out the measurement should master the correct sampling theory.

16.1 Sampling System

Sampling is generally divided into the planktonic method (the airborne state of sampled particles remains the same) and the capture method (airborne particles are captured).

In the capture method sampling system, there are a few instruments: the sampler (as the clamp of a filter material, it is preferably made of stainless steel with the commonly effective diameter 25 mm, as shown in Fig. 16.1), the sampling tube (usually plastic pipe), flowmeter (the float flowmeter is commonly used; the flow rate is 0–30 L/min), vacuum pump (vacuum degree $\geq$300 mmHg; the flow rate $\geq$30 L/min), and valve (the needle valve or other fine-tuned valve).

In the planktonic method sampling system, it is mainly composed of the dust analyzer (such as a particle counter) and the sampling tube.

When the sampling system is designed, there are two problems should be paid attention to. One is the orientation of the sampling probe, and the other is the position of the flowmeter.

16.1.1 Orientation of the Sampling Probe

The opening of the sampler or the sampling pipe should face the airflow direction. Otherwise, if there is an angle, due to the inertia effect some particles will deposit

Z. Xu, *Fundamentals of Air Cleaning Technology and Its Application in Cleanrooms*, DOI 10.1007/978-3-642-39374-7_16, © Springer-Verlag Berlin Heidelberg 2014

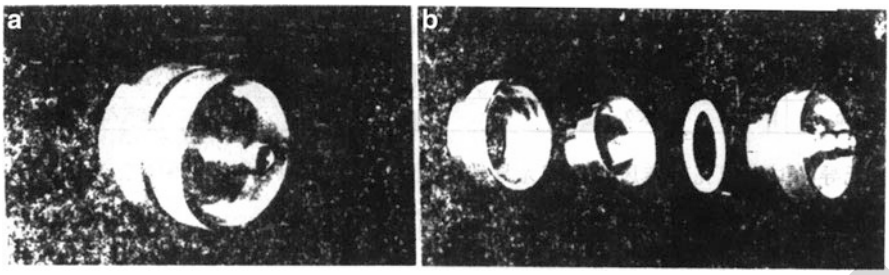

Fig. 16.1 Sampler. (**a**) Assembly sample. (**b**) Component sample

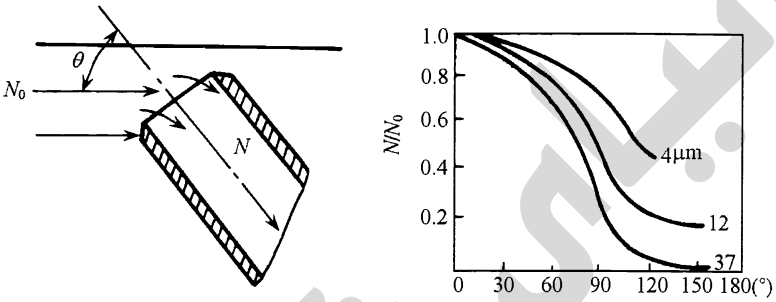

Fig. 16.2 Influence of the inclination between the sampling probe and the airflow direction

onto the inner wall of the tube or the mouth edge, while some cannot enter the sampler or the sampling tube, so that the resultant collected particle number is less than the actual value. Figure 16.2 shows the curve about the effect of the inclination angle between the sampling mouth and the direction of the flow [1]. When the angle is less than 30°, for particles with diameter less than 10 mm, the sampling error is less than 5 %. Figure 16.3 provides a curve which can be used to calculate this kind of error more accurately [2].

One accurate method is to obtain the direction with the maximum dynamic pressure, i.e., the airflow direction, when the pitot tube is used.

When sampling is performed outside, the filter material should be perpendicular to the ground to avoid the deposition of large particles or debris on the filter material.

16.1.2 Position of Flowmeter

The essence of this problem is the influence of additional resistance on the flowmeter. The calibration of flowmeter is carried out in the environment with certain resistance (i.e., the additional resistance at the entrance of the flowmeter), pressure, and temperature, but in the actual application period, all these conditions changed,

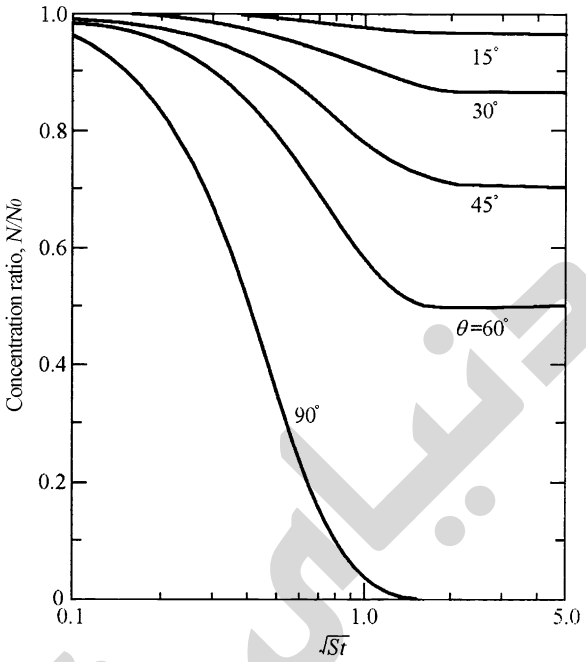

Fig. 16.3 Influence of the inclination of the sampling probe with the airflow direction on the sampled concentration when $u = u_0$

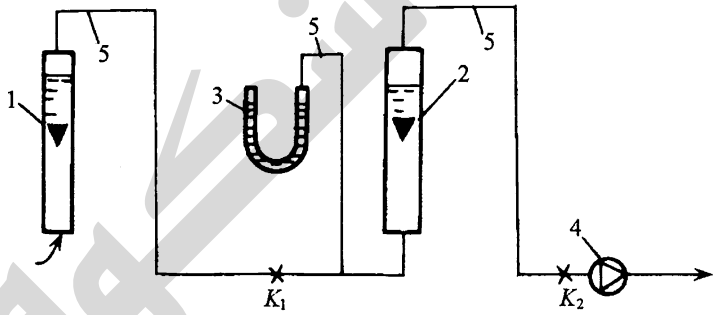

Fig. 16.4 Experimental system about the additional resistance. *1*, *2* Flowmeter, *3* pressure gauge, *4* vacuum pump, *5* rubber hose, K_1, K_2 spiral clamp

so it will certainly affect the original calibration value. In particular, the additional resistance caused by sampler, filter, and valve is often neglected, so it is necessary to emphasize this point.

Figure 16.4 shows the experimental system to investigate the influence of additional resistance caused by different installation positions of the flowmeter [3].

For the completely same flowmeters 1 and 2 (after calibration), they are connected in series and K_1 is placed in between to create resistance. Its value is indicated by 3. Flowmeter 1 reflects the standard flow, and flowmeter 2 reflects the flow under different resistances. When the vacuum pump is turned on, it can be found that the flow rates showed by the flowmeter 1 and 2 are different. The former

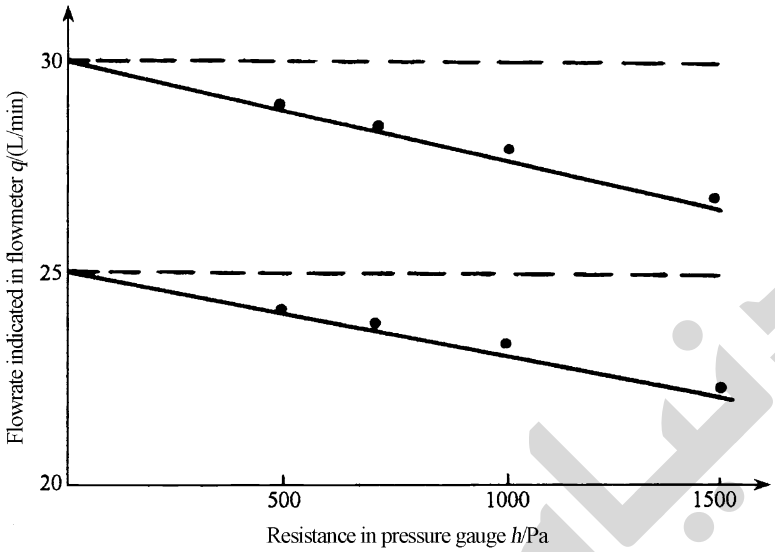

Fig. 16.5 Influence of additional resistance on the flow rate of the flowmeter. — Flow rate indicated by flowmeter 1, — Flow rate indicated by flowmeter 2

is less than the latter. The larger the resistance is, the larger the difference is. If K_1 and K_2 are adjusted in the way that the value indicated by the flowmeter 2 is fixed while the resistance of K_1 varies, the variation of the values indicated by flowmeter 1 is shown in Fig. 16.5.

The main reason for this result is that air pressures inside the two flowmeters are different due to the additional resistance caused by spiral clamp K_1. When air enters from the bottom of the flowmeter 1, there is almost no additional resistance (flowmeter calibration is often carried out in this case). When air goes through K_1, the resultant air pressure in the flowmeter 2 decreases. According to the principle for orifice flowmeter and float flowmeter, when the same gas under different conditions is measured with a flowmeter, the following relationship about flow rates can be obtained:

$$\frac{q_1}{q_2} = \sqrt{\frac{\rho_2}{\rho_1}} \tag{16.1}$$

where

q_1 and q_2 are the indicated flow rates under two kinds of working conditions;
ρ_1 and ρ_2 are gas densities under two kinds of working conditions.

It is known that the gas density ρ is proportional to the pressure P and is inversely proportional to temperature T. The above expression can be written as

$$\frac{q_1}{q_2} = \sqrt{\frac{P_2}{P_1} \times \frac{273 + t_1}{273 + t_2}} \tag{16.2}$$

where

P_1 and P_2 are the pressures upstream of the flowmeters under two different working conditions (The air pressure in calibration condition is generally one atmospheric pressure or 760 mmHg. The air pressure in measurement condition is the subtraction of the absolute value of the readings of the pressure gauge upstream of the flowmeter from the local atmospheric pressure B or the subtraction between B and the known additional total resistance before the flowmeter. Only in the circumstance with the sampler, the total resistance becomes the resistance of the filter media under the sampling velocity.);

t_1 and t_2 are air temperatures in two different working conditions, which is generally 20 °C in calibration condition.

There are two kinds of consideration methods for the application of this expression.

The first consideration method. Let the indication value q_2 represent the scale value in calibration condition, q_1 the indication value to be measured in the actual working condition, P_2 one atmospheric pressure in calibration conditions, and P_1 the pressure in the measurement condition; it is obvious that $P_1 < P_2$, and $q_1 > q_2$ (for the convenience of discussion, it is assumed that there is no difference for the temperature), namely, the actual flow through the flowmeter is greater than the indication value. This is because of the reduced density and the decreased air pressure in the flowmeter.

The second consideration method. Let the indication value q_2 represent the actual measured indication value, P_2 the actual measured pressure, and q_1 the indication value with the calibration pressure P_1; it is obvious that $P_2 < P_1$ and $q_1 < q_2$, i.e., the actual indication value q_2 in actual condition should be reduced to q_1 in the calibration condition, which is always easily neglected by people. The round dots in Fig. 16.5 are the indication values in the calibration condition after calculation (the temperature difference is ignored), and the value agrees well with the experimental data.

If the above two calculation results should be converted to other conditions, the following equation can be used:

$$q' = q_1 \frac{P_1}{P'} \frac{T'}{T_1} \tag{16.3}$$

where the superscript "′" in the equation represents the conversion state, such as the calibration state, standard state, sampling state, and special state in the flowmeter. The subscript "1" means the adopted symbol during the application of Eq. (16.2) with one of the two consideration methods.

As for what kind of the destination state of conversion, it depends on the need. For example, in inspection process of product quality or quality accident, the actual local particle concentration should be known, so it should be converted into the sampling state. For the general measurement, for the purpose of comparison, it should be converted to calibration state or standard state. So for the general

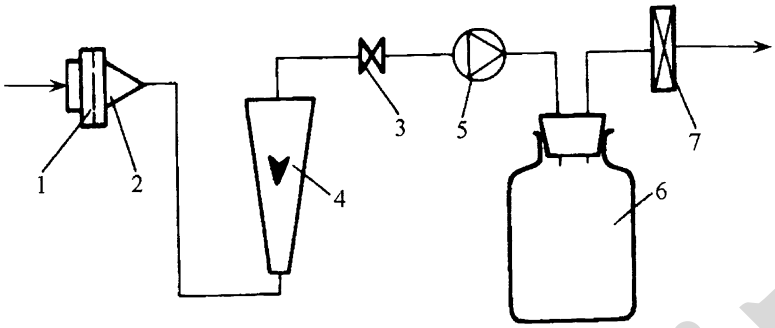

Fig. 16.6 Installation of flowmeter at the suction end of the vacuum pump. *1* filter membrane, *2* Sampler, *3* Valve, *4* Flowmeter, *5* vacuum pump, *6* buffer bottle, *7* HEPA filter

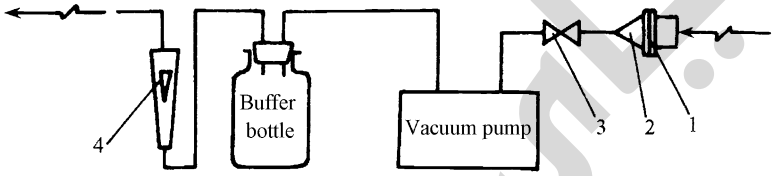

Fig. 16.7 Installation of flowmeter at the exhaust end of the vacuum pump. *1* Filter membrane, *2* Sampler, *3* Valve, *4* flowmeter

measurement, the second method to correct the flow rate should be used, because after correction the result under calibration state is obtained, which no longer needs state conversion.

According to the influence of the additional resistance on the flow rate, the following points in the sampling should be paid attention to:

1. When the particle concentration is measured with the filter method, under the premise of the particle collecting efficiency, the filter material with small resistance should be used, and the resistance of the pipeline should be reduced as much as possible.
2. When the flowmeter is installed at the suction end of a vacuum pump, the valve used to regulate the flow must be installed behind the flowmeter, as shown in Fig. 16.6. It should not be installed between the sampler and the flowmeter. If the flowmeter is installed at the exhaust end of the vacuum pump, there should be a buffer bottle between the flowmeter and the vacuum pump. Particularly for removing large oil drops during the use of mechanical pump, apparatus such as valve and filter cannot be placed outside of the buffer bottle, as shown in Fig. 16.7.

   If sampling is performed in the cleanroom, the vacuum pump can only be placed indoors. Because the exhaust of vacuum pump must pass HEPA filter, it is not suitable to place the flowmeter at the exhaust end.
3. When filter paper is used as the media, because the resistance during sampling is not more than 30 mmHg, so its influence can be neglected. When microporous

membrane filter is used for sampling, because its resistance during sampling is often more than 100 mmHg, the influence of this additional resistance on the indication value of flow rate will be more than 10 %. Therefore the result must be corrected.

Now examples for calculation will be given as follows:

Example 16.1. During the indoor sampling in a cleanroom, the indication value of the flowmeter is 20 L/min, and the sampling time is 16 min. The resistance of sampling filter material (microporous filter membrane) under the sampling flow rate is 150 mmHg. After calculation, the total number of particles is 102,000 under the air temperature 300 °C and the air pressure 750 mmHg during measurement. What kind of air cleanliness level can be achieved in the room?

Ans:

1. The flow without any corrections
   Total sampling flow rate is $q = 20 \times 15 = 300$ L
   The average particle concentration is $N = 102{,}000/300 = 340$ #/L
   So the air cleanliness in this room reaches Class 7.
2. Flow rate after correction
   With the first consideration method: (a). The actual flow rate through the flowmeter. The reading value of the flowmeter 20 L/min is the indication value in the calibration condition, so the actual flow rate q_1 through the flowmeter should be

$$q_1 = q_2\sqrt{\frac{P_2}{P_1} \times \frac{273 + t_1}{273 + t_2}} = 20\sqrt{\frac{760}{750 - 150} \times \frac{303}{293}} = 22.891 \text{ L/min}$$

   (b). The flow rate after conversion into other states

$$\text{Calibration state } q' = 22.89 \times \frac{293}{260} \times \frac{600}{303} = 17.47 \text{ L/min}$$

$$\text{Standard state } q' = 22.89 \times \frac{273}{760} \times \frac{600}{303} = 16.28 \text{ L/min}$$

$$\text{Sampling state } q' = 22.89 \times \frac{303}{760} \times \frac{600}{303} = 18.31 \text{ L/min}$$

   With the second consideration method: (a) The indication value in calibration condition

$$q_1 = q_2\sqrt{\frac{P_2}{P_1} \times \frac{273 + t_1}{273 + t_2}} = 20\sqrt{\frac{750 - 150}{760} \times \frac{293}{303}} = 17.47 \text{ L/min}$$

   (b) The flow after conversion into other states

$$\text{Standard state } q' = 17.47 \times \frac{273}{760} \times \frac{760}{293} = 16.28 \text{ L/min}$$

$$\text{Sampling state } q' = 17.47 \times \frac{303}{750} \times \frac{760}{293} = 18.31 \text{ L/min}$$

$$\text{Inner flowmeter state } q' = 17.47 \times \frac{303}{600} \times \frac{760}{293} = 22.89 \text{ L/min}$$

3. Particle concentration
   Now the particle concentration in sampling state becomes

$$N = 340 \times \frac{20}{18.31} = 371.4 \text{ \#/L}$$

According to the actual collected particle concentration 18.31 L/min after correction, the calculated indoor particle concentration is 371.4#/L, so the indoor air cleanliness level does not reach Class 7.

From the above calculation result, it is found that the influence of additional resistance cannot be overlooked.

16.2 Isokinetic Sampling

16.2.1 Sampling in Flowing Air

16.2.1.1 Principle of Isokinetic Sampling

When sampling is taken in the flowing air (especially when in the pipeline), the plane of the sampling mouth should be vertical to the direction of the air flow (namely, the axis of the sampling pipe and the direction of flow are the same), and the sampling velocity must be equal to the air flow velocity. Otherwise, the sampled concentration (i.e., the measured concentration) will be greater than or less than the true concentration, which will cause an error. This is the principle of the isokinetic sampling.

On the left of Fig. 16.8, the airflow velocity u_0 is greater than the sampling velocity u. In this case, the boundary limit of flow inhaled into the sampling tube is less than the diameter d of the sampling tube. If there are large particles outside the boundary limit of the inhaled flow or outside of the streamline with diameter D_0, it will not follow the streamline to flow along the tube wall when it approaches to the tube mouth; instead it will enter the tube due to the inertial effect. Small particles on this boundary limit will not enter the tube. In this way, in the same sampling air volume, particles outside this air volume will be carried to enter the tube, especially

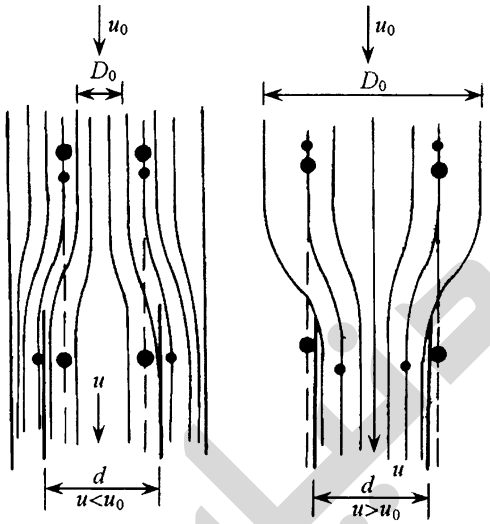

Fig. 16.8 Influence of non-isokinetic sampling

the large particles. So the sampled concentration of large particles increases, which means the whole sampled concentration will be higher than the actual concentration.

On the right in Fig. 16.8, the airflow velocity u_0 is less than the sampling velocity u. In this case, the boundary limit of the flow inhaled into the sampling tube is bigger than the diameter d of the sampling tube. Even if there are big particles within the boundary limit of the inhaled flow or within the streamline range with diameter D_0, when it approaches the tube mouth, it will not enter into the tube but instead flow away along the tube wall, and only small particles in the streamline can enter into the tube. So in the same volume of airflow entering into the tube, particles especially big particles will be lost. So the total sampled concentration will be less than the actual one.

Therefore, factors that affect the sampling concentrations mainly include the difference between the air flow velocity u_0 and the sampling velocity u (i.e., the velocity at the sampling mouth), the dimensionless inertial parameter describing the inertial effect (Stokes parameter) St. The form of the expression is

$$\frac{N}{N_0} = f\left(\frac{u_0}{u}, St\right) \tag{16.4}$$

where

N is the sampled concentration;
N_0 is the real concentration.

As for the error caused by non-isokinetic sampling, the following semi-theoretical formula [4–6] is now widely used:

$$\frac{N}{N_0} = 1 + [u_0/(u-1)]\alpha \tag{16.5}$$

In Refs. [4, 5] it provides:

$$\alpha = -\frac{\left(2 + \frac{0.617u}{u_0}\right)St}{1 + \left(2 + \frac{0.617u}{u_0}\right)St} \tag{16.6}$$

In Ref. [6] it provides:

$$\alpha = -\frac{\left(\frac{2 + 0.617u}{u_0}\right)St}{1 + \left(\frac{2 + 0.617u}{u_0}\right)St} \tag{16.7}$$

It is shown that the relationship between $\frac{N}{N_0}$ and $\frac{u_0}{u}$ is more obviously demonstrated directly in Eq. (16.6) (published in 1980) than Eq. (16.7) (published in 1994), so Eq. (16.6) was referred by 209E. The difference of the results with the two formulas is little, and the latter is slightly larger.

From Eq. (16.5), it is shown that the general characteristic is:

$$\frac{u_0}{u} = 1 \quad \frac{N}{N_0} = 1$$

$$St = 0 \quad \frac{N}{N_0} = 1$$

$St >> 1$ $\frac{N}{N_0} \approx \frac{u_0}{u}$ (for the situation when particles are very big, and the flow rate is large, and the diameter of the sampling tube is very small);

St = const (the larger the difference between u_0 and u is, the greater the concentration difference is)

u_0/u = const (the larger St is, the bigger the concentration difference is)

When both Eqs. (16.5) and (16.6) are plotted in Fig. 16.9 [7], the above feature can be vividly demonstrated.

It is shown that:

1. In the conditions of non-isokinetic sampling in the wide range u_0/u = 0.012–25.76, as long as $St \nearrow 0.001$, or u_0/u = 0.15–3 and $St \nearrow 0.01$, the sampling error$\nearrow$ 5 %.

   Because large particles are the sampled object in the field of dust removal technology, the requirement for the velocity deviation is less strict when error

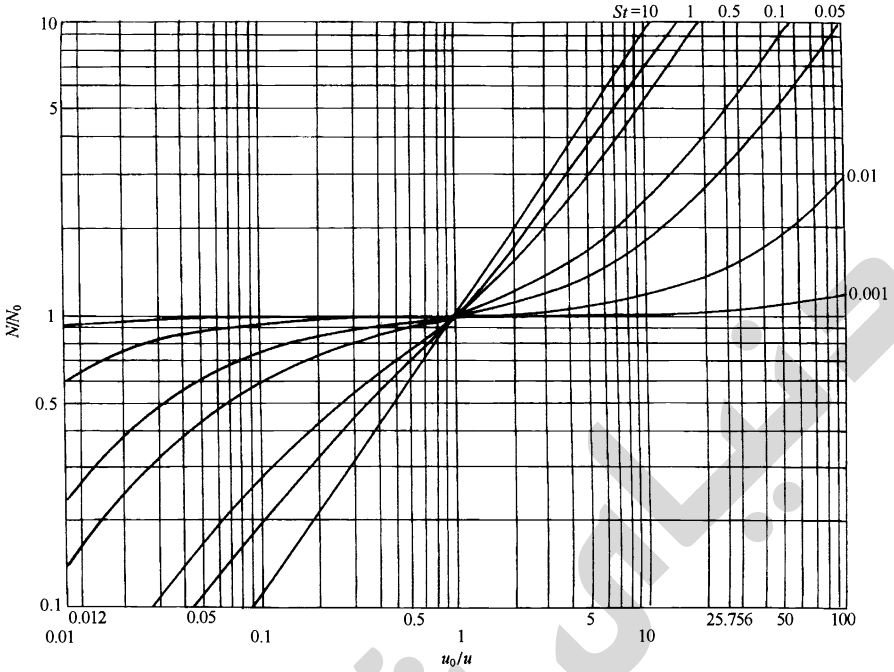

Fig. 16.9 Relationship among the sampled concentration, u_0/u and St

is ≯ 5 %. For example, in Japanese standard JIS Z8808, the sampling error for non-isokinetic sampling is within ±5 % when the error of non-isokinetic velocity is between −5 % ~ +10 %.

2. The influence at the situation $u_0/u > 1$ which has slower sampling velocity (as on the right of Fig. 16.9) is much larger than that at the situation $u_0/u < 1$ which has faster sampling velocity (as on the left of Fig. 16.9). This is also the reason why the negative deviation is less than the positive deviation specified in JIS Z88-8.

Professor Hinds (W.C. Hinds) at Harvard University of USA also obtained similar relationship diagram as Fig. 16.9 [2] based on Eq. (16.6). US Federal Standard 209E also gives the relationship between u_0/u and the error. The comparison is shown in Table 16.1.

Now one example is given as follows:

Suppose $d_p = 0.5$ and 5 μm, $u_0 = 0.5$ m/s, $D_0 = 6.5$ mm, $u = 1.42$ m/s (the sampling flow rate is 2.83 L/min) or 14.2 m/s (the sampling flow rate is 28.3 L/min), and $\rho_p = 1 \times 10^3$ kg/m^3.

At 20 °C, $\mu = 1.83 \times 10^{-5}$ Pa · s. From Table 6.4, it is found that $C = 1.33$ (0.5 μm) or 1.03(5 μm). The following results can be obtained with Eq. (3.7) (conversion of unit can be found in Sect. 6.2):

$$St_{(0.5\ \mu m)} = \frac{1.33 \times 1 \times 10^5\ \mathrm{kg/m^3} \times \left(0.5 \times 10^{-6}\right)^2 \times 0.5\ \mathrm{m/s}}{18 \times 1.83 \times 10^{-5}\mathrm{Kg.m.s/(s^2.m^2)} \times 6.5 \times 10^{-3}\ \mathrm{m}} = 0.00008$$

Table 16.1 Relationship between u_0/u and the sampling error

Source	u_0/u	St	Equivalent diameter (μm)	Error by non-isokinetic sampling (%)
Relationship diagram proposed by author based on Eqs. (16.5) and (16.6)	0.15–3	≯0.01	7	≯5
Relationship diagram proposed by Dr. Hinds (USA)	0.1–10	≯0.01	7	≯5
Illustration of the measurement error by non-isokinetic sampling in 209E (USA)	0.143 (=1/7)–3.33 (1/0.3)	≯0.006	5	≯5

$$St_{(0.5\ \mu m)} = 0.006$$

So from Eq. (16.6) we can obtain:

$$\begin{cases} \alpha_{(0.5\ \mu m)} = 0.00046 \\ \alpha_{(5\ \mu m)} = 0.033 \end{cases} \quad u = 1.42\ m/s$$

$$\begin{cases} \alpha_{(0.5\ \mu m)} = 0.0017 \\ \alpha_{(5\ \mu m)} = 0.105 \end{cases} \quad u = 14.2\ m/s$$

So

$$\begin{cases} \dfrac{N}{N_{0(0.5\ \mu m)}} = 0.9997 \\ \dfrac{N}{N_{0(5\ \mu m)}} = 0.979 \end{cases} \quad u = 1.42\ m/s$$

$$\begin{cases} \dfrac{N}{N_{0(0.5\ \mu m)}} = 0.9983 \\ \dfrac{N}{N_{0(5\ \mu m)}} = 0.9 \end{cases} \quad u = 14.2\ m/s$$

The calculated results about the big error with large flow rate are shown below:

0.5 μm	Relative error 0.17 %
1 μm	0.52 %
2 μm	2.03 %
3 μm	4.15 %
4 μm	7.1 %
5 μm	10 %

It should be emphasized that, as pointed out in Chap. 16 and relevant literatures [7], the unit of μ during calculation of St must be paid attention to. If the engineering unit in the past is used, the value of μ decreases by 9.8 times, which will increase the particle loss rate by 9.8 times and will draw different conclusions.

The above results show that the error with non-isokinetic sampling for $\leq$1 μm particles is less than 1 % even when particle counter with the sampling flow rate 28.3 L/min is used. But it reaches 10 % for $\geq$5 μm particles.

If the requirement of sampling error is not only for particles with a certain size, but also for whole particles with diameter larger than a certain size such as $\geq$0.5 μm, it should be calculated according to the standard distribution of particle size.

From Chaps. 2, 3, and 7, when suppose particles with diameter $\geq$ 0.5 μm occupy 100 %, particles with diameter 0.5 μm occupy33% ~ 38 %, so:

0.5–1 μm	83–86 %
1–3 μm	9–12 %
3–5 μm	2–4 %
5 μm~	1–3 %

It can be calculated that the error is 1–1.9 % for all the particles $\geq$0.5 μm with large sampling flow rate, and the average is 1.5 %. Apparently the error is much smaller with the small sampling flow rate. This result is much smaller than the experiment data in the wind tunnel, but the error of the experiment data is 4.2 % on average [8], which is also less than 5 %.

16.2.1.2 Application of Isokinetic Sampling

For sampling of large particles in the flow field with large velocity fluctuation, such as the sampling in the field of dust removal technology, the error will be 5 % by the velocity deviation 10 %. The application of isokinetic sampling is mentioned in all the monographs about this aspect, where the allowable error is also mentioned to be more than 10 % [9–12]. The velocity is required to be controlled strictly in these literatures. One method is the prediction of velocity. When a micromanometer is connected to both inside and outside of the sampling probe, the sampling velocity is adjusted so that the indication value is 0. Of course, when the sampling flow rate changes, it is necessary to use the cumulative flowmeter, and the rotameter is only for the purpose of surveillance and control. In addition, there is another method called isodynamic pressure method. Chinese Academy of Preventive Medicine has developed a specialized isokinetic sampling probe.

In cleanroom, it is obvious that the velocity field is stable. But it is not uncommon that the velocities at many positions are different from the average velocity by one time, or even much larger (e.g., in the blinder area below the shadowless lamp holder in the center of the operating table, where the air cleanliness must be measured). The transient change rate of velocity at each position can

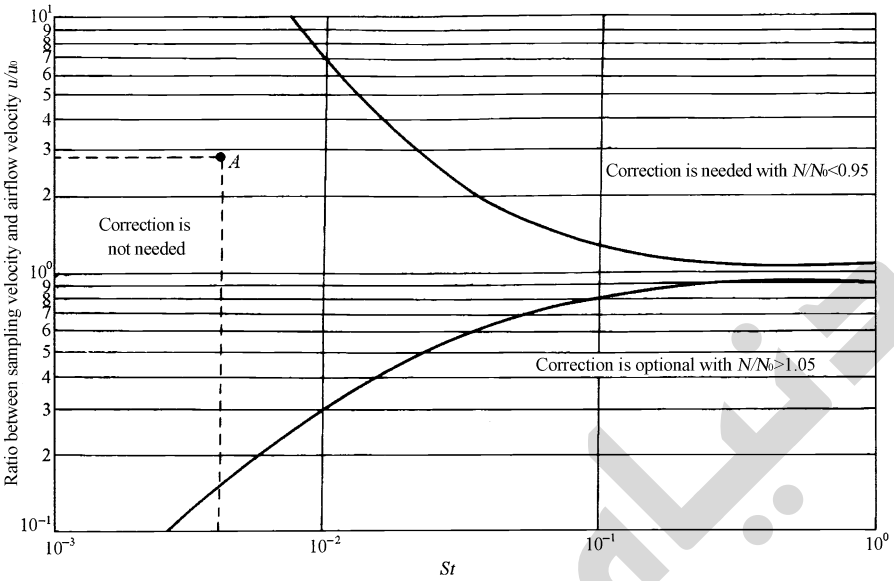

Fig. 16.10 Estimation diagram about the necessity to make correction for the sampling deviation in 209E

also be more than one time (as shown in Fig. 8.30). Because of the time difference at each sampling position, the variation of velocity may be offset with each other. Literatures have emphasized that the isokinetic sampling procedure must be followed. But the feasibility of isokinetic sampling at various measurement positions in large space is much less than that in the pipeline. In unidirectional flow cleanroom, the sampling velocity can be chosen to be the average velocity. But in turbulent flow cleanroom, it is meaningless to mention the average velocity. So for the measurement of the concentration field in space, the allowable error should be considered. All test results have errors. If the error is within the allowable range, the test results can be accepted. 209E proposed that the error less than 5 % is acceptable which is caused by non-isokinetic sampling. It also points out that when u:u_0 is between 0.3:1 and 7:1, the error is less than 5 %.

The diagram to make correction was also given as appendix C in 209E, which is shown in Fig. 16.10.

The example of the application of Fig. 16.10 is shown as follows:

When the particle counter with small sampling volume 2.83 L/min is used to detect particles with diameter 5 μm (only for this particle size) from airflow with velocity 0.5 m/s, should any correction be made?

Ans: We know that $u/u_0 = 1.42/0.5 = 2.84$, and $St = 0.006$ for 5 μm particles, so point A can be found on Fig. 16.10, which falls in the area where correction is not needed. So there is no need for correction.

Table 16.2 Specification of isokinetic sampling

	Specification			
Standard	Flow pattern	Particle size	Error	Isokinetic sampling
US 209D (1988)	Unidirectional flow			Needed
US 209E (1992)	Unidirectional flow	≥5 μm	>5 %	Needed
ISO14644 (1999)				Not specified

The specification of isokinetic sampling is listed below from the main standards, which is shown in Table 16.2.

It is shown that no matter what the particle size and the allowable error are, 209D required isokinetic sampling for unidirectional flow. But for 209E, isokinetic sampling is needed only when the error is >5 % for particles ≥5 μm, where the flow pattern is not specified. In fact it is turbulence flow. Because particle counter with small sampling flow is used, the sampling error is smaller and influence exists only for large size particles. So 209E clearly pointed out: "although isokinetic sampling is good, if it is not feasible, the sampling deviation should be estimated with the method in appendix C," "It is only meaningful for particles with diameter equal to or larger than 5 μm in clean area by non-isokinetic sampling." In ISO14644-1, it only kept the specification about the minimum sampling volume and the probe orientation which were given in 209E, while the requirement of isokinetic sampling is not explicitly mentioned. This is identical with the general opinion of 209E. Although the sampling error is big for particles ≥5 μm with non-isokinetic sampling, a lot of practice shows that 10 μm particles do not exist in cleanroom, and 5 μm particles do not exist in high-level cleanroom either, and only a few exist in low-level cleanroom. So the influence on the particle number is small, which can be used for the understanding of ISO specifications.

The next chapter will illustrate that the sampling error including the non-isokinetic sampling by particle counter will generally not exceed the standard estimation range.

Based on the above analysis, we can suggest that (sampling error ⊁ 5 % is used as the standard):

1. Under the condition of $u_0/u = 0.012–25.76$, as long as $St \not> 0.001$, isokinetic sampling is not required.
2. For sampling in cleanroom according to the current domestic and international standards, isokinetic sampling is not required for particles ≥5 μm.
3. If particle counter with large sampling flow rate is used in cleanroom, isokinetic sampling is required for particles ≥5 μm. (For particles less than 5 μm, calculation should be performed to determine whether isokinetic sampling is needed. Generally isokinetic sampling is needed for 4 μm particles.)
4. When isokinetic sampling is needed but it is impossible, correction of the result should be made with the estimation error on Fig. 16.9.

16.2.2 Sampling in Quiescent Air

Of course, it is absolutely impossible to obtain motionless air, and this is also the case even in some experimental device. Here the so-called quiescent state means that the air velocity is very low, and it is completely in natural state.

There are two kinds of errors when the sampling probe is facing upward in the still air:

1. Error caused by settlement of particles
   When the sampling rate is very low and the sampling mouth is upward, due to the settlement of particles, some particles outside the sampling volume will "fall" into the sampling probe. In the extreme case, the sampling flow rate is zero; sampling error will be infinite because of the natural sedimentation of particles.
2. Error caused by the inertial motion of particles
   This is similar to the sampling in flowing air. With the larger sampling flow rate and the larger particle size, these particles may not be collected.

In order to reduce the first kind of error, sampling with adequate sampling velocity must be performed. In order to reduce the second kind of error, sampling probe with large diameter should be used.

Davies provided a mathematical expression with the above two conditions [13]:
For the first kind of condition

$$\mu \geq 25\nu_s \tag{16.8}$$

where v_s is the settling velocity. Therefore the following expression can be obtained (where the slip boundary correction can be omitted)

$$D_0 \leq 4.1\frac{Q^{\frac{1}{2}}}{d_p} \tag{16.9}$$

where

D_0 is the diameter of the sampling probe;
Q is the sampling flow rate;
d_p is the particle diameter when $\rho = 1$.

For the second kind of condition (where the slip boundary correction can be omitted):

$$D_0 \geq 0.062Q^{\frac{1}{5}}d_p^{\frac{2}{5}} \tag{16.10}$$

With the mathematical expressions, Figs. 16.11 and 16.12 can be obtained [14], which facilitates the usage.

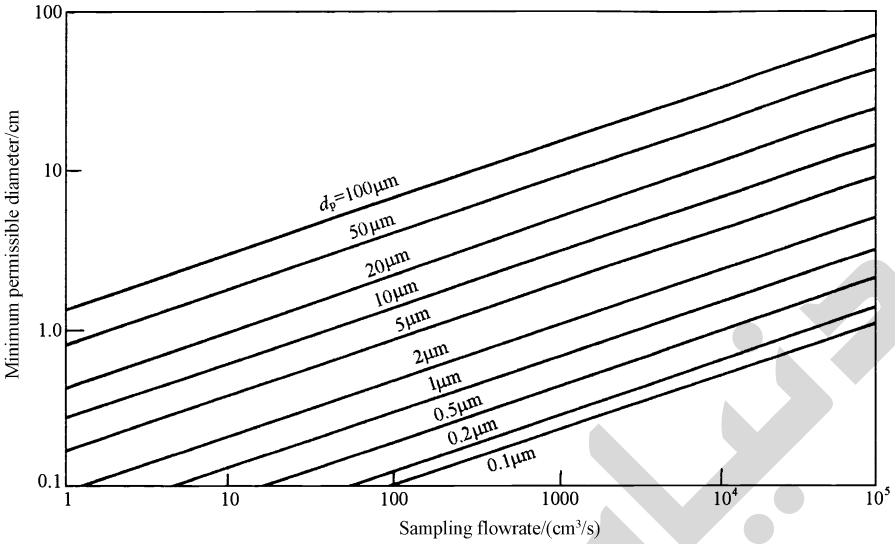

Fig. 16.11 The minimum permissible diameter of sampling probe in quiescent air

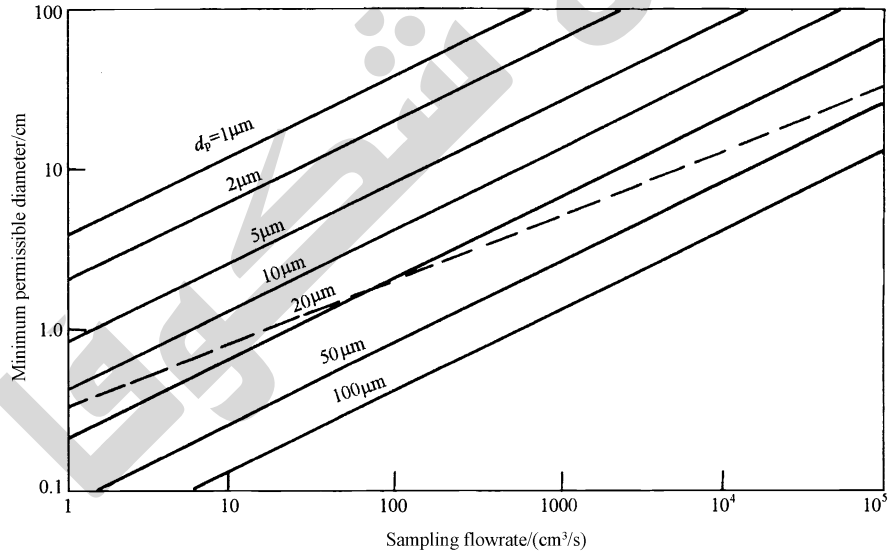

Fig. 16.12 The maximum permissible diameter of sampling probe in quiescent air

The sampling conditions below the dotted line in Fig. 16.12 show that the requirement for both the minimum and maximum allowable sizes of sampling probe cannot be simultaneously satisfied.

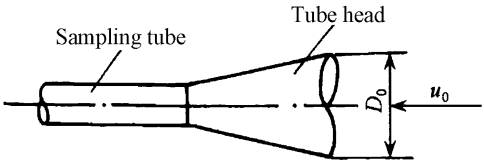

Fig. 16.13 Shape of sampling probe

16.2.3 Calculation of the Diameter of the Sampling Probe

When isokinetic sampling is required, it does not necessarily change the diameter of the whole sampling tube. It is fine as long as sampling probes with different diameters are placed at the head to the sampling tube, as shown in Fig. 16.13.

If air velocity u_0 is expressed with "m/s," the sampling flow rate q with "L/min," and the sampling probe diameter D_0 with "mm," we can obtain:

$$D_0 = \sqrt{\frac{q}{0.047u_0}} \tag{16.11}$$

16.3 Particle Loss in Sampling Line

It is a matter of concern about the measurement error caused by particles loss in the sample tube. It is serious when the sampling loss of microbiology reaches 38.2 % for a 2.8 m long sampling tube [15], which is not impossible. Except for the electrostatic effect during sampling and filtration processes because of the electrostatic charge, there are also other reasons for the particle loss, which mainly include the deposition of particles in the tube caused by diffusion, deposition, collision, and coagulation effect. They will be introduced separately as follows.

16.3.1 Diffusional Deposition Loss in Sampling Tube

Particles loss by diffusional deposition will occur since they will attach onto the tube wall by diffusional movement.

Expressions to calculate the particle loss by diffusional deposition are different according to the different flow states inside the tube. For the common particle counters with large, medium, and small sampling flow rates at home and abroad, Reynolds numbers Re in the sampling tube are shown in Table 16.3.

It is laminar flow when $Re < 2{,}000$. It is turbulent flow when $Re > 4{,}000$. So for the particle counter with large sampling flow rate, it should be considered as the

Table 16.3 *Re* numbers of the flow

Particle counter	Inner size of sampling tube R (m)	Q		u (m/s)	Re
		L/min	cm^3/s		
Large flow rate	0.5×10^{-2}	28.3	471.7	6	3,940
Medium flow rate	0.325×10^{-2}	2.83	47.2	1.42	605
Small flow rate	0.2×10^{-2}	0.3	5	0.4	105

turbulent flow, while the laminar flow should be considered for the particle counter with medium or less sampling flow rate.

16.3.1.1 Laminar Flow in Tube

According to the summary of the conclusions by Fuchs in 1955 [16], the following formula can be obtained. Let

$$\alpha = \frac{Dx}{R^2 u} \tag{16.12}$$

When $\alpha > 0.03$

$$\frac{N}{N_0} = 0.82e^{-3.66\alpha} + 0.097e^{-22.2\alpha} + 0.0135e^{-53\alpha} \tag{16.13}$$

When $\alpha < 0.03$

$$\frac{N}{N_0} = 1 - 2.57\alpha^{\frac{2}{3}} \tag{16.14}$$

where

N/N_0 is the penetration of particles through the sampling tube;
N_0 is the particle concentration at the entrance of the sampling tube, i.e., the sampling concentration, #/L;
N is the particle concentration at the distance x from the entrance of the sampling tube, #/L;
D is the diffusional coefficient of particles, m^2/s;
R is the radius of the sampling tube, m;
x is the length of the sampling tube, m;
u is the air velocity inside the sampling tube, m/s.

With the above formula, the dotted line shown in Fig. 16.14 can be obtained [17]. The relationship can be found between particle loss rates, particle size, and flow rate. But it is inconvenient to determine the required length of the tube from the theoretical curve.

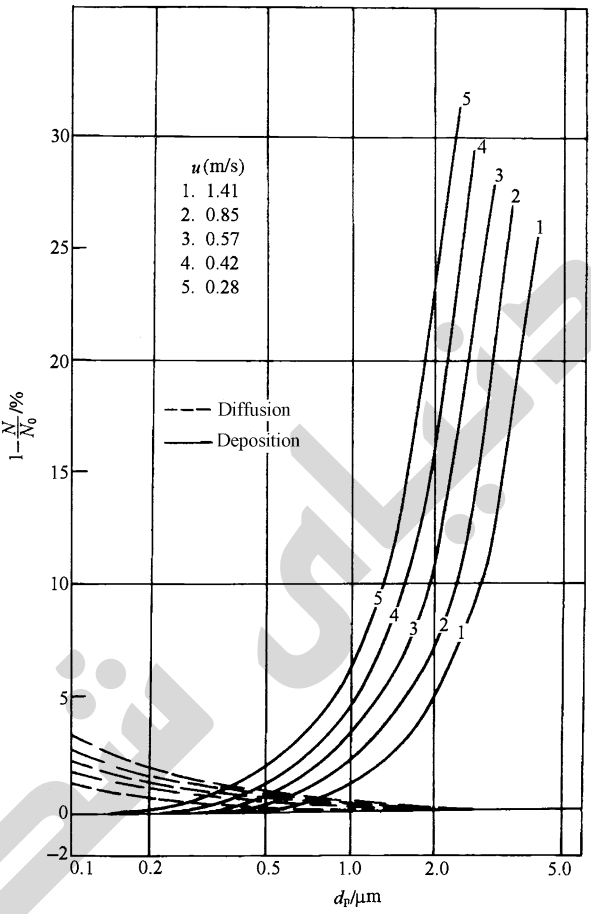

Fig. 16.14 Theoretical particle loss rate of DOP particles by diffusion and deposition in soft polyvinyl chloride tube with $R = 0.25$ m and length 4 m

Fuchs gave a slightly different equation in the published monograph in New York in 1964 [18] (in the past this equation was referred by author in relevant publications). When $\alpha > 0.04$,

$$\frac{N}{N_0} = 0.819e^{-3.657\alpha} + 0.097e^{-22.3\alpha} + 0.032e^{-57\alpha} \tag{16.15}$$

When $\alpha < 0.\ 04$,

$$\frac{N}{N_0} = 1 - 2.65\alpha^{\frac{2}{3}} + 1.2\alpha + 0.177\alpha^{\frac{4}{3}} \tag{16.16}$$

The α value above may also be 0.02 in some literatures [19].

By comparison, the result from Eq. (16.15) is slightly smaller than that from Eq. (16.13), and the result from Eq. (16.16) is slightly larger than that from Eq. (16.14). But the differences for these two situations are very small.

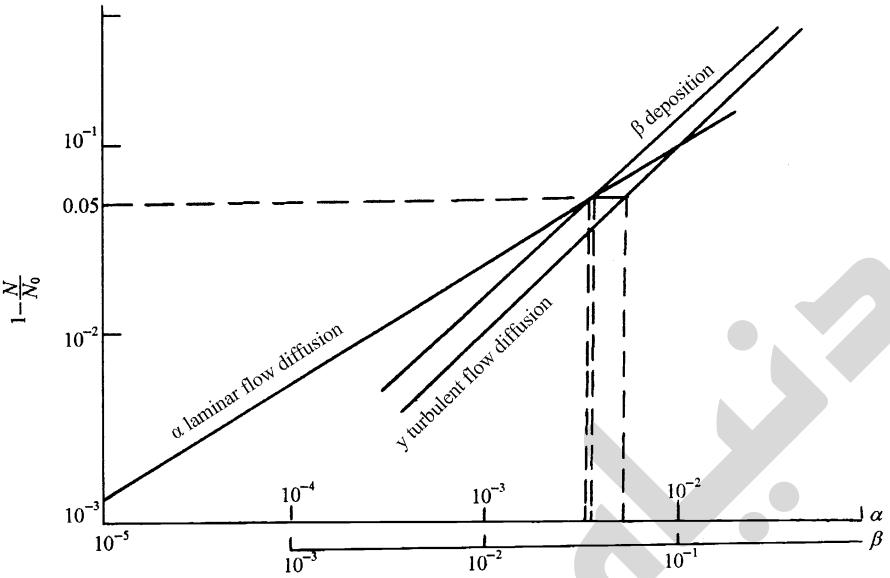

Fig. 16.15 Calculation curve of particle loss by diffusion and deposition

For particle counters with medium and low sampling flow rates, the value of α of the latter is greater than the former. The smaller the particles are, the larger the diffusion is, which is more disadvantageous. The most disadvantageous situation corresponds with $d_p = 0.1$ μm, when $D = 8 \times 10^{-10}$ m^2/s. We can obtain

$$\text{When } x = 5 \text{ m} \qquad \alpha = 2.5 \times 10^{-3}$$

$$\text{When } x = 50 \text{ m} \qquad \alpha = 2.5 \times 10^{-2}$$

So for calculating the diffusional loss of particles for particle counters with medium and small sampling flow rates, $\alpha < 0.04$.

Eq. (16.16) can be used to obtain the relationship diagram between α and $1 - N/N_0$, as shown in Fig. 16.15 [20]. In comparison of Fig. 16.14, this figure directly presents the relationship between α and the particle loss rate which is described in Eq. (16.16). It is convenient to calculate the particle loss rate and the pipe length with the known particle loss rate.

It is shown in Fig. 16.15 that as long as $\alpha \leq 0.0033$, the diffusional loss rate will be ≤ 5 %. Suppose the allowable maximum loss rate is 5 %, we know

$$\alpha = \frac{Dx}{R^2 u} \leq 0.0033$$

So the following requirement must be satisfied:

$$x \leq \frac{0.0033 R^2 u}{D} \tag{16.17}$$

Table 16.4 The allowable tube length in laminar flow sampling tube when the diffusional particle loss rate ≤ 5 %

		x (m)			
		0.1 μm	0.3 μm	0.5 μm	1 μm
R (m)	u (m/s)	$D = 8 \times 10^{-10}$ m^2/s	$D = 1.2 \times 10^{-10}$ m^2/s	$D = 0.7 \times 10^{-10}$ m^2/s	$D = 0.3 \times 10^{-10}$ m^2/s
0.325×10^{-2}	1.42	62	415	711	1,659
0.2×10^{-2}	0.4	44	295	506	1,181

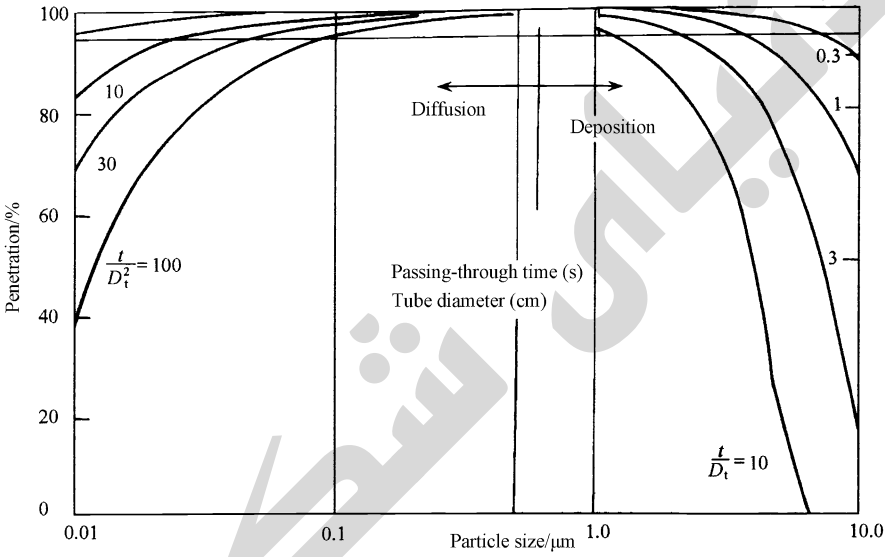

Fig. 16.16 The loss rate of aerosol through the sampling tube due to diffusion and deposition

For particle counter with medium and low sampling flow rates, calculation results are shown in Table 16.4.

Since the diffusional coefficient is independent of the particle density, the allowable tube length in Table 16.4 is also not related to the particle density.

From the calculated results, the diffusional loss for ≥ 0.5 μm particles is extremely small, which can be completely ignored.

In the literature from B.Y.H. Liu [19], similar equation as Eq. 16.16 was used to obtain the left part of Fig. 16.16 (only specified that $\alpha < 0.02$). Although it was pointed out that the formula was valid for laminar flow, it did not indicate in the figure that it is not suitable for the application in non-laminar flow such as the particle counter with large sampling flow rate. And example was given for this kind of particle counter (e.g., diameter $D_t = 1$ cm, and sampling velocity $u = 6$ m/s).

Taking the 0.1 μm as an example, line with the penetration 95 % is plotted to intersect with the line 0.1 μm at the place $\frac{t}{D_t^2} = 100$. According to the instruction of this parameter, we know that

$$\frac{t}{D_t^2} = \frac{100s}{(1\text{ cm})^2} \tag{16.18}$$

That means for a sampling tube with D_t 1 cm, when pass-through time of the flow is 100 s and particle loss rate by diffusion is 5 %, the allowable tube length is 100 s × 6 m/s = 600 m.

If Eq. (16.17) is used for calculation, when the particle loss rate is 5 %, we can obtain

$$x = \frac{0.0033 \times (0.5 \times 10^{-2})^2 \times 6}{8 \times 10^{-10}} = 618\text{ m}$$

There is little difference between these two results. So it is acceptable to consider that results are consistent with Fig. 16.16 and Eq. (16.17) for calculation of the turbulent flow.

But as mentioned before, the above formula and figure should not be used for the particle counter with large sampling flow rate where turbulent flow is inside. So it is incorrect to choose either 600 m or 618 m.

It is difficult to obtain the particle loss in the particle counter with medium sampling flow rate from Fig. 16.16. But it is convenient to use Eq. (16.17).

The allowable pass-through time t for the flow inside the tube can also be calculated with Eq. (16.12). Because

$$\alpha = \frac{Dx}{R^2 u} = \frac{D}{R^2} t \leq 0.0033$$

So

$$t \leq \frac{0.0033R^2}{D} \tag{16.19}$$

Because the particle loss by diffusion is known to be extremely small, the allowable tube length, i.e., the acceptable value t, is very big. The specific number of t will not be calculated. Of course, the value of t can be obtained with the known tube length and flow velocity.

16.3.1.2 Turbulent Flow in the Tube

The diffusional deposition onto the surface of tube wall by turbulent flow is much complex than that by laminar flow, and diffusional deposition onto the indoor wall

which is introduced in Sect. 6.5. As pointed out in Sect. 6.5, there is a very thin diffusional boundary layer close to the wall. Particle concentrations beyond the boundary layer will become uniform by turbulent flow. The boundary layer thickness is δ, which is difficult to determine. In Hinds' monograph [21], it is pointed out that Davis had already discussed the problem, and Fuchs provided the diffusional boundary layer thickness is δ inside the tube. So the whole penetration P through the tube with length x can be obtained with the following formula after the diffusional loss by the turbulent flow is considered:

$$P = \frac{N}{N_0} = \exp\left(-\frac{4V_{\mathrm{d}}x}{D_{\mathrm{t}}u}\right) \tag{16.20}$$

where V_{d} is the diffusional velocity (see Sect. 6.5) (m/s);

$$V_{\mathrm{d}} = \frac{D}{\delta}$$

$$\delta = \frac{28.5D_{\mathrm{t}}D^{\frac{1}{4}}}{Re^{\frac{7}{8}}\left(\frac{\mu}{\rho}\right)^{\frac{1}{4}}} \tag{16.21}$$

where ρ is the air density. Let

$$\frac{4V_{\mathrm{b}}x}{D_{\mathrm{t}}u} = y$$

Log-log paper can be used to plot the linear relationship between the loss rate 1-P and y. So the value of y can be obtained from the figure according to the required loss rate, and then the value of x can be calculated.

Suppose it is required:

$$1 - P \leq 5\%$$

Substituting it into the Eq. (16.20), we can obtain:

$$1 - \exp\left(-\frac{4V_{\mathrm{b}}x}{D_{\mathrm{t}}u}\right) \leq 0.05$$

$$-\frac{4V_{\mathrm{b}}x}{D_{\mathrm{t}}u} = \ln\ 0.95 = -0.0513$$

Table 16.5 Allowable length for turbulent flow with the diffusional loss rate ≤5 %

		x (m)			
		0.1 μm	0.3 μm	0.5 μm	1 μm
D_t (m)	u (m/s)	$D = 8 \times 10^{-10}$ m^2/s	$D = 1.2 \times 10^{-10}$ m^2/s	$D = 0.7 \times 10^{-10}$ m^2/s	$D = 0.3 \times 10^{-10}$ m^2/s
1×10^{-2}	6	16.7	68.8	103.3	195.1

Substituting $\mu = 1.83 \times 10^{-5}$ Pa · s and $\rho = 1.2$ kg/m^3 into the above expressions, we obtain:

$$y = \frac{0.00877 D^{\frac{3}{4}} Re^{\frac{7}{8}} x}{D_t^2 u} \leq 0.0513 \tag{16.22}$$

So

$$x \leq 5.85 \frac{D_t^2 u}{D^{\frac{3}{4}} Re^{\frac{7}{8}}} \tag{16.23}$$

With these above conditions, the loss rate ≤ 5 %.

If the value of y is obtained under a certain loss rate, we obtain:

$$x \leq \frac{114 y D_t^2 u}{D^{\frac{3}{4}} Re^{\frac{7}{8}}} \tag{16.24}$$

For the particle counter with large sampling flow rate where turbulent flow exists inside the sampling tube, the allowable lengths are specified in Table 16.5.

As shown in Table 16.5, the allowable tube length calculated according to the turbulent diffusion situation for 0.1 μm is much less than that with laminar flow diffusion. It is obvious that it's inappropriate to calculate by the latter situation.

And the allowable pass-through time t of the turbulent flow can also be obtained with Eq. (16.23), which is:

$$t = \frac{x}{u} \leq 5.85 \frac{D_t^2}{D^{\frac{3}{4}} Re^{\frac{7}{8}}} \tag{16.25}$$

For the sampling in turbulent flow by particle counter with large sampling flow rate, the allowable pass-through time through the sampling tube is shown in Table 16.6.

Of course, the allowable pass-through time can also be calculated with the division between the allowable tube length and the airflow velocity.

As mentioned before, B.Y.H. Liu just quoted the formula for diffusion loss in laminar flow [19]. He thought that the diffusional loss in the turbulent flow can be calculated according to the laminar flow at first, and then an additional item considering the vortex deposition is added. But the calculation method is very inconvenient for use, so it will not be introduced here.

Table 16.6 Allowable pass-through time for turbulent flow with diffusion loss rate ≤5 %

		t (s)			
		0.1 μm	0.3 μm	0.5 μm	1 μm
D_t (m)	u (m/s)	$D = 8 \times 10^{-10}$ m^2/s	$D = 1.2 \times 10^{-10}$ m^2/s	$D = 0.7 \times 10^{-10}$ m^2/s	$D = 0.3 \times 10^{-10}$ m^2/s
1×10^{-2}	6	2.8	11.5	17.3	32.6

16.3.2 Settlement Deposition Loss in Sampling Line

For laminar flow, Fuchs quoted the same formula of Г. Натансол in two versions of his monographs [16, 18]:

$$1 - \frac{N}{N_0} = \frac{2}{\pi}\left(2\beta\sqrt{1-\beta^{\frac{2}{3}}}\right) + \arcsin\ \beta^{\frac{1}{3}} - \beta^{\frac{1}{3}}\sqrt{1-\beta^{\frac{2}{3}}} \tag{16.26}$$

$$\beta = \frac{3v_s x}{8Ru} \tag{16.27}$$

For turbulence flow, Fuchs gave the following expression in his latter version [13]:

$$\frac{N}{N_0} = e^{-\frac{2v_s x}{\pi Ru}} \tag{16.28}$$

It has been pointed out that the difference is small between the calculation results when $N/N_0 \geq 0.9$ in two conditions. Here calculation for 5 μm particles is taken as an example:

The allowable tube length is as follows when $N/N_0 = 0.90$:

Calculate by laminar flow	$x = 0.095$ m
Calculate by turbulent flow	$x = 0.088$ m (deviation is 7.3 %)

The allowable tube length is as follows when $N/N_0 = 0.95$:

Calculate by laminar flow	$x = 0.046$ m
Calculate by turbulent flow	$x = 0.043$ m (deviation is 6.5 %)

Deviations for these two kinds of flow regime are both within 10 %, so they can be calculated by laminar flow.

The theoretical curve made by Eq. (16.26) has been shown in Fig. 16.14 [17], which is the solid line. It is also not convenient to determine the tube length by this curve.

The relationship diagram between β and $1 - N/N_0$ is shown in Fig. 16.15, which is very convenient for use to calculate the loss rate.

Table 16.7 Values of x/Ru when the sedimentation loss ≤5 % in the horizontal sampling tube

	x/Ru				
ρ (kg/m^3)	10 μm	5 μm	2 μm	1 μm	0.5 μm
2,000	≤0.1422	≤0.5686	≤3.555	≤14.22	≤56.88
1,000	≤0.2844	≤1.1376	≤7.11	≤28.44	≤113.76

Table 16.8 Allowable tube length when sedimentation loss ≤5 % in the horizontal sampling tube

	Q				x (m)				
R (m)	L/min	cm^3/s	u (m/s)	ρ (kg/m^3)	0.5 μm	1 μm	2 μm	5 μm	10 μm
0.5×10^{-2}	28.3	471.7	6	2,000	170.6	42.7	10.7	1.7	0.42
				1,000	341.2	85.4	21.4	3.4	0.84
0.325×10^{-2}	2.83	47.2	1.42	2,000	26.3	6.6	1.6	0.3	0.06
				1,000	52.6	13.2	3.2	0.6	0.12
0.2×10^{-2}	0.3	5	0.4	2,000	4.3	1.1	0.27	0.04	0.01
				1,000	8.6	2.2	0.54	0.08	0.02

From Fig. 16.15, if the sampling efficiency is required to be greater than 95 %, namely, the loss rate is less than 5 %, it must follow the condition that $\beta \leq 0.032$ [calculate by Eq. (16.26)]. "Arcsin" must be converted into radian. For example, $\arcsin 0.95 = 78.805^\circ = 78.5 \times \pi/180 = 1.253$ rad.

The value of x/Ru can be calculated, which is shown in Table 16.7. The allowable horizontal tube length of different particle counters during sampling are listed in Table 16.8.

The right part of Fig. 16.16 was made with the same formula (just specified that $\alpha < 0.02$) as Eq. (16.26) in B.Y.H. Liu's literature [19]. For the sampling tube with $D_t = 1$ cm, taking 1 μm, for example, when the particle penetration is 0.95, we obtain

$$\frac{t}{D_t} \approx \frac{13 \text{ s}}{1 \text{ cm}}$$

The allowable tube length for the particle counter with large sampling flow rate $u = 6$ m/s is

$$x = 13 \times 6 = 78 \text{ m}$$

The deviation is 8 % with the value 85.4 m in Table 16.8. Since interpolation is needed during the application of the figure, it is inconvenient to calculate specifically.

16.3.3 Collisional Loss in Sampling Line

In addition to vertical and horizontal tubes, the sampling tube generally has a certain degree of bending. Figure 16.17 shows a real photo. It forms a 90° bend in the extreme case, as shown in Fig. 16.18 [19]. The minimum bending radius is

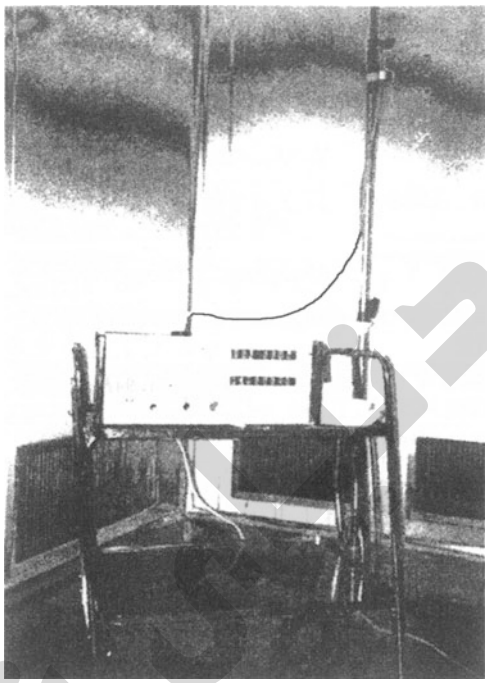

Fig. 16.17 Actual bending condition of sampling tube

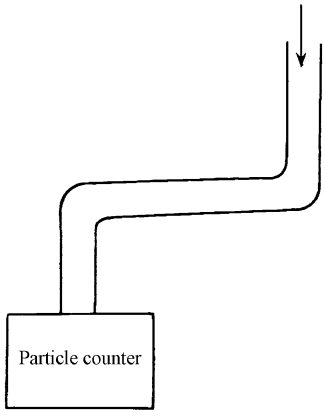

Fig. 16.18 Schematic of the extreme case for the sampling tube

only 2 ~ 3 cm. So particles will easily collide at the bending section and attached on the tube wall to cause loss.

B.Y.H. Liu quoted the following formula to calculate the penetration [19]:

$$P = \frac{N}{N_0} = 1 - St\left[1 + \left(\frac{\pi}{2R_0} + \frac{2}{3R_0^2}\right)\right] \tag{16.29}$$

This formula is only valid for $St < 0.1$.

$$R_0 = \frac{\text{Bending radius}}{\text{Tube radius}} \tag{16.30}$$

The calculation results of collision loss are listed in Table 16.9.

It is shown from the table that the larger the particle is, the greater the collisional loss is; the bigger the value St is, the bigger the collisional loss is; the smaller the value R_0 is, the greater the collisional loss is.

For particles with diameter equal to and less than 5 μm (this is the maximum controlling particle size in various recent standards), the collisional loss can be ignored. But for l0 μm particles, it should be taken into consideration.

16.3.4 Coagulation Loss in Sampling Line

Equation (6.49) has given the method to calculate the coagulation concentration of monodisperse particles. If it is used to estimate the coagulation concentration of polydisperse particles, separate calculation should be performed with different particle size. And further correction can be made according to the geometric standard deviation σ_g (see Chap. 1) of the group particles. The correction values from literature [22] are listed in Table 16.10.

Take the unfavorable 0.1 μm particles as an example:

$$\frac{N}{N_0} = \frac{1}{1 + K_0 N_0 t}$$

When $t = 10$s, and $N_0 = 10^3$ #/cm^3, the coagulation coefficient is found from Table 6.13 that $K_0 = 8.6 \times 10^{-10}$ cm^3/s. So

$$1 - \frac{N}{N_0} = 1 - \frac{1}{1 + 8.6 \times 10^{-10} \times 10^3 \times 10} = 1 - \frac{1}{1 + 0.0000086} = 0.000009$$

Suppose $t = 1$ h, we obtain:

$$1 - \frac{N}{N_0} = 0.0031$$

Even when polydispersity is taken into consideration with $\sigma_g = 2$, K_0 increases by 1.94 times. The result shows that the coagulation loss is very small, so it can be completely ignored.

Table 16.9 Collisional loss in the bending sampling tube

					$1 - N/N_0$				
					0.5 μm	1 μm	2 μm	5 μm	10 μm
D_t (m)	u_0 (m/s)	ρ (kg/m^3)	Bending radius/m	R_0	$St = 0.000052$	$St = 0.000204$	$St = 0.00082$	$St = 0.0051$	$St = 0.00204$
1×10^{-2}	0.5	1,000	2×10^{-2}	4	0.000075	0.00029	0.0012	0.0073	0.029
1×10^{-2}	0.5	1,000	20×10^{-2}	40	0.000054	0.00021	0.00085	0.0053	0.0021
					$St = 0.00008$	$St = 0.00032$	$St = 0.0013$	$St = 0.008$	$St = 0.032$
0.65×10^{-2}	0.5	1,000	2×10^{-2}	4	0.00011	0.00046	0.0019	0.011	0.046
0.65×10^{-2}	0.5	1,000	20×10^{-2}	40	0.000083	0.00033	0.0014	0.0083	0.033

Table 16.10 Correction of coagulation coefficient of polydisperse aerosol

	Coagulation coefficient		
d_p (μm)	$\sigma_g = 1$	$\sigma_g = 1.5$	$\sigma_g = 2$
0.1	K_0	1.22 K_0	1.94 K_0
0.2	K_0	1.18 K_0	1.77 K_0
0.5	K_0	1.13 K_0	1.53 K_0
~1.0	K_0	1.09 K_0	1.40 K_0
~2.0	K_0	1.09 K_0	1.34 K_0

Table 16.11 Experimental result of the particle loss rate by deposition in sampling tube

No.	Times	Size (μm)	Avg. concentration (#)	No.	Times	Size (μm)	Avg. concentration (#)
A	1	0.3–0.4	1,377	B	1	0.3–0.4	1,376
	2	0.4–0.5	1,071		2	0.4–0.5	1,074
	3	0.5–0.6	598		3	0.5–0.6	578
	4	0.6–0.8	180		4	0.6–0.8	186
	5	0.8–1.0	74		5	0.8–1.0	67

16.3.5 Comparison with Experiment

From the above theoretical calculation, the particle loss by collision, eddy, and coagulation for particles with diameter equal to and smaller than 5 μm inside the sampling tube is much smaller than that by diffusion and deposition, which generally can be ignored. It should be considered only for particles with diameter more than 5 μm and in special sampling conditions. For the particle loss by diffusion and deposition, the deposition loss is much important. The diffusional loss of large particles can also be negligible.

Comparison is performed between three experimental data and theoretical calculation results:

1. For the horizontal sampling tube with diameter 0.4 cm and length 15 cm (A) and 500 cm (B), respectively, particle counter with small sampling flow rate was used to measure the concentration of standard particles after steady state reached. The sampling velocities were both 27 cm/s. The test result is shown in Table 16.11 [23].

   For tube A with length only 15 cm, even for 1 μm particles, the theoretical deposition loss rate is much lower than 1 %, and the diffusional loss is even smaller. So the average concentration in tube A can be considered as the standard value without any particle loss, which can be used to compare with that in tube B (Table 16.11).
2. For a horizontal sampling tube with diameter D_t 1.09 cm and length 500 cm, measurement was performed to test the concentration of the standard particles when the sampling velocity was 0.44 m/s. The result is shown in Fig. 16.19 [24].

   By comparison of the particle loss rate in the figure with the theoretical particle loss rate, results are shown in Table 16.12.

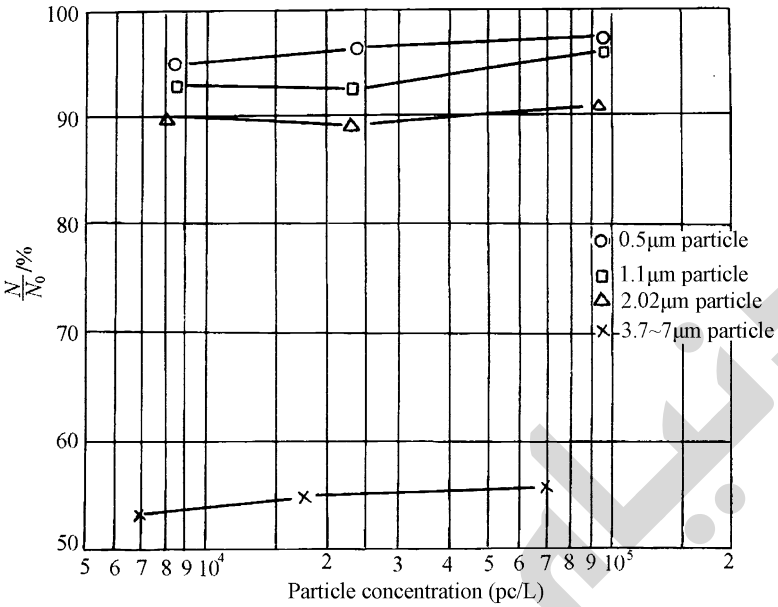

Fig. 16.19 Experimental result of the particle loss by deposition in sampling tube

Table 16.12 Results of comparison

Particle size range	μm	0.5–0.6	0.8–1.0
Calculation particle size	μm	0.5	0.9
Test loss rate	%	2	9.5
Calculated loss rate			
Diffusion	%	0.5	0.3
Deposition	%	2.5	11
Total	%	$[1 - (1 - 0.025) \times (1 - 0.005)] = 3$	$[1 - (1 - 0.11) \times (1 - 0.003)] = 11.3$

In the two experiments, small spherical PSL particles were used as the standard particles, whose density is 1.06 g/cm^3. From comparison, the actual particle loss rate is close to the theoretical value for particles with diameter less than 2 μm. But the actual loss rate is 70 % of the calculated value for particles with diameter larger than 2 μm. This is because the resuspension phenomenon is not considered in the formula after particles deposit. However, it cannot be ignored for big particles. Because the smaller the particles are, the larger the molecular force is. The corresponding suspension velocity is bigger, which needs bigger force to blow them up, and it is hard to resuspend again. As shown in Fig. 16.13, the suspension velocity suddenly decreases from about 2–25 μm. It showed that it is hard for particles with diameter more than 2 μm to resuspend, while it is quite easy for particles with diameter more than

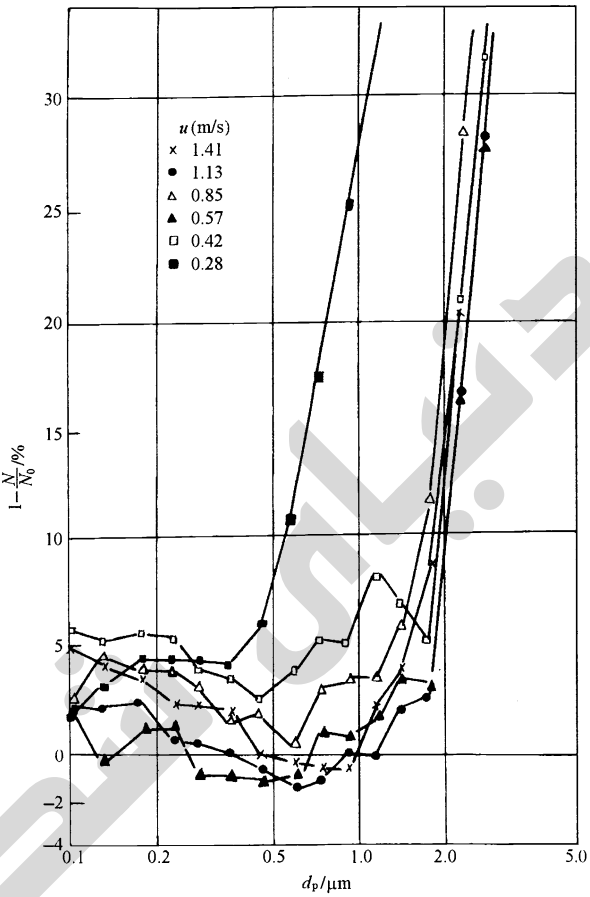

Fig. 16.20 Actual tested loss rate of DOP particles in the soft polyvinyl chloride tube with $R = 0.25$ m and length 4 m by diffusion and deposition

2 μm to resuspend again. It shows that the deposition loss rate is smaller than that of small particles.

3. For the horizontal sampling tube with diameter 0.5 cm and length 400 cm, when the sampling velocity is 0.28 m–1.41 m/s, the actual loss rate for polydisperse DOP particles in the tube is shown in Fig. 16.20 [17].

Taking $u = 0.42$ m/s, for example, comparison with theoretical results is shown in Table 16.13 (the particle density is 0.981 g/cm^3).

In the experimental results with six grades of velocity channels, most of the actual tested results are closed to the theoretical value, and both have the same trend. For example, the loss rate becomes bigger when the sampling velocity is small, and the loss rate increases quickly with the increase of the particle size. With the same sampling velocity, for most particle sizes, the particle loss rate in pipes with small diameter is bigger than that in big pipes.

Table 16.13 Comparison of results

Particle size range	μm	0.5	1.1	2.02	3.7–7
Calculation particle size	μm	0.5	1.0	2.0	5
Test loss rate	%	3	4.2	11	54
Calculated loss rate					
Diffusion	%	0.23	~0	~0	~0
Deposition	%	1.3	3.6	13	82
Total	%	$[1 - (1-0.013) \times (1 - 0.0023)] = 1.5$	3.6	13	82

Table 16.14 Comparison of results

Particle size	μm	0.1	0.5	1	2
Test loss rate	%	5.5	3	6	19
Calculated loss rate					
Diffusion	%	2.5	0.5	0.2	0.1
Deposition	%	~0	1.7	6.5	25
Total	%	2.5	$[1 - (1 - 0.017) \times (1 - 0.005)] = 2.2$	$[1 - (1 - 0.065) \times (1 - 0.002)] = 6.7$	$[1 - (1 - 0.25) \times (1 - 0.001)] = 25.1$

Through the comparison of three examples, it is reasonable to consider that the theoretical calculation is closer to the reality. Correct on the actual test data will be performed according to the theoretical calculation if necessary.

What should be emphasized is that, the theoretical calculation results are all obtained from the formula and the given parameters in this section, instead of directly in the Fig. 16.14. The values from this figure are a little smaller. Since the values of some parameters are unknown during the plot of the figure, the reason why it is smaller cannot be confirmed (Table 16.14).

16.3.6 Comprehensive Conclusion

Through the above analysis of particle loss inside the sampling tube, the following conclusions can be obtained:

1. For particles with diameter less than 5 μm, the length of sampling tube should be considered just according to the particle loss by diffusion and deposition.
2. For 0.5–5 μm particles, the deposition loss rate is gradually bigger than that by diffusion, so the length of the sampling tube should be considered according to the deposition loss.
3. For particles with diameter less than 0.5 μm, the length of the sampling tube should be considered according to the diffusional loss when only particle counter with large flow rate is used. When particle counters with medium and small sampling flows, the length should be considered according to the deposition loss.

4. The allowable pass-through time in the sampling tube is not a definite number.
5. According to the above conclusion, it is reasonable to believe that the recommendation in 209E about the length of the sampling tube is inappropriate.

In the appendix B 40.2 of FS209E, the sampling tube in the "air sampling system" for particle counters is required that "the size of the sampling tube should be determined in such a way that the flow time in the tube should not be more than 10s." And in the B40.2.1, further suggestion was given in the section about "the consideration for particle delivery." "For 0.1–1 μm particles, the maximum sampling tube could be 30 m. For 2–10 μm particles, the length of the sampling tube should not be more than 3 m. In this condition, the particle loss rate can be less than 5 % for small particles by diffusion and large particles by deposition and inertia (see appendix C)."

In the above references, the Reynolds number of sampling flow is required to be 500–2,500, and the diameter of the sampling tube is not specified. So in this *Re* conditions, when calculation is performed with the turbulent formula, if the diameter is bigger than that the diameter 1 cm for the particle counter with large sampling flow rate by 50 %, the allowable length could be 30 m for 0.1–1 μm particles. If the diameter is 1 cm, the maximum length could not be more than 17 m according to Table 16.5. The second channel should not be 2–10 μm, but instead it should be 2–5 μm as the interval, because 5 μm is the prescribed maximum control particle size in 209E. Therefore from Table 16.8, it is suitable that the length of the horizontal sampling tube is not more than 3 m (209E only mentioned it as the sampling tube, which is not accurate). If the diameter of control particles is 2–10 μm, it cannot be more than 1 m. For the special needs with the 5–10 μm particles as the control object, it should not be more than 1 m for the horizontal sampling tube. So for 209E, it is reconcilable that 2–10 μm is changed to 2–5 μm.

For the particle counter with so-called medium sampling flow rate 2.83 L/min in China, the control particle size generally begins from 0.5 μm. So the lower limit 0.1–0.5 μm can be classified as one channel (corresponding to 0.1–1 μm in 209E). Based on the results from Table 15.2 and the calculated results from Ref. [19] cited in 209E, the length of the allowable sampling tube can be long in terms of the diffusional loss. Therefore only the deposition loss should be considered. From Table 16.8, when the atmospheric particle concentration is large (2000), it is safe to set the length of the sampling tube within 30 m in theory. For cleanroom where the maximum control size is 5 μm commonly, it is more likely that only the deposition loss is considered. From Table 16.8, it is known that the horizontal sampling tube should be less than 0.5 m, which means that in order to ensure the loss rate less than 5 % for 5 μm particles, it is better that the length of the horizontal sampling tube is less than 0.5 m. As shown in Fig. 16.17, it is allowable that the length of the horizontal sampling tube is not more than the instrument length, and it is not suitable if the tube is longer. Ref. [20] gives the suggested length value of the sampling tube for domestic situation, as listed in Table 16.15.

Table 16.15 Suggested length values of horizontal sampling tube

Sampling flow rate of particle counter	Sampling particle size range and allowable length of sampling tube			
0.028 m^3/min	0.1–1 μm	2–5 μm	10 μm	
	30 m	3 m	1 m	
0.0028 m^3/min	0.1–0.5 μm	1 μm	2 μm	5 μm
	30 m	10 m	3 m	0.5 m

16.4 The Minimum Sampling Volume

16.4.1 Background of the Problem

For the environment with different air cleanliness levels, the sampling flow rates should be different. During the measurement with the balance meter, it is relevant to the sensitivity of the balance. During the dust sampling with membrane filter, the sampling flow rate is related to the background value of the membrane filter. An appropriate proportion must be kept between the captured particle number and the background value of the membrane filter. For both cases, appropriate sampling flow rates are needed. The minimum sampling volume put forward here is for the particle counter [25]. In the 1970s, particle counters with medium and big sampling flow rates had appeared. Due to the difference of the measurement results between large sampling flow rate and small sampling flow rate, this problem is naturally proposed. For measurement in cleanroom with air cleanliness level higher than Class 100, what is the requirement for the sampling flow rate of the particle counter? If requested, how to determine the minimum sampling volume? This is the new problem that is put forward by the development of air cleaning technology.

In US standards before 209C in 1987, including that from federal government, NASA, and air pollution control association, and in related standards from Britain and Germany, the problem of the minimum sampling volume, the minimum sampling times, and the necessary number of measuring points were not provided. Only in 1973, 209B generally put forward that for turbulent flow cleanroom, it is suitable to set the sampling flow rates 0.01, 0.1, and 0.25 ft^3/min, and for laminar (now unidirectional flow) cleanroom, it is suitable to set the sampling flow rates 0.25, 1.0, and 5.0 ft^3/min. In 1983, German Standard VDI-2083-III only put forward that it is better to use particle counter with sampling flow rate 1 ft^3/min for cleanroom with air cleanliness level above Class 100. In 1984 the standard IES-RP-CC-006 made by Institute of Environmental Sciences and Technology in USA pointed out the number of measuring points for the first time, and the method to determine the number of measuring points by the area of the cleanroom was proposed. For turbulence and laminar flow cleanroom, the area (ft^3) corresponding to each measuring point is $\leq \sqrt{\text{Air cleanliness level}}$, but the minimum sampling volume was also not mentioned.

In October of 1977, Sato [26] proposed to perform short-period sampling on several positions with small sampling volume particle counter for the first time. For Class 100 cleanroom, it is reasonable to doubt the accuracy of the measured results. But how to determine the sampling volume was not discussed.

It was the first time in China that the concept of the minimum sampling volume was officially put forward also in October of 1977. The nonzero principle to determine this minimum sampling volume was given, and the calculation method was also provided [25]. In 1980, the concept of necessary number of measuring points and the corresponding calculation method were put forward [27]. The minimum sampling volumes obtained by this method and by data (data from Japan JIS standard in 1987 adopted from US standard) from 209C later (in 1987) belong to the same class, which will be described in detail later.

16.4.2 Nonzero Sampling Principle

Particle counter can only display numbers which are positive integers such as 0, 1, 2, and 3. If the particle concentration of the measured space is extremely low, and the sampled air volume for each reading number every time, namely, the sampling volume is very small, the average concentration in the sampling volume may be a number that is less than 1. In this case, each reading may appear many times with the value of "0," or the majority is "0." For the occasion that the particle concentration is extremely low, when the average reading at each sampling point is "1" and there are few sampling points such as only three points, the average concentration should be "1." If there are errors, for example, there are two times of "1" and one time of "0," the average concentration becomes "0.7," so the difference between two concentrations reaches 1.5 times. In this case, the real particle concentration cannot be really reflected. If the sampling volume is big, each reading from every sampling volume may be more than 1, such as 2 and 3, then the frequency with number "0" in each sampling volume is few. Even if there are some particles, the average concentration is only affected in the magnitude of 0.01–0.1, so the difference from true concentration will be smaller. The above situation mainly appears in the place with high air cleanliness requirement (such as higher than Class 1000).

Therefore, the minimum sampling volume of the particle counter should have such characteristics. The possibility that particles fall into the minimum sampling volume is large, which means there is no possibility for the appearance of zero particle inside the sampling volume. This method can be called "nonzero inspection principle."

As pointed out in Chap. 1, if the average concentration in the sampling volume is set as λ, the particle distribution in the space can be described by the Poisson

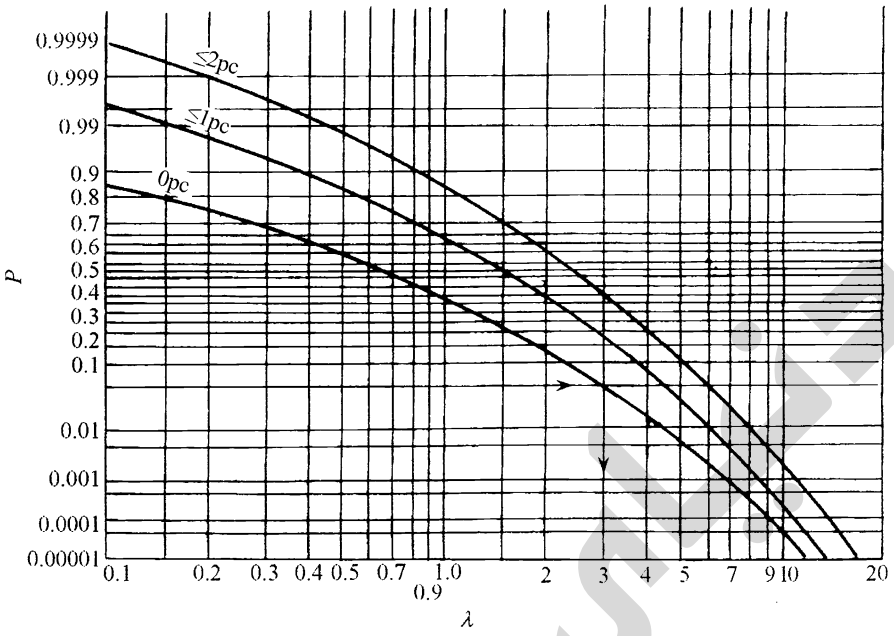

Fig. 16.21 Cumulative probability curve

distribution when $\lambda \leq 10$. Eq. (1.16) has given the probability P for the appearance of K particles at most in the sampling volume. It is rewritten here:

$$P(\zeta = K) = \frac{\lambda^K}{K!} e^{-\lambda}$$

So the probability for "0" particle is:

$$P(\zeta = 0) = e^{-\lambda} \tag{16.31}$$

The curve in Fig. 16.21 can be made with the two above formulas. The "0 particle" curve corresponds to the probability for the appearance of "0 particle." The "$\leq$1 particle" corresponds with the sum of appearance of "0" and "1" particle. The probability of appearance "1" particle is the difference between "$\leq$1" and "0," which is analogous for other cases.

From Fig. 16.21, if the probability of nonzero reading is required to reach 95 %, namely, the probability of the appearance of "0" particle is only 5 %, λ must reach 3. The sampling volume obtained is the minimum sampling volume.

The calculation example of the minimum sampling volume will be given below.

Table 16.16 The minimum sampling volume with "nonzero inspection principle"

Air cleanliness level	The lower limit of concentration at this level (≥0.5 μm) (#/L)	Minimum sampling volume	
		Calculated value (L (ft^3))	Suggest value (L)
100,000	351	0.0085(0.0003)	0.1
10,000	35.1	0.085(0.003)	0.1
1,000	3.51	0.85(0.03)	1
100	0.351	8.5(0.3)	8.5
10	0.0351	85(3)	85
1	0.00351	850(30)	850

Now the lower limit of the particle concentration for each air cleanliness level is used to represent the concentration for this level (which is safer than that with the upper limit of the concentration). We can obtain:

$$\text{The minimum sampling volume} = \frac{3 \text{ particles}}{\text{the lower limit of concentration at this level}} \tag{16.32}$$

The calculated results are shown in Table 16.16.
From Table 16.16, we can obtain:

1. In China, the legal unit system is used, while in air cleaning technology, "L" is used as the basic unit. So it is appropriate to take 0.1 L.
2. For the environment with the particle concentration less than 35#/L, when ordinary particle counter with small sampling flow rate is used, the sampling time should be extended to ensure adequate sampling volume and larger possibility of the appearance of nonzero particle. If the sampling time is not prolonged and the sampling volume is not increased, most of the measured results will be zero, which will reduce the reliability of the measurement results.
3. For the measurement in the space with high air cleanliness requirement with ordinary small sampling flow rate particle counter, if the extension of the required time is not long, the extension of time is feasible. If the extension of the time is too long, it is not only uneconomic, but also likely to cause other errors. So it is necessary to use the particle counter with large sampling flow rate in this case. But the effect of large sampling volume on the concentration field must be considered, which may be also likely to produce false phenomena. So in the above circumstances, it may not be necessary to use large sampling flow rate particle counter.

As already mentioned before, the Poisson distribution may not be suitable to describe the particle concentration distribution in the cleanroom. Although this aspect has been explained in Chap. 1, which believed that the Poisson distribution can still be used as the basic means to predict the particle distribution in space with high air cleanliness, if local serious leakage occurs in unidirectional flow

cleanroom, it will have effects. But this kind of influence also exists in the turbulent flow cleanroom, especially when the sampling points are close to the leakage airstream. So *Code for Construction and Acceptance of Cleanroom* (GB50591-2010) has required that air filters installed in the cleanroom must undergo the leakage detection one by one. After installation, leakage scanning must be performed along the frame of the air supply surface. When all the situations are confirmed, the statistical result is effective. Otherwise, if the frequency of a particle size is more than their due value, it is apparent that there are abnormal reasons, which means the data is not believable or the possible reason must be found. It does not mean that the Poisson distribution cannot be used to predict the particle distribution.

For example, during the measurement with 20 times (the sampling volume is 1 L), there are 19 times with "0" particle and one time with "1" particle. Please judge if this is a normal situation.

With Eq. (16.30), we can calculate $\lambda = 1/20 = 0.05$, which means the probability of the appearance of "0" particle should be 95 %, namely, it should be 19 times, which is consistent with the actual condition. So although the sampling volume is not enough according to the value of λ, the result can be considered as normal.

When the first measured value is "3" in the above example, please judge if this is a normal situation.

After calculation, we obtain $\lambda = 0.15$, so the frequency of the appearance of "0" particle should be 17 times. There are obvious differences.

From Eq. (16.30) we know:

$$P(\zeta = 0) = \frac{x}{k}\mathrm{e}^{-\lambda}$$

So

$$\lambda = -\ln\frac{x}{k} \tag{16.33}$$

where

k is the total times of measurement;
x is the times of the appearance with "0" particle.

If there are 19 times of the appearance of "0" particle in total 20 times, $\lambda = 0.051$, which means the average particle concentration in theory should be 0.051#/L, instead of 3/20 = 0.15#/L. Since the average concentration in the sampling volume 1 L is 0.051, the probability for the appearance of three particles is determined by Eq. (1.13) in this sampling volume, which is:

$$P(\zeta = 3) = \frac{0.051^3}{3!} = \mathrm{e}^{-0.051} = 0.000022 \times 0.95 = 0.000021$$

So the probability of the appearance of three particles is extremely small, which is impossible. If it appears, it is an illusion, and it cannot be used to calculate the average concentration.

Table 16.17 Different measurement results with two particle counters working simultaneously

	Average concentration (#/ft^3)				
	Instrument 1			Instrument 2	
Sampling position	≥0.2 μm	≥0.3 μm	≥0.5 μm	≥0.3 μm	≥0.5 μm
1	1.4	0	0	2.8	2.6
2	2.2	0	0	3.7	2.5
3	2.6	0	0	2.9	2.4
4	2.3	0	0	2.5	2.3
5	2.1	0	0	0.4	0.4
6	0.8	0	0	0.3	0.1
7	1.0	0	0	0.2	0.2
8	1.6	0	0	1.3	1.0
9	1.2	0	0	1.1	0.7
10	1.2	0	0	0.6	0.3
11	1.5	0	0	1.1	0.7
12	0.6	0	0	0.8	0.6
13	0.7	0	0	0.7	0.6
14	1.2	0.1	0	0.4	0.6
15	0.7	0	0	0.4	0.3

It is very likely that the occurrence of three particles is caused by leakage. But as illustrated in 209E, the statistics method is not aimed to changing multipoint leakage positions during sampling (the possibility of leakage at one place is very small), which means the application of statistical methods or the minimum sampling volume cannot modify the random abnormal error caused by the leakage. In other words, the abnormal situation of measurement results should not deny the particle distribution characteristic and the application of statistical methods.

Instrument performance may also become one of the abnormal reasons. Table 16.17 listed foreign measurement data (the data at each point is the average value of many sampling times), where air cleanliness Class 1 was realized in the cleanroom when Instrument 1 was used, while the conclusion was opposite when Instrument 2 was used [28]. The performances of these two instruments were compared, and it was found that the function to reset zero cannot be performed in Instrument 2. So it is inappropriate to conclude that the above particle distribution characteristic is not correct and the minimum sampling volume is not applicable when two instruments with different performances were used for measurement and the measured results do not follow the above distribution characteristics.

In Table 1.8, an example was presented where two instruments with identical performance after calibration were used to determine the particle distribution in three rooms, and the results are completely consistent. When statistical analysis is made on these data, it is more likely to conform to the distribution characteristic law.

The monograph *Air Cleaning Technical Measures* was published before the concept of "nonzero inspection principle." So the data of Table 16.15 were not adopted, but the empirical data were used. At that time the concept of the minimum

sampling volume was not established, and instead the concept of the sampling volume at every time was used. That is:

When particle concentration $<$ 30#/L (equivalent to Class 1000), sampling volume $\geq$0.9 L;
When particle concentration 30–300#/L (equivalent to Class 10000), sampling volume $\geq$0.3 L;
When particle concentration $\geq$300#/L (equivalent to Class 100000), sampling volume $\geq$0.1 L.

The *Code for Design of Clean Room* approved in 1984 and implemented in 1985 also adopted the similar data as the monograph "Air cleaning technical measures," which was later than the "nonzero inspection principle." The data are:

Class 100	Sampling volume each time $\geq$1 L
Class 1000–10000	Sampling volume each time $\geq$0.3 L
Class 100000	Sampling volume each time $\geq$0.1 L

The concept of the minimum sampling volume was also not given. It did not mention that particle distribution in cleanroom belongs to Poisson distribution, so the method with "nonzero inspection principle" was not cited to obtain the minimum sampling volume.

As for the sampling volume specified in *Code for Construction and Acceptance of Cleanroom* (JGJ 71-90) published in 1991 and *Code for Design of Clean Room* (GB50073-2001) published in 2002, it is consistent with related international standards (209D, ISO14644-1). The exact data will be presented later.

The above discussion is aimed to measure accurately, so the concept of the minimum sampling volume must be used. But it is still not enough only to use the minimum sampling volume; there must be enough sampling points, which have already pointed out in the past [27]. But the specification in this aspect in related foreign standards is not enough. The problem will be discussed in the next chapter.

16.4.3 The Principle of Minimum Total Particle Number [29–31]

Because sampling process is the collection of the counting data at every sampling point, it can be treated as the Poisson process. According to the Poisson distribution, the interval estimation of the average value for the test data can be made.

From Eq. (1.15), if the total number N obtained from the actual measurement is used to replace K, the distribution function of the estimation value λ_0 for λ is

$$F(0 < \lambda_0 < \lambda'_0) = \int_0^{\lambda'_0} \frac{\lambda_0^N}{N!} e^{-\lambda_0} d\lambda_0 \tag{16.34}$$

where λ'_0 is the upper confidence limit of λ_0, as shown in Fig. 16.22.

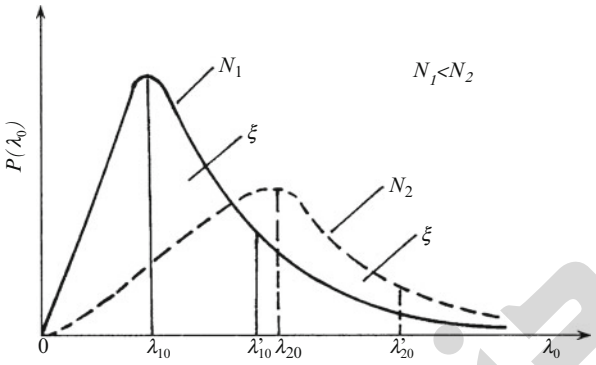

Fig. 16.22 Probability of λ_0

Table 16.18 Relationship among $N, \lambda'_0,$ and λ_0

	Confidence level 97.5 %		Confidence level 95 %	
N	λ'_0	R	λ'_0	R
5	11.67	1.334	10.51	1.03
10	18.89	0.839	16.96	0.696
15	24.74	0.649	23.10	0.540
20	30.89	0.544	29.06	0.453
25	36.91	0.476	34.91	0.397
30	42.83	0.428	40.69	0.356
35	48.68	0.391	46.40	0.326
40	54.47	0.362	52.07	0.302
50	65.92	0.318	63.29	0.266
60	77.23	0.287	74.39	0.240
70	88.44	0.263	86.40	0.220
80	99.57	0.246	96.35	0.204
90	110.62	0.229	107.24	0.192
100	121.62	0.216	118.08	0.181

When ζ is the probability (i.e., the confidence level) for the given value of $F(0 < \lambda_0 < \lambda'_0)$ and integration can be performed for the right expression of the above equation, the upper limit of λ'_0 of the estimation parameter λ_0 can be obtained with the value of N for different ζ. Results are shown in Table 16.18.

The random absolute error of this sampling is:

$$R' = \lambda'_0 - N \tag{16.35}$$

The random relative error is:

$$R = \frac{R'}{N} = \frac{\lambda'_0 - N}{N} \tag{16.36}$$

As shown in Fig. 16.22, for the given confidence level ζ, the more the sampled total particle number is, the bigger the upper confidence limit λ'_0 is. From Eq. (16.36), the relative error R decreases.

As for the minimum sampling volume in US 209C standard, it is based on the principle that the total sampled particle number is 20 for the corresponding air cleanliness level according to the explanation of 209B revision attendant. With this principle, when the confidence level is 95 %, the maximum concentration is 31 particles and the minimum is 12 particles. That means there is 95 % probability that the total particle number sampled is between 12 and 31. For example, when the upper concentration limit is calculated, it could be $30.89 \approx 31$ when Table 15.15 is used with the confidence level 97.5 %, which is consistent with the above explanation by 209B revision proposals. From the table, the sampling error is $R = 54.5$ %. If the confidence level reduces to 95 %, $\lambda'_0 = 29$ particles. Although the increased total sampled particle number can reduce error, the sampling time will be prolonged. It is completely artificial to set 20 particles. So we obtain:

$$\text{Minimum sampling volume} = \frac{20}{\text{Upper concentration limit with the air cleanliness}} \tag{16.37}$$

For Class 100, the upper concentration limit is 100#/ft^3, 20/100 = 0.2 ft^3.

For Class 1000, the upper concentration limit is 1,000#/ft^3, 20/1,000 = 0.02 ft^3.

According to the same principle, ISO14644-1 uses "L" to represent the sampling volume, so:

$$\text{Minimum sampling volume} = \frac{20}{\text{Upper concentration limit with the air cleanliness}/\text{m}^3} \times 1{,}000\,\text{L} \tag{16.38}$$

In *Code for Design of Clean Room* (GB50073-2001), the value 1,000 in the above equation was mistaken as 100.

The above results are shown in Table 16.19. The mantissa of L in 209E and ISO are different slightly. At the same time, ISO specified that the minimum value should not be less than 2 L.

From the comparison of Tables 16.16 and 16.19, we can know:

1. The above two principles to determine the minimum sampling volume are based on the collection of the point data. So all of them applied the Poisson distribution, but with different methods.

   The method with $\lambda = 3$ is aimed to guarantee that the probability of nonzero data is not less than 95 %. The method with total particle number = 20 is slightly optional. So although Eq. (16.32) and Eq. (16.37) have similar shapes, the nature is different. Only American literature [29] has not pointed out that the test statistics is based on the counting points' data when it comes to Poisson distribution. So when the statistical analysis about the average concentration

Table 16.19 The minimum sampling volume with the principle of least total particle number

Air cleanliness	Upper concentration limit (#/ft^3)	Minimum sampling volume		
		Calculated value (ft^3)	Value in 209C-209E[a] (ft^3)	ISO14644-1 (L)
100,000	100,000	0.0002	0.1(2.83)	2.0
10,000	10,000	0.002	0.1(2.83)	2.0
1,000	1,000	0.02	0.1(2.83)	2.0
100	100	0.2	0.2(5.66)	5.68
10	10	2	2(56.6)	56.8
1	1	20	20(566)	568

[a]The data in the bracket is expressed with "L"

(it will be introduced in detail in next chapter) was mentioned in this literature, it concluded that "both experience and theory have proved that Poisson distribution is seldom applicable for the actual concentration in the cleanroom," and *t* distribution was recommended, which will cause misunderstanding. It seems that *t* distribution may fit the particle concentration in the cleanroom. In fact, different principles were used to treat the statistical problems with two different features between the counting points' data and the average value.

From statistics theory, it is known that this is the problem with two different natures, and it is not a problem that which distribution is more suitable to describe the particle distribution in cleanroom. One is the density distribution, where the Poisson distribution is applicable. The other is the particle number distribution according to the particle size, which is aimed to calculate the error of the average value, namely, the so-called treatment of "actual measured concentration data from the cleanroom," so *t* distribution method reflects the average distribution characteristics from small subsamples. The method will be discussed in the next chapter.

2. The US Federal Standard 209C adopted the English unit, which chooses ft^3 as the basic unit. It is understandable that 0.1 of this unit, namely, 0.1 ft^3, is taken.
3. The minimum sampling volume specified in 209C is calculated according to the upper concentration limit. Although the concentration increased by 10 times, λ only improves 6.7 times. So in contrast, the minimum sampling volume of each air cleanliness level should be less than that in Table 16.15. Because the difference of the specific value represented by 0.1 unit for air cleanliness level lower than Class 100, the minimum sampling volume (L) is bigger than that in Table 16.16. But in all, the two values of the minimum sampling volume are very close.

16.4.4 The Minimum Sampling Volume of Airborne Bacteria

Like the measurement of particles, there is also the problem of the minimum sampling volume for airborne bacteria sampling. Now the minimum sampling volumes are calculated with "nonzero inspection principle" and the airborne bacterial concentration, which is shown in Table 16.20 [32].

Table 16.20 The minimum sampling volume of the airborne bacteria

Upper concentration limit of airborne bacteria (#/L)	Calculated minimum sampling volume (L)
10	0.3
5	0.6
1	3
0.5	6
0.1	30
0.05	60
0.01	300
0.005	600
0.001	3,000

16.5 The Minimum Deposition Area

As pointed out in Chap. 1, deposition of particles on surface follows the Poisson distribution. Therefore like the minimum sampling volume mentioned in the above section, there is also the minimum sampling volume problem during the measurement of particle settlement. If the deposition area is too small, it will reduce the reliability of the whole measurement because the probability of the appearance of "0" particle is extremely large. This problem is especially important during measuring the colony in biological cleanroom with the deposition method. As the minimum sampling volume analyzed in the previous section, in order to ensure 95 % of readings are nonzero, the particle deposition density must also reach or exceed 3. From Table 9.11, the allowable colony in the specified period in each Petri dish is known, which is the deposition density (take one Petri dish as the base). So the minimum deposition area needed for measuring the bacterial concentration with the deposition method in the environment with different air cleanliness levels can be obtained, which corresponds with the minimum number of Petri dishes. For example, when it is 3.5#/L from Table 9.11, the probable maximum settlement in each Petri dish is 0.239 CFU. Then in order to obtain three CFU, it needs 12.55 dishes, approximately 13 dishes. Results are listed in Table 16.21. If it is 3#/L, the number of Petri dishes is 14 and 4. That is the upper concentration limit corresponding with the air cleanliness level in Fig. 16.23 or the value used by author in the past.

The minimum number of Petri dishes should be adapt to the necessary number of sampling points or the number of sampling points specified in the regulation, which will be introduced later. If the minimum number of Petri dishes is bigger than the number of sampling points, the former value is adopted, and both the requirement of the number of sampling points and the minimum deposition area should be satisfied. If the minimum number of Petri dishes is less than the number of sampling points, the number of Petri dishes should choose the number of measurement points. If the sampling space is small and Petri dishes cannot be placed, the deposition period could be appropriately prolonged (not more than 1 h), and the number of the Petri dishes can decrease proportionally.

Table 16.21 The least number of Petri dishes to measure bacteria with the deposition method

Maximum particle concentration (#/L)	Number of Petri dishes needed (settling for 0.5 h)
0.35	40
3.5	13
35	4
350	2
3,500–35,000	1

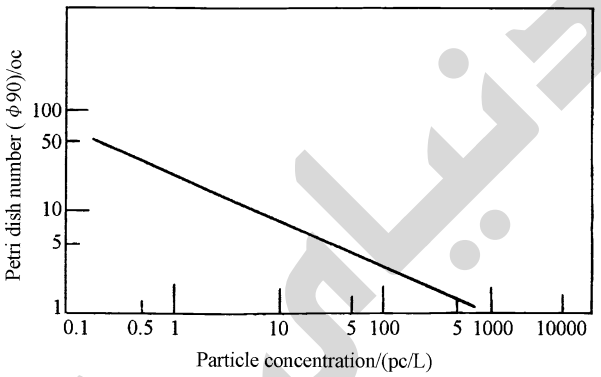

Fig. 16.23 Relationship between the number of Petri dishes and the particle concentration for the deposition period 0.5 h

References

1. Himi K (1972) Measurement method of particle concentration in exhaust air. Pract Pollut Control Manage 10(12):65–81 (In Japanese)
2. Hinds WC (1989) Aerosol technology (trans: Sun Yufeng). Heilongjiang Science and Technology Press, Harbin, p 132 (In Chinese)
3. Huang LM (1956) Influence of additional resistance on the flowrate calibration of the flow meter. In: Collected works on ventilation and dust prevention in metal mining, China Industrial Press, pp 245–246 (In Chinese)
4. Hinds WC (1989) Aerosol technology (trans: Sun Yufeng). Heilongjiang Science and Technology Press, Harbin, p 131 (In Chinese)
5. Hinds WC (1982) Aerosol technology: properties, behavior and measurement of airborne particles. John Wiley & Sons, New York, pp 187–194
6. Japan Air Cleaning Association (1981) Handbook of air cleaning. Japan OHM Press, p 29 (In Japanese)
7. Xu ZL, Zhang YZ, Zhang YG, Mei ZL, Shen JM, Guo DR, Jiang PC (1998) On the sampling error due to non-isokinetic sampling. Contam Control Air Cond Technol 1:14–17 (In Chinese)
8. Wei ZM, Li M (1990) Analysis of sampling problem in laminar flow cleanroom. In: Proceedings of the annual national conference on HVAC&R, Chengde, China, 1990, pp 344–347 (In Chinese)
9. Ono N (1982) Theory and practice of dust removal and collection (trans: Chan Wenchang). Scientific and Technical Documents Publishing House, Beijing, p 228 (In Chinese)
10. Chen GJ, Hu JM (1988) ESP test technology. China Water Power Press, Beijing, pp 53–55 (In Chinese)
11. Ku XJ, Li JY (1977) Dust removal in the workshop of crushing and screening. Metallurgical Industry Press, Beijing, pp 456–488 (In Chinese)

12. Tan TY, Liang FZ (1984) Industry ventilation dust removing technology. China Architecture & Building Press, Beijing, pp 487–504 (In Chinese)
13. Hinds WC (1989) Aerosol technology (trans: Sun Yufeng). Heilongjiang Science and Technology Press, Harbin, pp 134–135 (In Chinese)
14. Hinds WC (1989) Aerosol technology (trans: Sun Yufeng). Heilongjiang Science and Technology Press, Harbin, p 189 (In Chinese)
15. The fifth Institute of Military Medical College, Development of JWL-1 type sampler, 1983 (In Chinese)
16. Fuchs HA (1960) The mechanics of aerosols (trans: Gu Zhenchao). Science Press, Beijing, pp 198–199 (In Chinese)
17. Zhao RY, Qian BN, Xu WQ (1987) Particle loss in sampler. Tsinghua University (In Chinese)
18. Fuchs NA (1964) The mechanice of aerosols. The Macrailan Company/Pregamon Press, Inc., New York
19. Lin BYH, Pui DYH, Rubow KL, Saymanski WW (1985) Electrostatic effects in aerosol sampling and filtration. Ann Occup Hyg 29(2):251–269
20. Xu ZL, Shen JM, Zhang YZ (1998) Discussion of the sampling tube length of the particle counter. J Tongji Univ 4:447–452 (In Chinese)
21. Hinds WC (1989) Aerosol technology (trans: Sun Yufeng). Heilongjiang Science and Technology Press, Harbin, p 103 (In Chinese)
22. Hinds WC (1989) Aerosol technology (trans: Sun Yufeng). Heilongjiang Science and Technology Press, Harbin, pp 228–231 (In Chinese)
23. Niitsu Y et al (1966) Study on property of atmospheric aerosol (the 1st report). J SHASE (Soc Heat Air Cond Sanit Eng) Jpn 40(11):1–13 (In Japanese)
24. Tsukamatsu S (1979) Dust meter – light scattering particle counter. Jpn Refrig Air Cond Technol 30(352):1–6 (In Japanese)
25. Xu ZL, Gu WZ (1980) Calculation of the minimum detection volume of the particle counter with different air cleanliness levels. Contam Control Air Cond Technol 1:22–24 (In Chinese)
26. Sato E (1976) Status of industrial cleanroom. J Jpn Air Clean Assoc 13(8):32–41 (In Japanese)
27. Xu ZL (1980) Calculation of the necessary sampling points in cleanroom. Contam Control Air Cond Technol 1:25–28 (In Chinese)
28. Helander RD (1989) Certifying a Class 10 cleanroom using Federal Standard 209C. (trans: Zhang Yaping, checked by Feng Peiming). In: Collected works on design, construction and acceptance inspection of cleanroom, pp 292–302 (In Chinese)
29. Cooper DW (1989) Rationale for proposed revisions to Federal Standard 209B (Cleanrooms) (trans: Liu Xianzhe, Zhan Yingmin). In: Collected works on design, construction and acceptance inspection of cleanroom, pp 278–286 (In Chinese)
30. Liu XZ, Wang Q (1986) Interval estimation of particle concentration – process of measured data. In: Proceedings of the second academic annual conference by Chinese Contamination Control Society, pp 136–141 (In Chinese)
31. Qian BN, Xu WQ, Zhao RY (1988) Measurement of low concentration particles and evaluation of air cleanliness level in clean area, Tsinghua University (In Chinese)
32. Xu ZL (1992) Measurement of bacterial concentration. Handouts for the seminar on the specification of construction and acceptance inspection of cleanroom (In Chinese)

Chapter 17
Measurement and Evaluation

Under the guidance of the sampling theory, correct sampling procedures are taken, after which measurement can be performed with a variety of methods to determine the particle size, number, and distribution. After scientific evaluation is made on the measurement results, the correct conclusion can be finalized. This chapter will focus on the introduction of the principle of measurement and evaluation for particle concentration, filter, and cleanroom.

17.1 Particle Concentration Measurement

17.1.1 Particle Mass Concentration Method

Particle mass concentration method is the most basic method for determination of particle concentration. There are many kinds, and one of the precise methods is the filter paper weight concentration method, which will be mainly introduced here.

The basic principle of the filter paper weight concentration method is that airborne particles will be effectively captured on the filter media when the air with known volume passes through the filter media, and then the increase of weight on the filter media is weighted with the balance. The particle mass concentration in the sampled air is

$$C = 1,000 \times \frac{\Delta G}{qt} \tag{17.1}$$

where

C is the weight concentration (mg/m^3);
ΔG is increase of filter media weight, namely, the difference of filter media weight before and after the balance weighting process (mg);

Z. Xu, *Fundamentals of Air Cleaning Technology and Its Application in Cleanrooms*,
DOI 10.1007/978-3-642-39374-7_17,

q is the sampling rate (L/min);
t is the sampling time (min).

The most frequently used material of the measurement is the glass fibrous paper, because of its high efficiency.

When the glass fibrous paper is used as the filter media, there is a problem that humidity affects the weight of the filter. There are two aspects if the influence is considered:

1. The relative humidity is different between weighing location and measurement location.

Experiment performed at Institute of HVAC of China Academy of Building Research shows that in the actual operation, it takes more than 1–2 min for the adjustment of the balance for weighting the filter paper. During the period, equilibrium is reached quickly between the filter paper and the air within the balance chamber through direct contact and humidity exchange. In the weighting place, the influence of the moisture absorption and release remained is extremely small, which is within the fluctuation range of the balance. As long as enough time is provided for the equilibrium of the moisture, the influence of humidity can be ignored.

2. The change of relative humidity in weighing location.

Sometimes due to various reasons, the filter paper cannot immediately be weighed after sampling. During this period, the relative humidity within the balance chamber may change significantly, and the papers will absorb or release moisture, so the final weight measured does not reflect its true value. Experiment performed at Institute of HVAC of China Academy of Building Research showed that when the air relative humidity within the balance chamber changes from 65 to 70 %, the weight changes caused by moisture absorption were 0.074 and 0.02 mg for glass fiber filter paper and synthetic fiber filter paper with diameter of 60 mm and average weight of 180 mg, respectively. If the increase of the filter paper weight in the general environment is 0.25 mg, the error caused by absorption of moisture will be 30 % and 80 %, respectively. The experimental result curve is shown in Fig. 17.1. When the relative humidity within the balance chamber changes, it is necessary to make correction for the moisture absorption quantity on filter media. According to Fig. 17.1, the moisture absorption quantity on filter paper can be calculated as follows:

$$G_{\mathrm{p}} = G_1(\varepsilon_2 - \varepsilon_1) \tag{17.2}$$

where

G_p is the moisture absorption quantity on filter paper (mg);
G_1 is initial weight of filter paper (mg);
ε_1 and ε_2 are the moisture absorption quantity on filter paper per unit weight before and after and before weighting (mg/mg).

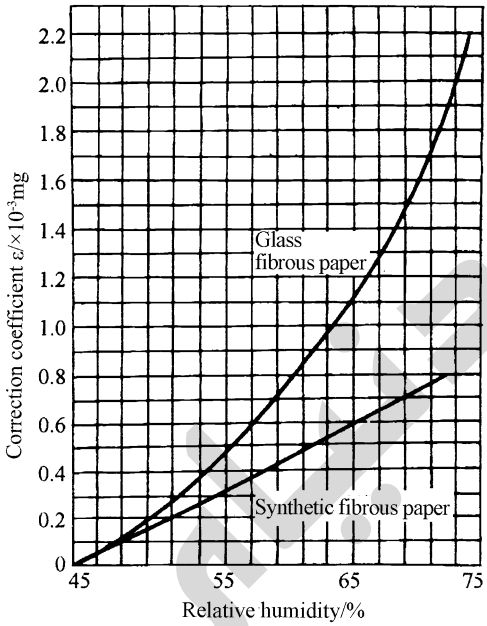

Fig. 17.1 Correction coefficient of the moisture absorption quantity

During the application of Eq. (17.2) to calculate the mass concentration, the moisture adsorption quantity G_p should be subtracted from the weight gain of the filter paper.

If the weighing process cannot be carried out in one place before and after particles are captured on the filter paper or if the relative humidity is not easy to determine, double sampling filter media method can be used in order to eliminate the influence of humidity. Because the weight efficiency of the first filter paper (top one) is 100 %, the increase of the weight on the second filter paper because of the dust collection should be zero in fact. If there is the moisture absorbing effect, the weight of the second filter paper should be varied before and after sampling. So the real weight gain of the filter media ΔG in Eq. (17.1) can be calculated with the following formula:

$$\Delta G = (G_1 - G_{01}) - (G_2 - G_{02}) \tag{17.3}$$

where

G_1 is the weight of the top filter media after sampling;
G_{01} is the weight of the top filter media before sampling;
G_2 is the weight of the bottom filter media before sampling;
G_{02} is the weight of the bottom filter media before sampling.

Calculation can be made according to Eq. (17.1) without correction of the relative humidity.

As for the detachment of fibers on the filter media under high sampling air velocity, it can be completely ignored according to experiment.

17.1.2 Particle Counting Method with Membrane Microscope

17.1.2.1 Principle

With the development of air cleaning engineering, it cannot meet the requirement with the weight concentration to describe the particle concentration. So the particle counting methods with both the chemical membrane microscope and the light scattering particle counter are widely used in the determination of particle concentration in clean environment. In the standards about cleanroom in some foreign countries, the particle counting method with membrane microscope was used as standard method for the determination of 5 μm particles. Before the development of photoelectric technique to measure particles, membrane counting method was once even used for measurement of particles with diameter ≥ 0.6 μm. Even today, it is still an available method for measurement under certain condition, because particles can be directly observed (size, shape, and color) with the membrane counting method, so in the certain condition.

To capture common aerosol particles, membrane with diameter 0.3–0.8 μm should be chosen, whose collecting efficiency is very high. Its efficiency is higher than the single-layer glass fiber paper by 2–3 orders of magnitude, but the resistance of membrane is also higher than that of the ordinary glass fiber filter paper by dozens of times.

In China, it was Research Institute of Mining and Metallurgy at China Academy of Science that firstly used the membrane technology in sampling of mine dust. Later Institute of HVAC of China Academy of Building Research studied the application of the membrane technology on the particle counting method of dust in air cleaning technology and developed the corresponding membrane. This particle counting method will be outlined as follows.

The principle to measure the particle counting concentration with membrane is that after the particles are trapped on the membrane surface, since membrane can be treated to be transparent under a microscope, particles are then observed and counted. Since membrane pores are filled with air, a number of optical boundaries are formed, which destroy the forward direction of light; membrane becomes opaque. In order to make the membrane transparent, the optical interface must be wiped out, which can be processed with the oil dripping method and the acetone steam fumigation method.

Oil Dripping Method

Oil with the same refraction rate as the membrane itself is dipped onto the membrane. Then oil will penetrate into the membrane, driving away the air in the micropore, so that the membrane becomes an optically homogeneous whole body and transparent. This method is suitable for observing particles with diameter more than 5 μm.

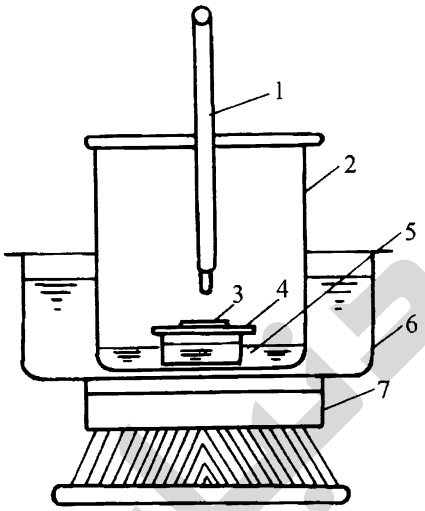

Fig. 17.2 Schematic diagram of membrane slide equipment. *1* thermometer, *2* beaker, *3* cover slip, *4* object slide, *5* base holder, *6* water tank, *7* electric furnace

Acetone Steam Fumigation Method

After acetone vapor immerses the membrane, the membrane becomes slightly soluble to expand and then contract, eliminating the air in the micropores, which makes the membrane transparent. This method makes the transparent performance of membrane good. But when the temperature and the volume of acetone vapor are not enough, the membrane edge is prone to curl. When the temperature and the volume are too much, the membrane will be dissolved too much, which affects the measured particle distribution on it. The method is also suitable for detecting small particles.

Specific fumigation device is shown in Fig. 17.2. The membrane is placed on a clean glass cover slip with the sampling face upward. It is fumigated in the beaker filled with 50 °C acetone vapor. (For the beaker with volume 600 mL, about 15 mL acetone is added. After operated with three samples, 5 mL acetone is added again.) Take the membrane out when it is transparent. Then fasten the cover slip onto the object slide in reverse (aluminum foil ring or a paper ring is used to separate the cover slip from the slide). Then, the cover slip is sealed around with glue or wax.

17.1.2.2 Particle Counting Method

Fix the prepared specimen slice on the proper position of the worktable of microscope. If particles with diameter above 5 μm are counted, the microscope with 100 times magnification ratio is used. If particles with diameter above 0.5 μm are counted, the microscope with high magnification ratio must be used, which is generally 1,500 times (100 times of immersion objective lens and 15 times for the eyepiece).

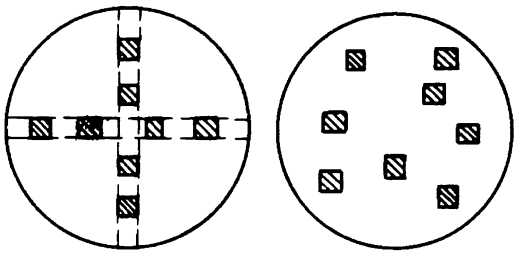

Fig. 17.3 Division of the counting area

During the counting process, the micrometer is adjusted vertical to the moving direction on the worktable of the microscope. When the worktable is moving slowly, specimens on the table will also move accordingly. In the microscopic field, we can see that particles continuously go through the micrometer. Particle sizes can be readout from the micrometer (see Fig. 1.2 in Chap. 1). Manual counter is used, and counting is performed according to the channel range.

Particle counting size can generally be classified as < 0.5 μm, ≥ 0.5 to < 1.0 μm, ≥ 1.0 to < 2.0 μm, ≥ 2.0 to 5.0 μm, and ≥ 5.0 μm.

The total counting area is about $0.02 \times (2\text{–}4)$ mm^2 on one specimen. Larger value is used when counting big particles, and smaller value is adopted when counting small particles.

In order to avoid too much focus of the counting areas, it should randomly measure with several segments that are not on the same straight line in a specimen. Edges of each segment should not stay too close to the edge of the specimen (Fig. 17.3). The readings on the micrometer on the worktable should be recorded when counting, which prevents the generation of error.

When immersion objective lens with 100 times of magnification ratio is used, big and small particles cannot be seen on the membrane simultaneously because of the small focus depth. So the focal distance needs to be continuously adjusted within a certain range. When the membrane sampling method is used and the sampling flow rate, the sampling time, and the membrane filtration area are known, the particle density on the membrane surface can be calculated, which can be used to obtain the particle concentration. But there is a problem which needs to be noticed; the effects of the background value should be considered. Because particles exist in the solution which is used for the manufacturing of the membrane, the prepared membranes also contain dust. This is called "the background density of membrane." Before measurement, we must determine the background density for the same group of produced membrane. In this way, the true sampling density can be obtained.

So, the particle counting concentration can be calculated by the following equation:

$$N = \left(\frac{c_1}{f_1} - c_0\right)\frac{f_0}{qt}\ (\#/\mathrm{L}) \tag{17.4}$$

where

c_0 is the background density of membrane (#/mm^2);
c_1 is the total number after sampling (#/mm^2);

f_0 is the effective filter area (mm^2);
f_1 is the total area for counting after sampling (mm^2);
q is the sampling rate (L/min);
t is the sampling time (min).

17.1.2.3 Applicable Condition

If the background density of the membrane is very big, in addition to the collected particles when counting after sampling, it also has the possibility to measure the intrinsic particles. The possibility is big if the background number is big. According to the result at Institute of HVAC of China Academy of Building Research, when the ratio between the counting density and the background density reaches above 4 times, the influence of the background density on the counting results is stabilized. In other words, the counting result is no longer different too much with different values of background densities.

For membranes manufactured in the general environment, the background density is often greater than 1,000#/mm^2. They can only be used in the environment where the airborne concentrations are greater than 1,000#/L. If the sampling rate is 15 L/min, the sampling time needed is generally only 2 h (suppose the filter sampling area is 490 mm^2). For membranes manufactured in the clean environment, the background density is still greater than 10#/mm^2. It should not be used in the environment where the airborne particle concentration is less than 10#/L. Otherwise the sampling time needed is more than 2 h. When it is used for the measurement of cleanroom with air cleanliness Class 100, half a day or even a day is needed, which is inconvenient.

By the counting method with membrane microscope, direct counting can be performed, and the properties of color, luster, and shape can be observed under the microscope, which can be used to identify if it contains metal fragments, fibers, or other impurities. When the airborne particle concentration is detected to be high suddenly with other fast dust detector, the microscopic counting method can also be used to observe the property of particles. It helps to determine whether the increase of dust particle is normal or abnormal, which can be used for further location of new dust source.

17.1.3 Particle Counting Method with Light Scattering Particle Counter

17.1.3.1 Principle

Both the filter paper weight method and the microscopic counting method are the method with particle capture, namely, airborne particles are captured with other measures, then the concentration is determined later. The instantaneous distribution

(or in a very short interval) of airborne particles cannot be understood. The method to measure the particle concentration when particles are still kept airborne is called the airborne measurement method. Light scattering particle counter is used for counting with this method.

The light scattering phenomenon appears when airborne particles are exposed in the light irradiation. It is related to the particle size, wavelength, particle refractive index, light absorption characteristics, and so on. But a basic law exists between the scattering light intensity and the particle size. The intensity of particle scattering light is proportional to the surface area of particles. Especially for 0.3–1.0 μm particles, this relationship is more obvious. Although this relationship to describe particles with diameter larger than 1 μm is relative poor, the difference between the nominal size measured with the above proportional relationship and the actual size is acceptable in practice, when the size of the instrument channel between 1.0 and 10 μm is relative coarse so that the deviation between the nominal size in the channel and the actual size in the channel is not small. By measuring the intensity of scattering light, the particle size can be obtained, which is the principle of light scattering particle counter. With the photoelectricity multiplier, the pulse by light scattering of particles is linearly transformed to the pulse signal with corresponding amplitude. Some electronic circuits are used to complete the counting of the electric pulse. Since a certain relationship exists between the scattering intensity and the particle size, photoelectricity multiplier has a linear relationship of conversion, the amplitude of various electrical pulses corresponds to different particle size, and the number of pulses corresponds to the particle number.

The relationship between the particle size and the output signal is [1]

$$d_p^{-n} = ku \tag{17.5}$$

where

d_p is the particle diameter;
k is the conversion coefficient;
u is the signal level (mV);
n is the coefficient dependent on the instrument structure, which is between 1.8 and 2 (the experimental value in Ref. [1] was 1.8).

The above formula can be converted to be:

$$n \lg d_p = \lg u + \lg k \tag{17.6}$$

It is apparent that a linear relationship exists between d_p and u in log-log paper. With the influence of the sensitivity performance of instrument, the calibration curve and the theoretical curve will be crossed, as shown in Fig. 17.4 [2].

This figure shows that if 0.60–0.69 μm standard particles are chosen to inspect the instrument sensitivity (the stipple line in the figure), 0.5 μm particles may be mistaken as 0.4 μm particles without recording by particle counter, so the output

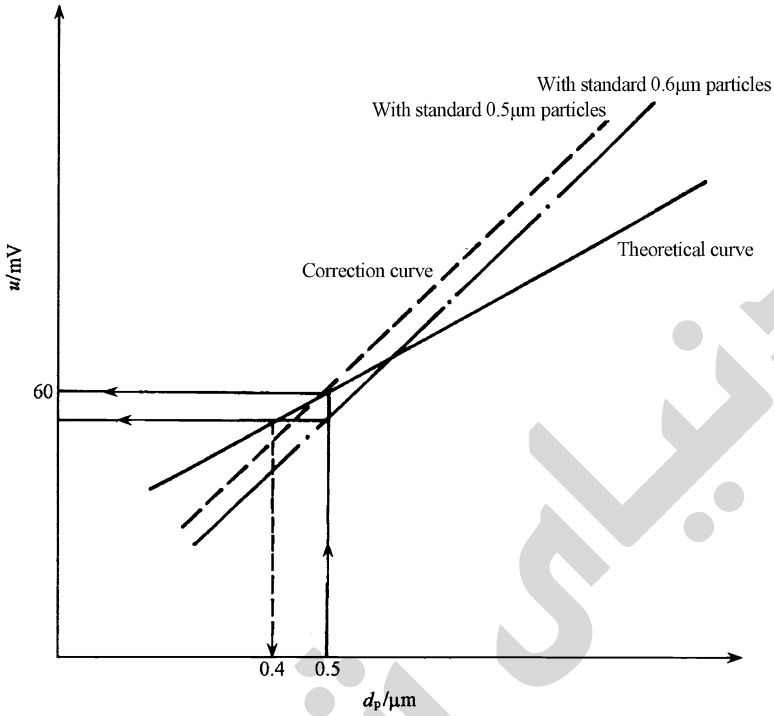

Fig. 17.4 Relationship between the signal amplitude and the particle size for particle counter

signal amplitude < 60 mV. On the contrary, if 0.40–0.49 μm standard particles are chosen for instrument calibration, 0.4 μm particles may be mistaken as 0.5 μm particles with recording by particle counter, which will cause error.

The specific working principle of the instrument is that the light from a light source is focused on measuring region by a group of lens; when every particle in the sampled airflow quickly passes through the region, the incident light scatters for once time, which forms a light pulse signal. This signal is sent to the negative pole of the photoelectricity multiplier by a group of lens (Fig. 17.5), where it is converted into electric pulse signal proportionally. After amplification and screening, signals required are sorted and then displayed by the counting system. The amplitude of electric pulse signal reflects the particle size, and the number of signals reflects the particle number, as shown in Fig. 17.6.

Various disturbance signals (the so-called noise signal) are generated with the common light source as the incident light of the particle counter itself, which affects the sensitivity of the instrument. The amplitude of signals generated by this kind of instrument with 0.3 μm particles is not much different from that of noise. It is hard to detect it from the noise. For example, the noise level is generally 20 mV, and the output signal under the sensitivity state for 0.5 μm particles is 0 mV, and that for 0.3 μm particles is 23 mV, which is very close to the noise level. So for the particle

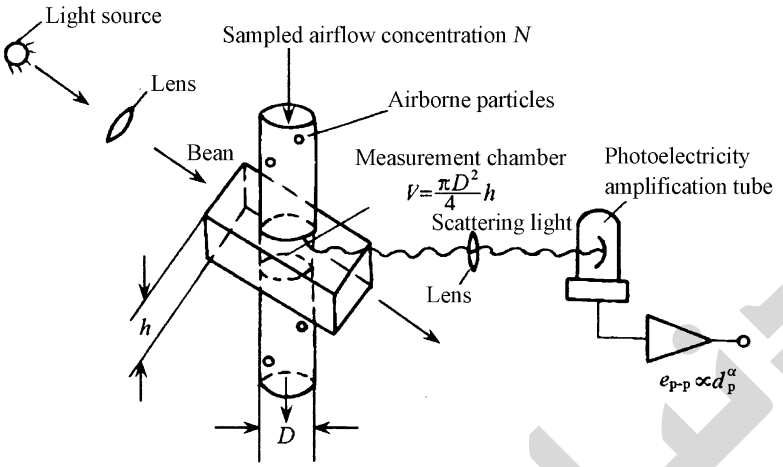

Fig. 17.5 Schematic diagram for the working principle of particle counter

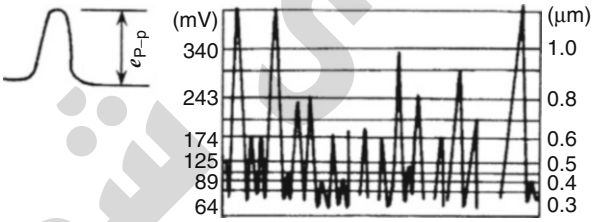

Fig. 17.6 Example of the relationship between the pulse signal and the particle size

counter with common light source as incident light (that is the so-called incandescent lamp light source particle counter), the sensitivity for particles with diameter less than 0.3 μm is very low, or the sampling efficiency is very low, which is from 10 % to 40–50 %. So although the channel with 0.3 μm is labeled, it is only suitable for detection of particles with diameter above 0.3 μm especially above 0.5 μm. In some product instructions manual, this is not mentioned, and sometimes it is noted that it is able to measure 0.3 μm particles, which is not appropriate.

17.1.3.2 Nominal Diameter and Diameter Channel

The particle size shown in the particle counter during the counting process is called the nominal size. This is just a representative of a certain particle size range. As for the actual particle size it represents, it is relevant with the standard particle size used during calibration. Table 17.1 is the first particle counter J-73 type developed by Institute of HVAC of China Academy of Building Research China. Taking the particle size range with 0.5 μm particles as the standard particles for calibration as an example [1], generally speaking, there are less particle size channels for simple instrument, which are often 5 channels, namely, 0.3, 0.5, 1, 2, and 5 (μm). Particle

Table 17.1 Particle size range of J-73 type particle counter (μm)

Channel	0.3	0.4	0.5	0.6	0.8	1.0	1.2
Particle size range	0.3526–0.4261	0.4261–0.5000	0.5000–0.6067	0.6067–0.7349	0.7349–0.8918	0.8918–1.067	1.067

Table 17.2 Particle size channels of LAS-226 type particle counter

Channel	1	2	3	4	5	6
Particle size (μm)	0.12	0.17	0.27	0.42	0.62	0.87
Range (μm)	0.12–0.17	0.17–0.27	0.27–0.42	0.42–0.62	0.62–0.87	0.87–1.17
Channel	7	8	9	10	11	12
Particle size (μm)	1.17	1.52	1.92	2.37	2.87	3.42
Range (μm)	1.17–1.52	1.52–1.92	1.92–2.37	2.37–2.87	2.87–3.42	3.42–4.02
Channel	13	14	15	16		
Particle size (μm)	4.02	4.67	5.37	6.12		
Range (μm)	4.02–4.67	4.67–5.37	5.37–6.12	Above 6.12		

size channels are more for some precision instrument, which are often for 15 channels, namely, 0.3, 0.4, 0.5, 0.6, 0.8, 1.0, 1.2, 1.5, 2, 3, 4, 5, 6, 8, and 10 (μm).

After the appearance of laser particle counter, smaller particle size can be measured, thus the particle size channels are finer and more. Table 17.2 is the particle size channels for Royco LAS-226 laser particle counter; there are 16 channels for particle size 0.1–6.1 μm. Later, there are also 16 channels for 236 type.

There are two specifications for another PMS LAS-x laser particle counter. One has 16 channels, and the other one has more and finer channels. There are 4 grades with 15 channels, which are equally divided into 60 channels. It is shown in Table 17.3.

17.1.3.3 Errors of Measurement

Overlapping Error

For the particle counter with the application of photoelectricity theory, the main error is the overlapping error caused by application of this theory. That means when there are 2 or more than 2 particles entering into the measuring space simultaneously (Fig. 17.5) – scattering cavity – only one enlarged signal is output from the instrument. This is the result of particles overlapping. At this time, the particle concentration indicated by the particle counter is less than the actual value.

According to Chap. 1, the density function of the situations when 1, 2, …, n particles appear in the detection space (i.e., the air column irradiated by the light beam) of the instrument follows the Poisson distribution in general. When particles

Table 17.3 Particle size channels of LAS-x type particle counter

The first type	Channel	1	2	3	4	5	6
	Particle size (μm)	0.09	0.11	0.15	0.20	0.25	0.30
	Range (μm)	0.09–0.11	0.11–0.15	0.15–0.20	0.20–0.25	0.25–0.30	0.30–0.40
	Channel	7	8	9	10	11	12
	Particle size (μm)	0.40	0.50	0.65	0.80	1.00	1.25
	Range (μm)	0.40–0.50	0.50–0.65	0.65–0.80	0.80–1.00	1.00–1.25	1.25–1.50
	Channel	13	14	15	16		
	Particle size (μm)	1.50	2.00	2.50	3.00		
	Range (μm)	1.50–2.00	2.00–2.50	2.50–3.00	Above 3.00		
The second type	Channel	1	2	3	4		
	Range (μm)	0.09–0.195	0.15–0.30	0.24–0.84	0.60–3.00		
	Interval (μm)	0.007	0.01	0.04	0.16		
	Channel No.	15	15	15	15		

overlap, no matter how many they are, they are only counted as 1 particle. So the total number in the detection space with overlapping, i.e., the counting concentration in the detection space, can be calculated with Eq. (1.16), so it should be

$$C = 1 \times P(1) + 1 \times P(2) + \cdots = 1 \times P(\zeta \geq 1) = 1 \times \{1 - P(\zeta = 0)\}$$
$$= 1 - e^{-\lambda} = 1 - e^{-VN} \tag{17.7}$$

$$\lambda = VN \tag{17.8}$$

where

$P(1)$ is the probability of the occurrence of 1 particle, and it is analogous for others;
λ is the average particle number in the detection space of the instrument for a long term, i.e., the mathematical expectation value;
N is the particle concentration of the airflow through the detection chamber (#/cm^3);
V is the volume of the detection chamber.

For incandescent light particle counter such as Royco 202, we can obtain:

$$V = \frac{\pi(0.1585)^2}{4} \times 0.1 = 0.00197\,\text{cm}^3$$

For laser particle counter such as LAS-x, we can obtain:

$$V = \frac{\pi(0.025)^2}{4} \times 0.02 = 0.00000982\,\text{cm}^3$$

The proportion of the particle number after and before overlapping is:

$$\frac{1 - \mathrm{e}^{-VN}}{VN} \tag{17.9}$$

Since non-overlapping particles are already contained in $1 - e^{-\mathrm{VN}}$ and $1 - e^{-\mathrm{VN}}$ is always less than VN, the ratio cannot be considered as the overlapping rate. Overlap rate can be 1, i.e., 100 %, which means all each measured particle is from the overlapping particles. For example, if each two particles overlap among the original 100 particles, the total number becomes 50, which can be thought that the overlapping rate for this group of particles reaches 100 % instead of 50 % (namely, half overlap).

If the particle loss rate after overlapping is β, we can obtain:

$$\beta = 1 - \frac{1 - \mathrm{e}^{-VN}}{VN} \tag{17.10}$$

When the specific values of V are inserted into the above formula and set $N = 100{,}000\#/\mathrm{L}$, the overlapping loss rate of particles for Royco 202 is 0.092, and that of LAS-x is 0.0005. The difference between them is large. The reason is that the incandescent light particle counter is suitable for testing low concentration because of its large test chamber, while laser particle counter is aimed to measure high concentration because of the small test chamber in order to make the laser beam finer. Therefore, the incandescent light particle counter manufacturers claim that in order to reduce the overlapping error, the maximum allowable detection concentration is 100,000#/L or 35,000#/L (the error β will be under 3.5 %). For laser particle counter, the maximum allowable concentration is 17,000#/cm^3 (such as the error for LAS-x is $\beta = 8$ %; it is indicated in product manuals from PMS company that in this condition, the overlapping error is under 10 %) or 5,000#/cm^3 (now $\beta < 2.5$ %).

Space-Time Error

Besides the overlapping error, there is a space-time error. For a particle counter, its response time from the output of electric pulse signal is certain. So the particle counter can only record these particles which pass through the scattering cavity with the time interval greater than the response time. But those particles with time interval less than the response time will not be recorded, which produces the error (set it δ).

Space-time error is derived as follows [3]:

$$\delta = 1 - \mathrm{e}^{\frac{1-\mathrm{e}^{-VN}}{VN}Nq\sigma_r} \tag{17.11}$$

where q is the sampling flow rate. For Royco 202 it is 5 cm^3/s. For LAS-x it is 1 cm^3/s;

Δt is the response time of the instrument(s). Reference [3] gave a complicated calculation method, but in general, it is in the range of 0.00001–0.000015.

Then, we can get:

Royco 202	$\delta = 0.0005$
LAS-x	$\delta = 0.005$

Since the space-time error is very small, which can be ignored, the detailed derivation process will not be introduced here.

Comprehensive Error [4]

If the error caused by the variation of the air change rate and the particle concentration is not considered, and the error caused by the particle counter's photoelectricity parameters is neither taken into consideration, while only the sampling error is considered, according to the error theory, this comprehensive error σ can be expressed as

$$\sigma = \sqrt{\sigma_1^2 + \sigma_2^2 + \sigma_3^2 + \sigma_4^2 + \sigma_5^2 + \sigma_6^2} \tag{17.12}$$

where

σ_1 is the error caused by the sampling flow rate of the particle counter, which is about ± 3 %;

σ_2 is the error caused by the non-isokinematic sampling, which is about -5 % (the maximum allowable value);

σ_3 is the error caused by settlement in the sampling tube, which is about -2 % (the maximum probable value);

σ_4 is the error caused by collision and coagulation in the sampling tube, which is about -1 % (the maximum probable value);

σ_5 is the error caused by the overlapping in the particle counter (for incandescence particle counter, it is -3.5 % when the concentration ≯35,000#/L, and it is -9.2 % when the concentration ≯100,000#/L; for laser particle counter, it is -0.05 % when the concentration ≯100#/cm^3, it is -2.5 % when the concentration ≯5,000#/cm^3, and it is -8 % when the concentration ≯17,000#/cm^3);

σ_6 is the error caused by the space-time interval in the particle counter (for incandescence particle counter, it is -0.05 %; for laser particle counter, it is -0.5 %).

Then, we can get the possible errors of the particle counter during every sampling process, which is listed in Table 17.4. From the table, when this maximum detection concentration 35,000#/L is taken as the basis, the maximum sampling error of the incandescence particle counter is 7.2 %, while that of the laser particle counter is 10.2 %.

Table 17.4 Comprehensive sampling error of particle counter

Particle counter	Maximum detection concentration		Comprehensive error (%)
	#/L	#/cm^3	
Incandescence light	35,000		7.2
	100,000		11.1
Laser		100	6.3
		5,000	6.8
		17,000	10.2

The above result is consistent with the conclusion in the national standard draft explanation of *Inspection Method of Particle Concentration Measurement Performance of Particle Counter*. In the conclusion, the error of the particle counter is between 7 and 10 % when both the sampling efficiency and the leakage flow rate of the instrument itself are considered.

It should be pointed out for the measurement error between two instruments. In some current research reports where results were obtained with two particle counters (the flow rate may be different), the calibration results of concentration between them is not given, and maybe the calibration process was not carried out. It seems to ignore the difference of the results between two instruments, which is unfair.

One example is the measurement of the cleanroom with 0.5 μm particles published by foreign countries [5]. With the first instrument, all the particle numbers among 15 sampling positions for particles larger than 0.5 μm are 0, through which the air cleanliness level reached Class 1 for 0.5 μm particles, but with the second instrument, the data among 15 sampling positions are between 0.1 and 2.6#/ft^3, through which the air cleanliness level belonged to Class 10. So the minimum difference is above 300 %. So the president of IES-RP-50, who was responsible for the revision committee of 209B in the USA, pointed out that "... the accuracy of the test method is very low. For the particle counters produced by different manufacturers, or even different particle counters produced by the same manufacture, the allowable error is 10–20%." Author's test experience also shows that it is not rare that the difference between measurement results is more than one time when particle counters produced by different manufactures are used. So when the measurement data are treated, the error of this aspect must be considered.

17.1.3.4 Measurement Methods

The measurement methods of the particle counter can be divided into single recording and total recording. The former only measures the number of particles in one particle size channel. The latter can determine the total number of the particles that is above one particle size channel.

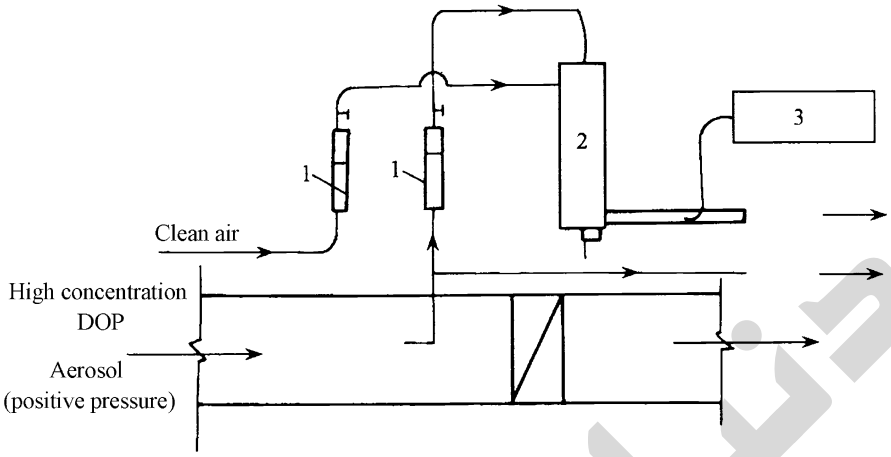

Fig. 17.7 Dilution system with only the mixer. *1* flowmeter, *2* mixer, *3* particle counter

The shifting ways can be divided into manual and automatic. For the automatic way, the sampling time is recorded automatically every time, which is specified alone for each instrument. For example, there are 20, 60, 120, 180, and 300 s. For the manual way, the sampling time is decided by the operator.

The sampling flow rate of particle counter first produced at home and abroad is usually 0.3 L/min, which is called small flow particle counter. Because of the small sampling flow rate, relative large effort will be caused during the measurement of the environment with very low particle concentration. And later the large flow particle counter came to the market in the USA (such as Royco 245 type). The sampling flow rate can reach 28.3 L/min (1 ft^3/L) and even bigger. This provides the convenience to measure the environment with low particle concentration. The relationship between the air cleanliness of the environment and the sampling flow rate will be discussed in detail later.

17.1.3.5 Dilution

When the overlapping error is required to less than 5 %, the dilution system is needed for the sampled air when the concentration for the incandescent light particle counter is more than 50,000#/L and when the sample concentration for laser particle counter is more than 10,000#/cm^3.

Dilution system has two kinds of forms:

1. Only with the flow mixer where the clean air and the sampled air are mixed, which is shown in Fig. 17.7 [6]. High-concentration DOP aerosol is sampled directly from the pipeline, which is powered by the positive pressure in the pipeline. When the pressure is insufficient, specialized exhaust fan should be supplemented so that the sampled air will not enter the mixer.

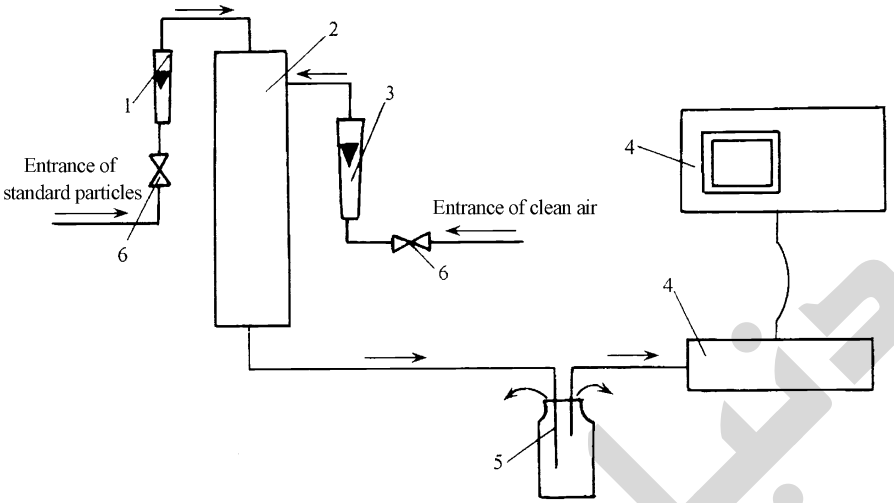

Fig. 17.8 Dilution system with both the mixer and the buffer bottle. *1* flowmeter, *2* mixer, *3* flowmeter, *4* particle counter, *5* buffer bottle, *6* adjustment valve

2. With the mixer and a buffer bottle, which is shown in Fig. 17.8 [7]. For example, this kind of system is used when the particle counter is calibrated with the standard particles. Positive pressure exists in both the standard particle flow and the clean airflow. They enter the mixer and then the buffer bottle so that the total flow rate is bigger than the sampling flow rate of the particle counter. A part of the excessive mixed airflow will spill over from the buffer bottle. The mixture performance of this system is better.

In addition to the dilution system, the dilution device of the particle counter itself can also be used, which is also produced in China. With the dilution system, the measured concentration should be multiplied with the dilution ratio. When the error of the dilution system is also considered, the actual concentration can be obtained. The dilution ratio for common instrument is 10 times, and some also has 100 times. But the small dilution ratio should be used.

17.1.3.6 Modulation of Light Source [2]

The main light sources of particle counter include the incandescent light bulb, the halogen lamp, and the laser source. After the light is emitted from the light source, it should focus as much as possible in the detection chamber of the scattering cavity through the optics system. But because of the error of the installation location for the light source and because the filament in some incandescent bulb are not winded homogeneously and concentrated consistently, the sensitivity of the instrument will be affected, which represents the measured aerosol concentration and the particle size distribution.

The method to judge whether the light source has been well adjusted is as follows:

1. After the light passes through the lens of the optical system, it will focus on the slit. The smaller the focus area is, the more concentrated the light is.
2. The light focusing area should face directly against the slit and cover it evenly.

A method to adjust is as follows:

1. Loose-related screws connected with the lamp bulb. Move the bulb forward and backwards. The optimal state is obtained when the light focus on the slit.
2. Then adjust the lamp position up and down. Observe the change of the counting by particle counter with standard aerosol. This is used to determine whether adjustment is fine.

17.1.3.7 Calibration

Particle counter can directly determine the particle size and number, but the values of both the size and the number are also converted from other signal, which is still not an absolute value. If the instrument sensitivity was not set properly, it will directly affect the true extent of measurement results. Therefore, the sensitivity of instrument needs correction, which is called calibration. Particle counter calibration should include two aspects: one is the calibration of particle size, and the other is the calibration of particle number or concentration.

Calibration of Particle Size

During the calibration process of particle size for particle counter, the "equivalent diameter" mentioned in Chap. 1 is used for comparison. Namely, when the scattering light intensity of the measured particles is the same as that of the standard particles, the size of the standard particles is treated as that of the measured particles. The closer the properties between the selected standard particles and the measured particles are, the larger the reliability of this "equivalent" is. At present polystyrene sphere latex (PSL) particles are chosen as the standard particles at home and abroad, whose physical properties are close to the atmospheric dust. The density of PSL is 1.059 g/cm^3, and the refractive index is 1.595 (at 20 °C). PSL particles are generated by polymerization of emulsion with polyethylene monomer. After dilution, spray and dry, monodisperse aerosol is generated, which is called PSL. Figure 17.9 is an electron microscopic photo of PSL standard particles developed by Wu Zhiyu et al. in China. Figure 17.10 shows the particle size distribution. It is clear that 70–95 % of particles focus on a certain size range, which means the monodispersivity performance is very good [8].

Usually PSL particles are stored in a cool place, which takes more than one year. During calibration operation, polystyrene latex is diluted with the secondary distilled

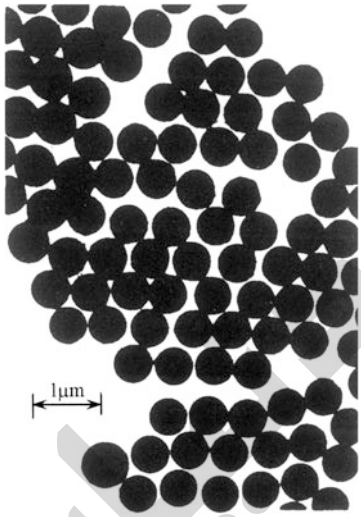

Fig. 17.9 Electron microscopic photo of PSL standard particles

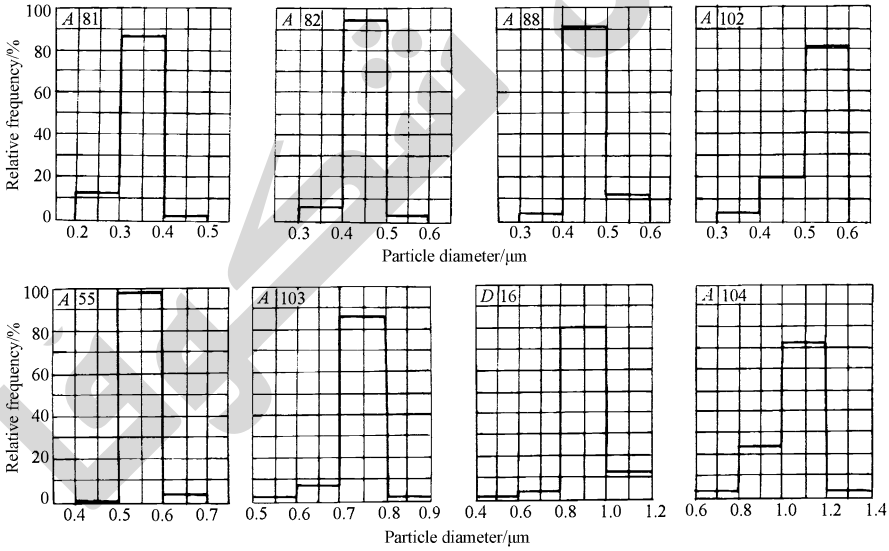

Fig. 17.10 Particle size distribution of PSL standard particles

water or the further filtered water with 0.3 μm microporous membrane. The concentration of dilution liquid is shown in Table 17.5 [9]. The diluted solution is sprayed and then introduced to the instrument. The spray process is shown in Fig. 17.11.

During the calibration of particle size for particle counter, when standard particles with known size are introduced into the particle counter, it will test

Table 17.5 Concentration of dilution liquid for spray

Diameter of PSL particles (μm)	Mass concentration (%)
0.5	0.001
1	0.005
2	0.1

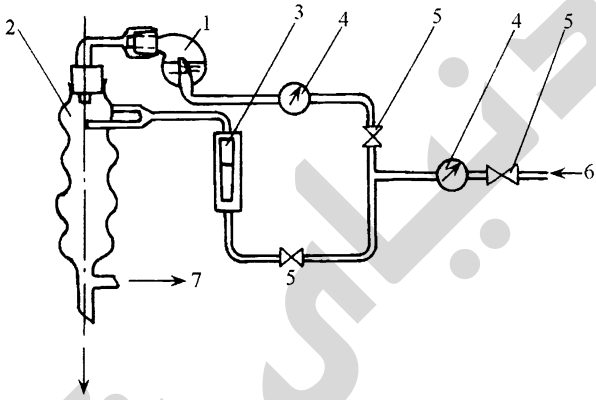

Fig. 17.11 Schematic diagram of particle generation process. *1* sprayer, *2* rotary drier, *3* flowmeter, *4* pressure gauge, *5* adjustment valve, *6* inlet of pressurized air, *7* outlet of aerosol

whether all the records of the instrument are in the known particle size range. For example, when the average particle size of standard particles is 0.555 μm and the standard deviation of size distribution is 0.0186, more than 95 % of particles are within the diameter range of 0.52–0.59 μm, which means the concentration degree is very high. Therefore, when these standard particles are used for instrument calibration, most of the measurement results data shall be recorded in the range 0.5–0.6 μm, which should have a prominent peak as shown in Fig. 17.12. But with the influence of factors such as the instrument and the aerosol generation condition, in some test results, there may be the particle size distribution with larger standard deviation than that of the standard particles themselves, and the peak value is much lower [2]. How big the peak value of the particle number frequency should be at least? According to the calibration work experience, it is equivalent with the conclusion by analysis of concentration. For a particle counter with 15 size channels, it should not be lower than 60 % during single recording process, namely, that the number of measured particles in the certain calibrated size channel range shall be not less than 60 % of the total number. If the calibrated peak value is lower than this standard value, or even abnormal distribution appears, the following reasons should be considered and then eliminated.

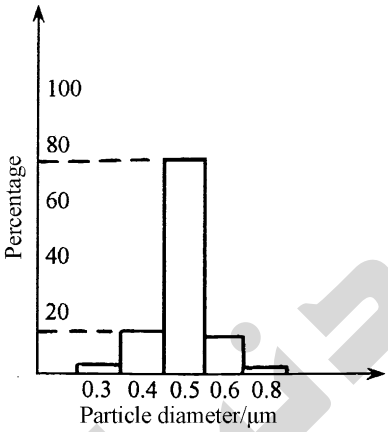

Fig. 17.12 Size distribution of standard particles with average size 0.555 μm

The pressure in the photoelectricity multiplier tube is high, which is not normal. This should be checked at first. If it is sure that the high pressure is not normal, the adjusting knob can be used to raise or lower the conversion sensitivity of the instrument. When the conversion sensitivity is adjusted appropriately, a prominent peak will appear in a predetermined size channel.

As for the light source problem, if the filament fails to align with the slit of the optics system when the lamp bulb is replaced, it should correct after discovery.

As for the problem of standard particle generation, we should consider whether the concentration of dilution liquid with PSL particles is appropriate, whether the flow rate of mixed air and its dry condition are enough, whether the spray pressure is appropriate, and whether the dilution solution needs to be cleaned. For this last point, pure distilled water can be used for check.

As for the problem of the counting component, when the above problems do not exist, the counting parts should be checked to find out if there are errors.

If all the problems above are not present, it is likely that the instrument itself has problem.

Calibration work of particle size should be carried out regularly. When particle counter is used to measure the concentration of some particles forever and when the refractive index between the measured particle and the standard particle is different a lot, correction with electron microscopy should be performed in advance. Figure 17.13 shows one corrected case [10].

Concentration Calibration

In order to know whether the measured particle counting concentration of particle counter is correct, it needs to calibrate the concentration of the instrument. Although there is standard about this aspect in China, this job has not been carried out yet.

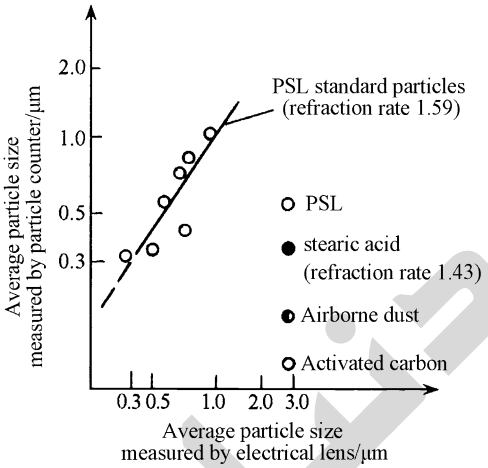

Fig. 17.13 Comparison of average particle size between the electron microscopic method and the particle counter

Among the calibration methods of concentration in foreign reports, vibration aperture method is one matured method [8]. In Fig. 17.14, aerosol jet flow is released from the orifice of the generator. Synchronous vibration occurs on the generator with the vibration effect of piezoelectric ceramic. The jet column is then fractured into small droplets, which mix with the air from the perforated plate after air passes through HEPA filter. The volume of each fractured droplet is:

$$V = \frac{Q}{f} = \frac{1}{6}\pi D_d^3 \tag{17.13}$$

So the particle size is

$$D_d = \left(\frac{6Q}{\pi f}\right)^{1/3} \tag{17.14}$$

where

Q is the liquid flow rate through the aperture (mL/s);
f is the perturbation frequency (s^{-1}).

The calculated droplet radius is slightly larger than the jet diameter. If it is a nonvolatile solute (such as sodium chloride) in the volatile solvent (such as ethanol), the solvent in the liquid drop becomes volatile after passing through the vibration aperture, then aerosol are generated with the nonvolatile solute. The particle size is determined by the following formula:

$$D_d = \left(\frac{6QC}{\pi f}\right)^{1/3} \tag{17.15}$$

where C is the volumetric concentration of solute in the solution.

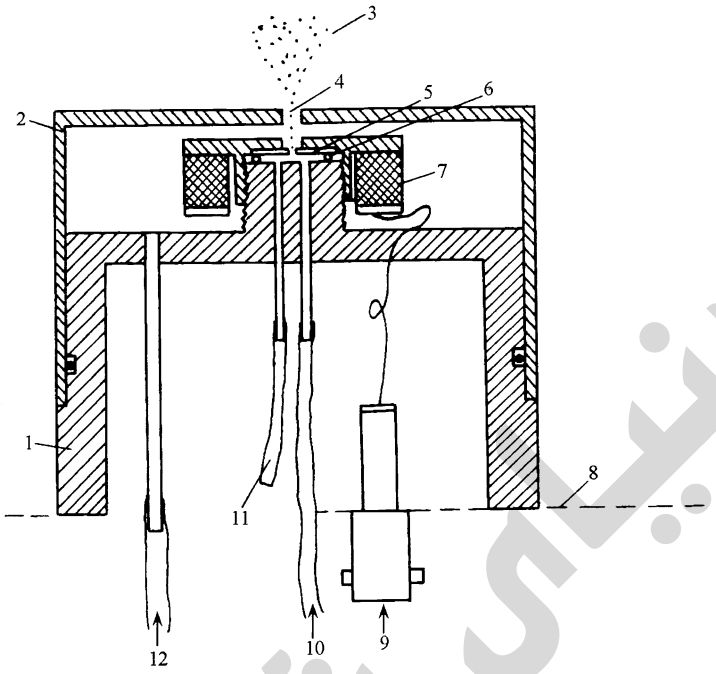

Fig. 17.14 Schematic diagram of dispersion system of vibration aperture generator. *1* bracket, *2* cover, *3* dispersed droplets, *4* holes, *5* hole plate, *6* PTFE O-ring, *7* piezoelectric ceramic, *8* perforation plate, *9* signal source, *10* fluid supply pipe, *11* exhaust pipe, *12* pressurized air pipe

It is clear that D_p is only $\sqrt[3]{C}$ times of D_d. This means D_p can reduce to one of scores of D_d.

Due to the synchronization of the jet fracture and the vibration of piezoelectric ceramic, the number of particles from aerosol generator is determined by the vibration frequency, and it is monodisperse. Because the vibration frequency can be accurately measured, the particle counting concentration can be known.

17.1.4 Other Particle Counting Method

Except for the above He-Ne laser particle counter, there are other counting methods that can be used to determine the concentration of ≤ 0.1 μm particles. Their principles are summarized later.

17.1.4.1 Electron Microscope Method

Particles with diameter above 0.01 μm are captured by the thermal or electrostatic type samplers. Then, the particle size and number can be measured through electron microscopy or automatically scanning electron microscope.

17.1.4.2 Condensation Nucleus Counters Method (CNC for Short)

Particles with different sizes are classified by other methods at first. Then, they pass through the saturated vapor (35 °C) of the medium liquid (such as *n*-butanol), where the saturated vapor encloses the particles. Then, they get into the condensation tube with the temperature maintained at 10 °C, where *n*-butanol vapor is condensed on the particles surface and particles become droplets with diameter 12 μm. But now only counting process can be performed. Other classification methods must be used together to measure the size of particles with diameter above 0.001 μm.

(a) Electrostatic Classifier (DMA). The distribution of migration can be measured when particles are charged so that the number of particles can be counted, which can be used to measure particles with diameter 0.003–1 μm. When the condensation nuclei counter is used, the method is expressed as DMA + CNC.
(b) Diffusion Classifier (DB). The smaller the particle is, the larger the diffusion distance by Brown motion is. When the condensation nuclei counter is used, the method is expressed as DB + CNC.

The detailed parameters about the two kinds of classification methods can be referred to Ref. [10].

17.1.5 Relative Concentration Method

The relative concentration method, the weight concentration method, and the particle counting concentration method are three kinds of basic methods. For the relative concentration method, there are the photoelectric colorimetry method, the photoelectric turbidity method, and so on. However, due to the development of light scattering particle counter, the two methods have been rarely used in air cleaning technology. But the latter method has transient characteristic as a leak detection method; it is more suitable than the particle counter at this point. Similar as the particle counter, the photoelectric turbidimetry method is also based on light scattering theory, and both of them belong to the floating measurement method. The scattering light of single particle is measured in particle counter, while the scattering light of the particle group is measured in the photoelectric turbidimeter. When the intensity of incident light is fixed, the total light scattering of particle group is not only related with the particle size but also related with the scattering particle number. Within a certain range of concentration, the total energy of scattered light is proportional to the concentration of particles. This measured result is represented

by the photoelectricity current value. For some aerosol often measured, if the weighing concentration is prepared in advance which is carried out during the concentration calibration of instrument, the equivalent weight concentration corresponding with the photoelectric current value can be directly obtained. If it is used to determine the filter efficiency, concentration calibration is not needed. In the past, the photoelectric turbidimeter for measuring particles has been produced, which will not be described in detail here.

17.1.6 Biological Particle Measurement Method

Measurement of biological particles (mainly bacteria) not only contains the measurement of all the particulate material but also must contain the necessary conditions of biology. The detailed discussion is not the scope of this book, so in this section, there is only a brief introduction.

Pay attention to the following questions when measuring biological particles:

1. Absolute sterilization must be performed on measuring instrument, measuring accessories, and operation appliances.
2. All measures should be taken to prevent the pollution of specimens from occupant.
3. It shall adopt the most suitable sampling method according to the applications. Detailed information about the use condition, culture medium, culture condition, and other parameters should be recorded.
4. In some cases, the contrast specimens must be used.

The commonly used measurement methods will be introduced as follows:

17.1.6.1 Settlement Method

This is the measurement method for sedimentation bacteria, which is the most convenient and simple method. The culture dishes filled with culture medium (diameter is usually 90 mm) are placed on the test locations. They are placed with the prescribed time for exposure, which can also be determined through trial test. Then, they are cultured according to the specified temperature and time, after which the colony number is counted with the naked eye.

In the past, the culture temperature was 37 °C, and the culture time was 48 h in general. The American Aerospace Standard specifies 32 °C and 48 h, respectively. But according to experiment [11], after 48 h of culture, the sequential relationship between the colony count and the temperature is: 25 °C $\geq$ 31 °C $\geq$ 37 °C $\geq$20 °C $\geq$43 °C. We can see that both 25 and 31 °C are the suitable culture temperature. Therefore, during the measurement of the general bacteria and the bacterial number, 48 h and 31–32 °C can be used for culture. For measurement of fungi, 96 h and 25 °C can be used for culture [12]. From the bacterial growth curve in Chap. 9, we can know that, 24–48 h corresponds to the stable growth period of bacteria. So, if

Table 17.6 Characteristics of Anderson sampler

Stage	Aperture size (μm)	Air velocity (m/s)	Lower size limit of capture particle (μm)	Particle size with 100 % capture efficiency	Main capture range (μm)	Average capture efficiency (%)
1	1.181	1.08	3.78	11.2	Above 7.7	–
2	0.914	1.79	2.76	8.29	5.5–7.7	60
3	0.711	2.97	1.44	4.32	3.5–5.5	63
4	0.533	5.28	1.17	3.50	2.3–3.5	63
5	0.343	12.79	0.61	1.84	1.4–2.3	66
6	0.254	23.30	0.35	1.06	0.75–1.4	66

the temperature for culture increases from 32 to 37 °C, 24 h can be used as the culture time, which also meets the requirements. For other tested bacteria methods, the data are also available.

17.1.6.2 Impactor Method

This is the method to measure the airborne bacteria.

Dry Method

(a) The Gap Method. Air is drawn through the slit. The air containing bacteria will hit and deposit on the fixed plate with culture medium. Then, the culture and the counting processes are performed. Cascade sampling device is one example of this method.
(b) The Rotation Method. Air is drawn through the slit. The air containing bacteria will hit and deposit on the rotating plate with culture medium. With the rotation of the culture medium, the variation of the concentration of airborne bacteria with time is measured. Rotary sampler is one example of this method.
(c) The Classification Method. It is a porous plate sampler. It is equipped with a multistage orifice plate. After ejected through each orifice, air impacts the plate culture base, where the biological particles deposit onto culture medium. Since the aperture diameters of each plate are different, the sizes of particles deposited on each section of the culture medium are different. So the size distribution of biological particles can be obtained. The Anderson sampler is one example of this method. It is taken as the standard sampler internationally. Table 17.6 shows the characteristics of Anderson sampler [13].
(d) The Centrifugal Method. Sampling head is the volute of an impeller. When it is turned on, air within the distance of 40 cm can be drawn into the sampler with the high rotating speed of the impeller inside the volute. A conical body with high rotating speed is formed after air enters the casing, where particles

containing bacteria impact onto the special plastic strip containing the agar culture medium due to the centrifugal acceleration force. Then, the air is exhaust to the outside of the volute in the annular shape.

Wet Method

(a) Injection Method. Inject the air that contains bacteria into the culture dish filled with culture solution, and then particles are trapped with liquid. And filter the culture solution containing bacteria through the membrane filter, and then culture and count on the membrane.
(b) Flow Method. This method is similar as the cascade impactor. The airflow ejected from the nozzle impacts with the high-voltage electricity collecting plate. Particles are captured with the electrostatic principle. At the same time the culture medium flows through the collecting plate, thus particles are trapped and then brought away by the culture solution. Then, the solution is filtered and cultured, after which counting can proceed. The characteristic of this method is the large sampling flow rate, which can shorten the sampling time.

17.1.6.3 Filtration Method

When air pass through the filter, which is 0.3 and 0.45 μm microporous membrane, microbial particles are trapped on the membrane. The membrane is placed directly on the culture medium, then counting can be made. Before sampling, membrane should be placed in the boiling water for sterilization. Take it out and then make it dry, after which it can be used. But someone thinks, with the blowing of sampling airflow, the weak microbe on the membrane surface may probably die due to dry. So it should be completed within the 5 min, and then culture it immediately. It is obviously that such a short sampling time for high air cleanliness environment is difficult. But when the sampling is on the culture medium, sampling time may be slightly longer.

Filtration media used in this filtration method include glass fibrous filter paper, gelatin sponge (after sampling, dissolve it in physiological salt water, then fall the water into the culture medium), and powdered glutamic acid alkali tablet (dissolve it in the water after sampling).

It is difficult to find out the regular relationship between different apparatus and methods for measuring the airborne bacteria both from theory and from practice. Results performed by different investigators are different a lot. Therefore, various measurement data will not be cited here. But the Anderson sampler is usually used as the comparison baseline. In addition, many data indicate that the sampling efficiency of filtration method is higher than that of other methods.

Figure 17.15 is the illustration of above methods and measurement of surface microorganisms.

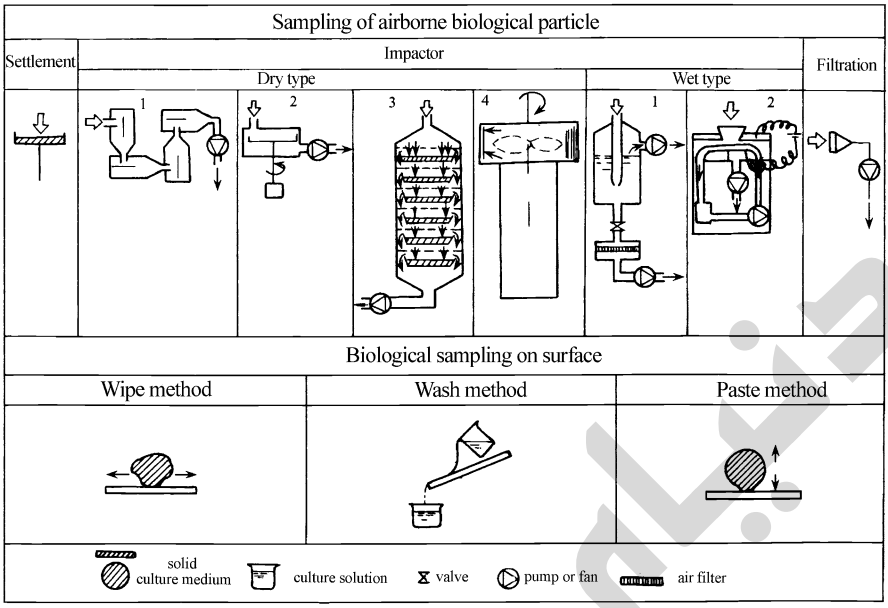

Fig. 17.15 Illustration of biological particle sampling

17.2 Air Filter Measurement

17.2.1 Measurement Range

There are usually three aspects for the measurement of air filter, which will be introduced as follows.

17.2.1.1 Measurement of Filter Media

It is aimed to the mechanism study of air filtration, the choice of filter media, the selection and comparison of filtration scheme, and the measurement needed as a reference for understanding the filter performance. It is known as the measurement of small sample. It includes the following items:

1. Efficiency. After the filter media is fixed by clamps, concentrations upstream and downstream are measured. Then, the efficiency can be calculated according to the formula. When the measured efficiency is provided, the corresponding specific velocity should be indicated.
2. Resistance. After the filter media is fixed by clamps, the difference of differential pressures upstream and downstream is measured, which is called the resistance.

When the measured resistance is provided, the corresponding specific velocity should be indicated.

3. Tensile strength. The tensile strength of filter media used in HEPA filter should be not less than 250 g. For the filter with the requirement of pressure resistance, the tensile strength should not be less than 450 g.
4. Content of combustible matter. For the filter with the requirement of fire protection, the combustible content of filter media should be not more than 5 %.
5. Heat resistance. After the filter media is heated under specified temperature, the tensile strength should be checked whether it has changed.
6. Water resistance. After the filter media is exposed in the humid steam flow for 5 min, the resistance is measured. For the filter media without the ability of water resistance or without hydrophobic treatment, pores are quickly blocked, which will increase the resistance significantly.

The above test items and related data are from the general literatures abroad, which are not all from domestic standards. All of them are described here only for readers' reference. The following content is the same.

17.2.1.2 Unit Measurement

These are the requirements during the developing and test of air filters, which include the following items:

1. Efficiency. Test is carried out according to the methods shown in Table 17.6. After air filter is tested, it should maintain the original efficiency or can still meet the requirements.
2. Resistance. Initial resistance is measured with rated airflow. The pipe diameters and velocities upstream and downstream of tested filter should be consistent. The measuring position from the local resistance component downstream should be larger than three times of the edge length, and the distance upstream is more than five times of the edge length.
3. Dust holding capacity. It will be described later.
4. Vibration resistance (applicable to HEPA filter). Tested filter is placed on the vibration table with the vibration amplitude below 10 mm and the vibration frequency about 300 times per minute. After vibration for the specified long time, the filter appearance should be checked to find out if it has changed.
5. Pressure resistance (applicable to HEPA filter). With the increased air velocity or increased dust holding capacity, the filter resistance is increased by more than 10 times. When this situation lasts 15 min, the efficiency is measured again. For HEPA filter with special requirements of pressure resistance, the ability to resist shock wave should be tested [13], such as the HEPA filter for breath of occupant.
6. Heat resistance. Filter is placed into an oven for several hours when the temperature increases slowly to the required value. Then, cool the filter till the room temperature. The shapes of the frame, the gasket, and adhesives should be

checked to find out whether there are unusual changes, and then the filter efficiency should be measured again. Or hot air is used to test the filter.
7. Flame resistance (applicable for filters with requirements of flame resistance). Flame should be used to face the windward side of the air filter at the nominal airflow rate for 5 min. Even when the filter is burnt, the filter can be considered to have the flame resistance ability when the combustion with the same degree of the windward side does not appear at the leeward side.
8. Water resistance (applicable to filters with requirements of water resistance). Immerse the filter vertically into 20 °C water for more than 5 min, and then take it out for less than 5 min to remove water. After water is removed, dry the filter with the air of the rated flow rate for 10 min. The resistance is measured, which should not be larger than two times of the initial resistance. The resistance after it is the completely dry should be half of the original value, and the increase of the most penetration should not exceed the requirement (generally it should not be more than two times of the original penetration).
9. Leakage performance (applicable to the sub-high-efficiency and HEPA filters). Test according to the requirement in Sect. 17.4.

17.2.1.3 Field Test

This is to check whether filters have been damaged during the installation process, whether the gasket is well sealed, or whether certain performance is kept during regular examination. There are the following items:

1. Efficiency. Test according to the methods in Table 17.7.
2. Resistance. The specific velocity should be indicated during the measurement of resistance.
3. Leakage performance. Test according to the requirements in Sect. 17.4 of this chapter.

The test items are summarized above. The following sections will mainly discuss the measurement of efficiency and dust holding capacity.

17.2.2 Measurement of Filter Efficiency

17.2.2.1 Measurement Method

Commonly used measurement methods for filter efficiency are listed in Table 17.7. The main difference between various methods is the standard dust source and the disparity of particles. As mentioned in the chapter about the filtration mechanism, according to the property and the application of air filters, standard dust source should be chosen to test the filter efficiency. For example, for study of HEPA filter, monodisperse particles are usually used as the dust source. Because it is difficult to

Table 17.7 Common test methods for efficiency of air filter

Test aerosol						
Name	Shape	Particle size distribution	Initial concentration (mg/m^3)	Test method and detectable efficiency	Application	Nation and region
DOP	Liquid, fog	Monodisperse, mass median diameter 0.3 μm occupies more than 85 % (mass percentage, and this applies below)	100	Light scattering method, particle counter for filter efficiency ≤99.9999 %	Sub-HEPA and HEPA filter. Applicable for unit test only	USA, Japan
DOP	Liquid, fog	Polydisperse, mass median diameter 0.8 μm 0.3 μm 24.77 % 0.4 μm 19.74 % 0.5 μm 15.80 % 0.6 μm 14.92 % 0.8 μm 13.04 % 0 μm 5.44 % 1.2 μm 4.13 % 1.5 μm 1.48 % ≥ 2.0 μm 0.68 %	100	Light scattering method, particle counter for filter efficiency ≤99.9999 %	Sub-HEPA and HEPA filter	USA, Japan
DOS	Liquid, fog	0.2 μm	–	Light scattering method, particle counter for filter efficiency ≤99.9999 %	Sub-HEPA and HEPA filter	USA, Japan
Paraffin oil	Liquid, fog	Polydisperse, 0.15–1.1 μm, where 0.3–0.5 μm occupies 80 %,mass median diameter 0.4 μm	10–80	Light scattering method, Dinter device for filter efficiency ≤99.995 %	Sub-HEPA and HEPA filter. Applicable for unit test only	Former Federal Germany
Turbine oil	Liquid, fog	Close to monodisperse, most are 0.28–0.34 μm. Mass-weighted diameter 0.31 μm	2,500	Light scattering method, turbidimeter for filter efficiency ≤99.99999 %	Sub-HEPA and HEPA filter. Applicable for unit test only	former Soviet Union, China

(continued)

Table 17.7 (continued)

Test aerosol						
Name	Shape	Particle size distribution	Initial concentration (mg/m^3)	Test method and detectable efficiency	Application	Nation and region
NaCl	Solid, dust	Polydisperse, 0007–17 μm,Mass median diameter 0.45–0.6 μm	3–5	Sodium flame method, flame photometer for filter efficiency ≤99.9999 %	Medium-efficiency and HEPA filter	EU, China
Atmospheric dust	Most are solid. Mixture of several shapes	Polydisperse, particle size distribution is shown in Chap. 2	Undefined	Arrestance method Balance for filter efficiency ≤99 %	Coarse and medium-efficiency filter	China, USA, Japan
				Dust spot method (NBS method).	Coarse and medium-efficiency filter	China, USA, Japan
				Chromometer for filter efficiency ≤99 %	Coarse and medium-efficiency filter	
				Particle counting method with membrane microscope ≤99.99 %	Medium-efficiency and HEPA filter	Sweden, China, Japan
				Particle counter ≤99.999 % (except dilutor)		
Radioactive atmospheric dust	Most are solid. Mixture of several shapes	Polydisperse, <1 μm	undefined	Condensation particle counter ≤99.99 %	Sub-HEPA and HEPA filter	USA, Former Federal Germany
Atmospheric condensation nucleus	Most are solid. Mixture of several shapes	Polydisperse, 0.001–0.1 μm	undefined	Condensation particle counter ≤ 99.99 %	Sub-HEPA and HEPA filter	USA, Former Federal Germany
Quartz dust	Solid, dust (SiO_2 72 %, Black carbon 25 %, Cotton fiber 3 %)	Polydisperse, mass median diameter 5 μm 0–5 μm 39 % 5–10 μm 18 % 10–20 μm 16 % 20–40 μm 18 % 40–80 μm 9 %	<70	Arrestance method (AFI method), balance for arrestance ≤99 %	Coarse and medium-efficiency filter. Applicable for unit test only	USA, Japan

Quartz dust	Solid, dust	Polydisperse Group A > 6 μm 0 % >4 μm 2 % >2 μm 26 % <1 μm 40 % Mass median diameter 1.3 μm Group B > 10 μm 1 % >6 μm 10 % >4 μm 26 % >2 μm 58 % <1 μm 21 % Mass median diameter 2.5 μm Group C > 10 μm 30% >6 μm 65 % >4 μm 78 % >2 μm 93 % <1 μm 2 % Mass median diameter 8 μm	2–10	Arrestance method Light scattering method for efficiency >99.5 %	Coarse and medium-efficiency filter. Applicable for unit test only. Or sub-HEPA filter and applicable for unit test only	Former Federal Germany
Japan JIS8 dust	Solid, dust	Polydisperse, mass median diameter 8 μm 0–5 μm 39 ± 5 % 5–10 μm 18 ± 3 % 10–20 μm 16 ± 3 % 20–30 μm 12 ± 3 % 30–40 μm 6 ± 3 % 40–74 μm >9 %	30 ± 10	Arrestance method	Coarse filter. Applicable for unit test only	Japan

(continued)

Table 17.7 (continued)

Test aerosol						
Name	Shape	Particle size distribution	Initial concentration (mg/m^3)	Test method and detectable efficiency	Application	Nation and region
Japan JIS11 dust	Solid, dust	Polydisperse, mass median diameter 2 μm 1 μm 65 ± 5 % 2 μm 30 ± 5 % 4 μm 22 ± 5 % 6 μm 8 ± 3 % 8 μm 3 ± 3 %	3 ± 1	Dust spot method	Medium-efficiency filter. Applicable for unit test only	Japan
Sodium fluorescein	Solid, dust	Polydisperse, average size 0.08 μm,mass median diameter 0.15 μm	0.01	Fluorescence method (fluorimeter is used to test the fluorescence from the scrubbing solution of filter media by ammonia) ≤99.9999 %	Sub-HEPA and HEPA filter. Applicable for unit test only	France

generate monodisperse particles, polydisperse particles are used for the field test of HEPA filter. In terms of penetration, the penetration with polydisperse particles is less than half of that with monodisperse particles. So the field test efficiency should be higher than that measured in factory or laboratory. But due to the leakage during installation, the conclusion is usually opposite.

It should be illustrated for DOP aerosol in the table that it got criticism recently in two aspects. One criticism is that DOP generated with the heating method is easily attached to the filter surface, and the generation device is huge, so it is suggested to change the generation method [14, 15]. The other one is that in some cases after the volatilization, DOP may enter the clean airflow and have the carcinogenic effect [16]. But there is also doubt on this criticism [17]. It is found through experiment under the normal temperature that the volatile DOP concentration from the filter material is only one tenth of the allowable concentration of harmful substances with the most strict control requirement, so it is too early to conclude that it is harmful. Based on the above reasons, attention has been paid on looking for the substitute of DOP recently. DOS in the table is one of the substitutes. DOS with molecular weight 427 is an aromatic colorless oily liquid. Its molecular expression is $(CH_2)_6(CH_2COOC_8H_{17})_2$. The dispersion characteristic is same as DOP, but it is relatively safer. Similar as DOS, DEHS (di-ethyl-hexyl-sebacat) is also one substitute. Besides, artificial aerosol also includes PAO (polyalphaolefin) and PSL (polystyrene sphere latex). Atmospheric dust can also be used.

As mentioned in Chap. 3, there is the most penetrating particle size (MPPS) d_{max}. The theoretical requirement is satisfied when particles with this size are used to test the efficiency of air filter during research studies. In European standard EN1822 published in 1998, it was proposed to use MPPS as the particle size to test HEPA filters before delivery from factory. But it did not specify the special aerosol. Under different conditions, d_{max} will be different. For glass fibrous HEPA filters, d_{max} is about 0.1–0.2 μm, and the difference of this value for different filters of this kind is small. As for the industrial standard, the comparable consistent standard should be found as the precondition. In this aspect, Chinese standard adopts 0.1–0.3 μm as shown in Table 4.37 to replace d_{max}, which seems more suitable to meet the requirement of consistent standard.

17.2.2.2 Comparison of Results with Several Measurement Methods

In Table 17.7, a simple comparison of results with several measurement methods published in literatures is shown.

Table 17.8 shows the difference of results with the weight method, the dust spot method, and the DOP method. The efficiency with the artificial dust and the weight method is the highest.

Figure 17.16 shows the relationship curve between the particle counting efficiency with atmospheric dust particle diameter $\geq$0.5 μm and the weight efficiency with artificial dust (the BF-2 dust mentioned above) in Ref. [18]. Equation (17.16) is the expression obtained from the curve.

Table 17.8 Comparison of the weight method, the spot method, and the DOP method

Filter type	Arrestance (with artificial dust) (%)	Dust spot efficiency (%)	DOP method efficiency (%)
HEPA filter	100	100	99.97
	100	99	95
	100	93–97	80–85
	99	80–85	50–60
	96	45–55	20–30
	92	30–35	15–20
Electrostatic filter	99	85–90	60–70
	76	8–12	2–5

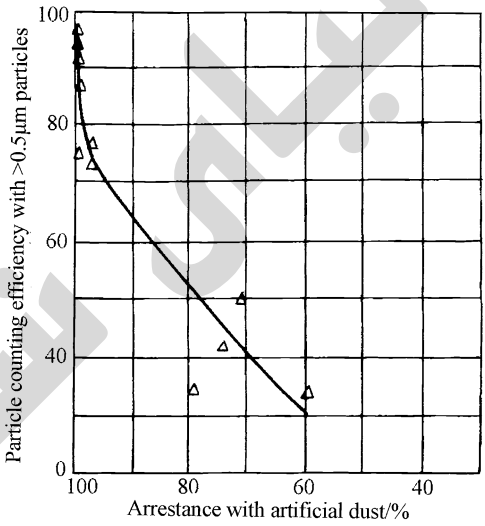

Fig. 17.16 Experimental relationship between the particle counting efficiency with atmospheric dust and the weight efficiency with artificial dust

$$\eta_g = 37.8 \ln \eta_d\text{-}68.5 \tag{17.16}$$

where

η_g is the weight efficiency with artificial dust;

η_d is the particle counting efficiency for particle diameter $\geq$0.5 μm with atmospheric dust.

Table 17.9 lists the test data on foreign filter [19].

Figure 17.17 is the comparison of the results among the DOP method, the spot method, and the weight efficiency with artificial dust in Ref. [20].

Table 17.10 shows the compiled data on HEPA filter according to the experimental data in China. Table 17.11 gives the measurement efficiency of coarse and medium-efficiency filters made with nylon and polypropylene.

Table 17.9 Comparison of the sodium flame method and the DOP method (air filter)

		Penetration			Efficiency	
Filter	Flow rate (m^3/h)	NaCl k_1 (%)	DOP k_2 (%)	k_2/k_1	NaCl	DOP
1	84	0.0045	0.007	1.5	0.999954	0.99993
2	84	0.0030	0.004	1.34	0.999970	0.99996
3	840	0.0040	0.004	1	0.999960	0.99996
4	840	0.0050	0.007	1.4	0.999950	0.99993
Average				1.31		

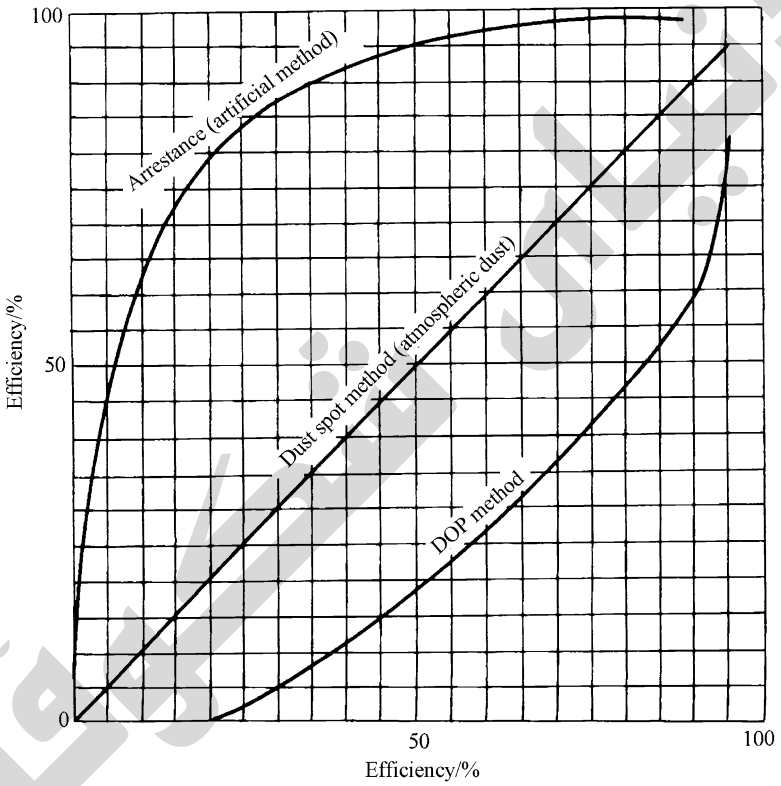

Fig. 17.17 Comparison of the efficiencies among the DOP method, the spot method, and the weight efficiency with artificial dust

Table 17.12 is the experimental result with high-efficiency filters [6].

The above relations come from the experience, through which theoretical conclusions cannot be made. But the relationship between several methods with domestic and foreign data is roughly as follows:

Penetration k_4 with the particle counting method with atmospheric dust > penetration k_2 with the DOP method > penetration k_1 with the sodium flame method > penetration k_3 with the oil mist method.

Table 17.10 Comparison of the sodium flame method and the oil mist method (air filter)

	Average penetration (%)		
Sample material	NaCl k_1	Oil mist k_3	k_3/k_1
Asbestos 149	0.000710	0.000220	0.31
Glass fiber 7001	0.000051	0.000031	0.61
Glass fiber 6901	0.008600	0.008700	1
фпп-15 from former USSR	0.240000	0.170000	0.71
Glass fiber (thick)	0.003300	0.000700	0.21
Glass fiber (thin)	0.051000	0.011000	0.27
Average			0.52

Table 17.11 Comparison of measured efficiency of coarse and medium-efficiency filters between the sodium flame method and the oil mist method

Filter media	NaCl η_1 (%)	Oil mist η_2 (%)	Filter media	NaCl η_1 (%)	Oil mist η_2 (%)
1	2	10	9	26	28.6
2	5	10.8	10	36	36.3
3	6	16	11	38	30.5
4	6	16	12	40	32.5
5	7	10	13	42	44
6	13	16	14	47	31.6
7	18	12.7	15	53	47.3
8	19	30.9	16	53	49.1

Table 17.12 Comparison of penetrations for several filter media

	Polydisperse DOP	Sodium flame method	Atmospheric dust method (laser particle counter)		
Filter media	k_2 (%)	k_1 (%)	k_4 (%)	k_2/k_1	k_2/k_4
I-2	0.000014	undetectable	undetectable	–	–
II-5	0.00302	0.0016	0.005	1.88	0.6
III-1	0.00476	0.0029	0.0059	1.61	0.81
III-2	0.0441	0.034	0.048	1.80	0.92
Average				1.6	0.78

The particle counting efficiency with atmospheric dust is slightly more than that with the DOP method, or the penetration of the former is slightly less by 20 %. The efficiency with the DOP method is lower than that with the sodium flame method, or the penetration of the former is larger by more than 1.4 times. The efficiency with the sodium flame method is greater than the oil mist method, or the penetration of the former is larger by more than 1 time.

The efficiency with the DOP method is less than that with the sodium flame method, which is consistent with the conclusions from the general literatures. This

is also consistent with the opinion that the efficiency with liquid particles is lower than that with the solid particles. But contradictory results appear when the oil mist method and the sodium flame method are compared. Liquid particle methods are used in both the DOP method and the oil mist method, where the average particle sizes are basically the same. But due to the different particle size distribution, it is possible that the measured efficiencies may not be entirely the same. But there may be other reasons for such big difference. According to the characteristic of the oil mist method, if parameters are not well controlled during the generation process of oil mist, both the dispersity and the average particle size may deviate a lot from the standard values. Furthermore, results are also affected by different filter media. In summary, further study is needed to compare the results with several measurement methods.

For measuring the coarse and medium-efficiency filters, the test efficiency with artificial dust is much higher than that with the atmospheric dust. For the same foam filter, the weight efficiency with atmospheric dust is 45 %, while the weight efficiency with artificial dust reaches 90 %. The reason why the efficiency with artificial dust is so high is that the artificial ground dust particles are angular and particles will be positively charged with the movement of airflow. When the particles are positively charged and the wall surface is negatively charged, the capture efficiency will be improved. Some artificial dust will easily coagulate due to the special ingredients, so it is more easily captured. In the nature, the dust particles formed are generally not angular, and the charged phenomenon is weak.

17.2.2.3 Standard Method in China

In national standard GB/T 14295-2008 *Air Filter*, test methods are included, which is suitable for dry air filter (including the electrostatic filter). It is shown in Table 17.13.

In national standard GB/T 13554-2008 *HEPA Filter*, HEPA and sub-high-efficiency air filters should be tested with the sodium flame method. ULPA filters should be tested with the particle counting method. The medium diameter of aerosol is 0.1–0.3 μm. There is no limit for the type of aerosol and its dispersity. This standard is not suitable for the military and nuclear applications. In the military application, the oil mist efficiency can be used.

17.2.2.4 Mixed Multi-position Test

For the efficiency test of filters especially HEPA filters, the most common practice at home and abroad in the past is that only one sampling position is placed in the center of both the upwind side and the downwind side, respectively. The measured efficiency in this way is often high. And it is also difficult to find the leakage phenomenon. This is caused by the nonuniform distribution of concentration in the pipe. There are two main reasons that cause the nonuniform distribution of

Table 17.13 Test methods of air filters

				Test method			
Method	Aerosol type	Name	Particle size range	Instrument	Instrument performance	Instrument No.	Reading
Particle counting method	Polydisperse solid particles 0.3–0.5 μm (65 ± 5)% 0.5–1 μm (30 ± 3)% 1–2 μm (3 ± 1)% >2 μm (>1)%	Potassium chloride KCl (charge neutralized after spray)	0.3–10 μm	Particle counter	Particle counting efficiency for 0.3 μm PSL ≥ 50 %	One particle counter is used upstream and downstream of tested filter alternatively when the efficiency <90 % (≥0.3μm); otherwise two are needed	The reading downstream should be >100. Average concentrations are obtained for sampling three times both upstream and downstream with two instruments, which can be used to calculate the efficiency. In total two times of efficiency should be calculated. The difference between two efficiencies is shown in Table 17.14. For one instrument only, five sampling times are needed while other requirements are the same as above situation
Weight method	Polydisperse solid artificial particles	Artificial dust (see Table 17.15)	see Table 17.15	The weighting method			

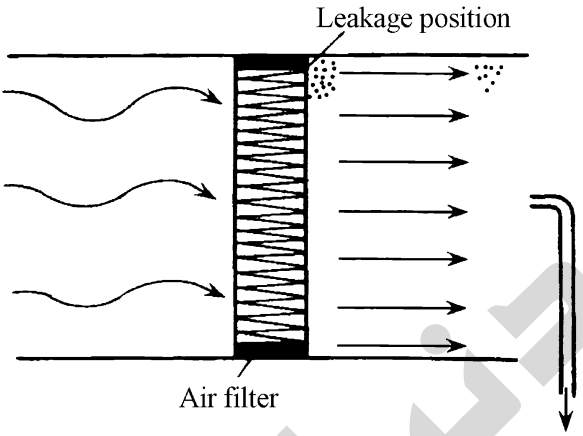

Fig. 17.18 Airflow state at the leeward side of the filter

Table 17.14 Particle counting efficiency

The 1st efficiency E_1	Difference between E_2 and E_1
< 40 %	$< 0.3E_1$
40–60 %	$< 0.15E_1$
60–80 %	$< 0.08E_1$
80–90 %	$< 0.04E_1$
90–99 %	$< 0.02E_1$
≥ 99 %	$< 0.01E_1$

concentration. First, the test aerosol particles generally come from a point source, so it is difficult to uniformly distribute on the cross section of the pipe. Second, with the effect of air filter, the airflow at the leeward side of the filter is much uniform, which is more significant for HEPA filters. With the characteristics of unidirectional parallel flow, the airflow with nonuniform distribution of concentration at upwind side passes through the filter, which will keep the original distribution. So it is difficult to mix fully at the cross section (see Fig. 17.18). So the result with this method will inevitably incorrect.

In order to improve this situation, experiment was performed to study different dust nozzles and different mixing methods [21]. Ten sampling points were placed along the center line at the cross section of the pipe. Concentrations N_t at each sampling point was measured. The arithmetic average value $\overline{N}$ of the measured concentrations was calculated. The deviation of the measured concentrations is expressed with $\left[\frac{N_t - \overline{N}}{\overline{N}} \times \frac{100}{100}\right]$. The bigger the deviation is, the worse the mixture effect is. The mixing effect on the upwind side of the filter is summarized in Table 17.16, which indicates that:

1. The mixing effect of the annular perforated nozzle, which is used to spray particles, is the best. The mixing effect of the linear perforated nozzle is almost

Table 17.15 Properties of artificial dust

Component	Mass ratio (%)	Specification of raw material	Particle size distribution		Property of raw material
			Size range (μm)	Percentage (%)	Chemical ingredients
Coarse particle	72	Road dust			SiO_2
			0–5	(36 ± 5)	Al_2O_3
			5–10	(20 ± 5)	Fe_2O_3
			10–20	(17 ± 5)	CaO
			20–40	(18 ± 3)	MgO
			40–80	(9 ± 3)	TiO_2
					C
Fine particle	23	Black carbon	0.08–0.13 μm		Iodine adsorption 10 mg/g–25 mg/g
					Oil absorption 0.4 mg/g–0.7 mg/g
Fiber	5	Short lint			Detached cotton fiber after treatment

Table 17.16 Comparison of mixing effect with various mixing means at the upwind side of filter

Generation location			Mixing means				
			Perforated plate (open ratio 0.2)		Stirring fan		
A (5*D* from filter)	B (2.5*D* from filter)	Nozzle shape	Without	With	Without	With	Max. deviation (%)
○		Ring multihole	○		○		20
○				○	○		12
○			○			○	17
○				○		○	4
	○		○		○		34
	○			○	○		7
	○			○		○	5
○		Linear multihole	○				28
○				○	○		11
○				○	○	○	4
	○		○				33
	○			○			19
	○			○	○	○	14
○		Single hole	○		○		24
○				○			13
○				○		○	10
	○		○		○		167
	○			○	○		55
	○			○		○	32

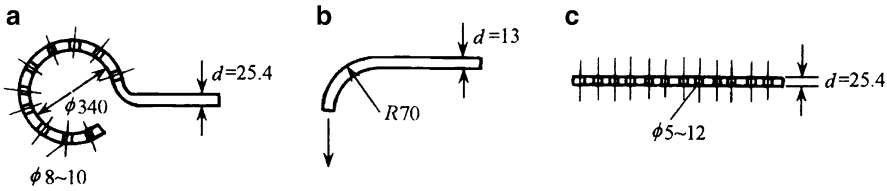

Fig. 17.19 Shapes of various nozzles

the same as that of the single-hole nozzle. The shapes of these nozzles are shown in Fig. 17.19.

2. It is better to place the sampling point at the windward side of air filter further. When the distance between this sampling point and the air filter is 5*D* (3 m, *D* is the pipe diameter), the biggest deviation is just 24 % even when single-hole nozzle is used without any other mixing means. But when the distance is 2.5*D* (1.5 m), the deviation reaches up to 167 %.
3. No matter what kind of dust nozzle is used and how much is the sampling distance is, the mixing effect improved when orifice plate or a mixing fan is used as the mixing method.

The uniform effect of the stirring fan is self-evident. The uniform effect of orifice plate is that the velocity field becomes uniform, which improves the uniformity of concentration field.

Let Δu_0 be the fluctuating velocity of the airflow upstream of the filter at the place far away from the orifice plate and Δu_1 the fluctuating velocity of the airflow downstream of the filter at the place far away from the orifice plate:

$$\frac{\Delta u_1}{\Delta u_0} = f \tag{17.17}$$

Obviously if $f = 0$, the fluctuation of airflow downstream is completely eliminated. Figure 17.20 is an experimental relationship between the air resistance coefficient ξ of the orifice plate and f [22]. Although the data are not concentrated, the curve such as the dotted line can still be plotted. It can be seen that ξ is about 2.5 when $f = 0$.

The value of ξ is closely related to the opening ratio. The differential pressure through the orifice plate is expressed as follows:

$$\Delta P = P_0 - P_1 = \frac{1}{2}\rho\left(u_1^2 - u_0^2\right) \tag{17.18}$$

$$u_1 = \frac{u_0}{cs} \tag{17.19}$$

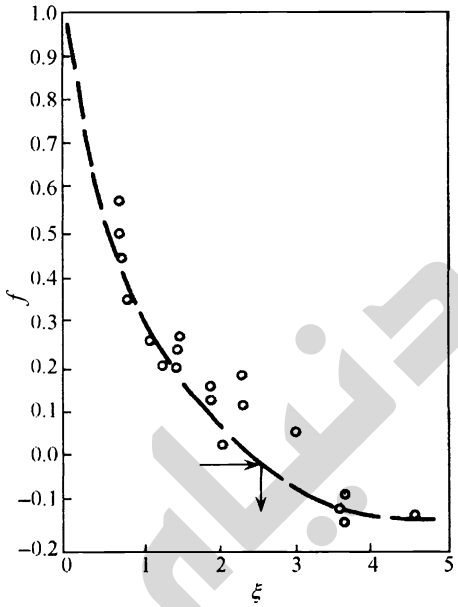

Fig. 17.20 Experimental relationship between ξ and f

where

u_0 and P_0 are the air velocity and the pressure at the windward side of orifice plate;
u_1 and P_1 are the air velocity and the pressure at the leeward side of orifice plate;
c is the contraction coefficient when airflow passes through the orifice plate, which is usually 0.9;
ρ is the gas density;
s is the opening ratio.

Substituting Eq. (17.19) into Eq. (17.18) becomes:

$$\Delta P = P_0 - P_1 = \frac{1}{2}\rho u_0^2 \left(\frac{1 - c^2 s^2}{c^2 s^2}\right) \tag{17.20}$$

Let

$$\xi = \frac{1 - c^2 s^2}{c^2 s^2} \tag{17.21}$$

It is the drag coefficient. In the above experiment, the opening ratio of the orifice plate is only 20 %, where only one plate was placed. If the opening ratio was increased or multiple orifice plates were placed in series, the effect will be better. Figure 17.21 shows the uniform velocity field with multiple orifice plates in series.

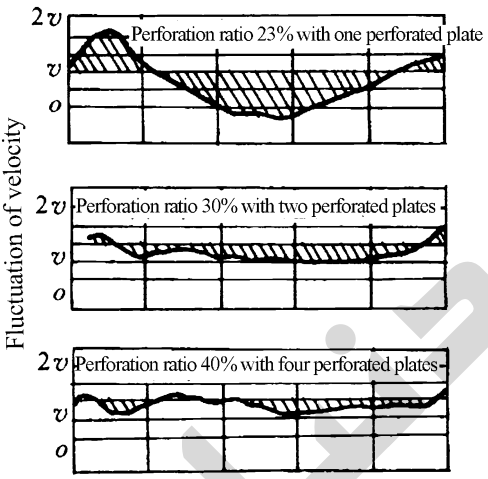

Fig. 17.21 Effect with orifice plates

Table 17.17 Comparison of the mixing effect with various means at the leeward side of filter

Sampler location	Leakage location			Mixing means				Max. deviation (%)
	Inner side of filter (close to the pipe center)	In the middle of filter	Outer side of filter (close to pipe wall)	Perforated plate (open ratio 0.4)		Stirring fan		
				Without	With	Without	With	
2.5*D* from filter (*D* is the pipe diameter)	○	○	○	○	○	○	○	65
	○		○	○	○	○	○	54
	○		○	○		○	○	75
				○			○	66
				○				140
								42
								58

Experimental results of the mixing effect at the leeward side of filter are summarized in Table 17.17. In the experiment, simulated leakage method was used so that leakage was forced from three positions of the cross section on the filter. (Leakage concentration is 0.03 mg/m^3. The leakage flow rate is for less than 0.2 % of the rated flow.) The results show that [23]:

1. The maximum deviation of measurement value appears when leakage appears on the edge of the filter and no mixing means was adopted.
2. When no mixing means is used at the leeward side of the filter, the maximum deviation of the measured results is about 65–140 %. By using the mixed means later, it reduces to 40–75 %, which is still not ideal.

When it is difficult to use any mixing means or the mixing effect is poor, the average method of three sampling positions is shown to be good at the consistent of the measured results [21]. The three sampling positions method is that sampling probes are placed in the central point of the trisection surface on the cross section of the pipeline, and then the mean value is calculated. From the measured data shown in Table 17.18, even if the single-hole nozzle is used, the maximum deviation at the windward side also drops from 167 to 11 %. Therefore, three sampling positions method is worthy consideration when filter efficiency is measured.

17.2.2.5 Total Measurement Error

If the measurement errors of air filter with upstream concentration N_1 and downstream concentration N_2 are σ_1 and σ_2, respectively, the maximum efficiency $\eta_{\max}$ and the minimum efficiency $\eta_{\min}$ can be expressed as:

$$\eta_{\max} = 1 - \frac{(1-\sigma_2)N_2}{(1+\sigma_1)N_1}$$

$$\eta_{\min} = 1 - \frac{(1+\sigma_2)N_2}{(1-\sigma_1)N_1} \tag{17.22}$$

So the positive error $\Delta\eta$ of efficiency and the negative error $-\Delta\eta$ can be deduced as follows:

$$\begin{aligned}\Delta\eta = \eta_{\max} - \eta &= \frac{(1+\sigma_1)N_1 - (1-\sigma_2)N_2 - (1+\sigma_1)(N_1 - N_2)}{(1+\sigma_1)N_1} \\ &= \frac{(\sigma_1+\sigma_2)N_2}{(1+\sigma_1)N_1} = \frac{\sigma_1+\sigma_2}{1+\sigma_1} \times \frac{N_1 - (N_1 - N_2)}{N_1} \\ &= \frac{\sigma_1+\sigma_2}{1+\sigma_1} \times \left(1 - \frac{N_1 - N_2}{N_1}\right) \\ &= \frac{\sigma_1+\sigma_2}{1+\sigma_1} \times (1-\eta)\end{aligned} \tag{17.23}$$

Also, we can get:

$$-\Delta\eta = \eta - \eta_{\max} = -\frac{\sigma_1+\sigma_2}{1-\sigma_1}(1-\eta) \tag{17.24}$$

According to the error theory, both σ_1 and σ_2 in the above formula can be expressed as follows:

$$\sigma_1(\text{or } \sigma_2) = \sqrt{\sigma_a^2 + \sigma_b^2 + \sigma_c^2 + \sigma_d^2} \tag{17.25}$$

Table 17.18 Effect of three sampling positions method

	Upstream			Downstream			
Nozzle	Generation location (distance from filter)	Max. deviation with the one sampling position method /%	Max. deviation with the three sampling positions method a' (%)	Leakage position	Max. deviation with the one sampling position method /%	Max. deviation with the three sampling positions method b' (%)	Comprehensive error with the three sampling positions method ($a' + b'$) (%)
Single hole	2.5*D*	167	11.3	a	65	12	23
				b	66	8.3	20
				c	140	12	23
	5*D*	24	0.8	a	65	12	13
				b	66	8.3	9
				c	140	12	13
Linear multihole	2.5*D*	33	11.3	a	65	12	23
				b	66	8.3	20
				c	140	12	23
	5*D*	28	4.3	a	65	12	16
				b	66	8.3	13
				c	140	12	16
Ring multihole	2.5*D*	34	0.3	a	65	12	12
				b	66	8.3	9
				c	140	12	12
	5*D*	20	2.2	a	65	12	14
				b	66	8.3	11
				c	140	12	14

where

σ_a is the error caused by the variation of the flow rate and the particle concentration through the air filter with time, weather conditions, or other factors. According to the practical experience, during the measurement time, the resultant error for particle concentration can reach 20 %. It can generally be considered as 10 %;

σ_b is the error of the sampling flow rate for instrument such as particle counter. As pointed out before it is about 3 %;

σ_c is the error caused by non-isokinematic sampling. According to the previous analysis, the average value is 5 %;

σ_d is the error caused by particle loss in sampling tubes. According to the previous analysis, in general it is not more than 3 %.

As for the overlapping error of particle counter, it should be considered under specific condition.

For efficiency test of air filter, we can consider that $\sigma_1 = \sigma_2$ and suppose $\sigma_a = \pm 10\,\%, \sigma_b = \pm 3\,\%, \sigma_c = \pm 5\,\%$, and $\sigma_d = \pm 3\,\%$. Substituting them into Eq. (17.25) becomes:

$$\sigma_1 = \sigma_2 = \sqrt{0.1^2 + 0.03^2 + 0.05^2 + 0.03^2} = \sqrt{0.0143} = 0.12$$

When it is inserted into Eqs. (17.23) and (17.24) and suppose $\eta = 0.999$, we obtain:

$$\Delta\eta = \frac{0.12 + 0.12}{1 + 0.12}(1 - 0.999) = 0.00021$$

$$-\Delta\eta = \frac{0.12 + 0.12}{1 - 0.12}(1 - 0.999) = -0.00027$$

So the filter efficiency should be within the range (0.999 − 0.00027)–(0.999 + 0.00021), namely, (0.99873–0.99921).

If σ_1 reaches 20 %, the efficiency is between 0.99847 and 0.99935.

It is clear that even with larger errors for individual measurement item, the total error for efficiency measurement is still acceptable.

17.2.3 Measurement of Dust Holding Capacity of Filter

Dust holding capacity W can be calculated by the following formula:

$$W = W_1 - W_2(\mathrm{g}) \tag{17.26}$$

where

W_1 is the weight of air filter at the end of the test, according to the requirement of dust holding capacity (see Chap. 4) (g);
W_2 is the weight of air filter quality (g) before the test for dust holding capacity.

With the value of W, we can calculate the dust holding capacity per unit area.

In order to shorten the test time, artificial dust is used as the test dust source for the dust holding capacity measurement, which is mainly the process dust and the simulated atmospheric dust. For the test of air filters in air-conditioning system and air purification technology, the simulated atmospheric dust is used as the test dust source. In terms of the blockage effect on air filter, three main components are contained to simulate the atmospheric dust. The first one is the mineral and the sand particles, which are the main component of atmospheric dust. Because they easily spread into the air, they are used to represent the inorganic noncombustible material, which occupies the most part in the simulated atmospheric dust. The second one is the carbon black. It is used to represent the free carbon in air, which is representative of the pollution effect of atmosphere and is the representative component of the atmospheric dust in industrial and urban region. Usually it occupies about 1/4. Because it is small and easy to coagulate, it is the important reason for the clogging of filter. It is also indispensable for the performance evaluation of the dust holding capacity. It is also essential in the simulated atmospheric dust. The third one is fiber. It represents the organic component in air, which can speed up the clogging of filter. So it should also be included in the simulated atmospheric dust. It only occupies several percentages.

AFI test dust was proposed by NAFA (National Air Filtration Association) in the USA, which is close to the urban atmospheric dust. It mainly contains mineral substances such as silica and others, and carbon black and batting.

Japan Air Cleaning Association specified the performance test method standard for air cleaning device. During the test of the dust holding capacity, the Type 15 dust from Japanese Industrial Standards (JIS) is used, which is made up of Type 8 dust, Type 12 dust, and cotton. Type 8 dust (also Type 7 dust and Type 11 dust) is the burnt East Asian clay which is ground to obtain the specified particle size distribution. The medium diameter is 8 μm, and the geometric standard deviation is $\sigma_g = 3.63$ (the composition and the real density of Type 7 dust and Type 11 dust are the same as Type 8 dust, and the particle size distributions are different). Type 12 dust is the carbon black. So East Asian clay is used as the test dust, because it does not easily adhere to the surface and easily disperse in the air and not easily coagulate.

The characteristics of the simulated atmospheric dust in the USA and Japan are shown in Table 17.19.

In order to compare the characteristics of the simulated dust and the atmospheric dust, the simulated dust is heated to 300 °C so that the carbon black is burnt off. Then, analysis is carried on. Some agencies in China have tried to use the simulated atmospheric dust which is made of 75 % anthracite-pulverized coal and 25 % carbon black. From the above analysis, the characteristics of this simulated dust are very different from that of the atmospheric dust. They are more likely to

Table 17.19 Characteristics of the simulated atmospheric dust in the USA and Japan

Test aerosol	Composition percentage					
Japan: JIS-15 type	JIS-8 type	72 %	JIS-12 type	25 %	Cotton fiber	3 %
Composition	SiO_2	34–40 %	Carbon black			
	Fe_2O_3	17–23				
	Al_2O_3	26–32				
	CaO	0–3				
	MgO	3–7				
	TiO_2	0–4				
	Scorching hot loss	0–4				
Particle size	0–5 μm	39 ± 5 %	0.03–0.2 μm		Smaller than 1.5 μm (diameter) × 1 mm (length)	
	5–10	18 ± 3				
	10–20	16 ± 3				
	20–30	12 ± 3				
	30–40	6 ± 3				
	40–74	below 9				
Density			2.7			
USA: AFI	Coarse particle	72 %	K-1 type carbon black	25 %	7 type cotton fiber	3 %
Composition	SiO_2	68.47 %	Airborne matter	3 %		
	Fe_2O_3	4.58	Non-airborne matter	95		
	Al_2O_3	15.98	Ash	2		
	CaO	2.91				
	MgO	0.77				
	Alkali	4.61				
	Scorching hot loss	2.68				
Particle size	0–5 μm	39 ± 2 %				
	5–10	18 ± 3				
	10–20	16 ± 3				
	20–40	18 ± 3				
	40–80	9 ± 3				
Density			2.2			

coagulate than the ordinary atmospheric dust. So filters are easily to be clogged. During the efficiency test, high value is likely to be obtained.

Before the year 2008, the artificial dust used for measuring the dust holding capacity in China was specified in the national standard *Test Method of Air Filter Performance in General Ventilation*, which is shown in Table 17.20. After 2008, the artificial dust specified in Table 17.15 is used.

Figure 17.22 shows the experimental curve [24], which explains what kind of the dust source can be used as the dust source for measuring the dust holding capacity. From three groups of curves among curves 1, 2, and 3, we can see that:

1. The filter is clogged very quickly by small particles.

Table 17.20 Leakage criteria with penetration in ISO 14644-3

Whole penetration (%)	Factor K	Calculated penetration for leakage position (%)
≤0.05	10	≤0.5
≤0.005	10	≤0.05
≤0.0005	30	≤0.015
≤0.00005	100	≤0.005
≤0.000005	300	≤0.0015

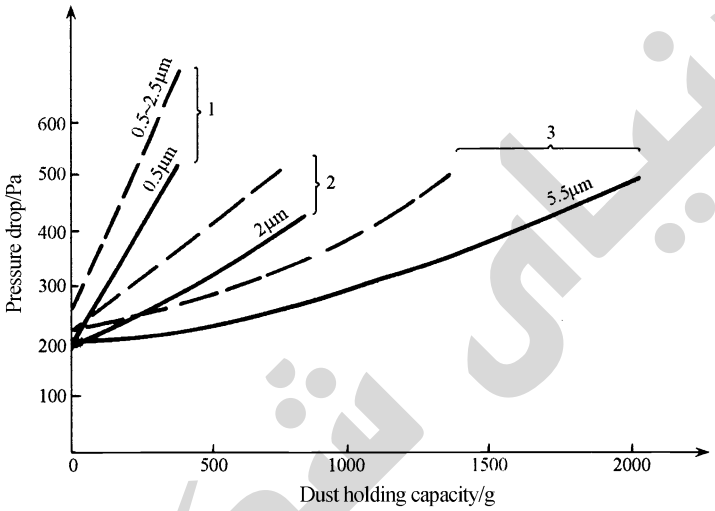

Fig. 17.22 Influence of different test dust on dust holding capacity. *1* carbon black, *2* atmospheric dust, *3* certain test dust

2. Carbon black is more likely to clog air filter than atmospheric dust.

It shows that filter's actual lifetime is longer than the experiment value with carbon black. Therefore, the characteristics of simulated atmospheric dust used for measuring the dust holding capacity must be close to that of the true atmospheric dust as much as possible.

17.3 Leakage Detection

17.3.1 Leakage Detection of HEPA Filter

17.3.1.1 Implication of Leakage on Air Filter

When leakage is mentioned for the air filter unit, it includes the leakage on the filter media and the glue between the filter media and the filter frame. When leakage is

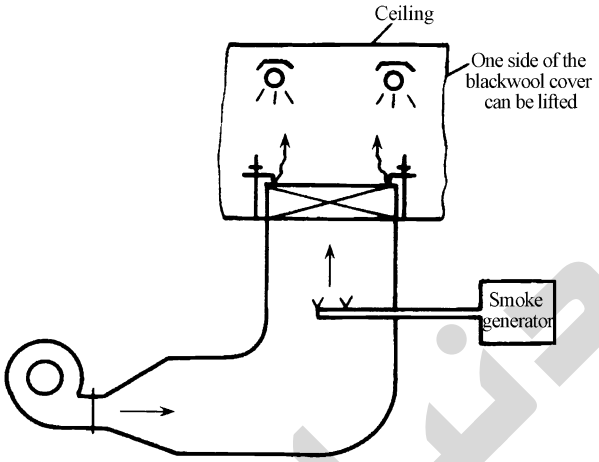

Fig. 17.23 Schematic diagram of the leakage detection equipment with light

mentioned for the air filter which is already installed, except for the above leakage positions, it also includes the leakage between the sealing surface of the filter frame and the installation frame and between the wall board where the installation box is placed and the installation frame.

Leakage on terminal air filter is a fatal quality problem for cleanroom and the air cleaning equipment. So the leakage of air filter is an important topic for the air cleaning technology.

17.3.1.2 Leakage Detection Method

There are usually several methods as follows to detect the leakage of HEPA filters:

Leakage Detection with Light

This method is only suitable for qualitative leak detection of air filter unit (or called initial check).

HEPA filter is installed on the leak detection device with light, which is shown in Fig. 17.23. It is covered with black velvet around. One side of the cover can be lifted so that the inspector can stretch out his head inside for visualization. Airflow with smoke passes through the filter with the velocity of 1 cm/s. If there is a leakage pore, the fume will be seen with the black background. This method is sensitive, and leakage with small flow rate can be detected. Smoke needs to be supplied continuously, so both the cigarette smoke and the incense smoke can be used.

Leakage Detection with Double Flow Rates

This method is also used for the leakage detection of air filter unit. With the condition of good mixture at leeward side of air filter, the efficiencies at both the

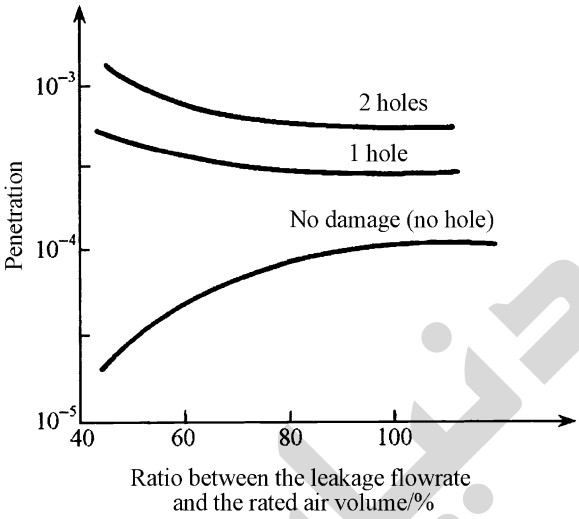

Fig. 17.24 Relationship between the leakage flow rate and the penetration

rated airflow and partial of the rated airflow are measured. If the latter is lower than the former, there is leakage hole on air filter, or the air filter is unqualified, or the scanning detection for leakage should be performed.

With the rated airflow, the resistance across the small hole is high, and the leakage cannot be detected with the leakage flow rate. The resistance of the filter paper is linearly proportional to the filtration velocity. According to the fluid dynamics, the resistance of the small hole is linearly proportional to the square of the air velocity. Suppose the ratio of air velocities before and after the flow rate is reduced is m, the resistance after the flow rate is reduced becomes $1/m^2$ of the original value. The flow rate through the small hole increases by about m times compared with the original value. The concentration at the cross section may increase, which means there is the leakage. Figure 17.24 proves the above reason [25].

For filters with no leakage holes, the lower the air velocity is, the lower the penetration is. The extent of decrease may be different (see the section about paper filter in Chap. 4). For filters with leakage holes, with the lower air velocity, the relative flow rate through the hole, namely, the leakage flow rate, becomes larger, so the penetration increases. In order to detect the leakage easily, it is hoped that two penetration values with these two air velocities differ a lot (because the fluctuation of the measurement data may also be 1 time). So in the US Federal Standard 209B, the flow rate for leakage diction was specified to be 20 % of the rated airflow. If the flow rate cannot be regulated to such low value, a little more flow rate can also be used. It is shown from Fig. 17.24 that if the airflow rate for leakage detection increases to 30 % of the rated airflow (try to extend the curve to the left side), the penetration can be more than 3 times of that with the rated airflow, which can be used to distinguish the leakage without any difficulty. Of course, since the leakage hole sizes are different, it is very difficult to determine the exact flow rate for leakage detection.

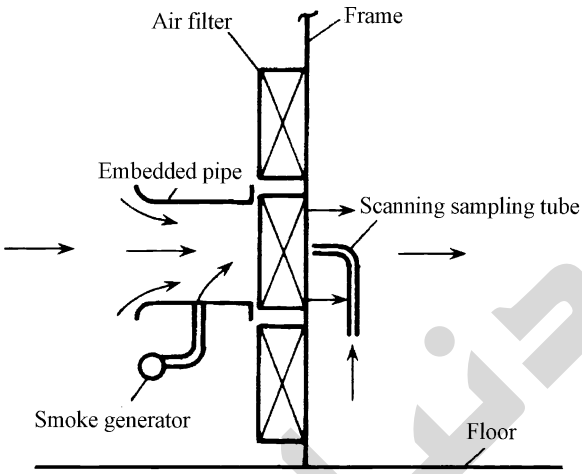

Fig. 17.25 Schematic diagram of leakage detection using smoke generation casing

Leak Detection with Scanning Method

This method is applicable for the leakage detection of both the filter unit and the mounted filter equipment. During the scanning process on filter unit, the leakage detection device with light can be used without the screen curtain. It is better to turn the device around so that filter is placed vertically to the ground, which facilitates the testing. When the combined equipment of air filter is tested and it is difficult to generate smoke upstream of the whole cross section since the upstream concentration needs to be increased, a smoke generation casing can be used at the back of each filter (see Fig. 17.25). Move it to the other filter when the measurement is finished on this filter.

During the leakage detection, it requires that the sampling probe is placed at 2–3 cm from the leeward-side surface of HEPA filter. Scanning is proceeded along the entire surface, the frame, and frame joint. Scanning speed should be 2–3 cm/s, which should not be larger than 8 cm/s and less than 0.5 cm/s. The scanning trajectory is shown in Fig. 17.26, where the trajectory can be overlapped to a certain extent.

When the leakage position is found, materials including the CPVC adhesive, No. 88 adhesive, No. 703 and No. 704 adhesive can be used to completely stop the leakage in site. However, the silicone rubber adhesive cannot be used in some electronic industrial production workshop, because they contain silicon component. Of course, this is only useful for surface leakage. When it is not allowed to seal the leakage hole, the air filter must be replaced.

One kind of leakage detection device for filter unit in foreign country is shown in Fig. 17.27 [26]. Of course, other aerosol can also be used as the artificial dust. This kind of special device is especially suitable for manufacturers and large project field.

Figure 17.28 shows the shape of automatic (also include the manual type) leakage detection device produced in China.

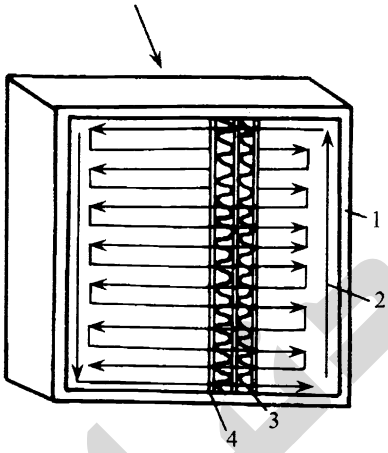

Fig. 17.26 Scanning trajectory. *1* outside frame, *2* scanning routine, *3* filter media, *4* separator

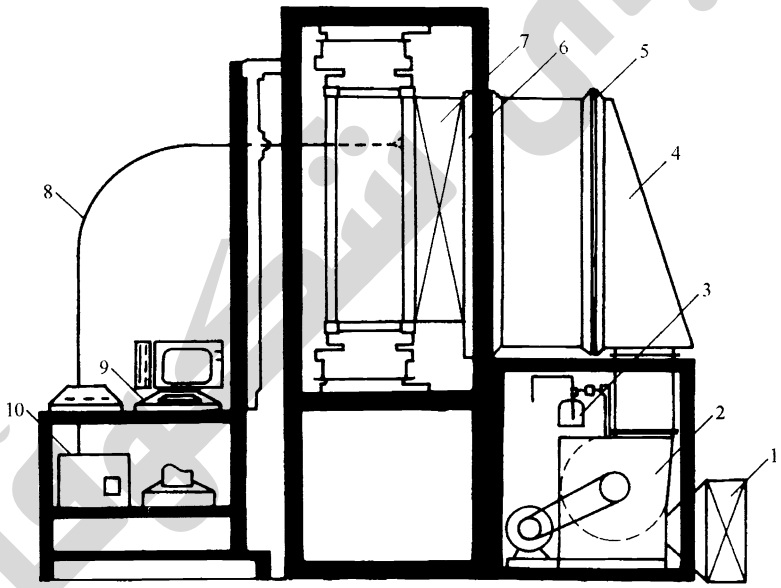

Fig. 17.27 Example of leakage detection device for HEPA filter. *1* prefilter, *2* fan, *3* Laskin DOP generator (also called as the cold generator, see page 353 of Ref. [11]), *4* transition section, *5* rectification plate, *6* separator, *7* tested filter, *8* sampling pipe, *9* computer, *10* particle counter

17.3.1.3 Leakage Detection Tester and Aerosol

There are two kinds of leakage detection testers, including the photometer and the discrete particle counter. ISO 14644-3 has already pointed out that:

Fig. 17.28 SX-F1260 on-site HEPA leakage tester

1. Photometer with DOP can be used to detect leakage for filters with penetration $\geq$0.005 %, which corresponds with HEPA filters whose MPPS efficiency is not larger than 99.995 % (which is equivalent with Type B and C filters in China).
2. Photometer with DOP can be used in the applications where the gas released from the volatile organic test aerosol deposited on filter and pipeline has no harmful effect on the product and the process inside the cleanroom, such as the leakage detection of air filter in nuclear facility.
3. Particle counter with artificial aerosol is suitable for the leakage detection of filter with penetration $\leq$0.0000005 %, which corresponds with filters whose efficiency is equal or larger than 99.9999995 % (with MPPS particles).
4. The method to use particle counter is more sensitive than the photometer. The resultant pollution is smaller. For leakage detection, it is more accurate and fast.
5. There are more than eight kinds of aerosol for leakage detection, such as phthalates, diethyl sebacate, PSL spheres, and atmospheric dust.

In the version published in 2008, it pointed out that when the atmospheric dust concentration is appropriate, particle counter can be used to detect the leakage with atmospheric dust.

17.3.1.4 Leakage Criteria with Penetration

For a long time, the leakage criteria are that when the penetration is larger than several times of the ordinary penetration of the whole filter media. As for the filter media, there is allowable common penetration. Once the penetration is larger than this value, it is considered as abnormal. But there is also fluctuation for common penetration. Therefore, the artificial magnification value is defined, and leakage occurs when the penetration is larger than it.

In the 1960s, the sampling flow rate of particle counter was 700 mL/min. Some foreign company specified that the leakage occurred when the penetration was five times larger.

In the Chinese Industrial Standard GB50591-2010 *Code for construction and acceptance of cleanroom*, the leakage criteria were also based on several times of the common penetration value.

In ISO 14644-3 published in 1999, the leakage criteria with penetration were specified, which is shown in Table 17.20. The factor in this table is the magnification of the leakage penetration compared with the whole penetration. When the magnification of penetration is larger than this factor, leakage occurs. At the same time, the sampling flow rate is specified as 28.3 L/min. This method is called the penetration method temporarily.

17.3.1.5 The Essence of Leakage

For a filter without leakage, no matter how much is the sampling flow rate, the particle number per unit liter of sampled air, namely, the concentration, is almost consistent (including the common fluctuation).

However, the penetration at the leakage position is related to the sampling flow rate. In the sampled airflow, there is the airflow from the leakage position, and there is also clean air through the filter ordinarily which occupies a large proportion. The larger the sample flow rate is, the more the clean air is. Since the number of particles through the leakage position is constant (for the given size of leakage hole and the given filter structure with known damage, when the differential pressure is constant, the leakage flow rate is constant), the penetrated particles will be diluted. In terms of this sample flow rate, when the local particle concentration decreases, the local penetration is correspondingly reduced.

For example, for a HEPA filter with the highest level according EU standard, if the penetration is 0.000005 % and the upstream particle concentration reaches 2×10^7#/L, the common penetration with the requirement in Table 17.20 is $\leq$1#/L.

According to ISO standard, the leakage appears when the penetration for the leakage position reaches 301 times of the ordinary penetration for this filter, while there is no leakage when it is 300 times.

Suppose there is a leakage hole with the leakage flow rate 8,490#/min. When the sampling flow rate downstream is 1 L/min, the sampled concentration at the leakage position is 8,490#/L. Since the factor is 8,490, it is of course considered as filter with leakage.

When the sampling flow rate downstream changes to 2.83 L/min, the sampled concentration at the leakage position is 3,000#/L. Since the factor is 3,000, it is of course also considered as filter with leakage.

When the sampling flow rate downstream is 28.3 L/min, the sampled concentration at the leakage position is 300#/L. Since the factor is 300, it is considered as filter without leakage according to the standard.

Since the leakage flow rate is a fixed value, i.e., 8,490#/min, the conclusions of the leakage detection cannot be different when the sampling flow rate is different.

It is shown that the leakage conclusion with the penetration is closely related to the sampling flow rate. So it is meaningless when the leakage conclusion is given when only the factor value is mentioned.

The reason is that the final sampled leakage concentration is diluted by the sampling flow rate 2.83 L/min or 28.3 L/min. The dilution factors by different sampling flow rates are of course different.

The most intuitional understanding is that leakage exists objectively. It exists when it is compared with non-leakage.

The essence of leakage is that under the certain differential pressure and the particle concentration upstream, the particle concentrations downstream are basically uniform for a complete air filter without leakage. If apparent nonuniform distribution appears, leakage is likely to exist. For a complete air filter, particles measured locally are almost continuous, and most of the time it is "0." This is the purpose to use HEPA filter. But if at local position particles can be detected, leakage hole exits at this place which is corresponding to the upstream concentration.

17.3.1.6 Leakage Criteria with the Leakage Flow Rate Through Hole

With the above analysis, we proposed the leakage criteria based on the particle penetration rate based on the flow rate through the leakage hole [27, 28]. This method is termed as the leakage hole method (also called the penetration rate method).

From the electronic microscopic photo of HEPA filter paper in Chap. 3, the grid formed by glass fiber is random with different sizes. But it is shown that the length of single layer of grid can reach 30 μm.

The so-called leakage means the passage or the hole is formed by friction and prick on the fibrous grid. The outflow is formed through the hole, where the flow rate is larger than that through the normal multi-layer fibrous grid.

The outflow Q through the hole can be expressed with the classical formula as shown in Eq. 17.27:

$$Q = \mu F \sqrt{\frac{2\Delta p}{\rho}} \tag{17.27}$$

where

F is the hole area, $A = 0.78 d_0^2$;
d_0 is the hole diameter;
Δp is the differential pressure across the air filter (also the leakage hole). For the initial resistance during leakage detection, it is 200 Pa;
ρ is the air density, 1.2 kg/m^3;
μ is the flow rate coefficient, which is calculated with the following expression:

$$\mu = \varepsilon\varphi$$

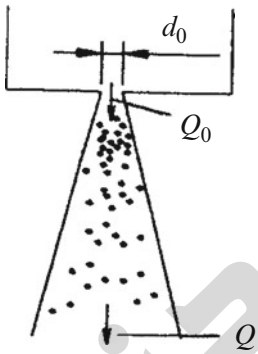

Fig. 17.29 Airflow through the leakage hole

where ε is the contraction coefficient. It is a kind of complete contraction since the surrounding area of the hole is spacious, according to the definition of the fluid dynamics. The value of ε is the minimum, i.e., 0.62.

φ is the flow rate coefficient, and the theoretical value is 0.82. The maximum value can be 1. The experimental maximum value is 0.97. For the expansion hole with the expansion angle 5°– 7°, it is 0.45. For the crack and the hole with complex structure, the average experimental minimum value is 0.29. For the small leakage hole, which is only several times larger than the single layer of fiber grid, the influence of the complex fibrous edge of the hole is large. So the resistance becomes larger, and the flow rate coefficient becomes smaller. With the minimum value of φ, we can obtain that $\mu = \varepsilon\varphi = 0.62 \times 0.29 = 0.18$ (in Ref. [27], the value for the hole with diameter larger than 0.1 mm was assumed $\varphi = 0.97$).

For the leakage hole shown in Fig. 17.29, it is simplified as a hole perpendicular with the surface of the airflow at the outlet face.

The cross section of the leakage airflow increases gradually, so the concentration is diluted gradually. This airflow is called the polluted airflow. This is caused by the induction of surrounding airflow. But this kind of expansion is not unlimited. When the air velocity at the boundary of the polluted airflow is close to that of the surrounding airflow, the induction effect stops.

Therefore, when the average velocity at the cross section of the polluted airflow decays to the supplied velocity at the outlet of the HEPA filter, expansion and dilution cannot be continued. Since the influence of the leakage airflow on the unidirectional flow is more prominent, the case with the unidirectional flow cleanroom is used as the basis. Suppose the supplied air velocity at the outlet of HEPA filter is 0.5 m/s, a series of parameters can be obtained with the jet flow theory, which is shown in Table 17.21.

In the table, Q_0 is the leakage flow rate; S is the air supply range, which is the distance when the boundary of jet flow does not expand; D is the diameter of the cross section when the boundary of jet flow does not expand; and Q is the flow rate of the polluted airflow at the place S after the leakage airflow expands and dilutes gradually.

Table 17.21 Various parameters for the jet flow of the leakage airflow

d_0 (mm)	Q_0 (L/min)	S (mm)	D (mm)	Q/Q_0
0.0085	0.000011	0.091	0.058	4.43
0.01	0.000015	0.11	0.068	4.43
0.05	0.00038	0.54	0.34	4.43
0.053	0.000427			
0.06	0.00054			
0.097	0.00144			
0.1	0.0015	4.02	2.29	4.43
0.11	0.0017			
0.15	0.0033			
0.17	0.0042			
0.19	0.005			
0.2	0.006	8.04	4.58	4.43
0.25	0.0094			
0.3	0.0135			
0.6	0.054	24.13	13.73	4.43
0.93	0.13			
1.0	0.15	40.22	22.28	4.43

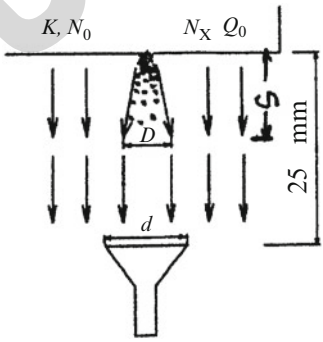

Fig. 17.30 The situation when the expansion distance is less than 25 mm, $D < d$

Reference [27] presented three types of situations for the sampling probe during leakage detection process. The most common situation is the place 1 mm from the leakage hole, which is shown in Fig. 17.30.

When the sampling flow rate is larger than the dilution flow rate during the arrival of the polluted airflow to the sampling probe, all the penetrated particles will enter the sampling probe. Since the leakage flow rate Q_0 is very small, most of the sampling flow rate is the clean airflow from the surrounding area, so the sampled concentration will be reduced greatly. Suppose the sampling flow rate is W L/min, the sampled concentration is

$$N_s = \frac{(W - Q)N_0K + N_x}{W} \tag{17.28}$$

where

N_s is the sampling concentration, #/L;
N_x is the penetrated particle number, $N_x = Q_0 N_0$, #;
W is the sampling flow rate, L/min.

According to the nonzero test principle for the minimum measuring volume introduced in previous chapter, the average concentration in each sampling volume should reach 3, and 95 % of the readings are nonzero values, which can be determined as leakage. This is the essence of the leakage hole method (also called the penetration method).

17.3.1.7 Leakage Detection with the Scanning Method

It is obvious that it is quite difficult to detect the real leakage position during the scanning process which goes on quickly. As mentioned before, most readings at the place without leakage are "0." When nonzero reading is found, the value is at least 1, which may be the possible leakage position. Reference [27] gives the characteristic parameter of the leakage, which is basically the same as ISO standard. The necessary upstream concentration N_0 for sampling particles $\geq$1# during the scanning process is calculated with the following formula:

$$N_0 Kt\left(W - Q_0 \frac{Q}{Q_0}\right) + Q_0 N_0 t \geq 1$$

where

t is the scanning time, min. $t = B/(60v)$;
W is the sampling flowrate, L/min, which is usually 2.83 or 28.3;
B is the side length of the sampling probe along the scanning direction, cm;
v is the scanning velocity, cm/s.

So we obtain:

$$N_0 \geq \frac{1}{\left[K\left(W - Q_0 \frac{Q}{Q_0}\right) + Q_0 N_0\right] \frac{B}{60v}} = \frac{1}{\frac{Q_0 B}{60v}} = \frac{60v}{Q_0 B} \tag{17.29}$$

It is shown from the above equation that when the leakage hole is smaller, Q_0 becomes larger and the value of N_0 needed is larger.

Only when $K > 0.0001$, $K\left(W - Q_0 \frac{Q}{Q_0}\right)$ is meaningful relative to Q_0. From HEPA filters, K decreases from 0.00001 (similar as Type A filter in China). So in above formula, $K\left(W - Q_0 \frac{Q}{Q_0}\right)$ can be omitted.

The upper limit of upstream concentration is related to the whole penetration of air filter. With this upstream concentration, the common penetration should be significantly different from the possible leakage value 1#, such as 0.1–0.2#. In this way, particles can be detected in all the leakage positions, while in other places, no particles will be detected.

According to the analysis of Sect. 4.7, HEPA filter is defined as those with particle counting efficiency larger than 99.9 % for 0.3 μm particles, which is the so-called three 9 filter. The efficiency for particles ≥0.5 μm can be approximated as 99.999 % (five 9 filter). (The three 9 filter has efficiency 99.9975 %.)

Therefore, the upstream concentration of HEPA filter should not be >20,000#/L, while the upper limit for the UPLA filter with eight 9 efficiency (for particles ≥0.5 μm) is extremely large, so no limit is made for this kind of filter.

17.3.1.8 Leakage Detection at Fixed Position

After possible leakage position is found, leakage detection at fixed position must be performed with Fig. 17.30. The sampling concentration at fixed position should be calculated with Eq. (17.29).

For example, when it is just determined as leakage with the leakage hole method, will it also be determined as leakage with the penetration method?

For a ULPA filter with $K \leq 0.000005$ %, when the sampling flow rate is 28.3 L/min according to ISO standard, the sampling concentration for the 0.5 mm leakage hole is

$$\begin{aligned} N_s &= \frac{(28.3 - Q)N_0K + Q_0N_0}{28.3} \\ &= \frac{(28.3 - 0.00038 \times 4.57) \times 8000 \times 5 \times 10^{-8} + 0.00038 \times 8,000}{28.3} \\ &= 0.107\#/\mathrm{L} \end{aligned}$$

So according to the penetration method, it is determined that the leakage penetration is 0.107/8,000 = 0.0013 % < 0.0015 %, which can be used to judge that there is no leakage.

But according to the leakage hole method in this section, when the upstream concentration is 8,000#/L, the sampled particle number is 3.42# when the particle counter with the sampling flow rate 28.3 L is used, which is ≥3#. It is judged as leakage.

When the size of the leakage hole increases to 0.053 mm, the sampling concentration becomes:

$$N_s = \frac{(28.3 - 0.00427 \times 4.37) \times 8,000 \times 5 \times 10^{-8} + 0.00427 \times 8,000}{28.3} = 0.121\#/\mathrm{L}$$

According to the penetration method, the leakage penetration is 0.121/8,000 = 0.00151 %, which is >0.0015 %. It is determined as leakage.

When the upstream concentration becomes 9,000#/L or 10,000#/L, the leakage penetration is still 0.00151 %. In the above examples, the upstream concentration changes while the leakage penetration remains the same.

For a ULPA filter with $K \leq 0.00005$ %, when the leakage hole size is 0.075 mm, it is determined as leakage with the leakage hole method. While the penetration is 0.003 %, which is <0.005 %, so it is without leakage with the penetration method.

When the leakage hole size increases to 0.97 mm, it is judged as leakage with the leakage hole method, and it is also determined leakage with the penetration method since the penetration is 0.0051 %, which is >0.005 %.

For a ULPA filter with $K \leq 0.0005$ %, when the leakage hole size is 0.1 mm, it is determined as leakage with the leakage hole method. While the penetration is 0.0053 %, which is <0.015 %, it is without leakage with the penetration method. When the leakage hole size increases to 0.17 mm, it is judged as leakage with the leakage hole method, and it is also determined leakage with the penetration method since the penetration is 0.0155 %, which is >0.015 %.

For a HEPA filter with $K \leq 0.005$ %, when the equivalent diameter of the leakage hole is 0.25 mm, the sampling concentration is:

$$N_s = \frac{(28.3 - 0.0094 \times 4.37) \times 400 \times 5 \times 10^{-5} + 0.0094 \times 400}{28.3} = 0.152\#/\mathrm{L}$$

With the leakage hole method, when the upstream concentration is 400#/L and the sampled particle number is 4.32# with the sampling flow rate 28.3 L/min, it is ≥3#, which can be determined as leakage.

According to the penetration method, the leakage penetration is 0.15/400 = 0.038 %, which is smaller than 0.05 %. So it is without leakage.

When the leakage hole size increases to 0.3 mm, we obtain:

$$N_s = \frac{(28.3 - 0.0135 \times 4.37) \times 300 \times 5 \times 10^{-5} + 0.0135 \times 300}{28.3} = 0.158\#/\mathrm{L}$$

With the leakage hole method, when the upstream concentration is 300#/L and the sampled particle number is 4.47# with the sampling flow rate 28.3 L/min, it is ≥3#, which can be determined as leakage.

According to the penetration method, the leakage penetration is 0.158/300 = 0.052 %, which is larger than 0.05 %. So it is also judged as leakage.

Although the penetration value changes, by the calculation of HEPA filter with $K \leq 0.05$ %, the conclusions with both methods for the leakage hole with diameter 0.93 mm are that there is leakage on the filter. When the upstream concentration is 30#/L and the penetrated particle number is 4.3# in the sampling air volume, the penetration is 0.51 %, which is >0.5 %, so it is judged as leakage. From the above calculation examples, we know that as only as the leakage flow rate remains the same, the penetration calculated with the penetration method is the same, no matter how much is the upstream concentration. This means the penetration is only related to the leakage flow rate. This also means it is the essence of leakage when the leakage flow rate through the leakage hole is used for determination.

According to the result from past research, no matter what the penetration is, the conclusion of leakage occurrence can be made when the detected particle number is ≥3# with the fixed detection position. It is of course the strictest requirement. But in order to be equivalent with ISO standard, the equivalent diameter of the leakage hole is specified for various HEPA filters when they are judged to have leakage, which is shown in Table 17.22.

Table 17.22 The minimum equivalent diameter of the leakage hole and Q_{0min}

K %	D_{0min} (mm)	Q_{0min} (L/min)
≤0.05	0.93	0.13
≤0.005	0.3	0.0135
≤0.0005	0.17	0.0042
≤0.00005	0.097	0.00144
≤0.000005	0.053	0.000427

Table 17.23 Possible minimum upstream concentration

K %	N_{0min} (#/L)
≤0.005–0.05	556
≤0.0005	1,786
≤0.00005	5,208
≤0.000005	17,564

Both v and B should be determined according to the specific condition and may be adjusted with Eq. (17.29), and the value of Q_{0min} should remain the same for this kind of air filters. The maximum value of B can be adjusted to 4 cm, and the minimum value of v can be adjusted to 0.5 cm/s. When values of Q_{0min} for various HEPA filters are inserted into Eq. (17.29), the minimum upstream concentrations can be obtained, which is shown in Table 17.23.

With the minimum upstream concentration, all the leakage particle numbers for various filters are $60 \times 0.5/4 = 7.5$# in the sampled air volume.

Under the condition of the minimum sampling concentrations, when the leakage detection with the scanning method is used for the above leakage hole size, the detected particles will be ≥1#, which may indicate the leakage position.

From the above analysis, we can know that:

1. For the particle counting concentration in the leakage hole method, the requirement for the upstream concentration is not high. According to ISO standard, atmospheric dust can also be used as one of the upstream dust sources. When atmospheric dust is used in the upstream, pollutions on the environment, test personnel and air filters can be avoided. When the atmospheric dust concentration is suitable according to 2008 version of ISO standard, it is recommended to use atmospheric dust as the upstream dust source. Usually the upstream concentration of HEPA filter in the general air cleaning system meets the above condition. Or measures can be taken to meet this condition. Before leakage detection, the upstream concentration should be checked.

   Since for most HEPA filters $K > 0.000005$ %, the least upstream concentration of channel 3 in Table 17.23, which is 5,208#/L, meets the requirement for most HEPA filters.

   If the upstream concentration is too big, which is not adjustable, particle sizes of ≥ 0.7 μm, ≥ 0.8 μm, ≥ 1μm and so on can be used. Contrarily, particle size of ≥ 0.3 μm can be chosen. Or the following measures can be taken:

   (a) Open the maintenance door at the downstream of air filter for fresh air in the air handling unit. Bypass the air filter for fresh air and draw the indoor air of the machine room.

(b) With the replacement method of air filter, uninstall one or two air filters for fresh air at one certain stage, or uninstall one or two air filters for fresh air at each stage.

2. The sampling flow rate of the instrument should not be specified for the leakage hole method. Results are the same no matter what kind of sampler is used.
3. Among the criteria, the leakage hole method is the most strictest. When three particles are detected in the sampling air volume, it is judged as leakage. It can be used to detect smaller leakage hole than the penetration method. When ISO standard should be followed as much as possible, criteria can be determined through simple calculation for any kind of HEPA filter or can be determined through negotiation (a certain amount of negative or positive deviation can be added on the equivalent diameter of the leakage hole).
4. It is not necessarily to choose particles with diameter $\geq$0.5 μm for measurement. According to the concentration, particles with diameter $\geq$ a certain value can be used.

Since for most HEPA filters, $K > 0.000005$ %, the minimum upstream concentration 5,208#/L in Table 17.23 can meet the requirement of most HEPA filters.

If the upstream concentration is too large, which cannot be adjusted, particles with diameter $\geq$0.7, $\geq$0.8, and $\geq$0.9 μm can be used. On the contrary, particles with diameter $\geq$0.3 μm can be used. Or the following methods can be used:

(a) Open the repair door after the fresh air filter in the air handling unit. Bypass the air from the fresh air filter. Air from the equipment room can be extracted.
(b) Similar to the replacement of air filter, one or two filters in the certain stage of fresh air filters are uninstalled, or one or two filters are uninstalled at each stage.

17.3.2 Leakage Detection of Isolation Bioclean Cabinet

Because dangerous biological particles are dealt with in the isolation bioclean cabinet, the requirement for its sealing performance is very high, which includes the sealing and the negative pressure maintenance ability of the device (containers). There are the following methods to detect leakage for these two aspects.

17.3.2.1 Leakage Detection of the Sealing

Pressure Decay Method

The test system is introduced in Chinese national standard *Code for construction and acceptance of cleanroom* (GB 50591-2010), which is shown in Fig. 17.31.

The test steps with this method are as follows:

(a) The cleanroom temperature is controlled in the design range and kept constant. The variation of room temperature during the pressure decay test process is

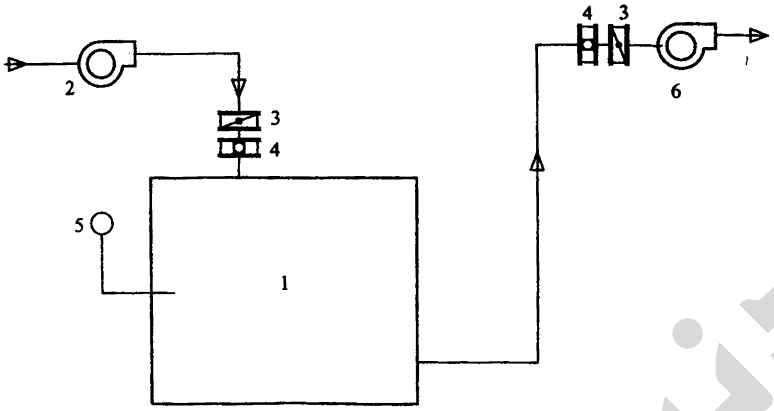

Fig. 17.31 System with the pressure decay method. *1* cleanroom, *2* air supply fan, *3* adjustment valve, *4* sealing valve, *5* pressure gauge, *6* exhaust fan

recorded (the minimum indication value on the thermometer or temperature sensor should not be larger than 0.1 °C).

(b) Close all the doors and the delivery windows on the envelope of the cleanroom. Switch off the sealing valve on the return air (or exhaust air) pipeline. Other sealing measures are not allowed to take at the air outlet. The sealing status of various apertures and cracks is maintained.

(c) Turn on the air supply system so that the room pressure increases to the specified test pressure. (The test range of pressure should be at least 1.5 times of the test pressure. The minimum indication value should not be larger than 10 Pa.) When the pressure is stable, stop the air supply fan and then close the air supply valve.

(d) Or close the valve on air supply pipeline. If there is no valve on the air supply pipeline or the valve is not sealed well, the air supply outlet should be sealed with the plastic membrane and the plate, then turn on the exhaust air system. When the room pressure decreases to the specified test pressure, which keeps stable, stop the exhaust system and then switch off the sealing valve on the exhaust air pipeline.

(e) Since the stop of air supply (exhaust), the variation of pressure decay with time is recorded. The differential pressure and the temperature are recorded once every minute. It continues till the room pressure decreases to half of the initial pressure.

(f) When test completes, switch on the valve slowly till the room pressure recovers to the common state.

(g) If repeated test is needed, it should restart in 20 min.

Cao Guoqing, author, and others performed measurement with this method [29]. The laboratory dimension is 4.5 × 4.5 × 2 m. It is the assembly structure. The floor is the field pouring concrete. The door is sealed. All the visible cracks are sealed with the sealing glue.

Experimental results are shown in Fig. 17.32.

At the same time, the theoretical calculation (with the same volume of the room) was performed. The result is shown in Fig. 17.33.

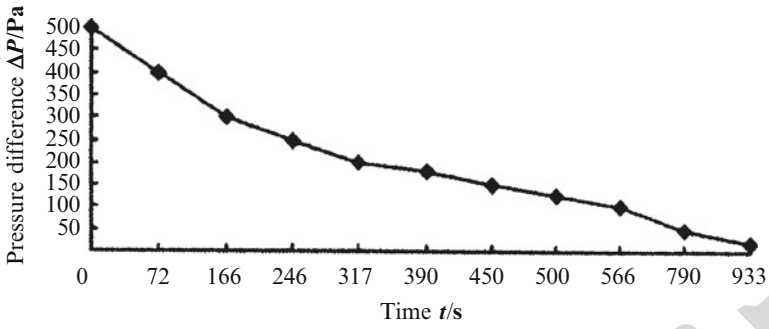

Fig. 17.32 Experimental result for the relationship between the pressure decay and the time

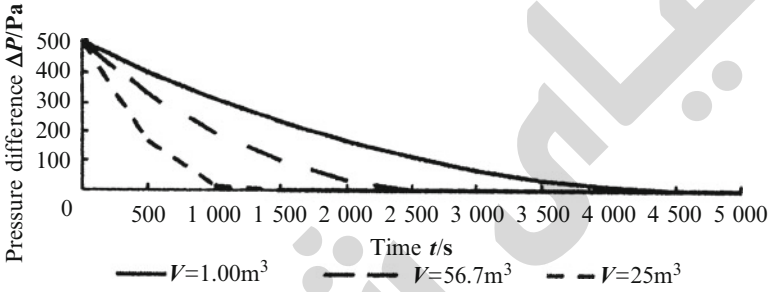

Fig. 17.33 Calculated result for the relationship between the pressure decay and the time

It is shown that the experimental data with the model is basically consistent with the decay curve of the pressure with the theoretical calculation. But the decay velocity of pressure with the model experiment is obviously larger than the theoretical value. The reason may be that when the differential pressure is relative large, the sealing performance of the envelope structure may be damaged. This also means that it is very difficult to maintain the pressure.

Constant Pressure Method

In the Chinese standard GB50591-2010 *Code for construction and acceptance of cleanroom*, the test system with this method is shown in Fig. 17.34.

The test procedures with this method are as follows:

(a) The cleanroom temperature is controlled in the design range and kept constant. The variation of room temperature during the pressure decay test process is recorded (the minimum indication value on the thermometer or temperature sensor should not be larger than 0.1 °C).
(b) Close all the doors and the delivery windows on the envelope of the cleanroom. Switch off the sealing valve on the return air (or exhaust air) pipeline. If there is no valve on the air supply pipeline or the valve is not sealed well, the air return

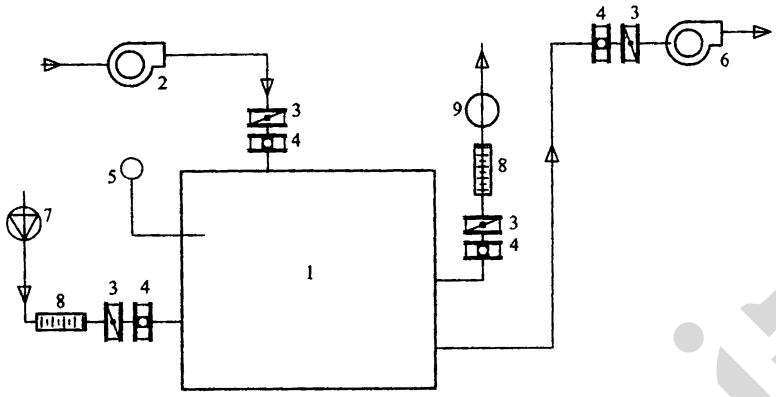

Fig. 17.34 Test system with constant pressure method. *1* cleanroom, *2* air supply fan, *3* adjustment valve, *4* sealing valve, *5* pressure gauge, *6* exhaust air fan, *7* air pump, *8* flowmeter, *9* vacuum pump. Note: Air pump is used for positive pressure test, while vacuum pump is used for negative pressure test

grille should be sealed with the plastic membrane and the plate on the return air (or exhaust air) system.

(c) Turn on the air supply system so that the room pressure increases to 500 Pa. Then stop the air supply fan, and close the air supply valve.

The makeup air is supplied into the room with the air supply fan and the air compressor by the aperture and the pipe on the envelope. The flow rate of the makeup air is varied with the adjustment value on the pipe so that the pressure inside the cleanroom is maintained constant and does not reduce. The readings on the floating flowmeter are recorded every 1 min. This value means the leakage airflow rate. The test should last less than 5 min. Average value should be calculated.

(d) On the contrary, close the air supply valve, and then turn on the exhaust air system. When the indoor pressure reduces to −500 Pa, close the exhaust air system. The vacuum pump is open to keep the indoor pressure. The leakage flow rate is recorded.

(e) When the test is finished, switch on the valve slowly so that the room pressure recovers to the common state.

(f) If needed, test can be repeated in 20 min.

The measured leakage ratios with above models are shown in Table 17.24.

The relationship between the leakage ratio and the pressure is thus obtained, which is shown in Fig. 17.35.

It is shown that the larger the test pressure is, the quicker the increase of the leakage ratio becomes. This is consistent with the pressure decay method.

The converted leakage flow rates in the above table are the corrected values with the readings of the leakage flow rates. The correction expression is shown in Eq. (16.2).

In the Chinese standard GB50591-2010 *Code for construction and acceptance of cleanroom*, it is suggested to distinguish the sealing extent according to the half-life time of pressure with the pressure decay method. It is shown in Table 17.25.

Table 17.24 Experimental relationship between the test pressure and the leakage ratio

Test pressure Pa	Leakage flow rate reading (m^3/h)	Converted leakage flow rates (m^3/h)	Leakage ratio (%)
150	1.61	2.79	4.92
250	1.80	3.12	5.50
360	2.00	3.46	6.11
500	3.20	5.54	9.78
660	4.95	8.57	15.12

Note: the room volume is 56.7 m^3

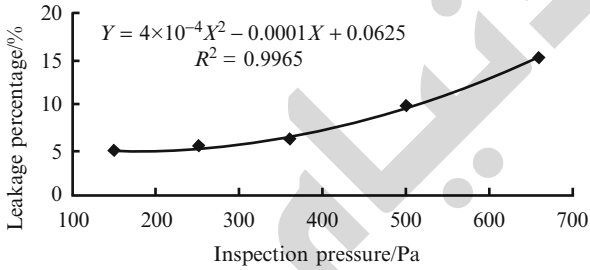

Fig. 17.35 Polynomial regression curve for the relationship between the test pressure and the leakage ratio

Table 17.25 Classification of the sealing extents with the half-life time of pressure

Sealing extent	Half-life time of pressure T (the time when test pressure decays to half) (min)
1	≥30
2	≥20
3	≥10
4	≥5

With the constant pressure method, it is also suggest in the above standard that the sealing extent is classified with the leakage ratio, which is presented in Table 17.26.

In the table, $\alpha = Q/V$, where V is the net volume of tested cleanroom (usually it is the room volume) (m^3); Q is the hourly leakage flow rate from the readings in the previous 5 min with the tested pressure (m^3/h).

For the industrial cleanroom, the requirement of the sealing is not so strict. The usual methods are as follows:

(a) For small apparatus, after it is pressurized, kerosene or soap liquid can be coated on various cracks. Bubble will appear at the place where leakage exists.
(b) After the pressurization system stops, the pressure decay within the specified time period should be observed to determine whether it is larger than the specified value. For example, in the American Aerospace Standard, when the large space is pressurized to 25 Pa, the pressurization system stops. If the pressure does not recover to the original value within 1 h, it is considered as sealed.

Table 17.26 Classification of the sealing extents with the leakage ratio

Sealing extent	The hourly leakage ratio α in the previous 5 min (h^{-1})
1	$\leq 2.5 \times 10^{-3}$
2	$\leq 10^{-2}$
3	$\leq 5 \times 10^{-2}$
4	$\leq 10^{-1}$

Halogen Method

The leakage detector made by the halogen effect can be used to detect the container filled with the halogen gas or the space with volume less than 30 m^3. Common halogen gases used include Freon 12 (or 22) and chloroform. The former is nontoxic, incombustible, and especially sensitive (the sensitivity of domestic-made halogen leak detector is 0.5 g/year). During the leakage detection process, the instrument is powered on at first, and then the end of the receiver probe is aligned with the gap and moved slowly. If there is leakage, the sound of the instrument increases and the pointer will also move with a larger magnitude. When leakage detection is performed on a certain device, the room air where the device is placed should be checked at first. Leakage detection starts when it is sure that there is no halogen pollution indoors.

The smelt copper wire can also be used, which moves near the gap. If any fluorine steam seeps and comes into contact with the copper wire, the copper wire will become dark green, which can be used as a qualitative check.

Sulfur Hexafluoride Method

SF_6 gas is injected into the container or the device, the leakage detector corresponding with this gas is used to check. This instrument is made according to the mechanism that the degrees of ionization are different for SF_6 gas in high-frequency electromagnetic field. The lower detection limit is higher than the halogen method.

Ammonia Method

Fill the container with ammonia. Phenolphthalein test paper is used to check the possible leakage place. If the leakage gas contacts the test paper, the test paper will be pink immediately. Ammonia method is more sensitive than the halogen method, but the risk is big. The safety operation manuals with ammonia must be followed.

17.3.2.2 Leakage Detection for the Maintenance Stability of Negative Pressure

In order to check whether there is airflow spillover at the opening position of the biological cleaning device in operation, leakage detection for the maintenance

stability of negative pressure is needed. High-concentration aerosol (smoke, spore fog, or other gas) is released in the interior of the instrument; detection is performed in the external of the device for leakage check. (According to the relevant standards in the USA, when Bacillus subtilis aerosol is used in the test, the total number of bacillus generated is hundreds of millions to billions. The sampling dish with narrow seam is used for the external sampling of the device. The colony should not be more than 5# in each sampling dish.)

17.4 Cleanroom Measurement

17.4.1 Measurement Types of Cleanroom

17.4.1.1 Acceptance Measurement (Characteristics Measurement)

This is aimed to find out whether the performance of the cleanroom meets the requirements of the design or to study the characteristics of the cleanroom. Through this kind of measurement, reasons for the failure of the requirement can be found whether problems exist in the design, construction or process. In addition, this kind of measurement can also be the foundation to establish reasonable maintenance management system.

Before the measurement, full preparation must be made. The general condition of cleanroom should be fully understood, which includes the following: various related drawings, the requirement of the designed air parameters, the air handling scheme, the flow rate and the air distribution method, cleaning schemes for human and object, the operational condition of cleanroom, and the surrounding environment of the cleanroom.

This kind of measurement is the most comprehensive, which includes the following items:

1. Leakage detection. It is performed according to the requirements in the previous section.
2. Air volume. It includes the supply air volume, the return air volume, the fresh air volume, and the exhaust air volume.
3. Velocity field. It includes the velocity field along the longitudinal cross section through the center of ventilation opening, the planar velocity field on the working area, and other velocity field at any cross section where it is required. The sampling positions for the velocity field are the same as that for the concentration field.

For unidirectional flow cleanroom, requirements are made for not only the average velocity on the working area but also the turbidity (namely, the nonuniformity of velocity).

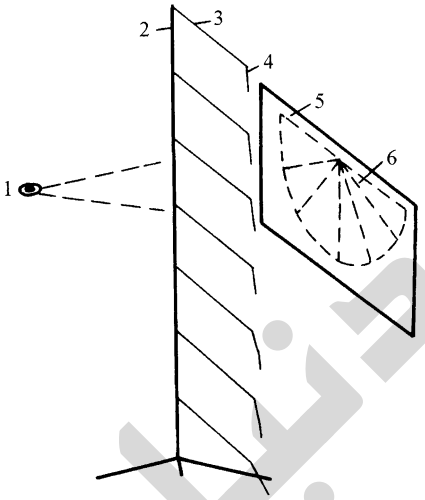

Fig. 17.36 Schematic diagram of the filament method for measuring the velocity field

4. Airflow pattern. The most commonly used method is that several filaments are fastened on different positions of the rod. During observation, the plate with black background and white lines is placed at the back of the filaments. The angles of the filaments are recorded point by point. It is shown in Fig. 17.36. Then, the flow directions are plotted on the paper point by point. The plotted cross section is the same as the velocity field.

When it is possible, tracer particles can be released to show the streamline, which can be recorded by taking photos. Tracer particles are commonly used in the visualization technology for airflow. Continuous tracer particles include smoke and fog generated by some liquid. Discontinuous tracer particles include feathers from some animals, plant seeds, and chemical crystals such as metaldehyde, foam plastic particles, the floccule by heating the solid alcohol, and bubbles produced by some foaming agent.

Figure 17.37 is the schematic diagram of the smoke generator with the smoke particles as the tracer particles, which is used for streamline measurement. The power supply for the smoke generator can be a blower or a handheld pinched ball. Observation of the streamlines with smoke generator is often performed with the velocity field measurement simultaneously.

Figure 17.38 shows a bubble generator. This is the first time that this kind of bubble generator is used in air cleaning technology in China for streamline visualization experiment [30]. The foaming agent is the Type 1227 surfactant produced in the detergent factory, which is diluted to the concentration 20 % and mixed with a small amount of foam stabilizer. The mixture gas with air and helium from the foam generator can produce many small bubbles with diameter 4 mm. When proper proportion of helium and air is kept, the bubble density can be equivalent with that of air.

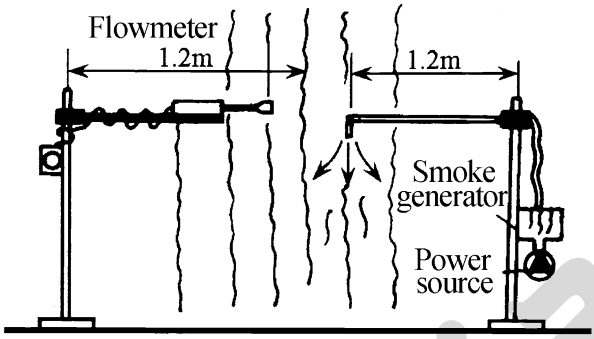

Fig. 17.37 Schematic diagram of the smoke generator for streamline measurement

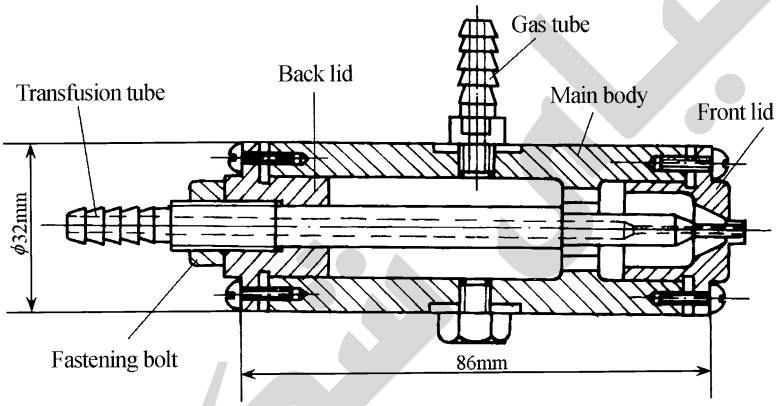

Fig. 17.38 Bubble generator

If the parallelism of the streamline is needed, it is measured with the concept of parallelism. The distance of lateral diffusion at the leeward side is measured, and the smoke is generated upstream.

5. Static pressure. The differential pressure between indoors and outdoors should be measured when the door is closed. Besides, according to the requirements for the positive pressure, the airflow direction should be inspected to find out if it can be kept in the outward flow when the door is open. Moreover, the particle concentration at the height of working area 0.6 m inside the door (this is also required in *Code for construction and acceptance of cleanroom* and related standard abroad [31]) should be checked whether it is higher than the required value corresponding to the air cleanliness level of cleanroom.
6. Filter efficiency at various stages. Measurement methods listed in Table 17.6 should be used.
7. Concentration field (including dust concentration and bacteria concentration). The sampling locations can be the same as that for measuring velocity field. For

cleanrooms with different cleanliness levels, the number of measuring positions is different, which should be determined with the relevant requirements introduced later. The measurement positions are placed in the cell centers which divide the measuring plane uniformly.

8. Self-cleaning time. Before the operation of the air cleaning system, the original concentration in the cleanroom is measured at first. Then, operate the system immediately. The variations of concentrations are measured with time during each sampling step. It continues until the concentration is obviously stable. If the original concentration is too low, smoke can be generated indoors at first. When particles are accumulated to a certain concentration, stop generating smoke and measure the concentration (usually in the center of the room) as the original value. Then, start up the system immediately, and measure the decay of concentration with time. The time from the starting up to the appearance of stable concentration is called self-cleaning time. The self-cleaning process curve can be plotted. Recently, in some standards for the application of air cleaning system in operating rooms, the time needed to remove 90 % or 99 % of the pollutant concentration is termed as the self-purification time.
9. Others. This includes temperature, humidity, air distribution and streamline, noise, illumination intensity, vibration, and other parameters, which can be referred to Ref. [11].

For the above items, some are compulsory, which are included in the content of "evaluation of comprehensive performance" and specified in detail in *Code for construction and acceptance of cleanroom* (GB50591-2010). It is the first time that formaldehyde is listed as the compulsory test item.

17.4.1.2 Monitoring Measurement (Daily Measurement)

This is aimed to determine whether the performance of the cleanroom can be kept. It also provides the basis for the parameter adjustment of the system. The measurement should be performed with the purpose of understanding the performance of cleanroom correctly. With the daily test data from several sampling positions, the whole indoor environment can be correctly derived. Otherwise, even if the measured data at certain places are obtained, it is hard to solve the problem with this kind of measurement, when the nonuniform distribution indoors is not understood, the daily variation data are not obtained, the limits of these main parameters (such as the design condition, the load condition, the operational condition of equipment) are unknown, and the influences of these basic factors are unclear.

As the sampling position for monitoring measurement, the controlling points should be chosen according to the performance of cleanroom or placed near the operating site. Usually sampling places can be arranged with the diagonal five-point layout method, which is shown in Fig. 17.39. The number of sampling points can be increased appropriately when the area of cleanroom is more than 40 m^2. For the turbulent flow cleanroom, sampling probe should not be placed right under the filter.

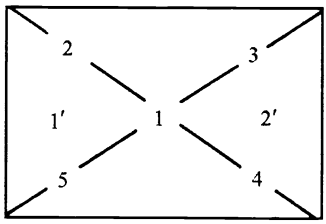

Fig. 17.39 Five sampling positions method

In order to reflect the characteristic and monitor the system, this kind of measurement should be performed in accordance to a predetermined plan. The representative sampling points or fixed points should be chosen during a regular time interval.

The monitoring measurement items should include the air volume or air velocity, the static pressure, the dust concentration, or bacteria concentration. The specific practice can be referred to the acceptance test. Other items can be measured according to the need.

17.4.1.3 Special Measurement (Temporary Measurement)

This is aimed to find out the temporary and local reason for problems. For example, when the production yield declines, in order to find out if there is a local pollution source, it is measured temporarily.

The main measurement items include the dust concentration and the air velocity. Sometimes the static pressure and the local streamline should also be measured.

17.4.2 Test Status of Cleanroom

In 1973, the test status of the cleanroom was first proposed [31]. It is the so-called empty status when the air cleaning system is already operated, when the process equipment is not installed. It is the so-called static status, once the process equipment is installed and put into operation, but there is no working staff indoors. It is the so-called dynamic status when the air-conditioning system and the process equipment are in operation with the presence of staff indoors. This classification method for the status was brought in the US Federal Standards 209C and 209D since 1987. It is also adopted in ISO 14644-1 EU GMP and GB50073-2001 *"Code for Design of Clean Room"* in China, which are shown in Tables 17.27, 17.28 and 17.29 [32].

It is obvious that any activity should exist in at-rest status. The implication of "at-rest" include "rest" and "still". If there is no personnel inside but there is production machine in operating condition, this is not the essence of "static".

Table 17.27 Definition of occupancy status in cleanroom by US federal standard

	Fed-Std-209C	Fed-Std-209D	Fed-Std-209E
At-rest cleanroom (facility)	A cleanroom (facility) that is complete and has the production equipment installed and operating, but without personnel within the facility.	A cleanroom (facility) that is complete and has the production equipment installed and operating, but without personnel within the facility.	A cleanroom (facility) that is complete, with all services functioning and with equipment installed and operable or operating, as specified, but without operating personnel in the facility.

Table 17.28 Definition of occupancy status in cleanroom by ISO standard

Occupancy status in cleanroom	ISO 14644-1-1999 and ISO 14698-1-2003
At-rest	Condition where the installation is complete with equipment installed and operating in a manner agreed upon by the customer and supplier, but with no personnel present.

Table 17.29 Definition of occupancy status in cleanroom by EU standard

Occupancy status in cleanroom	EU GMP
At-rest	The "at-rest" state is the condition where the installation is installed and operating, complete with production equipment but with no operating personnel present. "at-rest" state should be achieved after a short "clean up" period of 15–20 minutes (guidance value) in an unmanned state after completion of operations.

Therefore, it is suitable to call "empty status", "static status" and "dynamic status" as "completion status", "shutdown status" and "operational status", respectively.

It is quite common during the actual test process for cleanroom project that HAVC system runs normally while the installed process production equipment is not operating. The condition with operating equipment inside and without personnel can only be found in mechanized, automatic, and closed production cleanroom. It is ubiquitous in the workshop for semiconductors. But it is rare in other kinds of cleanrooms. GMP cleanroom workshop is one example.

In order to include several conditions, GB50591 "*Code for Construction and Acceptance of Cleanroom*" specifies three statuses, which are:

Process equipment is not operating and there are no personnel inside;

Process equipment operates with the mode agreed upon by the custom and the supplier, and there are no personnel inside;

Operation stops and steady state is reached after self-purification process.

17.4.3 Necessary Sampling Points

During the measurement of large clean space such as the cleanroom, because of the random particle distribution, coincidence rate is very large if the air cleanliness level was determined only with one sampling position. Obviously, the more the sampling positions are, the better it is. But there is a problem of economy and possibility, so the number of necessary sampling points should be found.

17.4.3.1 20 Points Reference Method [33]

It is already known that indoor dust distribution has some characteristics. The concentration of each sampling which contains more than ten particles in the sampling volume basically obeys the normal distribution. So 95 % of the measured data should fall in the range of $\overline{X} \pm 2\sigma = \left(1 \pm \frac{2\sigma}{\overline{X}}\right)\overline{X}$, where σ is the standard deviation. Based on the statistics of measured data, for applications with air cleanliness level between Class 100000 to Class 10000, $\left(\overline{X} \pm 2\sigma\right)$ is between 1.6 and 1.8 (here only the upper limit of the concentration deviation is used). As for the concentration of each sampling which contains more than 3.5 particles, 95 % of measured data are likely to be within the range of $2\overline{X}$. As for the concentration of each sampling which contains more than 1 particles, 94 % of measured data are likely to be within the range of $2\overline{X}$.

In addition, from the nonuniform distribution calculation theory of cleanroom introduced above, the biggest difference between the measured concentration and the room average concentration is about $2\overline{X}$ in cleanroom with air cleanliness levels Class 6 and higher, where $\overline{X}$ is the room average concentration. For cleanroom with air cleanliness levels Class 7 and Class 8, the difference is about $1.5\overline{X} \sim 1.8\overline{X}$. These theoretical conclusions are very close to the previous measurement results.

Therefore, for the normal measurement, it is allowable that 5 % of the data are more than the required values. If more than 5 % of the tested data are larger than the requirement, this measurement can be considered as abnormal and the reliability of the data is doubtful.

Since the number of measuring points is only an integer, when it should be assured that less than 5 % of the measured data are larger than the required value, the total number of measuring points should be 20 at least. If at each sampling place, it is required to sample at least two times, so there should be at least 10 test points. And in all the measured data, the frequency of the measured value which is more than $2\overline{X}$ should be at most once. So the method can be called 20 points reference method.

It is still not comprehensive to perform measurement with the number of measuring points determined in this way. For high cleanliness occasions, the second type of error may also easily appear because of less measuring points.

If the air cleanliness of the cleanroom has not reached a certain level, but a group of data within this air cleanliness level may be obtained as a result of randomness of dust distribution and shortage of the measurement times, it is possible to judge that

this cleanroom has reached this level. In this way, the unqualified cleanroom will be misjudged as qualified. This kind of error is the second type of error, whose probability is set as β. In project β is generally set less than 10–15 %. In order to make β smaller, there must be enough sampling points or sampling times. The probability is β for the occurrence of more than k times which is qualified ($k/m \geq 0.95$) for the unqualified cleanroom during the total sampling m times.

The probability of the appearance of k times with qualified conclusion and (m- k) times with unqualified conclusion can be described with binomial distribution, namely,

$$P(\xi = k) = C_m^k P^k (1-P)^{m-k} \tag{17.30}$$

$$C_m^k = \frac{m(m-1)\cdots(m-k+1)}{k!} \tag{17.31}$$

where P is the probability for the incident when it is not more than a fixed value.

Then the probability β of no less than k qualified samples in the total m samplers in the unqualified cleanroom is:

$$\begin{aligned}\beta &= P(\xi \geq k) \\ &= C_m^k P^k (1-P)^{m-k} + C_m^{k+1} P^{k+1} (1-P)^{m-k+1} + \cdots + C_m^m P^m (1-P)^0\end{aligned} \tag{17.32}$$

If β is very small, it means that the probability of the qualified conclusion from measurement is still very small, since the parent sample is unqualified. As we know, when the sampling positions are not enough, it is still very likely to obtain the qualified conclusion, which is out of our expectation. This also means that for a little qualified cleanroom, it is very likely that the measurement results show the qualified conclusion with great possibility and the probability to obtain qualified conclusion is very small.

In engineering, β is generally taken less than 10–15 %.

For example, in a clean space where the concentration is allowed to be 0.04#/L, when every sampling volume is 75 L, the detected particle number should not exceed 3#, which can be judged as qualified. According to the given formula in Chap. 1, the probability to obtain particles with number less than 3 in this clean space can be calculated, i.e., $P(\xi \leq 3) = 0.646$.

If the actual concentration is greater than 0.04 grains/L, the actual probability is $P < 0.64$, which can be assumed $P = 0.63$. However, in this occasion with unqualified cleanroom, even if the number of sampling points is not enough, samplers with the above probability can also be measured. With the above formula, trial calculation can be performed with the above 20 points (times) as the basis. The probability with k subsamples that are qualified is:

$$\begin{aligned}\beta = {} & C_{20}^{16} \times 0.63^{16} \times 0.37^4 + C_{20}^{17} \times 0.63^{17} \times 0.37^3 + C_{20}^{18} \times 0.63^{18} \times 0.37^2 \\ & + C_{20}^{19} \times 0.63^{19} \times 0.37^1 + C_{20}^{20} \times 0.63^{20} \times 0.37^0 = 0.086\end{aligned}$$

If $k = 15$, then $\beta = 0.18$.

If $m = 20$, $k = 8$, then $\beta = 0.18$.

This suggests that in 20 sampling points (times), if there are at least 16 sampling points (times) which contain no more than 3# and there is at most 1 sampling point (time) which contains more than $2 \times 3 = 6$#, then we can confirm that in the detection volume, there is less than 3#, so misjudgment will not be made. If in 20 sampling points (times), there are only 15 sampling points (times) which contain less than 3#, the possibility of appearance of the average concentration larger than 0.04#/L is large. If the number of sampling points decreases to 10 points (times), even if there are less than 3# in the sampling volumes of 80 % points, the possibility is still greater for the concentration larger than this value, so it is likely to make misjudgment for the unqualified cleanroom.

So, if both kinds of errors are required to be decreased or when one kind of error decreases at one place while the other kind does not increase, the number of samplers, namely, the sampling points (times) n, should be increased. The greater the number of sampler is, the more concentrated the average sampled distribution is.

If the concentration is as small as 0.02#/L, when the sampling volume 0.1 L is used, it contains 0.002# in each sampling volume. So more than hundreds of sampling points (times) may be needed. This is why cleanroom with high air cleanliness level cannot be measured with the sampling volume 0.1 L even when dozens of minutes or dozens of hours have been taken.

According to the above principle, the calculation results are shown in Table 17.30.

Before the test, λ is not given, so the number of necessary sampling points should be determined according to the estimated value of λ. If the measured λ is much smaller than the estimated λ, the number of necessary sampling points should be reconsidered according to the measured λ.

With the development of particle counter, λ will not be less than 1. So for general situation, it is most appropriate to place 20 points. If the space is small, the number of sampling times can be used to replace the number of sampling points. Suppose at least two times of sampling are performed for each point, the total sampling points can be 10. On contrary, when the space is very big, more sampling points can also be added on the basis of 20 points. This is all considered for engineering in the practical point of view.

Later, the number of sampling points proposed in Japanese standard is similar to the calculated value with the above method, which is shown in Table 17.31.

17.4.3.2 *t* Test Method

Detailed description is presented in Sect. 17.5 of this chapter.

17.4.3.3 Compromised Method in 209C

It is troublesome to determine the number of sampling points with the above statistic methods, and it is obviously not so convenient to place more than 20 sampling points. Therefore, two contradictory claims were put forward by revisers for the US Federal Standard 209B [5, 34]. One opinion is that the number

Table 17.30 Necessary sampling points

No.	Average measured concentration from every sampling volume/pc	Necessary sampling times	Necessary sampling points	Control value of concentration field/pc	Allowable times for concentration beyond control value	Due particle concentration/(pc/L)
1	$\lambda < 0.2$	120	120 (60)	1	1	λ/each sampling volume
2	$\lambda = 0.2$–0.3	100	100 (50)	1	1	
3	$\lambda = 0.3$–0.4	60 80	60(30) 80(40)	1	1 2	
4	$\lambda = 0.4$–0.5	30	30 (15)	1	1	
5	$\lambda = 0.6$–1	20	20 (10)	1 2	2 1	
6	$\lambda = 1$–2	20	20 (10)	3 3(λ–1.5) 4(λ–1.5)	3 1 1	
7	$\lambda = 2$–3	20	20 (10)	3 5(λ–2.5) 6(λ–2.5)	4 1 1	
8	$\lambda = 3$–10	20	20 (10)	λ 2λ	4 1	

Table 17.31 Specification of sampling points in related standard from Japan

Time	Standard	Title	Minimum sampling points	Suggested sampling points	Distance between points	Sampling times at each point
1987	JIS B 9920	Measurement method of airborne particles in cleanroom and evaluation method of cleanroom	6	20–30	In principle it should be $\leq$3 m. It can be larger for large space.	$\nless$ 3
	JACA Standard	Guideline for the evaluation of cleanroom performance	5	20–30	In principle it should be $\leq$3 m	–

of air cleanliness level should have the inverse relationship with the sampling points, so the numbers of sampling points between high and low air cleanliness levels are quite different. The other opinion is that sampling points has nothing to do with the air cleanliness level, and each sampling point corresponds with the air supply area 25 ft^2 or the number of area expressed in ft^2 is equal to the square root

Table 17.32 Necessary sampling points calculated with 209E

Air supply area (unidirectional flow) or room area (turbulent flow) (m^2)	Air cleanliness			
	Class 100 or higher	Class 1000	Class 10000	Class 100000
<10	2– 3	2	2	2
10	4	3	2	2
20	8	6	2	2
40	16	13	4	2
80	32	25	8	2
100	40	32	10	3
200	80	63	20	6
400	160	126	40	13
1,000	400	316	100	32
2,000	800	633	200	63

of the air cleanliness level. No matter which kind of opinions, the number of sampling points is far less than the number of the above 20 points. Finally, 209C adopted a compromised plan:

1. The number of sampling points should not be less than 2 (for any clean areas). At least one sampling time is needed at each point. In a zone, at least 5 times of sampling are needed.
2. According to the air supply area or the room area, the smaller value of the following results should be chosen as the number of sampling points (M is the number of air cleanliness level with the international unit system):

   For unidirectional flow

   (a)
   $$\frac{\text{Air supply area}(\text{ft}^2)}{25} \text{ or } \frac{\text{Air supply area}(\text{m}^2)}{2.32}$$

   (b)
   $$\frac{\text{Air supply area}(\text{ft}^2)}{\sqrt{\text{Air cleanliness level(English unit)}}} \text{ or } \frac{\text{Air supply area}(\text{m}^2) \times 64}{\sqrt{10^M}}$$

   For turbulence flow

   $$\frac{\text{Room area}(\text{ft}^2)}{\sqrt{\text{Air cleanliness level(English unit)}}} \text{ or } \frac{\text{Room area}(\text{m}^2) \times 64}{\sqrt{10^M}}$$

Table 17.32 shows the number of sampling points calculated with the above method.

From the above explanation, we can see that the specification of the necessary sampling points number between 209C and 209E is based on a kind of compromised

way [34]. In ISO 14646-1 published in 1999, the method to calculate the number of sampling points can be further simplified as:

$$\text{Minimum number of sampling points} = \sqrt{\text{Area of cleanroom}}$$

There is no specific statistical significance with these methods. Although they are convenient for use, the disadvantage is also obvious.

17.4.4 Continuous Sampling Method

For cleanrooms with air cleanliness level higher than Class 100, the dust concentration is extremely low. If the principle introduced in the previous chapter must be followed that 20 particles must be sampled, the sampling time must be very long. In order to shorten the sampling time, the US Federal Standard 209E put forward the "continuous sampling method." The essence of this approach is that the conclusion about the qualification of air cleanliness level is made with the appearance speed of particles (namely, the length of appearance time). Then, we can write as follows:

$$T = \frac{Q}{L} \tag{17.33}$$

where

T is the required sampling time (when 20 particles are detected) (s);
Q is the minimum sampling volume (m^3);
L is the sampling flow rate of the instrument (m^3/s).

Because

$$Q = \frac{20\ (\#)}{\text{upper limit of concentration with the corresponding air cleanliness level } (\#/m^3)}$$

So we know:

$$T = \frac{20}{NL} \tag{17.34}$$

Assume that the possibility with the time that particles are measured is uniform, the number of particles measured in unit time is:

$$\Delta N = \frac{20}{T} = \frac{20NL}{T20} = NL(\#/\text{s}) \tag{17.35}$$

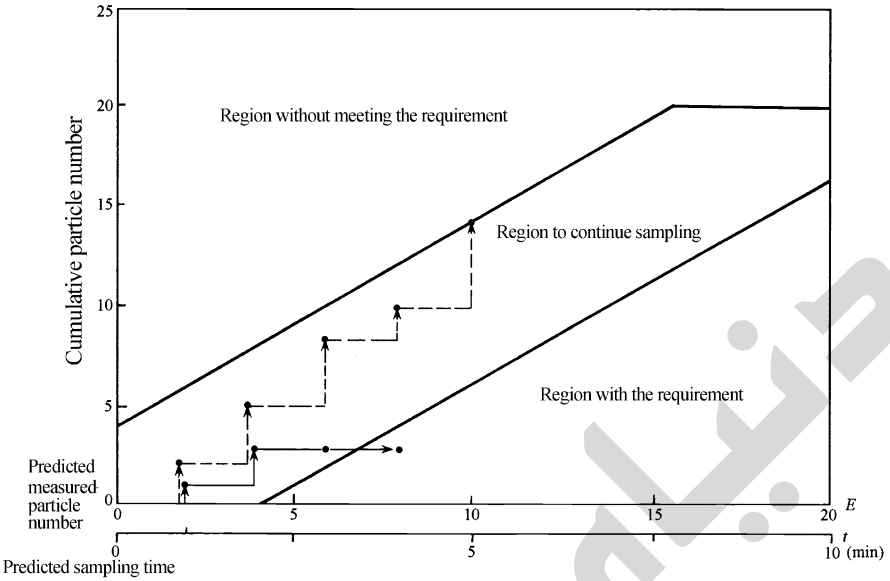

Fig. 17.40 Judgment diagram for continuous sampling

Then, the time that every particle is measured in turn is:

$$T = \Delta N \cdot E = NLE \tag{17.36}$$

where E is the measured particle number in turn (#).

Based on the relationship between the expected sampling time t and the measured particle number E, the judgment diagram given in 209E (see Fig. 17.40) can be used to judge whether the sampling is qualified.

Now let's take an example as follows [35]:

For the measurement of cleanroom with air cleanliness level Class M2.5 (the former Class 10 in 209E), the upper-limit concentration for $\geq$0.5 μm particles is 353#/m^3. Since the number of sampled particles should not be less than 20, the sampling flow rate is 20/353 = 0.056 m^3. If the flow rate of the instrument is 5.66 L (0.2 ft^3), it takes 1 min. When $E = 20$, the total sampling time is 10 min, so the total sampling volume needed should be 56.6 L. In the measurement:

1. When the sampling flow of the instrument is 5.66 L, if the counting numbers appeared in order are 1, 2, 0, and 0, four consecutive samplings are qualified. The qualification test purpose is obtained when the total sampled air volume is only 5.56 L × 4 = 22.64 L. So the measurement time is shortened.
2. With the same condition, if the numbers of sampled particles in order are 2, 3, 3, 2, and 5, the five consecutive samplings are unqualified. The total sampling flow rate is 5.66 L × 5 = 28.3 L. So when the sampling flow rate is less than the

Table 17.33 Particle generation tests of printer and printing paper

Sampling No.	Sampling times	Particle concentration [pc/(2.83 L · min)] ≥0.3 μm	≥0.5 μm	≥1.0 μm	≥2.0 μm	≥3.0 μm	Size of printing paper (length × width) (mm × mm)
1	1	7,096	6,657	3,562	2,735	610	1,470 × 44
	2	6,046	5,818	3,579	2,820	870	1,530 × 44
	3	9,328	8,867	5,600	4,492	1,267	1,590 × 44

predetermined value 56.6 L, it is concluded that the air cleanliness level has not reached Class M2.5.

3. If the cumulative counted particle number does not intersect with the upper and the lower boundaries when the total sampling volume has reached 56.6 L and the cumulative counted particle number is still less than 20, this cleanliness level can be reached.

Although continuous sampling method was given in 209E, the limitations of this approach were also pointed out, mainly:

1. The method is only valid when the number of each sampled particles is 20#.
2. During each measurement, the monitored data and data analysis are required as appendix (although it can be done by computer).
3. The average dust concentration calculated with the measured results is not very accurate, mainly because the sampling volume is too small.
4. When the sampling points are less than 10, the requirement with 95 % upper confidence limit is not generally easily achieved.

17.4.5 Factors Influencing Measurement Result

There are many factors affecting the measurement result of particle concentration in cleanroom, which mainly include the following: whether people wear clean clothes, whether people are at rest indoors and less active, whether it is located in the downwind, and whether people enter in and out. In addition, there are reports that the printer on the particle counter has a great influence on the measurement results [36], especially for high-grade cleanroom. Unqualified results are easily produced if the printer is used. The related experimental data are shown below.

Table 17.33 shows the concentration in the cover when both the printer and its printing paper were covered by clean covers, while only wires are connected to the instrument.

Table 17.34 shows the effect of two locations for the printer.

The above results indicate that if the printer is used, these printer and printing paper with less particle generation must be used or the printer should be kept away

Table 17.34 Influence of the printer on the measurement result

Printer location	Sampling No.	Particle concentration ([pc/(2.83 L · min)]) Printer turned off (measure 3 or 4 times after steady state is reached)	Printer turned on (measure 3 or 4 times after steady state is reached)	Ratio of concentration between printer turned on and turned off	Size of printing paper (length × width) (mm × mm)
Above the device	1	2 3 2	1 3 3	1	0
	2	4 2 4	6 2 4	1.2	160 × 44
	3	2 7 5	18 18 11	3.4	270 × 44
	4	6 6 10	12 11 15	1.7	500 × 44
	5	4 3 3	7 7 10	2.4	710 × 44
Near the device	1	2 2 1	8 5 2 3	3.6	1,030 × 44
Clean cover is used to mantle the printer and printing paper, except the electric line which connects with the device	1	3 0 2 0	0 1 1 5	1.4	1,220 × 44

from the sampling position. For cleanroom with higher air cleanliness level, it should be more careful with the application of printers. Of course, this should be noticed especially by the particle counter manufacturers.

17.5 Evaluation of Air Cleanliness in Cleanroom

17.5.1 Evaluation Standard of Air Cleanliness in Cleanroom

The air cleanliness level is evaluated with the particle concentration. So the evaluation of the air cleanliness level is the evaluation of the particle concentration.

17.5.1.1 Estimation Method with Fixed Value

The so-called estimation method with fixed value is the method to estimate the total average concentration N with the randomly sampled particle concentration values $N_1, N_2, \ldots$, and N_n. This parameter in the axis is a single position, so in the statistics it is called the estimation method with fixed value or the estimation method with fixed point.

Evaluation with the Sampled Mean Value

Estimation is performed with the sampled mean value, namely, the average particle concentration:

$$N = \frac{1}{n}\sum_{i=1}^{n} N_i \tag{17.37}$$

where N_i is the mean value at each point.

The standard deviation of the average value $\overline{N}$ is smaller than that of individual measured value. Only when the former is only $\frac{1}{\sqrt{n}}$ of the latter, it is closer to the true particle concentration N.

In order to obtain mean values at each position with greater credibility, the requirements in Table 17.18 should be satisfied. The purpose is to show that the distribution of concentration field has a certain pattern, which is not accidental.

If both the sampling volume and the number of measurements meet the requirement, but the number of the controlled value is larger than the required number, it is necessary to increase the average concentration. For example, there are some measurement data in a cleanroom (detection volume 1 L):

$$\ldots\#/\mathrm{L},\ \ldots 6\#/\mathrm{L},\ 7\#/\mathrm{L},\ 8\#/\mathrm{L}$$

There are 20 times of measurement (10 points) in total, and the average concentration $\overline{N} = 3\#/\mathrm{L}$. For concentration larger than $2\,\overline{N}$, there are only two times including 7#/L and 8#/L, which does not meet the requirement of the allowable number 1. So the average concentration should be increased to 3.5#/L, and the number of particle concentration larger than $2\,\overline{N}$ is only one time, which is 8#/L.

Evaluation with the Maximum Value of the Sample

With this method, any concentration in the cleanroom is not allowed to be larger than the required particle concentration with the corresponding air cleanliness level. This is specified in some foreign standards. But the necessary sampling points are not specified, so this method is also not strict, and sometimes larger error may be obtained.

17.5.1.2 Evaluation with Interval Estimation

Single-Side t Distribution Test

The so-called interval estimation is to estimate the overall average concentration N based on a random concentration interval. This interval is called the confidence interval or the confidence limits (upper or lower). It means the probability of the

overall N falling in a certain range. This probability is called the confidence probability, which is expressed as P.

In practice, they can be considered as continuous variables, whose average concentration $\overline{N}$ can be used to estimate the overall mean concentration N. According to the theory of mathematical statistics, there are two conclusions as follows:

(a) If the whole population is normally distributed, $\overline{N}$ is also normally distributed.
(b) If the whole population does not completely follow the normal distribution, as long as the number of samples (measured points) increases, which reached $n \geq 30$ in general, the distribution of N can be approximately considered as normal distribution. From Chap. 1, the characteristics of the normal distribution depend on its total average value N and the total standard deviation σ (or σ^2), that is,

$$\varphi(N) = \frac{1}{\sigma\sqrt{2\pi}} \mathrm{e}^{-\frac{(N-\overline{N})^2}{2\sigma^2}} \tag{17.38}$$

If $\overline{N}$ can be approximately described with the normal distribution, the standard deviation of the large samplers can be used to replace the total standard deviation σ (or σ^2). But in the actual test of dust concentration, the number of measurement points are rarely more than 30, which are all small samplers. In this case, it is the deduction with small samplers, where the value of σ is unknown. If the estimated value S of the standard deviation (in fact, it is the standard deviation of average value) is used to replace σ, it has been proved with mathematical statistics theory that the statistical variable $\mu = \frac{N-\overline{N}}{\sigma}$ in above expression will change to $t = \frac{N-\overline{N}}{S/\sqrt{n}}$ and it becomes t distribution instead of normal distribution.

According to the Bessel correction, we know for small samplers:

$$S = \sqrt{\frac{\sum \left(N - \overline{N}\right)^2}{n-1}}$$

It can be used to replace

$$\sigma = \sqrt{\frac{\sum \left(N - \overline{N}\right)^2}{n}}$$

Let

$$\frac{S}{\sqrt{n}} = \sigma_{\overline{N}}$$

It is called the error of the average value, then:

$$t_{(\alpha,f)} = \frac{N - \overline{N}}{\sigma_{\overline{N}}} \tag{17.39}$$

Table 17.35 t distribution coefficient

	Probability of t value larger than the indicated value in the table (bilateral side)				
$n-1$	0.2	0.1	005	0.02	0.01
1	3.078	6.314	12.706	31.821	63.657
2	1.886	2.920	4.303	6.956	9.925
3	1.638	2.353	3.182	4.541	5.841
4	1.533	2.123	2.776	3.747	4.604
5	1.476	2.015	2.571	3.365	4.032
6	1.440	1.943	2.447	3.143	3.707
7	1.415	1.895	2.365	2.998	3.499
8	1.397	1.860	2.306	2.896	3.355
9	1.383	1.833	2.262	2.821	3.250
10	1.372	1.812	2.228	2.764	3.169
15	1.341	1.753	2.131	2.602	2.947
20	1.325	1.725	2.086	2.528	2.845
30	1.310	1.697	2.042	2.457	2.750
40	1.303	1.684	2.021	2.423	2.704
∞	1.282	1.645	1.960	2.326	2.576
$n-1$	0.1	005	0.025	0.01	0.005
	Probability of t value larger than the indicated value in the table (single side)				

When $\overline{N}$ is bigger or smaller than N, we can get

$$N = \overline{N} \pm t_{(\alpha,f)}\sigma_N \tag{17.40}$$

where

t is the confidence factor, which can be found from the t distribution table (see Table 17.35). It varies with the significance level α and the degree of freedom $f = (n-1)$. It is also called the t distribution coefficient;

α is the significance level and also called the risk factor. It is the possibility of the estimated value falling out of the specified interval:

$$\alpha = 1 - P$$

P is the degree of confidence or the confidence coefficient, which reflects the reliability degree.

t distribution curve is not a curve; instead it is a group of curves with the change of f, which are symmetrical to the ordinate. When $n-1 < 10$, the curve is low and flat, which is greatly different from the normal distribution curve. When $n-1 > 30$, t distribution curve is similar with the normal distribution curve. When $n-1 > 100$, t distribution curve can be replaced with the normal distribution curve directly. When $t \to \infty$, they are strictly consistent with each other.

What should be noticed is that there are two forms of t distributions including the unilateral and the bilateral distributions. Bilateral distribution is used when both

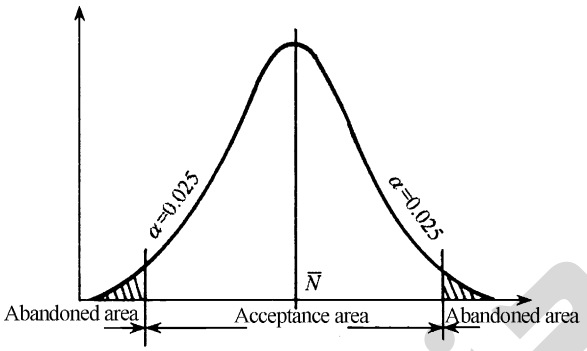

Fig. 17.41 Bilateral *t* distribution

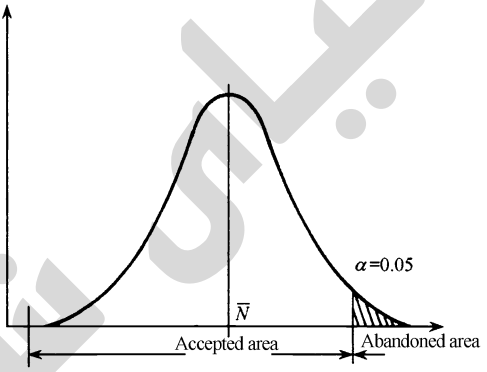

Fig. 17.42 Unilateral *t* distribution (upper limit)

upper and lower limits are required, which is shown in the Fig. 17.41. If it is assumed $\alpha = 0.05$, it occupies 0.025 at each side.

For the particle distribution in cleanroom, people only care about whether the highest concentration is more than the concentration limit corresponding with the air cleanliness level, while the lowest concentration does not affect. So unilateral *t* distribution should be used for the test. For example, in 209E the upper limit of confidence is 95 %; as shown in Fig. 17.42, $\alpha = 0.05$ for unilateral distribution. By comparing two figures, we can see that $t_{0.05}$ for unilateral distribution equals with $t_{0.1}$ for bilateral distribution and $t_{0.025}$ for unilateral distribution equals with $t_{0.05}$ for bilateral distribution.

As introduced before, when $n \leq 30$, *t* distribution should be used for the test. But when *t* distribution is used, the value of *n* can be different. The necessary measurement points can be calculated according to the calculation method about *t* distribution [37]. Here only the result derived by statistical methods is given. For normal distribution,

$$n \geq 8\left(\frac{t_{\infty,\alpha}}{K}\right)^2 \tag{17.41}$$

where

n is the necessary measurement points;
K is constant, which is the $1/\sigma$ of the estimated data distribution interval length, $K = 1/\sigma$. Usually it is 1;
t is the t distribution coefficient determined with the value of α and $f \to \infty$.

When the calculated n is a big value which corresponds with a big sample, t is close to normal distribution when $n \to \infty$, which does not need correction. If n is a small sample, t is close to the t distribution, which needs correction. The calculated value of n is used to obtain $t_{2n-2,\,\alpha}$, which is then substituted into the above formula to get the new value of n. The difference is usually small.

Example 17.1. When 95 % of the data for the unilateral t distribution are required to fall into the interval of one time of σ, how many measurement points are needed?

Solution. From the question, we know $1 - \alpha$ (unilateral) $= 0.95$. Looking up Table 17.35, we can get $t_{\infty,\,\alpha} = 1.645$. Since $K = 1$, so we get

$n \geq 8\left(\frac{1.645}{1}\right)^2 = 21.6$ (which can be taken as 22)

Because the number of samplers is small, correction is needed. Because $f = 2$ $n - 2 = 42$, we can look up the table and get $t_{42,\,0.05} = 1.684$:

$$n \geq 8\left(\frac{1.684}{1}\right)^2 = 23$$

It can also be seen from the results that both the former 20 points standard method and Japanese standards which require the number of measurement points to be between 20 and 30 are in accordance with the statistics, while the required number of measurement points and the total sampling times in 209C–209E are less. Even Mr. Peck, the committee chairman of IES-RP-50 who modified 209B, also pointed out that [5], "this will not reach the statistical qualified 95 % confidence. So there is no reason to make 95 % as a requirement. In these areas, a series of evaluation should be carried out." This comment should draw attention.

Assessment Standards

US Federal Standard 209C proposed two indispensable criteria with the interval estimation method to assess the air cleanliness. These two criteria are:

(a) The average concentration at each sample point with n sampling times $\leq$ upper limit of concentration corresponding with the air cleanliness level.
(b) 95% upper confidence limit of the average concentration of all sampling points, namely, the room average concentration (i.e., the room average statistical value) $\leq$ upper limit of concentration corresponding with the air cleanliness level.

When these two criteria are met, the air cleanliness has reached that level. ISO 14644-1 also made the same specification, which corresponds to the test with maximum concentration plus statistical test in fact.

The first criterion requires the existence of more than one measuring point. The number of sampling points specified in standard is a function of the measured area. As mentioned earlier, in fact, both the number of the measurement points and the total number of sampling times specified in 209C–209E are less than normal. Given the possible accidental error, the average concentration at one sampling point instead of one sampled concentration is used in this standard.

The second criterion requires the uniformity of measurement results (namely, the variation rate of concentrations at the measurement point is small). According to the specification in 209E, this has influence only for the application with less than 10 sampling points (209E has no limit for sampling points), because it is more difficult to reach the standard specified value. By this criterion, it shows that time is saved if the number of measuring points is less but at the expense of the air cleanliness. The statistic value with less point is higher than that with more points. In addition, if the measurement data is close to the upper limit of concentration corresponding with the air cleanliness level, or although there is a very low concentration data, the difference between the data is big; the statistic measurement result may be larger than the value specified in the standard. In this case, the number of measuring points should be appropriately increased.

According to 209E, *t* distribution will not be used when the number of measuring points is less than 10, so it is simplified to the test with maximum concentration.

17.5.2 Dynamic-to-Static Ratio

The particle concentration specified with the corresponding air cleanliness level is independent with the test state. But when the particle concentration under the as-built and at-rest status is compared with that under the operational status, the average concept should be introduced, namely,

$$\frac{\text{Particle concentration at operational status}}{\text{Particle concentration at at-rest status}}$$

It is called the dynamic-to-static ratio [38].

As mentioned before, the indoor particles in the cleanroom are mainly from the human activities. The ratio of the particle generation rate per unit volume (including the amount of surface particle generation) between the human activity and the human rest can be calculated. For a cleanroom with area larger than 1 m^2, it can be assumed two people inside for test, so the maximum occupant density during measurement is 0.2 p/m^2. According to the available information at home and

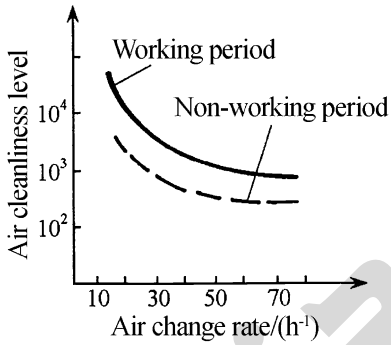

Fig. 17.43 Relationship of air cleanliness between working and nonworking periods

abroad, for turbulent flow cleanroom, the occupant density during work period is generally not more than 0.3; then we can obtain:

$$\frac{G_{n0.3}}{G_{m0.2}} = \frac{6.5 \times 10^4}{1.3 \times 10^4} = 5$$

If the area of cleanroom is more than 10 m^2, the ratio will be less than 5. When the staff density is greater than 0.3, the ratio will be greater than 5, but this is in a few situations. That means 5 is a relatively big number. Is it suitable to use the expression of G_n/G_m to represent the dynamic-to-static ratio of the particle concentration? First, N is proportional to G. Second, some experimental data also shows that most of the dynamic-to-static ratios are less than 5 [35]. Figure 17.43 shows the relationship summarized based on the operation experience of cleanroom with the published papers at both home and abroad [39]. It indicates that the difference of particle concentration is about 5 times between working and non-working periods.

In short, the operational particle concentration in general can be obtained when the as-built particle concentration measured for the acceptance test is multiplied by 5.

The above is about turbulent flow cleanroom. In the US Air Force Standard T.O.00-25-203, the ratio between the design standard and the operating standard for turbulent flow cleanroom is also 5 times.

For unidirectional flow cleanroom, there is no any foreign national standards which specify the dynamic-to-static ratio. In the US Air Force Standard above, the difference between the design standard and the operating standard for the unidirectional flow clean bench was stipulated with 10 times. But with the technical requirements for acceptance test in the USA for cleanroom with air cleanliness level Class 100 (ISO Class 5) [35], regardless of the as-built state or the at-rest state, the number of particles equal to and bigger than 0.5 μm per cubic foot is less than 10, and the number of the particles equal to and bigger than 1 μm is 0. This means the dynamic-to-static ratio for particle concentration in unidirectional flow cleanroom should be 10.

In China, there are two views on this issue. One view is that due to the characteristics of unidirectional flow, the particles generated can be removed immediately, so the dynamic-to-static ratio can be 1. Another point of view is that since the particle concentration for unidirectional flow cleanroom is very low, the concentration will change immediately once disturbance occurs. So for the safety reason, there should be a value for the dynamic-to-static ratio. As discussed before in the section about the lower limit of the air velocity, the pollution control ability of unidirectional flow cleanroom is really strong, which supports the first view. However, occasional factors cannot be excluded. For safety, it is also appropriate to define the dynamic-to-static ratio with a small value (such as 1 or 2 times). This value specified in "Air Cleaning Technical Measures" was 3, but now it seems that it is also feasible to set the value 2.

Here the example presented in Chap. 13 will be illustrated. The designed particle concentration cannot choose the maximum value corresponding with the air cleanliness level. For the cleanroom with air cleanliness level Class 7, the designed particle concentration cannot be 350#/L. As mentioned in Chap. 11, when other factors are taken into consideration, it is better to choose the upper limit of concentration with 1/2–1/3, namely, 175–120#/L.

17.5.3 Correction to Atmospheric Dust Concentration

For the cleanroom with air cleanliness level Class 5 or lower than Class 5, no matter how much is the atmospheric dust concentration during the test, the test results can be applied to all the conditions. While for cleanroom with air cleanliness higher than Class 5, it is necessary to make correction for the atmospheric dust concentration [40], namely,

$$\overline{N}' = AN_s + \overline{N} \tag{17.42}$$

where

$\overline{N}'$ is the average concentration in the cleanroom after correction (#/L);

$\overline{N}$ is the average concentration measured by normal methods before correction (#/L);

N_s is the particle concentration of the supplied air (#/L);

A is the atmospheric dust correction coefficient:

$$A = \frac{10^6 \#/L - M\#/L}{10^6 \#/L} \tag{17.43}$$

M is the atmospheric dust concentration during measurement.

References

1. Gu WZ (1980) Determination of the measuring capacity of the particle counter for 0.3 μm channel. Contam Control Air-Condit Technol 2:29–34 (In Chinese)
2. Wu ZY (1984) Discussion on the sensitivity adjustment for the particle counter. Institute of HVAC of China Academy of Building Science Research, Beijing (In Chinese)
3. Zhao RY, Xu WQ, Qian BN (1987) Particle counting error of the optical particle counter. Tsinghua University, Beijing (In Chinese)
4. Xu ZL, Shen JM, Chen CY, Zhang YZ, Zhang YG (2000) Aerosol sampling error about a particle counter. China Powder Sci Technol 6(1):15–19 (In Chinese)
5. Peck RD (1989) The proposed revision of Federal Standard 209B (trans: Tian Zhikun). In: Collected works on design, construction and acceptance inspection of cleanroom, pp 274–277 (In Chinese)
6. Zhao RY, Qian BN, Xu WQ (1987) Dilution and measurement of high concentration aerosol. Tsinghua University, Beijing (In Chinese)
7. No. 2 Design Research Institute of China National Nuclear Corporation, etc., Comparison of filtration performance with NaCl, DOP and atmospheric dust (exchange material, the data is missing) (In Chinese)
8. Wu ZY (1980) Generation of standard monodisperse aerosol. Contam Control Air-Condit Technol 2:35–38 (In Chinese)
9. JIS Draft Template (1975) Light scattering particle counter. J Jpn Air Clean Assoc 13 (2):48–53 (In Japanese)
10. Ventilation Committee and Subcommittee on Dust Measurement Method (1975) Measurement method of airborne particles in buildings (2). GA JAPAN 90(1098):849–866 (In Japanese)
11. Xu ZL, Shen JM (1989) Application of air cleaning technology. China Architecture & Building Press, Beijing, pp 396–398 (In Chinese)
12. Yamazaki S (1979) Measurement method of airborne bacteria. J Jpn Air Clean Assoc 17(7):26–33 (In Japanese)
13. Sugawara F, Yoshizawa S (1975) Study on microbial contamination indoors (1). Proc Jpn Build Instit 233:133–142 (In (In Japanese)
14. Institute of HVAC at China Academy of Building Research (1975) Two kinds of 300 type protective air filter. J HV&AC 1:23–35 (In Chinese)
15. JACA No.30-1994 (1994) Guideline for the generation method of aerosol used for contamination control. J Jpn Air Clean Assoc 32(2):60–82 (In Japanese)
16. Suemori T, IES-RP-CC001 (1994) 3 HEPA and ULPA filter. J Jpn Air Clean Assoc 32(1):57–68 (In Japanese)
17. Irie T, Mitsui Y, Saiki A (1992) Comment on volatilization quantity of DOP from filter media of HEPA filter. J Jpn Air Clean Assoc 30(1):13–19 (In Japanese)
18. Tu GB, Zhang SF (1990) Relationship between the filtration efficiency of microbe and particle for fibrous filter media. Contam Control Air-Condit Technol 2:20–21 (In Chinese)
19. Dorman RG (1968) European and American methods of testing air conditioning filters. Filtr Sep 1:24–28
20. Xu ZL (1995) Conversion method between particle counting efficiency and arrestance using atmospheric dust. Contam Control Air-Condit Technol 1:16–20 (In Chinese)
21. Yoshida F et al (1971) Study on the field test method of HEPA filter. J Jpn Air Clean Assoc 8 (7):54–65 (In Japanese)
22. Ji JW (1980) Precipitators. China Architecture & Building Press, Beijing (In Chinese)
23. Noso M (1973) The latest electrical dust collection device. Therm Manag Pollut 25(7):51–63 (In Japanese)
24. Linder P (1970) Air filters for use at nuclear facilities, International Atomic Energy Agency. Technical Reports Series, No. 122
25. Morkowski J (1972) Messtechnische Bewertung reiner räume. Schweizerische Blätter für Heizung und Lüftung 39:2 (In German)

26. Takizawa S (1994) Air filter in the pharmaceutical industry. J Jpn Air Clean Assoc 32(2):28–38 (In Japanese)
27. Xu ZL, Cao GQ, Feng X et al (2010) A theoretical analysis of atmospheric dust aerosol method for leak testing HEPA/ULPA filters installed in cleanroooms – Part 9 of the Series of research practice of the National Standard Task Group for the code for cleanroom construction and acceptance test. Build Sci 26(1):1–6 (In Chinese)
28. Xu ZL, Cao GQ, Feng X, Zhang YZ (2010) A novel qualitative leak scan test method for installed HEPA/ULPA filters used in China. In: Proceedings of 2010 International Symposium on Contamination Control, Tokyo, p 457
29. Cao GQ, Xu ZL, Zhang YZ et al (2008) Air tightness measuring method for cleanroom: Part 8 of the series of research practice of the national standard task group for the code for cleanroom construction and acceptance test. J HV&AC 38(11):1–6 (In Chinese)
30. Shen JM (1982) Discussion of the airflow visualization with bubble. Contam Control Air-Condit Technol 3:57–61 (In Chinese)
31. Philip WM (1973) Environmental control in electronic manufacturing, pp 278 –292
32. Xu ZL, Feng X, Zhang YZ et al (2008) Discussion of definition of cleanroom occupation status: Part 2 of the series of research practice of the national standard task group for the code for cleanroom construction and acceptance test. J HV&AC 38(2):1–4 (In Chinese)
33. Xu ZL (1980) Calculation of the necessary sampling points in cleanroom. Contam Control Air-Condit Technol 1:25–28 (In Chinese)
34. Cooper DW (1989) Rationale for Proposed Revisions to Federal Standard 209B (Cleanrooms) (trans: Liu Xianzhe, Zhan Yingmin). In: Collected works on design, construction and acceptance inspection of cleanroom, pp 278–286 (In Chinese)
35. Fan CY, Wang HP (1995) Air cleanliness level standard for cleanroom. J HV&AC 25(3):8–12 (In Chinese)
36. Feng HM (1997) Influence of the printer of the particle counter on the measurement results. Contam Control Air-Condit Technol 1:21–33 (In Chinese)
37. Zeng QC (1982) Technical mathematical statistics. Anhui Science & Technology Publishing House, Hefei, pp 71–73 (In Chinese)
38. Xu ZL (1980) Problem about the dynamic to static ratio of particle concentration in cleanroom. J HV&AC 3:16–19 (In Chinese)
39. Tanaka K (1972) Indoor air pollution and its countermeasures. J Jpn Air Clean Assoc 1:10–23 (In Japanese)
40. Xu ZL (1980) Evaluation standard and method for cleanroom. J HV&AC 2:27–29 (In Chinese)